ARGEO-C3 DJIBOUTI 2010

Organisé par
Organized by

CERD

Présidence de la République

IGA

UNEP

BGR

France coopération

IAHS AISH

République de Djibouti

3rd East African Rift Geothermal Conference ARGEO-C3
3ème Conférence Géothermique du Rift Est Africain ARGEO-C3

EXPLORING AND HARNESSING THE RENEWABLE AND PROMISING GEOTHERMAL ENERGY

EXPLORATION ET MAITRISE DE L'ENERGIE GEOTHERMIQUE RENOUVELABLE ET PROMETTEUSE

Djibouti, 22-25 November 2010

SYMPOSIUM PROCEEDING

3rd East African Rift Geothermal Conference ARGEO-C3

ACTES DU SYMPOSIUM

3ème Conférence Géothermique du Rift Est Africain ARGEO-C3

Djibouti, 22-25 November 2010

COMMITTEES

SCIENTIFIC COMMITTEE

LADISLAUS RYBACH

HORST RUETER

ARNASSON KNUTUR

MESERET TEKLEMARIAM

MWANGI MARTIN

GUDNI AXELSON

ORGANIZING COMMITTEE

JALLUDIN MOHAMED

NIMA GUELLEH

ABDOURAHMAN HOUMED-GABA

MAGUIDA HOUSSEIN

SAID AWALEH

BOUH HOUSSEIN

MAHAMOUD OSMAN

MAWASSEM AHMED

ABDOU MOHAMED HOUMED

MAGAREH HASSAN

SUMMARY

THEME I GEOLOGICAL EXPLORATION..... 7

GEOTHERMAL ENERGY: CURRENT STATUS AND FUTURE PROSPECTS 9
LADISLAUS RYBACH, HORST RUETER

GEOLOGICAL AND GEOCHEMICAL EXPLORATIONS OF GEOTHERMAL RESOURCES IN YEMEN..... 17
ABDULSALAM M. AL-DUKHAIN, TAHA A. AL-KOHLANI

YOUNG RIFT KINEMATICS IN THE TADJOURA RIFT, WESTERN GULF OF ADEN, REPUBLIC OF DJIBOUTI 19
MOHAMED A. DAOUD[1], BERNARD LE GALL2, RENE C. MAURY[2], JOËL ROLET[2], PHILIPPE HUCHON[3], HERVE GUILLOU[4]

GEOTHERMAL RESOURCE INDICATIONS OF THE GEOLOGIC DEVELOPMENT AND HYDROTHERMAL ACTIVITIES OF D.R.C. 27
GETAHUN DEMISSIE

HOW GEOTHERMAL EXPLORATION LED TO GOLD EXPLORATION: A CASE HISTORY - THE AFAR DEPRESSION 47
DAVID J. HALL

GEOLOGY OF KIBIRO, KATWE AND BURANGA GEOTHERMAL PROSPECTS OF UGANDA..... 53
JAMES FRANCIS NATUKUNDA

STRUCTURAL CONTROLS ON THERMAL ANOMALIES AND DIFFUSE SOIL DEGASSING AT MENENGAI GEOTHERMAL PROSPECT, THE KENYAN RIFT VALLEY 67
ISAACK KANDA

INTERGRATION BETWEEN GEOGRAPHICAL INFORMATION SYSTEM AND SERVICE, APPLICATION AND PRODUCTS CONTRIBUTION TO GEOTHERMAL DEVELOPMENT..... 73
JAMES KIMUTAI

SUCCESSFUL USE OF HYDROTHERMAL ALTERATION MINERALOGY IN APPRAISING A GEOTHERMAL RESERVOIR: CASE STUDY: OLKARIA DOMES GEOTHERMAL FIELD, KENYA 79
JOHN LAGAT .....

A PROTO-VOLCANIC MARGIN ALONG THE ASAL RIFT. THE MAKARASSOU FAULT SYSTEM, DJIBOUTI. 85
BERNARD LE GALL[1], MOHAMED A. DAOUD[2] & JOEL ROLET[1]

HYDROTHERMAL ALTERATION STUDIES OF THE TENDAHO GEOTHERMAL PROSPECT AREA, ETHIOPIA..... 91
MESERET TEKLEMARIAM

EPITHERMAL AU-AG- BI -TE MINERALIZATION IN THE SE AFAR RIFT, REPUBLIC OF DJIBOUTI 93
MOUSSA, N*. (1, 2,3); FOUQUET, Y. (1); LE GALL, B. (2); BOHN, M. (1); ETOUBLEAU, J. (1) ; GRASSINEAU, N. (4); CAMINITI, A. M. (3); ROLET, J. (2) ; JALLUDIN, M. (3)

THE MENENGAI CALDERA STRUCTURE AND ITS RELEVANCE TO GEOTHERMAL POTENTIAL 99
LUCY MUTHONI NJUE,

GEOTHERMAL WELL SITING USING GIS: A CASE STUDY OF MENENGAI GEOTHERMAL PROSPECT.....109
LEVI SHAKO

THOUGHTS ABOUT TECHNIQUES APPLICABLE IN EXPLORATION OF GEOTHERMAL RESOURCES OF UGANDA.....121
ISAIAH TUMWIKIRIZE

CONTRIBUTION TO FAVORABLE GEOTHERMAL SITE SELECTION IN THE AFAR TRIANGLE 139
JACQUES VARET

THEME II GEOCHEMICAL EXPLORATION..... 156

GEOCHEMISTRY OVERVIEW OF HOT SPRINGS FROM THE LAKE ABHE AREA: REPUBLIC OF DJIBOUTI 158
BOUH HOUSSEIN

GEOCHEMICAL CHARACTERISTICS OF HOMA HILLS GEOTHERMAL PROSPECT 170
CHARLES K. WANJIE

GEOCHEMISTRY OF RWENZORI HOT SPRING WATERS 172
VINCENT KATO1. DR. MICHAEL KRAML2

ISOTOPIC DETERMINATIONS OF BURANGA AND KATWE TRAVERTINE DEPOSITS, UGANDA 184
VINCENT KATO

WATER ISOTOPE GEOCHEMISTRY AS TOOLS FOR THE EXPLORATION OF A LOW-ENTHALPY COMPLEX RESERVOIR: THE CASE OF THE GEOTHERMAL FIELD OF HAINAUT (BELGIUM – NW EUROPE) 188
LUCIANE LICOUR

INTERPRETATION OF GEOCHEMICAL WELL TESTS DATA FOR OW-903B, OW-904B AND OW-909 - OLKARIA DOMES, KENYA. 196
Malimo, Sylvia Joan.

GEOTHERMAL PROSPECTING BY GEOCHEMICAL METHODS IN THE QUATERNARY VOLCANIC PROVINCE OF DHAMAR (CENTRAL-WESTERN YEMEN) 219
ANGELO MINISSALE[(1)], ORLANDO VASELLI[(1,2)], MOHAMED MATTASH[(3)], GIORDANO MONTEGROSSI[(1)], FRANCO TASSI[(2)], ABDULSALAM AD-DUKHAIN[(3)], ULRICH KALBERKAMP[(4)], ALI AL-SABRI[(3)], TAHA AL-KOHLANI[(3)]

GEOCHEMICAL ASSESSMENT OF KARISIMBI GEOTHERMAL PROSPECT, RWANDA.....221
JEAN NEPOMUSCENE NAMUGIZE[(1)*], UWERA RUTAGARAMA[(1)]

GEOCHEMISTRY OF KATWE-KIKORONGO, BURANGA AND KIBIRO GEOTHERMAL AREAS, UGANDA 223
GODFREY BAHATI, KATO VINCENT, NYAKECHO CATHERINE

USE OF A NEW SODIUM/LITHIUM (NA/LI) GEOTHERMOMETRIC RELATIONSHIP FOR HIGH-TEMPERATURE (HT) GEOTHERMAL FLUIDS DERIVED FROM SEAWATER/BASALT INTERACTION PROCESSES: APPLICATION TO THE DJIBOUTI CASE 231
BERNARD SANJUAN

GALLIUM AND GERMANIUM DISTRIBUTON IN GEOTHERMAL WATER.....249
SIKIE A. ELMI[A], STEFAN ARNORSSON[B] AND ANDRI STEFANSSON[B]

THEME III GEOPHYSICAL EXPLORATION 263

NEAR-REAL TIME INTERPRETATON OF MICRO-EARTHQUAKE DATA FOR RESERVOIR MODELING 265
LAWRENCE HUTCHINGS, KATIE BOYLE, STEVE JARPE*, BRIAN BONNER, AND NATHANIEL LINDSEY*

EVALUAITON OF HIGH RESOLUITON SOFTWARE FOR EARTHQUAKE LOCATIONS AND TOMOGRAPHY STUDIES.....267
LAWRENCE HUTCHINGS, KATIE BOYLE, AND NATHANIEL LINDSEY*

GEOPHYSICAL SURVEY IN KARISIMBI GEOTHERMAL PROSPECT, RWANDA 269
CONSTANTIN IRABARUTA, MAY BE INCLUDE OTHER PEOPLE

ACTIVITES VOLCANIQUES ET GEOTHERMIQUES EN REPUBLIQUE DE DJIBOUTI REVELEES PAR LES VALEURS *B* DE LA SISMICITE DE 1973 A 2009.....271
KASSIM MOHAMED KASSIM

ROLE OF TEMPERATURE CHANGE IN MICRO SEISMIC ACTIVITY DURING FLUID INJECTIONS IN FAULTED AND FRACTURED ZONES. PART 1: UPDATING THE THERMAL MODELLING IN A DFN MODEL USING A DOUBLE MEDIA APPROACH.....283
AHMED KAYAD MOUSSA[1], DOMINIQUE BRUEL[1]

JOINT 1-D INVERSION OF TEM AND MT DATA FROM OLKARIA DOMES GEOTHERMAL AREA, KENYA.....288
CHARLES MUTURIA LICHORO

THE PRELIMINARY RESULTS OF THE GEOPHYSICAL INVESTIGATION ON THE GHOUBBET PROSPECT. 303
HASSAN MOHAMED, NASROUDIN AHMED

EXPLORATION OF GEOTHERMAL RESOURCES USING MAGNETOTELLURICS CASE STUDY MENENGAI PROSPECT IN KENYA 307
RAYMOND MWAKIRANI

APPLICATION OF THREE-DIMENSIONAL MAGNETOTELLURIC IMAGING TO GEOTHERMAL EXPLORATION.....317
PASCAL TARITS[(1)] & SOPHIE HAUTOT[(2)]

INTEGRATED GEOPHYSICAL SURVEYS TO CHARACTERIZE TENDAHO GEOTHERMAL FIELD IN NORTH EASTERN ETHIOPIA.....323
YOHANNES LEMMA[1], ULRICH KALBERKAMP[2], AKLILU HAILU[3], MOHAMMEDNUR DESISSA[4] ,

GROUND WATER SURVEY WITH A NEW CAPACITANCE PROBE 335
IDRIS BEXI, XAVIER CHAVANNE, JEAN-PIERRE FRANGI

THEME IV GENERAL COUNTRY EXPLORATION..... 343

GEOTHERMAL ENERGY IN UGANDA, COUNTRY UPDATE 2010.....345
GODFREY BAHATI AND JAMES FRANCIS NATUKUNDA

PLANNING OF GEOTHERMAL PROJECT IN THE UNION OF COMOROS.....357
BOINAÏDI ALI SAÏD

GEOTHERMAL EXPLORATION ADVANCEMENT IN DJIBOUTI 359
MOHAMED JALLUDIN

THE POTENTIAL RELATIONSHIP OF SOME GEOTHERMAL FIELD IN UGANDA.....365
DEUS KATOMI MUHWEZI

THEME V. WELL TESTING, INJECTION, RESERVOIR ENGINEERING MODELLING 383

VOLUMETRIC RESSOURCE ASSESSMENT OF ASAL GEOTHERMAL FIELD, REPUBLIC OF DJIBOUTI.....385
DAHER E. HOUSSEIN

APPRAISAL OF GEOSTATISTICAL METHODS TO ESTIMATE HYDRAULIC PROPERTIES OF A COMPLEX BASALTIC RESERVOIR. THE GULF BASALTIC AQUIFER, DJIBOUTI, HORN OF AFRICA. 391
MOHAMED JALLUDIN[1] . AND MOUMTAZ RAZACK[2*]

THEME VI FIELD DEVELOPMENT PRODUCTION TECHNOLOGY, POWER, DRILLING AND WELL DESIGN, LOW ENTHALPY, DIRECT USE 405

DEVELOPMENT OF GEOTHERMAL ENERGY TECHNOLOGIES IN LOW-ENTHALPY REGIONS 407
PROF. DR. U. ARSLAN & DIPL.-ING. H. HUBER

GEOTHERMAL DEVELOPMENT IN ZAMBIA 409
KENNEDY MWANZA CLINT KOMBE

REHABILITATION OF THE ALUTO PILOT GEOTHERMAL POWER PLANT.....411
MARKOS MELAKU AND BOB THOMASSON

CURRENT STATUS OF THE GEOTHERMAL DEVELOPMENT IN KENYA 417
GEOFFREY MUCHEMI

Electricity and Freshwater Macro-project in the Arid African Landscape of Djibouti 425
RADU D. RUGESCU425

INFRASTRUCTURE DEVELOPMENT IN GEOTHERMAL FIELDS: A CASE STUDY FOR MENENGAI GEOTHERMAL PROSPECT, KENYA 437
WILSON RUTINU

THEME VII TRAINING AND CAPACITY BULDING 447

UNU-GTP AND GEOTHERMAL TRAINING FOR AFRICA 449
LÚDVÍK S. GEORGSSON

DEVELOPING CRITICAL HUMAN COMPETENCIES IN GEOTHERMAL ENERGY TECHNOLOGY 460
PETER OMENDA AND SILAS SIMIYU

CHALLENGES OF HUMAN CAPACITY BUILDING: GDC'S EXPERIENCE 464
IRENE N. ONYAMBU (MRS.)

CAPACITY BUILDING, THE GDC EXPERIENCE 468
ROSE OUGO TINDI

DEVELOPMENT OF A REGIONAL GEOTHERMAL TRAINING INSTITUTE IN KENYA 473
JAMES WAMBUGU

THEME VIII ECONOMICS FINANCING, PRIVATE SECTORS 481

NOTE ON THE PROGRAMME FOR INFRASTRUCTURE DEVELOPMENT IN AFRICA (PIDA) 483
MR. BERNARD BARANDEREKA,

OVERVIEW OF STATUS, STRATEGY AND GAPS IN THE COUNTRIES OF THE EAST AFRICAN RIFT SYSTEM (EARS) FOR DEVELOPMENT OF THEIR GEOTHERMAL ENERGY RESOURCE 485
MESERET TEKLEMARIAM (PH.D)

THE BUSINESS VALUE OF SERVER VIRTUALIZATION: THE GDC CASE 487
CHARLES SITONIK

THEME IX ENVIRONNEMENT, SOCIAL, LEGAL AND ECONOMICAL ASPECTS 497

THERMAL INFLUENCE OF SURFACE DISPOSAL OF HOT GEOTHERMAL WASTEWATER ON AQUATIC ECOSYSTEMS: WITH EXAMPLES FROM ICELAND 499
GABRIEL N. WETANG'ULA[1, 2, 3] AND SIGURDUR S. SNORRASON[1]

CHALLENGES IN PROVISION OF ADMINISTRATIVE SERVICES IN AN ACCELERATED GEOTHERMAL DEVELOPMENT PROCESS 510
PURITY GITUMA

EMPOWERING COMMUNITIES LIVING WITHIN GEOTHERMAL AREAS IN THE KENYAN RIFT 513
PASCAL MANAN

CORPORATE SOCIAL RESPONSIBILITY (CSR) IN GEOTHERMAL DEVELOPMENT: THE CASE OF THE GEOTHERMAL DEVELOPMENT COMPANY (GDC), KENYA 516
RUTH MUSEMBI

BIODIVERSITY CONSERVATION AND GEOTHERMAL DEVELOPMENT 522
THECLA M. MUTIA

THE NEED FOR ENHANCED ENVIRONMENTAL AUDITING OF GEOTHERMAL PROJECTS. A CASE STUDY OF KENYA ELECTRICITY GENERATING COMPANY LTD (KENGEN). 530
MS. PACIFICA F ACHIENG OGOLA,

STATUS AND STRATEGIC FRAMEWORK IN GEOTHERMAL DEVELOPMENT IN ETHIOPIA 535
SOLOMON KEBEDE

THEME X GEOTHERMAL COST - SIDE EVENT 543

POLICY IMPLEMENTATION TO ENABLE ACCELARATED GEOTHERMAL DEVELOPMENT 545
R. GORDON BLOOMQUIST, PH.D.

GEOTHERMAL ENERGY DEVELOPMENT OF L. ABBE AND CDM FOR DJIBOUTI 549
D CHANDRASEKHARAM[1,2] AND VARUN CHANDRASEKHAR[2]

GEOTHERMAL ENERGY IN THE LEAST COST ELECTRICITY SECTOR PLANNING IN DJIBOUTI 553
IDRISS AHMED HARED

DRILLING CHALLENGES TOWARDS COST EFFECTIVE DRILLING IN KENYA 555
STEPHEN KANGOGO

KENYA'S OPPORTUNITIES IN CARBON TRADING: A FOCUS ON THE ENERGY SECTOR 557
BENJAMIN KUBO, TECLA MUTIA, KENNEDY MOSS AND PATRICK OYUGI

REGULATORY FRAMEWORKS AND THEIR IMPLICATIONS IN GEOTHERMAL DEVELOPMENT PROJECTS - THE CASE OF KENYA. 565
CORNELIUS NDETEI

COSTING OF GEOTHERMAL WELLS 573
REUBEN NGOSI

A NEW KFW FUNDING AND RISK MITIGATION SCHEME FOR GEOTHERMAL PROJECTS IN
THE EAST AFRICAN RIFT VALLEY - STRATEGY AND STRUCTURE" 585
KATRIN KESSELS (KFW) HORST KREUTER (GEOT, GEOTHERMAL ENGINEERING GMBH) JAMES MUIR (SKM,
SINCLAIR KNIGHT MERZ) MARIETTA SANDER (BGR, BUNDESANSTALT FÜR GEOWISSENSCHAFTEN UND ROHSTOFFE, HANNOVER)

THEME I

GEOLOGICAL EXPLORATION

GEOTHERMAL ENERGY: CURRENT STATUS AND FUTURE PROSPECTS

Ladislaus Rybach, Horst Rueter
Geowatt AG Zurich, Dohlenweg 28, CH-8050 Zurich, Switzerland
rybach@geowatt.ch

ABSTRACT

Although geothermal energy is well positioned within the renewables (in 2008 geothermal power production exceeded more than three times that of solar photovoltaics), current growth is only steady but rather slow. While wind and solar PV show exponential growth, geothermal power develops rather linearly, so far provided by hydrothermal resources, located in special geological settings. The universally deployable Enhanced Geothermal Systems (EGS) technology could speed up geothermal growth, although substantial R&D efforts are needed to solve still open problems. Possible approaches are outlined.

Keywords: potential, power generation, direct use, development trends

INTRODUCTION

Geothermal energy is one of the contributors to any future energy mix. The advantages of geothermal energy are numerous: great, still only marginally developed potential, available around the clock (=provides base-load power), ubiquitous, indigenous, environmentally friendly, economically rewarding energy. Its two main utilization categories power generation and direct use are already introduced in many countries around the globe; further, expanding distribution is possible and should be increasingly enforced.

In the following a comparison is presented between geothermal and the other renewable energies, in terms of both potential and power generation. Development growth in power generation is presented for wind, solar photovoltaic and geothermal power and compared for the time period 1995 – 2008. Future growth estimates –for power generation as well as for direct use– are also given.

Technologic developments like Enhanced Geothermal Systems (EGS) are envisaged as the key to accelerating growth in geothermal development. There are still open questions about the universal applicability, long-term performance, and economic viability of EGS systems.

Geothermal direct use development is nowadays governed by the increasing deployment of geothermal heat pump systems. In several countries such systems already exhibits exponential growth; it is anticipated that this trend continues.

The future prospects of geothermal energy in general, and of power generation in particular, will depend on the gear-change in further growth: only if exponential growth is achieved can geothermal energy become a real player in future energy supply schemes.

LARGE GEOTHERMAL POTENTIAL

A highly respected source (World Energy Assessment – a collaborative effort between UNDP, UNDESA and the World Energy Council) attests the largest potential value to geothermal energy among all forms of renewable energy sources. The comparison is given in Table 1.

The values are given in capacity units, i.e. energy per unit time. It is obvious that geothermal energy has the largest capacity, although the accuracy of the reported number is limited. This potential is so far only marginally developed.

Table 1: Potential of renewable energy sources (WEA 2000).

Energy source	Capacity (EJ/yr)
Geothermal	5000
Solar	1575
Wind	640
Biomass	276
Hydro	50
Total	7541

GROWTH COMPARISON OVER THE TIME PERIOD 1995 – 2008

The comparison geothermal – other renewables is made for power generation. Geothermal power development data is available for the time period 1975 – 2008. The growth is practically linear, with only small increase rate changes (Figure 1, after Bertani in Fridleifsson et al. 2008).

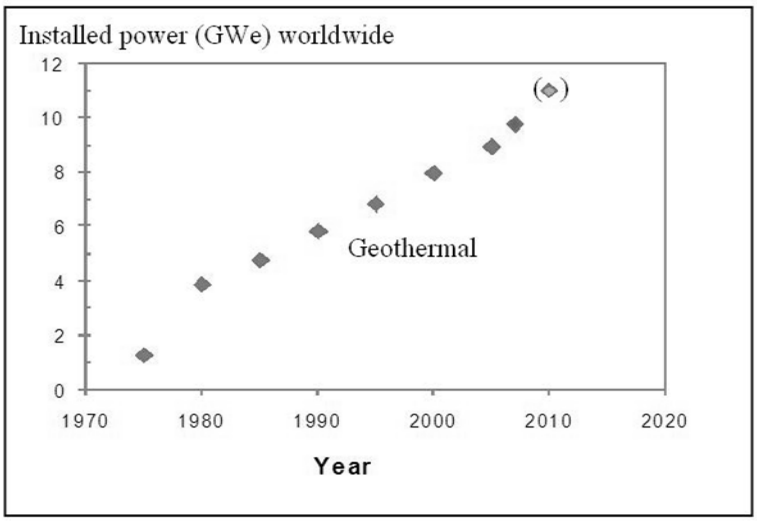

Figure 1: Growth in geothermal power development over the years 1975 – 2008. The number for 2010 (11 GWe) is estimated.

New data on the development of power generation from renewable sources is given in REN21 (2009). The installed capacity of wind power shows a clearly accelerating trend of an exponential nature (Figure 2).

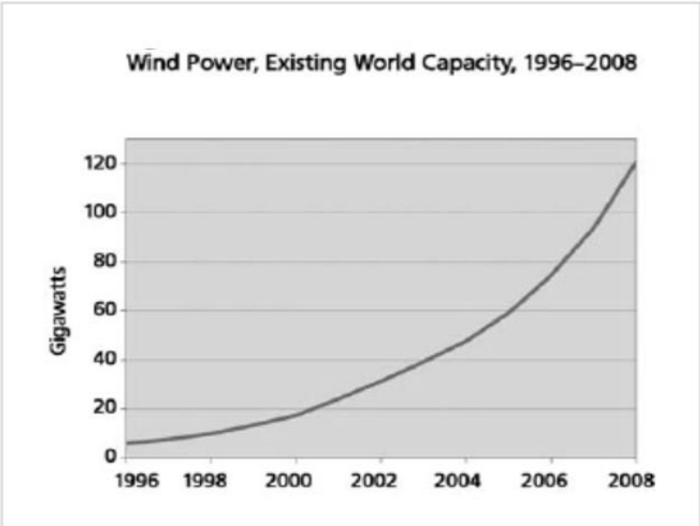

F**igure 2**: Growth in wind power development over the years 1996–2008. From REN21 (2009), modified.

A similar trend of exponential growth is reported for solar photovoltaic power, both grid-connected and off-grid production (Figure 3, from REN21, 2009). In Figure 3 the geothermal power growth -as depicted in Figure 1- is plotted for comparison. It is evident that geothermal had the lead over solar PV in the time before year 2006. Afterwards solar PV clearly takes over.

Here it must be emphasized that the plotted numbers refer to installed capacity, not to actual power production. Wind is not blowing all the time, the sun is shining only during daytime whereas geothermal production can go on at practically all times (except for production stops, for example during maintenance operations). This is reflected by the capacity factor (basically the percentage of yearly operating hours). Table 2 therefore clearly demonstrates that in terms of production geothermal is still by factors ahead of solar PV power generation.

Table 2: Renewable electric power production comparison. Installed capacity from REN21 (2009), capacity factors from Fridleifsson et al. (2008).

Technology	Installed capacity in 2008 (GWe)	Capacity factor (%)	Electricity produced (TWh)
Wind	121	21	222.6
Solar PV	16	14	19.6
Geothermal	10	75	65.7

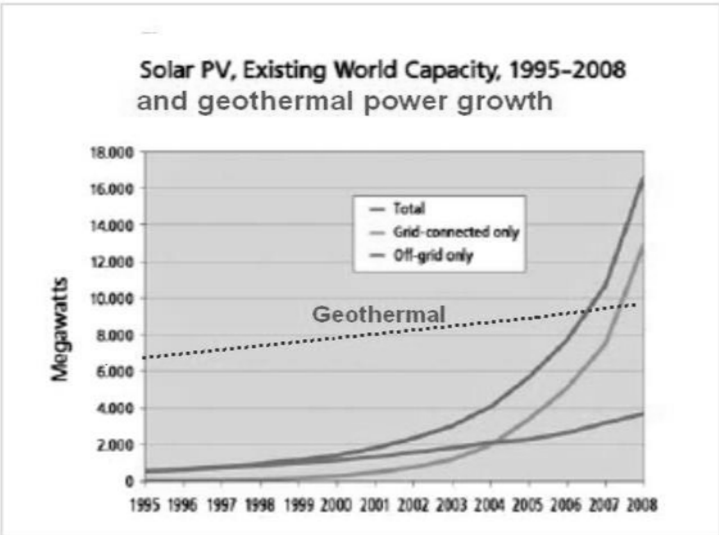

Figure 3: Growth in solar photovoltaic power development over the years 1995-2008 (from REN21, 2009). For comparison the geothermal growth trend is plotted (data of Figure 1).

From this comparison it is evident that currently geothermal power development is left behind wind and solar PV: whereas geothermal development growth is more or less linear (steady but slow growth – just a few percent increase per year), wind and solar PV exhibit accelerating growth with a clearly exponential tendency. To keep pace geothermal growth needs to be speeded up too; in the following some possible ways and means to accomplish this are addressed, primarily for power generation.

HOW TO SPEED UP GEOTHERMAL GROWTH?

In a study commissioned by the Intergovernmental Panel on Climate Change (IPCC) a team of authors estimated the growth curve in geothermal power development from the present to year 2050. Figure 4 from Fridleifsson et al. (2008) shows the result (installed capacity as well as power production). The curves in Figure 4 also exhibit exponential character.

How to achieve this accelerated growth? Until today the growth in installed geothermal power capacity originated entirely from “conventional”, hydrothermal resources. Such resources are found in numerous but special places, with high-temperature geothermal fluids present in the subsurface at relatively shallow depths (2 – 4 km). Such “anomalous” places can mainly be found in volcanic regions or in other regions, depending on their plate tectonic settings (details see e.g. in Fridleifsson et al. 2008). It can be expected that geothermal power development based on conventional high-enthalpy resources will remain more or less linear in the future; therefore some new technology is needed to provide the exponential growth component. In the following the case is made that EGS technology (Enhanced Geothermal Systems) could play this role.

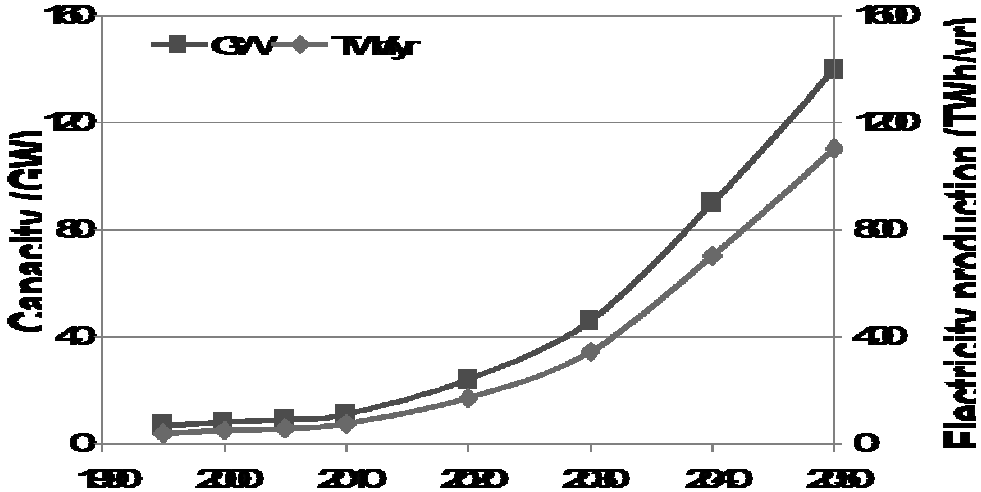

Figure 4: Installed capacity and electricity production 1995-2005 and forecasts for 2010-2050. From Fridleifsson et al. (2008).

ENHANCED GEOTHERMAL SYSTEMS – THE ACCELERATOR?

The widely renowned M.I.T. study "The Future of Geothermal Energy – Impact of Enhanced Geothermal Systems (EGS) on the United States in the 21th Century" (Tester et al., 2006) suggests that Enhanced Geothermal Systems will be the future of geothermal energy utilization. Enhanced Geothermal Systems is an umbrella term for various other denotations such as Hot Dry Rock, Hot Wet Rock, Hot Fractured Rock. The study M.I.T. study determined recoverable EGS resources > 200,000 EJ alone for the USA, corresponding to 2,000 times the annual primary energy demand.

The EGS principle is simple: in the deep subsurface where temperatures are high enough for power generation (150-200 °C) an extended fracture network is created and/or enlarged to act as new fluid pathways and at the same time as a heat exchanger. Water from the surface is transported through this deep reservoir using injection wells and recovered by production wells as steam/hot water. The extracted heat can be used for district heating and/or for power generation.

The core piece of an EGS installation is the heat exchanger at depth. It is generally accepted that it must have a number of properties in order to be technically feasible and economically viable. These refer to the total volume, the total heat exchange surface, the flow impedance, and the thermal and stress-field properties. The key properties are summarized in Table 3.

Table 3: Required properties for an EGS reservoir (after Garnish, 2002).

Fluid production rate	***50 - 100 kg/s***
Fluid temperature at wellhead	150 - 200 °C
Total effective heat exchange surface	> 2 x 10^6 m^2
Rock volume	> 2 x 10^8 m^3
Flow impedance	< 0.1 MPa/(kg/s)
Water loss	< 10 %

Although the minimum requirements for an economically viable EGS reservoir are herewith set, their realization in a custom-made manner to comply with differing site conditions is not yet demonstrated. The key issue is the development of a technology to produce electricity and/or heat from a basically ubiquitous resource, in a manner relatively independent of local subsurface conditions, i.e. to develop a technology for the creation of EGS downhole heat exchangers with the properties quantified above.

Therefore several still open questions about establishing and operating EGS heat exchangers need to be addressed and answered. Here some of the key issues are indicated:

- In creating EGS heat exchangers at several kilometers depth, questions of rock mechanics like the role of of anisotropy degree, stress change propagation/ transmission – fast / „dry“? slow / „wet“? (under different site conditions) – are unanswered;
- EGS induced seismicity (during stimulation in establishing the EGS heat exchanger but also during to production) becomes a real issue, also in terms of public perception. Social acceptance will be decisive (Majer et al. 2008).
- Uniform connectivity throughout a planned reservoir cannot yet be engineered;
- There is no experience with possible changes of an EGS heat exchanger over time.

A key property in this context is the recovery factor (fraction of extractable heat/heat in place). The recovery factor can change with time: permeability enhancement (e.g. new fractures generated by cooling cracks or dissolution of mineral species) could increase the recovery factor, while permeability reduction (e.g. due to mineral deposition) or short-circuiting could reduce recovery.

Without having field-scale experience with long-term EGS production the economic estimates about installation, production, and maintenance costs remain unsubstantiated. Onsite experience is needed with the production behavior of EGS heat exchangers at depth on the long-term, not least for acquiring economic data about installation, production, and maintenance costs. This is especially needed to judge the cost/benefit ratio of EGS power plants. Obviously the economic balance is most favorable when the waste heat of an EGS-based power plant can be sold locally, e.g. to an already existing district heating network.

So far the envisaged electric power capacity of an EGS installation (based on the properties of Table 3) is limited at a few MWe. But in order to play a significant role in local, regional and global electricity supply an EGS system capacity of at least several tens or hundreds of MWe would be essential.

One of the main future R&D goals will be to work out how the EGS power plant size could be upscaled. So far there are only some theoretical calculations available; see e.g. Vörös et al. 2007. In this publication an EGS scheme with 24 injection and 19 production wells is modelled, providing a net power output of around 60 MWe.

It is obvious that EGS is presently still at the “proof of concept” stage. More details about EGS status and problems can be found in Rybach (2010a).

R & D NEEDS, FINANCING

It is obvious from the above-described knowledge gaps that very substantial R & D efforts are still needed to make EGS become the future of geothermal energy. Whereas some of the problems could be tackled by broad-based international cooperation (the EU project ENGINE can be mentioned here; http://engine.brgm.fr), national R&D programs have to provide additional means for the challenge. Public funding, mainly by governmental agencies, will be indispensable. In Australia a veritable EGS boom is currently taking place (see e.g. Goldstein et al. 2009), its triggered only through through start-up financing, provided by the state budget.

Although envisaged for conventional geothermal resources, Ibrahim (2009) describes five steps to expedite development; four of them are based on fund allocations from national or regional governments. In any case it will be crucial to make rapid progress in tackling and solving the above-mentioned, still open problems.

GEOTHERMAL DIRECT USE

Geothermal direct use grows also steadily, but rather linearly (Table 4). The growth is increasingly dominated by the dissemination of geothermal heat pumps (GHP). This technology is versatile, can provide space heating as well as cooling and domestic hot water supply. Its world-wide growth is described in Rybach (2005).

Table 3: Growth of geothermal direct use world-wide. Data from Lund et al. (2005).

Year	MWth	TJ/yr
1995	8’660	112’441
2000	16’209	162’009
2005	27’825	261’418

Truly exponential growth is currently experienced in Switzerland. Here the borehole heat exchanger-coupled GHP systems are mainly used; their areal density is impressive (> 1 system per km^2) and so far the highest

worldwide. The corresponding drilling activities (meters drilled per year) are shown in Figure 5. Remarkable is also the rapidly increasing share of GHPs in retrofitting; replacing customary oil-fired burners provide real CO_2 emission savings (Rybach, 2010b).

Geothermal heat pumps can be installed in most geologic situations (except in groundwater protection areas) all around the world, due to the ubiquitous geothermal resource present in the shallow ground. It can thus be expected that the coming decades will show a clearly exponential growth of GHP installations.

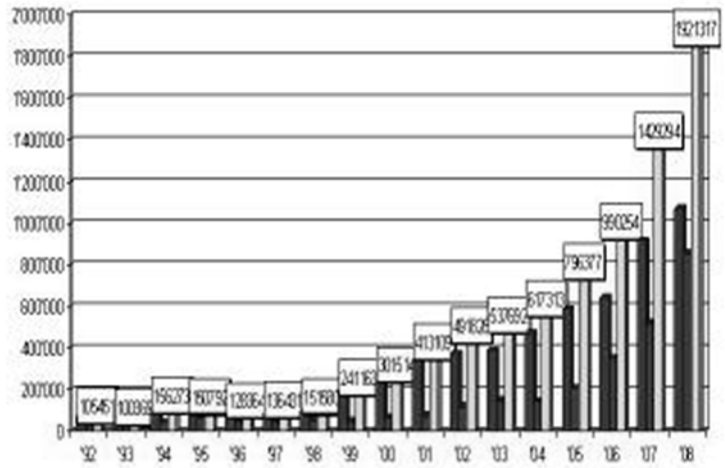

Figure 5: Development of borehole heat exchanger drillmeters in Switzerland 1992 – 2008.
Left bar: new installations, middle bar: retrofit, right bar: total. Data source: www.fws.ch

CONCLUSIONS, OUTLOOK

Enhanced Geothermal Systems have proven to have an immense theoretical potential. Presently EGS is still at the "proof of concept" stage; to reach the level of technical potential the it will be critical demonstrate that a technology can be created to establish EGS downhole heat exchangers with the needed properties independent of site conditions in the subsurface.

In addition, experience is needed about the production behavior of EGS heat exchangers at depth in the long-term, not least for acquiring economic data about installation, production, and maintenance costs. This is especially needed to judge the cost/benefit ratio of EGS power plants.

The future of geothermal energy will strongly depend on to what extent can geothermal power plant deployment can be accelerated. Other sources of renewable energy are developing rapidly (wind energy recently accomplished to install 25 GWe additional capacity per year; solar PV reached 6 GWe/yr; Renewables – Global Status Report 2009) whereas geothermal power growth remains clearly below 2 GWe/yr (Bertani 2009). Even when one takes into account the higher geothermal capacity factor the need for speeding-up geothermal development is obvious. Accelerating EGS development could provide a break-through, under the condition that the necessary significant funding needs can be met. This, in turn, will require heavy engagement of both the public and the private sector.

REFERENCES

Bertani, R. (2009): Long-term projections of geothermal-electric development in the world. In: Proc. GeoTHERM Congress, Offenburg/Germany, 5-6 March 2009.

Fridleifsson, I.B., Bertani, R., Huenges, E., J. Lund, J.W., Ragnarsson, A., Rybach, L. (2008): The possible role and contribution of geothermal energy to the mitigation of climate change. In: O. Hohmeyer and T. Trittin (Eds.) IPCC Scoping Meeting on Renewable Energy Sources. Proceedings (2008), Luebeck, Germany, 20-25 January 2008, 59-80.

Garnish, J. (2002): European activities in Hot Dry Rock research. In: Open Meeting on Enhanced Geothermal Systems, U.S. Department of Energy, Reno/NV, p. 8-9.

Goldstein, B., Hill, A., Long, A., Budd, A., Ayling, B., Malazavos, M. (2009): Hot rocks Down Under – Evolution of a new energy industry. GRC Transactions Vol. 43, p. 185-198

Ibrahim, H.D. (2009): Why is geothermal development slow – how to accelerate it? Petrominer no. 7, 28-29.

Majer, E., Baria, R. and Stark, M. (2008): Protocol for induced seismicity associated with enhanced geothermal systems. Report produced in Task D Annex I (9 April 2008), International Energy Agency-Geothermal Implementing Agreement (incorporating comments by: C. Bromley, W. Cumming, A. Jelacic and L. Rybach). Available at: www.iea-gia.org/publications.asp.

Renewables – Global Status Report (2009): REN21 (Renewable Energy Policy Network for the 21st Century). Avaliable at: www.ren21.net

Rybach, L. (2005): The advance of geothermal heat pumps world-wide. In: IEA Heat Pump Center Newsletter Vol. 23 No. 4, 13-18

Rybach, L. (2010a): "The Future of Geothermal Energy" and its challenges. In: Proceedings World Geothermal Congress 2010, Nusa Dua, Bali/Indonesia

Rybach, L. (2010b): CO2 Emission Mitigation by Geothermal Development – Especially with Geothermal Heat Pumps. In: Proceedings World Geothermal Congress 2010, Nusa Dua, Bali/Indonesia

Tester, J.W. et al. (2006) - The Future of Geothermal Energy – Impact of Enhanced Geothermal Systems (EGS) on the United States in the 21st Century, MIT - Massachusetts Institute of Technology, Cambridge, MA. 358 p. Available at: http://www1.eere.energy.gov/geothermal/future_geothermal.html.

Vörös, R., Weidler, R., de Graaf, L. and Wyborn, D. (2007): Thermal modelling of long term circulation of multi-well development at the Cooper basin hot fractured rock (HFR) project and current proposed scale-up program, Thirty-Second Workshop on Geothermal Reservoir Engineering, Stanford University, Stanford, California.

WEA (2000): World Energy Assessment Report: Energy and the Challenge of Sustainability. 500 p.

GEOLOGICAL AND GEOCHEMICAL EXPLORATIONS OF GEOTHERMAL RESOURCES IN YEMEN

Abdulsalam M. Al-Dukhain, Taha A. Al-Kohlani
Ministry of Oil and Minerals, Geological Survey and Mineral Resources Board, Geothermal Project, Sana'a, Yemen, P.O. Box 297

ABSTRACT

The Republic of Yemen is located on the south western part of Arabian Peninsula, between latitudes 12°N and 19°N, and longitudes 41.30°E and 54°E. The total area is 531,970 km2. The geographical sitting of The Republic of Yemen can be divided into

four principal physiographic provinces: Coastal Plains of the Red Sea (Tihama) and Gulf of Aden, Western Yemen Highlands and High Plateaus, Hadramawt-Mahra Uplands and Rub Al Khali and Ramlat Al Sabatayn.

Yemen is located at major geologic plate boundaries characterized by crustal spreading, active rift volcanism, and seismic activity. It is also dominated by major structures of the Gulf of Aden and the Red Sea. Occurrence of several late Miocene-recent volcanic fields at different locations throughout the country has encouraged searching for geothermal resources. The western Yemen volcanic province is characterized by several geothermal manifestations, such as hot springs, condensates, fumaroles and in many cases hot well waters. These geothermal manifestations are related to relatively shallow felsic magma chambers

Geochemical studies of all geothermal manifestations are carried out during 2001- 2006 and the chemical analysis of major components, trace elements, rare earth elements, and oxygen and hydrogen isotopes of the thermal waters and associated gases from Yemen has been already achieved. Temperature and pH values of the hot springs water range between 38 °C and 96 °C, and 6.3 and 8.7, respectively. The second phase of the studies represented by selection of three areas to executive the detail studies on it, these areas are Al-Lisi – Isbil area in Dhamar governorate, Al-Kafr area in Ibb governorate and Damt area in Ad-Dalea governorate. These areas are located in the western volcanic province of Yemen. Geochemical studies of Al-Lisi –Isbil area accomplished during 2007- 2009, and included the field measuring of temperature, PH and electrical conductivity, as well ammonia and silica analysis of 108 shallow wells. Major components of water (cations and anions) and oxygen, hydrogen and carbon isotopes has been analyzed. Geophysical studies which included 5 vertical electrical soundings (VES) have been achieved.

Preliminary interpretation of geochemical data and chemical analysis showed three sites characterized by high temperature values at depth 1000 m, therefore the exploration geothermal borehole drilling up to 1500 m depth will execute at one of these sites after the completion of geophysical data interpretation.

Key words: Volcanic, geothermal manifestation, Al-Lisi-Isbil, Yemen

YOUNG RIFT KINEMATICS IN THE TADJOURA RIFT, WESTERN GULF OF ADEN, REPUBLIC OF DJIBOUTI

Mohamed A. Daoud[1], Bernard Le Gall2, René C. Maury[2], Joël Rolet[2], Philippe Huchon[3], Hervé Guillou[4]
[1]*Institut des Sciences de la Terre, Centre d'Etudes et de Recherches de Djibouti, B.P. 486, Djibouti Ville, Djibouti.*
[2]*Université Européenne de Bretagne, Université de Brest, CNRS; UMR 6538 Domaines Océaniques, IUEM, place N. Copernic, 29280 Plouzané, France.*
[3]*UPMC Université de Paris 6, CNRS; UMR 7193, ISTeP, 4 place Jussieu 75252, Paris Cedex 05, France.*
[4]*UMR 1572, LSCE/CEA-CNRS, Domaine du CNRS, 12 avenue de la Terrasse, 91118 Gif-sur-Yvette, France.*

ABSTRACT.

The Tadjoura rift forms the westernmost edge of the westerly-propagating Sheba ridge, between Arabia and Somalia, as it enters into the Afar depression. From structural and remote sensing dataset, the Tadjoura rift is interpreted as an asymmetrical south-facing half-graben, about 40 km-wide, dominated by a large boundary fault zone to the north. It is partially filled up by the 1-3 Ma-old Gulf Basalts which onlapped the older Somali Basalts along its shallower southern flexural margin. The major and trace element analysis of 78 young onshore lavas allows us to distinguish and map four distinct basaltic types, namely the Gulf, Somali, Goumarre and Hayyabley Basalts. These results, together with radiometric age data, lead us to propose a revised volcano-stratigraphic sketch of the two exposed Tadjoura rift margins, and to discriminate and date several distinct fault networks of this oblique rift. Morphological and statistical analyses of onshore extensional fault populations show marked changes in structural styles along-strike, in a direction parallel to the rift axis. These major fault disturbances are assigned to the arrest of axial fault tip propagation against pre-existing discontinuities in the NS-oriented Arta transverse zone. According to our model, the sinistral jump of rifting into the Asal-Ghoubbet rift segment results from structural inheritance, in contrast with the *en échelon* or transform mechanism of propagation that prevailed along the entire length of the Gulf of Aden extensional system.

Keywords: Afar, Tadjoura rift, active/recent extension, faults, basalts, oblique rifting, rift propagation, inherited structures.

INTRODUCTION

The overall architecture of rift/ridge systems is controlled by several physical parameters which interact at various scales of times and space, and usually lead to intricate geometrical configurations. The large-scale spatial architecture of a propagating rift is known to depend merely on the absolute motions of the bounding plates, and on major lateral discontinuities in the strength of either the upper crust (e.g. inherited structures), or the lower crust (e.g. partial melt zones) (*Ziegler and Cloetingh*, 2004; *Wijns et al.*, 2005). At a smaller scale, the segmentation of the spreading axis within the rifted zone itself is commonly assigned to (i) its obliquity to the extension direction, and (ii) the angle between the axis of individual rift segments and the general trend of the rifted zone (*Abelson and Agnon*, 1997). The resulting complex multi-scale rift architecture is typically expressed along the Sheba westerly-propagating rift-drift system (Eastern Afar) by two nearly orthogonal first-order arms that, in turn, display specific segmented axial patterns (Figure 1A-B). Along most of its EW-trending path, the Sheba oceanic ridge is systematically offset to the southwest. This offset occurs through either a left-stepping ridge-transform network (up to the Shukra El Sheikh discontinuity, e.g. *Manighetti et al.* 1997) or oblique transfer zones with onlapping fault networks, up to the Tadjoura rift (TR) to the west (Figure 1B) (*Cochran*, 1981; *Tamsett and Searle*, 1988; *Manighetti et al*., 1997; *Dauteuil et al*., 2001). There, the nearly EW-trending axis veers abruptly counter-clockwise into the N120°E-oriented Ghoubbet rift, which is part of a submeridian, and partly emerged, rifted zone encompassing to the north the Asal and Manda Inakir *en échelon* subrifts (Figure 1B) (*Manighetti et al*., 1998). The structural link between the two sub-orthogonal rift arms in the TR has been variously interpreted, and assigned to either a large-scale dextral fault zone, in the prolongation of the NE-SW Maskali transform fault (Figure 1B) (*Ruegg et al*., 1980; *Arthaud et al.*, 1980; *Gaulier and Huchon*, 1991), or to an overlapping fault zone enclosing a network of *en échelon* structures (Figure 1D) (*Manighetti et al*., 1997).

The main goal of the present work is to address the mechanism of strain transfer between the Tadjoura and Ghoubbet rifts, with emphasis on the structure of the TR. Our study integrates (i) available seismic and bathymetric offshore data, (ii) sampling, geochemical analysis and K/Ar dating of young basalts from the Djibouti Plain, which lead us to propose a new geological map of the southern part of the TR, and (iii) structural analyses based on field studies and remote sensing interpretation.

These new data allow us to demonstrate that the TR typically displays a half-graben structure, which recorded a progressive shift of strain towards its inner part during the last 3 Ma. In addition, we propose that submeridian structural discontinuities, emplaced at an early stage of rifting in the Arta transverse zone (Figure 1B) may have locked the westerly propagation of extension in the TR, hence causing the jump of rift axis southwestwards into the Ghoubbet sub-rift.

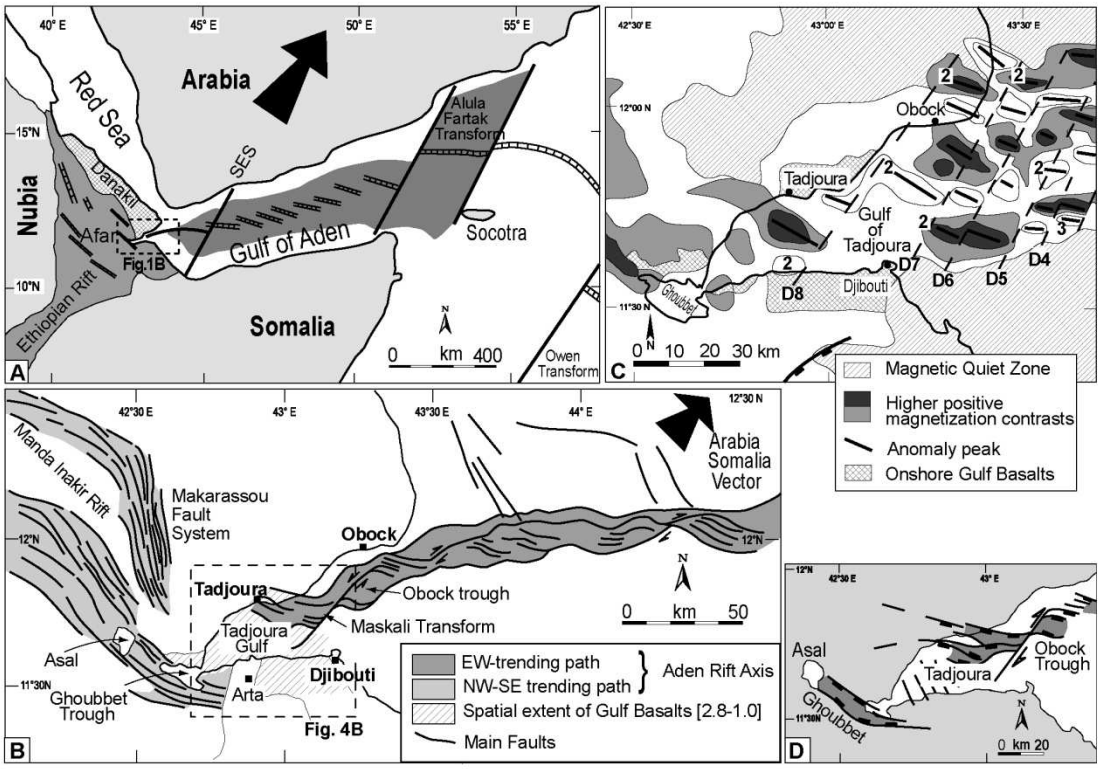

Figure 1: Various types of rift segmentation along the Gulf of Aden plate boundary between Arabia and Somalia. The active EW-trending Gulf of Aden (Sheba) rift-drift system evolves westwards into the sub-orthogonal Ghoubbet-Asal and Manda Inakir rifts. (A). Plate kinematic setting of the Afar Triple Junction. Thick arrows represent plate motion vectors, and the box indicates the study area. (B). Main physiographic features of the western Gulf of Aden rift system, modified from Manighetti et al. (1997). The revised spatial extent of onshore Gulf Basalts, as well as the Arta transverse zone (shown as the white NS domain centered on the Arta locality) are shown. (C). Aeromagnetic map of the Tadjoura Gulf, from Manighetti et al. (1997), with modified onshore parts. Dashed lines (D1-8) represent transform faults offsetting magnetic segments. Numbers refer to specific magnetic anomalies. (D). 'Overlapping subrift' model developed by Manighetti et al. (1997) to account for the relationships between the Tadjoura and Ghoubbet rifts. The inner floors of the rifts are shaded.

GENERAL RIFT SETTING AND VOLCANO-STRATIGRAPHY OF TADJOURA RIFT VOLCANIC

Geological context

The Sheba accretionary ridge within the Gulf of Aden forms, together with the Red Sea and the Ethiopian rift, one of the three diverging branches of the Afar triple junction (Figure 1A). According to magnetic anomaly data, mid-oceanic ridge segments and fracture zones initiated along its eastern part at 17-18 Ma *(Leroy et al.*, 2004; *d'Acremont et al.*, 2006), or possibly at 20 Ma (*Fournier et al*., in press), and then propagated westwards, obliquely to the N40°E direction of Arabia-Somalia plate separation (*Cochran*, 1981) (Figure 1A). Emplacement of incipient oceanic crust at the western tip of the Sheba ridge is recorded along the ~EW-trending Obock-Tadjoura Gulf by <2 Ma-old paired magnetic anomalies (Figure 1C). The anomalies partly coincide with the 3-1 Ma Gulf basaltic series which floor the Tadjoura Gulf, and outcrop onshore in its northern (Tadjoura) and southern (Djibouti Plain) margins (*Manighetti et al*., 1997) (Figure 1B). The EW-oriented TR-related structures intersect at high angle older tectono-magmatic fabrics displaying a submeridian orientation in the Mablas (15-11 Ma), Somali (7.2-3.6 Ma), and Ribta (3.6 Ma) substratum series, emplaced at an earlier stage of rifting.

The Gulf Basalts are a potentially accurate structural marker of the rift history recorded by the TR in the last 3 Ma, and it is therefore important to determine their spatial and temporal distribution for a better definition of the TR. That has been attempted by using new geochemical and age dataset obtained on basaltic units in the Djibouti Plain, i.e. on the southern margin of the TR. Combined with previously published K-Ar ages, this dataset allows us to discriminate four recent basaltic units, i.e. the Gulf, Somali, Goumarre, and Hayyabley Basalts, hence allowing significant revision of the 2D-map structure of the TR (Figure 2A). Finally, although they are younger than the Gulf and Somali Basalts which they crosscut, the Goumarre basalts were not recognized as a distinct type prior to this study.

NORTHERN MARGIN OF THE TADJOURA RIFT

In the Tadjoura-Obock area, the Gulf Basalts (2.8-1.0 Ma) occur in a 15 x 8 km faulted coastal plateau, less than 300 m high (Figure 3B). The main cartographic unit of the Gulf Basalts (the Roueli unit of *Gasse et al*., 1983, 1985) extends to the north as a 10 x 5 km faulted belt oriented N100°E, which swings to the north-east into a narrower N50°E strip. The Gulf Basalts lie further south as discrete inliers beneath locally faulted Quaternary alluvial fans, possibly as young as Holocene (*Manighetti et al*., 1997). Their rapid disappearance west of longitude 42° 50'E might result from a nearly NS-trending paleo-high, in the northern prolongation of the Arta zone (see below) (Figure 3A).

The southern margin of the TR (Djibouti Plain)

The Gulf Basalts are confined to a 10 x 20 km coastal faulted plateau which uprises southwards, via the EW-trending Ambouli topographic flexure (Figure 3E), to a northerly-tilted surface in the 7.2-3.6 Ma Somali Basalts.

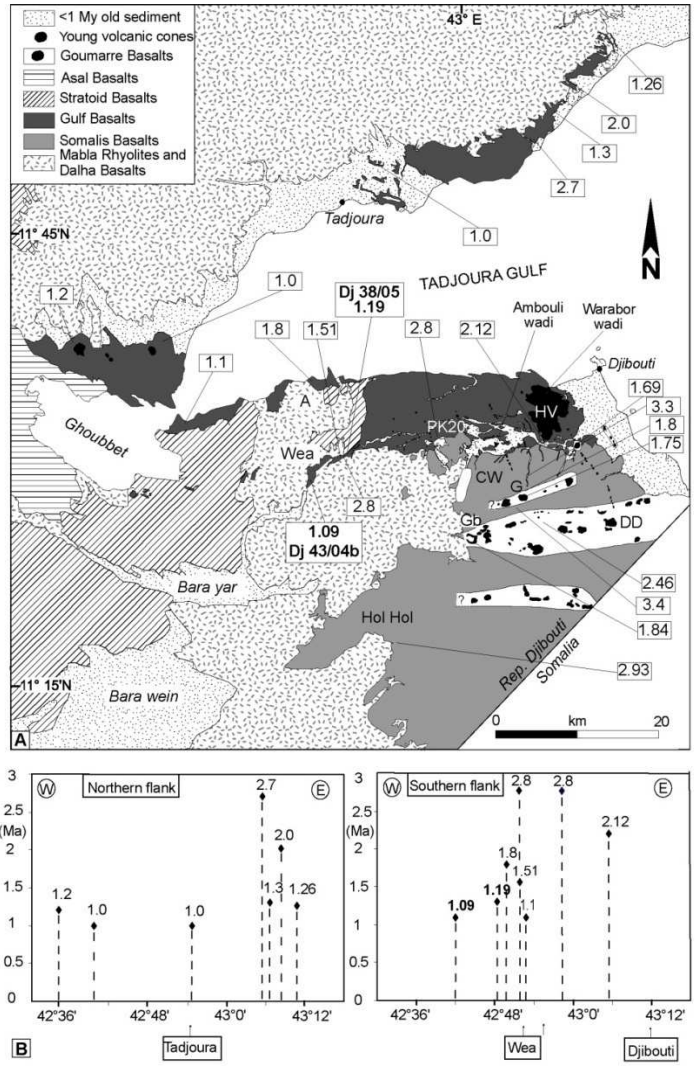

Figure 2: Revised geological sketch map of the onshore parts of the Tadjoura rift. (A). Revised map showing the distribution of the various basalt types and the location of dated basaltic rocks. Ages in Ma (numbers inside the squares) from published (Richard, 1979; Gasse et al., 1983; Zumbo et al., 1995), and new data (this study). Tectonic features are not shown on this simplified map. A, Arta; CW, Chabelley wadi; DD, Dey Dey wadi; HV, Hayyabley volcano; G, Goumarre; Gb, Goubbetto; PK20, "Point kilométrique" 20. (B). Longitude versus age plot for the southern and northern coastal strips of Gulf Basalts. A linear age progression is not clearly observed.

To the east, the Gulf Basalts are overlain by lavas of the ~1 Ma-old Hayyabbley shield volcano (*Gasse et al*., 1983; *Daoud et al*., 2010), the main axis of which follows a major N140°E fault scarp bounding the eastern coastal plain to the southeast. The western limit of the Gulf Basalts abuts against the NS-oriented eastern edge of the Arta reliefs, although they locally fill up the Wea paleo-valley (Figure 2A).

The Goumarre Basalts (2.46-1.69 Ma) forms three N80°E parallel arrays of basaltic vents crosscutting the Somali. These volcanic corridors, each of them a few km-wide, are sharply cut to the east by the N140°E coastal scarp. To the west, their tips remain within the Somali Basalts and do not reach the older substratum series of the Ali Sabieh range. It is therefore suggested that the Goumarre Basalts were emplaced during a relatively short time interval, concomitantly with the Gulf Basalts, but in a more southern, i.e. external, position with respect to the TR framework.

THE HALF-GRABEN STRUCTURE OF THE TADJOURA RIFT

2D-map structure

The TR is a ca. 60 x 40 km EW-trending topographically subdued domain, partly exposed onshore in the northern coastal fault belt (NCFB) and southern coastal fault belt (SCFB), on both sides of the Tadjoura Gulf (Figures 3A-B). Its inner offshore part is dominated to the north by the N120°E-oriented Tadjoura rhomb-shaped trough which is sinistrally offset from the Obock depression by ca. 30 km along the right-lateral Maskali transform fault system (*Arthaud and Choukroune*, 1976). The TR is surrounded by highlands involving older rift-related volcanics of the Mabla (18-11 Ma, in *Gasse et al*., 1985), Dalha (8.6-3.8 Ma), Somali (7.2-3.6 Ma), and Ribta (3.6 Ma) series. It is dissected by an inhomogeneously distributed fault pattern, comprising Gulf-parallel, NW-SE and NE-SW structures. The map-scale sigmoid trace of the entire fault pattern typically evokes an oblique rift setting. Two high-density fault zones occur on the eastern parts of the conjugate margins, in the Tadjoura trough and the NCFB to the north, and in the SCFB to the south. In the intermediate and less deformed zone, the preferred N60°E alignment of shield-like volcanoes might be controlled at depth by Maskali-type transverse structures (Figure 3B). To the west, the TR narrows markedly, north of the Arta transverse zone, where its floor shallows abruptly, up to 100-200 m below sea-level, through a submeridian scarp disrupted by an array of isolated NW-SE faults.

The TR fault system does not extend beyond the Gulf Basalts, e.g. into the substratum series which instead show evidence for earlier deformation (see discussion below).

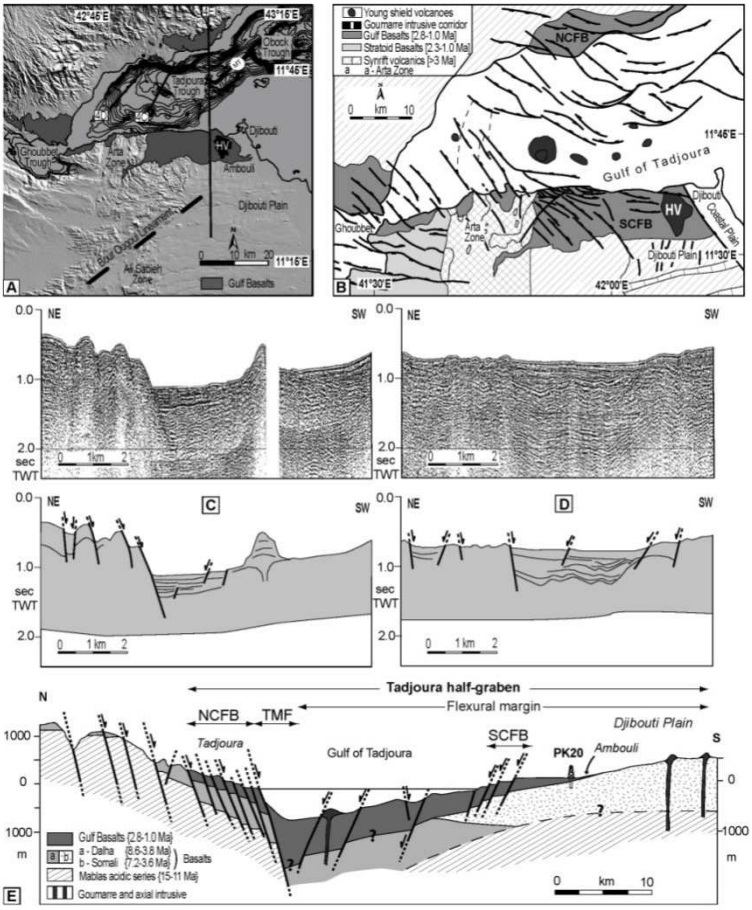

Figure 3: Overall structure of the Tadjoura rift. (A). Topography of the TR drawn from a bathymetric contour map (from *Audin*, 1999, modified) and a SRTM digital elevation model. Dashed lines represent the Maskali transform (MT) and Bour Ougoul transverse fault systems. Note the strong NS-oriented structural grain in the Arta zone. The traces of the structural cross-section in Figure 3E and the two interpreted seismic profiles in Figures 3C and D are shown. HV, Hayyabley volcano. (B). Structural map of the TR obtained (i) by merging onshore geology with offshore bathymetric dataset, and (ii) by using the Gulf Basalts as a rift marker (only drawn onland). ATZ, Arta transverse zone; HV, Hayyabley volcano; NCFB and SCFB, Northern and Southern coastal fault belts, respectively. (C) and (D). Raw (top) and interpreted (bottom) TADJOURADEN offshore seismic profiles (time-sections) perpendicular to the NW-SE-oriented fault-controlled Tadjoura inner trough (see traces in Figure 3A). (E). Interpretative structural cross-section showing the Tadjoura rift as a south-facing half-graben, partly filled up by Gulf Basalts. The elements of the deep structure of the Tadjoura rift are conjectural. The geometrical relationships between the underlying Somali and Dalha basalts are extrapolated from patterns observed onshore along the Bour Ougoul lineament on the NW flank of the Ali Sabieh antiform (see Figure 3A for location).

Half-graben cross-sectional structure

The composite structural cross-section in Figure 3E, drawn at high angle with respect to the dominant N110-120°E fault strike in the TR, is calibrated by TADJOURADEN bathymetric and seismic reflection data which have been merged with onshore geology. It shows a 35-40 km-wide half-graben structure, facing the SSW. Its inner and deeper part is occupied by the Tadjoura trough, which is bounded to the north by a prominent fault system, including the Tadjoura master fault, and its highly faulted footwall block, partly exposed in the NCFB. To the south, a ca. 20 km-long typical flexural margin shallows gradually southwards, up to the Djibouti Plain, where Gulf Basalts are locally dissected by a high density antithetic fault system in the SCFB. The flexure is locally punctuated by shield volcanoes.

The deep structure of the Tadjoura inner trough is constrained down to about 2 s (two-way travel-time), or depth of 4-5 km, by selected single-channel seismic reflection profiles striking NE-SW, orthogonal to the prominent bathymetric scarps (Figures 3C-D). To the north, the steep bathymetric scarp, >500 m-high and facing the SSW on the seismic line of Figure 3C, is interpreted as the upper part of the master fault. High amplitude reflectors lying, with an apparent gentle dip, in its immediate hangingwall are reliably correlated with Gulf Basalts dredged from the Tadjoura gulf (*Barrat et al*, 1990; 1993). Similar seismic facies present, with a reduced thickness, in the elevated footwall block correlate laterally with onshore Gulf Basalts in the NCFB (Figure 3B), hence confirming our seismo-stratigraphic interpretation. The volcanic infill sequence thickens markedly towards the boundary fault, just like synfaulting deposits, up to a maximum thickness of 7-800 m. This value is obtained by converting the 0.3 s (two-way travel-time) measurement, assuming an average seismic velocity for basalts of 4.5-5.0 km.s^{-1}.

The southwestern edge of the TR and the Arta zone

The sketch structural map in Figure 4A shows that very few transverse and Gulf-parallel TR-related faults crosscut the >3 Ma-old volcanic terranes forming the Arta zone. In this area, the 8.6-3.8 Ma-old Dalha Basalts and the overlying Ribta felsic lavas (3.6 Ma) are involved into a broad, 10 km-wide, upright arched structure, oriented N-S, i.e. nearly orthogonal to the E-W axis of the TR. This Arta anticline is in turn dissected by a dense network of NS-N20°E fault/fractures, parallel to the anticline axis and locally intruded by felsic bodies of the Ribta Fm. Most of these submeridian fractures were later reactivated as strike-slip faults (*Arthaud et al*., 1980).

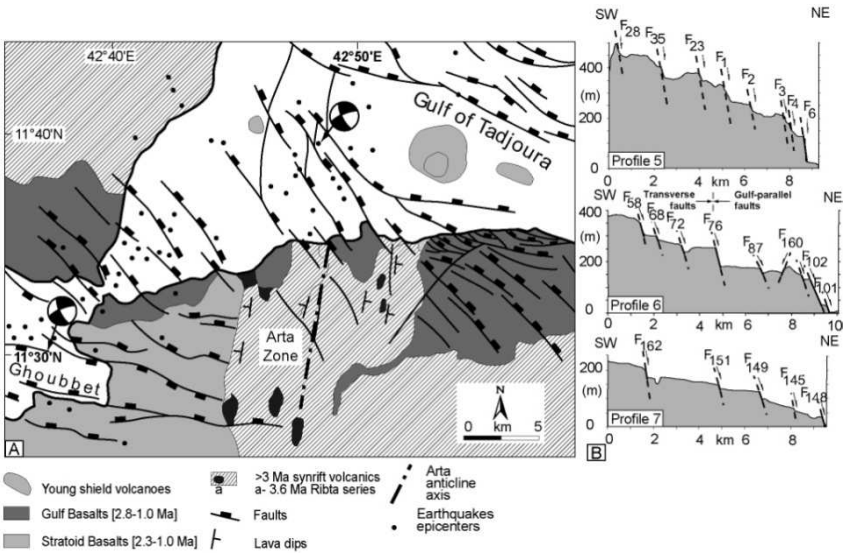

Figure 4: Onshore and offshore structural features in the transfer zone between the Tadjoura and the Ghoubbet rifts. (A) Structural sketch map showing the nearly underformed nature of the Arta transverse zone during recent (<3 Ma) rift stages. Note that most earthquakes and faults cutting through the Stratoid and Gulf basalts avoid the Arta NS-trending zone. The earthquake epicentres are from *Doubre* (2004) and the focal mechanisms of the 1978/21/12 and 1978/08/11 earthquakes, in the Tadjoura Gulf and Ghoubbet trough, respectively, are from *Lépine and Hirn* (1992). (B). Morpho-structural sections crossing the South Coastal Fault Belt, perpendicular to the N140°E transverse fault network.

From these structural relationships, the Arta anticline is inferred to have formed as a magma-driven structure overlying a felsic intrusion emplaced during the 3.6 Ma Ribta event.

KINEMATIC MODEL FOR THE <3 MA RIFT EVOLUTION OF THE TR

In response to the regional N40°E extension (*Jestin et al.*, 1994; *de Chabelier and Avouac*, 1994; *Vigny et al.*, 2007), the TR developed as a 60 x 40 km south-facing half-graben, filled up by a thick pile of syntectonic fissural Gulf Basalts. In map-view, the TR rhomb-shaped structure involves a composite network of dominantly extensional faults, striking EW (Gulf-parallel) and NW-SE.

The latter trend occurs in the western termination of the TR at the longitude of ca 42° 45', i.e. in the northern offshore prolongation of the Arta zone. The TR-related faults which exclusively involve the Gulf Basalt-filled half-graben recorded a complex history within an overall westerly migration of tectonic activity (*Manighetti et al.*, 1997). The dating of fault-controlled volcanic activity (Goumarre) across the flexural margin of the TR half-graben suggests that the onset of faulting along the master boundary fault to the north occurred at 1.7 Ma, concomitantly with active extension in the Tadjoura inner trough. At this stage, the master fault might have developed a number of splays into the footwall uplifted block (NCFB), probably coeval with localized antithetic faulting along part of the flexure to the south (SCFB). The long-lived development of the Tadjoura half-graben was accompanied by the temporal migration from old structures, in an external position, towards younger ones, closer to the Gulf axis. A similar evolution is reported from the Kenya rift, where a temporally progressive focus of strain into a narrow and inner trough has been documented (*Baker and Wohlenberg*, 1971; *Cerling and Powers*, 1977; *Vétel and Le Gall*, 2006). In addition to cross-rift migration of faulting, along-strike fault propagation also occurred, and resulted in contrasted fault patterns in the NCFB and SCFB. In the NCFB, the amount of displacement decreased regularly westwards along Gulf-parallel faults, towards a tip line located within the Gulf Basalts. Very few faults extended beyond the Gulf Basalts/substratum boundary, across the Mabla felsic series (Figure 5B). Small-scale (a few hundreds meters wide) jumping rift segments were assumed to occur in the NCFB (*Manighetti et al.*, 1997), where they turned into a network of *en echelon* fault swarms which connected the TR and the Ghoubbet rifted trough to the SW. These small-scale rift structures are here regarded as subsidiary structures on the northern flank of the TR half-graben documented in this work.

A more intricate fault pattern is present in the western part of the SCFB. There, the Gulf-parallel extensional faults deviate clockwise, from N90°E to N140°E, when approaching the Arta transverse zone. This fault map curvature is accompanied by a marked increase of fault density westwards, together with a decrease of individual fault length, hence resulting in over-displaced fault pattern.

Structural data suggest that strong submeridian terranes, including the Arta zone, transect orthogonally the western end of the TR (Figure 5B). To the south, these terranes extend towards the Ali Sabieh anticline (*Le Gall et al.*, 2010). They are bounded to the east by the so-called Arta-Asamo discontinuity, the > 60 km-long map trace of which is outlined by a variety of structures that indicate its long-lived history. To the north, the decrease of vertical motion along the NW offshore course of the N140°E transverse fault network (see Figure 3D) suggests the occurrence of a stronger substratum offshore the Arta zone.

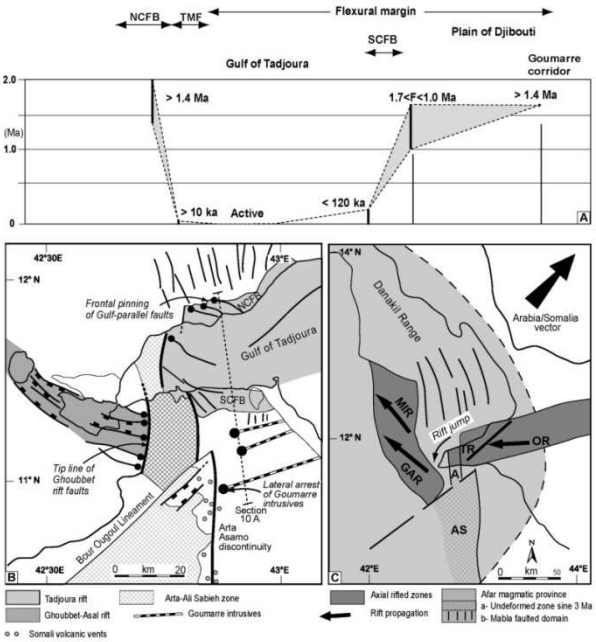

Figure 5: Kinematics of rift propagation throughout the Tadjoura-Ghoubbet connection zone. (A). Timing of faulting along a synthetic cross-section of the Tadjoura Rift. Despite age uncertainties, a pattern of younging of strain is observed from the margins to the inner part of the Tadjoura Rift, indicating progressive axial focusing of extension. NCFB: Northern Coastal Fault Belt; TMF: Tadjoura Master fault; SCFB: Southern Coastal Fault Belt. (B). Rift kinematic model in the Tadjoura-Ghoubbet linkage zone, emphazing the role of inherited submeridian structures in pinning the propagation of the Tadjoura and Ghoubbet rifts. C. Sketch rift pattern showing a major submeridian discontinuity at the transition zone between two variously-trending rift arms of the Aden plate boundary. The shaded area corresponds to the eastern edge of the Afar magmatic province (the initial 30 Ma-old flood basalts of Yemen are not considered). A., Arta zone; AS., Ali Sabieh range; GAR., Ghoubbet-Asal rift; MIR., Manda-Inakir rift; OR. Obock rift; TR., Tadjoura rift.

The strong mechanical behaviour of the Arta transverse zone during recent rifting is also confirmed by (1) the restricted location of earthquakes and aftershocks linked to the 1978 seismic crisis in the Tadjoura gulf (*Lépine et al.*, 1980; *Lépine and Hirn*, 1992; *Doubre*, 2004) (Figure 4A), and (2) the abrupt arrest of the EW-trending Ghoubbet rift fault network against its NS-trending western edge (Figure 5B).

Further south, the continuation of the Arta-Asamo discontinuity along the eastern flank of the Ali Sabieh anticline is deduced from the restricted distribution of the N80°E Goumarre fault-dyke corridors which do not penetrate westwards into the Ali Sabieh substratum series (Figure 5B). The inherited and deep-seated origin of the Arta-Asamo discontinuity is suggested by the NS alignment of Somali (7.2-3.6 Ma) volcanic vents along its inferred map trace (Figure 5B). This discontinuity might have been guided at depth by a large-scale Proterozoic fracture zone belonging to the Marda system (Boccaletti et al., 1991).

During the recent SE Afar rift history, the Arta preexisting submeridian structures are therefore assumed to have provoked the frontal pinning of axial fault growth in the TR, and then the lateral jump of rifting in the Ghoubbet area, in response to inferred higher strength contrast, together with their orthogonal orientation to rift propagation. This abrupt change in rift kinematics probably occurred at ca. 900 ka, when diffuse volcanism and associated faulting started in the Asal-Ghoubbet rift (*Manighetti et al*., 1998; *Audin et al*., 2001).

CONCLUSIONS

The major and trace element analysis of young basalts collected from onland Tadjoura Rift units (especially from the Djibouti Plain) allows us to distinguish four distinct types, namely the Gulf, Somali, Goumarre and Hayyabley Basalts. These results, together with new and previously published radiometric age data, lead us to propose a revised volcano-stratigraphic sketch map of the southern (SCFB) and northern (NCFB) margins of the TR. With respect to former studies (*Richard*, 1979; *Gasse et al.*, 1983, 1985, 1986), the Goumarre Basalts (2.46-1.69 Ma) are recognized as a distinct unit and the southern limit of the Gulf basalts in the Djibouti Plain is shifted ca. 10 km northwards. A consequence of this revision is that the progressive westerly younging of the Gulf Basalts suggested by previous authors (*Richard*, 1979; *Manighetti et al*., 2001; *Audin et al*., 2004) for the southern and northern borders of the TR is no more supported by the new longitude *versus* age trends for these basalts.

New structural data based on fieldwork and remote sensing analysis allow us to interpret the overall structure of the TR as an asymmetrical south-facing half-graben, about 35 km-wide, dominated by a large boundary fault zone to the north and extending southwards as a >20 km-long shallower flexural margin, partially exposed in the Djibouti Plain. There, it is locally disrupted by an antithetic southern coastal fault belt, and by the Goumarre transverse fault-dike corridors close to the inflexion point of the Somali Basalts monocline. Recent faulting is spatially restricted to the Gulf Basalts which form two narrow strips on the northern and southern margins of the TR.

The temporal change of the location of normal faults towards the inner trough of the half-graben indicates the progressive focusing of strain with time within the axial part of the rift. The geometrical and statistical analysis of onshore fault networks in the southern fault belt shows a westeryl increase of strain that is mechanically assigned to the frontal locking of axial fault tip propagation against sub-meridian discontinuities in the Arta zone. The arrest of fault propagation in the TR lastly resulted in the jump of rifting into the Ghoubbet-Asal trough system.

REFERENCES

Abelson, B.M. & Agnon, A. 1997. Mechanics of oblique spreading and ridge segmentation. Earth Planet. Sc. Letters, 148, 405-421.

Arthaud, F. & Choukroune, P. 1976. Mise en évidence d'une phase de compression à 3,5 Ma séparant deux épisodes d'ouverture du rift océanique de Tadjoura (T.F.A.I.). C.R.A.S., 283, 13-16.

Arthaud, F., Choukroune, P. & Robineau, B. 1980. Evolution structurale de la zone transformante d'Arta (République de Djibouti). Bull. Soc. géol. Fr., XXII, 909-915.

Audin, L. 1999. Pénétration de la dorsale d'Aden dans la dépression Afar entre 20 et 4 Ma. Unpublished Ph.D. Thesis, Univ. Paris 7.

Audin, L., Manighetti, I., Tapponnier, P., Métivier, F., Jacques, E. & Huchon, P. 2001. Fault propagation and climatic control of sedimentation on the Ghoubbet rift floor: insights from the Tadjouraden cruise in the western Gulf of Aden. Geophys. J. Int., 144, 1-28.

Audin, L., Quidelleur, X., Coulié, E., Courtillot, V., Gilder, S., Manighetti, I., Gillot, P.Y., Tapponnier, P. & Kidane, T. 2004. Paleomagnetism and K-Ar and 40Ar/39Ar ages in the Ali Sabieh area (Republic of Djibouti and Ethiopia): constraints on the mechanism of Aden ridge propagation into southeastern Afar during the last 10 Myr. Geophys. J. Int., 158(1), 327-345.

Baker, B.H. & Wohlenberg, J. 1971. Structure and evolution of the Kenya Rift Valley. Nature, 229, 538-542.

Barrat, J.A., Jahn, B.M., Joron, J.L., Auvray, B. & Hamdi, H. 1990. Mantle heterogeneity in northeastern Africa: evidence from Nd isotopic compositions and hygromagmaphile element geochemistry of basaltic rocks from the Gulf of Tadjoura and Southern Red Sea regions. Earth. Planet. Sci. Lett., 101, 233-247.

Barrat, J.A., Jahn, B.M., Fourcade, S. & Joron, J.L. 1993. Magma genesis in an ongoing rifting zone: the Tadjoura Gulf. Geochim. Cosmochim. Acta, 57, 2291-2302.

Boccaletti, M., Getaneh, A. & Bonavia, F. 1991. The Marda fault zone : a remnant of an incipient aborted rift in the paleo-African Arabian plate. J. Petroleum Geol., 14(1), 79-92.

Cerling, T.E. & Powers, D.W. 1977. Paleorifting between the Gregory and Ethiopian rifts. Geology, 5, 441-444.

Cochran, J.R., 1981, The Gulf of Aden: structure and evolution of a young ocean basin and continental margin. J. Geophys. Res., 86, 263-287.705

d'Acremont, E., Leroy, S., Maia, M., Patriat, P., Beslier, M.O. Bellahsen, N., Fournier, M. & Gente, P. 2006. Structure and evolution of the eastern Gulf of Aden: insigths from magnetic and gravity data (Encens Sheba Cruise). Geophys. J. Int., 165, 786-803.722

Daoud, M.A., Barrat, J.A., Maury, R., Taylor, R.N., Le Gall, B., Guillou, H., Cotten, J. & Rolet, J. 2010. A LREE-depleted component in the Afar plume: further evidence from Quaternary Djibouti basalts. Lithos, 114, 327-336.

Dauteuil, O., Huchon, P., Quemeneur, F. & Souriot, T. 2001. Propagation of an oblique spreading center: the western Gulf of Aden. Tectonophysics, 332, 423-442.

de Chabalier, J.B. & Avouac, J.P. 1994. Kinematics of the Asal rift (Djibouti) determined from the deformation of Fieale volcano. Science, 265, 1677-1681.

Doubre, C. 2004. Structure et mécanismes des segments de rift volcano-tectoniques; études de rifts anciens (Ecosse et Islande) et d'un rift actif (Asal-Ghoubbet). Unpublished Ph.D. Thesis, Univ. du Maine.

Fournier, M., Chamot-Rooke, N., Patriat, P., Petit, C., Huchon, P., Al-Kathiri, A., Audin, L., Beslier, M.O., d'Acremont, E., Fabbri, O., Fleury, J.-M., Khanbari, K., Lepvrier, C., Leroy, S., Maillot, B. & Merkouriev, S. (2010). Arabia-Somalia plate kinematics, evolution of the Aden-Owen-Carlsberg triple junction, and opening of the Gulf of Aden. J. Geophys. Res., in press.

Gasse, F., Fournier, M. & Richard, O. 1983. Carte géologique de la République de Djibouti, 1:100000. Djibouti. Notice explicative. ISERST, Ministère français de la Coopération, Paris.

Gasse, F., Fournier, M., Richard, O. & Ruegg J.C. 1985. Carte géologique de la République de Djibouti, 1:100000. Tadjoura. Notice explicative. ISERST, Ministère français de la Coopération, Paris.

Gasse, F., Varet, J., Mazet, G., Recroix, F. & Ruegg, J.C. 1986. Carte géologique de la République de Djibouti, 1:100000. Ali Sabieh. Notice explicative. ISERST, Ministère français de la Coopération, Paris.

Gaulier, J.M. & Huchon, P. 1991. Tectonic evolution of Afar triple junction. Bull. Soc. géol. Fr., 162 (VIII), 451-464.

Jestin, F., Huchon, P. & Gaulier, J.M. 1994. The Somalia plate and the East African Rift System : present kinematics. Geophys. J. Int., 116, 637-654.

Le Gall B., Daoud, M.A., Rolet, J., Maury, R.C., Guillou, H. & Sue, C. Magma-driven antiform structures in the Afar rift : the Ali Sabieh range, Djibouti. J. Struct. Geol., in press.

Lépine, J. C., Ruegg, J.C. & Anis, A. M. 1980. Sismicité du rift d'Asal-Ghoubbet pendant la crise sismo-volcanique de novembre 1978. Bull. Soc. geol. Fr., XXII, 6, 809-816.

Lépine, J. C. & Hirn, A. 1992. Seismotectonics in the Republic of Djibouti, linking the Afar Depression and the Gulf of Aden. Tectonophysics, 209, 65-86.

Leroy, S., Gente, P. & 10 others, 2004. From rifting to drifting in the eastern Gulf of Aden: A complete margin survey coverage of a young oceanic basin from margin to margin. Terra Nova, 16, 185-192.

Manighetti, I., Tapponnier, P., Courtillot, V., Gruszow, S. & Gillot., P.Y. 1997. Propagation of rifting along the Arabia-Somalia plate boundary: the Gulf of Aden and Tadjoura. J. Geophys. Res., 102, 2681-2710.

Manighetti, I., Tapponnier, P., Gillot, P.Y., Jacques, E., Courtillot, V., Armijo, R., Ruegg, J.C. & King, G. 1998. Propagation of rifting along the Arabia-Somalia plate boundary into Afar. J. Geophys. Res., 103, 4947-4974.

Manighetti, I., King, G.C.P., Gaudemer, Y., Scholz, C. & Doubre, C. 2001. Slip accumulation and lateral propagation of active normal faults in Afar. J. Geophys. Res., 13, 667-696.

Richard, O. 1979. Etude de la transition dorsale océanique – rift émergé: le Golfe de Tadjoura (République de Djibouti). Approche géologique, géochronologique et pétrologique. Thèse de 3ème cycle, Univ. Paris XI-Orsay, 149 pp.

Ruegg, J.C., Lépine, J.C. & Vincent, C. 1980. Sismicité et micro-sismicité de la dorsale de Tadjoura, tectonique et frontière de plaques. Bull. Soc. géol. Fr., 22, 917-923.

Tamsett, D. & Searle, R.C. 1988. Structure and development of the midocean ridge plate boundary in the Gulf of Aden: Evidence from GLORIA side-scan sonar. J. Geophys. Res., 93, 3157-3178.

Vétel, W. & Le Gall, B. 2006. Dynamics of prolonged continental extension in magmatic rifts: the Turkana Rift case study (North Kenya). In: Yirgu, G., Ebinger, C.J. & Maguire, P.K. (Eds), The Afar volcanic province within the East African rift system. Geol. Soc. London. Sp. Pub., 259, 209-233.

Vigny, C., de Chabalier, J.B., Ruegg, J.C., Huchon, P., Feigl, K., Cattin, R., Asfaw, L. & Khanbari, K. 2007. Twenty-five years of geodetic measurements along the Tadjoura-Asal rift system, Djibouti, East Africa. J. Geophys. Res., 112, B06410, doi:10.129/2004JB003230.

Wijns, C., Weinberg, R., Gessner, K. & Moresi, L. 2005. Mode of crustal extension determined by rheological layering. Earth Planet. Sci. Lett., 236, 120-134.

Ziegler, P.A. & Cloething, S. 2004. Dynamic processes controlling evolution of rifted basins. Earth Sci. Rev., 64, 1-50, doi :10.1016/50012-8252(03)00041-2.

Zumbo, V., Féraud, G., Vellutini, H., Piguet, P. & Vincent, J. 1995. First 40Ar/39Ar datings on Early Pliocene to Plio-Pleistocene magmatic events of the Afar – Republic of Djibouti. J. Volc. Geoth. Res., 65, 281-295.

GEOTHERMAL RESOURCE INDICATIONS OF THE GEOLOGIC DEVELOPMENT AND HYDROTHERMAL ACTIVITIES OF D.R.C.

Getahun Demissie
Addis Abeba, Ethiopia, geomet@ethionet.et

ABSTRACT

Published sources report the occurrence of more than 135 thermal springs in D.R.C. All occur in the eastern part of the country, in association with the Western rift and the associated rifted and faulted terrains lying to its west. Limited information was available on the characteristics of the thermal features and the natural conditions under which they occur. Literature study of the regional distribution of these features and of the few relatively better known thermal spring areas, coupled with the evaluation of the gross geologic conditions yielded encouraging results. The occurrence of the anomalously large number of thermal springs is attributed to the prevalence of abnormally high temperature conditions in the upper crust induced by a particularly high standing region of anomalously hot asthenosphere. Among the 29 thermal springs the locations of which could be determined, eight higher temperature features which occur in six geologic environments were found to warrant further investigation. The thermal springs occur in all geologic terrains. Thermal fluid ascent from depth is generally influenced by faulting while its emergence at the surface is controlled by the near-surface hydrology. These factors allow the adoption of simple hydrothermal fluid circulation models which can guide exploration. Field observations and thermal water sampling for chemical analyses are recommended for acquiring the data which will allow the selection of the most promising prospects for detailed, integrated multidisciplinary exploration. An order of priorities is suggested based on economic and technical criteria.

Keywords: Hydrothermal activities, Eastern D.R.C,

INTRODUCTION

The information which was available for this study was incomplete and mostly old. Moreover, it was believed that the systematic study of hydrothermal features from the geothermal energy development aspect was unlikely to have been carried out to date. Under circumstances where information on the occurrence and characteristics of hydrothermal features is insufficient to allow their study and the discovery of the associated geothermal resources, exploration is most effectively progressed by starting with the review of the available literature, the compilation of geologic information and hydrothermal feature inventory.

This paper aims to contribute to the literature research effort. It aims to provide a gross view of the subsurface geothermal conditions which are indicated by the occurrence of numerous thermal springs, and to identify areas where follow-up work may be warranted.

The effort involved:

- the compilation of hydrothermal feature occurrences based on published information;
- the review of this information in the context of the geologic settings of the activities; and,
- the identification of areas where follow-up work would be warranted to determine the most attractive sites for follow-up studies.

The work relied solely on literature research. However, the paucity of published information deterred the full characterization of the thermal springs and the prediction of the sub-surface conditions from which they derive. Moreover, the locations of only 29 thermal springs could be determined. The approach which was adopted was thus both general, to allow the appreciation of the gross subsurface geothermal conditions, and focused, taking advantage of the availability of some basic information on a few thermal spring areas.

The work resulted in the listing of 70 named thermal springs and of the general locations of another more than 65 un-named features. These are listed in the appendix. All features are situated in the eastern part of the country. The work also enabled an understanding of the large scale natural conditions which gave rise to this anomalously high concentration of hydrothermal features in that region. The features were found to be diagnostic of the hyper-thermalism of the subsurface under the region as inferred from its geologic, geophysical and physiographic characters. Of the areas where thermal springs were reported to have more than 50OC temperature, locations could be determined for only six. These are proposed to be the focal features around which further studies should be carried out. It is suggested that brief geologic reconnaissance surveys, and hydrothermal fluid sampling and chemical analyses be carried out in these areas in order to determine whether detailed investigations would be justified.

BACKGROUND: GEOLOGIC DEVELOPMENT OF EASTERN D.R.C.

Hydrothermal features occur in all tectonic terrains which date from as early as during the Archean. It is thus useful to gain an appreciation of the geologic development of D.R.C. since those times. Figure 1 shows the main tectonic terrains, lithologic types and structures of Eastern D.R.C. This geologic framework owes its origins to successive phases of continent construction and breakup.

Pre-East African Rift System (EARS) Developments.

The long history of geologic development of the D.R.C. till the Paleogene resulted in the creation of the basement terrain and structural framework on which took place the Neogene and Quaternary processes which determined the crustal geothermal conditions.

Congo craton (unit #1 in Fig. 1) formed during the Archean and served as the core around which this part of Africa was assembled during a succession of three major orogenic cycles. In D.R.C., the craton is mostly covered by sediments and outcrops in only a few places.

The Ubendian orogeny (2a) took place during the Paleoproterozoic and joined the Congo and Tanzanian cratons. The globally widespread Mesoproterozoic Kibaran orogenic belt (2b, in this wider sense also comprising other coeval orogens) formed during Rodinia supercontinent assembly during 1.36-1.00Ga. Rodinia broke up at the end of the period. During 800-550Ma, the Panafrican orogens, in D.R.C. comprising the Lindian (2c1) and Damaran-Lufilian (Katangan, 2c2) were raised between the Congo, Kalahari and East Saharan cratons resulting in the assembly of part of Gondwana supercontinent in the D.R.C. region.

The lithologic units which formed during these three orogenic cycles make up the Precambrian basement in most of the region of present interest. A protuberance of Congo craton occupies the northeast and extends into Uganda and C.A.R. The Ubendian and Kibaran make up the extensive Mitumba Mountains of Eastern D.R.C. and have contributed to determining the manner of Western rift development and the associated hydrothermal processes. The Panafrican orogenic belts occur in the north as part of the East Saharan Metacraton and host the Upemba and Moero rift zones in the south.

During the Cambrian to Carboniferous, the southern and equatorial regions of Africa were tectonically largely stable, remained above sea level and subjected to the denudation of high-standing orogenic ranges and sedimentation in low lying areas in and around Congo craton.

Fig. 1: Geologic outline, drainage and high temperature thermal spring areas in Eastern D.R.C. (modified from UNESCO/CGMW, 1985)

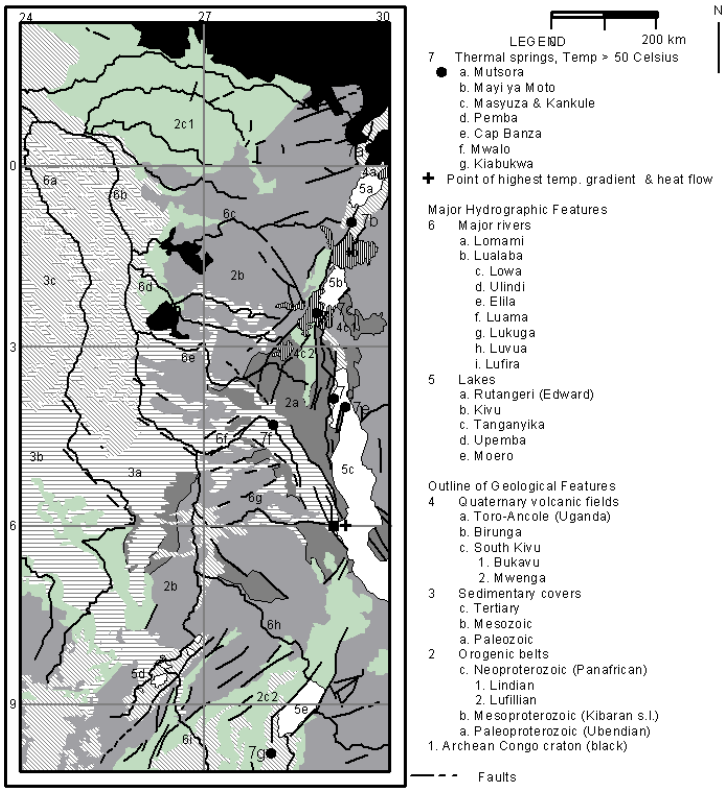

From the late Carboniferous onwards, Gondwanaland entered extensional tectonic phases which entailed a long period of intracontinental rifting followed by drifting phases during the Jurassic and early Cretaceous which respectively opened the Indian and Atlantic oceans. Extensive sedimentation took place in the rift basins. The Karoo continental sediments (3a) were deposited during the Carboniferous to Permian followed by the laying down of marine transgressive sediments during the Jurassic and Cretaceous (3b). These sediments are presently found in the Congo basin in the west and in the failed rifts of Eastern D.R.C. The sedimentary basins are reputed to host widespread hydrothermal activity.

The tectonic activities also resulted in the eruption of kimberlite in Southwest D.R.C. during the Jurassic and, during the Cretaceous, in the initiation of the periodic emplacement of small lava fields in Southern L. Kivu region.

Neogene and Later Developments

By the end of the Paleogene, Africa had attained its present outline. Since the Miocene however, as the core remnant from Gondwana breakup, it continued to rift and fragment along the Proterozoic orogenic belts in the context of EARS development.

Geodynamic studies show that much of the African lithosphere is underlain by a region of anomalously hot and upwelling asthenosphere, which was probably extant since about 45Ma, judging from the earliest volcanism in Northeast Africa which can be attributed to it. Asthenosphere upwelling heated and expanded a large region of the African lithosphere and caused it to isostaticaly rise to the high elevations, the "African Superswell", which especially characterize the region lying between Southern and Northeastern Africa. Eastern D.R.C. is situated on a particularly elevated part of the Superswell.

Seismic shear wave velocity tomography shows the asthenospheric temperature structure to rise to progressively shallower depths northeast-ward from Southern Africa. In the two regions where the upwelling has risen to shallow depths, it has spawned two mantle plumes which preferentially rose to still sallower depths along the Panafrican orogenic belts, the youngest and most mobile in the region. Mantle plume impact on the lithosphere caused further heating of the lithosphere which rose in isostatic adjustment to form the Ethiopian and East African domes. The two plumes are responsible for the extensive volcanism which characterized these regions starting during the Eocene. The Eastern rift developed on the softened and stretched terrains of these two domes starting during the middle of the Miocene. Plume driven within-rift volcanism has remained highly active since then. While much of it lies within the African Superswell, the Western rift developed outside the region of direct plume influence. This has given it a history of tectonic and magmatic development which is distinct from that of the Eastern rift.

The Western rift opened in a region occupied by diverse tectonic regimes. Its northern part lies in the Archean terrain of the Congo craton. Paleo- to Meso-Proterozoic orogenic belts make up its middle and southern parts while its southwestern branches developed in Neoproterozoic terrains. Its initiation is generally accepted as 10Ma: late Miocene, which appears to be the case for its central and southern parts. However, Abeinomugisha and Mugisha (2004) give an end-Oligocene to beginning-Miocene date for the initiation of its northernmost sector, the L. Albert rift, on the basis of the ages of rift bound sediments. Western rift development involved the opening of new rift zones following pre-existing rock fabrics in the metamorphic basement and the reactivation of structures that were initially setup during late Paleozoic and Mesozoic periods of crust extension. In addition to its main conspicuous physiographic expression lying between D.R.C and its eastern neighbors, the greater Western rift system also has a number of secondary rifted and faulted zones on its western side extending up to the eastern margin of Congo craton. This tectonic regime accounts for the great majority of the hydrothermal features of the country.

A distinctive feature of the Western rift is that it is segmented. It comprises rift zones, mostly half grabens which are separated from each other by rift-transverse faults. Quaternary volcanism took place solely along these faults while the interior parts of the rift segments remain amagmatic. In D.R.C., the Birunga and S. Kivu volcanic provinces are, from north to south, found between Lakes Rutangeri, Kivu and Tanganyika rift zones. To the north, the Toro-Ankole volcanic province in Uganda separates the Rutangeri and Albert rift zones.

The northernmost thermal springs in D.R.C. occur in L. Albert rift, a full graben which opened in Congo cratonic terrain. It is believed that this northernmost part of the Western rift is opening passively, with no in-field stress involved. Transform faulting along Aswa shear zone, which terminates the Western rift in the north, is believed to have transferred crustal movement from the Eastern rift. The tectonic event reported by Abeinomugisha and Mugisha (2004) predates the initiation of the main Kenya rift but rifting and volcanism in Turkana rift zone were already ongoing at that time. The Miocene age alkaline-carbonatite eruption centers in Eastern Uganda, e.g. Mt. Elgon, (Barifaijo, 2001) resulted from movement along this structure. The initiation of rifting by the agency of Aswa shear zone is thus plausible.

On the other hand, the high Mitumba Mountains region of Eastern D.R.C. is the part of the "African Superswell" which has undergone the most thermal uplift. The Ubendian basement terrain reaches 3,200m elevation along the Western rift margin on the western side of northern L. Tanganyika. This is the highest standing basement terrain of Africa attributed to thermal uplift. It is also marked by a regional gravity minimum (<-160mgal), a reflection of crustal density reduction by thermal expansion over tumescent asthenosphere.

In the region lying between Bukavu in the north and Kalemie about 400km to the south, the Western rift exhibits a complex structural pattern where faults of its three arms interact*:*

- a Northeastern arm: the L. Kivu rift zone which, in segmented form, extends to the northeastern termination of the rift branch at the Aswa shear zone in NW Uganda;
- a Southeastern arm: the Tanganyika-Rukwa-Malawi (TRM) rift zone which trends NW-SE to NNW-SSE; and,

- the Ruzizi rift zone: The N-S oriented structure which hosts the Ruzizi River and the northern L. Tanganyika basins and links the above two rift arms.

The L. Kivu rift zone is a half-graben extending from the NNE to the SSW between the Birunga and South Kivu volcanic fields. The earliest border faults are dated at between 7.5 and 4Ma (Furman and Graham, 1999). The WNW border faults extend to the region of Kamitunga in the Elila River basin in the SSW. Two lava fields are mapped as occurring in this rift zone: in Bukavu area and in Mwenga area situated about 100kms to the southwest.

A major NE-SW oriented, NW-facing regional fault could be discerned on SRTM-DEM of the L. Kivu-Elila River basin region. It extends from L. Kivu, where it forms the lake's southeastern coastline, to the northeastern border fault of Luama graben in the southwest. Its inferred disposition is shown in Figure 4. The fault appears to be more important than the NW border faults in forming an asymmetric graben in which Mwenga volcanic field is situated (here tentatively referred to as Elila graben). The graben is seismically active, discernibly more so in its southeastern part where this major fault is inferred to be situated. This fault may have contributed to the localization of volcanism in the Mwenga area, and possibly also in Bukavu area. The upper Elila River basin occupies the graben and is reported to be populated by 23 thermal springs of which the locations of only two, Kitutu (#24) and Kilenga (#31), could be determined. This inferred fault (here tentatively referred to as the S.E. Kivu fault) appears to form the northwestern structural boundary of the uplifted Ubendian basement.

The 200km wide TRM rift extends over a distance of 1,000km in the NE-SW to NNW-SSE direction between the southern part of L. Kivu rift and the northern end of Malawi rift, via L. Rukwa rift zone. It opened during Permo-Carboniferous times (Delvaux and Kervyn, 2004) following the Ubendian rock fabric, skirting the southwestern side of the Tanzanian craton. Crust extension across the TRM resulted in the opening of L. Rukwa graben in SW Tanzania and, in D.R.C. on the western side of the lake, the half graben which forms the upper Luama River basin. Permian Karoo and Cretaceous sediments were deposited in both rift zones. The opening of the part of TRM rift which houses L. Tanganyika's southeastern basin was initiated during late Miocene. The lake owes its formation to both crust extension and dextral displacement. The TRM was involved in transform movements at various times. The timing of these movements is subject to debate. As such, similarly to its northern counterpart, the Aswa shear zone, this structure is considered to be a transfer structure (CGMW, 2009) which facilitated the southward propagation of the EARS to by-pass the deep rooted and mechanically strong Tanzanian craton across which the Eastern rift failed to propagate. The structure is marked by late Miocene to Holocene volcanism in the areas where it terminates the L. Kivu and L. Malawi rift sectors.

The faults of Ruzizi rift zone have N-S trend, plausibly facilitating rifting to take place along the line of least mechanical resistance to link the above two rift arms. This rift zone includes the northern basin of L. Tanganyika which is characterized by N-S faulting extending as far south as Kalemie area. This basin is about 1,300m deep and it is separated from the lake's southeastern basin by a structural high where the depth of the lake is less than 750m (ILEC, 2009). From the structures which exist on both sides of the lake, it is evident that this structural high is cut by NW-SE trending faults which extend from the lake's northeastern side in Tanzania to Luama graben on the D.R.C. side in the northwest. Seismicity is particularly high in this zone (Fig.3).

The three sets of faults cross in the Kalemie-Bukavu region. Due to the above tectonic architecture, the Western rift exhibits an east-facing concave outline, with the Tanzanian craton nestled in the concave. This structural condition has given this part of the Western rift and its associated structures a distinctive geothermal character as discussed in Section 4 below. It is speculated here that the three fault systems form the structural framework within which the extraordinary thermal uplift of the Ubendian basement by about 2kms above the surrounding basement terrain occurred over a particularly buoyant sub-lithosphere region. The uplift of the Mitumba Mountains is greater in this area than elsewhere along the Western rift and cannot be accounted for solely by the rift shoulder uplift which is commonly said to accompany passive rifting. If this speculation is borne out to reflect the actual situation, it may explain why an anomalous geothermal regime prevails in this region, giving rise to a high density of hydrothermal activity and the occurrence of primary magmatic brines of very deep origin.

In the southeastern region of D.R.C., the incipient NE-SW trending Upemba and Moero rift branches are undergoing extension in the NW-SE direction (Fairthead, 1977). The structural development of the region dates from northeastward thrusting and the raising of the Lufilian Arc (Fig. 2) during the Panafrican orogeny. The Damaran-Lufilian orogenic belt is characterized by extensive faulting of this age with strikes oriented NE-SW, the direction of thrust. The structures which evolved to become rift faults thus seem to be attributable to Panafrican structuring. In contrast to other rift zones in the region (Luama, Rukwa, Malawi, Luangwa and Zambezi) these rift branches do not seem to contain Permian and Cretaceous sediments and thus appear to be newly opened during the EARS tectonic phase. Although situated in the mobile Neoproterozoic Lufilian (Katangan) greenstone belt, which is inherently most amenable to deformation, these two rift branches have failed to further propagate to the southwest. This is mainly attributable to the rheological barrier imposed across

the otherwise preferred path of rift propagation by the cross-cutting Lufilian Arc. Otherwise the rift zones exhibit a high level of seismic activity and extensional stress. A large number of areas of hydrothermal activity are reported to occur in the rifts and in the basins of the rivers in the region. During the early 1950s, Kiabukwa, situated in the southern L. Moero rift zone, was the site of the first geothermal power plant in Africa (Hochstein, 2000).

SUMMARY OF THE FINDINGS

Regional Distribution of Hydrothermal Activities.

All of the geologic terrains described above exhibit hydrothermal activity. Except for the fumaroles of Nyiragongo and Nyamulagira volcanoes, all other known hydrothermal features in D.R.C. are thermal springs. All of the features are found in the eastern part of the country, extending over nearly all of its latitudinal extent (Fig.2). None are reported to occur to the west of 24OE longitude.

The westernmost thermal spring, Tshapona (#35 in The appendix), discharges in the upper Kasai River drainage basin. Three others, Kibimbi, Lufubu and Piani Mimba (#25-27), occur close to Lualaba River. All of the rest are found to the east of that river. Of those features for which the locations are known, Kasongo occurs close to R. Lualaba but all of the rest are situated to the east of 28OE longitude. This distribution of most of the thermal springs indicates their large scale tectonic affiliation to the highlands of Eastern D.R.C.

Several thermal springs are found within the Western rift basin, including most of those that are hotter than 50OC. The largest number of the features is however found in the Mitumba Mountains region lying to the north of R. Lukuga, and most of them occur in the basins of the numerous rivers which drain westward into Lualaba River. In the southeast, numerous thermal springs are reported to occur in river and lake basins found in the Proterozoic terrain which makes up the plateaus and rifts of Katanga.

Sub-lithospheric Influence on the Hydrothermal Activities.

The different stages of tectonic and magmatic development reached by the various rift zones are due to the different degrees of sub-lithospheric influence which itself evolves in time. This is relevant to understanding the nature and characteristics of the hydrothermal features of the EARS in general and those of the Western rift in particular, including their associated geothermal resources (Getahun Demissie, 2010). The geothermal resource development prospects in Eastern D.R.C. are thus best viewed in this light.

The northernmost part of the Western rift lies outside and to the northwest of the East African dome, the region of direct mantle plume influence. The asthenospheric temperature structure has a more subdued aspect which is more akin to that prevailing in the Saharan zones of moderate thermal uplift. The gravity field is also similar to the pattern along these zones and matches the lower elevations which prevail in this part of the rift than further to the south. This part of the Western rift is situated in a region of old, thick and cooler crust than elsewhere and is undergoing a truly passive rifting process involving little or no in-field stress. Mantle influence is limited solely to the emission of volatile components released during the degassing of newly un-muffled mantle. There has not been any magmatism in the form of melt production.

On the other hand, in the Birunga and S. Kivu parts of the Western rift, asthenospheric impact is believed to occur, signaling two evolutionary stages of rift

Fig. 2: The known thermal spring locations of D.R.C.
(Thermal spring numbers are as in the appendix. Bold full lines are topographic contours for 2,400 and higher elevations)

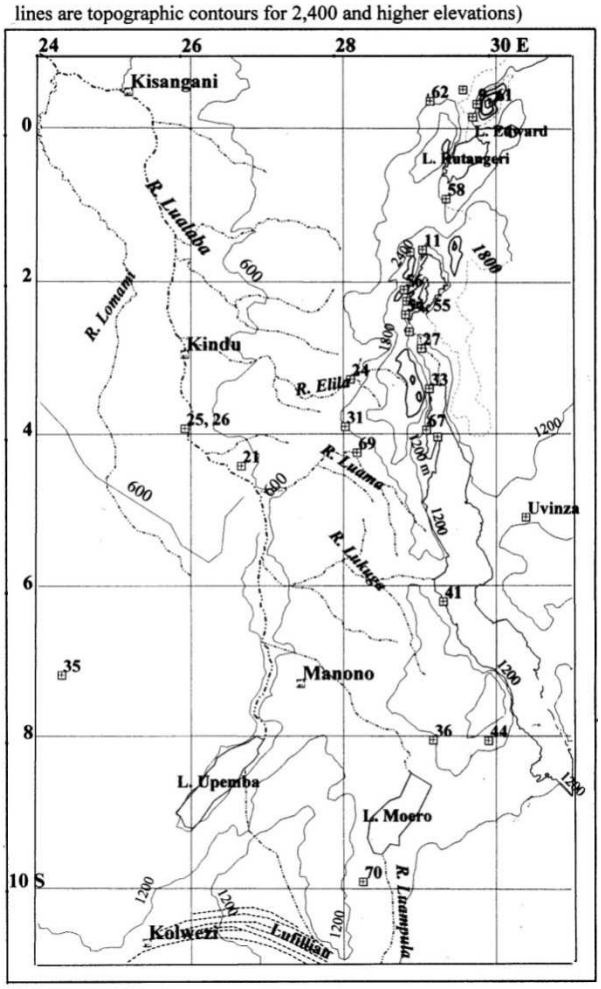

development. As further discussed under 3.3.4 below, the dominantly Potassic alkaline affinity of the volcanic rocks in the Birunga field (Rogers et al, 1998) represent the earliest phase of small scale melt production in a still passively rifting state. The mode of melt generation is metasomatic and not adiabatic melting which requires a higher more advanced scale of lithosphere structuring. On the other hand, volcanic petrogenetic data from Bukavu lava field (Furman and Graham, 1999) indicate the magma sources to be situated at the base of an already attenuating lithosphere at an estimated 65km depth, the shallowest depth in the Western Rift outside the Rungwe volcanic field in SW Tanzania. This state of lithosphere breaching can be taken as signaling the transition of Kivu rifting from the passive to the early active phase. The picture is broadly consistent with results from seismic shear wave velocity modelling work by Simiyu and Keller (1997) and Nyblade et al (2000). The models indicate the existence of a deep seated mantle plume arm rising westward from a plume head situated under the Tanzanian craton. Nyblade's model shows the plume arm apparently penetrating the lower lithosphere under the region of the Western Rift lying to the south of Kivu volcanic province. This may account for the significant extent of sub-lithospheric erosion which the petrogenetic evidence implies.

An evidence for this situation prevailing under Eastern D.R.C. is the occurrence of an anomalously large number of hydrothermal features, surpassed in density of activity only by regions of Africa which are traversed by the eastern and northern EARS sectors, the middle Zambezi rift and the Atlas Mountains belt of currently ongoing orogeny. The juvenile brine springs in the Ruzizi rift zone, indicate rifting in this region to be more advanced than in most other parts of the Western rift.

Crustal Influences on Hydrothermal Activity

Some Geophysical Features of the East D.R.C. Crust

Seismicity

Figure 3 shows the distribution of earthquake epicenters for the period 1973 to 2009 (NEIC, 2009). The three tectonic elements of the Lakes Kivu and Tanganyika region, discussed in 2.2 above, and the Upemba and Moero rift zones are schematically shown. Except for Upemba rift zone where the situation is unknown, most of the higher temperature thermal springs of Eastern D.R.C are hosted within this tectonic framework. The thickness of the seismogenic layer in the region is generally 33kms, showing the crust to be largely un-attenuated.

From the distribution of seismic epicenters, it is evident that the crust in the region is tectonically active. The high epicenter density shows not only that active faulting prevails in the rift zones that were newly opened during the late Miocene but also along the TRM fault system most parts of which date from the late Paleozoic and the Mesozoic.

The close association of areas of thermal spring activity in Eastern D.R.C. with these fault systems is discussed in 3.3.2 below and indicates that faults serve as channels of geothermal fluid ascent to the surface.

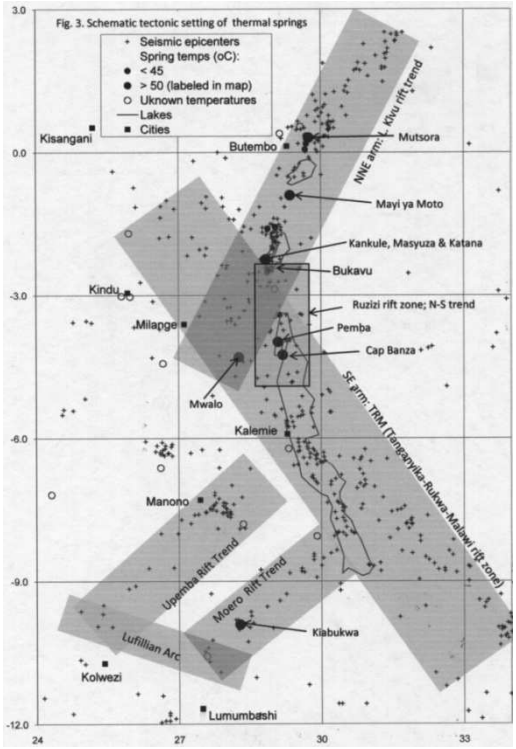

Heat Flow

Sebagenzi et. al. (1993, cited in Sebagenzi et. al., 2004) provided the two only known heat flow values on land in D.R.C.: 65mWm-*2* is reported for the rifted Kundelungu plateau terrain and 40mWm-*2* from Congo craton. These are comparable to values reported by Nyblade (1990, 1997) for the adjacent regions: 67+/-7mWm-2 for the Kibaran belt on the southwest side of L. Victoria, 76+/-14 mWm-2 for the Mesozoic Luangwa and Zambezi rifts in Zambia and 34+/-4mWm-2 for the Tanzanian craton.

The international heat flow data base contains only 17 values, all from Lakes Tanganyika and Kivu (Fig. 4, Table 1). Heat flow values range widely for both lakes, respectively from 17 to 151mWm-*2*, and 17 to 185mWm-*2*. Heat production values are 5.6 and 5.8µWm-*3* for L. Kivu and 3.3 to 3.5µWm-*3* for L. Tanganyika. There is no information on what rocks were tested for heat output. Therefore, it is not known if the higher values from L. Kivu are due to measurement in the young Panafrican rocks which occur in the lake's northwestern part. Granitic rocks in the Panafrican basement are much younger than the Ubendian and Kibaran rocks which make up the basement of L. Tanganyika and would still retain much of their original

radio-element contents. In the data from both lakes, there is no correlation between heat production and heat flow. Heat flow may thus have deeper sources and also appears to reflect the influence of faults. In L. Kivu, the higher values are from the zones of two east-facing faults: 99mWm-2 near a rift border fault to the east of Kabuno Bay and 181mWm-2 near the eastern border fault of Idjwi horst.

In L. Tanganyika, temperature gradient shows a wide range, all but one value exceeding the global average of 30*O*C/km. There is a linear relationship between heat flow and temperature gradient indicating the absence of near-surface influences. The highest temperature gradient and heat flow, respectively 190OC/km and 151mWm-2, are both from the shallow zone which separates the lake's two basins. This contrasts with usual sub-lacustrine heat flow value distributions in rift zones where the higher values typically are from the deeper parts the lakes, e.g. L. Baikal, Russia (Lysak and Sherman, 2002). This indicates that the high heat flow is due to a NW-SE trend fault which crosses this block. Another value of 57mWm-2 is from a nearby location on this block. The difference between these values seems attributable to the measurement points being located at different distances from fault zones.

Figure 4. Geology, known thermal spring locations and heat flow measurement points in Lakes Kivu-Tanganyika region.
(Geologic units are as in Fig. 1, Thermal spring and heat flow measurement sites are as in the Appendix and Table1)

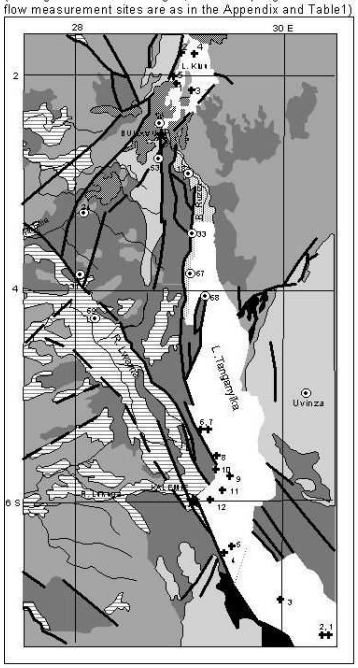

The Influence of Crustal Structures

As outlined under Section 2 above, the region of Eastern D.R.C. has a long history of structural development, mainly dating from Gondwana supercontinent rifting and break up during the late Carboniferous to Cretaceous. The dominant structural trends during those times appear to have been oriented NW-SE and NE-SW. This is discernible in the structural patterns engraved on the Proterozoic terrains and marking the outlines of sedimentary rock exposures. These structures also determine sections of the courses of the numerous rivers which drain the Mitumba Mountains. The latest phase of structural development however dates from the late Miocene initiation of EARS tectonics.

From the locations of thermal spring activity along fault zones and in the graben structures which house river basins, it is evident that faults serve as the preferred paths for thermal fluid up-flow from depth. This is particularly well illustrated by the locations of the sub-lacustrine juvenile brine springs of Pemba and Cap Banza (#67, 68). Tiercelin et al (1993) report that these features occur at the intersections of NW-SE and N-S trending faults, respectively designated above as the TRM and Ruzizi fault systems. Uvinza brine spring in Tanzania (Fig. 3) also occurs on a fault of the TRM system, and is believed to be of similar juvenile origin. Alleman et al (2003) reported water stratification in L. Tanganyika which is due to poor mixing. Hydrothermal fluid contribution to the deep lake water and particulate chemistry was seen to occur in the northern basin, from either upward fluid flow from beneath the basin itself or outflow from sources in the north. In either case, the importance of the N-S structures as conduits of hydrothermal fluids is demonstrated.

Table 1: Heat flow data from D.R.C.

A. From the IASPEI-IHFC database: Lakes Kivu (L-K) and Tanganyika (L-T),

Site	Location		Heat Production	Temperature Gradient	Heat Flow
No.	Long	Lat	µW m-3	oC km-1	mW m-2
L-K001	29.02	-1.99	-	-	41
L-K002	29.02	-1.75	5.8	-	99
L-K003	29.15	-2.13	5.6	-	185
L-K004	29.17	-1.80	5.8	-	25
L-K005	28.98	-1.93	5.6	-	17
L-T001	30.27	-7.22	3.4	49.0	35
L-T002	30.23	-7.22	3.3	54.5	39
L-T003	29.97	-6.85	3.4	77.0	55
L-T004	29.54	-6.44	3.5	24.0	17
L-T005	29.58	-6.38	3.4	33.0	22
L-T006	29.25	-5.33	3.3	48.0	35

L-T007	29.35	-5.30	3.3	57.0	67
L-T008	29.47	-5.54	3.3	58.0	41
L-T009	29.58	-5.77	3.3	55.0	39
L-T010	29.42	-5.73	3.5	65.5	46
L-T011	29.53	-5.92	3.3	72.0	57
L-T012	29.45	-5.97	3.4	190.0	151
B. From Sebangezi et al, 2004 (unspecified location coordinates)					
Kundulungu plateau,			-	-	65
Congo craton overlain by Paleozoic sediments				-	40

While the preceding accounts for the tectonic control on individual thermal spring occurrences, their general distribution in the key region affected by the above fault systems may be viewed in terms of the larger scale of crustal structural control. In this respect, the present perception is that the high standing block of Ubendian basement may be considered as a focal structural unit of geothermal anomaly with regional significance. This basement is believed to have been heated and thermally uplifted over a particularly tumescent mantle structure. The resulting thermal expansion and consequent density reduction of the Ubendian crust is reflected in a very strong negative gravity anomaly, as discussed in 2.2 above. This tectonic setting leads to the inference that the uplifted block has an anomalously high subsurface temperature. Its high internal heat content may be advectively flushed outwards by hydrothermal fluid flow which would have given rise to the numerous thermal springs which occur in the lower lying faulted areas of the surrounding region. Its conductive heating by a high standing mantle hot plate may also be augmented by the upward rise of juvenile hydrothermal fluids in the areas affected by the Ruzizi and TRM fault systems, elements of which are seen to extend into the uplifted block. The path of magma rise from lower lithosphere regions may have been refracted away from the uplifted block and into the faulted zone in the northwest to engender the volcanism of Bukavu and Mwenga areas. In this respect, the faults of Elila graben appear to be more amenable to the upward leakage of hot lower lithospheric materials, in the form of melt, than those of the amagmatic Ruzizi and TRM systems which facilitated only volatile component rise. From this may be inferred the possible geothermal attraction of Elila graben.

The Role of the Sedimentary Basins

Successive vertical movements have been followed by the erosion of uplifted blocks and sedimentation in tectonically subsided and rifted zones especially during the late Paleozoic and Mesozoic (lithologic units 3a and 3b in Fig. 1). The rivers which drain the Mitumba Mountains region lying between the latitudes of Bukavu and Kalemie wholly or partially flow in these sedimentary terrains. A number of the numerous thermal springs that are reported to occur in these river basins can thus be expected to be hosted in these structurally controlled sedimentary basins. The only thermal spring known to have such occurrence is Mwalo. It is reported to exhibit high energy of discharge. Continental clastic sedimentary basins tend to be associated with higher permeability than igneous and metamorphic terrains and to attain more extensive lateral continuity. They may thus support energetic hydrothermal activity as at Mwalo. If geothermal resources are hosted in such basins, as is supposed here to be generally the case on the western flank of the Mitumba Mountains, it can be expected that both the stored resources and well productivities may be sufficiently large to warrant economic geothermal resource exploitation. Deep sedimentary basins are also known to host geopressured geothermal resources which do not have surface expressions. The rift bound Paleozoic to Mesozoic sedimentary piles may thus also host such blind resources.

The influence of magmatism

As indicated earlier, coupled with it's more recent initiation than that of the Eastern branch, rifting in the thick and strong Paleo- to Mesoproterozoic crust in Eastern D.R.C. is insufficiently developed to trigger high volume adiabatic magma generation in the mantle. Rifting and crustal attenuation are thus at too early stages of development to engender the large scale and evolved magmatism which characterizes the more developed eastern and northern EARS sectors. Only small scale volcanism took place in the Birunga and South Kivu volcanic fields.

The oldest volcano in the Birunga volcanic field (unit 4b in Fig.1) is Mikeno and has been dated at 2.6Ma **(**Ranson and Demange, 1983**).** Two active volcanoes, Nyiragongo and Nyamulagira are of late Pleistocene age. These three volcanoes occur in the D.R.C. part of the volcanic field. Karisimbi and five other recently inactive volcanoes of similar age occur on the D.R.C.-Rwanda border. The Birunga field is characterized by alkaline, dominantly potassic, volcanism with limited total volume and areal distribution of eruptive products. The chemical and mineralogic compositions of the volcanic rocks in most cases show derivation from small fraction

metasomatic partial melting in the mantle and very little sign of magma differentiation or interaction with crustal rocks. Magma is thus believed to rise to the surface without undergoing significant intermediate storage in the crust.

Karisimbi, which is most favorably situated on the eastern rift border where it is crossed by a rift-transverse structure, shows a degree of magma differentiation reflected in the eruption of trachytic lava (Rogers et al, 1998). It is the only one which exhibits the possible presence of magma storage in the upper crust. Gisenyi thermal spring in Rwanda (70OC) may be associated with the magmatism which produced Karisimbi. The volcano's recent inactivity and the small volume of the total erupted products however indicate that magma size may not be large or to still be at high temperature. The other, warm, thermal springs which occur in the adjacent areas to the north of L. Kivu may owe their geneses to the circulation of meteoric waters in upper crustal regions that are heated conductively and by heat loss from ascending magma, and their mixing with hot juvenile volatile fluids which are common features of the Western rift region.

The nature of volcanism at Mayi ya Moto, situated to the north of the Birunga field, is not known although its tectonic setting suggests it to be an offshoot of that volcanic field and to broadly share its petrologic, and therefore genetic, characteristics. Its association with highly dynamic hydrothermal activity however lends it distinction which should be accounted for.

In the Southern Lake Kivu volcanic province, numerous episodes of small scale alkaline volcanism have been dated from as early as 70Ma (late Cretaceous) forming a pre-rift tholeiite flood basalt plateau (Ranson and Demange, 1983). The late Miocene lavas however date from the initiation of Kivu half graben opening at about 7.5Ma. The more evolved lavas are from Bukavu area (unit 4c1) where the above described three fault systems interact. The volcanic province is almost entirely made up of fissure lava flows with only a few relatively small volcanic centers occurring along the northwestern border faults. Tshibinda is the more prominent of these centers. Its last eruption was at 10Ka, at the same time as a small eruption on Idjwi Island.

The volcanic field in the general area of Mwenga (4c2) situated about 100 kms from Bukavu, forms the isolated, southernmost field of the South Kivu volcanic province. It is found in the area which is affected by the SW extensions of Kivu half graben border faults which, together with the S.E. Kivu fault described above form a graben. Information on the nature of the volcanic rocks was not available for this study.

A number of carbonate bodies, sometimes described as carbonatite, occur within and outside the rift basins. Evidence from Kibuye in Rwanda (Lavreau and Buyagu, 1989) shows it to be a product of hydrothermal remobilization of carbonates in the metamorphic and sedimentary rocks, rather than originating from metasomatic carbonatite volcanism. Thus, the many thermal springs which deposit travertine fronds should be viewed in this light for better understanding their geneses and chemical evolution.

Lithologic Affiliations of Hydrothermal Activity.

Hydrothermal activity takes place in areas made up of lithologic types of all ages.

Thermal Springs of the Volcanic Fields

Two of the high temperature spring areas, Mayi ya Moto and the Mahyuza-Kankule group, (respectively #58 and 54-55 in the appendix), occur in the areas of hydrologic discharge situated in Quaternary volcanic provinces.

The low temperature springs, Tingi, Sake, Kihira (collectively #11) and Kikingi (#63) occur on the northwestern shore of L. Kivu. It is uncertain if they are heated under the Birunga volcanic field to emerge on or near the lake shore at the lower end of the local hydrologic gradient, or if the waters rise from depth along the border fault limiting Kabuno Bay on the west. Published results (e.g. by Tietze et al, 1980; Tassi et al, 2005) show that L. Kivu discharges large volumes of CO_2 and CH_4, especially in Kabuno Bay. The CO_2 is of juvenile origin. Katana (#12) and Maziba (#56) occur near the northern end of the Bukavu sector of S. Kivu volcanic field, probably owing their location to the outer rift border faults. Nyangezi (#53) occurs near the southern edge of the lava field.

Kitutu (#24) is situated near Mwenga. It is the only thermal feature which may possibly be related to the volcanism there. Of the other 22 reported thermal springs in the Elila River basin, some may have similar association while others may be expected to occur in the graben marginal metamorphic or graben filling sedimentary rocks. No information was available on these thermal springs.

Thermal Springs of the Sedimentary Basins

The only thermal spring for which the location coordinates are known and that is believed to be situated in an area occupied by sediments is Mwalo (#69). It occurs in the upper Luama River basin in the piedmontain area on the northeastern side of the Luama half graben. Waring has reported the occurrence of 17 other thermal springs in this river basin (#28, 29 and the #29a group of 15 features). The main course of Luama River is situated within the extensive late Paleozoic and overlying Mesozoic graben filling sediments. Thus many of the features

may issue from these rocks. Two alternative modes of subsurface hot water circulation may tentatively be considered. Hot water may rise to the surface along faults from a reservoir situated within the sedimentary basin, or, it may emerge from a thermal water outflow structure originating from a heating and upwelling area situated under the high standing block of Ubendian metamorphic rocks lying to the northeast.

Pakundi spring (# 34) is reported to occur in the Lukuga River basin which is partly occupied by the same sedimentary rocks. Waring also reports that 7 named (#14-16 and 21-24) and 27 un-named thermal springs occur in the Ulindi and Elila River basins. The courses of these rivers traverse similar sedimentary basins as R. Luama. Thermal springs may thus discharge from sedimentary rocks if they happened to be situated in close proximity with the rivers in their middle courses. Others may issue from the metamorphic rocks which occupy the upper and lowermost parts of the river basins.

Thermal Springs of the Proterozoic Terrains

Many thermal springs, including half of those known to issue at high temperature (#68: Pemba, 69: Cap Banza and 70: Kiabukwa) occur in Proterozoic basement terrains. They rise from depth along crossing, rift forming faults and emerge where the near-surface hydrologic conditions allow them to occur. Pemba and Cap Banza brine springs occur in Ubendian basement rising along deep reaching faults, as discussed in the last paragraph of 2.3.2 above. Kiabukwa occurs in Panafrican terrain near the northwesters border fault of Moero rift zone.

A number of the thermal springs which are described by Waring as occurring in the Lowa (#10a group of 14 features), Luika (#30, 31), Luvua (#36-40) and Lufira (49-52) river basins as well as in the areas of Lakes Rutanzigi, Upemba and Tanganyika seem to all occur in similar terrains and under similar tectonic and hydrologic controls. Those features which occur in the non-volcanic, rift shoulder area to the northwest of L. Kivu (#64-66) seem to occur in areas of Kibaran basement. Some of the thermal springs in these areas may issue from Neogene sediments which may cover the basement rocks, as in Semliki River valley.

The thermal springs of Ruzizi valley (#17-20, 53) as well as Mutambula and Uvira (#32, 33) occur in Proterozoic metamorphic terrain. The hot waters issue from the border faults of the high standing metamorphics lying to the west. It is presently unknown whether, alternatively, the northernmost springs in this zone issue from hot water outflows from the Bukavu volcanic field to the north.

Thermal Springs of the Archean Terrain

Fourteen thermal springs (#1-9, 59-63) are reported to occur in areas of rifted Archean basement situated to the south, west and north of the Ruwenzori Mountains. The northern group (#1-4) are reported to occur in the vicinity of L. Albert but at unknown locations. Two of these (#1 and 2) are described as hot and sulfurous. Goda (#3) is reported to issue petroleum with its thermal water, which co-occurrence of the two fluids is reminiscent of Kibiro thermal spring area on the Ugandan side of the L. Albert rift zone. The southern group (#5-9, 59-63) are in the Semliki valley and are all reported to be sulfurous. The highest temperature, 57OC, was measured at Mutsora while for the rest of the #59-63 group temperatures range 39-43OC. No thermal water discharge rate is reported. No information is available for the #5-9 sub-group except for the location of Mutwanga (#9). The area found to the west of the Rwenzori Mountains is a low lying rift floor which is drained by R. Semliki which flows from L. Rutangeri to L. Albert in the north-northeast. Granted that temperatures are lower, the tectonic and hydrologic setting of this group is similar to those at Buranga in the Bundibugyo area of Uganda (Armannsson, 1994).

Other thermal springs of Unknown Affiliations

Tshapona (#35), the westernmost known thermal spring in D.R.C., occurs in a region of Mesozoic sediments. Kibimbi, Lufubu and Piani Mimba (#25-27) occur in Kibombo area near the Lualaba River. The area is made up of sediments which range in age from late Paleozoic to Quaternary. However, Piani Mimba (#27) is reported to issue from achiest (Kibaran?). Kasongo appears to be located about 100kms to the southeast of Kibombo and about 20kms east of Lualaba River. However, Waring reported it as occurring in Elila River basin, which is situated more than 200kms to the north.

These five areas are the westernmost places of thermal spring occurrence, far removed from the Mitumba Mountains region of high geothermal anomaly. It may be speculated that they owe their temperatures to crustal heat sources: either radioactive heat sources in the underlying basement rocks, or, exothermic diagenetic processes taking place in the sediments which may host some of them.

DISCUSSION

The information that was available for this study was insufficient to support conclusive interpretations. The principal source for hydrothermal feature occurrence was Waring (1965) who based his work on Belgian sources dating from 1879-1936. The available more recent information was bare on details. There had been a

professional paper on the thermal springs of D.R.C. by A. Le Bail and M. Buchstein which was presented at the International Geological Congress in 1969 under the title "Les sources thermales et thermo-minerales de la republique democratique du Congo.". The effort to locate a copy was not successful.

In spite of these shortcomings, a discussion of the findings of this study is believed to be useful for describing the picture which arose from it and for proposing explanations for the surface expressions of the subsurface geothermal situation. The testing and improvement of these explanations and the provision of answers to the uncertainties expressed by this study can provide a starting point for the systematic study of the hydrothermal manifestations.

It is evident that thermal spring occurrence in Eastern D.R.C. is associated with a variety of lithologic types. Overall, there is no fundamental distinction in the geneses of the thermal springs which is attributable to lithologic affiliation. A shared feature among the thermal springs is the combined control of fault tectonics and shallow subsurface hydrology on their regional distribution and individual occurrences.

The thermal springs which occur in the Archean cratonic and Quaternary volcanic terrains are the better known groups as they occur in the northeastern part of the country in areas of high population density and which are also the less challenging to field surveys by geoscientists from Kivu and elsewhere. Together these better known thermal springs make up about 20% of the reported number of thermal springs in D.R.C. More of these 20% occur in areas of Archean basement than in those of Quaternary volcanism. The least known thermal springs are those which occur on the western flank of the Mitumba Mountains which is highly dissected by the numerous rivers which descend toward Lualaba River, are sparsely populated and difficult of access. However, according to Waring's sources, about 50% of the thermal springs of the country occur in these river valleys. Another 30% occur in the river and lake basins of Katanga and Ruzizi valley. Thus about 80% of the thermal springs of D.R.C occur in areas made up of faulted Proterozoic metamorphic or Phanerozoic sedimentary rocks. A larger number of the known, most dynamic hydrothermal features occur in these terrains rather than in the volcanic fields. This is convincing evidence of the fact that magmatic melt transported to, and stored in, the upper crust, may account for the heating of only a few, if at all, of the hydrothermal features. Thus, magma storage in the shallow subsurface is not essential for the occurrence of high energy thermal spring activity in Eastern D.R.C. and, by extension, for engendering and maintaining the geothermal systems which they may indicate to exist in the subsurface.

Experience from within the region includes that from the better studied high temperature and high discharge thermal springs issuing in areas of no volcanic activity of any age: the Buranga and Kibiro thermal spring areas in Uganda. Experience from other parts of the world, includes that from the Basin and Range tectonic province of the Western United States (Edmiston and Benoit, 1984) which shows that Recent volcanism is either absent or of small volume and unrelated to the heating of the numerous medium and high temperature geothermal fields that have been successfully developed in the region. It is thus argued here that, while the question of to what extent various modes of magmatism may be involved in heating hydrothermal fluids should be addressed while exploring for geothermal resources in the volcanic fields of Eastern D.R.C., emphasis should also be given to exploring areas of high energy hydrothermal activity in the non-volcanic areas.

Crustal tectonic conditions which develop over regions of active tumescent mantle-crust interactions give rise to high temperature conditions in the upper crust. Meteoric waters which circulate in such crustal regions pick up heat from conductively heated crust, by the flushing of any residual heat transferred to country rocks during magma ascent to the surface, and by mixing with hot volatile components which are released during mantle degassing. These may give rise to hydrothermal features on the surface which may be associated with geothermal resources in the subsurface which may be economically exploitable.

Based on the information that was available for this study, thermal springs at eight named and two un-named areas are either described as "hot" or reported to issue at higher than 50OC temperature. However, only the locations of the eight features that are listed in Table 2 could be determined. It is possible that a more complete inventory would identify other high temperature hydrothermal features. A full inventory of these features in the whole of D.R.C. is essential and should be carried out in due course in order to create the basic data base which is needed for use in geothermal resource development.

However, the aim of the present exercise is to contribute to expeditious progression toward the identification of areas of most promising geothermal resource development prospect. It is thus found useful to focus present attention on starting with the existing state of knowledge of the high temperature thermal springs. It is proposed that this knowledge should be expanded by the follow-up study of the known features and others that may be found to share their tectonic and hydrologic settings.

The eight thermal springs occur in terrains occupied by the four lithologic units discussed under 3.4 above. They may thus be considered to be representative of other high temperature and high discharge springs which may be found under the same or similar natural conditions elsewhere and which may be included in the suggested studies. Table 2 is compiled with these objectives and scope in mind.

Table 2: Areas of the hottest known and related thermal spring activities in Eastern D. R. C.

No.	Main thermal springs	Unknown but possibly related thermal spring areas
54, 55	Mahyuza and Kankule	None
58	Mayi ya Moto	Waring's Kabusi volcano
61	Mutsora	Others in R. Semliki and L. Albert rift basins
68, 69	Pemba and Cap Banza	None others known
70	Mwalo	The easternmost of: 18 springs in R. Luama basin, 23 in R. Elila basin and Pakundi in R. Lukuga basin
71	Kiabukwa	17 named and 10 un-named thermal spring areas in Luvua and Lufira river basins and Upemba rift

The high temperature thermal springs of the volcanic areas

The Kankule-Mahyuza group

Vikandy's map of the area shows that the thermal springs occur near the southwestern shore of L. Kivu, near Bukavu, where Ruzizi River leaves the lake to flow south to L. Tanganyika.

Mahyuza, lies close to the lake shore and has a somewhat lower temperature (66OC) than Kankule springs (72OC) most likely due to cooling by mixing with cold water infiltrating from the lake. The springs produce near-neutral (pH 7.3) waters with TDS concentrations of less than 1,500ppm. The dominant ions are of Na and HCO_3 with the respective concentrations being about 200 and 800ppm. No travertine deposition is reported.

Their geologic setting indicates that the springs may be located closest to the focal area of geothermal water upwelling in the Bukavu lava field which is more centrally situated than the other parts of the volcanic field. Quaternary volcanism concentrated along the western Kivu rift border fault. Small volume Holocene volcanism occurred at Tshibinda situated about 15kms distance to the southwest and at a higher level of the local hydrologic gradient. Rancon and Demange (1983) report that some of the volcanic rocks in Bukavu area are products of differentiation from alkaline parent magma. However, the small volume of the volcanic rocks of Quaternary age and, as discussed above, the paucity of eruptive centers which are made up of magma differentiation products preclude the possible existence of a significant magmatic heat source.

The significance of the rifting and magmatic development in S. Kivu area seems to be less in its potential for spawning significant magma storage in the shallow subsurface, but more in its potential for installing a high temperature regime in the upper crust without significant contribution by magmatic mass and heat transport from sub-crustal sources. This region may be considered to be the exception in the Western rift in that it is situated over a sufficiently high standing mantle temperature structure which serves as a hot plate which maintains high upward thermal conduction through the overlying thinned lithosphere and as a source region for the upward leaking mantle volatiles as well as the small volumes of melt. Apart from heating conductively and by volatile fluid upwelling, the area may also contain residual heat that is released to the country rocks by magma rising to feed the Holocene volcanic eruptions at Tshibinda and Idjiwe. Circulating ground water may flush this stored heat over extended periods of time and sustain thermal springs.

Mayi ya Moto

The occurrence of these hydrothermal features in a discrete tectonic, volcanic and hydrologic setting lends the study of the features with a straightforward starting model which links them with the subsurface regions heated in connection with the activity of the presumably Holocene age Mayi ya Moto volcanic center and the hydrologic system maintained by Lakes Kivu and Rutangeri and River Rutshuru. Although the thermal water and steam output (natural heat energy release) is unknown, it appears that the hydrothermal activity may qualify as one of the most important volcanic field related activities of the Western rift. Hochstein (2000) reported that both hot water and steam discharges. Another spring, Bitangola (#10) which Waring reports as occurring in this river basin is at an unknown location.

Mayi ya Moto hydrothermal features occur along a major east-facing fault against which a within-rift horst is up-thrown in the west. The main body of Mayi ya Moto volcanic center is situated on the horst while the lower part of its eastern flank has been downthrown by the fault. It seems obvious that this structure controls the emergence of the thermal water at the surface. The springs occur in the western part of the Rutshuru River basin. The river starts in the uplands of the area of Rutshuru town and the eastern rift shoulder and flows north into L. Rutangeri. Ground water conditions in the area mirror the surface drainage pattern and are determined by the levels of Lakes Kivu and Rutangeri which respectively stand at elevations of 1,460 and 910 m a.s.l. Because of its impoundment in the north by the Birunga volcanic field since the Pleistocene, L. Kivu has stopped draining northward into L. Rutangeri and the Nile River system. However, there is a north-sloping ground water gradient.

This subsurface hydrologic regime may be thought to be favorable for the recharge of any subsurface geothermal reservoir that may be associated with the Mayi ya Moto hydrothermal features. An outstanding question is whether thermal springs occur on the southern shore of L. Rutangeri, being products of the northward flushing of thermal water from Mayi ya Moto area along this inferred ground water gradient.

Vikandy et al (2008) reported some major ion chemical analyses data. The field survey team does not seem to have been equipped to carry out on-site volatile component analyses. Additionally, a number of key components were not reported: SiO2, CO_2, CO_3, H_2S, and CH4. It is not known if the wide ranges in the reported chemical concentrations are due to sampling at different sources or during different seasons. However, all of the surveyed thermal springs surveyed are reported to be rich in CO_2, and this presumably includes those at Mayi ya Moto. However, travertine deposition, common among Western Rift thermal springs, is not reported, perhaps being absent due to low Ca concentration.

The pH of the thermal spring waters ranges 7.99 – 8.94. The lower range of temperatures reported, 94.5 - 96.4OC, are at the approximate boiling temperature of water for the elevation of the springs (about 1,000 m. asl). The reported 100OC temperature represents superheat but its significance is currently unknown. Laboratory analyses results show high concentrations of Na (2,170-2,745ppm), HCO_3 (3,400-5,096 ppm), Cl (1,070-1,140ppm) and SO_4 (400-590 ppm). Ca and Mg concentration s are low (respectively 1-9.6 and 0.9-2.0ppm). The higher of the above concentrations together with the very low concentrations of F, Br, NH_4 in comparison with Na and K show the waters to be of peripheral character to primary NaCl type waters and are of meteoric origin. Na/K geothermometer values of 163-177OC were calculated which are within the range for thermal springs with such chemical compositions.

The petrogenetic affiliations of the products of Mayi ya Moto volcanic center are not known. It is thus not possible to evaluate the likely heating mechanism for the hydrothermal fluids.

The Sedimentary Basin Hosted Thermal Springs: Mwalo and Others.

Mwalo was reported by Hochstein (2000, 2005) as one of the important areas of hydrothermal activity which were distinguished from other features by spring temperature and total heat energy output being respectively higher than 75OC and 3 MWt. There is no specific information on the characteristics of the thermal spring activity or on its geologic setting. Resort will thus be made to regional and generalized considerations for justifying the view that Mwalo may be the site of key hydrothermal activity.

The three major rivers: from north to south Ulindi, Elila and Luama drain the region of the thermally uplifted block of Ubendian metamorphic rocks, the highest standing range of the Mitumba Mountains. This region has a concentration of higher temperature springs and may be considered to be a regionally anomalous zone of hearting. Together, the three river basins account for the occurrence of a reported total of 54 thermal springs. The Locations of only three of these, Kitutu, Kilenga and Mwalo, are known and they are all located in the upper reaches of the river basins. The distribution of earthquake epicenters indicates that many of the structures which control the river valleys are active. These structures have potential for hosting thermal water flow and, under hydrologic influence, may give rise to widespread thermal spring occurrences, by a westward flushing of the high subsurface heat flux taking place in the east.

The regional drainage pattern in Eastern D.R.C. shows that the high topographic gradient descending toward R. Lualaba imposes a steep subsurface hydrologic gradient in that direction. The prevalence of high subsurface temperatures under the high standing block inferred from its geotectonic setting, suggests that the main heating areas of the hydrothermal features lie toward the east. It can be inferred from the above that the easternmost thermal; springs would be closer to their areas of heating and would be the hottest. Those lying toward the west may be expected, at least mostly, to emerge at the surface from subsurface hot water outflow structures from the east. The upper reaches of some of the river basins are situated in sediment filled basins in faulted Proterozoic basement and the easternmost thermal springs may issue from the sedimentary rocks. Any high temperature thermal springs which may be thus situated would have potential for high flow from aquifers which may sometimes be permeable and have large lateral extensions. Many of the thermal springs may share similar characteristics and it would thus be useful to carry out a survey of this group of thermal springs which appear to constitute a distinct generic type.

In the above generalized scheme, thermal spring activity at Mwalo offers one of the most promising starting points for the study of the geothermal resources associated with the river basins which traverse sedimentary rocks in their upper reaches. The reported large natural heat output at Mwalo indicates the prevalence of high permeability in the zone of hot water ascent to the surface and the existence of a voluminous source region in the subsurface. Its occurrence in an area of sedimentary infill in a reactivated half graben structure makes it attractive in that there is a possibility for the existence of a high temperature hot water reservoir system within the sedimentary sequences. There is also the possibility of such a reservoir system being replenished with hot

water as active faulting would keep channels of fluid ascent open and facilitate the rise of deep circulating geothermal waters to these levels.

High Temperature Thermal Springs of the Proterozoic Metamorphic Terrains

Cap Banza and Pemba brine springs

RIGFC (1982) quote a temperature of 96OC, pH 6.5 and SiO_2 concentration of about 210ppm for Cap Banza thermal spring (#68). It issues 1 l/s of NaCl type water along faults which define a narrow horst which is disposed in the N-S direction and projects into the northern part of L. Tanganyika from the D.R.C. side. Tiercelain et al (1993) report the occurrence of sub-lacustrine hydrothermal chimneys topped by vents at Cap Banza where aragonite and pyrite deposition is taking place. At Pemba (#67), located to the north of Cap Banza, Springs issue $NaHCO_3$ type water which deposits iron sulfide minerals. Temperatures of up to 103°C were measured. Chemical geothermometers yield temperatures at depth of 179 and 219°C respectively for Cap Banza and Pemba. Isotope data from the CO_2 released at the two sites show the gas to be of juvenile origin. The hydrothermal fluids emerge where TRM and Ruzizi trend faults cross. Hydrothermal fluids characteristically emerge above or at the levels of cold water bodies due to the low densities induced in them by thermal expansion and their usually dilute chemical contents. The Banza and Pemba brines issue below lake level because of their high density which is due to their high dissolved mineral content. These brines are typical of to ore transporting and depositing primary magmatic fluids. They are the precursors of near surface geothermal fluids, which result from the mixing of these parent fluids with much larger volumes of meteoric waters in the sub-surface. Thermodynamic evolutionary processes modify their original chemical and physical characteristics during their circulation and mixing in the subsurface.

The deposition of metal sulfides and carbonates at these features is analogous to mineral sulfide deposition from deep geothermal well discharges at Gale le Koma in the Asal Rift in Djibouti. Asal rift is the most advanced stage of EARS development. Mantle melt is estimated to undergo crystallization at about 4-5kms depth. The mineral content of the brine there is attributed to the exsolution of the volatile magma components (mainly water) together with metals which do not readily go into silicate mineral formation during magma crystallization. The segregated fluids leak upwards along fractures. Drill holes reduce the confining lithostatic pressures on the fluid and allow it to expand and rise. Mineral deposition occurs when brine density is reduced by boiling upon pressure release on brine entry into the geothermal well or upon its venting at the surface, in analogy to the natural processes of ore transport and deposition from primary magmatic fluids. The Banza and Pemba brines occur under favorable natural tectonic conditions. Deep reaching faulting allowed the buoyant rise to the surface of the primary magmatic fluids in a region of thick crust. Asal rift and the northern L. Tanganyika rift zone are the only two known zones of the EARS where primary brines reach the surface. The differences in the type of minerals that are deposited at Banza, Pemba and Asal are attributable to their initial chemical compositions as well as to the different brines having differently evolved during their rise from depth, including their internal chemical thermodynamic evolutions and, in the case of the former two features, their interactions with wall rocks and thermophylic microbial action.

The significance of the Banza and Pemba brines with respect to geothermal resource development does not lie in themselves or in the structures along which they rise to the surface. Their mode and places of occurrence make resource exploitation by drilling logistically impractical. Similarly to the situation in the Asal rift, the primitive chemistries of the brines are likely to render them challenging for direct utilization in economic power generation. Such fluids are economically exploitable for power generation where they are found lower down along their evolutionary paths. They are thus potentially important for their potential for spawning exploitable derivative geothermal resources and for the information which they may provide regarding the geothermal conditions in the larger area of Northern L. Tanganyika. The brines rise along Ruzizi and TRM structures. The importance of these structures as possible conduits for the primary brines into the adjacent areas may be important if, by mixing with meteoric waters in the subsurface, the brines generate derivative high temperature geothermal fluids suited to economic exploitation. It may be queried whether the numerous thermal springs which discharge to the west of Northern L. Tanganyika may have genetic relations with such deeply sourced primary fluids.

Kiabukwa

Kiabukwa (#70) has the distinction of having been the site of the earliest geothermal power plant in Africa but which has stopped operating at some unknown time in the past. It is reported to have had a generation capacity of 200kW. Although no other information is available on the resource, the fact that it had been developed in the past renders it significant.

Thermal Springs of the Archean Terrain: Mutsora and Others

As pointed out in 3.4.4 above, the 14 reported thermal springs which occur in this part of Eastern D.R.C. respectively share some of the hydrothermal fluid characteristics of Kibiro, in the case of the northern group, and the tectonic and hydrologic settings of Buranga, in the case of the southern group. These situations present opportunities for the exchange of experiences which can benefit the study of Mutsora and the region's other thermal springs.

CONCLUSIONS AND RECOMENDATIONS

The findings of the study encourage the conclusion that a number of thermal spring areas in Eastern D.R.C. warrant further study. It is recommended that the full complement of basic data on the hydrothermal activities which is essential for gaining greater certainty of the prospectivity of these areas should be collected. An order of priorities is also proposed among these areas based on need for geothermal power development and the likelihood of success in satisfying that need.

Candidate Prospects of High Priority

The priority areas are Mayi ya Moto, Kankule-Mahyuza and Mwalo and are the candidate targets which at this stage seem to offer better prospects for the discovery of exploitable geothermal reservoirs and also are important from the point of view of need for geothermal power generation, if possible.

Situations allowing, it is recommended that preliminary field and laboratory works be carried out consisting of geologic observations in the field and recording of conditions of thermal spring activity and their sampling for chemical analyses. In addition to these generic geoscientific due diligence surveys which apply to all three areas, it is recommended that studies be made in each area to clarify issues that are specific to it as follows:

Mayi ya Moto

A volcanic petrogenetic study should be carried out to determine if significant and sustained magma differentiation takes place at shallow crustal depth from which may be concluded that a geothermal resource which is associated with a shallow magma body heat source may exist. This will involve the sampling of young lava flow and pyroclastic units for major and trace element analyses.

The Mwalo-Bukavu-Kalemi Region

Two approaches are proposed for this region: a) specifically addressing the two high temperature thermal spring areas and, b) combining this with a preliminary evaluation of the regional context in which they occur.

Mwalo

Mwalo is a potentially attractive prospect, possibly together with other thermal springs which occur in Luama graben, not only because of its favorable attributes, but also because its position in the regional tectonic framework renders it important. An evaluation of the sedimentary stratigraphy which may influence the occurrence and character of the thermal water, estimation of sediment thickness, and determination of the character of contact areas with the metamorphic rocks would be of specific interest at Mwalo.

Kankule-Mahsyuza

Research on the volcanism of Bukavu area has provided good quality data which should be viewed in detail for the geothermal implications. Similar work should be carried out for the volcanic field in Mwenga area, especially in light of the integrated regional approach proposed below. Structural continuity between L. Kivu and the middle basins of Elila and Luama rivers justifies the adoption of an overall view of a unified geothermal system.

Regional Survey

The regional approach is based on the perception expressed in the last paragraph of 3.3.2 and encompasses the region described in 2.2 above. If that perception can be shown to be viable, a regional focal geothermal regime centered on the uplifted Ubendian terrain may give rise to the thermal springs which occur in the Ruzizi, Elila and Luama river basins and to those found along the western coast of L. Tanganyika's northern basin. This approach, while giving individual emphasis to the study of Mwalo and Kankule areas, would also involve the sampling of all of the thermal springs for chemical analyses and the cursory assessment of their geologic and hydrologic settings. This will contribute to the better understanding of the hydrothermal features of focal interest by viewing them in theirs regional context, at the same time that it clarifies the regional geothermal regime.

The Lower Priority High Temperature Thermal Spring Areas

Mutsora

The thermal springs of the region of Archean basement in North Kivu share a number of characteristics and geologic associations with those of the Buranga and Kibiro thermal springs in Uganda. The active effort to progress exploration work in these Ugandan prospect areas may produce results which work in North Kivu can learn from. It is believed to be useful to delay the investigation of the region of Mutsora area until that time, also with a view to deploying effort more gainfully in the high priority areas.

Kiabukwa

For reasons given under 4.3.3 above, Kiabukwa may be considered technically attractive. However, because its region is one of the most industrially developed in D.R.C., it is expected that hydro-electric power generation is well developed and there may not be a justification for granting priority to developing geothermal resources in the region in the short term.

ACKNOWLEDGEMENT

This study was initiated following brief exchanges with government officials and geoscientists from D.R.C. They are thanked for inspiring this interest in the country's rich geological heritage and its thermal springs.

REFERENCES

Abeinomugisha, D. and Mugisha, F., 2004, Structural analysis of the Albertine graben, western Uganda, extended abstract: International conference on the East African Rift System, Addis Abeba, Ethiopia, pp 4-6

Alleman, L. Y.; André, L. and Plisnier, P.-D., 2003, abstract #4102: Geochemical imprint on deep Tanganyika Lake water from hydrothermalism, groundwater or riverine sources, EGS-AGU-EUG Joint Assembly meeting, Nice, France, 6 - 11 April 2003.

Armannsson, H., 1994, Geochemical studies on three geothermal areas in west and southwest Uganda, final report.

Barifaijo, E., 2001, The petrology of the volcanic rocks of Uganda, GSU newsletter 1(1) 42-9

CGMW, 2009, The changing faces of Africa: Elements of African geology.

Delvaux, D. and Kervyn, F., 2004, Active tectonics of the Tanganyika–Rukwa–Malawi rift in Western Tanzania: a review, extended abstract, International conference on the East African Rift System, Addis Abeba, Ethiopia, pp 53-54

Edmiston, R.C. and Benoit, W.R.; 1984, Characteristics of Basin and Range geothermal systems with fluid temperatures of 150OC to 200OC; Geothermal Resources Council Transactions, Vol. 8, p. 417-424

Fairhead, J.D. and Reeves, C.V, 1977, Teleseismic delay times, Bouguer anomalies and inferred thickness of the African lithosphere, Earth and Planetary Science Letters, 36, 63-76

Fairhead, J.D., 1979, The gravity link between the domaly uplifted Cainozoic volcanic centers of North Africa and its similarity to the East African Rift System anomaly, Earth and Planetary Science Letters 42, 109-13.

Furman, T. and Graham, D., 1999, Erosion of the lithospheric mantle beneath the East African Rift system: geochemical evidence from the Kivu volcanic province, Lithos 48, 237-263

Getahun Demissie, 2010, Mantle Influence, rifting and magmatism in the East African Rift System (EARS): A regional view of the controls on hydrothermal activity, Proceedings, World Geothermal Congress, Bali, Indonesia, 25-29 April 2010

Hochstein, M. P., 2000, Geothermal resources of the western branch of the East African Rift System, IGA NEWS #42, pp. 10-12.

Hochstein, M. P., 2005, Heat transfer by hydrothermal systems in the East African rifts, Proceedings of the World Geothermal Congress, Antalya, Turkey.

IASPEI-IHFC, Heat flow database, accessed 14/12/2009

Lavreau, J. and Buyagu, S., 1989, Geochemical evidence for a non-alkalic origin for the carbonatic bodies of Kibuye, Rwanda, Journal of African Earth Sciences, 9 (2) 335-40.

Lysak S. V. and Sherman S. I., 2002, Terrestrial heat flow in areas of dynamic influence of faults in the Baikal rift zone, European Geosciences Union Stephan Mueller Special Publication Series 2, pp153–60

Morley, C.K., 1999, Tectonic evolution of the East African Rift System and the modifying influence of magmatism: a review, Acta Vulcanologica Vol. 11 (1) pp 1-19

Nyblade, A. A.; Pollack, H. N.; Jones, D. L.; Podmore, F. and Mushayandebvu, M., 1990, Terrestrial heat flow in east and southern Africa, Journal of Geophysical Research, Vol. 95, Issue B11, pp. 17371-84.

Nyblade, A.A.; Owens, T.J.; Gurrola, H., Ritsema, J. and Langston, C.A., 2000, Seismic evidence for a deep upper mantle thermal anomaly beneath East Africa, Geology, 28 (7) 599-602.

Rancon, J.–Ph. et Demange, J., 1983, Reconnaissance geothermique de la Republique du Rwanda, Rapport Geovolcanologique, BRGM, France.

RIGFC (Research Institute of the Geology of Foreign Countries, Moscow, Russia), transl. 1982, Hydrogeology of Africa, Nedra Publishers, Moscow 1978,

Rogers, N. W., James, D., Kelley, S. P. and De Mulder, M., 1998, The generation of potassic lavas from the eastern Virunga province, Rwanda, Journal of Petrology, 39 (6) 1223-47.

Sebagenzi, M. N.; Atekwana, E. et Lucazeau, F., 2004, Congo et fonctionnement de la cuvette centrale Congolaise, résumé, 20e colloque de géologie Africaine, Orléans, France.

Simiyu, S. M. & Keller G. R., 1997, An integrated analysis of lithospheric structure across the East African plateau based on gravity anomalies and recent seismic studies, Tectonophysics Vol. 278, Issues 1-4, 291-313.

Tassi, F., O. Vaselli, D. Tedesco, G. Montegrossi, T. Darrah, E. Cuoco, M. Y. Mapendano, R. Poreda, and A. Delgado Huertas, 2009, Water and gas chemistry at Lake Kivu (D.R.C.): Geochemical evidence of vertical and horizontal heterogeneities in a multibasin structure, Geochemistry, Geophysics, Geosystems. 10, Q02005, doi:10.1029/2008GC002191

Tiercelin, J-J; Pflumio, C.; Castrec, M.; Boulégue, J.; Gente, P.; Rolet, J.; Coussement, C.; Stetter, K. O.; Huber, R.; Buku, S.; and Mifundu, W., 1993, Hydrothermal vents in Lake Tanganyika, East African Rift system, Geology; 21 (6) 499-502.

Tietze, K., Geyh, M., Müller, H., Schröder, L, Stahl, W. and Wehner, H., 1980, The genesis of the methane in L. Kivu, International Journal of Earth Sciences, Vol. 69, No. 2.

UNESCO-CGMW, 1985, International Geologic Map of Africa, 1 :5,000,000 scale.

USGS-NEIC, Earthquake database, accessed 17/12/2009

Vikandy, M.S., Mahinda, K., Mapendano, Y. and Mifundu, W., 2008, Geothermal potential of eastern D.R. of Congo, ARGeo C-2 geothermal conference, Entebbe, Uganda.

Waring, G.A., 1965, Thermal springs of the United States and other countries of the world: USGs professional paper 492, United States Government Printing Office, Washington DC.

Appendix. The known thermal springs of D.R.C.

No.	Feature Name	Temp. OC	Reported Location, District l Province		Coordinates*		Observations; chemical features
					Long.	Lat.	
1	Kaswa	"Hot"	1. Vicinity of L. Albert				Deposits of sulfur
2	Mount Laba	"Hot"					Sulfurous
3	Goda						Water and petroleum
4	Pandju						Saline
5	Zumbia (Kwanjwa?)		2. Similiki River valley				
6	Molinglingo						Sulfurous
7	Katuka						
8	Vyatungo						
9	Mutwanga				29.750	0.351	
10	Bitagoha		3. Rutshuru	N. Kivu			
10a	*Un-named: 14 springs*		*4. Lowa River basin*				
11	Tingi/ Sake/ Kihira	30	5. L. Kivu volcanic area		29.041	-1.571	
12	Katana (Kakondo)				28.833	-2.225	Travertine deposit
13	Luiro						
13a	*Un-named: 1 spring*	*60*	*-do- Nr Kabusi volcano*				*Free CO_2, large travertine deposit*
14	Nyaluindja		6. Ulindi River basin				Sulfurous
15	Lualatshi						
16	Lubuka						
16a	*Un-named: 8 springs*						
17	Luwangi		7. Ruzizi River valley				
18	Luvungi				29.027	-2.871	
19	Mokindwa						
20	Minyove						
21	Mount Kasongo		8. Elila River basin		28.430	-3.543	
22	Pene Kabonde						
23	Tchavula						
24	Kitutu				28.100	-3.280	
24a	Un-named: 19 springs						

Appendix. The known thermal springs of D.R.C. (Continued)

No.	Feature Name	Temp. OC	Reported Location, District l Province		Coordinates*		Reported chemical features
					Long.	Lat.	
25	Kibimbi		9. Lualaba River basin, near Kibombo. Piani Mimba issues from schist		25.93?	-3.93?	
26	Lufubu				25.93?	-3.93?	Saline
27	Piani Mimba (Pene Sibo)						TDS: 33,360 ppm 55%NaCl, 11% $CaCl_2$, 5%$CaSO_4$
28	Basikabusi		10. Luama River basin				Sulfurous
29	Basimakule						
29a	*Un-named: 15 springs*						
30	Muesse		11. Luika River basin				
31	Kilenga				28.031	-3.908	
32	Mutambula	50	12. NW L. Tanganyika				Sulfurous
33	Uvira	44	Uvira	S Kivu	29.129	-3.406	
34	Pakundi		13. Lukuga River basin				
35	Tshapona		14 R. Lomami/ Luembe		24.317	-7.183	
36	Kisabi		15. Luvua River basin		29.181	-8.044	Saline
37	Luona						
38	Mbalai						
39	Sanga						
40	Luiboso						
41	Rutuku		16. South L. Tanganyika		29.314	-6.219	Saline
42	Kayungwa						
43	Kakonta						
44	Kianza (Near Tampa)				29.905	-8.055	
45	N'Ganza						
46	Kafungwe		17. L. Upemba area				Sulfurous
47	Katapena						
48	Konkula						
48a	*Un-name:10 springs*						

Appendix. The known thermal springs of D.R.C. (Continued)

No.	Feature Name	Temp. OC	Reported Location, District l Province		Coordinates*		Reported chemical features
					Long.	Lat.	
49	Moashia		18. Lufira River basin				
50	Tanda Mukola						
51	Kashiba						
52	Basumba						
52.a	*Un-named: Several sprs*	*c 60*	*Manjakito fault*				*Much free CO_2*
53	Nyangezi (Nya Ghezi)	40	#2. Walungu	S Kivu	28.871	-2.650	
54	Mahyuza	66	#3-5, 12 Kabare		28.841	-2.244	
55	Kankule 1 & 2	72			28.836	-2.249	
56	Maziba	40			28.8	-2.1	
57	Muganzo						
58	Mayi ya Moto	95	#6. Rutshuru	N. Kivu	29.350	-0.900	pH: 8.0-8.9, Na (HCO_3-Cl-SO_4) type water; T_{depth}=163-177°C
59	Kambo	40	#7. Kasindi		29.670	0.063	
60	Masambo	43	#8, 9. Beni		29.696	0.181	
61	Mutsora	57			29.742	0.306	
62	Mbau		#10, 11, Beni?		29.140	0.390	
63	Kikingi				29.570	0.540	
64	Kisuma	39	#15. Masisi		28.880	-1.600	
65	Nyabugezi		?				
66	Kalieri		Katale ?	?			
67	Pemba	103	NW. L. Tanganyika		29.092	-3.95	$NaHCO_3$ type water; massive sulfide deposit; T_{depth}=219°C
68	Cap Banza (Manza)	96			29.27	-3.97	NaCl type water; aragonite deposition; T_{depth}=179 °C
69	Mwalo	> 75	Upper Luama River basin		28.185	-4.248	
70	Kiabukwa	> 75	South of L. Moero		28. 266	-9.917	Site of a 200kW geothermal power plant during the 1950s

*Note: Some coordinates are approximate, except for those quoted from Mambo Vikandy et al (2008). Others may be those of nearby places with the same names as those of the thermal springs. There may also be more than one place in D.R.C. with the same name, e.g. Kasongo

Sources: # 1-52a: Waring (1965); 11, 33, 53-66: Mambo Vikandy S. et al (2008); 58, 67-70: Hochstein (2000); 69: RIGFC (1982); 67 & 68: Tiercelin et al (1993).

HOW GEOTHERMAL EXPLORATION LED TO GOLD EXPLORATION: A CASE HISTORY - THE AFAR DEPRESSION

David J. Hall
Executive Chairman
Stratex International plc.

Keywords: epithermal, bonanza, geothermal exploration, Afar depression, Megenta.

INTRODUCTION

The term epithermal derives from the genetic classification scheme for hydrothermal ore deposits proposed by Lindgren (1933). On the basis of stratigraphic relationships in volcanic sequences, and by analogy with mineral and metal occurrences and mineral textures in active hydrothermal systems, Lindgren inferred that epithermal deposits formed at <200°C and <100 atmospheres (~100 bars).

In New Zealand, Japan, Philippines, United States, and other countries, the demand for alternative sources of electricity encouraged geothermal exploration drilling and development from the 1980's. Temperatures and pressures similar to those in the epithermal environment were encountered at depths of less than 1 km (e.g., White, 1981; Henley and Ellis, 1983), and precious and base metals were found deposited in springs, wells, and surface pipes (e.g., Weissberg, 1969, Hedenquist and Henley, 1985a; Brown, 1986; Krupp and Seward, 1987). The rapid increase in understanding at the time was such that the first two volumes of *Reviews in Economic Geology* focused on the nature of epithermal environments (Henley et al., 1984; Berger and Bethke, 1985). Thus, by the mid 1980s, genetic models were formulated to explain the occurrence and zonation of metals and minerals, to define the physical-chemical conditions of ore deposition in several epithermal deposits, and to provide a basis for speculation on the sources of fluids and metals (e.g., Barton et al., 1977; Kamilli and Ohmoto, 1977; Sawkins et al., 1979; Buchanan, 1981; Berger and Eimon, 1983; Henley and Ellis, 1983; Hayba et al., 1985; Heald et al., 1987; Stoffregen, 1987). In these models, hydrology was seen to be an essential factor in producing ore deposits, with boiling and fluid mixing being recognized as causative agents for metal deposition.

It was early recognised (e.g., Lindgren, 1933; White, 1955) that clear parallels exist between the near surface (~500 m) depositional environment of these deposits and that of modern hot spring systems and these were emphasized by the results of exploration activity through the Western U.S.A. (e.g., McLaughlin deposit, California).

BONANZA GOLD, BI-MODAL VOLCANISM & RIFTING

In a comprehensive analysis of the tectonomagmatic controls and styles of epithermal gold mineralization in the northern Great Basin of the western United States John (2001) distinguishes two contrasting environments: first, high sulphidation and base metal bearing low sulphidation hosted by calc-alkaline andesitic and dacitic volcanic rocks as part of a conventional arc assemblage: second, base metal deficient low sulphidation deposits associated with a bi-modal basalt-rhyolite suite generated during rifting.

Bimodal volcanic suites and low sulphidation gold deposits characterise several extensional arcs: the Palaeocene are in the central Andes of northern Chile hosts the rhyolite dome related El Penon veins; the middle to late Jurassic arc in Patagonia of southern Argentina hosts Cerro Vanguardia vein systems. Most of the low sulphidation gold deposits (Ivanhoe, Sleeper, Mule Canyon, Midas) in the northern Great Basin of the western United States were generated over a 2 m.y. interval of the Miocene within and near the northern Nevada rift, a product of back-arc extension related by some investigators to the Yellowstone mantle plume (John, 2001).

Bonanza epithermal veins are defined informally by Sillitoe (2002) as those containing roughly 1 million metric tonnes or more averaging at least ~1 oz/t Au (i.e. ~ 30 metric tonnes gold) occur sparingly in the epithermal environment. However, somewhat surprisingly nearly 60 per cent of them occur in rifts with bimodal volcanism. This conclusion lead to Stratex reviewing such rift environments and areas of hot spring activity.

THE AFAR DEPRSSION

The Afar Depression lies within the Afro-Arabian Rift System. This rift system extends from Syria in the north and passes through Jordan valley, Dead Sea, Red Sea, Afar Depression and the East African Rift and terminates in southern Africa. The Main Ethiopian Rift, the southern Red Sea and the western Gulf of Aden lie within the Afar Depression forming a rift-rift-rift triple junction between the Nubian, Somalian and Arabian Plates.

The triangular shaped Afar Depression covers an area ~ 200,000 square kilometres and is bounded by marginal escarpments which close at narrow axial rift zones and ranges. It is flanked by the Ethiopian Plateau in the west and the Somalian Plateau to the SE. The Ali-Sabieh and Danakil Blocks bound the eastern and northeastern sides of the Afar Depression, respectively. Further south, the NE segment of the Main Ethiopian Rift separates the Ethiopian and the Somalian Plateaux. The Ethiopian Escarpment extends north into Eritrea and closes the AD against the Danakil Block at the Gulf of Zula, which is a re-entrant from the Red Sea. The Gulf of Tajura extends westwards from the Gulf of Aden and separates the Ali-Sabieh Block from the Danakil Block.

The central part of the Afar Depression is dominated by lowland plains corrugated by horsts and grabens and rare local high relief peaks representing shield volcanoes. It can be divided into northern, east-central, south-western and south-eastern regions on the basis of similar structural trends.

The east-central Afar is bounded by the Danakil Block in the east and the Tendaho-Gobaad Discontinuity in the west and south-west. It is dominated by north-west trending grabens and horsts between the south-east propagating Manda-Hararo-Gobaad and the north-west propagating Asal-Manda Inakir rifts.

The southwestern Afar is a continuation of the northern part of the Main Ethiopian Rift that is interrupted by the Tendaho-Gobaad Discontinuity. It is dominated by north to north-east trending structures manifesting a series of right laterally offset grabens and horsts (Beyene & Abdelsalam, 2005).

The volcanism is strongly bi-modal.

Petrological indications suggest that silicic rocks may have been generated by fractional crystallization of transitional basaltic magmas in shallow level magma chambers with some degree of crustal assimilation. The chemistry of the 28 to 2.5 Ma old silicic rocks indicate a possible increase in crustal involvement with time, suggestive of a progressive thermal and mechanical weakening of the crust in response to thinning and magmatic modification of the lithosphere as imaged by geophysical data (Corti, 2009).

At shallow levels, magmas can fractionate in predominantly small magma bodies (dikes) and some larger magma chambers (e.g. nested calderas), where zoned reservoirs are produced with a peralkaline silicic upper layer and basalts at the bottom. In this system, eruption preferentially taps the silicic layer giving rise to the abundant silicic activity, whereas mafic melts reach the surface when fractures intersect the lower layer of the shallow chamber or reach some deep underplated basalt reservoir.

A temporal evolution from silicic volcanism from the shallow magma chambers to basaltic activity within the Wonji segments has also been suggested. In this model, the successive cooling, faulting and fracturing of the silicic centres may allow the upraising and eruption of basaltic lava flows which may have led to an increase in basaltic activity in the last 0.65 Ma. This temporal trend mimics the northward increase in basaltic volcanism toward Southern Afar. In Afar, during the last 4 Myr magmatism has been bimodal, but with predominance of basaltic rocks over silicic products. Volcanism indeed mainly consisted in the eruption of a thick stratiform sequence of fissure fed basaltic to hawaiite lava flows – Stratoid Series. Silicic (trachy-rhyolites to pantellerites) central volcanoes locally grew o the upper part of the Stratoid Series. Further to the north, in Central and Northern Afar, the zone of Quaternary extension and magmatism is marked by clusters of voluminous fissure basalts and basaltic shield volcanoes of a transitional alkali/tholeitic composition. These axial basalt ranges are interpreted to be sub-aerial equivalents of oceanic spreading centres.

GEOTHERMAL EXPLORATION

Geothermal exploration has been undertaken in the Tendaho graben of Ethiopia (Gianelli et al, 1998) and in Republic of Djibouti (Zan et al, 1990).

Hydrothermal activity, both active and extinct, was reported by Gianelli et al (1998) in Tendaho. They reported that the extinct hydrothermal activity is indicated by silica deposition within NW to NNW sub-vertical fractures crosscutting the rift sediments. The veins are made up largely of microcrystalline quartz with minor calcite, stibnite and smectite. Ur-Th absolute dating was performed on a quartz–calcite vein and yielded an age of 12.5 ka (Abbate et al, 1995). Active surface manifestations are represented by steaming grounds at Ayrobera, mud pots and fumaroles at Dubti, as well as silica sinter and hot springs at Alalobeda near or at boiling point.

No extinct hydrothermal activity was reported by the geothermal work in Djibouti however, epithermal potential had been recognised by the USGS in 1991.

Epithermal mineral occurrences have been observed at three localities, (Corbetti, Gademsa and Aluto-CanCan). Associated features were reported on the surface and at depth in drill core. These include alteration patterns that display characteristic low sulphidation type epithermal occurrences. The low sulphidation alteration commonly displays a broad propylitised (chlorite, epidote, quartz) area that envelopes a core of pervasive potassic alteration, together extending to as much as several kilometers. Locally, intermediate argillic alteration

assemblages commonly overprint the potassic alteration. The alteration zone also displays broad propylitic zones, overprinted by advanced argillic alteration (kaolinite). Mineral phases include chlorite, kaolin, calcite, quartz and epidot, adularia, iron oxides, smectite and albite (Tadesse, 2001).

GOLD IN THE AFAR

Bonanza gold deposits make attractive targets because of their potential to yield high rates of return. The need for the discovery of high quality, high margin gold deposits (meaning higher grade) is essential to sustain a competitive industry position (Keith et al, 2010).

Stratex initiated a programme in January 2008 to prove the concept of gold potential of the African Rift valley. In March 2009 work commenced in the Lakes District of the Main Ethiopian Rift based on data from geothermal reports and that of Tadesse (2001). In October 2009 Stratex visited the Tendaho graben to investigate in and around known hot springs reported in Gianelli et al (1998). This resulted in the definition of the Megenta hot spring gold occurrence.

The Megenta prospect is the located at the triple junction where the north- and northeast-striking faults of the Main Ethiopian rift intersect the northwest-striking master fault that delimits the southern side of the Manda-Hararo-Gobaad rift, the position of the Tendaho-Gobaad discontinuity. The northwest-striking fault juxtaposes post-4-Ma basalt flows with a thick sequence of flat-lying, red-coloured, siliciclastic sedimentary rocks, which comprise claystone, siltstone, sandstone, grit and conglomerate. Some 2.5 km northwest of Megenta, a flow-foliated rhyolite plug is located along the rift-bounding fault, which may also have displaced it (Fig. 1).

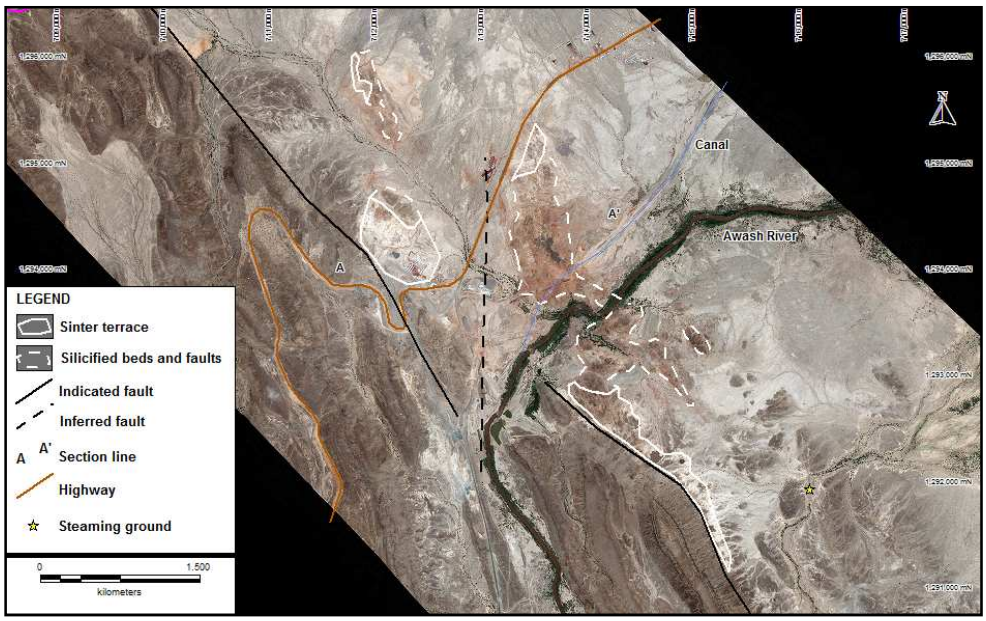

Fig. 1: Quickbird scene showing main geological features of the Megenta prospect

The rift-bounding structure and related subparallel faults immediately to the north localised an extensive hydrothermal system, which is roughly centred on their inferred intersection with one of the main north-striking faults (Fig. 1). The system, at least 6 km in a northwest-southeast direction and covering an area of >6 km^2 prior to dissection, is now extinct, although a small zone of steaming ground remains near its southern limit (Fig. 1). The Megenta system may have been active at ~4 Ka, the youngest accepted age for the host red-bed sedimentary sequence in the area.

The Alalobeda hot spring area, ~5 km southeast of the Megenta system, is localised by the same rift-bounding fault, and is highly active; it includes a geyser, fumarole, boiling mud pot and several thermal pools, all surrounded by an opaline sinter apron (Sillitoe, 2010).

The fossil Megenta hydrothermal system in outcrop comprises two closely related hydrothermal features: remnants of an extensive sinter terrace and immediately underlying silicification, the latter affecting both steeply dipping faults and subhorizontal sedimentary horizons, particularly coarse sandstone and grit beds (Figs. 1 and 2). In several places, the silicified faults, including tabular tectonic breccias, are observed to terminate at the base of the sinter terrace (Figs. 2). Elsewhere, silicified beds immediately underlie the sinter terrace.

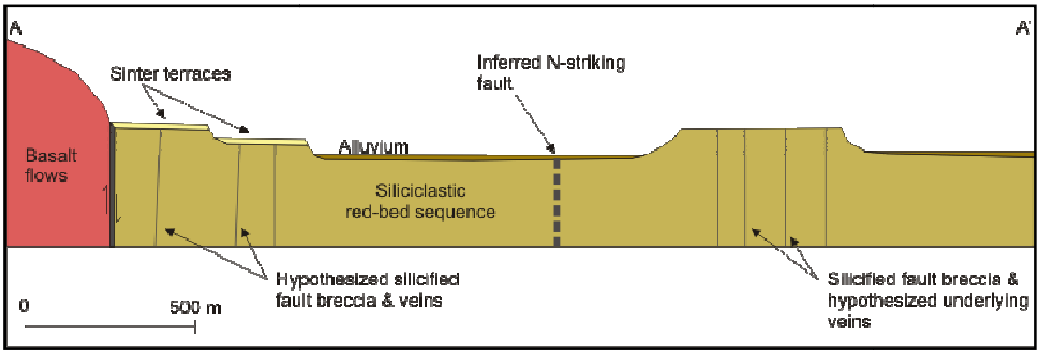

Fig. 2: Sketch section across the Megenta prospect (A–A' in Fig. 2)

The sinter terrace comprises two distinct components: typical banded opaline sinter containing a few reed stem moulds, and porous aggregates of reed stems transformed to opal. In the main Megenta area, where at least two sinter terrace levels may be distinguished in places (Fig. 2), the lower one is made up of the banded sinter and the upper one of the opalised plant matter. Although areally extensive, the sinter horizons generally do not exceed 2 m in thickness. Locally, the bacterial structure of the sinter is prominent and, in the northwesternmost sinter outcrop (Fig. 1), stromatolitic structures are evident. There, as well as locally elsewhere, paleo-water-table depression caused development of steam-heated alteration (probably mainly cristobalite) immediately beneath the sinter.

One or more individual siliciclastic beds beneath the sinter were preferentially silicified and comprise massive chalcedony. Similar chalcedonic silicification also affected the faults and their contained tectonic breccias, which range from <1 to >2 m wide. In places, at least four main, subparallel, silicified faults are present (Fig. 2). The chalcedony is everywhere limonitic as a result of supergene weathering of at least 5 volume % of contained pyrite and marcasite, which are locally preserved as disseminated grains within <1 m of the surface because of silica encapsulation.

The tectonic breccias defining parts of the faults comprise tightly packed, angular to subangular clasts of sedimentary rocks, including isolated larger pieces of reoriented sedimentary rock displaying prominent bedding. Very locally, short veins and veinlets of white chalcedony and/or crystalline calcite cut the silicified breccias. Smectite, indicative of relatively low-temperature hydrothermal conditions, is the only other alteration mineral recognised in and around the breccias.

Detailed rock channel sampling has returned highest grades of 16.7 g/t Au with anomalous gold values >0.1 g/t Au encountered over much of the prospect thus confirming the system as gold bearing.

Stratex intends to drill 3000 metres at Megenta in 2011 with view to defining if bonanza veins exist at depth within the controlling structures. In addition Stratex has taken up extensive exploration licences in the Afar of Ethiopia and also in the Republic of Djibouti.

REFERENCES

Abbate, E., Passerini, P., and Zan, L., 1995 Strike slip faults in a rift area: a transect in the Afar Triangle, East Africa: Tectonophysics, v. 241, p. 67-97

Beyene, A., & Abdelsalam, M.G., 2005. Tectonics of the Afar Depression: A review and synthesis: Journal of African Sciences v. 41 p. 41-59

Brown, K.L. 1986, Gold deposition from geothermal discharges in New Zealand: Geothermics: v. 32, p.619-625

Berger, B.R. and Bethke, P.M., Jr. eds. 1985 Geology and geochemistry of epithermal systems: Reviews in Geology 2 298p.

Barton, P.B., Bethke, P.M., Jr., and Roedder, E., 1977 Environment of ore deposition in the Creede Mining District, San Juan Mountains, Colorado: Part III. Progress towards interpretation of the chemistry of the ore-forming fluid for the OH vein: Economic Geology, v. 72, p. 1-24.

Buchanan, L.J., 1981 Precious metal deposits associated with volcanic environments in the south-west: Arizona Geological Society Digest, v. 14, p.237-262.

Berger, B.R. and Eimon, P., 1983 Conceptual models of epithermal precious metal deposits: Cameron volume on unconventional mineral deposits: Society of Mining Engineers of AIME p.195-205.

Corti, G., 2009, Continental Rift evolution: From Rift Initiation to Incipient break-up in the Main Ethiopian Rift, East Africa: Earth-Science Reviews v. 96, p. 1-50

Gianelli, G., Mekuria, N., Bataglia, S., Chersicla, A., Garafalo, P., Ruggieri, G., Manganelli, M., and Gebregziabher, Z., 1998 Water-rock interaction and hydrothermal mineral equilibria in the Tendaho geothermal system: Journal of volcanology and Geothermal Research, v. 86, p.253-276.

Hayba, D.O., Bethke, P.M.Jr., Heald, P., and Foley, N.K., 1985 Geologic, mineralogic and geochemical characteristics of volcanic hosted epithermal precious metal deposits: Reviews in Economic Geology, 2, p. 129-167

Heald, P., Hayba, D.O., and Foley, N.K., 1987 Comparative anatomy of volcanic-hosted epithermal deposits: Acid sulphate and adularia-sericite types: Economic Geology, v. 82, p.1-26

Hedenquist, J.W., and Henley, R.W., 1985a, Hydrothermal eruptions in

the Waiotapu geothermal system, New Zealand: Their origin, associated breccias, and relation to precious metal mineralization: Economic Geology, v. 80, p. 1640–1668.

Hedenquist, J.W. and Henley, R.W., 1985b, The Importance of CO_2 on freezing point measurements of fluid inclusions: Evidence from active systems and implications for epithermal ore depositions: Economic Geology, v. 80, p. 1379 – 1406.

Henley, R.W., and Ellis, A.J., 1983 Geothermal systems, ancient and modern: Earth Science Reviews, v. 19, p. 1-50

Henley, R.W., Truesdell, R.H., and Barton, P.B. Jr., 1984 Fluid mineral equilibria in hydrothermal systems: Reviews in Economic Geology 1, 267p.

John, D.A., 2001 Miocene and early Pliocene epithermal gold-silver deposits of the northern Great Basin, western United States: Characteristics, distribution and relation to magmatism: Economic Geology, v. 96, p. 1827-1853

Kamilli, R.J. and Ohmoto, H., 1977 Paragenesis, zoning, fluid inclusion and isotopic studies of the Finlandia vein, Colqui district, Central Peru: Economic Geology v. 72, p. 950-982

Krupp, R.E., and Seward, T.M., 1987 The Rotokawa geothermal system, New Zealand: An active epithermal gold depositing environment: Economic Geology v. 82, p.1109-1129

Lindgren, W., 1933, Mineral deposits: New York, McGraw-Hill, 4th ed., 930p.

Sawkins, F.J., O'Neil, J.R., and Thompson, J.M., 1979 Fluid inclusion and geochemical studies of vein gold deposits, Baguio district, Philippines: Economic Geology v. 74, p. 1420-1434.

Sillitoe, R.H., 2002, Rifting, Bimodal volcanism and Bonanza Gold veins: SEG Newsletter, January, p. 24-26

Sillitoe, R.H., 2010, Geology and Exploration of the Megenta Epithermal Gold Prospect, Afar Depression, Ethiopia: Internal Report for Stratex International plc.

Stoffregen, R.E., 1987 Genesis of acid sulphate alteration and Au-Cu-Ag at Summitville, Colorado: Economic Geology, v. 82, p. 1575-1591

Tadesse, S., 2001, Epithermal Gold Occurrences in the Lakes District of the Main

Ethiopian Rift and Tendaho Area of the Afar Rift; Discovery of a Metallogenetic Province: Ethiopian Journal of Science, v. 24, p. 69-91.

Weissberg, B.G., 1969, Gold-Silver-Ore grade precipitates from New Zealand thermal waters: Economic Geology, v. 64, p. 95-108

White, D.E., 1955 Thermal springs and epithermal ore deposits: Economic Geology 50th Anniversary Volume p. 392-424

Whire, D.E., 1981 Active geothermal systems and hydrothermal ore deposits: Economic Geology 75th Anniversary Volume, p. 392-424

Zan, L., Gianelli, G., Passerini, P., Troisi, C., and Omar Haga, A., 1990 Geothermal Exploration in the Republic of Djibouti: Thermal and Geological Data of the Hanle and Asal areas: Geothermics, v. 19, p. 561-582.

GEOLOGY OF KIBIRO, KATWE AND BURANGA GEOTHERMAL PROSPECTS OF UGANDA

James Francis Natukunda
Department of Geological Survey and Mines (DGSM), P.O. Box 9, Entebbe, Uganda. jfnatukunda@gmail.com

ABSTRACT

The three main Ugandan geothermal fields namely, Kibiro, Katwe and Buranga are located in East African Rift System (EARS) in its western arm (the Albertine Rift). The general strike of the Albertine Rift is NE-SW. Geophysical surveys indicate 2500 to 3000 m thickness of Pleistocene sediments in the rift floor.

The Kibiro geothermal prospect, which is located at the Eastern escarpment of Albertine Rift is comprised of hot springs that emerge at the base of the escarpment at the intersection of three oblique faults. The escarpment forms a boundary between the old basement rocks (to the east) and the young sedimentary formation of the rift (to the west). The basement consists of Precambrian granites, granitic gneisses, gneisses and N-S striking basic amphibolite intrusives. Mylonitic gneisses characterise the fault-controlled valleys. The NE striking faults in the area are oblique to main rift fault and crosscut E-W striking faults. All rocks are heavily fractured with crosscutting joints. The geothermal manifestations include; hot springs, solfatara, extinct clayey alterations and secondary hydrothermal minerals that include gypsum and calcite filling joints in altered mylonitic gneisses on escarpment among others. The maximum temperature of hot springs is 86.4^{0}C. The Katwe volcanic field is on the SE of Rwenzori massif and consists of 78 randomly distributed craters of which seven have water. The volcanics are deposited on Pleistocene sediments. Precambrian rocks of Toro system lie on the western side while on the eastern side; the sediments are underlain by Karagwe-Ankolean (K-A) metasediments. In the southeastern side of Katwe field, there is Bunyaruguru volcanic field that consists of tuffs mixed with K-A rock fragments. The Katwe volcanics are mainly phreatomagmatic pyloclastic deposits consisting of ash, tuff, lapilli, volcanic bombs and xenoliths of basement rocks. Basaltic lava flows and ejected lava blocks occur around Kyemengo and Kitagata craters. The volcanic material pile rises up to 420 m above surrounding sediments. NE-SW striking faults that characterize the field parallel the strike of the main rift fault. The carbon dating puts the age of volcanism as Pleistocene to Holocene. The Katwe geothermal manifestations include travertine deposits that indicate extinct hot springs, warm springs (30^{0}C) at L. Katwe and hot springs (70^{0}C) at L. Kitagata. The Buranga field is located at the NW end Rwenzori massif near the base of Bwamba escarpment. The hot springs emerge through Pleistocene sediments. Precambrian rocks underlie the sedimentts. The main rift fault strikes 45^0 and dips 60^0-65^0. The three hot spring areas namely Mumbuga, Nyansimbe and Kagoro lie on a line striking 40^0 parallel to main rift fault. Precambrian rocks form the northern half of Rwenzori massif that strike 10^0-30^0 and consists of migmatites and gneisses. The sediments consist of fine to medium-grained, poorly consolidated sands and clays, some of which are coated with calcareous material. The geothermal manifestations of Buranga field include three hot spring areas with a maximum temperature of 98^{0}C, travertine cones and some sulphur deposits at Kagoro spring area. The area is seismically active and frequent earthquakes in the region reactivate and create new manifestations like new hot springs near Nyansimbe pool.

Keywords: rifting, hot springs, fault permeability, geology

REGIONAL GEOLOGY

The geology of Uganda consists of an exposed pre-Cambrian basement dissected by the western branch of the East African Rift System in the western part of the country (Figure 1). The eastern branch, the Gregory Rift, passes through the central part of Kenya. The Western branch, the Albertine Rift, starts to the north along the Sudan border, and then curves to the west and then southwest along the border with the Democratic Republic of Congo, and south to Rwanda, Burundi and western Tanzania. Spreading began at least 15 million years ago in Miocene time. The western Rift is considered to be at an early stage in the development, and is younger (late Miocene-Recent) than the more mature eastern branch (Morley and Westcott, 1999). The Albertine rift is seismically active, characterized by deep-seated (27–40 km) large earthquakes. The region of the Rift has a markedly higher heat flow than the surrounding Pre-Cambrian terrain. Two different en echelon strands are found in the Western Rift Valley, separated by the Rwenzori Mountains, which rise from a base of less than 1,000 m in the Rift to over 5,000 m elevation. Within the Rift Valley there are thick layers of late Tertiary and Quaternary sediments, fresh water and saline crater lakes, volcanic, and plutonic bodies have been identified beneath L. Albert and L. Edward (EDICON, 1984). The three main geothermal areas of Uganda are Kibiro, Katwe, and Buranga.

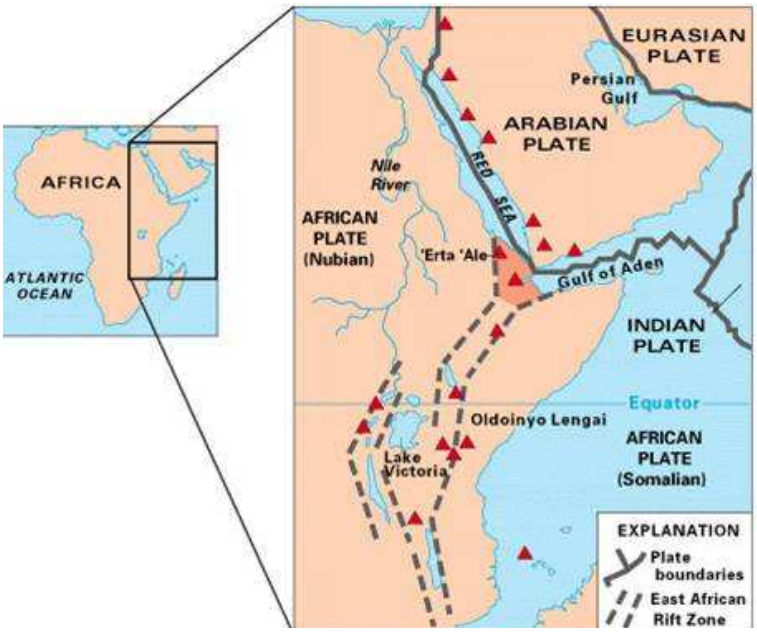

Figure 1: The East African Rift System.

LOCATION OF KIBIRO, KATWE AND BURANGA GEOTHERMAL AREAS

The Kibiro geothermal area is situated in Hoima district (Figure 2), on the eastern shore of Lake Albert. Kibiro is located at the foot of the escarpment of the western branch of the East African Rift System (EARS). The escarpment rises over 300 m above Lake Albert.

The Katwe-Kikorongo (here after only named Katwe) geothermal prospect is one of three geothermal areas, which have been studied by the Ministry of Energy and Mineral Development (MEMD), the other two being Kibiro and Buranga in Hoima and Bundibugyo districts respectively (Figure 2). Katwe is in the Kasese district. It is within the Queen Elizabeth National Park, south of the Rwenzori Massif and north of Lake Edward. Katwe is a volcanic area with many phreatic craters but very little lava at surface. Some of the craters have crater lakes. The most pronounced hot spring is on bottom of the crater lake in the Kitagata crater.

Being in a national park, the Katwe area is mostly uninhabited, except for the Katwe village, south of the saline lake Katwe. Considerable salt mining takes place in Lake Katwe.

THE GEOLOGY KIBIRO GEOTHERMAL FIELD

Introduction

The Kibiro area is located on the eastern escarpment of the western branch of EARS. It covers the small peninsula below the escarpment where the villages of Kachuru and Kibiro are located, the escarpment itself as well as the land extending from the escarpment shoulder towards the east. The area altitude is 620 m above sea level (asl) at the rift floor and Lake Albert to 1,100 m asl on the Rift shoulder. The area consists of deep and steep valleys (fault zones), especially closer to the escarpment. The temperature of the area is in the range of 32 – 38°C.

Description of rock units

The escarpment cuts through the field from SW to NE and divides the study area in two entirely different geological environments. To the east, the geology consists of crystalline basement, characterized by granites and granitic gneisses, where as in the rift there are thick sequences of sediments. The best rock outcrops are found in the escarpment face, but the rock is usually highly transformed by the fault movements. Good outcrops are also found along the numerous fault-lines in the block-faulted rock and on the eastern side, the outcrops are restricted to a few outcrops on hills. These are the hardest rocks, and therefore resistive to weathering. The softer rocks have weathered and formed depressions in the undulating landscape (Gislason et al., 2004).

Granite and gneiss

These Precambrian rocks form the entire basement east of the escarpment. They are fine- to coarse-grained composed of quartz, feldspars, amphiboles (mainly hornblende) and biotite. Their colour ranges from grey to

light brown and in some places pink hue depending on the type of feldspar present. Banding is common and is more pronounced closer to the escarpment, and usually dipping very steeply (60- 90°), and the most common direction of the strike is close to N20°E although E-W direction is also common (Gislason et al., 2004). Close to the escarpment and in association with fault line the granites are mylonitic or brecciated, typical of highly faulted environment.

The stage of weathering or alteration of the granites depends strongly on the structure and location of the rock. The massive, un-banded granites tend to be very fresh, and generally, the rock is less altered with distance from the escarpment.

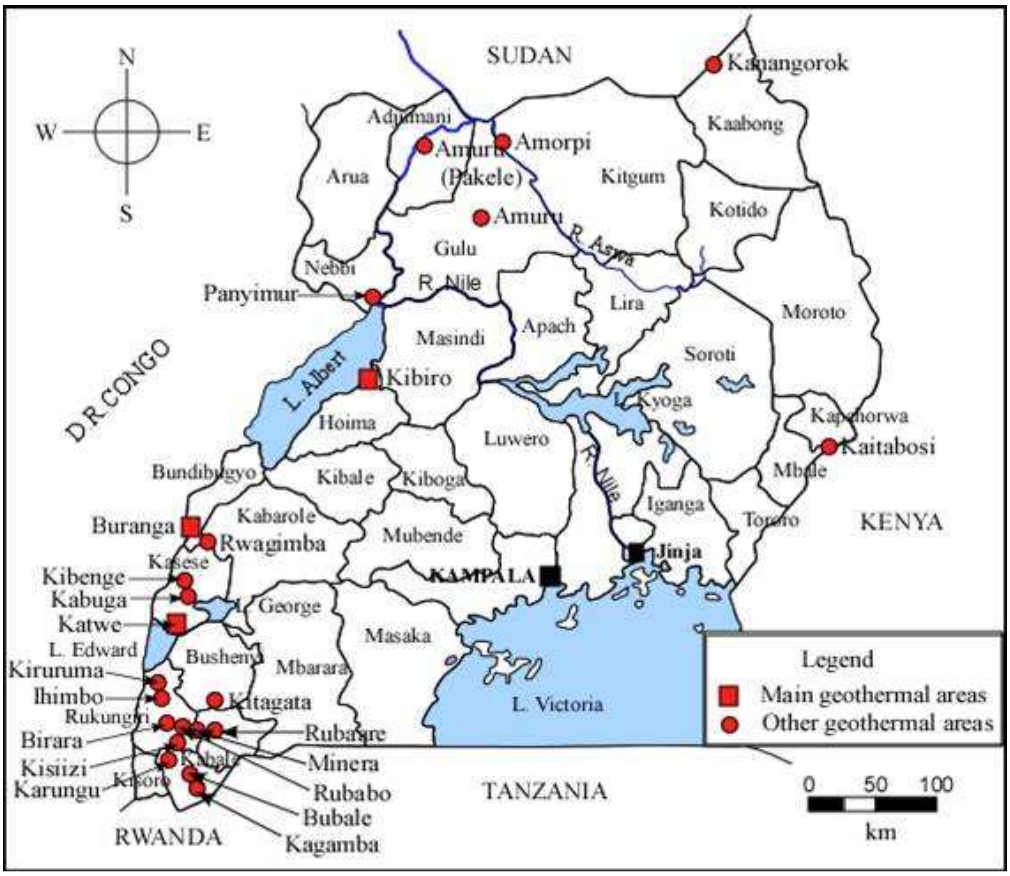

Figure 2: The geothermal areas of Uganda

Amphibolite dykes

Simmons (1921) is first to describe dyke-forming intrusives within the present study area and referred to them as "pyroxenites" as a field term, but later authors (Kakenga et al., 1994) have referred to it as diorites. This formation is black, angular blocks on the surface, forming a small, elongated ridge in the landscape (Figure 3). These outcrops are usually 10 – 20 m wide, but can be as long as a few km most commonly on the slopes and hilltops above Kibiro. Their strike varies from N-S to N20°E. In a hand specimen the rock is fine- to medium-grained, dark grey in colour and usually very fresh looking. No phenocrysts are seen, but joints are common. Microscopic examination of these intrusives in thin section reveals that the rock is composed of quartz, pyroxene (orthopyroxene and clinopyroxene), apatite and relatively large amount of an opaque mineral (Gislason et al., 2004). The dykes appear not to be associated with a heat source for the Kibiro geothermal system since there are no direct surface manifestations related to them (Natukunda, 2007).

Rift sediments

The studies been made on the sediments in the various parts of the EARS using geophysical methods indicate that the sediments are predominantly clastic, commonly fluvial and lacustrine deposits (Morley and Westcott, 1999). Little is known about porosity and permeability of the rift sediments. Their age is between 10 and 15 m.y. Although recent fluvial and lacustrine sediments usually have high porosity, with time these sediments become compacted and cemented, which reduces the initial porosity and permeability. Wayland (1925) described the stratigraphy of the sediments of the Albertine Rift as consisting of three units; Epi-Kaiso gravels;

predominantly arenaceous Kaiso beds and the underlying argillaceous Kisegi beds. In the Kibiro region, the Epi-Kaiso beds are about 20 m, the Kaiso beds are 500 m thick, and the total thickness is more than 1,200 m (Harris et al., 1956). The age of these two formations is uncertain, but Wayland (1925) considered the Kisegi to be possibly of Miocene age, and the upper part of the Kaiso beds to be late Pliocene or early Pleistocene.

A 684 m deep well was drilled close to the oil seepage about 1.5 km north of the Kibiro hot springs. The borehole log shows alternating layers of grey sand and grits with sandy clay and blue-green shales (Harris et al., 1956). At 120 m the sediments are predominantly sand and gravel, but between 120 and 250 m depth, layers of clayey sand and shales are dominant. Below 250 m the proportion of sand is high, until the hole hits the basement rock at 1,222 m.

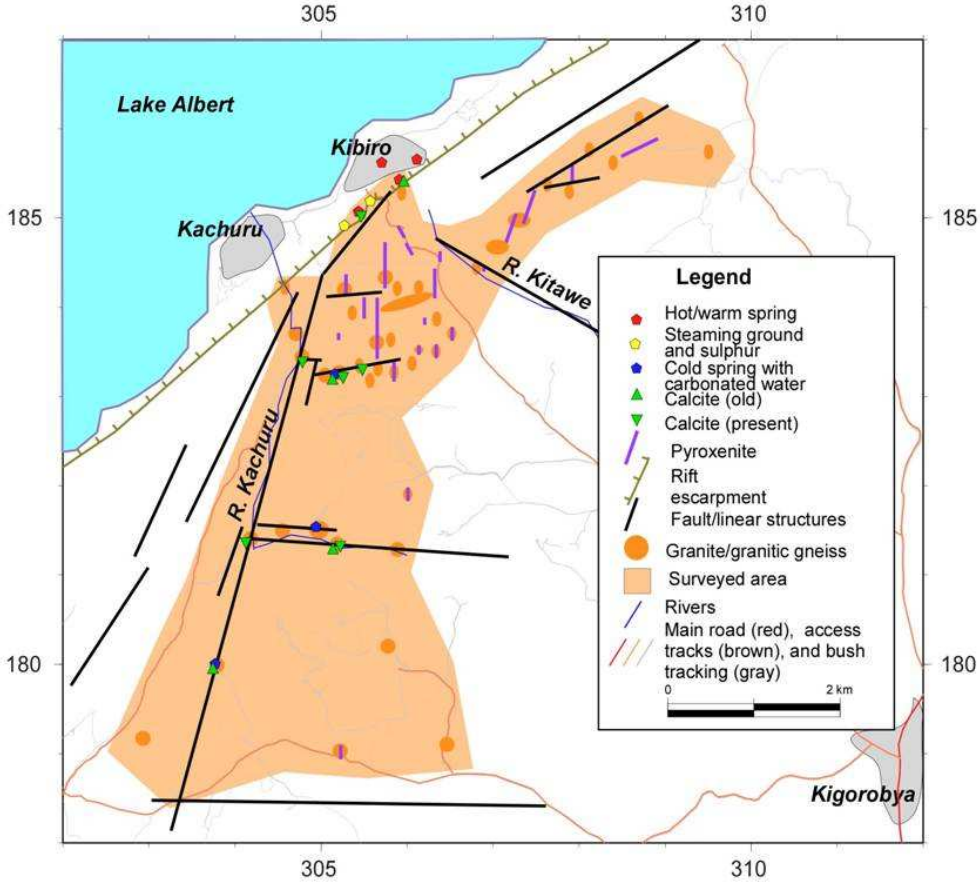

Figure 3: Geology map of the Kibiro area

Banding and jointing

The granites in the area are usually without any banding, it is commonly associated with increasing faulting of the granitic gneiss and mylonitic rocks. Several distinctive strike directions of banding have been observed, where east-west and N20°E are most prominent. A less common strike direction is N130°E. The dip is usually very steep, in the range from 60° to vertical. Closer to the escarpment the bedding tends to have near vertical dip, but farther "inland", the foliation in gneisses dips towards east and south. Banding is absent in the 'amphibolite' dykes. Joints are found in all rock types within the Kibiro, and have the same dominant direction as seen in the bedding. The joints and fissures are open or filled with secondary minerals such as quartz, calcite, kaolinite and sometimes pyrite.

A study of joints can reveal the stress field, which caused them. It shows the two prominent directions of joints in amphibolite outcrop, east-west and N20°E, intersecting at 60° angle. Also present is the less common joint with N130°E trend (Figure 4). A principal stress field with direction NW - SE, can explain this pattern of joints, more exactly with direction 140°E, which is exactly perpendicular to the direction of the rift in the area (N50°E) (Gislason et al., 2004).

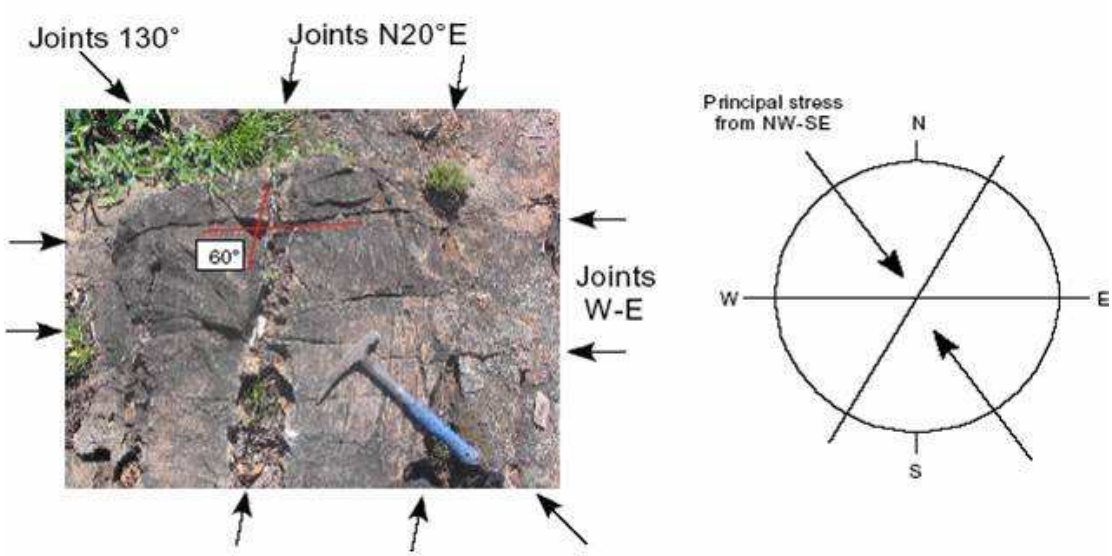

Figure 4: Joints in amphibolite outcrop. The main joints form a 60° angle, and the main stress field is from NW-SE as per stress diagram to the right. (After Gislason et al., 2004).

Figure 5: Kachuru fault-controlled valley viewed from its NE end.

Tectonics

The main faulting within the Kibiro area is the eastern escarpment of the rift, which cuts straight through the study area in N50°E. The visible vertical displacement at Kibiro, from Lake Albert at 622 m asl to about 960 m asl. on the shoulder of the escarpment above Kibiro (340 m). The land continues to rise towards the southeast, and at the village of Kigorobya the land elevation is about 1100 m asl. Seismic refraction data in the rift shows that the total thickness of sediments at Kibiro – Butiaba is about 5.5 km (PEPD, 2002), giving a displacement at Kibiro of at least 6 km in total. The visible part of the escarpment fault, the extension belt, is restricted to a narrow band, not more than 1 km, and often concentrated in one to two faults. Away from this narrow belt of rift faults no linear structures striking N50°E, i.e. the direction of the rift valley, have been found. The western branch of EARS is formed by series of half grabens, i.e. the main extension occurs on alternating sides of the rift, characterised by a dominant main boundary fault, but series of normal faults are hidden by lakes and sediments (Morley et al., 1999).

Drilling for oil north of Kibiro and at Butiaba showed that the escarpment dips at 65°E towards the rift (Harris et al., 1956). In the granites the most prominent landform within the study area is the valley of River Kachuru, which flows off the escarpment to Lake Albert via Kachuru village, south of Kibiro. The valley cuts straight through the granites, very steep and narrow and 200 m deep or more (Figure 5).

Its direction is N20°E, and parallel with it are series of smaller valleys and linear alignments. This Kachuru Fault Zone (KFZ), is oblique to the main rift fault, and intersects it at the villages of Kachuru and Kibiro. At this intersection several geothermal surface manifestations are located. Outcrops along the valley show strongly mylonitized rock, a characteristic fault rock, and the elongated fabric of the influenced rock is in the same direction as the fault. Mylonite are common in the vicinity of KFZ but are not found away from the fault zones. River Kachuru originates from a swampy area west of Kigorobya. It follows a direct course to the west until in flows in to the Kachuru valley (Figure 5) where it turns to NNE until it reaches the escarpment and flows into Lake Albert. The east-west direction of the upper parts of River Kachuru is a dominant linear structure in the study area, first described by Simmons (1921), who described an east-west fault just south of the study area and he associates it with a bend in the Rift just south of Kaiso peninsula in Lake Albert. Simmons interpreted the two fault line directions (i.e. N20°E and E-W) in the granites as block faulting associated with the formation of the Rift. Simmons also mapped and described two East-West faults west of Kigorobya (Figure 3), and these have also been mapped by later authors (Kakenga et al., 1994 and Gislason et al., 2004).

River Kitawe follows a fault-controlled valley just north of the Kigorobya – Kibiro road, and flows down the escarpment in a deep gully by the hot springs of Kibiro (Figure 3). The direction of this alignment is NW-SE (N120°E), intersecting the main escarpment at the Kibiro hot springs. Apparently, the NNE-trending Kachuru fault is the youngest one in the study area, as it cuts through the main rift escarpment. The Kachuru Fault apparently cuts off the east-west trending fault lines, indicating that they are older (Figure 3). On the other hand, the amphibolites, which have the same N-S trending lineament as the Kachuru Fault Zone, are clearly cut off by the E-W trending faults.

Geothermal surface manifestations

Hot and warm springs

There are three hot spring areas at Kibiro geothermal area. The main area of hot springs, Mukabiga, is located in a N-S trending ravine at the base of the main fault escarpment. A number of small springs issue from the boulder and gravel (Figure 6). Large amount of gas escapes from the springs, and there is a strong smell of H_2S in the air. There is little evidence for carbonate precipitation, but white thread-like algae are common in the stream. Close to the stream the threads are coloured black with sulphides. The springs are located on an elongated area, slightly oblique to the main fault. On the western side of the ravine is breccia outcrop related to a secondary fault, oblique to the main rift fault, and the springs are most likely controlled by the intersection of the two faults. Most of the springs drain into a small pool at the foot of the breccia outcrop, and gas bubbles continuously from the bottom of the pool. The total flow measured from the Mukabiga centre was 4 l/s, and the temperature range was 57^0C- 86.4^0C. A second group of hot or warm springs are found downstream, in an area of salt gardens called Mwibanda. The flow rate of 2.5 l/s is low, and the temperature range is 33^0C - 71.7^0C. Some of the seepages are on a straight N-S trending lineament, in a small dugout trench. Other springs are within the nearby Muntere salt gardens, which is directly north of the Mukabiga area. Its eastern side may be controlled by the secondary fault. Here the ground has been lowered down to the ground water level for the salt production. A number of small channels drain the area, and there are no well-defined springs. The highest recorded temperature at Muntere springs is 39.5^0C. Extinct clayey alterations occur in the breccia east of the Mukabiga hot spring area. They contain frequent colourless gypsum crystals.

Steaming ground and solfatara – surface alteration

In the lower slopes of the fault escarpment there are several sites of outcrops of highly brecciated fault rock. A faint smell of H_2S is in the air and a thin film of sulphur covers the rocks. In cracks a well-formed sulphur crystals grow in clusters. Also present is a black tar-like hydrocarbon substance (Figure 7). No steam is seen rising, but the smell and fresh deposits of sulphur demonstrate the presence of some gas being released. Calcite is found in cracks and fissures, indicating water discharge at earlier stages. A band of brecciated fault rock can be traced along the escarpment to both the north and south of this manifestation. About 175 m to the north, and about 50 m south of the track down the escarpment, the fault is well exposed in a shallow gully, and the rock is highly altered in a variety of colours. Sulphur and tar is present on rocks, but no smell is found. Another similar site is found on the same fault about 220 m south of the school, where both sulphur and tar deposits are found.

Figure 7: Black tar-like hydrocarbon substance and extinct clayey alterations on escarpment face.

Discharge into Lake Albert

From the salt works in the salt gardens of Kibiro, it is evident that some portion of the water seeps through the sediments towards the lake. It is therefore anticipated that some hot springs may occur in Lake Albert.

Carbonate springs

In the KFZ, there are three locations of small perennial springs in the granitic zones away from the escarpment (Figure 3). They are all on the fault lines in the block-faulted area. In all cases, the flow is small (<1 l/sec.) and the pH of the water is between 9 and 10. Calcite precipitates from two of the springs and forms few cm thick deposits on rock surface downstream from the springs. The springs issue from fissures in cross-jointed rock outcrops.

Figure 6: A view of the main Mukabiga hot spring area. The springs emerge from a foot of a fault breccia.

Calcite deposits

Calcite is not a primary mineral in granitic rock, and it is not expected to be present in the geological environment in the block-faulted granites. In this area it is present at some locations as secondary mineral in cracks and veins. Calcite is a common mineral in geothermal systems, especially in boiling zones and at the outer zones of the system. The calcite in the Kibiro area may be of geothermal origin, but this is yet to be proved. Three different formations of calcite occur. The first occurrence is calcite, which has formed from water flowing through joints and fissures in the rock, but the rock has now been brought to the surface due to fault movements and/or erosion. The second group is the calcite, which is currently being deposited at the carbonate springs. These two groups are here interpreted as geothermal manifestations, the former may be fossil but the latter is active. The water in the headwaters of River Kachuru is saturated with calcite, and a thin film forms on rocks in the river. This calcite forms the third group, and as its origin is less certain than the former two groups, it has not been mapped. If the calcites are geothermally related, it is apparent that the east-west faults are playing an active role in the geothermal system (Gislason et al., 2004).

GEOLOGY OF THE KATWE GEOTHERMAL FIELD

Introduction

The Katwe-Kikorongo Volcanic Field (KKVF) is located on the western escarpment of the Rift, south of the Rwenzori Massif which is a horst rising to an altitude of 5,109 m asl, with the equator running across the northern part of the field. Lake Edward and the Kazinga channel constitute the periphery of the Katwe field area in the south. In the east, the area reaches onto the flat plains of the Rift and in the west, the southern tail of the Rwenzoris borders it. Figure 8 shows a simplified geological map of the Katwe area. The geological history of the area begins from Precambrian base rock to Pleistocene-Pliocene volcanics to Quaternary lake sediments.

Basement rock

The basement rock outcrops on the rift shoulders to east of the rift, adjacent to the Bunyaruguru volcanic field, and in the Rwenzori Massif, immediately to the north of the KKVF. To the east of the rift is the Karagwe-Ankolean System (quartzites, shales, phyllites intruded by granites). Reece (1955) studied accidental blocks occurring in the tuffs and craters that this formation underlies the Bunyaruguru volcanic field. The rocks of the southern part of the Rwenzori Massif belong belong to the Toro system, which consists of schists, quartzites and intrusive rocks such as granites, pegmatite, amphibolites and dolerites. The strike of bedding and foliation in the southeastern Rwenzori has a similar strike to that of the main rift escarpment, 15° - 70°.

The Rwenzoris slope gently towards the south and their basement rock disappear under the volcanic pile of the KKVF close to the equator. In this area the volcanics are deposited directly on the pre-Cambrian rock, as outcrops can be seen in the northern part of the field like the northern inner slopes of the Mahiga crater. Towards the south, there is no direct evidence for the depth to the basement. The fresh water and temperature gradient boreholes drilled in the area have not intercepted the underlying basement rocks (Franzson, 2008).

Lake sediments

The present day Rift floor is covered by an unknown thickness of lake sediments. Near the KKVF two major lakes are found, Lake George and Lake Edward, connected by the slow-flowing Kazinga channel. Through its evolution, the Rift Valley has hosted lakes to a varying extent, depending on prevailing climate and other controlling parameters. The present day Lakes Edward and George are small in comparison with earlier lakes, which sometimes covered the whole breadth of the rift. Flat lying sediments from these periods cover the Rift Valley floor, and the best outcrops are along the Kazinga channel, which connects the two lakes. At the Mweya Lodge, there is 20 – 30 m high outcrop of lake sediments, fine silt or sand grain size with little or no layering with no volcanics. The outcrop at the bridge at the Katunguru village consists of volcanic pyroclastics, partly welded to form a 70 cm thick layer on top of the sediments. The land west of the crater area is outside the actual rift and is part of the southern slopes of the Rwenzori Mountains. Sediments can be seen in road cuttings and fault escarpments, and these are generally land deposits, interbedded with volcanic layers of pyroclastics, often rich of lapilli. In the crater area lake sediments are not exposed *in situ*, but can be found at few places as accidental fragments in the pyroclastics.

Volcanic rocks

The KKVF is dominated by pyroclastic material with rare occurrence of lavas and ejected lava blocks as accidental fragments. Lloyd at al. (1991) estimated that the bulk volume of tephra was 63 km^3 but only 0.07 km^3 of lavas.

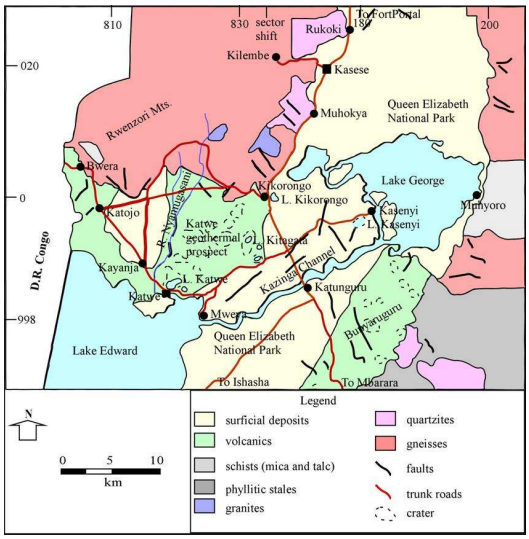

Figure 8: Geology map of Katwe area and its surroundings.

The Crater Area

The crater area is situated on the western escarpment of the rift, at the southern slopes of the Rwenzori Massif. The numerous craters are coarsely arranged in a north-easterly direction along the main rift alignment; the main crater area stretches over 30 km along the main fault lines, and is about 11 km from north-east to south-west at its widest. A few craters are found outside the main crater area, as far as the town of Kasese in the north, making the total length from north to south about 45 km. The craters are arranged very densely, often interlocking with each other, and many may be difficult to identify (Figure 10). A recent study identified over 140 eruptive centres within the Katwe area. The craters are generally of low relief, and were formed by a phreatic eruption, i.e. maars. Some of the craters, especially those on the lowland (Lake Katwe, Lake Kikorongo, and Lake Nyamunuka) or the deeper craters (Lake Kitagata, Lake Mahiga) have crater lakes, usually with high salinity waters due to evaporation. The phreatic nature of maars are caused by interaction of magma and shallow groundwater, leading to explosive type of eruption producing pyroclastic airborne deposits, often widely distributed and thus resulting in a low crater rims composed by loose airborne material, often mixed with fragments from the host rock, i.e. accidental fragments. It is believed that many centres of phreatic eruption were active at the same time, producing large maar type flat-bottomed depressions (Gislason et al., 2008).

Pyroclastics

Most of the primary magma of the volcanic pile is represented by pyroclastics, mostly tuff and to lesser extent lavas, but bombs are absent. This implies powerful explosions during eruptions, capable of tearing the magma to small particle sizes. The presence of lava flows with chemical composition identical to that of the tuffs shows that the explosive force is most likely due to external conditions such as direct contact of the parent magma with ground water. When magma and ground water interacts, the water is turned into steam, multiplying in volume, and breaking up the host rock formations where the interaction takes place. The angular forms of the abundant fragments of the basement rock in the pyroclastics indicate that the interaction takes place within the pre-Cambrian basement (Gislason et al., 2008). Accidental fragments of the sedimentary formations are found at low levels of the pyroclastics in the Lake Katwe crater.

The pyroclastic outcrops have a yellowish appearance, and may vary in fragment size, although generally rather fine grained. On some locations no bedding can be seen in thick sections, but generally the pyroclastic outcrops show sorted, stratified airborne character. The drilling of borehole for temperature gradient measurements indicate that the pyroclastic material extend up to 132 m depth (Natukunda, 2007). Commonly base surge structures are apparent, especially close to the crater of origin (Figure 9). No welding of the airborne material has been found, indicating lower temperatures, perhaps due to interaction of hot magma and cooler ground water (Gislason et al., 2008).

The most striking feature of the pyroclastic eruptions of the KKVF is the abundant occurrence of accidental fragments in the ejecta. The size of the fragments varies from being tiny fragments to over 3 m in diameter. The largest rocks are always found near a crater, all stones larger than 10-15 cm in diameter are found within 50 m distance from the nearest crater rim.

Figure 9: Surge structures in volcanic tuff.

Lava flows

Lavas make a very small part of the volcanic material of the KKVF. No lavas are seen on the present day surface, showing that the final volcanic phase was entirely of phreatomagmatic character. Lava flows can be seen *in situ* under a thick cover of pyroclastic material in four locations, in the inner slopes of two craters, namely the Lake Kitagata and Kyemengo craters. The main outcrops are on the northern side of the Nyabugando peak, which is located between the Kyemengo and Lake Kitagata. On its northern side, facing the Kyemengo crater at least six lava flows are exposed; their total thickness is about 120 m. The flows have scoreacous tops and bottoms, and are sometimes separated by thin pyroclastic layers. The lava outcrop rests on pyroclastic deposits, and the lavas are buried under some 150 m under the peak of the Nyabugando, which reaches to 1,225 m asl. On the eastern side the lava pile terminates abruptly, as the outcrop is bordering the main fault of the KKVF Fault Field, forming the western side of the peak.

On the eastern side of the Nyabugando peak, facing the Lake Kitagata crater is another outcrop of lavas, at least 30 m high, where four lava flows can be seen, and the steep wall is formed by the main fault of the KKVF. The hot springs of Lake Kitagata emerge at the foot of this. The third lava outcrop is found on the inner north wall of the Lake Kitagata crater. It is about 12 m thick and is level with the second outcrop, but their contact is hidden by vegetation and scree, and the fault, which controls the hot springs, runs through this span. The outcrop seems to consist of one thick lava flow, but no correlation between the two neighbouring outcrops can be made. Holmes (1952) found one 20 m thick lava flow in the Baboon cliff, which forms the western rim of the Kyemengo crater. The above locations are the only *in situ* lava flows, but lava blocks can be found in the ejecta of several of the craters surrounding the Lake Kitagata and Kyemengo craters. The blocks are angular and vary in size from few cm up to 2 m in diameter.

Based on the chemical analyzes of the rocks, which are low in silica ranging from 33.5 to 43.6 %, Holmes (1952) divided all the samples in two main groups based on the SiO_2/Al_2O_3-ratio. He identified the rock as being potash ankaratrites, leucite ankaratrites and melaleucitites. It is most likely that each lava block has been broken from its original place and ejected from the vent of the nearest crater.

O.B.P. series

The ultrabasic volcanic rocks found in the pyroclastic ejecta as accidental fragments in the KKVF (Figure 10) as well as in other volcanic fields around the Rwenzori Massif, are referred to as the O.B.P. series (Holmes 1952). The fragments are composed of olivine and/or biotite and/or pyroxene, hence the name O.B.P. In the KKVF O.B.P. is only found as fragments and never *in situ*. The crystals vary in size from fine grained to several cm in size, especially pyroxene and biotite. The latter is found as single crystals in the ejecta from many craters, up to 10 cm in diameter. The O.B.P. fragments tend to be round in appearance opposite to the lava blocks which are often angular. This might indicate that at the time of the explosive eruption, the O.B.P. host rock was semi-solid, where as the lavas in the root of the volcanic field was in a solid state (Gislason et al., 2008).

Accidental Fragments

The *maar* type of eruption, which is dominant in KKVF, is interpreted to be the product of an interaction between molten magma and groundwater, leading to violent steam explosions. The fragmented magma and voluminous steam tears lumps of material from the host rock where the explosion takes place and from the duct

walls as the steam/tephra mixture rushes to the surface. The map (Figure 10) shows that the basement rocks underlie almost the whole crater area, except at the Lake Kikorongo crater no basement fragments are found. The volcanic fragments are spread over the central part of the crater area, indicating that buried lava flows have formed a part of the volcanic pile in the central part of the volcanic system, but have not reached south to the Lake Katwe area, and the lavas have reached farthest to the north to Lake Mahiga. The O.B.P. series are shifted to the south compared to the lava distribution, and are found as far south as the Lake Katwe area, but are not found much north of the Kyemengo crater in the central part of KKVF. The large biotite crystals, which are presumed to be a part of the OBP series, are found in the southern part of KKVF, but overlapping with the occurrence of the O.B.P. fragments (Gislason et al., 2008).

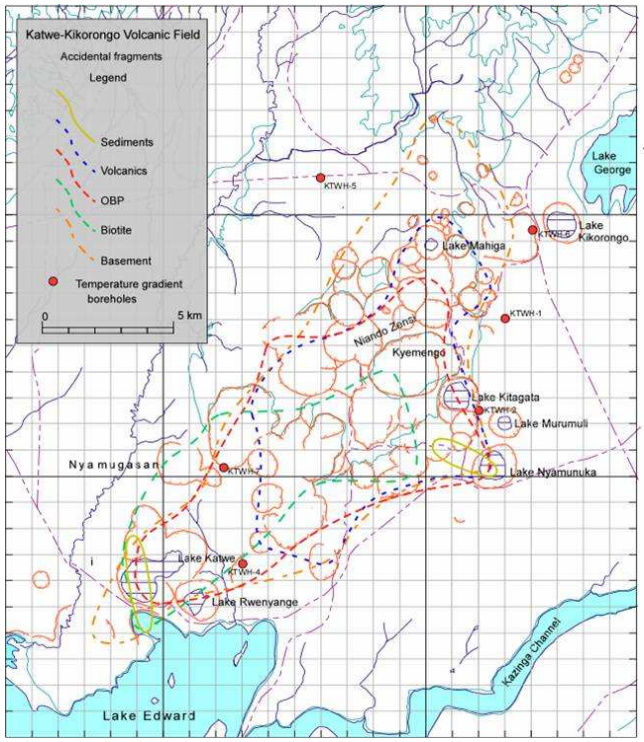

Figure 10: The Katwe-Kikorongo Volcanic Field. Outline of sub-surface distribution of rock formations as interpreted by distribution of accidental fragments in pyroclastics (after Gislason, 2008).

Lake sediments as accidental fragments are found in the Lake Katwe crater, and in situ under the pyroclastics in the Nyamunuka crater. The distribution of basement rocks not only show that the basement underlies the whole of the crater area, but also the interaction of magma and ground water takes place, at least to some extent, within the pre-Cambrian basement formation. The distribution of lavas coincides with the area of highest production of volcanic material in the crater area.

Faulting

Faulting plays an important role in shaping the study area, as it is located on the rift shoulder of one of the branches of the East African Rift System. The faults are draped by volcanics, and it appears that explosive volcanic activity was the latest events in the KKVF, covering any exposed faults. The Katwe faults have been mostly interpreted from aerial photographs, but in many cases confirmed by field observations. The dominant fault direction is parallel to the rift border, with a north-easterly direction. A major alignment in the pre-Cambrian basement in the north-western corner of the study area runs with a N150ºE direction under the volcanic field. This lineation marks the south end of the Rwenzori Massif. It is a product of foliation in schist, and faulting. South of this line the main faults of KKVZ have the direction N30ºE but to the north it changes to a more northerly direction, or N15ºE. Apparently, the intersection of these three structures influences the volcanic activity. The intersection coincides with the highest production of magma, and the distribution of lava blocks is centred on the intersection, and it is also the location of lavas found *in situ* (Figure 10). The main hot springs of the area, i.e. the springs in the Lake Kitagata crater are clearly controlled by NE-SW faults, and are as well located above the underlying basement lineation. It may be interpreted that although the transport of magma is along the faults of the rift; the intrusive magma is injected at relatively shallow depth from the main NE-SW faults to SE along the weaknesses of the older basement fault. Here the magma interacts with

considerable body of ground water to form the pyroclastic type of eruptions, only a small portion of the magma reaches the surface to form a normal lava flow (Gislason et al., 2008).

Geothermal manifestations

The geothermal surface manifestations in the Katwe prospect are hot springs located in the Lake Kitagata crater (Figure 11), and warm springs and travertine deposits that have built up tufas in the Lake Katwe crater, which is located 12 km southwest of Lake Kitagata (Figure 10). The maximum surface temperatures in the hot springs in Lake Kitagata crater is 70°C, while in Lake Katwe Crater it is 32ºC.

Figure 11: Kitagata crater in which lava flows occur under its highest Nyabugando peak and hot springs emerge at foothill and in the lake (eastern side of lake).

GEOLOGY OF BURANGA GEOTHERMAL PROSPECT

The Buranga geothermal area is located at the northwestern base of the Rwenzori Mountains in the Western Rift Valley (Figure 12). Exploration for oil around Buranga showed a Tertiary succession of sands, clays and boulder beds with occasional tuffs. Geophysical surveys confirmed the presence of these rocks down to a depth of 1,524 m. The boreholes showed that the Tertiary succession was terminated in the fault zone by a breccia cemented by calc-tuffs followed by mylonite (Harris et al., 1956). The clays are of various colours and the sands are fine-to medium-grained, varying in colour between white, brown, grey and green. The most common binding material is clay, although this may be patchily replaced by calcium carbonate, giving rise to calcareous sandstones and grits. Pebble beds are of rare occurrence. There are no fossils apart from plant fragments.

South of Sempaya and close to the Buranga hot springs, a fault line (striking between 20° and 45° and dipping 60-65° westwards) is exposed (Johnson and McConnell, 1951). The presence of mylonite along fault zone suggests movement along a very old fracture zone of compression. Traced further north, this fault system displays both a change of direction and reduction in magnitude. Step faulting is also present as per topographic features (Harris et al., 1956). The 13 structural lineament course is marked not only topographically, but also by masses of fossil calc-sinter covering 4 km^2 between Kibuku and Buranga (Sharma, 1971). Kibuku is located approximately 10 km north of Buranga hot springs.

Unlike Katwe, Buranga has no evidence of volcanism but is highly tectonically active.

Geothermal surface activity is intensive, with sprouting hot springs and high gas flow (Figure 5).The manifestations are found at the foot of the escarpments in a swampy area enclosed by a dense rain forest. Surface alteration is scarce but most of the springs have developed traces and mounds of travertine. Surface and geological observations carried out under UGA/8/003 project indicate the presence of extinct thermal features (travertine) along a 10 km stretch from Buranga hot springs to Kibuku. This shows that the area of thermal activity has been shifting from north to south and that the Buranga geothermal area may be somewhat larger.

Geothermal manifestations of Buranga

Buranga has the most impressive surface geothermal manifestations i.e. hot springs (Figure 13) with a wide areal coverage in the whole of the western branch of the East African Rift System. They include hot springs, calcareous tufa and recent surveys have reported small-scale seasonal fumaroles at Mumbuga spring area that appear in dry season when the water table is low. The surface temperature is close to 98˚C and the flow is approximately 10-15 litres/second, an indication of high permeability.

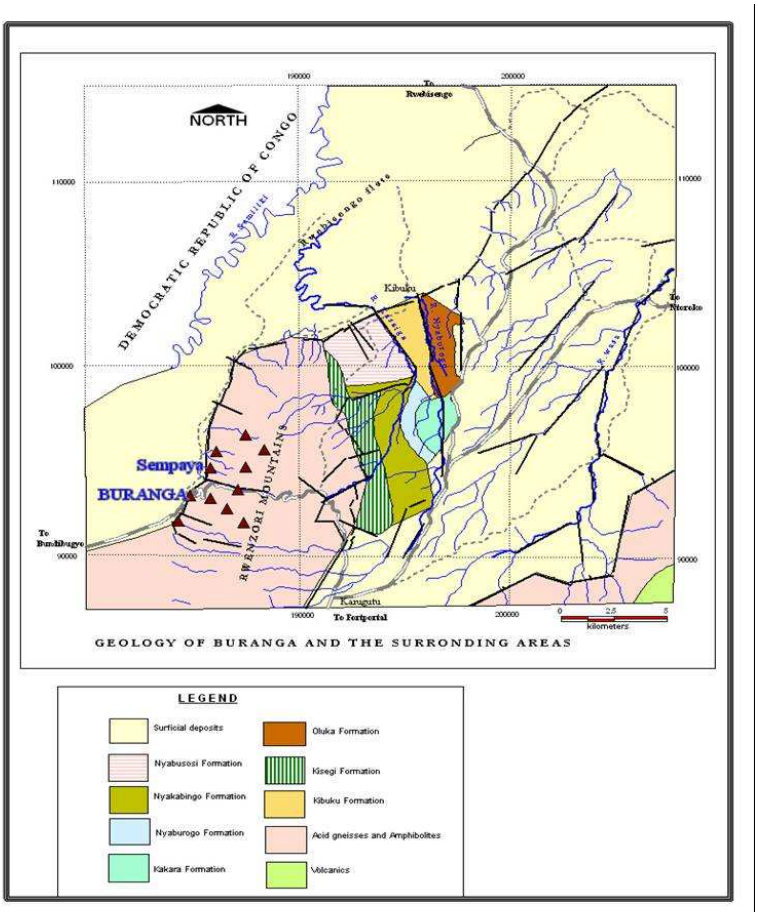

Figure 12: Geology map of Buranga showing location of hot springs.

Figure 13: The Mumbuga erupting hot spring in Buranga geothermal prospect. Note the developing travertine cone.

CONCLUSION

The Albertine Rift controls the geology of the three geothermal prospects. Katwe is the only prospect in a volcanic environment while the geology of Kibiro and Buranga is dominated by the crystalline basement and sedimentary formations. The fault system is most likely of the same age as the rift itself and results from the same forces. The tectonic pattern in the three areas is governed by the formation of the rift. The same forces that are tearing the Archaean shield apart in SE – NW direction and forming the Albertine Rift have block-faulted the semi-brittle granitic base rock east of Kibiro and Buranga prospects. In Katwe field, the geological evidence indicates that the magma-water interaction takes place within the pre-Cambrian basement and that the forces of the eruption demand that the access to groundwater is considerable. The presence of ample water in pre-Cambrian granites and gneisses suggests a secondary permeability, caused by the break up of the older formation during the evolution of the Rift Valley. The prerequisites for existence of geothermal reservoirs in the three prospects exist, namely a heat source, permeability and rechargeable water. This is supported by the existence of hot springs, fractured basement glaciers on top of Rwenzori Mountain (for Buranga and Kibiro) and appropriate precipitation. In Katwe, the hot springs are right in the middle of the field, where the geological evidence points to the highest magma production, an intersection of large tectonic system and therefore the highest permeability.

REFERENCES

EDICON.: Aeromagnetic interpretation of Lake Albert/Edward portion of the Western Rift Valley. Unpubl. Report, EDICON inc., Denver Colorado, (1984).

Fournier, R.O. and Potter, R.W. II..: A revised and expanded silica (quartz) geothermometer. Geotherm. Res. Council Bull., 11, (1982), 3-9.

Franzson, H.: Uganda Kibiro – Katwe. Geology of thermal gradient wells. Report, Project No. ISOR, Iceland Geosurvey: 590-110, (2008), 1-12.

Gislason, G., Árnason, K., and Eysteinsson, H.: The Kibiro geothermal rospect; Report, on geophysical and geological survey prepared for Icelandic International Development Agency and Ministry of Energy and Mineral evelopment, Uganda, (2004),1-109.

Gislason, G., Árnason, K., Eysteinsson, H., and Magnússon I.Þ.: The Katwe geothermal prospect; Report on a geothermal survey prepared for Icelandic International Development Agency and Ministry of Energy and Mineral Development, Uganda, (2008), 1-101.

Harris, N., Pallister J.W., and Brown, J.M.: Oil in Uganda. Memoir No. IX, Geological Survey of Uganda, (1956), 1-33.

Holmes, A.: Transfusion of quartz xenoliths in alkail basic and ultrabasic lavas southwest Uganda. Mineral Magazine, 24, 155, (1956), 408-421.

Holmes, A.: The potash ankaratrite-melaleucitite lavas of Nabugando and Mbuga craters, southwest Uganda. Trans. Edinb. geoL Soc., 15, (1952), 187–213.

Johnson, R.J., and McConnel, R.B.: Notes on the Geology of the northern parts of the Rwenzori Mountains. Geol. Magazine 88, (1951), 249-256.

Kakenga, J.W., Rubondo, E.N.T., Kato, V., Kabanda, F., Namukoye, P.N., Ssentomero, W.D., and Namisi, S.: Geology of Kaiso Tonya area. Unpublished geological map, Petroleum Exploration and Production Department, Uganda, 1994.

Morley, C.K., Ngenoh, D.K., and Ego, J. K.: Introduction to the East African Rift System, in C. K. Morley ed., Geoscience of Rift Systems – Evolution of East Africa, AAPG Studies in Geology, 44, (1999), 1 – 18.

Morley, C.K., and Westcott, W.A.: Sedimentary Environments and Geometry of Sedimentary Dodies Determined from Subsurface Studies in East Africa, in Morley, C.K. ed., Geoscience of Rift Systems – Evolution of East Africa, AAPG Studies in Geology 44, (1999), 211 - 231.

Natukunda, J.F.: Geology of Kibiro and Katwe gradient boreholes, Unpublished Report, Department of Geological Survey and Mines, Uganda (2007), 1-14.

PEPD.: A Report on Geophysical Surveys carried out by the Geophysical Division between 17th October and 7th November in Hoima Basin, Loose Minute, Petroleum Exploration and Production Department, Ministry of Energy and Mineral Development, Uganda, (2002), 1-16.

Reece, A.W.: The Bunyaruguru volcanic field: Geological Survey of Uganda, Records for 1953, (1955), 29-47

Sharma, V.: Preliminary survey of thermal anomalies of Western Uganda for the possible development of Geothermal Energy, Report DGSM, (1971).

Simmons, W.C.: A Rapid Geological Survey of Part of Bunyoro. Annual Report, Geological Survey Department, Uganda, (1921), 29 – 34.

Wayland, E.J.: Petroleum in Uganda. Memoir, 1, Geological Survey of Uganda, (1925), 61.

STRUCTURAL CONTROLS ON THERMAL ANOMALIES AND DIFFUSE SOIL DEGASSING AT MENENGAI GEOTHERMAL PROSPECT, THE KENYAN RIFT VALLEY

Isaack Kanda
Geothermal Development Company Ltd, P. O Box 17700-20100, Nakuru, Kenya. ikanda@gdc.co.ke

ABSTRACT

Regional exploration for geothermal resources in Kenya indicates that the Quaternary volcanic complexes of the Kenya rift valley provide the most promising prospects for geothermal exploration. A number of geoscientific studies have been conducted to assess the geothermal potential of this area. This paper reports the results of a survey of CO_2 soil fluxes and concentrations of thoron (Rn_{220}) in soil gases. Soil CO_2 concentrations measurements were performed using an Orsat apparatus whereas Rn_{220} soil gas concentrations were measured with a portable radon detector (emanometer). A total of 275 sampling points were measured. The obtained values ranged between zero to 12% of CO_2 in total gas and zero to 6425cpm of Rn_{220}.

Peak levels of soil CO_2 concentrations and thoron concentrations were identified to be located on major faults and within the caldera floor where hydrothermal fluids are rising and the rocks are highly fractured allowing the release of CO_2 and thoron locally marked by fumaroles. Areas identified with the highest anomalies for CO_2 and thoron soil gas concentrations can be seen in the contour maps presented. The caldera, Molo TVA and also Solai graben are the important geological structures associated with these anomalies.

Keywords: geothermal resource, thoron concentrations, CO2 concentrations, TVA and faults

INTRODUCTION

The Menengai Geothermal Prospect is located in the central section of Kenyan Rift Valley, the area north of L. Nakuru and south of Lake Bogoria. The extend of the prospect covers an area of approximately 600 km^2 characterized by a complex geological setting with Menengai caldera being notably the major geological feature in the area and is also important for its geothermal potential. Most part of this area, in particular the southern section is discussed in this study.

The general exploration for geothermal resources in Kenya indicates that the Quaternary volcanic complexes of the Kenya rift valley provide the most promising prospects for geothermal exploration, and as a result, intensive exploration work has focussed on areas with volcanic centres located within the rift valley. Studies show that these volcanic centres have positive indications of geothermal resource that can be commercially exploited. Menengai geothermal area is one of the priority prospects in the current prospects ranking. Eleven locations with fumaroles have been identified in the region (Figure 1).

A number of thermal anomalies and diffuse degassing assessments have been carried out in most of geothermal prospect areas in Kenya, including Menengai. Results for CO_2 and Rn_{-220} soil diffuse concentrations have been found to discharge more in areas that coincide with faults. The purpose of this study is to establish the soil gas concentration of CO_2 and Rn_{220} and relate with known geological structures.

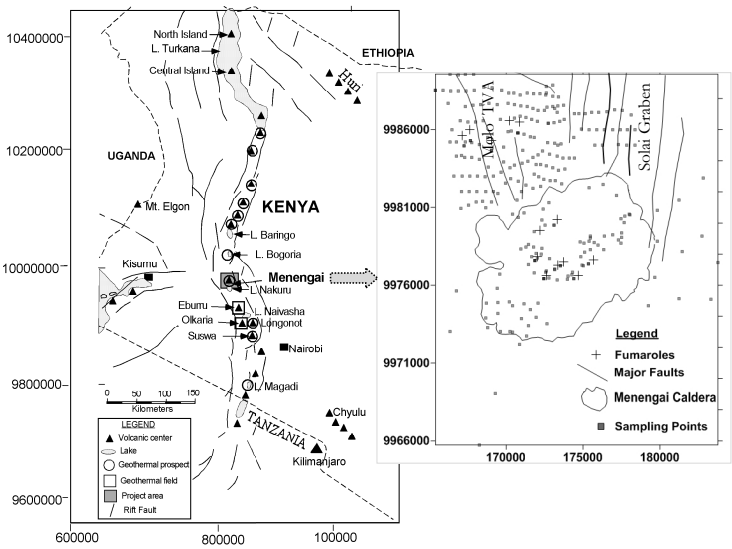

Figure 1. Location of Menengai Geothermal Prospect showing fumaroles, major faults and sampling points.

GEOLOGICAL AND STRUCTURAL PATTERN

The Kenyan Rift is characterized by extension tectonism where the E-W tensional forces resulted in block faulting (KenGen 2004). This included leant blocks as evident in both the floor and scarps of the rift. The rift trough is truncated by several normal faults, which evidently represent persistent and wide-ranging tectonism under the rift floor. Menengai Geothermal Prospect itself is located within an area characterized by a complex tectonic activity associated with the rift triple junction; the latter being a zone at which the failed rift arm of the Nyanza rift joins the main Kenya rift. Two rift floor tectono-volcanic axes (TVA) that are important in controlling the geothermal system in study area include the Molo and the Solai TVA.

Menengai has been active from about 0.4 -0.3 Ma B.P (Gislason 1989). The formation of the shield volcano began about 200,000 years ago and was followed by the eruption of two voluminous ash-flow tuffs, each preceded by major pumice falls. More than 70 post-caldera lava flows cover the caldera floor, the youngest of which may be only a few hundred years old. The caldera of Menengai volcano lies immediately north of Lake Nakuru, but ignimbrites and air-fall tuffs from the volcano cover some 1350km^2 (Leat & Macdonald 1984) extending into Molo area (Jennings 1971). The volcano is mainly composed of strongly peralkaline, Si-oversaturated trachytes and has had a complex geochemical evolution, resulting from the interplay of magma mixing, crystal fractionation and liquid state differentiation (Leat & Macdonald 1984).

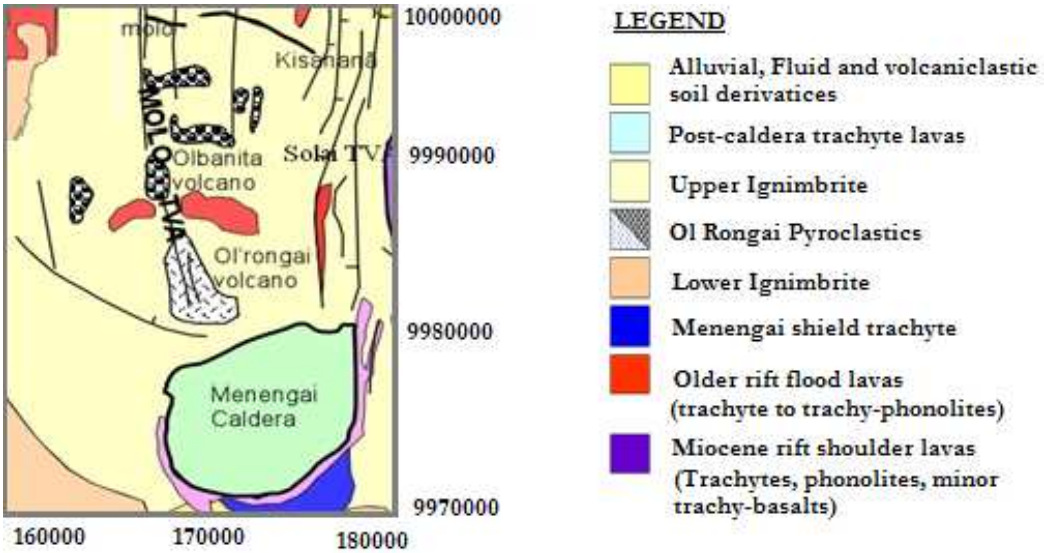

Figure 2. Geological map of Menengai Geothermal Prospect Area (after KenGen 2004)

METHODOLOGY

Early geochemical studies on diffuse soil degassing have been carried out in a number of geothermal areas. CO_2 soil gas investigations similar to the one used in this study have been conducted elsewhere in volcanic areas to examine unexpected rise in CO_2 flux (e.g. Farrar *et al.* 1995; McGee and Gerlach 1998; Gerlach *et al.* 1998), estimate total volcanic flux from volcanic vents and diffuse flank emissions (e.g. Allard *et al.* 1991; Chiodini *et al.* 1996), and to classify tectonic structures related to volcanic degassing (e.g. Giammanco *et al.* 1997; Bergfeld 1998).

The study area together with a total of 275 sampling points is presented in Figure 1. Sampling spacing relied mainly on accessibility of specific targeted points and the ease of getting samples, in particular on the rugged areas. Nonetheless, a random separation of about 300m in average was used. Areas covered by younger lava flow were almost impossible to sample and few samples thus represents such areas, as was seen with lava pond within the caldera. The survey involved measuring of CO_2 and Rn-$_{220}$ in the soil gas. All the measurements were done at the same point. In addition, soil temperatures were taken using an infra-red thermometer at the point where the soil gas survey was undertaken.

Measurement of CO_2 gas was done by the help of an Orsat apparatus after the soil gas was hand pumped from a depth of 1m below the surface via a hole made using a steel spike with jacket. The Orsat apparatus consist of absorption vessels, which measure about 100 mls and contain a 40% KOH solution for absorbing the acidic CO_2. The corresponding volume changes in the absorption vessel represent the corresponding amounts of the gases in volumes given as percent of the total gas as a percentage.

Radon radioactivity levels were measured in the soil gas using a portable radon detector (emanometer). The soil gas was passed into the emanometer by using a hand-operated vacuum pump and Rn_{-220} readings recorded in counts per minute (cpm). Three background counts were recorded at three-minute interval prior to introduction of sample into the emanometer. Upon introducing the sample, three more readings were taken at one-minute interval to give the total radon counts.

The CO_2 and Rn_{220} obtained in the survey (both 2004 and 2010 sampling programs) were corrected and used to construct concentrations contour maps (Figures 3 to 6). Natural neighbor contouring method was used because it interpolates scattered and irregularly spaced data effectively and hence produces better contours maps from irregularly spaced measurements (Ledoux & Gold 2005).

RESULTS AND DISCUSSIONS

The results of descriptive statistics of CO_2, Rn_{220} and Temperature collected are presented in Table 1. The frequency distributions are described by normal distribution. The range of values for these parameters spans several orders of magnitude.

Table 1: Descriptive statistics of CO_2, Thoron and Temperature from 275 sampling points.

	N	Range	Minimum	Maximum	Mean	Std. Deviation	Variance	Skewness		Kurtosis	
	Statistic	*Statistic*	*Statistic*	*Statistic*	*Statistic*	*Statistic*	*Statistic*	*Statistic*	*Error*	*Statistic*	*Error*
Rn220	275	6427	0	6427	386	603	363391	5.14	0.15	39.49	0.29
CO2	275	12.30	0.00	12.30	1.12	1.54	2.37	5.12	0.15	30.81	0.29
Temp	275	55.90	21.20	77.10	28.70	6.99	211.52	0.05	0.15	0.62	0.29

Soil Temperature Measurements

The mapping of temperature variations at or below the earth's surface is an essential geothermal exploration instrument. The spatial variation of soil temperature is illustrated in Figure 3. Quite a number of anomalies can be identified in relation to the major structural setting. And as indicted by results, a higher temperature anomaly in the caldera is evident around the fumaroles with the highest fumaroles temperature of 88°C. Similar to other soil surveys, soil temperature results in the caldera is mainly affected by the lava that covers the caldera floor and apart from the areas where the lava did not cover. The areas to the North outside the caldera gave an anomaly confirming the geothermal potential of the area coinciding with two major faults trending NW-SW.

Diffuse Degassing Measurements

The term volcanic gas defines a gas exsolved from a magmatic source of an active volcano whereas hydrothermal gas defines a gas exsolved from the envelope of hot water that surrounds the magmatic environment. Volcanic gases have composition different from the hydrothermal gases, the first is richest in SO_2 and the second in H_2S (Giggenbach 1996). CO_2 occurs in both magmatic and hydrothermal gases and is the most abundant gas after water vapor. The deep-seated faults in the crust tap magmatic CO_2, which is transmitted to the surface where it is naturally lost through the soil. Carbon dioxide (CO_2) of magmatic origin is normally channeled through deep-seated tectonic structures close to the surface of the earth and then seeps out of the ground through the soil. However, dealing with CO_2 anomalies especially in the Rift Valley ought to be treated with caution owing to the availability of localized sources of this gas as suggested by Darling *et al.* (1995). CO_2 may also originate from other sources like organic matter, which are likely to give false impressions of a geothermal source.

Thoron gas (Rn_{220}) is a short lived isotope of radon produced by the thorium (Th_{232}) decay series with a half-life of 55 seconds (Lopez *et al.* 2004). Due to its short half-life, thoron's transportation is limited to a few centimeters either by diffusive or convective flows, as compared to Rn_{222} (t ½ = 3.8 days) (Hutter 1993). As a result, the high concentrations of thoron are more likely to be due to convective movement of gases rather than diffusive processes and therefore it is difficult to achieve an exact quantitative measurement of its concentration. If we measure the disintegration of thoron, it shows a decrease during the first three minutes after collection of the sample, as opposed to the radon that presents a half-life of almost 4 days (Magana *et al.* 2002). High thoron values could be suggestive of enhanced permeability, as it may as well depend on other factors such as the degree of rock fracture and the ability of groundwater to circulate and remove thoron.

The CO_2 gas concentrations are plotted in Figure 4 while the results of radon emanations were recorded in counts per minute (cpm) for Rn_{-220} and plotted in Figure 5. To reduce interferences between CO_2 and Radon sources a ratio of Rn_{-220}/CO_2 have been plotted in Figure 6.

CO_2 Concentrations

The concentration of CO_2 in the soil gas in the surveyed area is given as a percentage of the total gas in the soil. The degassing of CO_2 through the soil in the prospect area is considered to be mainly supplied by two sources, the one of volcanic origin emanating from deep environment and a shallow one that result from organic activity. In this study, high CO_2 values (>2.5%) are found at a belt running in a NW-SE while other areas exhibit low values (<1 %). These areas coincide with the Molo Tectono-Volcanic Axis (Molo TVA), deep seated faults and the eruption centers in the prospect area which indicate that the source could be from a magmatic body. Highest CO_2 concentration in the soil gas was observed around Ol'Rongai Hill (located along Molo TVA) and the contiguous fumaroles with CO_2 >10% which could be indicative of good permeability in the area.

The central part of the caldera around the fumaroles, as well, displays relatively high values of CO_2 (>2.8%). There are also few highs of CO_2>5 % in the western part of the caldera. The presence of thick young lava that covers most parts of the caldera interfere with the movement of CO_2 to the surface and therefore makes sampling in these parts extremely difficult, and is also noticeable in the contouring of the CO_2 distribution as shown in Figure 4. Care ought to be taken while correlating thermal and diffuse degassing anomaly with subsurface permeability. This is because the cap of young lava that covers most part of the caldera might be directing the anomaly laterally beneath the lava bed and hence giving misleading impression as a result.

Thoron Concentrations

From the results of the absolute values of Rn_{-220}, north-western parts of the surveyed area show the highest concentrations (Figure 5). In addition, a more pronounced anomaly is evident in central part of the caldera in the areas adjoining fumaroles following similar pattern to the one revealed by CO_2 distributions. However, a mild rise in thoron values is seen in the eastern flank touching Solai Graben.

Thoron-CO_2 Ratios

The ratio of the Rn_{220}/CO_2 gases would be a good indicator of the magmatic source of the gases since the ratio is not expected to change if they are from the same source (see Figure 6). High values of these ratios are found towards the north, north-western to the north eastern parts outside of the caldera wall with two anomalous areas at the fumaroles in Ol'Rongai area. A mantle source of CO_2 as suggested by Darling et al. (1995) is a possibility of the source of this gas due to intense faulting in the area, and these faults around Ol'Rongai are of great importance in localizing degassing of CO_2 and $Rn\text{-}_{220}$ as well thermal manifestation anomalies. If a mantle source is inferred due to intense faulting, then the faults should be deep seated. These areas apparently coincide with high CO_2 and high Rn-220 absolute values.

The western part of the surveyed area, which shows high absolute values of CO_2, gives low value of this ratio. This is an indication of a source other than the one of magmatic origin. This coincides with an agriculture farm and consequently the CO_2 anomaly in this area is considered to emanate from organic source, as a result. Nonetheless, a higher ratio of these gases is seen within and to the east of the caldera.

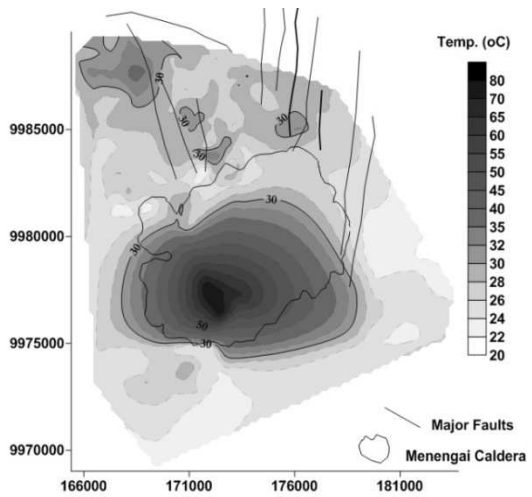

Figure 3: Temperature distribution in °C

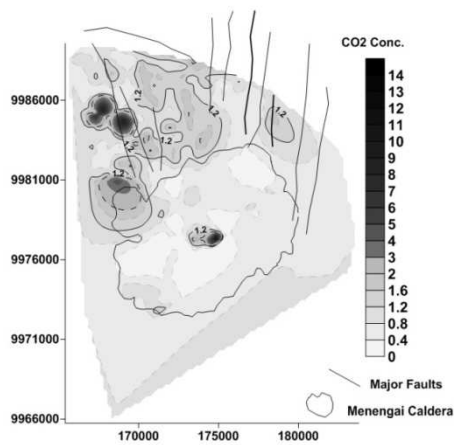

Figure 4: CO2 conc. distributions

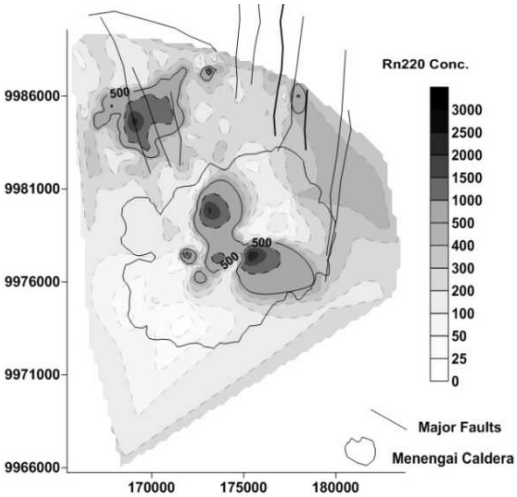

Figure 5: Rn220 conc. distributions

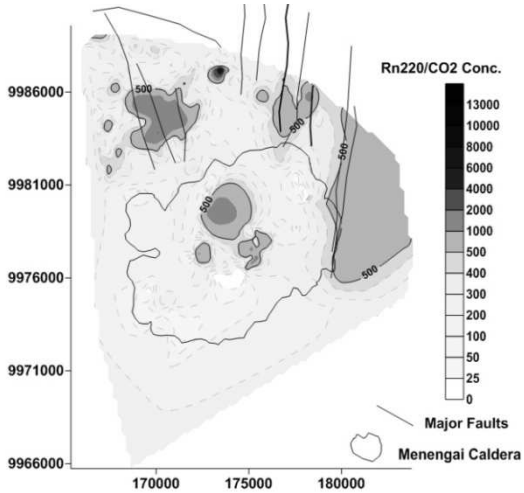

Figure 6: Rn220/CO2 conc. distributions

CONCLUSIONS

Despite the erratic distribution of sampling points, the results from acquired data can be used to make some conclusions relative to the objective. The fumaroles show close relations with geologic structures, which provides means of access for hydrothermal fluids to reach the surface. In the same way, most of the gas anomalies are located in fault zones. CO_2 and Rn_{220} emanations from the presently quiescent faults in Menengai were measured to be higher than background values.

The two fault-lines at Ol'Rongai are considered in this study to be of great importance in geothermal exploration and any future development as it reflects intensity of subsurface permeability in the area, and enhances the confidence to invest. The caldera itself as a geological structure displays a positive evidence of the existence of geothermal resource, with its thermal anomalies that coincides with CO_2 and thoron anomalies. Nonetheless, the picture portrayed by the contours within the caldera is hereby treated with caution as the pond of new lava spread across most part of the floor greatly influenced sampling spaces, and possibility of lateral flow of thermal fluids and diffuse gases at the upper zones restricted by the lava cap cannot be negated.

Generally, CO_2 concentrations are structurally controlled but may have been modified by changes in land use. As seen from the findings, the study of soil CO_2 and Rn_{220} composition as proved to be important geochemical method to identify vertical zones of high permeability. The employment of these methods in other geothermal fields could give important and relatively cheap information for field utilization and development.

ACKNOWLEDGEMENTS

The data used in this study belongs to Geothermal Development Company and some were obtained from KenGen. I acknowledge the two companies. I wish also to acknowledge the management and staff of Geothermal Development Company for their instrumental support during data acquisition and few personnel who helped in the write-up.

REFERENCES

Allard P., Carbonnelle J., Dajlevic D., le Bronec J., Morel P., Robe M.C., Maurenas J.M., Faivre-Pierret R., Martin D., Sabroux J.C. & Zettwoog P. 1991. Eruptive and diffuse emissions of CO2 from Mount Etna. Nature, 351, 387–391.

Bergfeld D., Goff F., Janik C.K. & Johnson S.D. 1998. CO2 Flux Measurements across Portions of the Dixie Valley Geothermal System, Nevada. Geothermal Resources Council Transactions, 22, 20-23.

Chiodini G., Frondini F. & Raco, B. 1996. Diffuse emission of CO2 from the Fossa crater, Vulcano Island _Italy. Bull. Volcanol., 58, 41–50.

Darling W.G., Griesshaber E., Andrews J.N., Armannsson H. and O'Nions R.K. 1995: The origin of hydrothermal and other gases in the Kenyan Rift Valley. Geochim. Cosmochim. Acta, 59, 2501-2512.

Farrar C.D., Sorey M.L., Evans W.C., Howle J.F., Ken B.D., Kennedy B.M., King C.Y. & Southon J.R. 1995. Forest-killing diffuse C02 emission at Mammoth Mountain as a sign of magmatic unrest. Nature 376, 675-678.

Gerlach T.M., Doukas M.P., McGee K.A. & Kessler, R., 1998. Three-year decline of magmatic CO2 emissions from soils of a Mammoth Mountain tree kill: Horseshoe Lake, CA, 1995-1997. Geophy. Res. Lett., 25, 1947-1950.

Giammanco S., Gurrieri S. & Valenza M. 1997. Soil CO2 degassing along tectonic structures of Mount Etna (Sicily): the Pernicana fault. Appl. Geochem., 12, 429–436.

Gislason G. 1989. Terminal Report of Exploration for geothermal energy KEN/82/002, United Nations DTCD.

Hutter A. R. 1993. Thoron/radon (220Rn/222Rn) ratios as indicators of soil gas transport: Geological Society of America Abstracts with Programs, p. A 195.

KenGen 2004. Menengai volcano: investigations for its geothermal potential. A Geothermal Resource Assessment (GRA) project. Internal Report.

Leat P.T. & Macdonald R. 1984. Geochemical Evolution of the Menengai Caldera Volcano, Kenya. U.S Geology Survey. Journal of Geophysical Research, 89, 8571-8592.

Ledoux H. & Gold H. 2005. An Efficient Natural Neighbour Interpolation Algorithm for Geoscientific Modelling. In Developments of Spatial Data Handling by Peter F Fisher. 11th International Sysmposium on Spatial Data Handling, pp. 97-109.

Lopez D.L., Ransom L., Perez N., Hernandez P. & Monterrosa J. 2004. Dynamics of diffuse degassing at Ilopango Caldera, El Salvador. Rose, W.I., Bommer, J.J., López, D.L., Carr, M.J., and Major, J.J. editors, Geological Society of America Special Paper No. 375 “Natural Hazards in El Salvador, pp.191-202.

Magaña M., Lopez D., Tenorio J. & Matus A. 2002. Radon and Carbon Dioxide Soil Degassing at Ahuachapan Geothermal Field, El Salvador. Geothermal Resources Council Transactions, 26, 341-344.

McGee K.A. & Gerlach T.M. 1998. Annual cycle of magmatic CO2 at Mammoth Mountain, California: Implications for soil acidification. Geology, 26, 463-466.

INTERGRATION BETWEEN GEOGRAPHICAL INFORMATION SYSTEM AND SERVICE, APPLICATION AND PRODUCTS CONTRIBUTION TO GEOTHERMAL DEVELOPMENT

James Kimutai
Geothermal Development Company
Taj Towers, 8th Floor, Box 100746-00101, Nairobi, Kenya. jkimutai@gdc.co.ke

ABSTRACT

Countries world over are seeking alternative renewable sources of energy which are cleaner and environmentally friendly. With the accelerated approach of the global climate-change point-of-no-return the need to address the pivotal role of renewable energy in the formation of coping strategies, rather than prevention, is more crucial than ever. Sustainability, green buildings, and the development of the large-scale renewable energy industry must be at the top of all development, economic, financial and political agendas. With estimated potential of over 7,000-10,000 MWe, geothermal energy from Kenya's geologically active Great Rift Valley forms the cornerstone of the government's initiative to realize 2000 MWe by 2018. To be able to achieve this, detailed surface exploration studies need to be conducted to be able to site good producer wells. The findings of the studies are then analyzed and interpreted by use of technologically advanced Information and Communication Systems housed at the Company's Laboratory. ICT systems can also be utilized to provide vital information during drilling at the rig and well testing on real time basis. Such interfaces are developed through proper integration of additional modules on both Geographical Information System (GIS)and the Enterprise Resource Planning software (SAP) to ensure that they are synchronized to communicate in a unified language. This abstract therefore outlays operational benefits of SAP/GIS/SCADA integration with well documented case studies discussed critically to suffice the reader with relevant information.

Some of the key points to be discussed are; (i) Integration dynamics between SAP, DMS, SCADA and GIS technologies in enhancing growth and development of Energy utilities and (ii) Communications network technology is needed to provide and support new operational applications (such as data acquisition and CCTV surveillance), enhancing efficiency and response time.

Keywords: GIS, SAP, WebMethods, EAI, geo-processing

INTRODUCTION

Geothermal Development Company is a newly formed government entity tasked with the responsibility of mining geothermal energy within the greater Rift Valley of an estimated 5000 MWe by 2030 in line with the Government's 2030 Vision. In such a dynamic environment, integration between key ICT systems becomes a necessity to facilitate smooth business flow of operation processes. Thus, integration of SAP, SCADA, DMS and GIS as the base is vital for GDC's core business operations ensuring that it meets its objectives.

In the mining industry, mapping and geography are most important decision making tools owing to factors such as routing, site selection, resource allocation, planning and asset management. GDC's mandate is to explore and mine geothermal potential power sites (GPP) in order to realize affordable and a continuous (renewable) source of power for Kenyans after which centralized power plants will be constructed harnessing power from the distributed wells within a geographical area. To accomplish this, geothermal drillings rigs have been acquired and commissioned in GPP sites lining the greater rift valley with a view of drilling wells generating a combined 400 MWe every year from 2013.

GIS therefore provides the base platform for which operations relating to daily business activities such as asset management, piping, site selection, etc are displayed graphically with their attributes and tools to manage the behavior of the mapped objects. GDC utilizes ESRI ArcGIS products

SAP is an ERP of choice when it comes to managing medium and large sized organizations. It enables businesses to make informed material procurements, generate workflows, monitor Key Performance Indexes (KPI), etc in-line with the company's objectives. SAP provides a unified platform whereby departments (Sales, Procurement, HR, etc) in an organization can access information form a centralized pool ensuring proper management, increased efficiency as well as productivity is achieved.

INFORMATION SYSTEMS AT GDC

GDC has already incorporated information systems in its activities within its short existence that is vital for its core business operations. However, much remains to be done with most of the information systems yet to be commissioned. Despite the setback, clear road maps have been identified and set in play that categorically covers all the information systems that the company intends to acquire for its activities.

GIS

GDC has implemented GIS for mapping and geographical work. The software (ESRI ArcGIS) is used quite extensively by the company's scientist in mapping potential well sites as well as displaying the topographical landscape of an area for routing purposes.

ERP (SAP)

The company chose to implement SAP due to its accommodative nature in mining operations. The modules selected by the company include:

Financial Modules

- FI (Financial Accounting) – Accounting and Financial processes
- AA (Asset Accounting) – Deals with Asset Management
- FM (Funds Management) – Manage funds in line with approved Budgets
- CO (Controlling) –

Logistical Modules

- PM (Plant Maintenance) – Used by Maintenance departments to run their activities and dispatch their work schedules with regards to mining and other related operations
- PS (Project System) – Used to manage large projects (water, mining, etc) and industrial projects
- MM (Material Management) – Used to facilitate procurement of materials with regards to forecasted demands, etc.

Human Resource Module

- HR-PA (Human Resources – Personal Administration) – Assists in the daily operation of the work-processes of the department such as payroll duties, leave days, Medicare, etc)

SCADA and DMS

SCADA (Supervisory Control and Data Acquisition) is yet to be commissioned. It is a real time data management system that will be used to remotely control the functioning of equipments on the Reservoir tanks. The SCADA system stores the needed information (readings of the level of water towers, pumps, valves, piping data, etc) that assists in decision making. It also has an alarm feature which it generates when certain unfavorable conditions are met and thereby warns SCADA administrators via email, sms, etc.

SCADA systems (4th generation) run on an Ethernet/IP architecture of a WAN nature that could be on WIMAX or Broadband depending on the company's infrastructure level DMS (Document Management Service)

BENEFITS OF INTEGRATION

Integration of the systems (GIS/SAP) allows a user to visualize the output of both systems on a single view rather than to switch back and forth between the systems. Data between the two systems is correlated enabling decision making process easier and more effective.

- Increases operational efficiency as it assists in identification of shortest map routes to working areas displayed as polygons on the maps
- Facilitates effective asset manageability and resource utilization through accurate deployment of staffs/crew based on the generated work order to the exact location as displayed on the map
- Enhances decision making process with the user being able to accurately access information from both systems on a single view
- Increases productivity by providing browser based access to GIS and SAP based assets, maintenance and customer information

METHODS OF INTEGRATION

ESRI and SAP, industry leaders of GIS and ERP respectively have identified five main technical ways of performing the integration. The interfaces are:

- SAP RFC Connectors – Remote Function Calls (RFC) allows for remote calls between SAP and any other software such as ESRI GIS as well as Basic Application Programmable Interfaces (BAPIs).
- Third Party Connectors – Include iWAY Control Broker from information builders which is component based and facilitates direct connection to packaged and backend legacy systems. Easy to deploy, no additional middleware and high performance.

- Third Party EAI (Enterprise Application Integration) – Combination of platforms, business processes, standards and applications that result in seamless integration of two or more enterprise systems. EAI platform for SAP and GIS can be utilized where there are non-standard processes that require custom development.
- SAP Exchange Infrastructure XI– EAI software used to facilitate exchange of information between SAP and ESRI GIS through mediating between entities with varying requirements with regards to format, connectivity and protocol.
- Pre-Packaged Solutions – Solutions such as IMPRESS facilitate integration of SAP and ESRI GIS through providing bundled solutions that limit custom development opportunities. This interface is best considered for data consistency, synchronicity and data linking. Another fully supported solution is SICAD-APX developed by AED-SICAD that is cost efficient for small and middle sized companies.

FACTORS FOR CONSIDERATION

- Identifying Workprocesses/Business process requirements resulting from GIS/SAP link
- Type of data exchange technology already adopted by the organization (third party integrators, application integrators, etc)
- Current/Available technology based on SAP modules to be incorporated
- Vendor recommendation on best integration method
- Corporate procedures in relaying business information either on real-time basis or using previously prepared reports.

It is worth noting that the integration methods that do involve further development of the software may result in additional costs from consultations and maintenance not to mention time consuming. Rapidly deployed integration methods may be expensive to purchase but cheaper in the long run.

CHALLENGES FACED IN GIS-SAPLINK

- **Security Permissions -** The challenge here would be to allow authorized users access to data on either system without many security login screens. The SAP Logon ticket should be the default gateway for access when calling SAPGui which will make the process straightforward and user friendly
- **Client-Server Application/Browser Application –** SAP runs on client-server environment and ESRI GIS runs on browser environments, which are technically different therefore resulting in security and application issues. One of the ways to circumvent these issues is by working on an intranet environment which offers fair amount of security.

INTERGRATION OBJECTS

SAP and GIS modules use different object identifiers with a certain format. GIS uses polygons, lines and points to represent an object. Thus when performing the integration, the business identifier in GIS could match up with SAP easily as it provides a lot of flexibility and the process can be initiated during system development.

Some of the elements of SAP that can be linked with GIS include:

- Plant Maintenance (Work & Maintenance orders)
- Locations (Pipelines, Pumping stations, Plants, Rigs)
- Equipment (Valves, etc)
- Health care

CASE STUDIES

GIS/SAP – Plant Maintenance

GDC already has four rigs deployed and by Year 2012, it is anticipated that there will be a total of twelve rigs. This represents a lot of related work such as piping networks for every area (Suswa, Menengai, Longonot, Menengai, etc), pump stations, etc. As a result, a lot of work orders and maintenance orders arising from scheduled maintenance or breakdowns will be generated using SAP PM Module and every order will be identified through a unique number that correlates with the activity and in sequence (Figure 1). Orders for large project will be generated using SAP PS module and identifier recorded in sequence too.

In this scenario, GDC will utilize a pre-packaged solution and in particular IMPRESS software to link GIS desktop tools with SAP PM hence allowing planners to schedule work orders and view maintenance history live from GIS. IMPRESS software will be used to create data mapping between SAP PM functional location and

GIS identifier for pipelines, valves, pumping stations, etc. The identifier also has a unique connection number that is represented as an attribute of the connection feature.

IMPRESS Geo I. Application a module of IMPRESS software will be used for the data mapping activities offering additional functionalities such as process scheduling and email alerts to support persons.

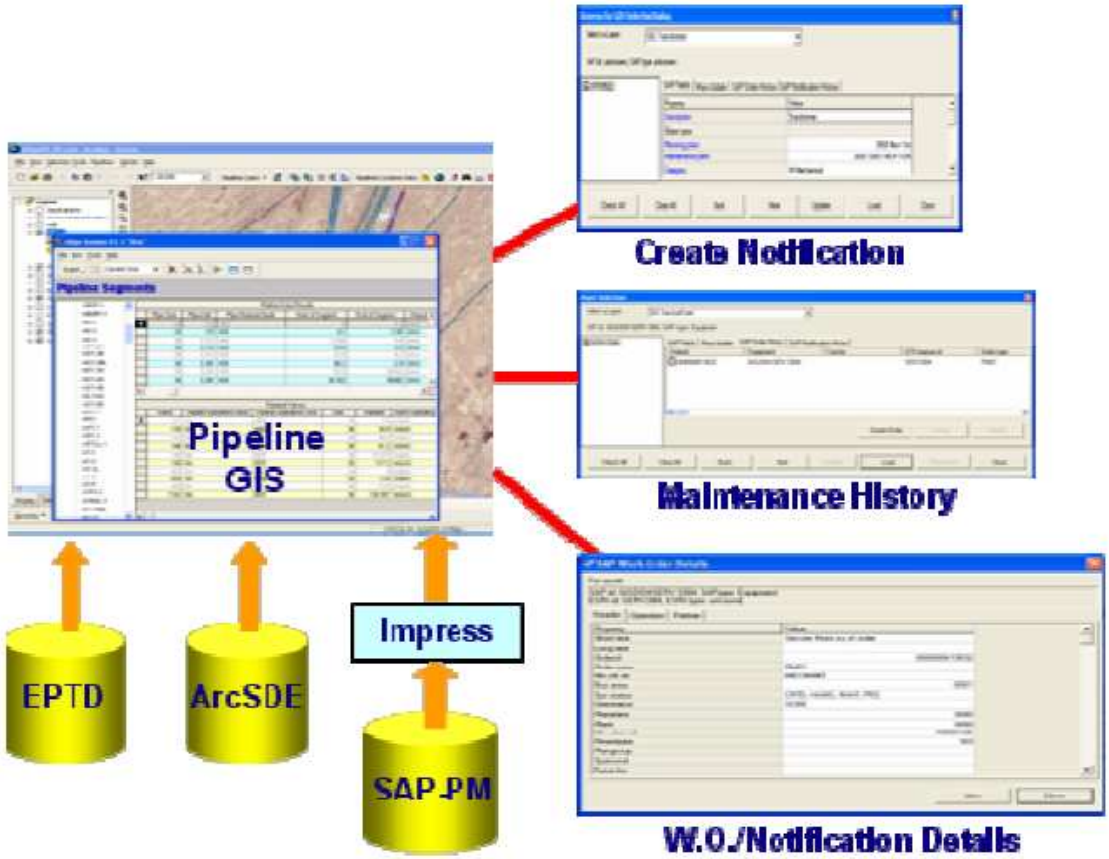

Figure 1: SAP/GIS Integration Using SAP PM Module. Source: Saudi Aramco Co.

GIS/SAP – Functional Locations

GDC has a lot of infrastructure in various regions of the country. These are office buildings, pumping stations, water reservoirs, rigs, and well-heads which in SAP are represented as **Work Area** which is a location of a work site. These elements are also represented in GIS and so the link with SAP can be generated by adding the work area ID as a feature attribute.

GIS spatial analysis feature will be used to identify parent polygons which will be classified as work areas and the data is sent back to SAP in real time. These will save a lot of time that would have been used to generate look-up-tables of work area in SAP. For this case an ArcIMS based GIS web application program will be used to design graphically the work areas with the assistance of ArcSDE Java API's online. A batch process will be triggered calling a Web function method to generate a work area in SAP once polygon is loaded in the geodatabase. The web function method calls to be developed will include create, delete, update, identify parent area, etc. Also a simple map viewer will also be embedded in SAP interface which will allow users to view the work areas instead of having to switch from system to system to verify location which safeguards data integrity during data entry.

GIS/SAP Healthcare

GDC has a staff capacity of about five hundred and is set to increase to one thousand by year 2011. The staffs are situated at various parts of the country and the healthcare system in place processes requests from main office.

The integration of SAP with GIS allows users to track and manage communicable and epidemic diseases of the company employees granting management the ability to accurately analyze the distribution of the diseases based

on a GIS map superimposed upon the base map in SAP (Figure 2). The analysis tools provided in the application allows color coding of the service area polygons by disease type, data range and patient location by work or residence.

A batch process will have to be developed which will push data from SAP HealthCare Master Data to GIS database on a scheduled basis using a Web Method Function calls which will write data into the Database. This process will assist in staff planning and deployment averting crises related to epidemic.

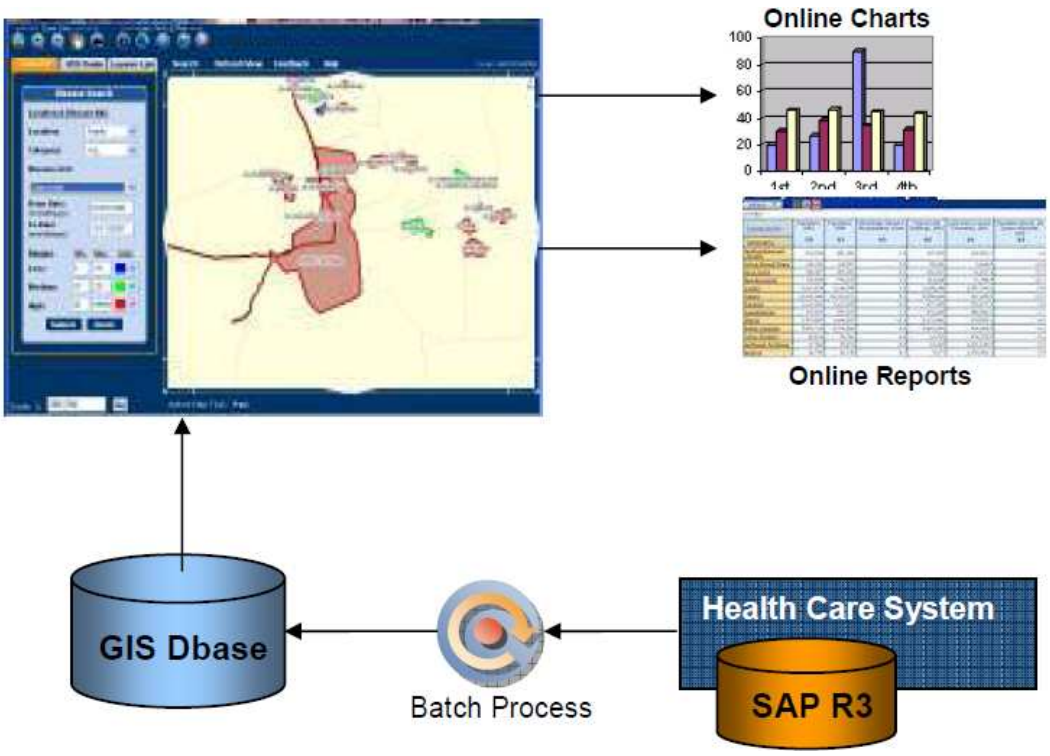

Figure 2: GIS/SAP Integration Displaying Healthcare System Using SAP R3. Source: Saudi Aramco Co

CONCLUSION

Enterprise services are beneficial when system integration is implemented correctly. With adoption of web services become the norm, the functionality of the systems broadens. As vector data is increasing in GIS, more analysis possibilities become available, supporting management in the decision making process. The myriad of possibilities GIS has to offer is not only restricted to network management, but can also perform thematic applications. Keyword for the future is further integration, respecting every information systems qualities and specific functionalities, but making this massive amount of information quickly available to the users via an intuitive connection between information systems.

REFERENCE

Best Practices Using GIS and SAP, Steve Benner, ESRI August 2007

Interfacing ESRI GIS to SAP R/3, ESRI Literature, ESRI June 1999

SUCCESSFUL USE OF HYDROTHERMAL ALTERATION MINERALOGY IN APPRAISING A GEOTHERMAL RESERVOIR: CASE STUDY: OLKARIA DOMES GEOTHERMAL FIELD, KENYA

John Lagat
Geothermal Development Company Ltd, P. O. Box 1770 Nakuru, 20100
E-mail: jlagat@gdc.co.ke

ABSTRACT

Three geothermal exploration wells OW-901, OW-902 and OW-903 were drilled in Olkaria Domes field to evaluate its geothermal potential. The three wells were drilled to a depth of 2200 m and all encountered a high temperature system and discharged on test. Completion tests and hydrothermal alteration mineralogy indicated a cold zone between 900-1150 m in all the three wells. Permeability of the wells was low compared to wells drilled in the neighbouring Olkaria East and Olkaria North East fields hence low productivity. The analyses of well completion tests and alteration mineralogy indicted that the resource was deeper compared to the other fields in Olkaria. Six appraisal wells OW-903A, OW-904A, OW-905A, OW-906A, OW-907A and OW-908 were recommended to delineate the geothermal reservoir and also site the best localities to drill production wells. Deep casing set at 1200 m recommended from the exploration wells studies for the appraisal wells was successfully, with the cold zone being isolated completely. Directional drilling was able to intersect the faults and fractures thus enhancing permeability and average production in the field increased from 2.5 MWe to 8 MWe per well, with the highest producer being over 14 MWe. Deep drilling to 3000 m was able to tap the deeper aquifers. Alteration mineralogy studies from the six appraisal wells were able to delineate the field and currently production drilling is underway to provide enough steam for a 140 MWe power plant. This paper therefore discusses the successful use of hydrothermal alteration mineralogy in to optimize the geothermal resource in Olkaria Domes field.

Key Words: Rift, Olkaria-Domes, Geothermal, Alteration

INTRODUCTION

The Greater Olkaria geothermal area is situated south of Lake Naivasha on the floor of the southern segment of the Kenya rift (Figure 1). The Kenya rift is part of the East African rift system that runs from Afar triple junction at the Gulf of Eden in the north to Beira, Mozambique in the south. It is the segment of the eastern arm of the rift that extends from Lake Turkana to the North to Lake Natron, northern Tanzania to the south (Figure 1). The rift is part of a continental divergent zone where spreading occurs resulting to the thinning of the crust hence eruption of lavas and associated volcanic activities.

The Greater Olkaria geothermal area is within the Greater Olkaria volcanic complex. It is subdivided into seven fields for geothermal development purposes namely Olkaria East, Olkaria Northeast, Olkaria Central, Olkaria Northwest, Olkaria Southwest, Olkaria Southeast and Olkaria Domes (Figure 2). Olkaria East field (Olkaria I) has been producing power since 1981 when the first of the three 15 MWe units was commissioned. The current generating capacity of the field is 45 MWe. Olkaria Northeast field (Olkaria II) is generating 70 MWe and an additional 35 MWe is under construction and is expected to be commissioned in 2010. Olkaria Northwest field (Olkaria III) which is being developed by an Independent Power Producer (IPP) was commissioned in 2009 and is currently producing 55 MWe. The rest of the fields are at various exploration stages. This paper therefore discus the results obtained from the analysis of samples recovered from the exploratory, appraisal and production wells drilled in the Olkaria Domes field, which is the field earmarked for development as Olkaria IV with an expected 140 MWe.

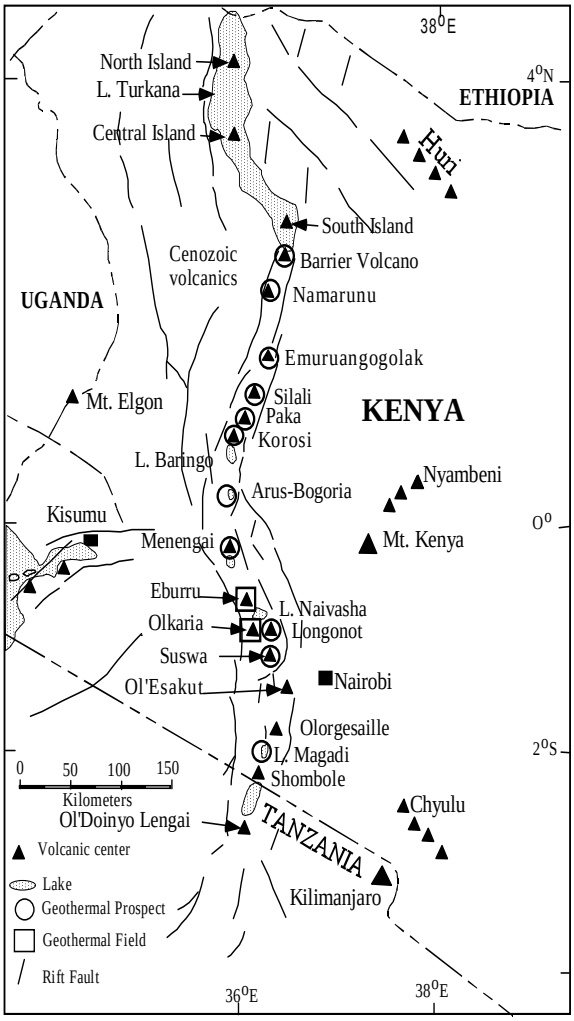

Figure 1: Map of the Kenya rift showing the location of Olkaria geothermal field.

OBJECTIVES OF THE STUDY

1. To identify the rocks and thereby understand the stratigraphy.
2. To identify the hydrothermal alteration minerals found in the field.
3. To determine the general location of the wells with respect to the upflow, outflow and the marginal zones of the system
4. Determine the appropriate casing depths in the field.

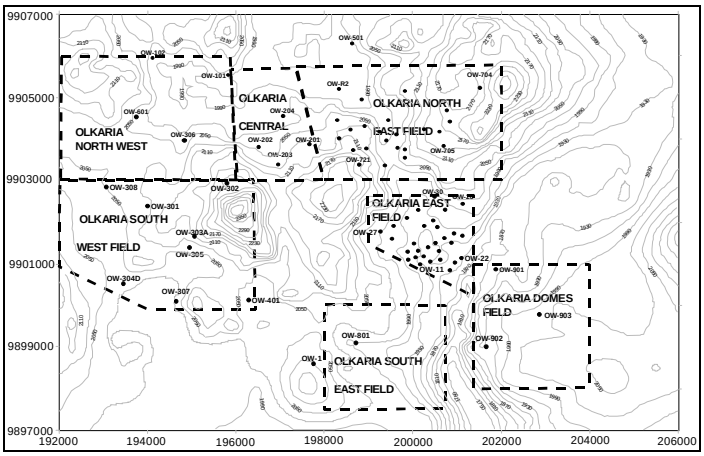

Figure 2: Map of the Greater Olkaria geothermal area showing the location of the fields.Geology

GEOLOGY

Geology of Olkaria volcanic complex

The Greater Olkaria volcanic complex is characterized by numerous volcanic centers of Quaternary age and is the only area within the Kenya rift with occurrences of comendite on the surface. Other Quaternary volcanic centers adjacent to Olkaria include Longonot volcano to the southeast, Suswa caldera to the south, and the Eburru volcanic complex to the north. Whereas the other volcanoes are associated with calderas of varying sizes, Olkaria volcanic complex does not have a clear caldera association. The presence of a ring of volcanic domes in the east and south, and southwest has been used to invoke the presence of a buried caldera (Clarke et al., 1990, Mungania, 1992).

Magmatic activity associated with Olkaria volcanic complex commenced during the late Pleistocene and continues to Recent as indicated by Ololbutot comendite, which has been dated at 180±50 yrs B.P using ^{14}C from carbonized wood obtained from a pumice flow associated with the lava (Clarke et al., 1990).

The litho-stratigraphy of the Olkaria geothermal area as revealed by data from geothermal wells and regional geology can be divided into six main groups; namely Proterozoic "basement" formations, Pre-Mau volcanics, Mau tuffs, plateau trachytes, Olkaria basalt and Upper Olkaria volcanics (Omenda, 2000).

Structures in the Greater Olkaria volcanic complex

Structures in the Greater Olkaria volcanic complex include; the ring structure, the Ol' Njorowa gorge, the ENE-WSW Olkaria fault and N-S, NNE-SSW, NW-SE and WNW-ESE trending faults (Figure 3). The faults are more prominent in the East, Northeast and West Olkaria fields but are scarce in the Olkaria Domes area, possibly due to the thick pyroclastics cover. The NW-SE and WNW-ESE faults are thought to be the oldest and are associated with the development of the rift. The most prominent of these faults is the Gorge Farm fault, which bounds the geothermal fields in the northeastern part and extends to the Olkaria Domes area. The most recent structures are the N-S and the NNE-SSW faults. Hydroclastic craters located on the northern edge of the Olkaria Domes area mark magmatic explosions, which occurred in submerged country (Mungania, 1992). These craters form a row along where the extrapolated caldera rim trace passes.

Dike swarms exposed in the Ol' Njorowa gorge trend in a NNE direction further attesting to the recent reactivation of faults with that trend. The development of the Ol' Njorowa gorge was initiated by faulting along the trend of the gorge but the feature as it is known today was mainly due to catastrophic outflow of Lake Naivasha during its high stands (Clarke et al., 1990). Volcanic plugs (necks) and felsic dikes occurring along the gorge further attests to the fault control in the development of this feature. Subsurface faults have been encountered in most Olkaria wells (KenGen, 2000). The wells encountered drilling problems when these faults were dissected due to cave-ins and loss of drilling fluids and cement. Materials recovered from these zones were mainly fault breccia.

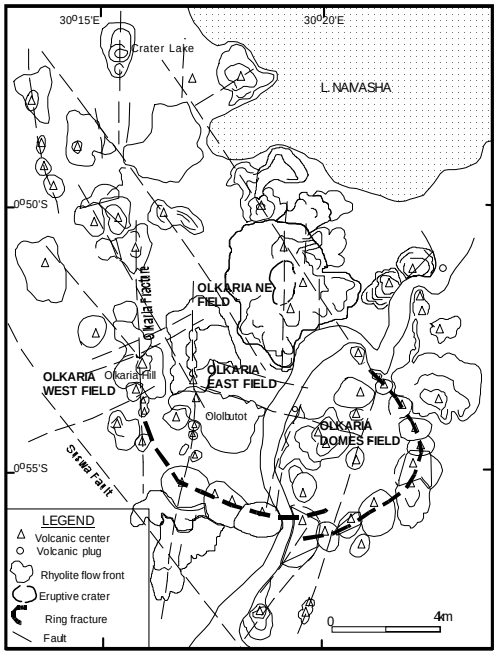

Figure 3: The volcano tectonic map of the greater Olkaria volcanic complex showing the structures in the area.

SAMPLING AND ANALYTICAL METHODS

Cuttings samples from Olkaria Domes wells were taken at every 2 m interval. Very few and unrepresentative cores were cut in Olkaria Domes field and therefore nearly all the descriptions and interpretations are based on cuttings samples. Binocular analysis of the cuttings samples was done using the Wild Heerbrugg binocular microscope. A sample is scooped from the sample bag into a petri dish and washed with clean water to remove impurities and dust. Wetting the cuttings is necessary to enhance visibility of samples and obscure features such as finely disseminated sulphides e.g. pyrite.

Representative samples from all the lithologic units encountered in wells were selected and thin sections prepared for petrographic studies. The thin sections were analyzed using the Leitz Wetzler petrographic microscope.

The X-ray Diffractometer is used to identify individual minerals especially clays. Samples were selected from all the lithologic units and analysed for clays. The <2 microns fractions were prepared for X-ray diffraction by crushing the rock into fine powder and dissolving in a test tube half full of distilled water. The test tube is left in a rack so that the <2 microns phylosilicates are left in suspension. A few drops are placed in marked glass slides and left to dry so that the sample can be run using the XRD machine. A Shimandzu 6000 Diffractometer, with CuKα radiation (at 40 kV and 50 mA), automatic divergence slit, fine receiving slit, and graphite monochrometor was used for the analyses.

RESULTS

Lithology

The drilled lithological column in Olkaria Domes field is composed of unconsolidated pyroclastics that are dominant in the shallow levels overlying a volcanic sequence whose lithological composition is dominated by comenditic rhyolite, trachyte, basalt, tuff and some granitic and syenitic dykes. Below is a brief description of the lithology, The drilled lithological column in Olkaria domes is composed of unconsolidated pyroclastics that are dominant in the shallow levels overlying a volcanic sequence whose lithological composition is dominated by comenditic, rhyolite, trachyte, intrusives and basalt (Lagat 2007, Lagat 2008, Lagat 2009). Petrochemical analysis indicates that most rocks from Olkaria domes plot in the region of rhyolite, trachyte and basalt. A summary descriptions of the lithologic units encountered in the Olkaria domes are as follows.

Pyroclastics

The pyroclastics are yellowish to brown and form the upper pats of Domes field. The rock unit is unindurated and consists of lithic fragments of rhyolite, trachyte and ash. The formation is mostly unconsolidated matrix dominated by ash size particles, crystals of glass, quartz, feldspars, amphiboles, obsidian and pumice.

Tuffs

The tuffs are brownish grey, grey to white in colour and occur in two types; the glassy and the fragmental tuff. The glassy (vitric) tuff is wholly glassy whereas the fragmental tuff is made up of lithics of lava fragments as well as subhedral to anhedral crystal lithics of quartz and feldspars.

Rhyolites

Rhyolites are of two types; (i) the granular non-porphyritic to quartz and sanidine porphyritic with abundant riebeckite and occasional hornblende and (ii) the spherulitic rhyolites with bands of volcanic glass enriched with quartz and feldspar crystals. The first type is light grey to brownish grey in colour, mainly comenditic and occurs at shallow depths and the second type occurs at depth.

Trachytes

Trachyte occurs alternating with tuff, basalt and rhyolite and is the dominant rock type, with minor tuff intercalation at greater depths. The rock is grey to brownish grey, fine grained and is composed of phenocrysts of sanidine, arfvedsonite-riebeckite, and aegirine. The matrix consists of flow oriented feldspar microlites in a fine grained to glassy groundmass. Sanidine crystals are the most common phenocryst and occur in crystals measuring up to 5 mm.

Basalts

Basalt is light greenish grey to black, with holocrystalline groundmass composed of plagioclase laths and anhedral clinopyroxene and magnetite. It is porphyritic with plagioclase phenocrysts, some of which are zoned, clinopyroxene and glomeroporphyritic clots of pyroxene. Olivine occurs in unaltered basalts, but at depth the mineral has undergone metasomatism and its presence is revealed by the crystal outline of the alteration products.

Hydrothermal alteration

In the Olkaria Domes geothermal field, hydrothermal alteration minerals appear both as replacement of the primary minerals, as well as fillings in vesicles, vugs and fractures. Factors that influence the distribution and kind of mineral assemblages present in hydrothermal systems include permeability, rock and water composition, temperature, pressure and duration of hydrothermal alteration (Browne and Ellis, 1970). These factors are largely independent, but the effects of one or more of the factors can exert a dominant influence in the location and extent of hydrothermal alteration. Permeability of the rocks controls the access of thermal fluids, which cause hydrothermal alteration of the rocks and precipitation of secondary minerals in open spaces. The chemical composition of the host rock determines the availability of components to form alteration minerals as well as possible fugitive components from the presumed magmatic heat source. Temperature is the most significant factor in hydrothermal alteration because most of the chemical reactions require elevated temperatures and also minerals are thermodynamically stable at high temperatures. Pressures at the depths penetrated by Olkaria Domes drill holes, like in other geothermal fields elsewhere in the world are not sufficient to greatly affect hydrothermal alteration minerals transformation (Browne and Ellis, 1970).

Although hydrothermal alteration has changed the primary minerals in different ways and magnitude, often the original textures and minerals are still recognizable. The main hydrothermal minerals in Olkaria Domes field are albite, amphibole (actinolite), biotite, calcite, chlorite, chalcedony, epidote, fluorite, garnet, illite, K-feldspar (adularia), mordenite, secondary Fe-Ti oxides, sulfides (pyrite), titanite (sphene) and quartz. In addition, minor amounts of wairakite and prehnite are present. Mineral associations in vesicles are common and consist of two or more of the following minerals; chlorite, quartz, calcite, epidote and pyrite with the paragenetic sequence varying with depth and from one well to another. Table 1 below shows the primary minerals observed in Olkaria Domes geothermal field and their alteration products.

Table 1: Primary minerals, order of replacement and alteration products of Olkaria Domes volcanics (modified from Browne, 1984a)

Primary phases	Alteration products
Volcanic glass	Zeolites, clays, quartz, calcite
Olivine	Chlorite, actinolite, hematite, clay minerals
Pyroxenes, amphiboles	Chlorite, illite, quartz, pyrite, calcite
Ca-plagioclase	Calcite, albite, adularia, quartz, illite, epidote sphene
Sanidine, orthoclase, microcline	Adularia
Magnetite	Pyrite, sphene, haematite

Distribution of hydrothermal alteration minerals

The distribution of hydrothermal alteration minerals in Olkaria Domes show that at shallow depths, low temperature phases occur with mainly silica, smectite, calcite, zeolites, phyllosilicates, oxides and sulphides being the alteration minerals present. In the deeper parts of the wells, however, hydrothermal alteration to ranged from high to extensive. Hydrothermal zeolites, calcite, epidote, phyllosilicates, silica, sulphides, epidote, albite, adularia, biotite, garnet, fluorite, prehnite, oxides and titanite are the alteration minerals observed. The hydrothermal alteration mineralogy patterns show prograde alteration with increase in temperature and depth with the low temperature phases disappearing as the high temperature phases appear.

Case study wells

Well OW-905A

Well OW-905A was drilled as an appraisal well in Olkaria Domes field. The rock types encountered consist of rhyolite, tuffs, trachyte, basalt and syenitic intrusives at depth. The rocks at shallow depths exhibit little or no hydrothermal alteration at all with mainly smectite silica, calcite, clays, oxides and pyrite being the alteration minerals present. Smectite a low temperature clay occurs from the surface to 1494 m depth, indicating temperatures of <200ºC above that depth. First occurrence of crystalline epidote was encountered at 1362 m indicating expected formation temperatures below this depth is >250ºC Unlike the nearby wells OW-904A and OW-903A where biotite and actinolite were encountered at depth, it was conspicuously absent in this well indicating probable formation temperatures of <300°C. Deeper casing therefore managed to isolate the low temperature zones, however when the well was discharge tested, it produced low pressure steam. Hydrothermal alteration mineralogy indicates that the well is at the resource boundary. This well is drilled N90°E and the next well to be drilled in the sector, OW-907A had to be drilled at N150°E and is a good producer (7 MWe).

Hydrothermal alteration mineralogy was therefore successfully used to set the production casing in this well and determine the boundary conditions.

Well OW-910A

Well OW-910A was drilled as a production well in Olkaria Domes field. The rocks at shallow depths exhibit little or no hydrothermal alteration at all with mainly smectite silica, calcite, clays, oxides and pyrite being the alteration minerals present. Smectite occurs from the surface to 680 m depth, indicating temperatures of <200ºC above that depth. Appearance of chlorite and illite below 680 indicate temperatures of over 220ºC. First occurrence of crystalline epidote was encountered at 820 m indicating expected formation temperatures >250ºC below this depth. In this well, the casing initially was to be set at 1200 m, but after careful study of hydrothermal mineralogy patterns, the well was cased at 850 m depth. The well is a good produces with an output of 12 MWe. Hydrothermal alteration was therefore successfully used to set the production casing in this well.

DISCUSSIONS

In any geothermal system, there is always some uncertainty whether observed minerals distribution reflect current formation temperatures or are related to some previous thermal events or regimes. In the Greater Olkaria geothermal area as in other geothermal fields throughout the world, hydrothermal alteration minerals are important indicators of subsurface thermal changes. Index minerals used to construct determine parameters in Olkaria domes include smectite, chlorite and crystalline epidote with stability temperatures of <200ºC, <220ºC and >250ºC respectively. Hydrothermal alteration mineralogy can be a cheaper way of determining the subsurface conditions of a geothermal well during drilling where decisions have to be made real time.

CONCLUSIONS

1. The Lithology of Olkaria Domes is made up of pyroclastics, tuff. Rhyolite, trachyte, and Basalts.
2. Stable formation temperatures of epidote, smectite and chlorite are <200ºC, >220ºC and >250ºC respectively.
3. Hydrothermal alteration has been used successfully to set production casing and also delineate the Olkaria Domes field.

REFERENCES

Browne, P. R. L., 1984: Subsurface stratigraphy and hydrothermal alteration of Eastern section of the Olkaria geothermal field, Kenya. *Proceeding*, 6th New Zealand Geothermal Workshop, Geothermal Institute, Auckland, 33-41.

Clarke, M. C. G., Woodhall, D. G., Allen, D. and Darling, G., 1990: Geological, volcanological and Hydrogeological controls of the occurrence of geothermal activity in the area surrounding

Lagat, 2007: Geological report of well OW-905A. KenGen Internal report

Lagat, 2008: Geological report of well OW-907A. KenGen Internal report

Lagat, 2009: Geological report of well OW-910A. KenGen Internal report

KenGen, 2000: *Conceptualized model of Olkaria geothermal field*. Compiled by Muchemi G. G. The Kenya Electricity Generating Company Ltd internal report p. 13

Mungania, J., (992: *Preliminary field report on geology of Olkaria volcanic complex with emphasis on Domes area field investigations*. Kenya Power Company internal report.

Omenda, P. A., 2000: Anatectic origin for Comendite in Olkaria geothermal field, Kenya Rift; Geochemical evidence for syenitic protholith. *African Journal of Science and Technology. Science and Engineering series*, Vol. 1, 39-47.

A PROTO-VOLCANIC MARGIN ALONG THE ASAL RIFT. THE MAKARASSOU FAULT SYSTEM, DJIBOUTI.

Bernard Le Gall[1], Mohamed A. Daoud[2] & Joel Rolet[1]
1Université Européenne de Bretagne, Université de Brest, CNRS; UMR 6538 Domaines Océaniques, IUEM, place N. Copernic, 29280 Plouzané, France.
2Institut des Sciences de la Terre, Centre d'Etudes et de Recherches de Djibouti, B.P. 486, Djibouti Ville, Djibouti.

ABSTRACT

The Makarassou fault system (MFS) is a 40 x 70 km submeridian structure connecting the Asal and Manda Inakir active-recent rift

axes, in Eastern Afar. Its previous interpretation as a transform fault structure is challanged on the basis of new structural field data and interpreted satellite images. The MFS involves 3-1 Ma-old basalts of the Stratoid series which onlapped Dalha basalts in the Asa Gayla plateau to the E, ie. on the southern part of the Danakil range. The overall structure of the MFS is dominated by a westerly-dipping monoclinal flexure, downflexed toward the Asal rift axis. It is further disssected by a dense network of extensional faults, dipping consistently outwards, to the E. Lava dips, as steep as 30°, locally occur in individual highly-rotated fault blocks. The causal mechanims of extensional flexuring along the Makarassou are assigned to isostatic loading caused by the >5 km-thick wedge of Stratoid and Dalha basalts that accummulated since 6 Ma beneath the Asal rift. The inward accummulation of mafic material, together with extensional and flexural strain, both resemble the pattern of Seaward Dipping Reflector Sequences that typically develop along volcanic rifted margins, worldwide. The structural interpretation of the MFS as outlining a nascent volcanic rifted margin along the eastern flank of the Asal-Manda Inakir rifted zone is consistent with available geochemical and geophysical records of the mafic crust flooring the Afar depression.

Keywords: East Afar, Makarassou fault belt, extensional flexure, Stratoid basalts, proto-volcanic margin.

INTRODUCTION

The Afar depression involves a number of large-scale fault-bounded blocks and transfer/transform structures (Barberi and Varet, 1977) that developed since less than 3 Ma, in the onshore prolongation of the Red Sea and Aden oceanic ridges (Fig. 1) (Laughton, 1966 ; Manighetti et al., 1998). One of these transform structures was assumed to lie along the Makarassou fault system (MFS), connecting the Asal and Manda Inakir active rift segments (AMIR) in Eastern Afar (Fig. 1) (Tapponnier and Varet, 1974 ; Courtillot et al., 1974). These early interpretations, based on fault map arrangement, and further compared to results of experimental modelling, are challenged in the present work from new structural data. Interpretation of field-calibrated ASTER satellite images suggest that the 3D-architecture of the MFS shares striking similarities with those of large-scale extensional flexures, typically developed along volcanic rifted margins (e.g. Brooks and Nielsen, 1982 ; Dessai and Bertrand, 1995 ; Geoffroy et al., 1998 ; Klausen, 2009). The new flexural model applied here to the MFS lends further support to the commonly accepted concept of the AMIR axis as forming an embryonic oceanic region (Barberi and Santacroce, 1980 ; Mohr, 1989 ; Dugda and Nyblade, 2006).

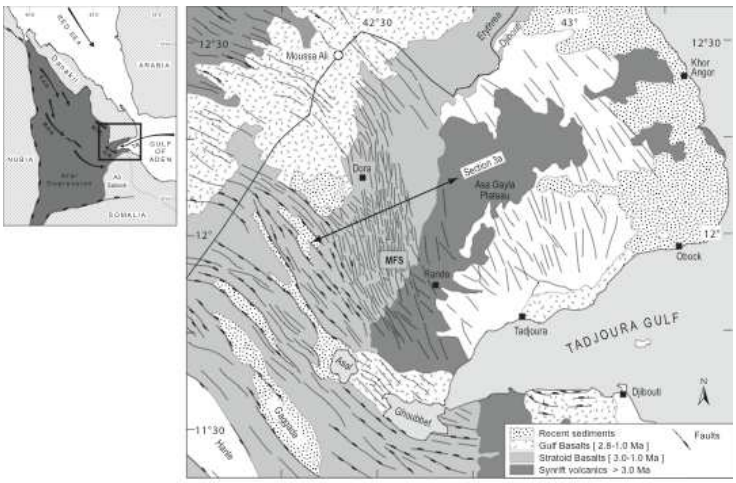

Figure 1: Simplified geological map of the Asal rift and the South Danakil range. The trace of the cross-section in Figure 2a is drawn. Top left inset shows location of Afar Triangle. The unstretched domains during the last 3 Ma are cross-ruled.

Rift context and methodology

On the map and cross-section of Figs. 1 and 2a, the MFS extends as a ca. 70 x 40 km submeridian fault belt that involves the 3.3-1.3 Ma Stratoid Basalts between the Asa Gayla volcanic plateau to the east, and the AMIR subsiding active axis to the west. The Stratoid faulted basalts give way westwards into younger rift volcanics, related to the AMIR disconnected right-stepping subrifts that propagated onshore, in the time-span 900-140 kyr, ahead of the Aden ridge (Manighetti et al., 1998). To the east, the Stratoid Basalts onlap a >800 m-thick pile of little deformed, and slightly tilted, older flood basalts of the 9.0-3.8 Ma Dalha Fm in the Asa Gayla plateau. The latter rest unconformably over 14.7-9.7 Ma Mablas acidic rocks which constitute the bulk of the South Danakil range. Further east, younger volcanic rocks of the Ribta (3.5 Ma) and Gulf Basalts (2.8-1.0 Ma) series lie over part of the coastal plain, at the foot of paleo-fault scarps following the eastern edge of the South Danakil range.

From field-calibrated ASTER satelitte imagery (15m vertical resolution), and corresponding digital elevation models, the structure of the exceptionally well exposed MFS is depicted, both in map-view and on a 25 km-long cross-section through its widest part. Vertical fault displacement is measured as minimum values from surface offsets along individual fault scarps, whilst fault lenghts, deduced from map traces on the ASTER image, are underestimated because of the lost of resolution below 10-15 m of vertical offset. Cumulate extension recorded by the MFS is estimated by summing individual fault heaves along the studied cross-section. Markers for sens of fault displacement have not been observed, because the lower parts of fault scarps are systematically concealed by slope deposits, whereas their exposed upper sections usually follow basaltic columnar jointing that rarely preserves the fault slip plane.

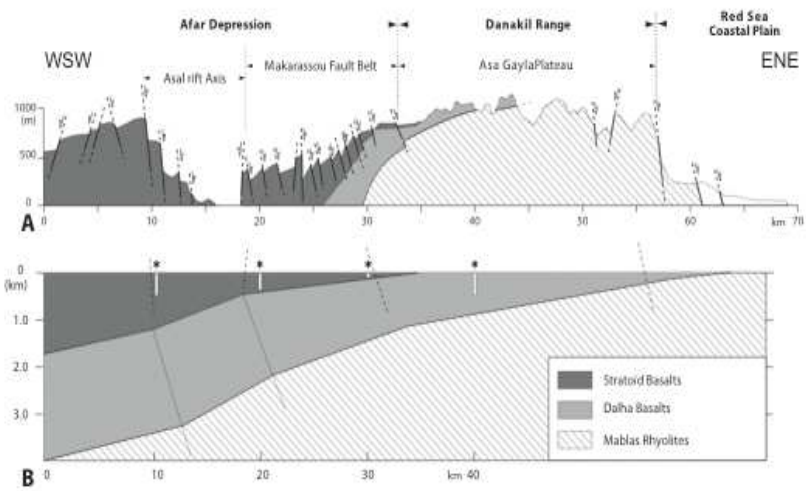

Figure 2: A. Structural section crossing the eastern side of the Afar depression from the Asal rift axis to the South Danakil horst and the Obock coastal plain. The Makarassou fault belt occurs close to the eastern edge of a rifward-thickening flood basalt package, involving the Dalha and Stratoid series. Volcanic thicknesses at depth are extrapolated from exposed sections. Vertical exaggeraration ~10. B. Restored 2D-sectional geometry (prior to extensional faulting) showing the wedge-shaped geometry of the 9.0-1.3 Ma Dalha-Stratoid flood basalt succession.

STRUCTURAL ANALYSIS OF THE MFS

On the DEM in Fig. 1b, the MFS is a fan-shaped fault belt, partly concealed to the NW, in the Dorra plain, by Holocene alluvial sediments and Pleistocene volcanics of the Moussa Ali volcanoe. To the east, the MFS comprises a narrow (20 km-wide) NS-trending belt of closely-spaced and colinear faults that swing counterclockwise to the NW, towards the Moussa Ali volcanic center, whilst merging into N130°-oriented Asal-type faults to the south. Fault strike rotates slightly (<10°) counterclockwise in the western part of the MFS, concomitantly to increasing fault spacing. There, wider fault-bounded blocks sharply cut, and thus post-date, N130°E Asal-type horst-graben structures extending continuously further west in the AMIR domain.

The 25 km-long structural cross-section in Fig. 2a cuts at high angle the MFS in its central part. It exhibits a westerly-dipping monoclinal flexure that lowers the exposed surface of the Stratoid Basalts to about 900 m, from the Asa Gayla plateau down to the Alol rifted zone to the west, with a regional dip of ~10°. The westerly-facing warp is dissected by a dense network of extensional faults, facing dominantly to the east (27 over a total of 38 faults), with an average dip of 70-80° (Fig. 3a). Their nearly consistent outward attitude (with respect to the Asal rift axis) is the most significant attribute of the entire MFS network. Antithetic faults, and associated

asymmetric horsts structures are present at the two extremities of the cross-section, and those occurring to the west, i.e. in the fan-shaped faulted subdomain, are Asal-type N130°E structures. Monoclinal flexuring is strictly focused on a 15 km-long high density fault section, enclosing a network of closely-spaced extensional faults, dipping exclusively to the east (F_{9-25}). The width of the resulting faulted blocks increases westwards from 480 m (F_{9-18}) to 700 m (F_{18-25}) (Figs. 3a and 4). Lava dips, as steep as 30° in highly rotated individual blocks (Fig. 3a), contrast with the regional dip of 10° of the envelop surface.

The spatial association of high tilt angles and closely-spaced faulted blocks typically characterizes high-strained extensional zones. Assuming that flexuring along the MFS took place at a late stage of the 900-140 kyr period (see above), in agreement with the involvement of <0.9 Ma-old volcanics of the Moussa Ali edifice (Piguet and Vellutini, 1991) into the curved extremity of the MFS to the north, indicates a minimum long-term cumulative extension rate of ca. 6 mm/yr. The finite geometry of the MFS thus results from the conjugate effects of large-scale flexuring an outward-verging extensional faulting, which are both characteristic structures of nascent volcanic margins. That leads us to discuss the tectonic *versus* isostatic origin of flexuring and associated structures along the MFS, as classically addressed about most volcanic rifted margins worldwilde.

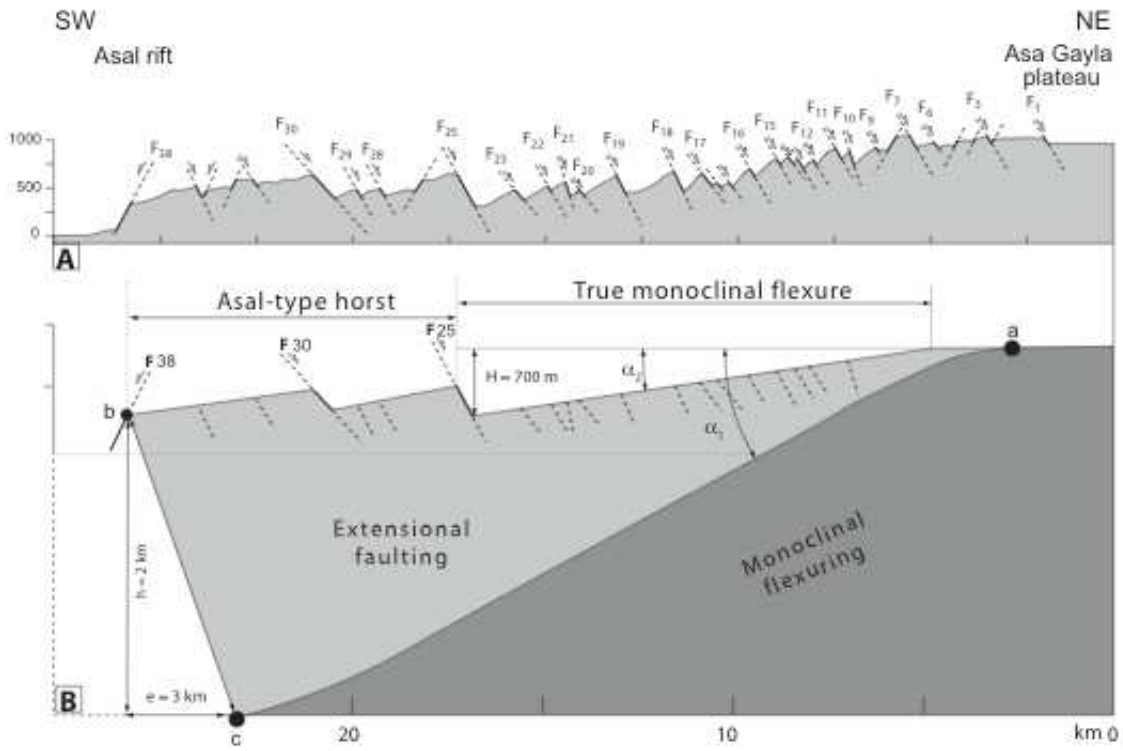

Figure 3: A. Structural cross-section of the Makarassou fault belt showing inward-dipping Stratoid blocks, arranged in a domino style, and bounded by a network of closely-spaced extensional faults dipping dominantly inward, toward the Asal rift axis. Numbers refer to individual faults identified from ASTER data interpretation. B. Structural sketch illustrating the respective role of flexuring and faulting during the development of the MFS on the eastern side of the Asal rifted zone. The envelop surface of the exposed Stratoid Basalts is used as a reference. Extensional faulting resulted in (1) the shallowing (estimated at 2 km) of the downflexed surface (from AC to AB) and (2) nearly 3 km of cumulate extension.

CAUSAL MECHANISMS OF THE MFS FLEXURE

The volcano-stratigraphic cross-section in Fig. 2b shows the restored architecture of the Dalha and Stratoid trap series, prior to the Makarassou flexuring event. The two basaltic successions are seen to thicken dramatically westwards through the South Danakil-Asal transition zone. The thickness of the Dalha Basalts increases from ca. 200 m in the coastal plain, up to >800 m over the Asa Gayla plateau, and > 1 km in the Doubye rift axis, north Asal (Vellutini, 1990). A much thicker sequence of Dalha Basalts might have once floored the Afar depression further west, in relation to a marked thinning of the Afar lithosphere in the time-period 8-3 Ma (Vellutini, 1990). Thickness distribution of the Stratoid basaltic cover also varies from a few 10's m on the western flank of the Asa Gayla plateau, up to >100 m throughout the MFS, >250 m north of the Asal rift (Gasse et al., 1985), and >1300 m in Central Afar (Barberi and Varet, 1975).

A wedge-shaped volcanic succession, >2-3 km thick, is thus assumed to have accumulated in the time range 9.0-1.3 Ma, at the transition between the proto-South Danakil horst and the Asal trough. It cannot be definitely ascertained whether the thickest volcanic accummulation, and corresponding attenuated and/or underplated crust at depth, were focussed along the AMIR and Manda Hararo axial ranges (Manighetti et al., 1998), or filled the entire Afar depression. In any case, the MFS flexure developed along the western edge of the Asa Gayla plateau, i.e. close to the hinge line marking the limit of pronounced lava thickness towards the active rifted domain. That is supported by aeromagnetic data from Eastern Afar (Courtillot et al., 1980) that show the trace of the MFS following the transition zone between an oceanic-type magnetic domain to the west (AMIR), and a continental-type (quiet) magnetic domain to the east (Danakil range).

The inward-dipping accummulation of mafic material erupted along the eastern edge of the AMIR resembles magmatic prisms, known as Seaward Dipping Reflector Sequences along most volcanic margins worldwide (see review by Coffin and Eldhom, 1992). The dyke swarms typically observed along volcanic margins are missing in the MFS, at the present erosion level, but they probably exist at depth beneath the Stratoid fissural-type flood basalts.

The accumulation of a km's-thick wedge of flood basalts along the South Danakil/AMIR transition zone leads us to envisage the key-role of isostatic loading on large-scale flexuring along the MFS, the old Dalha basaltic sequences being progressively depressed by weight of younger overlapping series (Stratoid) during volcanic deposition. The role of tectonic forces during flexuring cannot be totally ruled out. But, structural and geophysical evidence are currently missing for the presence of a large-scale antithetic detachment underlying the MFS, as commonly evoked in the roll-over anticline model applied to many volcanic margins (Nielsen and Brooks, 1981 ; Barton and White, 1997 ; Geoffroy et al., 1998).

The origin of the antithetic extensional fault network in the MFS is more satisfactorilly explained, using shear failure criterion, and applying the model of fault formation proposed by Forslund and Gudmundsson (1992) to the South Iceland rift. Assuming that the wedge-shaped pile of initially horizontal lava flows rotated westwards, towards the axis of the active magmatic zone, the cooling joint pattern, prone to act as tension fractures under tensile stress, evolved from an initially vertical attitude to an easterly-inclined position with time. The decreasing dip attitude of the joint pattern at depth resulted in a listric-shaped joint trajectory which might have later triggered the development of antithetic normal faults, dipping away from the subsiding rift axis to the west, once submitted to the N30°E horizontal extension. The obliquity of the submeridian MFS to regional extension might be partly explained by assuming its isostatic, instead of tectonic, origin.

CONCLUSIONS

ASTER satellite image interpretation, calibrated by field observations, leads us to interpret the Makarassou fault system, SE Afar, as an extensional faulted corridor, superimposed on a large-scale inward- (riftward-)facing flexure, involving the 3-1 Ma-old Stratoid basaltic trapp series. This monocline structure is assumed to result from isostatic adjustment related to the overloading of a >3 km-thick magmatic accumulation, composed of Dalha basalts and younger Stratoid lavas, at the transition between the South Danakil plateau and the Asal-Manda Inakir rifted domain to the East. The flexuring and outward-verging extensional faulting documented in the present work along this narrow transition zone are tectonic processes typically recorded by volcanic rifted margins, at an early stage of continental breakup. Our interpretation of the MFS as the shallow structure of a proto-volcanic margin fits with the kinematic model proposed by Wolfenden et al. (2005) for the conjugate West Afar margin (Fig. 1a). Once combined, these two structural works demonstrate the symmetrical 2D-architecture of the twin proto-volcanic margins, immediatly prior to, or even at an incipient stage of, plate separation between Nubia and Somalia.

ACKNOWLEDGMENTS

Funding and support from CERD (Study and Research Center of Djibouti) is appreciated. Dr Mohamed Jalludin, Director of CERD, is warmly thanked for his constant interest for the geological works carried out in Djibouti since many years by our team from Brest university.

REFERENCES CITED

Barberi, F., and Varet, J., 1975 : Nature of the Afar crust : A discussion, in Pilger, A., and Rosler, A., eds, Afar Depression of Ethiopia : Schweizerbart'sche, E., publisher, Stuttgart.

Barberi, F., and Varet, J., 1977: Volcanism in Afar: Small scale plate tectonics implications: Geological Society of America Bulletin, v. 88, p. 1251-1266.Barberi, F., and Santacroce, R., 1980 : The Afar Stratoid Series and the magmatic evolution of the East African rift system : Bulletin de la Société Géologique de France, v. 56, p. 903-915.

Barton, A.J., and White, R.S., 1997 : Volcanism on the Rockall continental margin : Journal of the Geological Society, London, v. 153, p. 530-536.

Brooks, C.K., and Nielsen, T.F., 1982 : The E. Greenland continental margin : A transition between oceanic and continental magmatism : Journal of the Geological Society of London, v. 36, p. 265-275.

Coffin, M.F., and Eldhom, O., 1992 : Volcanism and continental break-up : a global complication of large igneous provinces, in Storey, B.C., et al., eds., Magmatism and the causes of continental break-up : Geological Society of London, Special Publication, v. 68, p. 17-30.

Courtillot, V., Tapponnier, P., and Varet, J., 1974 : Surface features associated with transform faults : a comparison between observed examples and an experimental model : Tectonophysics, v. 24, p. 317-329.

Courtillot, V., Achache, J., Landre, F., Bonhomet, N., Montigny, R., and Féraud, G., 1980 : Episodic spreading and rift propagation : New paleomagnetic and geochronological data from the Afar nascent passive margin : Journal of Geophysical Research, v. 98, p. 3315-3333.

Dessai, A.G., and Bertrand, H., 1995 : The 'Panvel Flexure' along the Western Indian continental margin : an extensional fault structure related to Deccan magmatism : Tectonophysics, v. 241, p. 165-178.

Dugda, M.T., and Nyblade, A.A., 2006 : New constraints on crustal structure in eastern Afar from the analysis of receiver functions and surface waves dispersion in Djibouti, in Yirgu, G., et al., eds., The Afar volcanic province within the East African rift system : Geological Society of London, Special Publication, v. 259, p. 239-251.

Forslund, T., and Gudmundsson, A., 1992 : Structure of Tertiary and Pleistocene normal faults in Iceland : Tectonics, v. 11, p. 57-68.

Gasse, F., Fournier, M., Lépine, J.C., Richard, O., and Ruegg J.C., 1985 : Carte géologique de la République de Djibouti, 1:100000. Tadjoura. Notice explicative. ISERST, Ministère français de la Coopération, Paris.

Geoffroy, L., Gélard, J.P., Lepvrier, C., and Olivier, P., 1998, The coastal flexure of Disko (West Greenland), onshore expression of the 'oblique reflectors' : Journal of the Geological Society, London, v. 155, p. 463-473.

Klausen, M.B., 2009 : The Lebombo monocline and associated feeder dyke swarm : Diagnostic of a successful and highly volcanic rifted margin ? : Tectonophysics, v. 468, p. 42-62.

Klausen, M.B., and Larsen, H.C., 2002 : The East Greenland coast-parallel dyke swarm and its role in continental breakup, in Menzies, M.A., et al., eds., Volcanic rifted margins : Geological Society of America, Special Paper, v. 362, p. 133-158.

Laughton, A.S., 1966 : The Gulf of Aden, in relation to the Red Sea and the Afar depression of Ethiopia : Geological Survey of Canada, Special Paper, v. 66, p. 78-97.

Manighetti, I., Tapponnier, P., Gillot, P.Y., Jacques, E., Courtillot, V., Armijo, R., Ruegg, J.C., and King, G., 1998: Propagation of rifting along the Arabia-Somalia plate boundary into Afar: Journal of Geophysical Research, v. 103, p. 4947-4974.

Mohr, P., 1989 : Nature of the crust under Afar new igneous, not thinned continental : Tectonophysics, v. 167, p. 1-11.

Nielsen, T.F., and Brooks, C.K., 1981 : The East-Greenland rifted continental margin : an examination of the coastal flexure : Journal of the Geological Society , London, v. 138, p. 559-568.

Piguet, P., Recroix, F., and Vellutini, P., 1995 : Carte géologique de la République de Djibouti, 1:100000 Dorra, Notice explicative. ISERST, Ministère français de la Coopération, Paris.

Tapponnier, P., and Varet, J., 1974 : La zone de Mak'arrassou en Afar, un équivalent émergé des failles transformantes océaniques : Comptes Rendus Académie des Sciences, Paris, v. 274, p. 209-212.

Vellutini, P., 1990. The Manda-Inakir rift (Republic of Djibouti). Comparison with Asal rift. Geodynamic meaning : Tectonophysics, v. 172, p. 141-153.

Wolfenden, E., Ebinger, C., Yirgu, G., Renne, P.R., and Kelley, S.P., 2005: Evolution of a volcanic rifted margin: Southern Red Sea, Ethiopia: Geological Society of America Bulletin, v. 117 (7-8), p. 846-864.

HYDROTHERMAL ALTERATION STUDIES OF THE TENDAHO GEOTHERMAL PROSPECT AREA, ETHIOPIA

Meseret Teklemariam

ABSTRACT

The Tendaho geothermal Prospect area is one of the two more advanced geothermal prospect areas in Ethiopia which have under-gone shallow and deep exploratory drilling. The prospect area is located in the Tendaho geothermal graben in the inner part of the Afar Depression, about 600 Km NE of Addis Ababa.

This brief report deals with the distribution of alteration minerals, including clay minerals, in the Tendaho geothermal prospect areas of Alalobeda, Ayrobera and Dubti. It also deals with the distribution of alteration mineral assemblages in wells TD-5 and TD-6 of the Tendaho (Dubti) geothermal field.

Petrographic examinations and X-ray Diffraction analysis were performed on: (i) Seven surface altered rock samples collected from in and around the surface manifestations of Alalobeda, Dubti and Ayrobera geothermal prospect areas; and (ii) Ten rock samples from shallow wells of TD-5 and TD-6, Dubti geothermal field with a view to study and understand the different types of alteration minerals. The study was performed in the laboratory of International Institute for Geoscience and Georesources, Pisa, Italy.

Clay mineral assemblages observed in Alaolbeda, Ayrobera and Dubti prospect areas are: (i) smectite and Mixed layer clays of illite-smectite; (ii) Kaolinite, Alunite and smectite; and (iii) Mixed layer clays of illite-smectite respectively.

In wells TD-5 and TD-6, the main alteration mineral assemblage consists of calcite, zeolites, clays, sulfides, prehnite and wairakite. Epidote is found sporadically. Clay mineral assemblages observed in these wells are: (i) Smectite and Mixed layered lay minerals (Illite-Smectite) at a depth range of 0-300m; and (ii) Chlorite and epidote at a depth range of 350m-475 m. Alteration mineral assemblages indicate a progressively heating geothermal system, where the older zeolite assemblage are replaced by younger and high temperature alteration minerals . In thin sections, laumontite gives a clear indication of being replaced partly by wairakite and quartz. This indicates the presence of low temperature zeolites in the first phase of deposition at a lower temperature and followed by the second phase of deposition such as wairakite, prehnite and epidote at high temperatures.

The high temperature alteration minerals are in a good agreement with the measured in-hole temperatures of the wells (≈270°C). The temperature range shown by the alteration distribution in the Tendaho field compares in most cases with other geothermal fields.

EPITHERMAL AU-AG- BI -TE MINERALIZATION IN THE SE AFAR RIFT, REPUBLIC OF DJIBOUTI

Moussa, N*. (1, 2,3); Fouquet, Y. (1); Le Gall, B. (2); Bohn, M. (1); Etoubleau, J. (1) ; Grassineau, N. (4); Caminiti, A. M. (3); Rolet, J. (2) ; Jalludin, M. (3)
[1] IFREMER, Centre de Brest, BP 70, 29280 Plouzané, France
[2] UMR 6538 Domaines océaniques, UBO-IUEM, Place Nicolas Copernic, 29280, Plouzané, France
[3] IST, Centre d'Etudes et de Recherches de Djibouti, B.P. 486, Djibouti
[4] Department of Geology, Royal Holloway University of London, EGHAM Surrey TW20 0EX, U.K
**Correspondance Nima.Moussa.Egueh@ifremer.fr*

Epithermal gold mineralization were recently discovered in the SE part of the Afar volcanic Triangle, Republic of Djibouti. Mineralization generally occur as veins and are mainly associated with acidic volcanic intrusions along the faults at the edges of graben structures established during the last 4 Ma. Sixty samples were analyzed from 4 different sites representative of 4 major volcanic events. Mineralogical analyses based on optical reflected light microscopy, X-Ray diffractometry, X-Ray fluorescence, inductively coupled plasma mass spectroscopy, electron microprobe and scanning electron microprobe, led us to identify different types of gold mineralization (i) native gold, electrum, hessite ($Ag_{1,98}Te_{1,02}$), tetradymite ($Bi_{1,99}Te_{2,13}S_{0,88}$) and sulfides (chalcopyrite, pyrite, sphalerite, galena, bornite, digenite, marcasite) in massive quartz breccias and banded chalcedony, (ii) gold, electrum, pyrite, hematite, magnetite, traces minerals (argentite) and adularia in banded chalcedony. Gold-telluride associations are generally regarded as characteristics of low sulfidation epithermal gold deposits. Te is found in three different forms (i) Te occurs as invisible or submicrometer-size inclusions of hessite in pyrite where a high content (up to 41 wt %) of Te were measured; (ii) as visible independent telluride grains (hessite ($Ag_{1,98}Te_{1,02}$) and tetradymite ($Bi_{1,99}Te_{2,13}S_{0,88}$)) disseminated in quartz and (iii) as grains of hessite up to 50 µm with pyrite inclusions (10 µm). Tellurium is preferentially transported in a gas phase and may result from condensation of magmatically derived $H_2Te_{(g)}$ and $Te_{(g)}$ into deep-level of chloride waters [1]. At Hes Daba site, sulfur isotopic ratios of pyrite indicate values of $\delta^{34}S$ between

–9.20‰ to 1.45 ‰. The $\delta^{34}S$ values of pyrite close to 0‰ are typically reported to volcanic rocks and the negative $\delta^{34}S$ values classically indicate a source of sulfur from magmatic fluids. Thus in our samples telluride mineralization and sulfur isotopic studies of sulfides suggest that gold can be related to a magmatic fluid contribution and is precipitated in the deep high temperature part of the epithermal system.

[1] Cooke & McPhail., 2001, Econ Geol, v 96 pp 109-131

Keywords: Afar Rift, Epithermal System, Gold-Telluride, Djibouti

INTRODUCTION

Telluride minerals have long been regarded as rare mineral. The modern microanalytical methods have changed considerably this view (Oberthur and Weiser, 2008). Gold-telluride associations are typically regarded as characteristic of epithermal gold deposits as defined by Hedenquist et al. 2000 and Sillitoe and Hedenquist 2003. The most common occurrence of Te is the low sulfidation type that is spatially associated with alkaline igneous rocks (Voudouris, 2006). A Well known example is (i) the Emperor Mine, Fiji, (Ahmad et al 1987, Pals and Spry, 2003); and (ii) the Cripple Creek, Colorado (Thompson et al 1985). Telluride minerals can also be related to calc-alkaline rocks and intermediate sulfidation deposits such as the Baguio District, Philippines (Cooke and McPhail 2001), the Golden Quadrilateral, Romania (Cook and Ciobanu 2004); high sulfidation deposits at El Indio, Chile (Jannas et al 1990) and the mixed high-intermediate sulfidation deposit at Kochbulak, Uzbekistan (Kovalenker et al 1997). Te-bearing minerals offer potential for the understanding of the physicochemical conditions of ore formation because they are valuable indicators of changes in temperature and sulfidation state (Cook and Ciobanu, 2002). In fact, hydrothermal mineral ore deposits is the results of changes of physical and chemical variables such as temperature, pressure, acidity, redox, salinity and concentrations of sulfur, carbon and ligands (Cooke and McPhail, 2001).

In term of paragenetic assemblages; Te deposition is classically restricted to one or two stages that always follow initial deposition of sulfides (e.g. pyrite, chalcopyrite, sphalerite and galena; Afifi et al. 1998b).

The occurrence of Au together with Bi-telluride has long been observed in many ore deposits. Marcoux et al. (1996) considered this association as pathfinders for gold in the stringer zones of massive sulfide deposits (Iberian Pyrite Belt).

In this study, we report the first Au-Ag-Bi-Te-bearing ores, detailed mineralogical and chemical studies of gold-telluride minerals from 2 different sites representative of two major volcanic events consisting, in ascending

stratigraphic order, of (1) the 15-11 Ma Mabla acidic series (Ali Adde), and (2) the 3.3-1.0 Ma Stratoid basaltics series (Hes Daba). In order to understand the conditions of formation of ore deposits, we used sulfur isotope.

GEOLOGICAL SETTINGS

The Afar Depression resulted from the intersection of the Red Sea, Gulf of Aden and Ethiopian rift axes during the Miocene (Fig. 1). The main expression of the crustal rifting process in Afar is, in addition to extensional faulting, the bimodal magmatism. The volcanic activity started as early as 30 Ma with the emplacement of trap volcanism in Yemen and Ethiopia (Barberi and Varet 1977). The first evidence of synrift magmatism in SE Afar of the Republic of Djibouti, is the 28-19 Ma Ali Sabieh mafic complex, and the more widespread Mabla rhyolites which erupted at 15-11 Ma (Barberi et al. 1975; Varet and Gasse 1978; Gadalia 1980). The subsequent volcanic events were essentially basaltic, with locally minor acidic differentiates. They include 1) the Dalha (9-4 Ma), 2) the Stratoid (4-1 Ma), and 3) the Gulf (3-1 Ma) series (Gaulier and Huchon 1991). Dominantly felsic activity in a restricted area involving the Arta transverse zone (Fig. 2) is recorded by the Ribta volcanic products (4-3 Ma). The Stratoid trap-like lavas cover two thirds of the Afar depression and are commonly regarded as incipient oceanic crust (Barberi et al. 1975; Robineau 1979). There are numerous felsic silica centers near Lake Abhe (2 and 5 Ma): Babba Alou massif (1 and 8 Ma), and Egeraleyta massif (<1 Ma), immediately south of the Asal rift (Gaulier and Huchon 1991).

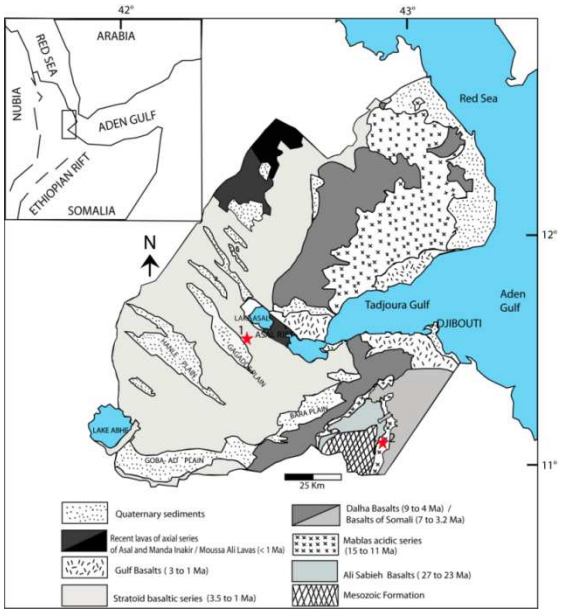

Figure 1 : Schematical geological map of the Republic of Djibouti (SE Afar Triangle) after Piguet & Velutini (1995). Red stars (and corresponding numbers) are the two hydrothermal sites studied in this work. 1 Hes Daba 2, Ali Addé.

METHODS

Polished-thin sections of ore samples were examined with a reflected-transmitted light microscope at magnification up to 1000 in dry air and oil. Additional studies were performed, using: (1) X-Ray Diffraction analyses to determine major minerals in gangue and alteration zones and (2) X-ray elemental mapping using CAMECA SX100 electron-microprobe with PAP correction program (Pouchou and Pichoir, 1984). To search telluride minerals, operating conditions consisted in accelerating voltage at 25 KV, beam current at 20 nA and beam size at 1 μm^3. The present work has been conducted at “Laboratoire de Géochimie et Métallogénie, IFREMER, Brest".

Sulfur isotopes were analyzed in mineralized samples at “Laboratory of Stable Isotopes, Royal Holloway University of London”. They were performed with the procedures using EA-IRMS which were developed by Grassineau et al. (2006).

RESULTS

From geological and mineralogical view, the two sites with Au-Ag-Bi-Te mineralization have been broadly detailed in Moussa et al. 2010 (submitted). Short descriptions of the hydrothermal alteration and mineralization of the areas studied are presented below and the results are summarized in Table 1.

Hes Daba

The mineralization is hosted by trachytic lavas and quartz constitutes the principal gangue in the veins. Early mineralization consists of sulfides (chalcopyrite, pyrite sphalerite, galena, bornite, digenite, covellite and marcasite) as disseminations and fracture fillings in quartz veins. The late-stage of mineralization is mainly composed of iron oxides (goethite and hematite). Late banded and massive quartz ± carbonate veins postdate and overprint a quartz stockwork. Telluride minerals have not yet been observed in this area. Fault controlled silicic alteration has 130 NW direction. Telluride minerals are expressed as (i) visible independent telluride grains (hessite ($Ag_{1,98}Te_{1,02}$)) disseminated in quartz (Fig. 2).

In term of sulfur isotope, pyrite is characterized by values ranging from -9.20 to 1.45 ‰.

Ali Addé

Pollymetallic sulfides such as chalcopyrite, pyrite sphalerite, galena, bornite, digenite, marcasite in massive quartz breccias; banded chalcedony and native elements; constitute the main expressions of the mineralization. Two stages of mineralization have been distinguished: initial deposition of sulfides followed by telluride minerals. Te is found in different forms (i) Te occurs as invisible or submicrometer-size inclusions of hessite in pyrite, (ii) as visible independent telluride grains (hessite ($Ag_{1,98}Te_{1,02}$), tetradymite ($Bi_{1,99}Te_{2,13}S_{0,88}$) disseminated in quartz and (iii) as grains of hessite up to 50 µm (Fig.2) with pyrite inclusions (10 µm). Native Te grains has been observed in this site. $\delta^{34}S$ values of pyrite correspond to -2.58 and 5.87 ‰ respectively.

Table 1: Microprobe analysis results of selected sulfide and telluride minerals (w %).

	Cu	Fe	Bi	Ag	S	As	Te
Pyrite FeS_2		45.97			53.32		
Hessite ($Ag_{1,98}Te_{1,02}$)				62.55			38.30
Tetradymite ($Bi_{1,99}Te_{2,13}S_{0,88}$)			56.96		3.86		37.12
Native Te							100

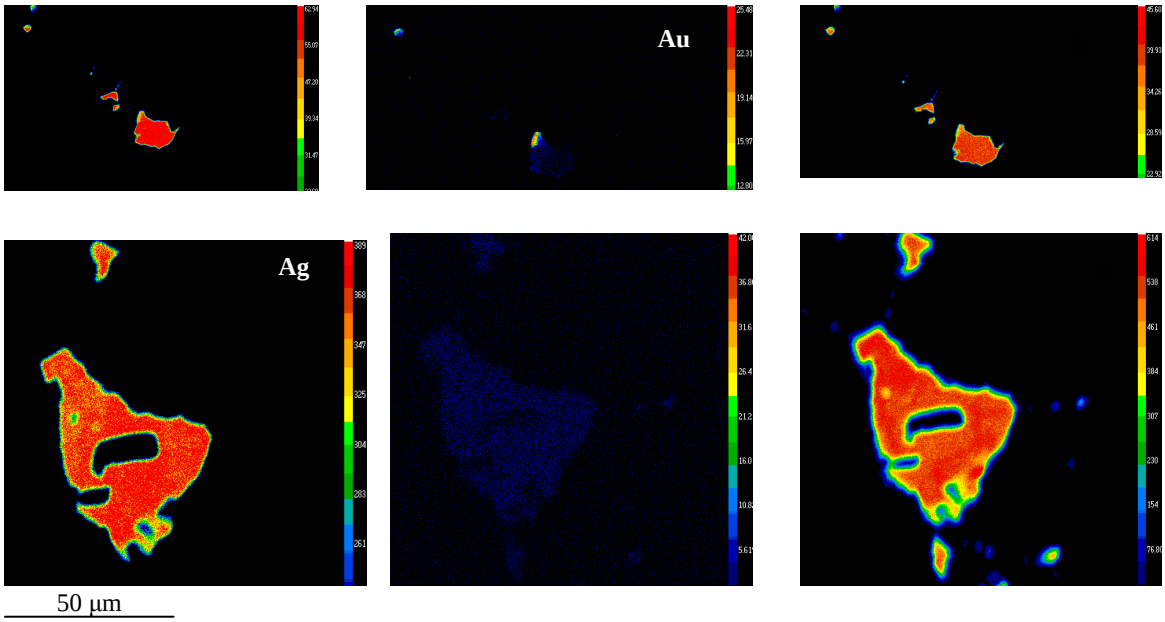

Figure 2: Electron Microprobe images illustrating Au-telluride assemblage in hydrothermal quartz veins from acidic volcanic lavas. A : Au-Ag-Te assemblages from Hes Daba hydrothermal site (Stratoid Fm). B : Ag-Te assemblage from Ali Addé hydrothermal site (Mabla Fm). Au lack in this assemblage.

DISCUSSION AND CONCLUSIONS

Mineralogical studies of the two hydrothermal sites show two major paragenetic sequences:

- High temperature paragenesis mainly composed by native gold, electrum, hessite, tetradymite, native tellurium and sulfides (chalcopyrite, pyrite, sphalerite, galena, bornite, digenite, marcasite) in massive quartz breccias and banded chalcedony.
- Lower temperature assemblage characterized by iron oxides (goethite, hematite, magnetite) in massive and breccias quartz.

Telluride minerals have long been considered, as a key of the understanding of the physicochemical conditions of ore formation. In fact, Zhang and Spry 1994 calculated the stability of (i) aqueous tellurium species and (ii) calverite and hessite. They conclude that

Te_2^{2-} is the most common important aqueous tellurium species in equilibrium with native tellurium in epithermal deposits and the stability of hessite covers most conditions of ore formation (e.g. oxidizing to reducing, and acid to alkaline) and is a less useful indicator of ore-forming conditions. Cooke and McPhail 2001 indicate that in Acupan, Philippines; the LS epithermal systems formed at lower T (<300°C), other precipitation mechanisms, e.g. condensation of Te vapor(s), followed by reaction with Au-Ag bearing fluids, is invoked to explain the presence of Au- (Ag)-telluride minerals.

By contrast, the occurrences of bismuth telluride have widely investigated by many workers. For Ciobanu et al 2005; bismuth telluride provides a "melt-precipitates window" for the formation of the main types of Au deposits. They suggest that Bi-rich melt-precipitates are constrained to reducing fluids and temperature >300°C whereas Te-rich form from oxidized fluids with temperatures of at least 400°C. Ciobanu et al. 2005; Tooth et al. 2008 defined that Bi-Te has the role of Au-scavenging in many gold deposits.

However in the most interpretation; Te is considered to be transported as aqueous species in epithermal fluids (Ciobanu et al. 2006).

The mineralogical assemblages of Hes Daba and Ali Addé sites, possess the highest sulfide content (chalcopyrite, pyrite, sphalerite, galena, bornite, digenite, marcasite). Bi and Te are also present. $\delta^{34}S$ values of sulfides spread between –9.2 to 5.87 ‰. The δ 34S values of pyrite close to 0‰ are typically reported to volcanic rocks whereas the negative $\delta^{34}S$ values of sulfides can be explained by the disproportionation of magmatic SO_2 that causes the enrichment of ^{32}S in the sulfides.

The occurrences of Bi-Te-bearing minerals and the negative values of sulfur isotopes suggest that gold can be related to a magmatic fluid contribution and is precipitated in the deep high temperature part of the epithermal system.

ACKNOWLEDGMENTS:

We thank the CERD (Centre d'Etude et de Reherche de Djibouti) for the help provided during the current study. The research has been supported by the CERD and the SCAC (Service de Cooperation et d'Action Culturelle).

REFERENCES

Afifi A, Kelly W, Essene E (1988) Phase relations among tellurides, sulfides, and oxides; I, Thermochemical data and calculated equilibria. Economic Geology 83: 377.

Ahmad M, Solomon M, Walshe J (1987) Mineralogical and geochemical studies of the Emperor gold telluride deposit, Fiji. Economic Geology 82: 345.

Barberi F, Ferrara G, Varet J (1975) Structural evolution of the Afar triple junction. Afar Depression of Ethiopia: Stuttgart, Germany, Schweizerbart, Scientific Report 14: 38-54

Barberi F, Varet J, (1977) Volcanism of Afar: Small-scale plate tectonics implications. Geol Soc Am Bull 88: 1251-1266

Ciobanu C, Cook N, Spry P (2006) Preface–Special Issue: Telluride and selenide minerals in gold deposits–how and why? Mineralogy and Petrology 87: 163-169.

Ciobanu C, Cook N, Pring A (2005) Bismuth tellurides as gold scavengers Springer, pp 1383-1386.

Cook N, Ciobanu C (2005) Tellurides in Au deposits: implications for modelling Springer, pp 1387-1390.

Cook N, Ciobanu C (2002) Tellurides: more than mineralogical curiosities, but also markers of fS2-fO2 evolution in zoned hydrothermal systems. IMA.

Cooke D, McPhail D (2001) Epithermal Au-Ag-Te mineralization, Acupan, Baguio district, Philippines: numerical simulations of mineral deposition. Economic Geology 96: 109

Gaulier J, Huchon P (1991) Tectonic evolution of Afar triple junction. Bull Soc Géol de France 162: 451-464

Grassineau N (2006) High-precision EA-IRMS analysis of S and C isotopes in geological materials. Applied Geochemistry 21: 756-765.

Hedenquist J, Arribas A, Gonzalez-Urien E (2000) Exploration for epithermal gold deposits. Reviews in Economic Geology 13: 245–277.

Jannas R, Beane R, Ahler B, Brosnahan D (1990) Gold and copper mineralization at the El Indio deposit, Chile. Journal of Geochemical Exploration 36: 233-266.

Kovalenker V, Safonov Y, Naumov V, Rusimov V (1997) Epithermal gold-telluride deposits of Kochbulak (Uzbekistan). Geol Ore Deposits 39: 127-152.

Marcoux E, Moelo Y, Leistel JM (1996) :Bismuth and cobalt minerals as indicators of stringer zonesto massive sulphide deposits, Iberian Pyrite Belt. Mineralium Deposita (31) 1-26.

Oberthur T, Weiser T (2008) Gold-bismuth-telluride-sulphide assemblages at the Viceroy Mine, Harare-Bindura-Shamva greenstone belt, Zimbabwe. Mineralogical Magazine 72: 953.

Pals D, Spry P (2003) Telluride mineralogy of the low-sulfidation epithermal Emperor gold deposit, Vatukoula, Fiji. Mineralogy and Petrology 79: 285-307.

Pouchou L J and Pichoir F (1984) New model quantitative x-ray microanalysis. Application to the analysis of homogeneous samples, Recherche Aerospatiale 3:13-38.

Sillitoe R, Hedenquist J (2003) Linkages between volcanotectonic settings, ore-fluid compositions, and epithermal precious metal deposits. Special Publication- Society of Economic Geologists 10: 315-343.

Thompson T, Trippel A, Dwelley P (1985) Mineralized veins and breccias of the Cripple Creek district, Colorado. Economic Geology 80: 1669.

Tooth B, Brugger J, Ciobanu C, Liu W (2008) Modeling of gold scavenging by bismuth melts coexisting with hydrothermal fluids. Geology 36: 815.

Varet J, Gasse F, (1978) Carte géologique de l'Afar central et méridional 'Ethiopie et République de Djibouti. CNRS Ed.

Vellutini P, Piguet P (1995) Carte géologique de la République de Djibouti au 1:100 000: feuille de Khor Angar. In: Les formations volcaniques Ministère Français de la Coopération et du Développement et ISERST BRGM

Voudouris P (2006) A comparative mineralogical study of Te-rich magmatic-hydrothermal systems in northeastern Greece. Mineralogy and Petrology 87: 241-275.

Zhang X, Spry P (1994) Calculated stability of aqueous tellurium species, calaverite, and hessite at elevated temperatures. Economic Geology 89: 1152.

THE MENENGAI CALDERA STRUCTURE AND ITS RELEVANCE TO GEOTHERMAL POTENTIAL

Lucy Muthoni Njue,
Geothermal Development Company.
P.O. Box 17700-20100 Nakuru, Kenya.
lnjue@gdc.co.ke

ABSTRACT

Calderas are considered to be depressions resulting from an underpressure and/or overpressure within the magma chamber and can be used to interprete the conditions of the subsurface Menengai caldera is located on the floor of the Kenya Rift Valley, 24 km south of the equator and is seen to be of great geothermal potential. Its location on major structures is seen to be advantageous in terms of a highly productive high temperature geothermal system.On the basis of geology the caldea is seen to have undergone multiple block collapse and is thus classified as a piecemeal caldera. The stages of its development include pre caldea volcanism, caldera susidence, post caldera volcanism and hydrothermal activity. The structure of the caldera and post caldera volcanism anf hydrothermal alteration imply a shallow and active magma chamber respectively.

INTRODUCTION

The word caldera in derived from the Latin word *caldaria* which means boiling pot (Cole et al, 2005). It is thus simple to understand in layman terms the basic features of a caldera and these comprise heat, a chamber and a conduit. A caldera is a cauldron-like volcanic feature usually formed by the collapse of land normally following a volcanic eruption. Acocella (2007) considers calderas to be depressions resulting from an underpressure and/or overpressure within the magma chamber. This term is sometimes used interchangeably with crater but the distinction is in the mode of formation. Calderas vary in size and shape based primarily on geological setting/tectonic control and composition of eruptives although the latter is not proven.

Calderas are thus interesting sites for geologists since they give information of the geological processes that have taken place on the surface and the subsurface. In the geothermal sector calderas are key indicators of the very sort after geothermal activity because they more or less imply an underlying heat source. Direct witnessing of the formation of a caldera is a minor setback in the formulation of a comprehensive model but is overcome with the use of geophysical methods and subsequent models.

Menengai caldera is located immediately north of Nakuru town and a few kilometres south of the equator (figure 1). It is one of five calderas in the Kenya Rift valley and is seen to be of great geothermal potential.

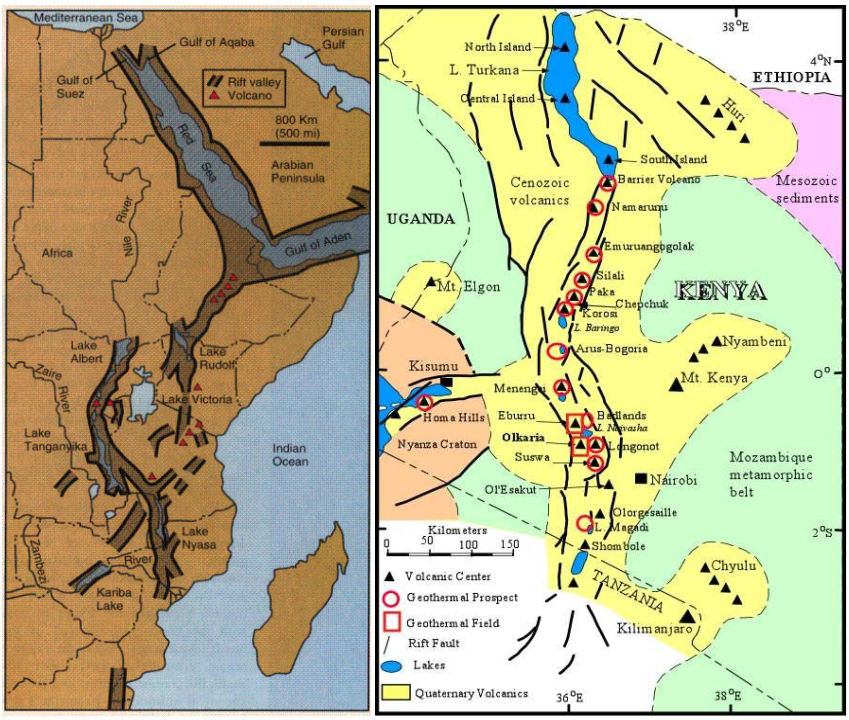

Figure 1: Tectonic setting of Menengai Caldera

The approximately 12 x 8 km summit caldera was formed about 8000 years ago following volcanic activity which begun almost 200,000 years ago (Seach 2009). This caldera is the major geological feature in the area and also an important structure in terms of occurrence of geothermal potential. The large caldera floor is partially covered by young rugged lava flows as shown in slide 1 below. The caldera rim forms a complete circular cliff that breaks at very few locations which makes it perfectly visible in areal and satellite images.

The apparent signatures of geothermal potential include the young volcanism represented by the numerous recent eruptions both inside and outside the caldera, the large caldera collapse and intense tectonics resulting in intense faults marking the area. Occurrence of active fumaroles, steaming ground, hot/warm water from boreholes and geothermal grass indicate hydrothermal activity and possibility of existence of geothermal reservoirs in this area.

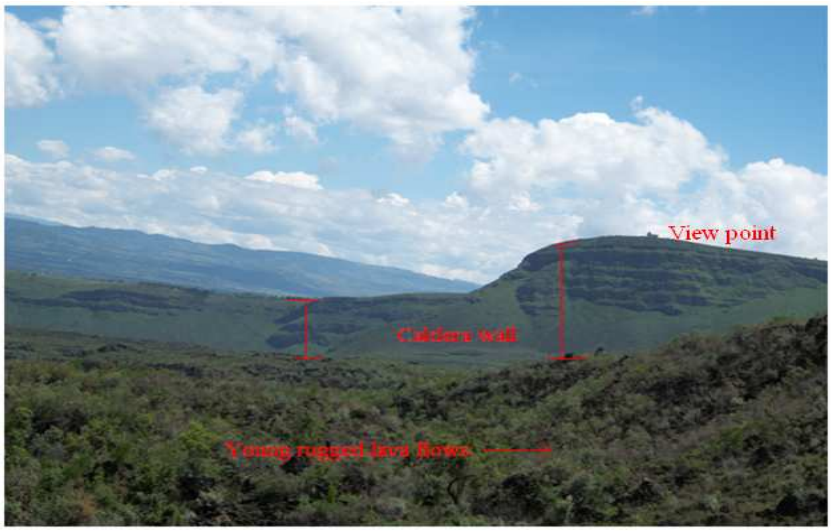

SLIDE 1: Image of Menengai caldera wall and some young lava flows.

TECTONIC SETTING

The Kenya Rift valley (Figure 1) is a very distinct feature of geographic and geologic interest that has developed along a rift, especially one bounded by normal faults in an area of lithospheric thinning. It is a tectonic feature that runs from Lake Turkana to the North down to Lake Magadi in the south splitting the country almost in half. It forms a classic graben averaging 40-80 km wide, is deepest at Naivasha area and shallowest at Lake Turukana area where there is no clear distinction between the rift and the surrounding desert. The Kenyan rift is part of the East African Rift system, which is an intra-continental divergence zone where the Somali and Nubian plates are rifting apart at a rate of 2cm per year (1cm in each direction) and creating a much thinner crust. Rift tectonism accompanied by intense volcanism, has taken place from late Tertiary to Recent (Kengen, 2004). Several Quaternary volcanoes occur within the rift floor of the Kenya segment of the rift. The extensional deformation occurs because the underlying mantle is rising from below and stretching the overlying continental crust. Upwelling mantle may melt to produce magmas, which then rise to the surface, often along normal faults produced by the extensional deformation (Odhiambo, 2010). Menengai is one of the volcanic centres that has had one or more explosive phase(s) including caldera collapse.

Menengai caldera is located within an area characterized by a complex tectonic activity associated with the rift triple junction. This is a zone at which the failed rift arm of the Nyanza rift joins the main Kenya rift. The Kenya rift is characterized by extension tectonism where the E-W tensional forces resulted in block faulting, which include tilted blocks as evident in both the floor and scarps of the rift (Jones and Lippard 1979).

The main rift is bounded by N-S running major rift scarps that depict different tectonic style on the two sides due to their morphological difference. Geotermica Italiana Srl (1987) proposes that this whole section of the rift is a crustal detachment generating a sequence of faults, which merge at a low angle at depth. Two rift floor tectono-volcanic axes Molo and Solai (TVA) that are important in controlling the geothermal system.

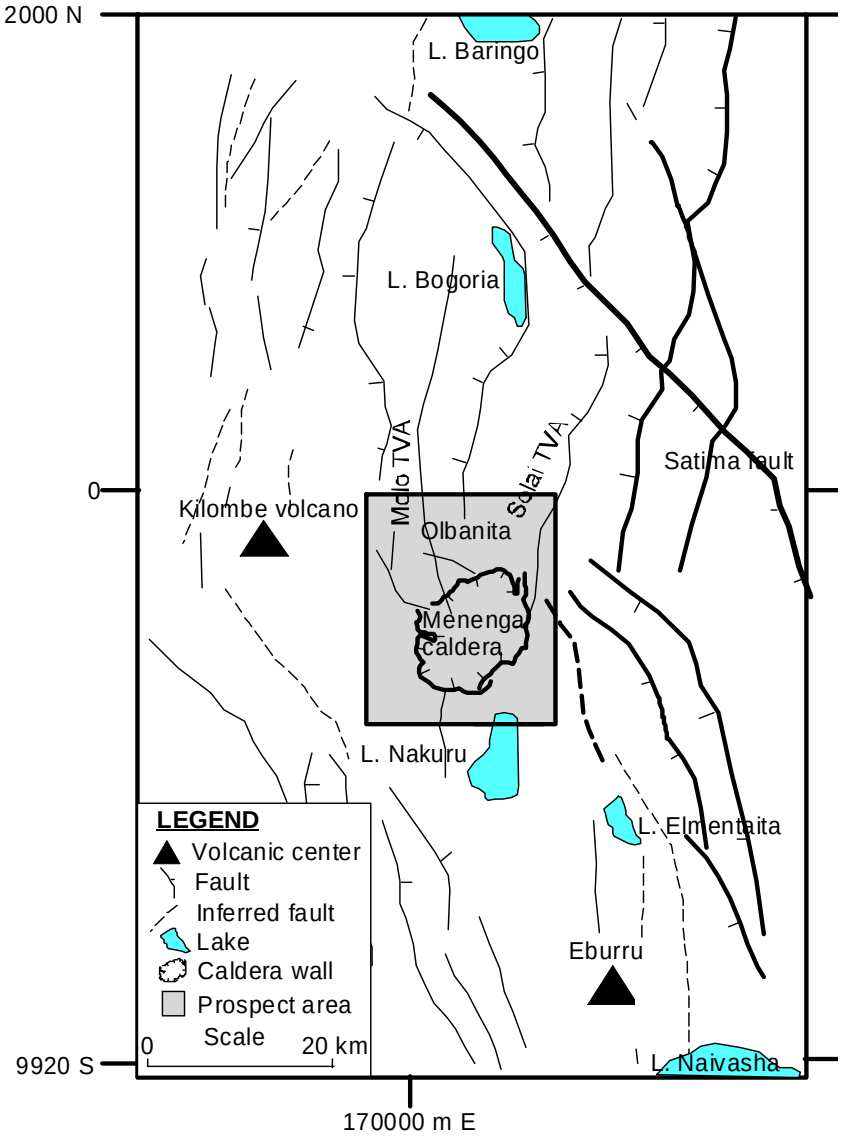

Figure 2: The tectonic setting of Menengai caldera

Although there is no direct link between type of eruptive and the type of caldera formed, there seems to be one between the type of eruptive and the tectonic setting. Peralkaline calderas such as menengai are associated with zones of rifting.

CALDERA CLASSIFICATIONS

Various caldera classifications have been suggested, published and adopted over time in an effort to reduce the numerous variations in their descriptions. The distinction of these classes is becoming more apparent with the availability of additional data and simulation of experimental models. The end member approach by Lipman (1997) is the most realistic as it recognizes and assimilates the wide range of features associated with these structures.

Classifications based on volcanic events, geophysical gravity anomalies and nature of magmas do not put clear boundaries on the calderas where for example a rhyolitic caldera may contain some mafic volcanism.

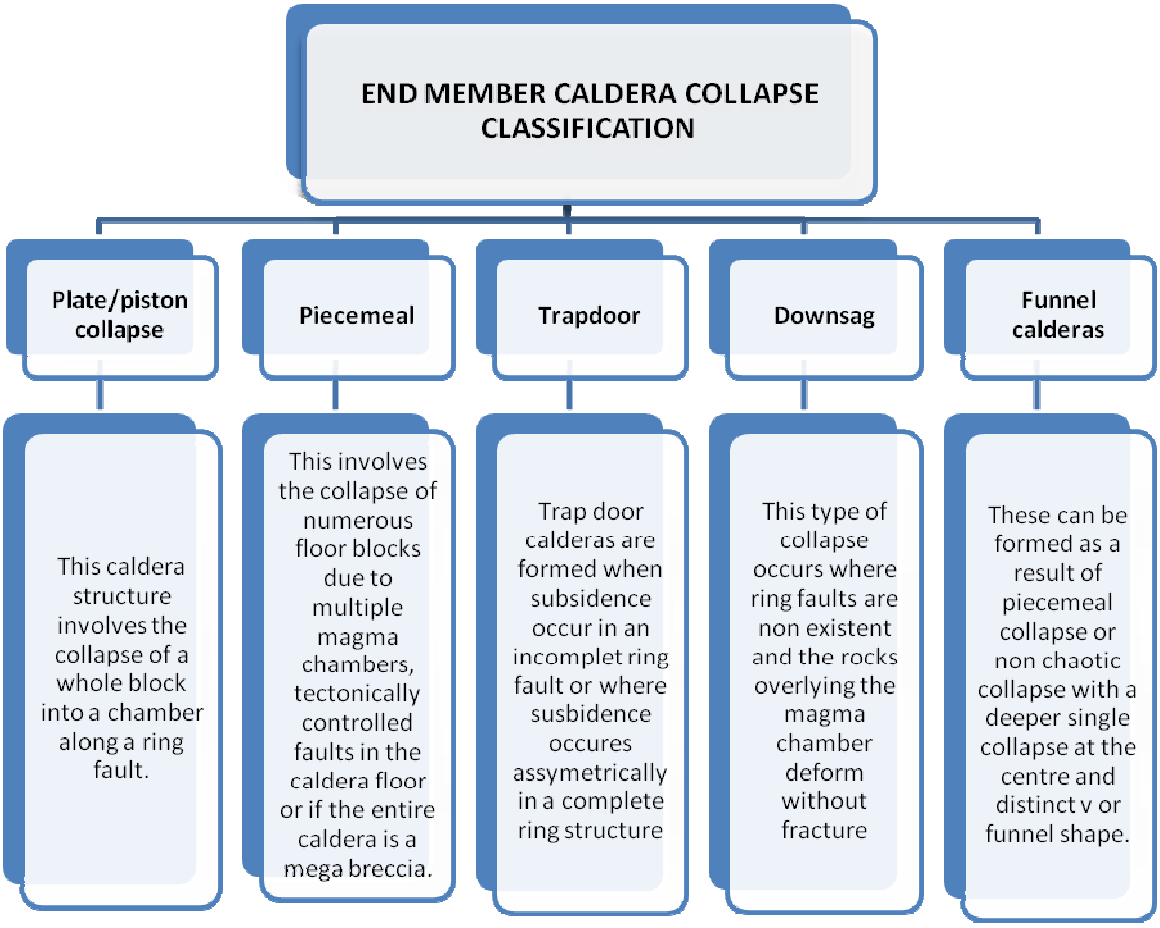

Figure 5: End member caldera classification after Lipman (1997)

The Menengai ring structure has only been disturbed by the Solai graben faults on the NE end and one another fracture at the SSW end. The caldera floor is covered with post caldera lavas such that it is not possible to estimate the collapse depth or any structures that may be marking the caldera floor (KenGen 2004). However, most of the caldera infill lavas are fissure eruptions that prefer fracture openings. These features therefore suggest a piecemeal collapse caldera as do the rock types and their respective ages.

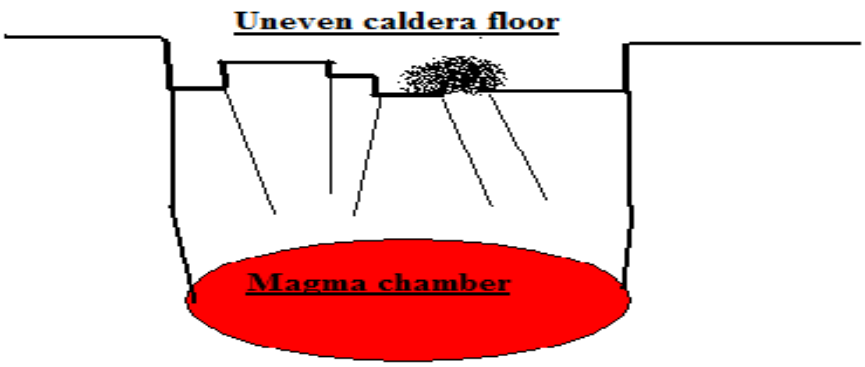

Figure 4: Piecemeal caldera

In the geothermal sector where structures are primary constituents of a good geothermal system, a piecemeal caldera is certainly ideal as the structures increase chances of recharge and permeability. Targeting these structures in the exploration drilling phase would certainly be an excellent plan as they also give additional information for use in the geothermal model.

MENENGAI CALDERA DEVELOPMENT

Lipman (1984, 2000) identified four stages which result in the development of a caldera based on his study of rhyolitic calderas in North America. This four stage cycle although applicable to other caldera types is not standard as some stages may not be pertinent to all formations.

TABLE 1: Stages in the formation of calderas (from Lipman 1984)

	Stage	Activity
1	Pre-collapse volcanism	Surface volcanism, frequently accompanied by tumescence, but this tumescence is not easily preserved and formation of pre-caldera lava domes and small explosive eruptions are often the only record of magma accumulation and migration to shallow crustal levels.
2	Caldera subsidence	Collapse associated with large-scale magma withdrawal (eruption). Eruptions often begin with a central vent phase and proceed to a ring vent phase coincident with caldera collapse
3	Post-collapse magmatism and resurgence.	Volcanism after caldera formation can be randomly scattered within the caldera or localised along regional structural trends. Renewed rise of magma may uplift the central portion of the caldera either by doming or block uplift. This uplift may also be caused by intrusion of sill complexes.
4	Hydrothermal activity and mineralisation.	This may occur throughout the life of the caldera, but begins to dominate activity late in the cycle creating geothermal systems.

The Menengai caldera although a peralkaline caldera fits perfectly into the four stages of formation described above with pre, syn and post caldera group volcanics being used to describe the geology of the area in various studies. The geology is subdivided into 3 based on caldera activity; rocks exposed at the surface, mainly the Menengai massif building lava (pre-caldera formations), the pyroclastics that accompanied the caldera collapse (syn-caldera) and glassy lavas that erupted after the collapse (post-caldera).

Pre- caldera volcanism

Activity in Menengai started shortly before 0.18 Ma, with the growth of a low-angle trachyte lava shield having a volume of about 30 km³ (Leat 1984). These volcanics are typical of any lava shield volcano where sequential piles of lava flow overlie each other (Slide 4). These rocks can be seen on the caldera walls such as at the lion hill where up to 250m of these lava piles are exposed despite the caldera wall being approximately 300m high. The rocks are trachytic in nature with the groundmass being comprised of mainly sanidine crystallites although riebeckite/ arfvedsonite are also present (Kengen, 2004). The chemistry of the rocks implies that there was periodic addition of new magma batches to the growing system. A series of Trachytic tuffs of similar age to the trachytes suggest that the chamber was zoned at that point of the chamber evolution (Mcdonald 2009).

Caldera Subsidence

Growth of the lava shield was truncated, at ~29 ka, by a period of caldera collapse, accompanied by the eruption of an ash flow tuff, preceded by pumice falls. The ash flow tuff had a volume of 20 km^3 and was erupted as a single flow unit (Leat, 1984). The rocks are exposed both at the upper parts of the caldera rim (east and northern rim), where they resemble an agglomerate deposit, which is rich in poorly sorted angular lithic and glassy/semi-pumiceous material (Kengen, 2004). Leat et al. (1984) inferred that the sequence was erupted from a compositionally zoned magma chamber. The ash shows flow texture indicative of pyroclastics flow mode of emplacement. This is the proximal phase indicating the source was at the caldera and its rim.

A second period of collapse occurred at ~8 ka, with the formation of a 12 × 8 km caldera associated with the eruption of 30km^3 of magma. A speculative sequence of the caldera formation during eruption of the second ash flow is shown below. The dot-dash area represents the volume of magma erupted as ash flow.

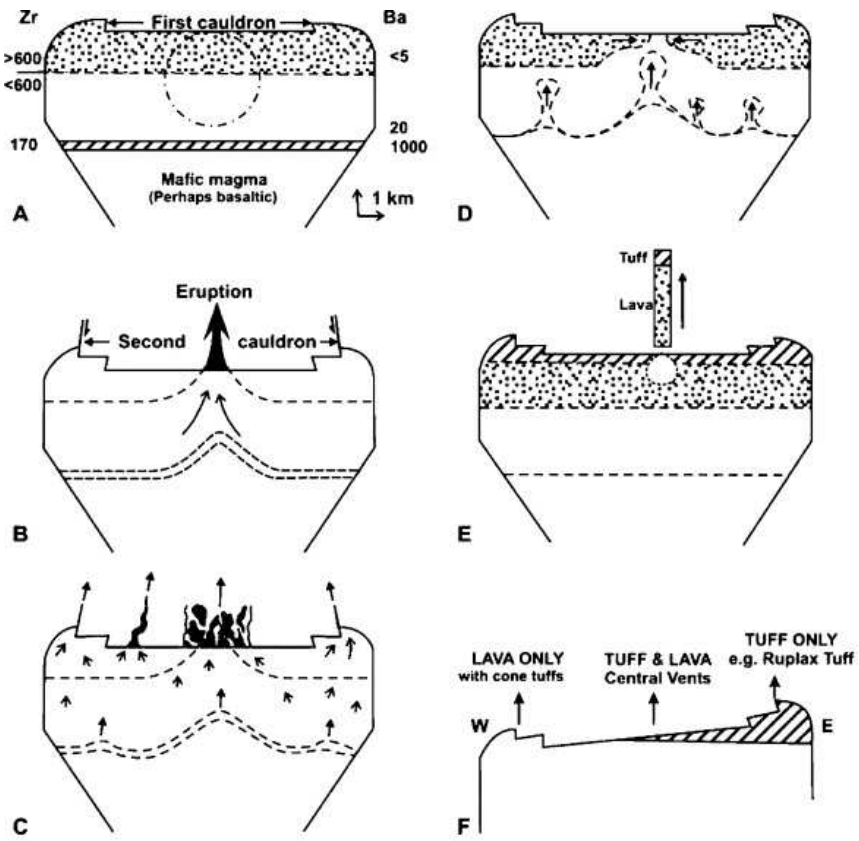

Figure 6: Phase two caldera collapse and post caldera volcanism

Post-collapse magmatism and resurgence

During post-caldera times, some 25 km³ of magma was erupted, mostly as lava flows which now cover the caldera floor and the eruption of these post caldera lavas may have been preceded by explosive episodes due to presence of ash and pumice products in the caldera floor (figure 4). About seventy distinct lava flows can be identified on the caldera floor, with most of the eruption centres emitting the flows being located in the central and the western parts. These lavas have built a huge pile inside the caldera rising to 2160 m.a.s.l. The lowest part of the caldera floor, which is also infilled with the same lavas stands about 1700 m.a.s.l. The lavas are dark in colour, holocrystalline, glassy and are vesicular (Jones 1985). The ropy flow texture, and the small undisturbed lava tubes which are still intact, indicates a young age and the low viscosity of the lavas. The groundmass is mainly made up of sanidine feldspar laths and occasional riebeckite crystallites.

SLIDE 2: Satellite image showing the post caldera lavas (darker in colour)

SLIDE 3: Lava tube.

Hydrothermal activity and mineralization

Hydrothermal activity is mainly what leads scientists to show interest in a geothermal field. The good thing is that in the feasibility stage of any mapping work, aerial photographs are required. Hydrothermal manifestations can be identifies from aerial photographs and thus thermal mapping mission was conducted in the Menengai area. Until then airborne exploration methods have scarcely been applied. As a result of this mission a total number of 2,400 thermal images with 5m pixel size were collected for an area of 510 km² (30 x 17 km) in the Menengai and surrounding areas. Additionally, 220 stereoscopic aerial photographs (1:20,000) were recorded. Eight thermally anomalous areas or "hot spots" were identified by KenGen. The digitally processed photographs were thereafter linked with temperatures from fumaroles steam discharge sampling, soil gas sampling and with several hundred temperature measurements in shallow boreholes (1m deep). The aerial thermal mapping technique proved to be a valuable additional exploration tool, particularly in relatively unknown prospect areas with limited vegetation. (BGR 2009)

Hydrothermal activity is manifested in this area by the occurrence of fumaroles, warm springs, steaming/gas boreholes, hot/warm water in boreholes and altered rock/grounds. Fumaroles are however located mainly inside the caldera floor (Slide 7) with some weaker ones outside the caldera. The fumaroles appear to be structurally controlled and are marked by silica and or chalcedonic deposition.

SLIDE 4: Pre caldera Trachytic lavas

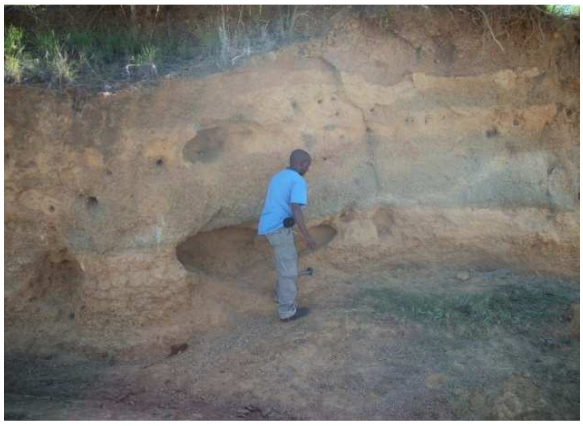

SLIDE 5: Syn caldera ignimbrite and tuff

SLIDE 6: Post caldera lava flows

SLIDE 7: Hydrothermal activity and mineralization

CONCLUSION

Regional and local structures are envisaged to be what created lines of weakness which lead to formation of the menengai caldera. These faults are also likely to be potential sites of magma accumulation and dyke formation which in turn provide heat to the geothermal system. The large diameter and circular shape of the caldera implies that the magma chamber is wide and shallow. Seismic studies in Menengai indicate that a dense body lies within 10 km below the surface (Simiyu and Keller, 2001). Studies further show that the caldera size is by no means an indication of the size of the magma chamber. This means that the chamber in Menengai is much larger and still active based on the active hydrothermal activity.

REFERENCES

Acocella Valerio. 2007:Understanding caldera structure and development: An overview of analogue models compared to natural calderas. Earth-Science Reviews Volume 85, Issues 3-4, December 2007, Pages 125-160

BGR.,2009: Geothermal Exploration at Menengai-Olbanita prospect From the World wide Web retrieved January 2010; www.bgr.bund.de

Cole et al., 2005 J.W. Cole, D.M. Milner and K.D. Spinks, Calderas and caldera structures: a review, Earth Science Reviews 69 (2005), pp. 1–96

Geotermica Italiana Srl., 1987 Geothermal reconnaissance survey in the Menengai- Bogoria area of the Kenya Rift Valley. UN (DTCD)/ GOK

Google earth: From the World wide Web retrieved January 2010;www.google.com

Seach J.,2009:Volanoes of Kenya, From the World wide Web retrieved January 2010 www.volcanolive.com/kenya.html

Jones, W.B., 1985 Discussion on geological evolution of trachytic caldera and volcanology of Menengai volcano, Rift Valley, Kenya. Journ. Geop\l. Soc. Lon, vol 142 pg 711

Jones, W.B. and Lippard, S.J., 1979 New age determination and Geology of Kenya rift-Kavirondo rift junction, west Kenya. Joun of Geol. Soc.Lon vol 136 pg 63

KenGen 2004: Menengai volcano: Investigations for its geothermal potential a geothermal resource assessment. KenGen internal report.

Leat, P.T., 1983 The structural and geochemical evolution of Menengai caldera volcano, Kenya Rift Valley. PhD thesis, University of Lancaster U.K.

Leat, P.T., 1984: Geological evolution of the trachytic caldera volcano Menengai, Kenya Rift Valley Journal of the Geological Society; November 1984; v. 141; no. 6; p. 1057-1069

Leat P,T 1985 Discussion on the geological evolution of the trachytic caldera volcano Menengai, Kenya Rift Valley Journal of the Geological Society, August 1, 1985; 142(4): 711 - 712

Lipman, 1984 P.W. Lipman, The roots of ash flow calderas in Western North America: windows into the tops of granitic batholiths, Journal of Geophysical Research 89 (1984), pp. 8801–8841 12.

Lipman P.W, 1997: Subsidence of ash-flow calderas: relation to caldera size and magma-chamber geometry, Bulletin of Volcanology 59 (1997), pp. 198–218

Macdonald .R., and Baginski B: The central Kenya peralkaline province: a unique assemblage of magmatic systems Mineralogical Magazine; February 2009; v. 73; no. 1; p. 1-16.

Odhiambo Amollo Joseph.,2005: East africa rift system, seismic activity, ground deformation and tsunami hazard assessment in Kenya coast.

Simiyu, S.M., and Keller, G. R., 2001: An Integrated geophysical analysis of the upper crust of the southern Kenya rift. Geophys. J. Int., 147, 543-561pp

GEOTHERMAL WELL SITING USING GIS: A CASE STUDY OF MENENGAI GEOTHERMAL PROSPECT

Levi Shako
Geothermal Development Company
P. O Box 17700-20100, Nakuru, Kenya. lshako@gdc.co.ke

ABSTRACT

Geothermal well site selection requires consideration of a comprehensive set of factors and balancing of multiple objectives in determining the suitability of a particular area for geothermal exploration drilling. The selection of geothermal well sites involves a complex array of critical multi-disciplinary factors and characterization. Geographic Information System (GIS), forms an invaluable link of field sample datasets from geologists, geophysicists, geochemists, reservoir scientists, and environmentalist. Geothermal spatial decision making could benefit from more systematic methods for handling multi- criteria problems while considering the physical and technical suitability conditions. Traditional decision support techniques lack the ability to simultaneously take into account these aspects which are achievable through geoprocessing and model builder tools in ArcGIS. GIS is the most efficient and effective modern technology used to make spatial multi criteria decisions that target potential geothermal resources. Comprehensive geo-scientific surface exploration was done in Menengai geothermal field prospect and multi-disciplinary data acquired through different spatial sampling techniques. The geo-scientific data from surface investigations was categorized into four key datasets; Geological (eruption centers, volcanic rocks, craters and faults), Geochemistry (soil gas, hot springs and acidic hydrothermal alteration zone), Geophysical (MT and TEM anomalies) and Surface heat loss (Heat loss anomalies). GIS was used to carry out spatial auto correlation of all the datasets, generation of trend surfaces and integrating and weighting all the four key datasets in a suitability model for geothermal well sites selection in Menengai prospect. Geoprocessing and Model builder tools were used for developing the suitabilitymodel and characterization. From the suitability model eight (8) geothermal well sites were eventually selected for exploratory drilling.

INTRODUCTION

Surface geothermal exploration projects entails in part identifying, analyzing and mapping of geothermal manifestations, such as fumaroles, altered grounds, and hot springs and other scientific survey techniques to determine prospective geothermal resources.For informed decision to be made there is need to combine and analyze the results from multi professional sample survey data and studies. Menengai area in the central rift was targeted for the accelerated development of geothermal resource. Surface geo-scientific measurements and data collection was done in order to determine the best area for drilling for subsequent reservoir assessment. The cost of drilling a typical geothermal well could range from KShs 400 Million to KShs 600 Million. Selecting suitable location for drilling a geothermal well will always remain a critical and a major decision by resource managers. The decision-making process need to combine and analyze the results of a number of different surveys and studies. GIS can be a powerful tool for minimizing human errors in identifying prospective areasfor drilling.ArcMap was used to develop a GIS Model for geothermal well drill site consisting of geoprocessing tools and a modelbuilder. Potential drill sites were defined and prioritized by assigning a weighted overlying selection query for geological, geophysical, geochemical, and heat loss data layers. GISwas used as an effective tool for the integral interpretation of geo-scientific data to determine best sites by combining various digital data layers.

Tabulated below is sample input data that was used from various surface measurements and studies in order to determine the best site location for a geothermal well:-

Data Type	Derived Parameter
Geophysics Dataset	
MT Anomaly	Heat source, reservoir extent
TEM Anomaly	Reservoir extent, permeability
Bouguer Gravity anomaly	Heat Source, Intrusive bodies
Geology Dataset	
Eruption Centers:	Heat Source
Structural setting:	Vertical Permeability
Petrological analysis	Geothermal Fluids/perm abilities
Geochemistry Dataset	
Soil gas (CO2, Radon)	Leakages, Heat source
Fluids Chemistry	Recharge, permeability
Reservoir Science	
Convective & Conductive Heat Loss	Heat Source & quantity
Boreholes Temperature Data	Reservoir Temperature
Others	
Civil dataset	Access, source of bulk construction materials
Environment dataset	Environmental Impacts

METHODOLOGY

GIS was used for integrated data modeling for selecting best area for geothermal well sites for Menengai prospect area. Spatial Analysis, a process that examines the locations, attributes and relationships of features in spatial data was run to produce various spatial models, such as suitability models, from which new information useful for geothermal resource development is derived. GIS is used to carry out a various geo-processes and analysissince it is designed to handle large amounts of data and information. In addition, it is used forvisualization of geo-scientific survey results that enhance sound decision making and allows the effective management of the data.

The model builder tools in ArcGIS were used as a graphical environment in which to develop a multi-step diagram of the complex geoprocessing tasks. When the model is run, the Model builder processes the input data in the specified order and generates output data layers.

Figure 1 displays a workflow process diagram of various data input for identification of the most suitable location of geothermal well sites in Menengai prospect. The data selection is dependent on the discipline expert and criterion selected is based on other interpretations. For instance, the considerations that areas with CO2 leakages of > 3.5% of soil gas as 'geochemical suitable areas' is based on the exploration Geochemist evaluation of the whole field data. Similarly the selection areas bound by Menengai caldera collapse as a geological suitable area is based upon the exploration Geologist's consideration of possible proximity to shallow hot magmatic bodies. Figure 1 below show the schema for selected parameters used for the suitability model.

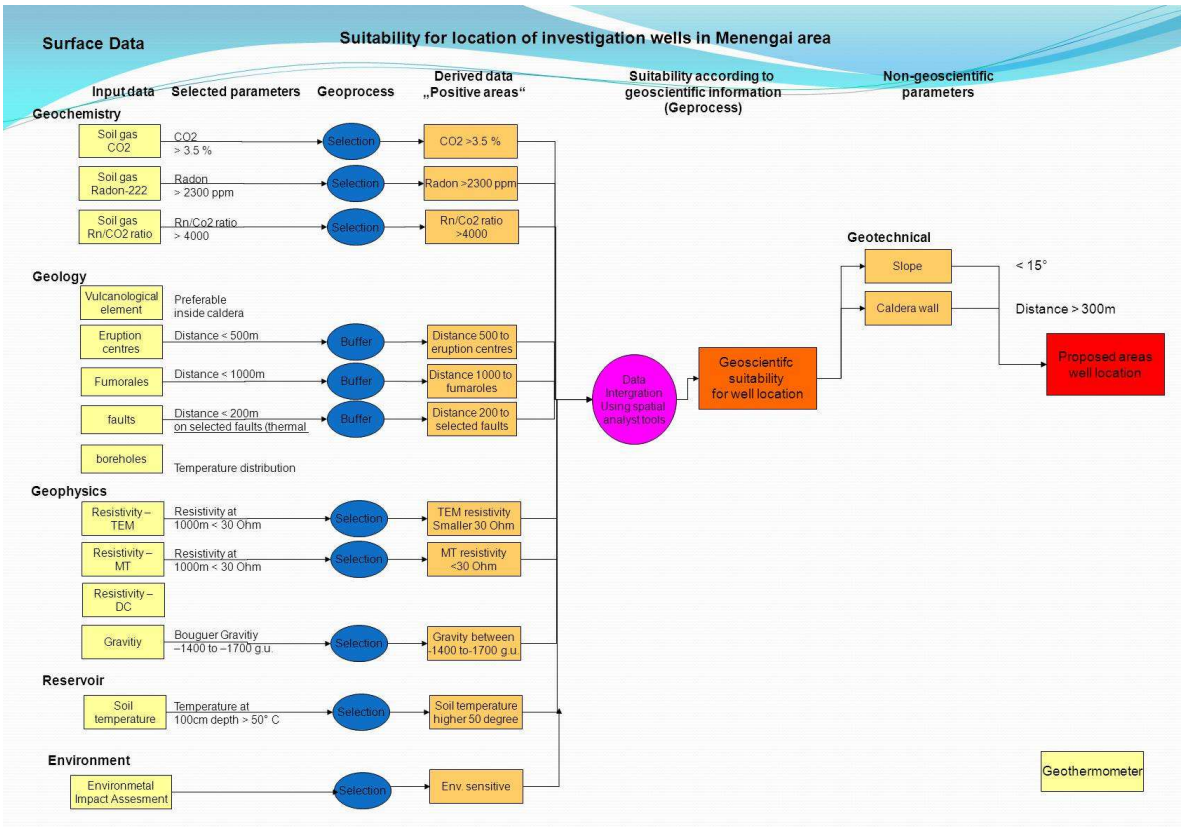

Figure 1: Workflow diagram: Data processing schema

GEOPROCESSED DATA LAYERS

Geothermal well site identification was carried out by using available digital datasets including reservoir science, geology, geochemistry and geophysics.Spatial analyst tools in ArcMap were used to derive 'positive' areas from all the scientific disciplines. Derivation of intermediate suitable areas requires creation of a geoprocessing model in ArcGIS model builder tool. The intermediate products are then integrated into a single suitability map. Data integration involves use of analysis tools in ArcMap to combine all derived information of suitable areas. Fig 2 shows an example of a geoprocessing model of some geology input data.

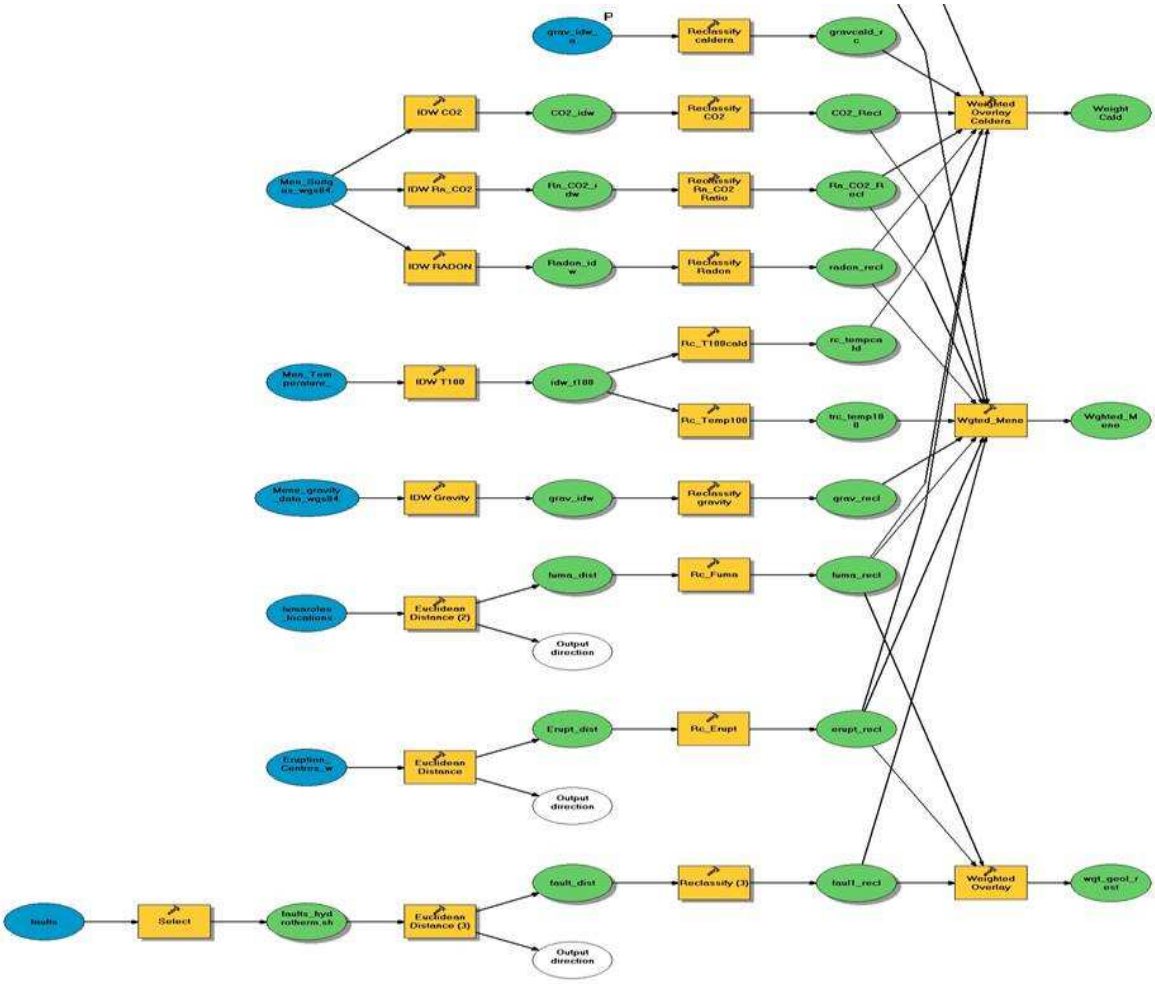

Figure 2: Suitability Model integrating geoscientic ‘positive areas’

Intermediate results

Geology Suitable Areas:

Geology dataset included classifications of faults into hydrothermal active or non-active, distances from fault and fracture due to subsurface permeability distribution, eruption centers and fumarolic activities (Figure 3)

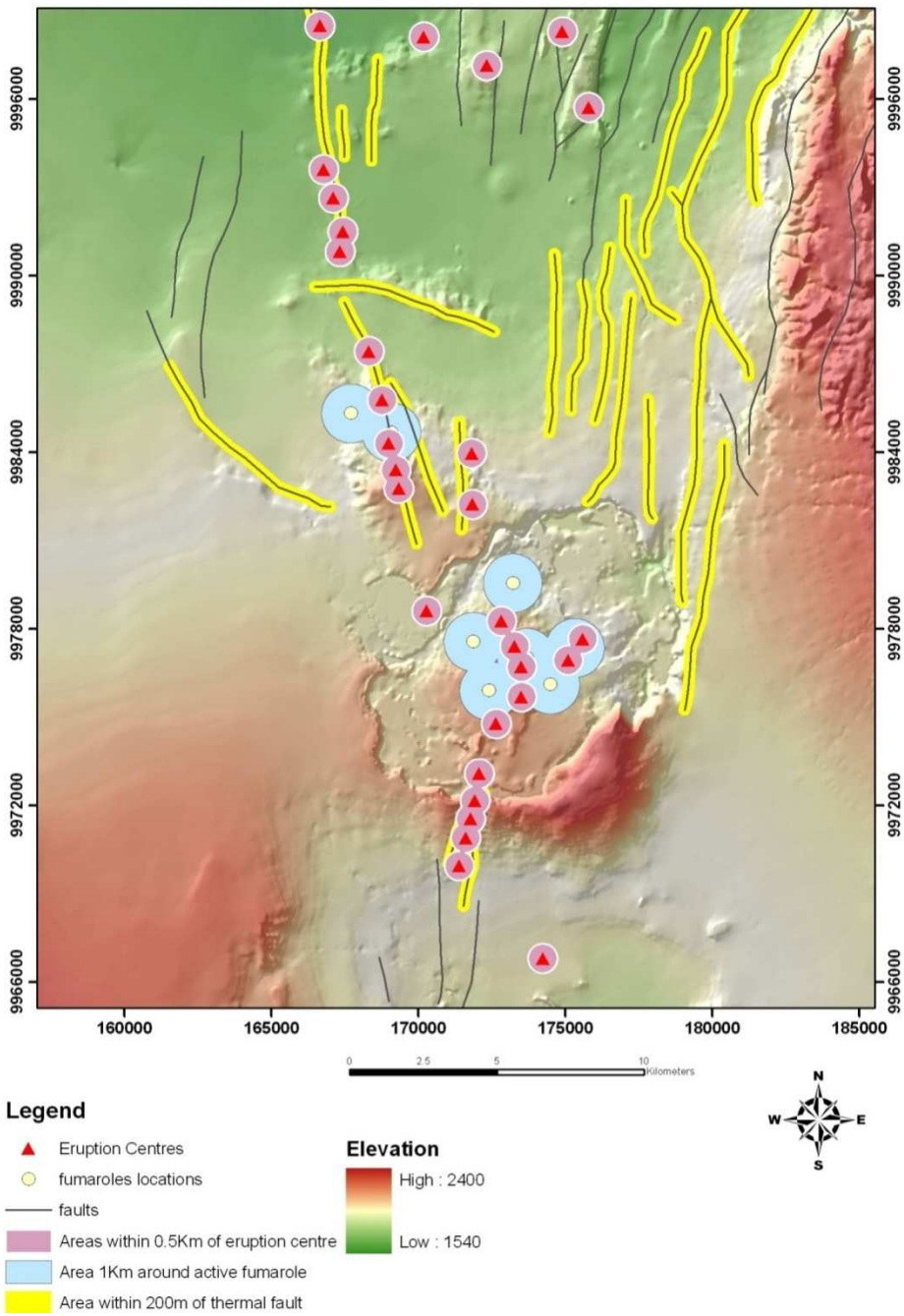

Figure 3: Showing geology data suitable areas.

Geophysics

Geophysics data used were MT and TEM anomaly maps integrated with Bouguer gravity map to derive positive areas

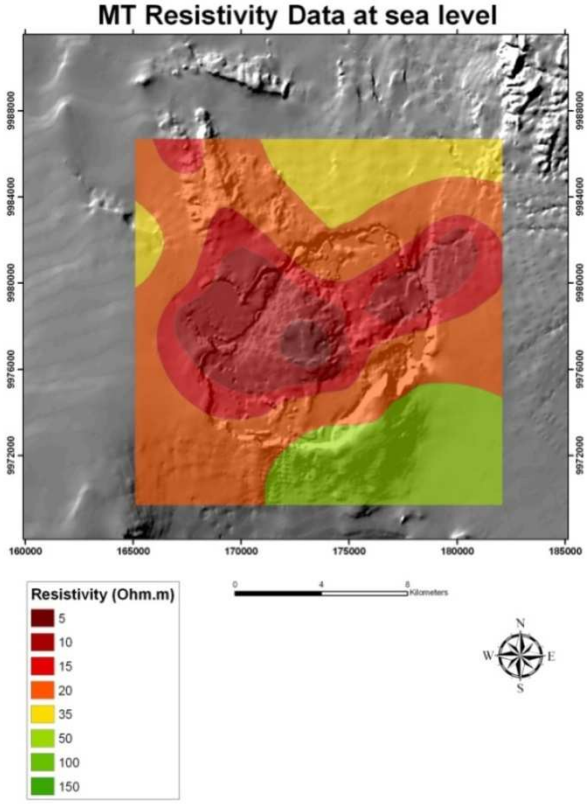

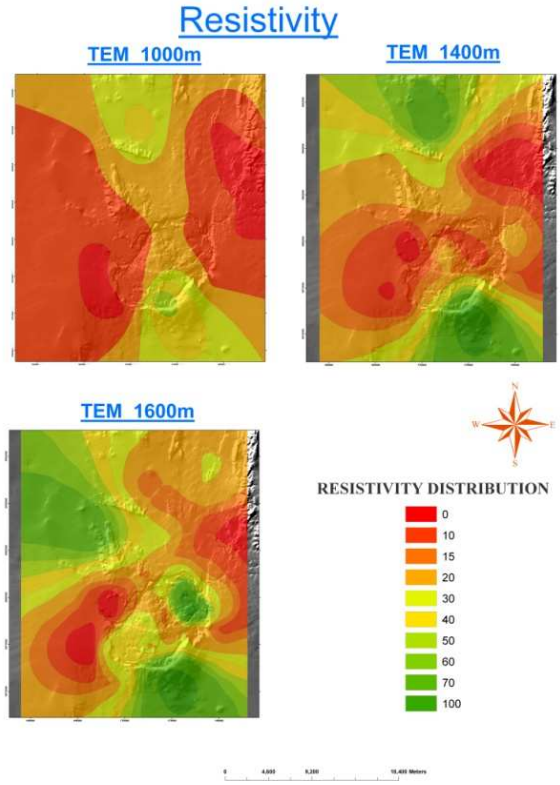

Bouguer Gravity Map of Menengai Caldera

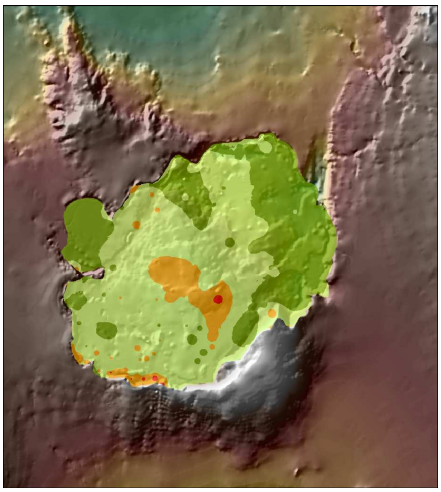

Figure 4: Geophysics data suitable areas:

Geochemistry

Geochemical parameters used include soil gas and fumaroles chemistry

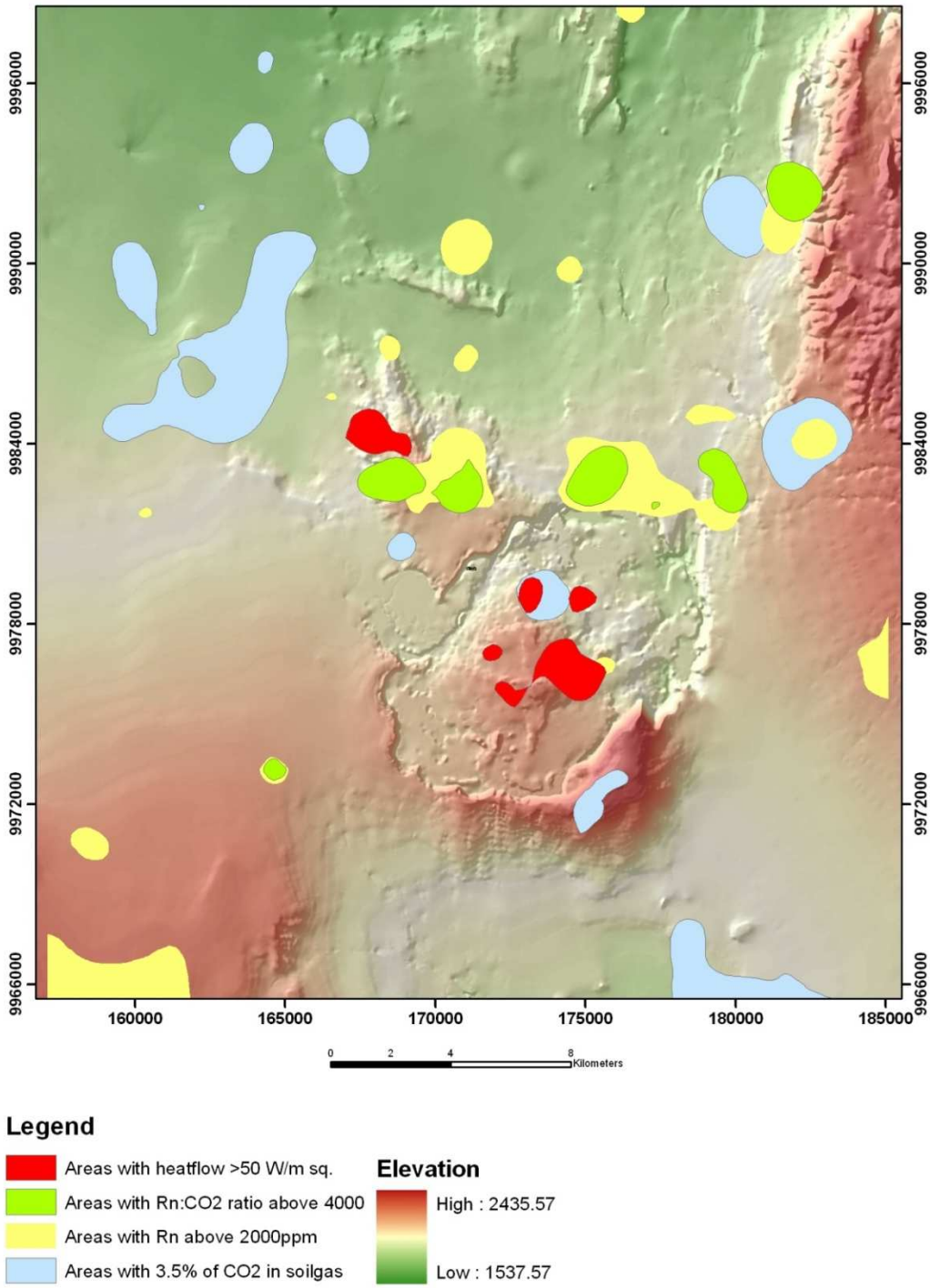

Figure 5: Geochemistry data and high heat flow suitable areas:

DATA INTERGRATION

Integration of data involves the logical combination of intermediate map products into a single suitability map. The procedure involves use of statistical and analysis tools to combine all information on the positive areas. Normally a

measurement from a given method may be given a higher confident on interpretation of a geothermal system than the other. For instance, MT resistivity sounding at 2km depth tells more on the hydrothermal activity at subsurface than fumarole temperatures measured on the surface. The suitable areas derived from the model are put through reclassification and weighted overlay process. Statistical weighting applied to the various data depends on the target depth and type of well. For shallow wells of less than 500m deep, derived data from some methods will have different weighting from wells that target 1500 m to 3000 m depth.

Geological suitable area was determined by integratingthe selected areas (buffered distances) based on eruption centers, fumarole locations and faults maps. These layers were overlain and the selected areas werecombined to identify geologically suitableareas. A suitability map based on geologicalinvestigations is shown in fig. 3. Geophysical suitable area was determined byoverlapping of the MT and TEM resistivity soundings together with bouguer gravity anomaly maps by using the analysis tools. The selected areas weremerged to identify the geophysical suitable area for siting geothermal wells. A Geophysics positive areas map is shown in fig. 4. Reservoir science derived positive area map, showing heat flow of > 50W/m sq. was combined with that of geochemistry suitable areas obtained by integratingselected areas of Radon and CO2 ratios maps. These layers were overlainand the selected areas were combinedto produce the geochemical and reservoir science suitable area map. A suitabilitymap based on reservoir science and geochemistry is shown in fig 5.

Weighted overlay table

Raster	% Influence	Field	Scale Value
Reclas_Rn222a	25	VALUE	
		1	1
		8	8
		9	9
		10	6
		NODATA	NODATA
Reclas Fumarole	15	VALUE	
		1	1
		6	6
		9	9
		10	1
		NODATA	NODATA
reclas_faults (2)	40	VALUE	
		1	1
		3	3
		9	9
		10	1
		NODATA	NODATA

Sum of influence 100 Set Equal Influence

Figure 6: Weighted Overlay statistical table

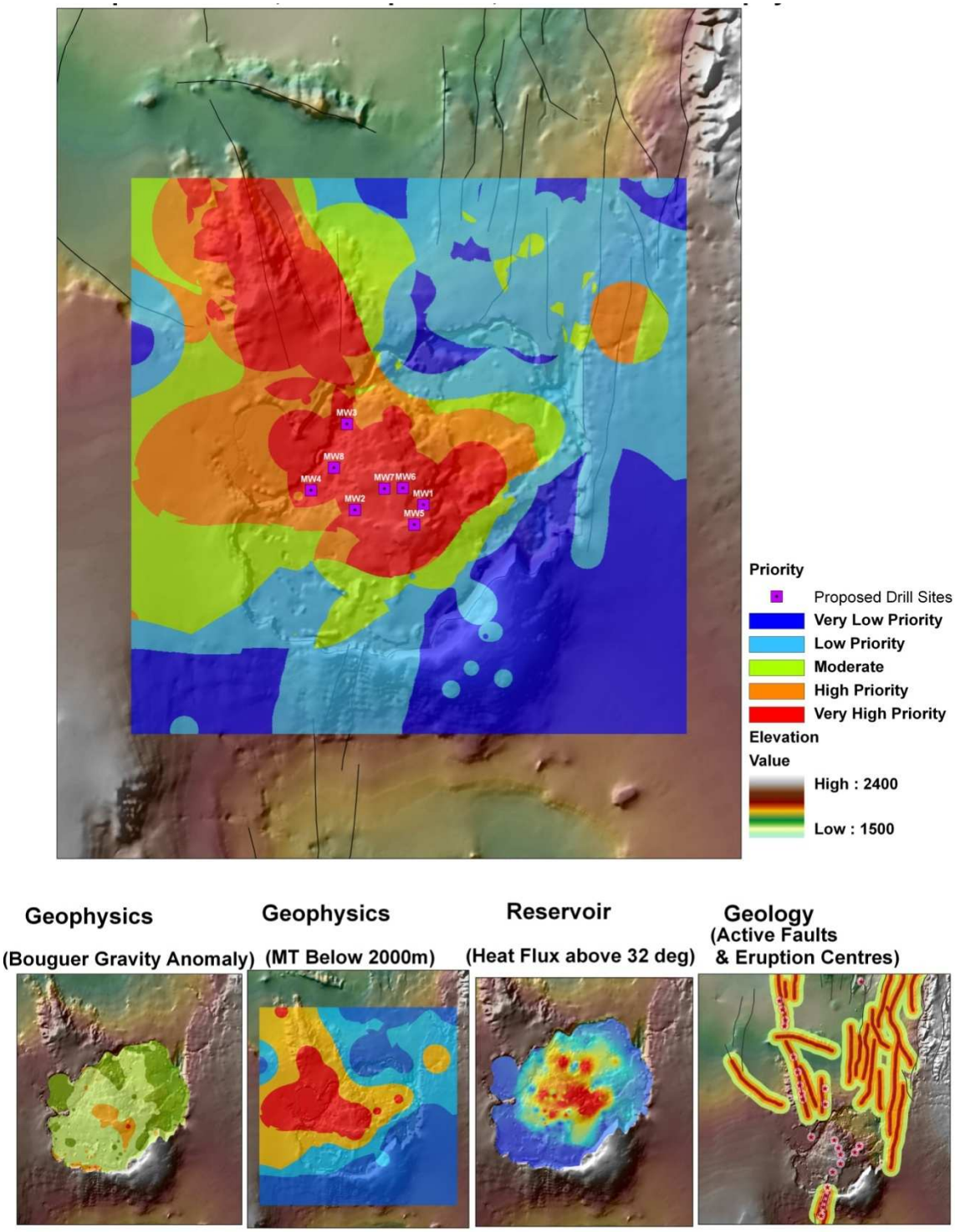

Figure 6: Shows priority areas for geothermal well sites in Menengai prospect

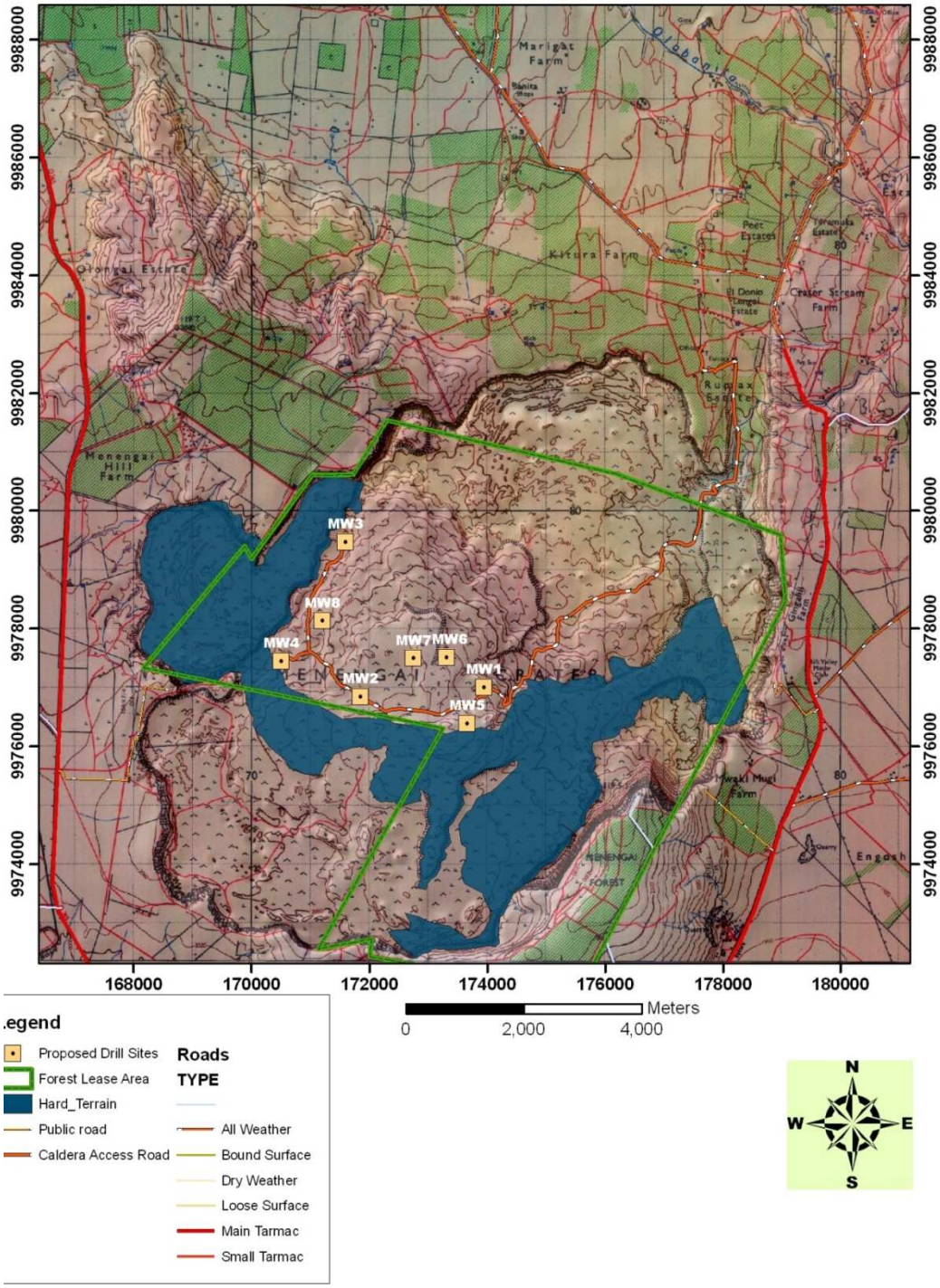

Figure 7: Map showing proposed geothermal well drill sites in Menengai prospect.

CONCLUSION

Geothermal exploratory drilling sites in Menengai prospect were investigated and identified by usingavailable geological data (structures, eruption centers, volcanic rocks, and faults), geophysical data consisting of Gravity, MT and TEM anomalies, and geochemical data such as soil gas samples, hydrothermalalteration zones, fumaroles and hot springs.

GIS was used to integrate these geo-scientific datasets in a suitability model for selecting best geothermal well sites.Eightgeothermal well drill sites werefinally identified.Observations on the final suitability model product show that the highest priority areas lie along zones of geological and tectonic significance. Since data integration process is quite automated, human bias is minimal and hence can be scientifically relied upon. The suitability model is dynamic andcan be enhanced even more by adding newdata layers to derive more relevant information useful for development of geothermal in Menengai prospect. The final priority map would normally be used by decision makers with emphasis on the available data.

REFERENCE

Bonham-Carter, 1991. Integration of geoscientificdata using GIS. In: Maguire, D.J., Goodchild, M.F., Rhind, D.W. (Eds.), Geographical Information Systems: Principles and Applications, Longman, Essex. pp. 171-184.

Bonham-Carter, G.F., (1994). “Geographical Information Systems for Geoscientists: modeling with GIS”. Computer Methods in the Geosciences 13, Pergamon, New York, 398 pp.

Geochemical evidence for syenitic protholith. African Journal of Science and Technology, Science and Engineering series, 1, 39-47.

KenGen, 2004. Menengai volcano: Investigations for its geothermal potential. Unpublished report of Geothermal Resource Assessment project

Lagat, J.K., 2004: Geology, hydrothermal alteration and fluid inclusion studies of the Olkaria Domes geothermal field, Kenya. University of Iceland, MSc thesis, UNU-GTP, Iceland, report 2, 71 pp.

Mariita, N.O. 2003.An integrated geophysical study of the northern Kenya rift crustal structure: implications for geothermal energy prospecting for Menengai area. A PhD dissertation, University of Texas at El Paso, USA

Muchemi, G.G., 1992: Structural map of Olkaria geothermal field showing inferred ring structures. Kenya Power Company, internal report, 27 pp.

Mungania, J., 1992: Geology of the Olkaria geothermal complex. Kenya Power Company Ltd., internal report, 38 pp.

Mungania J., 1999: Summary of the updates of the geology of Olkaria Domes geothermal field. KenGen, internal report.

Naylor, W.I., 1972: Geology of the Eburru and Olkaria prospects. U.N. Geothermal Exploration Project, report.

Omenda, P.A., 2000: Anatectic origin for Comendite in Olkaria geothermal field, Kenya Rift;

Wambugu, J. M., 1998: Geochemical Investigations of Longonot Geothermal prospect.

Yousefi. H, Ehara. S, and Noorollahi. Y., (2007), "Geothermal Potential Site Selection using GIS in Iran", 32nd workshop on Geothermal reservoir engineering, January 22 - 24, 2007, Stanford, CA, USA, Access site: http://pangea.stanford.edu/ERE/db/IGAstandard/record_detail.php?id=5061

THOUGHTS ABOUT TECHNIQUES APPLICABLE IN EXPLORATION OF GEOTHERMAL RESOURCES OF UGANDA

Isaiah Tumwikirize
Department of Geological Survey and Mines, P. O. Box 9 Entebbe Uganda. isaiah.tumwikirize@gmail.com

ABSTRACT

Some thoughts about the most important geophysical techniques used in geothermal exploration are presented. The exploration methods are Passive seismic, Transient Electromagnetic Magnetic (TEM) and Magnetotelluric (MT) and Gas geochemistry. Integrating the models from these techniques with geological and terrain models benefits the exploration strategy to the next step of prefeasibility and feasibility studies of the prospects respectively.

In Uganda, only surface exploration of the geothermal resources has been limited in extent and exploration techniques. Over the years, of all the available geothermal surface manifestations sites, only three prospects at Kibiro, Buranga and Katwe-Kikorongo have been studies using the geological and geochemistry methods but geophysical techniques were limited in extent and scope. TEM was used to explore the three prospects above, and covered extensively Katwe-Kikorongo. In Kibiro, fieldwork focused in the south, whereas very few TEM soundings are located in the northern part of the prospect. In Buranga, the TEM field work plan was inadequate and terrain is complex and mountainous. The results from the prospects caused the drilling of shallow wells for temperature gradient measurements in only Katwe-Kikorongo and Kibiro. Buranga was not subjected to temperature gradient measurements because the results from passive seismic and Direct Current resistivity methods alone were insufficient.

The geothermal techniques used in exploration of geothermal resources in Uganda are inadequate. The prospects need to be re-investigated using Gravity, TEM and MT.

Key words: Techniques, Geophysical Exploration, Geothermal Resources

INTRODUCTION

Geothermal resources (fig.1) in Uganda are located in the most seismically active western branch (fig.2) of the East African Rift System (EARS). On average more than 100 earthquakes a felt per year in Uganda. Its west border lies almost entirely in the western branch of the Rift System. Other tectonic features that have a great influence on earthquake occurrences and geothermal system in Uganda include:

a) The Ruwenzori Mountain: The Ruwenzori massif and tectonic movements cause stress accumulation that is released along the border and boundary faults to the mountain. The faults include:- the Nyamwamba, Kicwamba, Bwamba, and Kitimbi-Semuliki, Ruimi-wasa and Bunyoro –Toro.
b) Katonga Fault: This fault starts from foothills of the Ruwenzori Mountain, traverses Lake Victoria and connects to Kavirondo Gulf in western Kenya and Speke Gulf south of Lake Victoraia in Tanzania.
c) Aswa Shear Zone: the shear zone is observed in Uganda from Nimule at Uganda –Sudan Border and joins Mt Elgon in the north-east (see Kiatabosi Hotspring). The north – eastern volcanic fields is part of an array of tertiary and pre-tertiary that is composed of Mts. Moroto, Kadam and Napak (see Kanagorok hot spring fig.1).

The tectonic setting provides potential for geothermal resources and high seismic activity. Catastrophic earthquakes include the:

- 9th July 1912 Kitgum earthquake measured magnitude 6.7 (on Richter scale), with partial destruction of buildings in Northern Uganda;
- 18th March 1945 Sembabule earthquake measured 6.0, killed five people and destroyed buildings;
- 20th March 1966 Toro earthquake measured 6.6 and killed 150 people, injured 1,300 people and economic loss of 1million dollars;
- 5th February 1994 Kisomoro-Toro earthquake measured 6.2, killed 8 people and caused destruction of property worth 61 million dollars.
- 7th September 1990 Lake Victoria earthquake measured 5.0 destroyed semi-permanent buildings;
- 18th March 1945 Sembabule earthquake measured 6.0, killed five people and destroyed buildings.

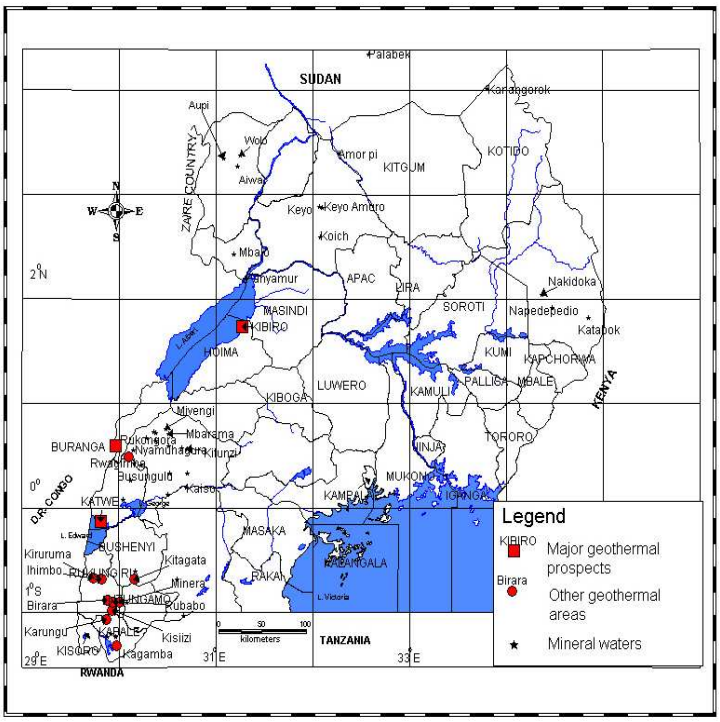

Fig.1: Geothermal prospects of Uganda

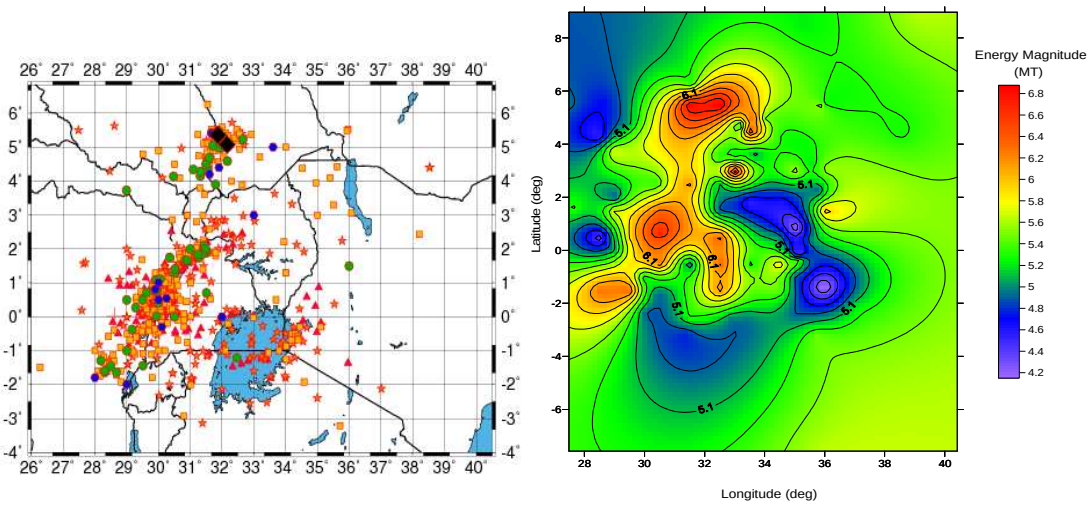

(a) (b)

Fig. 2: **(a)** Earthquakes (1840-1999).Earthquake magnitude is shown in range by symbols: 1.0 ≤ M≤ 1.9 red cross; 2.0 ≤ M≤ 2.9 red triangle; 3.0 ≤ M ≤ 3.9 red star; 4.0 ≤ M ≤ 4.9 orange square; 5.0 ≤ M ≤ 5.9 green circle; 6.0 ≤ M ≤ 6.9 blue hexagon; 7.0 ≤ M ≤ 7.9 black diamond symbols **(b)**: Seismic energy release.

Katwe –Kikorongo (Katwe) Prospect:

Katwe is located in the Kasese district (fig.1). It is within the Queen Elisabeth National Park, south of the Rwenzori Massif and north of Lake Edward. Katwe is a volcanic area with many phreatic craters but very little lava on surface. Some of the craters have crater lakes. The most pronounced hot spring is on bottom of the Crater Lake in the Kitagata crater. As being

in a national park, the Katwe area is mostly uninhabited, except for the Katwe village, south of the saline lake Katwe. Considerable salt mining takes place in Lake Katwe.

Kibiro Prospect

Kibiro is situated in Hoima district, on the eastern shore of Lake Albert (fig.1). Kibiro is located at the foot of the escarpment of the western branch of the East African Rift System (EARS), and is connected by a rough but motorable track up the escarpment from Kigorobya town council, which has road connection to Hoima in the south and Masindi to the north through Biiso. The escarpment, which rises over 300 m above Lake Albert, has a profound influence on land use in the area.

Buranaga Prospect

Buranga is situated at the western foot of the northern part of Rwenzori Mountains (fig.1) within the rift sediments of Semliki basin in the Semuliki National Park in Bundibugyo district.

PREVIOUS WORK

Geothermal investigations in Uganda were revived by the Ministry of Energy and Mineral Development (formerly Ministry of Natural Resources) in 1993 in co-operation with United Nations Development Programme (UNDP) under a project called Geothermal Exploration UGA/92/002 & UGA/92/E01. The project was co-funded by the Government of Uganda, UNDP, the Government of Iceland and Organisation of Petroleum Exporting Countries (OPEC) primarily focused on geochemistry and geology.

Isotope Hydrology for Exploring Geothermal Resources, UGA/8/003 & 005, in co-operation with International Atomic Energy Agency (IAEA), was initiated in 1999 and completed in 2007 Under the project, hydrological studies were carried out in the same three areas, Katwe, Buranga and Kibiro, as the earlier project and the findings regarding the Katwe area showed that the recharge is from the Rwenzori Mountains, subsurface temperature of 140 - 160ºC predicted by geothermometry.

In 2002 the Icelandic International Development Agency (ICEIDA) prepared a status report, where the current situation in the geothermal survey was reviewed, and recommended further actions to be taken to complete a pre-feasibility study in the three above-mentioned geothermal areas. Since then the Africa Development Fund (AfDF) funded a project to complete the study in two of the areas, Katwe and Buranga, but ICEIDA agreed to assist the Ministry of Energy and Mineral Development (MEMD) to complete the study in Kibiro. A project agreement was signed in 2003 and a work plan agreed upon, based on the recommendation set forward in the status report (ICEIDA 2004).

In 2004 and 2005 a geological and geophysical survey were carried out by professionals from Iceland and the DGSM in Kibiro. The surface exploration was later followed by a temperature gradient survey where the drilling cost was financed by the World Bank.

The AfDF funded project started in Katwe in 2003 and was continued in 2004. No work was however done in Buranga under that AfDF project. Later (2005 - 2006) The Germany Federal Institute for Geosciences and Natural Resources (BGR) financed and carried out a geothermal survey in Buranga in cooperation with the MEMD (BRG-MEMD, 2007).

The AfDF project in Katwe comprised geological investigation, TEM resistivity measurements, gravity- and ground magnetic measurements (Uganda-ARRDP 2004). The survey was mainly focused on three profiles. Densely spaced magnetic and gravity (271 stations) measurements were done along the profiles. TEM soundings were done along the profiles and some soundings spread over the whole crater area.

The AfDF survey gave some clear structural information but since the survey was mostly limited to three profiles, it was not considered as very conclusive and hence as insufficient geophysical survey of the area. The magnetic measurements did not provide any readily usable information but the gravity measurements and TEM soundings did.

GEOPHYSICAL TECHNIQUES

The geophysical methods presented here are the major ones useful in prospecting for heat source and associated structures in geothermal surveys.

Total Magnetic Field

The magnetic field is a dynamic entity and varies significantly on all temporal and spatial scales. The largest component 80 to 90% of the earth's magnetic field is believed to originate from convention of liquid iron in the earth's outer core. The remaining component of the field originates in rocks near the surface where temperatures are low, being less than 580°C in a region of upper crust (20-30) km (Nabighian et at., 2005, p. 34NB).

The magnetic method is discussed by many scholars for instance (Telford et al., 1976, pp.105-215; Nabighian et al., 2005, pp. 33ND-53ND). Magnetic method developed based on the earth's magnetic environment, because the earth has its own internally generated magnetic field, the bulk (99%) of which arises from a self-sustaining dynamo that operates in the liquid outer part of the core, and the remaining 1% arises from electric currents from ionosphere (radiation of particles) and solar winds due to the Sun. The method involves the measurement of earth's magnetic field and the interpretation of its variation in the survey area. The variations cause anomalies due to the field produced by the magnetic material within the earth.

The magnetic anomalies of geologic interest are of two types: induced magnetisation and remanent magnetisation. Induced magnetic anomalies are as a result of magnetisation induced in a body by the earth's magnetic field. The anomaly produced is dependent on the geometry, orientation and magnetic properties of the body as well as the direction and intensity of the earth's magnetic field.

Remanent magnetic anomalies are as a result of permanent magnetization of the body and are controlled by the direction of remanent magnetisation, and the geometry of the disturbing mass. Most magnetic anomalies are a combination of both types; however, usually one type is dominant and is used to interpret the results.

Gravity

Gravimetry is a geophysical method that measures the acceleration due to gravity. It 'involves measurement of variation of earth's gravitational field' (Telford et al., 1976, pp. 7-103). Gravimetry as a geophysical method is based on the universal law of gravitation. The law states that: every particle of matter exerts a force of attraction on every other particle that is directly proportional to the product of their masses and inversely proportional to the square of the distance between them. The other instrumental law in Gravimetry is Newton's second law which can be stated as: a body experiences an acceleration that is directly proportional to force and inversely proportional to the mass when a force is applied. The gravity variations associated with geologic bodies is measured in milligals. A gravity meter thus measures the maximum vertical component gravity difference between the earth's field (the main gravity of reference spheroid) and that is actually observed on the surface (gravity meter). The difference of the gravity value is the gravity anomaly and reflects the lateral density variations in rocks extending to a depth.

Resistivity method

Telford et al., (1976, pp. 632-700) discusses the resistivity method. This method uses electrical properties of the rocks, which also depend on the amount of water or pore-fluids within the rock, the salinity of the water and the distribution of water in the vicinity. The higher porosity of rocks saturated with water lowers the resistivity. High salinity of the saturating fluids too lowers the resistivity. The presence of clays and conductive minerals also reduces the resistivity of the rock. Thus saturated rocks have lower resistivities than unsaturated and dry rocks. The resistivity method is primarily facilitated by the ability of rocks to conduct electrical current and also the polarisation which occurs when electrical current is injected in the ground or the rocks. By injecting current into the earth, the electrical conductivity of the material that make up the earth are revealed by measuring the induced voltage between two potential electrodes by choosing appropriate array configuration. However, most commonly the geothermal water lowers the resistivity, but in some cases the resistivity increases again at very high temperatures.

Transient Electromagnetics

In the transient electromagnetics (TEM) method, the earth is excited by injecting electric current into the ground using a transmitter. A loop of wire is laid on the ground and a constant current is injected through the loop to build up a constant magnetic field of known strength. The current is turned off in a controlled manner by adjustments on the transmitter; the magnetic field starts to decay and, at the same time, induces secondary electrical currents in the ground. In turn, the induced a secondary magnetic field also decaying with time. The decay rate of the secondary magnetic field is then monitored by measuring the voltage induced in a receiver coil or a small receiver loop at the centre of the current transmitting loop. The distribution of the current and the rate of decay of the secondary magnetic field both depend on the resistivity structure of the earth.

Magnetotelluric

The Magnetotelluric (MT) method is a passive frequency-domain electromagnetic sounding technique that measures the earth´s response to natural electric (telluric) and magnetic fields to investigate the resistivity structure of the subsurface. The electromagnetic waves (EM) of the MT signals are mainly caused by distant lightning (above 1 Hz), and electric currents flowing in the ionosphere (below 1 Hz). The EM field caused by changing currents radiates around the earth,

reflected repeatedly between the conductive ionosphere and the relatively conductive earth. The MT method exploits naturally varying EM fields, spanning from 0.0001 Hz to 10 kHz. These primary fields induce secondary electric and magnetic fields in the conductive earth.

Telluric currents are caused to flow in the earth by the earth's varying magnetic field. As an electromagnetic wave propagates through the earth, its amplitude decays exponentially with depth at a rate dependent on the conductivity of the medium and the frequency of the wave. Longer periods (low frequencies) decay more slowly with depth and therefore penetrate deeper. The EM fields recorded at the surface of the earth are, therefore, diagnostic to the electrical properties of the earth. Hence, information about the near-surface and deep structure is deduced from high-frequency and low frequency variations, respectively.

MT surveys are conducted by measuring two perpendicular horizontal, *x* and *y* components of the electric and magnetic fields (***E*** and ***H***), and the vertical, *z* component of ***H*** as a function of time. The time series recorded are then Fourier transformed to the frequency domain for further processing, determining the impedance tensor, apparent resistivities and phases.

In the field, a typical layout of a five component MT unit consists of five (5) electrodes, four (4) of which measure two (2)-perpendicular horizontal components of the electric field (*Ex*,*Ey*), and the fifth electrode is used to ground the MT unit data logger at the centre. For magnetic field measurement, three (3) induction coils are involved, two (2) of which measure two (2)-horizontal perpendicular components *(Hx*,*Hy*), and one (1)-coil measures the vertical component (*Hz*) of the magnetic field. The MT sounding method, like all resistivity methods that are based on measuring the electric field in the subsurface, suffers the so called telluric or static shift problem. The static shift is caused by shallow resistivity inhomogeneities close to the electric dipoles, and can cause severe problems in the interpretation of MT data by shifting the apparent resistivity sounding curves (on a log scale) by a scale factor, which is independent of frequency. Telluric shift correction in the MT is achieved by jointly inverting the MT and TEM sounding data collected at the same location (Nyago 2009).

Seismic

Seismic methods are divided into two: (a) Passive seismic methods deal with the detection and recording of natural seismicity and induced seismicity due to ground fracturing associated with geothermal fluid extraction or injection. The seismic activity gives information about active faults and therefore permeable zones in geothermal systems. (b) Active seismic methods are concerned with seismicity generated by artificial wave sources. The propagation of the generated waves is used to study the geological structures and strata.

INSTRUMENTS FIELD PROCEDURE

TEM: Protem-67 instruments from Geonics Ltd. in Canada was used. The system comprises a PROTEM digital receiver, TEM67 transmitter with motor generator, a receiver coil with the effective area of 100 m2 and 800 m of cables for the source loop. The source loop used, was a single turn 200*200 m2 square loop. The transmitter transmitted 23 A half duty square wave current at the repetition rate of 2.5 Hz, with two 100 ms current off intervals in each cycle. The receiver and the transmitter are synchronised by connecting them by a signal cable such that the receiver records the induced voltage in the receiver coil, during the current off intervals, at 30 time gates, logarithmically spaced from 0.09 to 69.8 ms after the current turn-off. During recording, 75 to 150 transients were stacked in order to reduce external electromagnetic noise. Several tens of stacked transients were recorded and stored in an internal memory in the receiver, to be later downloaded to a PC computer.

Gravity: The gravity surveys were taken using Scintrex CG-3 Model-110196 Autograv gravimeter that was operating at a resolution of 0.005mGal. Positioning and determination of the elevation was done by differential GPS technique, using a pair (base and a rower) of Magellan Promarc x-cm (10 channels, single frequency, and carrier phase data) GPS system.

Magnetics: The instrument used was two Portable Invimag Proton Precession total filed magnetometers from Scintrex. One of the magnetometers was used as a reference station to correct for diurnal variations. The reference station was placed in the survey area at the coordinates 0308457E and 0181866N (UTM, Arc 1960). The rover was used to measure the total field at 5 m interval along profiles. The positioning was performed by a hand held GPS instrument and a measuring tape. Pre-calculated coordinates of stations at 50 m intervals along the profiles were loaded into the GPS instrument, which was used to navigate to these points. The absolute accuracy of these locations is of the order of +/-5 m.

DATA ACQUISITION

Katwe: TEM data was collected using Protem 67 Transmitter and Receiver reported here were collected under two projects: AfDF project from 4th to 13th April 2003 and 19th to 25th November 2004 (see red dots). ICEIDA/MEMD project started on August 19th to September 23$^{th.}$ 2005 (blue dots in fig.3).

Kibiro: The fieldwork started on 16th of February and was continued until March 26th 2004. TheTEM soundings were starting to reveal a N-S trending low-resistively anomaly to the south of Kibiro emphasis was put on that region and six relatively densely spaced E-W profiles (M6 to M11) were measured in order to see if a magnetic anomaly was associated with the resistively anomaly. A total of about 80 km were traversed amounting to over 16.000 magnetic stations. During the first days two gravity new base stations were established one at Kigorobya Health Centre and the other at Kabiribwa at the top of the escarpment above Kibiro. The gravity values at these reference stations were determined by connecting to an already established base station in Hoima. The new base stations were used for the GPS measurements and time dependent drift corrections for the gravimeter.

Large parts of the survey area are covered with dense bushes and some places the accessibility was further limited by deep gullies. Despite the difficult conditions a total of 75 soundings were made, amounting to an average performance of about three soundings a day.

Buranga

Ground geophysical field survey at the Buranga geothermal prospect started on 11th of February and ended on 4th of March 2005. Geoelectrical, TEM and gravity measurements were carried out. BGR installed seismic stations and between May 2005 and August 2006, earthquakes were rregistered at several seismological stations.

FIELD RESOURCES AND PLANNING

The field crew consisted of three experts from GSMD, one driver and two local helpers. ICEIDA expert supervised the fieldwork during the first week, but after that the field crew was properly trained and the ICEIDA expert could concentrate on data processing, interpretation and survey planning. The recorded data were downloaded to a PC computer at the end of each day and inspected and processed by the ICEIDA expert.

RESULTS

Katwe TEM

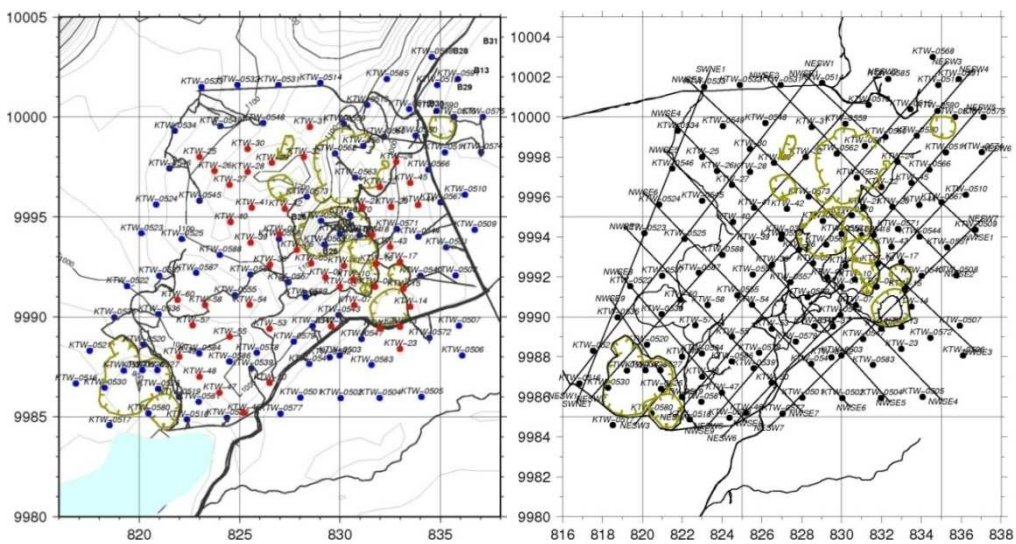

Fig. 3: Location of TEM stations in the Katwe area. Red points are stations from the ADF project and blue are stations from the ICEIDA/MEMD project.

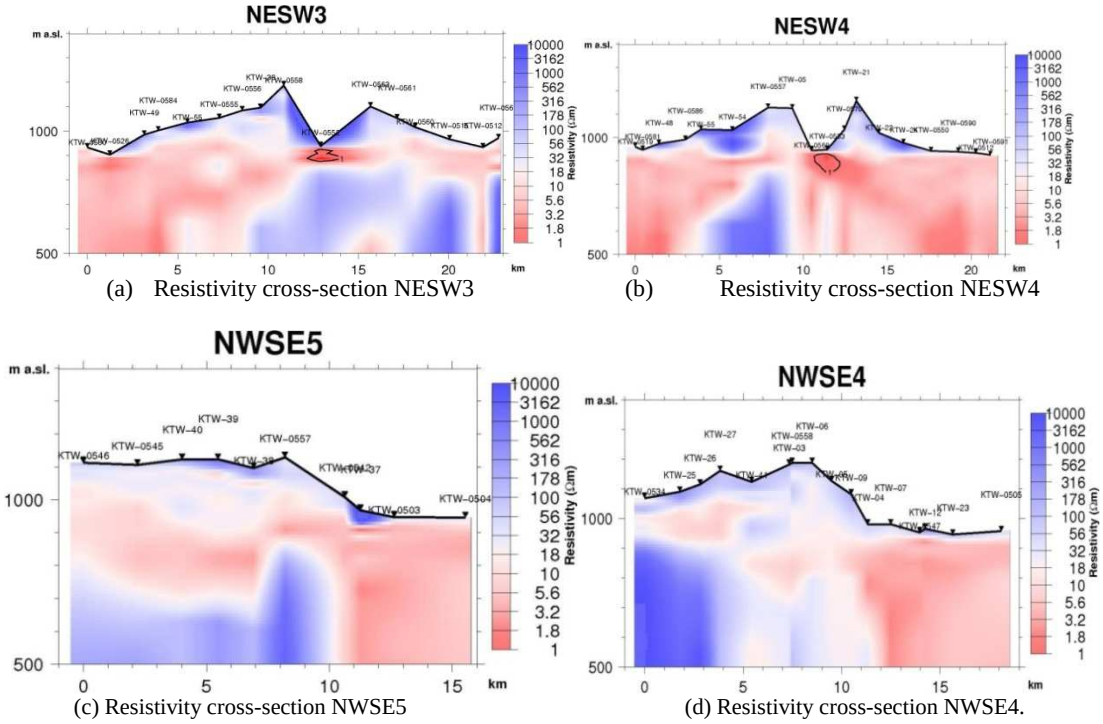

(a) Resistivity cross-section NESW3 (b) Resistivity cross-section NESW4

(c) Resistivity cross-section NWSE5 (d) Resistivity cross-section NWSE4.

Fig.4: Various section of TEM in Katwe prospect. The depth extent is limited in the rift sediments and anomalies are weakly resolved for deep well drilling.

Katwe Gravity

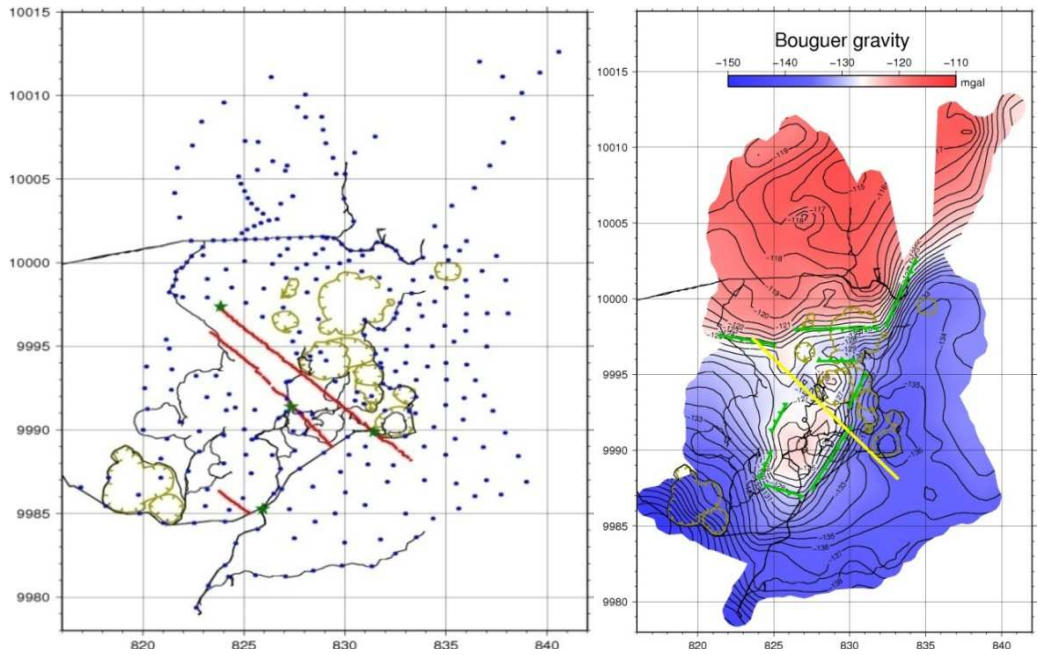

Fig.5: (a) Location of gravity stations in the Katwe area. Red points are stations from the ADF project and blue are stations from the ICEIDA/MEMD project. Green stars are local reference stations. (b) Bouguer gravity map of the Katwe area and inferred faults (in green). The location of the model profile is on by yellow line.

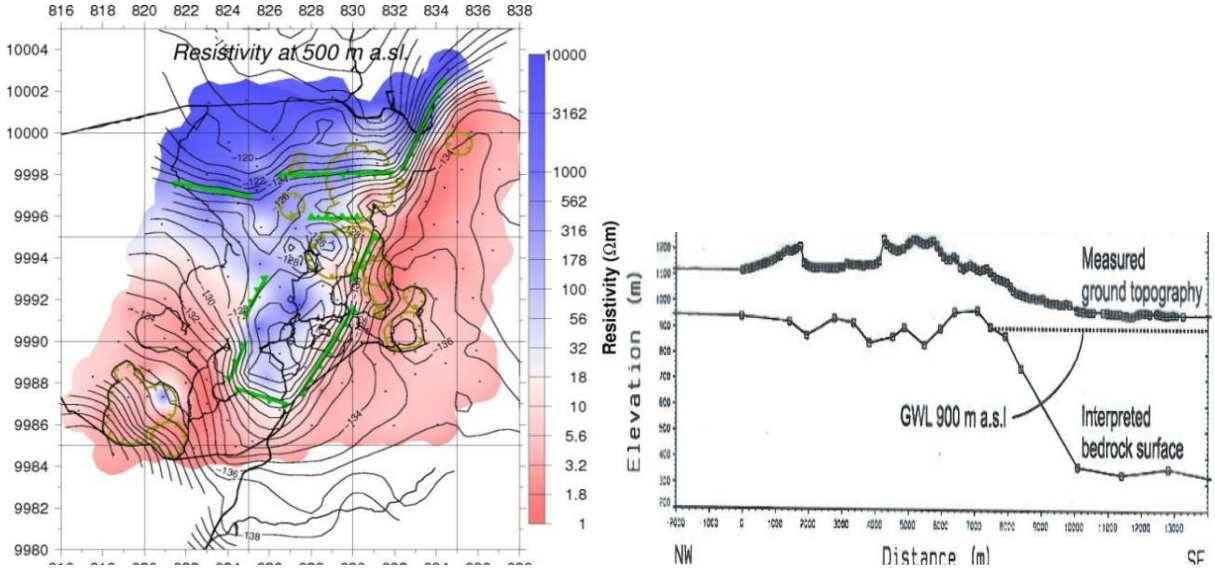

(a) (b)

Fig.6: Resistivity at 500 m a.sl; Bouguer gravity contours and inferred faults. (b) Model of sediment thickness and elevation of basement rocks (Uganda-AERDP 2004). Note that the thickness of the sediments is over 700m and all the drilling was done in the sediments.

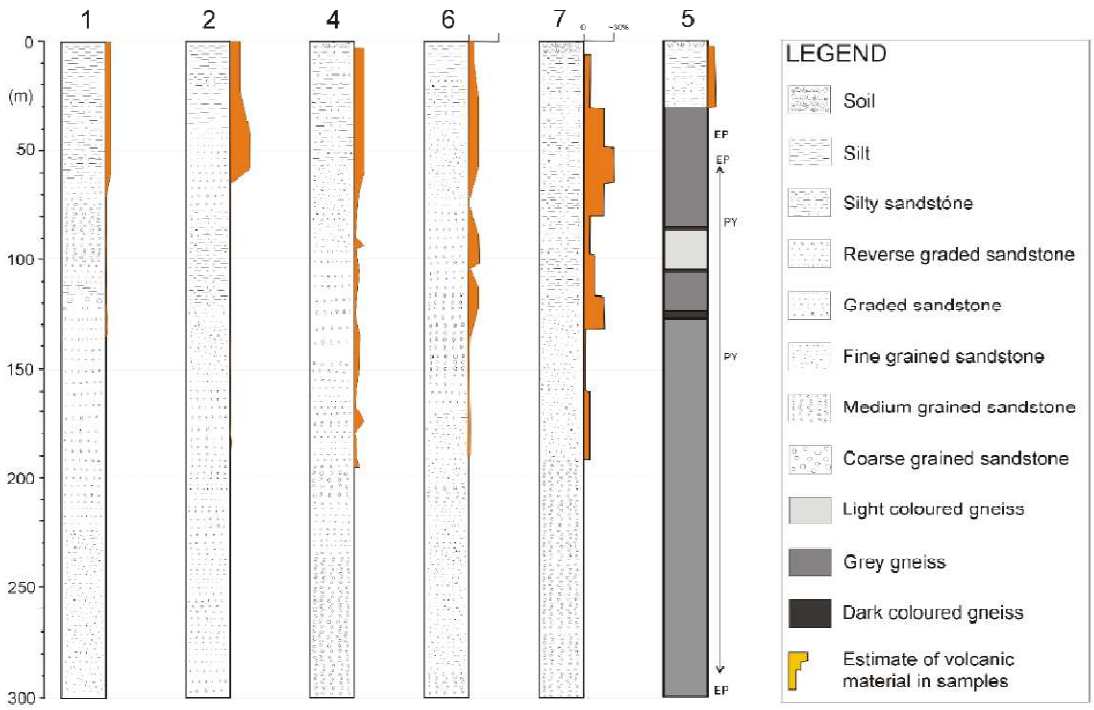

Fig.7: Katwe Stratigraphy of temperature gradient wells (ICEIDA 2008b). Note that drilling encountered rift sediments and volcanic except in borehole 5 in the north west of the prospect.

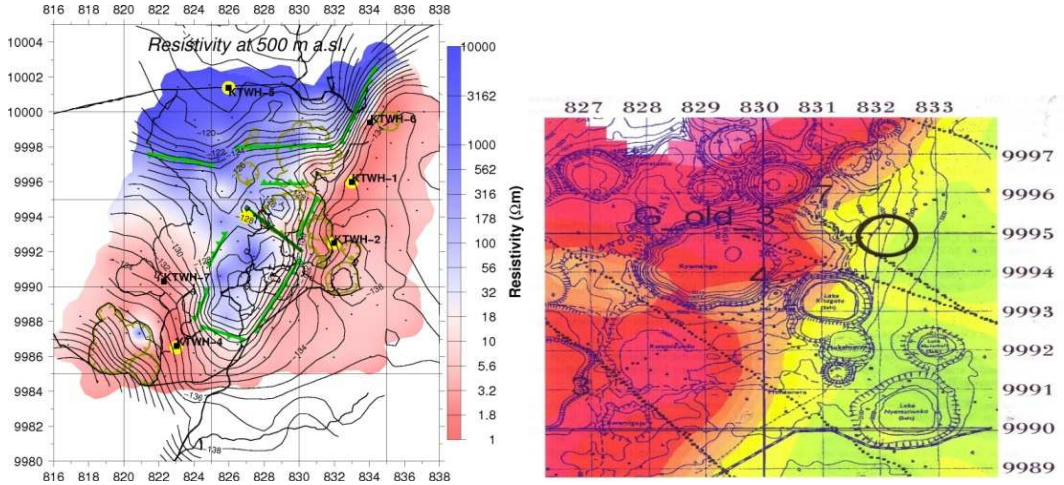

(a) Katwe temperature gradient sites (b) Katwe deep well site

Fig. 8: Locations of temperature gradient holes (yellow circles) and actual locations of the holes (black squares) (ICEIDA 2004) (b) Black Circle is a site recommended for drilling by Uganda-AERDP in 2004.

Table. 1: Temperature gradients in the boreholes in Katwe and extrapolated surface temperature.

Borehole	Gradient °C/km	Surf. temp. °C
KTWH-1	36.0	29.3
KTWH-2	36.0	27.8
KTWH-4	28.3	28.4
KTWH-5	13.0	24.7
KTWH-6	30.0	27.8
KTWH-7	33.5	28.2

The extrapolated surface temperatures are consistently about 28-29 °C at the lower altitudes and somewhat lower, about 25°C, for KTWH-5, which is at higher altitude. The extrapolated surface temperatures are consistently about 28-29 °C at the lower altitudes and somewhat lower, about 25°C, for KTWH-5, which is at higher altitude. The temperature gradients are all rather low, especially in KTWH-5. The temperature gradients in KTWH-5 and the other holes are not directly comparable. KTWH-5 is drilled into the granitic basement but the other holes are mainly drilled in sediments. The heat conductivity of granite is higher than that of sediments and equal heat flow would consequently have lower gradient in granite than in sediments (ICEIDA 2008b).

The temperature gradients are highest in holes KTWH-1 and 2, which are in the low resistivity anomaly South East of the main graben fault. This might indicate that the observed lower resistivity is due to slightly elevated temperatures. But the temperature gradients and estimated heat flow do not indicate that high temperatures are found in the uppermost few kilometres in the Katwe area (ICEIDA 2008b).

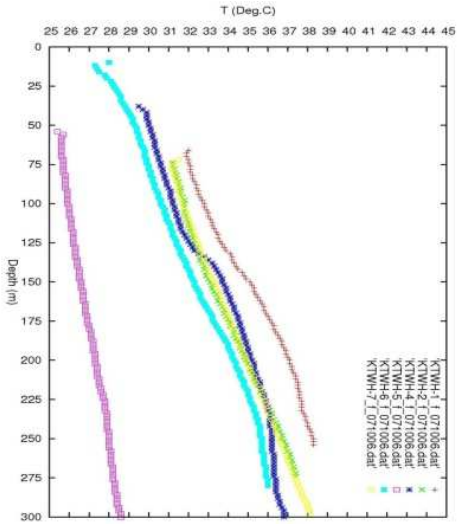

Fig. 9: The final temperature measurements in all the boreholes. Measurements in different holes are shown with different colours. The borehole numbers (KTWH-x) are shown in the lower right corner (ICEIDA 2008b).

Kibiro TEM results

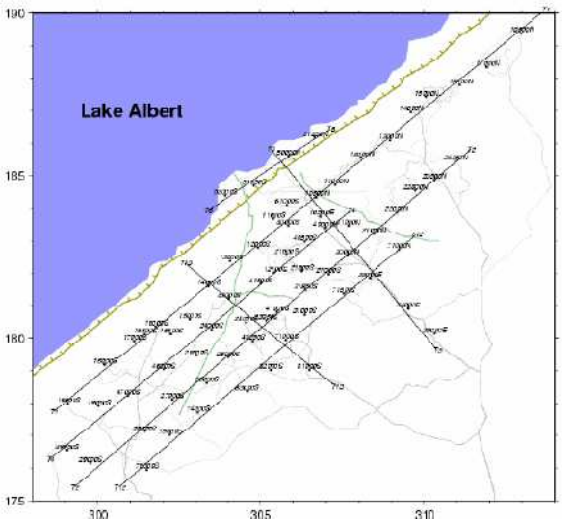

Fig 10: Location of TEM soundings and section lines in Kibiro Prospect

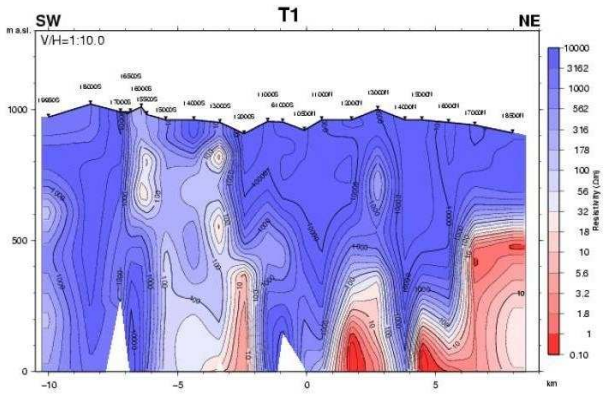

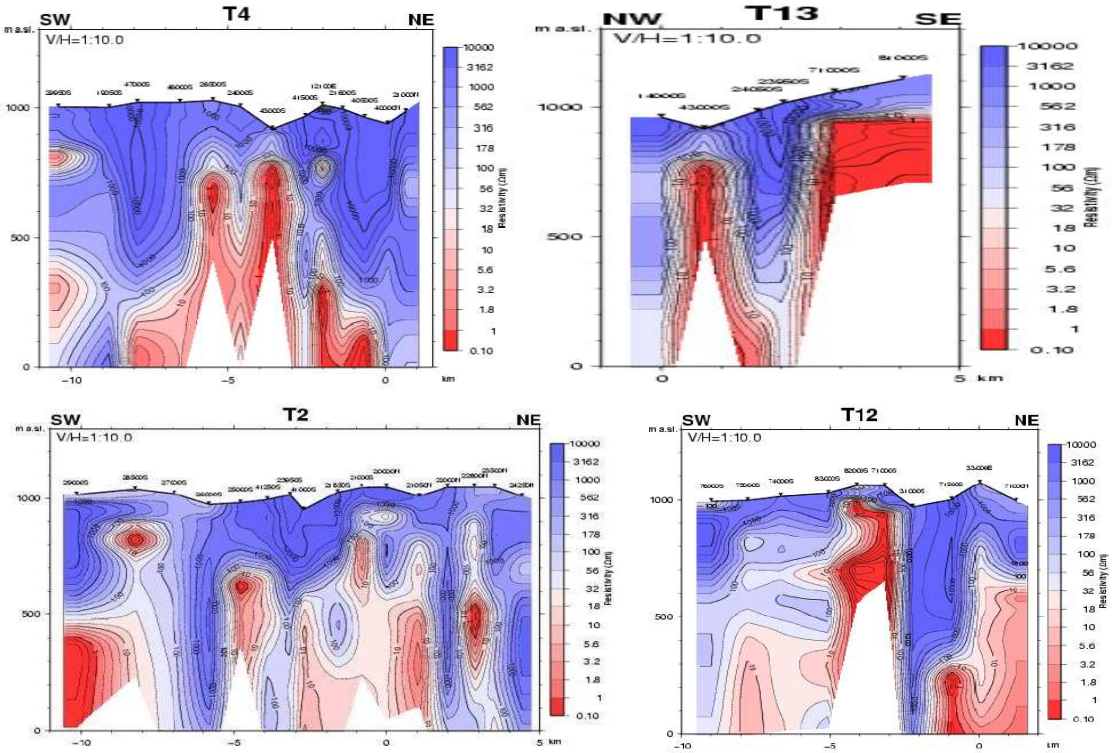

Fig.11: Various TEM sections in Kibro prospect. Note that the weak resolution at depth and gaps in the data. TEM only resolved the anomalies in few hundreds of metres above sea level (m. a. s. l). The observed low resistivity anomaly in shallow depth may be due to conductive minerals.

Kibiro Gravity

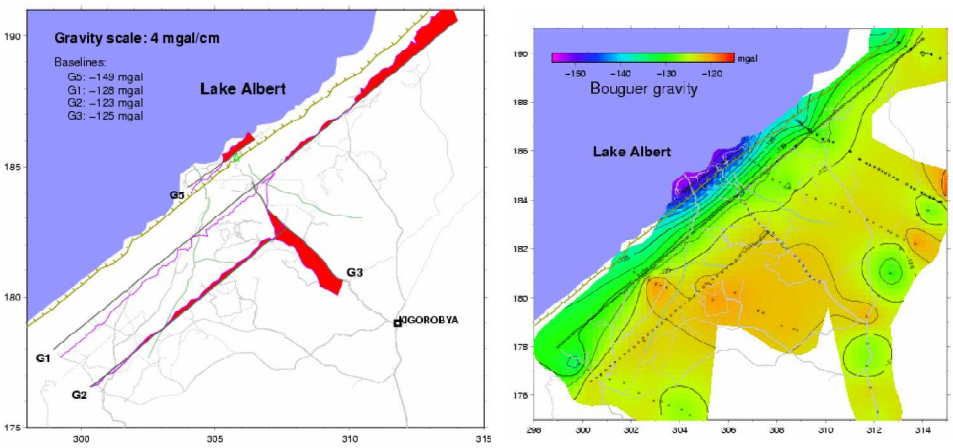

(a) Profiles and gravity response (b) Bouguer gravity map

Fig.12: The geothermal anomalies (b) are weakly resolved due to the few data samples (dots) collected and small gravity survey coverage.

Kibiro Magnetics

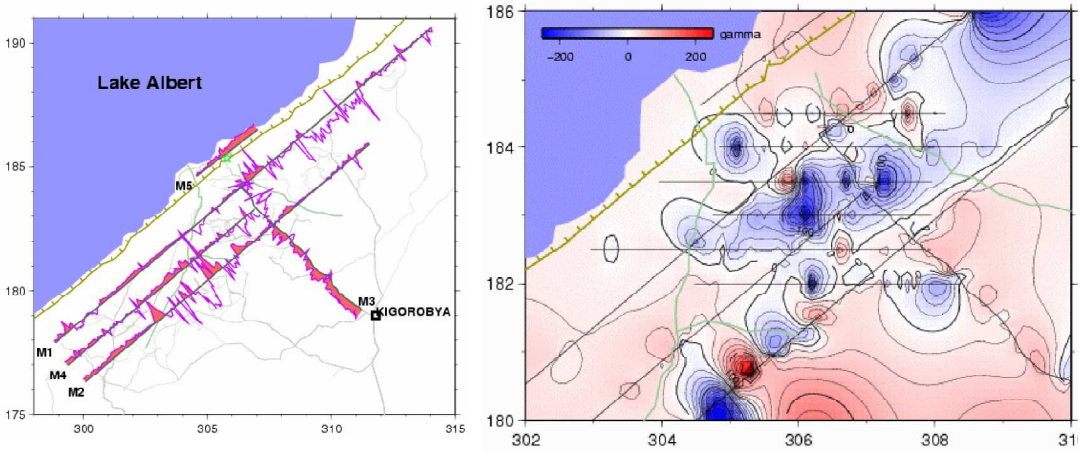

(a) (b)

Fig. 13: (a) Magnetic profiles and magnetic field (b) total field magnetic anomaly and major structures. The magnetic field strongly correlates with structural geology.

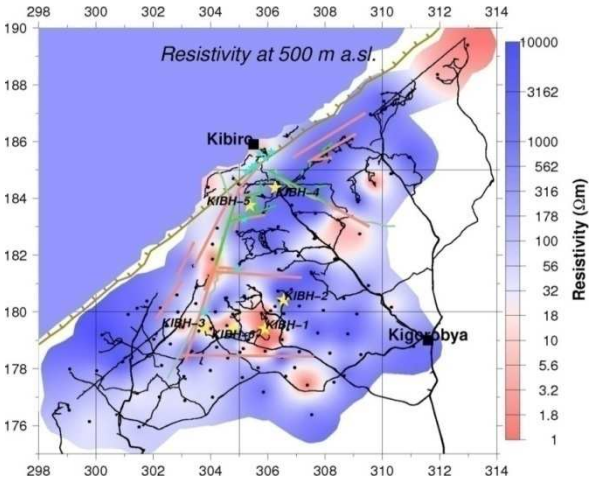

Fig.14: Locations of temperature gradient holes (yellow stars) and resistivity at 500 m above sea level. Inferred faults and fractures (pink lines), gullies (light green lines) and indications (Calcite, sulphur etc.) of geothermal activity(light blue stars).

Table. 2: Temperature gradients in the boreholes in Kibiro and extrapolated surface temperature.

Borehole	Gradient °C/km	Surf. temp. °C
KIBH-1	16.0	24.7
KIBH-2	16.0	24.4
KIBH-3	16.0	24.9
KIBH-4	27.3	27.9
KIBH-5 (deep)	31.3	25.7
KIBH-5 (shallow)	22.0	27.7
KIBH-6	16.0	24.8

The extrapolated surface temperatures are consistently between 24 and 25 °C for the holes away from the escarpment (KIBH-1, 2, 3 and 6). The holes at the escarpment (KIBH-4 and 5) have higher temperature gradients and extrapolated surface temperature.

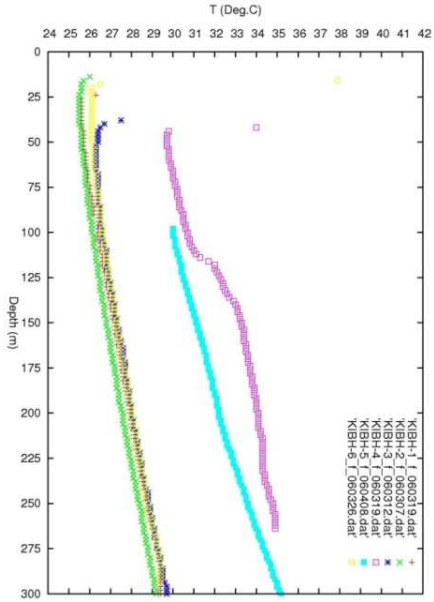

Fig. 15: Temperature gradient measurements in all the holes in the Kibiro area. The date is shown in the lower right corner [year month day] (ICEIDA 2004). Note that the wells can be categorised in two groups (KIBH-1, 2, 3 and 6) low temperature and (KIBH-4 and 5) high temperature.

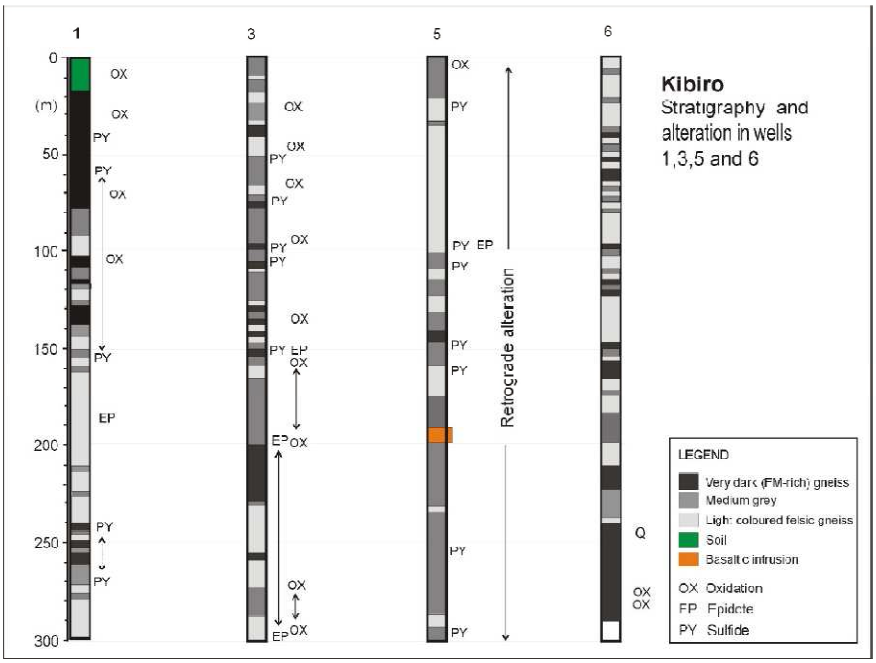

Fig. 16: Kibiro Stratigraphy of temperature gradient wells (ICEIDA 2008b). Note that the minerals Epidote and Sulfide are associated with high temperature.

Buranaga

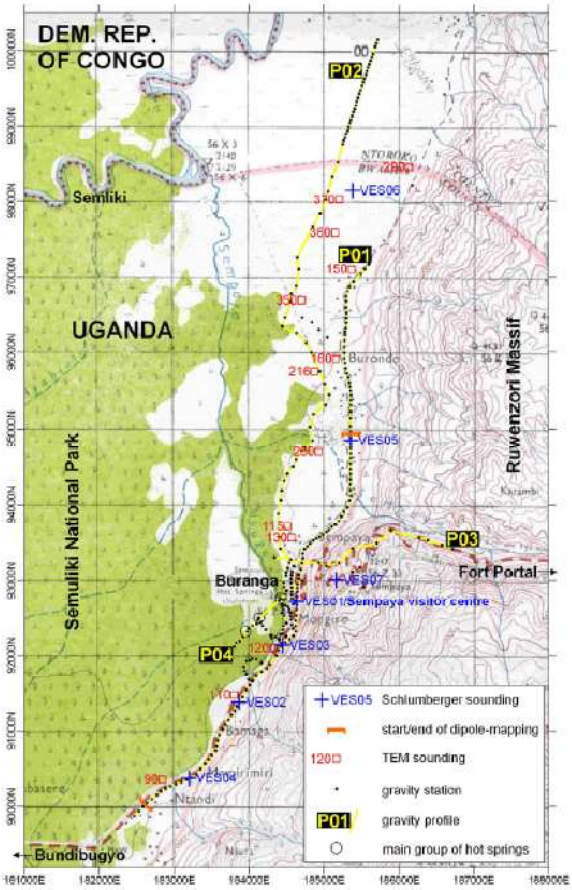

Fig. 17: Topographic map of Buranga Geothermal prospect and ground geophysics coverage.Note the limited extent in coverage of the geophysical surveys.

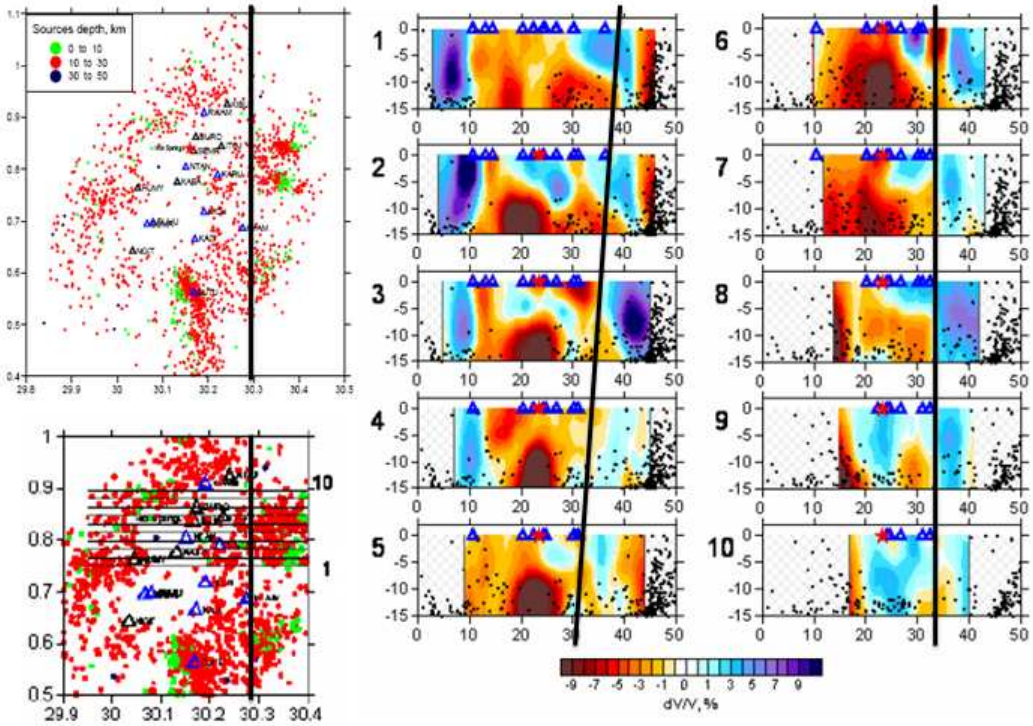

Fig. 18: Seismic activity and vertical topographic sections numbered from top 1 to 10. The thick black line sets a boundary of network coverage and limitation of the ray path to resolve a representative model and most of the data was left out. Red star is the location of Buranga hot spring. Brown-red show low velocities due to high heat flow and blue cold rocks.

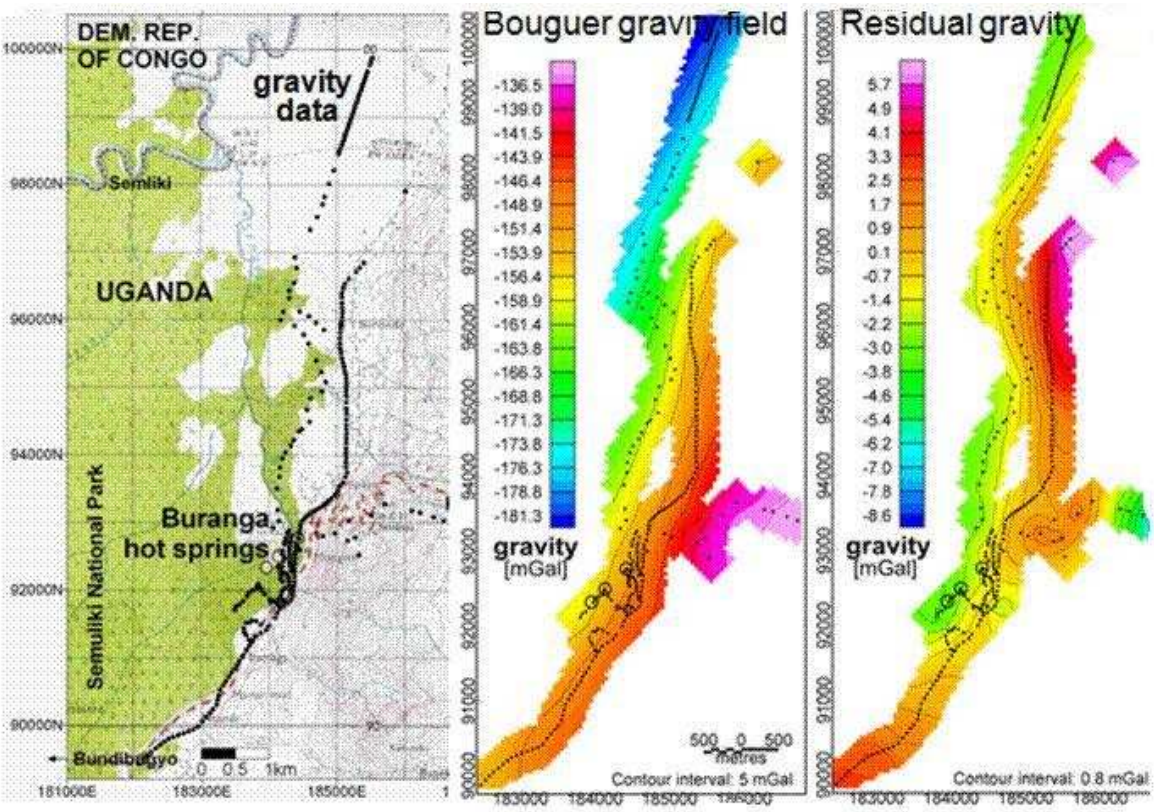

Fig. 19: Bouguer and residual gravity of Buranga. The gravity data coverage was not enough to resolve the geothermal anomaly.

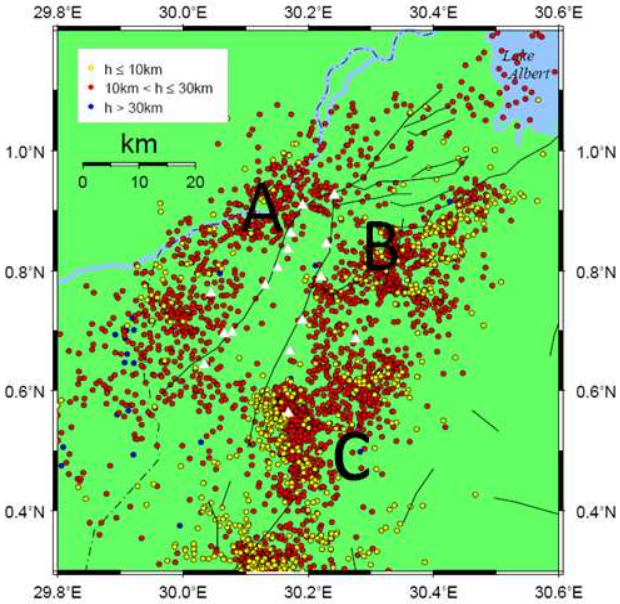

(a) Epicenters of natural earthquakes in Buranga

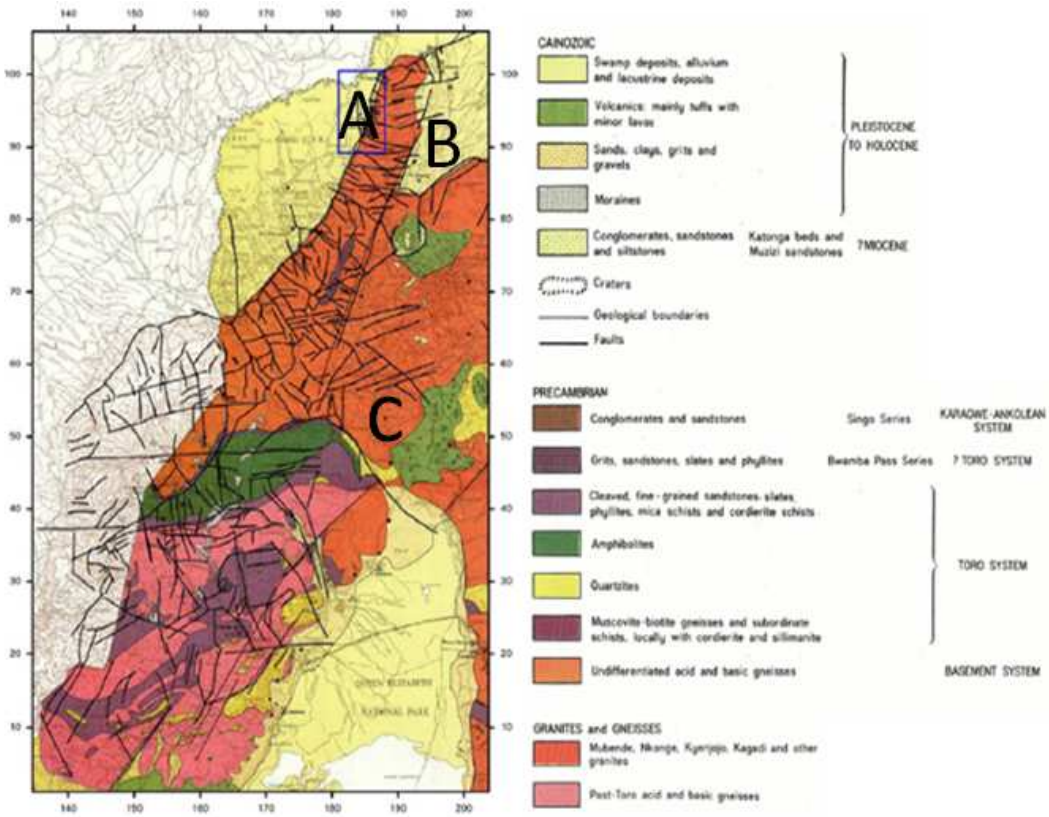

(a) Geological map of Rwenzori region and known faults

Fig.20: The seismic activity gives information about active faults and thus permeable zones in geothermal systems. However, in this case, there is no correlation between the known faults and the epicenter locations in (a). The observation may be due to geothermal activity in regions marked with A, B and C, because the seismic activity is clustered and diffuse.

Case study using Passive Seismic Method

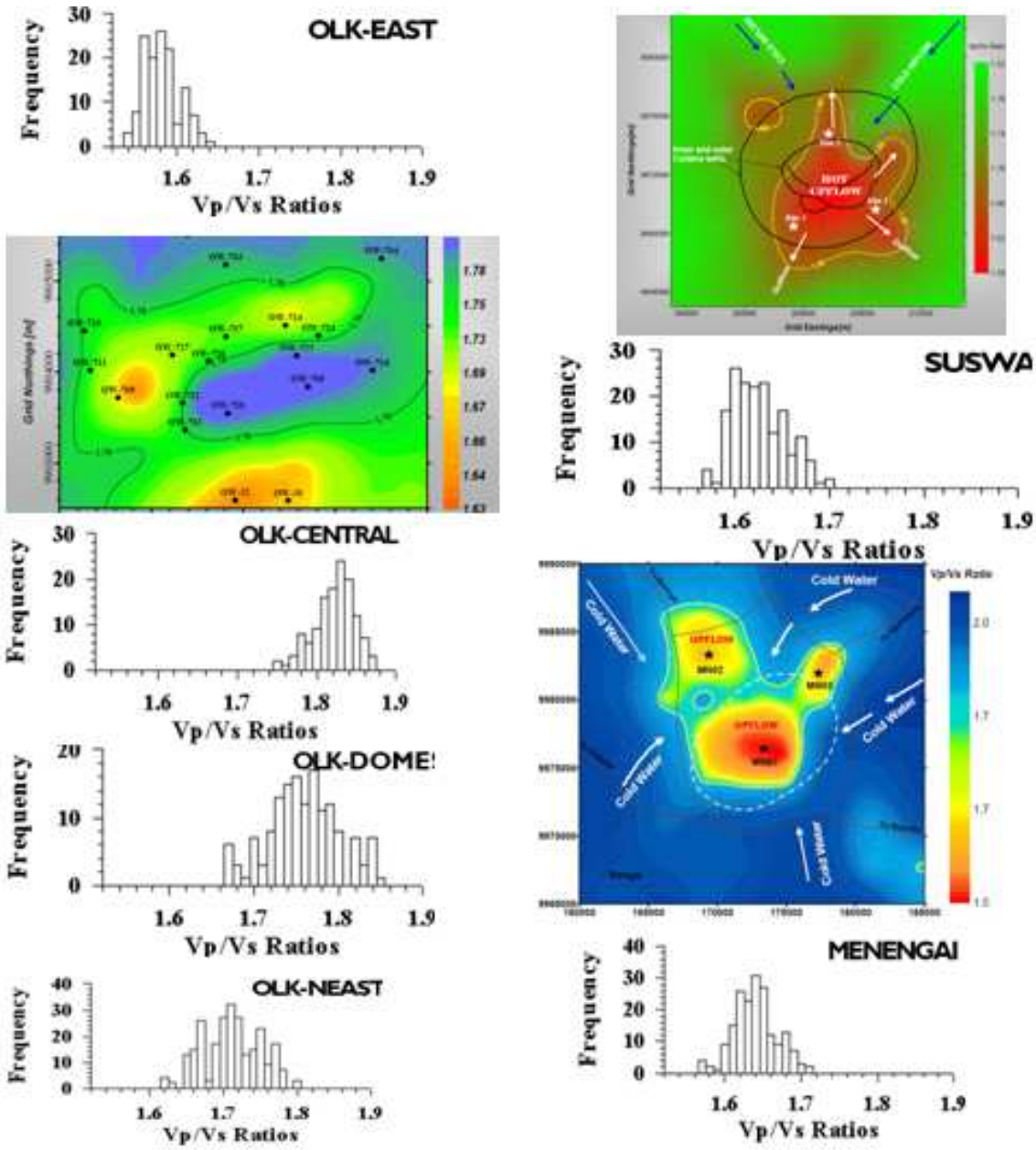

Fig. 21: P-wave and S-wave velocities ratios for Olkaria, Suswa and Menegai geothermal fields in Kenya Rift. Note a strong correlation of low velocity ratios with zones of high thermal anomalies. However such analysis was not carried out for Buranga Geothermal Prospect in Uganda.

LESSONS FROM CASE STUDIES OF OTHER GEOTHERMAL PROSPECTS

1. The geothermal resources in Uganda are largely located in the western branch of the rift which is volcanic and sedimentary as compared with Kenya, Ethiopia rifts which are highly volcanic.
2. The work done so far suggests that the heat source could be deep seated or off set from surface manifestation in Katwe, Kibiro and Buranga.
3. The current findings suggest that more detailed studies need to be done to map up flow zones and identify the heat source.
4. The geothermal fields in Uganda are different from most of the proven fields elsewhere so appropriate models should be developed.
5. The existing knowledge on the geothermal systems in Uganda is still limited and needs to be further expanded.

6. The concluded study has identified other areas which have geothermal potential and should be investigated further.

WAY FORWARD

The way forward is to continue investigating the geothermal resources

1. Carryout detailed geological, geochemical, hydrological geophysical including seismological and magnetotellurics investigations to probe deeper and identify the heat source.
2. Study in detail the structures that control the fluid flow mechanisms in geothermal areas.
3. Expand the areas of study to correlate extinct and active surface manifestations of geothermal systems.
4. Integrate the available geophysical and geological data at DGSM and PEPD to improve the existing knowledge, including the mineral content of the fluids.
5. Foster regional and international collaboration to enhance capacity building such as on-job training, short courses and formal qualifications, field attachments, equipment sharing and expertise.
6. Disseminate the results of the above initiatives at appropriate fora.
7. Funds should be mobilised both locally and through our Development Partners to support the above initiatives.

CONCLUSION

The geothermal studies in Uganda covered small areas and geothermal resources seem to be extensive with deep seated heat source.

Previous studies indicate that the heat source is deep seated in all cases. The geothermal anomalies are not adequately resolved to warrant the drilling of deep wells.

The prospects need to be re-investigated using good network coverage for Seismic, Gravity, TEM and MT techniques that can probe deeper to map the thermal anomalies for drilling.

The proposed geophysical techniques have proven to be the most successful mapping the geothermal system for development into steam production.

REFERENCES

BGR (2007). Project Final Report: Detailed surface analysis of Buranga Geothermal Prospect West Uganda. Unpul, Department of Geological Survey and Mines.

ICEIDA (2004). Kibiro Geothermal Prospects: A Report on a Geophysical and Geological Survey. Unpul. Department of Geological Survey and Mines Entebbe.

ICEIDA (2008a). Katwe Geotherml Prospect: A Report on a Geophysical and Geological Survey. Unpul. Department of Geological Survey and Mines Entebbe.

ICEIDA (2008b). Uganda Kibiro Katwe: Geology of thermal gradient wells. Unpubl. Department of Geological Survey and Mines.

Nabigani. N.M., Grauch .S.J.V., Hansen, R.O., LaFehr., R.T., Li.Y., Peirce.W. J., Phillips D.J., and Puder M.E. (2005). 75th Anniversary: The Historical development of the Magnetic method in exploration. Geophysics 70, 33ND-61ND.

Nyago Joseph (2009). 1-D inversion of MT and TEM data with examples from Krysuvik area Reykjanes Peninsula SW Iceland in Geothermal Training Programme 2009, No.22. Reports of the United Nations University.

Telford, M.W. Geldart, P.L. Sheriff, E. R and Keys, A. D. (1977). Applied Geophysics. Cambridge University Press, London.

Uganda-AERDP (2004). The Uganda Alternative Energy Resources Assessment and Utilization Study, Unpubl. Department of Geological Survey and Mines.

CONTRIBUTION TO FAVORABLE GEOTHERMAL SITE SELECTION IN THE AFAR TRIANGLE

Jacques Varet
Senior Advisor to the Chairman
- BRGM - 3, Av. Claude Guillemin. BP6009 - 45060 Orleans Cedex 02, France.
E-mail: j.varet@brgm.fr

ABSTRACT

The Afar triangle has been shown to be the surface expression of the Afro-Arabian plate boundary, having the surface expression of most of the characteristics of a mid-oceanic rift system (Barberi & Varet, 1977). Most of the heat is dissipated at the surface along these major geodynamic features and Afar, like Iceland, therefore represents an exceptional geothermal energy potential. Afar was therefore described as “the future Gulf region for geothermal energy” (Varet, 2006). Many sites have been shown to be of potential geothermal interest on the basis of geological criteria: the presence of a volcanic “axial range” (oceanic-type rift segment) combined with transverse fractures (the surface expression of transform faults) provides both a heat source and a fractured reservoir. In addition, central stratovolcanoes on the Afar Margins also develop favorable conditions similar to those prevailing in the rift valley.

Compared to Iceland, Afar suffers from a major handicap: the composition of the geothermal fluids in geothermal reservoir fed by meteoric water. Since there is much less rainfall in Afar (annual rainfall there being one of the world's lowest), and as a former branch of the Red Sea evaporated in Northern Afar in the Pleistocene, brines predominate over fresh meteoritic water both at and below the surface (Kebede et al. 2008), notably in northern and eastern Afar (where open faults allow the sea to penetrate the depression). The noticeable exception in the Awash valley fed by the river itself and its many tributaries descending from the Ethiopian plateau should be underlined. A new approach is proposed that takes into consideration the hydrological basins feeding the potential geothermal sites, as well as new hydrogeological considerations. This enables us to take a new look at potentially favorable geothermal sites.

The Dallol, Boina, Manda-Hararo and Asal-Ghoubet geothermal sites are particularly discussed.

The technical-economic challenge posed by how geothermal energy might satisfy local needs and aid in the development of this sparsely populated, essentially pastoral region is also addressed.

Key words: geothermal exploration, Afar, ridge, heat source, reservoir, fluid composition, local development

INTRODUCTION: WHY FOCUS ON AFAR?

Our generation will have to pass from a mode of development based essentially on fossil fuels to a “Green New Deal” based on renewable energy. This is imposed on us from “both ends”, by diminishing fossil fuel resources, and by the climate changes induced by CO2 emissions that result from there combustion (Varet, 2005). Geothermal energy will play a role in this new context. Just as the world economy has moved from Europe and North America to Asia due to cheaper labour costs, a similar movement will be observed in the future to meet energy needs. The reason for this is that, in the previous period, the abundance of fossil fuels (notably oil) enabled the cheap transport of energy throughout the world, benefiting regions far away from energy resources, whereas we will soon be constrained by local energy resources with much higher transportation costs.

In such a situation, countries and regions that have accessible, low-emission, renewable energy resources will be of interest for centralized energy-consuming activities. The time has come for regions provided with geothermal resources to develop. As geologists, we know that most of the planet's geothermal energy is dissipated along plate boundaries, with the highest heat flow located along zones of accretion, that is along mid oceanic ridges, and even more in regions affected by mantle plumes. In East Africa, the ARGEO programme organizing this meeting aims at developing the entire East African rift system, and Kenya is already showing the way with significant and steadily increasing geothermal energy production. But in this vast area, we must recognize that geodynamics offer various solutions, ranging from typical continental rift systems to typical emerged oceanic rift zones. Thirty years ago, it was shown (Tazieff et al., 1970; Barberi and Varet, 1977) that Afar is not the northern extension of the Ethiopian rift valley (Wonji Fault Belt, as proposed by Mohr, 1970), but rather the surface expression of the Red Sea – Gulf of Aden oceanic rift system.

The Afar region covering Djibouti, Ethiopia and Eritrea should, therefore, be regarded as being of specific interest for geothermal developers and likewise be of particular interest in the ARGEO programme. Afar and Iceland are the only places on our planet where such an exceptional geothermal energy potential, combining emerged rift zones and mantle plumes, occur. Many Afar sites have been shown to be of potential geothermal interest on the basis of geological and geodynamical criteria in this so called “future Gulf region for geothermal energy” (Varet, 2006). The presence of a volcanic “axial range” (oceanic-type rift segment) combined with transverse fractures (the surface expression of transform

faults) should provide both a heat source and a fractured reservoir – the two most favorable conditions for high enthalpy geothermal development (Fig. 1).

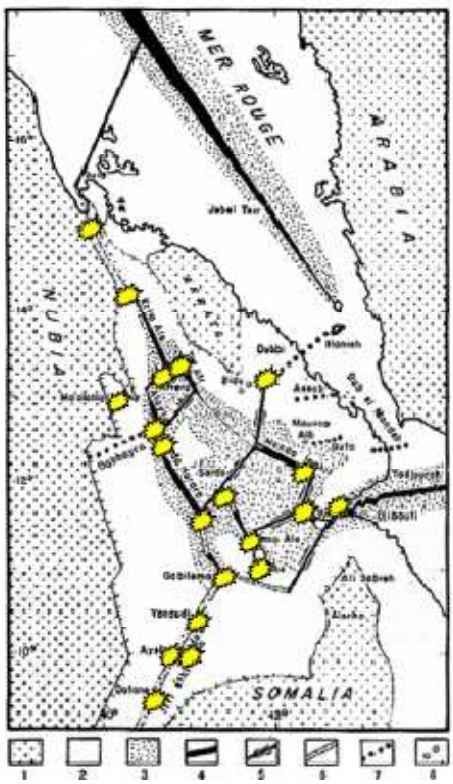

Fig.1: Geothermal sites in Afar, revisited selection by J.Varet (2006) on the basis of new geodynamic considerations, based on Barberi and Varet (1977) map of micro-plate boundaries.

Favourable geothermal sites

While Djibouti relies heavily upon fossil fuels for its energy production, Ethiopia has, to date, relied predominantly on hydropower plants. Although this energy is renewable and environmental friendly, power plant operation has already been affected by seasonal rainfall fluctuations and these are expected to increase in the future due to climate change. Furthermore, the hydropower potential is located in the western part of the Ethiopian plateau, whereas in the eastern part, the huge potential for geothermal energy has not yet been tapped. Northeastern Ethiopia is also an area where the population suffers from very low access to energy. Geothermal power might satisfy these needs as it enables modular development, with the great advantage of progressive investment. Moreover, this technology creates local jobs.

Studies carried out in the 1970s (Tazieff et al. 1970; UNDP, 1973) made it possible to identify several promising sites for geothermal development in the Ethiopian rift valley and Afar. A recent invitation by the Afar and Tigre regional governments, which included a joint field visit (Barberi & Varet, 2010), enabled us to precisely identify targets for providing electricity to rural and peri-urban communities and study the possibility of using these geothermal resources to contribute to the development of mining and agro-industrial activities.

The development of local geothermal projects will provide electricity and benefit rural communities, particularly those near the sites, and improve the socio-economic development of the entire region. Local populations would benefit from enhanced water supply, transportation, health, and other services fostered by the energy produced. In addition, the creation of new energy production sites, and the modular development enabled by geothermal power, would attract investments and induce future developments in various energy-consuming sectors such as mineral extraction and processing. The energy produced from this renewable source will, in the future, be connected to the main grid, thereby benefiting the entire regional energy sector – an important issue in an area that has, up until now, had to rely on seasonal hydroelectricity or costly fossil fuel, and future variable energy resources (wind or solar).

FACING A MAJOR HANDICAP: GEOTHERMAL FLUID COMPOSITION

At the first ARGEO conference in Addis Ababa, a proposal for a guide to geothermal exploration proposed for Afar (Varet, 2006) considered that favourable sites for high enthalpy geothermal development required the simultaneous occurrence of the following parameters:

- a high heat flow, linked with either a very shallow anomalous mantle or a superficial magma chamber
- a highly fractured area, allowing good reservoir permeability
- the recharging of the reservoir by meteoritic water or sea water, or a combination of both
- the development of a mineralised hydrothermal system

In the context of Afar, such sites were shown to offer suitable conditions for development in areas of junction between the axial ranges and the transverse tectonic systems. As described by Barberi et al. (1970), like in Iceland, transform faults are not observed in Afar. Nevertheless, Tapponier and Varet (1974) showed and Barberi and Varet (1977) more precisely confirmed that large oblique fracture systems are in many places the surface expression of a transform fault linking two distant axial ranges. This enables the interpretation of focal mechanisms of earthquakes, such as the Sardo event, in the Tendaho graben to the east of the southern extremity of Manda Harraro, the Afar axial range that is the most similar to mid oceanic ridges. Such a tectonic structure is particularly well developed north of Asal, in the junction area with the Manda Inakir axial range (Fig.2).

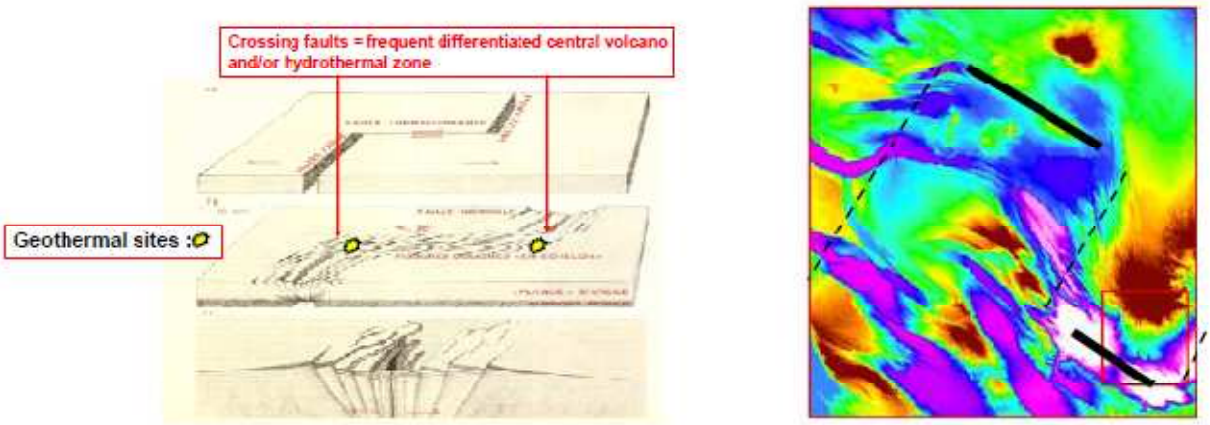

Fig. 2: The surface expression of transform faults in Afar is characterized by fault systems oblique with respect to the direction of the transform movement. Such features, conform to analogical models are particularly well developed on both extremities of Manda-Inakir axial range in Makarassou and Dobi regions (treatment by BRGM from NASA/SRTM).

However, compared to Iceland, Afar suffers from a major handicap – the composition of the geothermal fluids. Whereas in the North Atlantic climate of Iceland, due to high rainfall, geothermal reservoirs are predominantly fed by meteoric water, Afar has a dry tropical climate. Since there is much less rainfall in Afar (annual rainfall there being one of the world's lowest), brines predominate over fresh meteoritic water both at and below the surface (Kebede et al. 2008), notably in northern and eastern Afar.

A new approach is proposed that takes into consideration the hydrological basins feeding the potential geothermal sites and focuses on specific hydrogeological characteristics of the area. This enables us to take a new look at four potentially favorable sites selected among the many potential geothermal areas identified in 2006.

THE ERODED, FAULTED ESCARPMENT: AN EFFICIENT HYDRO-GEOLOGICAL SYSTEM FOR PROVIDING AN ADEQUATE GROUNDWATER SOURCE FOR GEOTHERMAL FLUIDS IN SELECTED SITES

In the escarpment bounding Ethiopia's northern Afar region, there are significant hydrological systems running from the upper part of the plateau down to the Afar floor (Fig.3). Typically endoreic, these basins feed the sedimentary and volcanic aquifers along the slope and under the plain. During the rainy season, the plains frequently turn into temporary lakes. This is the case of the great salt plain (locally called Dagad), where each year the salty crust at the surface is recrystallized after seasonal rains. At other times, the surface flow disappears in the flat-lying plains of the Afar floor. Along the flank of the active volcanic rift axis of Erta Ale, the Alayta and Manda Harraro ranges are notably developed, the largest being Dodom and Teru (Fig. 4).

Fig. 3: Satellite view of the numerous watershed feeding the Afar depression from the Ethiopian plateau and Danakil alps.

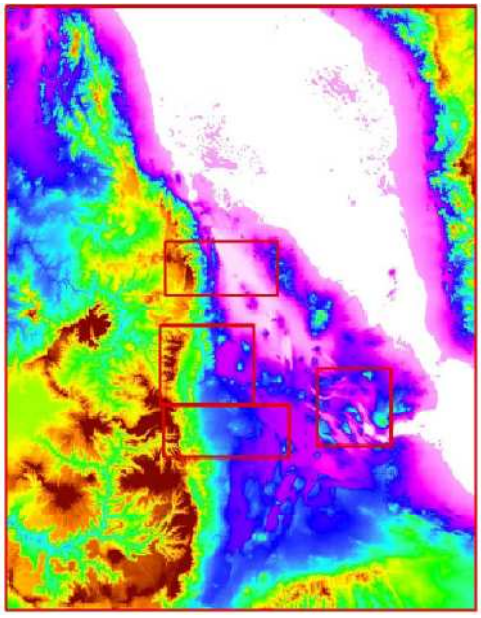

Fig. 4: relief map of Afar from NASA/SRTM, with BRGM processing; the basins feeding the reservoirs of the selected geothermal sites from the Ethiopian plateau are wider from north to south.

Therefore, although the rainfall is very low in the depression itself (a few millimeter to 100 mm/year, 129 mm being the average in Djibouti and 50 mm in Dallol), the western border of the Afar benefits from the much better hydrologic conditions of the Ethiopian plateau (up to 1,300 mm at an altitude of 3,000 m, figure 5 and table 1). As a result, a significant hydrological system developed in a complex array determined by both erosion (E-W direction, perpendicular to the scarp) and tectonics, which determines predominant NNE-SSW normally-faulted blocks and possibly marginal grabens (Fig. 6). The L-shaped (or rectangular drainage) river patterns (Fig. 7), the complex lithology of the faulted material and the intense and active extensional tectonics allow for a more efficient development of groundwater systems in fractures and possibly karst aquifers.

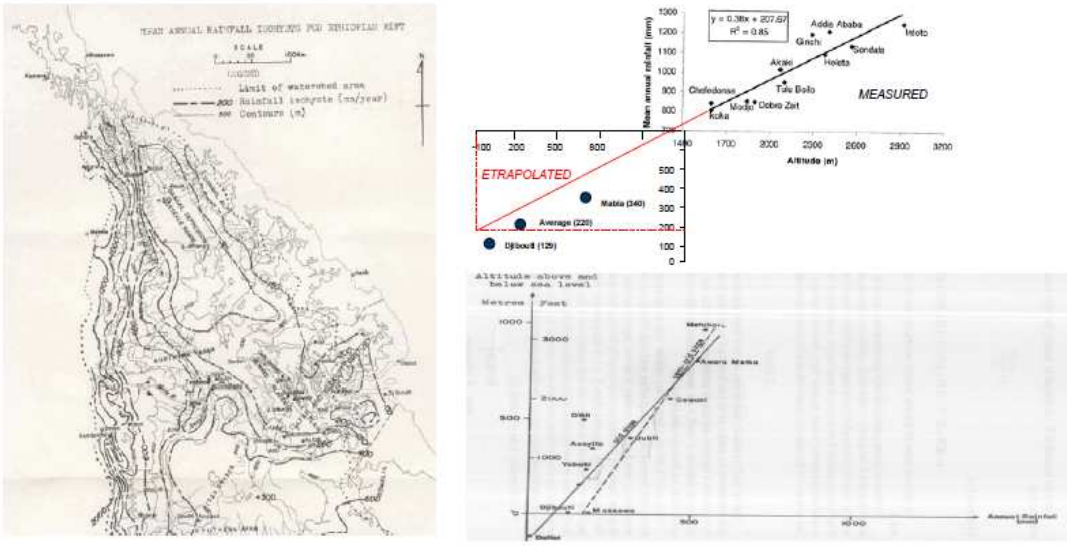

Fig. 5: Pluviometry in the Afar region: map of isohyets and correlation with altitude (UNDP, 1973 and Kebede, 2008)

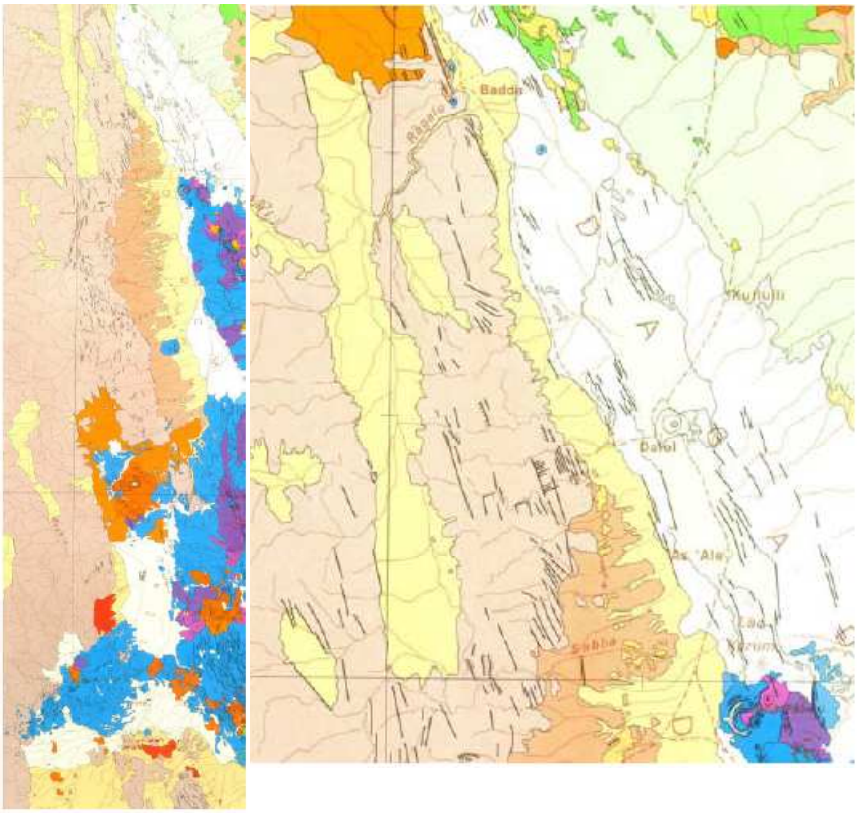

Fig. 6 : The basis of the faulted escarpment of the western Afar margin. Normal faults allow for the development of rectangular drainage and of marginal grabens, with “en echelon” arrangement (from CNR-CNRS map of the Danakil depression, northern sheet, J.Varet, 1978)

As a result, it is possible to select sites that meet the above mentioned criteria in terms of heat sources, transverse faulting, and hydrothermal development, that are also located in areas well fed by suitable hydrological basins crossing through the Ethiopian faulted scarp limiting the Afar depression to the West.

Two of these sites are located in NE Afar, in Ethiopia, i.e. Dallol and Boina. Note that similar contexts can be found in Eritrea (A. Michael, 2005), concerning the Alid volcanic and geothermal site (not studied here).

The third site is in the Djibouti republic, where the highlands of the Dalha plateau – with the well-known Day forest – also act as a meteoritic water source for the North Ghoubet site (Fig. 8).

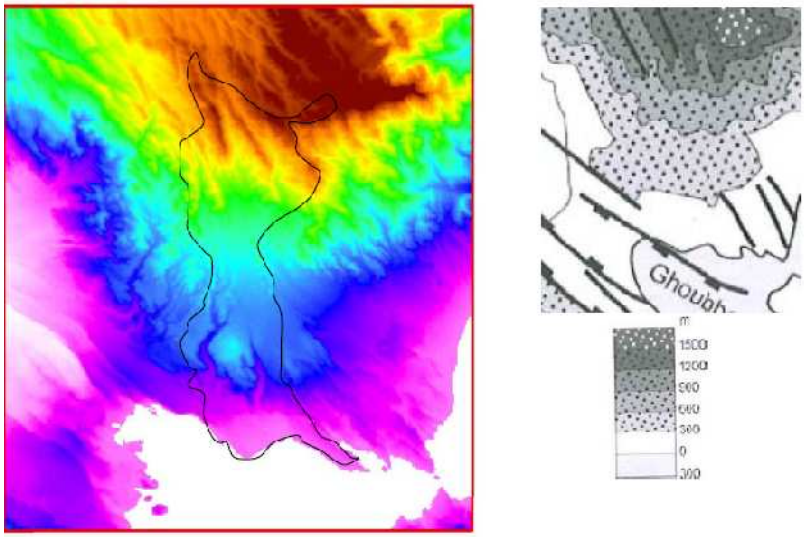

Fig. 7: The North Ghoubet site is fed by an hydrological basin with the head in the Day mountain (Dalha basaltic trapp series), the region in Djibouti Republic with the highest rainfall (processed NASA/SRTM data and current topographic map)

We do not address the geothermal area located near the southern extremity of the Manda Harraro axial range. The tectonic and magmatic crisis observed since 2005 (Ayele, 2006) has confirmed the very active nature of this axial range previously reported by Treuil and Varet (1973). Significant meteoritic water recharge of the entire Tendaho graben is provided by the wide Awash and Mille river basins (Fig. 9). The quality of the geothermal fluids was confirmed by exploration drilling (Aquater, 1996).

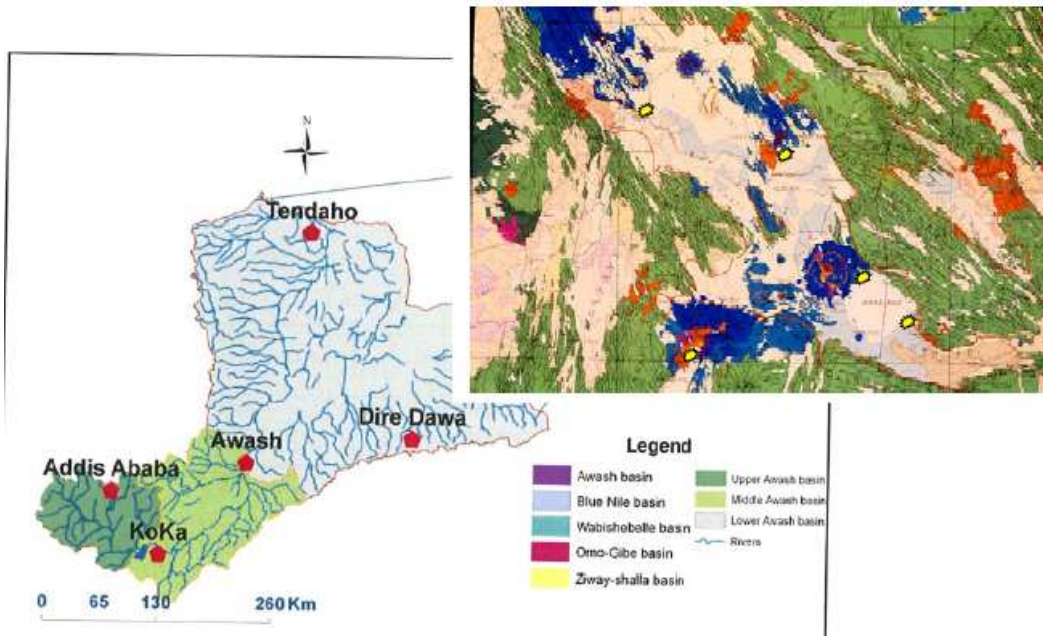

Fig. 8: The Awash river basin in Ethiopia (from Kebede et al. 2008) and the lowest part of the basin in the central Afar (Ethiopia and Djibouti, from CNR-CNRS geological map of central Afar).

DALLOL GEOTHERMAL SITE

The Dallol site is located in the middle of the vast Dagad salt plain. It is a former potash mining site (Holwerda and Hutchinson, 1966; ELMICO, 1984) and also a tourist destination due to the multicolored salt concretions that have developed as a result of spectacular hydrothermal activity. Hot water and fumaroles (the temperature of which may reach 120 °C) deposit sodium, potassium and magnesium chloride as well as metallic sulfurs, creating a wide range of colors at the emission sites, from black and green under reduced conditions, to yellow, red and brown after oxidation (Fig. 9). Springs and fumaroles are clearly aligned along NNE trending fissures, certainly linked with the opening of fissures on the rift axis. Vent locations change with time, as salt deposits plug old vents and new vents appear nearby along a new fissure. This confirms that Dallol is also located on the active Afar rift axis.

Fig. 9: black smoking fumaroles in Dallol, with successive stages of oxidation of the sulfurs offering a large variety of colors from green to yellow and red (Photo J.Varet, 2010).

The Dallol "dome" extends E-W, perpendicular to the rift axis. Rather than a real salt dome, it is a vertical uplift probably resulting from a deep magmatic intrusion. The regularly horizontal strata exposed in Dallol's eroded hills confirm this hypothesis. A similar feature is observed in the northern tip of the Erta Ale range, on the western side of the Kibrit Ale volcano (Barberi and Varet, 1970).

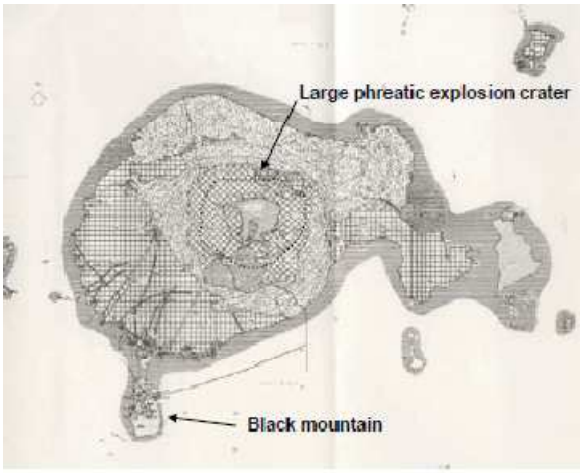

Fig. 10: magnetic field survey of Dallol site, showing a positive anomaly under the Black Mountain, and geologic map (ELMICO, 1984)

Geophysical data (magnetic and gravimetric) show that a magmatic body (most probably basaltic), a few kilometers deep, underlies the sediments, although no volcanic products are found in Dallol. With its location in the middle of the rift, right on the NNE alignment with the Erta Ale range, the presence of an active magmatic heat source is quite plausible. Geophysical data also show E-W anomalies that can be interpreted as being the result of transverse faults. Hence, although the existence of a well-developed and active geothermal system is obvious, we cannot be certain that suitable conditions for true geothermal development are to be found, due to the extremely salty environment, notably the saturation in salt of the geothermal fluids. The UNDP report (1973) concluded that Dallol was unsuitable for geothermal development on the basis of the geochemical content of the hot springs.

After new observations were made of the Dallol site, Barberi and Varet (2010) concluded that this site should be reconsidered as suitable for geothermal development for the following reasons:

1. Phreatic explosions are well-documented in the history of Dallol site and in the surrounding area. On the dome itself, a large crater – in which most of the active vents are located – indicates the presence of a very large phreatic explosion site probably a few hundred years old (Fig. 10) . Another phreatic explosion crater (100 m large) is well-documented in the Black Mountain site located SE of the Dallol dome, as observed in 1926 (Fig. 11). Between the Erta Ale range and Dallol, As Ale is also the expression of a former phreatic explosion, 55 m large. New craters and pools – apparently linked to the 2005 seismic event, according to local tribesmen – were observed during our last visit a few kilometers south from Dallol dome (Fig. 12), and show that phreatic explosions are still occurring. This clearly indicates the presence of a high-pressure, high-temperature (above 180 °C) geothermal reservoir currently active underneath this part of the salt plain.

Fig. 11: two phreatic explosion craters near Dallol :
As'Ale skating ring today (J.Varet, 2010), and
Black Mountain in 1926 (Italian archives, in L.Lupi, 2009)

Fig.12 : a new phreatic explosion crater appeared in 2005,
producing a lake still affected by hot springs and steam vents.

2. A closer look at the faulted scarp between Makale and Dallol shows that the whole series of the plateau collapsed along the many normal faults delineating the Afar margins. As a result, the Jurassic limestones and the Adigrat sandstones outcropping at 3000 m altitude on the Tigre plateau are observed at sea level and below, in tilted blocks emerging from tertiary detritic terrasses in the vicinity of the salt plain (Fig. 13). As a consequence, it is to be expected that these formations extend eastwards, at deeper depth, underneath the salt. In fact, they reappear on the eastern flank of the depression in the Danakil Alps (Arrata in Afar language).

3. Considering the hydrological and hydrogeological context, the Adigrat sandstones and the Jurasic limestones – the latter heavily karstified – both constitute efficient aquifers that would enable the infiltration of meteoritic water, itself facilitated by the intense normal faulting (and transverse fractures) affecting the escarpment (fig.14).

Fig.13: Tilted blocks of Jurassic limestone, downfaulted from the Ethiopian plateau, observed in the depression, emerging from tertiary detritic deposits, themselves also affected by normal faults.

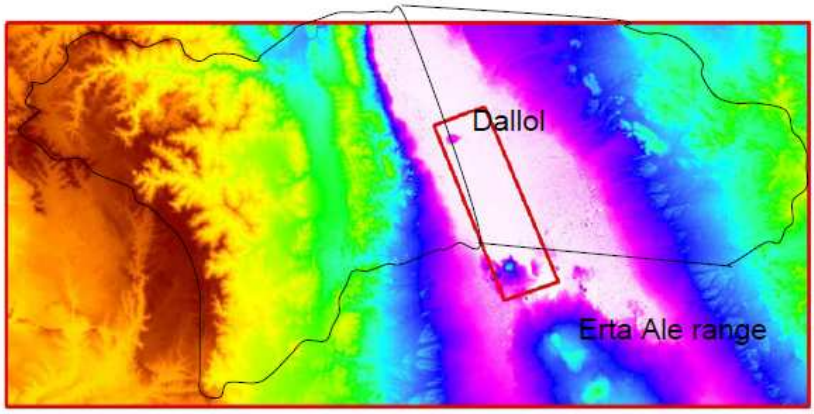

Fig. 14: hydrographic basins feeding the Dallol geothermal site, from Ethiopian plateau to Danakil alps

Under such conditions, a reasonably favorable geothermal model can be developed for the Dallol site where, underlying the salt plain and hyper-saline geothermal system, there might be a deeper aquifer in the Jurassic limestone characterized by both low salinity and regular recharge by meteoritic waters descending from the plateau. The presence of a high-pressure, high-temperature reservoir is evidenced by the numerous past and present phreatic explosions, as well as by the steam vents aligned on NNE trending open fissures frequently reopened though the salt cover (Fig. 15).

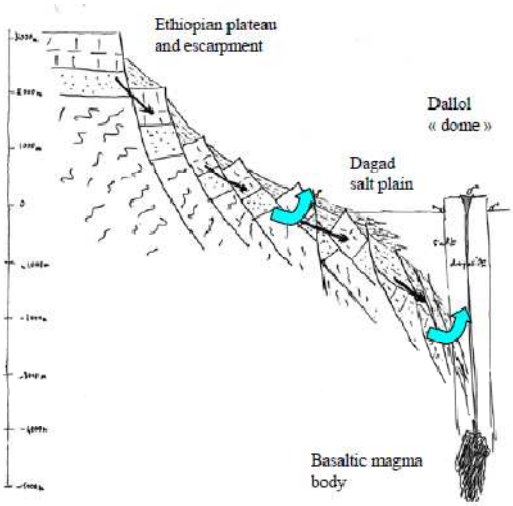

Fig. 15: Geological simplified model for Dallol geothermal system. The target would be to tap a deep aquifer in the Jurassic limestone and fed by the meteoritic water flowing down from the Ethiopian plateau.

Additional geochemical analyses and geophysical surveys should enable us to locate the best drilling sites, the cost of which would be low due to the ease of drilling through simple salt layers (Barberi and Varet, 2010).

In addition to meeting local needs in the surrounding Afar villages, this electrical energy production would also facilitate the re-opening of the Dallol potash mine. Instead of the costly ground mining techniques considered in previous feasibility studies (ELMICO report, PEC engineering, 1984), less expensive solution mining of the potash deposits could be done using the geothermal fluids (either directly or through heat exchangers).

BOINA GEOTHERMAL SITE

South of the Erta Ale range, the two axial ranges of Alayta and Manda Harraro represent the projection of the Red Sea-Gulf of Aden rift system into central Afar. The two active fissural basaltic ranges are not precisely aligned and the central Dabbahu volcano developed on this transition zone, probably a transverse fracture at depth (Fig. 16). This volcano (Fig. 16) is characterized by a complete magmatic series ranging from transitional basalts to hyper-alkaline rhyolites (comendites and pantellerites), described in detail by Barberi et al. (1975). The presence of a shallow magma chamber is evidenced by the series's crystal fractionation conditions. There are numerous fumaroles, locally called Boina (meaning fumaroles or steam vents in the Afar language), many of them exploited by the Afar tribesmen as a source of water with small artisanal steam-condensing units (Fig. 17). Such sites are so well-developed along the western margin of the Dabbahu volcano that Dabbahu may also be called Boina. Silica deposits are frequently observed on these hydrothermal sites, indicating high-temperature at depth.

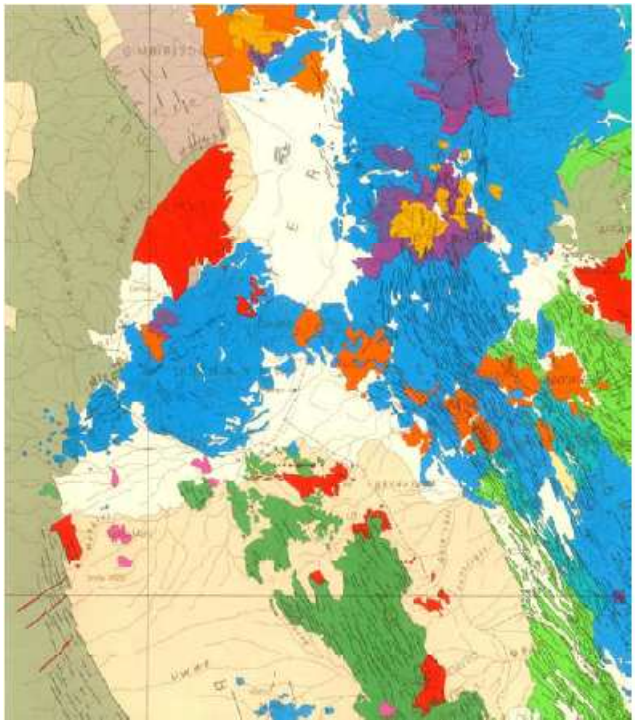

Fig. 16: Geological map of the foot of the Ethiopian escarpment and axial volcanic ranges of central Afar (CNRS-CNR, J.Varet, 1978). Dabbahu (also called Boina), located in area of junction (transverse structure) between Alayta and Manda Harraro axial ranges display a complete magmatic series from basalts to pantellerites. Numerous steam vents (locally called Boina) are observed along faults and open fissures affecting the lower part of the Dabbahu volcanic centre along the Teru plain.

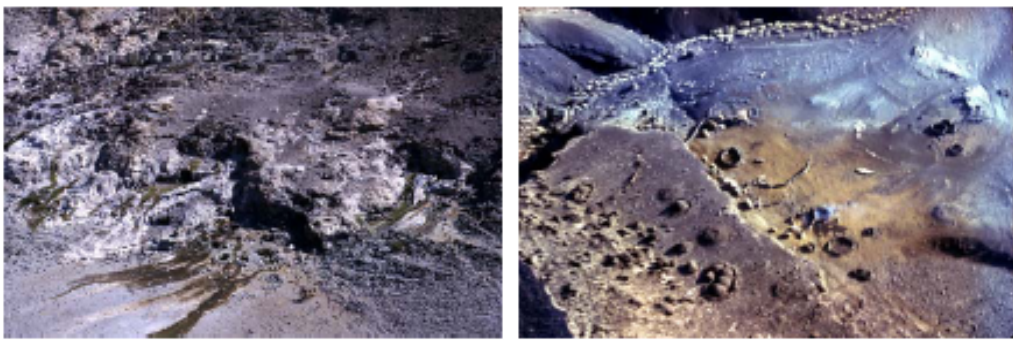

Fig. 17: Steam vents, fumaroles and hotsprings in Boina. Hydrothermal vents develop along faults and fissures affecting the basalts and the sediments of the Teru plain. The sites are frequently exploited by Afar people for steam condensation. Silica white deposits are observed.

The magmatic, geodynamic and hydrothermal characteristics of the site appear to be favorable and the hydrological context also confirms the interest of the area for further geothermal developments. The Teru Plain, one of the most extensive and fertile plains in NW Afar, extends along the foot of the volcano. The plain itself is fed by a large watershed descending from the Ethiopian plateau with several rivers crossing through normal faults and marginal grabens (Fig. 18). There is no outcropping of the Precambrian basement or Mesozoic

sedimentary cover in this area, but the thick trap basalt series of the Ethiopian plateau, heavily faulted and tilted along this transition zone between the highest part of the plateau and the Afar depression. The rainfall is higher here than in northern Afar and the surface of the basin is wider, so there is more water available to recharge aquifers. As opposed to the central part of Afar at the same latitude, around Tat'Ali (an axial range parallel to Alayta) where there are saline deposits, no such deposits are observed here.

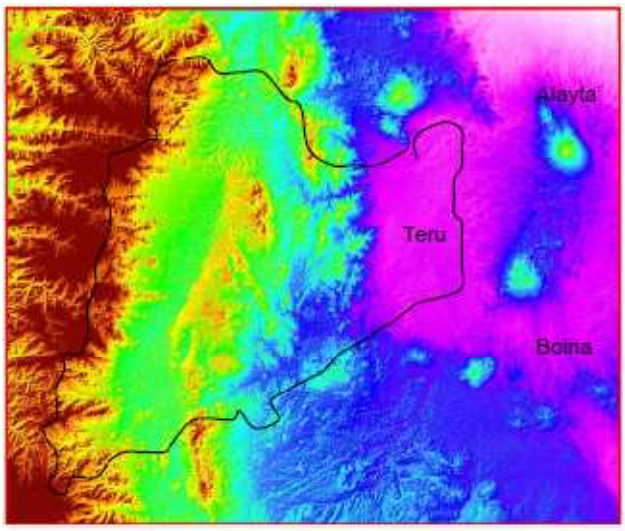

Fig. 18: Hydrographic basins feeding the Boina geothermal site, from the Ethiopian plateau. Observe the marginal grabens Along the foot of the escarpment.NASA/SRTM source, BRGM processing.

Due to these favorable hydrological conditions, this part of Afar also has a higher population density and the selection of this geothermal site would be of interest for local and regional social and economic development. Furthermore, since the resource is probably of high value in terms of quantity as well as quality, geothermal units of broader interest could be further developed on the Boina site. Additional prefeasibility work should include fluid hydrochemistry and geophysics, making it possible to site exploration boreholes. A small wellhead turbine and a local electricity grid should be installed during the feasibility phase in order to convince the local population of the benefits of developing this geothermal energy resource.

NORTH GHOUBET

In the Republic of Djibouti, following extensive surveys of the whole country, the Asal site was selected for geothermal developments (Farah, 2010). During three successive phases, led by BRGM (France) in the 1970s and by UNDP and Aquater (Italy) in the 1990s, the geothermal resource potential was tested and included deep drilling operations. A new approach has recently been developed by an Icelandic consortium (Reykjavik Energy Invest) and has led to the proposal of industrial development of a 50 MW plant on the Asal site (ISOR, 2008; Hjartarson et al., 2010).

The major problems encountered on the Asal site are not the heat source, which has already been certified by previous drilling campaigns (260 to 360 °C), but the permeability at depth and the fluid composition. Located between the marine gulf of Ghoubet and the halit- saturated Lake Asal, the geothermal fluid prevailing in the reservoir is a salty brine (Battisteili et al., 1990). Currently available technologies make it possible to exploit these geothermal fluids, as shown in the Salton Sea region in California. But finding a geothermal site where a less salty fluid could be tapped would be a real advantage.

The North Ghoubet site would merit more consideration. Located near the Asal-Ghoubet NW-SE trending axial volcanic range, it is also affected by transverse faulting resulting from the transition zone between Asal-Ghoubet range and the submarine rift segments identified along the axis of the Gulf of Tadjura (Fig. 19). This multiple faulting should be favorable to fracturation at depth and hence the development of hydrothermal reservoirs. Indeed, fumaroles have developed along faults in this area, with the development of recent silica deposits indicating the continuous exhaust from an active hydrothermal reservoir (CFG, 1993).

Fig. 19: photographic view of the Dalha basaltic series in the Day region. These trapp basalts are faulted to the south, dipping towards the Gulf of Tajourah and Ghoubet.

An additional consideration is reservoir recharge by meteoritic water. In North Goubhet, as opposed to Asal, a large basin is fed by rivers descending from the Dalha mountains, the highest and most humid part of the Republic of Djibouti. The Day Forest is a well-known tourist destination due to the exceptional climate prevailing in these highlands. Although dryer than the Ethiopian plateau, the conditions on the Dalha basaltic plateau are similar to those described above. Even if the annual rainfall does not exceed 200 to 300 mm, the small basin feeding the North Goubhet site allows not only for occasional flooding, but also for recharging deep aquifers developed in the unconformity between the deeply faulted and tilted basaltic trap series of the Dalha, and circulation within this trap series and in the underlying unconformity with the underlying Mabla rhyolitic unit. Since these successive geological units are characterized by different tectonic regimes (Marinelli and Varet, 1972), we can infer the development of well fractured reservoirs at depth. (Fig. 20, 21).

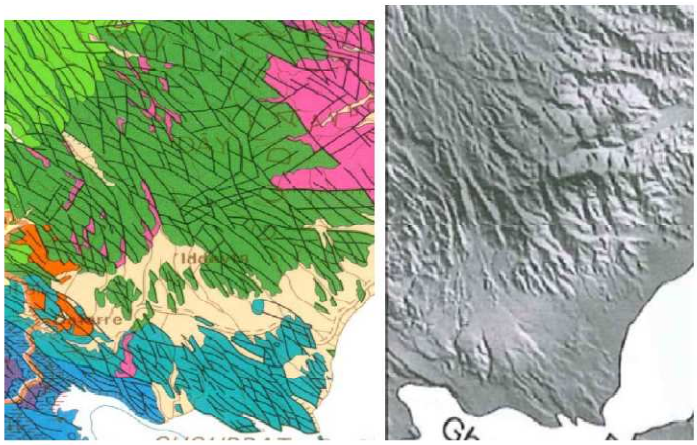

Fig. 20: The North Ghoubet site is fed by an hydrological basin with the head in the Day mountain (Dalha basaltic trapp series). The area is intensively eroded and faulted with normal faults trending NNW-SSE, NW-SE and E-W (from CNR-CNRS map of central Afar and NASA SRTM image).

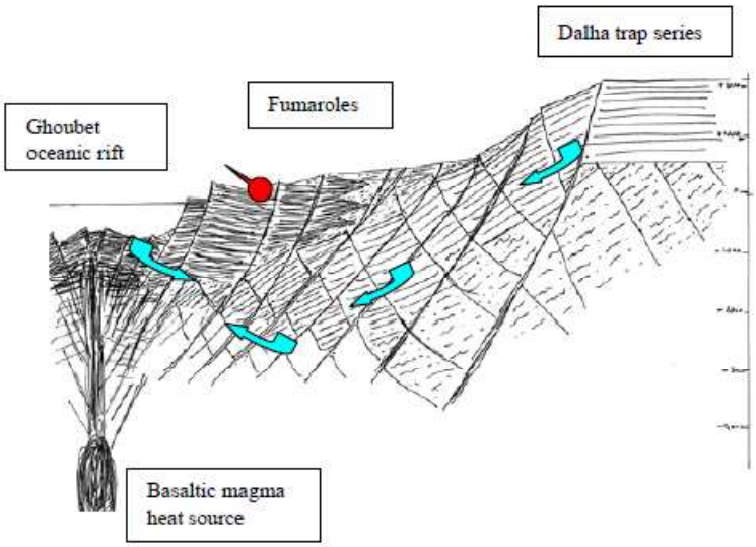

Fig. 21: geological qualitative Model of the North Ghoubet Geothermal site. Meteoritic Water descending from the Dalha plateau penetrates through.The numerous faults in the basaltic Aquifer, heated at depth by the Basaltic magma intrusions along the Ghoubet accreting oceanic ridge

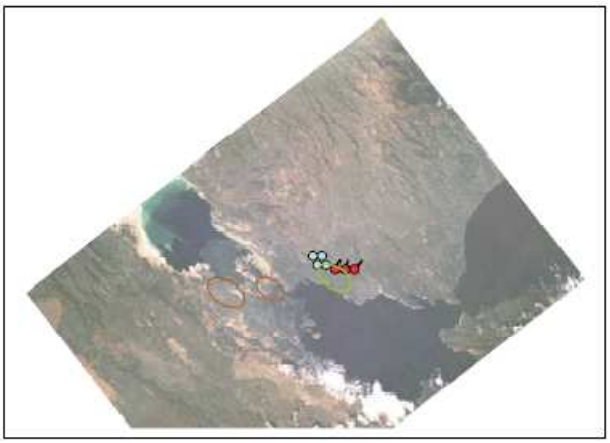

Fig. 22: proposed location for completing geophysical works before drilling exploration wells in the North Ghoubet site. Other geothermal sites in Asal previously drilled and proposed are also indicated.

Considering the active extensional tectonic regime affecting the North Goubhet area in two directions, as well as these hydrogeological considerations, suitable high enthalpy geothermal reservoir conditions should prevail in this area. A geophysical survey should help site exploration wells in order to better delineate this geothermal site (Fig.22).

CONCLUSION

While there are major geothermal sites all along the East African rift valley, several of which having already seen economic industrial developments, notably in Kenya, the Afar region has not yet demonstrated its capability. The purpose of this paper is to show that Afar – in Djibouti, Ethiopia and Eritrea – should possess the largest geothermal resources of the African continent. Due to its exceptional character as an emerged oceanic rift segment and zone of accretion of the Earth's crust, in addition to being affected by an active mantle plume, Afar certainly shares with Iceland the quality of having the world's highest geothermal potential.

As opposed to Iceland, however, climate conditions in Afar are not favorable for the recharging of the geothermal reservoir by meteoritic water. Geothermal brines with corrosive and scaling effects prevail in areas where hyper-saline lakes and salt deposits have developed, as in Assal. Nevertheless, deep aquifers in Afar can be recharged by meteoritic waters due to past wetter climate conditions and to the vicinity of high plateaus. Large water basins enable recharge of the fractured and permeable formations located on the sides of the axial ranges in transverse fracture zones where optimal conditions for geothermal reservoir development prevail.

If there is little doubt that Afar will, in the future, become a region of major renewable energy production, the transition period will be difficult due to the shortage of fossil fuels and the implementation of climate policies. The arid climate has not fostered the social and economic development of the Afar population and, as a first step, it is essential that the geothermal development benefit, first of all, local inhabitants. A well-adapted – probably specific – mode of development that involves the local population as much as possible should be considered. Afar workers presently building the steam condensers should, for instance, be offered employment in the drilling work. This sustainable development issue is a challenge for all, including local authorities, engineering and industrial firms, researchers as well as financing agencies.

To date, most of the prevailing financial schemes in such rural areas have been for smaller energy projects i.e. based on solar or wind energy. As a case in point, the 2010 call for rural energy development projects under the ACP-EU facility did not allow geothermal project to be selected. The capability of development agencies to support geothermal projects adapted to the conditions prevailing in Afar is a real challenge the ARGEO program should allow to master, as soon as possible.

ACKNOWLEDGMENTS

Most of the ideas presented in this paper developed during and after a recent visit to the northern Afar region, organized with Franco Barberi and Marisa Carapezza, at the invitation of the presidents of the regional states of Afar and Tigre, and the initiative of Ras Mengesha Seyoum, who supported CNR-CNRS expeditions to Afar between 1967 and 1975. A renewed interest for Djibouti was encouraged by Fouad Aye who wrote a stimulating thesis concerning energy issues in the Republic of Djibouti. The author also thanks Frederic Chêne BRGM, for the original NASA/SRTM satellite image treatment. We hope this work will contribute to the development of the Afar region and to the benefit of its warm and engaging local population.

BIBLIOGRAPHY:

M.Abraha (2006) Geothermal exploration opportunities. GRC Transactions, Vol.30, 643-647.

Aquater (1988) Djibouti Assal 3 well final report GEOT A 3237.

Aquater (1996) Tendaho geothermal project, final report. MME, EIGS – Gov. of Italy, Ministry of Foreign Affairs, San Lorenzo in Campo.

M.Asaye & M.Tassew (2006) Ethiopia geothermal activities – summary of rehabilitation of Alutu Langano geothermal power plant and Tendaho feasibility study. GRC Transactions, Vol.30, p. 649-653

A. Ayele et al. (2006) The volcano-seismic crisis in Afar, Ethiopia, starting september 2005, 11p, 6 fig.

F.Barberi, S.Borsi, G.Ferrara, G.Marinelli, R.Santacroce, H.Tazieff, J.Varet (1972) : Evolution of the Danakil depression (Afar, ethiopia) in light of radiometric age determinations. J.Geol. 80, 720-729.

F.Barberi, G.Ferrara, R.Santacroce, M.Treuil & J.Varet (1975) A transitional basalt-pantellerite sequence of fractional crystalliszation, the Boina centre (Afar rift, Ethiopia). J. Petrology, 16, 22-56.

F.Barberi & J.Varet (1970) The Erta Ale Volcanic range (Danakil depression) Northern Afar, Ethiopia. Bull. Volc. 34, 848-917.

F.Barberi & J.Varet (1977) Volcanism of Afar : small plate tectonics implications. Bull. Geol. Soc. Amer. 88, 1251-1266.

F.Barberi & J.Varet (1978) The Afar rift junction. In Neuman & Ramberg (Eds) Petrology ang geochemistry of continental rifts, 55-69.

F.Barberi & J.Varet (2010) Access to modern energy service using Geothermal Source in rural and peri-urban areas of Afar region Ethiopia. ACP-EU Energy facility call.

CFG (1993) Champ géothermique de Assal, Djibouti, synthèse des données, 93CFG06.

Battiteili, R.J. Rivera, R. Celati, A. Mohamed (1990) Study of the effect of several wellbore conditions on the output characteristics of wells at the Asal field, Rep. of Djibouti. Proc. XVth workshop on geothermal energy, Standford, Calif. SGP-TR-130, p. 71-79.

A.Y. Baye (2009) Hydrogeological and hydrogeochemical framework of complex volcanic system in the Upper Awash River Basin, Sentral Ethiopia. Thesis, Poitiers, 218p.

ELMICO (1984) Dallol Potash project. PEC Ingenierie, Mulhouse, France, 2 Vol, 280p.

A.A. Farah (2010) Djibouti potential status and prospectives in geothermal resources development. Proceedings WGC, Bali, apr. 2010.

ISOR (2008) The feasibility study of Lake Assal project. Confidential report

G. Hjartarson, V. Gisladottir, G. Gislason, K. Olafsson (2010) Geothermal Development in the Assal Area, Djibouti. Proceedings WGC, Bali, apr. 2010.

J.G. Holwerda & R.W. Hutchinson (1968) Potash bearing deposits in the Danakil area, Ethiopia. Econ. Geol. 63, 124-150.

S. Kebede, Y. Travi, K Rozanski (2008) The 18O and 2H enrichment of Ethiopian lakes. Jour. of Hydrology, 365, 173-182.

J..Lépine et al. (1980) Sismicité du rift d'Asal-Ghoubbet pendant la drise sismo-volcanique de novembre 1978. Bull. Soc. Géol. Fr. 809-816.

L.Lupi (2010) Dancalia, l'esplorazione del Afar, un'avventura italiana, IGM Firenze, 2 vol. 1488p.

Marinelli G. & Varet J., (1973) Structure et évolution du Sud du "horst Danakil" (TFAI et Ethiopie). C.R. Acad. Sci., (D) 276, 1119-1122.

A.Michael (2005) Country update on geothermal energy in Eritrea. Proceedings WGC Antalya, Turkey.

P.Mohr (1870) Afar triple junction and sea floor spreading. J. Geoph. Res. 75(35), 7340-7352.

P. Tapponier & J. Varet (1974) La zone de Mak'aeeasou en Afar : un équivalent émergé des « failles transformantes » océaniques. C.R. Acad. Sci., (D) 278, 317-329.

H.Tazieff, F.Barberi, S.Borsi, G.Ferrara, G.Marinelli et J.Varet (1970) Relationships between tectonics and magmatology in the Norther Afar (or Danakil) depression. Phil.Trans.Royal Soc. London. A.267, 293-311.

M.Teklemariam (2006) Overview of geothermal resource utilization and potential in Esat African rift system. JRC Transaction, Vol.30, p.711-716.

UNDP (1973) : Geology, geochemistry, and hydrology of the East Africa Rift System within Ethiopia. DDSF/ON/116. U.N. New York.

M.Treuil & J.Varet (1973) : critères volcanologiques, pétrologiques et géochimiques de la genèse et de la différenciation des magmas basaltiques : exemple de l'Afar. Bull. Soc. Geol. France, 7 (15), 506-540.

J.Varet et al. (1978) Geology of central and southern Afar (Ethiopia and Djibouti Republic) Edition CNRS, Paris.

J.Varet (2005) Les matières premières minérales. Flambée spéculative ou pénurie durable ? Futuribles, 308, 5-24.

J.Varet (2006) The Afar triangle, a future "gulf region" for geothermal energy? First African geothermal symposium, Addis-Abeba, 7p

.

THEME II

GEOCHEMICAL EXPLORATION

GEOCHEMISTRY OVERVIEW OF HOT SPRINGS FROM THE LAKE ABHE AREA: REPUBLIC OF DJIBOUTI

Bouh Houssein
Laboratoire de Géochimie du CERD - Route de l'Aéroport, BP : 486, Djibouti.
Email: bouhhoussein@yahoo.fr

ABSTRACT

The Abhé Lake site is located in the south-Western region of the Republic of Djibouti near the Ethiopian border. Geologically, the area is mainly composed of stratoïd basalts with a high plateaus and sedimentary plains. Several fumerolles and hot springs are identified in Abhe lake area. The temperature of the hot springs can exceed 100°C. Chemical analyses from 20 water sample, hot spring, shallow water well, lake and borehole from the Abhé Lake area were evaluated in order to investigate spring water origin, water–rock interaction mechanisms, and estimate the thermal potential of the geothermal areas. This study presents a preliminary geochemical data interpretation of the abhé area geothermal systems. Based on their hydrochemical facies, the water bodies are categorized into four main groups. The first group is Na-Cl type of water and represents all the boreholes catching the regional volcanic aquifer. Several springs located in Hanlé plain (Agna, Oudgini…) belong also to this group. The hot springs in abhe lake area are characterised by Na-Ca-Cl type of water and form the group 2. At last the waters from sedimentary aquifers are on the one hand characterized by Na-HCO3-Cl type of the shallow water well and on the other hand are characterized by Na-SO4-Cl type of water for deep well. The Lake Abhé waters belong to the Na-HCO3 type with high salinity (155 g/l) and high pH values (>9). The use of geothermometers suggested that the investigated geothermal areas have high enthalpy fluids at depth with temperature estimated by Chemical geothermometers are mostly 160°C.

Key Word: Abhe Lake, Hot springs, geothermometers, geochemistry, Djibouti, overview.

INTRODUCTION

The Republic of Djibouti is located in the arid zone of eastern Africa. Precipitation is randomly distributed on the coast and becomes monsoon in type in the inland (summer rains). Temperatures are high and show little monthly variation. The whole country is practically covered by lava and volcanodetrital deposits from Tertiary an Quaternary ages, some of them very recent. This volcanic activity is due to the location of the area on the southern part of the Afar rift (Fontes et al. 1980). Vertical movements along the faults on the rift structure give rise to isolated basins with internal drainage (Grand Bara, Abhè, Hanlé, Gobaad, Asal). During the upper Pleistocene and until 4000 years ago, lacustrine episodes took place in these depressions (Fontes et Gasses, 1973). At present two basins are still active, both occupied by highly saline lakes. Lake Asal represents the highest potential geothermal reservoir in Djibouti. Lake Abhè is the terminal lake of the Awash River system which comes from the Ethiopian Plateau. It is a sodium-bicarbonate type water (TDS~155g/l).

In Djibouti, different geothermal zone, revealed by numerous hot springs spread, are identified (**figure 1**). The study area is one of them. Located on the south western part of the country, it is a unique landscape in the world with hundreds of chimneys of ruiniform aspect forming a travertine chain on several kilometres (**figure 2**). Several hot springs and fumaroles are observed in this zone. The temperature of the hot springs can exceed 100°C.

Previous chemical and isotopic investigations on surface, groundwater and lake system in the Hanlé-Gaggadé geothermal fields were carried out during the 1970s and 1990s. The aim of this study is to present a preliminary result carried out to the hot springs from Lake Abhè area as well as estimation of the subsurface reservoir temperatures.

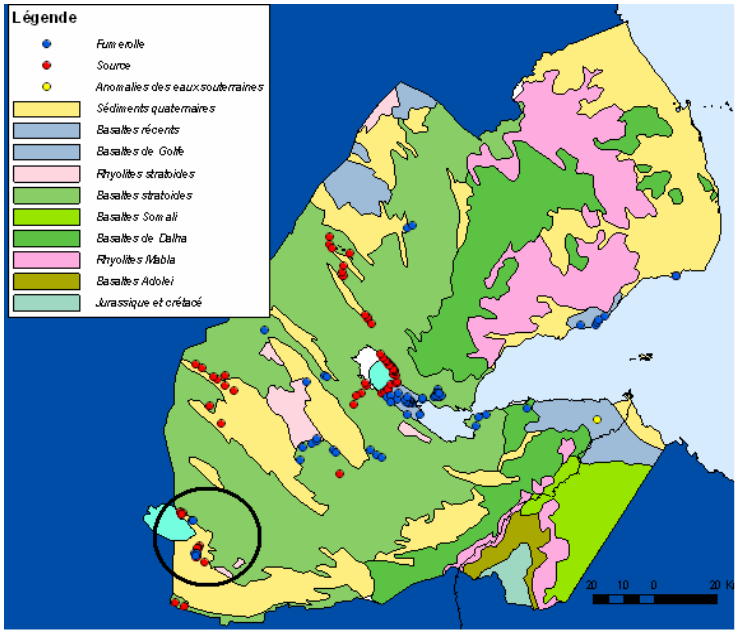

Figure 1: Gelogical map and hydrothermal manifestation in the Republic of Djibouti

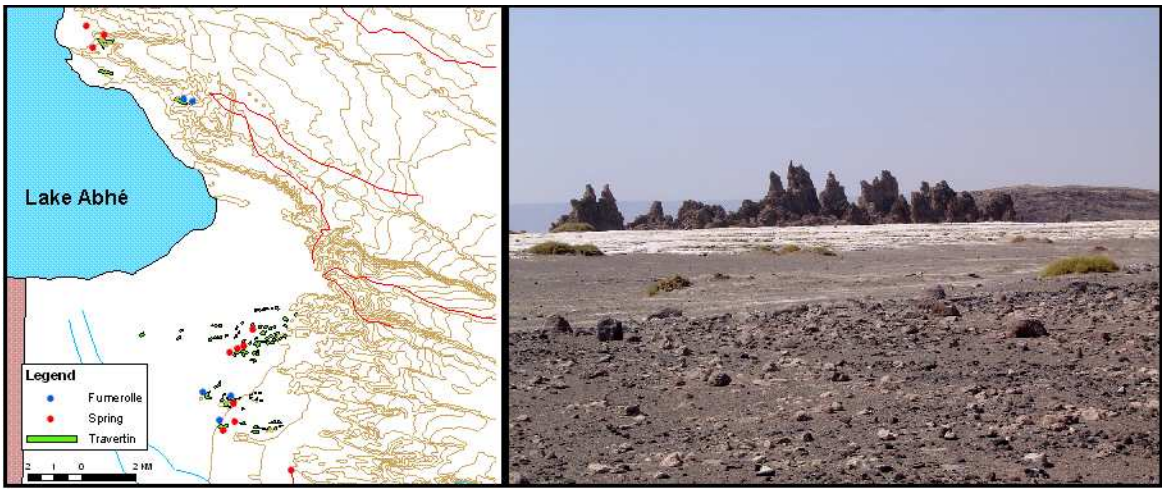

Figure 2: Location map of the thermal water from the study area. (Jalludin 2008)

GEOLOGICAL FEATURES OF THE STUDY AREA

The volcanic series overlie the basement rocks (Jurassic limestones and Cretaceous sedimentary rocks) as a result of the Red Sea, Aden gulf and East African rifts triple junction system, related to plate tectonic movements in the last 25-30 Ma. Adolei basalts characterize the first rupture movement within the Arabo-Nubian block which occurred during the later Miocene period (Figure 1). During these first movements the area is under an Ethiopian rift tectonic pattern with N-S extension faults system (Gaulier and Huchon 1991). There then followed a period of slow expansion during which the Mabla rhyolites outcrop formed (15 Ma) in a large senestral shear zone. Oldest Ethiopian structure oriented N-S to N20°E are reactivated as senestral strike-slip faults. Mabla rhyolite located in the Northern part of the country were then submitted to a diffuse extension phase with associated N160°E normal fault system. After an interval during which these rhyolites were eroded, the Dalha basalts were laid down with an angular unconformity (3.4 - 9 Ma). The Somali basalts outcrop was formed practically contemporaneously in the eastern part of the region. N160°E extension links to early movements during the emplacement of Dalha basalts. Progressively this extension turned to N20°E. Between 3.4 and 1.5 Ma, the Stratoid basalts and Gulf basalts poured out as the Gulf of Tadjourah opened (Black et al., 1974; CNRS-CNR 1973). At the early stage of the opening of the Gulf of Tadjourah the western border of Ali Sabieh horst acts as a wide dextral strike-slip zone with related N-S to N20°E extension which turned to N40°E. Recent volcanic formation are mainly located in the Asal rift and the Manda Inakir rift.

Sedimentay rocks are encountered in coastal areas, in tectonic basins in the southwestern part of the country and along the main stream beds. During the miocene-pliocene, sedimentary rocks (clays and alluviums) are interbedded in Dalha basalts. Alternative humid and arid climates went through the pliocene period with the outcrop of stratoid basalts. Limestones, clays and diatomites are interbedded in these basalts and fill tectonic basins. In the plains, the thickness of the sedimentary rocks can exceed several hundred of meters and in stream bed it remains between some meters to some tens of meters. During the quaternary period, marine sediments (coral limestones and limestones) were deposited in coastal areas. Since 100 000 years BP five phases of major extension of lakes in the tectonic basins were developped during the humid climates and has formed limestones, diatomites and clays outcrops (Gasse et al., 1980).

SAMPLING AND ANALYTICAL METHODS

For this report twenty one water samples from cold and hot springs and of lake water (**Table 1**) were used. These samples were collected in Janvier, 2009. During sampling, field measurements for pH, conductivity, spring temperature were carried out (**figure 3**). Samples were filtered through a 0.45 µm filter membrane and stored in two polyethylene bottles. One of the bottles was acidified with suprapure HNO3 for determination of cations and SiO2 analyses and the other was kept unacidified for anion analyses. The major chemical constituents were analyzed in the geochemical laboratory of the CERD. The δD and $\delta^{18}O$ values on the some sample were determined, at the "Laboratoire d'Hydrogeologie d'Avignon" (France), with standard deviations of 2 and 0.2‰, respectively. Additionally, isotopic (18O, 2H) analyses and some chemical analyses of waters from Hanlé and Gobaad area were used from previous studies. All the earlier and current analytical results were used to comment on hydrogeology and water chemistry.

Figure 3: Water sampling and field measurement

RESULTS AND DISCUSSION

Chemical results

The results of the chemical analyses of the hot spring, cold and Abhe lake waters from the study area are listed in Table 1. According to the *Piper diagram* (**figure 4**) the waters were classified into four groups. The first group is Na-Cl type of water and represents all the boreholes catching the regional volcanic aquifer. Several springs located in Hanlé plain (Agna, Oudgini…) at contact of sedimentary rocks and basalts fault scarp are also Na-Cl type and their chemistry is compatible with the chemistry of the volcanic rocks through which they flow.

The hot springs from the lake abhè area are characterised by Na-Ca-Cl type of water and form the group 2. One of the possible origins of these hot springs could be from waters of meteoric origin that circulates deep into the fault zones and rises to the surface once it is heated. The increase of the calcium contain in the water is the result of a reaction which produced at high temperature beetwen an chlorinate-alkaline water and basalts (albitisation of anorthite). The total dissolved solids of this group range from 1700 to 3400 mg/l. The temperature of the hot spring varies from 88,8 to 99,7°C.

The group 3 type is Na-HCO3-Cl and exhibit low mineralisation. It corresponds to the low depth waddi bed alluvium aquifers and is characterized by direct recharge from intermittent stream waters. The TDS range from 278 to 640 mg/l. The Abhé lake water belong to this group with high salinity (~155g/l) and high pH values 9,9.

The water catching the sedimentary aquifers are Na-SO4-Cl type of water form the group 4. This group represented by the sample koutabouya, Yoboki show moderate salinity (TDS=2200mg/l) with high SO4 contain in water. The enrichment SO4 is due to dissolution of evaporite minerals (gypsum) present in sediments lacustrine.

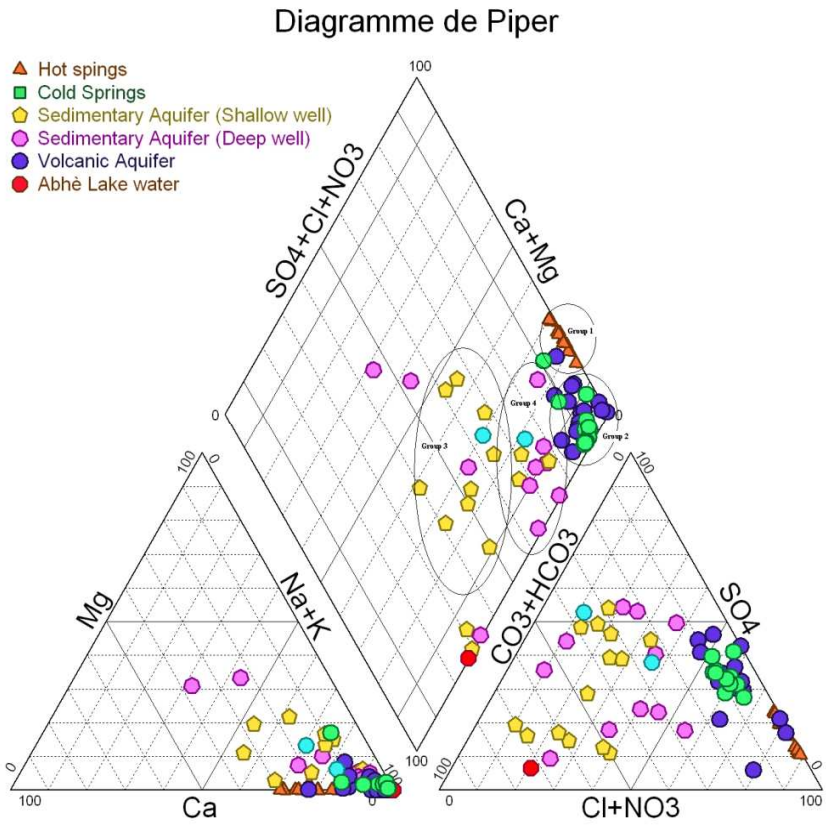

Figure 4: Distribution of the waters points from the study area in Piper diagram

The relations of the chemical constituents in the water samples from the study area are presented in Figure 5. The concentrations of the major ions were plotted against that of chloride, which is considered to be a conservative ion in thermal waters. The SO4 content increase with increase in Cl content. The Ca and HCO3 contents from the cold springs and volcanic aquifer wells seams controlled by the CaCO3 dissolution at high temperature. The Mg content for the hot spring waters is consistently low. The increase in SO4 and decrease in Mg in the hot springs can be explained by: (a) the increase in the solubility of CaSO4 with increasing temperature, and (b) the ion exchange at high temperature of Mg ions in several Ca-Mg-silicate minerals (Ellis, 1971) and subsequent re-equilibration in the solutions (Giggenbach, 1988). The increase of HCO3 could be explained by the reaction between the dissolved carbon dioxide and calcite from the rock that form HCO3.

Mineral saturation index (SI) are used to describe the extent to which a particular solution is saturated, supersaturated or undersaturated with respect to a particular mineral phase. The SI states with respect to calcite, dolomite and gypsum and other minerals were calculated for the water samples using the computer programWATQF, part of the parent code NETPATH (Plummer et al., 1994). The SI values indicate that the geothermal waters are saturated with respect to calcite and aragonite (except the lake abhe water which is supersaturated), and are undersaturated with respect to gypsum and anhydrite.

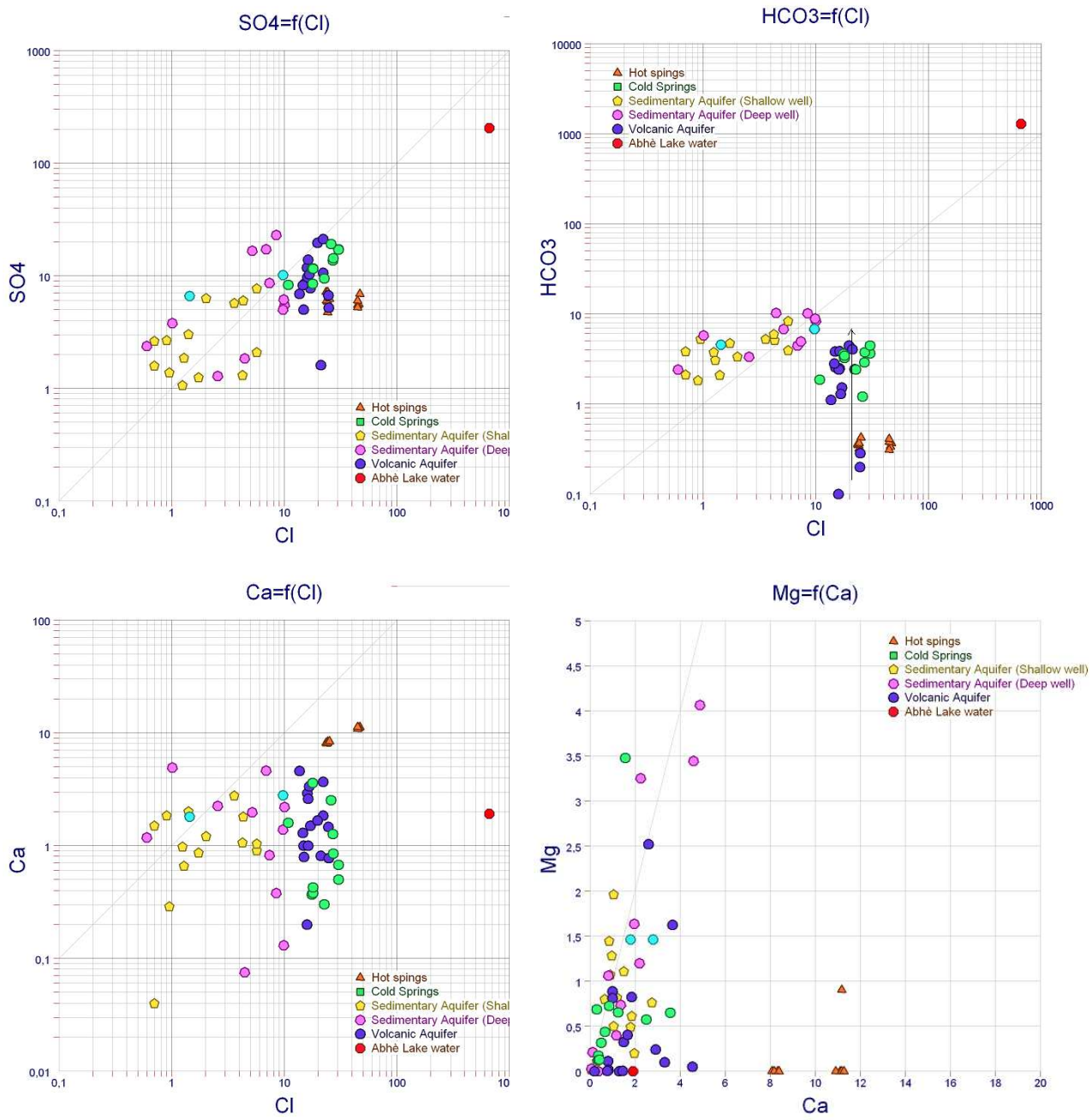

Figure 5: Plots of Ca, HCO3 and SO4 against Cl and Mg against Ca

Table 1: Chemical and physical data of the lake abhé hot springs area and Hanlé-Gobaad area cold water.

Nom	Libellé	T°C	Cond	pH	Cl	HCO3	CO3	SO4	NO3	Na	K	Ca	Mg	Li	B	SiO2	18O	2H
Asbahaltou	CS	36	3760	8,86	824,1	888,8	29,6	566,4	0,0	1426,0	12,9	5,6	0,0					
Abakara	CS	32,4	4540	8,52	1039,1	739,9	10,8	566,4	0,0	1058,0	21,5	6,8	0,0					
Agna	CS	43,7	2525	8,39	652,3	176,9	12,0	172,9	0,0	563,3	12,1	10,0	1,2	0,01		46,8	-3,27	-22,2
ALEYLOU	CS		8283		1816,0	1100,0	0,0	696,0		2012,0	35,0	9,0	3,0					
Dagirou	CS	41,5	5044	7,8	860,0	155,0	0,0	320,0	1,0	724,0	26,5	11,4	3,6	0,02		49,4		
Dahotto	CS	42	5290	7,85	890,0	216,0	0,0	330,0	1,5	806,0	31,5	8,1	4,6	0,02		40,3		
Dali	CS	42,9	6016	8,1	1060,0	220,0	0,0	400,0	1,5	904,0	54,8	6,1	3,3	0,02		58,5		
Eadara	CS	41,9	6151	8,2	1050,0	225,0	0,0	400,0	1,0	916,0	52,4	4,1	1,8	0,01		50,7		
Neinle	CS	68,3	2916	7,59	310,0	155,0	0,0	200,0	1,5	300,0	21,3	33,4	2,8	0,27		79,3	-1,90	-1,3
Oudgini	CS	43,2	4749	8,1	830,0	112,0	0,0	240,0	1,5	630,0	29,0	20,3	6,4	0,02		44,2		
S-AbP2	HS	95,6	4760	8,04	1658,0	22,6	0,0	331,0	0,0	906,2	31,6	224,0	11,0	0,265	1,059	**100,75**	-3,48	-23,74
S-AbP 3	HS	99,7	4710	8,1	1621,3	20,7	0,0	269,8	0,0	906,2	32,4	222,4	0,0	0,287		**114,7**		
S-AbP4	HS	98,6	4640	7,84	1578,0	23,2	0,0	264,0	0,0	1000,0	34,3	218,4	0,0	0,283		**111,4**		
S-AbP5	HS	88,8	4780	7,53	1584,4	25,0	0,0	288,0	0,0	1311,0	35,9	224,0	0,0	0,316	1,038	**119,54**	-2,92	-22,18
S-AbP 6	HS	97	4640	7,76	1575,8	18,9	0,0	251,5	0,0	772,8	24,6	226,0	0,0	0,249				
S-AbG1	HS	94,6	2800	8,32	861,6	19,5	0,0	228,5	0,0	460,0	17,2	166,8	0,0	0,133		**117,9**		
S-AbG3	HS	96,6	2770	8,26	848,5	21,4	0,0	288,0	0,0	743,4	16,4	163,6	0,0	0,133		**101,14**		
S-AbG5	HS	99,6	2720	8,3	848,5	21,4	0,0	282,2	1,2	529,0	16,4	162,4	0,0	0,134				
S-AbG6	HS	94,5	2720	8,5	844,2	21,4	0,0	290,9	0,0	552,0	14,4	161,6	0,0	0,129				
S-AbG7	HS	91,1	2750	8,14	835,3	22,0	0,0	345,6	0,0	644,0	13,3	163,6	0,0	0,132	0,664		-3,42	-24,78
S-AbG8	HS	96,8	2740	8,16	863,7	22,6	0,0	345,6	0,0	460,0	13,3	163,6	0,0					
S-AbG9	HS	93,9	2900	8,34	887,1	26,2	0,0	298,6	0,0	449,9	14,0	168,4	0,0		0,663		-3,03	-25,67
Abaïtou	INF		1072	8,08	150,7	361,2	0,0	62,4	22,3	223,0	9,8	21,2	23,8					
TeweoPuits	INF		720	8,43	33,7	319,1	20,4	66,3	19,8	174,7	2,0	5,8	1,3					
Checkeyti	INF		779	8,71	61,4	287,9	8,4	59,5	33,5	147,2	0,4	17,2	17,5					
Galafi	INF		1430	8,41	202,0	509,4	0,0	100,8	18,6	335,6	32,0	18,0	13,0					
Gagdé Puit	INF		495	8,06	45,7	186,7	0,0	89,3	18,0	102,1	2,0	13,2	9,7					

Teweo	INF		685	8,73	24,9	231,9	60,0	75,9	8,8	163,0	1,2	0,8	0,2					
Galafi 8	INF				202,3	509,8	0,0	201,9	0,0	335,2	31,9	35,9	25,7					
Koutabouya	SED	23	3610	8,52	302,8	622,2	9,0	1096,3	14,9	1133,9	0,0	7,6	0,0					
Gagadé	SED		1525	8,1	152,7	311,1	0,0	288,0	2,9	331,2	3,9	36,0	6,0		2,9			
Kimbire As	SED	30,8	900	7,99	71,4	205,6		303,4	0,0	227,7	5,1	24,0	10,0					
Yoboki1	SED		2370	8	184,6	413,1	0,0	792,5	164,3	598,9	7,8	39,7	19,9					
As Ela	SED		1270	7,56	127,3	319,7	0,0	273,8	1,9	252,9	3,9	54,9	9,2					
Koudi K	SED		530	8,27	44,4	229,4	0,0	50,9	10,5	81,7	3,9	19,6	15,6				-0,69	-1
LiLiya Bouri 1	SED		2030	8,6	261,6	302,6	0,0	412,1	20,5	445,5	6,3	16,4	12,9				-1,16	-0,4
LiLiya Bouri 2	SED		2770	8,16	354,5	511,3	0,0	265,1	446,4	620,7	5,1	44,1	14,6					
G2b Alo	SED		2000	8,1	345,7	414,9	0,0	242,1	11,2	443,5	6,3	27,7	9,0					
Gorabous	SED			7,85	38,0	314,0		74,5	14,0	62,0	5,5	64,0	22,0				-0,20	-0,9
Teweo 4	VOLC		2140	8,43	519,0	117,1	1,2	220,8	0,0	481,9	24,6	14,0	0,0				-2,75	-18,4
R1 bis	VOLC		2194		566,0	146,0	0,0	233,0	0,0	501,0	25,1	29,3	1,5				-2,92	-20,4
R-2	VOLC		2126		588,0	79,0	0,0	247,0	0,0	489,0	18,4	33,5	0,6				-2,86	-21,7
R-3	VOLC		3238		700,0	273,0	0,0	467,0	0,0	752,0	5,5	16,7	2,5				-2,23	-17,7
galafi1	VOLC	39,8	2200	8,9	158,0	624,0	82,0	88,0	18,1	400,0	16,6	1,5	0,4					
Koutabouya forage	VOLC	36	4500	8,1	785,0	149,0		507,0	20,0	740,0	27,0	37,0	10,0					
Gabaita	VOLC	37	2800	8,2	524,0	234,0		240,0	7,0	470,0	19,4	20,0	10,8	0,02		36,4		
Daoudouya forage	VOLC		758	7,99	124,1	210,5	0,0	84,5	26,0	153,6	8,2	33,3	16,5	0,01		35,1		
G2	VOLC				599,8	92,0	0,0	373,7	0,0	540,2	11,7	30,0	4,0					
T1	VOLC				560,8	0,0	0,0	565,6	0,0	589,3	21,8	4,0	0,0					
Hanlé1	VOLC				532,7	156,0	0,0	403,8	0,0	483,2	17,9	16,0	1,4					
Hanlé2	VOLC				481,6	67,2	0,0	333,8	0,0	367,2	7,5	91,4	0,6				-3,52	-21,9
Yoboki 3	VOLC				572,8	152,0	0,0	475,7	0,0	593,3	28,9	20,0	9,9					
Lake Abhé	LAKE	29	79100	9,94	23462	77763	31140	9768	0,0	43746	434,5	38,4	0,0	0,002	31,160		8,94	47,85

Geochemical geothermometry

Several chemical geothermometers have been developed to predict the subsurface reservoir temperatures in geothermal system (Fournier and Truesdell, 1973; D'Amore et al., 1987; Giggenbach, 1988). Dissolved silica and certain cation ratios in deep waters that have experienced prolonged interaction with rocks are usually controlled by temperature-dependent reactions between minerals and the circulating fluids (e.g. Fournier, 1973). Geothermometers represent the equilibria of these temperature-dependent reactions, and geothermometric analysis can indicate the temperature of the reservoir yielding the deep waters. These temperature variations may be due to the lack of equilibrium between solutes and minerals or due to additional processes (including mixing with cold water in the upflow).

Chemical analyses of thermal waters from the study area were used to estimate the subsurface reservoir temperatures by several solute geothermometers. Different geothermometers were applied to the thermal waters of the Lake Abhé hot springs area: chalcedony and quartz (Fournier, 1973 and 1977), Na/K (Giggenbach, 1988), Na-K-Ca (Fournier and Truesdell, 1973), Na-K-Ca-Mg (Fournier and Potter, 1979). Temperatures calculated by these geothermometers for the thermal waters discharged from springs are given in Table 2.

Tableau 2: Geothermometric temperatures (ºC) calculated using different methods

THERMOMETER								
Nom	**T°thermal springs**	**Chalcedony**	**Quartz**	**Quartz steam loss**	**Na/K (Fournier & Potter 1979)**	**Na/K (Fournier 1979)**	**Na-K-Ca (Fournier 1979)**	**Na-K-Ca Mg corrected**
S-AB-G1	**94**	**120**	**146**	**140**	**157**	**144**	**132**	
S-AB-G3	**96**	**111**	**138**	**133**	**123**	**113**	**116**	
S-AB-G5	**99**				**144**	**132**	**125**	
S-AB-G6	**94**				**133**	**122**	**119**	
S-AB-G7	**91**				**120**	**110**	**111**	
S-AB-G8	**96**				**140**	**128**	**120**	
S-AB-G9	**93**				**146**	**134**	**124**	
S-AB-P2	**95**	**110**	**137**	**133**	**152**	**140**	**136**	**132**
S-AB-P3	**99**	**119**	**145**	**139**	**154**	**142**	**137**	
S-AB-P4	**98**	**117**	**143**	**138**	**152**	**139**	**137**	
S-AB-P5	**88**	**121**	**147**	**141**	**136**	**125**	**130**	
S-AB-P6	**97**				**146**	**134**	**129**	
Lake Abhè	**29**	**60**	**91**	**93**	**83**	**76**	**152**	
Asbahaltou	**36**	**71**	**101**	**102**	**75**	**69**	**110**	

Results of the different solute geothermometers from de hot springs (**S-AB**) show that the subsurface reservoir temperatures varied between 110 and 157°C. Na/K and Na-K-Ca geothermometers gave the maximum reservoir temperatures (157°C). According to the chalcedony and quartz geothermometers (Fournier, 1977), the subsurface temperatures of the Lake Abhé hot springs area range between 110 and 147°C. In general, the quartz geothermometer is applied in high temperature reservoirs, and the chalcedony geothermometer in low temperature reservoirs. Chalcedony geothermometer gave temperatures close to the measured discharge temperatures (110 – 121°C), whereas quartz geothermometer gave the most reasonable subsurface temperatures (133 – 147°C) for all the investigated thermal waters.

Giggenbach (1988) is a method to discriminate mature waters, which have attained equilibrium with relevant hydrothermal minerals from immature waters and waters affected by mixing and/or re-equilibration at low temperatures along their circulation path. The graphical resolutions of this combined geothermometer for this study are illustrated in Figure 6. Most of the thermal waters in the Lake Abhé area fall into the immature fields or mixed waters (Figure 6), indicating that none of these waters have attained full equilibrium with their associated host rocks.

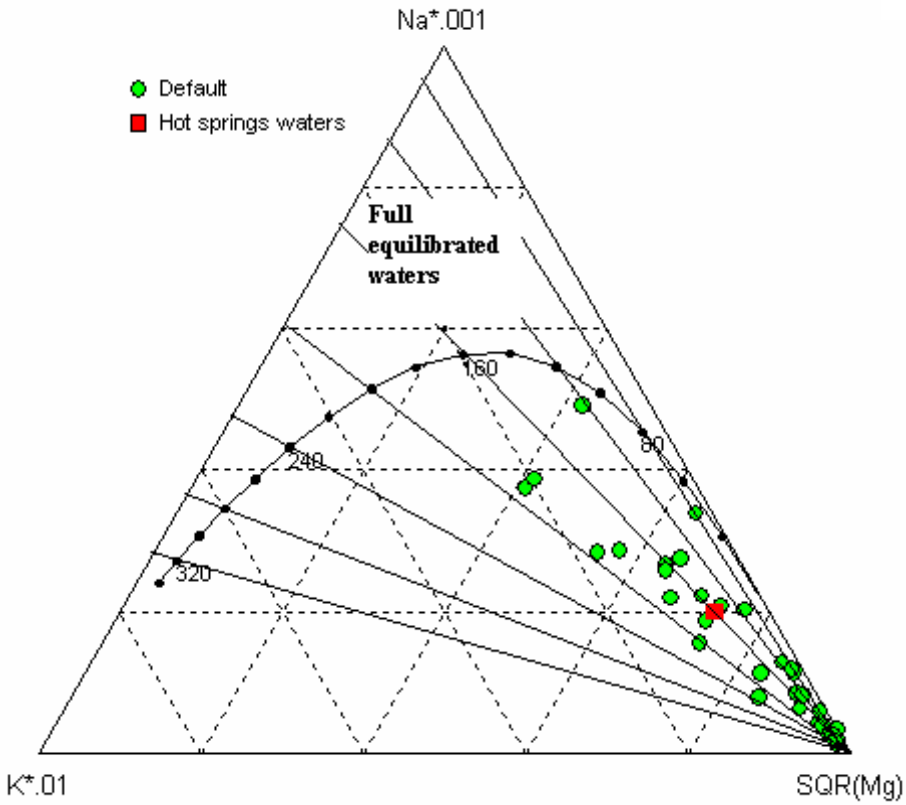

Figure 6: The Giggenbach (1988) Na-K-$Mg^{1/2}$ triangular diagram.

Stable isotope results

Stable 18O and D isotopic analyses were carried out to determine the origin of thermal waters and the geothermal reservoir recharge areas (**figure 7**). The Djibouti Local Meteoric Water Line (LMWL) is not yet available, thus the oxygen-18 and deuterium mean contents in precipitation were taken from stations of the International Atomic Energy Agency (IAEA) network near the studied area (Addis ababa).

The The Oxygen-18 and deuterium composition for 1980 and 2006 sampling ranges from -2 ‰ to 0 ‰, and from -6 ‰ to +2‰ respectively.

The Oxygen-18 and deuterium composition of thermal spring ranges from -2,92‰ to -3,48‰, and from -22,18‰ to -25,65‰ respectively.

Most of the values obtained by Fontes (1980) and Bouh (2006) fall on a range with a slope of 8 indicating that no significant evaporation occurred before or during infiltration; this fact is in agreement with the concept of a fast infiltration through fractured lavas.

The water from hot springs show and oxygen shift, indicating the occurrence of an exchange process with rocks at high temperatures. The following conclusions confirm the chemical observation. The increase of the calcium contain in the water is the result of a reaction which produced at high temperature between an chlorinate-alkaline water and basalts (albitisation of anorthite).

The Lake water show the effect of evaporation, the heavy isotope content between 1980 and 2010 is shifted. Also, the boiling sample from the lake abhé area between 1980 and 2010 show an oxygen and deuterium shift due to evaporation effect.

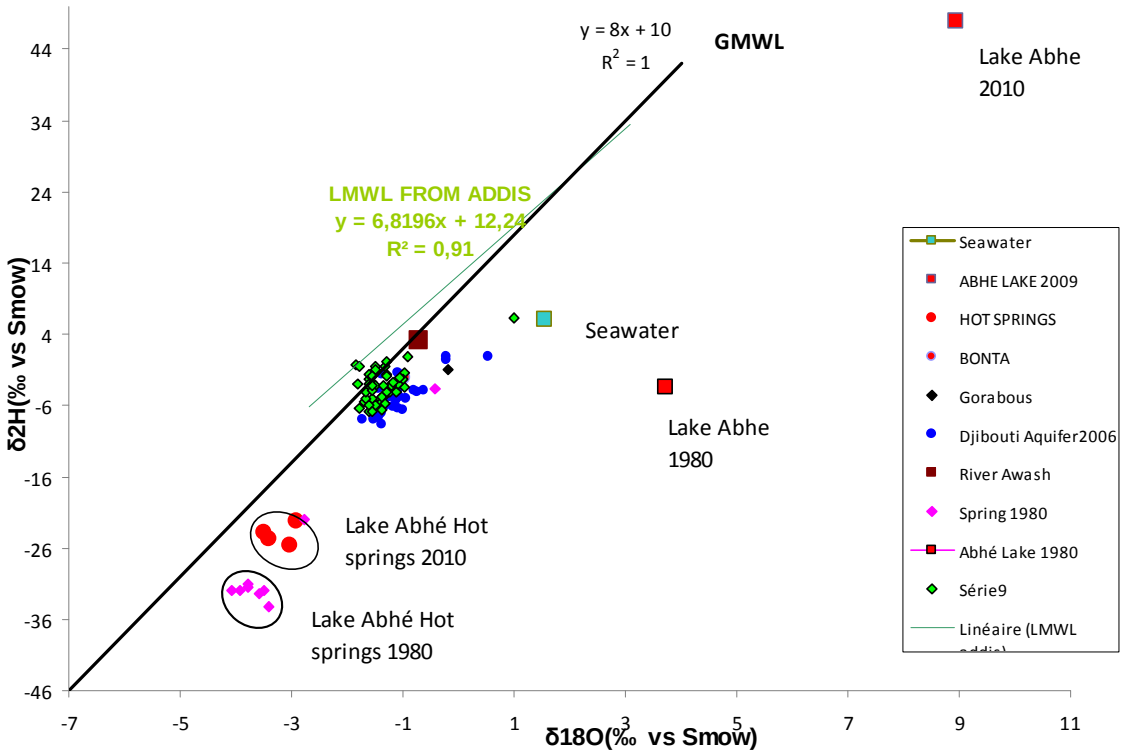

Figure 7: Plot of 18O-2H for the thermal waters from Lake Abhé, Hanlé-Gaggadé and Djibouti aquifer.

CONCLUSION

Geochemical study of thermal water from Abhè Lake area is carried out in order to investigate the origin and sources of solutes and estimate the subsurface reservoir temperatures. Four groups of type of water were found, the first are Na-Cl hydrochemical facies and represents the regional volcanic aquifer and several springs located in Hanlé plain. The hot springs from the lake abhè area are characterised by Na-Ca-Cl type of water and form the group 2. The group 3 type is Na-HCO3-Cl and corresponds to the low depth waddi bed alluvium aquifers. The Abhé lake water belong to this group with high salinity (~155g/l) and high pH values 9,9. The water catching the sedimentary aquifers are Na-SO4-Cl type of water form the group 4. The result of the geothermometer shows that the reservoir temperature can be reach up to 150 ºC.

The hot springs from Abhè Lake area are depleted in 18O and 2H, indicating the occurrence of an exchange process with rocks at high temperatures.

The hydrochemical and isotopic information combined with geological and hydrological data from the study area were used to build a conceptual model with the purpose of simplifying field problems (figure 8).

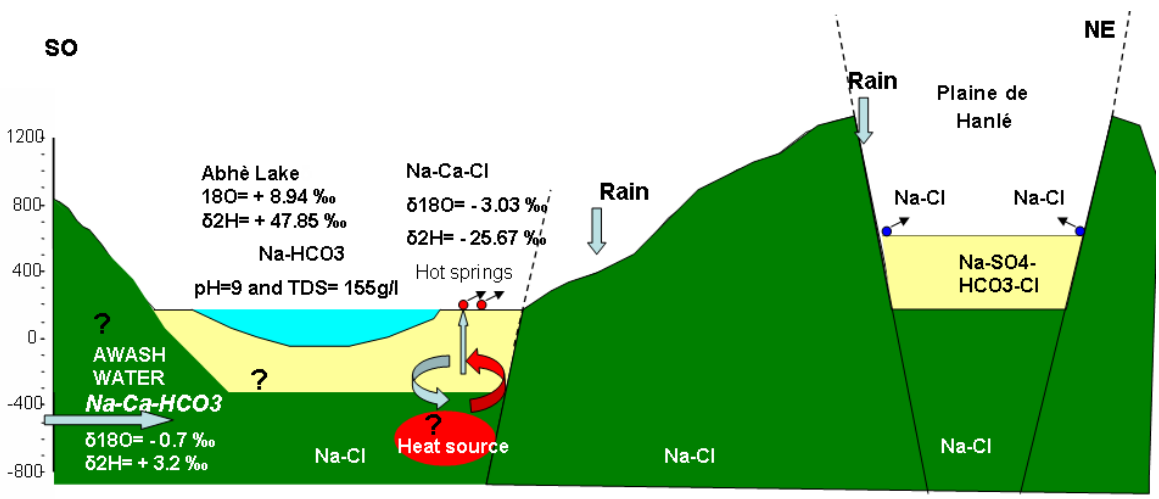

Figure 8: Conceptuel model

REFERENCES

Aquater (1981). Projet pour l'évaluation des ressources géothermiques. Government de Djibouti. ISERST. 137pp

Aquater, (1989). Djibouti geothermal exploration project Republic of Djibouti: final report. ISERST, 159 pp

Barberi, F., Ferrara, G., Santacroce, R., and Varet, J. (1975): Structural evolution of the afar triple junction. In: A. Pilger and A. Rösler Edition, Afar depression of Ethiopia. Vol. 1 Schweizerbart, Stuttgart, 38-54

BRGM (1970). Reconnaissance géothermique du Territoires Français des Afars et des Issas.70SGNGTM. 59pp.

Fontes J.Ch. (1980). Environmental isotope study of groundwater systems in the Republic of Djibouti. Extrait de "Arid zone hydrology" investigation with isotope techniques, "International Atomic Agency Vienne 237-263p.

Fournier, R.O. (1973). Silica in thermal waters: laboratory and field investigations. Proceedings International Symposium on Hydrogeochemistry and Biogeochemistry, Tokyo: 122-139.

Fournier, R.O. (1977). Chemical geothermometers and mixing models for geothermal systems, Geothermics, 5: 41-50.

Fournier, R.O. (1979). A revised equation for Na-K geothermometer, Geoth. Res. Council,

Transactions, 3: 221-224.

Fournier, R.O. and Truesdell, A.H. (1973). An empirical Na-K-Ca geothermometer for natural waters, Geochim. Cosmochim. Acta, 37: 1255-1275.

Fournier, R.O. and Potter, R.W. (1979). Magnesium correction to the Na-K-Ca chemical

geothermometer, Geochim. Cosmochim. Acta, 43: 1543-1550.

Gasse, F. (1975). « L'évolution des lacs de l'Afar central (Ethiopie T.F.A.I.) du Plio-Pleistocène à l'actuel » Reconstitution des paléomilieux lacustres à partir de l'étude des diatomées, thèses de Doctorat, Paris, 406p.

Giggenbach, W.F. (1988): Geothermal solute equilibria. Derivation of Na-K-Mg-Ca geoindicators. Geochimica et Cosmochimica Acta, 52, 2749-2765.

Houmed Gaba A. (2002). Modélisation préliminaire de l'Aquifère volcanique Régional de la Région de Hanlé en République de Djibouti. D.E.S.T.A.U.P., Université de Poitiers.

Houssein, I., Sanjuan, B., and Michard, G. (1993): Indices géochimiques de l'existence d'un fluide à 210°C dans la région d'Obock (République de Djibouti). C.R. Acad. Sciences de Paris, t. 316, série II, 771-776.

Jalludin Mohamed. An overview of geothermal prospections in the Republic of Djibouti. Results and perspectives. (Reprinted from Kengen Geothermal conference April 2003)

Jalludin, M. and Razack, M. 2004. Assessment of hydraulic properties of sedimentary and volcanic aquifer systems under arid conditions in the Republic of Djibouti (Horn of Africa). Hydrology Jour., 12, 159-170.

Sanjuan, B., Michard, G., and Michard, A. (1990): Origine des substances dissoutes dans les eaux des sources thermales et des forages de la région Asal-Ghoubbet (République de Djibouti). J. of Volcanol. and Geoth. Research, 43, 333-352.

Valette J.N. (1975). Le Lac Abhé (T.F.A.I.): Etudes morphologique et géochimique. Bulletin du BRGM (deuxième série) Section II, n°2, 1975, pp.143 à 155, 5 fig., 6 tabl.

Geochemical Characteristics of Homa Hills Geothermal Prospect

Charles K. Wanjie
E-Mail: cwanjie@gdc.co.ke

Solutes and gas composition of four hot water discharge areas are used in conjunction with deuterium and oxygen 18 to determine the chemical characteristics of geothermal fluids and to estimate the prevailing fluid temperatures in Homa Hills geothermal prospect, Kenya. A reservoir that consists of Na-Cl-HCO_3 water with temperatures in the range of 190-220°C exists. The heat sources are inferred to be intrusions in the form of plugs, dykes and sills. The water recharge is from Lake Victoria which lies east of the prospect area. The water discharging from the hot springs is a product of mixing of the Lake water and water from the rift scarps. The mixing leads to a dilution of the lake water by a factor of about 10 calculated using deuterium and oxygen 18 isotopes. The fluids from the prospect are ideal for binary cycle electricity generation and for locally based direct use depending on their geothermometry temperatures and chemical characteristics.

GEOCHEMISTRY OF RWENZORI HOT SPRING WATERS

Vincent Kato1. Dr. Michael Kraml2
1Department of Geological Survey and Mines, Entebbe, Uganda
2 Federal Institute for Geosciences and natural resources

INTRODUCTION

Rwenzori springs refer to hot and cold mineralized springs around Rwenzori Mountains. A chemical sampling campaign was undertaken as part of the GEOTHERM programme, a technical cooperation project between the Government of Uganda and Germany. The geochemical sampling programme was part of the field investigations, which included gravity survey, Transient Electromagnetic (TEM) survey and Schrumberger Sounding. Geological mapping was supplemented by Aster image interpretation.

Geophysical work was focused around Buranga hot springs, on the western side of Rwenzori. However, geochemical sampling was regional in scope, to understand the relationship of the neighboring thermal manifestations to Buranga hot spring system. Work was carried out between 21st February to 5th March 2005. It involved sampling hot spring water and hydrothermal deposits, measuring of surface temperature, conductivity and pH. The samples were to be analyzed for trace and major elements. Geothermal sites sampled included Lake Kitagata, Muhokya, Kibenge, Bugoye, Rwimi, Rwagimba, Nyansimbe, Kagoro, Mumbuga and Kibuku. This report is an integrated field and laboratory studies carried out on Rwenzori hot springs.

GENERAL GEOLOGY

Rwenzori region is a zone of crustal uplift and volcanism as evidenced by quaternary (young) alkaline volcanic centers around Fort Portal and Katwe-Kikorongo. Lithologically, it is made up of banded gneiss, granite and schist. Peaks are made up of amphibolites, hornblende gabbros and metasediments, which make up Stanley Series. The western boundary is made up of banded biotite gneiss. The axis of Rwenzori runs about N30^{o}E. The area is seismically active. The hot springs appear to be structurally controlled by faults and most of them are associated with travertine mounds. Hot spring tufa deposits are reported in some of the explosion craters around Fort Portal (Saka, Kasekere and Nyabusozi) on the eastern side of Rwenzori. Tufa deposits is reported on the northern end of Rwenzori nose, around Kibuku area, at Kikyo and are regarded as field-wide characteristics of Rwenzori thermal springs. Almost all springs are associated with tufa deposits with the exception of Kibenge and Muhokya.

FIELD ACTIVITIES

The fieldwork was carried on between 21st and 5th March 2005 and included chemical sampling of hot water samples, temperature, pH-field and conductivity measurements. Sampling points are shown in figure 1.

Hot springs with flow over 0.5 L/s were preferentially sampled since these were less likely to have been affected by dilution and evaporation (Mohan, 1963). Water samples were collected in a jug (on a rod, at Nyansimbe pool) so that they could be obtained from the center of the spring. Each spring was sampled at its hottest part, which was presumed to be the point where hot water enters the pool. The waters were transferred to a rinsed 100-ml plastic bottle.

The untreated water samples were to be analyzed for pH-lab, SO_4, and bicarbonate. pH was also measured at the time of field collection. Another set of water samples were treated at the time of collection (filtered through 0.4μm filters and acidified with a measured amount of Nitric acid, 1ml of acid per 100ml of water sample). This was to ensure that the analyses represent the chemistry of the thermal waters as closely as possible. This was collected into a rinsed 50-ml polythene bottles and was to be analyzed for chloride, silica and major cations. By bottling the samples at the sampling temperature, errors arising from evaporation were minimized (Mahon, 1961).

RESULTS OF CHEMICAL ANALYSIS

Laboratory analysis was carried out at BGR, Germany. The results are summarized in table 1 below. All samples are near neutral to slightly alkaline.

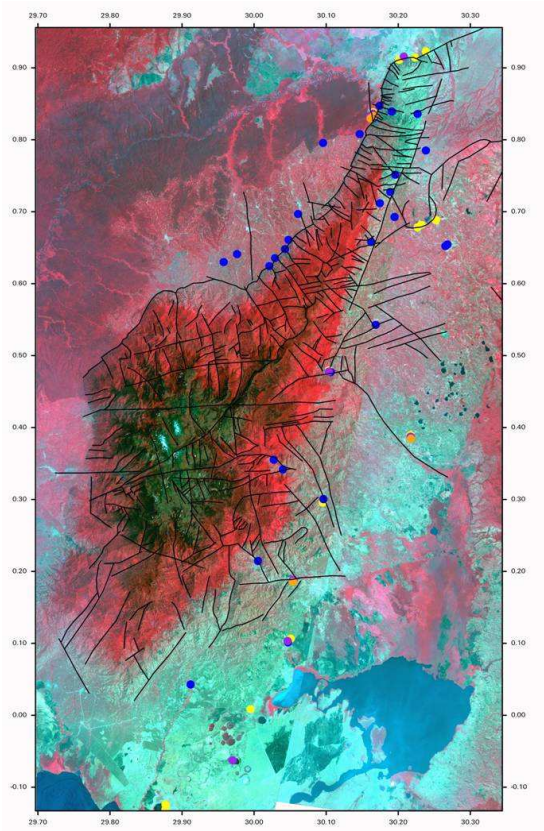

Figure 1: Sampling points of Rwenzori system

Table 1: Chemical composition of Rwenzori hot springs in ppm (mg/kg)

Location	Temp	Ph	Cond	SiO_2	HCO_3^-	Cl^-	SO_4^{2-}	Na^+	K^+	Ca^{2+}	Mg^{2+}	Li^+	B	Al	Fe
Mumbuga	94	8.7	17900	70	2850	3133	3222	4716	166	6.24	1.94	1.2	14.8	0.015	0.02
Nyansimbe	75.4	8.4	22400	77.4	3630	4019	4186	5991	218	6.55	1.97	1.51	18.1	0.02	0.02
Kagoro	88	8.6	21000	76.6	3360	3735	3842	5561	199	7.01	1.97	1.41	17.2	0.71	0.91
Well-1	62	8.3	21500	73.5	3440	3839	4001	5738	209	7.11	1.77	1.45	17.5	0.031	0.16
L. Kitagata	64	8.7	31300	81.7	4160	2447	12959	9237	634	2.41	0.86	0.048	3.22	0.02	0.02
Kibenge	42.5	8.2	3580	44.5	98	585	894	550	24.3	226	6.4	0.221	1.89	0.163	0.3
Muhokya	41	8.2	8460	50.9	143	460	1075	586	18.8	206	13.1	0.062	1.42	0.039	1.05
Rwagimba	69	8.1	6390	62.5	800	838	1468	1480	41.6	74.1	5.38	0.452	2.77	0.01	0.48
Rwimi-1	25.9	7.2	3880	92.7	2100	232	693	424	60.7	380	198	0.071	0.94	0.154	6.42
Rwimi-2	24.6	7.1	3640	84.8	2020	189	523	356	56.8	361	181	0.056	0.73	0.031	6.25

ION BALANCE

Ion balance was carried out to assess the quality of chemical analysis. This involved comparing the sum of the molal concentration of the major positively charged species times their valence (charge) against the sum of the molal concentration of the major negatively charged species. Prior to carrying out ion balance, chemical data was converted from ppm (mg/kg) to molal units. Again for convenience in determining the ion balance, molal units were converted to millimolal units (1 mole = 1000 millimoles).

Table 2: Chemical analysis in millimolal units

Location	HCO_3^-	Cl^-	SO_4^{2-}	Na^+	K^+	Ca^{2+}	Mg^{2+}	Δ charge %
Mumbuga	46.7	88.3	33.56	205	4.2	0.16	0.07	+1.83
Nyansimbe	59.5	113.2	43.6	260	5.6	0.16	0.08	+1.17
Kagoro	55.1	105.2	40.02	241	5.1	0.17	0.08	+1.29
Well-1	56.4	108.1	41.7	249.5	5.3	0.18	0.07	+1.47
L. Kitagata	68.2	68.9	134.9	402	16.2	0.06	0.04	+1.39
Kibenge	1.61	16.5	9.3	24	0.6	5.65	0.26	-0.39
Muhokya	2.34	12.9	11.2	25.5	0.5	5.15	0.54	-0.34
Rwagimba	13.1	23.6	15.3	64	1.06	1.85	0.22	+1.39
Rwimi-1	34.4	6.54	7.2	18	1.5	9.5	8.15	-0.49
Rwimi-2	33.1	5.32	5.4	15.5	1.5	9.03	7.44	+0.72

A reasonably adequate ion balance is good within 5%. According to table 2 above, all sample analysis fall within the acceptable range, that is below 5%. Hence, the analysis was generally good and of adequate quality. The results compares reasonably with earlier analysis (Sharma, 1971, Armannsson, 1994).

CLASSIFICATION OF WATERS USING RELATIVE CL-, SO42- & HCO3-

Chloride, sulphate and bicarbonate are the three major and most frequently analysed anions of thermal waters. These are used to characterize the thermal water and ascertain its evolutionary trend processes. The chloride and sulphate contents of Rwimi, Rwagimba, Mumbuga, Nyansimbe, Kagoro, Kibenge and Muhokya exhibit a high degree of co-variance (R^2 = 0.9935). Lake Kitagata is excluded in this compositional range and possibly belongs to a different geothermal reservoir.

The highest concentration of chloride and sulphate (Mumbuga, Nyansimbe, well-1 and Kagoro) are possibly influenced by magmatic HCl and SO_2 input. The lowest values at Rwagimba, Rwimi, Kibenge and Muhokya are reflecting little input from lithological sources (evaporates, sulphate-enriched) for these parameters. Mumbuga, Nyansimbe, Well-1 and Kagoro waters are chemically similar implying they are emanating from the same source and along the same migratory path. In their pure form, the various water types plot close to corners or along the axes of Cl-SO_4-HCO_3 ternary plot. **Partial equilibration** and **mixing** among the different water may have given rise to the formation of intermediate / hybrid waters as represented by Buranga hot water samples.

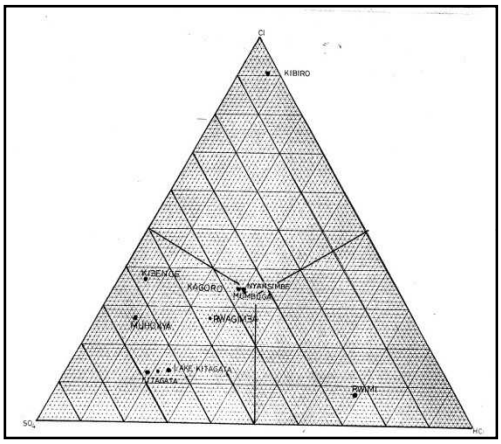

Figure 2: Relative contents of Cl, HCO and SO4 in ppm

Lake Kitagata, slightly alkaline, is characterized by high sulphate content possibly attributed to magmatic SO_2 input. The sample has the highest sulphate to chloride ratio possibly attributed to magmatic vapor input. Since it is plotting in the corners or along the axis, it must have been affected by mixing of sulphate waters with some meteoric waters. Sulphate waters sometimes contain appreciable amounts of chloride (>1000ppm Cl) as in case of Lake Kitagata

(2447ppm). The presence of high chloride contents, distinguish magmatic or volcanic sulpahte sources from sulphate waters of steam-heated origin, which have very little chloride content. The source of chloride like sulphate in Lake Kitagata hot water sample is possibly due to absorption of HCl bearing volcanic gas into meteoric water. This is supported by isotopic evidence (IAEA TC-PROJECT UGA/8/003).

Kibenge thermal waters are slightly alkaline with appreciable sulphate contents relative to other major anions. These can be described as **chloride-sulphate** waters, plotting almost on the axis. It appears to be of steam-heated origin rather than volcanic origin. The high magnesium contents might be attributed to mixing with meteoric ground-waters.

Muhokya thermal waters are slightly alkaline and can be classified as **chloride-sulphate** waters. High mg contents might indicate mixing with meteoric waters. It appears to be of steam-heated origin rather than volcanic origin.

Rwagimba thermal waters are slightly alkaline and have more sulphate than chloride and bicarbonate. These **chloride-sulphate** waters are possibly steam-heated waters rather than volcanic in origin.

Rwimi samples are **bicarbonate waters** (CO_2-rich waters) with appreciable amounts of bicarbonate. They have low chloride content and variable sulphate contents. Bicarbonate waters typically form in the marginal / peripheral zone and shallow subsurface region where CO_2 gas is absorbed and steam is condensed into cool ground waters.

RELATIVE NA, KAND MG CONTENTS

According to the ternary plot, Rwimi samples plot close to the Mg corner reflecting their high immaturity. Rwimi samples exhibit higher than equilibration Mg contents (181-198ppm). These are typical of low temperature environments created by the underground absorption of CO_2-rich vapours into meteoric groundwater. It is not justifiable to apply geothermometry on such non-equilibrated waters. Rwimi samples represent solutions affected largely by rock dissolution rather than fluid equilibration.

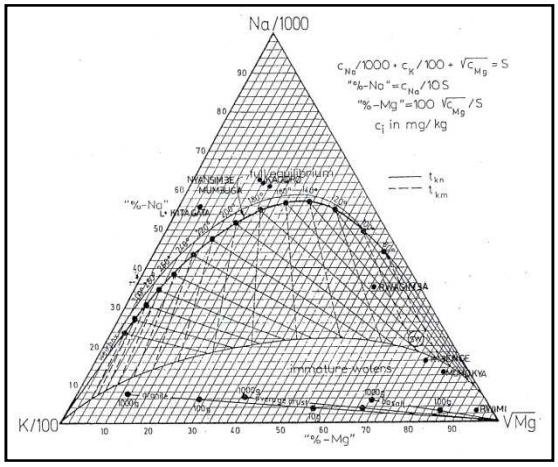

Figure 3: Relative contents of Na, K and Mg, showing dilution / mixing trend towards mg rich waters

Buranga samples plot above the full equilibrium line, possibly indicating boiling / steam loss which might have led to increase in the absolute solute contents.

Rwagimba sample occupy intermediate position reflecting partial attainment of equilibrium with rock at generally low temperatures. Indicated temperatures is between $T_{K\text{-}Na}$ 140-160°C and that of $T_{K\text{-}Mg}$ of 100-120°C, having acquired mg during their rise to lower temperatures without readjustment of K/Na ratios. Lake Kitagata waters plot above the equilibrium line possibly due to steam loss / boiling. Kibenge thermal waters plot on boundary between immature waters and partially equilibrated water, application of geothermometer is not justifiable on such immature waters. Muhokya waters are plotting in the immature zone and application of geothermometer is not justifiable also. All assumed steam-heated waters (Muhokya, Rwimi, Kibenge, Rwagimba) occupy positions close to the Mg corner, reflecting their highly immature state. In their case, application of solute geothermometers, based on assumption of attainment even of only partial equilibrium is not justified. These form end-members water-type.

Thermal waters from Kagoro, Mumbuga, Nyansimbe, Well-1, Rwimi, Muhokya, Kibenge and Rwagimba seem to be highly correlated (R^2=0.9978). Because of non-linear relationships among Na, K and Mg, the square root was taken for Mg contents. This high correlation might be attributed to genetic relationship and might point to single source of these thermal waters and the same migratory path-way, possibly reflect mixing between "dissolved rock" and fully equilibrated waters, obvious from the diagram.

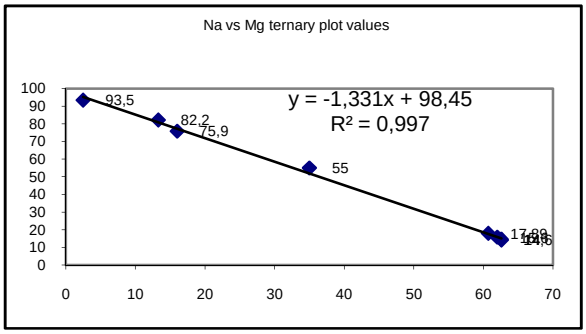

Figure 4: Graph showing sodium values plotted against magnesium values**.**

RELATIVE CL-LI-B CONTENTS

According to the ternary plot (figure 5), all thermal water samples plot close to the Cl corner. Since lithium tend to remain in solution, it is the relative Cl and B contents which are likely to change the B/Cl ratio. Low B/Cl ratio in steam is likely be brought about by addition of more chloride from a magmatic source not from simple rock leaching or from progressive boiling over time, which might have resulted in a low B/Cl ratio in a mature system. This might indicate that all chlorides are supplied after rock dissolution possibly absorption of low B/Cl magmatic vapors. A magma chamber is the most reasonable source of huge quantities of CO_2, B and Li.

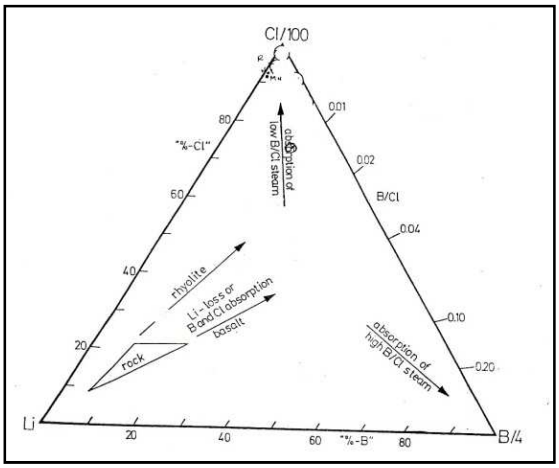

Figure 5: Relative contents of Li, B and Cl

CHEMICAL GEOTHERMOMETRY

Location	Qtz no steam loss	Qtz max steam loss	Na-K (Fournier)	Na-K (Giggenbach)
Mumbuga	118.3	116	140.9	161.4
Nyansimbe	123.4	121.1	143.7	162.7
Kagoro	122.9	120.7	142.3	162.7
Well-1	120.8	118.8	143.8	162.7
L.Kitagata	126.3	123.6	186.2	204.7
Kibenge	96.6	98	155.5	175.4
Muhokya	102.8	103.4	135.9	156.0
Rwagimba	112.6	119.2	128.6	148.2
Rwimi-1	132.2	128.6	249.3	262.0
Rwimi-2	128.5	125.4	260.7	272.1

The results indicated by Na-K geothermometers are not reliable for Rwimi waters, since they contain appreciable quantities of Ca (361-380ppm) and deposit travertine. Such geothermometer are not ideal for cool, CO_2-rich springs like Rwimi and hence results should be used with caution. Kibenge, Muhokya, Rwagimba and Rwimi do not contain reasonable contents of chloride, hence K/Na temperatures are not representative of those of the deeper neutral Cl water. Otherwise they are likely to reflect the lower temperatures (~150°C) typical of environments created by the underground absorption of CO_2-rich vapors into groundwater at the periphery or margins of a system.

RELATIVE PROPORTIONS OF B, CL AND NA

There is an indicated high correlation (R^2=0.9966) between sodium and chloride of thermal waters at Buranga, Rwimi, Muhokya, Kibenge and Rwagimba (Figure 6). This points a possible genetic relationship between these waters possibly influenced by mixing process.

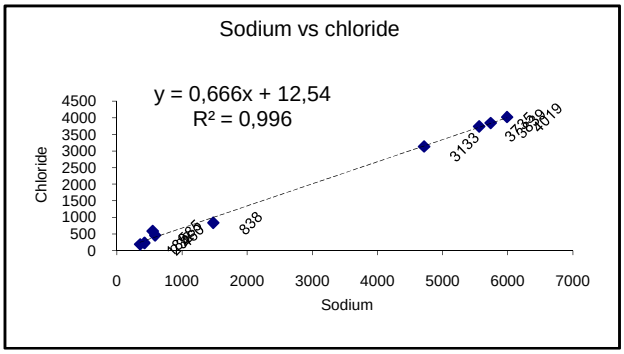

Figure 6: Graph showing chloride conc. (ppm) versus sodium conc. (ppm). Note the near linear relationship

There is a highly correlated linear trend (R^2=0.9976) between chlorine and boron values of Nyansime, Kagoro, Mumbuga, Rwimi, Muhokya, Kibenge and Rwagimba. Again this might point to a genetic relationship between these waters. A high correlation (R^2 = 0.9997) is observed between potassium and chloride, for springs Nyansimbe, Kagoro, Mumbuga, Rwagimba, Muhokya and Kibenge. Rwimi and Lake Kitagata hot springs plot in different compositional field. This correlation possibly points to the different environment, that is sediment starved systems versus sediment-hosted systems. There is a systematic change of K with respect to chloride. Potassium increases in a linear fashion with chloride in the sediment-starved systems, while sediment-hosted systems show high potassium with no systematic trend relative to Cl. The high K/Cl at Lake Kitagata and Rwimi possibly reflect the much greater concentrations of potassium relative to chloride in sediments relative to sediment-starved systems.

The increase in cationic charge from calcium exactly compensates the decrease in charge due to loss of sodium, which is especially evident at high chloride concentrations. This can be demonstrated by plotting Na plus two times Ca (**Na+2Ca**) versus Cl, which gives a highly correlated trend (R^2=0.9988) for springs at Mumbuga, Nyansimbe, Kagoro, Rwagimba, Muhokya and Kibenge. Rwimi and Lake Kitagata are out of the compositional range again due to anomalous Ca and K contents respectively.

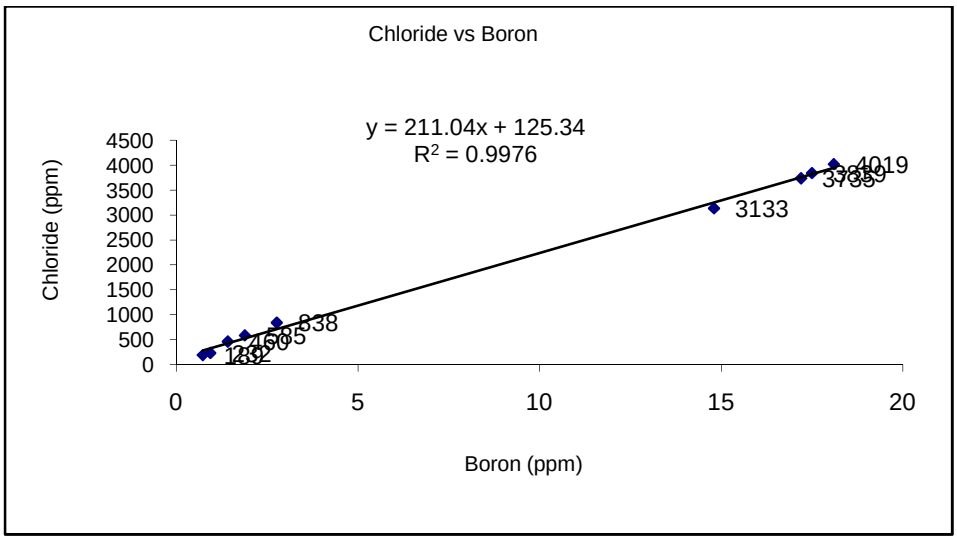

Figure 7: Graph showing chloride conc.(ppm) versus Boron conc. (ppm)

SALINITY ANALYSIS

A plot of bromine versus chlorine for waters of Nyansimbe, Mumbuga, Kagoro, Rwagimba, Rwimi, Muhokya and Kibenge reveal a high correlation (R^2=0.9976). This highly correlated linear trend points a possible genetic relationship possibly influenced by mixing and partial equilibration. The Br/Cl ratios fall in a range 0.00451 to 0.01120. This is somewhat higher than seawater (typically 0.00347). Br/Cl increased ratios might be due to increased Br or reduced Cl contents. The latter seems more probable. This may suggest that chloride salinity may be largely derived from silicate rock-water interaction / fluid inclusion leaching, rather than from modified seawater or from evaporates at depth. It points to a non-marine, non-evaporitic source of bromide and chloride (Andreasen & Fleck, 1997).

Sometimes higher Br/Cl ratios occur at lower chloride concentration due to analytical errors (i.e. greater relative error in Br determination in low salinity waters). However, for Buranga hot springs, the high salinity and presence of predominant sulphate may suggest that magmatic or volcanic sources are of major importance. This has been indicated by isotopic studies using strontium isotope $^{87}Sr/^{86}Sr$ (IAEA TC-PROJECT UGA/8/003). Sediment starved hot spring system like Kibenge have slightly higher $^{87}Sr/^{86}Sr$ values (0.7342) than in Buranga (0.7195-0.7287).

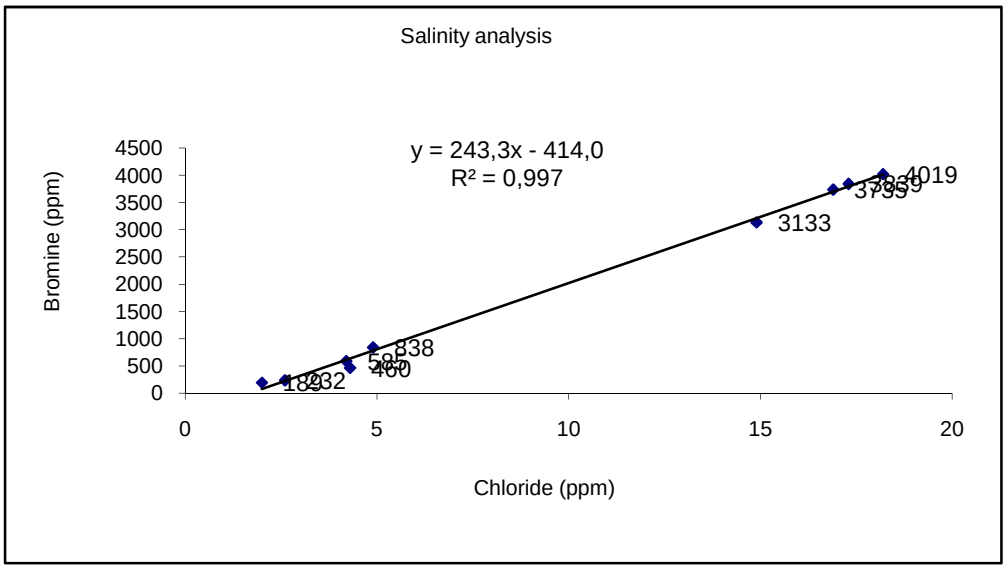

Figure 8: Bromine (ppm) versus Chlorine (ppm)

ISOTOPIC GEOCHEMISTRY

Carbon-13 and Oxygen-18 of travertine and limestone samples were analysed at the Institute of Geological and Nuclear Sciences, in New Zealand. Buranga travertine plot in carbonatite magma field (See figure 3), hence are a hydrothermal equivalent of carbonatite, i.e. the isotopic range of samples indicates magma-derived carbon as the probable origin of the carbon dioxide that dissolved into the fluid from which travertine precipitated.

(All measurements ± 0.1‰)

No.	Locality	$\delta^{13}C_{PDB}(CO_2)$	$\delta^{18}O_{PDB}(CO_2)$
1	Buranga	-3.78	-17.10
2	Buranga	-2.67	-16.04
3	Buranga	-2.54	-15.95
4	Buranga	-3.68	-15.21
5	Katwe	1.41	5.16
6	Katwe	2.87	7.36
7	Muhokya	0.89	-3.27
8	Lincoln carbonate	2.11	-6.55
9	GNS Marble	2.11	-6.55

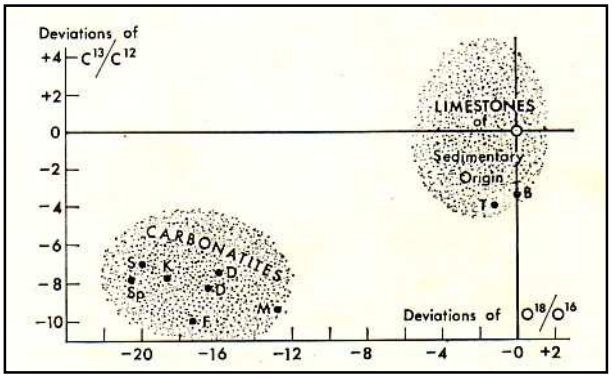

Figure 9: Buranga travertine plot in the carbonatite fields together with samples from Katwe, Mbuga crater, Fort Portal and Sukulu. Bunyrauguru and Muhokya limestone samples plot in the sedimentary field.

The points represent deviations of $^{18}O/^{16}O$ from arbitrary standard limestone (marked 0), plotted against the corresponding deviations of $^{13}C/^{12}C$, and fall into well-separated fields (shaded) for magmatic carbon and thermally derived sedimentary carbon respectively (Holmes, 1964). According to Allard et al, 1977; Allard, 1979; Rollinson, 1993, evidence for significant magmatic carbon input to a system should have a value of –4 to 8‰. Isotopic evidence favors meteoric recharge from Mt Rwenzori (Armannsson, 1994; Kato, 2000; IAEA TC-PROJECT UGA/8/003) possibly from melt water.

D/H values of geothermal waters are not controlled by the exchange processes, because the rocks contain so little initial hydrogen compared to the amounts of H_2O typically involved. Instead, the δD values remain constant. If it is assumed that Rwenzori thermal springs are genetically related, their δD values would reasonably compare, save for some processes due to no-equilibration evaporation of steam at temperatures of 70-90°C (Giggenbach, 1978). Kibenge δD values (-20.2) compares reasonably with Kagoro values (-19.4) according to IAEA TC-PROJECT UGA/8/003 (2003). The hot springs are nearly identical in deuterium content and indicate no appreciable oxygen shift that is observed in some high-temperature hot-springs. According to deuterium map, Buranga hot springs have deuterium values similar to Mubuku river, indicating a possible recharge from the glaciers.

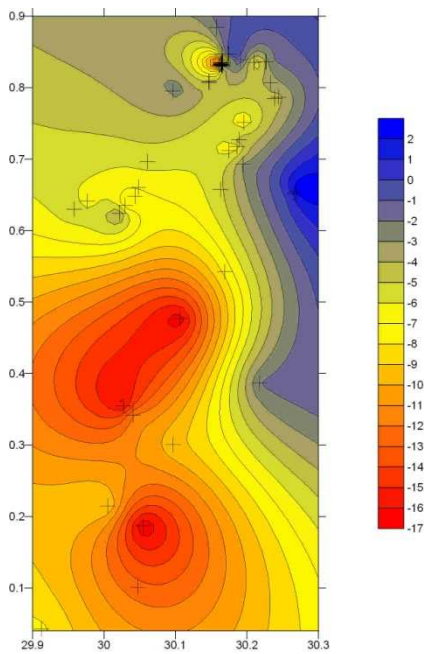

Deuterium map of Rwenzori springs

According to isotope geochemistry, Kibenge and Buranga thermal waters have no detectable tritium contents (IAEA TC-PROJECT UGA/8/003, 2003). These springs do not prove entry of meteoric water of high T content and very short subsurface travel time since they escape isotopic detection. Possibly, the greatly dominant component of these

thermal waters is concluded to be of meteoric origin (Armannsson, 1994; Kato, 2000; IAEA TC-PROJECT UGA/8/003, 2003) with an age of at least more than 88 years since isolation from direct contact with the atmosphere.

Thermal waters are on both sides of Rwenzori block and Rwenzori is made of crystalline basement rocks (granite / granitic gneiss, schist, amphibolite gneiss). These rocks are not sufficiently permeable to form a natural hydrothermal reservoir, hence the only plausible permeable structures indicated are faults or fractures. The geothermal reservoir is most likely to be fracture controlled not porosity controlled. Most of the Rwenzori rocks are not highly porous and thus hot water is likely to be located primarily in fractures. It is important to locate the orientation of the most important hot-water bearing fractures, to be consistent with the regional extension trend. Isotopic studies $^{87}Sr/^{86}Sr$ (IAEA TC-PROJECT UGA/8/003) point to water-rock interaction with granitic gneiss for Buranga thermal waters. Felsic type of igneous rocks (gneiss, granitic gneiss) tend to have high mean florine contents. This is also evidenced in the thermal waters of Buranga, possibly suggesting a fracture-controlled geothermal reservoir in the crystalline basement rocks.

DISCUSSION

According to isotopic evidence, Buranga geothermal system has a magmatic heat source. Since the chemistry of Rwenzori springs (Buranga, Rwimi, Kibenge, Muhokya, Rwagimba) is highly correlated, it might imply that there are genetically related and possibly influenced by partial equilibration and mixing. Lake Kitagata seems to belong to another geothermal system other than the Rwenzori hot spring system. The magma chamber is the most reasonable source of huge quantities of CO_2 discharged at Mulyambuzi cave (Fort Portal), Buranga and Rwimi. As Beall and Box (1993), noted, an increase in contents of CO_2, might be attributed to change in geothermal reservoir pressure, causing open-system flow of CO_2-rich gases into the Rwimi area, from below the geothermal reservoir.

Qualitatively high HCO_3 contents can be taken as an indication for comparatively low temperature system. Since most hot springs (Buranga, Rwimi, Rwagimba, Kibuku, Fort Portal craters) are depositing travertine, these are likely to be outflows of a system possibly in the Rwenzori mountain. This system is likely to be fracture controlled in a steep terrain of Rwenzori. This might be explained by an interaction of CO_2-rich waters with rock at shallow levels. Such CO_2-charged waters are formed by under-ground absorption of vapors separated from deeper Cl water into cooler groundwater (Hedenquist, 1990; Lonker et al., 1990). Isenthalpic expansion of steam, separated from a deeper liquid phase, to close to atmospheric pressures, is accompanied by a drop in temperature to about 160°C.

The temperatures of secondary bicarbonate waters formed in this way are therefore in the vicinity range of 150-160°C (Giggenbach, 1978; Cioni et al., 1984; Hedenquist, 1990). According to geothermometry, Buranga, Kibenge, Muhokya and Rwagimba fall in the range 150-160°C (Armannsson, 1994), possibly indicating that these are outflow of a geothermal system of Rwenzori. Travertine occurs at Rwimi, Buranga, Bugoye, Rwagimba, Kibuku, Kikyo and in volcanic craters at Fort Portal (Saka, Kasekere and Nyabusozi). Considering the geographical variation of bicarbonate, silica and chloride contents in Rwenzori hot springs, Buranga hot springs are nearer to the upflow zone than Rwimi, Muhokya, Rwagimba and Kibenge. More work should be concentrated around Buranga hot springs focused on Rwenzori.

Deuterium mapping shows that Buranga hot springs have relatively similar values with water from Mubuku hot springs indicating that glaciers drained by Mubuku are likely to be recharging source for this system.

CONCLUSION

The constancy of ratios as evidenced by high correlation values may indicate that Rwenzori thermal springs have a single geothermal reservoir. Buranga thermal waters cluster an evidence of single source system. Evidence for recharge of meteoric waters points at Rwenzori mountain while a fracture controlled crystalline basement reservoir is indicated by strontium ratio values. Buranga (Nyansimbe, Kagoro and Mumbuga) thermal prospect has impressive surface manifestations, occurring in steep mountain terrain hence could easily be mistaken for up flows of a reservoir system. The upflow system surface manifestation is still elusive. This is very common with high temperature systems in steep mountain terrain often associated with concealed outflow structures.

The springs indicate a low temperature system, possibly an outflow as indicated by low SiO_2 contents and high bicarbonates. The high salinity at Buranga could be explained by magmatic input not simple leaching of rocks. Contribution of magma-derived carbon to Buranga geothermal system has been indicated by carbon-13 vs Oxygen-18 analyses from Buranga, travertine falling between –2.54 to –3.78‰. Surface manifestation at Rwimi (high CO_2 contents) could be explained by magmatic gas contribution in a low-pressure zone. Geochemically, there are a number of chemical trends that differentiate Lake Kitagata from the Rwenzori thermal springs. Rwenzori thermal springs are as a result of different degree of mixing and partial equilibration.

Efforts should be directed to identify crustal magma bodies by means of innovative geophysical studies, including seismic tomography. Seismic-velocity data could give clues about rock type, geologic structures and temperature

beneath surface. Stable isotopes of the Rwenzori hot springs should be studied to investigate further their assumed relationship.

REFERENCES

Armannsson, H., 1994. Geochemical study on three geothermal areas in west and south west Uganda, UNDDSMS UGA/92/002 unpublished report.

Allard, P., 1979, 13C/12C and 34S/32 ratios in magmatic gases from ridge volcanism in Afar: Nature, v.282, p.56-58.

Allard, P., Guern, F. and Sabroux, J.C., 1977, Thermodynamics and isotopic studies in eruptive gases: Geothermics, v5., p.37-40.

Andreasen, D.C., & Fleck, W. B. 1997. Use of bromide: chloride ratios to differentiate potential sources of chloride in a shallow, unconfined aquifer affected by blackish-water intrusion. Hydrogeology Journal 5, No. 2 17-26.

Baertschi, P. 1951. Relative abundance of oxygen and carbon isotopes in carbonate rocks, Nature, 168 p288.

Chang, C. L., 1984. Triangular diagrams for prediction of aquifer chemistry: Geotherm, Res. Council Trans, 8. 373-376.

Cioni et al, 1984. The gas / steam ratio as an indicator of heat transfer at the Solfatara fumaroles, Phlegrean Fields (Italy): Bull. Volcanol. 47, 295-301.

Fournier, R. O., 1981. Application of water geochemistry to geothermal exploration and reservoir engineering. In Rybach, L.& Muffler, L.J.P. (eds), Geothermal systems: principals and case histories, John Wiley and Sons, 109-143.

Giggenbach, W. F., 1978. The isotopic composition of waters from the El Tatio Geothermal Field, Northern Chile, Geochem, Cosmochim, Acta 42. 979-988.

Hedenquist, J. W., 1990. The thermal and geochemical structure of the Broadlands-Ohaki geothermal system, New Zealand: Geothermics 19, 151-185.

Holmes, A., 1956. The ejectamenta of Katwe craters, S.W. Uganda.

Holmes, A., 1964. Principals of physical geology, University of Edinburgh, pp1069-1074, T. Nelson and Sons, London.

IAEA TC-PROJECT UGA/8/003, Terminal Report, Isotope Hydrology for Exploring Geothermal Resources, UGA/8/003, Department of Geological Survey and Mines, Uganda.

Kato, V., 2000. Geothermal field studies using stable isotope hydrology: case study in Uganda and Iceland, UNUGTP-IAEA Project UGA/8/003, Report 10.

Table: Rwenzori thermal springs field description.

Spring/pool No	UTM Coordinates	Location	Geologic setting	Description	Field analysis
Mumbuga	0184418E 0092769N	Located at Sempaya, just a few hundred meters on Fort Portal – Bundibugyo road, about 52 km from Fort Portal	The rocks surrounding the springs are mainly alluvial material washed down from Rwenzori.	Spouting hot springs with a large flow rate of about 1.5L/sec, clear water, but some milky water discharge into one of the pool of 2m diameter, temperature range between 41-94°C, moderate to vigorous gas bubbling, strong odor of H_2S, travertine moulds are found all over the place. Conductivity measured was 18.68ms/cm.	Slightly alkaline Gas-mainly CO_2 and H_2S
Nyansimbe pool	0184133E 0092497N	South of Mumbuga spring	The rocks surrounding the springs are mainly alluvial material washed down from Rwenzori.	A circular pool of hot water with a temperature of about 75°C, measuring 5 meters deep and about 30 meters in diameter. It reported that the base is about 60 m inferring a conical shaped body of hot water. Slight gas bubbling, some travertine deposits covering the pool of water,	Slightly alkaline Gas-mainly CO_2 and H_2S
Kagoro	0183950E 0092324N	South of Nyansimbe pool	The rocks surrounding the springs are mainly alluvial material washed down from Rwenzori	Temperature of about 84-88°C with a flow of about 0.8l/sec with slight gas discharge, faint H_2S gas smell, travertine deposits forming moulds.	Slightly alkaline Gas-mainly CO_2 and H_2S
Well-1	0184423E 0092288N	Located nearly between Mumbuga and Nyansimbe pool	The rocks surrounding the springs are mainly alluvial material washed down from Rwenzori	Flows ranging from 0.4-0.8l/sec clear hot water with temp 62°C,	Slightly alkaline Gas- mainly CO_2 and H_2S

Katwe-travertine	0820299E 09986260N	Located in the south western crater rims of Lake Katwe explosion crater.	Volcanic rocks possibly laid down in water.	Travertine moulds up to 10 meters high, scattered around the area. Others are included in the water laid tuffs.	No field analysis.
L. Kitagata hot spring	0830639E 9993296N	Located on the crater rims of Lake Kitagata, some seepages reported in the lake	Volcanic tuffs with visible blocks and bombs of crystalline basement rocks.	Clear hot water, Temp 64°C; a faint odor of H_2S. Salt crust deposits are found in the area.	Slightly alkaline , conductivity measured 29.0ms/cm
Kibenge hot spring	0172004E 0021030N	Located on Kasese – Kilembe road just after the junction to Marigerita Hotel	Alluvial material from Rwenzori.	Temp of about 43°C, clear water, in form of a pool, bubbling	Conductivity measured was 3.6ms/cm.
Muhokya	0171201E 0011651N	Located on Mbarara Kasese road just near Muhokya lime works.	Possibly in alluvial materials from Rwenzori.	Temp of about 41°C, clear water, gas bubbles.	Conductivity of 3.5ms/cm
Bugoye	0176634E 0032747N	Near Bugoye Gombolora head quarters.	Weathered Phyllitic schist rocks covered with terraces of travertine. No spring could be located. Possibly it is a cold spring.	Cold clear water was flowing over terraces of travertine. No bubbles were observed. It appears like fossil hydrothermal features. Geothermal glass covers the area.	No analysis
Rwagimba	0177588E 0053078N	Located in Rwenzori mountains along Rwagimba valley. You branch off at Kibito.	Crystalline granite gneiss of Rwenzori.	Hot clear water, with observable travertine, gas bubbles, reddish iron stains, with a maximum surface temp of 69^{0}C.	Slightly alkaline.
Rwimi (a)	0190150E 0042846N	Located in the land of Mr. Yozefu Buhanga, near Rwimi Town on Fort Portal-Kasese road.	No observable outcrops.	Cold water issuing with vigorous bubbling. Tem p recorded was 25.9^{o}C from a pool 5 x 2.5 m, iron oxides visible, reported to be used for healing diseases.	Near neutral with carbon dioxide bubbling
Rwimmi (b)	0190206E 0043062N	Just a few meters from Rwimi (a)	No observable outcrops	Travertine mould standing about 1.5m high, clear water flowing from the base of mould, temperature 24.6^{o}C, conductivity was 3.8ms/cm, iron oxide residues, few gas bubbles not as vigorous as in Rwimmi (a)	Near neutral with carbon dioxide bubbling.

ISOTOPIC DETERMINATIONS OF BURANGA AND KATWE TRAVERTINE DEPOSITS, UGANDA

Vincent Kato
Department of Geological Survey and Mines
Entebbe, Uganda

INTRODUCTION.

The report is a result of preliminary interpretation made on isotopic data as part of the GEOTHERM programme between BGR and DGSM. Isotopic determination was carried out on travertine samples from Buranga and Katwe to determine the likely source of heat being mined by Buranga and Katwe geothermal systems. The exercise was to determine whether there is any magmatic carbon input in the fluids or it was lacustrine carbonates / organic sedimentary rocks. Limestone (lacustrine origin) from Muhokya was also sampled for comparison purposes. Trace element analysis was also carried out on these samples to supplement the isotopic determination. Isotopic determination of $\delta^{18}O$ and $\delta^{13}C$ was carried out at the Institute of Geological and Nuclear Sciences Limited in New Zealand (Stable Isotope Laboratory) while trace analysis was carried out at Act lab Ultrace in Canada.

CARBONATITE AROUND BURANGA.

Since there is volcanic activity within the area (Fort Portal and Rusekere Volcanic fields, a magma body inferred north of the hot spring), the heat source might be a buried hot magma body related to young igneous rocks in the area. Toro-Ankole explosive eruptions began in Upper Pleistocene and stopped about 4,000 years ago. The volcanic field is small covering about 50 square miles and contains 49 undoubted volcanoes which are, however, much smaller than those of other fields (Nixon, 1969). The diameter of the crater rims is usually between 45m and 183m. The volcanoes lie along linear N.W. trending zones with steeper inner slope (mean angle of 33°) than the outer slope (Nixon, 1969). The tuffs are very recent and notably at Kalyango crater near Nyakasura, there are lavas with a high carbonate content with very little SiO_2 and alkalis.

Nixon describes volcanics at Fort Portal as highly carbonate rich ultra basic lavas formed by reactions of sialic rocks with carbonate magma. A magma chamber is the most reasonable source for large quantities of CO_2 observed at Buranga. Reaction between carbonatite magma and crustal rocks not only liberate vast quantities of carbon dioxide but would also produce highly basic and ultrabasic rocks like pyroxenites and peridotites as well as the alkaline rocks. Some of the later would become molten and being highly charged with gases would be readily erupted as a spray of lapili or vesicular lavas. The lavas in Fort Portal and Rusekere are carbonitic (Holmes, 1964, Dixon and Morton, 1967). Reaction between carbonatite magma and crustal rocks would only liberate vast quantities of CO_2 but would also produce highly basic and ultra basic rocks as well as alkaline rocks observed around Fort Portal and Rusekere volcanic fields.

PREVIOUS STUDIES

According to Holmes (1964) Lava flows are rare except from the isolated volcano of Katunga in the south and from the clustered volcanoes of Fort Portal in the north.

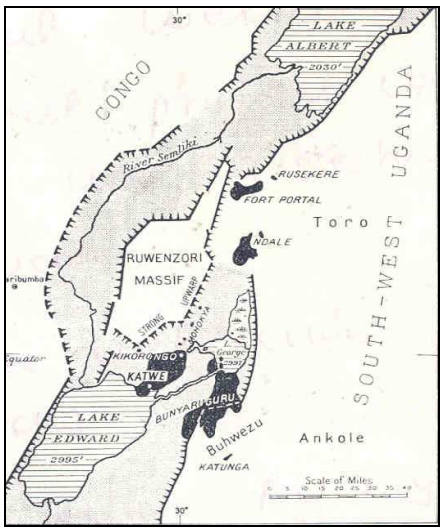

Figure 1: Map of part of the western Rift valley, showing the massif of Rwenzori and adjoining volcanic areas (black) after Holmes (1964).

Isotopic determinations made for Holmes by P. Baertschi show that travertine recently deposited from Hot springs around Lake Katwe is a hydrothermal equivalent of carbonatite magma. As shown by the data in figure below, ordinary limestone contain appreciably higher proportions of the isotopes ^{18}O and ^{13}C than carbonatites. Doubtful cases, such as Katwe Travertine (derived from Carbonatite) and some of the ejected blocks from craters in the Bunyaruguru field (sedimentary origin) were settled by isotopic analysis (Holmes, 1964).

Figure 2: Katwe travertine in background

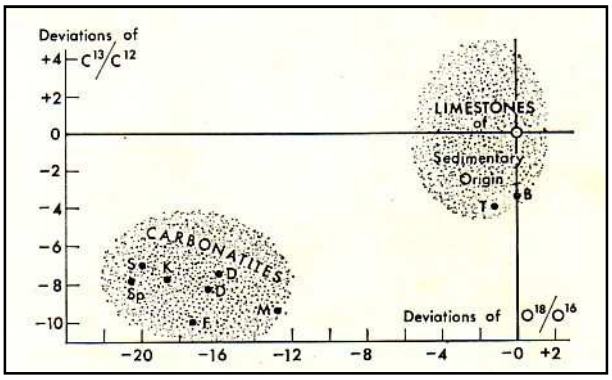

Figure 3: Isotopic determinations by P. Baertschi, abstracted from (Holmes, 1964)

The points representing deviations of $^{18}O/^{16}O$ from arbitrary standard limestone (marked 0), plotted against the corresponding deviations of $^{13}C/^{12}C$, fall into well-separated fields (shaded) for carbonatites and sedimentary carbonate rocks respectively (Holmes, 1964).

The travertine K from Lake Katwe falls within the carbonatite field, while an ejected block, B, from one of the Bunyaruguru craters falls within the sedimentary field. Similarly, Sp from the Spitzkop alkaline complex in the Bushveld South Africa can clearly be distinguished as a carbonatite from the sedimentary limestone, T, from the Transvaal System, with which it was formerly identified. The other carbonatites are D, dykes from the Pretoria Diamond Mine, South Africa, F, lava from the Fort Portal volcanic area, M, carbonatite lava from Mbuga crater, Katwe-Kikorongo volcanic area and S, carbonatite core from Sukulu volcano, eastern Uganda (Homes, 1964).

It is reported that hot waters from Buranga have trace values of tritium (IAEA TC-PROJECT UGA/8/003), which escape isotopic detection. This may indicate that the waters are older than 60 years (prebomb tritium values) or there was mixing of meteoric waters with higher tritium values and old connate waters with low tritium values to produce a hybrid, which could reasonably escape isotopic detection (diluted beyond isotopic recognition).

Isotopic evidence favors recharge of meteoric waters. The hot spring waters have different deuterium content from the spring waters in the area which might indicate the cold spring waters are not the source of recharge, but isotopically lighter meteoric waters possibly from the towering Rwenzori mountains (Kato, 2000). However, they plot on meteoric

line with hardly any major oxygen shift commonly observed in high temperature hot spring systems. This might imply there was no exchange of oxygen between circulating meteoric cold waters and silicate minerals that are being hydrothermally altered or possibly it might be related to high meteoric water flow and good permeable structures. Another possible explanation might be direct near surface dilution of the deep thermal chloride water by huge quantities of surface meteoric waters.

RECENT STUDY

The results in table 1 were analysed at the Institute of Geological and Nuclear Sciences, in New Zealand under the **GEOTHERM** programme. According to figure 3, Buranga travertine deposits plot in a zone of carbonatite magma, hence are a hydrothermal equivalent of carbonatite, i.e. the isotopic range of samples indicates a magmatic origin of the carbon dioxide that dissolved into the fluid from which travertine precipitated.

Table 1: Stable isotope results

(All measurements ± 0.1‰)

No.	Locality	$\delta^{13}C_{PDB}(CO_2)$	$\delta^{18}O_{PDB}(CO_2)$
1	Buranga	-3.78	-17.10
2	Buranga	-2.67	-16.04
3	Buranga	-2.54	-15.95
4	Buranga	-3.68	-15.21
5	Katwe	1.41	5.16
6	Katwe	2.87	7.36
7	Muhokya	0.89	-3.27
8	Lincoln carbonate	2.11	-6.55
9	GNS Marble	2.11	-6.55

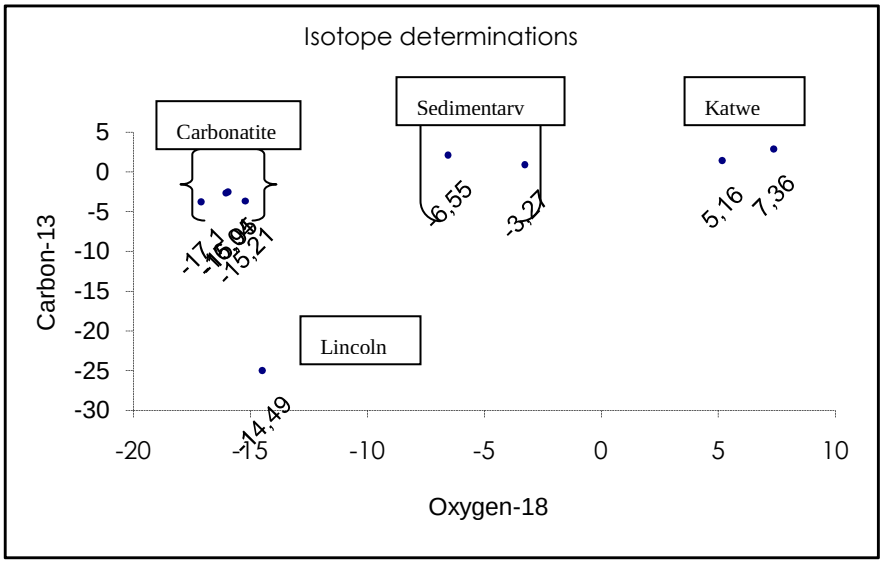

Figure 4: Samples from Buranga plot in the carbonatite field, while those from Muhokya plot in a sedimentary field. Samples from Katwe exhibit appreciably higher proportions of the isotopes oxygen-18 and carbon-13.

Muhokya limestone, a known fresh water lacustrine limestone deposits (figure 5) plots in a sedimentary limestone deposit (figure 4).

Figure 5: Muhokya fresh water lacustrine limestone deposit

Previous studies by Holmes (1964) indicated that travertine deposit from Lake Katwe falls within the carbonatite field. However, the recent analysis showed that Lake Katwe travertine was highly enriched in $\delta^{18}O$ and $\delta^{13}C$. It is ordinary limestone that contains appreciably higher proportions of the isotopes ^{18}O and ^{13}C than those derived from carbonatite (Holmes, 1964). This becomes an anomalous case, which needs further detailed study.

This study also reveals a marked difference between isotopic constitution of the Sr in Buranga travertine and that in limestone of sedimentary origin (Muhokya limestone). Once again Katwe sample had appreciably higher proportions of Sr, possibly being a reworked sample, which was found in cross-bedded tuffs of Katwe crater. Baertschi's results (1964) confirmed the marked difference between the isotopic constitution of the Sr in carbonatites and that in limestone of sedimentary origin.

CONCLUSION

Buranga travertine is derived from carbonatite according to isotopic range of samples. This points to a magmatic carbon dioxide (CO_2) input and infers a more recent intrusion as a likely source of heat that is being mined by Buranga geothermal field. This can be confirmed or disapproved by examining $^{3}He/^{4}He$ ratios in the Buranga geothermal fluids. Also $\delta^{34}S$ in H_2S can be applied to prove an igneous source of sulphur in Buranga geothermal field.

Muhokya limestone turned out, as expected, to be of sedimentary origin. Lake Katwe samples contained appreciably higher proportions of the isotopes ^{18}O and ^{13}O higher than the carbonatite varieties. This is contrary to what Holmes (1964) had found out. Isotopic determination made for Holmes by P. Baertsch showed that Lake Katwe travertine is a hydrothermal equivalent of a carbonatite magma falling within the carbonatite field (Holmes, 1964, pp1072). This needs further investigations. It is also likely that Holmes (1964) sampled moulds and pinnacles of travertine recently deposited from hot springs around Lake Katwe. The sample collected during GEOTHERM programme was probably from reworked seams of tufa interbedded with *cross-bedded* volcanic tuffs.

Isotopic evidence favors recharge of meteoric waters to Buranga geothermal system instead of connate or metamorphic waters. It is reported that hot waters from Buranga have trace values of tritium, which escape isotopic detection. This may indicate that the waters are older than 60 years (prebomb tritium values) or there was mixing of meteoric waters with higher tritium values and old waters with low tritium values to produce a hybrid, which could reasonably escape isotopic detection (diluted beyond isotopic recognition).

REFERENCES CITED.

Baertschi, P., 1964. Isotopic determinations of limestone.

Holmes, A., 1964. Principals of physical geology, University of Edinburgh, pp1069-1074, T. Nelson and Sons, London.

IAEA TC-PROJECT UGA/8/003, 2003. Terminal Report "Isotope hydrology for exploring geothermal resources", UGA/8/003.

Logatchev et al. 1972. East African Rift development, Tectonophysics, Elsevier Publishing Company, Amsterdam, The Netherlands.

Nixon, P. H., 1968. Notes on volcanicity in the western rift in Uganda, unpublished report, Geological Survey and Mines Department, Entebbe, Uganda.

Nixon, P. H., 1969. The carbonatites lavas and tuffs near Fort Portal, western Uganda, unpublished report, Geological Survey and Mines Department, Entebbe, Uganda.

Nixon, P. H., 1967. The geology of the Fort Portal and Kasekere volcanic fields, unpublished report, Geological Survey and Mines Department, Entebbe, Uganda.

Von Knorring, O., and DU Bois, C. G. B., 1961.Carbonatite lava from Fort Portal area in Western Uganda, Nature, vol. 192, pp1064-5.

WATER ISOTOPE GEOCHEMISTRY AS TOOLS FOR THE EXPLORATION OF A LOW-ENTHALPY COMPLEX RESERVOIR: THE CASE OF THE GEOTHERMAL FIELD OF HAINAUT (BELGIUM – NW EUROPE)

Luciane Licour
UMons – Faculté Polytechnique, Service de Géologie Fondamentale et Appliquée, Place du Parc, 20, 7000 Mons, Belgique – luciane.licour@umons.ac.be

Keywords: geochemistry – isotopes – karstic reservoir – low enthalpy – Belgium

INTRODUCTION

The geothermal reservoir of Hainaut is a mainly carbonated fissured and karstic aquifer, composed by Lower Carboniferous limestone and dolostone. It is located in the Mons region (see Figure 1), near the French border.

Figure 1 : Localization of the geothermal field of Hainaut

This geothermal resource was first discovered in 1976 thanks to a geological exploration borehole in Saint-Ghislain (Delmer, 1977). It encountered massive layers of anhydrite in the Upper and Middle Visean carbonate, overlying a thick productive layer of karstic breccias at 2.500 m deep. This borehole, that was turned into a production well ten years later, is the starting point of a district heating system. It gives 73°C hot water at an artesian flow rate of 100 m³/h.

Two other wells were drilled short after the Saint-Ghislain well, in Douvrain and Ghlin, a few kilometers North and North-East. The first one is exploited for heating buildings and sanitary water of a nearby hospital. The second one is still inactive. These two wells produce respectively 67°C and 71°C water, at 1.370 m and 1.575 m deep, from Upper Visean breccia. The flow is artesian as well as in Saint-Ghislain, and reaches the same value (100 m³/h). Another geothermal well drilled in 1985 in Condé (France), a few kilometers off the border, produced water at 29°C from 1.240 m deep, far from the expected temperature of 50°C. This heterogeneous temperature distribution demonstrates the necessity of investigating flow patterns in the deep reservoir before any new exploitation prospect.

Presently, the exploitation scheme of the reservoir is extremely simple. The two exploited wells draw water from the depths, use heat in a serie of heating applications, and then discharge cooled water to the hydrographic networks, thanks to its low salinity (less than 2g/l). Recent development programs involve present networks extension and new drilling works. Further investigations have to be led in the aim of avoiding other failure as it occurred in Condé and predicting the limitations of the single-well technique, amongst others.

The reservoir is thought to be recharged from infiltrating meteoric waters in the outcropping area. It has no natural exsurgence, except a few springs showing anomalies in temperature and/or chemical content. In the aim of assessing the influence of deep water on shallow water characteristics an extensive study has been made to gather chemical and isotopic data on both deep and shallow waters of this aquifer.

Figure 2 : Reservoir lithostratigraphy

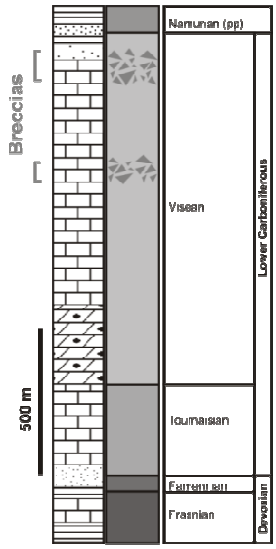

GEOLOGY OF THE GEOTHERMAL RESERVOIR OF HAINAUT

The rocks composing the geothermal aquifer are mainly Lower Carfoniferous carbonates. These strata outcrop at the North of the geothermal exploitation area, and the lithostratigraphical sequence is quite well known. Figure 2 gives a schematic log of the aquifer formations, as they have been described in Doremus and Hennebert (1995), and Hennebert (1999).

The aquifer includes Famennian and Upper Frasnian permeable strata. These formations show different lithologies, including sandstones and thin

shale layers. Tournaisian rocks are mainly limestones. Visean strata often show dolostones in the lower part, then limestones containing several breccia layers. Phtanites are the uppermost rocks considered that are part of the aquifer.

In the Mons region, the aquifer strata have an E-W direction and show a little dip of 10 to 15 degrees Southward. They can be found under Meso-Cenozoïc formations of the structure called “Mons Basin” and Pennsylvanian coal-bearing rocks that were intensively mined during the last two centuries. Figure 3 illustrates the geological context of the geothermal reservoir.

Figure 3 : Geological map and schematic cross-section of the exploited area

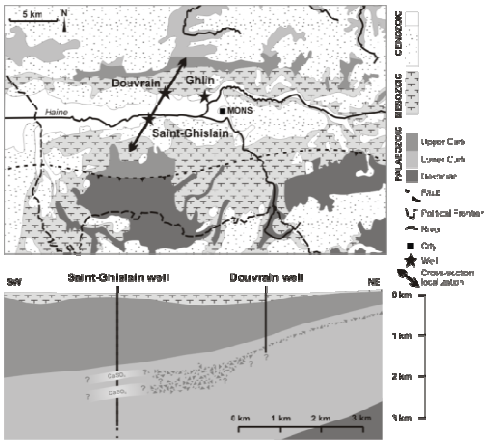

Palaeozoïc formations are shaped by Hercynian orogeny. The results of this influence are represented on figure 4. Palaeozoïc strata are divided in several tectonic units. The Ardennes Allochton overlays the Para-autochton unit, composed by Carboniferous and Devonian formations. The Para-autochton lies on the Cambro-Silurian autochton Brabant Massif.

Figure 4 : Schematic North-South cross-section

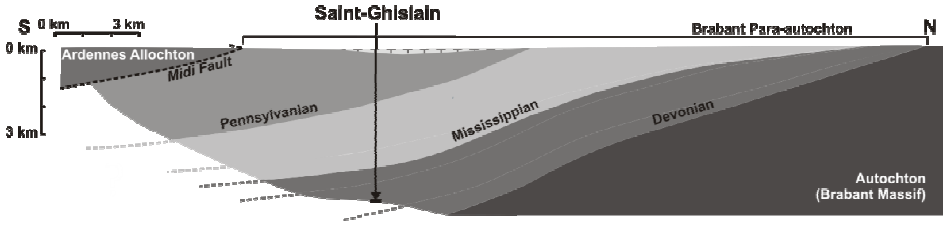

Hercynian tectonic only left rare traces on the reservoir strata, which show few faults and folds, but the overlying coal-bearing formations of Upper Carboniferous are heavily affected by thrust-faults. The Midi fault is the last of these numerous faults, and separates the Allochton from the Para-autochton unit.

The opening of the reservoir to meteoric waters is supposed to have taken place in Late Jurassic/Early Cretaceous times and to be related to fracturation of the carbonates under extensional tectonic regime (Quinif *et al.*, 1997). Penetration of fresh waters in the deep massif has induced anhydrite dissolution, which is one of the supposed origins of the basin-shaped top Palaeozoïc surface, where Cretaceous sediments have been conserved in the present Mons Basin (Dupuis and Vandycke, 1989).

The Saint-Ghislain well revealed thick anhydrite layers in Middle and Late Visean series, as described in Groessens *et al.* (1979) (see Figure 5). These anhydrites seem to correspond to breccia layers that appear at the outcrop and in the others geothermal wells of Douvrain and Ghlin. Anhydrite and gypsum pseudomorphs were found in most of these breccias, and indicate the contribution of anhydrite removal to their origin, though they may not be pure collapse breccias and be the result of several phenomena (Rouchy *et al.*, 1993; De Putter *et al.*, 1994).

The productive layer was crossed in Saint-Ghislain at a depth of 2.500 m, under the massive anhydrite strata, in a highly conductive

Figure 5 : Geological succession in the geothermal wells

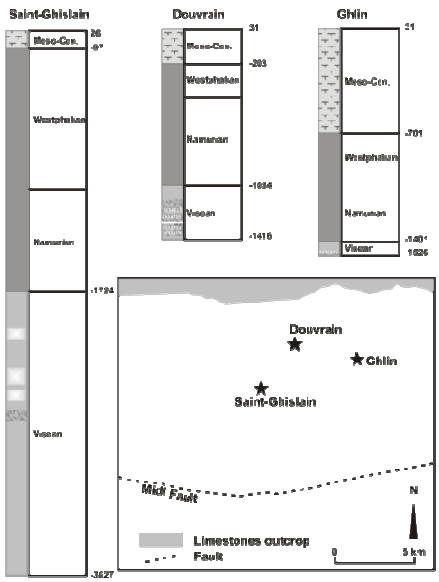

and probably karstified breccia. In Douvrain and Ghlin, large fissures in Upper Visean breccia give most of the hot water flow. Permeability and breccia layers related to anhydrite dissolution therefore seem strongly linked. On the other hand, natural springs of the Southern margin of the shallow aquifer, than issuing from to Upper and Middle Visean, tend to show temperature exceeding normal (10 – 12 °C), sometimes associated with high sulfate content.

The hypothesis has already been expressed in Delmer *et al.* (1982) that these springs can be influenced by deep water upflow. The investigations described below notably aim in confirming this hypothesis.

DEEP AND SHALLOW WATER GEOCHEMISTRY

Available data on Lower Carboniferous aquifer waters come from two main origins: shallow waters from springs,

Figure 6 : Piper and Schöeller-Berkaloff diagrams for geothermal water

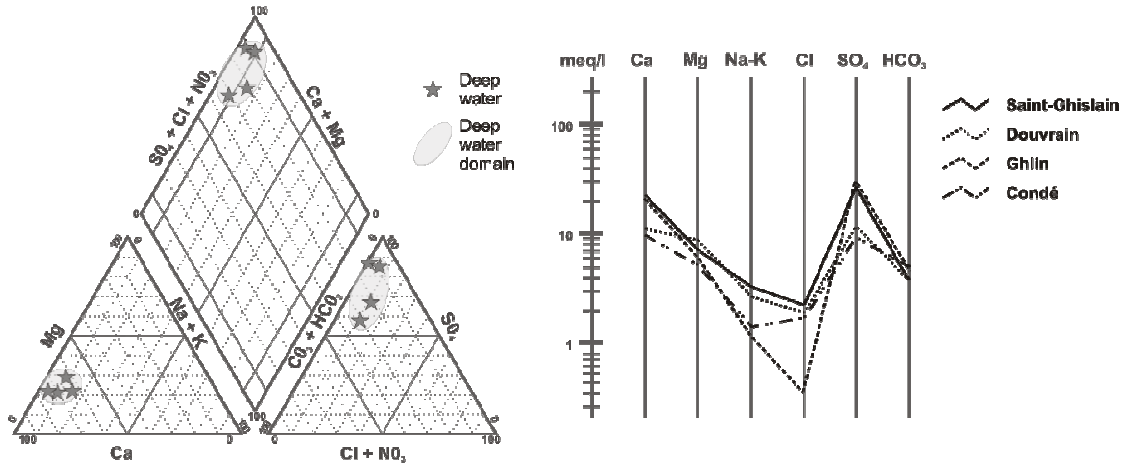

water catchment and quarries pumping on one hand, and, deep waters from the geothermal wells on the other hand.

The two active Hainaut geothermal wells waters are regularly sampled and analyzed since they were set in use. The third well has recently been opened for a several month flow test, and the water chemical content has then been analyzed. For the Condé well, data come from several unpublished reports.

Deep water, as illustrated by Figure 6, have a moderate chemical content, which does not exceed 2 g/l. Anhydrite leaching influence is obvious, with a strong sulfate content.

Shallow water can come from different lithologies: Limestone, dolostone, shaly limestone, sandstone… The calcium and carbonate influence is often well expressed (see Figure 7), with variations in magnesium content depending of the localization of the sampling point in relation with geology. Sulfate content can be quite heterogeneous, from 20 to 120 mg/l, but remains most of the time between 70 and 90 mg/l, which is normal for water issuing from these quite pyrite-rich formations.

Figure 7 : Piper and Schöeller-Berkaloff diagrams for shallow water

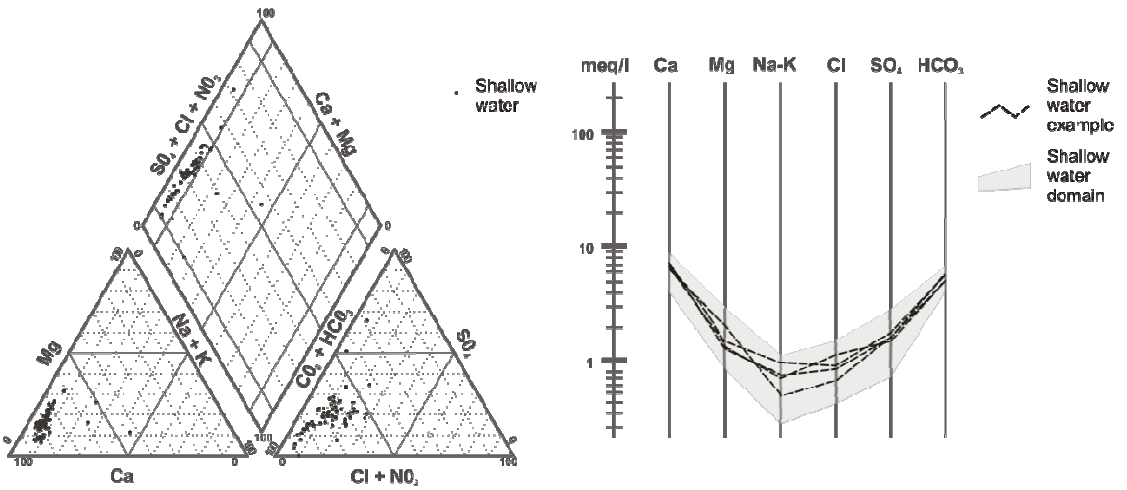

The normal temperature of shallow waters never exceeds 12°C. However, several natural spring mainly located at the Southern margin of the outcropping area show anomalies in temperature (over 13 °C), and/or in sulfate content (over 100 mg/l). These springs are represented on figure 8.

Figure 8 : Localization of Southern margin springs

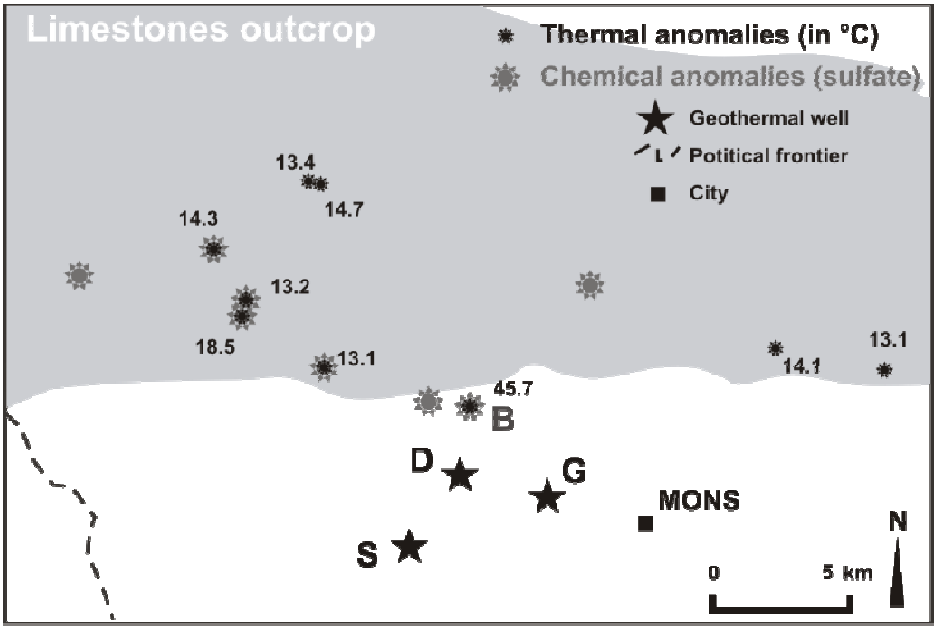

One of these spots show a temperature of more than 45°C, North from Douvrain well (marked "B" on figure 8). It represents the Baudour galleries, drilled at the beginning of the twentieth century by miners to reach coal seams without having to deal with Cretaceous aquifer, located above the coal basin. These galleries had to be abandoned because of hot water coming from fractures in Namurian sandstones. The initial temperature of the water was 53°C, at 300 m deep. Presently, water level is equilibrated with shallow aquifer piezometric level, and its temperature still reaches 45°C.

The springs represented on figure 8 have been sampled in the aim of confirming their chemical content (see Figure 9). Their sulfate content appears to be high, compared with the average content of shallow waters. The origin of this sulfate can be found in several origins. The two main suspected sulfate sources are anhydrite leaching and pyrite oxidation.

Temperature anomalies seem to indicate deep origin for some of these spring waters, and isotope analyses can validate or invalidate this hypothesis. Confirmation would implicate convection loops bringing hot and sulfated water in contact with fresh water at the Southern margin of the reservoir, along Upper Carboniferous impervious sediments,

Figure 9 : Piper and Schöeller-Berkaloff diagrams for anomalic springs

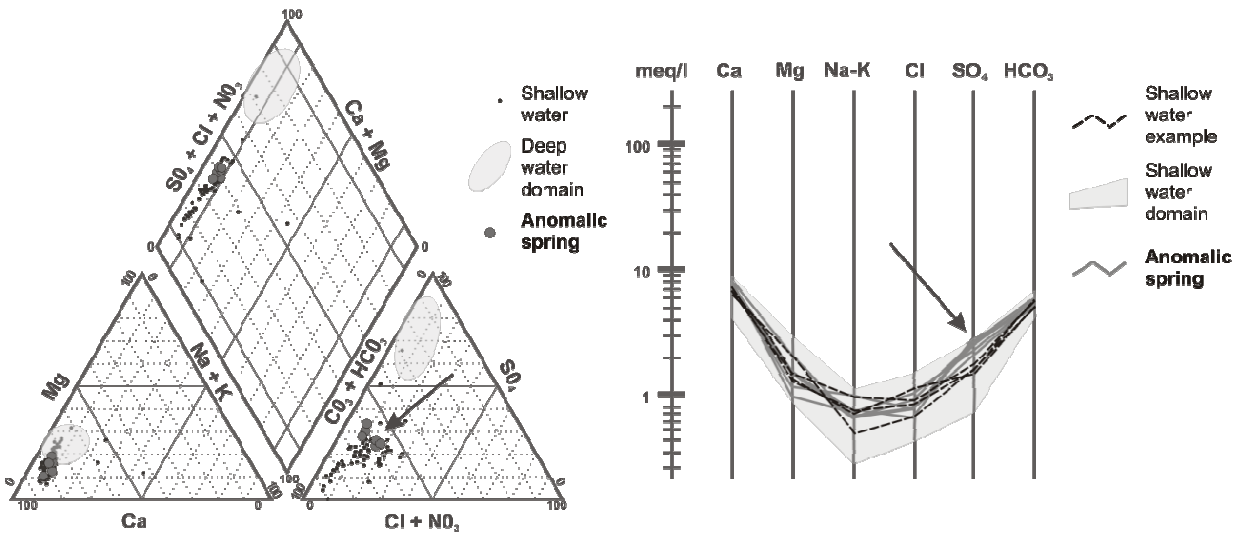

and sometimes reaching surface through them thanks to fractures, as in the Baudour galleries.

ISOTOPE INVESTIGATIONS IN LOWER CARBONIFEROUS RESERVOIR

Sampling points for isotope characterization of both shallow and deep Lower Carboniferous reservoir have been chosen as illustrated on Figure 10. Three main groups are represented :

1- quarry and water catchment pumpings, as reference of regular shallow water,
2- geothermal wells,
3- anomalic springs already mentioned.

The Condé geothermal well is located on this figure in a different grey tone because isotopical data that will be used below come from literature and not from recent sampling and analyses.

Figure 10 : Localization and type of sampling points for isotope analyses

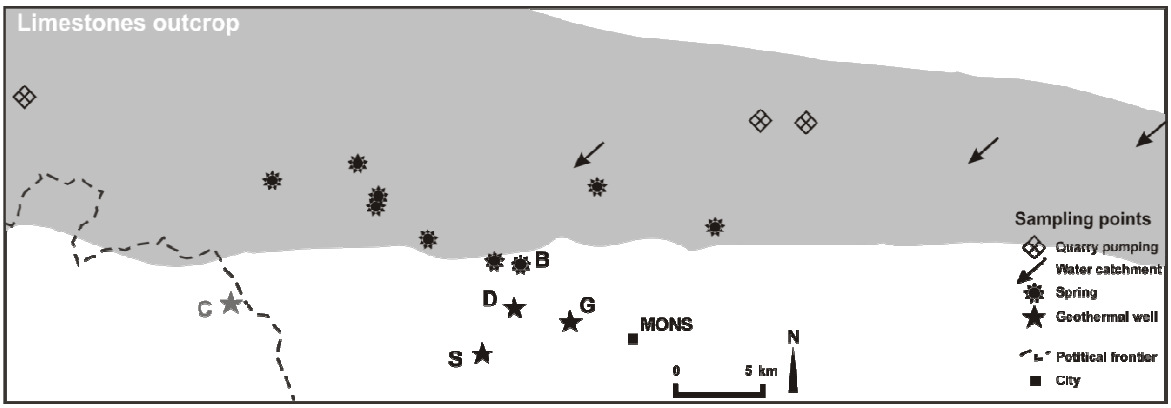

Stable isotopic ratios have been measured for deuterium and ^{18}O in water, ^{13}C of DIC in bicarbonate, and ^{34}S and ^{18}O of sulfates (except for ghlin well and Baudour galleries). The results are given in table 1. ^{14}C content has been analyzed for Saint-Ghislain and Douvrain geothermal waters.

Table 1: Isotopic content of deep and shallow water of the Lower Carboniferous reservoir

Locality	‰	H_2O		HCO_3^-	HCO_3^-	$SO_4^=$		$SO_4^=$	t°
		$\delta^{18}O$	δD	$\delta^{13}C$		$\delta^{34}S$	$\delta^{18}O$		
		± 0.20	± 2	± 0.20	mg/l	± 0.20	± 0.20	mg/l	°C
Saint Ghislain	PG - 01	-8.44	-55.35	-3.11	188.3	17.10	16.70	1316.0	65.5
Douvrain	PG - 02	-8.20	-57.47	-4.85	209.9	17.90	16.30	575.9	55.4
Ghlin	PG - 03	-8.29	-56.20	-3.60	274.7			1402.1	71.0
Condé	PG - 04	-8.50	-54.60	-7.60	303.0	14.80		440.0	27.9
Baudour	B - 01	-7.67	-52.05	-6.90	223.5			660.0	45.7
Stambruges	SAG - 01	-7.04	-49.13	-11.43	289.8	-0.20	9.90	129.8	18.5
Stambruges	SAG - 02	-7.08	-47.81	-12.18	305.0	-5.80	7.50	119.2	13.3
Wadelincourt	SAG - 03	-6.63	-45.81	-13.88	347.7	-4.20	6.10	120.7	11.1
Sirault	SAG - 04	-6.88	-47.86	-13.62	305.0	1.20	8.90	94.3	13.1
Beloeil	SAG - 05	-7.16	-49.93	-12.41	329.4	-6.80	7.20	113.7	14.3
Jurbise	SAG - 06	-7.03	-47.52	-14.11	311.1	-7.10	6.10	103.3	10.9
Feluy	PCCN - 01	-7.03	-47.19	-11.51		-5.10	5.00	718	
Lens	PCCN - 02	-7.07	-46.50	-13.35	340.3	-6.00	6.50	75.1	12.3
Buzet	PCCN - 03	-7.30	-48.96	-13.39	254.1	-3.60	1.70	77.6	10.6
Spy	PCCN - 04	-7.29	-49.01	-12.09	347.0	-3.90	6.80	77.1	12.5
Antoing	PCCN - 05	-6.80	-41.42	-13.76	355.0	-4.40	4.60	183.7	
Soignies	PCCN - 06	-6.67	-45.74	-9.35	327.6	-12.10	-1.20	595.6	
Soignies	PCCN - 07	-7.02	-48.11	-11.60	342.8	-7.00	1.70	85.5	12.1

Deuterium and ^{18}O content in sampled water are represented on Figure 11. The Global Meteoric Water Line (GMWL) according to Craig (1961) and Local Meteoric Water Line (LMWL) are illustrated as well. The d-excess of LMWL has been chosen to fit with experimental results, and is consistent with GNIP data (IAEA, 2001), which give a d-excess value of 8 to 9 in the area.

Figure 11 : δD and $\delta^{18}O$ vs. SMOW

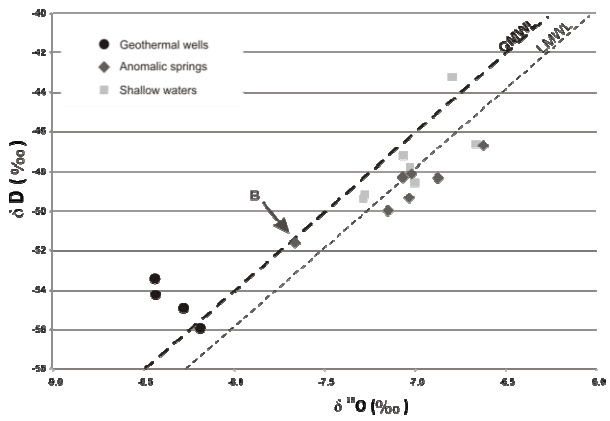

Meteoric origin of deep waters is confirmed. Heavy isotope depletion of deep water compared to that of shallow water suggests infiltration under cold climate.

The "B" marker represents the Baudour galleries. Its intermediate position between geothermal water and shallow water confirms a very strong contribution of deep water. Figure 11 shows that the other springs isotopic contents are too close to that of regular shallow water, forbidding any distinction between them.

$\delta^{13}C$ in bicarbonates is represented on Figure 12, compared to HCO_3^- concentration. DIC in water can come from several origins. Carbon resulting from dissolution of the aquifer carbonated matrix ($\delta^{13}C$ between 0 and +2 ‰) would show isotopic ratios between -0.7 and -2.7 ‰. Atmospheric CO_2 dissolved in water would be characterized by ratios between -15 and -17 ‰, depending on temperature (Mook, 2000).

Figure 12 : $\delta^{13}C$ vs PDB and HCO_3^- concentration

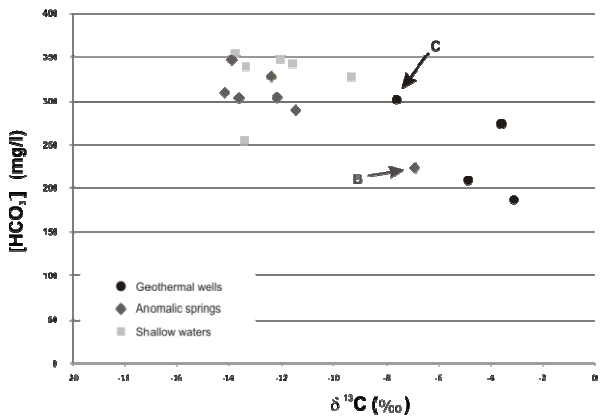

Geothermal water appears to be in equilibrium with carbonated matrix, except for Condé water ("C" marker), of which low ratio suggests mixing with fresh waters. The group of shallow waters shows ratios between -11 and -14 ‰, in good coherence with a situation where water is in contact with both atmosphere and carbonated rocks. Here again, the Baudour water ("B" marker) tends to join geothermal water area, and reveals a strong influence of carbonated aquifer.

^{14}C content has been measured on HCO_3^- in Saint-Ghislain and Douvrain deep waters. The residence time resulting from different interpretations ranges from 35.000 to 21.000 years

for Saint-Ghislain and from 20.000 to 8.000 for Douvrain (Ingerson and Pearson, 1964; Vogel, 1970; Tamers, 1975). This residence time is consistent with geothermal water depletion in ^{18}O and D, as they date infiltration back to the last ice age.

Figure 13 : $\delta^{18}O_{SO4}$ vs SMOW and $\delta^{34}S_{SO4}$ vs CDT

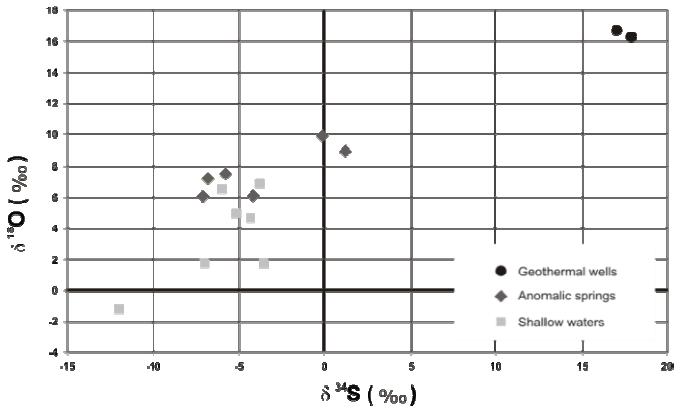

The two main origins of sulfate ion in Lower Carboniferous reservoir water are supposed to be sulfide oxidation and anhydrite leaching, which give totally different isotopic ratios. Sulfate from anhydrite would show high values for $\delta^{34}S$ as well as for $\delta^{18}O$ (more than +15 ‰), reflecting that of anhydrite itself, as measured by Langguth and Nielsen (1980), and Pierre (1986). Sulfate coming from sulfide oxidation would present typical negative values (Krouse, 1980).

Geothermal water, as Figure 13 shows, is the perfect example of anhydritic sulfate. On the opposite corner of this figure, one of the quarry pumping water, known for issuing from a pyrite-rich alteration zone in the Tournaisian limestone, shows quite negative values for $\delta^{34}S$.

On Figure 13, two anomalic springs clearly stand out from the shallow waters group and tend to show more positive ratios, indicating a significant anhydrite leaching influence. This effect is not obvious for the other springs, which stay close to the group of shallow waters.

Shallow waters isotopic ratios however show values that can't be the result of sulfide oxidation alone. Sulfate concentration in them indicates another participation that can be found in deep sulfated water. Mass balance for sulfate and resulting isotopic ratios have been calculated using three possible origins : anhydrite, sulfide and in a much lesser proportion, sulfate from meteoric water. Figure 14 gives the result of this treatment. With a meteoric sulfate having a +5 ‰ $\delta^{34}S$ for an average concentration of 2 mg/l (Mook, 2000), the shallow water markers spread along a straight line joining the 100 % sulfide corner to the opposite 100 % anhydrite corner. The gap to this line illustrates the influence of meteoric sulfate, which appears to be very limited, as expected.

Figure 14 : Origins of sulfate in the Lower Carboniferous aquifer water

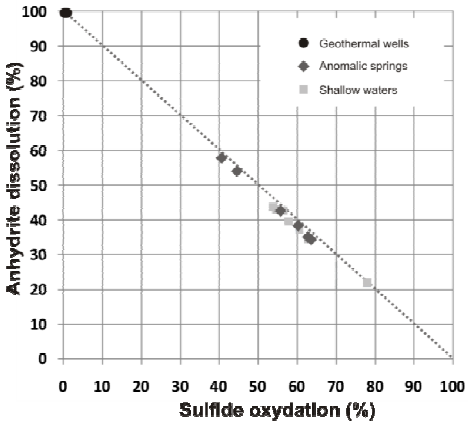

This figure confirms that two of the anomalic springs are clearly more influenced by deep water than the others. But it also indicates that even in regular shallow water, where sulfide oxidation remains the main sulfate provider, anhydritic sulfate enters as a part of the total sulfate content for 30 to 40 %. This proportion can finally be seen as an image of the mixing between shallow fresh water and deep warm and sulfated water in the shallow Lower Carboniferous aquifer.

Considering these results, the combined role of outcropping areas as both recharge and discharge zones is now proved. Further studies are presently going on to locate regions where recharge dominates and where deep water temperature could therefore be lower than in the presently exploited wells, as in Condé.

CONCLUSIONS

The Lower Carboniferous aquifer of Hainaut has been characterized in terms of water geochemistry and isotopic geochemistry, in both deep and shallow part of the reservoir. Deep geothermal water show strong sulfate content related to the leaching of Visean anhydrites still present in the deep strata. Oxygen and hydrogen isotopes analyses indicate its meteoric origin, and depletion in heavy isotopes suggests infiltration during or at the end of the last ice age, which is consistent with estimation of residence times based on ^{14}C. Stable carbon isotope ratios in bicarbonate confirm that geothermal water is in equilibrium with the carbonated rock matrix. Sulfur and oxygen stable isotopes on sulfate ion show the signature of Visean anhydrite dissolution.

Shallow water is not surprisingly a bicarbonate and calcium-rich water. Sulfate can appear in quite important quantities, and several natural springs, particularly on the South margin of the aquifer which corresponds to the top of the reservoir, also show temperature anomalies that lead to suspect a deep contribution to the shallow water chemical content. The Lower Carboniferous carbonates contain sulfides, especially pyrite, that is locally abundant (e.g. : in karstic altered fillings). In the aim of estimating the relative influence of each sulfur potential origin, $\delta^{34}S$ and $\delta^{18}O$ of

sulfate ion has been measured in anomalic spring water and in several quarry and water catchment pumping as a reference of regular shallow aquifer water. The results confirm mixed contribution of anhydritic sulfate and oxidized sulfite in shallow water, with a mixing rate that exceeds 50 % of deep sulfates in several cases.

These investigations confirm the double role of the shallow part of the aquifer, both as recharge and discharge area for the deeper part, presently exploited for geothermal heating. Flow patterns in the reservoir are not homogeneous, as temperature repartition tends to show, and further careful investigations have to be led before setting new exploitations to avoid regions where recharge dominates, and where deep temperature might be lower than expected.

REFERENCES

Craig, H.; 1961, Isotopic variation in meteoric waters, Science, 133, pp. 1702-1703.

Delmer; A. ; 1977, Le Bassin du Hainaut et le sondage de Saint-Ghislain, Service Géologique de Belgique, Professional Paper n°143.

Delmer, A., Leclercq, V., Marlière, R., Robaszynski, F. ; 1982, La géothermie en Hainaut et le sondage de Ghlin, (Mons-Belgique), Ann. Soc. Géol. Nord, 101, pp 189-206.

De Putter, T., Rouchy, J.-M., Herbosch, A., Keppens, E., Pierre, C., Groessens, E.; 1994, Sedimentology and palaeoenvironment of the Upper Visean anhydrite of the Franco-Belgian Carboniferous Basin (Saint-Ghislain Borehole, Southern Belgium), Sedimentary Geology, 90, pp 77-93.

Doremus, P., Hennebert, M. ; 1995, Carte géologique de Wallonie, 38/5-6, Blicquy-Ath, notice explicative, MRW-DGRNE.

Dupuis C. and Vandycke S. ; 1989, Tectonique et karstification profonde, un modèle de subsidence pour le basin de Mons, Ann. Soc. Géol. Nord, 112, pp 479-487.

Groessens, E., Conil, R., Hennebert, M. ; 1979, Le Dinantien du sondage de Saint-Ghislain, Stratigraphie et paleontology, Mem. Expl. Cartes Géol. Min. Belg., 22, 137 p.

Hennebert, M. ; 1999, Carte géologie de Wallonie, 44/3-4, Laplaigne-Péruwelz, notice explicative, MRW-DGRNE.

Ingerson, E., Pearson, F. J. ; 1964, Estimation of age and rate of motion of groundwater by the 14C method, Recent Researches in the Field of Hydrosphere, Atmosphere and nuclear chemistry. Maruzen Co, Tokyo, pp. 263-283.

Krouse, H ; 1980, Sulphur isotopes in our environment, Handbook of Environmental Isotopes, Geochemistry, pp. 435-471.

Langguth, H.R., Nielsen, H. ; 1980, Sulphur isotopes in thermal waters and anhydrites of the Dinantian at the Southern margin of the Brabant Massif: preliminary note, Meded. Rijks Geol. Dienst, 32-13, pp. 101-105.

Mook, W. G.; 2000, Environmental isotopes in the hydrological cycle, IHP-V Technical Documents in Hydrology, 39, 280 p.

Pierre, C. ; 1986, Données de géochimie isotopique sur les anhydrites (^{18}O, ^{34}S) et les carbonates (^{18}O, ^{13}C) des évaporites givétiennes et viséennes du Nord de la France et le la Belgique, Bull. Soc. Belg. Géol., 95, pp. 129-137.

Quinif, Y., Vandycke, S., Vergari, A. ; 1997, Chronologie et causalité entre tectonique et karstification. L'exemple des paléokarst crétacés du Hainaut (Belgique), Bull. Soc. Belg. Géol., 168, pp 463-472.

Rouchy, J.M., Groessens, E., Laumondais, A. ; 1993, Dislocation des formations évaporitiques par la tectonique et la dissolution: le modèle des évaporites dinantiennes du domaine varisque franco-belge, Bull. Soc.Belg.Géol.,164,pp39-50.

Tamers, M. A.; 1975, Validity of radiocarbonates on groundwater, Geophysical Survey, 2, pp. 217-239.

Vogel, J. C. ; 1970, Carbon 14 dating of groundwater, Isotope Hydrology IAEA, pp. 225-237.

CFG ; 1988, Rapport d'essais de longue durée realizes sur le forage géothermique en juillet et août 1988 – Recherche des causes de l'anomalie thermique, 12 p.

IAEA ; 2001, GNIP Maps and Animations, International Atomic Energy Agency, Vienna. Accessible at http://isohis.iaea.org.

INTERPRETATION OF GEOCHEMICAL WELL TESTS DATA FOR OW-903B, OW-904B AND OW-909 - OLKARIA DOMES, KENYA.

Malimo, Sylvia Joan.
Geothermal Development Company.
P.O Box 100746 -00101- NAIROBI, KENYA.smalimo@gdc.co.ke

ABSTRACT

Three production wells from the Olkaria Domes field (Kenya) were allowed to discharge for 3 months in early 2009 and this communication describes the chemical composition of the fluids from these three wells (OW-903B, OW-904B and OW 909). Down hole temperatures range from 250°C to 350°C for these three wells which agree with the solute and gas geothermometers. The wells produce fluids with high pH, deep fluid pH ranges from 6.9 to 8.3. OW 909 has higher deep fluid TDS, pH and concentrations of anions (B, Cl, F), Na and K as compared to OW 903B and OW 904B. Olkaria Domes wells have a sodium bicarbonate water type similar to those of Olkaria west and Olkaria central fields. Concentrations of most dissolved constituents were initially low but then increased with increasing enthalpy, a considerable range in observed concentrations. Deep fluids appear to be close to equilibrium with quartz and calcite. Very low Ca concentrations suggest that calcite scaling will not be a problem for the utilization of the Olkaria Domes geothermal fluids in electricity generation but fluid has to be separated at temperatures above 100°C to prevent silica scaling. There´s also low carbon dioxide emission from these wells.

INTRODUCTION

The Greater Olkaria Geothermal Area (GOGA) is situated south of Lake Naivasha on the floor of the southern segment of the Kenya rift (Figure 1). The Kenya rift is part of the East African rift system that runs from Afar triple junction at the Gulf of Eden in the north to Beira, Mozambique in the south. It is the segment of the eastern arm of the rift that extends from Lake Turkana to the North, and to Lake Natron northern Tanzania to the south. The rift is part of a continental divergent zone where spreading occurs resulting in the thinning of the crust hence eruption of lavas and associated volcanic activities (Lagat 2004).

The Greater Olkaria Geothermal Area consists of seven sectors namely, Olkaria North East, Olkaria East, Olkaria Central, Olkaria South West, Olkaria North West, Olkaria South East and Olkaria Domes. This report concentrates on part of the Greater Olkaria Geothermal Area – the Olkaria Domes field, which is being developed by the Kenya Electricity Generating Company (KENGEN), in addition to their other two producing fields - Olkaria East and Olkaria North East. This study aims at interpreting the geothermal fluid types, the chemical components and any recommendations resulting thereof in evaluating the chemistry of well discharges from three Olkaria Domes wells (OW 903B, OW 904B and OW 909). I also compare the waters of the Domes field to the other six fields in the Greater Olkaria Geothermal Area.

BACKGROUND

General and status of development

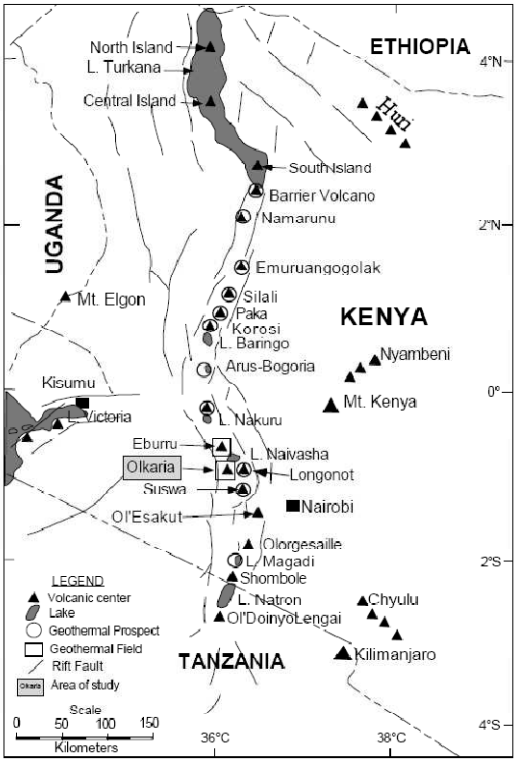

FIGURE 1: Map of the Kenya rift showing the location of Olkaria geothermal field and other quaternary volcanoes along the rift axis.

conducted and the fluids characterised. These were a mixed sodium bicarbonate–chloride–sulphate water type with very dilute chloride concentrations ranging from 178 to 280 ppm (Opondo 2008).

GEOLOGICAL SETTING

The volcanic activity in the Olkaria domes area has progressed from Miocene to the present with eruption producing rocks ranging from intermediate to acid with minor basic eruptions. Major volcanic and fissure controlled eruptions characterised by caldera collapse phases have resulted in uneven surface topography covered by fresh lava rocks and pyroclastics. Some of the volcanic centres are aligned on an arcuate structure that suggests that the Olkaria complex is a remnant of an older caldera which is commonly known as the ring structure. The presence of the ring of domes has been used to suggest the presence of a buried caldera (Mungania 1992). The surface outcrops mainly comprise alkali rhyolite lava flows, pyroclastic deposits, some trachytic and basaltic flows. Pyroclastic deposits comprise compacted and reworked beds and pumice rich deposits which are very thick on the Domes. Some lava dykes up to 6 m thick have been observed to cut across the pyroclastics a NS direction. The pyroclastic ash deposits are well layered and vary from weakly to highly weathered often imparting a brownish colour to the deposits (Omenda 1999).

Olkaria Domes Field is located within the GOGA and lies to the west of Longonot Volcano. Olkaria Domes is the latest of these seven sectors to be deep drilled. Three deep exploration wells were drilled between 1998 and 1999. An approximately 15 wells, both vertical and directional, have been drilled in the domes area (as of May 2009). Olkaria East and Olkaria North East are fully developed with installed capacities of 45 MWe and 70 MWe. Optimization for the two power plants operated by KENGEN in Olkaria East and Olkaria North East fields are underway with more wells being drilled in the Olkaria East field. Olkaria South West has a 50 MWe binary plant operated by Orpower4 Inc while a smaller binary plant of ~4 MWe is operated by Oserian Development Company (ODC).

Olkaria Domes Field lies to the east of the Olkaria East Field (Figure 2). It is bound approximately by the Hell's Gate National Park, Ol' Njorowa gorge to the west and a ring of domes to the north and south (Mungania 1999). Most of the Olkaria Domes Field lies within the less than 20 Ωm apparent resistivity zone that covers the central and western portions of the Olkaria Domes prospect. The rest of the field lies within the 30 Ωm apparent resistivity (Onacha 1993). Three initial exploration wells were sited in the Olkaria Domes Field and were drilled to depths varying from 1900m to 2200m vertical depth. These were wells OW-901, OW-902 and OW-903. These wells were sited to investigate the easterly, southerly and westerly extents of the reservoir and the structures that provide fluid flow into the field. Discharge tests were

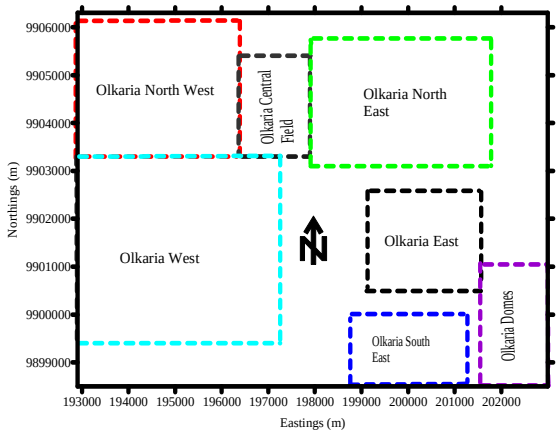

FIGURE 2: Geothermal Fields in the Greater Olkaria Geothermal Area (GOGA).

The Ol'Njorowa Gorge is probably an important structural feature that separates the Olkaria East Field from the Olkaria Domes field. Comendite is exposed in a few locations along lava fronts and along the Ol'Njorowa gorge. The rocks consist of unconsolidated pyroclastics, alkali rhyolite lavas with intercalations of tuffs, basalts interstratified with trachytes and synetitic intrusives at the bottom of the wells (Mungania 1999; Omenda 1999). The eruptive material covering Olkaria volcanic complex area is characterised by acid pyroclastics and alkali rich lavas to an elevation of about 1400 m.a.s.l. The high concentrations of incompatible trace elements imply that the volcanic activity tapped the upper parts of a highly fractionated magma reservoir rich in volatiles.

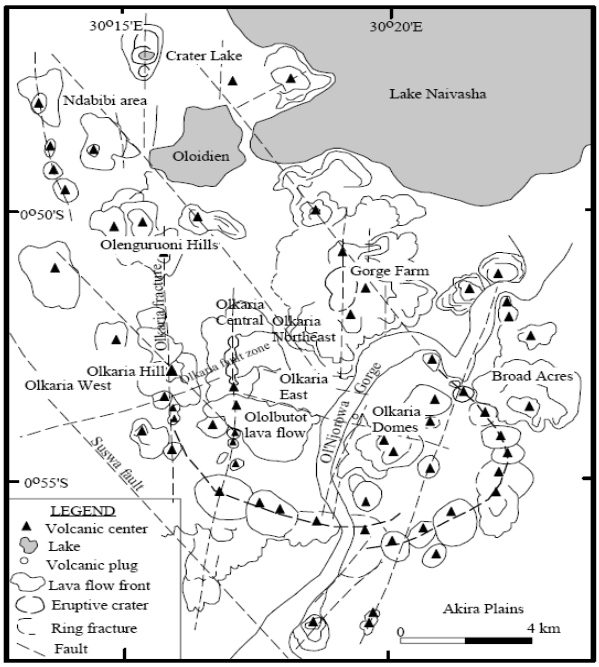

FIGURE 3: Volcano-tectonic map of the Greater Olkaria volcanic complex (modified from Clarke et al., 1990).

This is further supported by the presence of gas charged magmatic products like pumice and features of explosive volcanism like craters and caldera. According to Clarke et al., 1990, xenoliths of syenite in pyroclastics within the Domes and Longonot areas imply a possible cold or cooling upper part of a magma body which is interpreted to be shallower towards Longonot. The zone between 1400 m.a.s.l and 1000 m.a.s.l is dominated by thin basaltic and pyroclastics flows indicating quiet fissure eruptions and a period of strombolean type volcanism. Below 1000 m.a.s.l, trachytic lava dominates with associated pyroclastics and basalts. The trachytes are further divided into two types. The first is a quartz rich porphyritic type that extends to an elevation of 500 and may represent the remnant of the Olkaria mountain shield lavas. The second is a fine grained type having flow texture may indicate low viscosity associated with Pliocene plateau lavas.

Starting from these plateau lavas, the following volcanological model, (Figure 4), was first put forward:

a) The old Pliocene volcanic terrain covered by flood volcanics is characterised by block faulting associated with extensional tectonics.
b) The Plio-pleistocene shield volcano was built upon the shield quartz-trachyte lavas. The volcano then collapsed and formed a cauldron floor at about 1000 – 1200 m.a.s.l and due the emptying of the volatile rich parts, of the magma chamber during the explosive caldera collapse phase, more basic magma erupted effusively into the cauldron floor.
c) Reactivation of N-S faults during Pleistocene caused further explosive withdrawal of magma from a deep differentiated magma chamber. This phase may have been contemporaneous with activity in Longonot. (Onacha and Mungania 1993.)

Previous work.

Detailed geological, geophysical and geochemical work was conducted in the area by different workers (Mungania 1992). The surface exploration with emphasis in the Olkaria Domes field was conducted in the period 1992 to 1993 for geophysical, geological and geochemical surveys. This led to the development of a basic working model that resulted in recommendations to drill three wells. Exploration drilling started in June 1998 through June 1999 and three wells drilled to completion. Three geothermal exploration wells OW-901, OW-902 and OW-903 were drilled in Olkaria Domes field to evaluate its geothermal potential. The three wells (Figure 5) were drilled to a depth of 2200 m and all encountered a high temperature system and discharged on test. The highest recorded measured temperatures in the wells were; 342°C at -

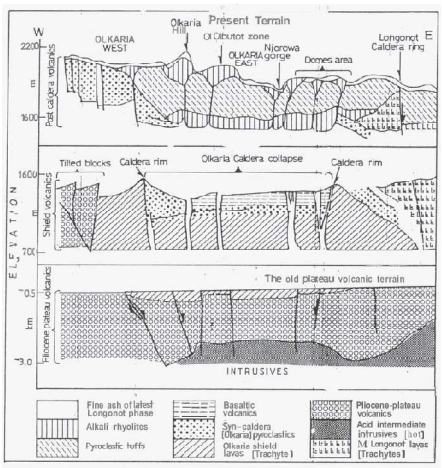

FIGURE 4: Volcanological model of Olkaria Domes area.

290 m.a.s.l, 248°C at 207 m.a.s.l and 341°C at -107m.a.s.l for wells OW-901, OW-902 and OW-903 respectively. Rocks encountered in the wells include pyroclastics, rhyolite, tuff, trachyte, basalt and minor dolerite and microsyenite intrusives.

Fractures, vesicles, spaces between breccia fragments, glassy rocks and primary minerals exhibit little or no hydrothermal alteration in the upper parts of the wells with mainly silica, calcite, zeolites, phyllosilicates, oxides and sulphides being the alteration minerals present. In the deeper parts of the wells, however, hydrothermal alteration to ranged from high to extensive. Hydrothermal zeolites, calcite, epidote, phyllosilicates, silica, sulphides, epidote, albite, adularia, biotite, garnet, fluorite, prehnite, oxides and titanite are the alteration minerals observed. The most important hydrothermal alteration controls in Olkaria Domes field are temperature, rock types and permeability (Lagat 2004).

FIGURE 5. Domes map showing the location of wells.

Four hydrothermal alteration zones were recognized in the field based on the distribution of the hydrothermal alteration minerals. They are in the order of increasing depth and temperature; the zeolite-chlorite, the illite-chlorite, the illite-chlorite-epidote and the garnet-biotite-actinolite zones. Feeder zones in the wells were found to be confined to faults, fractures, joints and lithologic contacts. Observations from hydrothermal alteration mineralogy, pressure and temperature profiles indicate that well OW-901 is close to the upflow whereas well OW-903 is in the outflow zone and well OW-902 is in the outflow and also the marginal zone of the field. The geochemical analysis found a mixed type sodium bicarbonate-chloride-sulphate water with dilute chloride concentration (chloride ~178-280 ppm). The pH of fluids discharged tended to be alkali (8.68 to 10.69) as sampled at atmospheric pressure and analysd at room temperature (25°C). Carbon dioxide gas concentration in steam, on average, was high relative to that of the Olkaria East Field. A less mineralised water component was found to exist in this field. Solute geothermometry offered a good estimate of temperatures where dilute fluids inflow into the wells between 1000m to 1200m. Gas geothermometry approximated to the deep temperature in the reservoir though these were less than measured temperatures at well bottom (Opondo 2008).

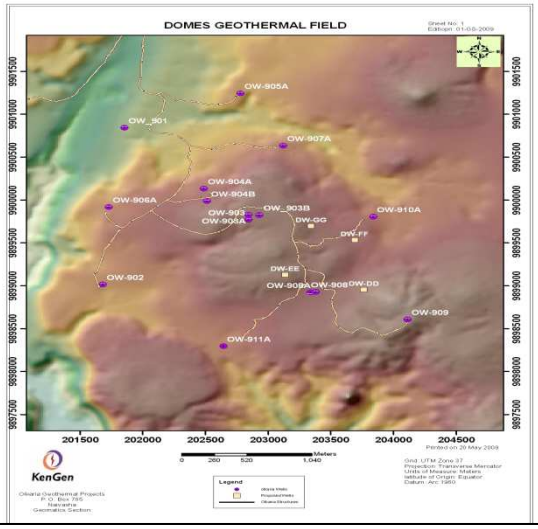

FIGURE 5: Domes map showing the location of wells.

Geology of OW 903B, OW 904B and OW 909

The major rock types found during drilling were trachytes with occurrences of epidotes and basalts for the three wells selected for this study. Trachytes dominate from shallow depths with secondary minerals of clays and pyrites. Basalts and tuffs were also observed in the drill cuttings with dominating clay, pyrite and calcite as the secondary minerals.

Reservoir temperature and pressure profiles

For the selected three wells from the Olkaria domes, the specifications of the wells are listed in Table 1. Figure 7 shows the temperature logs of the domes wells for different times during heating, injection and shut in. From these logs, I was able to choose reference temperatures that are necessary for computing deep fluid compositions from two phases chemical analyses.

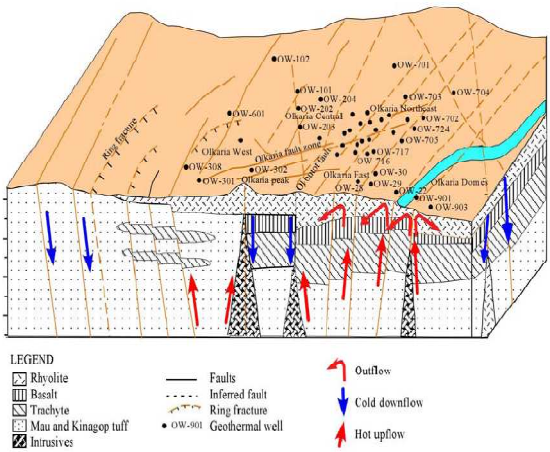

FIGURE 6: A conceptualized geological model of the Greater Olkaria Geothermal Area showing generalized geology and the locations of the fields with respect to downflow, upflow and the outflow zones. (Lagat, 2004)

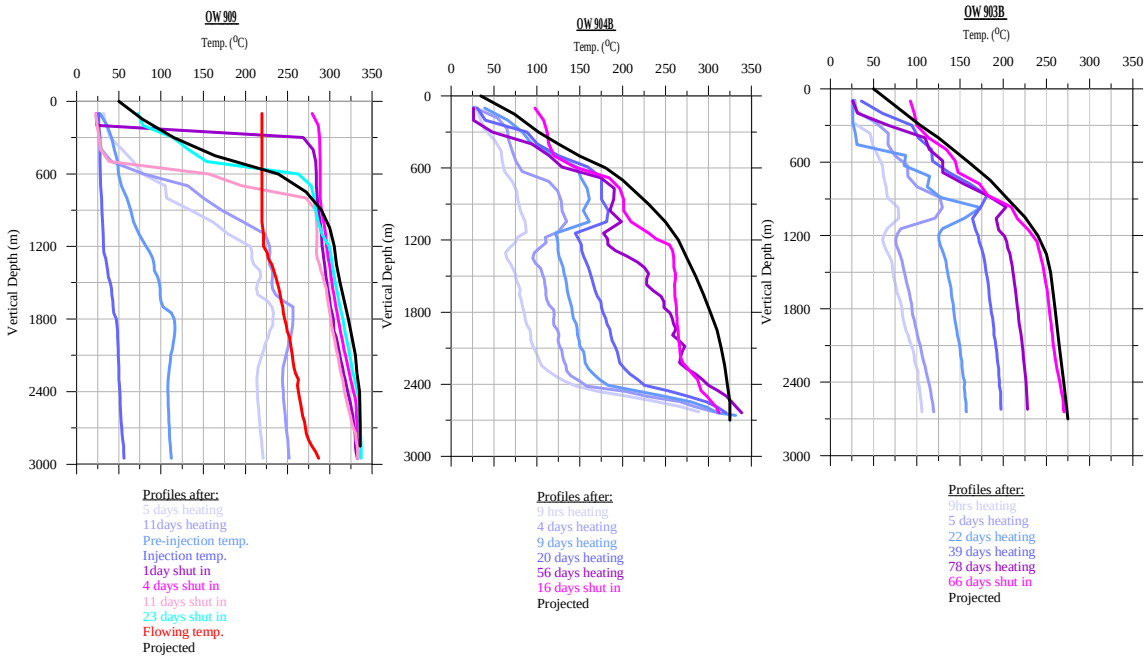

FIGURE 7. Temperature profiles of Olkaria Domes wells

Well	Type	Drilled Depth (m)	Production Casing Depth (m)	Reference temperature (°C)
OW 903B	Directional	2800	1200	250
OW 904B	Directional	2820	1200	260
OW 909	Vertical	3000	1200	300

TABLE 1: Well information

GEOCHEMICAL DATA AND TRENDS

Sampling and analysis

Water chemistry data is essential information required for the characterization of geothermal fluids and evaluation of energy potential of geothermal fields by geothermometry, and provides good indicators for monitoring reservoir changes in response to production and also allow us to evaluate and avoid scaling problems in wells and surface pipelines. Analytical results with good quality are the key to accurately evaluating geothermal resources and effectively solving reservoir management problems. Collection of samples for chemical analysis is the first step in a long process which eventually yields results that provide information that is used to answer different geochemical questions. In this study two-phase fluid samples from three discharging wells, OW 903B, OW 904B and OW 909 are considered. Steam samples were collected using the Webre separator on the wellhead while the liquid samples were collected at the weir box of the silencer. The liquid samples were collected in plastic bottles while the vapour samples were collected in evacuated double port glass bottles (Giggenbach flasks) containing 50ml of 40% NaOH. According to Ármannsson and Ólafsson 2006, different ways can be used to preserve the samples. Onsite analysis for H_2S in the water samples, acidification for cations and dilution for silica samples was done. The samples were then analysed for

the different elements and gases. Analytical methods for individual components in liquid samples are shown in Table 2. All the gases (CO_2, H_2S, CH_4, H_2, and N_2) were analysed using gas chromatography.

TABLE 2: Methods used for analysis of different elements in collected samples (Pang and Armannsson 2006).

Analysis for:	Method
a. pH	- pH meter
b. Conductivity / TDS	- Conductivity meter / gravimetry
c. CO_2	- Titrimetry
d. H_2S	- Titrimetry
e. B	- Spectrometry
f. SiO_2	- Spectrophotometry (with ammonium- molybdate)
g. Na	- AAS
h. K	- ISE
i. Mg	- AAS
j. Ca	- AAS
k. F	- ISE
l. Cl	- Spectrophotometry with thiocyanate
m. SO_4^{2-}	- Turbidometry with barium chloride

Results

The three selected wells in the domes area of the Olkaria geothermal field were sampled and tested for a period of about 5 months i.e. from February to June 2009. See data appendices I and II. From reservoir measurements, the enthalpy remained constant at about 2000 kJ/Kg while the discharge rates were as follows: steam discharge increased from 37 t/hr to 50 t/hr while water discharge was constant at ranges of 20 t/hr to 30 t/hr. A total of 88 samples were collected. The tables in appendix I show the raw water and gas data. Most of the samples from the wells had no detectable magnesium and the calcium concentrations were low (less than 10ppm).

In order to compute the deep fluid composition from the liquid sample (collected at atmospheric pressure) and the steam sample (collected at 1.2 to 7 bars) it was necessary to recalculate the steam sample composition to atmospheric pressure. The atmospheric steam composition was combined with the liquid sample composition in the computation of the deep fluid composition using the WATCH programme Version 2.1 (Arnórsson and Bjarnason 1994). Samples with good ionic charge balance (charge balance from -10 to +10) were then speciated using the WATCH program to give concentration of the deep fluids (Appendix II). For any solution, the total charge of positively charged ions will equal the total charge of negatively charged ions in reality. The net charge for any solution must equal zero. In the samples analyzed, though, the charge balances were not = 0 so the samples with the closest charge balance, i.e. ±10, were used.

GEOCHEMICAL DATA INTERPRETATION

Trends with time in the composition of well discharges

A total of 88 samples were used to compute the trends of the three wells sampled during discharge. The different solute and gas components were monitored and sampled to evaluate the recovery of the wells after shut in. Appendix shows the trends in the different components monitored for a period of about 100 days. OW 909 seems to have higher concentrations of the cation components as compared to OW 903B and OW 904B. Despite the limited time of recovery, the sulphate concentrations are declining with time as the H_2S concentrations increase showing good geothermal water inflow into the wells. The scatter in the data might in part result from non-equilibration of the geothermal water and the drilling fluids that had not totally been discharged from the wells and to some degree it might reflect analytical uncertainties.

Correlation of discharge components with chloride

Plots depicting the concentrations of several components such as B, SiO_2, Ca, Na, K and F as a function of Cl concentration are shown in appendix III. These plots seem to indicate that the ratios of chloride are close to linear with the other components except with calcium which is in very low concentrations in these new wells. This indicates that there is still mixing of the cold and hot water in the upflow. The concentrations of dissolved constituents in the fluids from wells OW 904B and OW 903B tend to be very similar whereas the fluids from well OW 909 tend to have higher concentrations of dissolved solids.

Cl-SO_4-HCO_3 ternary diagram

According to Giggenbach 1991, ternary diagrams are used for the classification of thermal water based on the relative concentrations of the three major anions Cl^-, SO_4^{2-} and HCO_3^-. Chloride, which is a conservative ion in geothermal fluids, does not take part in reactions with rocks after it has dissolved. Chloride, does not precipitate after it has dissolved; its concentration is independent of the mineral equilibria that control the concentration of the rock-forming constituents. Thus, chloride is used as a tracer in geothermal investigations. The Cl-SO_4-HCO_3 ternary diagram is one diagram for classifying natural waters (Giggenbach, 1991). Using this diagram, several types of thermal water can be distinguished: mature waters, peripheral waters, steam-heated waters and volcanic waters. The diagram provides an initial indication of mixing relationships. According to Giggenbach 1991, the chloride-rich waters are generally found near the upflow zones of geothermal systems. High SO_4^{2-} steam-heated waters are usually encountered over the more elevated parts of a field. Degree of separation between data points for high chloride and bicarbonate waters may give an idea of the relative degree of interaction of the CO_2 charge fluid at lower temperature, and of the HCO_3^- concentration increased with time and distance travelled underground.

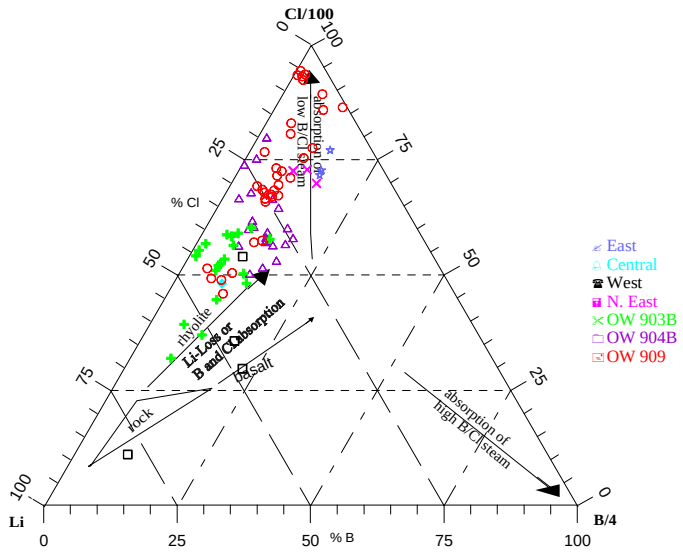

FIGURE 9: Comparative plot of relative Cl, Li, and B from wells in

Figure 8 shows that the three Olkaria Domes wells (OW 903B, OW904B and OW909) plot in the region with high HCO_3 peripheral waters with low chloride. This illustrates that the geothermal fluids in the Olkaria Domes reservoir are bicarbonate waters and correspond to peripheral waters (Giggenbach, 1991). The figure also shows the correlation of the waters with those of the other fields in the GOGA. The Olkaria Domes fluids seem to plot similar to those of Olkaria west and Olkaria central fields. From the relative abundance of chloride, sulphate and bicarbonate of the Olkaria wells, these waters would be classified as sodium-chloride and sodium-bicarbonate water, or mixtures thereof (Figure 8). Wells in the Olkaria East production field and in Olkaria Northeast discharge sodium-chloride type water that are classified as more mature according to the scheme of Giggenbach 1991.

Relative Cl, Li and B contents

Lithium is used as a tracer, because it is the alkali metal least affected by secondary processes for initial deep rock dissolution and as a reference for evaluating the possible origin of two important 'conservative' constituents of geothermal waters, Cl and B. Once added, Li remains largely in solution. The B content of thermal fluids is likely to reflect to some degree the maturity of a geothermal system; because of its volatility it is expelled during the early heating up stages. In such a case, fluids from older hydrothermal systems can be expected to be depleted in B while the converse holds for younger hydrothermal systems. It is, however, striking that both Cl and B are added to the Li containing solutions in proportions close to those in crustal rocks. At higher temperatures Cl occurs as HCl and B as H_3BO_3. Both are volatile and able to be mobilized by high temperature steam. They are, therefore, quite likely to have been introduced with the magmatic vapour invoked above to lead to the formation of deep acid brine responsible for rock dissolution (Karingithi 2000).

At low temperatures the acidity of HCl increases rapidly, and is soon converted by the rock to the less volatile NaCl. B remains in volatile form to be carried in the vapour phase even at lower temperatures. The Cl/B ratio is often used to indicate a common reservoir source for the waters. Care must however, be taken in applying such interpretation since waters from the same reservoir may show differences in this ratio, due to changes in lithology at depth over a field (example, the occurrence of a sedimentary horizon), or by the absorption of B into clays during lateral flow.

The fluid discharges from Olkaria Domes wells (OW-903B, OW-904B and OW-909) plot in the region along the Li-Cl axis but do not cluster around the same point. B/Cl ratios are in the intermediate region and could suggest the absorption of low B/Cl magmatic vapours. Discharges from the Olkaria –Domes wells show comparatively low lithium content. This is also shown in the other well discharges from the other GOGA wells. See figure 9.

Geothermometry

Chemical geothermometers are based on the assumption that temperature dependent mineral solute equilibrium is attained in the geothermal reservoir. In this report chemical geothermometers are used to assess the reservoir temperatures for the three wells chosen from Olkaria Domes. Studies indicate that geothermal water compositions are controlled by a close approach to mineral-solution equilibria with respect to various elements (Arnórsson et al., 1983a; Tole et al., 1993; Karingithi, 2000). Changes, which occur in temperature and water composition during boiling between aquifer and wellhead, generally lead to changes in mineral saturation. Such changes may result in mineral precipitation or mineral dissolution. Together with physical processes in the depressurization zone around wells, these changes may cause well discharge compositions to differ from the chemical composition of the aquifer fluid.

Solute Geothermometers

In geochemical studies, water chemistry and gas composition of geothermal fluids have proved useful in assessing the characteristics of geothermal reservoirs, both to estimate temperatures (Arnórsson and Gunnlaugsson, 1983; D'Amore and Truesdell, 1985) and to estimate initial steam fractions in the reservoir fluid (D'Amore and Celati, 1983; D'Amore and Truesdell, 1985).

The following solute geothermometers are used in this study:

Quartz - Fournier (1977)
- Fournier and Potter (1982)
- Fournier (1979)

Na-K - Arnórsson et al. (1983)
- Giggenbach (1988)

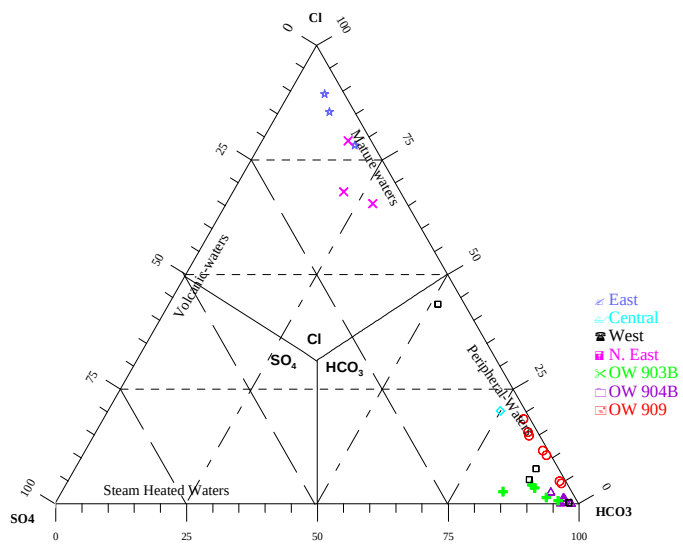

FIGURE 8: Comparative plot of relative Cl-SO4 -HCO3 contents from the discharges of wells in the GOGA fields.

Silica geothermometers

The silica geothermometers are based on experimentally determined solubilities of chalcedony and quartz. Usually the quartz geothermometer is applied to high-temperature reservoirs like the Olkaria geothermal field. Application of the silica geothermometers is based on the fact that the activity of dissolved silicic acid, H_4SiO_4, in equilibrium with quartz, is temperature dependent. The solubility reactions for silica minerals can be expressed as:

$$SiO_{2,solid} + 2H_2O = H_4SiO_4{}^{o} \tag{1}$$

However $H_4SiO_4^0$ is not only aqueous silica species in natural waters. $H_4SiO_4^0$ is a weak acid which dissociates, if pH of the fluid is high enough to yield $H_3SiO_4^-$:

$$H_4SiO_4{}^{0} = H^+ + H_3SiO_4{}^{-} \tag{2}$$

Analysis of silica in aqueous solution yields the total silica concentration, generally expressed as ppm SiO_2, which includes both un-ionized $H_4SiO_4^0$ and ionized ($H_3SiO_4^-$). The dissociation constant for silicic acid is about 10^{-10} at 25°C. Thus, at a pH of 10 ($H^+ = 10^{-10}$) the concentration of unionized silica equals that of ionized silica:

$$K_{H_4SiO_4^\circ} = \frac{[H^+][H_3SiO_4{}^-]}{[H_4SiO_4^\circ]} \tag{3}$$

When using quartz geothermometers, some factors should be considered (Fournier and Potter, 1982):

- The temperature range in which the equations are valid;
- Possible polymerization or precipitation of silica before sample collection;
- Possible polymerization of silica after sample collection;
- Control of aqueous silica by solids other than quartz;
- The effect of pH upon quartz solubility; and
- Possible dilution of hot water with cold water before the thermal waters reach the surface.

The quartz geothermometers used to estimate the aquifer temperatures in this report are:

Fournier (1977)

$$t\,(°C) = \frac{1309}{5.19 - logS} - 273.15 \tag{4}$$

Fournier and Potter (1982)

$$t(°C) = -42.2 + 0.28831S - 3.6686 \times 10^{-4}S^2 + 3.1665 \times 10^{-7}S^3 + 77.034logS \tag{5}$$

The results for the quartz calculations are shown in Table 3.

Cation geothermometers

Reactions between alkali feldspars and Na and K in aqueous solution have often been described as exchange reactions. At the temperature prevailing in geothermal systems, the reaction involves simultaneous equilibrium between Na^+ and K^+ in solution and quite pure albite and K-feldspar.

The reaction is expressed as:

$$NaAlSi_3O_8 + K^+ = KAlSi_3O_8 + Na^+ \tag{6}$$

The equilibrium constant, $K_{eq,}$ for reaction 4 is:

$$K_{eq} = \frac{[KAlSi_3O_8][Na^+]}{[NaAlSi_3O_8][K^+]} \tag{7}$$

The activities of the solid reactants are assumed to be unity and the activities of the dissolved species are about equal to their molal concentrations in aqueous solution.

Equation 5 reduces to:

$$K_{eq} = \frac{[Na^+]}{[K^+]} \tag{8}$$

In this report the following equations are used for calculating reservoir temperatures based on the Na/K activity ratio in the geothermal fluid:

Fournier (1979)

$$\mathbf{t}(℃) = \frac{\mathbf{1217}}{\mathbf{1.438 + \log\,(Na/K)}} - \mathbf{273.15} \tag{9}$$

Na/K temperature in the range of temperatures 250-350°C (Arnórsson et al., 1983) given by:

$$t(℃) = \frac{\mathbf{1319}}{\mathbf{1.699 + \log\,(Na/K)}} - \mathbf{273.15} \tag{10}$$

Na/K temperature by Giggenbach (1988) given by:

$$t(℃) = \frac{\mathbf{1390}}{\mathbf{1.750 + \log\,(Na/K)}} - \mathbf{273.15} \tag{11}$$

The reference temperatures chosen agree with the different chosen geothermometers. OW 903B has aquifer temperatures in the range of 220°C to 260°C; OW 904B has temperatures in the range of 230°C to 300°C while OW 909 temperatures are in the range of 250°C to 340°C indicating good production temperatures. The results for the calculations are shown in Table 3.

Gas geothermometers

Studies in many high-temperature geothermal fields (> 200°C) indicate that the concentrations (or ratios) of gases like CO_2, H_2S, H_2, N_2, NH_3, and CH_4 are controlled by temperature-dependent gas-gas and/or mineral-gas equilibria (D'Amore and Arnórsson, 2000). On this basis, data from chemical analyses of those gases have been used to develop relationships between the relative gas concentrations and the temperature of the reservoir. Such relationships are known as *gas or steam geothermometers*. Gas geothermometers are also based on certain chemical reactions between gaseous species and minerals which are considered to be in chemical equilibrium. For each chemical equilibria considered, a thermodynamic equilibrium constant may be expressed in terms of temperature, in which case the concentration of each gas species is often represented by its partial pressure in the vapour phase (D'Amore and Truesdell, 1985).

Geothermal gases are introduced into geothermal fluid with recharge water, from water-rock interaction in the reservoir or from magmatic fluid invasion. In an undisturbed reservoir, reactions in equilibrium at the reservoir temperature control the concentrations of these gases. On boiling, the partitioning of gases between liquid and vapour phase is controlled by the enthalpy of the geothermal fluid and the boiling temperature in cases where the vapour

travels without hindrance to the surface (in boreholes and wide open fissures), negligible changes in the gas concentrations and ratios will occur, and these can be used as gas geothermometers. There are essentially three types of gas geothermometers. The first group is based on gas-gas equilibria. The second group is based on mineral-gas equilibria involving H_2S, H_2 and CH_4 but assuming CO_2 to be externally fixed. The third group is based on mineral-gas equilibria. The first two groups of geothermometers require only data on the relative abundance of gaseous components in the gas phase, whereas the third group calls for information on gas concentrations in steam (D'Amore and Arnórsson, 2000).

When using gas geothermometry, it is important to keep in mind that several factors other than aquifer temperature may affect the gas composition of a geothermal fluid. In geothermal reservoir fluids, gas concentrations at equilibrium depend on the ratio of steam to water of that fluid, whereas the gas content of fumarole steam is also affected by the boiling mechanism in the upflow, steam condensation and the separation pressure of the steam from the parent water. Furthermore, the flux of gaseous components into geothermal systems from their magmatic heat source may be quite significant and influence how closely gas-gas and mineral-gas equilibria are approached in specific aquifers (D'Amore and Arnórsson, 2000). In this study, the gas geothermometers used are those based on gas concentrations in mmol/kg corrected to the atmospheric pressure. The geothermometers are based on mineral gas equilibria and the temperature equations for the thermodynamic data for the following reactions:

$$\boldsymbol{2Ca_2Al_3Si_3O_{12}(OH) + 2CaCO_3 + 3SiO_2 + 2H_2O = 3Ca_2Al_2Si_3O_{10}(OH)_2 + 2CO_{2,aq}} \tag{12}$$

$$\boldsymbol{FeS_2 + FeS + 2Ca_2Al_2Si_3O_{10}(OH)_2 + 2H_2O = 2Ca_2Al_2FeSi_3O_{12}(OH) + 3H_2S_{aq}} \tag{13}$$

$$\boldsymbol{4FeS + 2Ca_2Al_2Si_3O_{10}(OH)_2 + 2H_2O = 2Ca_2Al_2FeSi_3O_{12}(OH) + 2FeS_2 + 3H_{2,aq}} \tag{14}$$

Q in the gas geothermometry equations represents the gas concentrations in log mmol/kg. The equations, Arnórsson 1998, were:

For T_{CO_2}:

$$\mathbf{t}(°\mathrm{C}) = \mathbf{4.724Q^3 - 11.068Q^2 + 72.012Q + 121.8} \tag{15}$$

T_{H_2}:

$$\boldsymbol{t}(°\mathrm{C}) = \mathbf{6.630}\boldsymbol{Q^3} + \mathbf{5.836}\boldsymbol{Q^2} + \mathbf{56.168}\boldsymbol{Q} + \mathbf{227.1} \tag{16}$$

T_{CO_2/N_2}:

$$\boldsymbol{t}(°\mathrm{C}) = \mathbf{1.739}\boldsymbol{Q^3} + \mathbf{7.599}\boldsymbol{Q^2} + \mathbf{48.751}\boldsymbol{Q} + \mathbf{173.2} \tag{17}$$

The results in the table 3 below show the different geothermometer results found for the three wells. The samples used to calculate for the geothermometers are those that had all the elemental analysis , the samples used to calculate the geothermometers had been discharged for a while to give a good indication of the reservoir fluid and good charge balances per well were also considered.

Well	T_{q-1}	T_{q-2}	T_{NaK-1}	T_{NaK-2}	T_{NaK-3}	T_{qtz}	T_{NaK}	T_{CO2}	T_{H2}	$T_{CO2/N2}$	$T_{ref.}$	$T_{av.}$	T_{median}
OW903B	232	238	263	248	265	249	245	221	239	259	250	246	248
OW904B	254	266	271	255	272	276	307	244	228	263	260	263	263
OW909	274	294	339	351	332	264	340	253	300	268	300	301	300

TABLE 3: Various solute and gas geothermometers of Olkaria Domes Wells.

T_{q-1}	Fournier 1977	T_{q-2}	Fournier and Potter 1982
T_{NaK-1}	Fournier 1979	T_{NaK-2}	Arnórsson et al 1983

T_{NaK-3}	Giggenbach et al 1988	T_{qtz}	WATCH calculated quartz
T_{NaK}	WATCH calculated Na-K	T_{ref}	Observed temperatures
$T_{av.}$	Average Temperature	T_{median}	Median Temperature
TCO_2, TH_2, TCO_2/N_2	Arnórsson (1998)		

Deep fluid species, Log Q/K and saturation indices

As previously stated in the geothermometry section above, WATCH program was used to speciate for the deep fluids. Quartz in the deep fluids shows a slight undersaturation with a bit of scatter due to non-equilibration of the deep fluids and the drilling fluids during the discharge testing. The initial discharge samples are quite varied as compared to the later sampled ones which show equilibration with the quartz species. For the calcite deep fluid species, both the WATCH and SOLVEQ programs were used to speciated the samples. The SOLVEQ program was used to compute for the calcite WATCH results always predicted super saturation was not a realistic result for nature. With SOLVEQ, we get a more realistic result because it incorporates more Ca bearing species like $CaCl^+$, $CaCl_{2\,(aq)}$, CaF^+, and $Ca(HSiO_3)^+$ apart from the ones that both the programs incorporate (Ca_2^+, $CaSO_{4(aq)}$, $CaHCO_3^+{}_{(aq)}$ and $CaOH^+$).

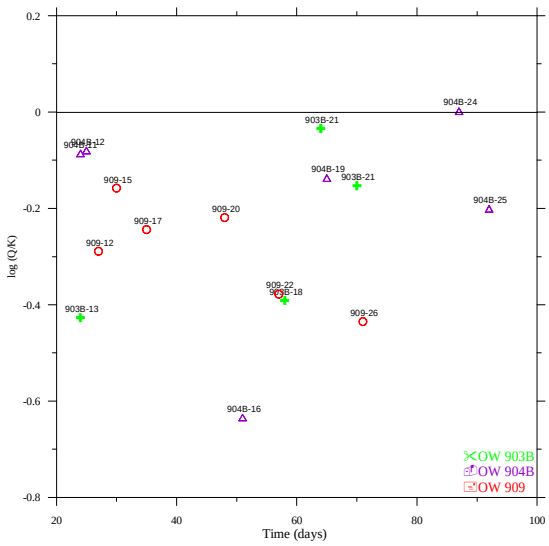

FIGURE 10: Quartz saturation of the deep fluids from Olkaria Domes field.

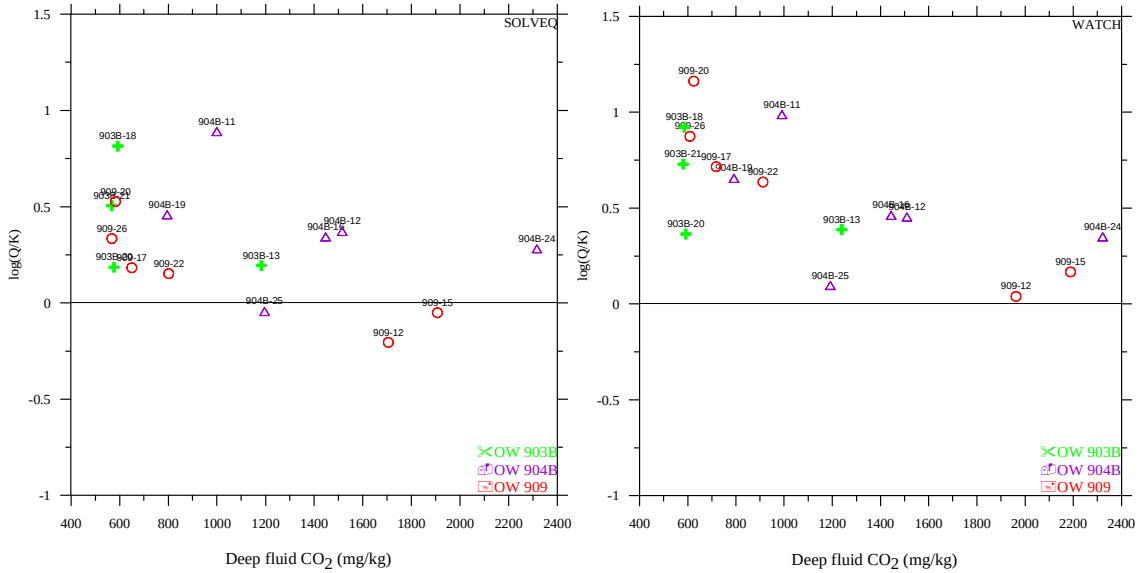

FIGURE 11: Calcite saturation of deep fluids from Olkaria Domes field.

Using the results of the aqueous speciation calculations, the saturation indices (SI) of minerals in aqueous solutions at different temperatures were computed. The SI value for each mineral is a measure of the saturation state of the water phase with respect to the mineral phase. Values of SI greater than, equal to, and less than zero represent, super saturation, equilibrium and under-saturation, respectively for the mineral phase with respect to the aqueous solution. Equilibrium constants for mineral dissolution often vary strongly with temperature. Calcite seems to be close to the super saturation line with few exceptions (Figure 10). In this samples although low calcium concentrations were detected the concentration is expected to equilibrate with time as the well flows and the chemical composition of the deep fluids equilibrates.

PRODUCTION PROPERTIES

Brine handling can be hard in geothermal operations. It is frequently described as the entire periodic table of elements in a pipe. The high temperature solution of elements and compounds, however, causes operational limitations in geothermal power plants. These limitations are due to the severe scaling and corrosion characteristics of geothermal brine and steam. Because of these characteristics, plants may experience extreme plugging and corrosion in wells, lines and equipment. Curtailment in power plant production and even complete plant shutdown are often the end result from these conditions. Different types of brine with differing chemistry conditions are found in various areas around the world. Substantial differences can even be found within the various wells of a given field, just like we have seen in the new Olkaria Domes field. The chemistry of these different brines varies and the differences will depend on several factors including the geology of the resource, temperature, pressure, and water source. Depending on the resource, steam and water ratios in the brine can vary significantly.

The scaling characteristics of brine and steam cause difficult problems in geothermal operation. The variety of problems associated with handling geothermal brine can be extreme – making it critical to understand the chemistry of the brine for successful plant operation. Geothermal brine causes a variety of operational problems and includes the following:

- Equipment Damage and Failure
- Equipment Repair and Replacement
- Well and Line Plugging
- Reduced Steam/Brine Flow
- Power Production Losses
- Complete or Partial Plant Shutdown

The effectiveness of the development of geothermal energy will be determined by the amount of geothermal power that is made available, and this amount will be influenced by the effect that materials problems have on efficiency and downtime. Since every technological effort is limited to some extent by the performance of materials, it is prudent to

consider scaling and corrosion and materials problems which may limit the development of geothermal energy. The availability of durable and cost-effective construction materials for processing geothermal fluids has a definite impact on the development of geothermal energy. Geothermal resources include steam-dominated sources, liquid dominated sources, geo-pressurized sources, and dry (hot rock) sources. Scale is a major problem in geothermal operation. The plugging and deposit problems caused by scale can reduce power plant production, and create expensive cleaning costs. The reduction in power and increased operating costs caused from difficult scale conditions can directly impact a plants financial outcome. Different types of scales are found in various geothermal areas and sometimes, even within the various wells of the same field. The major species of scale in geothermal brine typically include calcium, silica and sulphide compounds. (Stapleton 2002)

To be able find the production properties of the three Olkaria Domes wells, three samples were used to analyse the deep fluid calcite and silica saturation. The species selected for this speciation were those sampled later in the discharge testing period. This was so as to get the close to equilibrium fluids and thus the silica and calcite concentration. The samples selected for silica analysis also had good charge balance and the highest silica concentrations to speciate for the silica deep fluid concentration. The species selected for calcite scaling had the lowest calcium concentration but a representative pH values and CO_2 concentration.

Scaling

Geothermal waters are saturated with silica and are frequently close to saturation with calcite, calcium sulphate and calcium fluoride. Some acid hot water also contains appreciable concentrations of heavy metals. Changes in temperature and pressure disturb the equilibria and will generally lead to scale formation. Calcite and silica deposits are the most frequent scale formation materials. The most troublesome calcite deposits usually occur in the well casing at the level of first boiling (bubble point) with heavy bands of calcite depositing over a short length. (Moller et al, 2004).

Silica scaling

Silica related scale is arguably one of the most difficult scales occurring in geothermal operation. Silica is found in virtually all geothermal brine and its concentration is directly proportional to the temperature of the brine. As brine flows through the well to the surface, the temperature of the brine decreases, silica solubility decreases correspondingly and the brine phase becomes over saturated. When pressure is dropped in the flash vessel, steam flashes and the temperature of the brine further decreases. In the flash vessel, the brine phase becomes more concentrated. Under these conditions, silica precipitates as either amorphous silica or it will react with available cations (e.g., Fe, Mg, Ca, Zn) and form co-precipitated silica deposits.

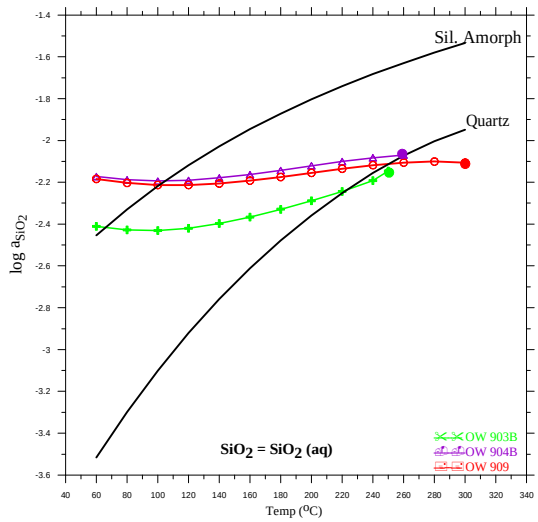

FIGURE 12: Temperatures indicating probable silica scaling in Olkaria Domes.

Scale formation in plant equipment and porosity losses in injection well formations created by the precipitation of amorphous silica have been identified as important problems in some geothermal power operations. In high temperature hydrothermal systems, the formation water is frequently in near equilibrium with quartz. Since the solubilities of pure silica minerals decrease rapidly with decreasing temperature, large amounts of quartz would be expected to precipitate as the brines in these systems are cooled upon production and energy extraction. However quartz rarely precipitates because of the slow kinetics involved in this reaction. Although amorphous silica has a higher solubility than quartz, it is a much more common precipitate in geothermal operations. (Moller et al, 2004). The solubility reactions for silica minerals are invariably expressed in equation (1) and (2).

Since geothermal waters may boil in the upflow of the geothermal system if reservoir temperatures are above 100°C, the boiling causes the concentrations of aqueous solutes to increase in proportion to steam fraction. It also causes the pH of the water to increase because the weak acids dissolved in the water, CO_2 and H_2S, are transferred into the steam phase. To estimate the silica scaling in the new wells drilled in the Olkaria Domes field, WATCH program was used to speciate the analysis and the results indicated on the graphs. From equations 2 and 3 above, $H_4SiO_4^0$ is not the only aqueous silica species in natural waters. $H_4SiO_4^0$ is a weak acid which dissociates, if pH of the fluid is high enough to

yield $H_3SiO_4^-$. Boiling the fluids thus affects the silica concentration leading to the activity of silica to decrease and finally precipitation as amorphous silica at the temperatures shown on the figure 11.

Calcite scaling

Calcite a major scale-forming mineral in many geothermal systems precipitates from a brine according to the following reaction:

$$Ca^{2+}(aq) + 2HCO^{-}{}_{3} \leftrightarrow CaCO_3(s) \downarrow + H_2O + CO_2 \uparrow \quad (18)$$

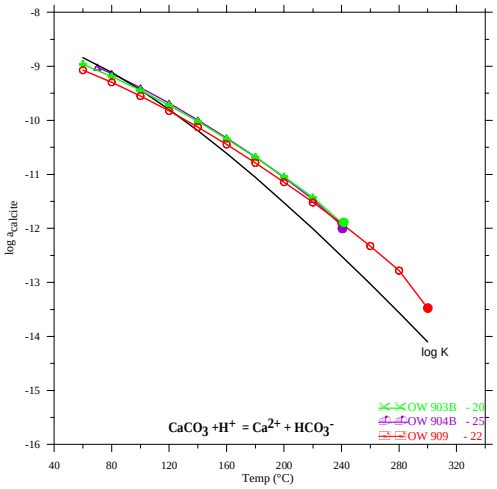

FIGURE 13: Temperatures indicating probable calcite scaling in Olkaria Domes wells.

Ocampo-Diaz et al 2005 found that scale deposition, especially calcite ($CaCO_3$), is a complex function of physical chemistry (for example, total salinity, pH and concentration of calcium and dissolved CO_2) and the pH change upon boiling compared to the rate of cooling upon boiling. Calcite is commonly saturated in the reservoir fluid, and when such fluids boil there is generally a chemical potential to form calcite. However, unlike silica and the sulphides, calcite becomes more soluble as temperature decreases. As result, the most severe calcite scale deposition tends to occur from lower temperature geothermal fluids below 220°C to 240°C.

When reaction 18 is forced to the right by the loss of CO_2 from the liquid phase into a gas phase on flashing, calcite is deposited. In complex brines there may be many other reactions taking place, some of which interact with the calcium and carbonate ions. For this prediction, a sample from each well was selected. The samples selected 20, 25 and 22 for wells OW 903B, OW904B and OW909 respectively had a representative pH and CO_2 with reference to the others from the wells. Although the general calcium concentration is low for these wells, the CO_2 and pH were considered for sample selection. The results from the wells during the initial discharge seemed to have low concentrations of calcium (and high pH values) but trends indicate that with further discharge, the calcium concentrations will increase though not to a great extent. From the WATCH calculations, the calcite saturation is over estimated but considering the deep fluids shown (Figure 12) had been at equilibrium with calcite when the boiling started, then less super saturation would have been experienced during boiling. Calcite scaling will not be a problem in these Domes wells as the low calcium concentrations and high pH, (which affects calcite saturation) indicates.

CONCLUSIONS

- OW 909 seems to have higher concentrations of the cation components as compared to OW 903B and OW 904B. Despite the limited time of recovery, the sulphate concentrations are declining with time as the H_2S concentrations increase showing good geothermal water inflow into the wells.
- Solute and gas geothermometry indicate high temperatures in the range of 250°C to 350°C.
- Olkaria Domes wells have a sodium bicarbonate water type and plot similar to those of Olkaria west and Olkaria central fields. Unlike the wells in the Olkaria East production field and in Olkaria Northeast discharge sodium-chloride type water of mature nature.
- With low calcium concentrations and high pH, calcite scaling can be expected to be minimal in these wells but fluid has to be separated at temperatures above 100°C to prevent silica scaling. There´s also low carbon dioxide emission from these wells.

ACKNOWLEDGEMENTS

I would like to extend my sincere gratitude to Dr. Ingvar B. Fridleifsson, the Director of the UNU Geothermal Training Programme for giving me the chance to take part in the Programme, and to the Deputy Director Lúdvík S. Georgsson for his ever present help. To Thorhildur Isberg for her essential and valuable assistance during my stay in Iceland. To Dorthe Holme and Markus Wilde for their expertise in making the studies and project work go easy.

My great and sincere appreciation to my project supervisor Dr. Thrainn Fridriksson (ISOR, Iceland) for his ever present guidance and hand in each page of this project paper. For his wise counsel, encouragement and efficiency in the supervision of this project paper. To the 2009 UNU fellows who were always supportive and the friendships forged. To the entire Orkustofnun community, thank you for all the assistance and support. I am grateful to the Kenya Electricity Generating Company, for the data from the geothermal wells and the opportunity to study the Olkaria Domes field. A big thank you to Kizito Opondo for updating me with geochemical data. To my parents, Dr & Mrs W.O. Wanyanga, for their love, support and encouragement. Finally, to God the Almighty for granting me the wisdom and guidance always.

REFERENCES

Ármannsson, H. and Ólafsson, M., 2006: Collection of geothermal fluids for chemical analysis. Iceland GeoSurvey-ÍSOR, Reykjavík report ISOR-2006/016, 17 pp.

Arnórsson S., 1998: Interpretation of chemical and isotopic data on fluids discharged from wells in the Momotombo geothermal field with notes on gas chromatography analysis, IAEA Project report NIC/8/008-05, 28 pp.

Arnórsson, S. and Bjarnason, J.Ó., 1994: Icelandic Water Chemistry Group presents the chemical speciation programme WATCH Program upgrade: Version 2.1. Science Institute, University of Iceland, Orkustofnun, Reykjavík, 7 pp.

Arnórsson, S. and Gunnlaugsson, E., 1983: Gas chemistry in geothermal systems. Proceedings of the 9th Workshop on Geothermal Reservoir Engineering, Stanford University, Stanford, California, 231-237.

Arnórsson, S., Gunnlaugsson, E., and Svavarsson, H., 1983: The chemistry of geothermal waters in Iceland II. Mineral equilibria and independent variables controlling water compositions. Geochim. Cosmochim. Acta, 47, 547-566.

Clarke, M.C.G., Woodhall, D.G., Allen, D., and Darling, W.G., 1991: Geological, volcanological and hydrogeological controls on the occurrence of geothermal activity in the area surrounding Lake Naivasha, Kenya. Ministry of Energy, Nairobi, Kenya, report, 138 pp. + 3 maps.

D'Amore, F. and Arnórsson, S., 2000: Geothermometry. In: Arnórsson, S.(ed.), Isotopic and chemical techniques in geothermal exploration, development and use. Sampling methods, data handling, and interpretation. International Atomic Energy Agency, Vienna, 152-199.

D'Amore, F. and Celati, C., 1983: Methodology for calculating steam quality in geothermal reservoirs. Geothermics, 12. 129-140.

D'Amore, F., and Truesdell, A.H., 1985: Calculation of geothermal reservoir temperatures and steam fractions from gas compositions. Geothermal Resources Council, Trans., 9, 305-310.

Fournier, R.O., 1977: Chemical geothermometers and mixing model for geothermal systems. Geothermics, 5, 41-50.

Fournier, R.O., 1979: A revised equation for the Na/K geothermometer, Geotherm. Resources Council Trans., 3. 221 -224.

Fournier, R.O. and Potter, R.W.II., 1982: A revised and expanded silica (quartz) geothermometer. Geoth. Res. Council, Bull., 11-10, 3-12.

Giggenbach, W.F., 1988: Geothermal solute equilibria. Derivation of Na-K-Mg-Ca geoindicators. Geochim. Cosmochim. Acta, 52, 2749-2765.

Giggenbach, W.F., 1991: Chemical techniques in geothermal exploration. In: D'Amore, F. (coordinator), Application of geochemistry in geothermal reservoir development. UNITAR/UNDP publication, Rome, 119-142.

Karingithi, C.W., 2000: Geochemical characteristics of the Greater Olkaria geothermal field, Kenya. Report 9 in: Geothermal Training in Iceland 2000. UNU-GTP, Iceland, 165-188.

Lagat, J.K., 2004: Geology, hydrothermal alteration and fluid inclusion studies of the Olkaria Domes geothermal field, Kenya. University of Iceland, MSc thesis, UNU-GTP, Iceland, report 2, 71 pp.

Moller, N., Greenberg, J.P., Weare, J.H., 2004: Computer modelling for geothermal systems: predicting carbonate and silica scale formation, CO2 breakout and H2S exchange. Transport in Porous Media Journal, 33-1/2. 173-204.

Mungania, J., 1992: Surface geology of Olkaria- Domes field. Kenya Power Company, unpublished internal report.

Mungania, J., 1999: Reservoir model of Olkaria- Domes field. KenGen, unpublished internal report.

Ocampo-Díaz J.D., Núñez, Q.M., Moya-Acosta, S.L., 2005: Silica scaling as a predominant factor of the production in Cerro Prieto geothermal wells, Mexico. Proceedings of the World Geothermal Congress 2005, Antalya, Turkey, 5pp.

Omenda, P.O., 1999: Borehole geology of Well OW-901. KenGen, unpublished internal report.

Onacha, S.A., 1993: Resistivity survey of Olkaria- Domes field. Kenya Power Company, unpublished internal report.

Onacha, S.A., and Mungania, J., 1993: Surface exploration of Domes Area: An extension of Olkaria Geothermal Field. Proceedings of the 14th New Zealand Geothermal Proceedings, Auckland, NZ. 6 pp.

Opondo, K.M., 2008: Fluid characteristics of three exploration wells drilled at Olkaria Domes field, Kenya. Proceedings of the 33rd Workshop on Geothermal Reservoir Engineering, Stanford University, Stanford, Ca, 6 pp.

Pang Z.H., and Ármannsson, H. (editors), 2006: Analytical procedures and quality assurance for geothermal water chemistry. UNU-GTP, Iceland, Report 1, 172 pp.

Stapleton, M., 2002: Scaling and corrosion in geothermal operation. GeoChemical Services - PowerChem Technology. 7 pp.

Tole, M.P., Ármannsson, H., Pang Z.H., and Arnórsson, S., 1993: Fluid/mineral equilibrium calculations for geothermal fluids and chemical geothermometry. Geothermics, 22, 17-37.

Appendix I

Water and Gas analysis

	OW 903B Water Analysis (ppm)																			Gas Analysis (ppm)				
Day	GSP	WHP	Temp	Enth. kJ/kg	Cond	TDS (ppm)	pH	B	SO_4	Cl	CO_2	F	H_2S	SiO_2	Ca	Li	Na	K	Mg	CO_2	H_2S	CH_4	H_2	N_2
1	2.1	3.8	94.0	1307	2776	1390	9.5	0.9	717.7	196.7	266.2	41.6	0.1	281.3		1.5	512.6	55.1	0.7	4382	9.2	15.8		418
2	2.3	3.8	90.0	1325	2924	1462	9.4	0.1	699.0	175.7	225.3	46.5	0.3			1.4	482.3	61.6	0.2		3.2	15.0	0.2	2033
3		4.0	94.5	1466	2740	1368	8.7	1.7	677.6	178.2	436.7	45.6	0.2	285.3			549.6	71.6		4580	4.0	27.6	0.2	1980
9		4.0	90.0	1516	2310	1156	9.6	1.8		202.0	243.3	43.8	1.2	287.5		1.4	498.5	83.8		5091	11.9	41.8		1273
10	2.3	3.8	89.5	1425	2967	1481	9.6	0.1	679.4	189.6	290.4	58.0	1.0	184.5	3.6	1.4	589.2	80.8		6189	2.8	0.2		16
13	1.8	3.6	89.0	1567	2954	1490	10.2	0.6	497.2	201.6	341.0	50.4	1.7	251.8	8.3	1.2	538.4	90.7		5221	42.4	8.0	0.3	764
14	1.2	3.6	92.0	1595	2968	1525	9.5	0.7	472.2	203.1	385.9	55.8	1.4		0.7	1.2	564.7	82.8		8080	5.5	5.6	0.2	452
15	3.4	5.2	89.0	1461	2993	1497	9.6	0.9	639.4	199.5	281.1	51.2	3.4	266.3		1.6	535.8	94.8		5227	9.4	18.9	1.8	1603
16	3.7	5.7	85.0	1434	2942	1471	9.5	1.0	708.1	224.7	303.4	60.4	0.7	413.0		1.4	513.3	92.2			1.3	9.8	0.9	678
17	4.1	7.5	84.1	1334	2870	1431	10.1	0.8	655.2	195.6	330.0	50.0	2.4		0.1	1.1	482.7	49.7			7.2	9.5	0.9	664
20	4.1	7.6	86.0	1253	2897	1422	9.4	0.7	624.8	202.4	338.4	64.0	0.5	585.0	1.6	1.2	411.5	87.0		5753	7.0	7.0	0.7	469
21	3.8	7.9		1453	2897	1442	9.6	0.2	538.2	220.8	280.5	53.8	1.0	273.5	1.6	1.5	431.9	0.0						
24	4.1	7.6	85.0	1247	2880	1450	9.2	1.0	446.4	211.6	274.2	66.5	1.2	250.0	1.5	1.5	571.7	94.0		12788	10.9	27.6	0.7	465
30	4.1	7.2	88.0						380.8						7.2									
35	3.8	5.9	93.0	1007			10.2	0.4	481.1	224.0	273.5	79.0	0.7	304.5	1.5	0.0	526.5	105.1		6665	11.3	1.3	0.4	480
43	3.4	5.6		1916	2966	1483	10.1	1.3	418.0	220.0	322.3	67.5	0.9	677.0	1.0	2.9	533.0	112.1		11275	2.4	4.9	42.6	17
50	3.4	4.8		1591	2954	1477	9.5	1.3	310.0	243.0	351.1	73.0	0.7	627.0	1.0	1.2	483.1	95.7		14197	2.3	2.7		12
58	2.1	3.8		1307	2775	1390	9.5	0.9	718.0	197.0	317.0	42.0	0.1	281.0	1.9	1.5	717.0	55.0	0.7	4383	9.3	95.6	29.8	
62	3.9	6.2		1490	2887	1444	10.3	2.2	336.0	252.0	348.0	82.0	1.9	621.0	1.2	1.2	614.0	124.0		3396	33.4	1.5	26.2	9
64	4.1	6.3		1414	2980	1488	9.4	2.7	333.0	252.0	359.0	75.0	1.5	649.0	0.3	1.9	634.0	106.0		4146	99.9	1.8	26.3	9
70	3.4	6.2		1638	2880	1450	9.6	2.3	306.0	209.0	365.0	80.0	4.8	499.0	0.6	2.8	628.0	127.0		3941	267.7	1.1	16.8	6
72	4.6	8.3		1487	2906	1455	9.7	2.5	350.0	281.0	383.0	59.0	4.8	587.0	0.1	0.1	613.0	138.0		4292	144.6	0.9	16.9	
79	4.1	8.1		1535	2945	1472	9.9	2.3	323.0	262.0	362.0	77.0	5.0	449.0	0.2	4.7	612.0	124.0		4229	29.1	4.4	39.4	8
84	5.5	10.3		1466	2842	1421	10.1	2.2	310.0	267.0	374.0	62.0		726.0	0.3	2.6	612.0	129.0		9604	120.6	2.8	16.0	7
86	2.8	10.3		1488	2902	1451	9.9	2.0	278.0	587.0	360.0	61.0	5.8	623.0	1.2	0.2	620.0	139.0		10134	32.2	3.4	22.3	10

	OW 904B Water Analysis (ppm)																			Gas Analysis (ppm)				
Day	GSP	WHP	Temp	Enth. kJ/kg	Cond	TDS (ppm)	pH	B	SO_4	Cl	CO_2	F	H_2S	SiO_2	Ca	Li	Na	K	Mg	CO_2	H_2S	CH_4	H_2	N_2
1	2.1	3.2	94.0	1307	2222	1106	6.0		782.5	124.3		36.8	3.4	212.0		0.4	322.0	52.9	0.5		3.4			
3	3.6	7.9	87.0	1325	2183	1092	5.7	1.4	686.1	124.6		48.9	0.4	106.5		0.5	298.5	19.2	0.5	9166	8.6	45.0	2.4	3570
4	2.4	4.0	90.0	1466	2090	1045	5.9	1.0	732.2	133.5	172.6	49.1	0.2	238.8			359.0	48.4		10034	6.4	20.7	2.3	869
10	2.4	5.0	90.0	1516	3085	1540	8.8	0.9	591.2	177.1		49.4	0.2	207.7	3.4	0.8	347.3	46.3		8719	36.7	143.1	1.4	420
14	2.8	4.6	89.0	1567	2061	1037	9.7	0.9	401.6	168.3	337.9	61.8	0.8	285.7	1.1	0.6	350.7	42.4		8248	2.1	14.5	6.3	984
15	2.8	4.9	89.0	1595	2275	1137	9.1	1.0	515.3	182.8	171.6	51.8	1.4	0.0	2.0	0.9	434.3	45.0		21770	1.9	19.5	7.3	1090
16	4.4	6.5	83.0	1461	2286	1143	9.2	0.3	562.9	198.8	124.9	50.1	3.4	243.0		0.9	446.2	47.3		13084	13.0	29.4	3.7	1042
17	5.1	6.5	81.3	1434	2253	1126	9.2	0.5	556.1	203.8	171.8	59.1	0.5	326.0		0.8	419.4	45.0		4359	8.2	37.0	4.6	1270
18	5.0	6.9	85.0	1334	2259	1129	10.0	0.1	647.2	192.8	255.4	52.2	0.3	0.0	1.0	0.4	413.9	47.2		21677	26.5	32.7	3.7	1051
21	5.0	6.7	84.0	1253	2203	1102	9.4	1.0	524.1	198.4		52.3	0.3	546.0	1.8	1.0	350.6	46.6		10421	5.8	34.4	3.9	1094
24	4.5	6.7	84.0	1471	2031	1010	9.6	2.0	160.0	207.0	144.6	62.0	5.8	621.0	3.1		428.2	52.0		8993	15.6	29.9	3.8	846
25	5.1	6.9	85.0	1525	2271	1139	9.4	0.2	429.6	178.6	156.9	60.6	2.2	625.0	2.3	0.5	497.8	44.6		14065	13.5	31.5	4.3	1190
31	5.0	6.5			2894	1138	9.5	0.2	381.2	200.6	199.3	55.3		247.5	2.8		408.1	49.8		199				
36	3.6	5.4		1676			10.0	1.5	414.0	213.0	197.6	50.8	1.4	220.0	0.2		421.9	48.5		9525	8.9	3.5	10.3	362
44	3.5	6.2		1560	2366	1183	9.7	2.1	289.6	209.5	237.6	57.6	1.3	516.0	1.0	1.4	426.2	51.1		12243	120.6	3.8	20.7	136
51	4.1	5.2		2178	2390	1196	9.7	1.2	277.5	216.7	265.5	57.7	1.4	175.0	1.4	1.3	479.9	56.8		12744	6.3	3.4	23.0	103
58	3.5	7.6		1824	2350	1181	9.6	2.7	278.4	226.4	330.0	73.5	1.4	420.0	1.0	1.2	500.1	64.0		7937	2.5	3.0	22.2	311
63	3.9	7.6		2009	2341	1169	10.3	2.4	241.4	240.2	253.0	54.0	2.8	492.0	0.6	1.2	489.6	62.6		6458	74.6	6.8	3.4	337
65	4.3	7.2		2043	2376	1199	9.4	2.0	244.2	240.5	276.5	54.3	4.8	559.0	0.9	1.2	487.3	60.3		6240	28.3	6.3	2.3	
71	6.9	9.7		1535	2062	1029	9.8	2.1	217.9	186.7	290.8	50.6	8.2	446.0	0.7	1.1	460.8	78.3		5631	164.9	7.8	2.3	370
73	7.6	10.3		1690	2386	1193	9.7	1.7	232.4	255.0	294.4	53.5	8.1	677.0	0.7	0.9	454.9	71.8		7735	135.6	6.9	2.2	331
80	5.4	10.3		1481	2380	1190	10.0	1.8	214.7	227.0	262.9	57.9	9.5	502.0	0.7	1.1	457.3	76.7		9418	77.7	5.1	2.0	321
85	5.5	17.9		1812	2295	1147	10.2	2.0	189.1	231.3	290.2	54.4	8.5	652.0	1.1	1.2	459.1	87.6		12541	271.1	13.5	5.7	283
87	5.2	17.9		2168	2366	1182	9.9	1.9	208.0	249.0	275.9	53.2	7.8	758.0	0.8	1.1	455.0	128.1		21428	177.9	10.4	5.3	338
92	5.5	17.0		1924	2287	1143	9.7	2.8	193.1	247.9	286.9	54.1	8.2	479.0	0.3	1.1	495.1	142.5		10159	160.7	13.7	6.3	289
94	2.9	17.9		1857	2298	1140	9.6	3.0	206.5	303.6	278.1	52.9	6.9	473.0	1.4	1.2	455.9	131.1		8396	210.7	16.0	8.8	851

Water and Gas analysis (Cont)

	OW 909 Water Analysis (ppm)																		Gas Analysis(ppm)				
Day	GSP	WHP	Temp	Enth. kJ/kg	Cond	TDS (ppm)	pH	B	SO_4	Cl	CO_2	F	H_2S	SiO_2	Ca	Li	Na	K	CO_2	H_2S	CH_4	H_2	N_2
1	3.7	2.8	86.0	1552	3910	2737	9.6	0.1	177.3	652.8	294.4	229.0	0.3	358.0	1.6	0.4	779.0	215.7	8710.2	5.4	0.0	1.1	3188.0
5	3.1	6.2	89.0	2001	4000	2800	10.1	0.6	250.3	732.4	203.1	250.0	1.0	530.0	2.6	0.4	641.7		11302.9	2.8	2.3	12.3	380.1
8	2.9	6.9	86.0	1697	3999	2000	9.9	0.1	152.6	743.4	162.8	284.9	1.4	395.0	6.6	0.3	732.4	222.5	162.8	1.4	0.0	0.0	0.0
9	3.4	6.5	90.0	1875	4230	2961	9.4	0.4	179.8	765.7	202.8	323.6	1.2	652.0	0.4	0.4	852.9	255.5	3983.4	5.5	1.0	15.9	223.5
14	3.4	6.2		1904	4350	3045	10.0	1.0	85.0	772.3	275.7	310.7	0.3	436.5	0.4	1.9	770.0	270.7	5386.6	0.9	1.2	29.6	414.1
16	3.4	7.0		1783	4430	3101	9.8	0.6	109.4	875.4	255.4	305.5	0.5	441.0	0.1	0.3	869.1	274.2	4116.5	2.7	1.3	26.9	375.6
19	2.2	3.6		1831	4450	3115	10.0	0.0	0.0	827.9	230.6	235.0	0.3	943.0	0.3	0.4	900.0	260.4	9347.8	5.6	0.0	0.0	0.0
21	3.5	7.0		1696	5420	2711	10.3	2.9	81.2	817.6	179.1	292.4	0.7	932.0	0.2	2.8	850.8	304.3	13494.2	12.5	1.8	32.9	68.4
22	3.5	7.0		1990	5032	2516	10.0	2.7	69.9	786.6	218.7	257.4		898.0	0.2	2.0	913.4	287.4	6479.0	7.0	1.1	28.9	32.4
23	3.0	7.0		2220	6168	3100	10.1	2.2	95.8	803.7	261.6	191.9		738.0	0.2	2.8	905.8	280.2	13937.0	4.9	1.0	24.9	23.0
26	3.1	7.0		2051	2223	1104	10.0	1.6	132.3	780.5	255.0	287.8	0.5	950.0	0.5	1.1	909.3	286.0	8735.3	12.0	1.0	27.0	31.0
27	3.5	6.3		2015	3999	2000	9.6	3.3	116.7	803.6	226.8	263.9	0.7	598.0	0.1	0.4	954.4	270.0	12924.5	10.6	0.7	20.0	15.4
28	3.5	6.3		2070	4972	2486	10.0	3.9	116.6	806.8	248.2	249.0	0.5	664.0	0.2	2.7	954.0	274.6	7409.8	4.8	1.1	20.6	247.9
29	3.3	6.3		2050	2316	1155	10.0	3.5	115.6	822.0	230.6	261.7	0.3	831.0	0.2	2.1	962.6	374.6	5364.8	3.5	9.8	3.6	413.1
30	4.0	7.0		2028	4480	2000	9.8	2.5	112.5	812.3	266.9	264.5	0.7	812.0	0.1	0.2	950.2	357.8	14369.4	2.1	12.1	38.9	544.6
33	3.9	6.9		2029	4490	2000	10.0	2.7	114.2	810.9	289.7	250.7	0.7	760.0	0.1	6.6	939.2	398.3	2937.6	6.0	6.4	3.0	284.8
35	3.7	6.9		1955	4712	2358	9.9	5.9	88.2	810.2	232.3	244.9	0.7	693.0	0.2	6.1	903.3	388.5	4255.7	2.4	6.2	2.6	279.2
40	3.5	5.7		2273	5348	2674	10.6	3.3	83.7	816.1	202.2	270.3	0.9	950.0	0.1	2.2	925.5	360.3	7665.0	21.8	5.5	0.4	448.7
42	3.5	6.5		1834	5858	2929	10.3	4.7	82.4	849.2	216.7	287.1	2.4	645.0	0.2	0.0	909.6	373.1	3572.9	287.5	9.6	3.8	282.3
48	3.2	6.6		2089	9750	3750	10.1	5.8	62.6	682.5	294.1	236.7	0.9	769.0	0.3	6.2	893.6	396.5	3393.2	30.4	9.6	18.1	53.9
50	3.3	6.5		2065	5360	2690	10.0	4.1	46.1	847.1	280.3	263.9	3.1	965.0	0.2	7.3	863.9	387.6	3483.6	22.1	7.5	3.3	214.2
57	4.1	7.9		1985	5192	2598	10.2	4.6	46.9	822.2	183.5	259.7	3.0	500.0	0.2	2.0	911.0	380.4	5725.9	50.0	5.1	2.3	208.5
62	4.1	8.0		1993	4656	2328	10.3	2.2	51.6	843.0	265.0	273.2	1.2	886.0	0.1	1.3	912.1	434.1	4840.7	55.8	8.8	6.2	161.6
64	5.2	8.1		1991	4825	2420	10.2	4.7	42.7	719.5	286.2	272.0	3.4	926.0	0.1	6.0	892.9	340.2	8309.6	53.1	8.9	6.0	133.0
69	4.5	8.3		2016	4794	2398	10.0	5.0	38.9	872.7	222.4	289.8	3.4	835.0	0.7	2.8	951.6	281.5	4851.9	7.7	12.0	7.8	87.5
71	2.6	8.5		2235	2364	1181	9.8	4.7	41.6	836.4	245.7	230.7	3.4	443.0	0.3	1.1	974.1	363.2	3441.6	63.1	25.5	19.2	623.5
78	1.8	8.4		2150	5175	2550	9.9	4.6	25.8	836.4	251.7	226.0	3.4	569.0		1.4	942.7	165.3	4761.6	58.9	0.9	2.0	115.4
84	3.1	8.5		1996	4524	2260	10.5	4.6	47.4	936.0	184.4	230.2	3.4	716.0		2.7	1047.0		3942.0	72.3	13.4	3.5	674.2
85	3.7	8.4		2153	3243	1623	10.1	4.1	26.0	853.7	237.8	263.2	3.0	746.0		2.7	1003.0		6011.4	31.6	16.6	6.3	113.2
90	7.0	10.4		2168	5302	2651	10.6	4.3	47.2	848.9	170.9	257.9	2.9	884.0		2.9	995.0		6672.4	46.2	9.0	3.9	83.7
92	4.8	10.0		2219	4364	2680	9.9	4.7		591.3	199.3	235.0	3.7	725.0		3.0	1056.0		5314.3	74.6	2.9	1.3	165.3
97					5378	2689	10.3	3.3	50.7	824.7	244.0	244.0	2.7	512.0		2.9	807.5		4780.6	61.6	0.2	0.5	88.1
104	5.4	14.3		1527	6420	3210	10.7	3.4	7.7	545.3	213.0	305.2	2.8	831.0		3.0	734.0		6163.2	38.1	1.1	2.5	267.2
106	4.8	14.3		2072	4320	2200	10.5	3.8	24.5	545.3	192.1	260.9	3.0	583.0		2.9	1040.0		4186.4	14.9			132.4
112	5.2	23.1		1872	4980	2490	11.0	3.7	27.5	812.1	165.2	307.6	2.4	703.0		3.0			165.2	2.4			
118				1994			11.0	3.8	21.3	799.2	147.4	255.6		560.0		3.0			147.4				
121	1.7	7.2		1232			10.9																

Deep fluid concentrations

Well/Sample No.	pH	B	SiO_2	Na	K	Mg	Ca	F	Cl	SO_4	TDS	CO_2	H_2S	H_2	CH_4	N_2
903B - 13	7.0	0.7	176.2	402.8	66.2	0.0	1.1	46.9	149.1	314.5	1021.7	1239.6	1.7	0.1	2.3	38.1
903B - 18	7.5	0.6	198.0	505.2	38.8	0.5	1.3	29.6	138.8	505.9	979.4	585.9	0.8	2.5	7.9	0.0
903B - 20	7.7	1.9	457.3	446.7	74.7	0.0	0.2	52.8	177.6	234.6	1048.4	592.2	9.2	2.2	0.1	0.7
903B - 21	7.8	1.6	351.6	442.5	89.5	0.0	0.4	56.4	147.3	215.6	1021.7	580.8	25.4	1.4	0.1	0.5
904B - 11	7.2	1.4	424.0	292.4	35.5	0.0	2.1	42.3	141.3	109.3	689.6	991.3	5.0	0.4	3.0	85.4
904B - 12	6.9	0.1	426.8	339.9	30.5	0.0	1.6	41.4	122.0	293.3	777.7	1510.0	2.6	0.4	3.2	120.1
904B - 16	7.0	0.8	119.5	327.7	38.8	0.0	1.0	39.4	148.0	189.5	816.6	1443.9	1.5	2.3	0.3	10.4
904B - 19	7.4	1.4	381.7	332.7	41.2	0.0	0.6	37.1	164.2	166.7	818.7	792.2	5.7	0.2	0.6	0.0
904B - 24	7.1	1.3	517.6	310.7	360.6	0.0	0.6	36.3	170.0	142.0	807.1	2321.9	22.5	0.5	1.0	34.1
904B - 25	7.3	1.9	327.1	338.1	97.3	0.0	0.2	36.9	169.3	131.9	780.5	1191.7	21.0	0.6	1.4	29.2
909 - 12	7.3	1.9	352.7	562.8	159.2	0.0	0.1	155.6	473.9	68.8	1179.0	1962.3	1.8	2.9	0.1	2.2
909 - 15	7.4	1.5	478.9	560.4	211.0	0.0	0.1	156.0	479.0	66.3	1179.5	2188.3	0.6	5.6	1.7	78.4
909 - 17	8.0	3.5	408.7	532.7	229.1	0.0	0.1	144.4	477.8	52.0	1390.6	718.1	0.7	0.4	0.9	40.3
909 - 20	8.3	3.4	453.5	527.0	233.8	0.0	0.2	139.6	402.5	36.9	2211.5	624.8	4.9	2.6	1.4	7.9
909 - 22	7.8	2.7	294.9	537.5	224.3	0.0	0.1	153.2	484.9	27.7	1532.1	912.3	8.6	0.3	0.7	30.0
909 - 26	7.9	2.8	261.3	574.5	214.2	0.0	0.2	136.0	493.2	24.5	696.5	609.1	10.7	2.8	3.7	90.6

Appendix II

Trends in the discharge contents of Olkaria Domes wells

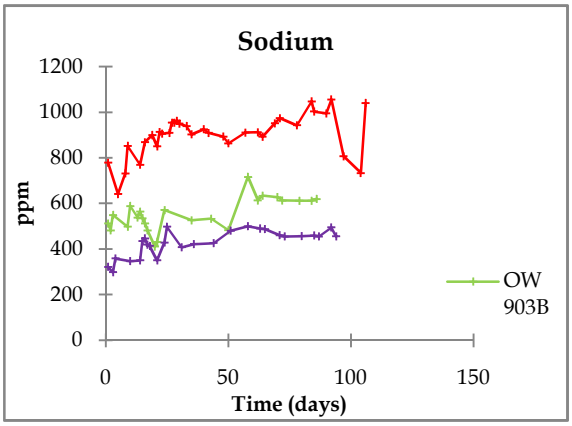

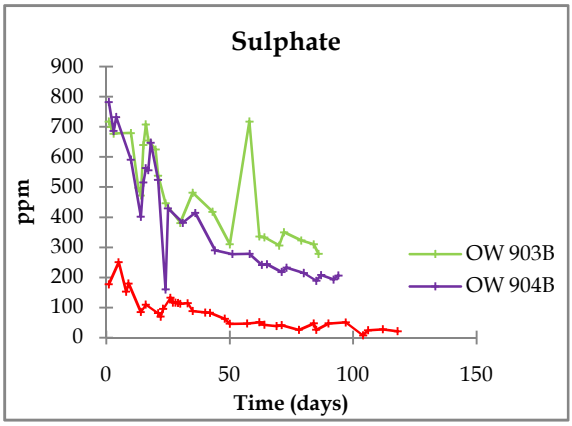

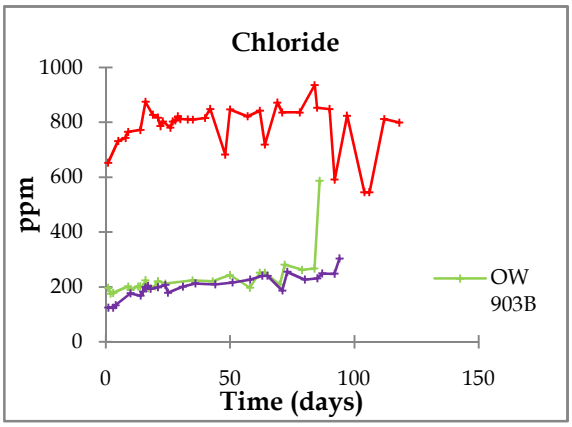

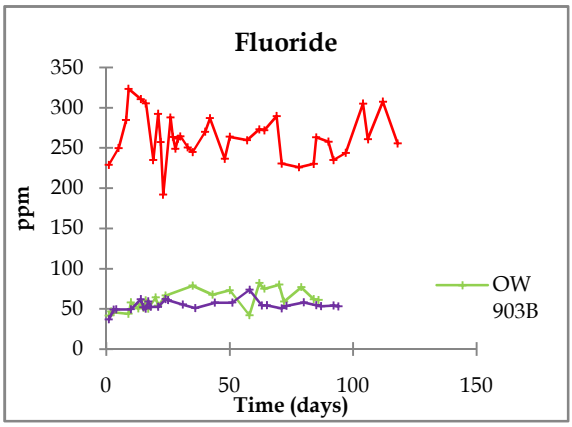

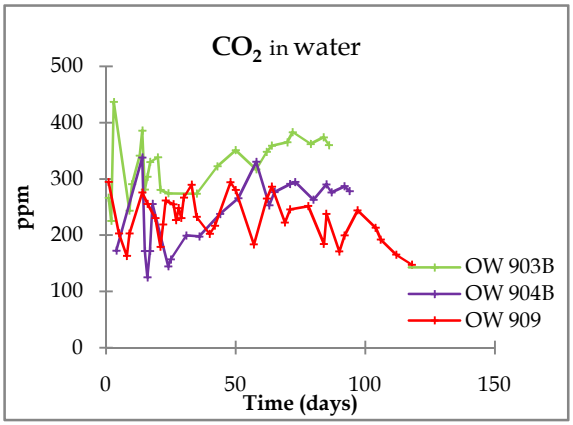

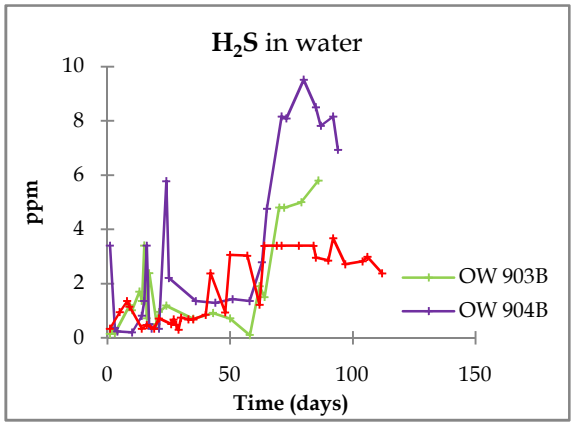

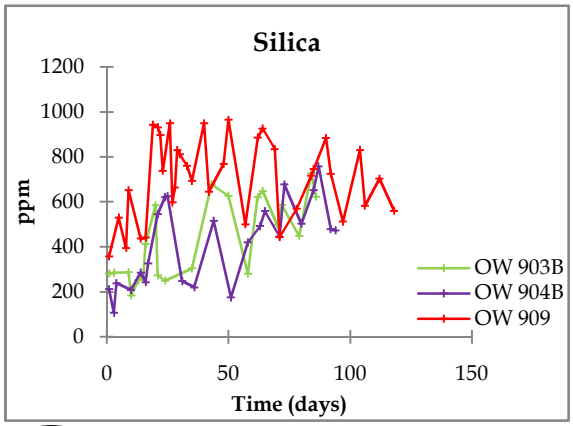

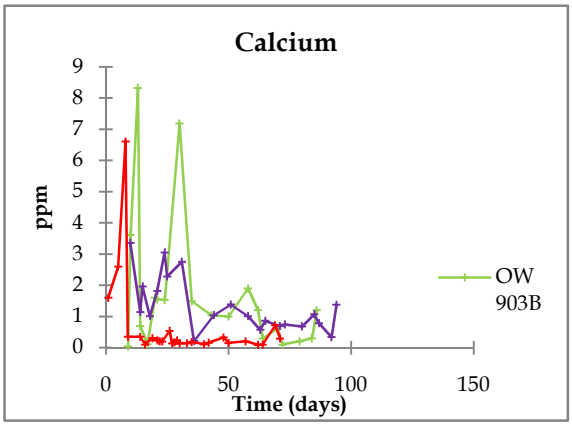

Trends in the discharge contents of Olkaria Domes wells (Cont.)

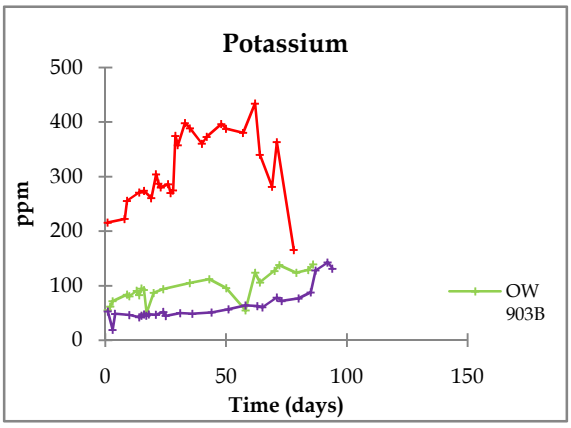

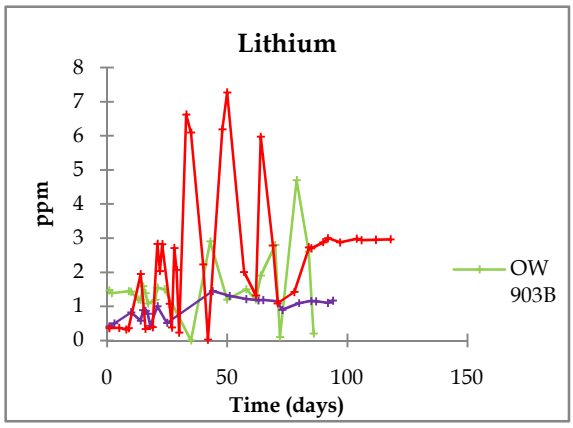

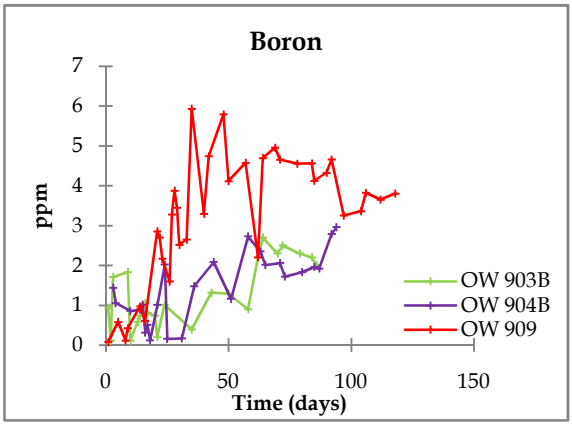

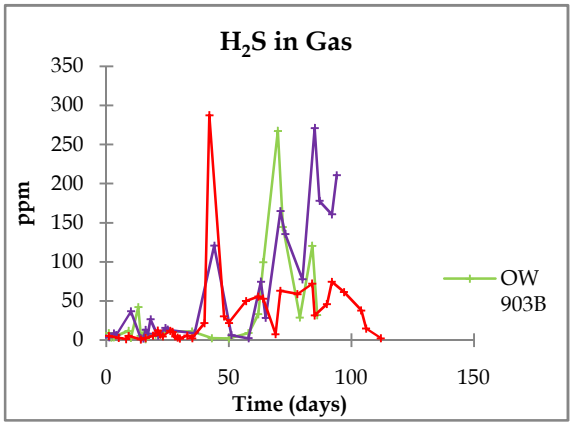

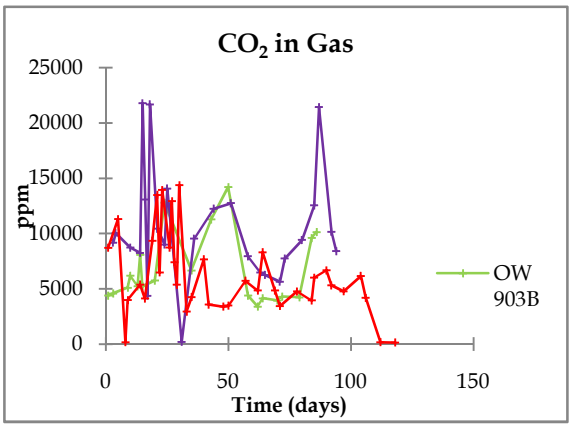

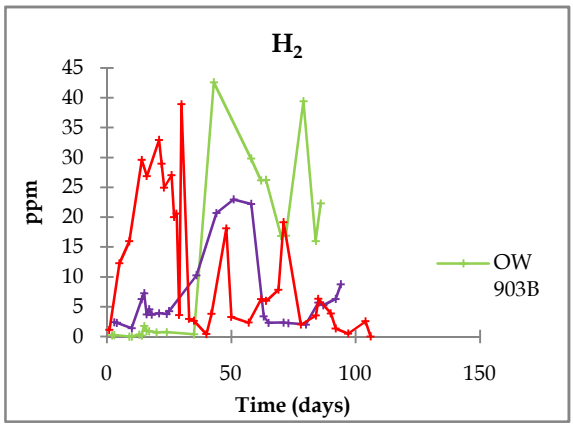

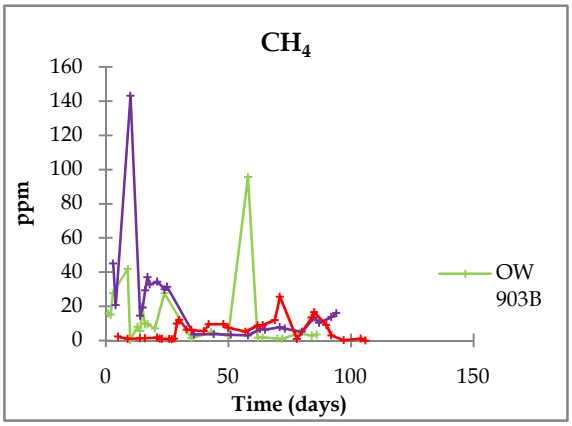

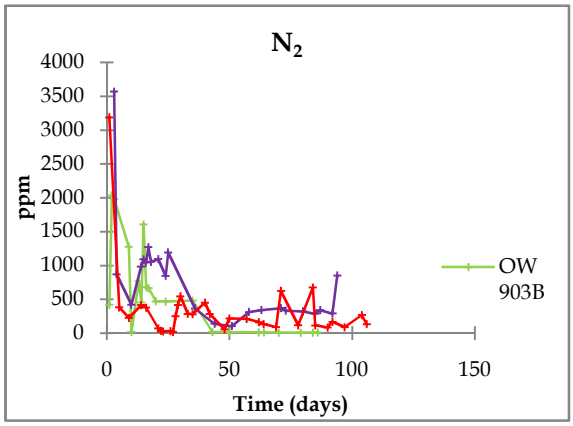

Appendix III

Deep fluid chloride correlation with other elements.

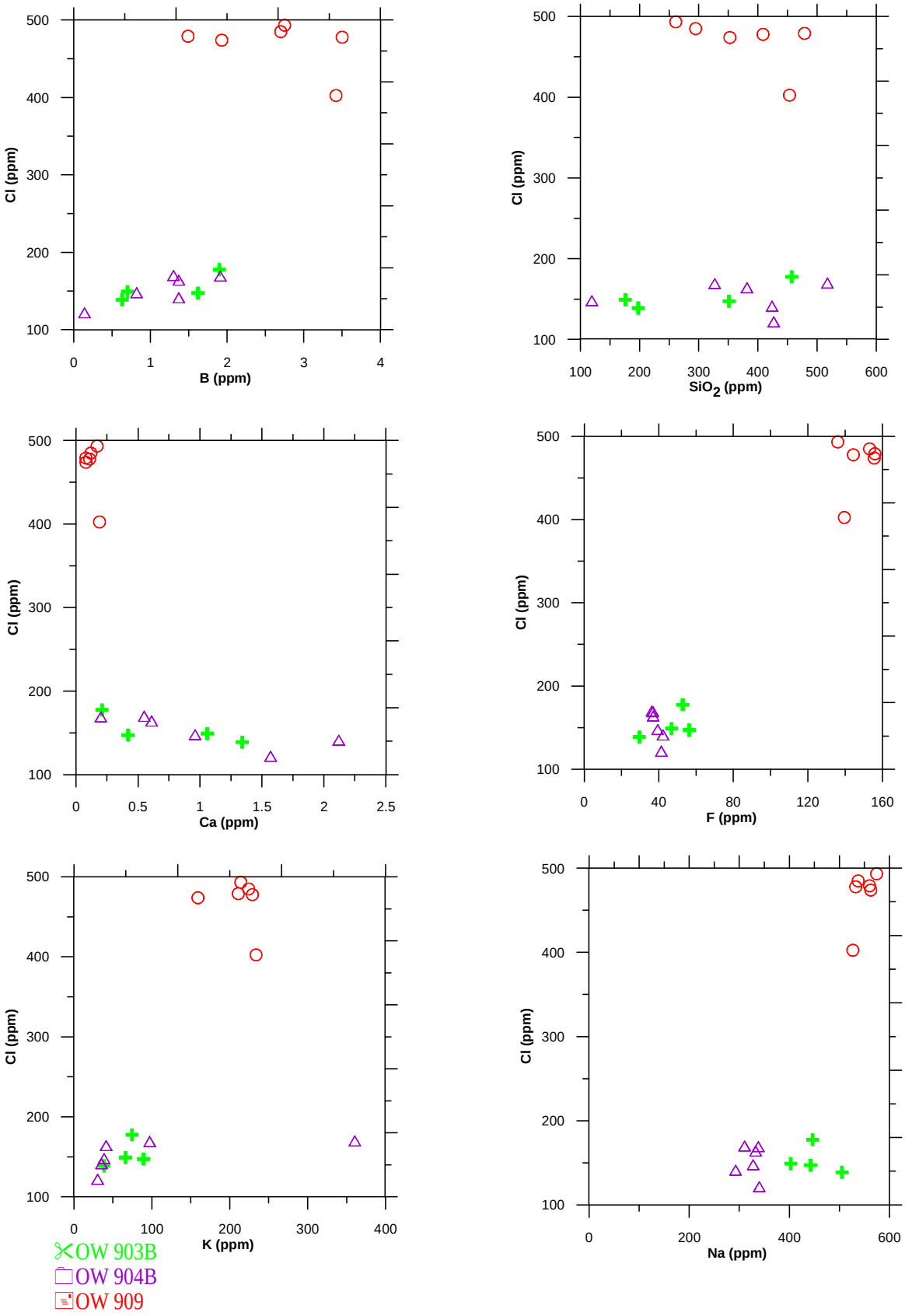

GEOTHERMAL PROSPECTING BY GEOCHEMICAL METHODS IN THE QUATERNARY VOLCANIC PROVINCE OF DHAMAR (CENTRAL-WESTERN YEMEN)

Angelo Minissale[(1)], Orlando Vaselli[(1,2)], Mohamed Mattash[(3)], Giordano Montegrossi[(1)], Franco Tassi[(2)], Abdulsalam Ad-Dukhain[(3)], Ulrich Kalberkamp[(4)], Ali Al-Sabri[(3)], Taha Al-Kohlani[(3)]

(1) CNR-Italian Council for Research, Institute of Geosciences and Earth Resources of Florence,Via La Pira 4 - 50121 Firenze (Italy)
(2) Department of Earth Sciences, University of Florence, Via La Pira 4 - 50121 Firenze (Italy)
(3) Ministry of Oil and Mineral Resources, Geological Survey and Minerals Resources Board, P.O. Box 297, Sana'a (Yemen)(4) Federal Institute for Geosciences and Natural Resources (BGR), Stilleweg 2 - 30655 Hannover (Germany)

ABSTRACT

This paper deals with geothermal prospecting carried out in the Quaternary volcanic field of Dhamar, which is located almost in the centre of the main Oligo-Miocene basaltic trap plateau of Yemen.

By applying geochemical and thermometric techniques in domestic wells producing from a shallow unconfined aquifer that is prevalently hosted within the Quaternary volcanics, a thermal anomaly associated with the Quaternary volcanic activity was well delineated. Although the aquifer has a Ca-Na-HCO_3 composition, that is typical of shallow aquifers, there are several anomalies in the thermal area compared to typical aquifers: the *p*H is lower and the calculated partial pressure of CO_2 in solution, electrical conductivity, salinity and fluoride ion concentration are higher. Such chemical anomalies are not generated by the rising and/or mixing of deep hydrothermal components into the aquifer, but rather produced by enhanced water-rock interaction processes resulting from the higher temperature of the aquifer.

The application of calculations based on the likely temperature of rainfall in the area and the depth and temperature of individual wells, the local thermal gradients in the area have been calculated. The thermal gradient varies from 41 °C/km at the periphery of the thermal anomaly to more than 250 °C/km, within an extensive area (exceeding 200 km^2) where the gradient is greater than 100 °C/km.

KEYWORDS: Yemen, Dhamar, geothermal prospection, thermal anomaly

GEOCHEMICAL ASSESSMENT OF KARISIMBI GEOTHERMAL PROSPECT, RWANDA

Jean Nepomuscene Namugize[(1)*], Uwera Rutagarama[(1)]
(1) Unit of Geothermal Development, Energy Sector, Ministry of Infrastructure, P.o.Box 24 Kigali, Rwanda.
**Corresponding author e-mail: jnepo.namugize@mininfra.gov.rw*

ABSTRACT

Karisimbi geothermal prospect is located in border between Rwanda and Democratic Republic of Congo, with an elevation of 4,507 m above sea level. Karisimbi is a strato and young volcano with recent lava age varying between 240,000 and 90,000 years and comprised in the Western Branch of East African Rift System. Moreover the Virunga complex has some active volcanoes, latest Nyamuragira eruption in January 2010 and Nyiragongo in 2002. This work presents the available geochemical data within the Karisimbi Prospect.

Water chemistry analyses of rainwater, snow, rivers, lakes, cold springs, mineralised springs and hot springs were carried out. In total 24 sampling sites were chosen for stable isotopes, cations, anions, strontium and tritium by the Federal Institute for Geosciences and Natural Resources (BGR).

Analytical results showed significant concentrations in trace elements such as Rubidium, Cesium, Baryum, Beryllium, Gallium, Germanium concentrations in the six locations which suggest a geothermal character. Results for anions measurements in waters except one site draining into Karisimbi crater are predominantly bicarbonate waters representing cold ground water. The results of precipitation, cold ground water and hot springs have indicated a good permeability and subsurface temperatures in excess of 100°C at six locations thus making production of electricity using a binary fluid possibility.

Key words: Karisimbi volcano, Easter African Rift System, stable isotope, Virunga complex

GEOCHEMISTRY OF KATWE-KIKORONGO, BURANGA AND KIBIRO GEOTHERMAL AREAS, UGANDA

Godfrey Bahati, Kato Vincent, Nyakecho Catherine
Department of Geological Survey and Mines, P.O Box 9, Entebbe, Uganda
Email: gbahati@gmail.com, kato_vicent@hotmail.com, ncathy.geology@gmail.com.

ABSTRACT

Reconnaissance surveys have been carried out on the geothermal areas of Uganda since 1935 when the first documentation of Uganda's hot springs was made. Recent studies have focused on three geothermal systems of Katwe, Buranga and Kibiro all located in the active volcanic belt in the Western Rift valley along the border of Uganda and the Democratic Republic of Congo. The Western Rift Valley is characterised by geothermal systems and saline and fresh water lakes. The three areas were chosen for the study because of their volcanic and tectonic features that indicate a powerful heat source and high permeability. The objective of the study is to develop geothermal energy to supplement hydro and other sources of power to meet the energy demand of rural areas in sound environment.

The results from geological and geochemical studies indicate that all the three areas are potential geothermal prospects. Their hydrothermal systems appear to be relatively old and rise from volcanic basement rocks rather than from the young overlying sediments. Stable isotope data suggests a similar origin of the geothermal fluids and the meteoric water. The high carbonate contents and salinity in the range of 25,000 - 30,000 and 14,000 - 17,000 mg/kg total dissolved solids of the geothermal waters from Katwe and Buranga respectively, affect their magnesium and calcium concentrations hence throwing the validity of some conventional methods of interpretation into doubt. Taking these doubts into account, reservoir temperatures of 150 - 220˚C and 120 - 150˚C are inferred by geothermometry for Katwe and Buranga respectively. Mixing models applied to the Katwe waters predict a reservoir temperature of about 230˚C. The chemistry of the surface fluids from Kibiro on the other hand suggests a mixture of thermal and cold waters with a pH of 6 to 8, and salinity of up to 4,000 - 5,000 mg/kg total dissolved solids. The fluids are relatively dilute compared to those of Katwe and Buranga and would probably cause a few problems on exploitation. Geothermometry and mixing models predict a reservoir temperature of 200˚C and above for Kibiro.

The predicted reservoir temperatures for the three areas could be suitable for electric power generation and direct use in industry and agriculture.

Key Words: Western Rift Valley, Katwe, Buranga, Kibiro, Geothermometry.

INTRODUCTION

The three geothermal areas namely Katwe-Kikorongo (Katwe), Buranga and Kibiro are situated in the Western branch of the East African Rift System that runs for most of its length along the border of Uganda with the Democratic Republic of Congo (DRC) (Figure 1). The Western Rift valley is marked by intensive faulting, often accompanied by volcanic and seismic activities, and commonly geothermal systems. Geothermal resources are estimated at about 450MW in the Ugandan Rift System (McNitt, 1982).

Since 1992 systematic exploration has been going on in three geothermal areas of Katwe-Kikorongo, Buranga and Kibiro located in the districts of Kasese, Bundibugyo and Hoima respectively. The three areas were chosen as priority areas because of their volcanic and tectonic features that are indicators of heat sources and high permeability. The exploration has been centered on geological, geochemical, hydrological and geophysical investigations with the aim of locating suitable sites for drilling. This paper presents the current status of the geochemical model of the three study areas.

THE STUDY AREAS

Katwe Geothermal Prospect

The Katwe geothermal prospect is situated in the Katwe-Kikorongo Volcanic Field (KKVF), south of the Rwenzori massif in Kasese district. The KKVF is bordered to the south by the Lake Edward and Kazinga Channel and to the east by Lake George (Figure 2). The prospect stretches from Lake Katwe to Lake Kikorongo and is bordered to the south by Lake Edward and the Katwe – Katunguru road, to the west by River Nyamugasani, to the north by the Kikorongo – Bwera road and to the east by the Katunguru – Kasese road.

The geology of the Katwe geothermal prospect is dominated by explosion craters, ejected pyroclastics, tuffs with abundant granite and gneissic rocks from the basement (Figure 2). The volcanic rocks, composed mainly of pyroclastics and utramafic xenoliths, are deposited on the extensive Pleistocene lacustrine and fluvial Kaiso beds and in some places directly on Precambrian rocks. Minor occurrences of lava are found in the Lake Kitagata and Kyemengo craters. The age of the volcanic activity has been estimated as Pleistocene to Holocene (Musisi, 1991).

The deposit is greyish, generally coarse-grained and calcareous. Travertine cones (Tufa), which are indicators of extinct hot spring activity, are a common feature in the Lake Katwe crater. Other travertine deposits have been found in Lake Nyamunuka, Lake Kasenyi, and Lake Kikorongo and at Kikorongo junction. The volcanic setting of this prospect gives an indication of a heat source.

Outside the crater area the geology is characterized by surficial deposits to the east and the west, and to the north lie the Rwenzori Mountains whose geology is dominated by gneisses and in some places granites and quartzites along the Kikorongo - Kasese road. South of Lake George lies the Bunyaruguru volcano which has a number of craters and crater lakes, believed to have been formed at the same time as the KKVF but has no surface geothermal manifestations. East of the Bunyaruguru volcano and Lake George from south to north are phyllitic stales, quartzites, gneisses and schists (mica and talc).

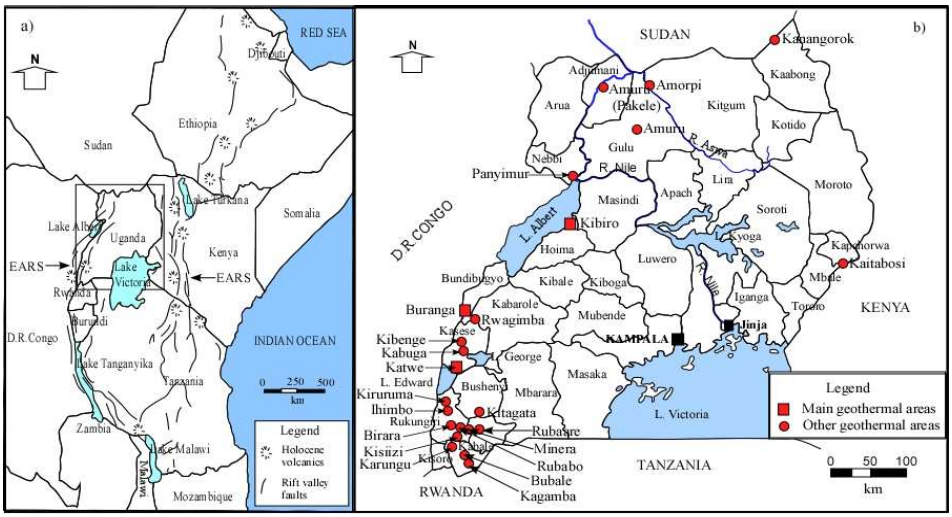

Figure1: **a)** East African Rift Systems (EARS) **b)** Location of the geothermal areas in Uganda.

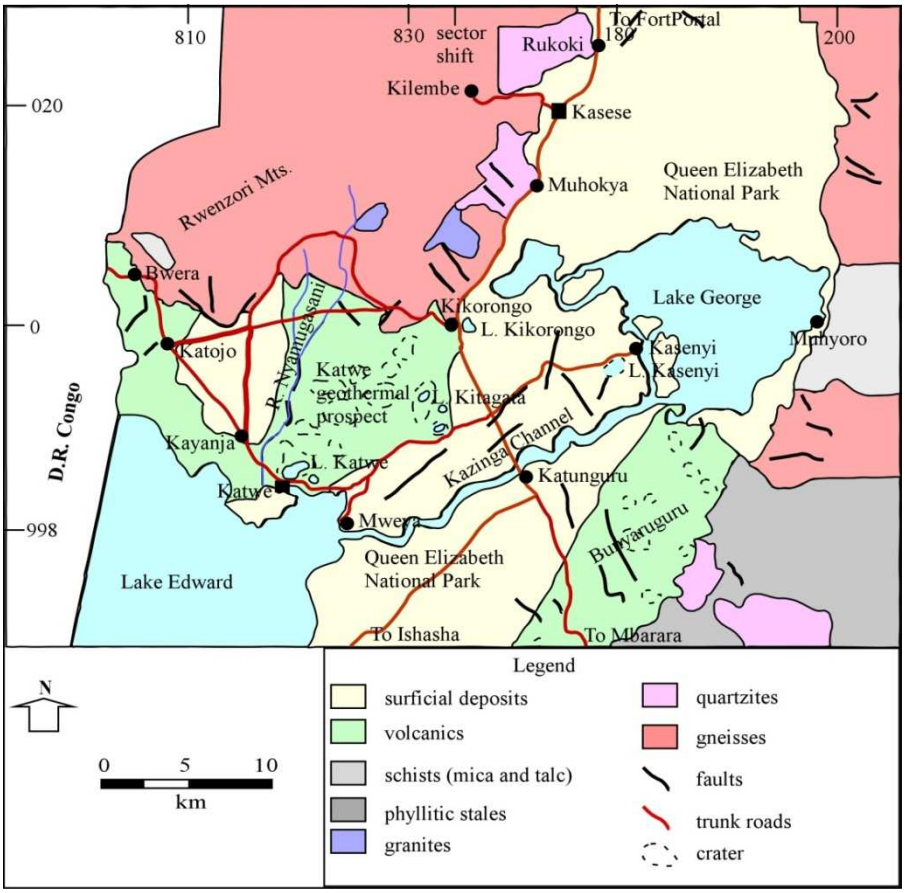

Figure 2: The geology of the Katwe-Kikorongo volcanic field and surroundings

Buranga Geothermal Prospect

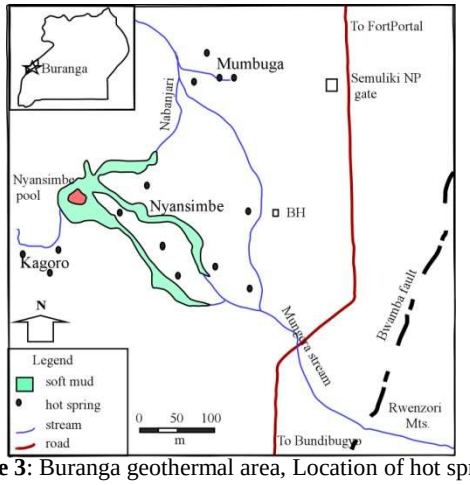

Figure 3: Buranga geothermal area, Location of hot springs.

The Buranga geothermal prospect is located at the foot of the Rwenzori massif in Bundibugyo district, West Uganda (Figure 3).

Buranga is localized by the major Rift Valley faults. It has a simple geology characterized by 'Epi - Kaiso' beds and 'Peneplain Gravels' (of Upper to Middle - Tertiary age), sediments which consist of boulder beds and unsorted scree overlying sands and clays. These sands and clays are described as Kaiso - Kisegi beds. They have been thrown against Pre-Cambrian migmatites and gneisses by the main fault, which strikes at 45˚ azimuth and dips at 60 - 65˚NW. Buranga has no evidence of volcanism but is highly tectonically active.

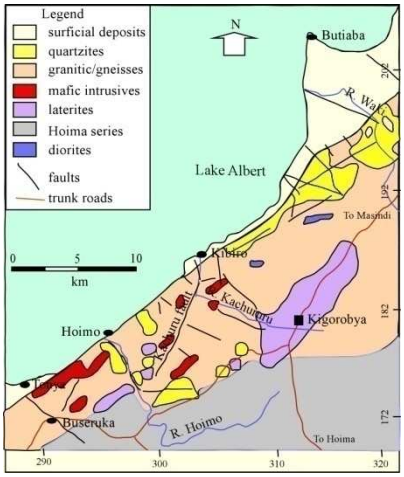

Kibiro Geothermal Prospect

The Kibiro geothermal prospect is located on a small peninsula in Lake Albert under the Rift Valley escarpment in Hoima district (Figure 4).

The Kibiro geothermal prospect is divided into two entirely different geological environments by the escarpment, which cuts through the field from SW to NE. To the east of the escarpment the geology is dominated by an ancient crystalline basement, characterized by granites and granitic gneisses. To the west lie a thick accumulation of thick sequences of rift valley sediments of at least 5.5 km, but without any volcanic rock on the surface (Figure 4).

Figure 4: The geology of the Kibiro geothermal prospect and surroundings fault.

Along the escarpment and NE of Kibiro is a stretch of quartzites, which are also found SW of Kibiro. Laterite is the main feature along the Kigorobya–Biiso–Masindi road. Also present are mafic intrusives along the Kachuru Kigorobya–Kibiro road and extreme SW near Buseruka and Tonya. South of Kigorobya lie the Bunyoro (Hoima) series which are sedimentary beds (meta-sediments) mainly represented by phyllites, tillites and sandstone.

Recent geological and geophysical studies show that the geothermal resource can be traced along faults in the block faulted granites to the east away from the rift. The Albertine rift is seismically active, characterized by deep-seated (27–40 km) large earthquakes. The tectonic pattern within the Kibiro geothermal area is very complex, and this complexity may well be the main contributor to the existence of a potential geothermal reservoir (Gislason et. al., 2004).

FIELD ACTIVITIES

The main activities of the geochemical investigation centred on chemical sampling of geothermal surface manifestations (hot springs), surface and ground waters temperature, pH-field and conductivity measurements; analysis of the samples for major and minor components and stable isotopes; and data analysis and interpretation. The sampling was done in 1993-1994 during the Geothermal Energy Exploration I project. The sampling locations are presented in figures 5, 6 & 7.

Hot springs with flow over 0.5 L/s were preferentially sampled since these were less likely to have been affected by dilution and evaporation (Mohan, 1963). Water samples were collected in a jug (on a rod, at Nyansimbe pool) so that they could be obtained from the center of the spring. Each spring was sampled at its hottest part, which was presumed to be the point where hot water enters the pool. The waters were transferred to a rinsed 100ml plastic bottle.

The untreated water samples were to be analyzed for pH-lab, SO_4, and bicarbonate. PH was also measured at the time of field collection. Another set of water samples were treated at the time of collection (filtered through 0.4µm filters and acidified with a measured amount of Nitric acid, 1ml of acid per 100ml of water sample). This was to ensure that the analyses represent the chemistry of the thermal waters as closely as possible.

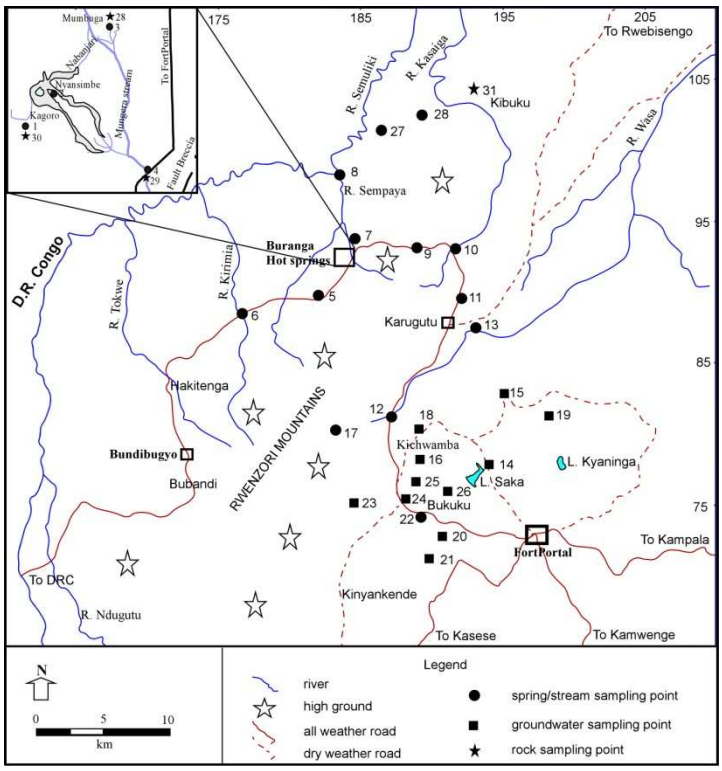

Figure 5: Buranga Geothermal, surface and ground water sampling points.

These samples were then collected into a rinsed 50-ml polythene bottles and was to be analyzed for Chloride, silica and major cations. By bottling the samples at the sampling temperature, errors arising from evaporation were minimized (Mahon**, 1961).**

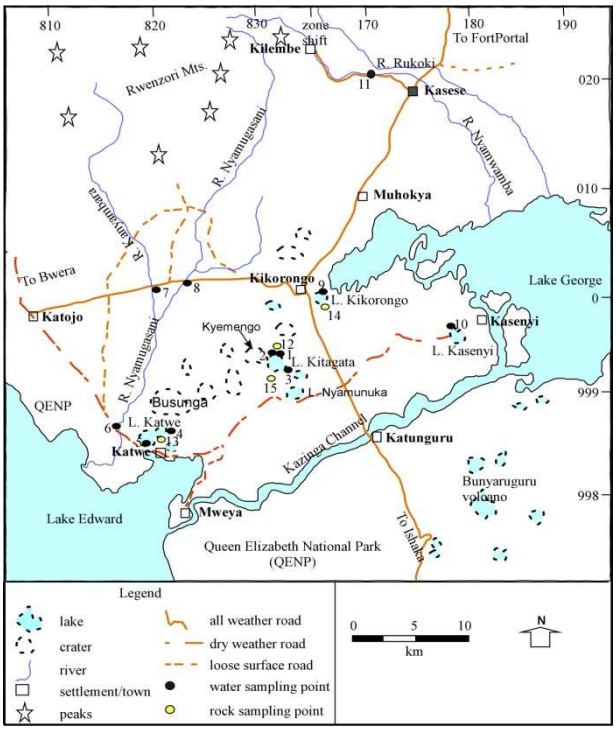

Figure 6: Katwe Geothermal, surface and **ground water sampling points**

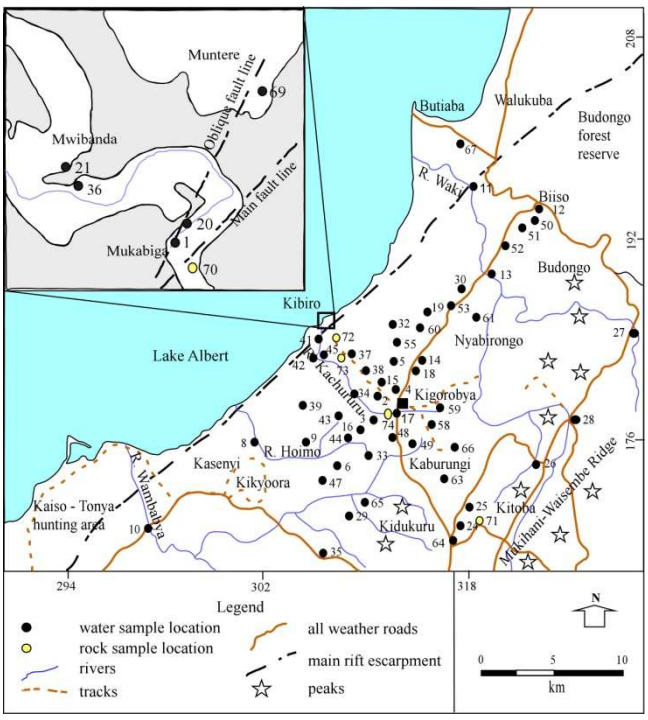

Figure 7: Kibiro Geothermal, surface and ground water sampling points.

RESULTS OF CHEMICAL ANALYSIS AND DISCUSSION

Laboratory analysis was carried out at BGR, Germany. The results are summarized in table 1 below. All samples are near neutral to slightly alkaline.

Katwe

The geochemistry results reveal the existence of a geothermal system in the Katwe prospect. The geothermal fluids are characterized by high

Carbonate contents and salinity, two of the hot springs sampled in the Lake Kitagata crater, HS-02 and HS-05 have a salinity of 19,410 and 27,770 mg/kg total dissolved solids respectively. The high carbonate affects the concentrations of Ca and Mg which are less mobile and tend to precipitate out of solution as Ca and Mg carbonates rendering the geoindicators involving the two cations unreliable. Solute geothermometers have been difficult to use in Katwe due the high salinity of the fluid. The sulphate concentrations are relatively high and all indications suggest that the geothermal system is relatively old. Relatively low B values compared to Cl and Li suggest that the fluids are more likely to originate from volcanic basement rocks rather than from the young overlying sediments. Some indications of possible mixing with groundwater were inferred from log (Q/K) diagrams (Ármannsson 1994) predicting a temperature of 140 - 160°C. The NaK geothermometer (Arnórsson et al., 1983b) and quartz geothermometer (Fournier and Potter, 1982) give temperatures of 140 – 160°C and 120 - 140°C respectively for the on shore hot spring waters in the Lake Kitagata crater (Ármannsson (1994). It was difficult to get a representative sample from the offshore hot springs in Lake Kitagata during the study. The samples collected at different times were variable mixtures of the geothermal water and lake water. However high levels of H2S (7 - 40 ppm) measured in the mixed water at the different times suggest the source of the geothermal water to be volcanic and hydrothermal.

Buranga

The fluids are neutral with a PH of 7-8 and salinity of 14,000 – 17,000 mg/kg total dissolved solids. In the earlier study by Ármannsson (1994) a good agreement was obtained for all solute geothermometers tested for several hot springs and pools in Buranga and it was concluded that the subsurface temperature was 120-150°C. Gas analysis did not show presence of hydrogen indicating that the subsurface temperature cannot exceed 200°C. There are no indications of mixing of the geothermal and cold water.

Kibiro

The geochemistry results suggest a high temperature geothermal system in the Kibiro geothermal prospect. The fluids are characterised by a neutral pH, and salinity of up to 4,000 - 5,000 mg/kg total dissolved solids. Cl of the geothermal waters is high compared to the SO4 and HCO3 concentration and is classified as mature waters suitable for application of geoindicators. Relatively low B values compared to Cl and Li suggest that the fluids are more likely to originate from volcanic basement rocks rather than from the young overlying sediments. Ármannsson (1994) found that results for different geothermometers for hot water samples from Kibiro fell into two groups, one showing a temperature of about 150°C and another 200 - 220°C. The geothermometers that gave the lower temperature were one component solute geothermometers, e.g. quartz, and geothermometers based on ratios of components that equilibrate fast, e.g. K-Mg. The higher temperature was obtained by geothermometers based on ratios between components that equilibrate more slowly, e.g. Na-K, and gas geothermometers. The use of mixing models (SiO2-enthalpy, SiO2-CO2) and the construction of log (Q/K) diagrams supported this model. These observations suggest that the geothermal fluid is a mixture of a hot water component at 200 - 220°C and cold water producing a second equilibrium at 150°C. A subsurface temperature of 200 - 220°C is therefore inferred by geothermometry and mixing models for Kibiro. The fluids are relatively dilute and would probably cause few problems on utilization.

CONCLUSIONS

From the chemistry of the waters from the surface manifestations, hot springs, there are indications of high subsurface temperatures in the Katwe geothermal prospect. Geothermometry has predicted reservoir temperatures in the range of 150 - 200˚C. The fluids in the crater lakes and springs are saline and alkaline and are probably concentrated by evaporation and/or modified by near surface processes, but the reservoir fluids may be more dilute. This is supported by the low salinity of the geothermal waters sampled from the hot springs in the Lake Kitagata crater as compared to its lake water. The fluids would be suitable for direct power production.

The reservoir temperatures for Buranga are estimated at 120 - 150˚C by geothermometry. There is plentiful supply of fluid, which is fairly saline with total dissolved solids of up to 14,000 - 17,000 mg/kg. This fluid would be suitable for binary turbine power production and industrial use.

Chemistry and stable isotope data interpretation has indicated mixing of geothermal water and cold groundwater in Kibiro. A subsurface temperature of 200˚C and above is predicted by geothermometry and mixing models. The geothermal fluid is less saline, neutral, with total dissolved solids of approximately 4,000 - 5,000 mg/kg. This fluid would be suitable for direct power production.

REFERENCES

Ármannsson, H., 1994. Geochemical Studies on three geothermal areas in West and Southwest, Uganda. Geothermal Exploration UGA/92/003, UNDESD, GSMD, Uganda, 85pp.

Arnorsson, S., Gunnlaugsson, E., and Svavarsson H. (1983). The chemistry of Geothermal Waters in Iceland III. Chemical Geothermometry in Geothermal Investigations. Geochim. Cosmochim. Acta, 47, 567 - 577.

Fournier, R.O., and Potter, R.W. II. (1982). An equation correlating the solubility of quartz in water from 25°C to 900°C at pressures up to 10,000 bars. Geochim. Cosmochim. Acta, 46, 1969-1974.

Gislason, G., G. Ngobi, E.M. Isabirye, and S. Tumwebaze, 1994. An Inventory of three Geothermal Areas on West and Southwest Uganda. Prepared by the United Nations for a Project of the UNDP.

Gíslason, G., K. Árnason, H. Eysteinsson, 2004. The Kibiro Geothermal Prospect. A Report on a Geophysical and Geological Survey. Prepared for the Icelandic International Development Agency and the Ministry of Energy and Mineral Development, Uganda. Unpublished report, June 2004. 109 pp.

Groves, A.W., 1930. Report on the nature, origin and available supply of the salt of Lake Katwe, Kasenyi, with notes on Lake Kikorongo and an appendix of the petrography of volcanic bombs of the district.

Kato, V., 2003. Geology of Katwe – Kikorongo Prospect. Unpublished DGSM Report KVK-22.

McNitt. J.R. (1982). The geothermal potential of East Africa. Proceedings of the Regional Seminar on Geothermal Energy in Eastern and Southern Africa held in Nairobi, Kenya. p 3 - 8.

Musisi, J., 1991: The neogene geology of the Lake George-Edward basin, Uganda. PhD. thesis.

Table 1: Katwe analytical results. Concentrations in (mg/kg) and (‰) for stable isotopes

Location	Sample No.	Temp. (°C)	pH	CO_2	H_2S	SiO_2	Na	K	Ca	Mg	SO_4	Cl	B	Li	$\delta^{18}O$	δD	TDS
LKatwe13	UG-93-01	28.6	7.61	156	0	29.3	44.7	35.1	10.1	5.92	7.0	3.9	0	0.003	-3.52	-9	132
L.Katwe6	UG-93-02	28.5	9.64	11316	5.3	88.6	25600	3500	0.1	0.95	9940	19000	1.9	0.067	1.9	-6	72000
L.Nyamunu1	UG-93-03	27.5	9.42	5523	0	32.2	8950	722	0.13	0.49	6450	3340	0.27	0.025	1.12	9.1	24690
L.Edward1	UG-93-04	23.3	8.55	223	0	18.2	83.7	41.5	16.8	27.3	18	20.2	0	0.01	2.52	22.1	254
Katunguru1	UG-93-05	26.6	6.95	1000	0	53.7	952	89.7	296	232	1800	723	0	0.023	-1.88	-8	4870
L.Kitagata5	UG-93-06	66.6	8.41	3105	0	91	9310	644	0.6	0.85	13400	2430	0.82	0.063	-0.73	0.5	27770
L.Kitagata2	UG-93-07	56.6	8.03	2544	0	105	6510	523	1.45	6.27	8970	1770	0.59	0.031	-0.6	3.2	19410
KazingaCh1	UG-93-08	26.2	8.28	108	0	21.5	38.5	7.8	22.9	11.2	11	10.3	0.06	0.005	0.98	12.6	180
L.Kitagata1	UG-96-06	61.1	9.33	10350	19.4	210	33600	1840	4.1	2	44000	8370	2.77	0.16	2.2	0	99515
L.KitagataW	UG-93-28	36	9.57	19470	0.3	389	87300	4780	4.3	1.47	110300	22200	6.9	0.08	10	24	256000
L.KatweW	UG-93-29	28	9.55	9008	4.8	237.6	124500	22500	5.3	32.5	71300	86600	17.5	0.11	9.6	24.5	372000

Table 2: Buranga analytical results. Concentrations in (mg/kg) and (‰) for stable isotopes

Location	**Sample No.**	**Temp (°C)**	**pH**	**CO_2**	**H_2S**	**SiO_2**	**Na**	**K**	**Ca**	**Mg**	**SO_4**	**Cl**	**B**	**Li**	**$\delta^{18}O$**	**δD**	**TDS**
Mumbuga2	UG-93-09	93.4	7.87	2445	0	76.9	5320	195	2.45	2.13	3720	3580	4.3	1.34	-3.6	-17.1	14600
Mumbuga5	UG-93-10	93.6	7.73	2411	0	76.4	5160	190	2.56	2.27	3570	3490	4.2	1.3	-3.49	-12.8	14030
Nyansimbe9	UG-93-16	95.8	8.15	2638	0	87.7	5940	222	0.95	1.74	4180	4010	4.71	1.48	-3.21	-12.2	16250
Nyansimbe13	UG-93-11	80.3	7.61	2889	0	88.6	6160	230	2.1	2.63	4330	4160	4.96	1.51	-3.54	-12.4	17050
Nyansimbe17	UG-93-32	98.2	8.57	2635	0	85.1	6270	235	0.39	0.28	4400	4210	4.96	1.51	-3.45	-13.4	17080
Nyansimbe19	UG-93-13	85.8	7.81	2878	0	85.7	6300	234	2.04	1.98	4420	4240	4.8	1.54	-3.46	-12.9	17050
Kagoro20	UG-93-12	89	7.50	2798	0.3	81	5950	219	2.69	2.19	4160	4030	4.7	1.47	-3.69	-12.7	16400
R.Mungera	UG-93-15	21.8	7.52	57	0	37.2	11.1	3.7	11.2	3.61	1.7	1.8	0	0.008	-2.24	-3.7	74
Kyakatimba1	UG-93-17	23.8	7.54	197	0	36.3	21.2	8.1	54.7	14.3	27.6	2.1	0	0.034	-2.57	-4.6	208

Table 3: Kibiro analytical results. Concentrations in (mg/kg) and (‰) for stable isotopes

Location	Sample No.	Temp. (°C)	pH	CO_2	H_2S	SiO_2	Na	K	Ca	Mg	SO_4	Cl	B	Li	$\delta^{18}O$	δD	TDS
Mukabiga2	UG-93-19	86.5	7.06	146	10.4	129	1530	169	62	8.14	46.7	2500	2.26	1.5	-2.01	-11.3	4576
Mukabiga5	UG-93-20	81.1	7.14	155	13	125	1490	164	62.9	7.96	26.4	2450	2.23	1.48	-2.08	-11.8	4436
Mwibanda 14	UG-93-21	71.8	7.14	155	17.3	122	1480	165	65.7	9.21	15.4	2440	2.21	1.46	-1.98	-10.6	4384
Muntere15	UG-93-22	39.5	8.05	115	0	135	1570	182	75.9	8.71	49.9	2580	2.47	1.53	-1.01	-3.9	4548
L.Albert	UG-93-23	30	8.93	236	0	0.5	72.3	49.4	9.75	27.3	19.3	24.2	0	0.012	5.47	39.8	338
Wantembo	UG-93-24	29.8	6.89	367	0	90.5	87.5	7.7	75.8	39.5	139	31.2	0	0.016	-3.58	-15.2	662
Kiganja1	UG-93-25	23.6	6.26	130	0	70.8	12.4	2.6	14.8	8.03	5.3	5.2	0	0.003	-1.57	-4.1	124
Ndalagi1	UG-93-26	24.9	6.72	232	0	76.1	50.6	7.5	138	39.5	227	123	0	0.015	-2.08	-5.2	680

USE OF A NEW SODIUM/LITHIUM (NA/LI) GEOTHERMOMETRIC RELATIONSHIP FOR HIGH-TEMPERATURE (HT) GEOTHERMAL FLUIDS DERIVED FROM SEAWATER/BASALT INTERACTION PROCESSES: APPLICATION TO THE DJIBOUTI CASE

Bernard Sanjuan
Department of Geothermal Energy - BRGM - 3, Av. Claude Guillemin. BP6009 - 45060 Orleans Cedex 02, France.
E-mail: b.sanjuan@brgm.fr

ABSTRACT

This study has allowed improving the Na/Li geothermometric relationship for High-Temperature (HT) fluids derived from seawater and basalt interaction processes existing in emerged Rifts such as those of Djibouti (Asal-Ghoubbet and Obock geothermal areas) and of Iceland (Reykjanes, Svartsengi and Seltjarnarnes geothermal fields), or in numerous Oceanic Ridges and Rises (Middle-Atlantic Ridge, East Pacific Rise, etc.). The best adapted Na/Li relationship for this type of fluids seems to be:

$$T\ (°K) = 920 / [\log (Na/Li) - 1.105] \quad (r^2 = 0.994)$$

where Na and Li are the aqueous concentrations of these elements given in mol/l.

This relationship which can give estimations of temperature for a value range from 0 to 365°C, with an uncertainty of ± 25°C, is very different from the three main relationships known in the literature (Fouillac and Michard, 1981; Kharaka and Mariner, 1989) and from that recently found for the HT dilute geothermal fluids from Iceland (Krafla, Namafjall, Nesjavellir and Hveragerdi geothermal areas; Sanjuan *et al.*, 2010) in the framework of the European HITI project (HIgh Temperature Instruments for supercritical geothermal reservoir characterization and exploitation). The existence of different Na/Li geothermometric relationships seems to indicate that the Na/Li ratios not only depend on the temperature but also on other parameters such as the fluid salinity and origin, the nature of the geothermal reservoir rocks in contact with the deep hot fluids or the equilibrium reactions between these fluids and the reservoir mineral assemblages. Some case studies in the literature and thermodynamic considerations suggest that the Na/Li ratios for the HT geothermal fluids derived from seawater and basalt interaction processes could be controlled by a full equilibrium reaction involving a mineral assemblage constituted, at least, of albite, K-feldspar, quartz and clay minerals such as kaolinite, illite (or muscovite) and Li-micas.

Moreover, this study confirms the presence of a deep seawater-derived geothermal fluid indicating a temperature close to 210°C and salinity of about 35 g/l, which would supply the littoral hot springs located in the Obock area (Houssein *et al.*, 1993). It also suggests that the fluid collected from the thermal spring located near the Ghoubbet Channel ("Passe du Ghoubbet"; Sanjuan *et al.*, 1990) results from a mixing between a marine origin fluid which would interact with basalt rocks at a temperature value close to 160°C and cold seawater.

Key words: geothermometer, marine geothermal fluid, basalt, Asal-Ghoubbet, Obock

INTRODUCTION

Since 1965, several chemical and isotopic geothermometers such as dissolved silica, Na/K, Na/K/Ca, Na/K/Ca/Mg, K/Mg or $\delta^{18}O$ (H_2O-SO_4) are used as geochemical tools in geothermal exploration to estimate the fluid temperature in the deep reservoirs (White, 1970; Fournier, 1979; Michard, 1979; Giggenbach, 1988; Nicholson, 1993; Serra and Sanjuan, 2004). Unfortunately, these classical geothermometers, based on empirical or semi-empirical laws derived from known or unknown equilibrium reactions between water and reservoir minerals, do not always give concordant temperature estimations for the deep geothermal fluid. Different surface processes such as a mixing of this fluid with shallow waters, or the occurrence of mineral precipitation/dissolution reactions during its rising to the surface and its cooling, can be responsible of these discordances. For example, the Na/K geothermometer can give overestimated reservoir temperatures for dilute thermal waters from volcanic and granite areas. On the other hand, erroneous temperatures can be estimated using Na/K and Na/K/Ca for seawater-derived fluids not equilibrated with the reservoir rocks.

In order to obtain auxiliary geothermometers, several relationships combining major and trace elements were investigated. The most known and efficient geothermometric relationships are those associating Na and Li (Fouillac and Michard, 1981; Kharaka and Mariner, 1989). The two empirical and statistical relationships determined by

Fouillac and Michard (1981), dependant on the fluid salinity, were obtained from numerous data relative to several world geothermal fields mainly located in volcanic and granitic areas. The relationship given by Kharaka and Mariner (1989) was determined for hot saline fluids discharged from sedimentary basins, using many data collected from world geothermal and US oil-fields. Given the low Li reactivity during the ascent of the geothermal fluid up to the surface, this auxiliary geothermometer can be considered as a very useful tool to help to select the best estimation of the reservoir temperature, even if the running of this geothermometer is still poorly known.

Unfortunately, this geothermometer seems to be dependant not only on temperature but also on other parameters such as the fluid salinity or the nature of the reservoir rocks. Recent studies carried out in the framework of the European HITI project (HIgh Temperature Instruments for supercritical geothermal reservoir characterization and exploitation) show that two new Na/Li relationships were determined for HT geothermal fluids from Iceland (Sanjuan and Millot, 2009; Sanjuan *et al.*, 2010). One of these relationships was obtained using HT dilute fluids collected from wells located in four Icelandic geothermal fields (Krafla, Namafjall, Nesjavellir and Hverargerdi). The other Na/Li relationship was determined from literature data about HT fluids circulating in several oceanic Ridges and Rises (Middle-Atlantic Ridge, East Pacific Rise, etc.) and using HT saline geothermal fluids sampled in emerged Rifts such as those of Djibouti (Asal-Ghoubbet and Obock geothermal areas) and Iceland (Reykjanes geothermal field). All these fluids are derived from seawater and basalt interaction processes.

The main objectives of this study are:

- to improve the Na/Li relationship relative to this last type of fluids, and investigate the mechanisms involved in this relationship;
- to confirm or invalidate the temperatures estimated for this type of fluids discharged from littoral hot springs located in the Obock and North-Ghoubbet areas of Djibouti (Sanjuan *et al.*, 1990; Houssein *et al.*, 1993).

STUDIED AREAS

Republic of Djibouti

In order to obtain data from geothermal fluids derived from seawater-basalt interaction processes, two geothermal areas of this country located in the horn of Africa, at the Afar triple junction between the Red Sea, Gulf of Aden-Tadjourah and East African Rift systems, were studied.

Asal-Ghoubbet area

The distension system which separates the two plates from North to South of Tadjourah Gulf (Arabian and Somalia plates) belongs to the largest and most complex Rift system of the East part of Africa (Fig. 1). The separation of these plates induces a relative decrease of the crust thickness in the central area of the Gulf and a submarine volcanism, which produces a new oceanic crust. As a consequence, an anomalous heat flow which can be 4 to 6 times higher than the mean terrestrial flow occurs. The spreading area (with active volcanism) is segmented and dislocated by a system constituted of relatively long transform faults (Fig. 1). More recent studies indicate the importance of active structures with 130-140°N directions (Chouckroune *et al.*, 1988; Lépine and Hirn, 1992; Dauteuil *et al.*, 2001).

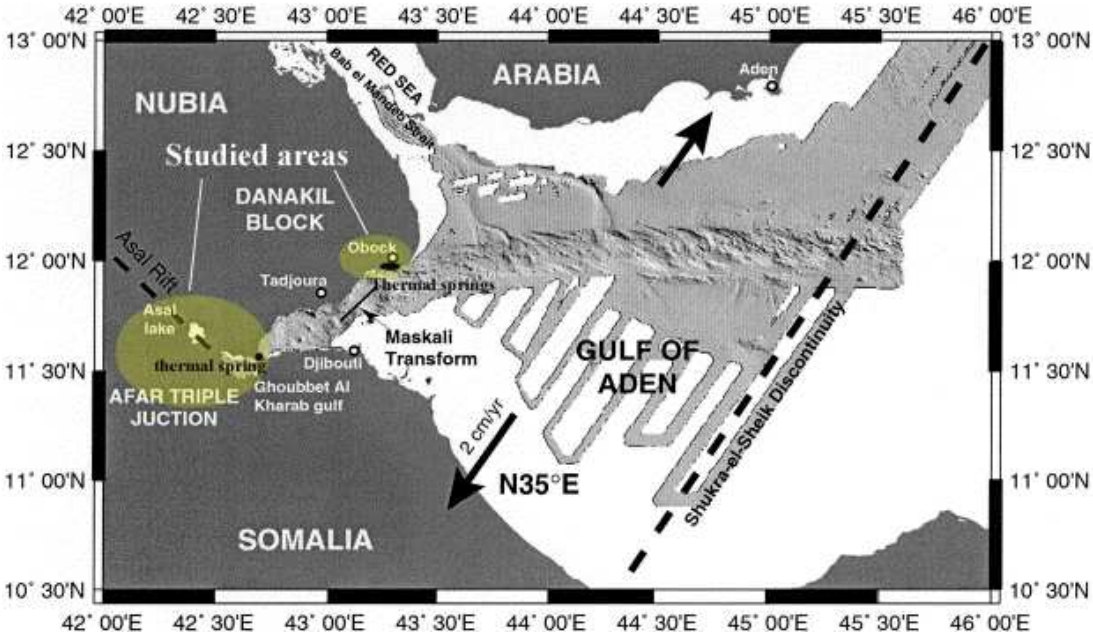

Figure 1: Location of the studied areas in the Republic of Djibouti and of the littoral thermal springs of Goubbet Channel and Obock. Black arrows show the direction of spreading between the Somalia and Arabia plates (figure extracted from Dauteuil et al., 2001)

The Asal-Ghoubbet emerged Rift occurs within the vast Danakils depression, an area still referred to as the Afar triangle (Fig. 1). In the southern part of this depression, within the frontiers of the Republic of Djibouti, this Rift forms a 12 km long axis which separates Asal Lake to the Northwest from the Gulf of Ghoubbet-Al Kharab to the Southeast. The Asal Lake is 155 m below sea level and is 9-10 km wide.

The Asal-Ghoubbet Rift seems to be largely underlain by pre-Asal crust not replaced by newly formed one, and to be still in a pre-oceanic stage. However, it presents remarkable analogies (morphology, volcanism, tectonic) with the axial valley of the oceanic ridges (Stieljes, 1973). At surface, it is exclusively constituted of volcanic rocks with a Quaternary age lower than 1 My. Its opening is recent and has not more than 1 My (Barberi *et al*., 1975). Most of the faults are normal and symmetrical on both side of the Rift and indicate a general NW-SE direction. However, some reverse faults are also present. Out of the axial Rift area, the normal faults intersect some previous normal N350 and N280 direction faults. Open fissures with or without vertical offset are largely responsible for the horizontal extension.

The Asal Rift is markedly asymmetrical with respect of its median axis. The most active and recent part of the Afar depression is the so-called Inner Rift where the volcano axial chain is observed and the last eruption (Ardoukoba volcano) occurred in 1978. It is about 3 km wide and is shifted to the NE part of the main Rift. This Inner Rift is characterized by intense fracturing and recent lava flows. The axis of crustal divergence of the Rift seems to migrate from SW to NE. The rise of hot material beneath the Rift is thus considered to proceed from SW to NE by successive pulses. The existence of an area of crust fusion at low depth, the important seismic activity, the presence of fumaroles and hot springs suggest that this region has a high geothermal potential.

The southern flank of the Asal-Ghoubbet Rift has been explored by six geothermal wells drilled at depths ranging from 1150 m to 2000 m. Beneath the Asal series formed during rifting (basalts and hyaloclastites less than 1 My old), all the wells encountered basalts with some rhyolithes 1-4 My old attributed to the Afar Stratoid series and basaltic lava flows with some intercalations of rhyolithes and trachytes 4-9 My old corresponding to the Dalha basalt series. The maximum temperatures were measured around 340-350°C in the bottom-hole of Asal 4 and 5 but these wells were considered as unproductive (Houssein and Axelsson, 2010). These temperatures indicate strong geothermal gradients which may be related to the presence of magma chambers below about 4000 m in the central part of the Rift. Geothermal brine (TDS about 120 g/l) with a temperature close to 255-265°C was encountered in the wells Asal 1, 3 and 6, at depths ranging from 1050 to 1350 m. This saline geothermal reservoir is located in the fractured Dahla basalt series.

Numerous thermal springs (Fig. 2) and fumaroles are present in the Asal-Ghoubbet Rift. These surface manifestations and the fluids collected from the geothermal wells were studied by several teams of researchers since 1973 (Bosch *et al.*, 1977; Fontes *et al.*, 1979; Fouillac *et al.*, 1983; Marini, 1987; Sanjuan *et al.*, 1990 ; D'Amore *et al.*, 1998). From a chemical and Strontium isotopic study, Sanjuan *et al*. (1990) conclude that the hot waters collected from this area result from basalt-seawater interaction, associated with variable evaporation rates due to the aridity of this region. Some thermal waters result from a mixing between deep geothermal water and seawater or Asal lake water. Dissolution from evaporitic rocks appears unimportant.

For this study, only the waters for which the deep temperature was well known were selected. So, according to Sanjuan *et al*. (1990), the brines collected from the geothermal wells Asal 1, Asal 3 and Asal 6 are in equilibrium with a mineralogical assemblage at a temperature close to 255-265°C, temperature which was also measured into the wells. For the three wells, the selected water samples were collected after the phase separator. Only one water sample was directly sampled at the Asal 3 bottom-hole (BH in table 1).

The results of the chemical analyses of these waters which were corrected taking into account the concentration factor due to the phase separation were extracted from Sanjuan *et al.* (1990) and are reported in table 1. The results obtained using different classical chemical geothermometers such as Na/K, Na/K/Ca, K/Mg or Silica (quartz) are presented in table 2 and are close to the measured temperatures. The chemical composition given by these authors for three water samples collected from Asal Lake (Fig. 2) is also reported in table 1.

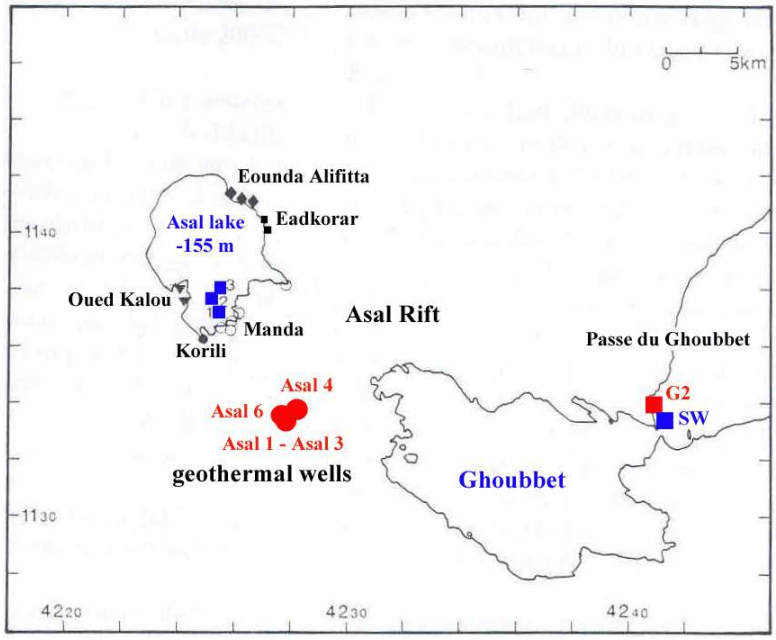

Figure 2: Location map of the geothermal wells studied in this study and of main thermal springs (Eounda Alifitta, Eadkorar, Manda, Korili, Oued Kalou, Ghoubbet Channel) in the Asal Rift and the North-Ghoubbet. Three water samples collected from Asal Lake and a sample of seawater (SW) were also integrated in this study.

During the collection of the water sample from the littoral thermal spring located near the Ghoubbet Channel (Figs. 1 and 2), tide was high and this spring was recovered by seawater. Consequently, the collected water sample (G2) is a mixing with a high proportion of cold seawater (Tab. 1; Sanjuan *et al.*, 1990). As the Chloride concentration of this mixing is slightly lower than for seawater (see table 1), it can be concluded that a small proportion of shallow freshwater, estimated to be close to 1%, is also present. As noticed by Sanjuan *et al.* (1990) and Houssein *et al.* (1993), the hot seawater-derived solutions reacting with basalt in submarine hydrothermal springs, in geothermal wells or in laboratory are characterized by a strong depletion in Magnesium and Sulfates, and enrichment in Calcium, Potassium, Silica and Lithium. In the figure 3, the Mg/Cl and SO_4/Cl ratios extrapolated to zero, using the best linear regression coefficients, lead to the same Li/Cl value. This result suggests that the collected sample of

thermal water would be also constituted of a hot end-member without Mg and SO_4, reacting with basalt (probably Gulf basaltic series 1 to 3 My old).

The graphical determination of the Na/Cl, Ca/Cl and SiO_2/Cl ratios for the hot end-member can be obtained using the previously determined Li/Cl value (Fig. 4). The chemical composition of the hot end-member was reconstructed using the Chloride concentration of seawater (Tab. 1). Contrary to the literature observations, the K/Cl ratio determined in the G2 thermal water sample is lower than for seawater. In order to discard this anomalous result (probably due to an uptake of K by mineral precipitation/adsorption reaction during the rising and cooling of the hot end-member or eventually, to an analytical error because the difference relative to seawater is low), we have preferred to select a K/Cl ratio close to that of seawater (Fig. 4). Moreover, this ratio allows estimating a temperature for the hot end-member using the Na/K and Na/K/Ca geothermometers similar to that given by the Silica (quartz) geothermometer (Tab. 2). The temperature selected for the hot end-member was 160°C. This value is close to those (160-180°C) estimated by Marini (1987) using chemical geothermometers applied to non condensable gases collected from several fumaroles located in the vicinity of this thermal spring, in the North-Ghoubbet. The temperature and the chemical composition of a Ghoubbet seawater sample, collected near the thermal spring (SW in figure 2) by Sanjuan *et al.* (1990), are also reported in table 1.

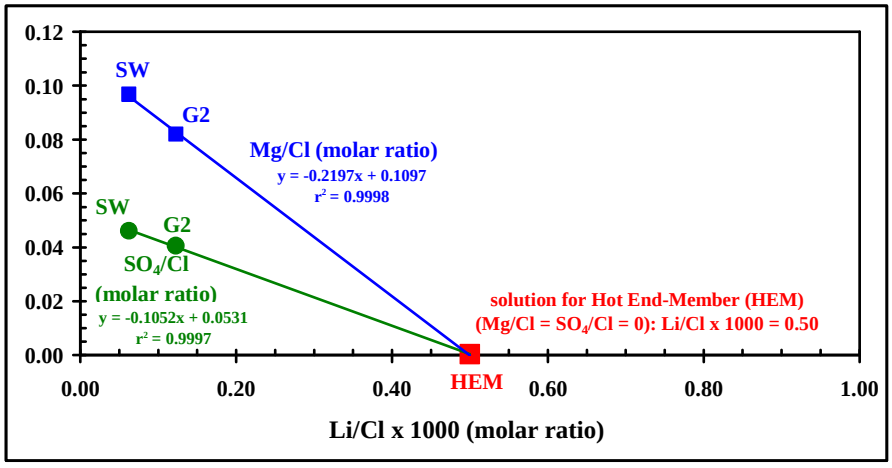

Figure 3: Determination of the Li/Cl ratio for the Hot End-Member (HEM) of the thermal spring Ghoubbet Channel (G2) using the Mg/Cl and SO4/Cl variations.

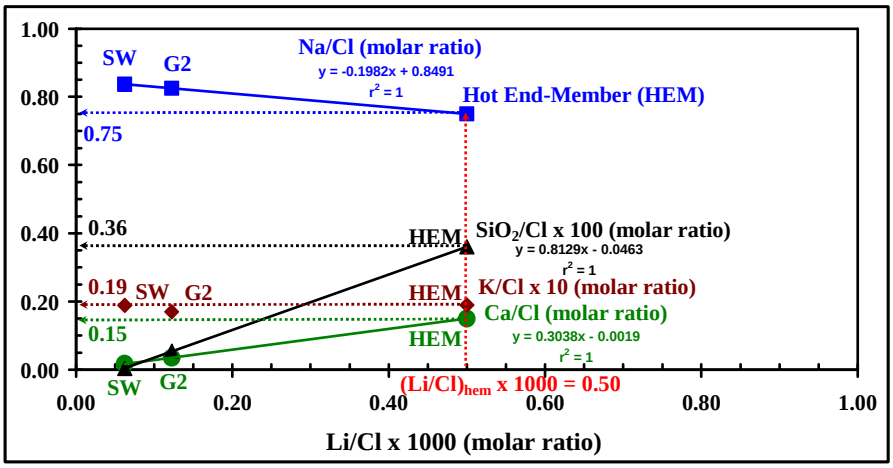

Figure 4: Determination of the Na/Cl, SiO2/Cl, Ca/Cl and K/Cl ratios for the hot end-member of the thermal spring G2 using the Li/Cl determined in figure 3.

Table 1: Chemical and isotopic compositions of geothermal seawater-derived fluid samples collected from Djibouti and Iceland selected for this study. These data were extracted from Sanjuan et al. (1990), Houssein et al. (1993), Bjornsson et al. (1972), Olafsson and Riley (1978), Truesdell et al. (1981), Sanjuan et al. (2010; in prep.).

Geothermal area	Sample	Fluid sampling date	T °C	pH	Eh_{nc} mV	Na mg/l	K mg/l	Ca mg/l	Mg mg/l	Cl mg/l	Alk. meq/l	SO_4 mg/l	SiO_2 mg/l	Li µg/l	TDS g/l	Na/K molar	Na/Li molar	$\delta^{18}O_{(SO4)}$ ‰	$\delta^{34}S_{(SO4)}$ ‰
Djibouti																			
Asal wells	**Asal 1**	1983	255			28507	4888	16393	24	77997	0.33	21.1	514	12976	128	10	663		
	Asal 3	9/11/1987	260	4.65		26254	4692	15431	23	72076		19.2	520	14156	119	10	560		
	Asal 3 (BH)	1/9/1988		5.22		26438	4497	14268	23	69842	0.11	44.2			115	10			
	Asal 6	10/1/1988	260	4.64		27588	4927	15511	23	74593	0.01	27.9	574	13878	123	10	600		
Asal Lake	**S1**	1987				81959	4340	2553	9795	173720				4857	272	32	5093		
	S2	1983	32	7.10		94718	4731	2469	11472	184001	2.05	4304	170	4649	302	34	6149		19.3
	S3	1983	32	7.00		101155	5161	2677	12493	198891	2.20	4400		5551	325	33	5500		18.9
Ghoubbet Channel thermal spring (Tadjourah)	**G2**	1987	60			11265	391	834	1172	20846		2296	19.2	500	36.8	49	6806		
Hot end-member	**HEMGC**	1987	160			10253	438	3571	0	21059		0	129	2061	35.5	40	1502		
Seawater	**SW-TA**	1987	30			11426	438	409	1398	21059		2632	1.20	257	37.4	44	13432		
Obock thermal springs	**O1**	1989	70	6.63		9541	579	1126	729	18081		1614	83.5	1388	31.8	28	2075	9.2	19.4
	O2	1989	63	6.70		10230	544	878	987	18896		2056	60.7	1041	33.7	32	2967	9.4	19.8
	O3	1989	74	6.52		10805	657	1050	792	19712		1777	92.5	1665	34.9	28	1958	9.2	20.2
	O4	1989	54	6.75		10230	559	902	941	19003		2037	63.1	1110	33.7	31	2781	9.1	20.2
Hot end-member	**HEMO**	1989	210			10529	1216	2409	0	20705		0	266	4025	35.1	15	790		
Seawater	**SW-OB**	1989	30	8.22		11495	442	449	1429	20705		3122	0.90	250	37.6	44	13878	9.1	19.9
Iceland																			
Svartsengi wells	**SV-07**	10/9/2007	244	6.15	-165	7043	1049	1128	0.4	13696	0.29	37.0	531	2580	23.5	11	824		
	SV-07	6/10/2008	244	6.09	-201	7483	997	1156	< 0.25	14942	0.32	32.6	465	2897	25.1	13	780	4.3	16.6
	SV-18	10/9/2007	244	7.29	-120	7498	1154	1163	0.5	14366	0.31	39.4	563	3060	24.8	11	740		
Reykjanes wells	**H2**	Bjornsson *et al.* (1972)	260			14506				19500				7440			588		
	H2	Olafsson and Riley (1978)	?	6.60		11930	1820	2239	12.7	23702		3.2	462	5950	40.2	11	605		
	H8	Olafsson and Riley (1978)	?	7.10		12730	1990	2249	9.8	25054		2.4	943	6590	43.0	11	583		
	H8	Tuesdell *et al.* (1981)	283			9629				18785			572	5100			570		
Reykjanes wells	**RN-10**	10/9/2007	319	4.95	-84	12644	1825	1886	2.1	25015	0.02	25.9	1023	5830	42.4	12	655		
	RN-21	6/10/2008		5.82	-6	12675	1748	1372	< 0.25	23795	0.19	20.9	789	5500	40.4	12	696	4.2	19.8
	RN-22	10/9/2007	305	5.17	-120	12263	1814	2087	2.4	23620	0.09	29.8	788	5068	40.6	11	730		
	RN-22	6/10/2008	305	5.17	114	13911	1763	1581	< 0.25	25293	0.11	25.3	800	5951	43.4	13	706	4.8	20.8
	RN-24	10/9/2007	286	5.66	-192	11310	1646	1889	1.0	21807	0.31	27.5	744	4700	37.4	12	726		
Seltjarnarnes wells	**SN-04**	6/5/2009	114	6.23	284	643	13	548	< 0.25	2020		340	109	63	3.7	84	3078		
	SN-05	6/5/2009	114	8.27	149	677	13	408	< 0.25	1870		259	105	61	3.3	91	3362		
Seawater (Grindavik)	**SW-GR**	6/10/2008	10			11427	374	386	1204	19108		2847	0.50	158	34.1	52	21829		

Table 2: Measured temperatures, temperatures of deep geothermal fluid estimated using chemical geothermometers and values of temperature selected for this study.

Geothermal area	Sample	T °C	$T_{Na/KM}$ °C	$T_{Na/KF}$ °C	$T_{Na/K/Ca}$ °C	$T_{K/Mg}$ °C	T_{Qz} °C	$T_{Qz\ vapor}$ °C	$T_{Chalc.}$ °C	$T_{Na/Li}$ °C	$T_{sel.}$ °C	$1000/T_{sel.}$	log(Na/Li) molar
Djibouti													
Asal wells	**Asal 1**	255	262	267	251	278	255			263	260	1.88	2.82
	Asal 3	260	268	271	253	277	256			287	260	1.88	2.75
	Asal 3 (BH)		261	266	251	274	256			286	260	1.88	
	Asal 6	260	268	271	254	280	266			277	260	1.88	2.78
Ghoubbet Channel thermal spring (Tadjourah)	**G2**	60	107	140	166	98	62			64	60	3.00	3.83
Tadjourah hot end-member	**HEMGC**	?	122	153	163		152			171	160	2.31	3.23
Obock thermal spring	**O3**	74	150	177	193	118	133			148			
Obock hot end-member	**HEMO**	?	213	229	223		201			240	210	2.07	2.90
Iceland													
Svartsengi wells	**SV-07**	244	243	253	240	310	258	230		235	243	1.94	2.92
	SV-07	244	230	242	233		246	221		242	235	1.97	2.89
	SV-18	244	248	256	243	309	264	234		248	245	1.93	2.87
Reykjanes wells	**H2**	260								279	260	1.88	2.77
	H2	?	247	255	246	241	245			275	250	1.91	2.78
	H8	?	250	258	249	252	318			281	292	1.77	2.77
	H8	283					265			284	283	1.80	2.76
Reykjanes wells	**RN-10**	319	239	250	245	292	328	283		265	283	1.80	2.82
	RN-21		234	245	246		298	261		256	261	1.87	2.84
	RN-22	305	243	252	245	288	298	260		250	260	1.88	2.86
	RN-22	305	224	237	240		300	262		255	262	1.87	2.85
	RN-24	286	241	251	243	310	292	256		251	256	1.89	2.86
Seltjarnarnes wells	**SN-04**	114	73	109	104		142	137	113	113	114	2.58	3.49
	SN-05	114	68	105	103		140	135	111	107	114	2.58	3.53

$T_{Na/KM}$: Na/K geothermometer (Michard, 1979)

$T_{Na/KF}$: Na/K geothermometer (Fournier, 1979)

$T_{Na/K/Ca}$: Na/K/Ca geothermometer (Fournier and Truesdell, 1973)

$T_{K/Mg}$: K/Mg geothermometer (Giggenbach, 1988)

$T_{Qz\ vapor}$: Silica-quartz geothermometer taking into account the water vaporisation before water sampling (Fournier and Rowe, 1966)

$T_{Chalcedony}$: Silica-Chalcedony geothermometer (Arnorsson, 1983)

$T_{Na/Li}$: Na/Li geothermometer (this study)

Obock area

The Obock area, located in the northern part of the Republic of Djibouti, is practically constituted of a quaternary formation of coralline limestone, 120-130 Ky old (Faure *et al.*, 1980) with a thickness probably lower than 50 m. Other present calcareous formations and detrital materials are also observed. All these formations are above basalt formations of the Tadjourah Gulf, 2 My old (Varet, 1975). During the 1980 years, the regional tectonic was considered to be as dominated by the famous normal-transform system of the Tadjourah Gulf in which the normal faults were E-W direction and the transform faults were NE-SO direction (Richard and Varet, 1979). However, more recent studies indicate a different configuration (Fig. 5) and the importance of active structures with 130-140°N directions (Chouckroune *et al.*, 1988; Lépine and Hirn, 1992; Dauteuil *et al.*, 2001).

The four littoral thermal springs, which were studied by Houssein *et al.* (1993), are located in an intensively fractured area (Fig. 1). They were sampled during low tide. The temperatures of emergence range from 50 to 80°C. The results of the chemical and isotopic analyses presented by Houssein *et al.* (1993) are reported in table 1. Using these data and chemical geothermometers, these authors showed that the origin and the evolution of these thermal waters seem to be:

- seawater which reacts with basalt at 210°C for enough time to reach equilibrium;
- a mixture of this hot fluid with cold seawater while it emerges through the fractures;
- dilution with small quantities of freshwater which may explain the lower Chloride concentration of these springs

The isotopic $\delta^{18}O$ and $\delta^{34}S$ marine signature of the dissolved Sulfates determined by BRGM for the four water samples (Tab. 1) confirms the mixture of a hot seawater-derived fluid (absence of Sulfates) with cold seawater. Only the hot end-member was used in this study.

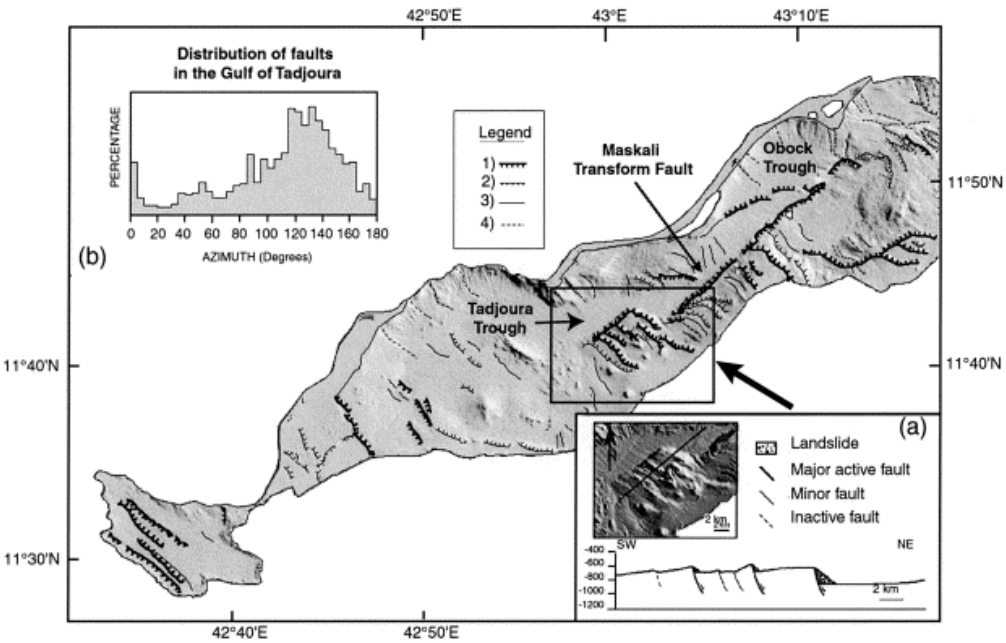

Figure 5: Fault pattern of the Gulf of Tadjourah deduced from detailed analysis of shaded relief, stereoscopic and acoustic reflectivity images. Four kinds of structures are identified (main active faults, minor active or inactive faults, inactive faults, and canyons) (figure extracted from Dauteuil et al., 2001).

Iceland

This study focuses on two high-temperature areas that have been extensively drilled for electrical power generation and are being exploited today. These are Reykjanes and Svartsengi, southwest Iceland (Fig. 6). These areas are located within the active volcanic belts, the axes of which represent the plate boundary between the Eurasian and North-American lithospheric plates. Another studied area is the medium-temperature Seltjarnarnes geothermal field, which is sited outside the active volcanic zone, in Quaternary flood basalts (Fig. 6).

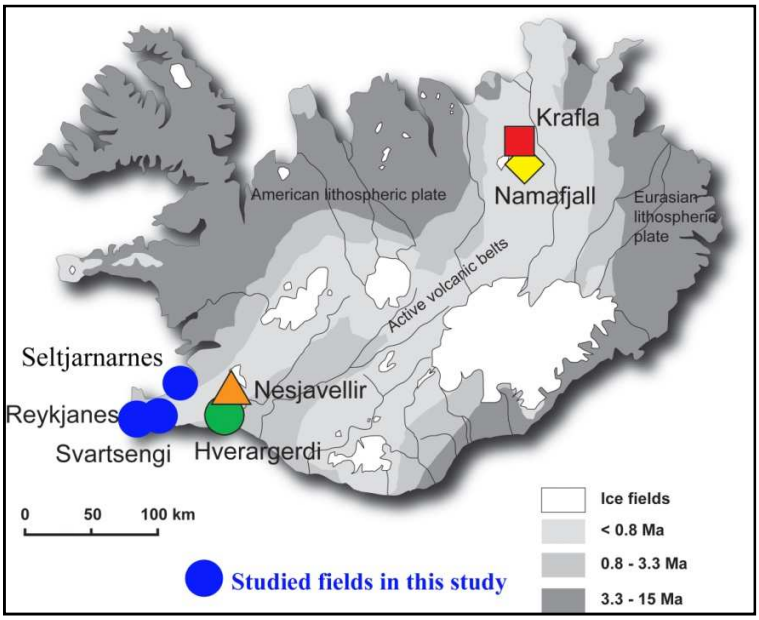

Figure 6: Location map of the three Icelandic geothermal fields selected for this study and of the other geothermal fields studied in the framework of the European project HITI (Sanjuan et al., 2010).

The three geothermal fields are both located on the Reykjanes peninsula in southwestern Iceland which represents the landward continuation of the Reykjanes Ridge (Fig. 6). This Ridge is itself a projection of the Mid-Atlantic Ridge (Olafsson and Riley, 1978). The peninsula consists mostly of Holocene lavas protruded by hyaloclastite hills formed by sub-glacial eruptions during the last glaciation (Clifton and Kattenhorn, 2006). They lie astride setting, the heat source to these systems are considered to be shallow (1-3 km) sheeted dyke complexes and the permeability is fracture controlled. The two high-temperature geothermal systems are hosted by basaltic rocks, subglacial hyaloclastites, breccias, and pillow lavas as well as tuffaceous sediments (Giroud, 2008). Abundance of intrusions increases with depth and dominate the succession at the greatest depth reached by the wells.

At Reykjanes, the measured temperatures at the bottom-hole can vary from 225 to 320°C. The highest temperature recorded in the geothermal wells is close to 320°C, at a depth of 2000 m. The aquifer is two-phase above 1000 m but sub-boiling at greater depths. The Svartsengi geothermal field is classified as high-temperature and liquid-dominated (Gudmundsson and Thorhallsson, 1986). The temperature in Svartsengi is very homogeneous. Between 500 and 2000 m depth, it is close to 240°C, reflecting good vertical permeability in the system which presents abundant vertical fractures. At Seltjarnarnes, the maximum measured temperature was 114°C (Arnorsson and Andresdottir, 1995).

The geothermal fluids selected for this study are those found in the literature for the Reykjanes field (Bjornsson *et al.*, 1972; Olafsson and Riley, 1978; Truesdell *et al.*, 1981) and those sampled by Sanjuan *et al.* (2010, in preparation) with the collaboration and help of ISOR on October 2007, June 2008 and June 2009, in the framework of the European HITI project (HIgh Temperature Instruments for supercritical geothermal reservoir characterization and exploitation). These fluid samples were collected at the well-head using a stainless steel (N316) Webre separator to separate water (Sanjuan *et al.*, 2010, in prep.) from the wells:

- RN-10, RN-21, RN-22, and RN-24 in the Reykjanes geothermal field,
- SV-07 and SV-18 in the Svartsengi geothermal field,
- SN-04 and SN-05 in the Seltjarnarnes geothermal field.

A sample of seawater was also selected. The results of the corresponding chemical analyses are reported in table 1. The chemical composition of the geothermal fluids sampled by Sanjuan *et al.* (2010, in prep.) was not corrected taking into account the concentration factor due to the phase separation because most of the chemical geothermometers are based on element concentrations ratios. However, for the temperatures estimated using the Silica (quartz) geothermometer, the relationship considering the water vaporization was selected (Tab. 2). Contrary to the Svartsengi and Seltjarnarnes geothermal fields where the temperatures measured at the bottom-hole are close to those estimated using the chemical geothermometers, the bottom-hole temperatures in the Reykjanes geothermal field are often different from the estimations (Tab. 2). For the geothermal waters of this field, we have considered that they were not always in equilibrium with surrounding rocks at the temperature measured in the bottom-hole and have preferred to select the average temperature estimated using the chemical geothermometers as the most representative of these waters (Tab. 2).

The geothermal fluids at Reykjanes represent seawater which has reacted with basalt (Arnorsson, 1995) and experienced stable isotope exchange with alteration minerals (Pope *et al.*, 2009; 2010). The Cl concentration of the unboiled aquifer water is thus close to that of seawater. The Svartsengi geothermal system has a mixed meteoric-seawater fluid origin with Cl content corresponding to about 2/3 that of seawater and the deuterium content of this water is consistent with such an origin (Giroud, 2008). This mixture has reacted with basalt at 240°C for enough time to reach chemical equilibrium. The geothermal fluids at Seltjarnarnes represent seawater highly diluted by freshwater (about ten times), which has interacted and would be in equilibrium with basalt at relatively low temperature (114°C).

Mid-Ocean Ridges and Rises

Numerous chemical and Li isotopic data from literature were obtained for the very hot fluids circulating in Mid-Ocean Ridges (Mid-Atlantic Ridge, Middle Valley Ridge, etc.) and Rises (East Pacific Rise…), in the bibliographical review done by Sanjuan and Millot (2009) in the framework of the European project HITI. The data selected for this study were extracted from the bibliographical review and are reported in Appendix 1. The temperatures given in the literature are often close to those estimated using the silica geothermometer (quartz). Depletion in Lithium can be observed for the fluids circulating in old and much altered MAR and EPR, such as vent fluids from the Lucky Strike field or vent fluids at 13°N...

NA/LI RELATIONSHIP FOR GEOTHERMAL FLUIDS DERIVED FROM SEAWATER-BASALT INTERACTION PROCESSES

As shown in figure 7, a Na/Li thermometric relationship can be statistically defined for seawater and geothermal waters derived from seawater-basalt interaction processes such as those discharged from the emerged Rifts of Djibouti and Iceland. This relationship:

$$T\ (°K) = 920 / [\log (Na/Li) - 1.105] \quad (r^2 = 0.994)$$

can be considered as the most reliable and accurate for temperature values ranging from 0 to 365°C. Absolute uncertainty on the estimated temperatures is close to ± 25°C. This uncertainty is in good agreement with the temperatures estimated using this geothermometric relationship in this study (Tab. 2). For seawater, several examples were selected (see Table 1 and Appendix 1). The data for the hot fluids circulating in the Mid-Ocean Ridges and Rises (Appendix 1) have not been integrated for determining this relationship in order to obtain a more accurate relationship for the fluids discharged from emerged Rifts. However, except the fluids from old and much altered MAR and EPR, depleted in Li, most of them fit this relationship very well (Fig. 7).

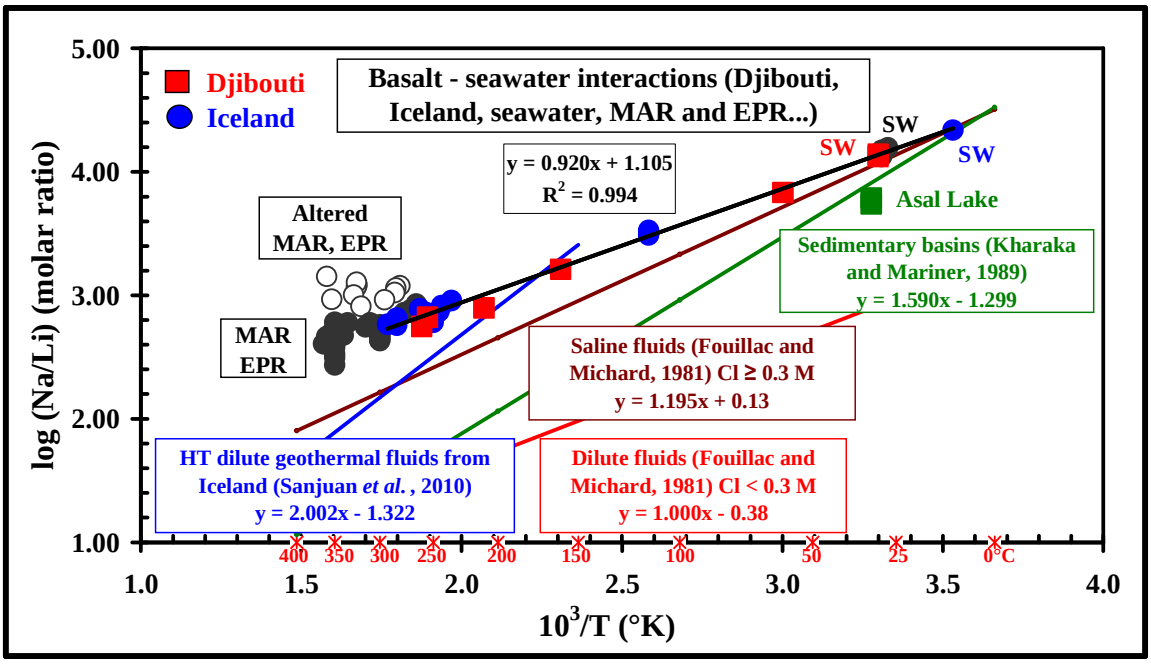

Figure 7: Sodium/Lithium geothermometric relationships existing in the literature and new Na/Li relationship determined for geothermal fluids derived from basalt-seawater interaction processes in this study.

The excellent regression coefficient obtained for this relationship confirms the temperatures estimated for the hot marine end-member of the thermal waters collected from the Ghoubbet Channel (160°C) and Obock (210°C), using the other chemical geothermometers (Tab. 2).

This thermometric relationship is slightly different from that determined by Sanjuan and Millot (2009):

$$T\ (°K) = 855 / [\log (Na/Li) - 1.275] \qquad (r^2 = 0.967)$$

which integrated most of the literature data about HT fluids circulating in Oceanic Ridges and Rises as well as data from Djibouti, but used limited data from Iceland.

This thermometric relationship is very different from that determined by Fouillac and Michard (1981) for saline geothermal waters in volcanic and granite environments (Cl concentrations ≥ 0.3 M):

$$T\ (°K) = 1195 / [\log (Na/Li) - 0.13] \qquad \text{(brown line in figure 7).}$$

and from that described by Kharakha and Mariner (1989) for hot saline fluids discharged from sedimentary basins located in world geothermal and US oil fields:

$$T\ (°K) = 1590 / [\log (Na/Li) + 1.299] \qquad \text{(green line in figure 7).}$$

However, we can note that the data relative to the brines collected from the Asal Lake, reported in table 1, fit this last relationship very well (Fig. 7).

Finally, the Na/Li relationship determined for geothermal fluids derived from seawater-basalt interaction processes is also very different from those determined for:

- the HT dilute geothermal waters (Cl concentrations < 0.3 M) in volcanic and granite environments by Fouillac and Michard (1981; Fig. 7);
- the HT dilute geothermal waters from Iceland by Sanjuan *et al.* (2010; Fig. 7).

THERMODYNAMIC CONSIDERATIONS

The sodic feldspar is commonly observed in the rocks of the volcanic and granitic geothermal reservoirs and is often involved with K-feldspar in the control of the aqueous Na/K ratios (see Na/K thermometric relationships). However,

in other environments such as sedimentary rocks, clay minerals can be also involved (D'Amore and Arnorsson, 2000).

As discussed in Sanjuan *et al.* (2010), dissolved Li generally increases with increasing temperature which can be interpreted as mainly caused by rock leaching or dissolution. However, Shaw and Sturchio (1992) noted that Li was also preferentially trapped in illitic alteration products when temperature increased and that, consequently, the retention of this element was favoured by abundant illitic alteration. Li can be also scavenged by other clays such as smectites, mixed layer clays or micas.

In order to understand the mechanisms involved in the thermometric Na/Li relationship determined for geothermal waters derived from seawater-basalt interaction processes in this study, a thermodynamic approach was carried out. As muscovite ($KAl_3Si_4O_{10}(OH)_2$) is relatively easily available as mineralogically pure phase, and consequently is chemically and thermodynamically better defined, it is widely used as a proxy for illites in the system K_2O-Al_2O_3-SiO_2-H_2O (Manning, 2003; Sanjuan *et al.*, 2003). Consequently, muscovite replaced illite in the thermodynamic calculations of this study.

If we consider the following equilibrium reaction:

$$NaAlSi_3O_8 \text{ (albite)} + KAlSi_3O_8 \text{ (K-feldspar)} + 2\ Al_2Si_2O_5(OH)_4 \text{ (Kaolinite)} + Li^+ = KAl_3Si_3O_{10}(OH)_2 \text{ (Muscovite)} + LiAl_3Si_3O_{10}(OH)_2 \text{ (Li-Mica)} + 4\ SiO_2 \text{ (Quartz)} + 2\ H_2O + Na^+,$$

the equilibrium constant for this reaction at temperature T (K_T) is given by:

$$K_T = (Na^+)/(Li^+)$$

where (Na^+) and (Li^+) are the activities of the dissolved Sodium and Lithium ions.

If we consider that Na and Li are essentially in form of Na^+ and Li^+ and the activity coefficients for these ions are very close, K_T can be then expressed as:

$$K_T \approx [Na^+]/[Li^+] \approx Na/Li$$

where [Na^+] and [Li^+] are the concentrations of the dissolved Sodium and Lithium ions and Na and Li are the concentrations of total dissolved Sodium and Lithium.

For this reaction, the integration of the Van't Hoff equation: $\partial \ln K_T/\partial T = \Delta H°_R/RT^2$ allows expressing the equilibrium constant K_T as a function of temperature following the relationship:

$$\log K_T = \log K_{298} - \Delta H°_R/(2.303 \times R) \times (1/T - 1/298.15)$$

where K_{298} is the equilibrium constant at 298.15°K (25°C), $\Delta H°_R$ ($J.mol^{-1}$) is the standard molar enthalpy of reaction assumed to be constant in function of temperature, and R is the perfect gas constant (= 8.3143 $J.K^{-1}.mol^{-1}$). Temperature T is given in °K.

We can then write:

$$\log (Na/Li) \approx \log K_{298} + \Delta H°_R/5709 - \Delta H°_R/(19.1478 \times T)$$

If we compare the Na/Li thermometric relationship obtained in paragraph 3 with this last equation, we can estimate the values of the corresponding reaction enthalpy and equilibrium constant at 298°K (25°C) as follows:

$\Delta H°_R/19.1478 \approx -920$ (slope of the straight line in figure 7) and:

$\log K_{298} + \Delta H°_R/5709 \approx 1.105$ (constant of the straight line in figure 7)

This implies that $\Delta H°_R \approx -17616\ J.mol^{-1} \approx -17.6\ KJ.mol^{-1}$ and $\log K_{298} \approx 4.191$.

Knowing this last parameter, we can determine the value for the corresponding standard Gibbs free energy of reaction $\Delta G°_R$ following the fundamental thermodynamic relation:

$$\Delta G°_R = -\log K_{298} \times R \times 298.15 \times 2.303 \approx -23924\ J.mol^{-1} \approx -23.9\ KJ.mol^{-1}.$$

The $\Delta G°_R$ of this reaction can be also calculated using the following fundamental thermodynamic relationship:

$$\Delta G°_R = \Sigma\, n_i\, \Delta G°_{f\,(right\ compounds)} - \Sigma\, n_i\, \Delta G°_{f\,(left\ compounds)}$$

where n_i is the reaction coefficient of each compound and $\Delta G°_f$ refers to the standard Gibbs free energy of formation of each compound of the reaction and for which the values are reported in table 3.

We can then write:

$$\Delta G°_R = \Delta G°_{f\,(muscovite)} + \Delta G°_{f\,(Li\text{-}mica)} + 4\,\Delta G°_{f\,(quartz)} + 2\,\Delta G°_{f\,(H2O)} + \Delta G°_{f\,(Na^+)} - \Delta G°_{f\,(albite)} - \Delta G°_{f\,(K\text{-}feldspar)} - 2\,\Delta G°_{f\,(kaolinite)} - \Delta G°_{f\,(Li^+)}$$
$$= -23.1\ KJ.mol^{-1}.$$

Most of the $\Delta G°_f$ values (Tab. 3) were selected from the thermodynamic data base data0.com.R2 of the EQ3/6 code (Wolery, 1995) which relies heavily on the SUPCRT92 consistent data base (Johnson *et al.*, 1992), a reference software package for calculating the standard molal thermodynamic properties of minerals, gases, aqueous species and reactions.

However, for micas, in the absence of data for Li-Mica, all the values (Tab. 3) were extracted from the paper written by Tardy and Duplay (1992), who use a method of estimating the standard Gibbs free of formation of clays minerals and thermodynamic values similar to those found in the EQ3/6 data base. Note that for muscovite (K-mica), the $\Delta G°_f$ value is identical to that proposed in the EQ3/6 data base. As shown in Sanjuan *et al.* (2010), the values of standard Gibbs free energy of formation found in the literature for the alumino-silicate minerals, especially for clay minerals, can have large variations. It is why the most important requirement is the consistence and the coherence of the selected data base.

The value found for $\Delta G°_R$ close to that determined from the relationship obtained in paragraph 3 (-23.9 $KJ.mol^{-1}$) suggests that the Na/Li ratios are most probably controlled by this type of equilibrium reaction, where the formulae of the clay minerals (K- and Li-micas) are certainly simplified but represent relatively well the interacting phases. Consequently, the Li concentrations could be well controlled by clay alteration products, partially constituted of illitic and mica minerals, at high temperature. As shown by Sanjuan *et al.* (2010), other equilibrium reactions involving slightly different mineral assemblages could explain the other existing Na/Li relationships.

The $\Delta H°_R$ value relative to the considered equilibrium reaction can be calculated using the values of standard molar enthalpy of formation ($\Delta H°_f$) for each compound following the fundamental thermodynamic relationship:

$$\Delta H°_R = \Sigma\, n_i\, \Delta H°_{f\,(right\ compounds)} - \Sigma\, n_i\, \Delta H°_{f\,(left\ compounds)}$$

where n_i is the reaction coefficient of each compound.

We can then write:

$$\Delta H°_R = \Delta H°_{f\,(muscovite)} + \Delta H°_{f\,(Li\text{-}mica)} + 4\,\Delta H°_{f\,(quartz)} + 2\,\Delta H°_{f\,(H2O)} + \Delta H°_{f\,(Na^+)} - \Delta H°_{f\,(albite)} - \Delta H°_{f\,(K\text{-}feldspar)} - 2\,\Delta H°_{f\,(kaolinite)} - \Delta H°_{f\,(Li^+)}$$
$$= -17.5\ KJ.mol^{-1}.$$

As for the $\Delta G°_f$, the $\Delta H°_f$ values (Tab. 4) were selected from the thermodynamic data base data0.com.R2 of the EQ3/6 code (Wolery, 1995), except for Li-mica and muscovite, which were those proposed in Sanjuan *et al.* (2010). The $\Delta H°_f$ value selected for muscovite was determined by Vieillard (1994) and is very close to that of the EQ3/6 data base (Tab. 4). The $\Delta H°_f$ value selected for Li-mica was estimated by Sanjuan *et al.* (2010) because it was not available in the literature.

In spite of the inaccuracy related to the $\Delta H°_f$ values (Sanjuan *et al.*, 2010), the value determined for $\Delta H°_R$ is very close to that estimated using the Na/Li relationship determined in paragraph 3: -17.6 $KJ.mol^{-1}$. This result is in good agreement with that obtained from the $\Delta G°_R$ values and strengthen the conclusions drawn up from these last. It is concordant with the $\Delta H°_f$ value estimated for Li-mica by Sanjuan *et al.* (2010).

Table 3: Values of the standard molar Gibbs free energies of formation $\Delta G°_f$ selected for the compounds used in this study.

Compound	Chemical formula	Authors	$\Delta G°f_{selected}$ KJ.mol^{-1}	EQ3/6 data base
Water	H_2O	Johnson *et al.* (1992)	-237.17	X
Aqueous Lithium ion	Li^+	Robie *et al.* (1978), Tardy and Duplay (1992)	-293.30	
Aqueous Sodium ion	Na^+	Shock and Helgeson (1988) and Johnson *et al.* (1992)	-261.88	X
Albite	$NaAlSi_3O_8$	Helgeson *et al.* (1978) and Johnson *et al.* (1992)	-3708.31	X
K-Feldspar	$KAlSi_3O_8$	Helgeson *et al.* (1978) and Johnson *et al.* (1992)	-3746.24	X
Illite	$K_{0.6}Mg_{0.25}Al_{2.3}Si_{3.5}O_{10}(OH)_2$	Wolery (1978)	-5455.81	X
Kaolinite	$Al_2Si_2O_5(OH)_4$	Helgeson *et al.* (1978) and Johnson *et al.* (1992)	-3789.09	X
Li-Mica	$LiAl_3Si_3O_{10}(OH)_2$	estimated by Tardy and Duplay (1992)	-5596.80	
Muscovite (K-Mica)	$KAl_3Si_3O_{10}(OH)_2$	estimated by Tardy and Duplay (1992)	-5591.10	X
Quartz	SiO_2	Helgeson *et al.* (1978) and Johnson *et al.* (1992)	-856.24	X

Table 4: Values of the standard molar enthalpies of formation $\Delta H°_f$ selected for the compounds used in this study.

Compound	Chemical formula	Authors	$\Delta H°f_{selected}$ KJ.mol^{-1}	EQ3/6 data base
Water	H_2O	Robie *et al.* (1978), Johnson *et al.* (1992)	-285.84	X
Aqueous Lithium ion	Li^+	Shock and Helgeson (1988) and Johnson *et al.* (1992)	-278.45	X
Aqueous Sodium ion	Na^+	Robie *et al.* (1978), Shock and Helgeson (1988) and Johnson *et al.* (1992)	-240.30	X
Albite	$NaAlSi_3O_8$	Helgeson *et al.* (1978) and Johnson *et al.* (1992)	-3931.62	X
K-Feldspar	$KAlSi_3O_8$	Helgeson *et al.* (1978) and Johnson *et al.* (1992)	-3971.40	X
Illite	$K_{0.6}Mg_{0.25}Al_{2.3}Si_{3.5}O_{10}(OH)_2$	Wolery (1978)	-5835.29	X
Kaolinite	$Al_2Si_2O_5(OH)_4$	Helgeson *et al.* (1978) and Johnson *et al.* (1992)	-4109.61	X
Li-Mica	$LiAl_3Si_3O_{10}(OH)_2$	no data found in the literature - proposed in this study	-5992.00	
Muscovite (K-Mica)	$KAl_3Si_3O_{10}(OH)_2$	Krupka *et al.* (1979), value also selected by Vieillard (1994)	-5971.60	
Quartz	SiO_2	Helgeson *et al.* (1978) and Johnson *et al.* (1992)	-910.65	X

CONCLUSION

In the framework of this study, a specific Na/Li thermometric relationship was statistically obtained for HT fluids derived from seawater and basalt interaction processes existing in emerged Rifts such as those of Djibouti (Asal-Ghoubbet and Obock geothermal areas) and of Iceland (Reykjanes, Svartsengi and Seltjarnarnes geothermal fields), or in numerous Oceanic Ridges and Rises (Middle-Atlantic Ridge, East Pacific Rise, etc.). This relationship, which can be applied at temperature values ranging from 0 to 365°C, with an uncertainty of ± 25°C, can be described as:

$$T\ (°K) = 920 / [\log (Na/Li) - 1.105] \quad (r^2 = 0.994)$$

This relationship is slightly different from that determined by Sanjuan and Millot (2009) which integrated numerous literature data about HT fluids circulating in Oceanic Ridges and Rises as well as data from Djibouti, but used limited data from Iceland. The use of the thermometric Na/Li relationship determined in this study is recommended.

The excellent regression coefficient obtained for this relationship confirms the temperatures estimated for the hot seawater derived end-member of the thermal waters collected from the Ghoubbet Channel (160°C) and Obock (210°C), using the other chemical geothermometers.

This thermometric Na/Li relationship is very different from the three relationships previously described and known in the literature and that proposed by Sanjuan *et al.* (2010) for the HT dilute geothermal waters from Iceland.

The existence of new Na/Li thermometric relationships confirms that the Na/Li ratios not only depend on the temperature but also on other parameters such as the fluid salinity and origin, the nature of the geothermal reservoir rocks in contact with the deep hot fluids or the equilibrium reactions between these fluids and the reservoir mineral assemblages.

Some case studies found in the literature and thermodynamic considerations suggest that the Na/Li ratios for the HT geothermal fluids derived from seawater and basalt interaction processes could be controlled by a full equilibrium reaction involving a mineral assemblage constituted, at least, of albite, K-feldspar, quartz and clay minerals such as kaolinite, illite (or muscovite) and Li-micas. Other equilibrium reactions involving slightly different mineral assemblages could explain the other existing Na/Li relationships (Sanjuan *et al.*, 2010).

This study shows that it is essential to well define the environment in which the Na/Li geothermometer is applied before its use. Additional developments relative to this auxiliary geothermometer in different environments and regions are necessary in order to improve its use, which can be more reliable than other classical geothermometers in many cases and consequently, very useful for geothermal exploration. Experimental works in laboratory involving water-rock interaction processes as a function of temperature and integrating chemical, isotopic and mineralogical analyses should allow improving the knowledge and understanding of the running of this geothermometer.

Aknowledgments: I would like to thank the International Division of BRGM, especially J.-Ph. Rançon and J.-C. Guillaneau, who supported financially this study. This study benefited from the results obtained during my stay in Djibouti (1986-1990), at ISERST (presently CERD), and in the framework of the FP6 European project HITI (2007-2010). My colleagues from BRGM (especially R. Millot and M. Brach), CERD (especially A. Abdallah, A. Abdillahi and I. Houssein), Prof. G. Michard (University of Paris 7) as well as ISOR (especially, R. Asmundsson and N. Giroud) are also thanked.

REFERENCES

Arnorsson, S. (1983): Chemical equilibria in Icelandic geothermal systems. Implications for chemical geothermometry investigations. *Geothermics*, **12**, n°2-3, 119-128.

Arnorsson, S. (1995): Geothermal systems in Iceland: Structure and conceptual models. 1. High-temperature areas. *Geothermics*, **24**, 561-602.

Arnorsson, S., and Andresdottir, A. (1995): Processes controlling the distribution of boron and chlorine in natural waters in Iceland. *Geochimica et Cosmochimica Acta*, **59**, n°20, 4125-4146.

Arnorsson, S., and Stefansson, A. (1999): Assessment of feldspar solubility constants in water in the range 0 to 350°C at vapor saturation pressures. *American Journal of Science*, **299**, 173-209.

Barberi, F., Ferrara, G., Santacroce, R., and Varet, J. (1975): Structural evolution of the afar triple junction. *In: A. Pilger and A. Rösler Edition, Afar depression of Ethiopia. Vol. 1 Schweizerbart, Stuttgart*, 38-54.

Bjornsson, S., Arnorsson, S., and Tomasson, S. (1972): Economic evaluation of the Reykjanes thermal brine area, Iceland. *Bull. Am. Assoc. Petrol. Geologists*, **56**, 2380-2391.

Bosch, B., Deschamps, J., Leleu, M., Lopoukhine, M., Marcé, A., and Vilbert, C. (1977): The geothermal zone of Lake Asal (T.F.A.I.). Geochemical and experimental studies. *Geothermics*, **5**, 166-175.

Calvet, R., and Prost, R. (1971): Cation migration into empty octahedral sites and surface properties of Clays. *Clays and Clay Minerals*, **19**, 175-186.

Clifton, A., and Kattenhorn, S. (2006): Structural architecture of a highly oblique divergent plate boundary segment. *Tectonophysics*, **419**, 27-40.

Choukroune, P., Francheteau, J., Auvray, B., Auzende, J.-M., Brun, J.-P., Sichler, B., Arthaud, F., and Lépine, J.-C. (1988): Tectonics of an incipient oceanic rift. *Mar. Geophys. Res.*, **9**, 147-163.

D'Amore, F., Arnorsson, S. (2000): Geothermometry. *In Isotopic and chemical techniques in geothermal exploration, development and use, Edited by S. Arnorsson, International Atomic Energy Agency, Vienna*, **10**, 152-199.

D'Amore, F., Giusti, D., and Abdallah, A. (1998): Geochemistry of the high-salinity geothermal field of Asal, Republic of Djibouti, Africa. *Geothermics*, **27**, n°2, 197-210.

Dauteuil, O., Huchon, P., Quemeneur, F., and Souriot, T. (2001): Propagation of an oblique spreading centre: the western Gulf of Aden. *Tectonophysics*, **332**, 423-442.

Faure, H., Hong, T., and Lalou, C. (1980): Datation ^{235}Th/^{234}U des calcaires corallines et mouvements verticaux à Djibouti. *Bull. Soc. Géol. France, TXXII*, **6**, 959-962.

Fontes, J.-C., Florkowski, T., Pouchan, P., and Zuppi, G.M. (1979): Preliminary isotopic study of lake Asal system (Rep. of Djibouti). In: "Isotopic Lake Studies". Proc. Adv. Group Meeting, Vienna, IAEA, 163-174.

Fouillac, Ch., Fabriol, R., and Iundt, F. (1983): Champ géothermique d'Asal. Synthèse des données disponibles au 1er janvier 1983. *Report BRGM 83SGN022GTH*, 71 p.

Fouillac, C., and Michard, G. (1981): Sodium/Lithium ratio in water applied to geothermometry of geothermal reservoirs. *Geothermics*, **10**, 55-70.

Fournier, R.O. (1979): A revised equation for the Na/K geothermometer. *Geothermal Resources Council Transactions*, **3**, 221-224.

Fournier, R.O., and Rowe, J.J. (1966): Estimation of underground temperatures from the Silica content of water from hot springs and wet-steam wells. *American Journal of Science*, **264**, 685-697.

Fournier, R.O., and Truesdell, A.H. (1973): An empirical Na-K-Ca geothermometer for natural waters. *Geochimica et Cosmochimica Acta*, **37**, 1255-1275.

Giggenbach, W.F. (1988): Geothermal solute equilibria. Derivation of Na-K-Mg-Ca geoindicators. *Geochimica et Cosmochimica Acta*, **52**, 2749-2765.

Giroud, N. (2008): A Chemical Study of Arsenic, Boron and Gases in High-Temperature Geothermal Fluids in Iceland. *Dissertation for the Degree of Doctor of Philosophy, University of Iceland*, 110 p.

Gudmundsson, J.S., and Thorhallsson, S. (1986): The Svartsengi reservoir in Iceland. *Geothermics*, **15**, n°1, 3-15.

Helgeson, H.C., Delany, J.M., Nesbitt, H.W., and Bird, D.K. (1978): Summary and critique of the thermodynamic properties of rock-forming minerals. *American Journal of Science*, **278a**, 229 p.

Houssein, D.E., and Axelsson, G. (2010): Geothermal resources in the Asal Region, Republic of Djibouti: An update with emphasis on reservoir engineering studies. *Geothermics*, **39**, 220-227.

Houssein, I., Sanjuan, B., and Michard, G. (1993): Indices géochimiques de l'existence d'un fluide à 210°C dans la région d'Obock (République de Djibouti). *C.R. Acad. Sciences de Paris*, t. 316, série II, 771-776.

Johnson, J.W., Oelkers, E.H., and Helgeson, H.C. (1992): SUPCRT92: A software package for calculating the standard molal thermodynamic properties of minerals, gases, aqueous species, and reactions from 1 to 5000 bar and 0 to 1000°C. *Computers Geoscience*, **18**, 899-947.

Kharaka, Y.K., and Mariner, R.H. (1989): Chemical geothermometers and their application to formation waters from sedimentary basins. *In: Naeser, N.D. and McCulloch, T.H. (Eds), Thermal history of sedimentary basins: methods and case histories. Springer-Verlad, New York*, 99-117.

Krupka, K.M., Robie, R.A., and Hemingway, B.S. (1979): High-temperature heat capacities of corundum, periclase, anorthite, $CaAl_2Si_2O_8$ glass, muscovite, pyrophillite, $KAlSi_3O_8$ glass, grossular, and $NaAlSi_3O_8$ glass. *American Mineralogist*, **64** (1-2), 86-101.

Lépine, J.-C., and Hirn, A. (1992): Seismotectonics in the Republic of Djibouti, linking the Afar depression and the Gulf of Aden. *Tectonophysics*, **209**, 65-86.

Manning, D.A.C. (2003): Experimental studies of clay mineral occurrence. *In clay mineral cements in Sandstones, Intern. Assoc. Sedimentol. Spec. Publ., Edited by R. H. Worden and S. Morad and published by Blackwell Publishing*, **34**, 177-190.

Marini, L. (1987): Geochemistry of North Ghoubbat - Asal region. *Report Geotermica Italiana srl - ISERST, April 1987*, 28 p.

Michard, G. (1979): Géothermomètres chimiques. *Bull. BRGM*, Section III, **2**, 183-189.

Nicholson, K. (1993): Geothermal fluids. *Chemistry and Exploration Techniques, Springer-Verlag Berlin, Heidelberg*, 260 p.

Olafsson, J., and Riley, J.P. (1978): Geochemical studies on the thermal brine from Reykjanes (Iceland). *Chemical Geology*, **21**, 219-237.

Pope, E.C., Bird, D.K., Arnorsson, S., Fridriksson, T., Elders, W.A., Fridleifsson, G.O. (2009): Fluid origin and evolution in the Reykjanes geothermal system, Iceland. A stable isotope study of hydrothermal epidote. *Geochimica et Cosmochimica Acta, 73, 4468-4488.*

Pope, E.C., Bird, D.K., Arnórsson, S., Fridriksson, T., Elders, W.A. and Friðleifsson, G.O. (2010): The Iceland Deep Drilling Project: Stable Isotope Evidence of Fluid Evolution in Icelandic Geothermal Systems. *Proc. World Geothermal Congress, Bali, Indonesia*, April 25-29.

Richard, O., and Varet, J. (1979): Study of the transition from deep oceanic to emerged rift zone: Gulf of Tadjourah, Republic of Djibouti. *Intern. Symp. Geodyn. Evol. Afro-Arabian rift system, Roma, April 1979.*

Robie, R.A., Hemingway, B.S., and Fisher, J.R. (1978): Thermodynamic properties of minerals and related substances at 298.15°K and 1 bar pressure and at higher temperatures. *U.S. Geological Survey Bulletin*, **1452**, 1-456.

Sanjuan, B., Girard, J.-P., Lanini, S., Bourguignon, A., Brosse, E. (2003): Geochemical modelling of diagenetic illite and quartz cement formation in Brent sandstone reservoirs: example of the Hild Field, Norwegian North Sea. *In clay mineral cements in Sandstones, Intern. Assoc. Sedimentol. Spec. Publ., Edited by R. H. Worden and S. Morad and published by Blackwell Publishing*, **34**, 425-452.

Sanjuan, B., Michard, G., and Michard, A. (1990): Origine des substances dissoutes dans les eaux des sources thermales et des forages de la région Asal-Ghoubbet (République de Djibouti). *J. of Volcanol. and Geoth. Research*, 43, 333-352.

Sanjuan, B., and Millot, R. (2009): Bibliographical review about Na/Li geothermometer and Lithium isotopes applied to worldwide geothermal waters. *Report BRGM/RP-57346-FR*, 56 p.

Sanjuan, B., Millot, R., Brach, M., Asmundsson, R., and Giroud, N. (2010): Use of a new Sodium/Lithium (Na/Li) geothermometric relationship for High-Temperature dilute geothermal fluids from Iceland. *Proceedings World Geothermal Congress 2010 (WGC2010), Bali, Indonesia, 25-29 April 2010*, 12 p.

Sanjuan B., Millot, R., Brach, M., Asmundsson, R., and Giroud, N. (2010): Use of two new Sodium/Lithium (Na/Li) geothermometric relationships for High-Temperature geothermal fluids from Iceland *(In preparation).*

Serra, H., and Sanjuan, B. (2004): Synthèse bibliographique des géothermomètres chimiques. *Report BRGM/RP-52430-FR*, 80 p.

Shaw, D.M., and Sturchio, N.C. (1992): Boron-Lithium relationships in rhyolites and associated thermal waters of young silicic calderas, with comments on incompatible element behaviour. *Geochimica et Cosmochimica Acta*, **56**, 3723-3731.

Shock, E.L., and Helgeson, H.C. (1988): Calculation of the thermodynamic and transport properties of aqueous species at high pressures and temperatures: Correlation algorithms for ionic species and equation of state predictions to 5 Kbar and 1000°C. *Geochimica et Cosmochimica Acta*, **52**, 2009-2036.

Stieljes, L. (1973): L'axe tectono-volcanique d'Asal (T.F.A.I.). Thèse 3ème cycle, Université de Paris Sud.

Tardy, Y., and Duplay, J. (1992): A method of estimating the Gibbs free energies of formation of hydrated and dehydrated clay minerals. *Geochimica et Cosmochimica Acta*, **56**, 3007-3029.

Truesdell, A.H., Thompson, J.M., Coplen, T.B., Nehring, N.L. and Janik, C.J. (1981): The origin of the Cerro Prieto geothermal brine. *Geothermics*, vol. 10, n°3/4, 225-238.

Varet, J. (1975): Carte géologique de l'Afar centrale et méridionale au 1/50000. *CNRS Edition*.

Vieillard, Ph. (1994): Prediction of enthalpy of formation based on refined crystal structures of multi-site compounds. Part 2: Application to minerals belonging to the system Li_2O-Na_2O-K_2O-BeO-MgO-CaO-MnO-FeO-Fe_2O_3-Al_2O_3-SiO_2-H_2O. Results and discussion. *Geochimica et Cosmochimica Acta*, **58**, 4065-4107.

White, D.E. (1970): Geochemistry applied to the discovery, evaluation, and exploitation of geothermal energy resources. *Geothermics, Special Issue 2 on U.N. Symposium on the development and utilization of geothermal resources, Pisa, Italy*, **vol. 1**, section V, 58-80.

Wolery, T.J. (1978): Some chemical aspects of hydrothermal processes at mid-oceanic ridges: A theoretical study. I. Basalt-sea water reaction and chemical cycling between the oceanic crust and the oceans. II. Calculation of chemical equilibrium between aqueous solutions and minerals. *Unpublished Ph.D. Diss., Northwestern Univ., Evaston, IL*, 263p.

Wolery, T.J. (1995): EQ3/6, A software package for geochemical modelling of aqueous systems: Package overview and installation guide, Version 7.2b. *Laurence Livermore National Laboratory*.

Appendix 1

Review of Lithium chemical and isotopic data relative to worldwide hydrothermal submarine fluids (extracted from Sanjuan and Millot, 2009). The data in italic do not fit the Na/Li geothermometric relationship determined in this study.

Hydrothermal springs	T °C	1000/T °K^{-1}	pH	Na mg/l	Li mg/l	Cl mg/l	SiO_2 mg/l	Alk. mg/l HCO_3	Na/Li	log (Na/Li)	Li/Na x 1000	Li/Cl x 1000	Na/Cl	δ^7Li ‰	T Sil.-Qz °C	Reference
Vent fluids Bent Hill (Middle Valley Ridge, 1990)	**265**	**1.86**	5.13	7242	2.57	14607	619	88	851	2.93	1.17	0.90	0.76		**273**	Butterfield *et al.* (1994)
Guaymas Basin hydrothermal solution 9 (Gulf of California, USA)	**270**	**1.84**	5.90	11035	4.37	20598	559		762	2.88	1.31	1.08	0.83	10.0	**263**	Von Damm *et al.* (1985) - Chan *et al.* (1994)
Vent fluids Dead Dog (Middle Valley Ridge, 1990)	**276**	**1.82**	5.50	9150	3.82	20492	637	122	724	2.86	1.38	0.95	0.69		**276**	Butterfield *et al.* (1994)
Vent 6X (Escanaba Through, Gorda Ridge hydrothermal system, 1988)	300	1.74	5.40	12874	8.92	23683	415	189	435	2.64	2.30	1.93	0.84	9.1	**236**	Campbell et al. (1994)
Vent 6X (Escanaba Through, Gorda Ridge hydrothermal system, 2000)	300	1.74	< 5.81	12460	8.74	22406	382	< 145	430	2.63	2.32	1.99	0.86		**229**	Von Damm *et al.* (2005)
Vent 6X (Escanaba Through, Gorda Ridge hydrothermal system, 2002)	300	1.74	< 5.75	12736	7.70	22725	379	< 128	499	2.70	2.00	1.73	0.86		**228**	Von Damm *et al.* (2005)
Guaymas Basin hydrothermal fluid 7 (Gulf of California, USA)	**300**	**1.74**	5.90	11265	7.47	20598	769		455	2.66	2.20	1.85	0.84		**295**	Von Damm (1988)
Guaymas Basin hydrothermal fluid (South Field, Gulf of California, USA, 1982)	**300**	**1.74**	5.90	11265	7.36	20917	775	641	462	2.66	2.16	1.80	0.83	5.0	**296**	Campbell *et al.* (1988b) - Chan *et al.* (1993)
Guaymas Basin hydrothermal fluid (South Field, Gulf of California, USA, 1985)	**300**	**1.74**	5.90	10851	6.89	20563	811	586	475	2.68	2.10	1.71	0.81	2.6	**301**	Campbell *et al.* (1988b) - Chan *et al.* (1994)
Guaymas Basin hydrothermal fluid (East Hill, Gulf of California, USA, 1982)	**300**	**1.74**	5.90	11150	6.06	21236	829	494	556	2.74	1.80	1.46	0.81	7.6	**303**	Campbell *et al.* (1988b) - Chan *et al.* (1994)
Guaymas Basin hydrothermal fluid (East Hill, Gulf of California, USA, 1985)	**300**	**1.74**	5.90	11219	5.89	21378	829	543	575	2.76	1.74	1.41	0.81	10.2	**303**	Campbell *et al.* (1988b) - Chan *et al.* (1994)
Vent fluid 6 at 11°N (East Pacific Rise)	**310**	**1.71**	3.10	6667	3.36	11983	859		599	2.78	1.67	1.43	0.86	10.7	**307**	Bowers *et al.* (1988) - Chan *et al.* (1993)
Guaymas Basin hydrothermal solution 4 (Gulf of California, USA)	**315**	**1.70**	5.90	11150	6.06	21236	829		556	2.74	1.80	1.46	0.81		**303**	Von Damm (1988)
MARK-1 vent fluid (Mid-Atlantic Ridge)	**335**	**1.64**	3.70	11702	5.89	19818	1100	< 4	600	2.78	1.67	1.52	0.91	6.3	**336**	Campbell *et al.* (1988b) - Chan *et al.* (1993)
OBS (21°N, East Pacific Rise, 1985)	**340**	**1.63**	3.40	10093	6.43	17727	1057		474	2.68	2.11	1.85	0.88	8.9	**332**	Campbell *et al.* (1988b) - Chan *et al.* (1993)
Vent fluid 1 at 11°N (East Pacific Rise)	**347**	**1.61**	3.10	10851	6.13	19960	1130		534	2.73	1.87	1.57	0.84	10.9	**340**	Bowers et al. (1988) - Chan et al. (1993)
MARK-2 vent (Mid-Atlantic Ridge)	**350**	**1.60**	3.90	11725	5.85	19818	1094	< 15	605	2.78	1.65	1.51	0.91	8.5	**336**	Campbell *et al.* (1988a) - Chan *et al.* (1993)
Clambake (Ridge crest hydrothermal activity at Galapagos Spreading Center)	**350**	**1.60**		11196	7.92	21095	1316		427	2.63	2.34	1.92	0.82		**359**	Edmond *et al.* (1979)
Garden of Eden (Ridge crest hydrothermal activity at Galapagos Spreading Center)	**350**	**1.60**		10368	7.92	19251	1316		395	2.60	2.53	2.10	0.83		**359**	Edmond *et al.* (1979)
Dandelions (Ridge crest hydrothermal activity at Galapagos Spreading center)	**350**	**1.60**		7196	7.92	14004	1316		274	2.44	3.65	2.89	0.79		**359**	Edmond *et al.* (1979)
Oyster Beds (Ridge crest hydrothermal activity at Galapagos Spreading Center)	**350**	**1.60**		5954	4.78	11416	1316		376	2.58	2.66	2.14	0.80		**359**	Edmond *et al.* (1979)
OBS (21°N, East Pacific Rise, 1981)	**350**	**1.60**	3.40	9932	6.18	17337	1057	< 24	485	2.69	2.06	1.82	0.88	9.2	**332**	Von Damm *et al.* (1985) - Chan *et al.* (1993)
NGS (21°N, East Pacific Rise, 1981)	**350**	**1.60**	3.80	11725	7.17	20527	1172	< 12	494	2.69	2.03	1.78	0.88	10.0	**344**	Von Damm *et al.* (1985) - Chan *et al.* (1993)
NGS (21°N, East Pacific Rise, 1985)	**350**	**1.60**		11656	7.57	20421	1166		465	2.67	2.15	1.89	0.88		**344**	Campbell *et al.* (1988b)
SW (21°N, East Pacific Rise, 1981)	**350**	**1.60**	3.60	10093	6.24	17585	1039	< 18	488	2.69	2.05	1.81	0.89	9.6	**330**	Von Damm *et al.* (1985) - Chan *et al.* (1993)
SW (21°N, East Pacific Rise, 1985)	**350**	**1.60**	4.00	10621	6.72	18613	1033	< 10	477	2.68	2.10	1.85	0.88	8.6	**329**	Campbell *et al.* (1988b)
HG (21°N, East Pacific Rise, 1981)	**350**	**1.60**	3.30	10184	9.17	17585	937	< 31	335	2.53	2.98	2.67	0.89	6.6	**317**	Von Damm *et al.* (1985) - Chan *et al.* (1993)
HG (21°N, East Pacific Rise, 1985)	**350**	**1.60**	3.60	10414	10.05	17939	1009	< 24	313	2.50	3.20	2.86	0.90	6.8	**326**	Campbell *et al.* (1988b) - Chan *et al.* (1993)
OBS (21°N, East Pacific Rise, 1981)	**355**	**1.59**	3.60	10093	6.24	17585	1040		488	2.69	2.05	1.81	0.89		**330**	Von Damm *et al.* (1985)
Vent fluid 5 from the Broken Spur site (29°N Mid-Atlantic Ridge)	**356**	**1.59**		9679	6.98	16627			418	2.62	2.39	2.14	0.90			James *et al.* (1995)
Plume (Southern Juan de Fuca Ridge)	**360**	**1.58**	3.20	18300	11.92	38537	1400		463	2.67	2.16	1.58	0.73		**368**	Von Damm and Bischoff (1987)
Vent fluid 3 from the Broken Spur site (29°N Mid-Atlantic Ridge)	**360**	**1.58**		9702	7.17	16627			409	2.61	2.45	2.20	0.90			James *et al.* (1995)
Vent fluid 4 from the Broken Spur site (29°N Mid-Atlantic Ridge)	**364**	**1.57**		9633	7.18	16627			405	2.61	2.47	2.21	0.89			James *et al.* (1995)
Vent fluid from the Menez Gwen Field (Mid-Atlantic Ridge, 37°50'N, Mean values, 1993)	***280***	***1.81***	*4.20*	*7242*	*1.82*	*13259*	*601*		*1198*	*3.08*	*0.83*	*0.70*	*0.84*		***270***	*Charlou et al. (2000)*
Vent fluid from the Menez Gwen Field (Mid-Atlantic Ridge, 37°50'N, Menez flank site, 1993)	***284***	***1.79***	*4.20*	*7196*	*1.90*	*13508*	*619*		*1142*	*3.06*	*0.88*	*0.72*	*0.82*		***273***	*Charlou et al. (2000)*
Hydrothermal fluid from the 17°S active site on the North Fiji Basin Ridge (SW Pacific)	***285***	***1.79***	*4.70*	*4828*	*1.39*	*9041*	*841*		*1050*	*3.02*	*0.95*	*0.78*	*0.82*		***305***	*Grimaud et al. (1993)*
Brandon vent - brine Be.5 (Southern East Pacific Rise)	***295***	***1.76***	*3.30*	*10322*	*3.39*	*19747*	*751*		*920*	*2.96*	*1.09*	*0.88*	*0.81*		***293***	*Von Damm et al. (2003)*
13°N hydrothermal site (East Pacific Rise)	***320***	***1.69***	*3.20*	*12874*	*4.77*	*26235*	*1322*		*814*	*2.91*	*1.23*	*0.93*	*0.76*		***360***	*Michard et al. (1984)*
Vent fluid from the Lucky Strike Field (Mid-Atlantic Ridge, 37°17'N, Eiffel Tower site, 1994)	***324***	***1.67***	*3.70*	*7977*	*1.98*	*14784*	*799*		*1213*	*3.08*	*0.82*	*0.69*	*0.83*		***299***	*Charlou et al. (2000)*
Vent fluid from the Lucky Strike Field (Mid-Atlantic Ridge, 37°17'N, Eiffel Tower site, 1993)	***325***	***1.67***	*4.07*	*8161*	*2.10*	*15528*	*943*	*< 1.2*	*1172*	*3.07*	*0.85*	*0.69*	*0.81*		***318***	*Von Damm et al. (1998)*
Vent fluid from the Lucky Strike Field (Mid-Atlantic Ridge, 37°17'N, Mean values)	***325***	***1.67***	*3.65*	*8966*	*2.13*	*16486*	*865*		*1270*	*3.10*	*0.79*	*0.66*	*0.84*		***308***	*Charlou et al. (2000)*
Vent fluid from the Lucky Strike Field (Mid-Atlantic Ridge, 37°17'N, 2608 Vent site, 1996)	***328***	***1.66***	*3.78*	*9633*	*2.89*	*18648*	*1051*	*< 35*	*1005*	*3.00*	*1.00*	*0.79*	*0.80*		***331***	*Von Damm et al. (1998)*
Vent fluid 2 at 13°N (East Pacific Rise)	***354***	***1.59***	*3.10*	*12667*	*4.11*	*25243*	*1166*		*931*	*2.97*	*1.07*	*0.83*	*0.77*		***344***	*Bowers et al. (1988)*
Hydrothermal fluid from Trans-Atlantic Geotraverse (TAG, 26°08'N)	***360***	***1.58***		*13426*	*2.85*	*23364*	*1322*		*1421*	*3.15*	*0.70*	*0.62*	*0.89*	*11.5*	***360***	*Campbell et al. (1988a) - Chan et al. (1994)*
Seawater (Diamant, Martinique)	**29**	**3.32**	8.19	11400	0.23	20200	0.19	143	14960	4.17	0.07	0.06	0.87	30.5		Sanjuan *et al.* (2003)
Seawater (Bouillante, Guadeloupe)	**29**	**3.31**	8.23	11000	0.25	20181	0.43	169	13280	4.12	0.08	0.06	0.84	29.3		Sanjuan (2001)
Seawater (Lamentin, Martinique)	**29**	**3.31**	8.20	11400	0.23	21307		148	14960	4.17	0.07	0.06	0.83	30.1		Sanjuan *et al.* (2002)
Lake Bogoria (Kenya)	**27**	**3.33**	10.10	39300	0.76				15608	4.19	0.06					Cioni *et al.* (1992)

$T_{Sil.-Qz}$: temperature estimated using the Silica-quartz geothermometer (Fournier and Rowe, 1966).

GALLIUM AND GERMANIUM DISTRIBUTON IN GEOTHERMAL WATER

Sikie A. Elmi[a], Stefan Arnorsson[b] and Andri Stefansson[b]
[a] *: Centre d études et de recherches de Djibouti.*
[b] *: University of Iceland, Institute of Earths Science.*

ABSTRACT

The geochemistry of gallium and germanium was studied in geothermal waters from the low-temperature fields in the Southern Lowlands and the Geysir high-temperature field in Iceland. Germanium concentrations in waters with temperatures below 225°C were in the range <0.05-24 ppb whereas those of gallium lie in the range of <0.01-21 ppb. Both elements show positive relationships with temperature, in particular Ge. Based on aqueous speciation studies, the dominant forms of Ge and Ga in the water are $H_4GeO_4^0$ and $Ga(OH)_4^-$, respectively, but $H_3GeO_4^-$ and $Ga(OH)_3^0$ are also important. The mobility of Ge relative to Si and of Ga relative to Al is much higher than the respective primary rock ratios. The cause of this is considered to be either non-stoichiometric dissolution of the primary basalt rock-forming minerals with respect to Ge and Si and Ga and Al and/or exchange of Ge into silicates and Ga into aluminium silicates in ratios that differ from those of fresh basalt. An example of such an exchange is given for Si and Ge.

INTRODUCTION

Gallium and germanium are trace elements in geothermal waters. They are positioned below Al and Si in the Periodic Table and exhibit many similar chemical properties. Germanium is enriched in geothermal water and some non-thermal groundwater relative to the ocean and river water. Only 0.06 ppb Ge are present in oceanic water (Burton et al., 1959). By contrast, Ge concentrations reported for geothermal waters are much higher, or between 2 and 30 ppb for Icelandic geothermal waters (Arnórsson, 1984), 0.4-43.8 ppb for geothermal waters in Japan (Uzumasa et al., 1959), 2-20 ppb in Vichy, France (Criaud and Fouillac, 1986) and on the Juan de Fuca Ridge they lie in the range 10.9-18.9 ppb (Mortlock et al., 1993). Much less data are available on Ga concentrations in geothermal waters. The values, however, seem to be lower compared to Ge. Gallium concentrations in geothermal waters at Broadlands and Wairakei, New Zealand, were estimated to be ~0.6 and ~0.2 ppb, respectively (Goguel, 1988) and in some Japanese geothermal waters values between 0.11 and 72 ppb have been reported (Uzumasa and Nasu, 1960).

The purpose of this study is to establish the distribution of Ga and Ge in geothermal waters from the Southern Lowlands in Iceland and to delineate the processes that may control the concentrations of these trace elements in these waters. The study is based on analyses of 72 samples of thermal waters from the Southern Lowlands and the Geysir high-temperature field and 22 samples of cold ground and surface waters, collected and analysed by Arnórsson and co-workers in 2002-2005. The cold waters mostly have temperatures below 10°C whereas the thermal waters are from slightly above ambient to >200°C. The waters from the Southern Lowlands are associated with basaltic rock formations, but in the Geysir field both basaltic and silicic volcanics outcrops.

GEOLOGICAL SETTINGS

Iceland is located on the North-Atlantic Ridge that separates the North-American and Eurasian plates (Vink, 1984). The volcanic succession pile of Iceland can be divided into four zones based on the age of the rocks: the Upper Tertiary flood basalt formations which are older than 3.1 m.y., the Upper Pliocene and Lower Pleistocene grey basalt formation, which are between 0.7 and 3.1 m.y., the Upper Pleistocene palagonite (hyaloclastite) formation that is younger than 0.7 m.y., and Postglacial lavas which formed during the last 9,000 to 13,000 years (Saemundsson, 1979).

Geothermal systems in Iceland have been divided into two groups, high-temperature fields (volcanic geothermal systems) and low-temperature fields (non-volcanic systems). The high-temperature fields are located within the active zone of volcanism and rifting and temperatures exceed 200°C at less than 1000 m depth. The low-temperature fields are widely distributed in Quaternary and Tertiary formations and have much lower temperatures, less than 150°C in the uppermost 1000 metres (Arnórsson et al., 2008).

In the Southern Lowlands, low-temperature activity is widespread, and sometimes divided into three distinct areas (Arnórsson, 1995). It mostly occurs to the north of an east-west running zone of intense seismic activity (Einarsson,

1991) (Figures 1). Hot springs are typically associated with young fractures. The Geysir field, which is of the high-temperature type, is located in the northernmost part of the Southern Lowlands. Great Geysir of Haukadalur is in the area, one of the more famous geysers in the world (Barth, 1940). The bedrock in the Southern Lowlands is basaltic, for the most part lavas, pillow lavas and hyaloclastite of Quaternary age. They are overlain in places by sediments formed at the end of the last glaciation and in early Holocene times. The same types of rocks outcrop in the Geysir field, i.e. hyaloclastites, in addition to relatively abundant rhyolites (Arnórsson, 1985).

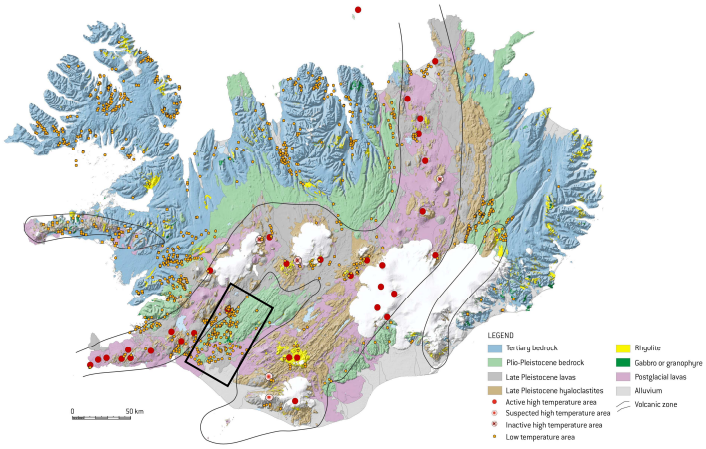

FIGURE 1: A geological map of Iceland with geothermal areas (modified from ISOR database)

SAMPLING AND ANALYTICAL METHODS

The present study is based on data on the chemical composition of 91 samples of ground and geothermal waters from the Southern Lowlands and the Geyser geothermal field (Figure 2). Of these, 66 are of geothermal waters from springs and wells and 25 are non-thermal groundwater, also from springs and wells. The data constitute a part of an unpublished database of the Institute of Earth Science of the University of Iceland, the University of Akureyri and Iceland GeoSurvey. The samples from the Southern Lowlands were collected and analysed in 2002-2005, whereas the samples from the Geysir geothermal field were collected and analysed in 2001. The samples were collected and analysed by Stefán Arnórsson and co-workers. The results for elements relevant for the present study are shown in Table 1.

The samples were collected and treated according to the procedures described by Arnórsson et al. (2002) and Arnórsson and Óskarsson (2007). The samples were filtered on-site through a 0.2 µm acetate cellulose membrane followed by acidification by 1 ml Suprapur HNO_3 (Merck) to a 100 ml sample. Aluminium, Ga, Ge and Si, as well as a number of other major and trace elements, were determined by ICP-MS, ICP-OES and ion chromatography. The detection limit for

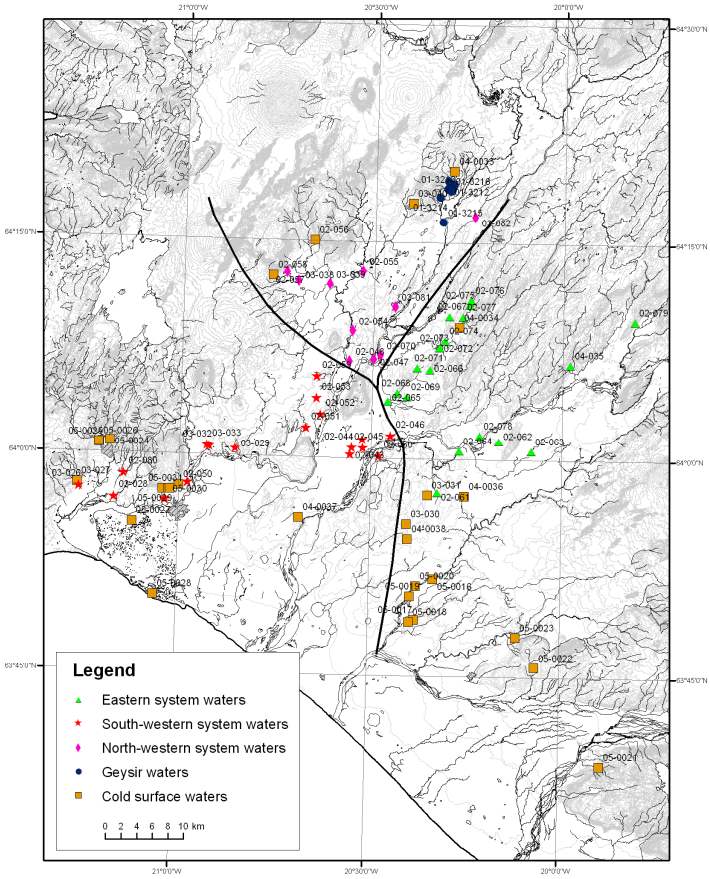

FIGURE 2: A map of the Southern Lowlands of Iceland showing sample locations and the division of the low-temperature activity into three fields; The Geysir high-temperature field is located at the northern periphery of the area

Ge and Ga are ~0.01 and ~0.05 ppb, respectively.

AQUEOUS SPECIATION

Thermodynamic data

To quantify and understand the Ga and Ge accumulation in geothermal waters requires knowledge of the thermodynamic properties of important aqueous Ga and Ge species. The most important aqueous Ge species are germanic acid ($H_4GeO_4^0$) and its dissociation products ($H_3GeO_4^-$ and $H_2GeO_4^{2-}$).

TABLE 1: The concentrations of SiO2, Al, Ga and Ge in cold groundwater and geothermal waters from the Southern Lowlands and the Geysir high-temperature field; also shown are measured surface temperature , and silica and Na/K geothermometer temperatures.

Sample No.	Location	Coordinates	t_{meas}/°C	t_{NaK}/°C	t_{cal}/°C	SiO_2 ppm	Al ppb	Ga ppb	Ge ppb
01-3201	Geysir	64.31387/-20.29934	87.0	197	233	533.9	742.0	9.10	21.40
01-3202	Blesi	64.31352/-20.30140	87.5	188	230.7	517.3	300.0	7.94	21.10
01-3203	Ótherrishola	64.31208/-20.30237	98.0	188	230.5	519.0	243.0	13.00	20.30
01-3204	Litli-Geysir	64.31180/-20.30126	93.0	143	214.4	416.1	394.0	20.50	23.60
01-3205	Litli-Strokkur	64.31115/-20.30230	88.0	141	207.3	364.7	156.0	14.90	17.90
01-3206	Smidur	64.31057/-20.30184	99.0	142	204	358.5	165.0	20.90	17.50
01-3207	Konungshver	64.31386/-20.30186	95.0	184	226.2	488.9	386.0	10.30	21.30
01-3208	Helludalur 1	64.32171/-20.30826	30.1	187	81.1	62.7	8.8	0.11	2.05
01-3209	Laugarfell west	64.31280/-20.31019	38.8	155	101.4	88.5	8.0	0.06	2.62
01-3210	"82-015"	64.31833/-20.30478	26.0	155	72.3	51.7	11.7	0.21	1.25
01-3211	Spring by Beiná	64.31793/-20.29345	19.6	161	39.2	24.6	7.2	0.14	0.17
01-3212	Laugarfell east	64.31390/-20.30607	97.5	132	208.1	373.8	564.0	19.90	18.10
01-3213	Strokkur	64.31269/-20.30095	86.0	156	214.2	416.7	543.0	14.90	22.80
01-3214	Nedridalur 1	64.30280/-20.33033	65.2	256	142.2	176.2	11.7	0.12	7.45
01-3215	Múli 1	64.27408/-20.32108	48.0	196	123	126.3	5.6	0.05	2.99
01-3216	Nyihver	64.31039/-20.30155	98.0	144	210.2	392.4	525.0	20.70	21.60
02-041	Blesastadir		69.0	74	70	66.7	48.2	2.22	2.20
02-042	Brautarholt	64:01.3137/20:31.3048	68.8	82	74	64.7	43.2	2.81	2.18
02-043	Brjánsstadir	64:00.2642/20:33.1877	63.9	137	117	125.1	3.6	0.11	2.41
02-044	Hlemmiskeid	64:00.7290/20:32.9498	68.5	87	64	67.3	71.5	3.55	1.48
02-045	Húsatóttir	64:01.5925/20:31.2093	73.5	87	66	68.1	51.9	2.96	2.26
02-046	Reykir, Skeid	64:02.6440/20:26.9037	68.3	85	75	64.7	41.3	2.38	3.37
02-047	Laugarás	64:06.8750/20:29.4882	97.3	108	98	110.4	120.0	4.98	6.21
02-048	Thorlákshver	64:06.7325/20:33.6703	97.0	104	109	104.6	109.0	3.92	6.73
02-050	Ingólfsfjall	63:57.8318/20:59.9705	3.8	133	12	13.1	14.8	0.45	<0.05
02-051	Vatnsendi	64:02.0740/20:40.2103	80.0	129	117	136.6	28.6	1.03	6.29
02-052	Hamrar	64:03:008720:37.9740	48.0	102	81	63.6	1.7	0.04	1.65
02-053	Sólheimar	64:04.1362/20:38.6425	79.0	110	107	96.5	16.3	1.63	6.82
02-054	Spóastadir	64:08.8410/20:33.2123	76.4	106	102	100.5	25.6	1.22	9.30
02-055	Sydri-Reykir	64:12.9550/20:31.7545	98.6	140	145	183.5	325.0	5.57	9.17
02-056	Ljósuár	64:15.0405/20:39.5447	4.3	137	-2	13.3	31.8	1.05	0.07
02-057	Laugarvatn I	64:12.8182/20:43.7842	97.0	136	118	140.0	139.0	3.84	6.70
02-058	Laugarvatn II	64:12.5493/20:45.9553	4.8	133	10	15.6	20.3	1.06	0.05
02-059	Kringla	64:05.6357/20:38.7160	81.3	103	86	83.3	66.1	2.95	8.15
02-060	Kaldárholt	64:00.1680/20:28.7383	62.4	71	57	51.9	35.8	1.90	1.06
02-061	Skammbeinsstadir	63:57.7073/20:19.4503	50.6	60	33	76.6	187.0	10.30	1.80
02-062	Hvammur, Skardsfjall	64:01.3134/20:09.8485	57.0	79	54	71.6	143.0	6.42	1.32
02-063	Stóri-Klofi	64:00.6440/20:04.7430	54.6	74	46	61.5	57.8	3.30	0.54
02-064	Flagbjarnarholt	64:00.5940/20:16.0819	60.4	69	49	71.4	146.0	8.45	2.69
02-065	Ósabakki	64:03.9940/20:27.4518	60.0	81	67	68.9	37.5	2.55	5.05
02-066	Midfell	64:06.1992/20:20.9337	62.0	80	96	91.9	11.9	0.85	5.25
02-067	Kópsvatn	64:09.9104/20:18.0108	94.0	122	133	156.6	64.3	2.66	8.84
02-068	Sydra-Langholt	64:04.5701/20:26.0099	64.2	91	78	69.3	45.3	2.46	4.95
02-069	Birtingaholt	64:04.3251/20:24.4410	61.0	88	73	69.9	26.0	1.87	5.18

TABLE 1: Continued

02-070	Audsholt, Bisk.	64:07.1811/20:28.7419	84.1	102	87	91.0	106.0	4.85	3.84
02-071	Ásatún	64:06.3328/20:22.9470	82.4	98	102	93.4	51.8	2.38	5.33
02-072	Flúdir	64:07.7525/20:19.4240	95.2	111	128	137.6	90.4	3.55	6.93
02-073	Flúdir	64:07.7530/20:19.4070	99.8	119	127	155.0	103.0	3.77	7.07
02-074	Vadmálahver	64:08.2195/20:18.5758	99.3	116	133	147.7	143.0	4.05	7.13
02-075	Thórarinsstadir	64:10.7200/20:14.7742	98.9	125	133	174.3	233.0	6.10	10.50
02-076	Laugar, Hrun	64:11.0508/20:14.5958	98.4	146	172	278.5	315.0	4.96	14.10
02-077	Reykjadalur	64:09.8834/20:15.8153	97.8	119	119	138.3	119.0	4.09	7.45
02-078	Thjórsárholt	64:01.6751/20:12.9245	63.2	90	56	70.2	175.0	7.89	2.15
02-079	Thjórsardalur	64:09.6914/19:48.6926	67.5	98	50	60.0	18.4	1.34	7.41
02-080	Gljúfurholt	63:58.5928/21:08.6710	82.1	128	118	116.9	63.7	1.50	5.91
03-026	Thóroddstadir, Ölfus, 1	63:57.6230/21:15.6159	120.0	124	122	129.4	93.4	1.23	9.40
03-027	Thóroddstadir, Ölfus	63:57.8611/21:15.9083	4.7	192	21	15.7	16.4	0.07	0.005
03-028	Audsholt, Ölfus, 1	63:56.9405/21:10.0430	59.5	73	55	50.7	52.3	1.84	4.85
03-029	Vadnes, 1	64:00.5292/20:51.2214	73.8	84	72	80.9	86.4	2.65	2.21
03-030	Laugaland, Holt	63:55.5150/20:24.1664	4.6	192	47	29.0	2.3	<0.005	0.014
03-031	Skammbeinsstadir	63:57.4965/20:20.9695	5.1	202	43	27.0	3.5	0.014	0.013
03-032	Öndverdarnes, 27	64:00.6458/20:55.3309	83.8	105	90	88.1	52.9	1.67	2.09
03-033	Öndverdarnes, 18	64:00.6994/20:55.6627	72.0	100	85	72.3	32.1	1.26	1.41
03-038	Útey	64:12.2125/20:41.9244	90.2	124	113	133.1	74.1	2.89	10.30
03-039	Austurey 1	64:12.0392/20:36.9789	88.2	104	93	103.9	125.0	3.06	9.77
03-040	Bjarnarfell water supply	64:17.7149/20:24.0784	6.7	144	31	22.5	15.5	0.24	0.22
03-081	Reykholt, 1	64:10.5379/20:26.5587	133.0	128	145	173.0	188.0	4.87	10.60
03-082	Gýgjarhólskot, 1	64:16.8487/20:14.2051	22.7	138	47	37.7	12.4	0.20	0.23
04-031	Árbaer	63:56.8582/21:02.0727	59.9	83	62	59.7	101.0	1.99	1.75
04-032	Árbaer	63:56.8410/21;02.0771	59.7	83	62	59.5	114.0	2.05	1.60
04-033	Haukadalur	64:20.0035/20:17.6668	5.9	162	24	17.5	16.9	0.16	0.08
04-034	Flúdir	64:09.1498/20:16.3752	6.7	230	51	31.9	6.4	<0.005	0.02
04-035	Ásólfsstadir, 1	64:06.6545/19:58.7788	51.6	70	68	79.1	34.3	0.835	4.36
04-036	Laekjarbotnar, Land	63:57.4585/20:15.2132	5.3	162	37	22.9	7.9	0.037	0.03
04-037	Urridafoss	63:55.8115/20:41.1091	4.4	205	44	27.4	4.3	<0.005	0.02
04-038	Bjálmholt	63:54.4677/20:23.9866	5.5	174	48	30.1	4.6	0.012	0.04
05-019	Hella	63:50.5288/20.23.4507	5.0	237	49	30.6	1.7	<0.005	0.007
05-020	Hella	63:51.2504/20:22.5616	7.0	212	47	29.1	2.4	<0.005	0.004
05-023	Hvolsvöllur	63:47.8123/20:06.8407	3.8	196	27	17.8	6.6	0.040	0.002
05-024	Hveragerdi	64:00.8208/21:10.9586	11.1	238	33	20.7	1.8	<0.005	0.009
05-025	Hveragerdi	64:00.6758/21:12.6596	6.6	173	21	15.3	9.4	0.052	0.055
05-026	Hveragerdi	64:00.7022/21:12.7003	6.6	174	19	14.6	10.0	0.052	0.040
05-027	Kaldadarnes	63:55.2541/21:07.1673	5.8	205	42	25.9	0.6	<0.005	0.011
05-028	Stokkseyri	63:50.2814/21:03.5478	9.0	181	31	22.4	1.5	<0.005	<0.001
05-029	Selfoss 1	63:57.5389/21:02.4961	4.0	127	18	13.9	13.3	0.247	0.020
05-030	Selfoss 2	63:57.5478/21:01.6121	3.6	117	19	14.2	10.3	0.196	0.017
05-031	Selfoss 3	63:57.5626/21:01.3249	3.4	129	13	13.8	15.3	0.203	0.016

Experimental data on the first dissociation constant of germanic acid were summarised by Wood and Samson (2006). The data show considerable discrepancies. For this study the data of Pokrovski and Schott (1998) were selected. They are summarised in Table 2. Experimental data on the second dissociation constant of germanic acid is available at 25°C only. They indicate that the $H_2GeO_4^{2-}$ species only occurs in significant concentrations at pH above 12, meaning that this species is not expected to contribute significantly to the total germanium concentration in the water considered for the present study. This species was, therefore, ignored and it was assumed that practically all aqueous germanium occurs as $H_4GeO_4^0$ and $H_3GeO_4^-$. The most important Gallium species are Ga^{3+}, $GaOH^{2+}$, $Ga(OH)_2^+$ and $Ga(OH)_4^-$ (Wood and Samson, 2006). The thermodynamic properties of the Ga species were selected from Wood and Samson (2006) and Shock et al. (1997).

The temperature dependence of the equilibrium constants for Ga and Ge species was calculated from the following equation, using the data in Table 1 (see Arnórsson et al., 1982):

$$\log K = 0.0523 \times \Delta_r S° + (33.043\ \Delta_r S° - 0.2185\ \Delta_r H°)/T + 0.623 \times 10^{-6} \times \Delta_r S° \times T^2$$

In the above equation, $\Delta_r S$ and $\Delta_r H$ represent the entropy and enthalpy of the respective reaction at 25°C, and T is in Kelvin. The resulting dissociational reactions are summarised in Table 2.

TABLE 2: Thermodynamic data used in the present study

Reaction	$\Delta_r S°(T_r)$ (cal/mol.K)	$\Delta_r H°(T_r)$ (cal/mol)	Log K(Tr)	Log K (T)
$GaOH^{2+} = Ga^{3+} + OH^-$	-20.33	9153.6	-11.85	$-1.063-2671.9 / T-12.666\times10^{-6}\times T^2$
$Ga(OH)_2^+ = GaOH^{2+} + OH^-$	-22.24	6104.1	-9.34	$-1.163-2069.36 / T-13.86\times10^{-6}\times T^2$
$Ga(OH)_3 = Ga(OH)_2^+ + OH^-$	-44.86	-340.0	-9.56	$-2.346-1409.50 /T- 27.95\times10^{-6}\times T^2$
$Ga(OH)_4^- = Ga(OH)_3 + OH^-$	-3.52	12975.5	-9.91	$-0.184-2951.58 / T-2.19\times10^{-6}\times T^2$
$H_4GeO_4 = H_3GeO_4^- + H^+$	-20.69	6500		

Speciation calculation

Calculation of the aqueous speciation distribution was carried out with the aid of the WATCH programme, version 2.3 (Arnórsson et al., 1982; Bjarnason, 1994). For a selected temperature, the programme calculates individual aqueous species activities, activity coefficients and selected mineral activity products as well as mineral solubility constants for the same minerals. This involved simultaneous solution of mass balance and mass action equations. Gallium and Ge are not included in the database of the WATCH program but were added to the calculation routine for the present work. The species included were $H_4GeO_4^0$ and $H_3GeO_4^-$ for germanium, and Ga^{3+}, $GaOH^{2+}$, $Ga(OH)_2^+$, $Ga(OH)_3$ and $Ga(OH)_4^-$ for gallium. The hydrolysis reactions for the respective species are given in Table 2. The activity coefficient is obtained from the Debye-Hückel equation:

$$-\log \gamma_i = \frac{A z_i^2 \sqrt{I}}{1 + B \mathring{a}_i \sqrt{I}}$$

where γ_i is the activity coefficient, A and B are temperature and pressure dependent solvent parameters, z_i is the species charge and I is ionic strength given by:

$$I = 0.5\ \Sigma m_i z_i^2$$

where m_i represents concentration in moles/kg.

The speciation calculations were solved by combining the equilibrium constants (Table 2) and the mass equations for Ge and Ga given by

$$m_{Ge} = m_{H_4GeO_4^0} + m_{H_3GeO_4^-}$$

and

$$m_{Ga} = m_{Ga^{3+}} + m_{GaOH^{+2}} + m_{Ga(OH)_2^{+}} + m_{Ga(OH)_3^{0}} + m_{Ga(OH)_4^{-}}$$

These calculations need selection of a specific temperature. For the present work, chalcedony geothermometer temperatures, as computed by the WATCH program, were used as the selected reference temperature in the low-temperature areas of the Southern Lowlands as well as for the mixed waters in the Geysir field, whereas quartz equilibrium temperatures were used for reference for boiling hot springs for Geysir (Table 1). Measured temperatures were used for reference for non-thermal waters.

GERMANIUM AND GALLIUM DISTRIBUTION IN WATERS

The concentrations of Ga and Ge in all the water samples considered for the present study are given in Table 1 together with the concentrations of Si and Al. Gallium was detected in all but 8 cold spring samples and Ge in all but 2 samples, also of non-thermal waters. The Ge concentrations in the geothermal waters were between 0.17 and 24 ppb but in the non-thermal waters they were generally below or close to the detection limits, the highest Ge concentrations in these waters being 0.22 ppb. The Ge concentrations increased with increasing temperature (Figure 3). Accordingly, the samples from the Geysir geothermal field have the highest Ge concentrations. In the Southern Lowlands low-temperature areas the Ge concentrations showed complete overlap between the three recognized geothermal systems. Most samples had 1-10 ppb Ge.

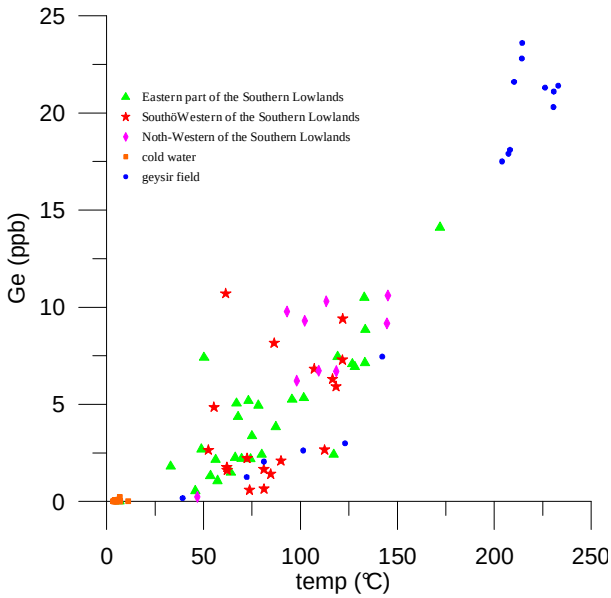

FIGURE 3: Germanium concentrations in geothermal waters as a function of aquifer temperature. For the high-temperature waters of the Geysir field, this temperature was taken to be representedby the quartz geothermometer but for the mixed waters in this field as well as in thelow-temperature systems by the chalcedony geothermometer. For non-thermal groundwaters the measured temperature was used for reference.

The Ga concentrations in the geothermal waters ranged between 0.04 and 21 ppb. In the Southern Lowlands, they were, however, mostly between 1 and 5 ppb. Non-thermal groundwaters contained less Ga, the highest concentration being 1 ppb while a third did not contain detectable Ga (<0.005 ppb). The Ga concentrations increased with increasing temperature (Figure 4). The Ga concentrations in waters from the Southern Lowlands generally registered between 0.5 and 3 ppb. A considerable range in the concentration range was observed for

samples from boiling hot springs in the Geysir area. This was considered a result of mixing between non-thermal waters containing low Ga concentrations and deep geothermal waters containing elevated Ga concentrations. In warm waters from the Geysir field that contain a large cold water component. Ga concentrations were very low.

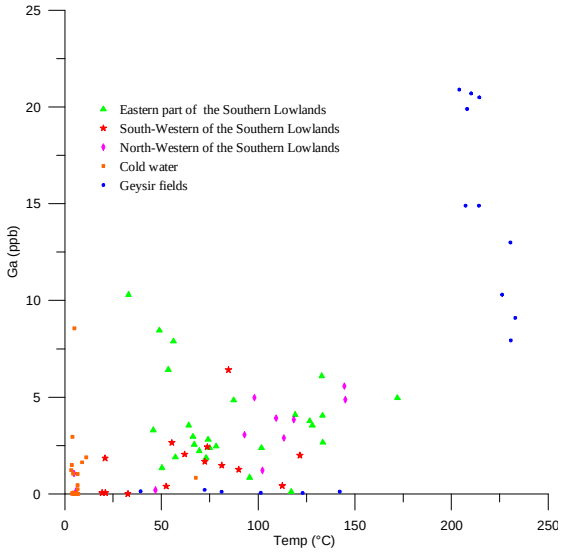

FIGURE 4: Gallium concentrations as a function of temperature; for selection of aquifer temperature see Figure 3

The results of the aqueous speciation calculations indicate that the dominant Ge species is $H_4GeO_4^0$, whereas the dominant Ga species is $Ga(OH)_4^-$. Germanium and Ga show similar chemical behaviour as Si and Al, respectively. The predominant species of Ge and Ga are tetra-coordinated hydroxy complexes, just like for Si and Al or $H_4SiO_4^0$ and $Al(OH)_4^-$. The ratios of $H_4GeO_4^0$ / $H_4SiO_4^0$ and $Ga(OH)_4^-$ / $Al(OH)_4^-$ are plotted against temperature in Figures 5 and 6. From Figure 5 it is seen that the ratio $H_4GeO_4^0$ / $H_4SiO_4^0$ increased with increasing temperature. This suggests that the chemical behaviour may not be exactly the same. Silicade was incorporated into smectites, zeolites and chalcedony at temperatures below about 150°C, whereas at higher temperatures it could also enter quartz, chlorite, epidote, prehnite and some other silicates. The observed variation in the $H_4GeO_4^0$ / $H_4SiO_4^0$ ratio with temperature might possibly be caused by its incorporation into different minerals and their rates of formation. Germanium has an ionic radius of 0.53 Å which is somewhat larger than that of Si (0.39 Å). This limits substitution of Ge for Si in silicate minerals, and the mineral structure is more compact. For the primary minerals of basalt, it was demonstrated by Harris (1954) that substitution of Ge for Si is easiest in olivine (iron silicate), less so in pyroxene (chain-silicate) and least in the plagioclase (framework silicate). The increase in the $H_4GeO_4^0$ / $H_4SiO_4^0$ ratios with rising temperature may thus be explained by the fact that hydrothermal minerals forming at high temperature have a more compact or rigid crystal structure than the secondary minerals formed at lower temperatures. However, the extent of the water-rock interaction would have the same effect; the more particular water has precipitated secondary or hydrothermal minerals, the higher the $H_4GeO_4^0$ / $H_4SiO_4^0$ ratio. It is to be expected that the higher the temperature a particular geothermal water has attained, the more extensive the water-rock interaction.

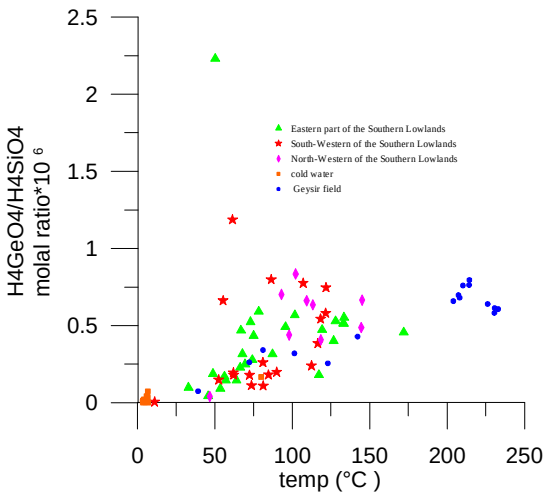

FIGURE 5: H_4GeO_4/H_4SiO_4 species ratios versus aquifer temperature in geothermal waters in the Southern Lowlands and the Geysir field; for selection of aquifer temperature see Figure 3

The $Ga(OH)_4^-$ / $Al(OH)_4^-$ activity ratio is shown in Figure 6 as a function of temperature. No temperature variations were observed. Instead, significant differences were observed for this ratio at any temperature between the three main low-temperature geothermal systems of the Southern Lowlands. In the Geysir field, the ratio was very low for warm waters that contained a large cold groundwater component. For the hot springs, the ratios were highly variable, largely caused by the removal of Al from the solution. Gallium concentrations were near-constant in these waters. The reasons for this may be the same as for Ge and Si. Gallium has an ionic radius of 0.62 Å whereas that of Al is 0.50 Å. Evidently the mineral that removes Al from the hot spring waters at the Geysir field does not consume Ga. Thus, $Ga(OH)_4^-$ / $Al(OH)_4^-$ activity ratios may be much affected by which mineral precipitates from the solution and its rate of formation as well as the extent of water-rock interaction. The distribution of the $Ga(OH)_4^-$ / $Al(OH)_4^-$ ratios between the different low-temperature geothermal systems in the Southern Lowlands may be the consequence of the formation of different hydrothermal minerals in different systems, likely zeolites and/or clay minerals.

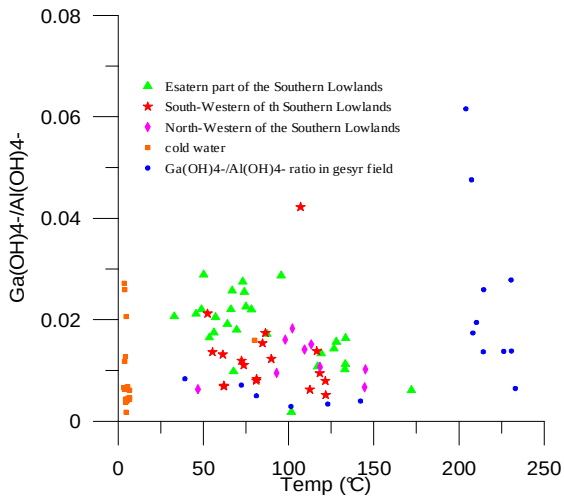

FIGURE 6: $Ga(OH)_4^-$ / $Al(OH)_4^-$ species ratios versus aquifer temperature in geothermal waters in the Southern Lowlands and the Geysir field; for selection of aquifer temperature see Figure 3

MOBILITY AND SATURATION OF GERMANIUM AND GALLIUM IN GEOTHERMAL WATERS

The mobility of one element relative to another may be used to gain insight into its geochemical behaviour. The concentration of $H_4GeO_4^0$ vs. $H_4SiO_4^0$ is shown in Figure 7. In addition, the Ge/SiO_2 ratio in basaltic rocks is shown (line). This line was obtained from data on Ge in selected Icelandic basalts as given by Arnórsson (1984) and assuming its SiO_2 content to be 50%. The $H_4GeO_4^0$ concentrations in the waters relative to $H_4SiO_4^0$ are much higher than the average Ge/SiO_2 ratio of basalt. This indicates that Ge is more mobile than Si by a factor of about 20. This does not, however, imply that Ge is mobile. The cause of the high mobility of Ge as compared to Si likely is its non-stoichiometric substitution for Si into secondary minerals due to its larger size. By the terminology of Goldschmidt, Ge is permitted into the structure of silicates where it replaces silica, but the substitution is not free.

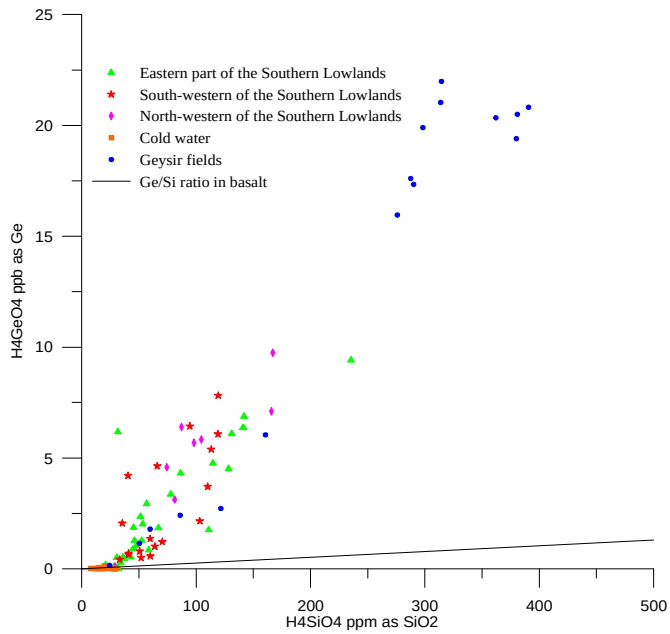

FIGURE 7: The relationship between Ge and Si in geothermal waters in the low-temperature field of the Southern Lowlands of Iceland and the Geysir field; the black line represents the Ge/Si ratio in basalts

Following Arnórsson (1984), an exchange equilibrium between Ge and Si involving solid SiO_2 (chalcedony or quartz) may be defined as $H_4GeO_4^0 / H_4SiO_4^0 = X_{SiO2}$ where X represents the mole fraction of the subscribed species (quartz). At equilibrium with respect to $SiO_2(s)$ we have $H_4GeO_4^0 = = H_4SiO_4^0 \times X_{SiO2} \times K_{SiO2}$ where $K_{SiO2}(s)$ is the solubility of quartz or chalcedony as a function of temperature. Geothermal waters in Iceland are known to be undersaturated with respect to germanium oxide (Arnórsson, 1984). However, exchange with other minerals like quartz or chalcedony containing up to 10 ppm Ge may explain the Ge concentrations in the waters at >100°C. For waters of the present study a similar trend was observed (Figure 8). A very good agreement was observed suggesting that the possible exchange of reactions between Ge and Si in minerals like chalcedony might explain the geochemical behaviour of Ge.

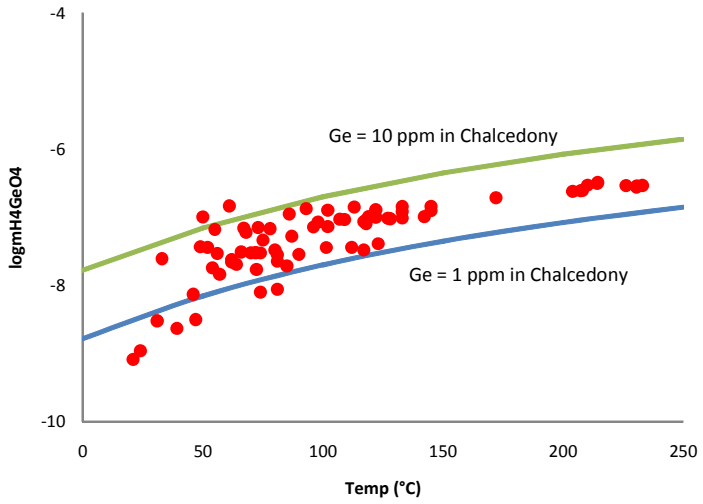

FIGURE 8: Saturation state with respect to chalcedony assuming 1-10 ppm Ge; the solubility constant for chalcedony was selected from Arnórsson et al. (1982)

The mobility of Ga compared to Al is shown in Figure 9. A similar trend as for Ge and Si was observed: Ga had a higher mobility than Al. The cause for this may be the same as for Ge, non-stoichiometric dissolution of the primary rock-forming minerals or exchange of Ga with Al into secondary minerals in proportions other than those found in the unaltered rock. Aluminium is incorporated into many secondary aluminium silicates. Therefore, assigning a particular mineral or ratio may be difficult to assess the trace impurities of Ga in secondary minerals containing Al.

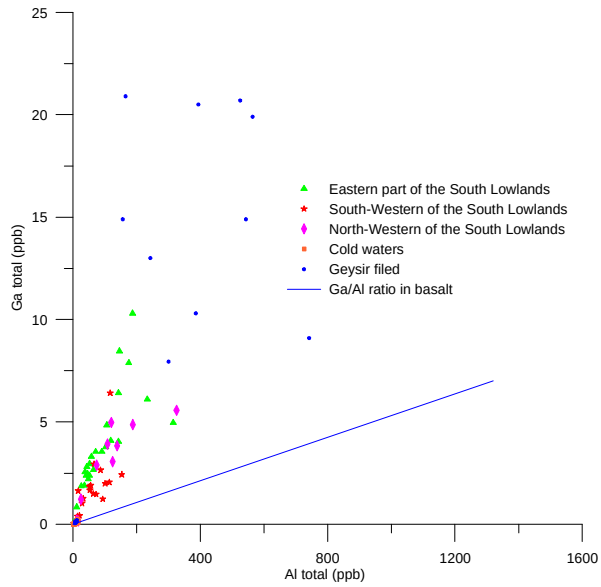

FIGURE 9: The relationship between Ga and Al in geothermal waters on the Southern Lowlands and the Geysir field; the black line represents the average Ga/Al ratio in basalt

SUMMARY AND CONCLUSIONS

The geochemistry of gallium and germanium was studied in geothermal waters in the low-temperature fields of the Southern Lowlands in Iceland and the Geysir high-temperature field. Germanium concentrations in water samples ranged between <0.05 and 24 ppb but those of gallium the ranged between <0.01 and 21 ppb. Germanium showed a good positive correlation with temperature whereas for gallium it was poor.

The mobility of Ge was studied relative to Si. The two elements showed very similar chemical behaviour. Germanium was observed to be 20 times more mobile than Si for the samples considered for this study. The cause is considered to be either non-stoichiometric rock dissolution or incorporation of Ge into Si containing secondary minerals with a molal exchange ratio that differs from that of the fresh basalt. An example of Ge exchange for Si into chalcedony indicated that Ge concentrations between 1 and 10 ppm in chalcedony matched the observed Ge concentrations. Similar trends were observed for Ga relative to Al, i.e. Ga showed much higher mobility than Al relative to primary rock composition.

ACKNOWLEDGEMENTS

My sincere thanks are due to many people without whose help this report would not have been completed. I would like to express my sincere gratitude, assistance and kindness to the UNU staff, Dr. Ingvar B. Fridleifsson, Mr. Lúdvík S. Georgsson and Mrs. Dorthe H. Holm during the whole training period. My sincere thanks go to the UNU, the Government of Iceland and Orkustofnun for granting me the opportunity to participate in the UNU Geothermal Training Programme. I am very grateful to Dr. Stefán Arnórsson and Dr. Andri Stefánsson for guidance, advice and teaching for the preparation of this report.

Finally, my deepest gratitude to my family for their unconditional support during my six month stay in Iceland.

REFERENCES

Arnórsson, S., 1984: Germanium in Icelandic geothermal systems. Geochim. Cosmochim. Acta, 48, 2448-2502.

Arnórsson, S., 1985: The use of mixing models and chemical geothermometers for estimating underground temperature in geothermal systems. J. Volc. Geotherm. Res., 23, 299-335.

Arnórsson, S., 1995: Geothermal systems in Iceland: structure and conceptual models – II. Lowtemperature areas. Geothermics, 24, 603-629

Arnórsson, S., Sigurdsson, S. and Svavarsson, H., 1982: The chemistry of geothermal waters in Iceland I. Calculation of aqueous speciation from 0°C to 370°C. Geochim. Cosmochim. Acta, 46, 1513-1532.

Arnórsson, S., Axelsson, G., and Saemundsson, K., 2008: Geothermal system in Iceland. Jökull, 58, 269-302.

Arnórsson, S., Gunnarson, I., Stefánsson, A., Andrésdóttir, A., and Sveinbjörnsdóttir, A.E., 2002: Major element chemistry of surface- and ground waters in basaltic terrain, N-Iceland. I. Primary mineral saturation. Geochim. Cosmochim. Acta, 66, **4015-4046.**

Arnórsson, S. and Óskarsson, N., 2007: Molybdenum and tungsten in volcanic rocks and in surface and <100°C ground waters in Iceland. **Geochim. Cosmochim. Acta., 71, 284-304.**

Arnórsson, S., Sigurdsson, S., and Svavarsson, H., 1982: The chemistry of geothermal waters in Iceland I. Calculation of aqueous speciation from 0° to 370°C. **Geochim. Cosmochim. Acta., 46**, 1513-1532.

Barth, T.F.W., 1940: Geysir in Iceland. Amer. J. Sci., 238, 381-407.

Bjarnason, J.Ö., 1994: The speciation program WATCH, version 2.1A. Orkustofnun, Reykjavík, 7 pp.

Burton, J.D., Culkin, F., and Riley, J.P., 1959: The abundance of gallium and germanium in terrestrial materials .Geochim. Cosmochim. Acta, 16, 151-180.

Criaud, A., and Fouillac, C., 1986: Study of CO2-rich thermomineral waters from the central French massif. 2. Behaviour of some trace-metals, arsenic, antimony and germanium. Geochim. Cosmochim. Acta, 50, 1573–1582.

Einarsson, P., 1991: Earthquakes and present-day tectonism in Iceland. In: Björnsson, S., Gregersen,

S., Husebye, E.S., Korhonen, H., and Lund, C.E. (editors), Imaging and understanding the lithosphere

of Scandinavia and Iceland. Tectonophysics, 189, 261-279.

Fridleifsson, I.B., 1979: Geothermal activity in Iceland. Jökull, 29, 47-56.

Goguel, R., 1988: Ultra-trace metal analysis of New Zealand geothermal waters by ICP-MS. *Proceedings of the Conference on Trace Elements in New Zealand: Environmental, Human and Animal, New Zealand Trace Elements Group, 30 November–2 December, 1988, Lincoln College, Canterbury*, 263–270.

Harris, P., 1954: The distribution of Germanium among co-existing phases of partly glassy rock. Geochim. Cosmochim. Acta, 5, 185-195

Mortlock, R.A., Froelich, P.N., Feely, R.A., Massoth, G.J., Butterfield, D.A., and Lupton, J.E., 1993: Silica and germanium in Pacific Ocean hydrothermal vents and plumes. Earth Planet. Sci. Let., 119, 365–378.

Pokrovski, G.S., and Schott, J., 1998: Thermodynamic properties of aqueous Ge(IV) hydroxide complexes from 25 to 350°C: implications for behaviour of germanium and the Ge/Si ratio in hydrothermal fluids. Geochim. Cosmochim. Acta, 62,1631-1642.

Saemundsson, K., 1979: Outline of the geology of Iceland. Jökull, 29, 7-28.

Shock, E.L., Sassani, D.C., Willis, M., Sverjensky, D.A., 1997: Inorganic species in geologic fluids: correlations among standard molal thermodynamic properties of aqueous ions and hydroxide complexes. Geochimica et Cosmochimica Acta 61, 907–950.

Uzumasa, Y., and Nasu, Y., 1960: Chemical investigations of hot springs in Japan: LVII. Gallium in hot springs. Nippon Kagaku Zasshi, 81, 732.

Uzumasa, Y., Nasu, Y., and Toshiko, S., 1959: Chemical investigations of hot springs in Japan: XLIX. Germanium contents of hot springs. Nippon Kagaku Zasshi, 80, 1118–1128.

Vink, G.E., 1984: A hotspot model for Iceland and the Voring Plateau. J. Geophys. Res., B 89, 9949–9959.

Wood, S.A., and Samson, I.M., 2006: The aqueous geochemistry of gallium, germanium, indium and scandium. Ore Geol. Rev., 28, 57-102.

THEME III

GEOPHYSICAL EXPLORATION

NEAR-REAL TIME INTERPRETATON OF MICRO-EARTHQUAKE DATA FOR RESERVOIR MODELING

Lawrence Hutchings, Katie Boyle, Steve jarpe*, Brian Bonner, and Nathaniel Lindsey*
Lawrence Berkeley National Laboratory, University of California
**Jarpe Solutions, Prescott Arizona*
***University of Rochester*

We are developing instrumentation, data processing, and inversion programs in order to obtain high resolution reservoir properties in near real-time utilizing passive seismic recordings. Geothermal, CO2 sequestration, oil, and gas reservoir modeling depends on identifying reservoir properties, including: geology, fractures, fluids, and permeable zones. Our approach is to extract as much information as possible from recordings, use this to develop three-dimensional models of physical properties of the reservoir, and use rock physics (including effective medium theories) to derive reservoir properties. We have developed an inexpensive recording system to gather data from large numbers of stations at 500 sps for high resolution and an automated system to process this data in near real-time.

The data used as input to operate several programs include P- and S-wave: arrival time picks, waveforms, pulse widths, and spectral content. The computer programs provide: high-resolution double-difference earthquake locations, 3-D velocity (Vp andVs) and attenuation (Qp and Qs) structure, moment tensor solutions, seismic moments, and stress drops. We utilize a three-dimensional visualization program to examine spatial associations and correlations of these physical properties. Modeling is typically in the depth range of reservoirs of interest, usually surface to 5 Km depth, and depends upon sufficient numbers of earthquakes, usually 100 – 500 events. This can be updated regularly to monitor temporal changes.

Keywords: rock physics, real time, reservoir modeling, micro-earthquake

EVALUAITON OF HIGH RESOLUITON SOFTWARE FOR EARTHQUAKE LOCATIONS AND TOMOGRAPHY STUDIES

Lawrence Hutchings, Katie Boyle, and Nathaniel Lindsey*
Lawrence Berkeley National Laboratory, University of California
**University of Rochester*

We evaluate and perform parameter sensitivity tests on high-resolution earthquake location and tomography software using synthetic data sets and actual micro-earthquake recordings from the Salton Sea Seismic Network, Imperial Valley California. The purpose is to determine the best strategy for obtaining high resolution results which can be used to understand reservoir properties. We also developed an automated data processing system to provide accurate, rapid data analysis for this and future studies and tested it using the Salton Sea data. The programs will be used to develop 3-D velocity and attenuation models and high-precision earthquake locations. We compared hypoDD (Waldhauser & Ellsworth, 2001) locations obtained with a 1-D velocity model to locations obtained using a standard tomography approach for earthquake location and 3-D geologic model (SimulPS, Thurber, 1983). We found that even though both absolute and relative locations can be refined with a double difference approach, absolute locations are highly dependent on the 3-D geological model. We conclude that a coupled solution for 3-D velocity model and double-difference earthquake locations is the best approach for high-resolution earthquake locations and 3-D geologic modeling in a geothermal environment. We evaluate tomoDD (Zhang, 2009) for this purpose.

Keywords: micro-earthquake locations, tomography, automated processing, hypoDD, tomoDD

GEOPHYSICAL SURVEY IN KARISIMBI GEOTHERMAL PROSPECT, RWANDA

Constantin Irabaruta, may be include other people
Rwandan Ministry of Infrastructure-P.O. Box 24, Kigali-Rwanda
E-mails: constantin.ira@gmail.com, constantin.irabaruta@mininfra.gov.rw

ABSTRACT

Karisimbi Geothermal Prospect is located on the border between the Republic of Rwanda, the Democratic Republic of Congo and the Republic of Uganda. The prospect is part of the Virunga National Park, touching the Western branch of the East African Rift System. The prospect is in an area with complex geological and tectonic structures due to intense multiple volcanic and tectonic events. The area is known to have few surface manifestations but some geothermal activity and gas release occur through hot springs. Detailed Geophysical Exploration such as MT (Magnetotellurics) and TEM (Transient Electromagnetic) have been used to explore the geothermal potential and recommend a strategy for proving whether a viable geothermal resource exists. The results of the geophysical survey indicate that a geothermal resource could exist in the southern and southeast slopes of the Karisimbi volcano. Results of geophysical and geochemical surveys have been used to recommend sites for drilling exploration wells. The drilling will be done after a microearthquake survey to locate fluid-filled fracture zones as targets for drilling. The biggest problem is the discrepancy between the interpreted heat source at a depth of 5km using the electric resistivity data and the interpreted low temperatures using the quartz geo-thermometer.

ACTIVITES VOLCANIQUES ET GEOTHERMIQUES EN REPUBLIQUE DE DJIBOUTI REVELEES PAR LES VALEURS *B* DE LA SISMICITE DE 1973 A 2009.

Kassim Mohamed Kassim
Observatoire Géophysique d'Arta, CERD

RESUME:

Le catalogue de la sismicité de 1973 à 2009 de l'Observatoire Géophysique d'Arta (Djibouti), a été analysé par la cartographie des valeurs *b* de la distribution fréquence-magnitude des séismes.

Plusieurs zones avec des valeurs *b* élevées (de 1.4 à 1.8) ont été trouvés aussi bien à terre comme dans le rift d'Asal-Ghoubbet et en mer, dans le golfe de Tadjoura, plus particulièrement à l'ouest du golfe de Tadjoura. Ces zones aux valeurs *b* élevées, pourraient être en relation avec les activités des fluides geothermiques ou magmatiques en circulation . Par contre, les valeurs *b* faibles (*b* autour de 0.6) observées dans la région de Damerlà pourrait être due à la zone de fortes contraintes et donc susceptible de donner un fort tremblement de Terre (magnitude voisine de 6).

ABSTRACT:

The seismicity calalogue from 1973 to 2009 of the Arta Geophysical Observatory (Djibouti), was analysed by mapping the *b* values of the distribution frequency-magnitude of earthquakes.

Several areas with high *b* values (1.4 to 1.8) were found both on land as in the rift of Asal-Ghoubbet and offshore in the Gulf of Tadjoura, particularly in the western Gulf of Tadjoura. These areas with high b values could be related to the activities of the geothermal or magmatic fluids in circulation. By cons, low b values (b around 0.6) observed in the region of Damerla could be due to the high stress area and therefore likely to give a strong earthquake (magnitude about 6).

Mots clefs: Golfe de Tadjoura, sismicités, magnitude de complétude, les valeurs *b*.

INTRODUCTION

La République de Djibouti, située dans l'Afar méridional, occupe une place particulière dans le schéma de la tectonique des plaques, puisque c'est un des rares lieux où l'on peut observer la pénétration à terre d'une dorsale océanique (Barberi et al., 1972; Tisseau, 1978; Courtillot, 1980; Cochran, 1981) en l'occurrence celle du golfe d'Aden qui se prolonge dans le golfe de Tadjoura pour sortir en surface dans de le rift d'Asal-Ghoubbet (voir fig. 1). La manifestation de cette activité sous forme de séismes est suivie (Lépine and Hirn, 1992; kassim, 2009) depuis plus d'une trentaine d'année par l'observatoire géophysique d'Arta (Djibouti) .

Le paramètre "*b*" est la pente de la distribution fréquence-magnitude (Ishimito and lida, 1939; Guthenberg and Richter, 1944) pour une population des séismes donnée et exprime la proportion des petits par rapport aux gros séismes dans une région donnée pour une période de temps donnée.

Des variations spatiales aussi bien que temporelles de la valeur *b* ont été observées depuis des décennies. Plusieurs facteurs peuvent être à l'origine des variations de *b* de sa valeur standard qui est d'environ 1 (Kanamori, 1975). Un milieu matériel dans lequel l'hétérogénéité est importante produit des valeurs de *b* élevés (Mogi, 1962a). C'est ce que l'on rencontre souvent en milieu volcanique, où en présence de fluides ou de progression d'un dyke, la pression de pore augmente en provoquant une fracturation hydraulique de la roche encaissante. L'augmentation d'un gradient thermique peut aussi être la cause de l'augmentation de la valeur *b* (Warren and Latham, 1970). A l'inverse une diminition de la valeur *b* est associée à une augmentation des contraintes locales ou régionales (Wyss, 1973; Schorlemmer et al., 2004; Wiemer and Schorlemmer, 2007), phénomène qui a pu être aussi observé en laboratoire (Sholz, 1968; Amitrano, 2003).

DONNEES UTILISEES ET METHODE D'ANALYSE

Nous avons sélectionné la sismicité des zones les plus actives de la République de Djibouti (le golfe de Tadjoura, le rift d'Asal-Ghoubbet et le nord-ouest du lac Asal) comprises dans une boîte rectangulaire qui couvre la zone 42.2°E ≤ longitude ≤ 44°E et 11.2°N ≤latitude≤ 12.2°N. Pour la période 1973 à 1975, il y a très peu de données surtout pour

les séismes de magnitude ≤ 3. Nous avons donc préféré commencer à partir de 1976, date à laquelle la couverture en nombre de stations autour du golfe de Tadjoura commence à s'améliorer et les données du catalogue d'Arta ne comporte plus de lacune. Nous y avons denombré 15441 événements de magnitude $M \geq 2$ localisés durant la période 1976 à décembre 2009 (voir fig. 2). Ces données ne sont pas homogènes dans le temps aussi bien en quantité qu'en qualité. En effet nous avons par exemple 5401séismes pour la période 1976-1992.5, et le double, soit 10040 événements pour la période 1992.5-2009. Ceci s'explique facilement par l'évolution technique du matériel tant au niveau de l'observatoire qu'au niveau du réseau de stations déployées sur le terrain. Par exemple, l'année 1991 a vu le début de l'enregistrement direct des signaux su PC (système IASPEI et format PC-SUDS), et *ipso facto* celui du dépouillement sur l'écran, en remplacement des anciens systèmes qui demandaient de nombreuses manipulations avant d'obtenir un sismogramme, puis un foyer. Tenant compte de cette réalité, nous avons choisi une méthode d'analyse robuste ayant déjà fait ses preuves pour pouvoir estimer la variabilité spatiale du paramètre *b* de la loi de Gutenberg-Richter à l'échelle locale.

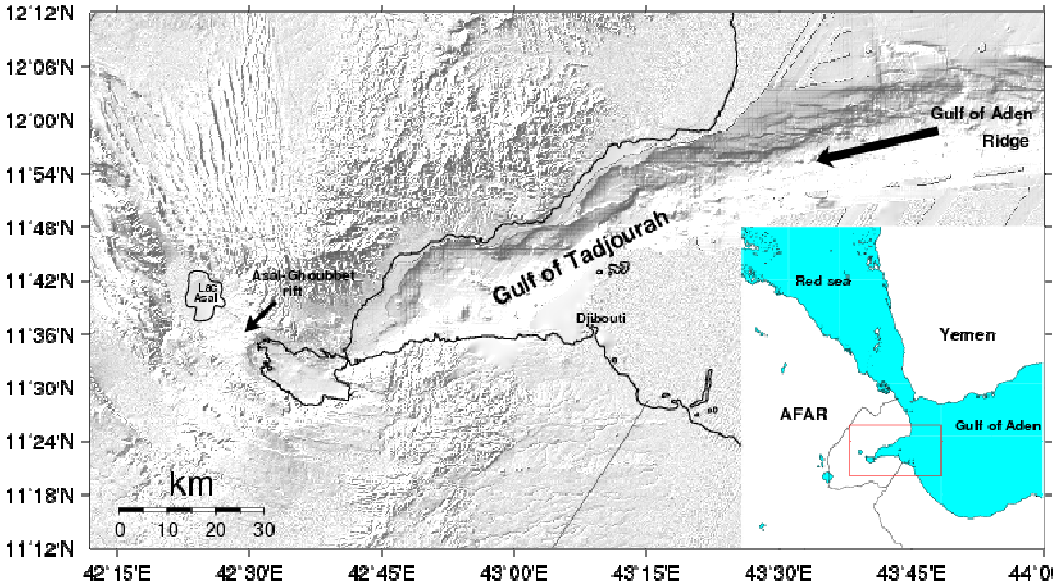

Fig. 1 : Bathymètrie du golfe de Tadjourah + topographie des zones côtières de la République de Djibouti qui représentent le zoom de la partie encadrée en rouge sur la carte régionale en bas à droite. La grande fléche en haut à droite indique le sens de propagation de la ride du golfe d'Aden dans le golfe de Tadjoura et sa sortie à terre au niveau du rift d'Asal-Ghoubbet.

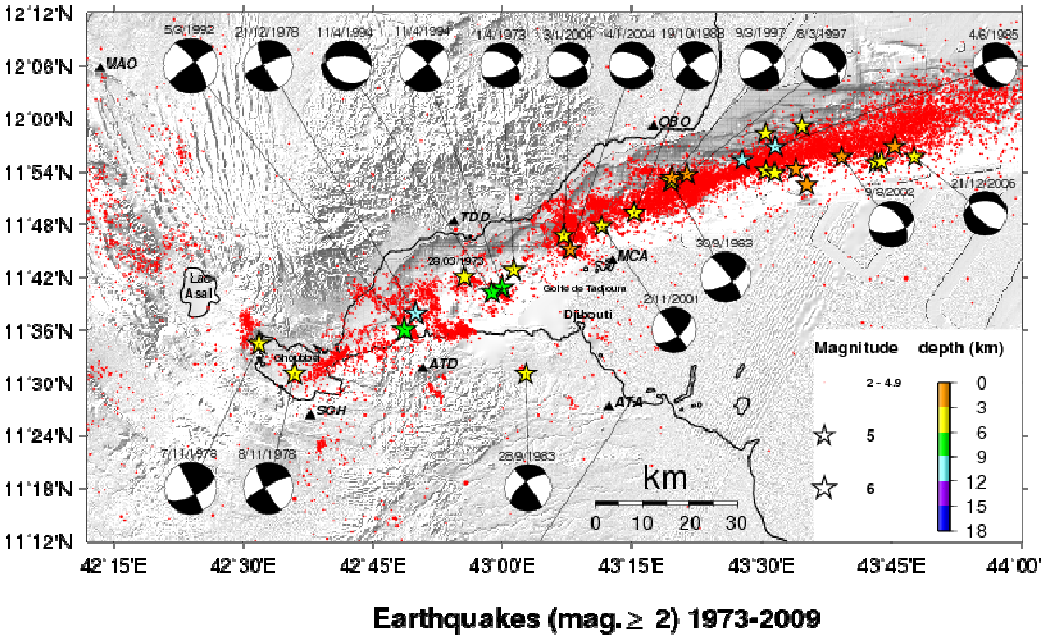

Fig. 2 : Séismes de magnitude ($M \geq 2$) qui se sont produits entre 1973-2009. Les mécanismes aux foyers de séismes de magnitude ($M \geq 5$) proviennent du CMT Harvard. Les triangles noirs sont des stations sismologiques de l'observatoire. Les stations sismologiques du rift d'Asal-Ghoubbet ainsi que celle du grand-bara (GBR) ne sont pas répresentés ici.

DISTRIBUTION FREQUENCE-MAGNITUDE

La distribution fréquence-magnitude (Ishimito and lida, 1939; Guthenberg and Richter, 1944) est tirée de la loi de puissance qui relie la fréquence d'occurrence et la magnitude des séismes dans un volume sismogénique selon la formule:

$$\log_{10} N = a - bM ,$$

où N est le nombre de séismes de magnitude $\geq M$ dans une période de temps donné, et a et b des constantes. Le paramètre "a" décrit la productivité du volume sismogénique, c'est-à-dire le nombre théorique de séismes de magnitude zéro, que l'on aurait pu enregistrer, si on avait été en mésure de le faire. Le paramètre "b" est la pente de la distribution fréquence-magnitude, elle depend des conditions de contraintes.

CALCUL DES VALEURS *B*

Le calcul des valeurs b dans cette étude est effectué d'après le logiciel ZMAP (Wemer, 2001) qui utilise la technique de MLE (Maximun Likelihood Estimation) suivant l'équation (Utsu, 1965; Aki, 1965; Bender, 1983) comme:

$$b = \frac{\log_{10}(e)}{\overline{M} - M_{min}}$$

où e=2.71828183,

$\overline{M}$ est la magnitude moyenne de l'échantillon,

$M_{min} = M_c - \frac{\Delta M_{bin}}{2}$, où M_c est la magnitude de complétude[1] et ΔM_{bin} est la largeur de la boite du catalogue (Aki, 1965; Bender, 1983; Utsu, 1999).

Une estimation de la déviation standard σb de la valeur *b* est calculée suivant la formule de Shi and Bolt, (1982):

$$\sigma(b) = 2.30b^2 \sqrt{\sum_{k=1}^{n} \left(M_i - \overline{M}\right)^2 / n(n-1)}$$

où n est le nombre total des événements d'un échantillon donnée.

Pour la détermination du volume échantillonné par les séismes, nous employons la technique avec le rayon *R constant* qui correspond a un volume de forme cylindrique centré sur chaque noeud d'une grille.

Une bonne estimation de la valeur "*b*" depend fortement de la magnitude de complétude M_c car la relation de Gutenberg-Richter (1944) est seulement valable pour $M \geq M_c$. En effet si M_c est sous déterminée dans le catalogue de la sismicité, il en résulte une valeur de *b* trop faible par rapport à sa vraie valeur.

ESTIMATION DE LA MAGNITUDE DE COMPLETUDE

La plupart des méthodes qui estiment la magnitude de complétude des catalogues de sismicité supposent la self-similarité du processus de production des séismes, qui implique en conséquence une distribution des séismes suivant une loi de puissance dans le domaine de magnitude et dans celui du moment sismique (Woessner and Wiemer, 2005).

Dans cette étude nous utilisons la méthode MAXC (Maximum curvature) de Wiemer and Wyss (2000) qui fait une estimation rapide et sûre de M_c à partir du point défini comme le maximum de la courbure obtenu en calculant la valeur maximale de la dérivée première de la courbe fréquence/magnitude. En pratique, cela correspond à la boîte de magnitude avec la plus haute fréquence d'événements dans la distribution non-cumulative de la fréquence-magnitude comme indiqué sur la figure 3. Lorsque l'on applique cette méthode MAXC, il est recommandé de le faire avec bootstrap[2] en ajoutant une correction de 0.2 à M_c, qui est justifiée par l'analyse des catalogues synthétiques.

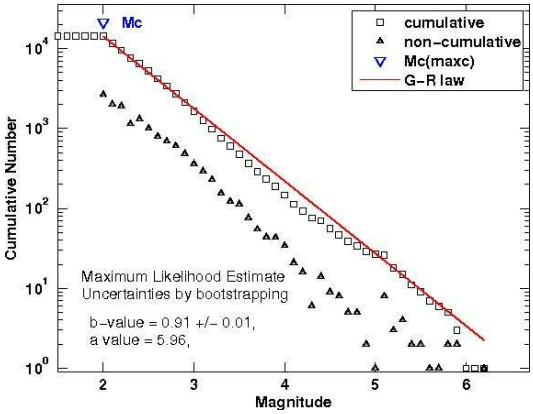

Fig. 3 : Nombre de séismes en fonction de la magnitude (calalogue de l'observatoire 1976-2009).

1 M_c Est défini comme la plus petite magnitude à laquelle 100% des événements sont détectés dans un volume espace-temps (Rydeleck and Sacks, 1989; Taylor et al., 1990; Wiemer and Wyss, 2000).

2 L'échantillon boostrap des catalogues des séismes est généré en faisant le tirage aléatoire avec remise d'une quantité équivalente d'événements du catalogue original. Pour chaque échantillon boostrap des cata de séismes, M_c et b sont calculés ainsi que δM_c et δb qui sont définis comme étant le moment d'ordre deux de l'évolution des distributions empiriques M_c et b. Comme résulat final, nous utilisons les valeurs moyennes de M_c et b pour faire l'imagerie.

Imagerie de la magnitude de complétude

Pour pouvoir distinguer visuellement la distribution spatiale de M_c et de son incertitude ΔM_c dans le plan longitude-latitude à travers le golfe de Tadjoura, le rift d'Asal-Ghoubbet et au nord-ouest du lac-Asal, nous avons choisi le rayon *R=5 km* pour le volume cylindrique échantillonné par les séismes et la distance de *d=0.5 km* entre chaque noeud de la grille. Il faut noter que lorsque le nombre de séismes sur un noeud de la grille est inférieur à $N_{min} = 50$, M_c n'est pas calculée car l'incertitude sur la valeur de M_c devient trop importante (Schorlemmer, 2004). Les résulats de ces calculs sont représentés sur la figure 4.

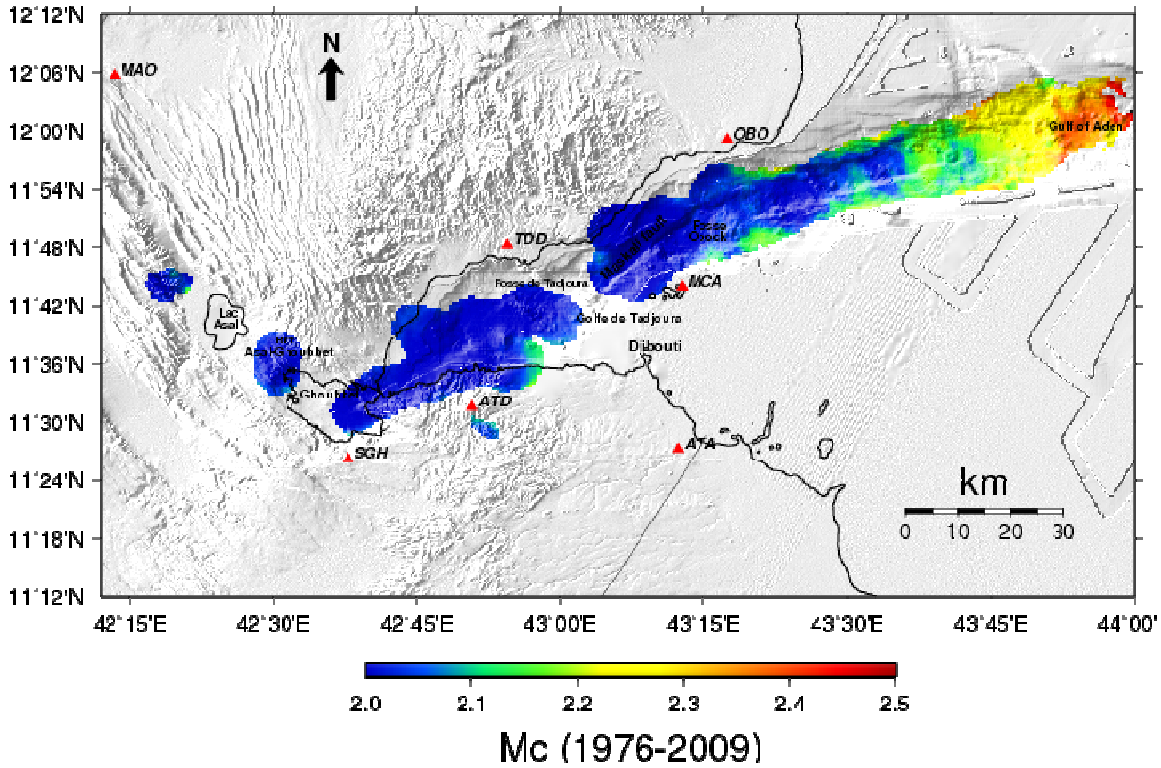

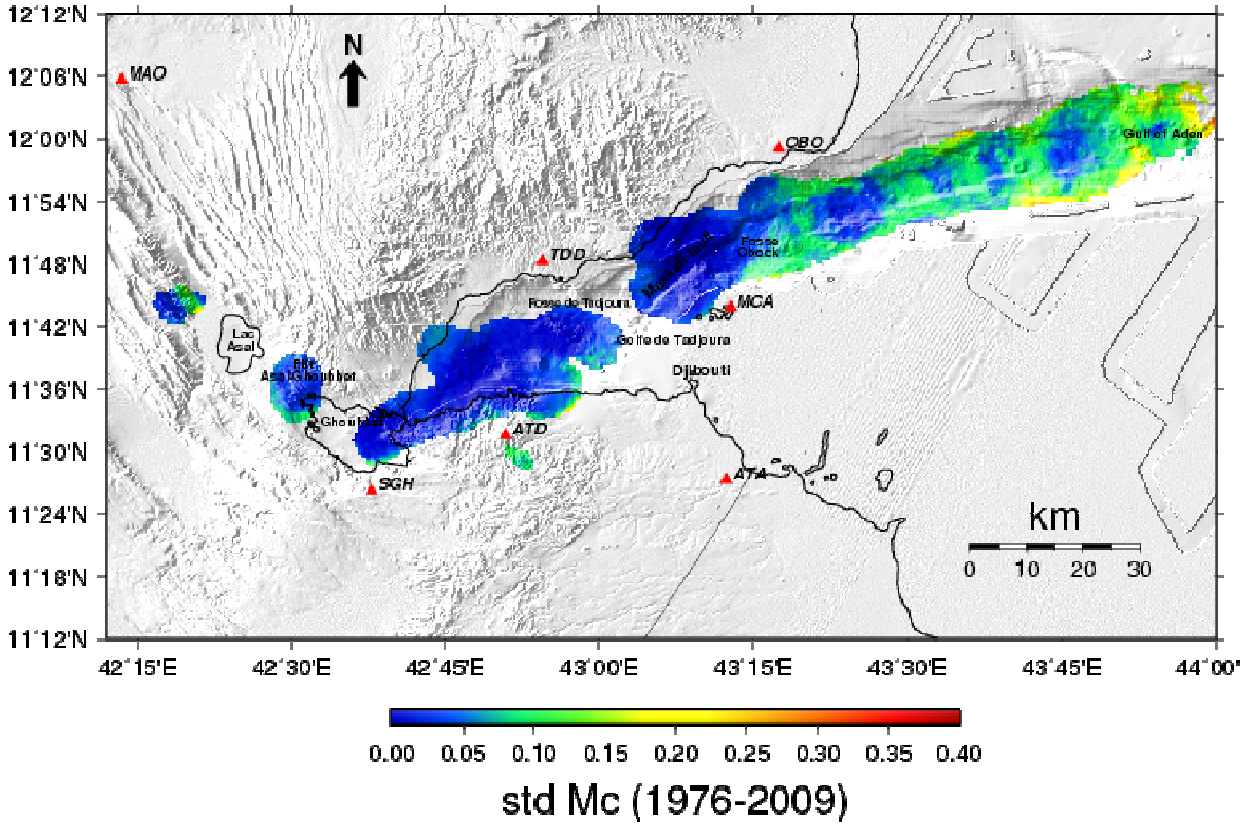

Fig. 4 : Variations spatiales de M_c et δM_c pour la période 1976 à 2009.

Nous constatons que la magnitude de complétude est d'environ $M_c = 2$ sur la plus grande partie de la région en question, bien couverte par le réseau de surveillance sismologique. Deux zones de la "dorsale" apparaissent en blanc, l'une dans le Ghoubbet, l'autre au SE de la station TDD. Ceci ne signifie pas qu'elles soient totalement exemptes d'activité sismique, mais seulement que le nombre de séismes dans le rayon *R* choisi est inférieur à 50 sur les 33 dernières années. D'autre part, lorsqu'on s'éloigne d'Obock vers le golfe d'Aden, M_c ainsi que δM_c augmentent progressivement, ce qui s'explique facilement par le fait que la distance aux stations augmente, et donc que le seuil de détection diminue.

IMAGERIE DE LA VALEUR *B* ET SON INCERTITUDE

La figure 5 présente le résultat des calculs des valeurs b et δb. La variation spatiale de la valeur *b* est très hétérogène sur l'ensemble des zones golfe de Tadjoura, rift d'Asal-Ghoubbet et au nord-ouest du lac Asal. Tout d'abord, l'observation à travers le golfe de Tadjoura montre que la valeur *b* varie beaucoup : ses valeurs limites sont entre 0.6 et 1.5 et se trouvent réparties globalement en 2 blocs. (1) Au niveau de l'extrémité orientale du golfe de Tadjoura, depuis la fosse d'Obock jusqu'à sa connexion avec le golfe d'Aden, la valeur *b* est relativement stable et reste inférieure à 1 (souvent au x alentours de 0.8 à 0.9). (2) En revanche depuis la faille transformante de Maskali jusqu'au Ghoubbet, la valeur *b* est très hétérogène et souvent supérieure à 1 (typique 1.2). Ses valeurs extrêmes vont de 1.4 (au niveau de la passe du Ghoubbet et au sud-ouest de la fosse de Tadjoura) à 0.6 (nord-est de la station ATD, Damerla).

La limite entre la zone de $b \approx 0.8$ de la partie orientale du Golfe et celle incluant la faille transformante de Maskali (autour de 1.0) est curieusement très nette. Elle est orientée $N\,15°E$, mais ne correspond à une direction tectonique reconnue dans la zone.

Dans le rift d'Asal-Ghoubbet, la valeur *b* est partout élevée avec une tendance à des valeurs plus élevées au nord (*b* autour de 1.8) qu'au sud du rift (*b* autour de 1.6), c'est à dire dans la zone dite du Petit Rift Nord, connu pour être la plus active du rift et enfin au nord-ouest du lac Asal, *b* est plutôt homogène de l'ordre de 1.0.

Au NO de la station ATD, près du lieu dénommé Demerla, existe une zone de *b* faible (0.8-0.6) qui contraste fortement avec le Golfe de Tadjoura qui est dans des valeurs 1.0-1.4.

Interprétations

Dans le rift d'Asal-Ghoubbet :

Les caractères volcaniques associé à l'hydrothermalisme d'un tel milieu sont bien connus. Pour plus des détails voir Lépine (1987), de Chabalier (1993), Jacques (1995), Abdallah (1997), Doubre (2004), Pinzuti (2006). Les valeurs de *b* élévés y sont dues principalement à une sismicité se développant sporadiquement, sous forme d'essaims au centre du rift (plancher interne) et plus particulièrement à l'aplomb du volcan Fiale. On peut seulement invoquer l'effet de fluides dans cette zone (champ géothermique prouvé par forages profonds, éruption fissurale de l'Ardoukoba en 1978 et cratères récents), mais pouvoir distinguer les signatures d'une activité hydrothermale (eau + chaleur) de clle d'une activité purement magmatique (dykes). Cependant on remarque que l'essentiel de la sismicité des trente dernières années se localise presque uniquement sur l'axe du rift, en fait sur un point de l'axe du rift, sous le volcan Fiale, et pas sous d'autres zones, par exmple sud-ouest du rift, où des champs géothermiques ont été reconnus.

Les séismes du “petit rift nord” à proximité de la station DAF paraissent beaucoup plus liés à l'activité tectonique de la faille bordière nord du rift d'Asal.

Au niveau de Damerla :

Selon Wiemer et al., (2005), les zones à valeurs *b* basses sont soumises à des contraintes élevées (aspérités), et que des ruptures futures pourraient préférentiellement s'y produire. Cette

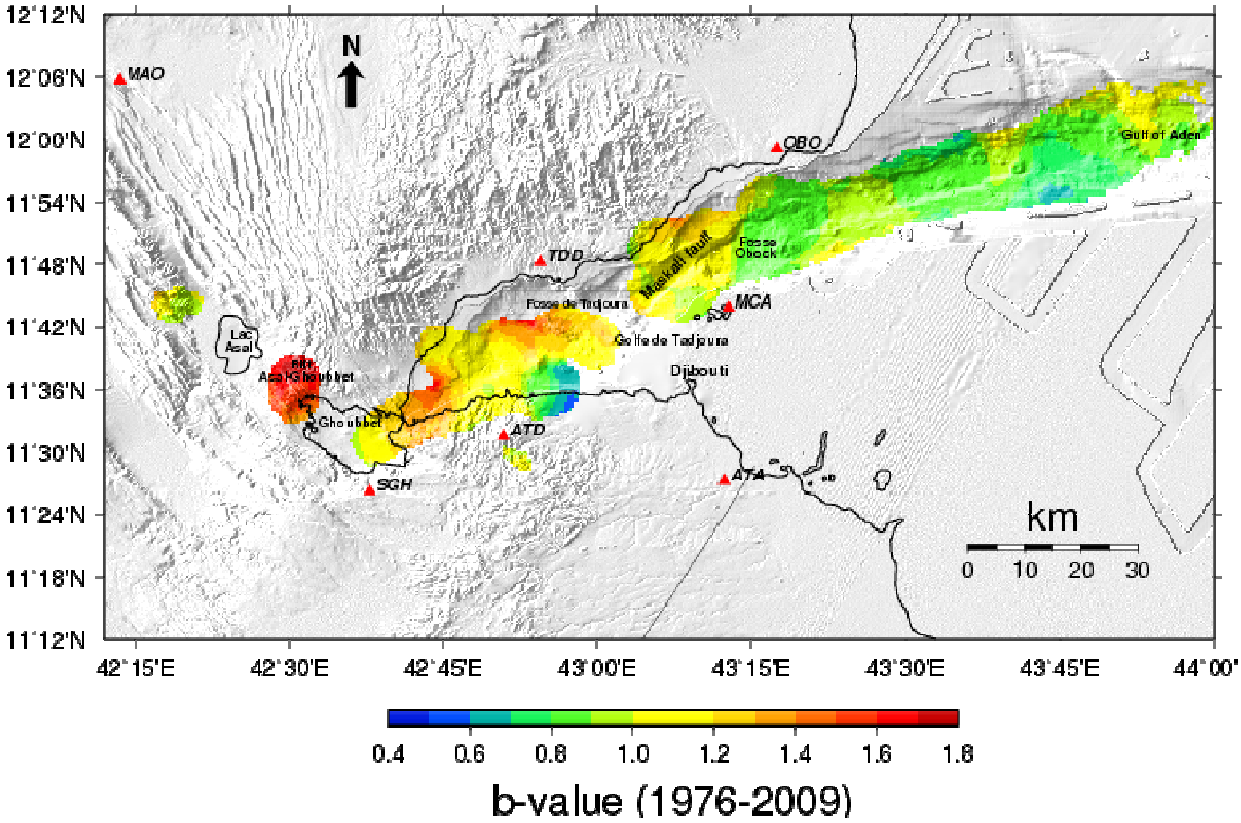
12°12'N
12°06'N
12°00'N
11°54'N
11°48'N
11°42'N
11°36'N
11°30'N
11°24'N
11°18'N
11°12'N
42°15'E
42°30'E
42°45'E
43°00'E
43°15'E
43°30'E
43°45'E
44°00'
N
MAO
OBO
TDD
MCA
ATD
SGH
ATA
Gulf of Aden
Maskali fault
Fosse Obock
Fosse de Tadjoura
Golfe de Tadjoura
Djibouti
Lac Assal
Rift Asal-Ghoubbet
Ghoubbet
km
0
10
20
30
0.4
0.6
0.8
1.0
1.2
1.4
1.6
1.8
b-value (1976-2009)

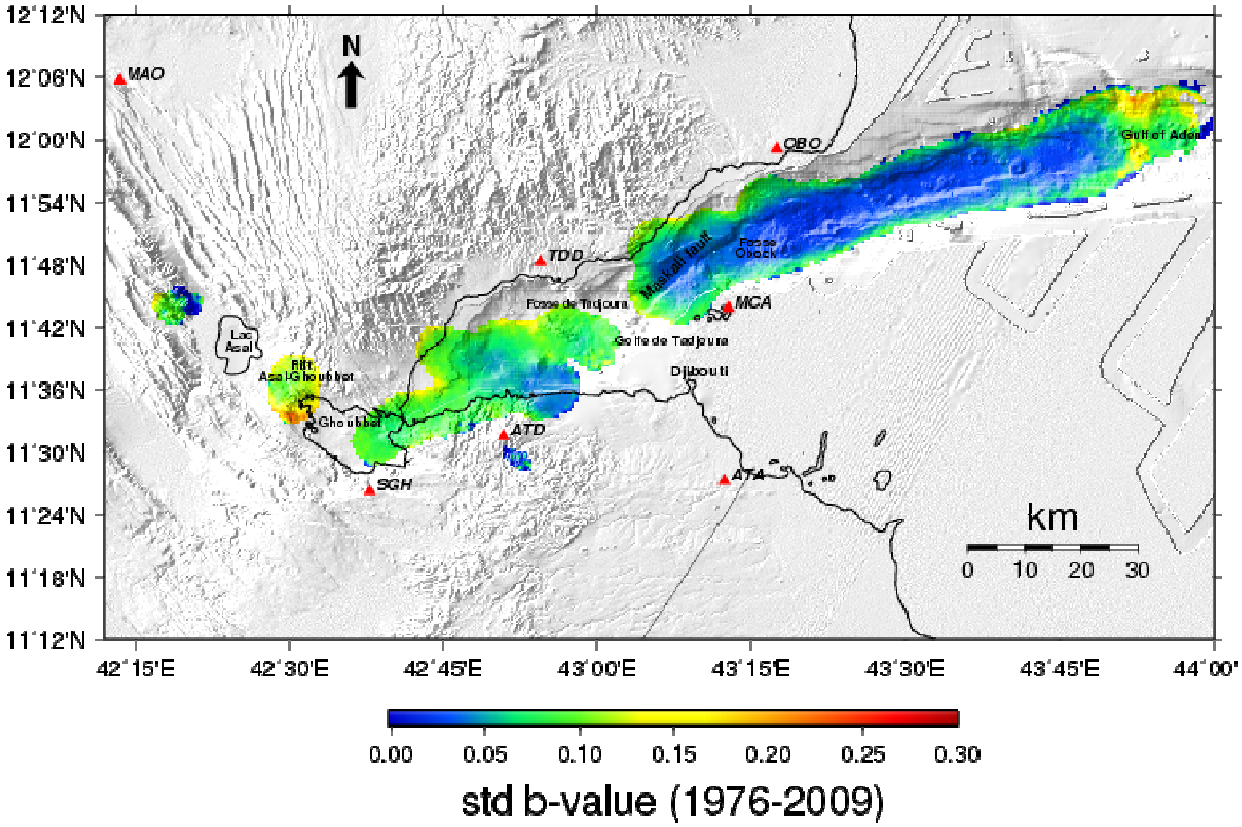

Fig 5 : Valeurs de *b* et erreur standard à travers le golfe de Tadjoura

hypothèse de contrainte élevée au niveau de la région de Damerla est en accord avec une étude tectonique très récente (Daoud, 2008) de la zone qui indique que la région de Damerla subit une déformation importante.

Au niveau de la faille de Maskali

La zone de discontinuité tectonique que représente la faille transformante de Maskali, présente aussi une discontinuité très nette en ce qui concerne la valeur *b* ($b > 1$) sur toute sa longueur, sauf sur une petite portion de bande (en couleur verte) vers l'extrémité sud en allant dans la direction de la fosse de Tadjoura où la valeur *b* est inférieure à 1 (voir fig. 5). En effet , nous savons d'après les études bathymétriques effectuées dans le golfe de Tadjoura par Choukroune et al., (1986), Audin (1999) que la faille transformante de Maskali assure le transfert de la propagation de la ride du Golfe d'Aden à travers le golfe de Tadjourah, en reliant la fosse d'Obock à celle de Tadjourah.

En partant de l'hypothèse, comme dans Wiemer et al. (2005), que les zones à valeurs *b* basses sont soumises à des contraintes élevées (aspérités), où les ruptures sismiques futures pourraient préférentiellement se produire et s'arrêter dans les zones ayant des valeurs *b* élevées (à contrainte faibles), la partie NE de la faille transformante de Maskali qui exhibe les valeurs de *b* supérieures à 1, pourrait constituer une barrière qui arrête toute rupture sismique en provenance de la fosse d'Obock se propageant vers l'ouest.

Pour illustrer ce dernier point de l'hypothèse, nous pouvons prendre l'exemple de la crise sismique de mars 1997 qui avait débuté dans le golfe d'Aden et qui s'est ensuite rapidement déplacée dans la fosse d'Obock sans toutefois franchir la faille transformante de Maskali.

D'après cette dernière hypothèse et son illustration, il est plus probable que la faille transformante de Maskali flue au niveau de sa terminaison NE, du côté de la fosse d'Obock. En effet, pour la période 1976à 2009, la sismicité est

quasi absente sur une partie au niveau de la zone NO de la faille transformante de Maskali, comme cela est illustré par la figure 6.

Il faut noter qu'il y a cependant des séismes qui s'alignent sur cette faille trandormante de Maskali durant la même période. Ceci peut suggérer que cette faille n'est pas totalement inactive à cette endroit. Donc, l'hypothèse que cette faille puisse fluer à ce niveau n'est pas fortuite au vue de la valeur *b* assez élevée de la zone.

Passe du Ghoubbet et sud de la fosse de Tadjoura

Pour ces deux zones, au vu de leur proximité avec les différents édifices volcaniques dans le golfe de Tadjoura, il n'est pas impossible que la valeur *b* élevée observée soit directement ou indirectement en relation avec les fluides géothermiques ou magmatiques en circulation. Mais à ce stade, nous n'avons pas de confirmation qui permette de privilégier telle ou telle hypohèse.

CONCLUSION

La cartographie de la valeur *b* à travers le golfe de Tadjoura indique une forte variation depuis le golfe d'Aden jusqu'à l'extrémité sud de la fosse d'Obock, zone où apparaît la faille transformante de Maskali. La valeur *b* élevée de l'extrémité nord de la zone qui englobe la faille de Maskali est interprétée comme la mainifestation possible de fluage de cet accident tectonique sur sa partie nord-est.

Par ailleurs, nous remarquons qu'il existe une importante structure volcanique active dans la zone fosse de Tadjoura, qui ainsi que la région de la passe du Ghoubbet, se signalent par des valeurs *b* élevée, confirmant ainsi la nature volcanique (ou hydrothermale) de leur activité. Enfin la zone de Damerla au nord-est d'Arta, qui affiche une valeur de *b* très faible et très localisée indiquant de fortes contraintes locales, pourrait être affectée par des séismes “forts”.

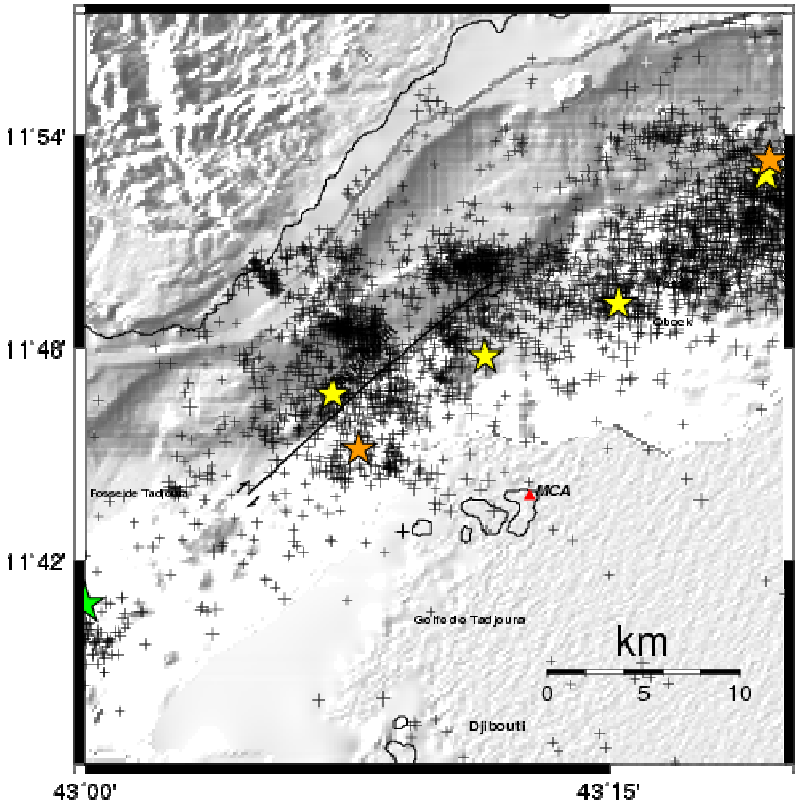

Fig. 6 : Sismicité de la période 1976-2009. Les étoiles représentent les séismes de magnitude $M \geq 5$.

RÉFÉRENCE BIBLIOGRAPHIQUES

Abdallah, A., V. Courtillot, M. Kasser, A.Y. Le Dain, J.C. Lépine, B. Robineau, J.C Ruegg, P. Tapponnier, and A. Tarantola, Afar seismicity and volcanism: relevance to the mechanics of accreting plate boundaries, *Nature, 282*, 17-23, 1979.

Abdallah, A. (1997), Champ géothermique d'Asal, République de Djibouti. *Thèse de doctorat, Université Paris 7.*

Akaike, H., 1974. A new look at the statistical model identification. *IEEE Trans. Automat. Contr. 19,* 716–723.

Aki, K., 1965. Maximum likelihood estimate of b in the formula log N=a−bM and its confidenc limits. *Bull. Earthq. Res. Inst. Univ. Tokyo 43,* 237–239.

Amitrano, D. (2003), Brittle-ductile transition and associated seismicity: Experimental and numerical studies and relationship with the *b* value, *J. Geophys. Res. 108*(B1), 2044,10.1029/2001JB000689.

Audin, L., 1999. Pénétration de la Dorsale d'Aden Dans la Dépression Afar Entre 20 et 4 Ma. *Thèse de doctorat, Université Paris 7*

Bender, B., 1983. Maximum likelihood estimation of b values for magnitude grouped data. *Bull. Seismol. Soc. Am. 73,* 831–851.

Barberi, F., H. Tazieff and J. Varet, Volcanism in the Afar depression: Its tectonic and magmatic significance. *Tectonophysics, 15*, 19-29, 1972.

Chabalier, J.B., (1993), Topographie et déformation tridimentionnelle du rift d'Asal (Djibouti): de la disparition d'un volcan à la naissance d'un volcan, *Thèse de doctorat, Université de Paris 7.*

Choukroune, P. et al., 1986. Tectonics of the westermost Gulf of Aden and the Gulf of Tadjoura from submersible observa-tions, *Nature, 319*, 396-399.

Cochran, J. R., The Gulf of Aden : Structure and evolution of a youg ocean basin and continental margin, *J. Geophys. Res., 86*, 263-288, 1981.

Courtillot, V., Opening of the gulf of Aden and Afar by progressive tearing, *Physics of the Earth and Planetary Interiors, 21*, 343-350, 1980.

Daoud, M.A., (2008), Dynamique de rift continental de 30 Ma à l'actuel dans la partie Sud Est du triangle Afar. Tectonique et magmatisme du rift de Tadjoura et des domaines Danakil et d'Ali Sabieh, République de Djibouti. *Thèse de doctorat , Université de Bretagne Occidentale.*

Doubre C. (2004), Structure et mecanisme des segments de rift volcaniques, Etudes des rifts anciens (Ecosse, Islande) et actifs (Asal-Ghoubbet), *thèse de doctorat de l'Université de Maine.*

Guthenberg, B., and C. F. Richter, Frequency of earthquake in california, *Bull. Seismo. Soc. Am., 34,* 185-88, 1944

Ishimoto, M., and K. lida, Observations of earthquakes registered with the microseismograph constructed recently, *Bull. Earthquake Res. Inst. Tokyo Univ., 17,*443-473, 1939.

Jacques, E., Fonctionnement sismique et couplage élastique des failles en Afar, *Thèse de doctorat de l'Université Paris 7,* 1995.

Kanamori, H., and D. L. Anderson, Theoretical basis of some empirical relations in seismology, *Bull. Seismol. Soc. Am., 65*, 1073-1095, 1975,

Kassim, M.K., (2009), Fonctionnement sismique du golfe de Tadjoura: Approche statistique (1973-2007) et deterministe (cas la séquence 2004). *Thèse de doctorat, Institut de Physique du Globe de Paris.*

Lépine, J.C., Répartition de la sismicité dans la zone d'extension de Djibouti (1972-1986), Relation entre activité sismique et éruptions volcaniques au Piton de la Fournaise (Réunion, 1985-1986), *Thèse de Doctorat, Université de Paris 6*, 1987.

Lépine, J.C., and A. Hirn, Seismotectonics in the Republic of Djibouti, linking the Afar depression and the Gulf of Aden, *Tectonophysics, 209,*65-86, 1992.

Mogi, K., Relations between the eruptions of various volcanoes and the deformation of the ground surfaces around them, *Bull., Earthq. Res. Inst, 36*, 99-134, 1958.

Pinzuti, P. (2006), Croissance et propagation des failles normales dans le rift d'Asal-Ghoubbet par datation cosmogénique . ^{36}C -Relation avec le magmatisme, *thèse de doctorat, Institut de Physique du Globe de Paris.*

Rydelek, P.A. and Sacks, I.S. (1989). Testing the completeness of earthquake catalogs and the hypothesis of self-similarity. *Nature, 337*. 251-253.

Scholz, C. H., The frequency-magnitude relation of microfracturing in rock and its relation to earthquakes. *Bull. Seism. Soc. Am. 58*, 399-415, 1968.

Schorlemmer, D., Weimer, S., Wyss, M., 2004. Earthquake statistics at Parkfield: 1. Stationarity of b values. *J. Geophys. Res. 109*, B12307. doi:10.1029/2004JB003234.

Schorlemmer, D., Wiemer, S., 2005. Microseismicity data forecast rupture area. *Nature 434,* 1086.

Schorlemmer, D., Wiemer, S., Wyss, M., 2005. Variations in earthquake-size distribution across different stress regimes. *Nature 437,* 539–542.

Shi, Y., Bolt, B.A., 1982. The standard error of the magnitude–frequency b-value. *Bull. Seismol. Soc. Am. 72,* 1677–1687.

Taylor, D. A., J. A. Snoke, I. S. Sacks, T. Takanami (1990). Nonlinear frequency magnitude relationship for the Hokkaido corner, Japan,*Bull. Seism. Soc. Am. 80*, 340–353.

Tisseau, J., Etude structurale du golfe d'Aden et du bassin de Somalie (océan Indien occidental nord), *Thèse de Doctorat, Université Paris-Sud, Paris XI*, 1987.

Utsu, T., 1965. A method for determining the value of b in a formula log N=a−bM showing the magnitude frequency for earthquakes. *Geophys. Bull. Hokkaido Univ. 13*, 99–103.

Utsu, T., 1992. On seismicity. Report of the Joint Research Institute for Statistical Mathematics: *Inst. For Stat. Math., Tokyo, vol. 34*, pp. 139–157.

Utsu, T., 1999. Representation and analysis of the earthquake size distribution: a historical review and some approaches. *Pure Appl. Geophys. 155*, 509–535.

Warren, N. W. and Latham, G. V. An experimental study of thermally induced microfracturing and its relation to volcanic seismicity. *J. Geophys. Res., 75,* 4455-4464, 1970.

Wiemer, S. and Wyss, M. (2000). Minimum magnitude of completeness in earthquake catalogues. Examples from Alaska, the western United States and Japan. *Bull. Seism. Soc Am. 90*:4, 859-869.

Wiemer, S., 2001. A software package to analyze seismicity: ZMAP. *Seismol. Res. Lett. , 72* , 373-382.

Wiemer, S., D. Schorlemmer, J. Woessner, (2005), Lessons learned from Monitoring b-value of micro-seismicity at Park-field throughout the seismic cycle, www.earthquake.ethz.ch/docs/presentations/talk_wiemer2005c.pdf

Wiemer, S., Schorlemmer, D. (2007): ALM: An asperity-based likelihood model for California, *Seismol. Res. Lett. 78*: 134-149.

Woessner, J., Wiemer, S., 2005. Assessing the quality of earthquake catalogues: estimating the magnitude of completeness and its uncertainty. *Bull. Seismol. Soc. Am. 95 (2*), 684–698. Doi: 10.1785/0120040007.

Wyss, M., 1973. Towards a physical understanding of the earthquake frequency distribution. *Geophys. J. R. Astr. Soc. , 31* , 341-359.

ROLE OF TEMPERATURE CHANGE IN MICRO SEISMIC ACTIVITY DURING FLUID INJECTIONS IN FAULTED AND FRACTURED ZONES. PART 1: UPDATING THE THERMAL MODELLING IN A DFN MODEL USING A DOUBLE MEDIA APPROACH

Ahmed KAYAD MOUSSA[1], Dominique BRUEL[1]
[1]*Centre de Geosciences –MinesParis-Tech*
Fontainebleau (France)
Dominique.bruel@mines-paristech.fr ; ahmed.kayad_moussa@mines-paristech.fr

Keywords: induced seismic, heat transfer; fracture system; geothermal system; hot dry rock.

INTRODUCTION

According to the general agreement that carbon emissions use should be strongly controlled, governments are now committed to diversify the primary fossil energy resource and particularly use more renewable resources. This is even more vital for countries that depend on imported oil products. Developing electricity production obtained from geothermal fields is therefore a priority at many places in the world. A step forward in this domain has been achieved with the Enhanced Geothermal System (EGS) concept, which was demonstrated at a pilot plant scale at the Soultz sous Forêts site (Genter et al., 2009). In such reservoirs, developed in deep hard rocks, the overall flow pattern is controlled by the pre-existing network of geological discontinuities. Access to the reservoir can be improved thanks to hydraulic stimulation techniques resulting in better connections between boreholes and these natural pathways. Controlling the efficiency of stimulation techniques upon the natural structures forming the bulk part of the reservoir is still a matter of research, as results obtained at various sites are highly variable. In all cases, raising the pore pressure, thereby reducing the shear strength of fractures zones and promoting shear failure and some increase in fracture permeability, is accompanied by micro seismic activity and acoustic emissions (AE). These signals are recorded and analysed. The spatial localization of rupture sources often delineates planar structures where pressure perturbations were propagated. It is therefore confirmed that flow occurs in a 3D network of 2D structures and that specific quantitative models are required to capture the coupled hydraulic-mechanical processes at issue. During the past decade, attention was first given to the engineering of the reservoir using various combinations of hydraulic tests, and to the evaluation of the hydraulic improvement of the pathways developed the fractured system, using tracer tests (Sanjuan et al., 2006). Recent works are re-focussing at physical processes, such as the determination of fracture/matrix transfer area, (K. Pruess and C. Doughty, 2010) or at comparisons of tracer and thermal transport in fractured reservoirs (Juliusson et Horne, 2010) to investigate the extent to which tracer return can be used to predict thermal breakthrough. Very few new programmes were dedicated to long term thermal behaviour, assuming that a reservoir with sufficient size would last long enough for industrial purposes. The phenomenon of large induced seismic events (LISE) then received considerable interest after the generation in 2003 of a Magnitude 2.9 earthquake at Soultz sous Forêts (France). In 2006, a M 3.4 earthquake was generated during the hydraulic development of a new EGS reservoir, near the Swiss city of Basel, that stopped the project.

This issue of large seismic event is also raised at other places where natural steam reservoirs exist and are exploited for decades. At the Geysers site (California) it is clearly observed that earthquakes with magnitudes larger than 4 become more frequent, in correspondence with continuous re-injection of fluid performed to maintain the reservoir pressure. In this case, it was argued and demonstrated (Rudqvist et al., 2002) ° that the thermal poro-elastic cooling below re-injection zone is responsible for mechanical changes, sufficient to activate dislocation mechanisms along pre-existing fractures. However the working hypothesis of equivalent porous media did not offer the possibility to the authors of going further ahead with fracture failure analysis in a realistic fractured reservoir. Other pioneer 3D modelling works can be mentioned. Conceptual models based on deterministic regular fracture patterns or simplified geometries (Swenson 1997, Hicks *et al.*, 1996, Kolditz and Diersch, 1993, Kolditz and Clauser, 1998) were first developed. Since fractures are unevenly distributed in space, forming clusters, with widely variable size (see Genter *et al*., 2000 at Soultz sous Forêts site), and since the heat to mine out is stored in the matrix surrounding the fractures, continuum models based on equivalent porous materials are not adequate. Randomly distributed networks (Robinson, 1990; Bruel, 1995, 2002; Willis-Richard *et al.*, 1996) embedded in the rock mass have been developed. Most of the recent efforts are attempts to mix both representations, a discrete randomly distributed network embedded in a porous system. A recent example is given by (E. Juliusson and R.N. Horne, 2010) using Finite

Element type numerical methods, and working on sophisticated unstructured computational grids. One of their conclusions is however that numeric for a realistic (2D) network was at the margin of being feasible, and the authors claim for the need of new appropriate upscaling algorithms and new non meshing techniques.

The purpose of this paper is to go back to the understanding of the long term potential impacts of coupled Thermo-Hydro-Mechanical processes (THM) in EGS geological settlements, using a discrete fracture network (DFN) specific approach. This discrete approach is able to handle the specific geometrical characteristics of fracture networks and faulted zone. Such an approach was already introduced for EGS modelling by Bruel (1995, 2002) for the study of a 3 year long circulation test at the Rosemanoves site (UK) and for the simulation of a four months long circulation tests at 3.5 km depth performed in 1997 in the upper reservoir of the Soultz sous Forets site (France). For the latter case, no long term fluid circulation was planned for this EGS sites, so that only local thermo-elastic couplings were considered, with no interactions in between temperature changes and fluid properties.

The work presented here after is an update of the FRACAS DFN code (Baujard et Bruel, 2006) where a double media is introduced to solve for thermal conductive heat transfer at the reservoir scale coupled with local heat exchange along the fractures embedded in the rockmass and heat convection along the flowing pathways. These efforts are clearly required to tackle new research aspects concerning long term seismic risk analysis. This should be also particularly useful for new sites as those planned in faulted rift zones of eastern Africa, where the prevailing tectonic regime makes fractures very close to instability. As an example, C. Doubre et G. Peltzer (2007) analyse natural micro-seismic activity and show that present day fracture propagation at Asal rift (Djibouti) is probably linked with natural flow along fractures. The Asal hydrothermal region has been identified as a favorable area to develop the geothermal resources and projects are already underway. But the first evaluation of the production potential considers that re-injection of (cold) fluids will be necessary to compensate for reservoir drawdown (Houssein and Axelsson, 2010).

THEORITICAL BACKGROUND OF THE FRACAS DISCRETE FRACTURE NETWORK FLOW CODE

The FRACAS modelling approach is based on the assumption that fluid moves through a rock mass within a system of interconnected fractures and that flow in the rock matrix is negligible by comparison. The three-dimensional hydraulically conductive network of planar, disc-shaped fractures generation is inherited from Cacas et al.(1990) modelling work. Series of individual fractures are generated within a rectangular block of rock, based on stochastic descriptions of fracture density, fracture orientation, and fracture size. Improvements were achieved to capture more realistic geological systems. Specific fracture sets can be defined as models of faults zones. Relay structures or simple planar fault segments can be generated as well as combinations of adjacent blocks with different fracture network properties.

FLOW RULES

Hydraulic conductivities

The overall flow model is based on the premise that flow in granitic basements primarily occurs on channels within fractures. The 3D structure resulting of the superimposition of the connected portions of planes is thus treated as a 3D network of 1D pipes. Equivalence of this channel flow approach with others solving true 2D flow in planes has been discussed (Dershowitz and Fidelibus, 1999).

Time-dependant analysis requires assumptions to be made concerning the form of fluid flow within the fracture network. The general form of fluid flow assumed in each fracture is based on an analytical solution, known as the « cubic law », for fluid flow between approximately parallel surfaces. Modified forms of the cubic law are used to account for the effects of changes in the morphology of contact between fracture surfaces. As the effective stress across a fracture increases flow through the fracture becomes confined to a limited number of channels. Thus, in FRACAS, the single phase volumetric flux (m^3s^{-1}) in the *x*-direction through a length *l* (m) of a fracture has the form :

$$Q=\frac{-a_0^3}{12\nu}glF\frac{dh}{dx} \qquad (1)$$

where a_0 is the hydraulic aperture (m) of the fracture at zero effective stress, *g* is acceleration due to gravity (ms^{-2}), ν is the kinematic viscosity (m^2s^{-1}), *dh/dx* is the hydraulic head gradient driving flow through the fracture, and *F* is a

dimensionless function dependent on effective stress. The effective stress is defined as $\sigma' = \sigma_\pi - p$, where σ_π (Pa) is the rock stress normal to the fracture surface and p (Pa) is the fluid pressure in the fracture. Empirical expressions for the closure law F, in which F decreases as the effective stress increases (F=1 at zero effective stress) are presented by Jeong (2006). This coupled approach was tested against various *in situ* experiments performed in hard rocks in the frame work of a nuclear waste storage research program, and predictive results were compared with those of other numerical approaches (Rejeb and Bruel, 2001). The approach was extended (Bruel, 2007) to account for shear loading and Coulomb frictional failure, in an attempt to simulate reservoir hydraulic stimulation processes and micro-seismic predictions.

However, in this paper the objective is to incorporate the potential effects of a short term thermal perturbation to evaluate how significantly it may alter the reservoir performances. Therefore F will be re-derived later, according a new procedure described in the section devoted to the thermo-hydro-mechanical interactions, after the basics for heat exchange modeling in the FRACAS discrete fracture network model have been introduced.

Specific storage of the fractures

The specific storage S (m^{-1}) of a fracture with R as radius (m) is given by:

$$S = \rho g \frac{1}{a_0} \frac{da}{d\sigma'} + S_0 \qquad (2)$$

where ρ is the fluid density (kgm^{-3}) and g the acceleration due to gravity (ms^{-2}). S_0 denotes the potential specific storage of the adjacent weathered rock that can be identified on cores and in situ, using sonic logs. These zones exist on both fracture sides and can extend up to a metric scale (Genter *et al*., 2000). In deriving the specific storage term, the rock stress has been assumed constant, such that changes in effective stress are caused only by fluid pressure changes. Also, fluid compressibility is generally much smaller than fracture compressibility and, thus, has been neglected. The form the of the term $da_i/d\sigma'$ calculated at the center of the fracture disc, depends on the assumed form of the relationship between the hydraulic fracture aperture and the effective stress, as discussed above.

THERMAL MODELLING

Convective and conductive heat transfer along individual fractures

Heat exchange along the circulated fractures can be evaluated assuming that heat conduction develops perpendicular to each fracture plane. No energy is retained by the volume of fluid within the fractures. The conservation of energy is written at each fracture centre as a balance between energy transferred by convection from or to neighbouring fractures and energy dissipated by conduction in the current cell. At any time, continuity of the temperature at the fracture wall is assumed, that is :

$$\theta_f = \theta_m(y=0) \qquad (3)$$

Subscript f and m respectively stand for fluid and matrix. If q_{ij} and q_{ik} [m3s-1] denotes fluxes entering and leaving a given disc i at time t, with respective temperatures $\theta_{fi}(t)$ and $\theta_{fi}(t+dt)$, the energy exchanged during dt is dQ_i [J], given by :

$$dQ_i = \Sigma_j \rho_f C_f q_{ij} \theta_{fj} dt - \Sigma_k \rho_f C_f q_{ik} \theta_{fi} dt \qquad (4)$$

This energy is related to the heat flux at the fracture wall, Φ_i , across the exchange area S_i [m^2], that has to dissipate in an adjacent rock volume according to a diffusive equation. The shape of this adjacent block is cylindrical, with a radius equal to that of the fracture-disc and a length l_i chosen so that the total volume cumulating all the cylinders is equal to the reservoir volume in order to fulfil the global heat capacity conservation.

The temperature at the face opposite to the circulated fracture is a new variable. $\theta_{ml} = \theta_m(y=l)$. This initial value of this local variable is set to the temperature estimated at depth for the corresponding fracture, given the natural measured temperature profile..

The developments insuring block to block thermal interactions for predicting long term thermal depletions are proposed in the next section. We will assume that interactions are controlled by the thermal diffusivity coefficient, which is in the order of 1. $m^2\ s^{-1}$ for rocks. Temperature changes may propagate at significant distances greater than 10 m within time periods no longer than a year. The equations presented here below are solved sequentially.

$$dQ_i = \Phi_i\ S_i\ dt, \quad \textbf{(5)}$$

$$\Phi_i = K_m\ (d\theta_m/dy)_{y=0} \quad \textbf{(6)}$$

$$\frac{K_m}{\rho_m C_m}\Delta\theta_m = \frac{\partial\theta_m}{\partial t} \quad (7)$$

At each disc i in the network, the diffusivity equation is written in a discrete form following a standard finite difference scheme, and the set of equations is solved for θ_{fi} and θ_{mi} at time $t+dt$ knowing similar quantities and boundary θ_{mli} values at time t. The temperature of the injected fluid is continuously prescribed. Parameters are matrix heat conductivity K_m [W m^{-1} K^{-1}], heat capacity C_f, C_m [J kg^{-1} K^{-1}] for both fluid and matrix, density ρ_f, ρ_m [kg m^{-3}] for both fluid and matrix.

CONDUCTIVE HEAT TRANSFER AT THE GLOBAL SCALE AND DERIVATION OF INTERNAL BOUNDARY VALUES θ_{ML}

The basic idea suggested in this section is that the heat extracted during a given time step from a sub volume containing a number of connected fractures by a fluid forced to circulate along these fractures can be approximated by an equivalent density term, source or sink, depending on the sign of the calculated heat balance. Therefore, the method consists at any time step, when fluxes, fluid temperature and local matrix temperature profiles are known at each fracture disk i,, in solving a succession of tasks as follows:

- Define a regular 3D grid, with cells cubic in shape, overlapping the fractured reservoir, each cell being large enough to contain a sub-network of fractures
- Identify the discs belonging to each cell
- Calculate the net heat balance per cell, from the differences in temperature profiles at t and t+dt at each disc within the cell
- Derive a source term from the temperature change for each cell, accounting for cell volume and time step duration.
- Solve for a heat conduction problem over the 3D grid, using prescribed temperature at the top of the reservoir, regional geothermal heat flux at the base of the reservoir, heat conduction and capacity coefficients for the rock mass, and the discrete volumic heat source at each cell.
- Use the temperature obtained at each cell at date t as the new θ_{ml} value for all the discs belonging to that cell.

The two step algorithm is sequential, but the time stepping for the conductive behaviour at large scale can be larger than the time stepping for solving the local convective-conductive heat exchange at the local scale. This new algorithm has been iùplemented in our FRACAS code. Numemerical verifications are now focussing on the hydro-thermal global behaviour of the double media, using benchmarking against other numerical codes that can handle some fracture patterns (GEOFRACK, TOUGH2). An outcome of the FRACAS code development is that experimental testing programmes running over years but combining successions of injection/production phases separated by month long rest periods can be modelled in a single run.

PRELIMINARY CONCLUSION

Apart from standard numerical checking, a series of verification examples against true data sets is under construction. The first one will be based on results obtained on one of the first Hot Dry Rock research programme run at the Rosemanoves quarry site (Cornwall, UK), extensively documented by RH Parker (1988).

A main aspect in this data base is that it contains a long term circulating test that lasted about 3 years and that shows a thermal breakthrough partly due to thermo mechanical interactions. Fracture network is well described, as a dense regular network made of 3 directional sets (blocky pattern). A large number of hydraulic tests in between the

different wells have been performed as well as tracer tests to discuss heterogeneity and role of main flow paths. A main interest in running a model in such a system is to revisit the potential impact of fracture stimulation at the network scale and rediscuss some of the remarks concerning single well injection-withdrawal tracer tests done by Pruess and Doughty (2010), stating that temperature return is insensitive to fracture aperture changes. As thermal processes may combine with mechanical processes, we also intend to derive rock thermal shrinkage at the reservoir scale, and obtain the dramatic short-circuit effect observed at Rosemanoves site. Given shear rupture modelled along thermo-mechanical perturbed pathways, we will suggest, as done in Bruel(2007), a catalogue for the thermally induced micro-seismicity.

REFERENCES:

Baujard. C et Bruel D, (2006) Numerical study of the impact of fluid density on the pressure distribution and stimulated volume in the Soultz HDR reservoir Geothermics Volume 35, Issues 5-6, October-December 2006

Bruel, D. (2007) Using the migration of the induced seismicity as a constraint for fractured hot dry rock reservoir modelling. Int. J. Rock. Mech. Mining Sci., vol. 44, n°8.

Bruel D., (2002), Impact of induced thermal stresses during circulation tests in an engineered fractured geothermal reservoir. Example of the Soultz sous Forêts, European hot fractured rock geothermal project, Rhine Graben, France, Oil & Gas Science and Technology, Rev. IFP, vol. 57, n°5.

Bruel D. (1995) - Heat extraction modelling from forced fluid flow through stimulated fractured rock masses. Application to the Rosemanoves Hot Dry Rock reservoir. Geothermics, 24(3).

Cacas, M., E. Ledoux, G. de Marsily, A. Barbreau, B. Tillie, E Durand, P. Feuga, and P. Peaudecrf (1990). Modeling fracture flow with a discrete fracture network ; calibration and validation. 1. the flow model. Water Resource Research 26 (3), 491-500.

C. Doubre,G.Peltzer (2007) Fluid-controlled faulting process in the Asal Rift, Djibouti, from 8 yr of radar interferometry observations. *Geology* January 2007 v. 35 no. 1.

Daniel Swenson and Brian Hardeman The Effects of Thermal Deformation on Flow in a Jointed Geothermal Reservoir Int. J. Rock Mech. & Min. Sci. Vol. 34, No. 3/4, NYRocks '97, ISRM International Symposium Columbia University, NY, June 29-July 2, 1997

Dershovitz, W and C. Fidelibus (1999). Derivation of equivalent pipe network analogues for three dimentional discret fracture networks by the boundary element method. Water Ressources Research 35 (9), 2685-2691.

Egill Juliusson and Roland N. Horne Study and Simulation of tracer and thermal transport in fractured reservoirs., Thirty-Fifth Workshop on Geothermal Reservoir Engineering Stanford University, Stanford, California, February 1-3, 2010 SGP-TR-188.

Daher. E. Houssein and G. Axelsson, 2010. Geothermal Resource Assessment of Asal Field, Republic of Djibouti Geothermics, 39 (2010), 220-227.

Genter, A., Traineau, H., Bourgine, B., Ledesert, B., Gentier, S.Over ten years of geological investigations within the HDR soultz project, France (2000) *World Geothermal Congress 2000*

Genter, A., Fritsch, D., Cuenot N., Baumgartner, J., Graff, J.J.,Overview of the current activity of the European EGS SOultz project: from exploration to electricity production. Proc. of Thirty-Fourth Workshop on Geothermal Reservoir Engineering Stanford University, Stanford, California, February 9-11, 2009

Hicks, T.W., Pine, R.J., Willis-Richards, J., Xu, S., Jupe, A.J., Rodrigues, N.E.V.A hydro-thermo-mechanical numerical model for HDR geothermal reservoir evaluation (1996) *International Journal of Rock Mechanics and Mining Sciences and Geomechanics*, 33 (5).

Jeong, W.C. Bruel D., and Cho, C.H.O. (2006) Numerical experiments of flow and transport in a variable-aperture fracture subject to effective normal stresses. Journal of Hydraulic Research, 44, n°2.

Kolditz, O., Clauser, C.Numerical simulation of flow and heat transfer in fractured crystalline rocks: Application to the hot dry rock site in rosemanowes (U.K.) (1998) *Geothermics*,27 (1).

Kolditz, O., Diersch, H.-J.Quasi-steady-state strategy for numerical simulation of geothermal circulation in hot dry rock fractures (1993) *International Journal of Non-Linear Mechanics*, 28 (4).

Pruess, K. and C. Doughty. Thermal Single-Well Injection-Withdrawal Tracer Tests for Determining Fracture-Matrix Heat Transfer Area, Thirty-Fifth Workshop on Geothermal Reservoir Engineering, Stanford University, Stanford, California, February 1-3, 2010.

Rejeb, A. and Bruel , D., (2001), Hydromechanical effects of shaft sinking at the Sellafield site, International Journal of Rock Mechanics and Mining Sciences, 38.

Robinson, B.A A discrete fracture model for a hot dry rock geothermal reservoir (1990) *Camborne School of Mines International Conference on Hot Dry Rock Geothermal Energy*, pp. 315-327.Ed. Roy Baria (1989), Robertson Scientific, London

Rutqvist J., Y.-S. Wu, C.-F. Tsang, and G. Bodvarsson A Modeling Approach for Analysis of Coupled Multiphase Fluid Flow, Heat Transfer, and Deformation in Fractured Porous Rock Int. J. Rock Mech. & Min. Sci. 39, 429-442 (2002).

Sanjuan, B., Pinault, J. L., Rose, P., Gerard, A.,Brach, M., Braibant, G., Crouzet, C., Foucher, J.C., Gautier, A. and Touzele, S. (2006), "Tracer testing of the geothermal heat exchanger at Soultz-sous-Forêts (France) between 2000 and 2005", Geothermics, 35 (5-6), 622-653

Willis Richards et al., Progress toward a stochastic rock mechanics model of engineered geothermal systems. Journal of Geophysical Research, vol.101, noB8, Aug. 1996

JOINT 1-D INVERSION OF TEM AND MT DATA FROM OLKARIA DOMES GEOTHERMAL AREA, KENYA

Charles Muturia Lichoro
Geothermal development company Ltd. (GDC),
cmuturia@gmail.com

ABSTRACT

Joint one-dimensional (1-D) inversion of magnetotelluric (MT) and central loop transient electromagnetic (TEM) data was done by fitting both data kinds using the same 1-D resistivity model. It is well known that in the presence of small-scale surface or near-surface resistivity inhomogeneities the magnetotelluric (MT) apparent resistivity can be shifted by a multiplicative factor which is independent of frequency. In this regard TEM has been used to correct for the static shift factor to restore the MT curve where it should have been without the effect of shift for this project.

The 1-D joint inversion results reveals three main resistivity zones, a shallow high resistivity zone (> 100 Ωm) to about 300 metres below the surface, an intermediate low resistivity zone (10 Ωm) to depths of about 1 kilometre and a deeper high resistivity (> 50 Ωm), up to 3-4 kilometres depth. Below the high resistivity zone a relatively low resistivity zone at depth is evident possibly indicating a high temperature which is a likely source of crustal fluids for this field.

A good correlation is found between the resistivity structure, hydrothermal alteration and reservoir temperatures. The low resistivity is dominated by conductive minerals in the smectite-zeolite zone at temperatures of 100-200°C. In the temperature range of 200-240 °C zeolites disappear and smectite is gradually replaced by resistive chlorite. At temperatures exceeding 250 °C chlorite and epidote are the dominant minerals and the resistivity is probably dominated by the pore fluid conduction in the high-resistivity core provided that hydrothermal alteration is in equilibrium with the present temperature of the reservoir.

Key words: resistivity, alteration, static shift, joint inversion

INTRODUCTION

Scope of work

This report presents the geophysical work performed in Olkaria-domes in Kenya. It covers Magnetotelluric (MT) and Transient electromagnetic (TEM) data acquisition, processing and interpretation using a one dimensional joint inversion of those data sets (based on a nonlinear least-squares inversion of the Levenberg-Marquardet code, Árnason, 1989). The result is presented both by iso–resistivity maps at different elevations and resistivity cross-sections along profiles. The goal of this study is to establish the resistivity structure of this field and correlate it with the alteration mineralogy and the reservoir characteristics from wells that have been drilled and suggest possible locations for future drill holes.

An attempt has been made to relate the modelled geophysical parameters to the geological and tectonic structures and the geothermal reservoir characteristics from wells in the area.

Geological and tectonic setting

Olkaria Domes geothermal field is located on the South-eastern part of the Greater Olkaria geothermal area. The area approximately bound by Ol'Njorowa gorge to the west and a ring of domes to the east and south of the field (Figure 1).

The Greater Olkaria volcanic complex is characterized by numerous volcanic centres of Quaternary age and is the only area within the Kenya rift with occurrences of comendite (a type of white rhyolite comprising the minerals amphibole and pyroxene) on the surface (Lagat, 2004). Other volcanoes in Kenya are associated with calderas of varying sizes. Olkaria volcanic complex does not have a clear caldera formation, which might suggest younger in age compared to other volcanic areas in Kenya. However as seen on figure 1, the volcanic domes in the east, south and southwest appear to be located on a ring shaped structure. This observation has been used to suggest the presence of a buried caldera (Figure 1); Naylor, 1972, Virkir, 1980, Clarke et al., 1990, Mungania, 1992). In support of the caldera theory micro-seismic studies have indicated possible attenuating bodies under the ring of Domes (Simiyu, et.al., 1998).

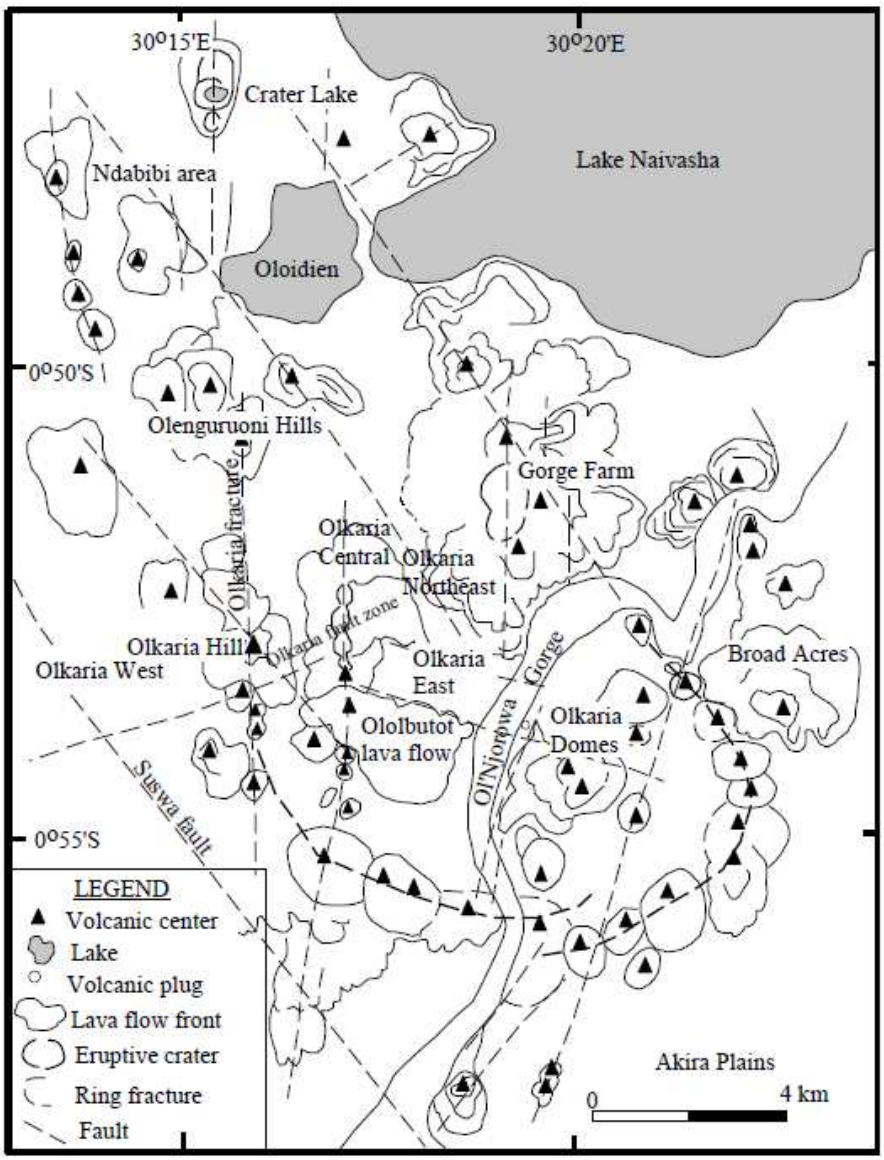

FIGURE 1: Volcano-tectonic map of the Greater Olkaria volcanic complex (modified from Clarke et al., 1990)

RESISTIVITY STUDY OF OLKARIA DOMES GEOTHERMAL FIELD

TEM survey

In this study a total of 52 Central Loop TEM soundings were carried out in the Domes area spread over about 45 km^2. The stations are scattered within the prospect area with denser coverage in the areas where wells have been drilled as can be seen on Figure 2.

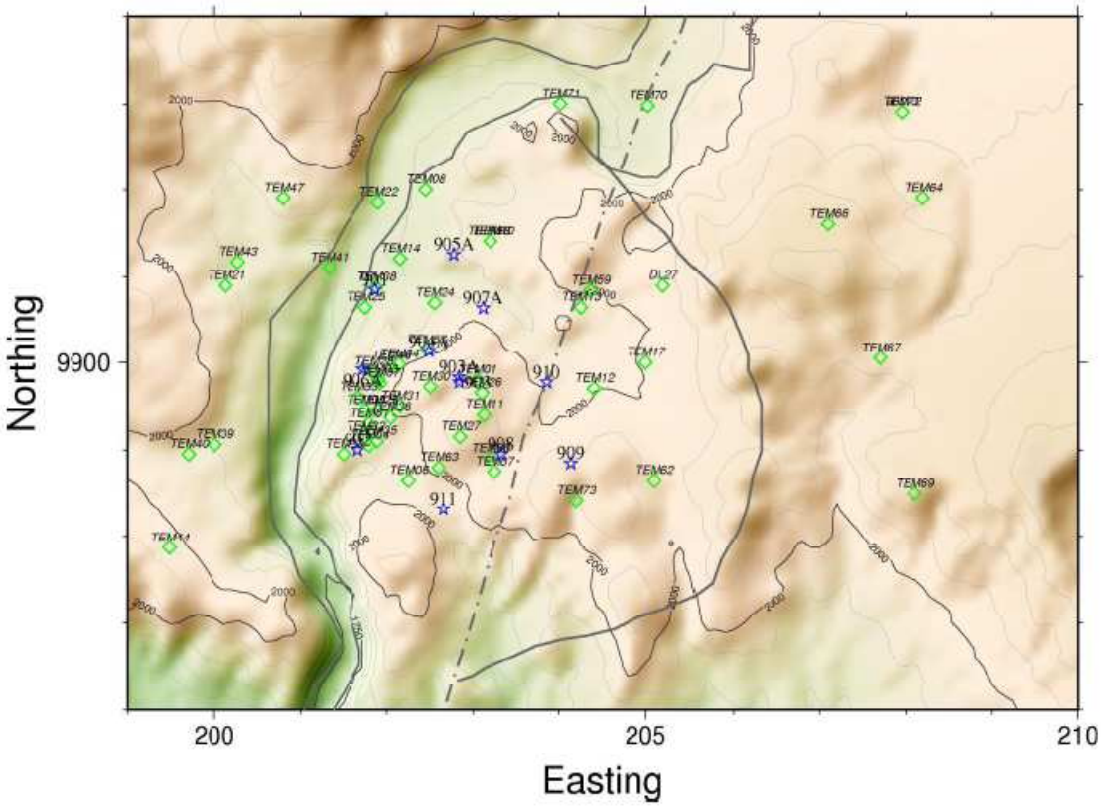

FIGURE 2: TEM sounding locations

TEM data processing and 1-D interpretation

The raw TEM data was processed by the program TemZ, a modified version of Temx to handle Zonge data (Árnason, 2006). This program averages data acquired at same frequency and calculates late time apparent resistivity as a function of turn-off time. It also enables visual editing of raw data to remove outliers and unreliable data points before the data can be used for interpretation.

1-D inversion of TEM is achieved by software called TEMTD a UNIX program. This software assumes that the source loop is a circular source field and that the receiver coil/loop is at the centre of the source loop. Practically a square loop is used with equal area to that of the circle. The current waveform is also assumed to have equal current-on and current-off time segments. The transient response is calculated both as induced voltage and late time apparent resistivity as function of time.

All the TEM soundings in the Domes area have been interpreted by 1-D inversion. The inversion was done by the Occam inversion (Figure 3), with as smooth models as possible. In 1-D inversion it is assumed that the earth consists of horizontal layers with different resistivity and thickness. The 1-D interpretation seeks to determine the layered model whose response best fits the measured responses.

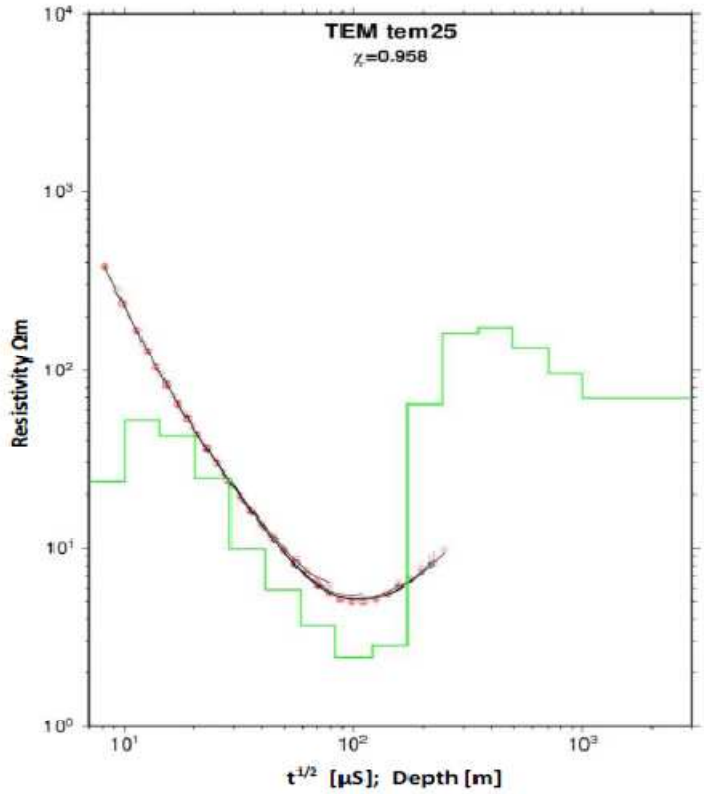

FIGURE 3: TEM sounding from Domes area and its 1-D inversion. It illustrates the TEM apparent resistivity curve and its interpretation.

MT survey

A total of 70 MT soundings are considered for interpretation in the Domes prospect covering an area of about 45 km^2 as can be seen in (Figure 4). The data was acquired using 5-channel MT data acquisition system (MTU-5A) from Phoenix Geophyics.

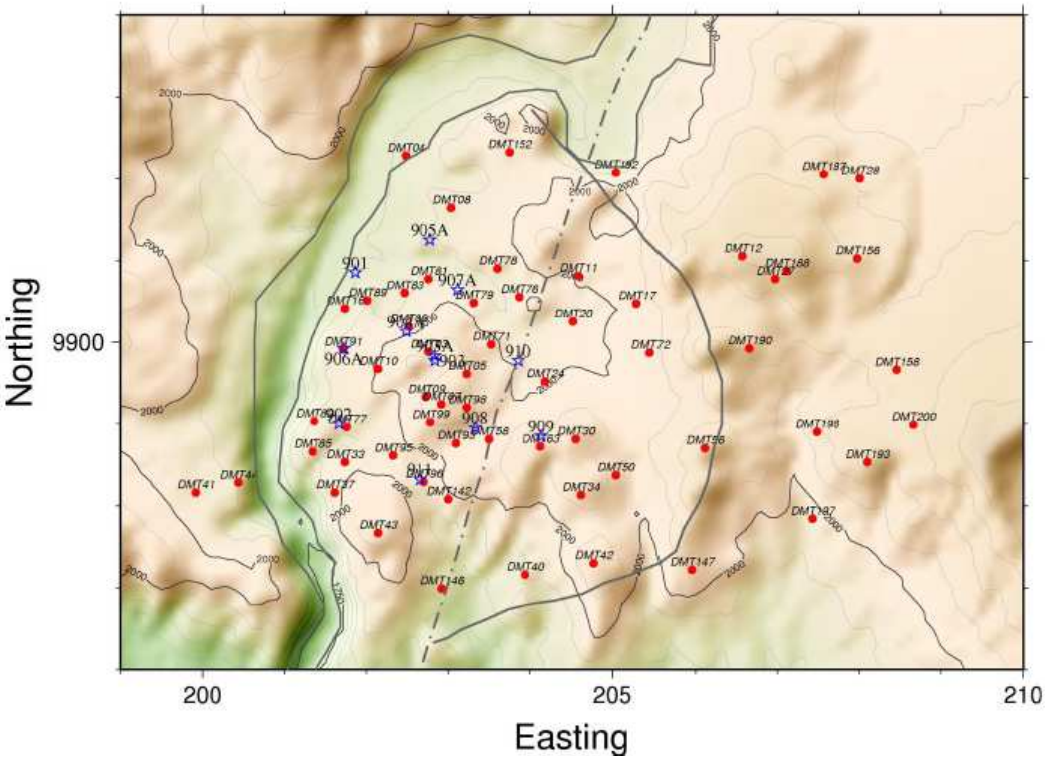

FIGURE 4: The MT sounding distribution over the prospect area

The MT static shifts

The MT method suffers from the so called static shift problem. This phenomenon is caused by local resistivity inhomogeneities which disturbs the electrical field. The main cause is the accumulation of charges at resistivity boundaries causing the Electrical field not to be continuous close to this boundary. The static shift is expressed by scaling of the apparent resistivity by an unknown factor (shifted on log scale). This shift is independent of frequency, at least for those frequencies generally used in MT soundings (Jones, 1988). The static shifts can be a big problem in volcanic environments where resistivity variations close to the surface are often extreme. These parallel shifts in apparent resistivity curve can lead to large errors in inverted data.

In this interpretation Central loop-induction TEM sounding have been used to correct for static shift in MT data by jointly inverting both MT and TEM data. This is based on the fact that, for TEM measurements at late time there are no distortions due to near surface inhomogeneities since they do not involve measuring electrical field. This has been tested by model calculations (e.g. Sternberg et al., 1988) and shown to be a useful method to correct for static shifts in MT soundings, at least for 1-D resistivity environment.

Static shift analysis of MT data in Domes

Static shift analysis of the 62 MT sounding was done in the Domes area where shifts factors in the range of 0.2 to 2.1 have been observed. This outcome indicate that about 57% of all the MT determinants were shifted down whereas 23% were shifted up with only 20% not showing any static shift (Figure 5). Therefore if interpretation was to be done without the static shift correction then we would have an error of 80% in resolving the resistivity structure for this field.

Figure 6 shows the spatial distribution of the shift multipliers in the Domes area. The map shows that there are some large areas where the MT apparent resistivity is consistently shifted downwards and other areas where it is shifted upwards. The orientation of shift spread could probably be used to infer certain geological structures since the shifts are as a result of near surface inhomogeneities.

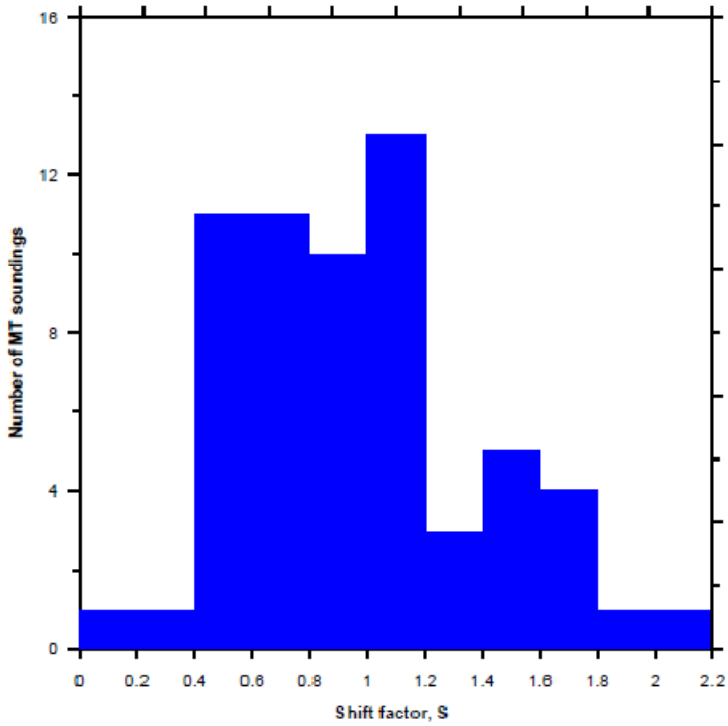

FIGURE 5: Histogram of static shift parameters for determinant apparent resistivity in the Domes area.

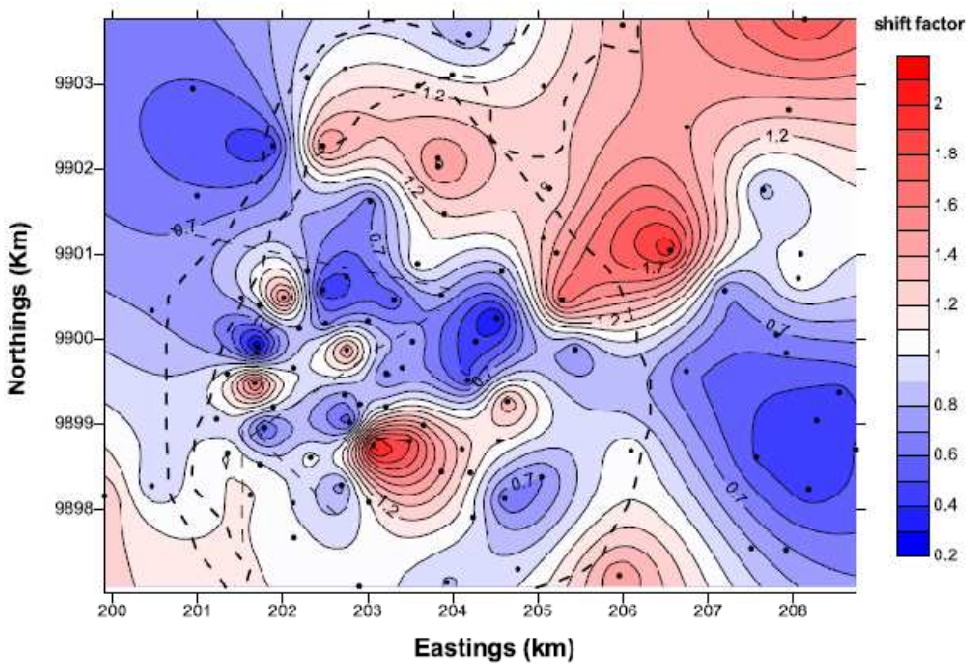

FIGURE 6: Spatial distribution of static shift parameters for determinant apparent resistivity in the Domes area.

JOINT 1-D INVERSION OF TEM AND MT SOUNDINGS

The one-dimensional joint inversion is performed simultaneously for both TEM and MT data by fitting one inversion on both data sets to obtain one model. This is achieved by use of an algorithm which determines the appropriate shift factor to be used to constrain the MT data to fit the TEM response. Both the MT and TEM data collected on approximately the same location are brought together in a joint inversion where TEM 1-D inversion obtained earlier was used for static shift correction on MT data.

The TEMTD program was used to invert MT apparent resistivity and phase derived from the rotationally invariant determinant of the MT tensor elements. In the joint inversion, one additional parameter was also inverted for, namely a static shift multiplier needed to fit both the TEM and MT data with the response of the same model, (Árnason, 2006).

An example of a 1-D joint inversion of MT and TEM data is shown on Figure 7, where the red diamonds are measured TEM apparent resistivities and blue squares are the MT apparent resistivities and phase. Solid lines show the response of the resistivity model to the right. The shift multiplier is shown in the upper right hand corner of the apparent resistivity panel.

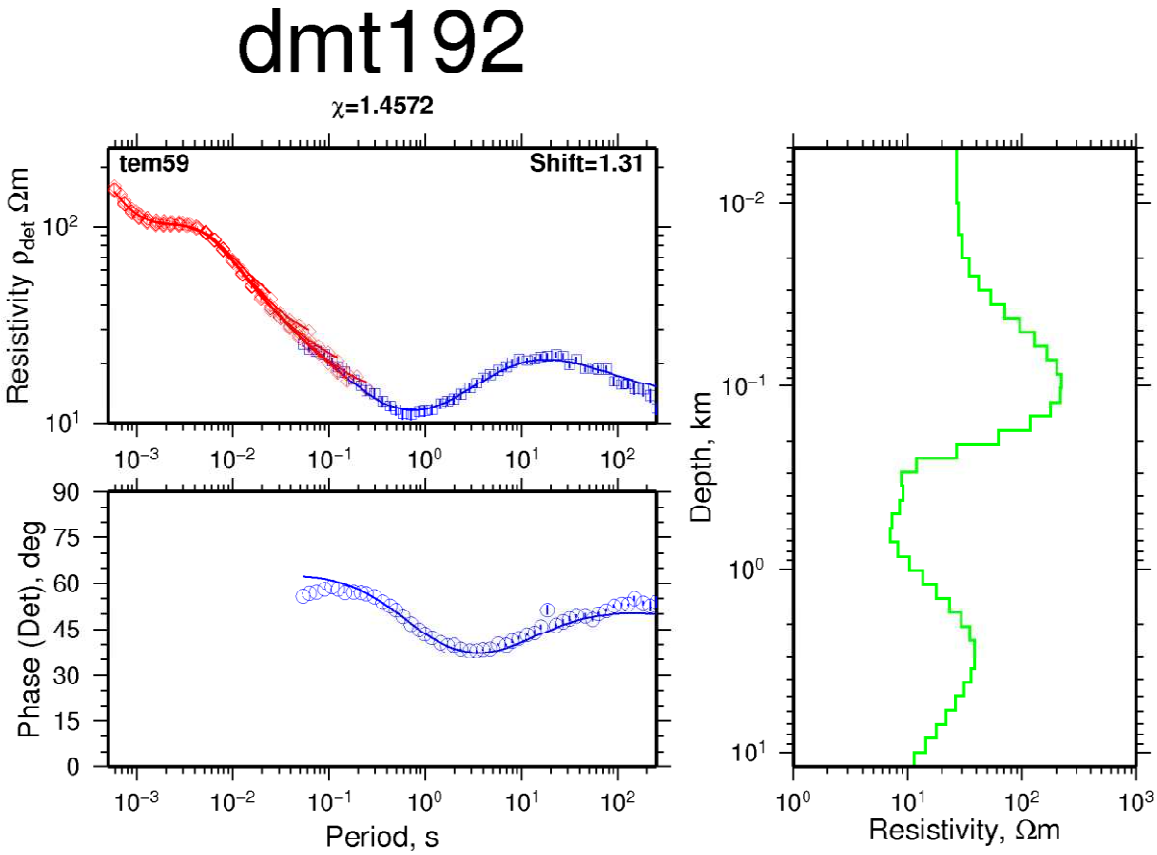

FIGURE 7: Typical result of a joint 1-D inversion of TEM and MT soundings

Cross-sections

Resistivity cross-sections are plotted from 1-D inversion results by a program called TEMCROSS (Eysteinsson, H., 1998). The program calculates the best line between selected stations on a profile, and plots resistivity isolines based on the 1-D model generated for each sounding. Several vertical cross-sections were made through the survey area and their locations are shown on Figure 8. A sub-program called MAXDEPTH has been used to clip soundings to match their longest periods so that they do not give misleading depths of penetration.

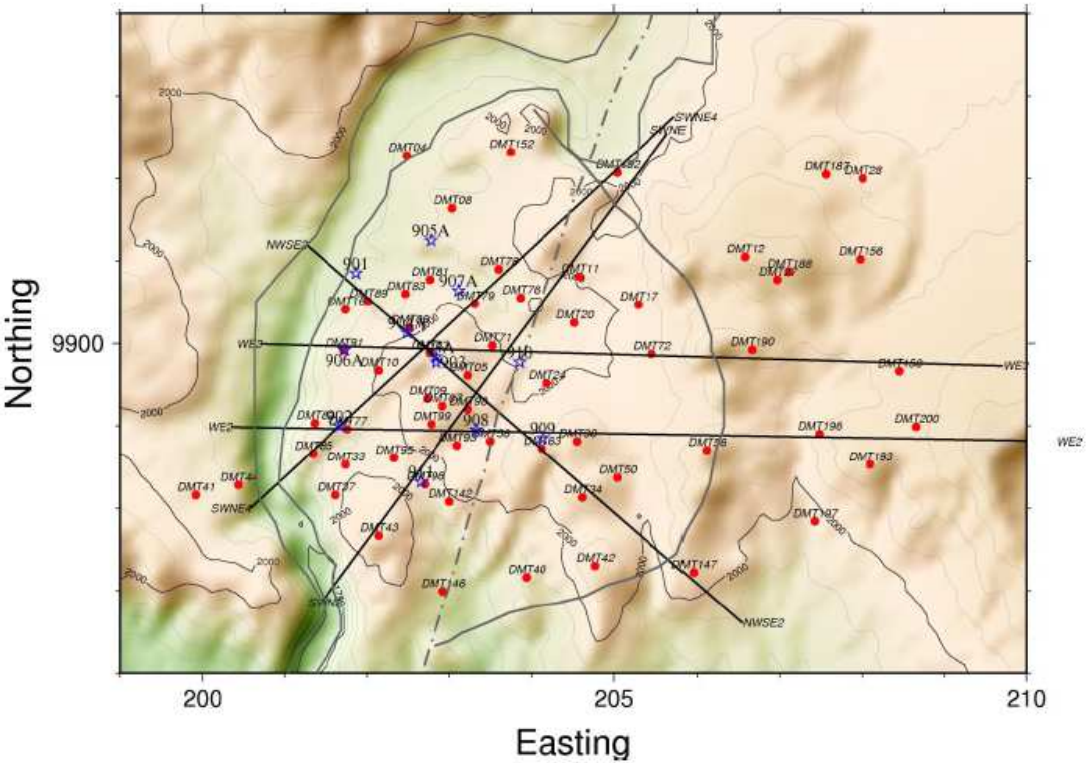

FIGURE 8: Domes profile map, red dot show location of MT stations and the blue stars are location of wells.

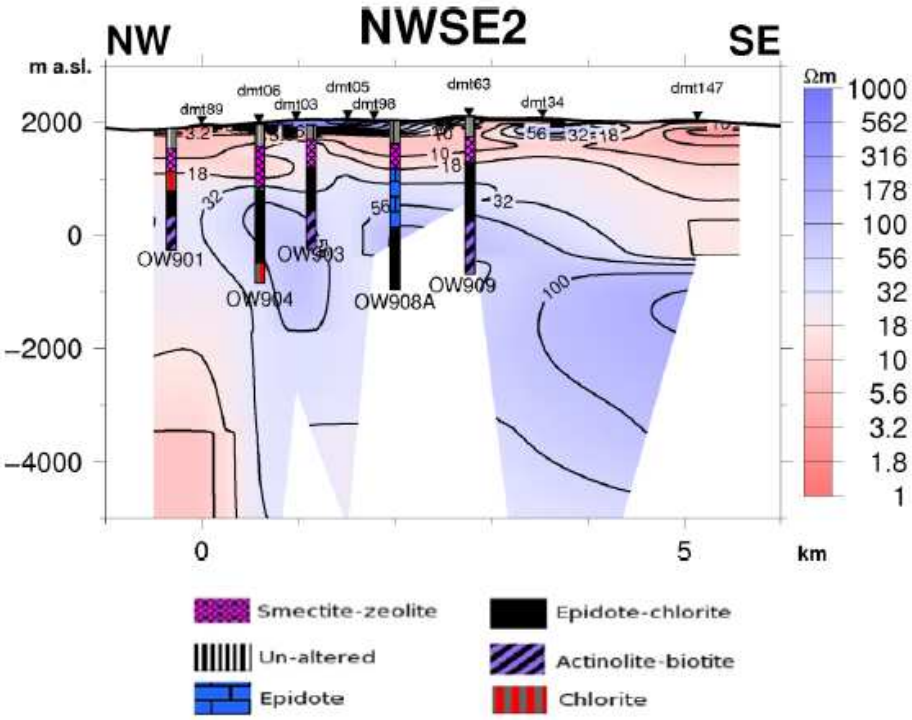

FIGURE 9: Resistivity Cross-section NWSE2 according to joint 1D inversion of TEM and determinant MT data.

Cross-section NWSE2 is shown on figure 9; cutting through wells OW901, OW904, OW903, OW908A and OW909. A high resistivity (> 100 Ωm) occurs close to the surface below some of the sites, overlaying a low resistivity extending down to 0.5 to 1 km. This high resistivity could be reflecting unaltered rocks near the surface. The low resistivity (< 10 Ωm) here correlates well with the alteration clay minerals as seen in the wells close to the profile. Below the low resistivity zone is a high resistivity, with resistivity close to 50Ω m and increases to above 100 Ωm and stays relatively high in the chlorite and chlorite-epidote zones as evidenced from the drill holes.

Cross-section SWNE is shown in Figure 10. It shows a high resistivity in the uppermost 300 metres. The uniformly low resistivity layer of about 10 Ωm correlates well with the smectite zone as seen in the alteration mineralogy of well OW910. Below the low resistivity layer is a high resistivity layer reaching 100Ω m at about 2 kms depth. To the south west of well OW909 a low lateral resistivity discontinuity can be seen protruding up to depth of 1000 m.bsl below soundings dmt93. This low resistivity anomaly could be reflecting a fault-like structure. Also below OW909 a low resistivity can be seen at about 6 km depth which could probably be related to the heat sources for this part of the field.

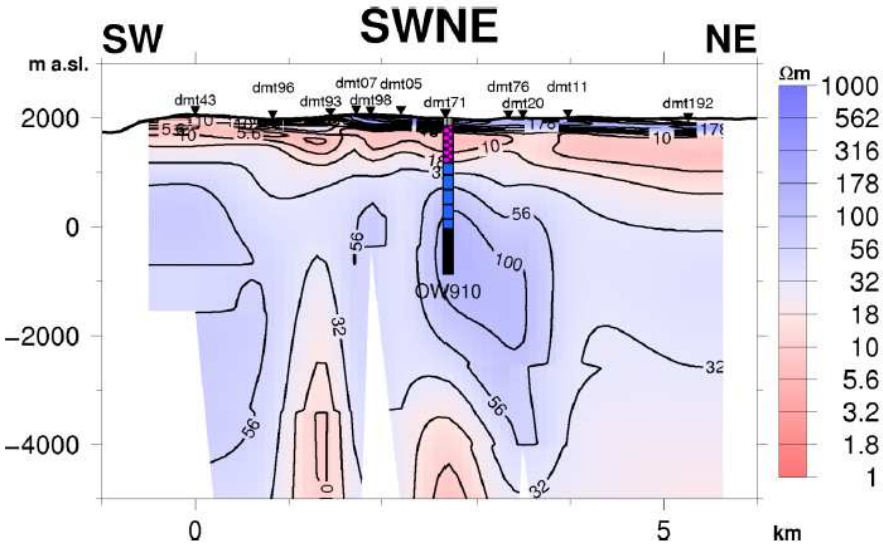

FIGURE 10: Resistivity Cross-section SWNE according to joint 1D inversion of TEM and determinant MT data

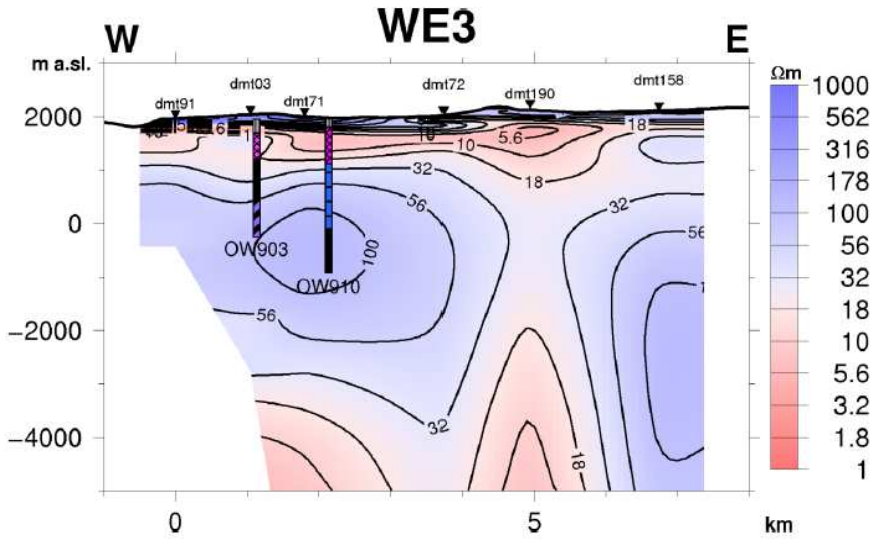

FIGURE 11: Resistivity Cross-section WE3 according to joint 1D inversion of TEM and determinant MT data

Cross-section WE3 as shown in Figure 11 presents a typical resistivity phenomenon expected in a high temperature geothermal system. Where at the top of a high enthalpy geothermal system a clay cap with expandable clay minerals occur. Its resistivity is generally lower than in the overlying rocks exposed to lower subsurface. At depths of 4000 m.bsl, a low resistivity is emerging below the wells, this is the same low resistivity seen from cross-section SWNE and could probably be the heat source for this field though it's not well resolved at depth. To the east of the well OW910 and below sounding dmt190 another low resistivity can be clearly seen at depths of 4 km below the surface. This low resistivity body could be a magmatic intrusion earlier inferred by seismic studies as an attenuating body below the ring structure (Simiyu, et.al., 1998).

Iso-resistivity maps

Iso resistivity maps are made by the TEMRESD program, which generates iso-resistivity maps at different elevations from the 1-D Occam models (Eysteinsson, H., 1998). In this report Iso-resistivity maps are presented from 1950 m a.s.l down to 5000 m.bsl, with the upper isomaps reflecting the TEM resistivity structure and the deeper ones representing the depth of penetration of the MT soundings.

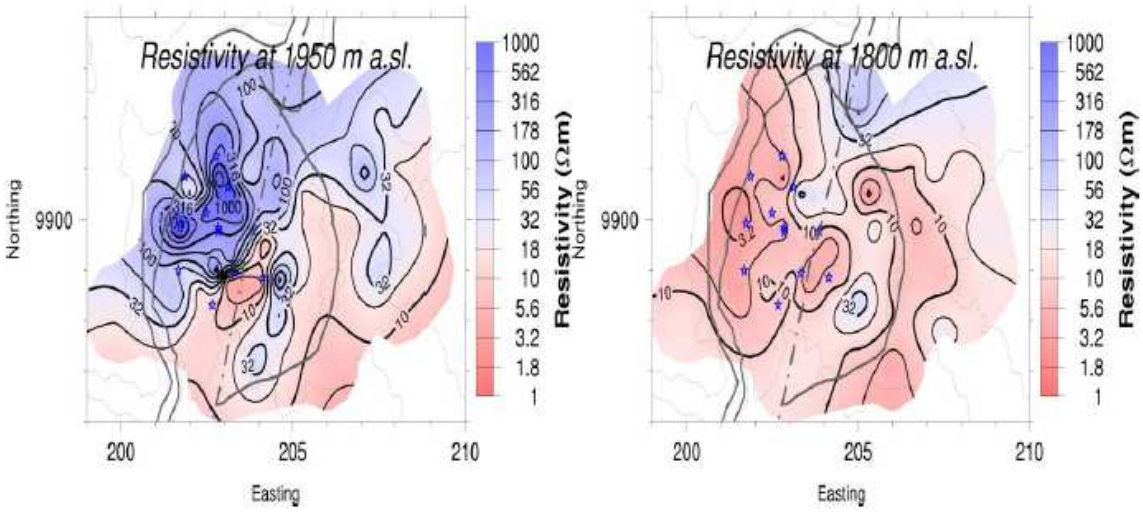

FIGURES 12 and 13: Resistivity in the Domes area at 1950 and 1800 m a.s.l respectively, the blue stars shows the drilled wells and the black dots are the MT stations.

Resistivity map at 1**950 m a.s.l,** is shown on figure 12. This elevation is generally between 50 to 250 m below the surface within the study area. The map shows high resistivity (100 to about 1000 Ωm) on the western and northern sectors of the study area, the high resistivity is probably due to un-altered formations that overlay the low resistivity region. Low resistivity anomalies are seen one along the ring of Domes from the south and the other in the middle of the study area in NNE-SSE direction superimposed between high resistivity zones.

Resistivity map at **1800 m a.s.l,** is shown on figure 13. This elevation is at about 400 m depth from surface. The low resistivity appears on the eastern and central part with a linear low resistivity (< 10 Ωm) anomaly aligning N-S in the eastern portion of the map. These low resistivity spread over the area are associated with the alteration low resistivity clay region overlaying the high resistivity core of the geothermal system. The high resistivity anomaly patches seen in the middle portion of the map are probably remnants of the un-altered zone at this depth.

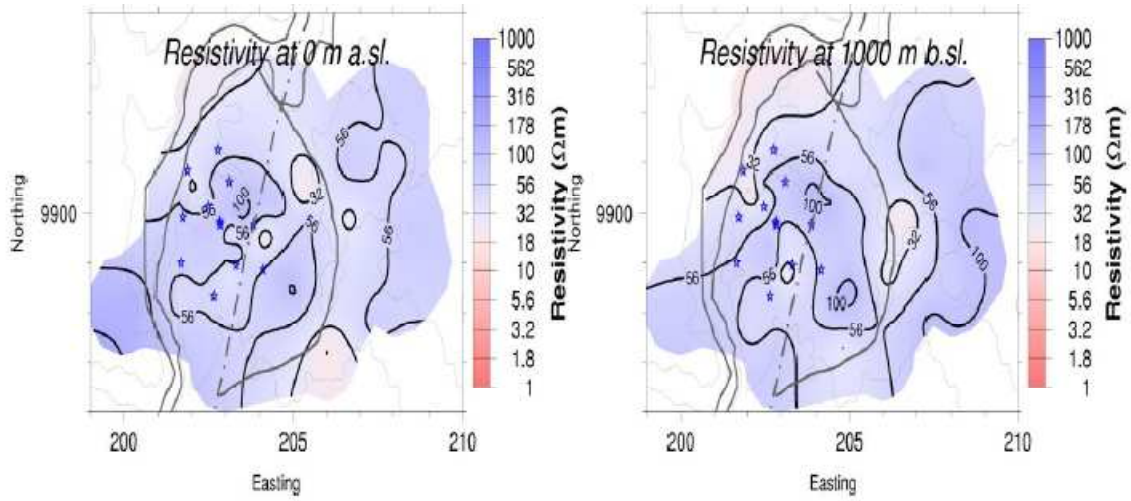

FIGURES 14 and 15: Resistivity in the Domes area at sea level and 1000 m.bsl respectively

Resistivity map at **sea level,** at this depth the high-temperature alteration (resistive zone) has fully set in with more dominance in the central Domes area where wells have been drilled and to the eastern sector of the survey area. This high resistivity perhaps reflects relatively high temperature zone where geothermal fluids may be prevalent. Superimposed between the high resistivity core is a lower resistivity aligned in NE-SW direction, this could probably be a zone of high permeability where hydrothermal alteration is not advanced, suggesting a possible up-flow zone beneath. A medium to low resistivity anomaly is starting to show up between Easting 205 and 207 aligned in North-South direction along the Domes ring structure.

Resistivity map at **1000 m.bsl,** is shown on figure 15. The resistivity is still high in most of the survey area. The low resistivity anomaly seen in the previous elevation is still present along the geological ring structure. A relatively low resistivity is also seen in the north-western sector of the study area, along the northern part of the Ol'Njorowa gorge.

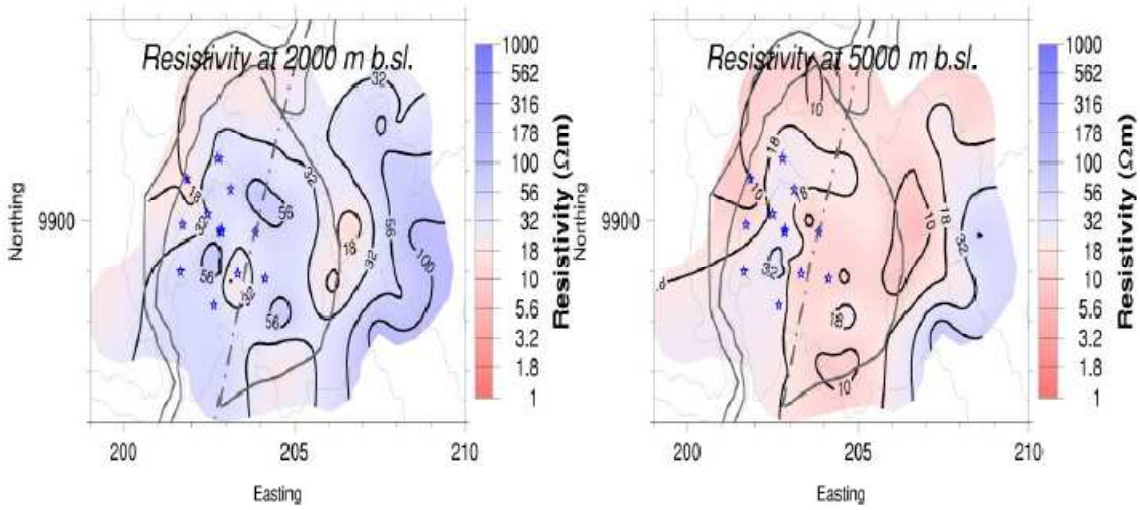

FIGURES 16 and 17: Resistivity in the Domes area at 2000 and 5000 m.bsl respectively

Resistivity map at 2**000 m.bsl,** is shown on figure 16. The high resistivity is still dominant in the central sector of Domes field and to the East. The low resistivity anomalies seen 1000 m.bsl are more expressed here, one to the west

of the field running in NNE-SSW along the Ol'Njorowa gorge and the other aligning in N-S direction along the Domes ring structure.

Resistivity map at 5**000 m.bsl,** At this depth the low resistivity is seen in almost the whole study area with the lowest resistivity (< 10 Ωm) aligning in NNE-SSW direction. This low resistivity could be reflecting the heat source. However it is not well observed in many MT sites due to lack of long enough period data.

Correlation of the resistivity structure with well temperature data and alteration

This section describes observed relationship between electrical resistivity, alteration mineralogy and reservoir temperatures. The data presented is temperature logs from wells

901 through 910 and lithology from wells 901, 902, 903, 904, 908A, 909 and 910. A resistivity cross-section passing through wells 901, 904, 903, 908A and 909 is shown on Figure 18 with alteration mineralogy and temperature from those wells.

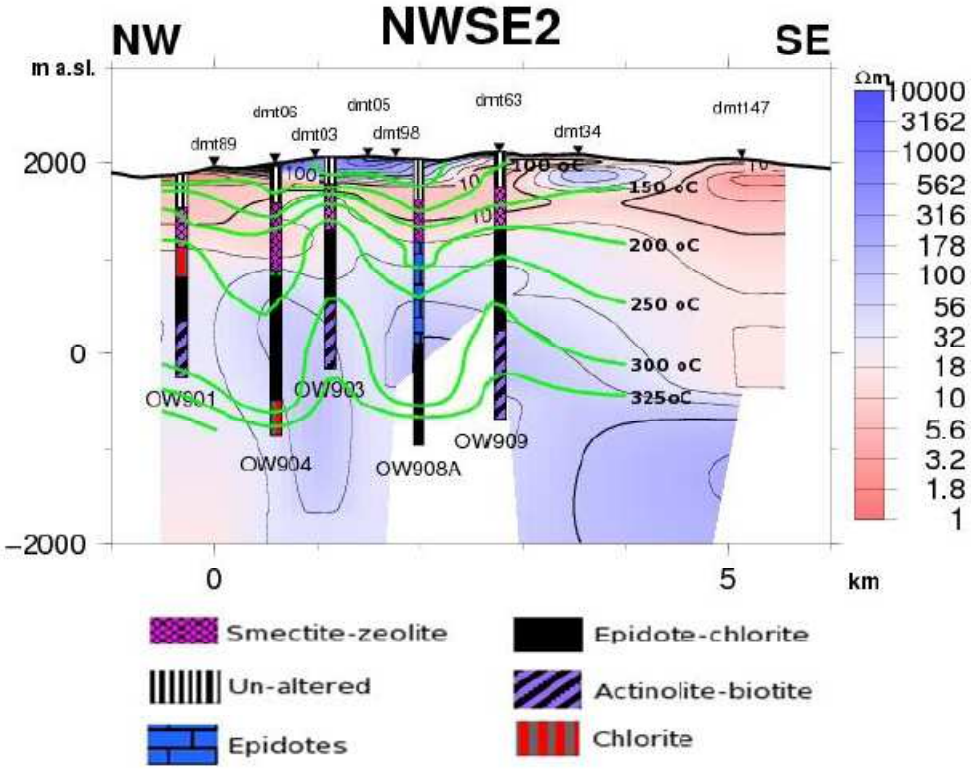

FIGURE 18: Resistivity cross-section, alteration zoning in wells and well log temperature.

A low resistivity zone of the order of 10 Ωm is observed between the surface high resistivity and the higher resistivity below at about 1-2 km depth. Five wells have been drilled along this profile showing the zones of dominant alteration minerals. Formation temperature isotherms, based on temperature logs from the wells are also projected into this profile. The figure shows very good correlation between the resistivity, temperature and alteration for the wells 904, 903, 908A, and 909. The resistivity is high in the cold, unaltered rocks outside the reservoir and decreases considerably as geothermal alteration, in the smectite-zeolite zone sets in. The bottom of this region correlates with temperature of about 100 °C and resistivity of about 10 Ωm. At around the 200°C isotherm the smectite-zeolite zone is slowly disappearing and is replaced by the mixed-layered clay zone, with resistivity in the range of 30 Ωm after which the resistivity increases considerably again and stays relatively high in the chlorite and chlorite-epidote zones at temperatures exceeding 250°C.

On the other hand well 901 show a very consistent correlation between the alteration mineral zones and resistivity. The low-resistivity cap (resistivity lower than 10 Ωm) coincides with the smectite-zeolite zone, which extends to about 800 m below the surface. In the chlorite-epidote zone also there is good correlation between resistivity and alteration though the resistivity is not as high as in the high resistivity core to the SE. The correlation with

temperature in the well (and partly also in well 904) is not as good, thus the alteration mineralogy is not in equilibrium with present temperature in the system which probably could be as result of cooling having occurred in that zone.

Studies have shown that the appearance of hydrothermal minerals can be used as indicators of past or present temperature and at the same time becomes an indicator of the impermeable behaviour of geological units because of the sealing of open fractured spaces. Therefore, hydrothermal mineralogy can be used as a support in defining the extent of the reservoir.

DISCUSSION

In the Olkaria-Domes study area, the results show fairly good correlation with the available geological information. The compiled resistivity model from the 1-D inversions reveals that Domes geothermal area is generally characterized by a high-resistivity surface layer (>100 Ωm), which is interpreted as fresh un-altered rocks possibly due to the thick pyroclastic cover from the adjacent Longonot volcano. Below that is a low resistivity layer of about 10 which correlates very well with the mineral alteration of smectite-zeolite zone of the geothermal reservoir. This zone also correlates very well with the temperature in the range of 100-200 ^{o}C.

Underlain below the low resistivity cap is the high resistivity core which is evident in all the cross-sections within the study area. The existence of a high resistivity core indicates reservoir temperatures exceeding 250°C, which has been confirmed by the drilled wells. Alteration mineralogy also is in agreement with resistivity structure confirmed by the presence of Epidote-chlorite zone. In the region around well OW901 the reservoir temperature is not in equilibrium with the alteration of the rocks.

The low resistivity seen at sea level in the middle zone of domes may be due to the low resistivity fluid in the pore spaces. Moreover, there is a consistency between the distribution of the relatively low resistivity zone at depth (>2 km bsl.) and the ring of domes alignment in the Domes sector. Therefore, this relatively low resistivity zone at depth possibly indicates a high temperature zone representing a major source of crustal fluids.

Comparison of well data with the resistivity structure shows a good correlation between the resistivity and alteration mineralogy. The low resistivity is dominated by conductive minerals in the smectite-zeolite zone at temperatures of 100-200 ^{o}C. In the temperature range of 200-240 °C zeolites disappear and smectite is gradually replaced by resistive chlorite. At temperatures exceeding 250 °C chlorite and epidote are the dominant minerals and the resistivity is probably dominated by the pore fluid conduction in the high-resistivity core.

CONCLUSIONS AND RECOMMENDATION

For geothermal exploration, MT method targets deep brine reservoirs and hot rocks that act as the heat source for a geothermal system under survey.

Results from the resistivity cross-sections derived from the 1-D joint MT and TEM inversions in Domes area reveals three layers namely: a very shallow high resistivity layer of > 100 Ωm, an intermediate low resistivity layer of > 10 Ωm underlying the upper high resistivity layer, and a deep high resistivity layer with values greater than 50 Ωm underlying

the low resistivity layer. MT resistivity cross-section also shows low resistivity at few kilometres depth below sea level that could be related to heat sources for this part of the field.

Based on these results it can be concluded that the Domes geothermal field host a much larger geothermal system than previously thought. The system appears to cover much larger area than the coverage of soundings. If there is equilibrium between the hydrothermal alteration of the rock and the present temperature in the reservoir, then the temperature in the high resistivity core is expected to be more than 250 °C as evidenced from the well data.

It is recommended that more long period MT and TEM data at the same location be acquired in order to define the extent of this field

REFERENCES

Árnason, K., 1989: Central-loop transient electromagnetic sounding over a horizontally layered earth. Orkustofnun, Reykjavík, report OS-89032/JHD-06, 129 pp.

Árnason, K., 2006. TEMTD, a programme for 1-D inversion of central-loop TEM and MT data. Short manual. Iceland GeoSurvey - ISOR, internal report, 17 pp.

Árnason, K., 2008: The Magneto-telluric static shift problem. Iceland GeoSurvey - ISOR, report, ISOR-08088, 17 pp.

Árnason, K., Karlsdóttir, R., Eysteinsson, H., Flóvenz, Ó.G., and Gudlaugsson, S.Th., 2000: The resistivity structure of high-temperature geothermal systems in Iceland. Proceedings of the World Geothermal Congress 2000, Kyushu-Tohoku, Japan, 923-928.

Eysteinsson, H., 1998: TEMMAP and TEMCROSS plotting programs. Iceland GeoSurvey - ÍSOR, Unpublished programs and manuals.

Jones, A.G., 1988: Static shift of magnetotelluric data and its removal in a sedimentary basin environment. Geophysics, 53-7, 967-978.

Lagat, J.K., 2004: Geology, hydrothermal alteration and fluid inclusion studies of the Olkaria Domes geothermal field, Kenya. University of Iceland, MSc thesis, UNU-GTP, Iceland, report 2, 71 pp.

Mungania, J., 1992: Geology of the Olkaria geothermal complex. Kenya Power Company Ltd., internal report, 38 pp.

Mungania J., 1999: Summary of the updates of the geology of Olkaria Domes geothermal field. KenGen, internal report.

Naylor, W.I., 1972: Geology of the Eburru and Olkaria prospects. U.N. Geothermal Exploration Project, report.

Simiyu, S.M., Oduong, E.O., and Mboya, T.K., 1998: Shear wave attenuation beneath the Olkaria volcanic field. KenGen internal, report.

Sternberg, B.K., Washburne, J.C., and Pellerin, L., 1988: Correction for the static shift in magnetotellurics using transient electromagnetic soundings. Geophysics, 53, 1459-1468.

THE PRELIMINARY RESULTS OF THE GEOPHYSICAL INVESTIGATION ON THE GHOUBBET PROSPECT.

Hassan Mohamed, Nasroudin Ahmed
Centre d'Etudes et de Recherches de Djibouti (CERD)

ABSTRACT

A combined Magneto telluric (MT) and Time Domain Electromagnetic (TDEM) investigations have been carried out in the Ghoubbet prospect in the north of the republic of Djibouti to determine the distribution of the electrical resistivity of the subsurface. The objective of this geophysical study was to delineate the boundaries of the geothermal reservoir. On this site, we carried out 21 MT soundings and 26 TDEM soundings around a horst delimited by normal faults where the principal thermal manifestations are localised. The data from these soundings are interpreted with a one-dimensional (1D) approach to determine the conceptual model of the geothermal system.

Keyword: Magneto telluric, Time Domain Electromagnetic, electrical resistivity, geothermal reservoir

INTRODUCTION

There exist several techniques for measuring the resistivity of subsurface rocks. They can be divided into galvanic or direct-current (DC) methods and electromagnetic (EM) methods. Some decades ago, the DC methods (mainly Shlumberger soundings) were widely used. Nowadays, the electromagnetic methods are largely used, mainly the Time Domain Electromagnetic method and the Magnetotelluric method.

The MT method is based on measuring currents induced in the ground by time variations in the Earths magnetic field. The fundamental theory was first developed by Cagniard (1953) and Tikhonov (1986).The time varying magnetic field and the electric field generated in the surface are measured simultaneously. The electric field is measured in two perpendicular horizontal directions and the magnetic field in the same horizontal and the vertical direction. The measured time series are Fourier transformed into harmonic components with different periods. The harmonic components of the electric field are related to the magnetic field by the so-called impedance tensor, which depends on the subsurface resistivity. For short periods the tensor is mainly dependent on shallow resistivity structure, but for long periods it is mainly dependent on deep resistivity structure. The MT method has the greatest depth of exploration of the available EM methods (some tens or hundreds of kilometres) and is practically the only method for studying deep resistivity structures particularly in volcanic medium.

TDEM Method as for it admits a depth of investigation from 200 to 300 m according to the size of the transmitting loop and provides a geoelectrical model with a good resolution. The fundamental principles of the Time domain electromagnetic method were developed by Kaufman (1983) and Decloîtres (1998). This technique also makes it possible to correct the static shift which affects the apparent resistivity of the MT method in the near surface. The principle of this method consists to injecting an electric current in the ground by a loop of wire (transmitting loop). This electric current will induce a magnetic field in the ground. Then, this current is abruptly off and there is creation an electromotive force (f.e.m) which will generate electric currents called eddy currents in the ground. These currents induce in the ground a second magnetic field which will be to measure by a one second loop wire (receiver loop) posed on the ground.

GEOLOGICAL SETTING

The republic of Djibouti is located in the Horn of Africa where three major extensional structures, the Gulf of Aden, the East African Rift and the Red Sea, meet and form the Afar Depression. Most of Djibouti is covered by volcanic rocks, mainly basaltic. There exist most geothermal sites in Republic of Djibouti as shown in the figure 1. The Ghoubbet prospect was selected for its proximity with the Asal prospect where a geothermal reservoir was identified and existence a possible recharge of the system by the high plateaus located in north contrary with Asal. The Ghoubbet prospect is located in the nord-east of the north-westward extension of the Gulf of Aden-Tadjura, from the Gulf of Ghoubbet in the sud-east and to Lake Asal in the nord-west which is 155 m below sea level. This area is presently the most active part of the Afar Depression. The Ghoubbet field is approximately 4-5 kilometers broad and the most currently active part is contitued by a horst bounded by the impressive normal faults. The thermal manifestations are widespread which form a NE and SW tendency. These thermal manifestations are primarily fumeroles with a hot spring.

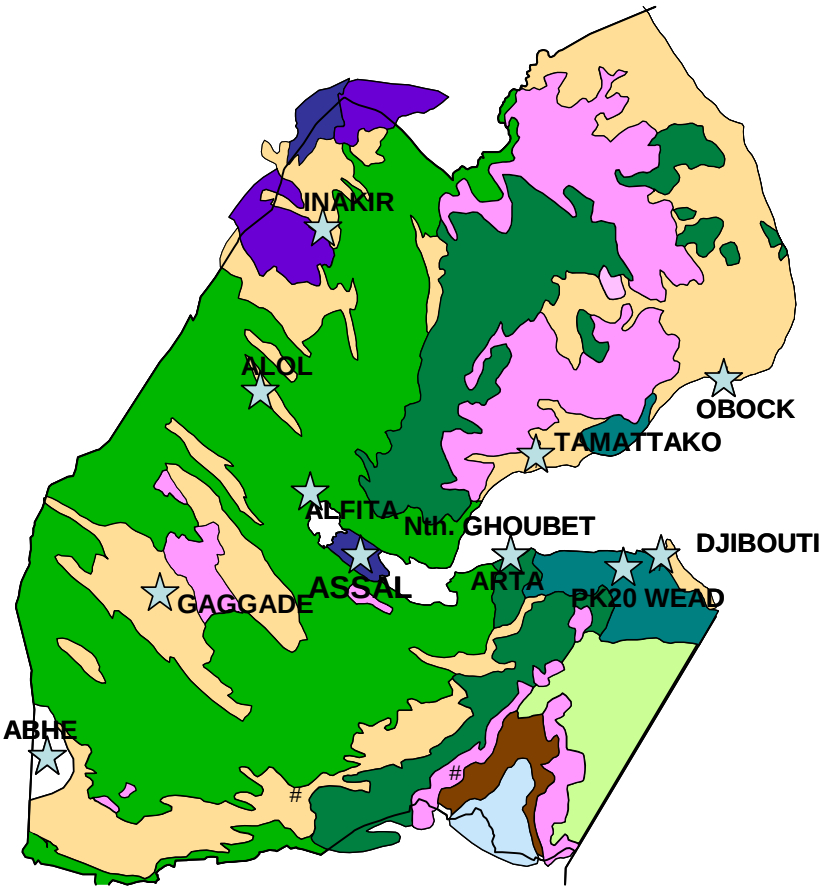

Figure 1: Geothermal sites in Republic of Djibouti.

FIELD WORK

During this geophysical survey on the Ghoubbet prospect, 21 MT soundings and 26 TDEM soundings have been carried out as shown in the figure 2.In this field work, the system used to record the MT data was Metronix, MT system, with ADU-06 data logger, MFS-07e induction coil magnetometer and EFP-06 electrodes. In order to record the desired frequency range, the time series at each sounding was recorded in three different bands representing different frequency intervals. These three different bands are described in the table 1. For the Sampling frequency 128 Hz, we have applied a digital filter to obtain the sampling frequency 32 Hz.

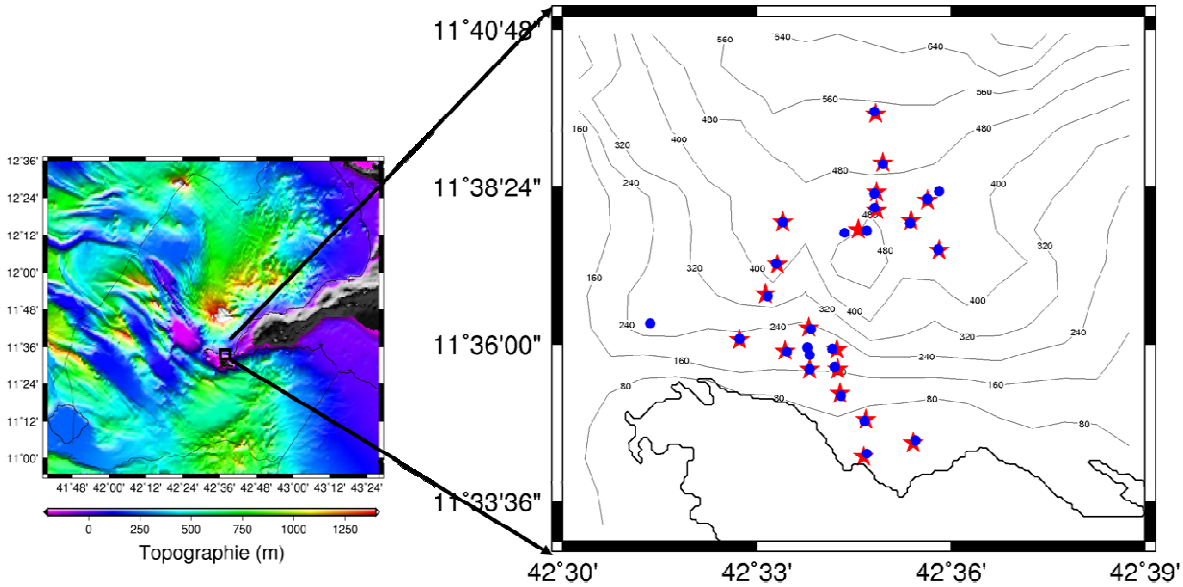

Figure 2: Location map of the study area (topography map). Stars: MT soundings. Cercles: TDEM soundings.

Band name	Sampling frequency	frequency	Recorded length
HF	2048 Hz	200000-500 Hz	2 m
LF1	256 Hz	1000-10 Hz	40 m
LF1	128 Hz	1000-10 Hz	20 h

On the field, the data measured were the time data. Then, these time series were transformed to the frequency domain impedance tensor using magneto telluric programme MAPROS (Friedrich 2007). The figure 3 shows an example of the transfert function for a MT sounding realised on the Ghoubbet prospect. On this figure are represented the apparent resistivities (in top) and the phase (in bottom) in directions XY and YX.

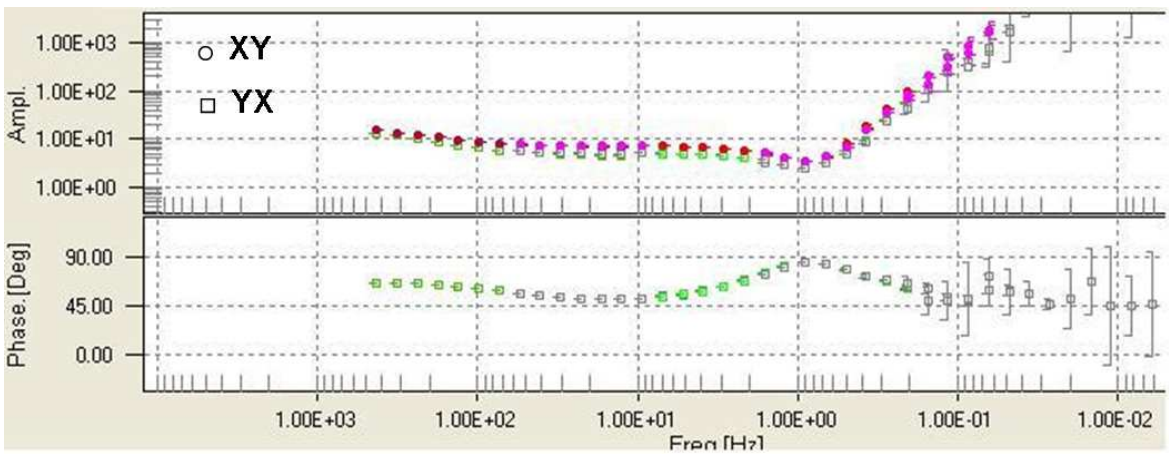

Figure 3: Apparent resistivity and phase responses for a MT sounding carried out on the Ghoubbet prospect.

For TDEM method, the system used during this study was terraTEM system. This instrument is a new transient electromagnetic survey system constructed by Australian firm. With this equipment, there exist a several configurations to measure the distribution of the electrical resistivity of the subsurface. In our case, we have used a coincident loop configuration with a size loop 100 x 100 meters.

CONCLUSION

The geothermal reservoir on the Ghoubbet prospect has been studied on the basis of the electromagnetic data (MT and TDEM). These data are in the course of treatment in order to determine a conceptual model of deep structure.

REFERENCES

Cagniard, L. 1953. Basic theory of the magnetotelluric method of geophysical prospecting. Geophysics, 18, 605-645.

Descloîtres, M. 1998. Les sondages électromagnétiques en domaine temporal (TDEM): Application à la prospection d'aquifères sur les volcans de Fogo (Cap-vert) et du piton de la fournaise (La Réunion), Thèse, Université Pierre-et-Marie-Curie, Paris, 228p.

Friedrichs, B. 2007. MAPROS, Software Manual.

Kaufman, A.A and Keller G.V. 1983. Frequency and Transient Sounding, Elsevier, Amsterdam, 686p.

Tikhonov, A.N., 1986. On determining electrical characteristics of the deep layers of the Earth's crust. Dokl. Akad. Nauk. USSR, 73, 295-297.

EXPLORATION OF GEOTHERMAL RESOURCES USING MAGNETOTELLURICS CASE STUDY MENENGAI PROSPECT IN KENYA

Raymond Mwakirani
Geothermal Development Company Ltd,
P. O. Box 1770 Nakuru, 20100
E-mail: rmwakirani@gdc.co.ke

ABSTRACT

Geothermal energy sources are formed by heat stored in rocks at depth. In regions with high heat flow, like at volcanically active plate margins, high total thermodynamic energy is accumulated in the so called high enthalpy resources. Unaltered volcanic rocks generally have high resistivity which can be changed by hydrothermal activity. Hydrothermal fluids tend to reduce the resistivity of rocks by altering the rocks or by increasing salinity. Initial regional exploration for geothermal resources in Kenya indicated that the Quaternary volcanic complexes of the Kenya rift valley provided the most promising prospects for geothermal exploration. Consequently, detailed exploration for geothermal power has been concentrated around volcanic centres within the rift valley. Studies show that these centres have positive indications of geothermal resource that can be commercially exploited. The geothermal potential of the area is associated with these magma chambers that constitute the heat sources. Magnetotellurics (MT) data show that the heat sources are shallow beneath the volcanic centres. This abstract concentrates on the geophysical work that has been carried out in the Menengai Geothermal prospect using Magnetotellurics (MT). Data collected using magnetotellurics is used to determine the resistivity distribution within the earth to depths of many kilometers which is then interpreted in terms of lithology. The contrast in resistivities provides an excellent tool for identifying geothermal targets. So magnetotellurics is the standard method for mapping the alteration cap and via 3D inversion the underlying reservoir.

INTRODUCTION

Initial regional exploration for geothermal resources in Kenya indicated that the Quaternary volcanic complexes of the Kenya rift valley provided the most promising prospects for geothermal exploration. Consequently, detailed exploration for geothermal power has been concentrated around volcanic centres within the rift valley. Studies show that these centres have positive indications of geothermal resource that can be commercially exploited. The geothermal potential of the area is associated with these magma chambers that constitute the heat sources. Magnetotelluric (MT), seismic and magnetic data show that the heat sources are shallow beneath the volcanic centres. This abstract concentrates on the geophysical work that has been carried out in the Menengai Geothermal prospect. Static shifts of the resistivity curves have been removed by means of the MT response derived from TEM measurements at the same locations.

The Magnetotellurics (MT) technique, a natural electromagnetic method, has proved effective in mapping the characteristics of geothermal fields due to its lateral resolution and also greater depth of investigation. Magnetotellurics survey is more appropriate for difficult topography due to its simple logistics and low cost compared to seismic survey. MT provides useful information about the lateral and vertical resistivity variations in the earth's subsurface from surface measurement of two horizontal electric field and three magnetic field variations over a typical 10^{-3}-10^{3} Hz frequency range. MT results along a profile can be used to evaluate the resource potential of the area. Data collected using magnetotellurics is used to determine the resistivity distribution within the earth to depths of many kilometers which is then interpreted in terms of lithology. The contrast in resistivities provides an excellent tool for identifying geothermal targets. So magnetotellurics is the standard method for mapping the alteration cap and via 3D inversion the underlying geothermal reservoir. This resistivity survey identified three zones, separated by discontinuities, which are suitable for geothermal production.

The role of electrical resistivity

Unaltered volcanic rocks generally have high resistivities which can be changed by hydrothermal activity. Hydrothermal fluids tend to reduce the resistivity of rocks:-

- by altering the rocks,
- by increase in salinity or
- due to high temperature.

In high enthalpy reservoirs, i.e. fluid temperatures above 200 °C, hydrothermal alteration plays the predominant role (Figure 1.1). In a volcanic terrain the acid-sulphate waters lead to different alteration products depending on the temperature and thus on the distance from the heat source. With basalts as country rock smectite becomes the dominant alteration product in the temperature range from 100 °C to 180 °C. At higher temperatures mixed layer clays and chlorite become dominant

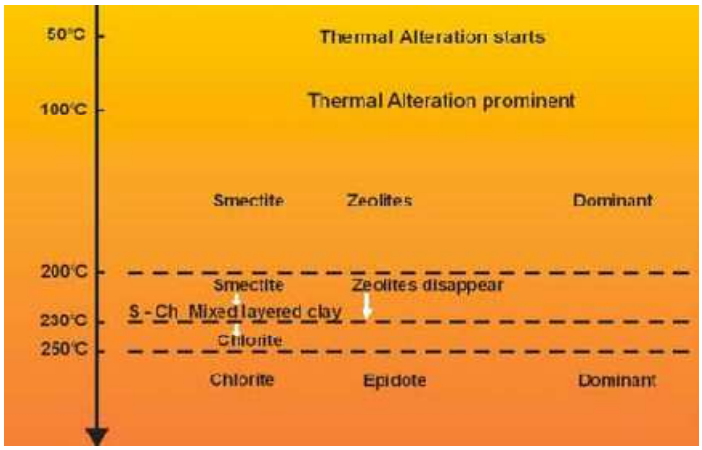

Figure 1: Alteration mineralogy with increasing temperature in basaltic country rock. In the temperature range 100°C to 180°C smectite becomes the dominant alteration product and generally forms a smectite/bentonite clay cap (source: Geological Survey of Iceland ISOR).

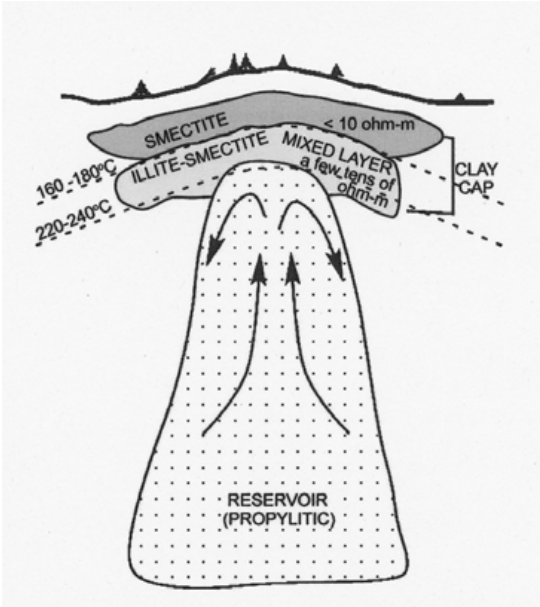

Figure 2: Schema of a generalised geothermal system. The smectite cap formed exhibits resistivities in the range of 2 Ohm*m, the mixed layer around 10 Ohm*m.

METHODOLOGY

MT Sounding

MT techniques measure over a frequency range. The lower the frequency, the greater the depth of investigation possible at a given site. MT techniques acquire data in frequencies ranging from about 400-0.0000129 Hz (over a

period of about 21.5 hrs), and are suitable for deeper investigations. The survey was planned so that work crews could set up one or more sites each day (depending on the nature of the terrain), allowing the equipment to acquire data for a period of time and then retrieving the equipment to re-deploy it at another site. In this survey, the equipment was left to acquire data overnight and retrieval usually happened the next morning.

Although an MT can be used alone, best results are achieved when a remote or far remote site is available for noise-reduction techniques. Apart from the 50 Hz or 60 Hz grid frequency, electrical noise from human activities tends to vary considerably over distance. The natural magnetic signal, though, tends to be the same over large distances; the lower the frequency, the less variation. The MT equipment system employed took advantage of these characteristics by collecting data simultaneously at the survey ("local") sites and at one reference ("remote") site.

MT equipment and sensors must be calibrated before acquiring data. Calibration took place at the beginning of the survey, and was repeated in the course of the survey when equipment problems arose (e.g., damaged cables). The field layout comprised of two orthogonal electric dipoles to measure the two horizontal components, and two magnetic sensors parallel to the electric dipoles to measure the corresponding magnetic components. A third sensor measured the vertical magnetic component. Thus, at each station, five parameters were measured simultaneously as a function of frequency. By measuring the changes in the magnetic field (H) and electric (E) field over range frequencies, an apparent resistivity sounding curve can be produced, analogous to that produced for electrical resistivity sounding but measured as a function of frequency rather than inter-electrode separation. The data are displayed on log-log plots as apparent resistivity versus either frequency (f) or period ($1/2\pi f$)

DATA PROCESSING AND ANALYSIS

Resistivity

Both MT and TEM data can be analysed in different ways according to the manner in which they have been acquired. Measured parameters may be plotted as profiles or as gridded and contoured maps on which anomalous zones can be identified. These approaches tend to be qualitative and of first order interpretations. The data was processed, inverted and produced in apparent resistivity plots in form of contours maps at various elevations. The aim was to locate a possible sub-surface resistivity anomaly on the basis of relevant parameters such as apparent resistivity values, shape and size.

Time series processing included visual inspection of the recorded data and excluding disturbances and heavily noise affected parts of the time series. Although very time consuming this approach proved to be the best means to extract maximum information from the noise contaminated time series. These preconditioned time series were then transformed into the frequency domain by a FFT using adapted window lengths. With a coherency based algorithm the Fourier spectra were thenaveraged and the impedancetensor estimated. The impedance tensor has been rotated mathematically by a constant angle derived from the swift angle at low frequencies. This results in a data set with consistent orientation with one axis approximately along the valley which is taken as direction for the E-field. Static shifts of the resistivity curves have been removed by means of the MT response derived from TEM measurements at the same locations.

Figure 1.3 shows the map of the areal distribution of the resistivity soundings from the greater Menengai prospect area. Since resistivity of the subsurface varies with depth as well as horizontally, several iso-resistivity maps were constructed at elevations from 1800 masl to 5000mbslas shown in Figures 1.4,1.5,1.6,1.7,1.8,1.9, and 2.0 respectively.

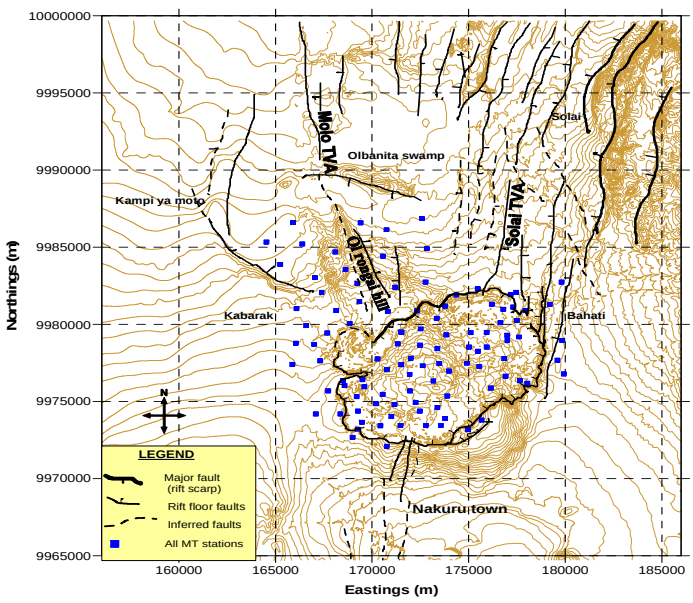

Figure 3: The areal distribution of MT resistivity soundings from the Menengai prospect area

Resistivity at 1800 masl

At 1800 masl(Figure 1.4), most of the area is covered with moderately high resistivity values particularly the Menengai caldera and to the North-west towards the Ol' Rongai area, except for localized low resistivity appearing in the north west towards the direction of KampiYa Moto and another in the south-east of the caldera. Relatively lower resistivity discontinuity can also be seen in the central part of the caldera. The high resistivity is probably as a result of un-altered rocks near the surface.

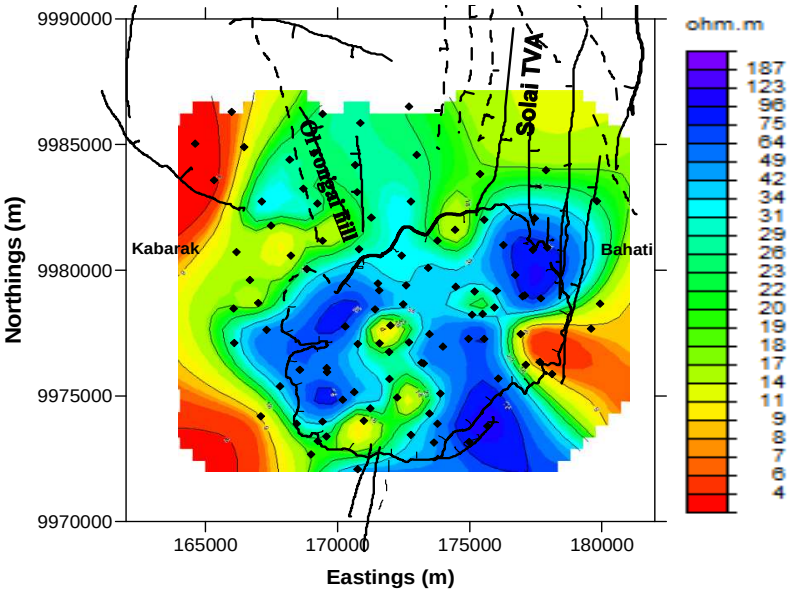

Figure 4: Resistivity distribution at 1800 masl. within Menengai prospect

Resistivity at 1400 masl

Deeper down, at 1400 masl (Figure 1.5), the high resistivity is still dominant within the caldera and to the Ol' Rongai hill except the low resistivity discontinuity that appears in the centre of the caldera and localized low resistivity anomalies in the north-west and south-east of the caldera as seen in the layer 400m above.

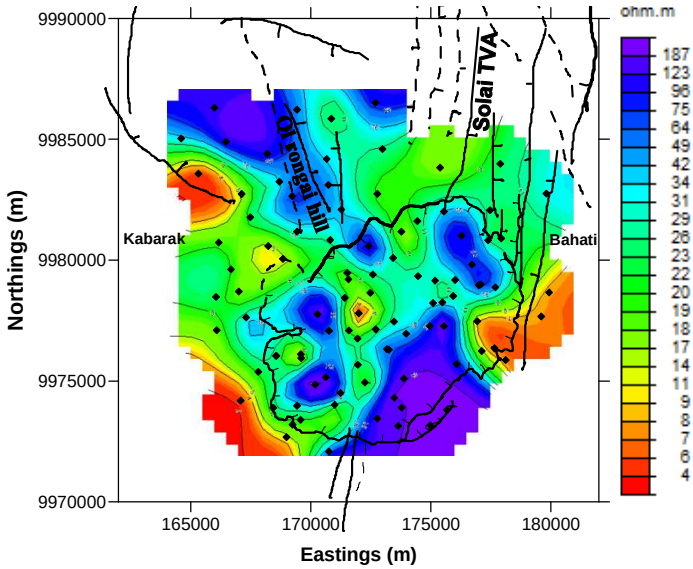

Figure 5: Resistivity distribution at 1400 masl. around Menengai

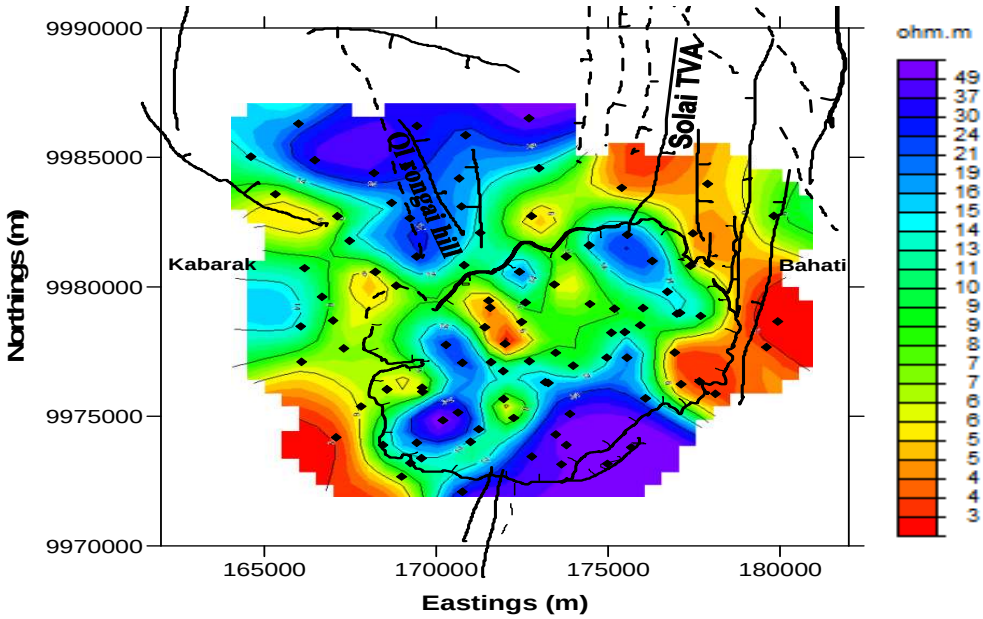

Figure 6: Resistivity distribution at 1000 masl within Menengai prospect

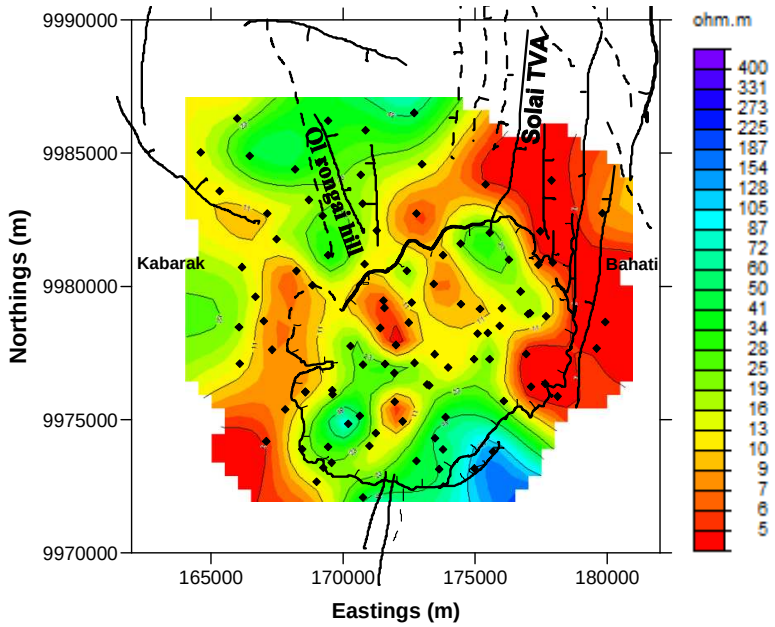

Figure 7: Resistivity distribution at 800 masl. in the Menengai prospect

Resistivity at 1000 masl and 800 masl

At 1000 masl (Figure 1.6) three distinct low resistivity (≤ 10 Ωm) areas are clearly seen; one large region to the east of the caldera towards Bahati area, one to the west of the caldera and a small low resistivity anomaly in the central

portion of the caldera. High resistivity values, just as in the previous higher elevations, are still present in the Ol' Rongai area and the other to the southern rim of the caldera.

At 800 masl (Figure 1.7), low resistivity is smeared out in almost the entire plot with more prominence in the eastern, western and central part of the caldera. These low resistivity zones could probably be as a result of low temperature hydrothermal clay minerals like smectite and zeolite. On the other hand, the south-east of the caldera and north-west area around Ol' Rongai area is characterized by high resistivities.

Resistivity at Sea level

At Sea-level (Figure 1.8), the general resistivity structure of the prospect indicate a moderate high resistivity (about 49 ohm-m) particularly within the caldera and in the north west in tha Ol' Rongai area. This high resistivity portion could probably be associated with high temperatures alteration minerals such as chlorites and epidotes. Some higher resistivity zones can be seen appearing from the South and of the caldera and another in the North-East portion of the caldera aligning in the NW-SE direction. Low resistivity seen in the previous levels towards Bahati and in the north east along the Solai TVA is still present here.

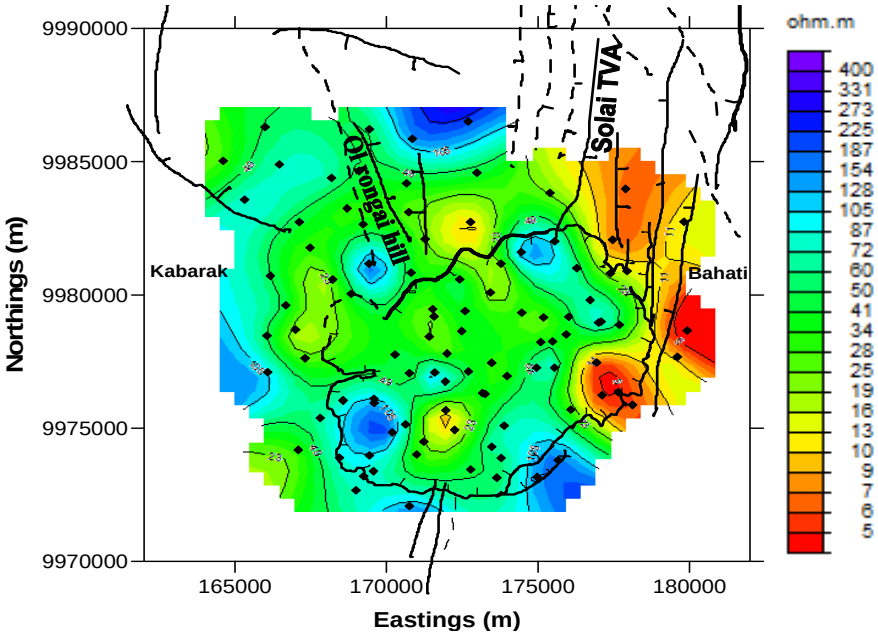

Figure 8: Resistivity distribution at sea level within the Menengai prospect

Resistivity at 3000 mbsl and 5000 mbsl

Figures 1.9 and 2.0 shows resistivity at 3000 mbsl and 5000 mbsl respectively. These figures reveal low resistivity bodies at depth that could be related to magmatic heat sources. Three distinct low resistivity anomalies can be seen in the prospect area, one in the central part of the caldera, the other in the Ol' Rongai area and the third towards Kabarak.

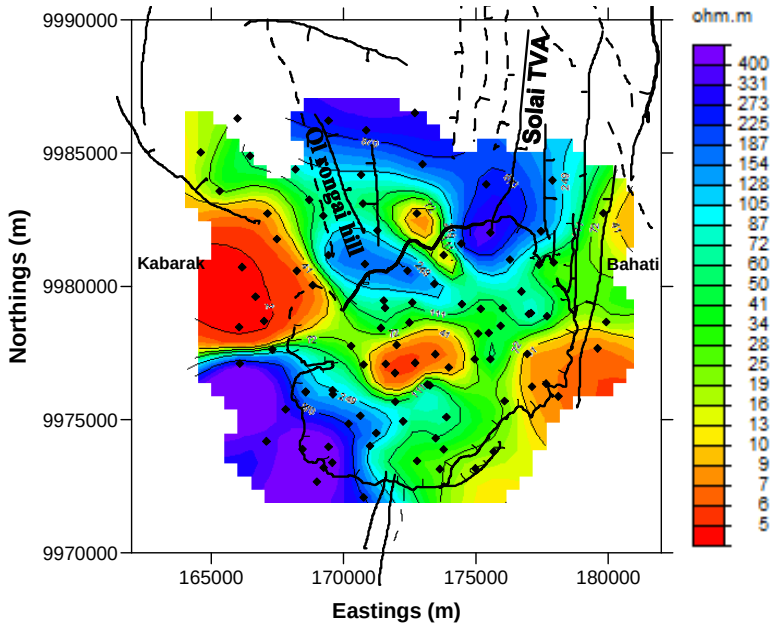

Figure 9: Resistivity distribution at 3000 mbsl within the Menengai prospect

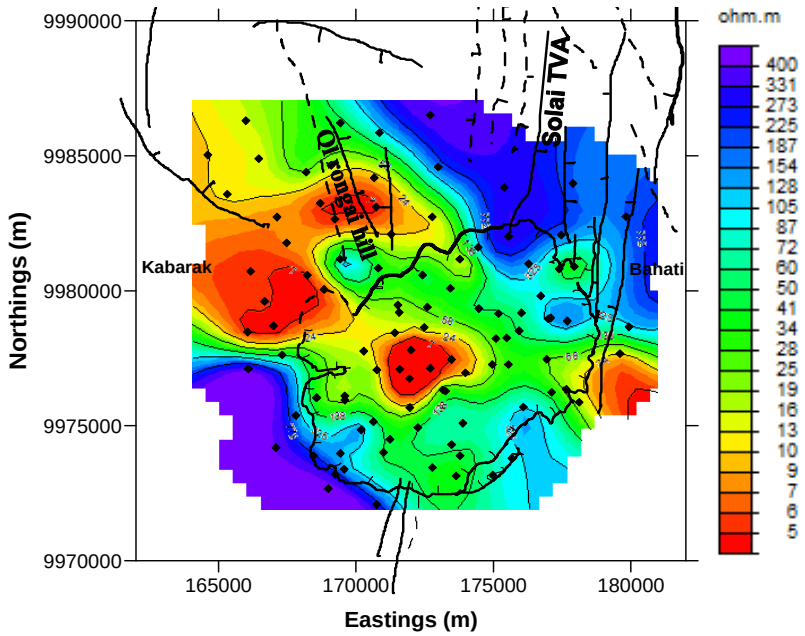

Figure 10: Resistivity distribution at 5000 mbsl within Menengai Prospect

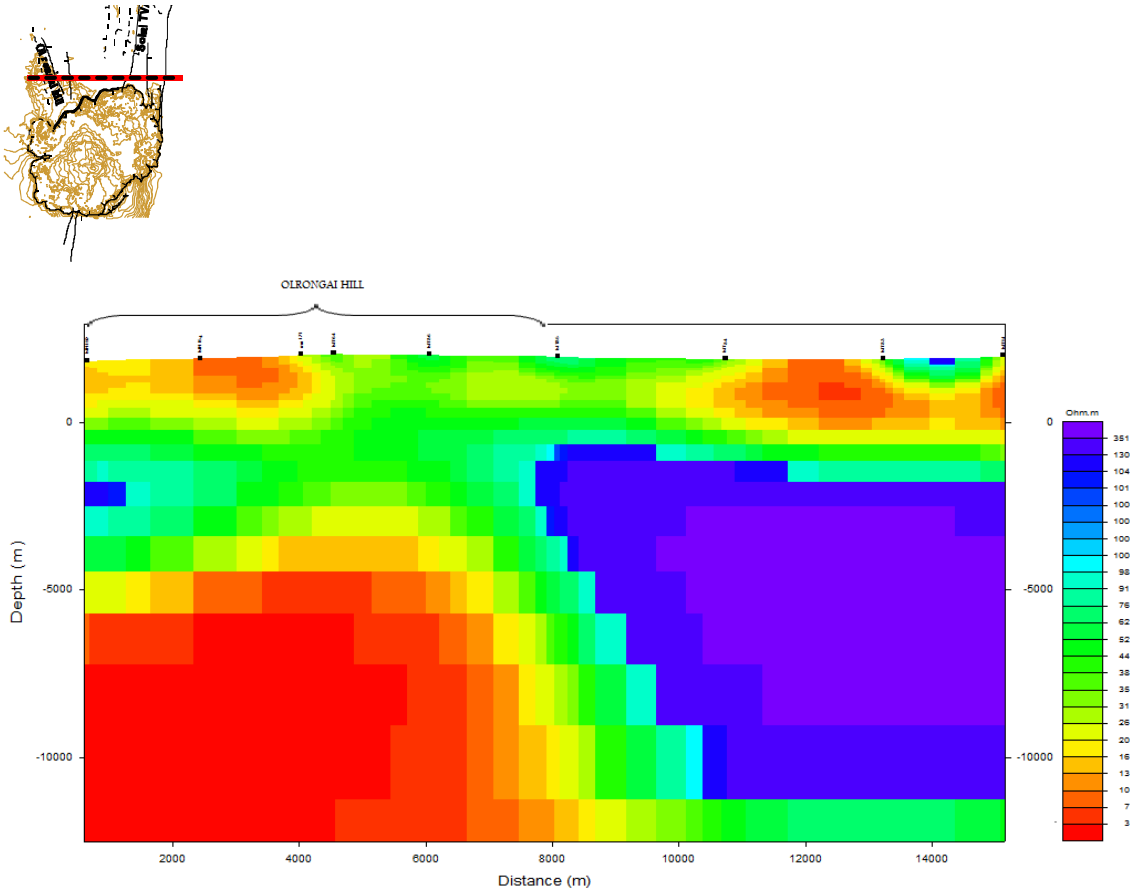

Figure 11: 2D East-west MT resistivity cross-section

Resistivity cross-section through Ol' Rongai area

Figure 2.1is the cross section through the Ol' Rongai area north of the caldera. It shows a low resistivity layer that is about 1.5 km deep below Ol' Rongai area. This shallow low resistivity layer on this profile defines a combination of conductive sediments and alteration zones around Ol' Rongai area. Below this zone a higher resistivity layer is seen overlaying a low resistivity starting at about 6 km below the surface. This is probably a magmatic heat source for the Ol' Rongai area.

Resistivity cross-section passing through the Menengai caldera

Figure 2.3 shows MT resistivity cross-section E-W 2 passing through Kabarak, the caldera and Bahati. This profile shows generally higher resistivity near the surface which is probably due to un-altered rocks in the near sub-surface. Underlain is a low resistivity layer about 1 km thick which run accross the entire cross-section. This shallow low resistivity layer on this profile defines the clay layer formed due to hydrothermal alteration at the upper zone of the geothermal system in Menengai prospect and the outflow zones. A localized low resistivity anomaly is also observed at a depth of about 4 km. This low resistivity body could be associated with magmatic intrusion which is a probable source of crustal fluids for this Prospect.

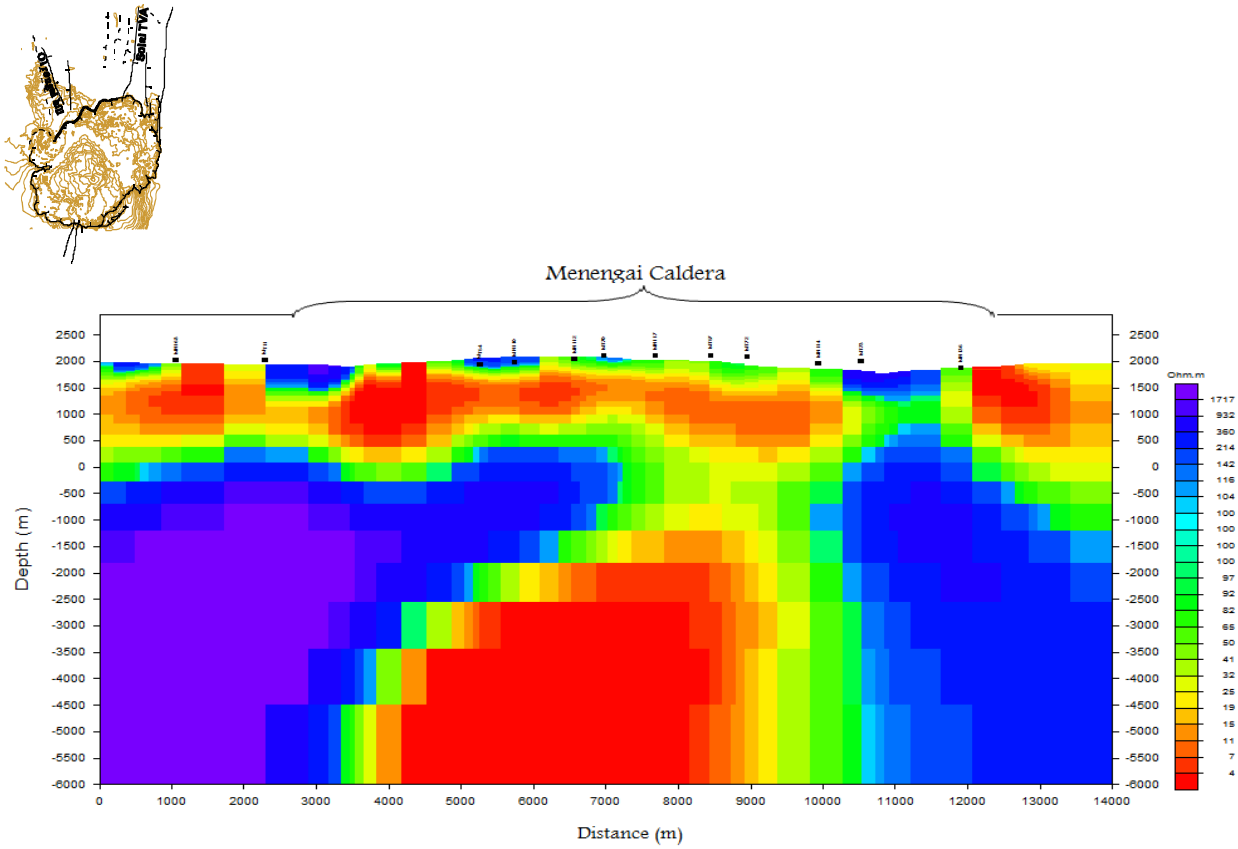

Figure 12: 2D East-west MT resistivity cross-section

DISCUSIONS

This resistivity survey has identified three zones, separated by discontinuities, which are suitable for geothermal production. These are:

(1) The central part of the caldera which shows a low resistivity (< 10 Ωm) anomaly at depth.
(2) The Ol' Rongai area where steaming and dry hot wells are located also with low resistivity at depth.
(3) The western domain towards Kabarak which is separated from the central one by a structural discontinuity has a homogenous electrical response and low resistivity (<10 Ωm). The low resistivity is attributed to primary (lithology) rather than secondary alteration, probably due to intense hydrothermal alteration. However, the top of the resistive basement is shallower.

The total heat estimated from the caldera alone is in excess of 2690 MWt. This high heat flow from the Menengai caldera could be indicative of a big hot body underneath, which can be explored further for production of steam. Areas around Ol' Rongai and Ol' Banita are also interesting even though the overall heat flow estimated is low. The low heat flow could be due to the fact that they are older systems. The orientation of the high temperature areas is in a NNW-SSE direction. This suggests that a major fault/fracture zone could be aligned in this direction and allows deep hot fluids to flow close to the surface causing localized heating of the shallow fluids. Another possible structure seems to occur in NE-SW direction as can be observed from the orientation of the high temperature areas within the caldera.

CONCLUSION

It is recommended that four deep directional exploratory wells be drilled in Menengai caldera as was initially proposed and three more to be drilled on Ol' Rongai and Kabarak area as indicated in the findings**(**Figure 2.4**)**. The resource area based on the anomaly is about 84 km^2 which can yield about 1260 MWe based on the world average of 15 MWe/km^2

Figure 13: Menengai proposed exploratory well sites and resource area

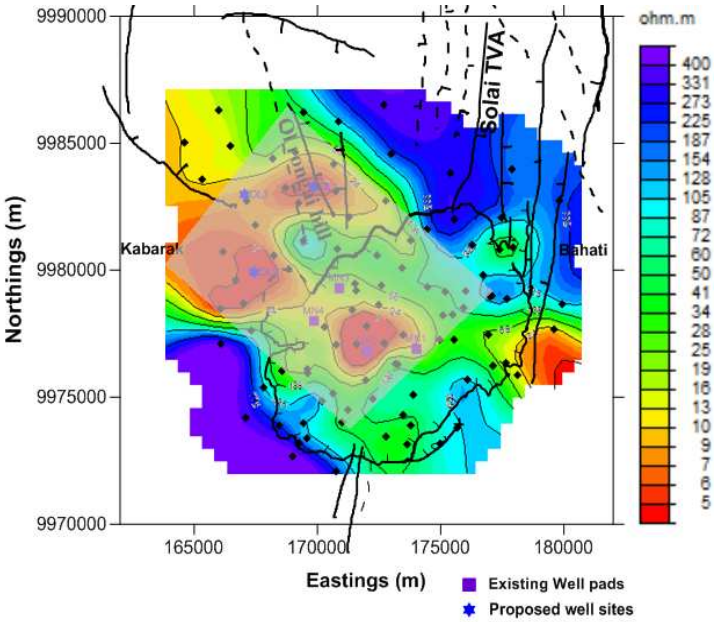

Resource area

APPLICATION OF THREE-DIMENSIONAL MAGNETOTELLURIC IMAGING TO GEOTHERMAL EXPLORATION

Pascal Tarits[(1)] & Sophie Hautot[(2)]
Laboratoire Domaines Océaniques, IUEM, Place Nicolas Copernic, Plouzané, France
IMAGIR sarl, IUEM, Place Nicolas Copernic, Plouzané, France

Keywords: magnetotelluric, three-dimensional, heterogeneity, geothermal exploration

INTRODUCTION

Eastern Africa geothermal fields are associated with the recent to actual volcanism in the Rift region. As a result, the geometry of the geothermal source is complicated. Water and vapor flow in fractures within the lava flows often interlaced with hydrothermal and/or sediment deposits. How geophysical imaging techniques could provide accurate models of the plumbing system and the nature of fluids circulating in it is a central question in geothermal exploration. Electromagnetic techniques and in particular Magnetotelluric (MT) is one of the geophysical technique used in this domain. The method provides information about the electrical conductivity down to several kilometers in depth.

Electromagnetic techniques complete seismic techniques for oil, gas, mining, geothermal or hydro-geological exploration. These complementary techniques are particularly useful in areas with complex structures such as geothermal regions. Furthermore, although seismic methods provide the best possible reservoir descriptions, they remain poorly informative on fluids properties, MT methods provide reservoirs electrical resistivity information, thus enabling to better describe and understand fluids in the pore space. .

New tree-dimensional imaging (or inversion) tools are now available to improve the accuracy of the conductivity models retrieved from the MT data. For 3-D inversion, it is best to acquire data over a fine 2-D surface grid with a regular spacing. It is in general difficult to acquire MT data on a such a grid over a volcanic geothermal field. In this study, we present results of three-dimensional (3-D) MT inversion for various types of MT sites distribution, including 2-D profiles which show that accurate local 3-D structures can be recovered. We test the approach with synthetic examples and demonstrate the feasibility with a series of 3-D MT studies carried out in Eastern Africa.

THREE-DIMENSIONAL INVERSION

We developed a robust full tensor 3D MT data inversion scheme with a coarse-to-fine lattice parameterization approach (Hautot et al. 2000, 2007). The technique was developed to provide a detailed geological image of sedimentary basins in complicated geological contexts such as thick basaltic screen covers. It is now extended to complex geothermal and volcanic regions. The 3-D inversion technique is based on an iterative procedure to minimize a misfit function between the observed data and the model response using a non-linear steepest gradient method with a regularization term. The data is the MT tensor (the four complex components and tipper when available) at all available frequencies and at all sites.

As MT inversion is a non-linear problem, the misfit obtained for the best-fitting model is not an absolute minimum but is some compromise between all sites, periods, and data quality. Therefore, the parameters of the model may not be equally constrained by the data. The large number of parameters to be processed makes the 3-D inversion procedure complex. In order to limit the number of these parameters, the 3-D model is parameterized by blocks. The size and the initial meshing of the 3D volume are determined according to the MT sites distribution and the depth of investigation of the data. Then the inversion is controlled by increasing the number of parameters treated as iterations on increasingly sensitive areas. This procedure tends to increase the number of voluntary iterations but with shorter and more effective iterations.

The coarse-to-fine approach provides a final grid that reflects the resolution of geological targets in the model. Compared to other available techniques, the number of parameters is much smaller, adapted to the actual number of data and fully flexible in terms of site/frequency distribution, hence providing accurate 3D structures resolution information. The approach makes the technique flexible and allows dealing with unevenly distributed sites, topography or bathymetry (for marine MT) effects and any number of periods. This iterative and incremental parameter approach enables an easy integration of parameters from other sources (drilling) into the procedure to add geophysical information.

SYNTHETIC INVERSION OF COMPLEX RESERVOIR

Figure 1 is the result of 3-D inversion for a synthetic test for a complex structure embedded in a uniform half space. MT data at 100 sites were generated (Miensopust et al., 2008) and inverted with our code. The results for a fairly coarse grid was quite good. The quality of the results may be measured by the fit between the data and calculated MT tensor (Figure 2).

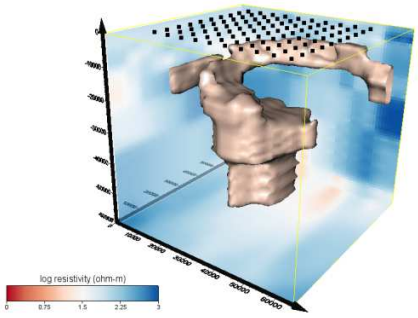

Figure 1: 3-D inversion of complex structures. Dots are the sites were synthetic data were generated.

One the characteristics of 3-D geothermal structures is to generate quite heterogeneous data set with significant diagonal terms in the MT tensor data. The later are difficult to fit but provides a very good constraint on the geometry and conductivity of the 3-D structures.

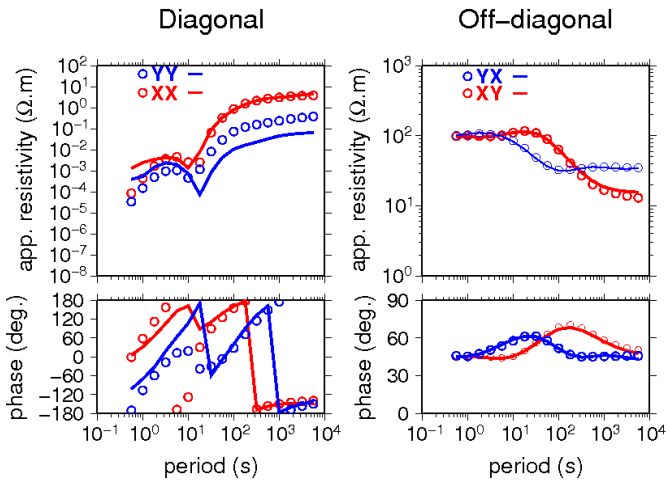

Figure 2: Example of fit between data (circles) and model responses (lines) for all four components of the MT tensor, expressed as apparent resistivity and phases. The term X means North and Y East.

3-D MT IMAGING FROM A HETEROGENEOUS NETWORK

Surveys in difficult areas such as volcanic regions or remote access areas generally leads to very heterogeneous networks of MT sites from which one has to obtain some ideas about the 3-D structures. As an example, we present here a project funded by industry to study the thickness of sediments in the basin of the River Omo in Southwest Ethiopia (Whaler and Hautot, 2007). For political and practical reasons, the actual network of MT sites is not homogeneous as planned (Figure 3).

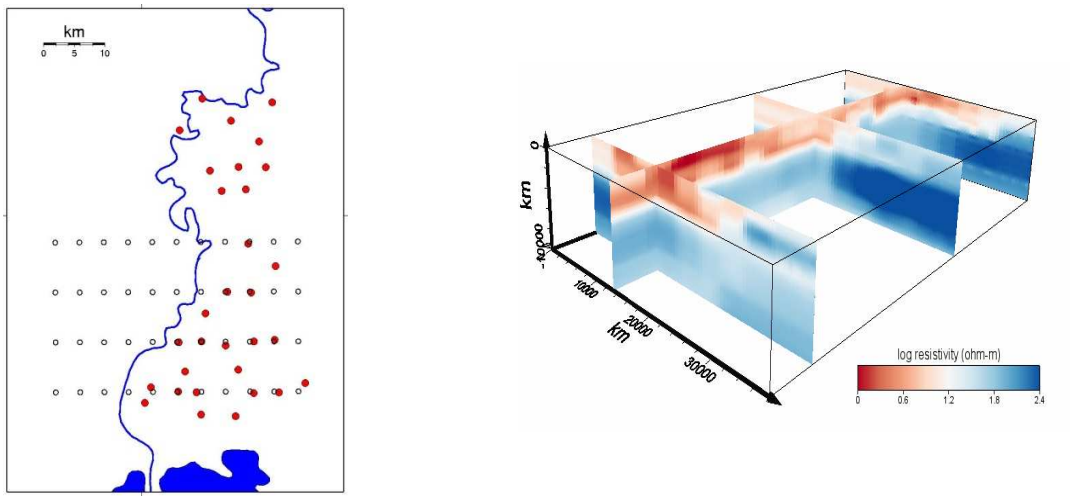

Figure 3: Left: MT network for the OMO basin experiment. The open circles are the original plan while the red dots are the actual 31 sites which were possible to collect. Right: The final 3-D resistivity model obtained from the inversion of the data from the 31 sites.

A total of 31 magnetotelluric (MT) sites were occupied over the Omo basin in South west Ethiopia. The inversion was run on the 31 full MT tensors at 16-33 frequencies depending on the sites, with a total of 6840 data values to recover 1000 resistivity parameters. The final model is shown to the right. In Omo Basin, the structures are fairly smooth and the diagonal terms of the tensor are small and easy to fit at all frequencies. The model indicates a N-S geo-electrical strike, in agreement with the geological strike, with up to 4km of sediments in the southern part of the basin, but no more than 2km in the northern part, underlain by more resistive material, assumed to be the basement.

3-D IMAGING OF A MAGMATIC CHAMBER IN AFAR (NORTH ETHIOPIA)

As part of a major program of research into the processes and controls involved in the break-up of continents and the generation of new oceanic crust, we have collected broadband magnetotelluric (MT) data along a ~50km long profile in the Afar region of Ethiopia (Hautot et al. 2009).

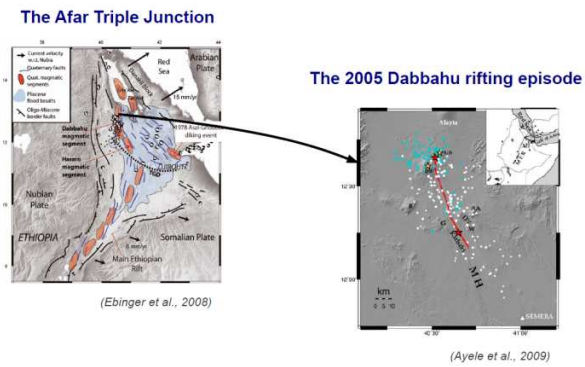

Figure 4: The Dabbahu volcanic event in Afar (Ethiopia)

The Dabbahu rift segment (Figure 4), in Afar is active since 2005 with volcanic eruptions and seismic tremor associated with a 60 km long dike intrusion in major tectono-magmatic episodes along the same segment. MT data

have been collected in 2008 at 17 sites along the profile across the Dabbahu segment in order to image beneath the volcanic layers. The method can provide new and additional information on the relationships between the crustal structure and the deep processes that control the deformation of the rift. While the data are broadly consistent with a two-dimensional interpretation, with geoelectrical strike along the segment's axis of rifting, three-dimensional effects are seen primarily at sites beneath the rift axis. We have inverted the data using a 3-D inversion technique (Hautot et al. 2000, 2007) in order to account for conductivity variation along the rift segment (Figure 5).

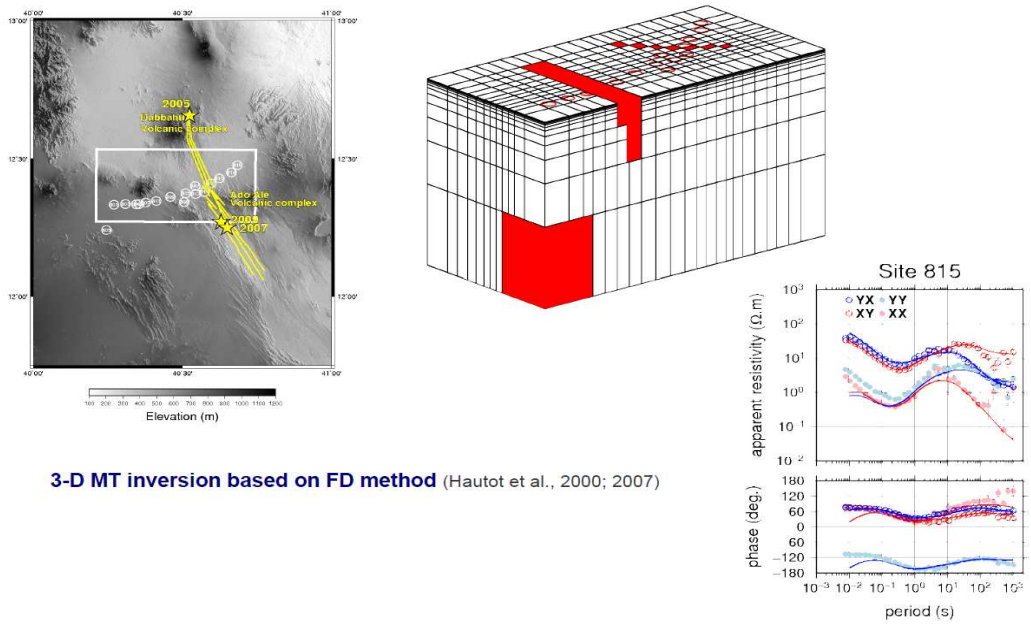

Figure 5: Left: MT profile across the Dabbahu segment. Top right: 3-D parameterization of the model for the Mt inversion. Bottom left: Example of fit for one site showing the significant diagonal MT tensor components.

Significant departure from a 2-D structure are observed in the depth range 5-10 km and in the shallow (0-2 km) part of the model. The 3-D approach refines the observation of high conductivity at depth beneath the segment axis in a zone ~10 km wide close to the surface and in a much broader zone at depths straddling the crust-mantle interface (Figure 6).

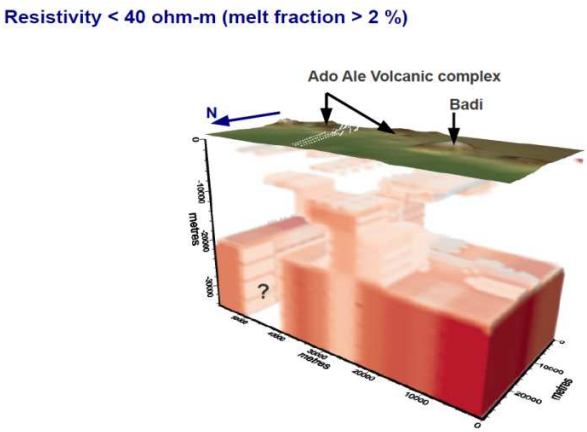

Figure 6: Iso-contour of resistivity values less than 40 Ohm-m that depict a possible limit of partial melting.

CONCLUSION

The 3-D MT inversion is now becoming a tool that may be used to obtain accurate models of the geological structures in complex areas. The 3-D MT is proven to provide useful information even if the network of MT sites is heterogeneous or only along a profile provided the full MT tensor is available. MT surveys for geothermal exploration should make use of these methods to provide the best resistivity models to geologist and geothermal scientists and managers.

REFERENCES

Ayele, A., D. Keir, C. Ebinger, T. J. Wright, G. W. Stuart, W. R. Buck, E. Jacques, G. Ogubazghi, and J. Sholan, September 2005 mega-dike emplacement in the Manda-Harraro nascent oceanic rift (Afar depression), *Geophys. Res. Lett.*, 36, L20306, doi:10.1029/2009GL039605, 2009.

Ebinger, C. J., Keir, D., Ayele, A., Calais, E., Wright, T. J., Belachew, M., Hammond, J. O. S., Campbell, E. and Buck, W. R., Capturing magma intrusion and faulting processes during continental rupture: seismicity of the Dabbahu (Afar) rift. Geophysical Journal International, 174: 1138–1152. doi: 10.1111/j.1365-246X.2008.03877.x, 2008.

Hautot, S., Tarits, P., Whaler, K., Le Gall, B., Tiercelin, J.J, and Le Turdu, C., The deep structure of the Baringo Rift basin (central Kenya) from 3-D magnetotelluric imaging : Implications for rift evolution, Journal of Geophysical Research, 105, 23493-23518, 2000.

Hautot, S., R. Single, J. Watson, N. Harrop, D. A. Jerram, P. Tarits, K. A. Whaler,, and G. Dawes, 3-D magnetotelluric inversion and model validation with gravity data for the investigation of flood basalts and associated volcanic rifted margins, Geophysical Journal International, 170(3), 1418-1430, 2007.

Hautot S., K. Whaler, M. Desissa, G. Dawes, S. Fisseha, N. Johnson, 3-D conductivity structure of an active magmatic segment associated with the final stage of continental break-up: Afar, Ethiopia. Eos Trans. AGU 90(52), Fall Meet. Suppl., Abstr. T43F-07, 2009.

Miensopust, M. P., P. Queralt, A. Jones, and the "MT 3D inversion workshop attendees, MT 3D inversion: a recapitultation of a successful workshop, IAGA WG 1.2 on Electromagnetic Induction in the Earth, 19th Workshop, Beijing, China, October 23-29, 2008.

Whaler, K., and S. Hautot, Final report on the magnetotelluric study of the Omo Valley JSA, report for White Nile Company, RPS Energy, and The Ministry of Mines and Resources of Ethiopia, 2007.

INTEGRATED GEOPHYSICAL SURVEYS TO CHARACTERIZE TENDAHO GEOTHERMAL FIELD IN NORTH EASTERN ETHIOPIA

Yohannes Lemma[1], Ulrich Kalberkamp[2], Aklilu Hailu[3], Mohammednur Desissa[4] ,
[1,3,4] Geological survey of Ethiopia, P.O.BOX 2302, Addis Ababa, Ethiopia
[2] Geological survey of Germany, GEOTHERM Programme, Stilleweg 2, 30655 Hannover, Germany
yohanesle207@gmail.com or yohlema@yahoo.com

ABSTRACT

Tendaho geothermal field is a high temperature geothermal resource in Afar regional state North Eastern Ethiopia. Gravity, magnetic, transient electromagnetic and magneto- telluric survey were carried out. The objective of the geophysical survey was to delineate the boundaries of the geothermal reservoir and geological structures that control flow of geothermal fluids.

The complete Bouguer anomaly map has reveled two distinct broad high (in NW sector) and low (in SE sector) Bouguer anomalies. These contrasting Bouguer anomalies may indicate the presence of ENE-WSW trending regional crustal discontinuity (fault). The Tendaho graben is mapped as a NW-SE trending prominent magnetic low feature and corresponding high residual gravity anomaly. The geothermal manifestations at Tendaho geothermal field lie on NW-SE trending fault system on magnetic and gravity surveys.

TEM data from the same site was used to correct for static shift in MT data. MT data were analysed and modelled using 1D Occam inversion of the determinant of the impedance tensor. In the MT cross sections, the low resistivity at shallow depth is interpreted as a sedimentary formation, lateral flow of geothermal fluids or a fracture zone. The high resistivity below the low resistivity can be associated to less permeable Afar stratoid series basalts. A low-resistivity zone bounded between high resistivity is interpreted as a fracture zone in the Afar stratoid basalts which may give rise to higher permeability and higher temperature and may indicate upflow of geothermal fluid. The fracture zones inferred from MT correlate with NW-SE trending structures from gravity and magnetic surveys and the surface geothermal manifestations in the area. The fracture zones are not well resolved because of large MT station spacing..

Keywords: Tendaho, Gravity, Magnetics, transient electromagnetic (TEM) and magnetotelluric (MT) survey

INTRODUCTION

The Dubti (Tendaho) geothermal field is located in the central part of Afar Depression about 600 kilometers from Addis Ababa in the northeastern part of Ethiopia (Figure 1). Structurally the area is part of the Tendaho graben, which is about 50 km wide, 100 km long and oriented in the NE-SW direction. Gravity and magenetics surveys were conducted to study the geological structures and dimension of subsurface lithology of Tendaho geothermal field. The gravity survey was conducted using a Lacoste and Romberg model 819G gravimeter having a reading accuracy of 0.01mGal. The position and elevation of the survey stations were obtained using the Magellan 315 GPS and Barometric Altimeter. The Scintrex made portable proton precession magnetometer MP-2 was used to measure the total magnetic field.

Magnetotelluric (MT) and Transient Electromagnetic (TEM) surveys were conducted by joint collaboration of experts from BGR (German geological survey) and Ethiopian Geological Survey from January 23 – February 23, 2007. A total of 51 MT soundings were measured using ADU-06 Metronix MT units.

REVIEW OF PREVIOUS WORK

Geologic and Tectonic Setting

Tendaho graben is trending in a NW direction as a southern portion of the Erta-Manda Hararo rift system in the Afar region (Aquater, 1995). The rift joins the Ethiopian rift close to volcano Dama Ale, west of Lake Abhe. The Tendaho rift, however does not merely swerve into the Main Ethiopian rift, but is prolonged east of the latter by Gobaad structure (Aquater, 1996).

The borders of the Tendaho rift are constituted by the Afar Stratoid Series and the rift is filled with lacustrine and alluvial deposits and with post stratiod basalt flows. This filling is topped by recent volcanoes, including the

historically active Kurub and Damal Ale volcanoes (Aquater, 1996). The Tendaho graben is bounded by Logya fault to the west and Gamare fault to the East. In the Tendaho region NW and NNE trending faults predominate (UNDP, 1973).

NNE trending faults may have played only a minor role in the evolution of the Tendaho graben, where the dominant structural element is NW (UNDP, 1973). The intersection of these two faults trend appears to be a controlling factor governing the locations of current hydrothermal activity (UNDP, 1973).

Inside the Tendaho Rift, lacustrine and alluvial plains alternate with zones where basalts crop out as NW-oriented elongated fault blocks. Evidence for active NW-striking faults includes aligned steaming grounds, fumaroles and hydrothermal deposits in the sediments within the Dubti plantation (Aquater, 1995).

According to the stratigraphy under the graben floor (revealed by geophysics), the rock units are grouped into:

- Upper unit: thick sedimentary sequence consisting of fine to medium grained sandstone, siltstone and clay probably intercalated by basaltic lava sheets; and
- Lower unit: basaltic lava flows of the Afar stratoid series.

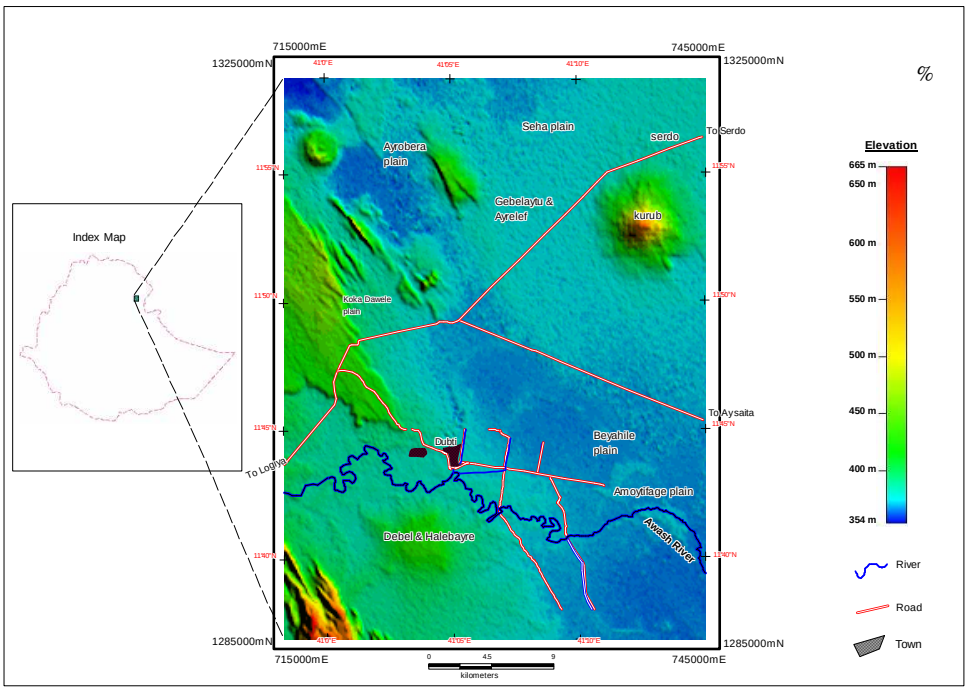

Figure 1: Location map of the study area

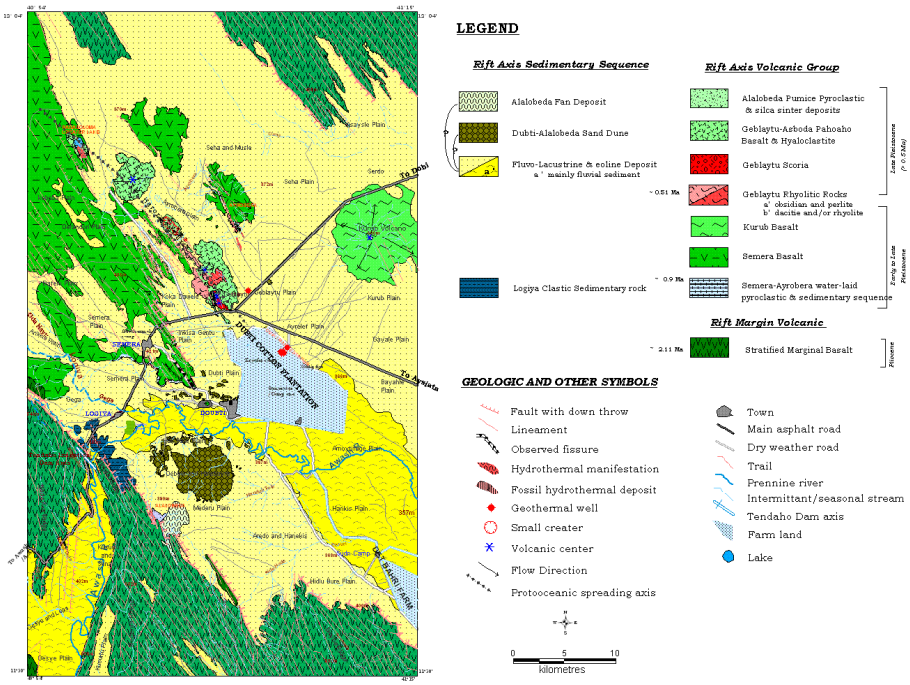

Figure 2: Geological map of Tendaho Graben (After Megersa and Getaneh, 2006)

The geology of Dubti-Semera area was mapped at a scale of 1:50,000 and the following units were identified (Megersa and Getaneh, 2006) and (Figure 2). The Rift margin complex of the study area represented by Stratified Rift Margin Basalt and the Rift Axis complex comprises of volcanic and sedimentary sequences. The Rift Axis Volcanic Group of the study area, found in the axial range of Tendaho rift, includes: Ayrobera-Semera Water-laid Pyroclastic and Sedimentary Sequence, Semera Basalt, Kurub Basalt, Geblaytu Rhyolitic Rocks, Geblaytu Scoria and Geblaytu-Asboda fresh Pahoehoe Basalt and Hyaloclastite. Sedimentation of fluvial, lacustrine and eoline have been simultaneously carried with the axial volcanic activity, mainly in the graben area. Eolian deposit is the dominant surface sedimentary unit at present. The measured surface temperatures in geothermal manifestations mainly fall in the ranges from 65 to 100.3ºC (Megersa and Getaneh, 2006).

In Tendaho geothermal field six wells were drilled from 1993-98. Wells TD1, TD2 and TD3 are deep wells with depth of 1550, 1881 and 1989 m respectively. Wells TD4, TD5, and TD6 are shallow wells with depth of 466, 516 and 505 m respectively. Wells TD2, TD4, TD5 and TD6 are productive.

Previous Geophysical Work

Regional and semi-detailed geophysical studies have been carried out in the Afar Depression and Tendaho geothermal field, with the aim to investigate the deep structures and to delineate possible geothermal reservoir. The methods include Magneto-telluric (MT) (e.g. Berktold, 1975); Vertical Electrical Sounding (VES), Magnetics and Gravity survey (e.g. Aquater, 1980) among others.

In 1971 MT survey was carried out in the Afar region to investigate the deep electrical resistivity distribution (Berktold, 1975). The survey included measurement of the electric field in 36 temporary stations along three profiles for a total length of 900 km. Profile I of the MT survey which is trending East-West (Dessie-Bati-Serdo) intersect the study area. Results indicate that in the Afar Depression and the marginal parts of the Western plateau, the resistivity is decreasing from 200-500 Ohm-m in the uppermost kilometers to 10-50 Ohm-m at a depth of about 15 km (Berktold, 1975). The anomalously low resistivity beneath the Afar and the marginal parts of the Western plateau was interpreted as an anomalously high temperature of 800-1000˚C at a depth of about 15 km and a temperature gradient of about 60˚C/km (Berktold, 1975).

In 1972 five deep seismic refraction profiles 120-250 km long were run in the Afar lowland and on the western Ethiopian plateau (Berckhemer and Baier, 1975). In one profile, the crustal thickness is estimated beween 22 and 25

km with a 7.7 km/s mantle velocity; whereas in other profile the estimated crustal thickness is about 24 km and mantle velocity 7.6 km/s. According to Berckhemer et al., 1975, the interpretation suggests a crustal thinning and upwelling of hot upper-mantle material beneath Afar.

A gravity survey (between Tendaho, Serdo and Asayita) was conducted by Searle and Gouin (1971) in an area 1000 km². The authors produced a Bouguer anomaly map using an average crustal density of 2.67 Mg/m³. The main feature of the map is a decrease in Bouguer gravity from -40 mGal to the north to -55 mGal along the Awash River in the south, mainly caused by the accumulation of sediments in the Awash Basin. A few localized Bouguer gravity anomalies are observed along the southern edge of the surveyed area. A relative positive Bouguer anomaly is located near Tendaho village and a negative one near Dubti plantation.

An aeromagnetic map produced by Aquater (1979) showed a complex pattern of short positive and negative lineations. These were interpreted by Aquater (1979) being related to short spreading segment that have been active in the last four million years. One of such anomalies is located in the survey area along the Manda-Hararo Volcanic range.

In 1971 the Hunting Geology and Geophysics Ltd. conducted an airborne infrared survey of the geothermal prospects in Ethiopia including the Tendaho area. The infrared survey was able to detect hot grounds in Tendaho that were not recognized by previous ground surveys.

Vertical Electrical Sounding (VES) data was acquired by Aquater (1980). In this survey, depth of investigation reached only to a maximum of one km and the data lacked resolution in differentiating layers within the sedimentary and basaltic sequences. In addition, Aquater (1980) occupied 2086 gravity stations in the Tendaho area. The NW-SE trending gravity low near Tendaho plantation is related to a depression of the high-density substratum. A strong positive Bouguer gravity anomaly centred over the Ayrobera area may be due to a dense intrusive body in the fluvial-lacustrine sediment system (Aquater, 1980).

Aquater (1980) has also produced total field magnetic map that shows a general NW-SE magnetic anomaly. The anomaly extends from northwest to southeast following the Tendaho graben axis with minor anomaly interruptions attributed to near surface inhomogeneities.

Aquater (1980, 1994) drilled nine temperature gradient wells to map the subsurface temperature distribution in the Tendaho Graben and Logiya area. But, due to shallow depths of the boreholes (76.6-173.5 m) the reservoir temperature is masked by the thick sediment layers and the presence of hot or cold shallow aquifers. The micro seismic survey (Aquater, 1995) in the Tendaho graben has indicated that the hypocenters of the seismic events are distributed in a NW-SE direction and to a depth between 5 and 10 km.

A geophysical survey by Oluma et al. (1996) consist of Schlumberger traversing, Head-on resistivity profiling, vertical electrical sounding (VES) at three well sites (TD1,TD2,TD4) and 60 line km gravity surveys were conducted centring the active thermal manifestations of the Tendaho graben. The result of AB/2=500 m resistivity map indicated a prominent anomaly with its roots in the SE part**.** The result of resistivity map for AB/2=1000 m showed a narrow NE elongation of low resistivity zone. The dominant regional trend, i.e., NW and NE ones are the major structures controlling the flow of hot geothermal fluids.

RESULTS

Bouguer Anomaly Gravity Map

Broad and relative positive Bouguer gravity anomalies (above -25 mGal) characterize the northwestern part (Ayrobera and Gebelaytu plain) of the study area (Figure 3). They are narrow and negative high on southwestern part of Debele plain and Serdo area. Strong negative Bouguer anomalies (less than -35 mGal) are observed on Beyahile and Amoytifage plain. Intermediate Bouguer anomalies of about -30 mGal separated the two Bouguer anomalies. Seha plain to the north is characterized by intermediate Bouguer value.

The low Bouguer anomalies of Beyahile plain are associated with sedimentary basin and apparently the thickness increases towards Amoytifage plain. The high positive Bouguer anomalies (greater than -29.8 mGal) of Ayrobera and Gebelaytu plain appear to be related to basaltic upper extrusive complexes. The most positive Bouguer anomaly, near Ayrobera plain geothermal manifestations is possibly associated with deposition of some hydrothermal minerals (hydrothermal alteration) on the volcanic rocks.

The narrow postive Bouger anomalies in the north east of Serdo and south west of Debel plain are associated to rhyolites and basalts (middle extrusive complexes). The area between Koka Dawele plain and Dubti is characterized

by relatively low Bouguer gravity anomalies. This may indicate the area is covered by loose, low density sediment below, which probably a basaltic body exists (Aquater 1980). Broadly, the thickness of the sedimentary rocks decreases from southeast to northwest in the Tendaho rift, which is also observed from the Bouguer anomaly features (relative positive to the North West and a relative negative to the south east).

The geothermal manifestations at Ayrobera plain and Alelo bade area correlate to the north west- southeast trending fault systems (Figure 3).

The complete Bouguer anomaly map has revealed two distinct broad high (in the north western sector) and low (in the south eastern sector) Bouguer gravity anomalies. These two contrasting Bouguer anomaly features may indicate the presence of regional crustal discontinuity (fault) in between. The probable structure has ENE/WSW orientation. The low Bouguer anomaly in Beyahile plain is also separated from another high Bouguer anomaly over Debele plain by a probable NW-SE trending structure. The aforementioned high Bouguer zone is characterized by nearly circular contour of increasing magnitude towards the center. This may suggest the presence of high density volcanic up doming, which could be the reason for thin sediment deposit. Since the survey area is located in an area where lithosphere is thinned by stretching**,** an increased heat flow and doming **(**Berckhemer et al., 1975**)** are the consequences.

Total Field Magnetic Anomaly Map

High total magnetic field relief is observed in Koka Dawele plain, Dubti town, Kurub plain and Serdo area (Figure 4). Low magnetic relief characterizes the Ayrobera plain, Gebelaytu plain, Beyahile plain and Dubti plantation.

The high magnetic anomalies are related to upper extrusive complex and middle extrusive complex basalts and rhyolites. The low magnetic anomalies of Dubti plantation and Beyahile plain are associated to thick sedimentary rocks. The Tendaho graben is mapped as a NW-SE trending low magnetic feature and corresponding high residual gravity anomaly. Low magnetic anomaly near the geothermal manifestations in Ayrobera plain is interpreted as result from alteration effects on magnetic minerals (Aquater, 1980)

Possible lineaments inferred from the total field magnetic map is shown in Figure 4.

The manifestations are well correlated with the NW-SE trending structure (possible fault). The magnetic gradient at Dubti plantation (geothermal manifestation) could be interpreted as possible fault NW-SE. The Alalobeda thermal manifestations also lie on magnetic gradient SW of Debel plain, which is interpreted as fault.

Comparison of the Bouguer and total magnetic field anomaly maps (Figure 3 and 4), the total magnetic field anomaly is very low and the Bouguer anomaly is high at Ayrobera and Gebelaytu plain. . The high Bouguer anomaly indicates the presence of high density probably caused by deposition of hydrothermal minerals on basaltic body (e.g. Hochestein and Hunt, 1970). Consequently, the magnetic response of the basalt has to be high too (e.g. A. Manzella). But, the total magnetic field anomaly is low. This may show that the basaltic unit has lost its ferromagnetic nature due to high temperature underneath. This geophysical information help to infer the presence of heat source which could be one of the causes for the existence geothermal potential in the area.

MT Soundings Cross Section

MT cross section, L1, (Figure 5 and 6), runs from Dubti in the SW, passes the geothermal manifestations near shallow well TD4 and ends SE of Kurub volcano. A low resistivity of about 1 Ω m is observed across the cross section to a depth of 100 m a.s.l. This resistivity structure can be associated to sediments. On northeast part of the cross section a relatively high resistivity is observed from a depth of 0 to 200 m b.s.l. This is correlated to basalts intercalated in sediments. Another low resistivity of 1 Ω m is observed from 200 to 500 m b.s.l. This is associated to sediments or lateral flow of geothermal fluid or fracture zone. A high resistivity of anomaly > 100 Ω m is observed under TDO0106 from a depth of 1000 m. to 2000 m b.s.l. A similar anomaly is observed under TDO0103 and TDO0107 from 1200 m to 2000 m b.s.l. This high resistivity can be associated to the less permeable Afar stratoid basalts. Between these two high resistivity structures, there is a low-resistivity zone under soundings TDO0107 and TDO0108 at bottom part of the cross section. This can be due to presence of fracture zone in the basalts which may give rise to higher permeability and higher temperature and may indicate upflow of geothermal fluid into the system.

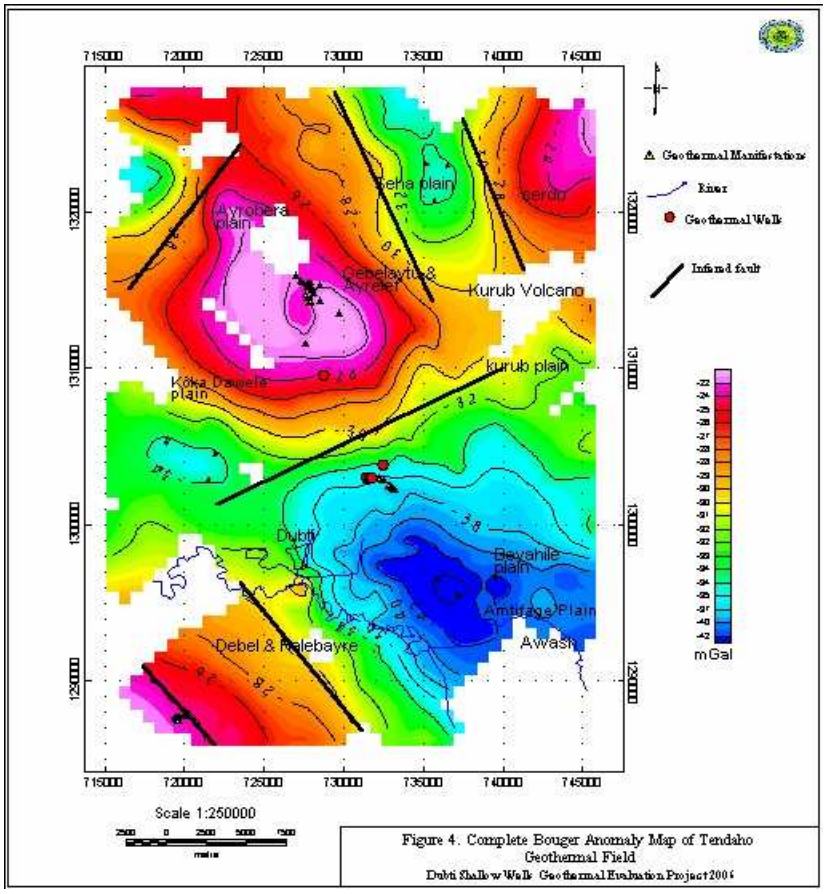

Figure 3: Bouguer Anomaly map of Tendaho Geothermal field

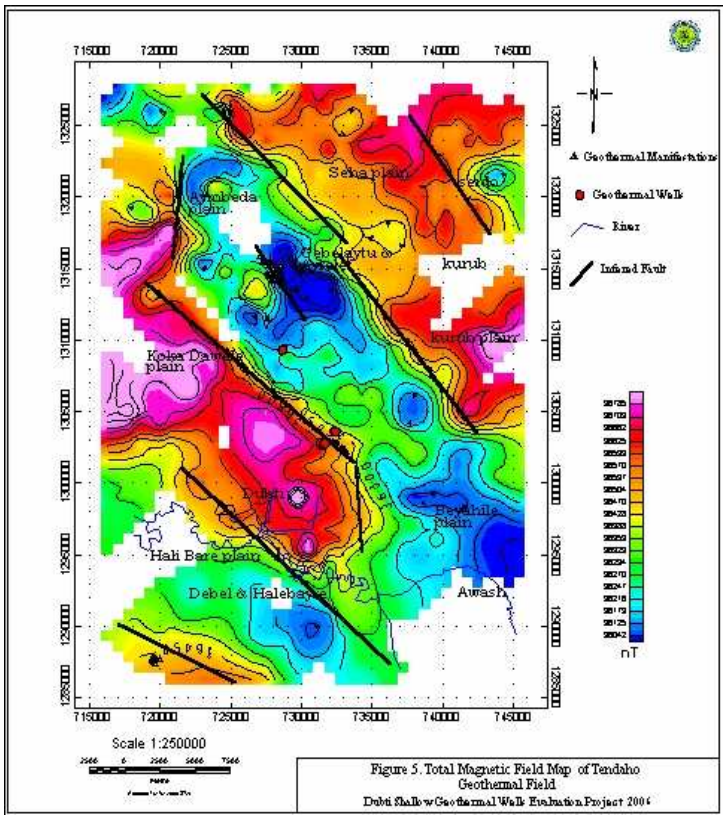

Figure 4: Total Field Magnetic Anomaly Map of Tendaho Geothermal Field

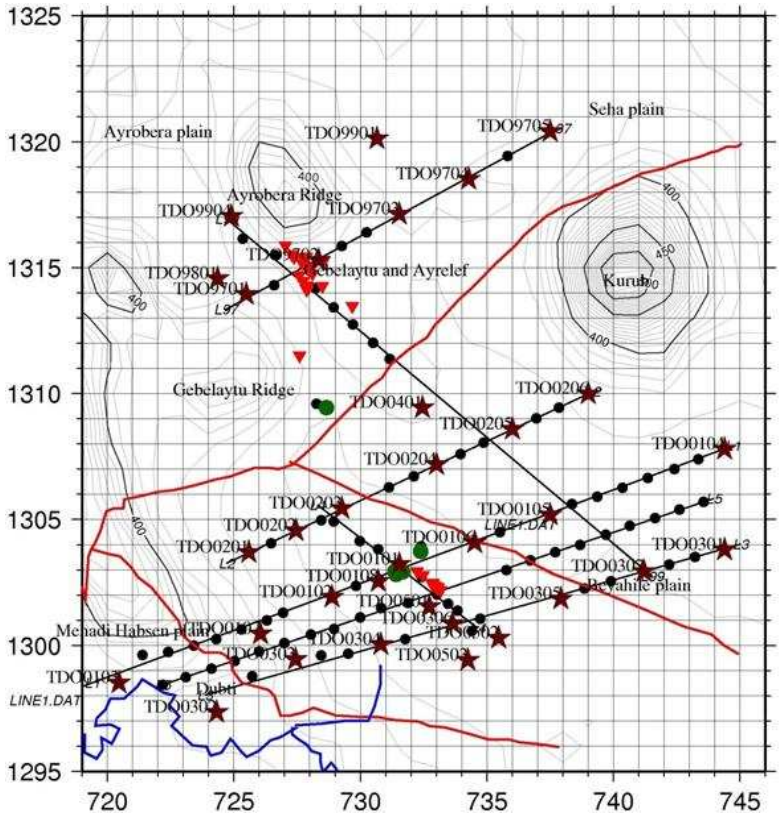

Figure 5: Location of MT and TEM soundings (UTM 37, datum: ADINDAN-Ethiopia, in km)

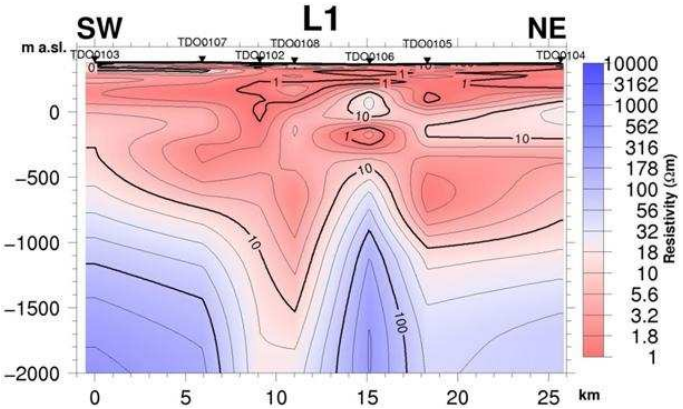

Figure 6: MT resistivity cross section L1

MT cross section L2, Figure 7, runs from Mehadi Habsen plain in SW to Kurub volcanic complex in the NE. A low resistivity ≤ 10 Ω m is observed along the whole cross section to depth of 0 m at sea level. This low resistivity extends to a depth of 1000 m b.sl at southwest section under sounding TDO0201 and TDO0202. The same resistivity structure extends to 800 m b.s.l at northeast part of the cross section under soundings TDO0205 and TDO0206. This low resistivity structure can be correlated to sediments. A broad high resistivity of ≥ 100 Ω m is observed along the cross section at an average depth of 1000 m b.s.l. This high resistivity is up doming near southwest sector of the section especially under TDO0203. The high resistivity at the bottom part of the cross section is associated with Afar stratoid series basalts.

MT cross section L3, Figure 8, runs from Dubti in SW to Behyahile plain in NE. A low resistivity ≤ 10 Ω m is observed to a depth of 0 m at sea level. A broad high resistivity of ≥ 100 Ω m is observed under the low resistivity to a depth of 2000 m b.s.l. The low resistivity can be associated with sediments and the high resistivity to Afar stratoid basalts.

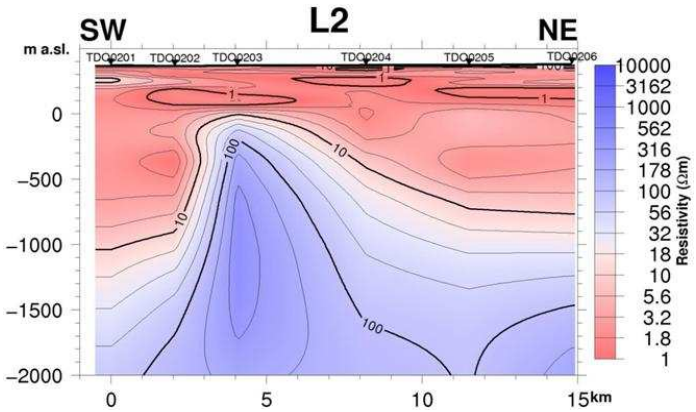

Figure 7: MT resistivity cross section L2

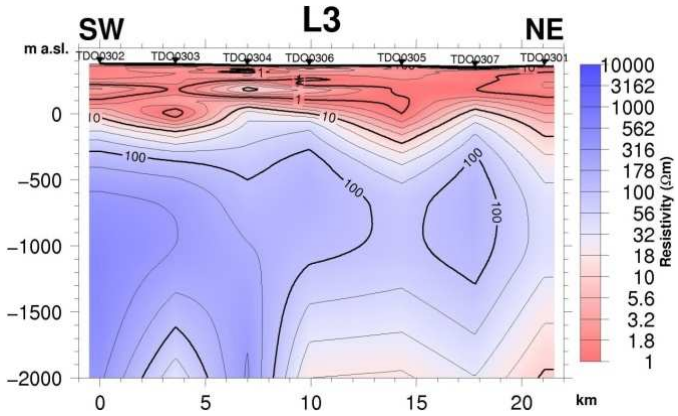

Figure 8: MT resistivity cross section L2

MT cross section L97, Figure 9, runs from Gebelaytu ridge in SW to Seha plain in the NE. A high resistivity anomaly ≥ 100 Ω m is observed at shallow depth of about 200 m a.s.l in

the southwest part of the cross section under sounding TDO9712. A relatively high resistivity of ≥ 10 Ω m is observed on the northeast part of the cross section at the same depth. This high resistivity can be correlated to basalts in the area. The rest of the cross section is characterized by low resistivity ≤ 10 Ω m to a depth of 300 m b.s.l. This low resistivity is associated with sedimentary formation or geothermal fluid circulation in the formation. A high resistivity of anomaly > 100 Ω m is observed under TDO9712 from a depth of 400 m. to 2000 m b.s.l. A similar anomaly is observed under TDO9704 and TDO9705 from 500 m to 2000 m b.sl. This high resistivity is associated to less permeable Afar stratoid basalts. Between these two high resistivity structures, there is a low-resistivity zone under soundings TDO9702 and TDO9703 in the Afar stratoid basalts. This anomaly is interpreted as fracture zone in basalts where geothermal fluids circulate.

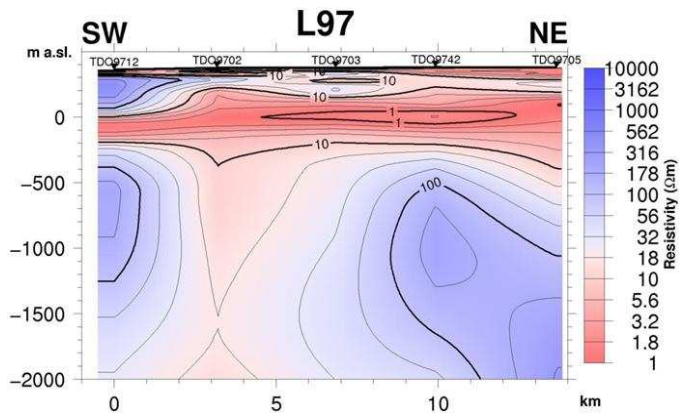

Figure 9: MT resistivity cross section L97

CONCLUSIONS

The geological structures controlling the flow of geothermal fluids are dominantly NW-SE trending regional system. The mapped geological structures are in line with Aquater, 1990. The density distribution of the Tendaho geothermal field is predominantly volcanics in NW sector and sedimentary in SE sector from gravity surveys.

Since both volcanic and sedimentary rocks cover the survey area, it is difficult to indicate the boundaries of geothermal reservoir by magnetic method. Even though the geothermal manifestations in Dubti, Ayrobera and Alelobade lie on a fault, it is not possible to infer that they are connected in anyway structurally because of data scarcity in some areas.

In MT cross sections L1 and L97, the low resistivity at shallow depth can be correlated to sedimentary formation (clay, siltstone and sand stone), lateral flow of geothermal fluid, fracture zone or alteration mineralization. The high resistivity at depth below the low resistivity can be associated to the less permeable Afar stratoid series basalts. A low-resistivity zone bounded between high resistivity in the basalts is interpreted as a fracture zone which gives rise to higher permeability and higher temperature and may indicate upflow of geothermal fluids. The fracture zone inferred from MT cross sections coincides with the surface geothermal manifestations in Dubti and Ayrobera area.

On MT cross section L1 the low-resistivity zone between MT soundings TDO0107 and TDO0106 may represent shallow sedimentary reservoir at depth of 200 m b.s.l and deep basaltic reservoir at 1000 m b.s.l which was also observed on well testing and reservoir engineering studies results of Tendaho geothermal field (Amdebrhan and Bjornsson, 2000).

The fracture zones interpreted from MT cross sections L1 and L97 (Figures 6 and 9) correlates to NW-SE trending structures inferred from the gravity and magnetic survey for the area (Figures 3 and 4). The fracture zone inferred from the MT cross sections also coincides with the surface geothermal manifestations in Dubti and Ayrobera area.

In MT cross sections L2 and L3, a low resistivity is underlain by high resistivity formation. The low resistivity can be correlated to sedimentary formation. The high resistivity can be associated to the Afar stratoid series basalts.

REFERENCE

Amdeberhan, Y., and Björnsson, G., 2000: Well testing and reservoir engineering studies at the Tendaho geothermal field. Proceedings of the World Geothermal Congress 2000, Kyushu - Tohoku, Japan, 901-907.

Aquater, 1979: Geothermal Resources Exploration Project Tendaho Area-Prefeasibility Study. EIGS and Ministry of Foreign Affairsof Italy, San Lorenzo in Campo.

Aquater, 1980: Geothermal resource exploration project Tendaho area, feasibility study- phase II. EIGS and Ministry of Foreign Affairs of Italy, San Lorenzo in Campo.

Aquater, 1995: Micro seismic study, final report. EIGS and Ministry of Foreign Affairs of Italy, San Lorenzo in Campo.

Aquater 1996: Tendaho geothermal project, final report. MME, EIGS - Government of Italy, Ministry of Foreign Affairs, San Lorenzo in Campo.

Árnason, K., 1989: Central loop transient electromagnetic sounding over a horizontally layered earth. Orkustofnun, Reykjavík, report OS-89032/JHD-06, 129 pp.

Árnason, K., 2006: TEMTD (Program for 1D inversion of central-loop TEM and MT data). ISOR, Reykjavík, short manual, 16 pp.

Berckhemer, H., and Baier, B, 1975: Deep seismic sounding in the Afar Region and on the highland of Ethiopia. Proceedings of the International Symposium on the Afar Region and Related Rift Problems. Schweizerbart,I, Stuttgart, 89-107.

Berktold, A., 1975: Magnetotelluric measurements in the Afar area. Afar Depression of Ethiopia. Proceedings of the International Symposium on the Afar Region and Related Rift Problems, Schweizerbart, I, Stuttgart, 262-275.

Berktold, A., 1983: Electromagnetic studies in geothermal regions. Geophysical Surveys, 6, 173-200.

Friedrichs, B., 2005: MAPROS (version 0.876b freeware), manual. Metronix, 123 pp.

Geonics, 1999: Operating Manual for PROTEM 67 D. Geonics Ltd, Ontario, 58 pp.

Lemma, Y., and Hailu, A., 2006: Gravity and magnetics survey at the Tendaho geothermal field. GSE, Addis Ababa, unpublished internal report, 23 pp.

Megersa, G., and Getaneh, E., 2006: Geological, surface hydrothermal alteration and geothermal mapping of Dubti-Semera area, Tendaho geothermal field. GSE, Addis Ababa, unpublished report, 66 pp.

Oluma, B., Ayana, D., and Demisse, Y., 1996: Geophysical survey of Tendaho geothermal field. MME, EIGS, geothermal exploration project, unpublished report, 23 pp.

Searte, R., and Gouin, P., 1970: Gravity survey of the Tendaho-Asayita-Sardo region, Wollo, Ethiopia. Geophysical Observatory of Addis Ababa University, Addis Ababa, technical report.

UNDP, 1973: Geology, geochemistry and hydrology of hot springs of the East African Rift System within Ethiopia. UNDP, NY, technical report DD/SF/ON/11.

GROUND WATER SURVEY WITH A NEW CAPACITANCE PROBE

Idris Bexi, Xavier Chavanne, Jean-Pierre Frangi
Equipe Géomatériaux & Environnement
Institut de Physique du Globe de Paris / Université de Djibouti

ABSTRACT

Original in-situ HF technique of material dielectric characterization in the 1-20 MHz have been developed and validated in order to estimate the moisture content of soils. The 1-20 MHz device is based on 2 electrodes put into the soil and separated from a distance of up to 30 cm. As the probe system is able to investigate several layers constituting a stacking of electrodes, a moisture profile of the soil can be obtained. The system is based on the determination of the complex impedance (ratio voltage/current through the soil impedance) in a variable frequency from 1 to 20 MHz. The measurement requires a calibration on several soil types to reach acceptable accuracy for water content. The design and data processing as well as preliminary results obtained from laboratory experiments are presented.

Keywords: dielectric measurement, impedance, permittivity, conductivity, moisture content, soil, capacitor, electromagnetic waves

INTRODUCTION

Soil moisture is a key variable in controlling the exchange of water and heat energy between the land surface and the atmosphere through evaporation and plant transpiration. The unsaturated zone between the Earth's soil surface and the water table –known as the "vadose" zone – is penetrated by the roots of vegetation, which take up some of the water. Hence, the amount of water in this zone, which determines the "soil moisture", varies with time as a function of the amount of precipitation and the root water take-up, governed by the degree of vegetation cover, the energy being received from the Sun, and run-off and percolation. As the properties of the soil determine its storage capacity and the transport process within the soil, such a topic concerns a wide range of scientists: hydrologists, climatologists, geophysicists, agronomists, geomorphologists. Among various techniques currently used (gravimetric, nuclear, electromagnetic, tensiometric, hygrometric, remote sensing processes), electromagnetic methods appear particularly attractive as they allow to infer soil moisture content by measuring the effective real or imaginary parts of the complex permittivity at different locations using reflected or transmitted waves [1, 2, 3, 4, 5]. Such techniques are generally divided into two categories, surface and drill-hole based measurements, which use open-ended transmission line or free-space methods. Among surface techniques, new developments have been performed which concern a capacitive probe HYMENET. This probes appear as a particularly simple and efficient tools to characterize the dielectric properties of the near surface of soft soils in broad frequency bands [0.1; 20] MHz.

In the present study, the dielectric characterization of soils and particularly their volumetric moisture content rely on the estimation of the real permittivity because of the great difference between the relative permittivity of water close to 80, and the relative permittivity of common dry soils ranging from 4 to 15. Afterwards, a non trivial relation between the real permittivity measured by the probe and the soil moisture content has to be found. The use of a mixture law allows us to solve a nonlinear inverse problem to obtain the parameters characterizing the constituents of the surrounding medium. In general, soil forms a heterogeneous material made of a mineral-air-water mixture. Thus, its dielectric properties are closely dependent on the dielectric constants of the individual constituents, the volume fractions of the components, the geometric characteristics of the constituents, and the electrochemical interactions between the constituents.

Concerning the dependence of a medium with moisture, several models have been proposed, each with its own characteristics and variables. Fundamental developments have been associated to the empirical formula of Topp et al. [6], to a three-phase model formulated by by de Loor [7], and to a four phase model proposed as a semi-disperse model by Wang and Schmugge [8], a semi-empirical power-law model by Dobson and Ulaby [9], and Peplinski et al. [10], and a generalized refractive dielectric model by Mironov et al. [11]. Recently, Boyarskii et al. [12] have suggested a model of the complex permittivity of bound water versus frequency in wet soils, and Jones et al. [13] have studied the effects of particle size on the bulk dielectric constant. In the present study, the volumetric moisture content (free water) of the soil has been deduced from the real part of the complex permittivity using parametric relations based on the polynomial Topp's formula, and an extended version of the CRIM (Complex refractive Index

Model) formulation [14]. The validation of experimental setup have been performed on experimental measurements associated with different types of sands. This article is focused on the development and the validation of the following novel in-situ device: the capacitive probe HYMENET. The design, the methodology, the data processing, as well as experimental results obtained from laboratory or in-situ experiments are detailed.

THE CAPACITIVE PROBE

Probe geometry and general considerations

The probe HYMENET (Figure. 1) works as an impedance meter working in the range [1; 20] MHz. Its measurement principle is based on the electrokinetic's theory where the scanned soil is considered as a capacitor (C) in parallel with a resistor (R). Because of the device main aim to study porous media filled with some fluids like water, air, or others constrains on its geometry and working frequency f have been imposed upon it. The geometry of the probe allows us to relate the permittivity measurement to a representative volume of the electrical properties of the medium [15]. The geometry must be also simple to derive easily the intrinsic properties of the medium (relative permittivity ε_r and conductivity σ) from R and C. The design consists on two parallel cylindrical electrodes for the probe as shown on Fig. 1. A tension of excitation V_{ex} is applied between the two electrodes plunged inside the medium to be characterized. Both V_{ex} and the resulting current are measured by an electronic board placed inside the ground electrode to deduce the impedance through the generalized Ohm's law. Thus, the impedance meter is able to determine separately the dielectric and conductive properties of the medium (ε_r and σ). This reduces interferences between both variables. One of the electrodes is divided vertically in equal parts of height h, or channels, electrically isolated from each other. This configuration allows to measure the current at different heights and hence to deduce the medium properties at these heights. It is used to study fluid vertical flows. The top and bottom parts assure that the electric field around electrodes is horizontal at the intermediate levels (this has been shown by numerical simulations, e.g. [16]). The two extreme channels constitute these shields while for each intermediate channels, ε_r and σ can be computed. Hence the electrode geometry can be considered as vertically infinite and the following formula can be applied for the impedance determined at each intermediate channel [17]:

$$C = \frac{h\pi\varepsilon_0\varepsilon_r}{\arg ch(\frac{D}{\phi})} \qquad \frac{1}{R} = \frac{h\pi\sigma}{\arg ch(\frac{D}{\phi})} \qquad (1)$$

with ε_0 is the absolute permittivity ($8.85\ 10^{-12}$ $F.m^{-1}$) and ε_r the relative permittivity, argch is the inverse of hyperbolic cosine, D is the distance between two electrode axis, Φ is the electrode diameter and h the height of one channel of the ground electrode, and σ is the conductivity. For our current sensor h equals 45 mm, D is 90 mm and Φ is 50 mm. From relation 1, we deduce C(pF) = $1.04\times\varepsilon_r$ and R(Ω) = $9.2/\sigma$. Typical values of ε_r expected for soils range from 3 to 50 [5], giving a capacitance between 3 and 50 pF. For soil bulk conductivity ranging from nearly 0 up to 0.5 $S.m^{-1}$ the associated resistance value varies from infinity down to 20 Ω.

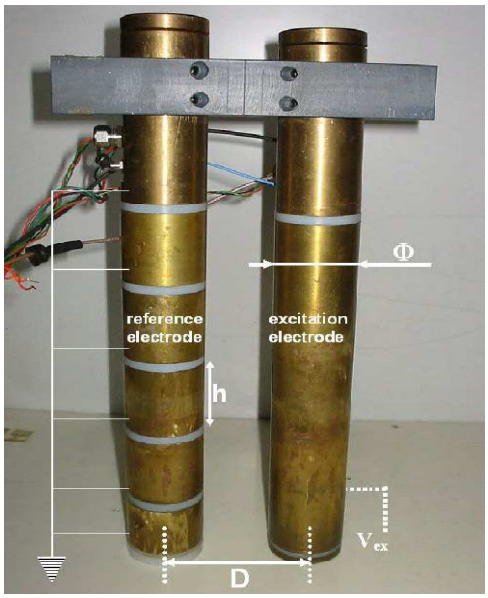

Figure 1: The HYMENET probe. D is the distance between the two electrodes axis, Θ the electrode diameter and h the height of one channel of the ground electrode.

Data acquisition and data processing

Different devices are used to power the apparatus (DC power supply HP E3631A), send the exciting voltage (Agilent generator up to 80 MHz HP 33250A), digitalize and record the different signals (Tektronics numerical scope TDS 3012B with analogue filter at 100 MHz, sampling frequency up to 1 GS/s, 8 bit nominal resolution and sensitivity down to 10 mV in full scale). The scope works with a numerical filter at 20 MHz and performs an average over 512 scope recordings to reduce the noise to signal ratio. Data are stored in a computer for further signal analysis (conversion in impedance and electric properties). Thanks to the overall system the medium properties can be monitored over a large period of time (from one hour to more than a month, depending also on the record capabilities of central unit) at different sampling frequencies down to 1 Hz, and the sensor is operating at frequencies up to 20 MHz. The reason is to reduce the sensitivity of εr to other parameters of the porous medium than the fluid permittivity like pore size and shape, or ionic content of fluids. Thus, εr appears as a good indicator of medium water content or fluids showing a strong permittivity contrast as compared with the dried medium. A system of relays and switches remotely operated allows to measure successively voltage and current (via a transimpedance) for each channel. Relays are controlled by a shift register driven by a computer with TTL signals. The same program also controls signals acquisition. The technical details of measurement chains are described in the patent above mentioned. We underline that high frequencies induce major electronic drawbacks like parasitic self inductances of conductors. Moreover, these disturbances grow roughly linearly with the size of the sensor. Consequently capacitors and self inductors will form resonators amplifying high frequency noises that induce voltage drops modifying the signal. A careful circuit design, avoiding some ground loops, plus some low band filters have permitted to control instabilities. The reference change between the different voltages is corrected by analog trim; for each the reference potential is measured and then subtracted to the voltage by on board integrated components placed before sensor output.

Calibration method

Calibration tests consist in connecting standard impedance between electrodes to determine probe systematic errors. Remaining systematic errors of the voltage after analog trim are due to self inductance of conductors (leads are necessary to connect the standard impedances at both electrodes, introducing other parasitic components to be removed), parasitic capacitance between close conductors, probe radiation losses and wire skin effect, and interferences between channels. Such errors are increased by frequency and impedance discrepancy between channels. The numerical program converting voltages into impedance includes parasitic effects corrections. It is

based on a physical model (equivalent electric circuit) in which parasitic effects is represented by self-inductances and capacitances. Thus, for instance, coupling two electrodes next to each other corresponds to a capacity up to 10 pF. The model parameter values are determined through standard electronic components (capacitors composed of porcelain multilayer by American Technical Ceramics, accuracy +/- 1%; resistors are 1206 thick film components manufactured by Vishay, accuracy 0.1 %). This calibration is made using resistors values and reference capacitances. The parameters interfering in this model are thus also becoming instrument parameters highly independent of the studied area. This apparatus can then be used for measurements of unknown impedances, be they artificial (e.g., electronics components) or natural (e.g., soils).

Tests and experimental results

Various experiments have been set up to qualify the instrument. One should bear in mind that the moisture measures in probed area are obtained through in-situ calibration curves (like all capacitive methods) by relating relative permittivity to volumetric water content of the medium. The relative permittivity being obtained through probe impedance measurements, the first serial measures have been set up to determine the apparatus capacity to evaluate artificial impedances. To this aim, electronic components (such as resistors and capacitances) have been connected to electrodes using a large value scale ranging from 25 to 5000 Ω as for resistors and from 5 to70 pF as for capacitances. Different configurations have been tested: resistor or capacity alone or combinations of resistors and capacities on a single channel (complex impedance then created), and analyzing the influence of impedance measurements on a single channel when other impedance is present on other one (cross-talk test). Figure. 2 enables us to compare connected impedances and impedances measured by the probe. It reveals that HYMENET probe measurement corresponds precisely to the impedance values obtained through the electrodes whatever the frequency. We can determine the impedance with a resistive part from 0.025 to 5 kΩ and with a capacitive part between 5 to 70 pF. The precision margin arises maximum 5% when dealing with the extreme case of high impedance difference between two neighboring channels (as well as scarce case as for soil measurements). For further details on the calibration processus, the reader is referred to Chavannes 2009 [19].

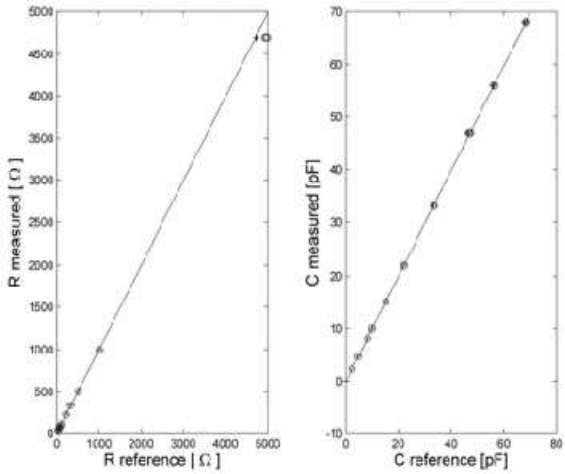

Figure 2: Impedance measurements (resistance on the left, capacitances on the right) for 10 MHz (cross) and 20 MHz (circles) with HYMENET probe.

The next stage consists in comparing the medium characteristics (εr, σ) obtained through those impedance measurements using relations 1. Such comparison entails the use of another apparatus as reference, which is very difficult since no apparatus has up to date been recognised reliable as to its permittivity measurements when electrodes are deported. In the absence of such apparatus, we have chosen the probe developed and commercialised by INRA (HMS9000 probe of SDEC company [20], Figure 3).

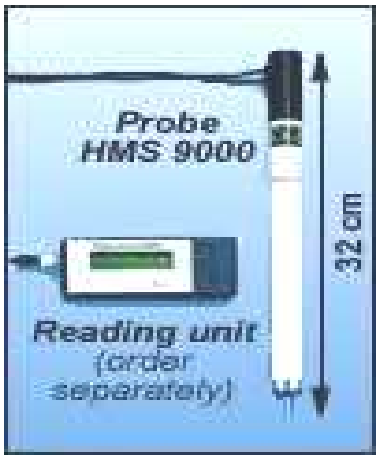

Figure 3: Capacitance probe HMS9000 of SDEC company.

The advantages of this probe are that it has already been studied and that its working frequency is 39 MHz, being then not too far from the frequencies used by HYMENET probes. The studied soil is a Fontainebleau sand (SiO2 > 99.8%, grain size distribution between 150 and 250 µm), which permittivity has been varied by modifying its moisture content. A certain quantity of dry sand has been put into a rectangular tub measuring 560×360×70 mm (to limit skin effect), into which two holes have been pierced for the introduction of the HYMENET probe Figure 4.

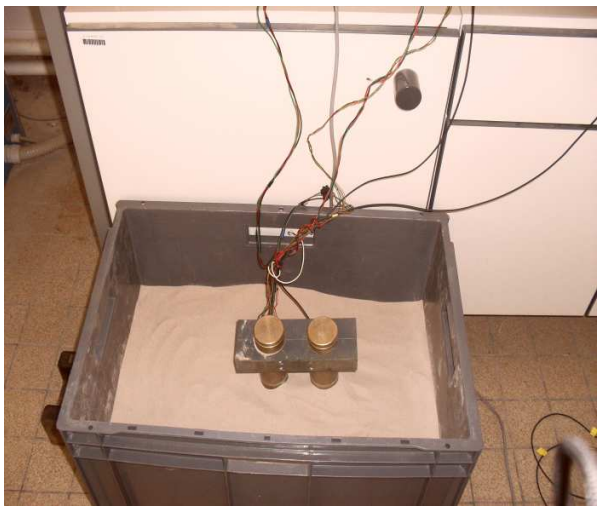

Figure 4: Rectangular tub measuring 560×360×70 mm, containing sand soil and HYMENET.

The height of the sand discharged into the tub corresponds to the height of a measurement channel (i.e. 50 mm). Distilled water has been added successively so as to obtain a volumetric humidity up to de 0.45 cm3.cm-3. Ten measurements have been taken for each water content so as to obtain a medium permittivity value, the probe HMS9000 being highly sensitive to the spatial heterogeneity due to its very low measure volume. Figure 5 shows the results obtained for two frequencies by the HYMENET probe (10 and 20 MHz).

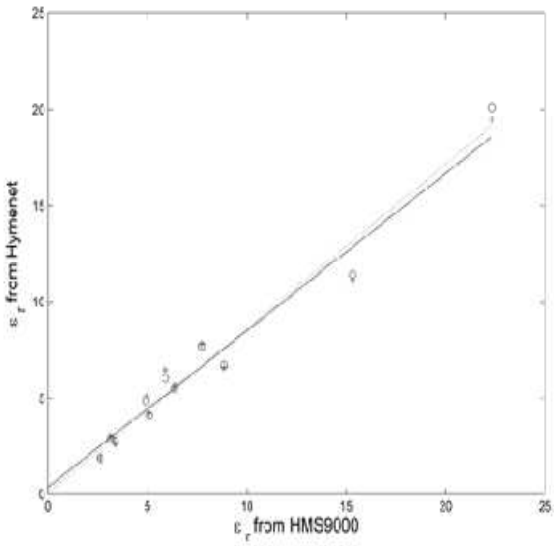

Figure 5: Relationship on the measured permittivity between HMS9000 probe (in abscissa) and HYMENET probe (in ordinate) at the 10 MHz frequency (cross) and 20 MHz (circle). Straight-lines are plotted for both (solid line for 10 MHz and dotted line for 20 MHz).

A very good correlation between the εr values between the two instruments is observed. For the measurements obtained at 10 MHz, the coefficients of the straight-line fit give a slope of 0.833 ± 0.051 and an intercept of -0.174 ± 0.580 with R^2=0.9906. For those obtained at 20 MHz, one have a slope of 0.871 ± 0.052, an intercept of -0.413 ± 0.586 with R^2=0.9912. The existence of a bias between the HYMENET et HMS9000 probes cannot be argued, even if at this stage determining which one is responsible is impossible. The HMS9000 measurements can be disturbed by the proximity of the electric field created by the HYMENET probe. Similarly, the latter can be disturbed by the current injection of the HMS9000 probe. This could be minor since moisture measurements entail calibration relation with in situ permittivity. However, further experiments using other apparatus (e.g. TDR) will soon be realised to clarify this point. The measurements obtained by the HYMENET probe can be reasonably considered as correct (with a very few percent of error). Experiments as to the medium moisture can then be carried out. This type of experiments are common (e.g. [21, 22]), and, as a first step, the relation between moisture content vs permittivity of Fontainebleau sand has been studied. This experiment has followed an experimental protocol identical to that used for the permittivity. Like permittivity measurements, Fontainebleau sand dried in drying oven has been humidified successively with a certain volume of distilled water and then homogenized. It appears useful to compare HYMENET measurements with the well-known "Topp curve" as a reference. Topp's calibration curve is generally accepted calibration equation for TDR water content measurements which is accurate for sand in general, but represents an average for a number of sandy-loam and clay-loam soils.

Figure. 6 shows the first results of this experiment and comparison with the Topp relation [23] valid for an average soil. $\varepsilon_r = 3.03 + 9.3\theta + 194\theta^2 - 76.6\theta^3$

It reveals that HYMENET measures do not depend on the frequency (corrections brought to the signal appearing as coherent), and that experimental curve trend follows that of Topp modelisation. The differences found between the calibration curve of Topp and the HYMENET data may be attributed to the dielectric behaviour of soils as a function of frequency due to Maxwell-Wagner effect, counterion polarisation and the impact of air bubbles, as highlight by Hilhorst [24].

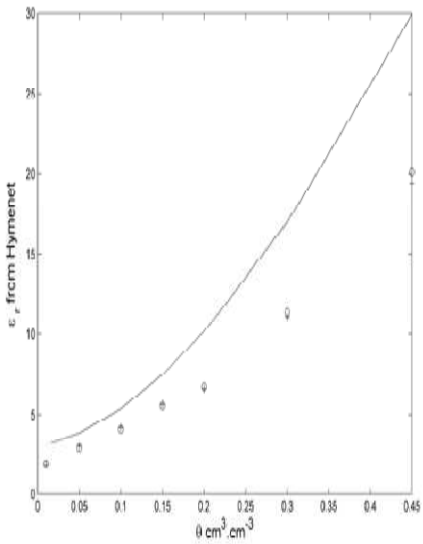

Figure 6: Volumetric water content relationship with measured permittivity by HYMENET probe at 10 MHz (cross) and 20 MHz (circle). The Topp (1980) relation is plotted (solid line).

CONCLUSION

This paper presents new instruments to characterize the moisture content of soft soils using two types of probes in a large frequency range 1-20 MHz and 0.1-4 GHz respectively. As far as the HYMENET probe is concerned, parasitic effects on the impedance measurements by the probe due to the frequency domain used imposed a sophisticated design of the electronics. However, an analog trim coupled with a physical model to take into account self-inductances and parasitic impedances enables the probe to measure the capacitance and the resistance of a medium at different frequencies. The model parameters have been estimated through a calibration process with standard capacitors and resistors. The model allows a determination of the impedance over its operating range of less than 5 % and mainly less than 1 %. An impedance profile can be traced since the conductors are separated along their length in different sections electrically insulated. It must be emphasized that the device determine the effective permittivity and conductivity (computed from the capacitance and the resistance) of the medium surrounding the electrodes, for a large area around the electrodes unlike others devices. This medium can be any porous medium filled with fluids, like a soil or a fresh concrete. Contrary to the TDR regarding which many studies have shown that relative permittivity is influenced by the conductivity (e.g., [2]), the measurement of the complex permittivity of soil with our device is not affected by the conductivity of the soil. Nevertheless, other experiments will be carried out to test the probe more precisely. Calibration tests with standard electronic components will be completed by using standard liquids (ethanol C2H5OH εr=24.3 at 25°C, methanol CH3OH εr=32.63 at 25°C, and acetic acid CH3COOH εr=6.18 at 24°C). To insure the independency of the permittivity measurements to the conductivity, dedicated experiments will soon be realised by using distilled water with different ionic conductivities. The present system is intended for laboratory works. A more compact and rugged system with self-balanced bridge will substitute the present one and will be more convenient and cheaper for field studies. It will also allow a faster sampling frequency.

REFERENCES

[1] J., Behari, Microwave dielectric behavior of wet soils. Springer, 2005.

[2] J. E Campbell, Dielectrics properties and influence of conductivity in soils at one to fifty Meghertz, Soil Sc. Soc. Am. J. 54 (1990) 332-341.

[3] M.A. Hilhorst, Dielectric characterisation of soil, PhD Thesis, Wageningen, Holland, 1998, 141 p.

[4] J.A. Huisman, S.S. Hubbard, J.D. Redman, A.P. Annan, Measuring soil water content with ground penetrating radar: A review, Vadose Zone J. 2, Nov. 2003, pp. 476-491

[5] D.A. Robinson, S.B. Jones, J.M. Wraith, D. Or, S.P. Friedman, A review of advances in dielectric and electrical conductivity measurement in soils using time domain reflectometry, Vadose Zone J. 2, Nov. 2003, pp. 444-475

[6] G.C. Topp, J.L. Davis, A.P. Annan, Electromagnetic determination of soil water content: Measurements in coaxial transmission lines, Water Resour. Res. 16 (1980) 574-582.

[7] G.P. de Loor, The dielectric properties of wet soils, IEEE Trans. Geoscience Remote Sensing GE-21 (3), July 1983, 364-369

[8] J.R.Wang, T.J. Schmugge, An empirical model for the complex dielectric permittivity of soils as a function of water content, IEEE Trans. Geos. Remote Sens. 18 (1980) 288-295.

[9] M.C. Dobson, F. Kouyate, F.T. Ulaby, M.T. Hallikainen, M.A. El Rayes, Microwave dielectric behaviour of wet soil - Part II: Dielectric mixing models. IEEE Trans. Geoscience and Remote Sensing, 23 (1985) 51-61.

[10] N.R. Peplinski, F.T. Ulaby, M.C. Dobson, Dielectric properties of soils in the 0.3-1.3 GHz range, IEEE Trans. Geos. Remote Sens. 33 (3) (1995) 803-807.

[11] V.L. Mironov, M.C. Dobson, V.H. Kaupp, S.A. Komarov, V.N. Kleshchenko, Generalized refractive mixing dielectric model for moist soils, IEEE Trans. Geos. Remote Sens. 42 (2004) 773-785.

[12] D.A. Boyarskii, V.V. Tikhonov, N.Y. Komarova, Model of dielectric constant of bound water in soil for applications of microwave remote sensing, PIER 35 (2002) 251-269.

[13] S.B. Jones, S.P. Friedman, Particle shape effects on the effective permittivity of anisotropic or isotropic media consisting of aligned or randomly oriented ellipsoidal particle, Water Resour. Res., 36 (2000) 2821-2833.

[14] JM.C. Dobson, F. Kouyate, F.T. Ulaby, M.T. Hallikainen, M.A. El Rayes, Microwave dielectric behaviour of wet soil - Part II: Dielectric mixing models. IEEE Trans. Geoscience and Remote Sensing, 23 (1985) 51-61. [15] G. de Rosny, A. Chanzy, M. Pardé, J.C. Gaudu, J.-P. Frangi, J.-P. Laurent, Numerical Modeling of a Capacitance Probe Response, Soil Sci. Soc. Am. J. 65 (2001) 13-18.

[15] J.-P. Frangi, G. de Rosny, X. Chavanne, D. Richard, A. Bruère,. Device for measuring electrical properties of a water-containing medium. World Intellectual Property Org. WO/2008/006973, Patent PCT/FR2007/01180, publication date: 17.01.2008.

[16] G. de Rosny, A. Chanzy, M. Pardé, J.C. Gaudu, J.-P. Frangi, J.-P. Laurent, Numerical Modeling of a Capacitance Probe Response, Soil Sci. Soc. Am. J. 65 (2001) 13-18..

[17] E. Durand, Electrostatique, Masson, Paris, 1966, 389 p.
J. E Campbell, Dielectrics properties and influence of conductivity in soils at one to fifty Meghertz, Soil Sc. Soc. Am. J. 54 (1990) 332-341.

[18] A. Chanzy, J. Chadoeuf, J.-C. Gaudu, D. Mohrath, G. Richard, L. Bruckler, Soil moisture monitoring at the field scale using automatic capacitance probes, Eur. J. Soil Sci. 49 (1998) 637–648.

[19] Chavannes X,Frangi, A new device for *in situ* measurement of an impedance profile at 1 to 20 MHz, Instrumentation and Measurement, IEEE Transactions on(2009), 1850 - 1859

[20] A. Chanzy, J. Chadoeuf, J.-C. Gaudu, D. Mohrath, G. Richard, L. Bruckler, Soil moisture monitoring at the field scale using automatic capacitance probes, Eur. J. Soil Sci. 49 (1998) 637–648.

[21] C.M.K. Gardner, T.J. Dean, J.D. Cooper. Soil Water Content Measurement with a High-Frequency Capacitance Sensor, J. agric. Engng Res. 71 (1998) 395-403.

[22] G.C. Topp, J.L. Davis, A.P. Annan, Electromagnetic determination of soil water content: Measurements in coaxial transmission lines, Water Resour. Res. 16 (1980) 574-582.

[23] M.A. Hilhorst, Dielectric characterisation of soil, PhD Thesis, Wageningen, Holland, 1998, 141 p.

THEME IV

GENERAL COUNTRY EXPLORATION

GEOTHERMAL ENERGY IN UGANDA, COUNTRY UPDATE 2010

Godfrey Bahati and James Francis Natukunda
Department of Geological Survey and Mines
Plot 21-29 Johnstone Road, P.O Box 9, Entebbe, UGANDA
gbahati@gmail.com, jfnatukunda@gmail.com,

ABSTRACT

Exploration for geothermal energy in Uganda has been in progress since 1993. The studies have focused on three major geothermal areas namely Katwe, Buranga and Kibiro. The three areas are in advanced stages of surface exploration and will soon be subjected to exploratory drilling that will pave the way for a feasibility study. The overall objective of the study is to develop geothermal energy to complement hydro and other sources of power to meet the energy demand of rural areas in sound environment.

The current study has focused on geology, geochemistry, hydrology and geophysics with the aim of elucidating subsurface temperatures and the spatial extent of the geothermal systems. The results indicate that the geothermal activity in the three areas is related to the volcanic and tectonic activities of the Rift Valley, which has a higher heat flow than the surrounding Precambrian crust. Subsurface temperatures of approximately 140-200˚C for Katwe, 120-150˚C for Buranga, and 200-220˚C for Kibiro have been predicted by geothermometry and mixing models. Anomalous areas have been delineated in Katwe and Kibiro prospects using geophysical methods. Drilling of shallow boreholes to a depth of 200-300m for temperature gradient measurement has been completed and the temperatures measured (30-36˚C/km) are slightly above the global average of 30˚C/km, which suggests deep reservoirs in Katwe and Kibiro or geothermal reservoirs offset from the drilled areas. Additional geophysical measurements to locate the deep reservoirs and drill sites in the two areas are recommended. The results will then be used to update the geothermal models that will be a basis for drilling of deep geothermal wells in the two areas. The Buranga area still needs detailed geophysical surveys to delineate anomalous areas that could be targets for drilling.

The fourth area, Panyimur in Nebbi district, West Nile region, has indications of a geothermal prospect following the results of the petroleum drilling programme that has encountered high temperature gradients (maximum 80˚C/km) in the vicinity of the thermal area.

The results of the preliminary geothermal investigations on other areas predict subsurface temperatures of 100 - 160˚C suitable for small scale electricity production and direct uses. These areas have been ranked based on predicted subsurface temperatures and other geothermal features for further exploration and development.

Keywords: Uganda, geothermal, surface surveys, feasibility.

INTRODUCTION

Geothermal resources were estimated at about 450 MW in the Ugandan Rift System (McNitt, 1982). The main geothermal areas are Katwe-Kikorongo (Katwe), Buranga and Kibiro, all located in the Western Rift Valley that runs along the border of Uganda with the Democratic Republic of Congo, and is part of the western branch of the East African Rift System (Figure 1).

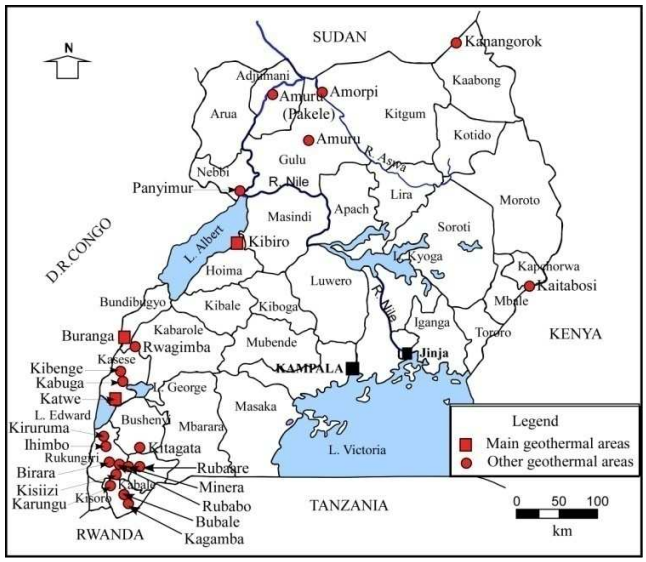

Figure 1: The geothermal areas of Uganda.

Geothermal resources exploration in Uganda is still at the pre-feasibility phase with three most promising prospects Katwe-Kikorongo (Katwe), Buranga and Kibiro in advanced stages of surface exploration and will soon be subjected to the drilling of the first deep exploration wells and feasibility studies. Subsurface temperatures of approximately 140-200˚C for Katwe, 120-150˚C for Buranga, and 200-220˚C for Kibiro have been predicted by geothermometry and mixing models. The temperatures are suitable for electricity production and for use in industry and agriculture. The temperature gradient results (30 - 36˚C/km) suggest deep reservoirs in Katwe and Kibiro prospects. However, there is a need for additional geophysical surveys using methods which probe deeper into the subsurface to locate the heat source and its extent, in order to complete surface exploration in the three areas.

The fourth area, Panyimur in Nebbi district, West Nile region, has indications of a geothermal prospect following the results of the petroleum drilling programme that has encountered high temperature gradients (maximum 80˚C/km) in the vicinity of the surface manifestations (hot springs). This area needs to be investigated. After completing surface exploration in the four areas, one of the areas will be selected for the feasibility study that will involve drilling of three exploration wells and well testing. The feasibility study will then lead to the establishment of the first geothermal power plant in the country.

The country is endowed with considerable hydropower resources with the potential estimated to be in excess of 2,500 MW. Uganda presently has a total installed capacity of electricity production of 565 MW of which 387 MW is hydropower, 160 MW is generated from thermal power plants and 18 MW from cogeneration in sugar industries. Hydropower capacity has been reduced to a mere 150 MW due to climatic fluctuations resulting in lowering of water levels in Lake Victoria, that serves as the reservoir for two major hydropower dams at Jinja; the Nalubale (formerly Owen Falls) and Kiira (Owen Falls extension) dams on the River Nile. The demand for electricity is estimated at 540 MW. To offset the demand, the Government is constructing Bujagali hydropower dam (250 MW) and in 2011 construction of Karuma (700 MW) also along the River Nile will start. In addition, other small hydros in the western part of the country are under construction. Two more dams, Ayago (500 MW) and Isimba (100 MW), also along the River Nile are at the feasibility stage. Other proposed hydropower developments on the River Nile have raised socio-economic and environmental issues and therefore a need to diversify the energy sources. Alternatives being investigated are mainly renewable sources that include geothermal, biomass, wind, peat, mini and small hydros, and solar energy.

The country's *per capita* energy consumption of 30.116 Kwh is among the lowest in the world (Energy statistics, 2006). The grid electricity access rate is very low: 12% for the whole country and about 6% for the rural areas. Electricity production is approximately 2,280 GWh per year with a demand for power growing by 8% per anuum.

The Ministry of Energy and Mineral Development (MEMD) implements the national energy policy with two departments i.e. Energy Resources (ERD) and Geological Survey and Mines (DGSM) involved in geothermal exploration and development. The DGSM is responsible for exploration and development of the geothermal

resources while the ERD is responsible for the energy policies formulation and implementation, and administration of energy laws.

The Uganda Energy Policy was enacted in 2002 and is implemented by the Uganda Electricity Act 1999. This Act provides for an independent Electricity Regulatory Authority (ERA), private sector participation in power generation and distribution with transmission remaining a government parastatal in the medium term. The major goal of the Energy Policy 2002, is to meet the energy needs of Uganda's population for social and economic development in an environmentally sustainable manner. To achieve the above goal, there is need to tap all possible sources of energy in the country, including the new and renewable sources, to which geothermal belongs. Accordingly, one of the Energy Policy, 2002 objectives is to establish the availability, potential and demand of the various energy sources.

To further focus on the above objective, a New and Renewable Energy Policy, 2007 has been put in place. The Policy aims to provide a framework to increase in significant proportions the contribution of renewable energy in the energy mix. The policy has: 1) Introduced the feed in tariffs, 2) Standardized Power Purchase Agreements, 3) Obligation of fossils fuel companies to mix products with biofuels up to 20% and 4) Tax incentives on renewable energy technologies.

This paper presents the current status of the geothermal exploration project, and planned exploration and development activities on the geothermal systems of Uganda.

STUDY AREAS

The main geothermal areas are Katwe, Buranga and Kibiro (Figure 1). The three areas were chosen for study because of their volcanic and tectonic features that indicate heat sources and high permeability.

Other areas are located within or on the outskirts of the Rift Valley in southwest, west, and north and in isolated places in east and northeast Uganda (Figure 1).

CURRENT STATUS

Katwe geothermal prospect

Geology

The results of geological surveys in the Katwe prospect indicate that explosion craters, ejected pyroclastics, tuffs with abundant granite and gneissic rocks from the basement dominate the area (Figure 2). The volcanic rocks, mainly composed of pyroclastics and ultramafic xenoliths, are deposited on the extensive Pleistocene lacustrine and fluvial Kaiso beds and in some places directly on Precambrian rocks. Minor occurrences of lava are found in the Lake Kitagata and Kyemengo craters. The age of the volcanic activity has been estimated as Pleistocene to Holocene (Musisi, 1991). The deposit is greyish, generally coarse to fine-grained, calcareous and mixed with sand and silt of Pleistocene sediments. Travertine deposits have been found in Lake Katwe, Lake Nyamunuka, Lake Kasenyi, and Lake Kikorongo (Groves, 1930) and in the vicinity of Lake Kikorongo at Kikorongo junction (Kato, 2003). The lava flows, craters and extinct hydrothermal deposits give an indication of a heat source for the geothermal activity. The prospect stretches from Lake Katwe to Lake Kikorongo and occupies an area of approximately 150 km^2. Outside the crater area, the geology is characterized by surficial deposits to the east and the west, and to the north lie the Rwenzori Mountains whose geology is dominated by gneisses, granites, granulites, amphibolites, schists and in some places quartzites.

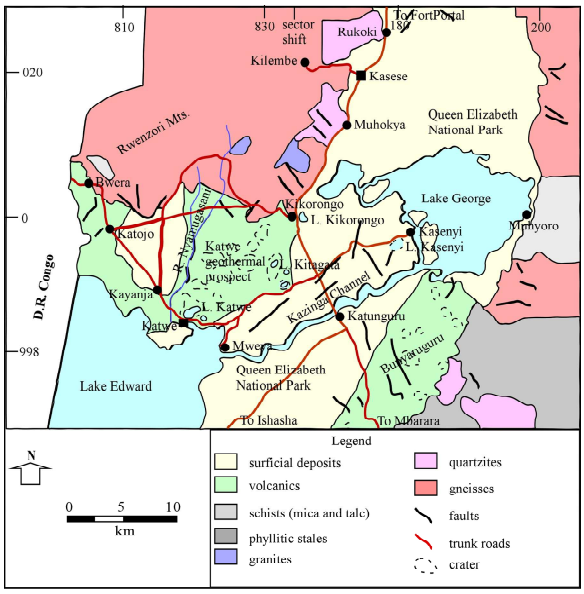

Figure 2: Geology of Katwe volcanic field and surroundings.

Geothermal manifestations

The geothermal surface manifestations in the Katwe prospect are hot springs located in the Lake Kitagata crater, and warm springs and travertine deposits that have built up tufas in the Lake Katwe crater, which is located 12 km southwest of Lake Kitagata (Figure 2). The maximum surface temperature in the hot springs in Lake Kitagata crater is 70°C, while in Lake Katwe Crater it is 32ºC.

Geochemistry

The geothermal fluids are characterized by high carbonate and sulphate, and salinity of 19,000 - 28,000 mg/kg total dissolved solids. High carbonate and sulphate in the geothermal water tend to invalidate solute geothermometer results in Katwe. Subsurface temperatures are estimated at 140-200˚C using plausible solute geothermometers (Armannsson, 1994). The thermal fluids from Lake Kitagata and Lake Katwe craters are characterized by the presence of high levels of hydrogen sulphide of about 30-40 ppm which suggests the source of the geothermal water to be volcanic and hydrothermal (Bahati, 2003).

Isotope hydrology

A number of water samples from hot springs, cold springs, rivers and lakes as well as rock samples were collected and analyzed for isotopic compositions. The objective was to provide hydrological information essential to the exploration for geothermal resources using isotopes. Isotopes analyzed for included those of hydrogen ($\delta^{2}H_{H2O}$, $^{3}H_{H2O}$), oxygen ($\delta^{18}O_{H2O}$, $^{18}O_{SO4}$), sulphur ($\delta^{34}S_{SO4}$), and strontium ($^{87/86}Sr_{H2O}$, $^{87/86}Sr_{Rock}$).

The results indicate that the Katwe geothermal system is most likely recharged from high ground in the Rwenzori Mountains. The tritium concentration in the thermal waters from the Katwe area is minimal suggesting that the hot spring water is not mixed with cold groundwater. The isotopic composition of sulphur ($\delta^{34}S$), and oxygen ($\delta^{18}O$) in sulphate suggests a magmatic and hydrothermal source for the geothermal water. Strontium isotopes in water and rock ($^{87/86}Sr_{H2O}$, $^{87/86}Sr_{Rock}$) indicate an interaction between the rocks sampled and the geothermal fluids. The rocks interacting with the fluids, i.e the reservoir rock types, in Katwe are basalt. The major source of salinity is rock dissolution, but some magmatic input is suggested (Bahati, et. al., 2005).

A temperature of 140 - 150°C was obtained for the sulphate-water ($S^{18}O_4$-$H_2{}^{18}O$) isotope geothermometer (Bahati, et. al., 2005) which compares reasonably well with that from solute geothermometers.

Geophysics

Geophysical surveys; Transient Electromagnetic (TEM) and Gravity were conducted in the Katwe geothermal prospect (Gislason, et. al., 2005). The results indicate the existence of two low resistivity anomalous areas (Figure 3). The first one is located around Lake Katwe and the second stretches from Lake Kitagata to Lake Kikorongo. The gravity data agrees with the TEM resistivity data and indicates that the two low resistivity anomalous areas are controlled by a N-S fault east of Lake Katwe and a NNE-SSW fault in the Lake Kitagata – Lake Kikorongo area (Figure 3).

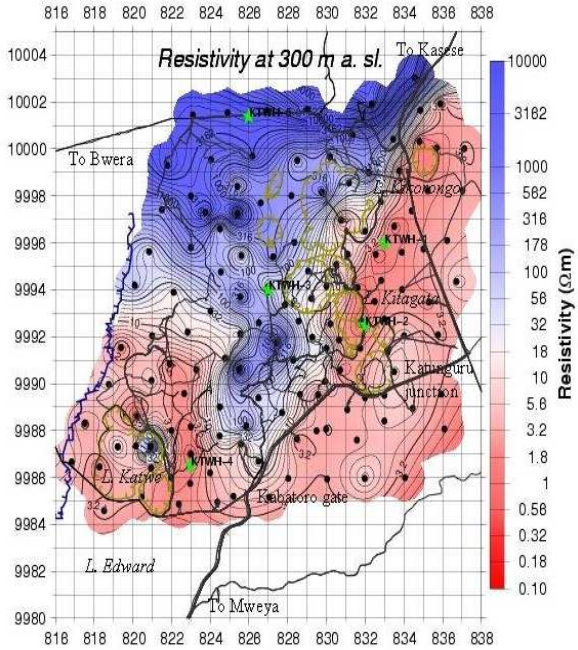

Figure 3: Katwe. Resisitivity at 300 m a.s.l., (from Gislason et. al., 2005).

Temperature gradient drilling

The drilling of six thermal gradient wells up to a maximum of 300m depth in the volcanics did not show any indication of Olivine-Biotite-Pyroxene (OBP) series. This confirms that the depth to the intrusive source of heat is greater than 300m to which the wells were drilled (Gislason et.al., 2008).

The results from the temperature gradient measurements give almost linear profiles indicating conductive heat transfer (Gislason et.al., 2008). However, the values between 30 and 36˚C/km are slightly above the global average of 30˚C/km suggesting that the geothermal reservoir is either deep-seated or offset from the drilled sites.

Kibiro geothermal prospect

Geology

The Kibiro geothermal prospect is divided into two entirely different geological environments by the escarpment, which cuts through the field from SW to NE (Figure 4).

To the east of the escarpment, the geology is dominated by Precambrian crystalline basement, characterized by granites and granitic gneisses that are mylonitic in the fault controlled valleys. To the west lies an accumulation of thick sequences of Rift Valley arenaceous Kaiso and argillaceous Kisegi sediments of at least 5.5 km thickness, but without any volcanic rocks on the surface. The faults of the escarpment that strike N50^{0}E constitute the main structures in the tectonic environment. The forces causing the rifting of the Archaean plate have put stress on the granitic rocks resulting in block faults with two main directions, N20^{0}E and N90^{0}E.

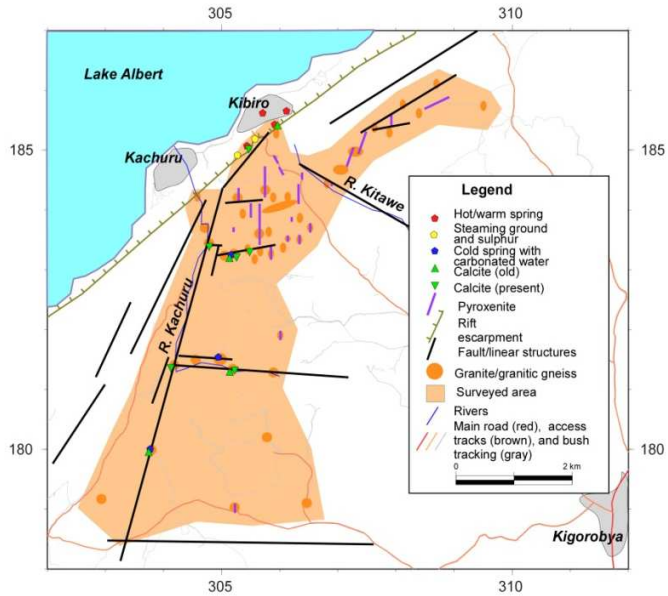

Figure 4: Kibiro. Geology and geothermal surface manifestations (from Gislason, et. al., 2004).

Crosscutting joints striking mainly E-W and N20^{0}E with vertical dips are found in all the rock types. A less common joint set of N130^{0}E also occurs (Gislason et.al., 2004) (Figure 4).

Some joints are open while others are filled with secondary minerals commonly quartz or siliceous material and rarely by calcite. The faulting and jointing in the crystalline basement constitute high yielding aquifers as evidenced by the shallow thermal gradient wells drilled in the area.

Recent geological and geophysical studies show anomalous areas that can be traced along faults in the block faulted granites to the east and away from the Rift escarpment (Gislason, et. al., 2004).

Geothermal manifestations

The geothermal surface manifestations in the Kibiro geothermal prospect are mainly concentrated at Kibiro and Kachuru, west of the escarpment, on the shores of Lake Albert. They comprise hot and warm springs at Kibiro, and fumarolic activity at Kachuru (Figure 4). The fumarolic activity is heavily pronounced in the Kachuru area and along the escarpment for approximately 1.5 km from the intersection of the Kachuru fault and the main escarpment to the Kibiro hot springs. Calcite deposits are observed in cracks and fissures in many locations along the escarpment, Kachuru fault, Kitawe fault and in the crystalline rocks located south-southeast of Kibiro, indicating extinct thermal fluid discharges (Figure 4).

The hot springs at Kibiro are apparently related to a secondary fault, oblique to the main Rift fault, and most likely controlled by their intersection (Figure 4). The total flow measured from the hot springs is approximately 7 l/s and the maximum surface temperature is 86.4˚C (Gislason et. al., 1994).

Geochemistry

The fluids are characterized by a neutral pH, and salinity of 4,000 - 5,000 mg/kg total dissolved solids. A subsurface temperature of 200 - 220°C is inferred by geothermometry and mixing models (Armannsson, 1994).

Isotope hydrology

Stable isotope results show that two groups of waters located east and south of Kibiro represent the groundwater that could be the source of recharge for the Kibiro hot springs (Figure 5). A massive flow of groundwater from a higher elevation than all the cold-water sampling points is also suggested. This high ground is represented by the Mukhihani-Waisembe Ridge in Kitoba subcounty, located 20 km southeast of Kibiro.

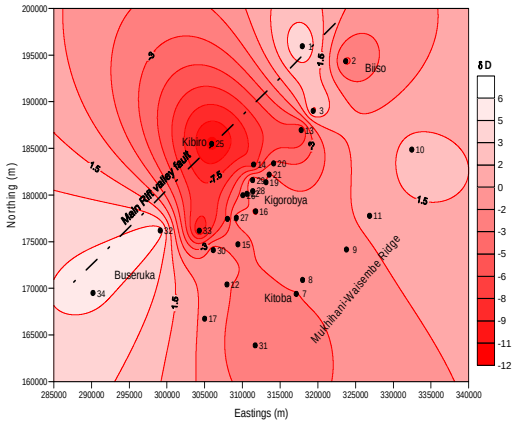

Figure 5: Kibiro. Deuterium variation in surface and groundwaters, dots represent sampling points.

The tritium concentration of the Kibiro hot spring water is 1.25 TU similar to that of the groundwaters (0 - 3.5 TU), and indicates that the hot spring water has cold groundwater contribution as suggested by geochemical modelling and is therefore a mixture of a hot water component and cooler water (Ármannsson, 1994). However, it should be noted that the tritium background in precipitation for the area is rather low, up to a few tritium units only, and indications of mixing may not always be clear.

The isotope composition of sulphur and oxygen in sulphates expressed in $\delta^{34}S$ (SO_4) and $\delta^{18}O$ (SO_4) suggest a magmatic contribution. Strontium isotopes in water and rock ($^{87/86}Sr_{H2O}$, $^{87/86}Sr_{Rock}$) indicate an interaction between the granitic gneisses and the geothermal fluids. The reservoir rock types in Kibiro are, therefore, granitic gneisses (Bahati, et. al., 2005).

Geophysics

The results of the geophysical surveys indicate the existence of anomalous areas in the Kibiro prospect (Gislason et. al., 2004). A low resistivity anomaly trench was traced into the crystalline basement, following the fault lines of the block-faulted granites, first to the SSW away from Kibiro and then following W-E fault lines toward Kigorobya Town (Figure 6).

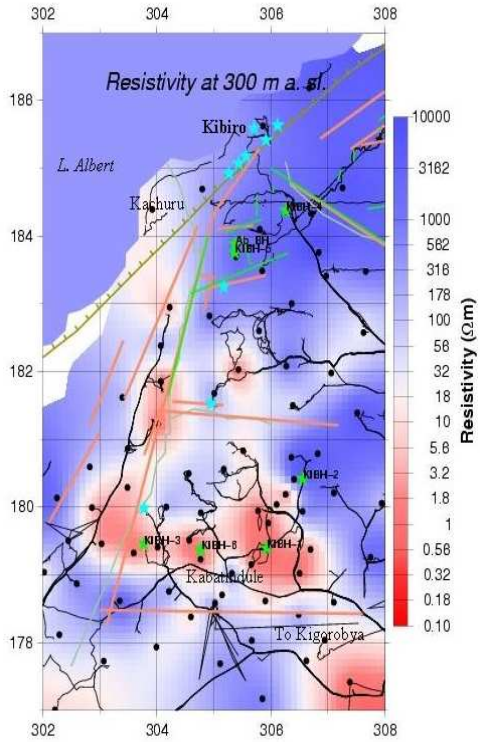

Figure 6: Kibiro. Resisitivity at 300 m a.s.l., faults and fractures, geothermal surface manifestations (stars) (from Gislason et. al., 2005).

The gravity data does not show any distinct density variations, except for the large density contrast between the sediments in the Rift Valley and the granites east of the escarpment. There is, however, an indication of a higher gravity field in an area roughly coinciding with the W-E low-resistivity anomalous area (Figure 6). This might indicate a deep higher density intrusive acting as a heat source for the geothermal activity producing the low-resistivity anomaly.

The cause of these low-resistivity anomalies can, at the moment, not be stated with certainty, but the most likely explanation is conductive alteration minerals in fractures in the otherwise resistive base-rock. Saline water in fractures could also be a possible candidate, but the relatively low salinity of the water discharges from hot springs at Kibiro and other cold springs in the area makes this rather unlikely.

Temperature gradient drilling

Six thermal gradient wells were drilled up to 300 m in the geophysical anomalous areas in the crystalline basement. The lithological analysis and the temperature gradient results indicate absence of a geothermal gradient east of the escarpment (16˚C/km) but slightly elevated towards the escarpment (31˚C/km). The results indicate that the anomalous area in the crystalline basement east of the escarpment is not caused by a geothermal activity or represents an old geothermal system that has cooled down.

Buranga geothermal prospect

Geology

Buranga is located at the foot of the Rwenzori massif near the base of Bwamba escarpment and localized by the major Rift Valley faults (Figure 7). Buranga has no evidence of volcanism but is highly tectonically active.

The hot springs emerge through sediments of Kaiso beds and peneplain gravels. The Kaiso beds and peneplain gravels consists of variable sands and gravels with irregularly distributed boulders containing sub-angular fragments.

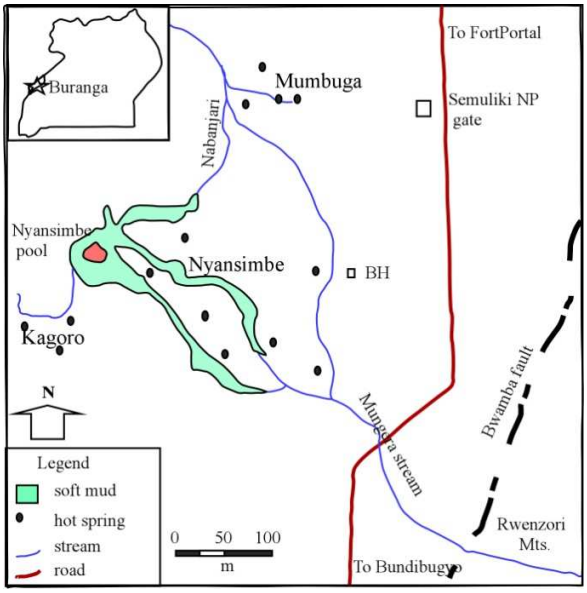

Figure 7: Buranga geothermal area.

The Kaiso sediments are underlain by fine to medium-grained, poorly consolidated sands and clays; some coated with calcareous material. Precambrian rocks of the main rift fault, which strikes N45^{o}E and dips N60-65°E, underlie the sediments. The rocks form the northern half of Rwenzori massif and consists mainly of migmitites, gneisses and amphibolites. They strike N10-30°E and have complex joint systems. The hot springs seem to lie on a fracture/fault line striking N40^{o}E parallel to main rift fault.

Geothermal manifestations

Buranga has the most impressive surface geothermal manifestations with a wide areal coverage in the whole of the western branch of the East African Rift System. They include hot springs that are close to boiling and calcareous tufa. The surface temperature is close to 98˚C and the flow is approximately 10-15 litres/second, an indication of high permeability.

Geochemistry

The fluids are neutral with a pH of 7-8 and salinity of 14,000 – 17,000 mg/kg total dissolved solids. In the earlier study by Ármannsson (1994) a good agreement was obtained for all plausible solute geothermometers tested for several hot springs and pools in Buranga and it was concluded that the subsurface temperature was 120 - 150°C.

Isotope hydrology

The results from stable isotopes suggest that the geothermal water is from high ground in the Rwenzori Mountains like in Katwe (Figure 8).

There is no tritium in the thermal water from Buranga which implies that it is not mixed with cold groundwater. The strontium ratios in rocks indicate that the geothermal water, most likely, interacts with granitic gneisses. The source of sulphate is minerals or rock (terrestrial evaporates) with a possible magmatic contribution (Bahati et. al., 2005). Studies by the Federal Institute for Geosciences and Natural Resources (BGR) of Germany and the Government of Uganda using helium isotopic ratio ($^{3}He/^{4}He$) in gaseous discharges from hot springs also suggest a magmatic source of solutes for Buranga (BGR-MEMD, 2007).

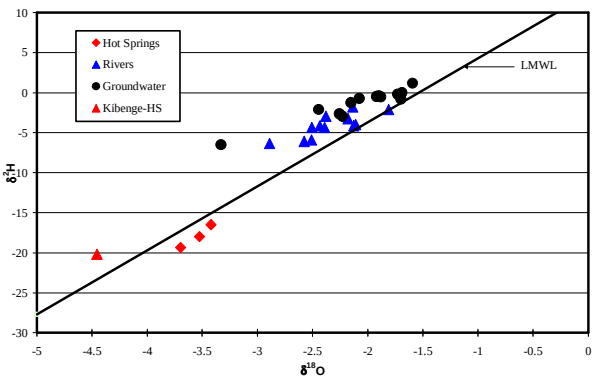

Figure 8: Buranga. Stable isotopic composition of hot and cold water samples.

Panyimur geothermal prospect

Geology

Panyimur hot springs are located on escarpment front just near the shores of Lake Albert, in Panyimur subcounty, Nebbi district (Figure 1).

The area is characterized by fractured crystalline basement rocks such as coarse hornblende gneisses, coarse hornblende garnet rocks, talcose rocks and pegmatitic veins in a gorge that dips into the escarpment from the hot springs. A foliation/basement schistose trends NNE-SSW. Others schistose trend almost NE, parallel to the local major faults.

Rocks in the area include crystalline basement rocks (coarse jointed granitic-gneiss outcrops to the west) and Pleistocene sediments to the east of the Rift fault boundary.

Surface manifestations

The thermal area can be divided into three groups of hot springs namely; Amoropii, Okumu and Avuka, all along the escarpment of the Rift Valley. The hot springs are aligned in a northwest direction possibly controlled by the major normal boundary rift fault for a distance of approximately 1.5 km with Amoropii further east and Avuka further west. It is anticipated that the springs rise at or close to the fault. Other surface manifestations reported include deposits of travertine, sulphurous algae and smell of hydrogen sulphide characteristic of a high temperature area. The surface temperature ranges from 35˚C to 58˚C. The maximum surface temperatures at Avuka is 35˚C, at Okumu is 44˚C and 58˚C at Amoropii.

The Okumu hot spring is tapped through a protected spring which is surrounded by inactive travertine mounds (old spring deposits). The Avuka thermal area is characterized by thermophyllic (geothermal) grass in a boggy environment. All the discharges are characterized by gas bubbling.

Geochemistry

The fluids are slightly above neutral with a pH of 7-9 and low salinity of 300 – 900 mg/kg total dissolved solids (Armannsson et. al., 2007). Presence of hydrogen sulphide in Okumu (2.48 ppm) and Amoropii (5.61 ppm) hot spring waters indicates that the source of heat is volcanic and, therefore, the possibility of a high subsurface temperature in the area. But the Quartz and NaK predicted geothermometer temperatures of 100-115°C and 100-140°C for Panyimur are low suggesting that the sampled waters may not be in equilibrium and most likely contaminated with surface cold waters. A repeat of the sampling is needed to get more representative samples which could assist in delineating the subsurface temperature of the area.

Other geothermal areas

The rest of the geothermal areas of Uganda are at a preliminary level of investigation. The current results predict subsurface temperatures of 100 - 160˚C suitable for electricity production and direct uses. Four areas have been selected for detailed surface exploration and they include Rubaare in Ntungamo district, Kitagata in Bushenyi district, Ihimbo in Rukungiri district, and Kanangorok in Kabong district.

CONCLUSIONS

Subsurface temperatures of 140-200°C, 120-150°C and 200-220°C are inferred by geothermometry for Katwe, Buranga and Kibiro respectively. These temperatures, if confirmed, are high enough for electricity production and for direct use in industry and agriculture.

Anomalous areas have been partially mapped by geology and geophysical studies in Katwe and Kibiro prospects.

Temperature gradient measurements (30 - 36°C/km) suggest deep geothermal reservoirs in Katwe and Kibiro that are either deep seated or offset from current drilled positions.

Isotope hydrology results indicate the source of the geothermal fluids to be from high ground in the Rwenzori Mountains for Katwe and Buranga, and from the Mikihani-Waisembe ridge for Kibiro. Reservoir rock types are most likely basalt in Katwe, and granitic gneisses in Buranga and Kibiro.

Three areas, Katwe, Buranga and Kibiro, have reached advanced stages of surface exploration.

The fourth area, Panyimur, has indications of a geothermal prospect following the results of the petroleum drilling programme that has encountered high temperature gradients (maximum 80˚C/km) in the vicinity of the thermal area. Presence of H_2S in the thermal waters is an indication of a volcanic source of heat and a high temperature area but predicted sub surface temperatures are as low as 100-140 ˚C.

In other areas, the current study has identified other potential geothermal areas with subsurface temperatures of 100-160˚C good for further exploration and development.

RECOMMENDATIONS

Katwe: Before the feasibility study is undertaken, the following need to be done: 1) Carry out additional geophysical surveys using the Magnetotellurics (MT) and Transient Electomagnetics (TEM) methods to delineate the boundaries of the low resistivity anomalous areas, probe in the deeper layers of the crust and identify the heat source, 2) Structural geological and hydrological mapping focused on locating drill sites, 3) Updating of the geothermal models and location of drill sites.

Kibiro: Before the feasibility study, the following need to be done: 1) Carry out additional geophysical surveys using the MT and TEM methods to delineate the boundaries of the geothermal anomalous areas from the current large anomalous area, 2) Structural geological and hydrological mapping focused on locating drill sites, and 3) Updating of the geothermal model and location of drill sites.

Buranga: Has not reached advanced stages in surface exploration like Katwe and Kibiro. The following activities need to be done before the area is recommended for the feasibility study: 1) Carry out detailed geophysical surveys using MT and TEM, Gravity and Micro-seismics to delineate geothermal anomalous areas and 2) Updating of the geothermal model and location of drill sites.

Panyimur: This area is still at the reconnaissance stage of investigation. The following activities need to be done before the area is recommended for the feasibility study: 1) Carryout detailed geological, geochemical and geophysical (MT, TEM and Gravity) surveys at Panyimur to delineate geothermal anomalous areas, identify the source of heat and targets for deep drilling, 2) Carryout hydrological and hydrogeological surveys to study in detail the structures that control the fluid flow mechanisms, 3) Updating of the geothermal model and location of drill sites.

Feasibility study: Drilling of 2-3 wells to discover a reservoir in the most promising prospect(s); Katwe, Buranga, Kibiro and Panyimur. The objective of the feasibility study is to drill at selected sites; prepare technical and financial/investment plans for the installation of an appropriately sized power plant and feasibility of direct use in industry and agriculture.

The rest of the geothermal areas should be investigated in detail for the possibility of installing binary geothermal power plants. The most promising areas from the current results include Rubaare in Ntungamo district, Kitagata in Bushenyi district, Ihimbo in Rukungiri district, and Kanangorok in Kabong district.

Institutional Model: The current institutional model for geothermal activities is inadequate since the activities are divided between two departments making the execution of geothermal projects difficult. There is therefore a need for a single independent institution that should take the resposibility for geothermal exploration and development.

ACKNOWLEDGEMENTS

The authors wish to thank all the organisations/governments that have supported the Uganda geothermal exploration and development programme since 1993. They include the United Nations Development Programme (UNDP), Organization of Petroleum Exporting Countries (OPEC), International Atomic Energy Agency (IAEA), African Development Bank (AfDB), World Bank (WB), Federal Institute for Geosciences and Natural Resources (BGR) of Germany, and Governments of Iceland and Uganda.

REFERENCES

Ármannsson, H., 1994. Geochemical Studies on three geothermal areas in West and Southwest, Uganda. Final Report. Geothermal Exploration UGA/92/003, UNDESD, GSMD, Uganda, 85pp.

Ármannsson, H., G. Bahati, V. Kato, 2007. Preliminary investigations of geothermal areas in Uganda, other than Katwe-Kikorongo, Buranga and Kibiro Final Report. ICEIDA, MEMD, Uganda, 19 pp

Bahati, G., 2003. Geothermal Energy in Uganda, Country update. International Geothermal Conference, Reykjavik, Iceland. S04 paper 124, p. 48-53.

Bahati, G., Z. Pang, H. Armannsson, E.M. Isabirye, V. Kato, 2005. Hydrology and reservoir characteristics of three geothermal systems in Western Uganda, Geothermics, 34, p.568-591.

BGR-MEMD, 2007. Detailed surface analysis of the Buranga geothermal prospect, West-Uganda. Final terminal report, 168 pp.

Gislason, G., G. Ngobi, E.M. Isabirye, and S. Tumwebaze, 1994. An Inventory of three Geothermal Areas on West and Southwest Uganda. Prepared by the United Nations for a Project of the UNDP.

Gíslason, G., K. Árnason, H. Eysteinsson, 2004. The Kibiro Geothermal Prospect. A Report on a Geophysical and Geological Survey. Prepared for the Icelandic International Development Agency and the Ministry of Energy and Mineral Development, Uganda. Unpublished report, June 2004. 109 pp.

Gíslason, G., K. Árnason, H. Eysteinsson, 2005. The Katwe and Kibiro Geothermal Prospects. A Draft Report on a Geophysical and Geological Survey. Prepared for the Icelandic International Development Agency and the Ministry of Energy and Mineral Development, Uganda.

Gíslason, G., K. Árnason, H. Eysteinsson and Ingvar T. Magnusson, 2008. The Katwe Geothermal Prospect. A Draft Report on a Geophysical and Geological Survey. Prepared for the Icelandic International Development Agency and the Ministry of Energy and Mineral Development, Uganda.

Groves, A.W., 1930. Report on the nature, origin and available supply of the salt of Lake Katwe, Kasenyi, with notes on Lake Kikorongo and an appendix of the petrography of volcanic bombs of the district.

Kato, V., 2003. Geology of Katwe – Kikorongo Prospect. Unpublished DGSM Report KVK-22.

McNitt. J.R., 1982. The geothermal potential of East Africa. In proceedings of the Regional Seminar on Geothermal Energy in Eastern and Southern Africa, Nairobi, Kenya. P. 3 - 8.

Musisi, J., 1991. The neogene geology of the Lake George – Edward basin, Uganda. *PhD thesis*.

Wayland, E.J., 1935. Notes on thermal and mineral springs in Uganda. UGSM Bull. 2, p. 44-54

PLANNING OF GEOTHERMAL PROJECT IN THE UNION OF COMOROS

Boinaïdi Ali Saïd
Energy Ministry of Comoros
BP. 1762 MA-MWE, Moroni,COMOROS
boinaidalisaid@yahoo.fr

ABSTRACT

The Comoros archipelago is composed of four islands (Grand Comore, Moheli, Anjouan and Mayotte) all of which are of oceanic volcanic origin. Grande Comore Island is composed of two large shield volcanoes known as Karthala and La Grille. A heat source for the geothermal system exists under the volcano. There are geothermal manifestations include fumaroles on the northern side of Karthala volcano, hot springs and gas emissions from existing boreholes.

The reconnaissance study of geothermal resources that have been conducted in April 2008 by KenGen in Grande Comore show the possibility of exploiting the existing geothermal potential. And thanks to these studies the Comorian government made the decision to complete the exploration surveys, build capacity for geothermal energy, mobilize funds and make a generic plan for the development of geothermal resources.

1) The action plan of the project consists of four phases each dependent for a period of 5 years:
2) The realization of preliminary studies,
3) Appraisal study,
4) Project design,
5) Construction and field development,
6) Operation (Production and resource management).

The objective of this project is to install a geothermal energy between 10-15 MW.And the Comoros government is subject to request the admission of the Comoros to ARGeo.

GEOTHERMAL EXPLORATION ADVANCEMENT IN DJIBOUTI

Mohamed JALLUDIN
CERD, Centre d'Etudes et de Recherches de Djibouti, P.O. Box: 486, tel: (253) 35 27 95
Email: jalludinmak@yahoo.com, Djibouti, Republic of Djibouti

ABSTRACT

The Republic of Djibouti is located within an exceptional geodynamic situation, the Afar Depression, an emerged triple junction of the Red Sea, Gulf of Aden and East African rifts, where volcanic and tectonic activity occurs since 30 My, and numerous current and past hydrothermal activities are identified mostly in the Western part of the country. Twelve prospects are recognized from which there are Asal rift, lake Abhe and others.

Although geothermal explorations began from the early 1970s, the generation of the geothermal energy is still at the stage of programming.

Given that energy is a key sector for the economical and social development of the country to alleviate poverty, the Government of the Republic of Djibouti is strongly committed in developping as much as possible the geothermal resources. Over the years 2000, Djibouti conducted a significant policy of capacity building of CERD, the national research center, in order to give the capability to prepare faisability studies reports for the geothermal prospects. As a results CERD has launched such studies on the Djibouti aquifer thermal anomalies and the prospect of Nord-Goubhet.

In addition, being active for the promotion of the geothermal energy, private sector has been involved on different geothermal prospects: Asal rift and lake Abhe.

INTRODUCTION

Two main phases are identified for the geothermal exploration in the Republic of Djibouti over the last thirty years but the underground geothermal energy has not yet reached the stage of exploitation. However, today a new era can be considered within the frame of the third phase where several prospects are under study to prepare the faisability phases with exploration drillings.

The commitment of the Government of Djibouti to tackle the energy sector with geothermal energy as a priority has led to this new phase with the involvment of private sectors and the capacity building at all levels of the national research institution, CERD.

After a short review of the past activities, the paper describes the advancement of the geothermal exploration sector in the Republic of Djibouti.

BRIEF SUMMARY OF THE PAST ACTIVITIES

The geothermal exploration can be divided in two main phases. The first phase concerns the exploratory survey conducted by BRGM (1970), which showed possible potential geothermal areas as Lake Asal, Lake Abhé, Allols, Nord-Ghoubet, Arta and Obock to be prospected by drillings (fig. 1). The two initial drillings in the rift of Asal in 1975 (BRGM) recognized a deep reservoir at 1000 m depth with a high mineralisation (180 g/l) fluid and 260°C. The low production of the well Asal 1, located in the Southern area of Asal rift, decreased relatively quickly because of mineral deposits in the wellbore casing and in the surface tubings.

The second phase beginning in 1981 (AQUATER) delt with the exploration of Hanlé-Gaggadé area, recent tectonic basins, located between Abhé and Asal. Results from Hanlé plain drillings reported a good permeability aquifer but containing a low temperature fluid (AQUATER 1989). The fresh water underground flow from the downstream Awash river valley would explain the low temperature of the reservoir. With respect to the new drilling capacities the exploration continued in the Asal area with four new wells. Although Asal 3 located nearby Asal 1, revealed a maximum well head pressure of 21 bars and a maximum discharge rate of 350 ton/h, it is still accompanied by scaling and also by decreasing of the discharge rate. Except Asal 6 located in Asal 3 area, the other wells located toward the axial rift area, did not recognized the reservoir.

If technical solutions to exploit the deep Asal reservoir are still to be found, there exist an alternative geothermal resource with the low depth reservoir in the Asal area. The latter has not been tested but the preliminary data (50 g/l;

130°C to 190°C) of the fluid and the extension of the reservoir as it has been recognized by all Asal wells, gives the possibility of a geothermal resource development using binary systems.

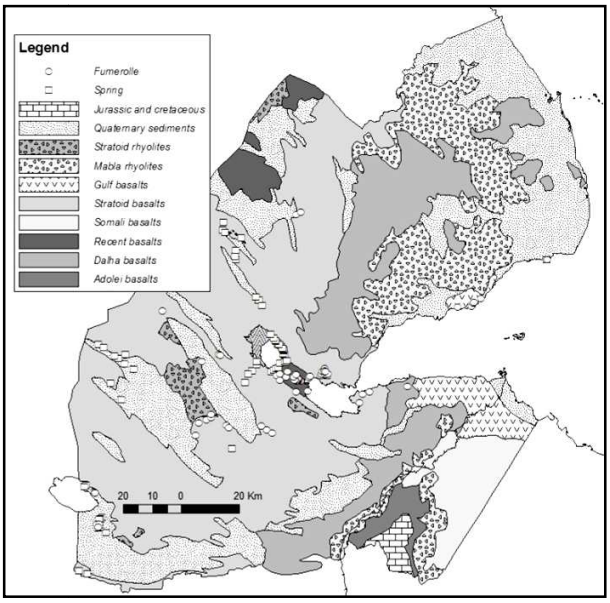

Figure 1. Geothermal surface manifestations in Djibouti

ASAL RIFT GEOTHERMAL PROSPECT

Since the last exploration by drillings in 1988 and other few studies by the 1990 on the corrosion and scaling in the Asal rift geothermal prospect new exploration activities have taken place only by 2008. Such activities were initiated by the cooperation of Djibouti and Iceland Governments and the involvement of a private sector, Reykjavick Energy Invest, REI. Within the frame of this new exploration phase, agreements including general agreement, the head of terms of the document project and the head of terms of the power purchase agreement were signed.

The programme realized a new and complete geophysical coverage of the Asal rift using TEM and MT methods. From this 106 TEM and 102 MT soundings were executed. In addition a tectonic/structural survey was conducted based on aerial and satellite images and field works (fig. 2).

The analysis of the results brought REI to propose a more targeted area of exploration within the Asal rift, known as Fiale and represented by a collapsed large caldera. The previous explored area of the well Asal 1 is located close to the Southern margin of the Asal rift. Based on those results, a faisability study programme was prepared including deviated exploratory wells.

An Environmental Impact Assessment study has been also undertaken by the programme of REI for the Asal rift region.

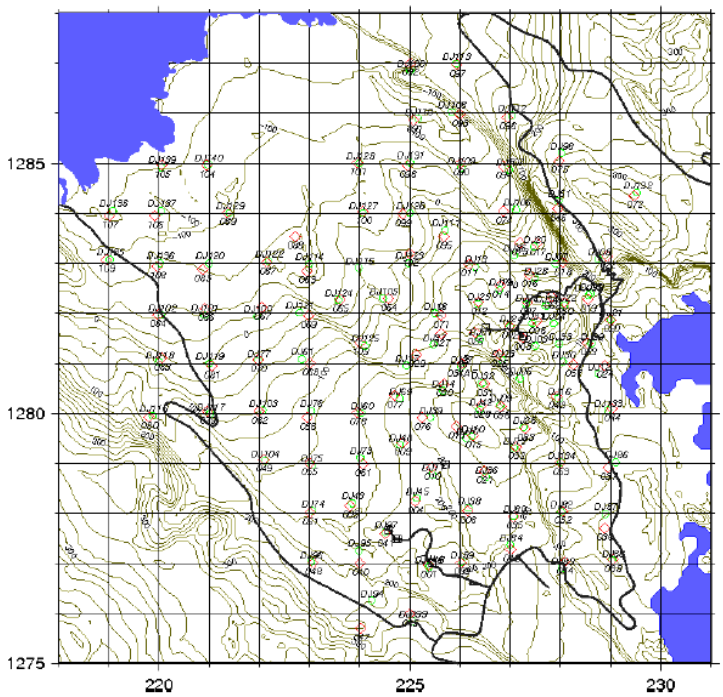

Figure2: TEM and MT surveys of Asal rift (REI-ISOR 2008)

Given the complex Asal geothermal reservoir with the presence of brine a modeling project has been undertaken. The PhD-project (Daher 2010) involves the study of the Asal geothermal resources based on the analysis of existing and new field data collected by REI. The principal tool used is a detailed numerical reservoir modelling, while other methods of reservoir analysis are used as well as interpretation of underground resistivity data. Chemical data also provide input for the project. The aim of the study is to:

- Significantly improve understanding of the nature of the complex Asal brine geothermal system. Asal geothermal reservoir capacity assessment between 115 and 329 MWe with 95% interval confidence is done by using the Volumetric method.
- Develop a conceptual model of the system on the basis of all available old and new data (geological logs, hydrothermal alteration, chemical analyses, well production). The resistivity data collected from October to December 2007 are of major importance here.
- Develop a numerical model of the Asal system based on forward modelling with TOUGH2. TOUGH2 is a numerical simulator for non-isothermal flows of multicomponent, multiphase fluids in one, two, and three-dimensional porous and fractured media (fig. 3). It is widely used and considered the most advanced and powerful geothermal reservoir simulator available.
- Inverse modelling with iTOUGH2 is applied, which helps in the development of the conceptual model. This inverse modelling software was developed for the non-isothermal, multiphase, multicomponent numerical simulator TOUGH2 to facilitate automatic history matching and parameter estimation based on data obtained during testing and exploitation of geothermal fields. The iTOUGH2 code allows one to estimate TOUGH2 input parameters based on any type of observation for which a corresponding simulation output can be calculated.
- Underground resistivity is incorporated in the modelling study, during forward modelling, and is attempted during the inverse modelling phase.
- The numerical model will furthermore be used to select the most appropriate region for future reinjection.

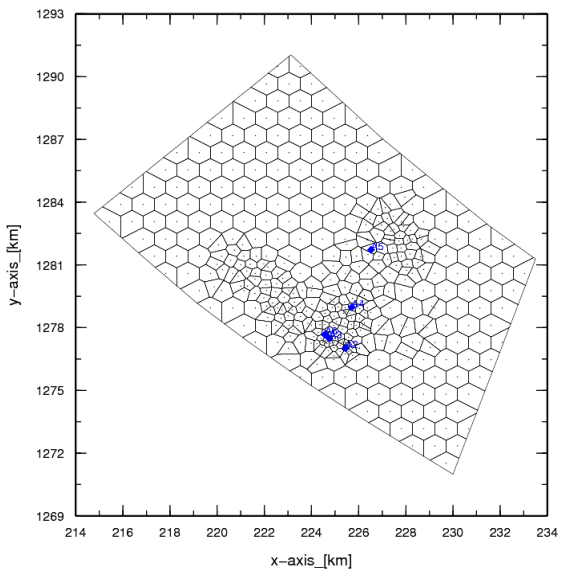

Figure 3: Mesh for the Asal rift geothermal system modeling

The next immediate step for the Asal rift prospect is the faisability study with at least three deviated wells in the Fiale area (REI 2008). Such exploration drillings might lead to the development of the geothermal energy with a minimum of 50 MW power plant.

NORD-GOUBHET

The Nord-Goubhet area is located North-Eastward but close to the Asal rift. Goda mountain and Makarassou region are found in the Northern part and the study zone is limited by the sea in the South. The geology is marked by the Dalha basalts outcrops covered by the more recent Gulf basalts and pleistocene sediments (fig. 4). The fracture network is well developped. The area is situated between different zones of different tectonic pattern and therefore is affected by several tectonic trends: Asal rift NW-SE faults, Makarassou N-S trends and old trends identified in the Goda mountain.

Along the scarped valleys of the wadis several fumaroles and one boiling spring are found at the bottom of the volcanic cliffs. Different methods applied to the chemical data from the condensate of the fumaroles give estimations for the possible reservoir temperature: 220°C and 170°C. Stable isotopes analysis of the fumaroles describe an assumption of the origine of the waters. Compared to the fumaroles of the Asal rift zone, Nord-Goubhet fumaroles have significantly lower Deuterium and Oxygene18. It is suggested that no primary steam from undiluted or diluted deep water exist in this zone. Fumaroles would be more likely the result of a secondary steam from previously condensated steam or boiling groundwater (Geothermica 1987).

Three geophysical surveys were conducted in the area of Nord-Goubhet: gravimetry, AMT and electric (rectangle method) (BRGM 1983). The gravimetric results point out several heavy and light anomalies not distributed regularly. Although these anomalies are of low amplitudes they are more or less clearly delimited by the different linear trends, correlated to the tectonic of the area. From their analysis, BRGM retain three main guidelines. First, the Southern Asal rift system delimits light anomalies. Parallel to it and Northward, a large axis comprises a succession of heavy and light anomalies. In the central part, a similar axis is identified along a NNW-SSE trend. It can be noticed that the major part of the hydrothermal activity is located between these two axis. Finaly, light anomalies cover the Eastern part of the prospect. The geoelectrical survey shows globaly low resistivities and three main zones can be observed. The first one is located on the Eastern part of the prospect. The second low resistivty area is located on the South-Westrn zone but higher resistivities are found along a NNW-SSE axis. The last and very conductive area is located in the North-Western part. It has been estimated that the bottom of the conductive zone

would reach around 1000 meters. The AMT survey identifies in the central zone of the prospect an uplifted conductive body. The results from the three geophysical surveys cannot be completely intercorrelated. However, findings from the gravimetric and the geoelectrical methods bring out interesting approach of the underground structures in relation with the surface hydrothermal activities that can guide a drilling exploration.

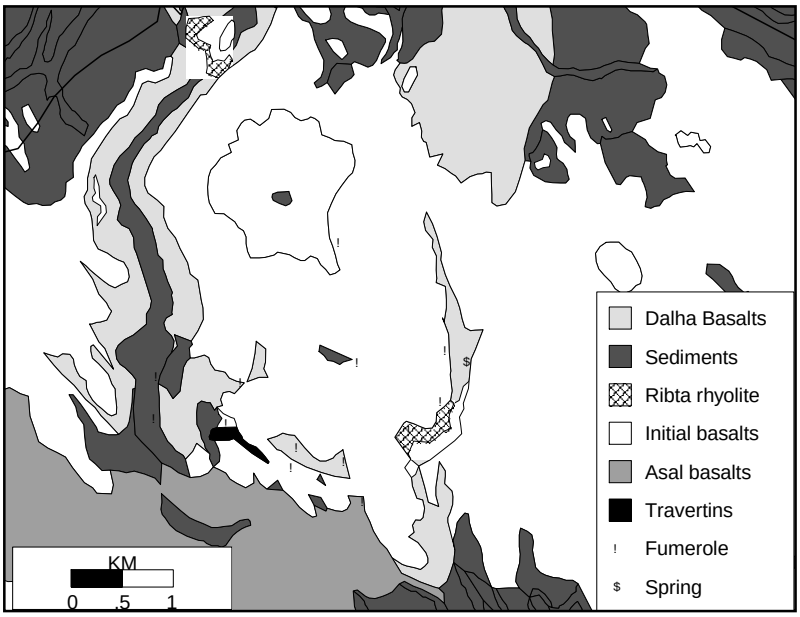

Figure 4. Nord-Goubhet prospect

A new phase of exploration is undergoing by CERD to complete the exploration with new data. This prospection comprise firstly a geophysical survey that applies TDEM and MT methods. Up to now 25 TDEM and MT stations were realized in the area of Nord-Goubhet. Surface manifestations as fumaroles and hot springs are also sampled for geochemical and isotopic analysis. A pecular analysis is undertaken of the surface manifestations and the weathered zones according to the geology and the structural features. These prospections will be completed by the environmental impact assessment of the study area in order to finalise the prefaisability study that will allow the exploration drilling in the frame of the faisability study.

LAKE ABHE AND DJIBOUTI PROSPECTS

Lake Abhé zone is located in the South-Western region of the country, on the border with Ethiopia. This hypersaline lake is the Western end of the Gobaad plain and the Eastern end of the dowstream valley of Awash river coming from the Ethiopian plateau. The geology is characterized by th stratoid basalts plateaus limited by E-W faults configuring the Gobaad plain, filled by quaternary and probably late pliocene sediments. The lake area is particularly rich of surface hydrothermal manifestations with fumaroles and hot springs but also travertine constructions, some of them being elevated at more than 60 m above ground level. The travertines are aligned on the main fracture trends. Fumaroles are located on those travertines and the hot springs occur at the bottom of these travertine chimneys. The temperature of resurgence of the hot springs is generaly higher than 90°C. Only geochemical preliminary studies cover this prospect and give mainly two types of waters. Most of the hot springs are alkaline-chloride-sulfated and few of them present also a bicarbonated type as a result of surface water mixing. The surface hydrothermal manifestations are spread over an area of about one hundred square kilometers. This observation suggest that in lake Abhé zone there exist an important thermal anomaly representing potential geothermal reservoir.

The lake Abhe prospect is under an agreement with the private sector, Hydrocarbon Co., since 2009. The environmental impact assessment study has been launched but the prefaisability study might begin in the next future.

The Djibouti prospect is represented by the aquifer of Djibouti exploited for fresh water supply to the town of Djibouti. It is located around the capital and extends over an area of about 500 km². The recent basalts of Gulf constitute the fractured and heterogeneous aquifer. There are no surface manifestation in this prospect but there are few thermal anomalies on the groundwater wells at Awrawsa and Wead in the Northern part of the aquifer. The temperatures between 100 meters and 150 meters reaches 60°C.

Therefore some preliminary studies were programmed and undertaken by CERD with the cooperation of University of Brest. Previous large grid MT and recently MT and TDEM methods results are under interpretation for the temperature anomaly zones.

CONCLUSION

The energy sector in Republic of Djibouti needs a clean and cheaper energy in order to boost the social and economical development of the country. However most of the geothermal prospects are not studied and slow down the resources evaluations. Therefore, the Government of Djibouti conducted an intensive programme and actions to build up the capacities of CERD, the national research center, to be able to undertake the prefaisability studies of the geothermal prospects.

Those studies are already in progress on the prospects of Nord-Goubhet and the Djibouti aquifer and the others will be covered progressively.

The commitment of the Government of Djibouti has brought private sectors on two main prospects, Asal rift and lake Abhe. Asal rift faisability programme with deviated exploration wells is on the stage to be launched. In the case of lake Abhe prospect prefaisability studies, surface studies, would start in the next future.

REFERENCES

AQUATER 1981. Projet pour l'évaluation des ressources géothermiques. Gouvernement de Djibouti. ISERST. 137pp

AQUATER 1989. Djibouti geothermal exploration project. Republic of Djibouti. Final Report. ISERST. 159pp

BRGM 1970. Reconnaissance géothermique du Territoire Français des Afars et des Issas. 70SGNGTM. pp59

BRGM 1975. Territoire Français des Afars et des Issas: rapport de fin de sondage: résultats des premiers essais de production. 75SGN442.GTH. 18pp

BRGM 1983. Reconnaissance géothermique par prospections gravimétrique-électrique, audio-magnétotellurique dans la région du Nord-Goubhet (République de Djibouti). 83GPH014. 27pp.

Daher Elmi Houssein. 2010. Reservoir study of the Asal geothermal system. Djibouti. PhD, University of Reykjavick, under preparation

Reykjavick Energy Invest. 2008.The Asal geothermal field, Djibouti. Geothermal surface exploration 2007-2008. ISOR

THE POTENTIAL RELATIONSHIP OF SOME GEOTHERMAL FIELD IN UGANDA.

Deus Katomi Muhwezi
Department of Geological Survey and mines
Ministry of Energy and Mineral Development. P.O. Box 9, Entebbe UGANDA
deuskatomi@yahoo.com

ABSTRACT

Detailed geological work has been concentrated on three main geothermal areas of south western Uganda that is Katwe-Kikorongo, Buranga and Kibiro Hot springs. This included geochemical exploration, isotope hydrology, geological mapping and geophysics. Resistivity located an anomaly in Katwe and Kibiro thought to be a geothermal reservoir. However, drilling to the depth gave no sign of geothermal activity hence a need to expand on the previously drilling targeted areas and probing deeper. Under this project, study has been made to correlate different geothermal hot springs with the aim of grouping them into geothermal fields. The characteristics of the geothermal fluids were studied using Cl-SO_4-HCO_3, Na-K-Mg , Cl-Li-B ternary diagrams, Speciation using WATCH 2.1 version, isotopes, ratio of conservative elements and mixing models. Cl-SO_4-HCO_3 ternary diagram classifies Amoropii, Okumu, and Kibiro as chloride waters, Kitagata and Kanangorok, as steam heated waters, Kibenge, Kabuga and Rwagimba as Volcanic waters, Amuru as bicarbonate waters while Amuru (Pakele) and Avuka as peripheral waters. The geothermal fluids come from old base rock rather than underlying sediments and are also partially or fully equilibrated. The δ^2H versus δ^{18}O plots, Cl/B, Cl/Li, Na/K, Na/Cl ratios and plots show that Kibenge, Rwagimba and Kabuga are correlated to Buranga with fluids of similar origin while Kibiro and Panyamur appear to be linked, with Avuka at the peripheral of Kibiro-Panyamur geothermal area. SiO_2-CO_2 mixing model show that there was no boiling in the studied hot springs but with some evidences of mixing. The log Q temperature plots of minerals shows Kanangorok, Kabuga, Kibenge, Rwagimba, and Okumu are saturated with calcite and could be prone to scaling if utilised.

INTRODUCTION

Uganda is one of the east African counties crossed by the East African rift valley. Several geological surveys, including shallow drilling have been carried out on three geothermal areas of Uganda which include Katwe-Kikorongo, Buranga and Kibiro. Preliminary work has also been carried out in other geothermal areas of Uganda, aimed at the development of geothermal energy for rural development. Biomass represents 93% of the energy used in the country, thermal power installed capacity is 100MW_e and installed hydro electric power is 380MW_e that has

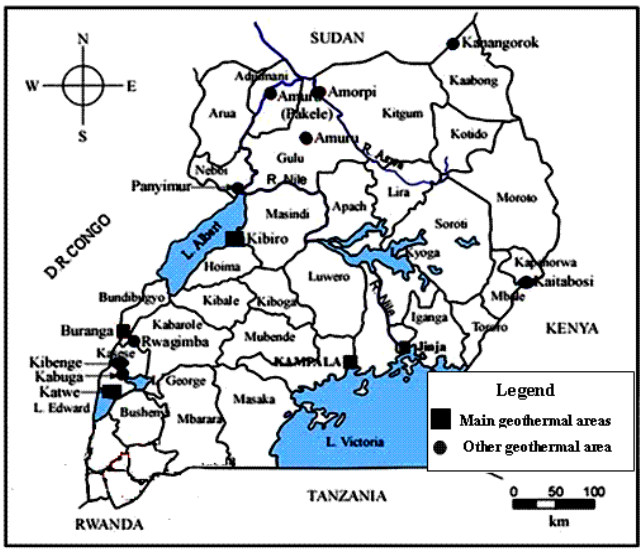

Fig. 1: Map of Uganda showing the hot springs studied

diminished to150MW_e in the past few years due to climatic changes. This has made and unaffordable in addition to electricity expensive being scarce

Since all the oil products are imported. This has made the government consider the development of renewable energy among which is geothermal energy with an estimated capacity of 450MW_e (McNitt 1982)

Study Areas

This study is of the main three geothermal areas, that is Katwe-Kikorongo (Katwe), Buranga and Kibiro, but also Kibenge, Kabuga, Rwagimba and northern Uganda hot springs i.e. Amuru, Avuka Amuru(Pakele), Amoropii, and Kanangorok. These are all located in the Western Rift Valley in the Albertine graben that runs along Uganda-Democratic Republic of Congo border (Fig. 1)

Aim / Scope of the Study

During geological, geophysical, and geochemical exploration anomalies for drilling have been located in the Katwe-Kikorongo, Buranga and Kibiro geothermal fields. However, drilling to a depth indicated by the geophysical methods in Katwe-Kikorongo and Kibiro gave a much lower geothermal gradient than expected and there was no sign of geothermal activity in the drill cores. It was however thought that the low resistivity could be due to an ore mineral body in the case of Kibiro and salt deposits in the case of Katwe-Kikorongo. It was therefore concluded that the source of heat is likely to be deep or outside the area previously interpreted as drilling target. The future plan is to use geophysical methods that probe deeper and compare geothermal hot springs to find if there could be a link between the main geothermal hot springs with other neighbouring hot springs to expand the study area.

The objective of the present project is to analyse and correlate the geochemical data for different hot springs, to find a possible potential with reference to geological location and structural controls. These were considered in two groups, Firstly, Buranga, Katwe-Kikorongo, Kibenge, Kabuga and Rwagimba, and secondary Kibiro and Northern Uganda hot springs (Amuru, Amuru(Pakele), Amoropii, Avuka and Kanangorok). To find out whether there is a relationship between fluids of different hot springs, their chemical composition was studied by looking at the conservative constituents that can be regarded as tracers. These include Li, Rb, that are highly mobile, Cl, B, and Br which form soluble minerals and their sources of supply to geothermal fluids limited to saturate it with any mineral (Anórsson,2000b).

Deuterium was also used as conservative isotope in the geothermal fluids due to its mobility. The formation of secondary minerals containing water can cause deuterium to fractionate between mineral and water. However the amount of water held in secondary minerals in insignificant compared to amount flowing through a given rock hence fractionation between the phases will have negligible effect on the deuterium content of the flowing water through it. Also water with temperature below100°C generally shows no oxygen shift and hence the ^{18}O isotope can be used as a tracer. Sulphate can also be reactive in some geothermal systems as it can react and be precipitated as anhydrite but conservative in others (Anórsson, 2000b)

BACKGROUND

The Geology of the geothermal fields

Geology of Kibiro

Kibiro geothermal field is divided into two geological environments by an escarpment of the western branch of the east African rift valley that runs from SW to NE. The eastern side is mainly crystalline basement with granites and granitic gneisses while the western part is characterised by rift sediments. The hot springs are found in the rift sediments (Fig. 2). Kachuru fault trending NNE is oblique to the main rift fault and intersects it at Kachuru and Kibiro Villages. Several surface manifestations are found at the intersection of the two faults (Fig. 3). The surface manifestations entail hot and warm springs, which include Mukabiga and Mwibanda; there are also salt gardens such as the Muntere salt garden. Other manifestations include smell of hydrogen sulphide in the air, steaming grounds, calcite and

Fig. 2: Kibiro hot springs in rift sediments

sulphur deposits (Gíslason et al., 2004, Gíslason, 1994)

Geology of Katwe-Kikorongo geothermal field.

Katwe-Kikorongo volcanic field is located on the escarpment of the western branch of the East African rift valley south of Rwenzori massif. The field has a number of craters that lie on the NE-SW striking main fault. It characterised by basement granite and granite gneisses (Fig. 4) explosion craters, ejected pyroclasts and tuffs (Fig. 5). The craters are believed to have been formed by phreatic eruptions and in some of them like Lake Katwe, Kikorongo and Nyamunuka there are crater lakes with high salinity due to evaporation (Fig. 5) there are also minor occurrences of lava near Lake Kitagata and Kyemengo crater areas.

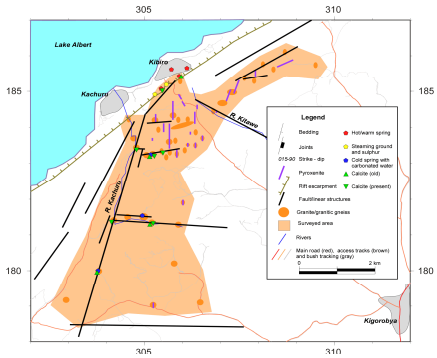

Fig. 3: Geology of Kibiro area

Geothermal surface manifestations are scarce and only found in the Katwe and Kitagata craters.

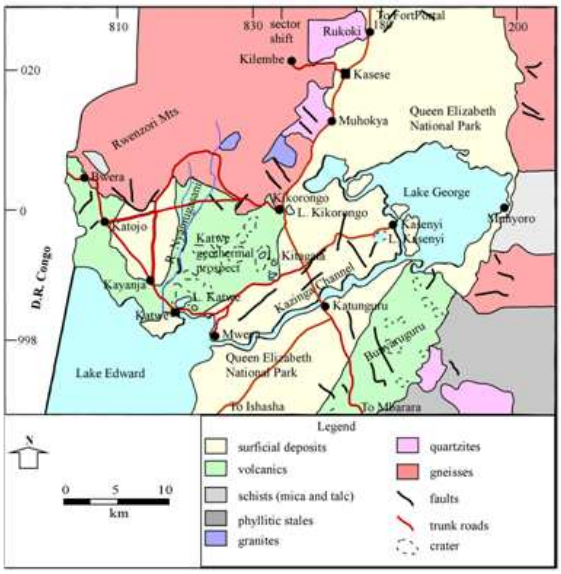

Fig. 4: Map of the geology of Katwe-Kikorongo area

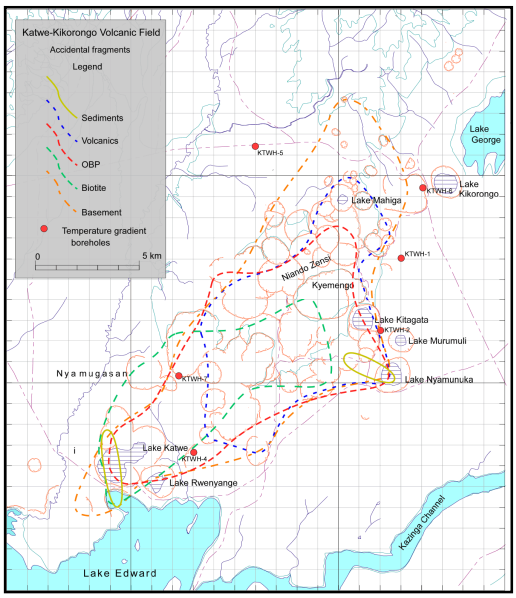

Fig. 5: Katwe-Kikorongo geothermal field showing springs and craters

Geology of Buranga geological field

This field is also in the western branch of the East African rift valley. It is situated in a sedimentary environment and despite the high tectonic activity; Buranga has no evidence of volcanism. It is a geothermal field with sprouting hot springs and high gas flow and travertine

Geology of other geothermal hot springs

Kabuga hot spring (also called Muhokya warm springs) has a temperature of about 40°C and a flow rate of 1 l/s. It has no rock exposure but the surface geology indicates that the springs issue from alluvial and pediment gravel material at the base of Rwenzori mountains. Kabuga is also thought that it is controlled by the major Rwenzori fault that extends from Lake Kitagata in the Katwe geothermal field (Ármannsson, et al., 2005).

Panyamur Hot springs are located on the escarpment near the shores of Lake Albert. They are divided into three hot springs which include Amoropii, Okumu and Avuka. All the three lie on the Rift Valley escarpment. They extend in a northwestly direction and are likely to be controlled by a major boundary fault.

The manifestations include hot springs, travertine deposits, and sulphurous algae and hydrogen sulphide smell. From the hot spring lies a gorge that dips into the escarpment in which fractured crystalline basement rocks like coarse hornblende gneiss, coarse hornblende garnet rock, talcose rock have been reported. There are two directions of foliation that is NNE-SSW and NE in the direction of the local major fault. Okumu is characterised by basement rocks of granitic gneiss and Pleistocene sediments to the east of rift fault boundary. Amur is underlain by fractured basement rocks with foliation trending in NNE-SSW and joints trending NE-SW in quartzite.

SAMPLING AND ANALYSIS

The analytical results used under this project were analysed in 1993, 2002, 2003 and 2005**.** In 1993 under UNDP project (UGA/92/002), geological work was done on Kibiro, Buranga and Katwe- Kikorongo geothermal areas. The samples were analysed both at the department of geological survey and mines (pH, conductivity, CO_2, H_2S and NH_3) while the rest of the results were an analysed at Orkustofnun (Ármannsson, 1993).

In 2005 under the project of the government of Uganda with support from World Bank and international development Bank, geochemical investigation involving sampling of hot springs was done. The collected samples which include water and rock samples were analysed at the institute of Geological and Nuclear science New Zealand (Ármannsson, 2005).The areas covered whose results are considered under this project include Kabuga, Kibenge, Amuru, Amuru(Pakele) Avuka Amoropii, Kanangorok and Okumu.

The project UGA/8/003(1999-2002) was renewed under isotope hydrology UGA/8/005(2005-2006) with the objective of obtaining origin of geothermal fluids, recharge mechanism, resident time, predicting of subsurface temperatures using isotope geothermometers and delineate source of salinity and mixing processes. The work was done by International Atomic Energy Experts (IAEA) and Ugandan professionals. It involved sampling of hot springs, groundwater boreholes and streams which started in 1999. Volatiles were measured in field for hydrogen sulphide and Carbondioxide, temperature and conductivity while environmental isotopes were measured by IAEA Isotope laboratory in Vienna. In 2001 more samples were collected and analysed for isotopes in the IAEA laboratory Vienna, Institute of Hydrology (GSF) in Munich, Germany and Institute of Geosciences and Earth Resources (CNR-IGG) in Pisa, Italy. In 2002 sampling was done in Katwe and Buranga geothermal areas as the last sampling during the project. This was done in 2005 in Kibiro, Buranga and environmental isotopes were also analysed in IAEA Isotope laboratory in Vienna.

DISCUSSION

Classification of geothermal waters

The CL-SO_4-HCO_3 triangular plot was used for the classification of geothermal fluid with respect to the major anions Cl, SO_4 and HCO_3 (Fig. 6). The Kibiro, Amoropii, and Okumu samples plot close to the chloride corner and are classified as mature neutral chloride water. These are likely to be formed from discharge from the geothermal reservoir associated with neutral chloride and represent equilibrated fluid from the upflow. Avuka and Amuru (Pakele) are peripheral bicarbonate waters likely to be spring waters with high Carbondioxide at the peripheral of the geothermal system. Kanangorok and Lake Kitagata plot in the field of steam heated waters. Steam heated waters are usually formed as a result of absorption of magmatic gases into ground water and are characterised by a low pH (Giggenbach, 1988). However, fluids of the hot springs considered here are neutral to alkaline (Kanangorok 7.37, Lake Kitagata 8.03 - 8.61) and

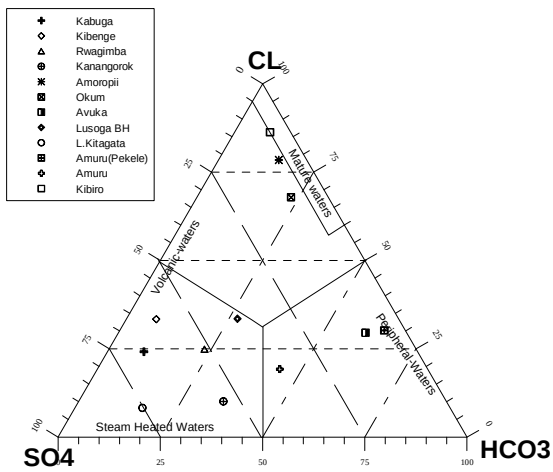

Fig. 6: Classification of geothermal water using CL-SO4-HCO3

are likely to be volcanic fluids in which hydrogen sulphide has been oxidised to sulphate by other processes other than oxidation by oxygen in ground water. Kabuga, Rwagimba, Kibenge and Lusoga borehole samples plot as volcanic waters but the Amuru sample is bicarbonate water.

The Cl-Li-B ternary plot, use Li as a tracer for rock dissolution processes and evaluating the possible origin of B and Cl. Kabuga, Kibenge, Rwagimba, Amoropii, Okumu, Lake Kitagata and Kibiro samples plot close to the chloride corner indicating that these constituents originate in old hydrothermal systems (Fig. 7). Due to either very low values of boron or lithium in geothermal fluid samples (below detection limit) Amuru (Pakele), Amuru, and Kanangorok (apart from waters from the Kanangorok borehole) waters could not be plotted on the diagram. However, they have almost 100% chloride and therefore would plot on the chloride vertex.

The low values of lithium and boron may be an indication that fluids come from old base rock rather than from the underlying sediments.

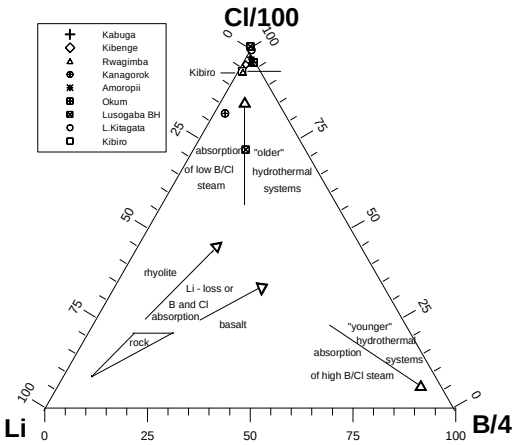

Fig. 7: Classification of geothermal waters using a Cl-Li-B ternary diagram

In the Na-K-Mg ternary plot, the geothermal fluids are divided into immature, partially equilibrated, and fully equilibrated waters. It shows which fluids are suitable for geothermometry that is partially and fully equilibrated fluids. Kibiro, Rwagimba, Lake Kitagata, Kibenge, Kabuga, Amuru, Amuru(Pakele), Amoropii, Kanangorok, Avuka and Kaitabosi waters are fully or partially equilibrated and therefore can be comfortably used for ion geothermometry(Fig. 8A). The equilibrium curve is based on Icelandic basalt results (Arnórsson et al., 1983). Lake Kitagata and Kaitabosi water samples plot above equilibrium line. The reason could be that they are derived from rocks that are not close in composition to the basalts used by Arnórsson et al. (1983). However, Kaitabosi plot on fully equilibrated curve based on andesitic rocks (Giggenbach, 1988), while Lake Kitagata plots close to it (Fig. 8B). Na-K-Mg ternary diagram was used to estimate temperature of the geothermal springs (Table 3) using Na/K and K/Mg geothermometers. However there are some differences in the values from the two geothermometers. This could be due to the fact when geothermal fluids ascend and cool without boiling there is a decrease in pH and temperature. This causes undersaturation with respect to primary igneous rocks that eads to more dissolution lowering K/Mg compared to Na/K tending towards the ratio in the rock. This K leads to different values for Na-K and K-Mg geothermometers with K-Mg indicating a lower temperature (Arnórsson and D'Amore, 2000). The difference is also caused by the fact that the K/Mg geothermometer adjusts to changes in temperature faster than Na/K even for Carbondioxide rich waters. The K-Na geothermometer tends to preserve deep equilibrium of Na/K ratios (Giggenbach, 1991).

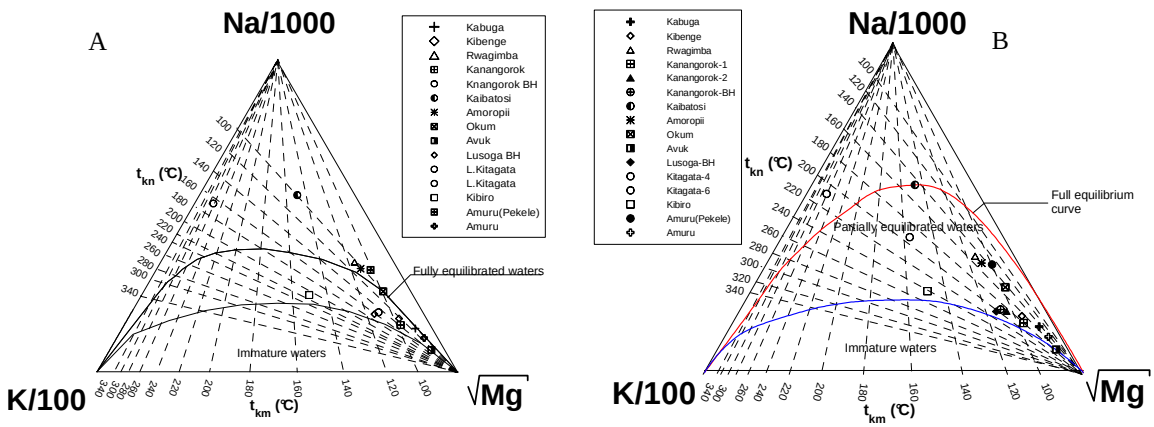

Fig. 8: Classification of geothermal waters using Na-K-Mg ternary diagram a) With Arnórsson et al. (1983) equilibrium line; b) With Giggenbach(1988)equilibrium line.

TABLE 1: Temperature estimated from the Na-K-Mg Triangular diagram.

Hot spring	Kabuga	Kibenge	Rwagimba	Kanangorok	Kaitabosi	Amoropii	Kitagata	Kibiro
Na/K	130	130	108	150	100	105	170	210
K/Mg	90	60	115	110	150	110	260	150

FLUID MINERAL EQUILIBRIA

The Cl-Li-B ternary diagram shows that Okumu geothermal water is fully equilibrated while Kabuga, Amuru, Amoropii and Rwagimba waters plot close to the full equilibrium curve. It would be expected for these fluids to give a clear convergence of minerals that are believed to be in equilibrium. This may be a test to prove that the fluids are in equilibrium with respect to some minerals in the rocks but not others. Due to relatively low temperatures, it takes a long time for the fluid to be in equilibrium with solutes. Water that is far from equilibrium with hydrothermal minerals shows no convergence of minerals at any specific temperature.

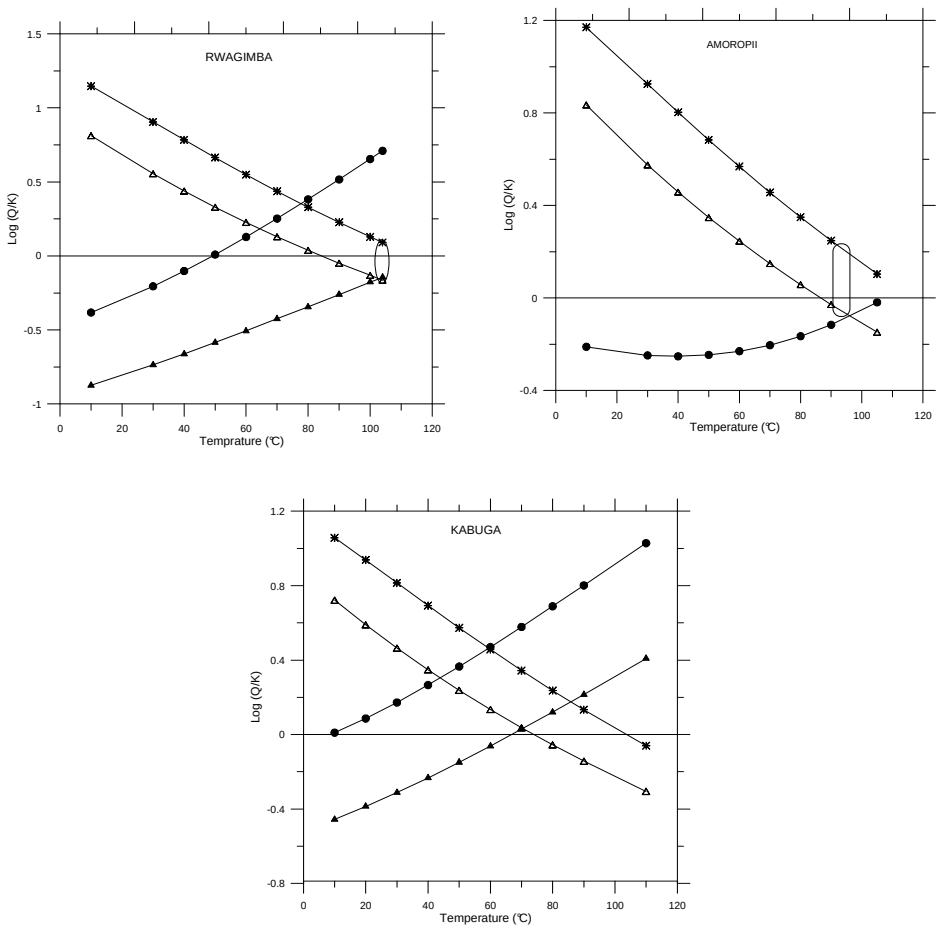

Fig. 9: Saturation index diagram log Q/K versus temperature

It differentiates between equilibrated geothermal fluids and those that have departed from equilibrium due to boiling or mixing with cold water. The geothermometer temperatures below are estimated by using the WATCH speciation programme (Table 2). In some geothermal fluids of Kibenge, Kabuga and Okumu the mineral curve intersect above the zero line giving a positive value of Log (Q/K). This can be possible if boiling happened before sampling due to loss of vapour and gases that leaves residual solution with a simple non volatile component (Arnórsson, 1985). However, this is not the case since the silica-carbonate mixing model indicates that there was no boiling in these hot springs. Amuru curves intersect below the zero line giving a negative log (Q/K). This happens when the mixing of the fluid with dilute solutions lowers the log (Q/K) value. The Amoropii sample shows no clear convergence of mineral curves. The geothermal fluid could have mixed with fluids of different composition which disturbs its equilibrium. Also if it mixes with fluid with solutes in a proportion very different from that of geothermal fluid there is a complete lack of any equilibrium (Fig. 9). In plotting Log (Q/K) versus temperature plots, minerals considered to be in equilibrium were considered. Amorphous silica was not was not used as equilibrium was thought to be controlled by quartz or chalcedony. Also because of dilute fluids of mainly northern Uganda hot springs, calcite and anhydrite were not used for locating the point of intersection or equilibrium point as there no enough calcium to saturate anhydrite and calcite. Few minerals are in equilibrium with the fluids. The low temperature of the fluids makes it require a long time to interact with fluids for equilibrium to be attained. Rwagimba and Kanangorok, geothermal temperatures from WATCH are higher than the average measured temperature using Quartz, chalcedony and Na/K geothermometers that was used in WATCH and the temperatures in the table was got by extrapolation.

Kabuga, Kibenge, Okumu and Amoropii show equilibrium at the chalcedony temperature while Rwagimba and Amuru show equilibrium at the quartz measured temperature. Kanangorok temperature is greater than the average measured temperature.

TABLE 2: Temperature estimated with WATCH and calculated temperature with geothermometers.

Location	Sample No.	T(WATCH)	Ionic balance (%)	Quartz temp. °C	Chalcedony temp. °C	Na/K temp. °C	Mean temp. °C
Kabuga	UG-05-29	62-70	2.53	104.0	73.8	100.2	102
Kibenge	UG-05-30	67-73	2.97	97.5	66.8	121.6	110
Rwagimba	UG-05-33	118	0.35	114.3	85.0	93.1	104
Kanangorok-1	UG-05-58	157	2.85	138.4	111.6	139.4	129.8
Kanangorok-2	UG-05-59			145.0	119.0	146.0	136.8
Kanangorok-BH	UG-05-60			144.9	118.9	153.2	139
Kaitabosi	UG-05-61	-		26.9	-3.1	93.7	-
Amoropii	UG-05-62	?	-0.28	111.3	81.8	98.5	105
Okumu	UG-05-63	70-90	3.05	112.9	83.6	95.4	104
Avuka-2	UG-05-64	-	15.21	104.6	74.5	139.6	
Amuru (Pakele)	UG-05-117		-17.76	78.7	46.7	82.5	81
Amuru	UG-05-118	100	-2.44	114.0	84.7	106.8	110

Kibiro, Panyamur, Amuru, Amuru (Pakele) and Kanangorok hot springs

Kibiro fluid flow is controlled by two intersecting faults, with the main one trending in the NE-SW direction and the other is oblique to it. Panyamur (Avuka,Amoropii, and Okumu) lie along the escarpment of the rift valley and appear to be controlled by it. The altitude of Kibiro and Panyamur springs is not so different that it will stop the flow in either direction

The isotope ratio plot (Fig. 10) shows excess hydrogen in Panyamur and other springs in northern Ugandan. However, samples from Panyamur hot springs (Okumu, Amoropii and Lusoga BH) plot together with Kibiro groundwater and close to Kibiro geothermal samples. The water samples plot in a line together with samples from other geothermal areas of Uganda apart from Katwe, Buranga and Kibiro. This together with a small oxygen shift could mean high permeability and interaction of geothermal fluids with Kibiro groundwater. The plotting of Panyamur samples close to Kibiro samples may be an indication of correlation between the geothermal fluids of Kibiro and Panyamur hot springs.

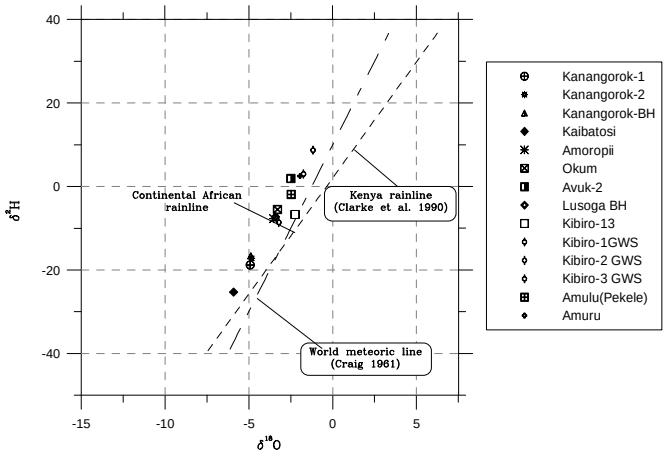

Fig. 10: Isotope ratios of Kibiro and northern Uganda hot springs.

The differences and similarities were further tested by studying conservative elements in the fluids from Kibiro (Mukabiga, Muntere and Mwibanda) and Panyamur. The conservative elements form soluble minerals and some of its supply is limited to saturate the fluids (Arnórsson, 2000b). The concentrations can vary as a result of dilution but the ratio remains the same. The ratios considered include Cl/B, Cl/Li, Na/Cl and fluids of similar origin should have same ratios.

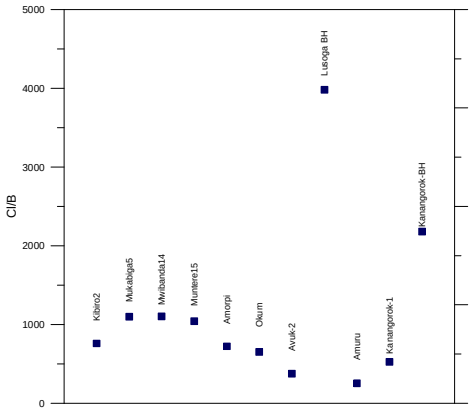

Fig. 11: Cl/B ratio in Kibiro and northern Uganda hot springs

Kibiro geothermal hot spring samples which including samples from Mukabiga, Muntere and Mwibanda have B/Cl ratios ranging from 759-1104(Fig 11). This is not very different from Panyamur hot spring samples with a range of 653-723 despite being analysed in different years, while others outside the rift have very low values. However boreholes samples have a high ratio due to high chloride values. Amuru (Pakele) has low detectable value of boron hence its ratio could not be calculated. The Lusoga borehole contains groundwater while the Kanangorok BH sample is likely to be intermediate between groundwater and geothermal water. The Cl/B ratio plot shows Amoropii and Okumu samples plotting close to Kibiro samples (Fig. 11) while Amuru and Kanangorok samples have considerably lower ratios except for borehole samples. Amuru (Pakele) samples have a low boron concentration, below the detection limit.

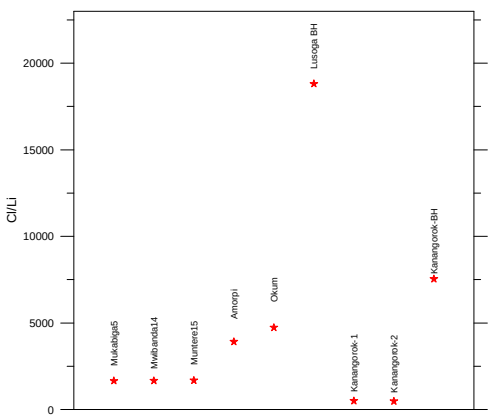

Fig. 12: Cl/Li ratio in Kibiro and northern Uganda hot springs

The concentration of boron is affected by both temperature and permeability of rocks in reservoirs. Literature shows that Cl is incompatible in alteration phases in all natural water-

rock environments whether at ambient or elevated temperatures. It is also not adsorbed on a mineral surface (Hem, 1970). It does not enter any common forming mineral either due to its large size. Also when temperatures are high, B is mobile and incompatible as observed from many rock- water interaction experiments (Mahon, 1970). However at lower temperatures, below 100-150°C experiments have shown that B is incorporated in secondary minerals (Arnórsson and Andrésdóttir, 1995). It is adsorbed and incorporated in clay minerals, mainly illite (Harder, 1970) and behaves as incompatible in geothermal systems above 150°C (Ellis and Mahon, 1964, 1967, and Ellis 1970). These could be the reasons for the lower values of B in Panyamur geothermal hot spring water where temperatures are as low as 84 °C according to geothermometers. Therefore B might have been scavenged from the solution and even some samples have no detectable concentrations like Amuru Pakele and could be the cause of a slight variation in Cl/B ratios compared to those of Kibiro.

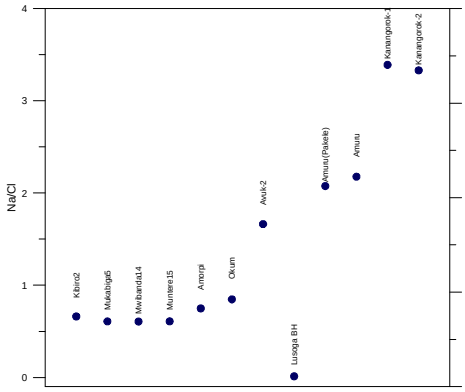

Fig. 13: Showing Na/Cl ratio in Kibiro and northern Uganda hot springs

The Cl/Li ratios are lower for Kibiro hot spring samples than Panyamur hot spring samples Okumu and Amoropii (Fig. 12.) The difference in Cl/Li can be attributed to very low values of lithium (Okumu 0.08 mg/kg) that may increase error in analysis.

Kibiro hot spring waters have a Na/Cl ratio close to that of Amoropii and Okumu waters samples while the rest have a high ratio due to a small concentration of chloride (Fig. 13). Okumu and Amoropii have the same range of Na/Cl ratios as Kibiro geothermal fluid samples.

From the Cl- SO_4-HCO_3 triangular diagram for classification of geothermal fluids (Fig. 6), Kibiro, Amoropii, and Okumu are classified as mature chloride waters, while Amuru, Amuru (Pakele) waters are classified as bicarbonate peripheral waters and Amuru bicarbonate geothermal waters.

Another similarity between Kibiro, Amoropii, and Okumu waters is that they all contain hydrogen sulphide and ammonia whereas the rest of the hot springs in northern Uganda does not have detectable concentrations of these constituents.

However there appears to be no clear temperature gradient between Kibiro, Okumu and Amoropii. This could be due to short distance between Okumu and Amoropii. Kibiro has an estimated subsurface temperature of 200°C and its geothermal fluid has mixed with cold groundwater to give a subsurface temperature of about 150°C**.** Okumu quartz temperature 113.3, chalcedony 83.6, and Na/K 95.4 while Amoropii quartz temperature 113.3, chalcedony temperature 81.8, and Na/K temperature 98.4.

A Na/K plot (Fig. 14) shows that Kibiro water has low Na/K ratios and hence high temperatures while the Panyamur hot springs have high Na/K ratios suggesting that they are low temperature fluids. High temperatures tend to increase dissolution but give low Na/K ratios (Arnórsson, 1985)

Kanangorok1 and Kibiro (Mwibanda, Mukabiga) waters have high concentrations of silica and high surface temperature

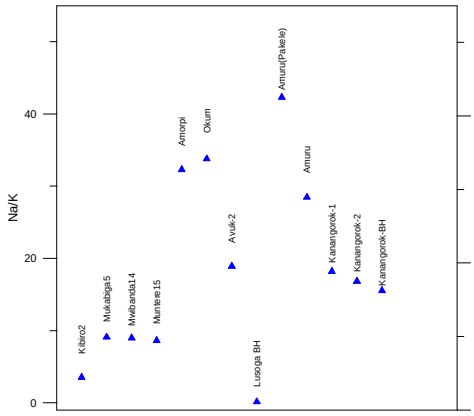

Fig. 14: Showing Na/K in Kibiro and northern Uganda hot springs

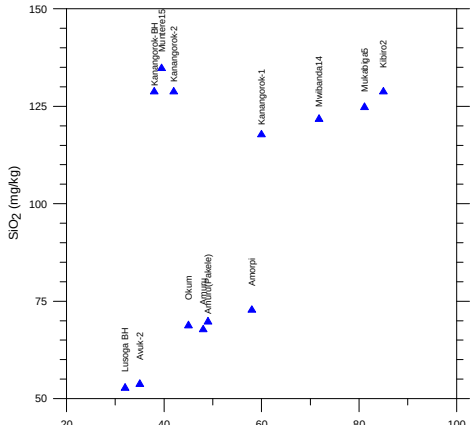

Fig. 15: Variation of SiO_2 with surface temperature.

compared to other hot springs (Fig. 15). Kanangorok 2 and Kanangorok borehole waters have a low sampling temperature with relatively high silica.

This together with almost equal quartz and Na/K temperatures shows that the low surface temperature is a result of conductive cooling rather than mixing with cold ground water.

Kanangorok and Kibiro have high concentration of silica and high sampling temperature compared to other hot springs (Fig. 15). The low sampling temperature of Kanangorok with relatively high silica and almost equal quartz and Na/K temperatures (Table 2) shows the low sampling temperature is a result of cooling rather than mixing with cold ground water.

The plots of Cl versus B and Cl versus Li show a strong correlation between Kibiro, Okumu and Amoropii waters (Fig. 16). The Panyamur and other northern Uganda hot springs have lower concentrations. The lower concentrations can be attributed to low temperature of the fluids which require a long time to increase their concentrations through dissolution of rocks. The plots show that as you move away from Kibiro the concentration decreases.

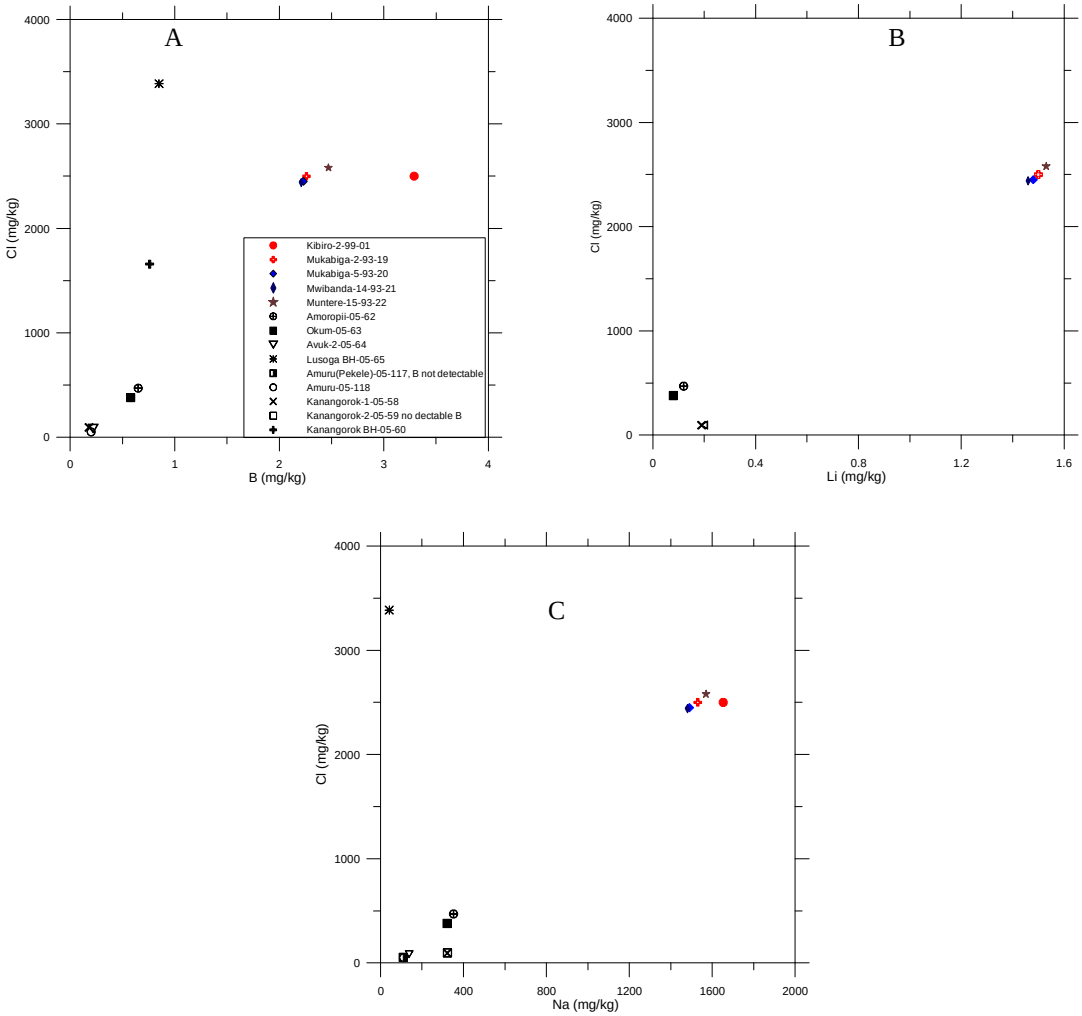

Fig. 16: Graphs showing a) Cl B, Cl versus Li, and c) Cl versus Na in Kibiro and northern Uganda hot springs

The results of geochemical study show that Kibiro waters are likely to be linked to Amoropii and Okumu waters. Carbondioxide rich waters have also been found to develop at the boundaries of geothermal reservoirs in New Zealand (Herderquist, 1989) and Olkaria geothermal field in Kenya (Arnórsson 1991**).** Therefore Avuka which is part of Panyamur which is one of the Panyamut hot springs is likely to be at the peripheral of the 'Kibiro-Panyamur' geothermal field. This is also supported by the Cl-SO_4-HCO_3 diagram in which the sample from Avuka, plots as peripheral water (Fig. 6)

Evidences of mixing

A positive correlation between the conservative elements and a linear relationship between them are typical of mixed waters (Fig. 16). However for fluid to be considered mixed the there is likely be a difference of about 50°C between the Na/K and quartz geothermometers (Fournier, 1981). Therefore using this criterion of measured temperature by the Na/K and quartz geothermometers it is Avuka water (Quartz temperature, 104.6 and Na/K temperature 139.6) that is considered to have mixed

The Na-K-Mg ternary diagram classifies geothermal fluids into immature, partial and full equilibrium (Giggenbach, 1991). However, most of the hot spring samples (Kibiro, Kanangorok) plot in partial equilibrium with only Avuka-2 plotting at the boundary of immature water and partially equilibrated water. The Log Q/K versus temperature diagram for the samples which plot close to equilibrium (Amoropii, Amuru, and Amuru (Pakele) does not show equilibrium with the minerals in the analysed geothermal sample (Okumu and Amoropii) at the expected temperatures. Lack of clear intersection of saturation mineral curves could be due to mixing with either solution of different concentration or ground water that is not dilute. Amuru, Kanangorok whose curves intersect at a negative value for Log Q/K, suggests mixing with dilute water.

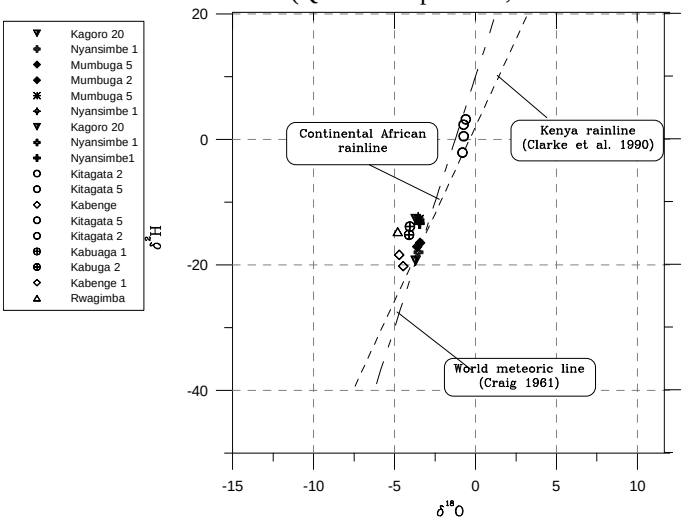

Fig. 17: Variation of ∂^2H with ∂^{18}O for Katwe-Kikorongo and Buranga geothermal field

Mixing also involves lowering of concentration without effectively lowering the CL/B ratio. The lowering of concentration of Amoropii and Okumu without too much lowering of the Cl/B ratio is also an indication of mixing. The mixed water is low in chloride relative to the water within the same reservoir it also tends to be high in CO_2/H_2S (Okumu 44, Amoropii 12.7) while the ratio for Kibiro waters varies from 9-14. This could be due to reactions caused by mixing that tend to remove H_2 and H_2S from solution relative to CO_2 (Hedenquist, 1990). The high value for Okumu water may also be an indication of mixing.

Avuka, Amuru, and Amuru (Pakele) waters have HCO_3 as a major anion. Carbon dioxide may form by mixing of fluid that has not undergone fluid phase separation with cold ground water (Arnórsson 1985). Carbon dioxide rich waters can also form by mixing of mantle derived magmatic or metamorphic CO_2 with ground or surface waters (Arnórsson and Barnes, 1983).

The dissociation constant of carbonic acid increases with increasing temperature and thus the H^+ concentration increases. Mixed waters have low pH with high carbonic acid and with a pH of 6-7 for chloride concentrations less than100 ppm. Avuka water has a pH of 7.56 with Cl of 83 ppm. The increased H^+ concentration also causes rock dissolution that may lead to a drastic change in initial equilibrium and approach the one dictated by rock stoichiometric dissolution. This leads to an increase of Mg and Ca concentrations (mainly Mg) relative to the Na concentration (Árnorsson, 1991). The cooling by mixing affects exchange reactions with rock minerals and thus causes increases in the Na/K and Mg/Na ratios (Truesdell, 1991). The Mg/Na ratio for the Kibiro water varies from 0.002 to 0.006, Kanangorok 0.008, Amuru 0.007 and Avuka 0.022 which is the highest of the samples studied.

Geochemistry isotope studies have also shown that Avuka appears to be recharged locally or has a component of lake water while the values for Okumu and Amoropii are lower suggesting recharge from a higher altitude or mixing with local ground water (Ármannsson et al., 2005). Therefore the mixing model has only been considered for Avuka, Okumu and Amoropii by taking account of gas ratios, Log Q/K-Temperature plots, and difference between Quartz and Na/K temperatures.

However the interpretation of Avuka and Amuru (Pakele) waters needs more work since they have high ionic differences (Amur (Pakele) 11.9% and Avuka 15.12%) from WATCH speciation programme.

Katwe-Kikorongo, Buranga, Rwagimba, Kibenge and Kabuga geothermal springs.

Effort has been made to study the geochemistry of the above geothermal springs to see if there is any possible correlation between them. The Plot of δ^2H versus δ^{18}O (Fig. 17) shows that Buranga (including Kagoro), Kibenge, Kabuga can be grouped together as one geothermal field different from that of Katwe-Kikorongo field. For the isotope ratio plot, results of 1993, 1994, 2002 and 2005 were used. The results from plotting of Cl versus Li, Cl versus Li and Cl versus Na for Katwe-Kikorongo Kabuga and Rwagimba show that 1993 results from Kitagata-1 plot higher on the graph than the rest and once plotted with other results bring out a pseudo correlation mostly for Cl/B and Cl/Na plots. However, when these points are removed the other points scatter (Fig. 20).

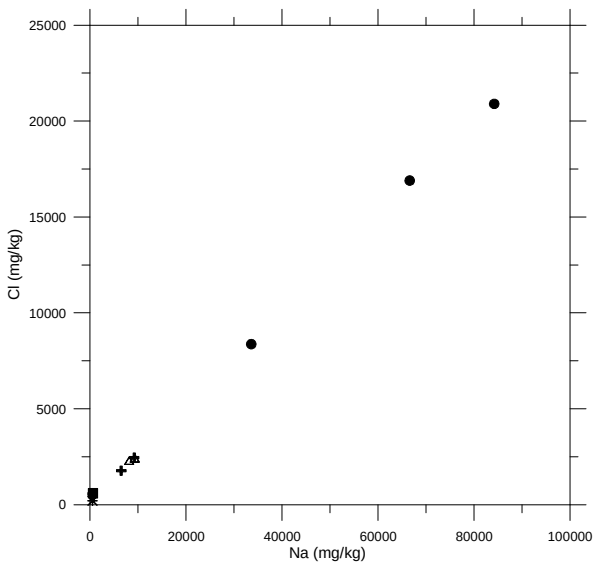

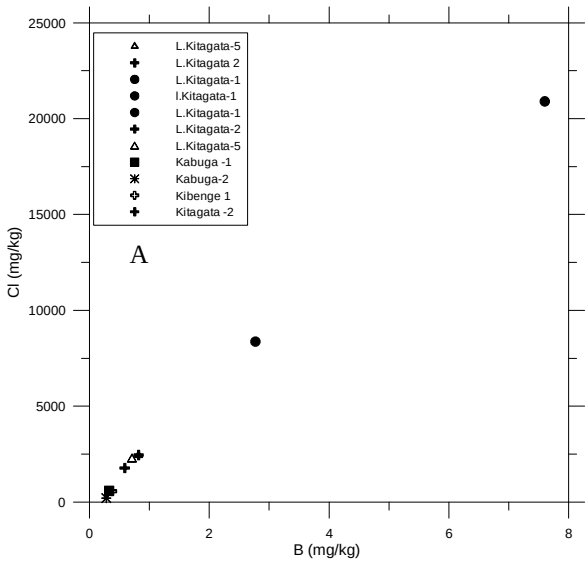

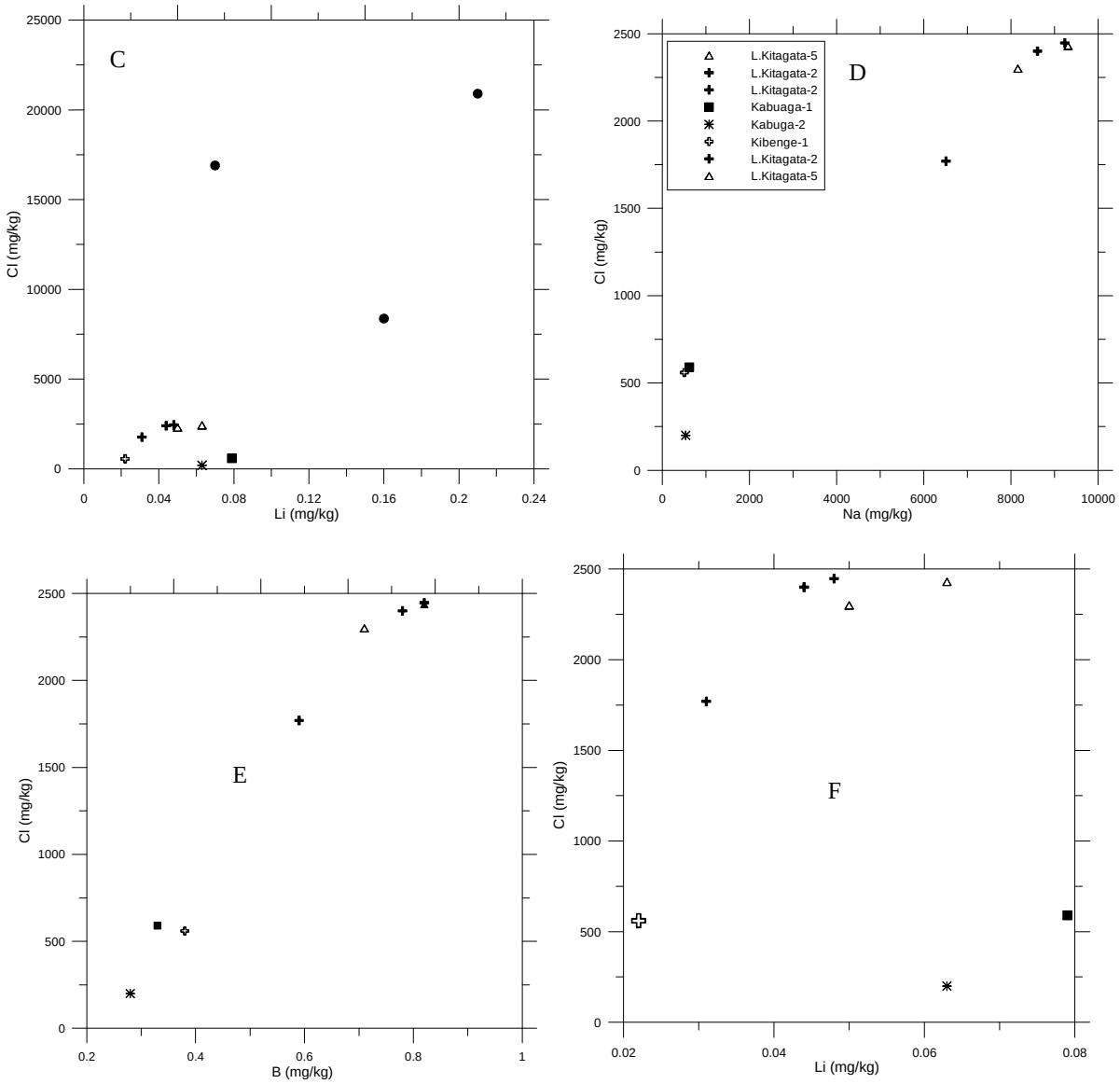

Fig. 18: Variation of Li, B, and Na with Cl in Katwe-Kikorongo, Rwagimba, Kibenge and Kabuga hot springs; graphs a-c) include the Kigata-1 1993 results, while graphs d-f) do not include these.

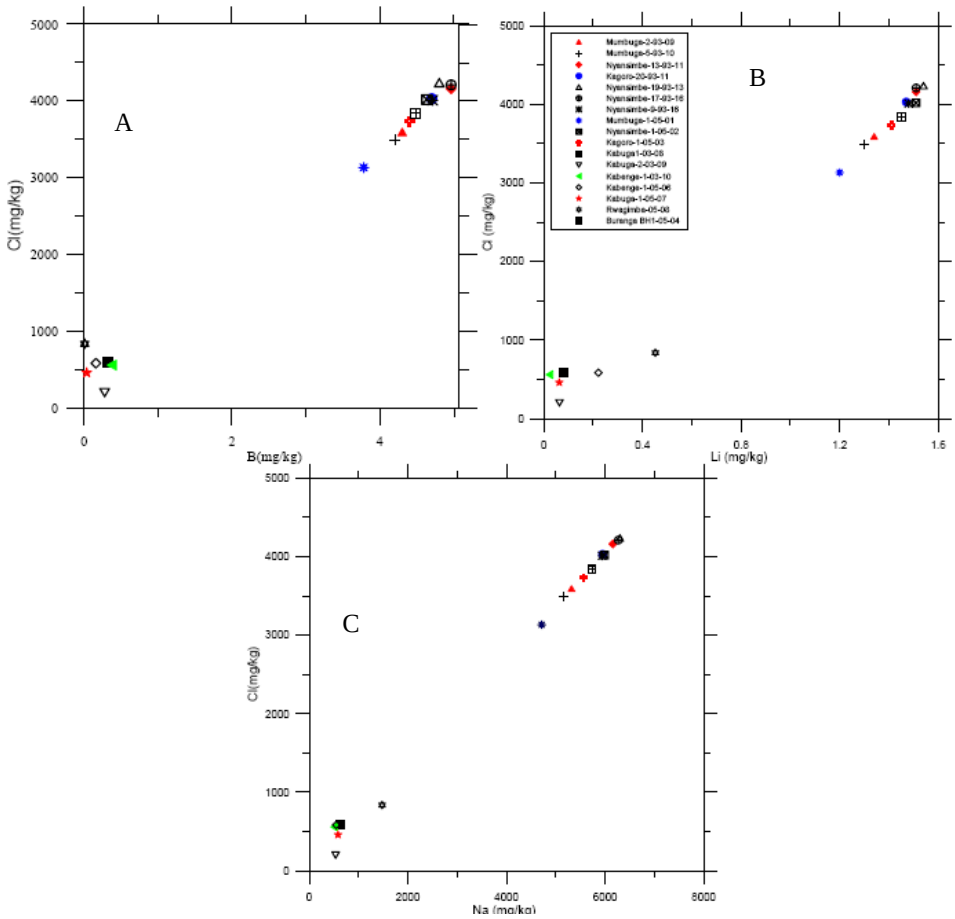

Fig.. 19 Graphs showing a) Cl vs. B, b) Cl vs. Li, and c) Cl vs. Na, in Kibiro and northern Uganda hot springs

However, the plots of Cl versus Na, Cl versus Li, Cl versus B for Buranga, Kibenge, Kabuga, and Rwagimba show a strong correlation (R^2 >0.995)between the conservative Cl, Li and B elements indicating that the different hot springs are genetically related (Fig. 18). Kabuga, Kibenge and Rwagimba waters are more dilute than those of Buranga and this is due to low temperatures and the long time needed for the fluids to interact with the rocks as earlier seen.

This grouping is also supported by different ratios between conservative elements. The ratios of different conservative elements from a geothermal fluid with a similar source of origin are constant or close despite changes in concentration. The conservative element ratios studied include Cl/B, Cl/Li, and Na/K. Katwe-Kikorongo Cl/B values vary from 2963.4 to 2984, higher than Buranga ratios varying from 830.95 to 868.03. The Kabuga1 water's Cl/B ratio varied from 1787.9 in the 2003

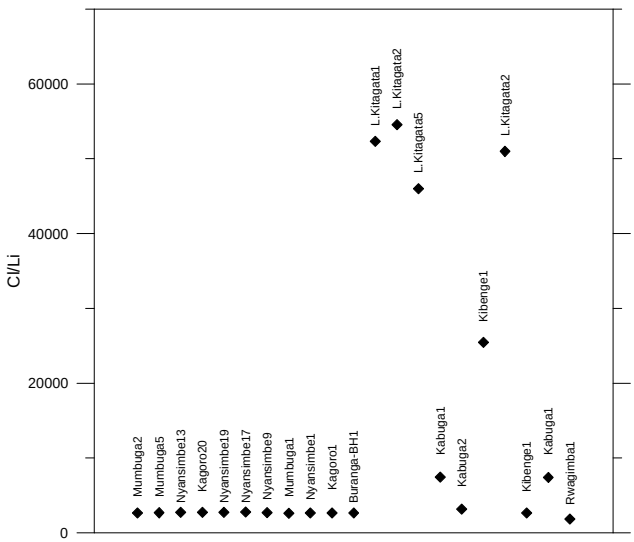

Fig. 20: Cl/B ratio in Katwe-Kikorongo and Buranga hot springs

analysis to 1277 in the 2005 analysis while Kabuga-2 water has a Cl/B ratio of 714.3, close to that of Buranga water. Kibenge values varied from 1218.75 to 1473.7 and the Rwagimba value is 1180.28, close to that of Buranga.

A plot of Cl/B ratios (Fig. 20) shows the geothermal field samples plotting close to Buranga samples with Katwe samples plotting at high ratios.

The Cl/Li ratio depicts a similar relationship. The Cl/Li ratio of Kibenge water (2647.059 analysed in 2005) is close to that of Buranga water (2610.83 to 2788.08) but lower than the high ratios of Katwe waters (46000-54545.5). The plot (Fig. 21) shows that Kibenge, Rwagimba and Kabuga and Buranga may be grouped together as one geothermal field. The K/Na ratio of Kibenge, Rwagimba and Kabuga (0.04 -0.05) waters is close to the Buranga water (0.04) ratio but lower than the Katwe water K/Na ratio of 0.06 to 0.09 with an average of 0.0714.

The Buranga Na/Cl ratio varies from 1.48 to 1.51 while that of Kitagata varies from 3.5 to 4.0. The rest of the hot springs vary from 0.9 to 1.77 close to Buranga than Kitagata (Katwe-Kikorongo) with Kitagata plotting above all other hot spring samples (Fig. 22).

The Na/K ratio for Buranga waters varies from 26.68 to 27.8 in the 1993 to 2005 analysis which shows that they are consistent, Katwe water gives 11.8-19.0 in the 2003 analysis with an average of 15.98, Kabuga1 water 21.2 to 24.9 (in the 2003 analysis) and 31.2(in the 2005 analyses), Kibenge water 18.7 according to the 2003 results, but 22.6 in the 2005 analysis while Rwagimba water gives 35.6. Therefore Kabuga and Kibenge waters correlate more closely to Buranga than Katwe waters. The results show that Buranga hot spring (Nyansimbe and Mumbuga), and Ruwenzori hot spring (Kagoro) hot spring waters have Na/K ratios in the range 26.78 to 28.41 for the samples analysed in 1993 to 2005 thus showing consistence in the Na/K ratios. The plot of Na/K ratios (Fig. 23) shows that correlation although there are few discrepancies which could be due to results obtained in different years. This shows that Katwe-Kikorongo is a higher temperature geothermal field than Buranga.

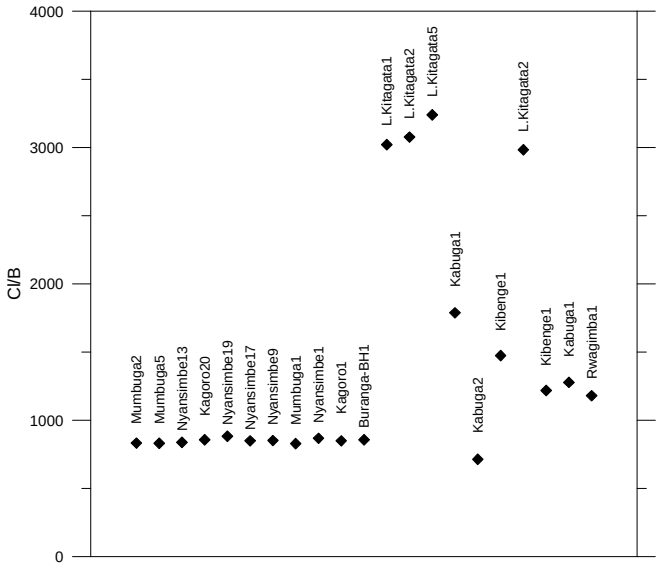

Fig. 21: Cl/Li ratio in Katwe-Kikorongo and Buranga hot springs

Evidences of mixing

Whereas the concentration of other elements in the

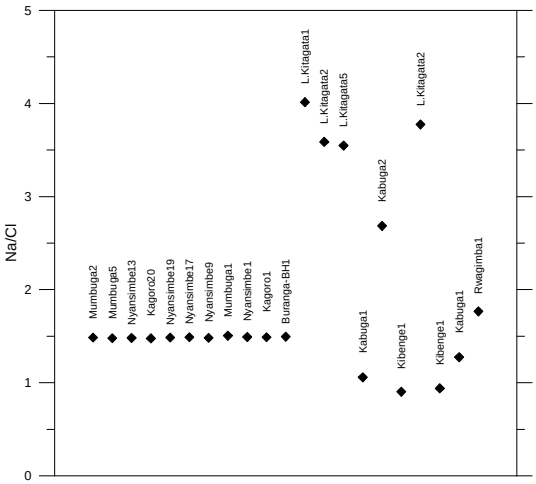

Fig. 22: Variation of Na/Cl ratio of Katwe -Kikorongo and Buranga hot springs

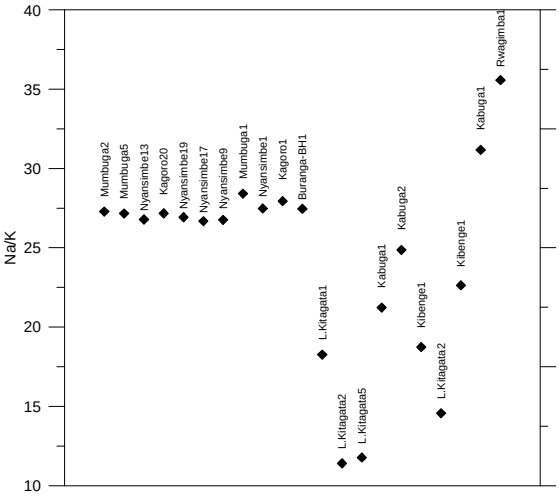

Fig. 23: Variation of Na/K ratio of Katwe-Kikorongo and Buranga hot springs

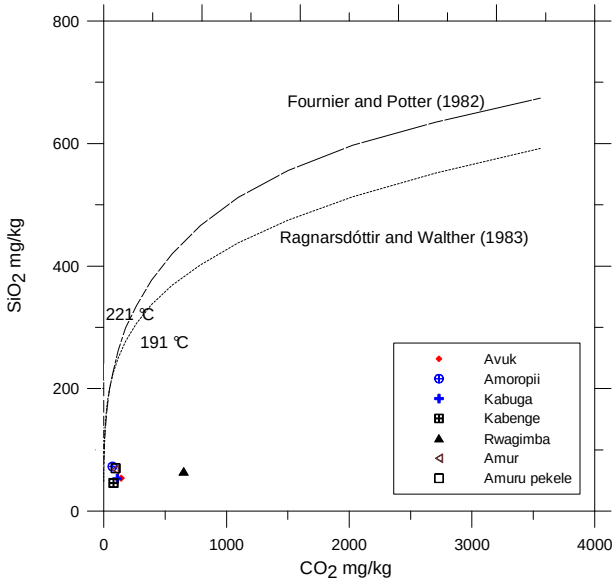

Fig. 24.The silica-carbonate mixing model

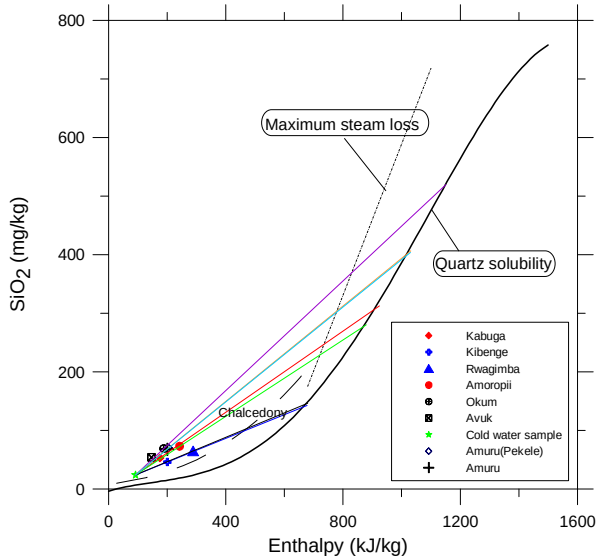

Fig. 25: Silica-carbonate mixing model for Buranga and northern Uganda hot spring samples.

geothermal fluids of Katwe and Buranga are higher than the concentration of Kabuga and Kibenge fluids, the concentration of Mg and Ca are higher in the two geothermal hot springs. This could be due to mixing with cold water and could be the reason why their predicted subsurface temperatures are lower than either that of Buranga geothermal field. Magnesium in geothermal fields rapidl y decreases as temperature increases. However as geothermal fluids flow from a high-temperature environment to a low temperature environment they pick up relatively easily and quickly significant amount of magnesium from rocks (Fournier, 1991). Therefore Kabuga, Kibenge and Rwagimba waters have been considered for mixing models.

Mixing models.

Silica carbonate mixing model temperatures

The silica carbonate model was used to determine whether the fluids boiled. The data plotted below the curve region representing unboiled or degassed waters (Fig. 24). It shows that Avuka, Amoropii, Kabuga, Kibenge, Rwagimba, Amuru and Amuru (Pakele) waters never boiled.Silica-Enthalpy model for calculating silica mixing model temperatures.

Enthalpy silica model for calculating silica mixing temperatures.

The silica concentration and the enthalpy of these unboiled samples were then plotted on a silica-enthalpy diagram together with the same parameters for a sample of cold water from the area (non thermal water). A line was drawn joining the cold sample point to each of the hot spring sample points. The line was extrapolated until it intersected the quartz solubility curve. The point of intersection represented the enthalpy and silica of geothermal water before mixing (Fig. 25). The maximum steam curve was not used since silica carbonate mixing model showed that there was no boiling. The Kibenge and Rwagimba samples give a reading reasonably close to the temperatures for the Buranga samples. The rest of the samples give very high values and even the extrapolated line for Avuka did not intersect the solubility curve. This could be due conductive cooling without loss of silica for the case of non boiling springs that shifts data points to the left giving a steep line, or boiling (Arnórsson, 2000). The boiling possibility is ruled out as silica carbonate models shows that there was no mixing. The higher temperatures of other geothermal samples could be due to dissolution of silica after mixing as this leads to estimation of high temperatures.

TABLE 3: Estimated temperature by SiO_2-Enthalpy mixing model

Location	Kabuga	Kibenge	Rwagimba	Amoropii	Okumu	Amuru(Pakele)	Amuru
T(°C)	214	160.5	161	205	263	238	238

CONCLUSION

The main objective of the study was to find possible potential relationships between geothermal hot springs in Uganda. The major conclusions of the study include:

- The geochemistry study of the geothermal fluids show that Kibenge, Kabuga, and Rwagimba are linked to Buranga and form one geothermal field.
- The Kibiro geothermal area is likely to be linked to Panyamur hot springs (Okumu, Amoropii, and Avuka) with Avuka likely to be at the periphery of the Kibiro-Panyamur geothermal field.
- Kabuga, Kibenge waters with measured temperatures of 100.2 and 126°C respectively are mixed with ground water and the SiO_2-Enthalpy mixing model indicates a temperature of 161°C.
- The geothermal samples studied come from old hydrothermal system rather than young underlying sediments since they plot near chloride corner on Cl-Li-B ternary diagram.
- Comparing the Na-K-Mg ternary diagram with Log (Q/K) versus temperature the geothermal fluids are in equilibrium with rocks rather than minerals since the samples that plot as partially and fully equilibrated on the Na-K-Mg ternary diagram do not show clear convergence of mineral saturation curves.
- The silica-carbonate mixing model shows that there was no boiling in Avuka, Amoropii, Kabuga, Kibenge, Rwagimba, and Amuru (Pakele) hot springs.

RECOMMENDATIONS

- More sampling should be carried out for Avuka and Amuru (Pakele) because of the poor ionic balance of the present samples and may reflect problems during sampling and analysis. The results from these two hot springs samples may not be reliable.
- More detailed work should be done on Kibiro and Panyamur hot springs to confirm their link and the possible common geothermal source. This is because correlation was done basing on a single analysis for every hot spring in Panyamur.

REFERENCES

Ármannsson, H., 1994: Geothermal studies on three geothermal areas in West and Southwest Uganda. UNDESD, UNDP project UGA/92/002, report, 85 pp.

Ármannsson, H., Bahati, G., Kato, V., 2005: Preliminary investigation of geothermal areas in Uganda, Other than Katwe-Kikorongo, Buranga and Kibiro.

Arnórsson, S., 1981: Mineral deposition from Icelandic geothermal waters, environmental and utilisation problems. Jour. Petroleum technology, 33, 181-187

Arnórsson, S., 1985: The use of mixing models and chemical geothermometers for estimating underground temperature in geothermal systems. J. Volc. Geotherm. Res., 23, 299-335.

Arnórsson, S., 1991: Geochemistry and geothermal resources in Iceland, In: D´Amore, F. (co-ordinator), Applications of geochemistry in geothermal reservoir development. UNITAR/UNDP publication, Rome, 145-196.

Arnórsson, S., 2000a: Mixing processes in upflow zones and mixing models. In: Arnórsson, S. (ed.), Isotopic and chemical techniques in geothermal exploration, development and use. Sampling methods, data handling, and interpretation. International Atomic Energy Agency, Vienna, 200-211.

Arnórsson, S., 2000b: Reactive and conservative components. In: Arnórsson, S. (ed.), Isotopic and chemical techniques in geothermal exploration, development and use. Sampling methods, data handling, and interpretation. International Atomic Energy Agency, Vienna, 200-211.

Arnorsson,S., Andresdottir, A., 1985: Processes controlling the distribution of Boron and Chlorine in natural waters in Iceland. Geochemi. Cosmochim. Acta, 59 4125-4146

Arnórsson S, Barnes I., 1983: The structure of Carbondioxide waters in Snaefellsnes, Western Iceland. Geothermics 12:171-176).

Arnórsson, S., Gunnlaugsson, E., and Svavarsson, H., 1983b: The chemistry of geothermal waters in Iceland III. Chemical geothermometry in geothermal investigations. Geochim. Cosmochim. Acta, 47, 567-577.

Bahati, G., 2007: Isotope hydrology for exploring geothermal resources. Dept. Geol. Surv. and Mines, Uganda, IAEA TC, project terminal report, UGA/8/005, 47 pp.

Bahati, G., Pang, Z., Armannsson, H., Isabirye, E.M, Kato, V., 2005: Hydrology and reservoir characteristics of three geothermal systems in western Uganda. Geothermics 34 , 568-591.

D'Amore, F., and Arnórsson, S., 2000: Geothermometry. In: Arnórsson, S.(ed.), Isotopic and chemical techniques in geothermal exploration, development and use. Sampling methods, data handling, interpretation. International Atomic Energy Agency, Vienna, 152-199.

Ellis A. J. (1970) Quantitative interpretation of chemical characteristics of hydrothermal systems. Geothermics 2, 516-527.

Ellis A. J. and Mahon W. A. J., 1964: Natural hydrothermal systems and experimental hot water/rock interactions. Geochim. Cosmochim. Actu 28, 1323-1357.

Fournier, R.O., 1973: Silica in thermal waters. Laboratory and field investigations. Proceedings of the International Symposium on Hydrogeochemistry and Biochemistry, Tokyo, 1, Clark Co., Washington D.C., 122-139.

Fournier, R.O., 1981: Application of water chemistry to geothermal exploration and reservoir engineering. In: Rybach, L., and Muffler, L.J.P. (editors), Geothermal system: Principles and case +

histories. John Wiley and Sons Ltd., Chichester, 109-143.

Fournier, R.O., 1991: Water geothermometers applied to geothermal energy. In: D'Amore, F. (coordinator), Application of Geochemistry in Geothermal Reservoir Development. UNITAR/UNDP publication, Rome, 37-69.

Fournier R.O and Rowe J.J., 1966: Estimation of underground temperatures from the silica content of water from hot springs and well steam wells. Amer. J. Mineral. 6, 459-464.

Giggenbach, W.F., 1988: Geothermal solute equilibria. Derivation of Na-K-Mg-Ca geoindicators. Geochim. Cosmochm. Acta, 52, 2749-2765.

Giggenbach, W.F., 1991: Chemical techniques in geothermal exploration. In: D'Amore, F. (coordinator), Application of geochemistry in geothermal reservoir development. UNITAR/UNDP publication, Rome, 119-142.

Gíslason, G. 1994: Geothermal Exploration – I, UGA/92/002 & UGA/92E01: Terminal Report. UNDDSMS – Geol. Surv. & Mines Dept., Uganda.

Gíslason, G., Árnason, K., Eysteinsson, H., 2004: The Kibiro geothermal report. A report on Geophysical and Geological survey prepared for the Icelandic international Development Agency and the ministry of Energy and Mineral Development, Uganda, unpublished report, p.109

Gíslason, S.R., Heaney, P.J., Oelkers, E.H. and Schott, J. 1997: Kinetic and thermodynamic properties of moganite, a novel silica polymorph. Geochim. Cosmochim. Acta, 61, 1193-1204.

Heaney P.J., 1995: Moganite as an indicator for vanished evaporates: A testament reborn? J. Sediment. Res. A65, 633-638

Heaney P.J and Post J.E 1992: the widespread distribution of a novel silica polymorph in microcrystalline quartz varieties. Science 255, 441-443

Hedenquist, J.W., 1990: The thermal and geochemical structure of the Broadlands-Ohaaki geothermal system, New Zealand. Geothermics, 19: 151-185.

Hem, J. D., 1970: Study and interpretation of the chemical characteristics of natural water. U.S. Geol. Survey, water supply paper 1473.

Henley, R.W., Ellis, A.J., 1983: Geothermal systems ancient and modern: a geochemical review. Earth-Sci. Rev. 19, 1–50.

Harder H. (1970) Boron content of sediments as a tool in facies analysis. Sediment Geol. 4, 153-175

McNitt. J.R., 1982. The geothermal potential of East Africa. In proceedings of the Regional Seminar on geothermal energy in Eastern and Southern Africa, Nairobi, Kenya. P. 3 - 8.

Paces, T., 1975: A systematic deviation from Na-K-Ca geothermometer below 75°C and above 10-4 atm PCO2. Geochim. Cosmochim. Acta, 39, 541-544.

Reed, M.H., and Spycher, N.F., 1984: Calculation of pH and mineral equilibria in hydrothermal water with application to geothermometery and studies of boiling and dilution. Geochim. Cosmochim. Acta, 48, 1479-1490.

Tole, M.P., Ármannsson, H., Zhong-he, P., Arnórsson, S., 1993: Fluid/mineral equilibrium calculations for geothermal fluids and chemical geothermometery Geothermics, Vol. 22pp. 17-37

Truesdell, A.H., 1991: Effects of physical processes on geothermal fluids. In: D'Amore, F. (coordinator), Application of geochemistry in geothermal reservoir development. UNITAR/UNDP publication, Rome, 71-92.

Truesdell, A.H., and Fournier, R.O., 1976: Calculations of deep temperatures in geothermal systems from the chemistry of boiling spring waters of mixed origin. Proceedings of 2nd U.N. Symposium on the Development and Use of Geothermal Resources, San Francisco, 1, 837-844.

Petrovic I., Heaney P.J., and Navrptsky A., 1996: Thermochemistry of the new silica polymorph moganite.Phys.chem. Minerals 23, 119-126

THEME V.

WELL TESTING, INJECTION, RESERVOIR ENGINEERING MODELLING

VOLUMETRIC RESSOURCE ASSESSMENT OF ASAL GEOTHERMAL FIELD, REPUBLIC OF DJIBOUTI

DAHER E. HOUSSEIN
Centre d'Etude et de Recherche de Djibouti, CERD, Djibouti

ABSTRACT

Three geothermal fields were identified in Asal geothermal field. Based on USGS volumetric estimation method together with Monte Carlo simulations is used to provide estimates of the probable power potential capacity of the geothermal system. The estimated power generation potential of all Asal high-temperature hydrothermal systems is between 115 and 329 MWe for a 25-year exploitation period.

Keywords: Asal, Resource, Assessment, Simulation

INTRODUCTION

Different methods used to assess geothermal resources are described by Muffler and Christiansen (1978) and Muffler and Cataldi (1978). These authors also discuss the theoretical background, assumptions and development of the equations used in these models. The most commonly used, particularly during the initial phases of a geothermal project mainly because of lack of sufficient data, is the volumetric method. Due to the simplifying assumption made, the volumetric method tends to be much less accurate than the numerical models.

from Mt and TEM survey made later in December 2007 (Arnason et al., 2008), three geothermal sufields is recognized in Asal area (Fig. 1)

The USGS volumetric method (Sabodh, 2010) is applied to the Asal area to get an initial capacity estimate. The purpose of this assessment is to estimate the electricity generation capacity for the region assuming a 25-year power plant life. Because most of the parameters assumed in the calculations are associated with considerable uncertainties, a Monte Carlo technique is used.

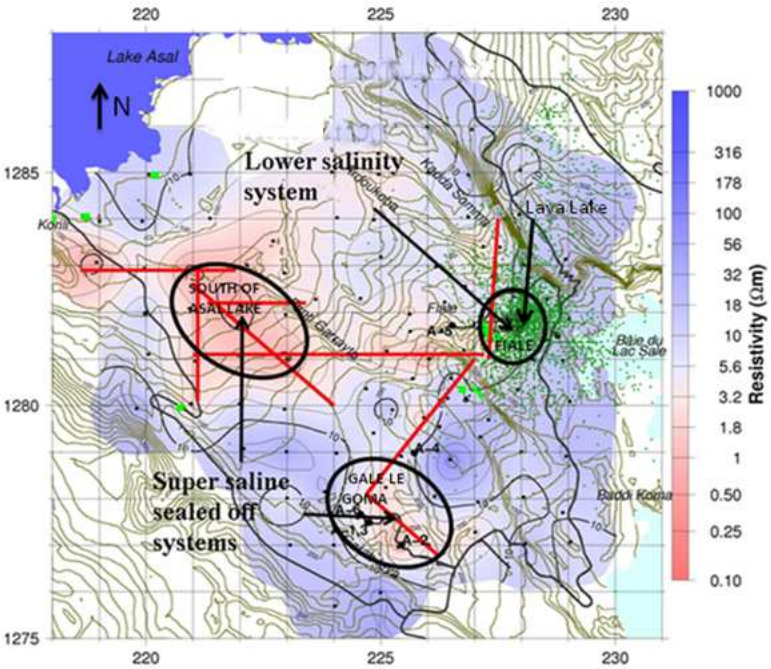

Fig. 1: Map showing the location of the three known geothermal systems (Gale le Goma, Fiale and South of Lake) in the Asal region. The figure also shows the resistivity at 3000 m b.s.l., inferred lineaments in low resistivity (red lines), seismicity (dark green dots) and geothermal surface manifestations (light green). The two super saline and sealed-off Gale Le Goma and South of

Asal Lake systems are indicated, as is the more open, lower salinity Fiale system under Lava Lake (modified from Arnason et al., 2008).

PARAMETERS USED IN THE MODEL

Based on the resistivity surveys conducted by ISOR (Arnason et al., 2008), the median estimated surface areas of the three geothermal systems, Gale le Goma, Fiale and South of Lake Asal, are 4, 4 and 3 km^2, respectively. From the temperatures profiles (Fig. 2) and the MT and TEM) data (Arnason et al., 2008), the thickness of these reservoirs is assumed to vary between 1500 and 2000 m.

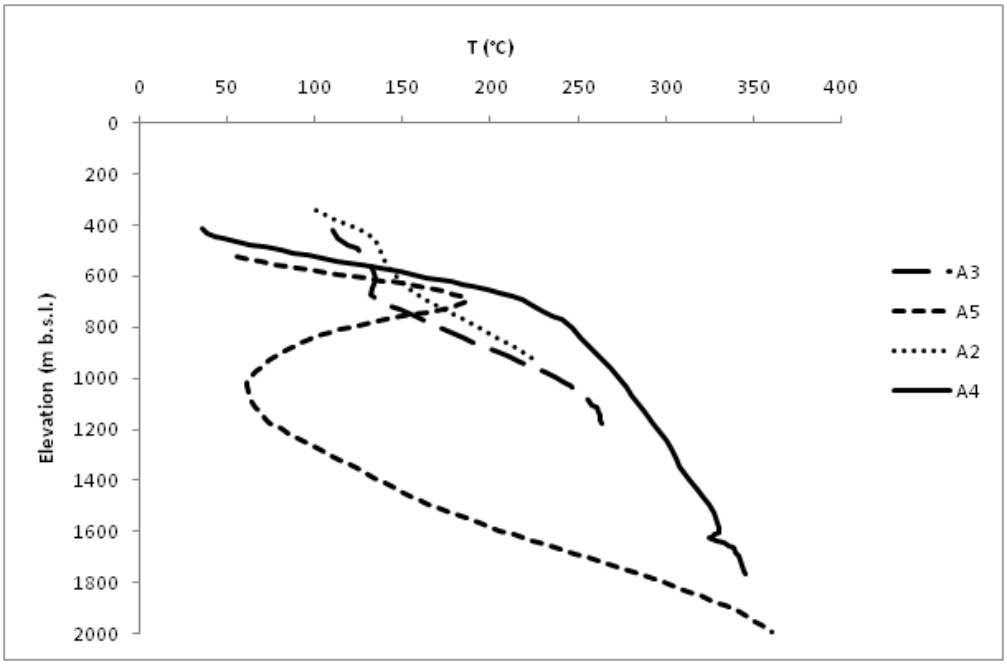

Fig. 2: Temperature profiles of Asal wells A2-A5.

In the calculations, a rejection (condenser) temperature (T_{ref}) of 40°C was selected (MIT, 2006). The reservoir temperature (T_{res}) was assumed to be homogenous, 280°C being the most likely, 265°C the minimum, 290°C the maximum for both Gale le Goma and South and 350°C the maximum for Fiale. This temperature range was based on the temperature profiles of wells A6, A3 and A4 drilled in the Gale le Goma area (Fig. 2).

Because of the high salinity of the fluid in the deep Asal reservoir, our calculations assume a fluid average density (ρ_{fluid}) of 890 kg/m^3 (Aquater, 1989) and a heat capacity ($ß_{fluid}$) of 4800 J/(kg°C).

The deep Asal reservoirs are considered to be composed mostly of metamorphic rocks (Aquater, 1989); therefore, the value for the heat capacity of the rock, $ß_{rock}$, is chosen to be between 0.8 and 1 kJ/kg°C, the values measured experimentally by Vosteen and Schellschmidt (2003). The porosity φ of the basalt rocks in the Asal area is of the order of 10% (Aquater, 1989). The average density of the rock (ρ_{rock}) is set at 2870 kg/m^3 on the basis of the gravity data collected by BRGM in 1979 (Aquater, 1989).

The geothermal recovery factor R_f, which represents the ratio of extracted thermal energy (measured at the wellhead) to the total thermal energy contained in a given subsurface volume of rock and water (Muffler and Cataldi, 1978), is assumed to be between 0.05 and 0.2, with 0.1 being the best guess. The electrical conversion efficiency (η) is taken to be 40%, like in the case of the Wairakei power plant (Thain and White, 1993). A 95% load factor L is used, based on 18 days of preventive maintenance per year.

All the input parameters used in the volumetric assessment are listed in Table 1.

Table 1: Most likely values and probability distributions for the patameters used to estimate power generation capacities in the different Asal geothermal fields

Input parameter	Units	Assumed distribution	Best guess	Minimum	Maximum
Area	km^2	Triangular	4 Gale	2	6
			4 Fiale	2	6
			3South	2	8
Thickness	m	Triangular	1500	1000	2000
Reference temperature (T_{ref})	°C	Constant	40		
Reservoir temperature (T_{res})	°C	Triangular	280 Gale	265	290
			280 Fiale	265	350
			280 South	265	290
Time period (Δt)	Years	Constant	25		
Recovery factor (R_f)	%	Triangular	0.1	0.05	0.2
Fluid density (ρ_{fluid})	kg/m^3	Constant	890		
Fluid heat capacity ($ß_{fluid}$)	J/(kg°C)	Constant	4800		
Rock density (ρ_{rock})	kg/m^3	Constant	2870		
Rock heat capacity ($ß_{rock}$)	J/(kg°C)	Triangular	900	800	1000
Reservoir porosity (ϕ)	%	Constant	10		
Conversion Efficiency (η)	%	Constant	40		
Load factor (L)	%	Constant	95		

RESULTS AND DISCUSSION

The results of the volumetric assessment of the electricity generation potential of the three geothermal fields in the Asal region are summarized in Table 2 and Fig. 3. These estimated generation capacities are only preliminary estimates since they are based on parameters with considerable uncertainties (in the South Asal Lake area, no wells have been drilled), particularly in the size of the reservoirs and in the assumed recovery factor.

At the present time, the Fiale field is under development. A 50- MWe geothermal power plant might be installed there in the next few years. This size of plant might be realistic as the mean power capacity for the Fiale field is estimated to be 71 MWe and the 10% -90% confidence interval of the estimate is 42-116 MWe (Table 2).

Table 2 :Estimated power generation capacity of the three Asal geothermal fields based on the volumetric method and Monte Carlo calculations

Geothermal field	Estimated capacity (MWe)		
	Minimum	**Median**	**Maximum**
Gale le Goma	37	62	99
Fiale	42	71	116
South of Asal Lake	36	65	114
Total	115	198	329

Minimum, median and maximum are the P90, P50, and P10 values. Here Pxx indicates that there is a xx probability that the power generation capacity is at least the estimated value.

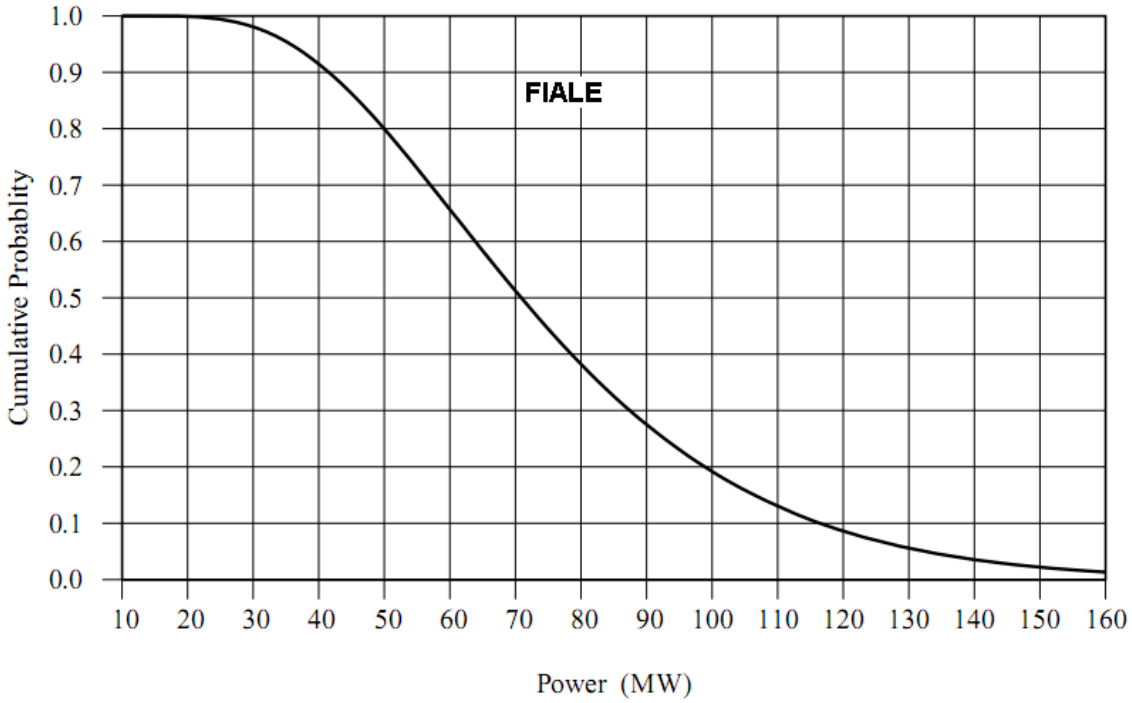

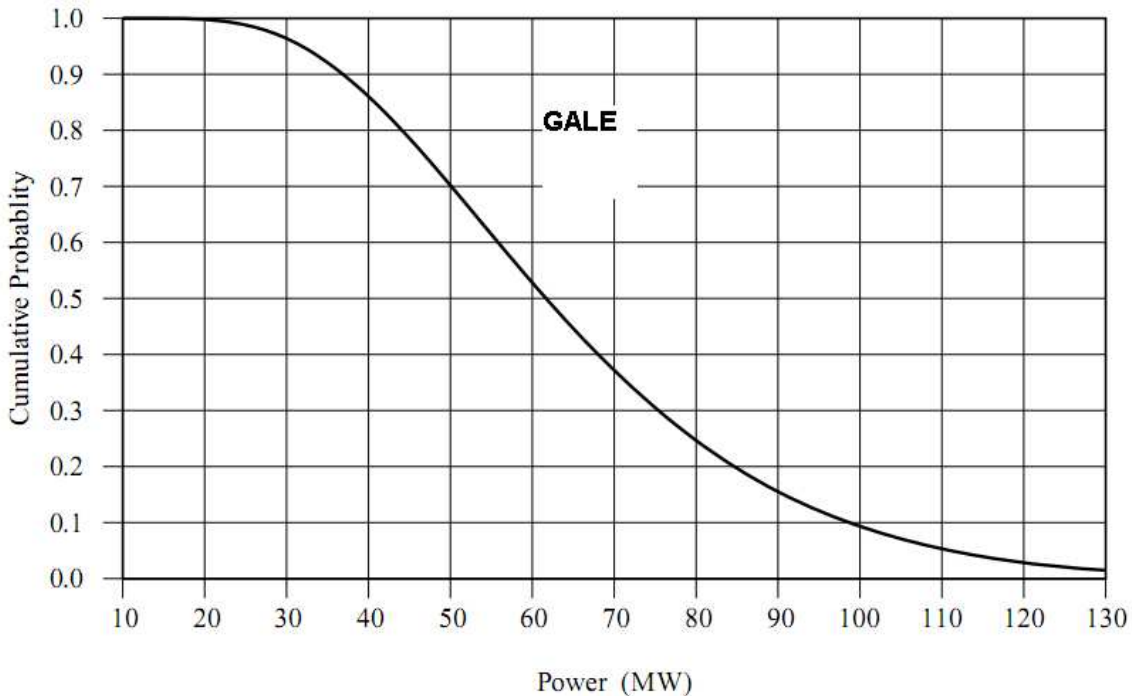

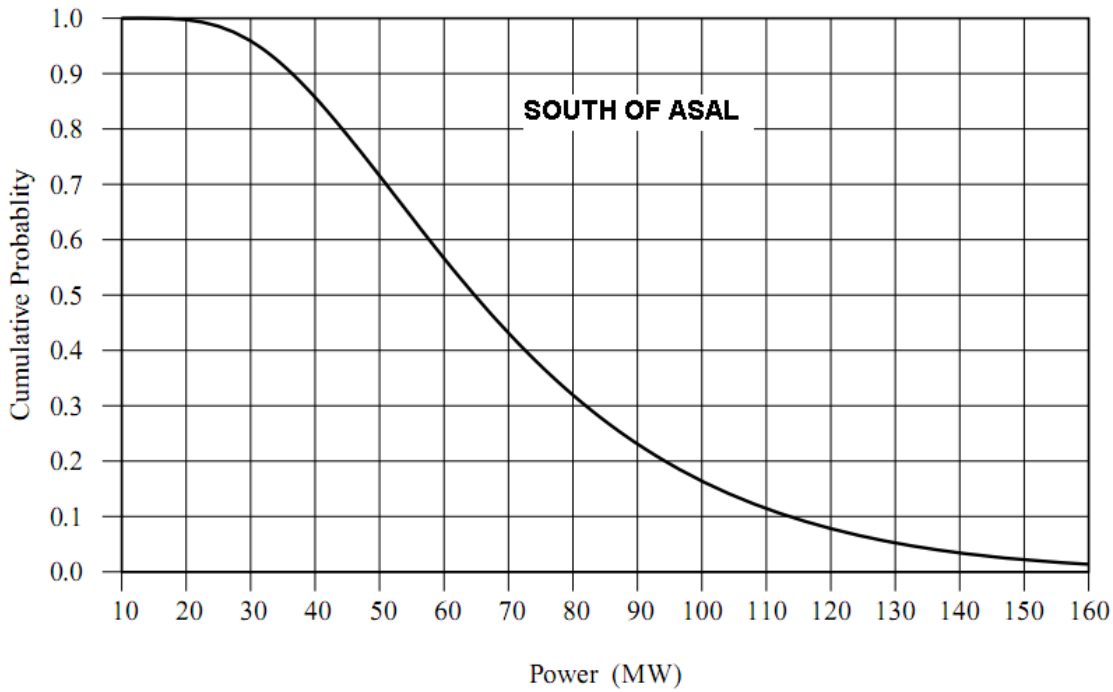

Fig. 3: Cumulative probability of energy reserves in three geothermal subfield of Asal area.

CONCLUSIONS

Using a volumetric method, the combined electricity generation potential of the three Asal geothermal systems is estimated to be between 115 and 329 MWe (Table 6). As more data on these areas become available, numerical studies should be performed to better determine electricity generation capacity of the Asal region.

ACKNOWLEDGEMENTS

Thanks to Reykjavik Energy Invest for allowing me to use data from the geophysical survey made in the Asal geothermal system. My appreciation goes also to Dr. Sabodh K. Garg for his help with calculations using volumetric method.

REFERENCES

Aquater, 1989. Djibouti geothermal exploration project Republic of Djibouti: final report. Aquater SpA, Lorenzo in Campo, Pesaro, Italy, 159 pp.

Arnasson, K., Eysteinsson, H., Vilhjalmsson, A.M, 2008. The Asal geothermal field, Djibouti. ISOR geophysical surface exploration. ISOR report 2008/019, 70 pp.

MIT, 2006. The future of geothermal energy: impact of enhanced geothermal systems [EGS] on the United States in the 21th Century. Massachusetts Institute of Technology , Cambridge, MA, USA. Available on World Wide Web at: *http://www1.eere.energy.gov/geothermal/future_geothermal.html*

Muffler, L.J.P., Cataldi, R., 1978. Methods for regional assessment of geothermal resources. Geothermics 7, 53-89.

Muffler, L.J.P., Christiansen, R.L., 1978. Geothermal resource assessment of the United States, Pure and Applied Geophysics 117, 160-171.

Sabodh, K.G., 2010. Appropriate use of USGS volumetric "heat in place" method and Monte Carlo calculations. Proceedings of the 34th Workshop on Geothermal Reservoir Engineering, Stanford University, Stanford, CA, USA, SGP-TR-188.

Vosteen, H.D., Schellschmidt, R., 2003. Physics and Chemistry of the Earth 28, 499–509.

APPRAISAL OF GEOSTATISTICAL METHODS TO ESTIMATE HYDRAULIC PROPERTIES OF A COMPLEX BASALTIC RESERVOIR. THE GULF BASALTIC AQUIFER, DJIBOUTI, HORN OF AFRICA.

Mohamed Jalludin[1] . and Moumtaz Razack[2*]
[1]*CERD, Centre d'Etudes et de Recherches de Djibouti, PB 486, Djibouti, Republic of Djibouti. email: cerd@intnet.dj*
[2]*University of Poitiers, Departement of Hydrogeology UMR 6962, 40 avenue du Recteur Pineau, 86022 Poitiers Cedex, France. email: moumtaz.razack@univ-poitiers.fr*
**corresponding author*

ABSTRACT

Estimating hydraulic properties of highly heterogeneous reservoirs is still a problem difficult to solve, especially when available data are few and poorly distributed. Such an estimate is still necessary to develop numerical models for resource management of these reservoirs. In the Republic of Djibouti, the basaltic reservoirs are the main source of water supply. Djibouti, the capital city, is especially supplied with water from the Gulf basaltic aquifer. The sustainable management of this reservoir is currently a priority, since its resources are overexploited. The objective of this work is to analyze several geostatistical methods (ordinary kriging, cokriging and kriging with external drift) and compare their performances to estimate the properties of highly heterogeneous reservoirs.

The Gulf basaltic aquifer is strongly heterogeneous. The transmissivity (T, m²/h) data are few and clustered mainly along the coastline. However, several geophysical surveys were undertaken over this basaltic reservoir. At present, a great deal of geoelectric data (transverse resistance, R ohm.m²), almost uniformly distributed, are available. Performances of the geostatistical methods are assessed using the cross-validation procedure. The results show that ordinary kriging, which is a univariate method, is the least suitable method to assess the transmissivity of the basaltic aquifer. The use of the transverse resistance (R), as an auxiliary variable, much more densely sampled than the principal variable (T), can significantly improve the estimation of T. Comparing the cokriging and the kriging with external drift, shows that KED is the best estimation procedure of the transmissivity of this highly heterogeneous reservoir.

INTRODUCTION

Basaltic volcanic rocks form aquifers which can contain significant groundwater resources and represent the major water supply source (Krivochieva and Chouteau, 2003). The structure of these aquifers can however be strongly heterogeneous and show high variability in reservoir properties (Livet et al., 1999 . Sruoga et al., 2003 ; Jalludin and Razack, 1994), which actually constitutes a real difficulty when one aims at the identification of these aquifers. The resources of these aquifers can accordingly be wrongly exploited, resulting in overexploitation and quality deterioration.

This situation prevails in the Republic of Djibouti, a country of 23000 km² and 650000 inhabitans located in the Horn of Africa at the crossing of the Red Sea and the Indian Ocean (Fig.1). The territory of Djibouti is mainly covered by volcanic rocks (more than 75%) as a result of the Red Sea, Gulf of Aden and East African rifts spreadings. The country undergoes an arid climate and does not possess perennial surface waters. Thus water resources are almost solely provided by aquifers located in volcanic rocks.

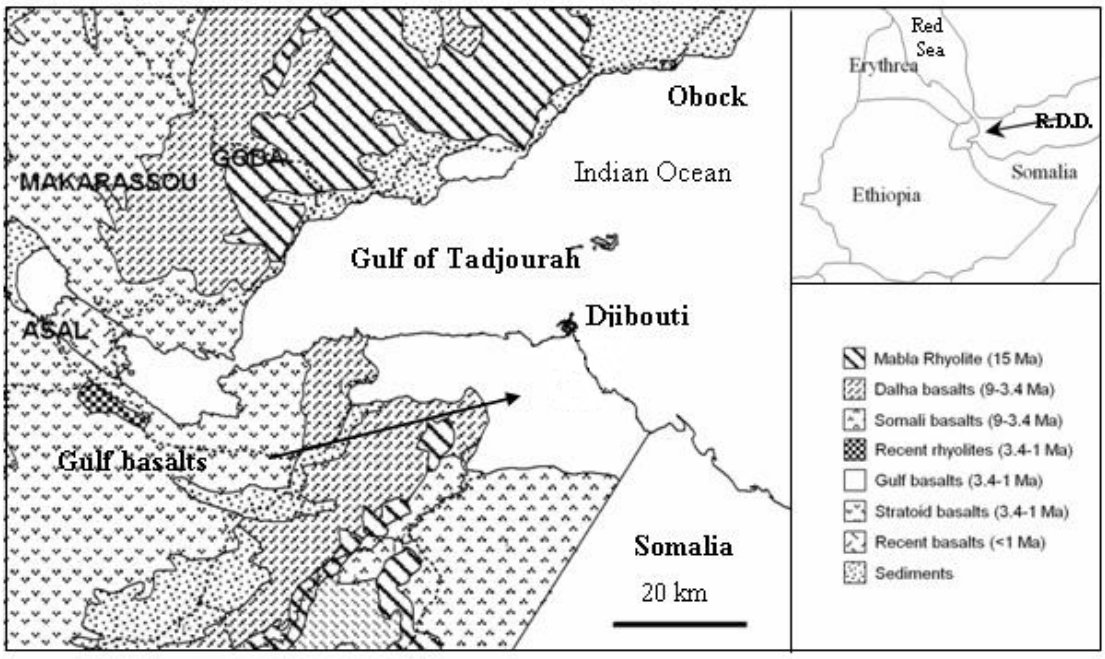

Figure 1: Geological setting of the Gulf basaltic aquifer.

The city of Djibouti, capital of the Republic, is supplied with drinking water, abstracted from the Gulf basaltic aquifer. The steady and drastic increase in water demands, due to the rapid development of the capital particularly during the last two decades, has led to an intensive exploitation of this aquifer and has severely depleted its reserves and deteriorated its quality (Houssein and Jalludin, 1996 ; Jalludin and Razack 1997). An optimal and sustainable management of this aquifer must be undertaken in order to prevent an irreversible deterioration of its resources. The evaluation of this aquifer hydrogeological properties and the elaboration of a management numerical model are the principal objectives of a large research program launched by the authorities. All the transmissivity data available since the Sixties were assembled in a database (Jalludin & Razack, 2004). However, transmissivity data of the Gulf aquifer are still few and irregularly distributed (Fig.2). Upscaling these few data at the scale of the aquifer is a prerequisite, before undertaking a valuable modeling task.

This paper is focused on the estimation of the transmissivity of this strongly heterogeneous aquifer, with the use of geostatistical methods (Isaak and Srivastava, 1989; Kitanidis, 2000). A noteworthy advantage of geostatistics is that these estimation procedures take into account the spatial variability of the data. This propriety is essential when dealing with very highly heterogeneous medium such as the Gulf basaltic aquifer. Three methods are compared, ordinary kriging (OK), cokriging (COK) and kriging with external drift (KED). OK is a univariate estimation method, which uses only the available data of the principal variable to estimate. COK and KED are multivariate estimation methods as they use the principal variable but also one or more secondary variables which are sampled at much more locations over the study area. In the latter case, the principal and secondary variables should display significant correlations.

In this study, the availability of a large number of geoelectrical data covering the aquifer system was exploited as secondary data in the COK and KED procedures. The Gulf basaltic aquifer was subjected to a number of geoelectric surveys in the Sixties. Accordingly, geoelectric data are quite numerous and are distributed almost over the whole area of the aquifer (Fig.3). Comparison of the different estimation methods, (OK, COK, KED) is made using the cross-validation procedure (Isaak and Srivastava, 1989; Clark, 1986). The following points will be developed : statistical analysis of available transmissivity (T, m²/h) and transverse resistance (R, ohm.m²) data; statistical

regression between T and R data ; variographic analysis of T and R data; comparison of the three geostatistical estimation methods ; estimation of the transmissivity using the best geostatistical method. .

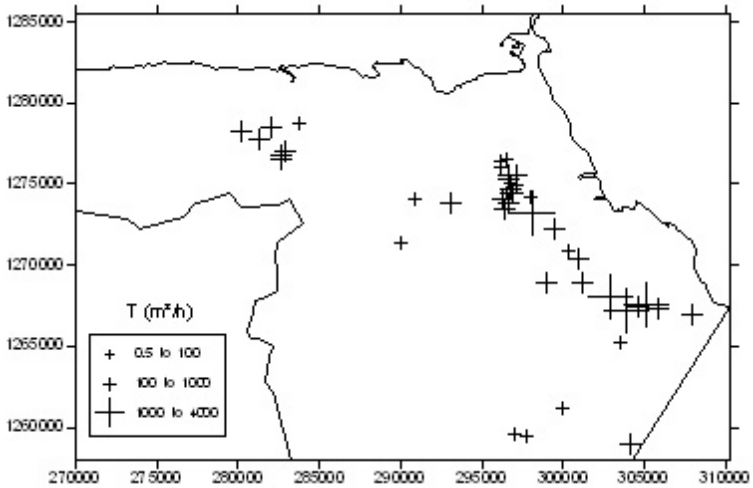

Figure 2: Distribution of the transmissivity data

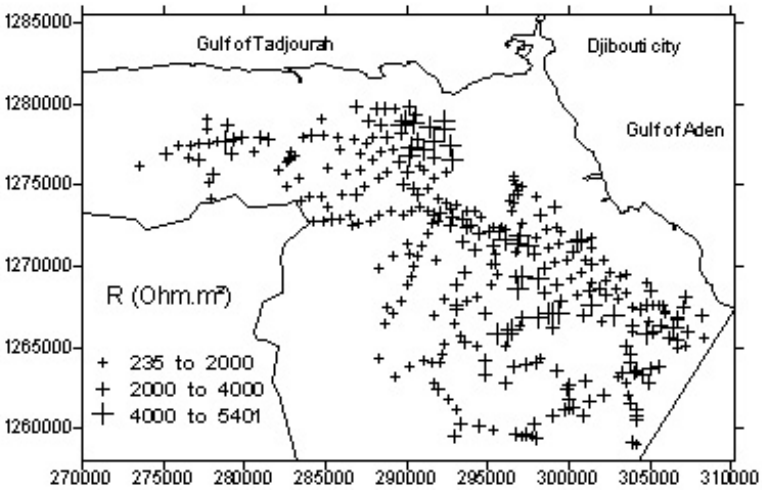

Figure 2 – Distribution of the transverse resistance (R, ohm.m²) data

Summary of univariate and bivariate geostatistical analysis

A few noteworthy features regarding the geostatistical methods used in this study are highlighted hereunder. A detailed presentation can be found in basic geostatistics references (Isaaks and Srivastava, 1989 , Kitanidis, 2000; Clark and Harper, 2000).

A geostatistical estimation procedure is twofold. When the variable of interest is unique (say Z), the first objective is to describe the spatial correlation between sample points. This is achieved by calculating the variogram, which is defined by the following equation:

$$\gamma_Z(h) = \frac{1}{2} E\left[(Z(x+h) - Z(x))^2\right] \qquad [1]$$

where $h=x_i-x_j$; E: mathematical expectation. The variogram is the basic tool for geostatistical analysis. It shows the spatial variability of the regionalized variable. The second objective is to provide the best estimation of the variable Z at unsampled points. Contrary to other estimation techniques, Geostatistics takes into account the observable spatial correlation between sample points to predict the variable at unsampled points. The geostatistical univariate estimation method used in this study is the ordinary kriging (OK). The kriging estimator (Eq.2) at a point x_0 is written:

$$Z^*(x_0) = Z_0^* = \sum_{i=1}^{N} \lambda_i Z(x_i) \qquad [2]$$

Z_0^* is a linear weighted estimator, N is the number of values involved in the estimation within the searching neighbourhood and λ_i are weights. The OK estimator should satisfy two major conditions, called the unbiasedness and optimality conditions. These conditions stipulate that the errors of estimate (differences between the true values and the estimated values) should have a mean equal to zero and a minimum variance. They are written, respectively:

$$\mathrm{E}(\mathrm{Z}^* - \mathrm{Z}_0) = 0 \qquad [3]$$

$$\mathrm{Var}(\mathrm{Z}^* - \mathrm{Z}_0) \text{ minimum} \qquad [4]$$

In many cases, the principal variable Z is undersampled, whereas one (or more) secondary variables are available at much more sample points. In such cases, the secondary variables, which should be correlated with the principal one, can be used to improve the estimation of the principal variable Z. Two bivariate geostatistical methods, which use one secondary variable densely sampled, are implemented in this study : cokriging (COK) and kriging with external drift (KED).

Cokriging requires the variogram of the principal variable Z (Eq.1), the variogram of the secondary variable Y (Eq.5) and the cross variogram (eq.6) of both variables Z and Y :

$$\gamma_Y(h) = \frac{1}{2} E\left[(Y(x+h) - Y(x))^2\right] \qquad [5]$$

$$\gamma_{ZY}(h) = \gamma_{YZ}(h) = \frac{1}{2} E\left[(Z(x+h) - Z(x))(Y(x+h) - Y(x))\right] \qquad [6]$$

The variogram, $\gamma_Z(h)$ or $\gamma_Y(h)$, as stated above, shows the spatial variability of one variable, whereas the cross variogram, $\gamma_{ZY}(h)$, shows the spatial covariability of one variable with the other.

Cokriging is the multivariate extension of kriging that allows the inclusion of more readily available and inexpensive attributes in the prediction process. The cokriging estimator is also a linear estimator of weights λ_i (principal variable) and β_i (auxiliary variable) and is written:

$$Z^*(x_0) = \sum_{i=1}^{N} \lambda_i Z_i + \sum_{j=1}^{M} \beta_j Y_j \qquad [7]$$

where Z_i and Y_j are the values of variables Z and Y measured at points i and j respectively ; N and M are the number of points of measurement of variables Z and Y within the searching neighbourhood ; λ_i and β_i are unknown. The COK estimator should also satisfy the unbiasedness and optimality conditions.

Developing equations [3, 4] leads to a system of kriging (or cokriging) equations written in terms of the variograms and cross-variogram. Solving these systems yields the N weights λ_i to be used for OK estimation [eq.2] or the N weights λ_i and and M weights β_j to be used for COK estimation (Eq. 7). The kriged estimate (Eq.2) or cokrigged estimate (Eq.7) can be calculated.

The variance of the errors of estimate (kriging variance) is given as:

$$\sigma^2(x_0) = Var(Z^* - Z_0) = \sum_{i=1}^{N} \lambda_i \gamma(x_i - x_0) + \mu_0 \qquad [8]$$

where μ_0 is the Lagrange multiplier. The expression of the co-kriging variance can be found in geostatistical basic references.

The variance of the errors of estimate is an indicator of the confidence to be granted to the kriging or cokriging estimates. The lower the variance, the higher the confidence.

One should note that OK and COK takes well into account : i) the spatial positions of the point to be estimated and the known points; and ii) the spatial variability of the variables through the variograms and the cross-variogram.

Kriging with external drift (KED) is an alternative to co-kriging. In this case, the auxiliary variable Y(x) is considered as a second random variable and is interpreted as a drift or trend that may follow the principal variable Z(x) throughout the study area. Z(x) may thus be expressed as (Wackernagel 1995):

$$Z(x) = a + b\,Y(x) + R(x) \qquad [10]$$

where a and b are constants, Y(x) is the auxiliary variable (or drift function), R(x) is a residue.

To be useful the drift function either need to be everywhere known or can be easily and precisely interpolated throughout the study area. KED assumes that, rather than being constant, the mean E[Z(x)] is a function of location, specifically a linear combination of one drift function which varies according to location :

$$E[Z(x)] = a + b\,Y(x) \qquad [11]$$

The residue R(x) is assumed to be an intrinsic residue :

$$E[R(x)] = 0 \qquad [12]$$

The principal variable Z(x) is then modeled as a nonstationary variable whose non-constant average is locally equal to the external drift. The KED estimator should, as the OK and COK estimators, satisfy the unbiasedness (Eq.3) and the optimality (Eq.4) conditions.

Cross validation

The performances of the estimation methods are assessed using the cross-validation procedure (Isaaks and Srivastava, 1989 ; Clark, 1986). This procedure compares actual values with estimates and comprises the following steps : i) eliminate a single value from the data set, ii) estimate a new value at this location vs. the surrounding values using OK, COK or KED, iii) calculate the actual error using (Z_i^* - Z_i) (actual value-estimated value), and iv) find out the theoretical error using the estimation variance (or its square-root, the standard deviation). This procedure is repeated for all the data set. If the estimation is accurate, the following results should be obtained : i) the average of the actual errors should be zero (Eq.3) ; ii) their variance should be a minimum (Eq.4) ; iii) the ratio of the variance of the actual errors to the average estimation (kriging or cokriging) variance (Eq.13) should be one :

$$\left\{\frac{1}{N}\sum_{i=1}^{N}(Z_i^*-Z_i)_2\right\}/\frac{1}{N}\sum_{i=1}^{N}\sigma_i^2=1 \qquad [13]$$

A standardised W statistic can also be calculated as follows (Clark, 1986) : each actual error is divided by the appropriate estimation standard error. This W statistic should then average zero and have a standard deviation of one.

GEOLOGICAL AND HYDROGEOLOGICAL SETTING OF THE GULF BASALTIC AQUIFER

The regional geodynamic framework is related to the expansion of the tectonic plates of Africa, Arabia and Somalia since 30 My, during which the principal volcanic series, basalts and rhyolites, that are found in the area of Djibouti, were laid down (Jalludin, 1993). Basalts of the Gulf (2.8-1 My), which are the subject of this study, are located close to the town of Djibouti (Fig. 1). They cover a surface of 560 km2 until the town of Arta and the massif of Bour Ougoul towards the West, and until Hindi and Loyada towards South-west. They are presented in the form of a plateaus which go up to 200 meters in altitude. Several principal wadis (temporary rivers), Ambouli, Atar, Damerdjog and Douda, cross this formation and sometimes sculpt canyons whose cliffs exceed several tens of meters. Many volcanic cones of different sizes strew the plateaus, in particular in the Southern part.

The Gulf basalts are composed of basaltic flows with intercalation of sedimentary layers, scoria and paleosoils. They are characterized on the surface by a significant weathering in balls. The thickness of this formation is very variable because of the play of the normal faults and the paleoreliefs highlighted by geophysics (CGG, 1965-1987) and drillings. It must reach 200 meters at least, in particular near the well PK20.

Basalts of the Gulf lie in discordance on Somalis basalts (7.1-3 My) in the South and on Dalha basalts (9-3.4 My) and Mabla rhyolites (15 My) in the West. This contact is well determined by the geomorphological criteria in the West and South-west.

Several networks of fractures affect the Gulf basalts. The East-West fracturing direction is the most significant and results probably from the first deformations linked with the pouring of the basaltic formation and which would have been reactivated until recently. The other directions of fracturing are N140°-150° and NS-N040°. The outcrops are characterized by weathering and hydrothermalism. Their effects are all the more marked as the formation is older. The hydrothermal activities result in secondary mineral deposits and accordingly reduce the permeability of the basalts.

The Gulf basaltic aquifer is prone to an intense exploitation for the drinking water supply of the town of Djibouti. This exploitation has increased regularly with the social and economical development of the Capital and amounts to about 35 000 m^3 per day (12.7 millions m^3 per year) provided by 32 wells. The abstraction rate of the wells is included between 20 and 100 m^3/h. One notes a regular degradation of the quality of water highlighting the overexploitation of the aquifer.

Because of the arid climate, annual precipitations reach only 150 mm on average. The surface of basalts being impermeable because of surface weathering, the recharge of the aquifer occurs exclusively in the stream beds occupied by alluvial deposits which represent an intermediary aquifer before basaltic aquifer recharge (Jalludin and Razack 2004). Recharge of the aquifer has been estimated by BGR (1982) as the equivalent of 5 % of the precipitations (150 mm). The annual average recharge is estimated between 10 and 15 millions cubic meters per year indicating that there might be overexploitation of the aquifer.

Transmissivity data. Statistical and variographic analyses

Jalludin & Razack (2004) elaborated a database of all the transmissivity data available regarding the Gulf basaltic aquifer and other basaltic aquifers in the Republic of Djibouti. Since then this database has constantly been kept updated. At present, 42 (forty two) data of transmissivity characterizing the Gulf basaltic aquifer are available (Fig.2). The summary statistics of these transmissivity values deduced from these tests are provided in Table 1. The transmissivity values of the Gulf basaltic aquifer range between 0.5 m^2h^{-1} and 3600 m^2h^{-1}. The average is 402 m^2h^{-1} , the standard deviation is 676 m^2h^{-1} and the variation coefficient is 168 %. These statistics emphasize the strong heterogeneity of this aquifer.

Table 1. Summary statistics of the transmissivity (T, m^2/h) database for the Gulf basaltic aquifer including T values deduced from pumping test data and estimated from corrected specific capacity.

maximum	**minimum**	**average**	**Standard deviation**	**Coefficient of variation (%)**
3 600,0	0,5	402	676	168

The frequency distribution of the transmissivity data set is reported on a log-probability diagram (Figure 4). Most of the data are plotted along a line, which indicates that the data are lognormally distributed. No fitting test is provided here. However lognormality of the transmissivity has widely been demonstrated in the literature (Delhomme, 1979 ; Neumann, 1979) and is at present accepted as an intrinsic property of heterogeneous media.

The experimental variogram of the log-transmissivity (logT) is reported in figure 5. It is characterized by no drift, a sill and an autocorrelation between the points for low distances It shows that logT has a regionalised variable behaviour. No nugget effect was depicted which means that there is no lower scale structure. The theoretical model fitted to the experimental logT variogram is an exponential model, whose general equation is :

$$\gamma(h) = C_0 + C_1 [1 - \exp(-\frac{3h}{a})] \qquad (14)$$

where C_0 is the nugget effect, $C = C_0 + C_1$ is the sill, a is the practical range (distance at which 95% of the sill has been reached) , h is the distance between sampling points. The nugget effect represents any small-scale data variability or possible sampling (measurement and/or location) errors. The sill indicates the total variance. The range is the distance between sampling points at which the sill is reached. Beyond the range, the variance measured between the data points is independant from the respective data points and there is no longer a correlation between the points.

The expression of the exponential variogram of log(T) is :

$$\gamma(h) = 0.0 + 0.63 \ [1 - \exp(-\frac{3h}{5160})] \qquad (15)$$

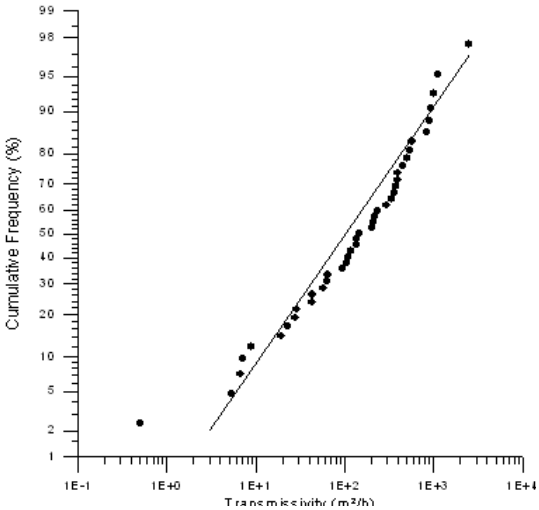

Figure 4: Frequency distribution of T(m²/h)

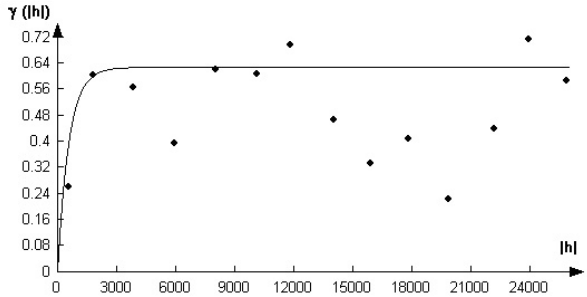

Figure 5: Experimental variogram of logT and fitted exponential model.

Geophysical prospection and transverse resistance data

Several geophysical studies were undertaken on the Gulf basaltic aquifer in order to develop the groundwater resources supply for Djibouti town (BGR 1982, 1996; CGG 1965-1987; ARLAB 1984; ISERST 1997). Progressively, these geophysical surveys covered almost the whole Gulf basaltic aquifer. The Schlumberger electrical method (Astier 1971) has been almost exclusively applied. For the present study, all the available transverse resistance (R, Ohm.m²) data were collected, as they are reported in these surveys. The raw electrical soundings were not reinterpreted. A number of 322 transverse resistance data were thus collected. They are quite homogeneously scattered over the aquifer surface (Fig.3).

Statistics on the transverse resistances data are given in Table 2. The average is 2265 ohm.m² and a coefficient of variation of 55%.Transverse resistance values vary between 235 ohm.m² and 5400 ohm.m². Low values are generally significant of the presence of clay material, while high values would result from impervious basalts.

Table 2. Summary statistics of the transverse resistance (R, Ohm.m²) database for the Gulf basaltic aquifer .

maximum	minimum	average	Standard deviation	Coefficient of variation (%)
5400	235	2168	1257	58

The frequency distribution of the transverse resistance is plotted on a log-probability diagram (Figure 6). As for transmissivity, this diagram shows that the transverse resistance data are lognormally distributed. This result is consistent with those previously published in the litterature (Razack and Sinan, 1988 ; Ahmed et al., 1988)

The experimental omnidirectional variogramme of the logarithm of transverse resistance (logR) is presented in figure 7. It is characterized by no drift, a sill and an autocorrelation between the points for low distances showing that the transverse resistance has a regionalised variable behaviour. It also indicates the presence of a second-order stationnarity for an h of about 6 km.

The theoretical model fitted to the experimental logR variogram is an exponential model, whose equation is :

$$\gamma(h) = 0.0 + 0.081 \ [1 - \exp(-\frac{3h}{10080})] \qquad (16)$$

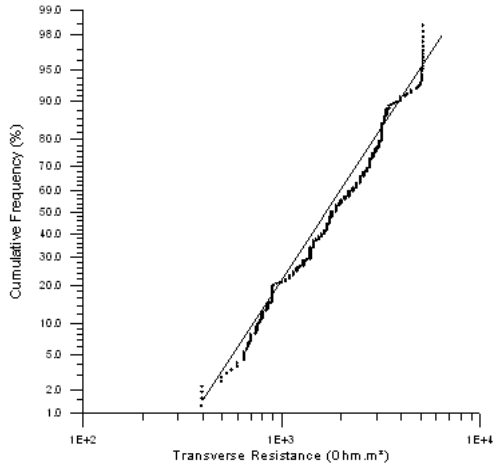

Figure 6: Frequency distribution of R(Ohm.m²)

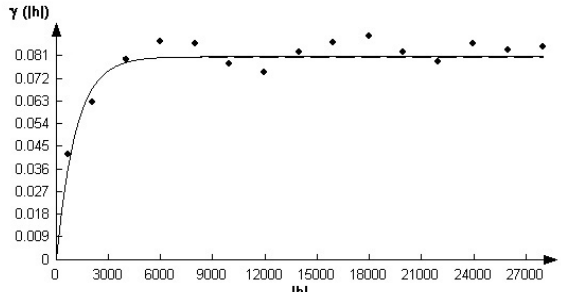

Figure 7: Experimental variogram of logR and fitted exponential model

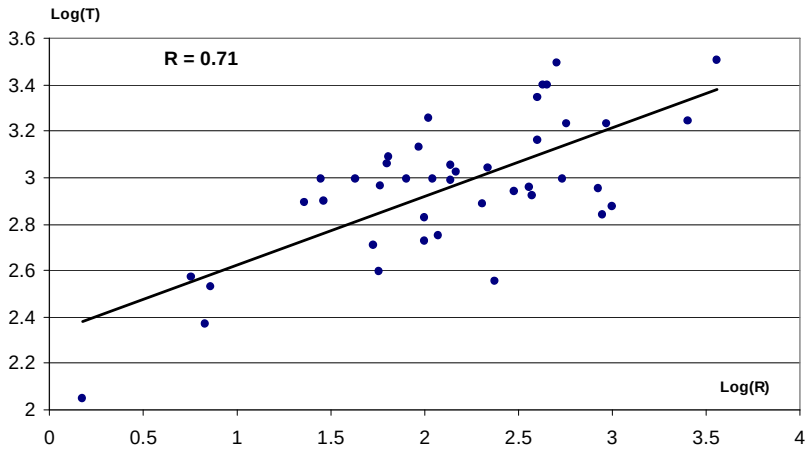

Figure 8: Correlation diagram between log(T) and log(R)

REGRESSION ANALYSIS OF LOG (TRANSMISSIVITY) VS. LOG(TRANSVERSE RESISTANCE)

Previous studies on the relationship between transmissivity and transverse resistance investigated three types of statistical relationships : linear form T = a + bR, exponential form $T = ab^R$ and log-log form logT = a+blogR (i.e. geometrical) (Razack and Sinan 1988 ; Kosinski and Kelly 1981; Heigold et al., 1979 ; Mazac et al., 1985). However when the variables are lognormally distributed, a log-log regression yields the best estimates (Huntley, 1986 ; Razack and Huntley, 1991).

The log(T) data vs. log(R) data are reported in figure 8. The diagram shows that both variable are linearly correlated. The value of the coefficient of correlation is R = 0.71, which is quite significant. Such a significant correlation between log(T) and log(R) allows thus to undertake estimation of the undersampled principal variable (log transmissivity) using the widely sampled auxiliary variable (log transverse resistance).

Cross validation results and discussion.

The cross validation results are summarized in Table 3. The following comments can be drawn :

- The errors average (Eq.2) is close to zero. The lowest values are provided by OK and KED.
- The errors variance (Eq.3) is the lowest for KED.
- The average of the Wi statistics is close to zero and its standard deviation close to one for the 3 methods. Best values are however related to OK and KED.
- The ratio Errors variance/estimation variance (Eq.13) is close to 1 for the 3 methods.

The correlation coefficients between observed and predicted values of log(T) are not significant for OK [R_{OK}(obs, pred) = 0.10] and COK [R_{COK}(obs, pred) = 0.13]. The highest correlation is provided by the KED procedure [R_{KED}(obs, pred) = 0.50].

Table 3: Comparison of the cross-validation performances using the OK, COK and KED estimation procedures

	OK	**COK**	**KED**
R(obs, pred)	0.1	0.1	0.5
W Average	0.04	0.34	0.08
W SD	1.05	1.16	1.08
Error Average	0.04	0.24	0.06
Error SD	0.78	0.79	0.69
Error Variance (1)	0.61	0.62	0.48
Estimation Variance (2)	0.52	0.46	0.41
(1)/(2)	1.2	1.3	1.2

Accordingly, the cross validation clearly demonstrates that OK and COK are the least performing estimation methods. Cokriging, though using a densely sampled auxiliary variable, does not provide in this study, the best estimation, contrary to what was observed in previous studies (Aboufirassi & Marino, 1984).

The best estimation of the logT is provided by the KED procedure. The use of logR data, as auxiliary variable, proved quite useful when performing estimation using KED.

Estimation of the logT of the Gulf basaltic aquifer using KED

Estimation of the Gulf basaltic aquifer log(transmissivity) using KED has been carried out on a grid with a mesh size of 1 km x 1 km. As transmissivity is assumed isotropic, the KED is performed with a moving neighbourhood that uses a circle radius search. The KED procedure produces an unbiased estimation of logT. This is the best estimation of logT that can be presently achieved, on the basis of the available transmissivity and transverse resistance data.

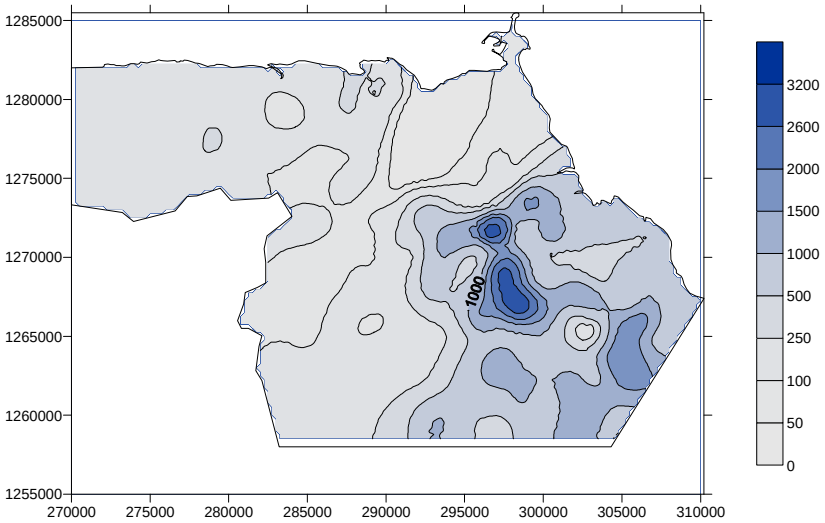

Figure 9: Distribution of the transmissivity (T, m²/h) of the Gulf basaltic aquifer, obtained by backtransform of the estimated logT using KED

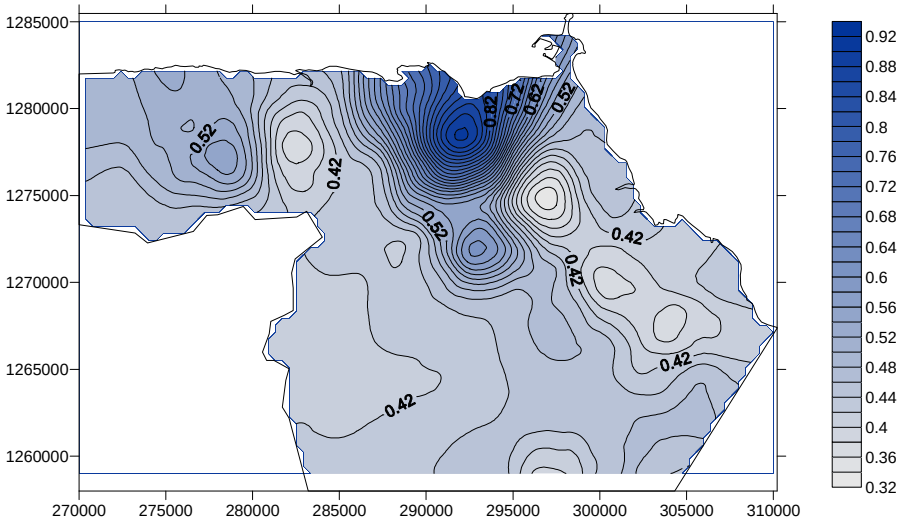

Figure 10: KED variance associated with the estimation of logT

Figure 9 shows the distribution of the transmissivity (T, m²/h) throughout the Gulf basaltic aquifere. This distribution is obtained by backtransform of the estimated logT distribution using KED. This estimation will be used in forthcoming numerical modeling works of the Gulf basaltic aquifer.

Figure 10 shows the estimation variance associated with the estimation of logT. The higher the variance, the more uncertain the estimation of logT. The figure reveals however that the places where the estimation is highly uncertain, are rather few. This might be due to the densely sampled auxiliary variable (transverse resistance, R ohm.m²) used with KED.

CONCLUSION

The determination of the transmissivity fields is one of the most critical issue to which the hydrogeologists are faced. An attempt has been undertaken on the basis of geoelectrical properties to estimate the transmissivity field of the Djibouti basaltic aquifer using geostatistical procedures. Three estimation procedures have been compared, ordinary kriging (OK), cokriging (COK) and kriging with external drift (KED). OK is a univariate method, as it uses only the data of the principal variable, while COK and KED are bivariate method as they use the data of an auxiliary variable, which can be much more densely sampled than the principal variable. The auxiliary variable used in this study is the transverse resistance.

The main findings of this study are summarized as follows :

1. Transmissivity (T, m²/d) and transverse resistance (R, ohm.m²) are lognormal variables.
2. Both variables are spread over several orders of magnitude, revealing the strong heterogeneity of the aquifer.
3. A significant statistical relationship was found between logT and logR, along with a correlation coefficient R=0.71.
4. The geostatistical procedures estimation performances were assessed using cross-validation. This test showed that the best logT estimates are provided by KED.
5. An estimation of the logT of the Gulf basaltic aquifer was performed on a regular grid of 1 km x 1 km using KED.

The geostatistical approach proved useful to provide a reliable estimation of the log(transmissivity) of the Gulf basaltic aquifer. This approach incorporates all the available data on transmissivity and transverse resistance. This transmissivity estimation will be used as an input in forthcoming modelling of this important aquifer, the water resources of which need to be optimally managed.

REFERENCES

Aboufirassi M. and M.A.Marino, 1984. Cokriging of aquifer transmissivity from field measurements of transmissivity and specific capacity. Math.Geol. v.16, no.1, pp.19-35.

Ahmed, S., de Marsily, G., Talbot, A., 1988. Combined use of hydraulic and electrical properties of an aquifer in a geostatistical estimation of transmissivity. Ground Water 26 (1), 78–86.

ARLAB 1984. Etude géophysique de la zone du PK20. Rapport final de projet. *Unpublished*.

Astier J. 1971. Géophysique appliquée à l'hydrogéologie. Masson, Paris, 277p.

BGR 1982 Bundesanstalt für Geowissenschaften und Rohstoffe. Inventaire et mise en valeur des ressources en eau de la République de Djibouti. Coopération Hydrogéologique Allemande. 4 volumes. *Unpublished*.

BGR 1996. Bundesanstalt für Geowissenschaften und Rohstoffe. Assistance auprès de l'Office national des Eaux de Djibouti (ONED. Résultats de la campagne des forages de reconnaissance effectué dans la plaine de hanlé. *Unpublished*.

Clark I., 1986 The art of cross validation in geostatistical applications. Proc. 19th International APCOM Symposium, Penn. State Univ., April, 211- 220.

Clark I. and Harper W.V., 1982. Practical Geostatistics 2000. Ecosse North America, Columbus Ohio (USA).

CGG 1965-1987. Etudes géophysiques en République de Djibouti. Rapports d'étude. *Unpublished*.

CPGF 1987. Etude géophysique de la région de Mouloud. Rapport d'étude. *Unpublished.*

Delhomme J.P. 1979. Spatial variability and uncertainty in groundwater flo parameters : a geostatistical approach. Water Res. Research, 15 :269-280.

Heigold P., Gilkeson R., Cartwright K. and Reed P. 1979 Aquifer transmissivity from surficial electrical methods. Ground Water, 17(4):338-345.

Houssein I. and Jalludin M. 1996. The salinity of Djibouti's aquifer. Journal of African Earth Sciences, vol.22, n°4, p 409-414.

Huntley D. 1986. Relations between permeability and electrical resistivity in granular aquifers. Ground Water, 24(4):466:474.

Isaak E. and Srivastava R., 1989. An introduction to applied Geostatistics. Oxford Univ.Press, New York, NY.

ISERST 1997. Etude hydrogéologique. Localisation des points deau pour les camps de régugiésà Assamo, Ali Adé et Holl Holl.UNHCR-ISERST. Rapport final. *Unpublished*.

Jalludin M. 1993. Propriétés géométriques et hydrodynamiques des roches volcaniques fissurées sous climat aride. République de Djibouti. Thèse de Doctorat, Poitiers, décembre1993

Jalludin M. and Razack M. 1997. Modélisation de l'aquifère fissuré basaltique. Nappe de Djibouti. 5ème Assemblée Scientifique de l'Association Internationale des Sciences Hydrologiques. Rabat, Maroc, 23/04-3/05 1997.

Jalludin M. and Razack M. (1994) Analysis of pumping tests in fractured Dalha and stratoid basalts with regards to tectonics, hydrothermal effects and weathering. Republic of Djibouti. Journal of Hydrology., 155:237-250.

Jalludin M. and Razack M. (2004) Assessment of hydraulic properties of sedimentary and volcanic aquifer systems under arid conditions in the Republic of Djibouti (Horn of Africa). *Hydrogeology Journal, Vol.12:159-170.*

Kitanidis P.K., 2000. Introduction to Geostatistics. Application in Hydrogeology. Cambridge Univ. Press, Cambridge, UK.

Kosinski W.K. and Kelly W. 1981. Geoelectrical soundings for predicting aquifer properties. Ground Water, 19(2):163-171.

Krivochieva S. and Chouteau M., 2003. Integrating TDEM and MT methods for characterizing and delineation of the Santa Catarina aquifer (Chalco Sub Basin, Mexico). J. of Applied Geophysics, 52, 23-43.

Livet M., Blavoux B., d'Arcy D. and Mishellany A., 2000. Capture et emmagasinement sous coulée au site volcanique de Beaunit (Puy de Dôme). C.R.A.S. Sc.Terre et des Planètes, 330, 47-52.

Mazac J., Kelly W. and Landa I. 1985. A hydrogeophysical model for relations between electrical and hydraulic properties of aquifers. J. Hydrol., 79:1-19.

Neuman S.P. 1979. Statistical characterization of aquifer heterogeneities, an overview of recent trends in hydrology. Proc. Symp. Honoring Prof. Witherspoon's 60th birthday, Lawrebce Berkeley Laboratory, Brkeley, CA, USA.

Razack M. and Huntley D. 1991. Assessing transmissivity from specific capacity in a large and heterogeneous aquifer. Ground Water, 29 :856-861.

Razack M. et Sinan M. 1988. Possibilités statistiques de prédiction des propriétés aquifères à l'aide des paramètres géoélectriques en milieu sédimentaire fortement hétérogène, Plaine du Haouz, Maroc. Journal of Hydrology, 97: 323-340.

Sruoga P., Rubinstein N. and Hinterwimmer G., 2004. Porosity and permeability in volcanic rocks: a case study on the Serie Tobifera, South Patagonia, Argentina. J. of Volcanology and Geothermal Res., 112, 31-43.

Wackernagel, H., 1995, Multivariate geostatistics : An introduction with applications, Springer, Berlin, 256 p.

THEME VI

FIELD DEVELOPMENT PRODUCTION TECHNOLOGY, POWER, DRILLING AND WELL DESIGN, LOW ENTHALPY, DIRECT USE

Development of geothermal energy technologies in low-enthalpy regions

Prof. Dr. U. Arslan & Dipl.-Ing. H. Huber
Faculty of Civil Engineering and Geodesy, Technische Universität Darmstadt,
Petersenstraße 12, 64287 Darmstadt, Germany, Arslan@IWMB.TU-Darmstadt.de

ABSTRACT

While other renewable energies arise more or less from the sun, geothermal energy sources its heat from the earth's interior, which is caused mostly by radioactive decay of persistent isotopes. This means a possibility of a base-loadable form of energy supply. Especially efficient is the use of geothermal energy in high-enthalpy reservoirs, which means a high energy potential in low depths. In Germany no high-enthalpy reservoirs are given. To use the given low-enthalpy potential efficiently inventions and improvements need to be performed. An important part of geothermal progresses is performed by universities with multidisciplinary research of geothermal design. Numerical calculations are essential for a correct dimensioning of the geothermal system. Therefore German universities and state aided organizations are developing numerical programs for a detailed use of application on geothermal systems. The history of this multidisciplinary research of geothermal design performed by German universities is shown in this paper. Outstanding shallow geothermal research projects of German scientists are pointed out. Currently the Technical University Darmstadt is performing a research program supported by the Ministry of Economics and Technology (BMWi). Main aim of this research program titled "*experimental investigation for the verification of a Finite-Element-Multiphase-Model*" is to analyze the subsoil as a three-phases-model with separated consideration of conduction, convection and advection and their subsequent interaction. The latest developments of shallow geothermal projects as well as the current state of the before mentioned research program are pointed out in the paper.

Keywords: Shallow geothermics, low-enthalpy, finite-element-multiphase-model, research

GEOTHERMAL DEVELOPMENT IN ZAMBIA

Kennedy Mwanza
Clint Kombe
ZESCO Limited
Great East Road, Stand No. 6949 - P.O. Box 33304, Lusaka. ZAMBIA

ABSTRACT

The Government of Zambia carried an inventory of potential geothermal prospects between 1970 and 1984. The program was aimed at undertaking a countrywide reconnaissance study of all known geothermal occurrences to establish their potential to generate electricity for small rural communities off the national power grid. Among the sites targeted for further investigation and development was the Kapisya and Chinyunyu hot springs. There are several identified hot springs located in different areas across the country.

In 1988, a pilot 200kWe geothermal Turboden binary power generating plant was constructed, but has remained non-operational for an extended period of time. The Kapisya binary plant is based on the organic Rankine thermodynamic cycle (ORC). The plant was not fully commissioned due to the absence of transmission and distribution reticulation to the load centres. The plant has remained dormant leading to loss of functional capacity due to equipment degradation. The plant is earmarked for resuscitation and supply power to the nearby communities and industries.

In view of the need to assess the geothermal resources of the Kapisya and Chinyunyu fields, and investigate the possibility of increasing the Kapisya plant capacity, ZESCO has partnered with a power utility with experience for technical assistance. The objective of the assessments is to rehabilitate and re-commission the Kapisya plant, and to assess the reservoir characteristics and to recommend a development plan for the two geothermal fields.

The geo-scientific investigations of the geothermal fields to determine the two fields' potential for geothermal power generation have already been carried out. The geoscientific works carried out included geological, geophysical and geochemical investigations. Geophysical investigations involving the use of the magneto-telluric (MT) and transient electromagnetic (TEM) methods, and geochemical surveys involved radon and carbon dioxide (CO2) gas measurements in soil, sampling of hot and cold springs and borehole water. The studies have shown that the two prospects are low-enthalpy fields and there is a high chance of getting more than 2MWe at each site using binary system of generation.

The plant will undergo rehabilitation with a view to overhaul existing production wells and electro-mechanical equipment, including construction of transmission line to load centres. The plant's surface facility conditions have already been undertaken. The plant resuscitation works are being followed by plant capacity expansion works to meet energy needs of the nearby communities and industries. The preparatory works for the erection of transmission/distribution lines have commenced.

Keywords: Binary plant; low-enthalpy; electricity

REHABILITATION OF THE ALUTO PILOT GEOTHERMAL POWER PLANT

Markos Melaku and Bob Thomasson
Geothermal Development Associates
mmelaku@gdareno.com, bthomasson@gdareno.com

SUMMARY

The Aluto Pilot Geothermal Power Plant was built and commissioned in late 1998 but stopped operation after a very short period due to various technical problems. Failure of the heat exchanger tubes caused the premature shutdown of the OEC unit after about a year of operation. A number of resource related problems also caused reduction in the power output of the GCCU which was eventually shut down in 2002.

The rehabilitation of the plant began in early 2006 which included overhaul of the wellhead valves, inspection of the steam turbine rotor and bearings, testing and identifying failed tubes of the OEC heat exchangers and rectifying plant PLC control system.

Significant work was carried out during 2006 and 2007 which resulted in the GCCU unit becoming operational in June 2007.

Failure analysis of the OEC heat exchanger tubes revealed that they need to be replaced with more corrosion resistant material. Subsequently, retubing of the heat exchanger tubes was undertaken in early 2009 and the unit was commissioned in June 2009. Both of the Aluto power plant units have been under operation since commissioning.

Keywords: Aluto project, plant rehabilitation, pilot power plant, binary and combined cycle unit

INTRODUCTION AND BACKGROUND

The Aluto geothermal field is located in the lakes district region of Ethiopia, about 200km south of the capital Addis Ababa. Access to the site is along the main southern high way which proceeds to Kenya.

The Aluto Langano Geothermal Pilot Plant is the first geothermal plant to be built in Ethiopia. The power plant is owned and operated by the state power company, Ethiopian Electric Power Corporation (EEPCO). The plant is composed of two units, the geothermal combined cycle unit (GCCU), which uses the geothermal steam from the hotter wells LA3 and LA6, and the Ormat Energy Converter (OEC unit) which uses steam from the lower temperature wells LA4 & LA8 and brine from all four wells. The objectives of the pilot plant were to test the Aluto resource, identify any resource or plant-related issues that could affect the further development of geothermal power at Aluto, allow EEPCo personnel to gain operation and maintenance experience on a geothermal power plant, and to provide power to the national grid. The project was also designed to act as a catalyst for the development of larger follow-on geothermal plants in the area.

Although the production wells were drilled during the early 1980's, as exploration wells, the decision to build a geothermal pilot plant was made more than a decade later in the mid 1990's. During the exploration program, a total of six wells were drilled on the Aluto volcano of which five were found to be productive.

Ormat Industries Ltd of Israel built and installed the power plant under a turnkey contract from early 1997 until the middle of 1998. EEPCo assumed formal responsibility for the operation and maintenance of both the plant and well field after commissioning in the middle of 1998.

The designed power output of the pilot plant was 8.52 MWe (gross) and 7.28 MWe (net). Shortly after commissioning, the resource and plant began experiencing problems that eventually led to its shutdown in 2002.

In 2005, EEPCo issued an international tender for the rehabilitation of the Aluto plant and wellfield that was won by Geothermal Development Associates of USA. The primary objectives of the contract was to investigate the reported problems and carry out repairs on the plant, wellfield, gathering system, transmission line, plant control system and provide training for EEPCO personnel. Any additional failure discovered during the rehabilitation was to be given as a recommendation. The main rehabilitation contract was implemented beginning in February 2006 through June 2007 when the GCCU unit was put back into operation. Under a contract amendment, the retubing of the OEC unit was carried out from late 2008 until early 2009 and the unit was put back into operation in July 2009.

PROBLEMS IDENTIFIED

A number of problems were identified during the initial operation of the plant and subsequent to its shut down in 2002 which formed the contract terms of reference for the rehabilitation work. These problems can be generally classified into two groups: those relating to the resource and those relating to the plant/steamfield.

Resource related problems:

- Wells unable to deliver steam at design pressure
- Solid emission from some of the production wells
- Mineral deposition down hole and is surface fluid gathering system

Plant/ steamfield related problems

- Leakage of wellhead valves
- Steam turbine bearing wear and high bearing temperature
- Heat exchanger tube failure
- Cooling tower fan problems
- Operational difficulties with plant control & monitoring software
- Transmission line problems

REHABILITATION WORK PERFORMED

Resource related rehabilitation works

Low operating pressure of wells LA3 & LA6

The most serious problem observed during the initial operation of the plant was that the operating pressure of wells LA-3 and LA-6 falling significantly lower that the design inlet pressure of the steam turbine. Subsequent well tests performed by GDA, as part of this contract, also showed that the wells are unable to sustain the operating pressure that the turbine was originally designed for. To address this problem, it was necessary to review the design of the turbine and implement necessary engineering measures so that it can operate at lower steam inlet pressures. After thorough review of the characteristics of the wells a recommendation was made to remove the first two stages of the turbine blades to enable the turbine accept the design flow rate of steam at the reduced inlet pressure. This measure of removing some of the stages (de-staging) would allow the wells to operate reliably, although at a slight reduction in power generated from the steam turbine.

The recommendation to remove the stages was also based on other practical issues. For example during the rehabilitation work, visual inspection of the first and second stages showed that they would required major repairs or outright replacement with new components. The de-staging process is reversible and if the operating pressure of future new wells reaches and maintains the original design pressure, the removed stages can be reinstated.

Solid emission from wells:

Some of the production wells were reported as emitting solids into the fluid gathering system resulting in blockage of the piping and parts of the plant. Most of the wells only discharge solids during the initial opening; however, well LA8 tends to produce sand & debris even during normal operation. In order to resolve this problem, two solutions were proposed. The first was to design & implement an operational procedure that will ensure that wells are vented to atmospheric discharge vessels (silencers) during initial opening until the flow stabilizes and become clear of solids. The second solution is to install strainers on the wells which continuously discharge solids such as well LA8.

Mineral deposition:

Due to the reported blockage in some wells and the suspected decline in flow, detail investigation of the condition of the well bores was carried out using go-devil tool and sinker bars to determine the open diameters and current total depths of the wells. The sinker bar/go-devil logging in well LA-4 conclusively showed that the well has a major scale deposition with the greatest restriction probably near a depth of 1000 m. The sinker bar/go-devil logging in LA-8 discovered a major blockage of uncertain nature at a depth of 700 m. LA-3 had little or no loss of total depth but LA-6 had lost some total depth. It was determined that the thick scale recovered from go-devils in LA-4 would

explain a large reduction in the output of LA-4. The recovered fragments of scale from LA4, along with the depth and shape of the diameter reduction, strongly suggests that this scale is carbonate scale that formed as a result of flashing of the liquid in the wellbore. A major blockage of uncertain nature was also observed at 1,461.7 m in LA-7. As this is a reinjection well, it is not known how this blockage will impact the well's ability to accept fluid. Well work-overs were proposed for those wells with blockage.

Plant and steamfield related works

Rehabilitation of the steam turbine

The major repair work undertaken on the plant involved the work done to rectify the problems on the GCCU steam turbine. During inspection of the turbine rotor, in addition to the repairs defined in the rehabilitation contract, significant damage to the rotating blades, seal hub and shaft journal area was observed. Damages to the rotor shaft and bearing were also noted. Subsequently, a recommendation to repair the turbine blades and the hub were made to EEPCO.

There was heavy corrosion and deposits on parts of the rotor blades (Figure 1). The interstage drains were clogged and filled with hard deposits which were later cleared of the deposition and cleaned.

There was very little scale deposited on the first stage nozzles, where it normally is found. A soft scale was found in the first stage rotating blades and it was deposited along the outer section of the blades, near the shrouds.

Figure 1: Corrosion of the turbine blades

A section of the rotor labyrinth steam seal appeared to have been damaged due to wear from contact with a heavy scale deposit or a foreign object. However, there was no corresponding wear on the mating stationary labyrinth seal (Figure 2).

Other than the damage to shaft bearing journal, and to oil and steam seals and corrosion on rotating and stationary blades, the rest of the turbine appeared to be in reasonably good condition and the design and build quality appeared to be good.

Figure 2: Worn Labyrinth seal

The stationary labyrinth steam seals were in generally excellent condition.

An investigation was conducted to decide whether it would be better to repair the rotor in Ethiopia or send it overseas.

Several facilities in Addis Ababa were visited and the Ethiopian Airlines (EA) shop appeared to be an excellent and well-equipped facility and a strong candidate for a local repairs. However, it was discovered that the EA shop repairs damaged shafts by a plating process and the maximum thickness they could plate was 1 mm. The scoring on the turbine shaft was deeper than that.

The decision to repair the shaft in Addis was further complicated in part because the rotor must be disassembled for repair and drawings or experience with this particular rotor design were not available. The needed turbine drawings were not provided as part of the original plant contract.

GDA's recommendation was that the rotor be shipped to Texas, USA, where identical turbines from other US geothermal plants are routinely repaired.

Wellhead valve repairs

The wellhead valves at Aluto had been in service ever since the wells were drilled and completed in the early 80's. Major problems observed included, severe corrosion of the valve stem, corrosion and in some instances jamming of the gate-segment assembly, erosion & wear of the body-seats, damage of the valve gland and bearings. Despite these problems, the valve bodies were in very good condition. It was decided that the most cost-effective solution was to procure valve spare parts and carry out maintenance of the valves in stead of buying new wellhead valves, which also involve long lead times. Accordingly, spare parts enough to service most of the 10" and 2" wellhead valves at the project site were purchased and the maintenance carried out. After completing the repair each valve was pressure tested to the applicable pressure to ensure that the repair work was satisfactory. The reconditioned valves were subsequently installed on the geothermal wells.

Repairs to Heat Exchanger Tubes

The OEC was taken out of service in 1999 due to vaporizer tube leaks. Originally, a total of twenty (20) leaking tubes were reported by EEPCo.

The vessel is a shell and tube heat exchanger with approximately 1,641 tubes of welded 316L stainless steel and 20 mm (¾") OD by 0.035" wall thickness (20 gages) dimensions. The tube length is approximately 11.6 m (38').

GDA was tasked with identifying the cause of the leaks, repairing the leaks, if possible putting the unit into operation and making recommendations for a long-term solution.

A tube failure analysis of two leaking tubes was carried out by Jonas Inc. laboratories of Wilmington, USA. The major finding of this analysis was that the root cause of the pitting was the use of wrong tubing material, 316L austenitic stainless steel, which seemed to be not suitable for the chemistry of the Aluto wells. It also found that the tube leaks were caused by tube ID pitting, which occurred during the initial service of the heat exchanger. Additional pitting could have happened during the subsequent six years of unprotected layup. The pitting seemed to be more frequent at the bottom part of the tubes where there was a liquid layer of condensed steam. It was expected that pits were present on the ID of most of the heat exchanger tubes. Jonas concluded that, with the same composition of steam and operating conditions, the pitting will continue and the heat exchanger will be unusable within a few years, therefore total replacement of the tubes would be necessary.

A second analysis was carried out by PowerChem, of Minden, Nevada, USA. PowerChem's final report provided a number of recommendations that related to operator training in order to improve the steam quality, testing and startup procedures, etc as well as implementation of a corrosion mitigation treatment program. The practicality and feasibility of isolating (by plugging) the failed tubes and putting the unit into operation, as a temporary solution, was extensively investigated. However, successive pressure tests after plugging leaky tubes proved to be unsuccessful due to discovery of more leaky tubes after each pressure test. It was decided to replace the failed tubes on the vaporizer and the first two passes of the preheater with more corrosion resistant tube material – 2205 Duplex stainless steel.

Other Rehabilitation Works performed

Various additional tasks and reviews were carried out during implementation of the rehabilitation phase. A number of recommendations on well work-over, staffing and training, establishment of plant & resource monitoring program, required plant spare parts were submitted.

In addition, investigation of the problems and putting the plant control system (Programmable Logic Control) back into operation was carried out.

The Fiber Optic communication link between the plant and the Adami Tulu sub station was repaired

Investigating the problem and undertaking the necessary repair, including supply of parts, for the cooling tower fans & proposing long-term solutions was made.

Inspecting the problems and reviewing the design of the 15 kV transmission line between the power plant and the substation and providing recommendations to enable reliable operation was done.

FUTURE WORKS

A number of follow-on tasks are required to be implemented to complete the rehabilitation work and ensure long-term reliable operation of the plant and resource. Some of these follow-on tasks include:

- Work-over of wells which have blockage in the wellbore
- Implement chemical inhibition system for those wells with chemical deposition
- Implement resource (reservoir & geochemical) and plant performance monitoring program

CONCLUSION

Geothermal energy is one of the available renewable energy sources in Ethiopia and can play an important role in supporting the current generation. Geothermal power is capable of providing a base load to supplement the existing mainly hydro-based power generation system. Unlike hydro power plants, geothermal power also has the benefit of not being affected by drought patterns.

Based on the experience gained during the rehabilitation work, the following observations and suggestions are made:

1. The Aluto plant is a relatively complex plant to operate and maintain when compared to back pressure or even condensing flash plants of similar size. Due to its complexity, it requires oversight and maintenance by an experienced team of plant and resource specialists.
2. In order to expand the use of geothermal energy in Ethiopia, training of Ethiopian personnel in the various aspects of plant and wellfield operations and maintenance should be an ongoing process.
3. An experienced geoscientist, responsible for the long-term operability of the wellfield, including resource monitoring, scaling monitoring and mitigation would be beneficial.
4. Successful operation of a geothermal plant requires adequate and timely supply of tools, equipment and consumables, therefore a well-organized spare parts procurement and storage/retrieval system must be put in place.

ACKNOWLEDGEMENTS

The rehabilitation work described in this paper was possible due to the participation of a number of GDA engineers and scientists in addition to EEPCO personnel. The input of Dick Benoit and Martin Booth on the resource side, Bob Thomasson, Larry Bandt, Dave Mendive and Sean Geffert on the power plant aspects was crucial. The input of EEPCO project coordinators Mulugeta Asaye and Merga Tassew and several other personnel through out the implementation period was significant. Thanks are due to Yvette Hamacek for reviewing the draft of this paper.

REFERENCES

Geothermal Development Associates, Unpublished Report Submitted to EEPCO, “Final Project Completion Report - Consultancy Services and Repair of the Aluto Langano Geothermal Pilot Power Plant, Contract RHGP 1/97”, June 2008.

Geothermal Development Associates, Unpublished Report Submitted to EEPCO, “Contract TOR Reports – Volume 1 - 3”, July 2008.

Jonas Inc. Unpublished Report Submitted to EEPCO “Analysis of Heat Exchanger Tube Pitting - Aluto-Langano Geothermal Pilot Plant”, June 2006

PB Power, Unpublished Report Submitted to EEPCO “Aluto-Langano Geothermal Pilot Plant Project Power Plant and Resource Review Report”, May 2000.

Powerchem, Unpublished Report Submitted to EEPCO “Aluto-Langano Geothermal Pilot Plant OEC Vaporizer Corrosion - Evaluation and Mitigation Plan”, September 2006.

CURRENT STATUS OF THE GEOTHERMAL DEVELOPMENT IN KENYA

Geoffrey Muchemi
Geothermal Development Manager
Kenya Electricity Generating Company Limited -P.P. Box 785, Naivasha
Email: gmuchemi@kengen.co.ke

ABSTRACT

Kenya is accelerating the development of geothermal resources to meet the increasing power demand. Power demands now stands at 8% with only about 1 % of the rural population having access to electricity. For a very long time, growth of geothermal was slow as the country relied more on the hydro power production because there was adequate precipitation. With the current changes in climate and the dwindling rainfall, overreliance on hydro power production has proved to be expensive. Geothermal energy capacity ratio does not depend on the weather conditions and therefore it is more reliable. The Government has fasttracked the development of geothermal resources in the country as a source of affordable and clean power. The Government established the Geothermal Development Company with the sole purpose of making available enough steam for electricity generation by Independent Power producers (IPPs) and KenGen.

Key words: Geothermal energy, hydropower.

INTRODUCTION

Kenya is endowed with a huge geothermal resource due to the presence of the Kenya rift which is part of the East African rift system. Geoscientific instigations indicate that the potential is over 7000Mwe if fully exploited. The geothermal activity is attributed to Neogene volcanic activity which has resulted to the presence of near surface heat generating sources. Geothermal fields of the Kenya rift occur in two types of environments, in Quaternary volcanoes or in fissures. The main geothermal fields are associated with Quaternary volcanoes. The second type is associated with fissures that are related to active fault zones. In either case, these fields are dissected by numerous rift faults that give rise to a number of geothermal springs and fumaroles, See Figure1.

Exploration for geothermal resources in Kenya started in 1950's and gained momentum in the 1960's, when two wells were drilled at Olkaria. From 1967, the United Nations Development Programme (UNDP) in collaboration with the Kenya Government and the then East African Power and Lighting Company Ltd., conducted geological and geophysical surveys in the area between Lake Bogoria and Olkaria. The studies identified Olkaria as the most prospective area for further investigations. As a result, more wells were drilled from 1973. The Government and KenGen, and now together with the Geothermal Development Company have undertaken to ramp up the development of geothermal resources in the country especially for electricity generation.

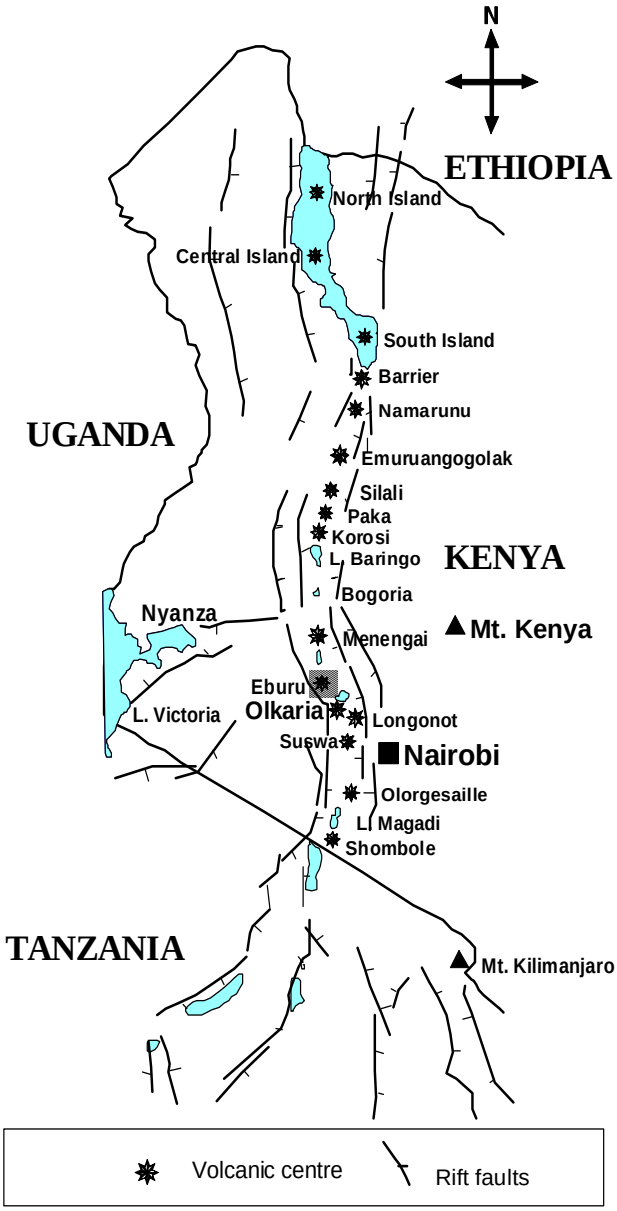

Figure 1: Map showing location of the geothermal fields and the Quaternary volcanoes and Rift faults along the Kenya rift axis.

GREATER OLKARIA GEOTHERMAL AREA

Olkaria 1 Power Plant (45 MW)

The Olkaria 1 Power Plant is the first geothermal power plant in Kenya and in Africa. It was commissioned in 1981 at the time producing 15MW and by 1985, the plant was producing 45MW. The power plant is owned by KenGen has been in operation since then. The power plant is currently using steam from the Olkaria East field.

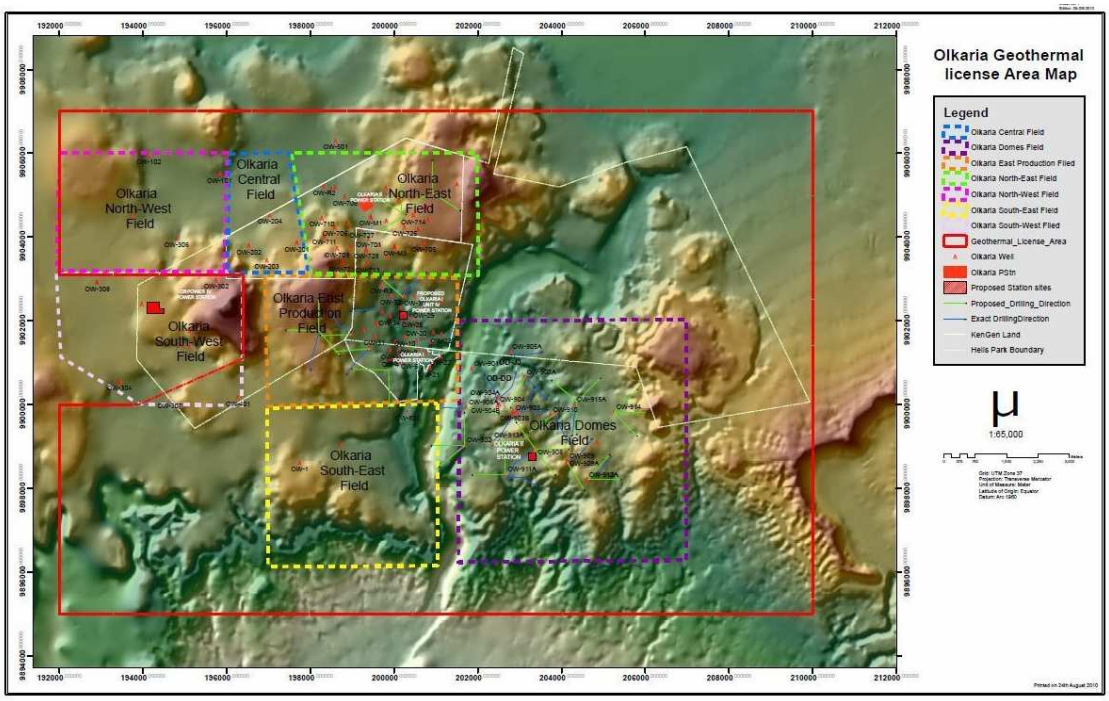

Figure 2: The Greater Olkaria geothermal field showing seven production fields.

Olkaria II Power Plant (105 MW)

More wells were drilled in the Olkaria East geothermal field. This culminated into the construction of a 70 MW power plant, the Olkaria II Power Plant. The Plant was commissioned in 2003. Due to the availability of excess steam, KenGen decided to add a third unit to Olkaria II Power Plant to generate an additional 35 MW. Construction of the unit commenced in 2009 and was completed in May 2010, bringing the total combined output at Olkaria II Power Plant to 105 MW.

Olkaria IV Power Plant (140 MW)

Plans are at advanced stage to construct a 140 MW Olkaria IV Power Plant. KenGen has secured funding for the Power Plant from bilateral donors.

Olkaria I unit 4 & 5 (140 MW)

Funding has also been secured from bilateral donors for construction of units 4 &5 at the Olkaria East Geothermal field with a total capacity of 140 MW. Consultancy services have already been procured for the project, together with that of the Olkaria IV Power Plant.

Wellhead generation

The Company has adopted use of wellhead generation units. These units will generate electricity from single wells before construction of large power plants. The electricity generated will then be transmitted to the national grid. This

technology was adopted so that the costs incurred in the drilling of the wells can be offset and funds made available for further development and or construction of the large power plants. This early generation will make available more power to the country thus help mitigate against the effects of drought and resultant high cost of power from diesel generation

Olkaria III

In Africa, the only binary plant in Kenya is OrPower4, which is producing 48 MW. The power plant is located in Olkaria South West (See Figure 2). The Ormat® Energy Converter (OEC) is a modular binary power plant that consists of heat exchangers, turbine/generator, motive fluid, lubrication pumps, valves, controls and instruments. The operation of OEC's is based on the Rankine cycle. Heat is transferred from the geothermal fluid to the organic fluid via heat exchangers (vaporizer and per-heater) where the organic fluid is heated and vaporized. The organic fluid is then expanded in the turbine to a lower pressure and temperature after which it is then condensed in the air cooled condenser. The organic fluid now in the liquid phase is pumped back to the heat exchangers – either vaporizer or pre-heater. After the heat has been extracted from it, the geothermal is reinjected to replenish the aquifer and ensure sustainability *(Mabwa, 2007)*.

Greenhouse heating at Oserian Flower farm

By the year 2000, global statistics on non-electric uses of geothermal energy showed Kenya had a capacity of 1.3 MWt with a capacity factor of 0.25. The annual heat produced then was 10 TJ/yr with 3 GWh/yr of utilization mainly from well OW 101 on the Olkaria field leased to Oserian by KenGen. Lagat (2003) has documented non-electric uses of hot water from well OW-101 at Olkaria Central field in green house heating, soil fumigation and addition of carbon dioxide to green houseplants at Oserian. Steam from the well is used to heat fresh water through heat exchangers and the water is then circulated to heat the greenhouses.

EBURRU PILOT PLANT

The Company has engaged a consultant and contractor for the construction of the Eburru Pilot plant that will initially generate 2.5 MW. The generation capacity will finally be upgraded to 25 MW. The Eburru geothermal field has a greater potential estimated to be more than 50Mw. Figure 3 shows MT resistivity anomaly map at -3000m above sea level with the low resistivity values indicating the geothermal resource.

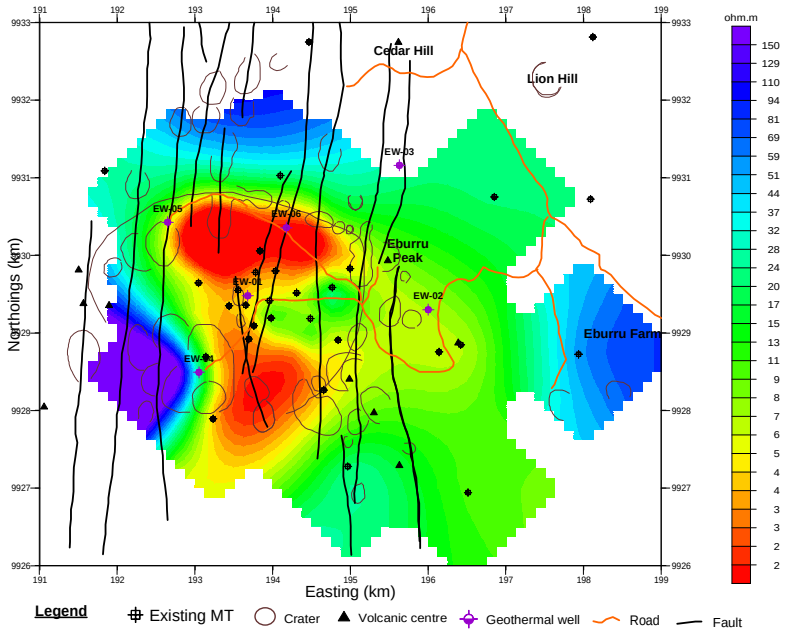

Figure 3: MT Resistivity plot at -3000 meters above sea level of Eburru Geothermal field.

OTHER GEOTHERMAL FIELDS

Suswa

The Kenya Electricity Generating Company undertook detailed surface exploration studies in the Suswa prospect. Suswa prospect has a central volcano with an inner and outer caldera. The diameter of the outer caldera is 10 km while that of the inner is 4 km. Surface manifestations in the prospect are fumaroles, steam jets, steaming and hot grounds with temperatures of over 93ºC. Plateau Trachyte Formation comprises flood trachytes that erupted on the developing graben. (Omenda et al, 2000). Suswa is a Quaternary caldera volcano in the southern part of the Kenya rift. The prospect has a central volcano with an outer and inner caldera (Simiyu, 2010). The next phase is for exploratory drilling to be carried out.

Longonot

The Longonot geothermal prospect is a Quaternary caldera volcano in the south of Olkaria prospect and is within the Longonot volcanic complex. The volcano is has summit crater and is largely a central volcano. Detailed surface exploration work in Longonot was carried out in 1998 by KenGen. In 2005, additional geophysical studies were conducted in order to delineate the areal extent of the anomaly. Exploratory drilling is yet to be done in the area to confirm the subsurface conditions.

Menengai

The Menengai prospect is located at Nakuru area and is geologically located at a triple junction of the Kavirondian Rift trending East west and the Major Kenyan Rift which trends North South. Detailed surface exploration was carried out in 2004 by the Kenya Electricity Generating Company Limited and it is one of the most promising prospects with a potential of over 700MW. Menengai volcano caldera is one of the high potential prospects in Kenya. It is Located in Nakuru and therefore is close to high power transmission lines and is situated close to a populated town. Menengai is a major Quaternary caldera volcano located within the axis of the central segment of the Kenya Rift. The volcano is located within an area characterized by a complex tectonic activity characterized by confluence of two tectono-volcanic axes (Molo and the Solai). The volcano has been active since about 0.8 Ma to present. The volcano is built of Trachyte lavas and associated intermediate pyroclastics. Most of the pyroclastics activity accompanied caldera collapse. Post caldera activity (<0.1 Ma) mainly centred on the caldera floor with eruption of thick piles of trachyte lavas from various centre (Simiyu, 2010)

Arus Bogoria

Arus and Lake Bogoria is an area with no observable central volcano. Geothermal manifestations mainly hot springs, geysers, hot grounds, fumaroles and steam jets occur along the shore of Lake Bogoria and at Arus. From the geoscientific work done in the area done in 2006 by KenGen, the prospect is ideal for a binary system as the prospect is considered to have low to intermediate temperature system which can generate to up to 400MW. The prospect is also ideal for direct uses of recreation and within the area a hotel has utilized the hot water for its swimming pools and other local use within the hotel.

Figure 4: Geysers at the Lake Bogoria prospect.

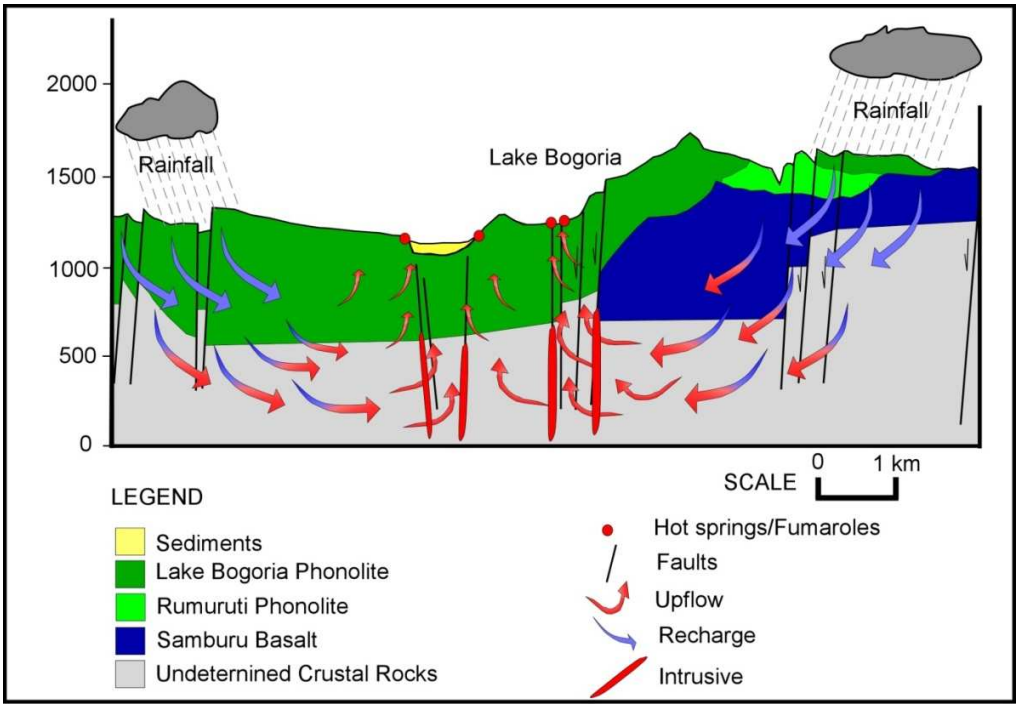

Figure 5: Conceptual model of the Arus- Bogoria prospect.

Paka

Detailed surface investigations to determine the geothermal potential of Paka was carried out between 2006 and 2007 by Kengen in collaboration with the Ministry of Energy. Paka volcano is one of the localities in the Kenya Rift endowed with geothermal resource potential. Occurrence of a geothermal system at Paka is manifested by the widespread fumarolic activity, hot grounds and hydro thermally altered rocks.

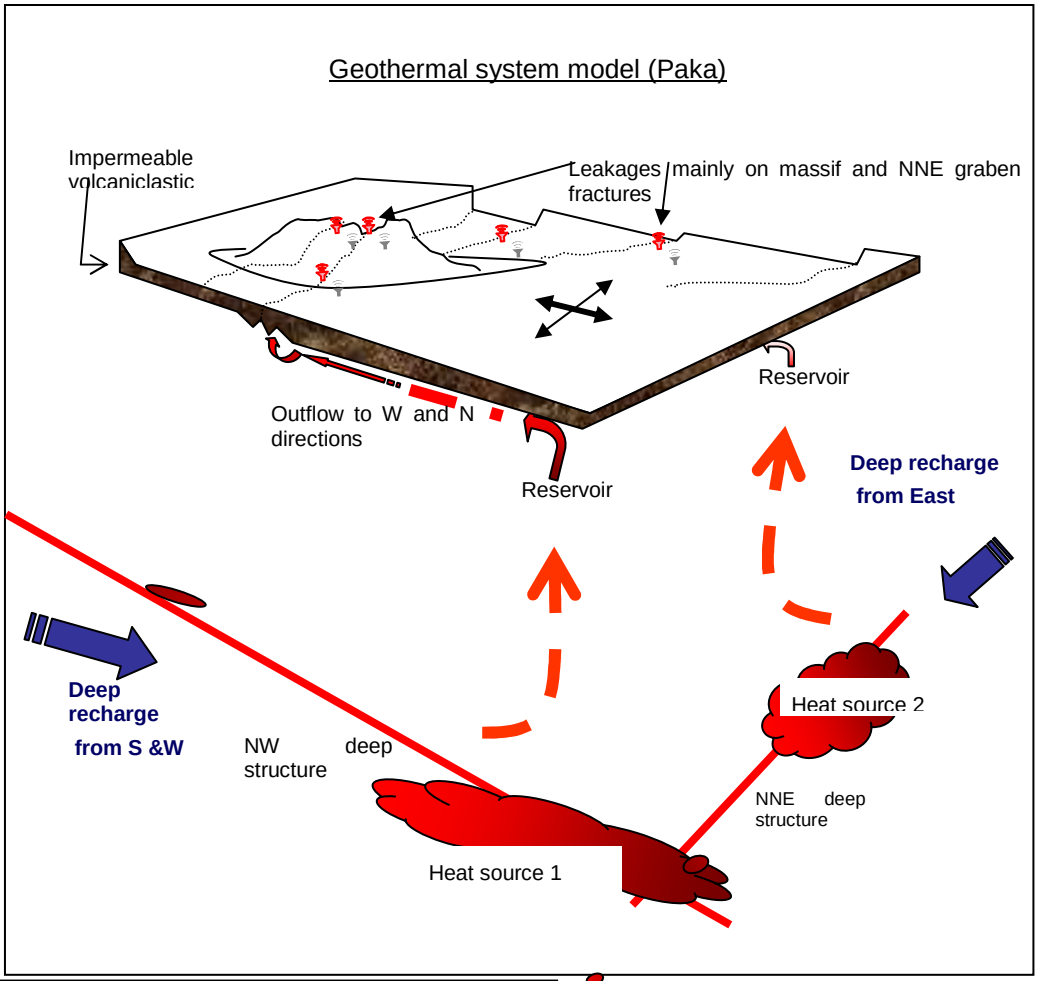

Figure 6: Conceptual model of the geothermal systems at Paka (after KenGen and MOE assessment report.)

Exploratory wells to confirm the geothermal reservoir have been sited. Estimated potential of the prospect is >500 MWe.

LAKE BARINGO PROSPECT

Lake Baringo geothermal prospect located in the North of the Menengai prospect and is characterized by hot springs, fumaroles and highly altered grounds. Surface manifestations include fumaroles, hot springs, thermally altered hot grounds and anomalous ground water boreholes. The Kenya Government and KenGen carried out detailed surface studies in 2004 (Mungania et al, 2005).

The geology of this area can be summarized culmination of trachytes, trachy-phonolites, basalts and alluvial and fluvial deposits on the lower parts. There is no evidence of a centralized volcano or a caldera in this prospect. The temperatures for this prospect are low and hence due to this it is ideal for a binary cycle generation. Exploration drilling is recommended to confirm the viability of the prospect.

Korosi-Chepchuk

KenGen carried out detailed surface exploration in Korosi-Chepchuk prospect in 2006. The geology of Korosi is mainly dominated by the intermediate lavas mainly trachytes and trachy-andesite, which cover the central and eastern sectors of the prospect area and basalts dominating the south, northland western sectors. The southwestern plain is, however, dominated by fluvial and alluvial deposits whereas the pumice deposits dominate the western plains. Chepchuk volcanic complex consists of a sequence of flows of trachyte with inter-layering of basaltic lavas of various ages and pyroclastics. The geothermal manifestations in Korosi are seen in the elevated surface temperatures, steaming grounds and fumaroles. Hydrothermal alteration is associated with the Korosi volcano with reservoir temperatures in excess of 300°C as deduced from gas geothermometry. Exploration studies indicate that the power potential for the prospect is over 450 MWe. In the North of the Rift there are other geothermally active areas which little exploration work has been done. These are Emuruangogolak, Namarunu, Barrier.

CONCLUSION

Kenya has a great potential in geothermal resources when exploited would generate over 7000Mw. In Olkaria it has been a success story and Kengen is optimizing this field with incorporation of new technologies to ensure maximum output from the steam from the field. Of all the fields in the Kenyan Rift only Olkaria is being exploited and that is why the government has given priority to the geothermal by incorporating the Geothermal Development Company to ensure that the exploitation is achieved. Geothermal development is a very expensive affair and therefore to ensure the fast growth in this sector is to ensure that funding is secured early and the proper planning of the projects to ensure money is not lost in delays. Kengen has a fine track record ensuring that project are completed ahead of schedule and hence has enabled to ensure addition of Megawatts to the national grid. There is need to do more geoscientific work on the other fields outside of Olkaria to ensure the realization of vision 2030 of achieving 4000Mw of electricity from geothermal.

REFERENCES

Geothermal Assesment report (2007) Ministry of Energy and Kengen.

Lagat, J., (2003) Geology And The Geothermal Systems Of The Southern Segment Of The Kenya Rift International Geothermal Conference, Reykjavík, Sept. 2003

Mabwa, E.S (2007) Olkaria III – A Successful Technology Transfer to Kenya. GRC *Transactions*, Vol. 31, 2007

Mungania J., Omenda .P.(Dr), Mariita N., (Dr.), Karingithi C., Wambugu J., Simiyu S., Ofwona C.,Ouma P., Muna Z., Opondo K., Kubo B., Wetangu'la G., Lagat J.: Geo-scientific resource evaluation of the Lake Baringo geothermal prospect., Kenya Electricity Generating Company Limited, internal report, (2004)

Omenda .P.A., Opondo K., Lagat J., Mungania J., Mariita N., Onacha S., Simiyu S., Wetang'ula G., Ouma P.,(2000) Ranking of geothermal prospects in the Kenya rift. Kenya Electricity Generating Company Limited,internal report. pp 121, (2000) Simiyu, S.M., (2010) Status of Geothermal Exploration in Kenya and Future Plans for Its Development Proceedings World Geothermal Congress 2010 Bali, Indonesia, 25-29 April 2010

ELECTRICITY AND FRESHWATER MACRO-PROJECT IN THE ARID AFRICAN LANDSCAPE OF DJIBOUTI

Radu D. Rugescu
Richard B. Cathcart
Dragos Ronald Rugescu
Sergiu Paul Vataman

INTRODUCTION

Bordering the Gulf of Aden and the Red Sea, the economically underdeveloped Republic of Djibouti gained its independence on June 27, 1977 from the former territory of the French Somaliland (later called the French Territory of the Afars and Issas), which was created in the first half of the 19th Century as a result of French interest in the Horn of Africa. It is a 23,200 km^2 coastal dryland ecosystem-nation without any perennial rivers, generally described as a drab and hot desert-type landscape of ochre-colored geomorphology situated near the Bab-al-Mandab Strait, international shipping's southernmost Red Sea entrance/exit (Fig. 1).

Figure 1: Map of the Republic of Djibouti indicating its most pronounced physical features as well as its immediate surroundings.

A Bab-al-Mandab dam-construction macro-project has been proposed to regulate the Red Sea for the purpose of electricity generation on a truly monumental scale (Schuiling et al 2007); were the Bab-al-Mandab Dam built it might induce further seaport development in Djibouti. Macro-engineers have already proposed a plan to "tent" most of the Sahara, which lies to the west of Djibouti (Cathcart and Badescu, 2004).

The DESERTEC Foundation is actively formulating a macro-engineering concept to produce electricity and freshwater on a spatially semi-continental scale (Strahan, 2009). During 2010, DESERTEC's geographical planning boundaries, encompassing spatially widespread industrial-scale electricity generation installations (concentrating solar power, photovoltaics, wind-power, geothermal, biomass and hydropower), do not yet include any Republic of Djibouti territory. Djibouti has an estimated mid-2010 human population of fewer than one million citizens (~750,000 persons).

Most of land-locked Ethiopia's imports and exports pass through Djibouti's well-developed seaports, so improvement of road, railway and ocean-shipping access should be very helpful with the future economical and social progress of several other inland East Africa countries. The Republic of Djibouti and Ethiopia share a 337 km border (Mugnier, 2008). Ethiopia is among the most recent of states to become land-locked and is trying to cope successfully with its dependency on coastal Djibouti; its external trade stability will, thus, be tied to the crucial infrastructure and vital economic prosperity of the littoral state of Djibouti. (By 2007, Djibouti's domestic electricity supplier, Electricite de Djibouti, had entered into an agreement with the Ethiopian Electric Power Corporation to share any power surplus that either country may develop.) The metric-gauge (1,000 mm) railway

Chemin de Fer Djibouti-Ethiopian (CDE) connects the Port of Djibouti with Dire Dawe, Ethiopia. Djibouti's coastline length is 314 km. DESERTEC's service region expansion could foster a spin-off regional development, a Republic of Djibouti macro-project we have dubbed the "Lac Assal Freshwater Distillatory and Energy District" (LAFDED), technically detailed herein. The CDE strategically terminates at the Port of Djibouti and is likely to serve the hinterland of East Africa, perhaps as a regional multi-modal transport hub. Djibouti endures a domestic freshwater shortage, which curtails its progress as a sustainable ecosystem-nation; its arable land is but 0.25% of that ecosystem-nation's territory. The offered LAFDED macro-project is meant to readily, comprehensively, and permanently remedy this unfortunate circumstance of a pervasive civilian potable water limitation and to produce low-cost electrical power.

The oval-shaped Lac Assal (located at 11^0 28' to 11^0 23' North latitude by 42^0 23' to 42^0 28' East longitude), at a negative global sea-level elevation of minus 155 m, is the lowest and geologically the youngest dry-land place on the continent of Africa and is also Africa's most saline lake. Its easternmost shoreline lies ~11-12 km from the Gulf of Aden, separated by a strip of faulted volcanic land ~5 km wide by 12 km long with a maximum above sea-level topographic elevation of ~98 m. Las Assal proper, consisting of syrup-like brine volume—nearly ten times more concentrated than the nearby Gulf of Aden seawater—amounting to ~420 x 10^6 m^3, is approximately 54 km^2 in area and is faced by a vast white-colored crystallized sea salt plain (a flat terrain of 60 km^2) on its northern shoreline. The salt pan is quarried commercially, with sea-salt production at Lac Assal started on a semi-industrial scale in 1998. On average, the brine in Lac Assal is ~300 g/l of sodium chloride (NaCl), with another 100 g/L of various other salts (Brisou et al 1974). Derived mostly from hot springs, the lake's high temperature brine, 33-34^0 C, has a surface density of ~1.204. The mean annual air temperature in this tectonically closed, below world sea-level, basin is a torrid ~33^0 C with maximum monthly means of nearly 40^0 C in June and July. The mean annual rainfall is <200 mm. In other words, per year, freshwater evaporation from Lac Assal must be in the range of ~250-290 x 10^6 m^3 (Gasse and Fontes, 1989). The maximum wind, ~14-15 m/second, impinging Lac Assal is onshore (easterly) 66% of the time and offshore (westerly) 23% of the time; the onshore wind carries more water vapor than the offshore wind over Lac Assal.

Figure 2: A speculative chart of Lac Assal converted to anthropogenic gulf filled to the current local level of the nearby ocean. Connecting 12 km-long filling canal is not drawn.

Filled to today's global sea-level, the volcano-tectonic crater-basin of Lac Assal, shaped like an ellipse, would be a 340 km^2 body of evaporating seawater amounting to, probably, <50 km^3 (Fig. 2). However, in that unique connected state, its usefulness would likely be restricted to simply functioning as an anthropogenic ocean gulf, perhaps a new commercial and naval harbor with a maximum navigational depth in excess of 150 m and a controllable, but unlocked, seawater canal shipping access route. Since the sill between the Ghoubbat-al-Kharab Strait (Fig. 3), situated immediately to the east of the 12 km-long land barrier that isolates the existing Lac Assal, and the Gulf of Aden lies at 4.5 m below extant sea-level, then any large-scale harbor development would necessitate dredging of a harbor approach channel leading to the man-made gulf's proposed canal. Most large 21st Century ships require 40 m of nautical depth to maneuver safely. So, the proposed canal, measuring 12 km long by 100 m wide with a navigational depth of 40 might necessitate the removal of >192,000,000 m^3 of material (>0.192 km^3) which can be done economically, we think, by nuclear-powered dredgers (Cathcart, 2008).

Figure 3. Lac Assal, fringed on the northwest by a massive arid terrain of air-exposed sea-salt, is separated from the Gulf of Tadjoura (bottom right), by a 5 km-wide volcanic land form known as the Ghoubbat-al-Kharab ("navel of the world"). Satellite image.

There is a network of some 30 GPS sites established in the Republic of Djibouti to monitor the Lac Assal-Ghoubbet Rift System (Vigny et al, 2007) which seems to be widening at a current measured yearly rate of ~16 mm; Djibouti endures the focused devastation of earthquakes—extensional faults accommodate 5-15% of the total extension of the Lac Assal Rift. It is widely assumed that, in a million years possibly, a geological rift will permit the ocean to flood the low-lying Lac Assal Basin with seawater (Backer et al 1973). Sub-aerial geological rift zones in Iceland—where volcanic eruptions of airborne ash, starting in 2010, interfered with scheduled transatlantic air traffic—and in Djibouti afford geoscientists glimpses of dyke injections at Earth's divergent plate tectonic boundaries. The two month-long 1978 Lac Assal-Ghoubbet Rift event-process commenced with a 5.3 Richter Scale temblor near the "…center of a 60 km-long segment followed by a week-long volcanic eruption…" (Rowland et al 2007). Deep-drilling, at least six wells completed so far (Asal 1-6), has been conducted in Djibouti on the landform named Ghoubbet-al-Kharab that separates Lac Assal from a gulf facing the Indian Ocean and a technical study, financed by The World Bank Group as Project P000612 for USD 9.2 million related to the feasibility of a 30 MW power-plant at Assal was completed by 1992. The estimated installation cost of the power-plant was USD 117 million. Since the GDP of the Republic of Djibouti is only about one billion US dollars, materialization of that project would have to be realized by international monetary help. The national resource of geothermal energy is estimated at 230-860 MW and Lac Assal's wind-power potential is estimated at 100 MW.

Figure 4, below, will give the reader a necessary understanding of the broad relationships amongst the most significant terrain features, some of which are (such as the glaring white salt flats northwest of Lac Assal) almost vegetation-less. The near sterility of the arid desert landscape is clear (Fig. 4).

Figure 4. Lac Assal and its salt flat—so tantalizingly close to the global ocean! *Image source:* http://commons.wikimedia.org/wiki/Atlas_of_Djibouti.

A greening of this East African ecosystem-country could serve as an inspiration to many peoples living in similar landscapes to research and develop the sub-surface geothermal energy resources via the technologies we present in this article.

CANALS AND DOMES

Not long after Lac Assal was first mapped topographically, macro-engineering proposals were made public that an 12 km-long canal, excavated through the land barrier between the inland, permanent body of syrupy brine 155 m below global sea-level and the Gulf of Tadjoura, would permit the massive generation of hydropower locally. (A gravity-fed canal must be used because 10 m is the maximum for seawater transfer by siphon.) Inflowing seawater from the Gulf of Aden would, of course, mix with Lac Assal's gushing geothermal spring water where the stagnant water's temperature is 80-100^0 C during the daytime and nighttime. Pierre Gandillon (1931) proposed a canal-enabled hydro-solar facility in the Republic of Djibouti and he was followed by George A. Whetstone (1954), L. Le Grain (1955) and, finally, by El Sayed M. Hassan (1961). Significantly, long-distance international electricity transmission lines were an unconsidered option by these famously imaginative hydrological and hydrogeological investigators.

Macro-engineers have proposed city-covering inflatable (and geodesic) domes. Buckminster Fuller, in the 1960s, suggested a hemispherical geodesic dome 3 km-wide and 1.6 km-tall could enclose a part of New York City (USA) from the East River to the Hudson River at 42nd Street, and, north and south, from 62nd Street to 22nd Street. His dome, composed of wire-reinforced, one-way transparency, shatter-proof glass mist-plated with fine particles of aluminum to reduce internal solar glare whilst admitting sunlight would mass at 4,000 tonnes and cost ~200 million 1960 US dollars; adjusting for inflation since 1960, the *circa* 2009 cost would be ~1.433 billion dollars!

On 8 December 1992, Robin Berg and Timothy Berg were awarded a US Patent, #5168676, for their "Horizontally Ribbed Dome for Habitation Enclosure". The Bergs imagined "…domes having a minimum radius of one-half mile [~0.804 km]" composed of graphite-reinforced composite trusses and panels of clear plastic. Alexander A. Bolonkin and R.B. Cathcart (2007) have described huge inhabitable domes for use in the Arctic and in Antarctica. We assert here that a single dome or a series of small interconnected domes could cover Lac Assal and its adjacent bedded sea-salt terrain, approximately 115 km^2, with the macro-engineering aim of creating a huge distillation installation!

The key positive impacts of our LAFDED (the "Lac Assal Freshwater Distillatory and Energy District") in the East African Republic of Djibouti are:

(1) help create useful jobs and gainful employment

(2) increase export potential (made freshwater, generated electricity)

(3) improve the national standard of living and boost the nation's GDP

(4) services and infrastructure nationwide will be enhanced

(5) provide a new and unique tourist industry attraction

(6) cause the implementation of new Green landscape management measures

Some of the key negative impacts of LAFDED are:

(1) permanent loss of open and unblemished desert landscape to seawater flooding and new buildings

(2) some incidental decrease in aesthetic value of the distinctive salt flats and Lac Assal

(3) land vehicle movements of automobiles and trucks on newly-paved highways will induce smog in the air and cause additional road accidents

(4) new unplanned human settlements (spontaneous village type) may spring up

(5) seaport development, and the attendant increase in oceanic-shipping arrivals and departures, will cause some offshore damage to the seafloor and seawater in the Gulf of Tadjoura and even the Gulf of Aden

Nevertheless, we propose a new kind of freshwater distillation and geothermal energy tower in the next section of this article.

GEOTHERMAL RESOURCES

Most of Africa's geothermal resources are located in its Rift Valley, one of the geologic wonders of the world. The Rift Valley spans roughly 6,000 kilometers across East Africa and runs through Kenya, Ethiopia, Djibouti a. s. o. (Poole, 2010). Kenya and Djibouti have the highest potentials for geothermal resources in East Africa. The technically exploitable geothermal potential in the different Djiboutian regions is currently estimated to range between 350 and 650 MW. The economically exploitable capacity for the Lac Assal-Ghoubbet region only is >100 MW; that is much more than the current requirements of Djibouti. The studies done on the territory showed that there are two kinds of reservoirs; a deeper one (over 2,000 m depth with >350°C) and a super-incumbent zone (between 300 m and 600 m with a 200°C resource). Other estimates are ten times more optimistic and range from 2,000 MWe (megawatts electric) to 7,000 MWe. This unmistakably shows that further investigations of the potential are required. Lately, there has been keen interest by many American investors, especially in infrastructure projects. Kenya was one of the first African states to develop its geothermal energy potential. The KenGen (Kenya Electricity Generating Company) has built three plants—Olkaria I (45 MW), Olkaria II (65 MW), and Olkaria III (48 MW)—with its American investing partner company Ormat Technologies, located in Nevada, USA. Among the companies competing for geothermal resources in other parts of the Rift Valley are Mitsubishi Heavy Industries, a global manufacturer of power equipment, and Reykjavik Energy (REI), which has developed geothermal energy macro-projects in Iceland.

So far, only about 200 MW of geothermal power have been installed in Kenya and 4 MW in Ethiopia. In Djibouti, research had been going on for the last 30 years. Exploratory wells have been drilled that strongly imply the presence of an exploitable geothermal resource. A TAA funded project on Djibouti geothermal exploration study was financed and completed between 1986 and 1992. However, no utilization has been commissioned yet. In Ethiopia, the R&D history is similar, but 4 MW are already installed. Reykjavik Energy is currently implementing a contract with the Government of Djibouti for a 50 MW geothermal power plant in the Lac Assal Area, about 100 km west of Djibouti City. Djibouti currently derives all its electricity from diesel generators, so power from geothermal plants in this country is intended for the general market. There are also large naval bases in Djibouti that generate their own electricity that are potential customers. There are also some other prospects for the development of Djibouti geothermal resources (Chideh, 2006). As part of the Lac Assal Project, REI intended geothermal power-plant is estimated to start production in 2012. The plant will supply Djibouti with Green electricity, replacing its costly current diesel-generated electricity supply.

The regions of Assal, Dikhil, Obock and Arta are quite rich areas and could enable the production of geothermal power fluid-direct use. The promising region of Lac Assal can, early on, supply a first increment of 30 MW; the studies completed in the Obock region showed that there is a possibility to project in a short term, the creation of a pilot geothermal central plant producing 5 MW. In a 2008 study, carried to conclusion by a team from Iceland in the Fiale region of Lac Assal is considered the most promising, with favorable geological setting, including a 3-4 km^2 reservoir with temperatures >240 °C. As the reader shall soon see, this working fluid temperature is ideal for driving the gravitational drought tower of a complex power plant with cold air turbine.

THE LAFDED GEOTHERMAL GRAVITY DRAUGHT POWER-PLANT

It is a demonstrated fact that the most efficient means to transform heat, namely enthalpy, into mechanical work is derived by adding a gravitational acceleration of the hot air by thermal draught in the gas-dynamical chain (Günter 1931, Unger 1988, Rugescu 2005). The source of heating was first considered as by the solar energy, although any type of heater may be considered (geothermal, nuclear, biofuel). The possibility to efficiently extract work from a geothermal resource of heat through a gravitational draught amplification was previously suggested (Rugescu and Tsahalis, 2007). The block-diagram of the draught tower in Figure 5 is considered for modeling its working efficiency in the LAFDED scheme. The air intake with the laminator device is the first element of the gas-dynamical chain, followed by the one-stage air turbine of Zoelly type (the continuous cascade of accelerating vanes plus the turbine rotor), the air heater and the air column within the tall part of the tower at last. An unrestricted upper opening for atmospheric release is closing the circuit. In order to exploit the geothermal heat resource, the heating scheme is different from the solar tower concept. In the present macro-project, the solar receiver is replaced by the geothermal water-air heat exchanger. Otherwise the working principle of the draught tower is identical. From the macro-engineering point of view, the removal of the solar array of helliostats considerably reduces the necessary land surface and the problem of mirror system maintenance. The geothermal version of GIGANT is called LAFDED and

makes no use of the entire solar array because the thermal energy is introduced only from the geothermal source by the classical method of underground water pumping.

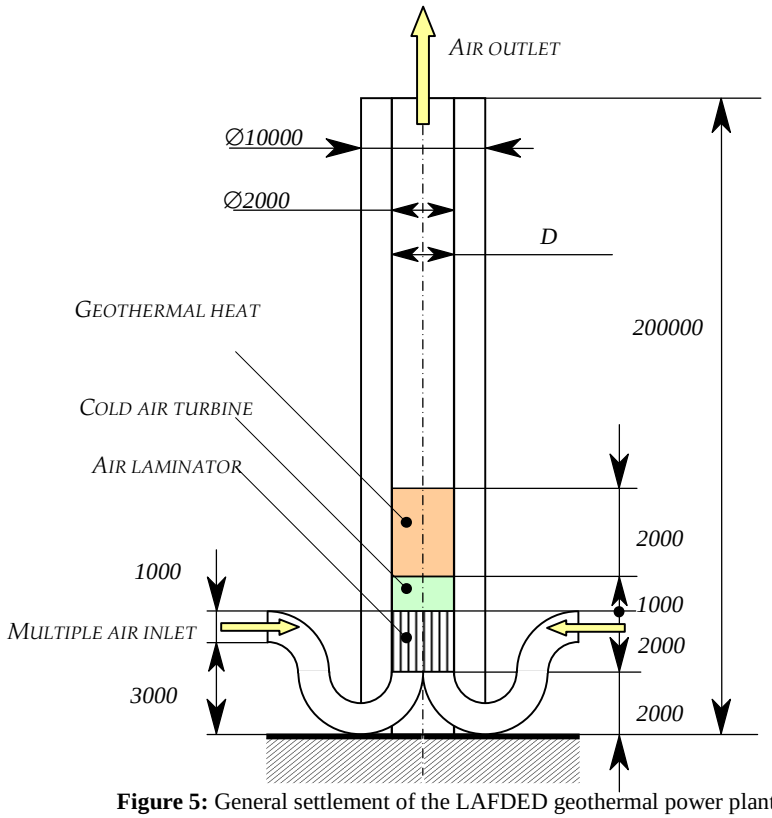

Figure 5: General settlement of the LAFDED geothermal power plant.

(All stations are entered in mm.)

It induces the extra gravitational energy amplification when the air is expanded by heating and by further acceleration in the turbine stator. The scheme is given in Fig. 6. Due to practical reasons, the order between the turbine and the air heater within the two heating solutions could be reversed. The unsteady models of these parts are based on the simplest approaches to avoid unnecessary computations. The physical size of the tower is informative and only used to derive the LAFDED framework's computational scheme.

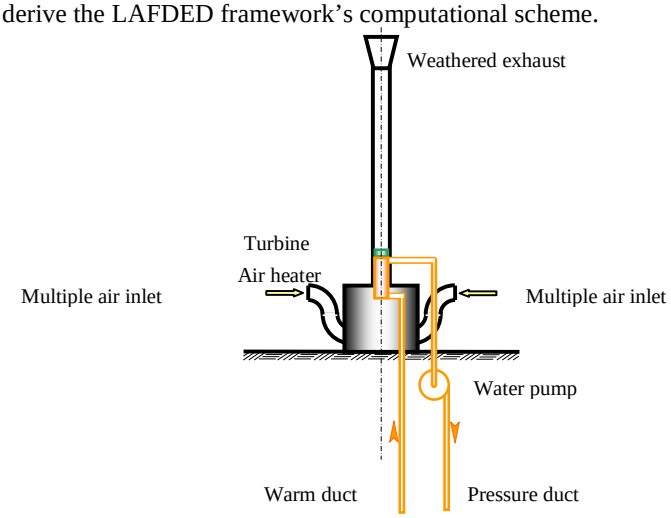

Figure 6: Scheme of the geothermal-gravitational LAFDED power-plant set-up

Under these assumptions, the efficiency of the gravitational draught in the tower was already thoroughly investigated (Unger 1988, Rugescu 2005), without the involvement of the turbine however. A minute unsteady characterization of the turbine tower has already been developed (Cirligeanu et al., 2010). A simplified and fast assessment method of the tower efficiency is considered in the following.

Into the simplified 1-D computing scheme the main stages of the tower with turbine, corresponding to the set-up scheme from figure 1-*a*, are nominated in Figure 7.

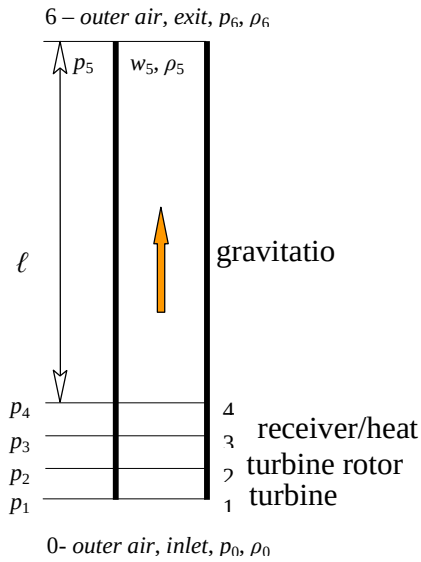

Figure 7: Main stations of the GIGANT draught tower model (Rugescu et al., 2005).

It succeeds in imparting a near sonic velocity c_2 to the airflow at rotor entrance "2". The rotor of Zölly turbines is of equal pressure type and consequently the magnitude of the blade angle $|\beta|$ at entrance and exit is the same (equal angles rotor), while their sign is opposite. This forces the magnitude of the relative velocity inside the blades' channel to preserve constant magnitude at a given instant, still opposite relative to the axis. A continuous turn of the airflow occurs into the channel. As a result, the high absolute velocity c_2 at rotor entrance reduces to the value and direction of the axial velocity c_{3a} at rotor exit (Figure 7, $c_3 \equiv c_{3a}$). This way the kinetic energy is sharply reduced by transfer of the equal amount of work to the turbine shaft, which means to the consumer (electric generator) from outside. From the mass continuity condition the axial speed c_{3a} can never be zeroed and it remains as a small, intrinsic and unavoidable loss of power into the gravity accelerator. All the other thermal parameters preserve constant along the rotor. To reduce pressure and friction losses to a minimum, the position angle of the blades at entrance is set equal to the nominal β value and the things are going that well for the nominal flow and rotational rate.

At non-equilibrium the air enters the blades under different angles, producing a lot of turbulence, friction losses and a reduction in the absolute velocity c_1. At turbine start for example, due to the blunt turn of the speed from the direction of c_1 to the direction of w_1 a lower kinetic energy is delivered to the shaft. As the rotor gains speed this difference is gradually diminishing and finally ends into the steady-state condition described above. The model of the turbine that describes this start-up transient behavior simply reads

$$J_s \frac{d\omega}{dt} = M_N (1 - \overline{\omega}) \tag{1}$$

where J_s is the moment of inertia of the entire rotating shaft, M_N the nominal driving couple, ω_N is the nominal circular frequency and $\overline{\omega} = \omega / \omega_N$ is the relative circular frequency.

For the simplest case when the driving couple is given as constant, the angular acceleration $\varepsilon = d\omega / dt$ becomes a linear function of the circular frequency lag, ceasing at the nominal rate. Although simplifying, this case is useful to estimate the time constant T_N of the turbine shaft itself. The equation of motion (1) is re-written as

$$J_s \frac{d\omega}{dt} = M_N - m_N \omega \tag{2}$$

with $m_N = M_N / \omega_N$. It manifests the solution

$$\omega = \omega_N \left(1 - e^{-\frac{m_N}{J_s} t} \right) \equiv \omega_N \left(1 - e^{-\frac{t}{T_N}} \right). \tag{3}$$

Consequently, the linear rotor presents a time constant given by

$$T_N = \frac{\omega_N \cdot J_s}{M_N}. \tag{4}$$

The estimate for the moment of inertia of the STRAND shaft gives $J_s \cong 200\ kg \cdot m^2$ and this ends in $T \cong 2\ s$, which means the same order of magnitude with the airflow itself. It is observed in these computations that the nominal power output relates the shaft couple and the frequency by

$$P_N = M_N \cdot \omega_N .$$

In fact the unsteady motion is not that simple, and the driving moment must be computed at each moment from the equation of impulse, with $\bar{r}$ for the mean value of the radius within the rotor, as

$$M_N = 2 \cdot \rho_2 A \cdot \bar{r} c_{2a} (c_{2t} - \bar{r}\omega). \tag{5}$$

From this parabolic dependence, it is found again the known fact that the power output goes through a maximum ($\partial P_N / \partial(\bar{r}\omega) = 0$) for

$$\bar{r} \cdot \omega_N = \frac{c_{2t}}{2}$$

from where the optimal turning rate and size of the turbine are derived. In these relations the magnitude and inclination of the absolute velocity of the air at stator exit $\mathbf{c}_2$ is a given parameter that depends upon the optimal level allowed by the entire tower under its best working conditions.

These relations are not directly involved in the computational scheme, because the significant sudden jump of the axial velocity through the turbine is of macro-engineering interest. When given by a steady thermal equation

$$\Delta c_{13} \equiv c_3 - c_1 = c_1 (A_1 \rho_1 / A_3 \rho_3 - 1), \tag{6}$$

it hides the transient regime of the start and other unsteady variations, that must be added through extra equations. The connection between the local velocity at rotor entrance c_2 and the rotating rate ω results, for example, from the triangle of speeds, where the direction β of the relative velocity $\mathbf{w}$ is imposed by the geometry of the rotor blades, as drawn in Figure 8, below.

From the geometry of the triangle the relation results $c_2 \sin(\beta_2 - \alpha_2) = \bar{r}\omega \sin \beta_2$, or

$$c_2 \cos \alpha_2 - c_2 \sin \alpha_2 \cot \beta_2 = \bar{r}\omega . \tag{7}$$

The moment of the impulse must be introduced in order to show up the fast transient effects. The formula (5) will be used with consideration of (7) to write

$$J_s \frac{d\omega}{dt} = 2 A_1 \rho_1 c_1 \bar{r} c_2 \sin \alpha_2 \cot \beta_2 \cdot (1 - \bar{\omega}) \equiv 2 \dot{m} \bar{r} c_{2a} \cot \beta_2 \cdot (1 - \bar{\omega}). \tag{8}$$

At each moment the rotating rate reaches the value that satisfies this equation, while the local speed c_2, its angle α_2 and the air density ρ_2 should result from the local conditions, considered an isentropic expansion.

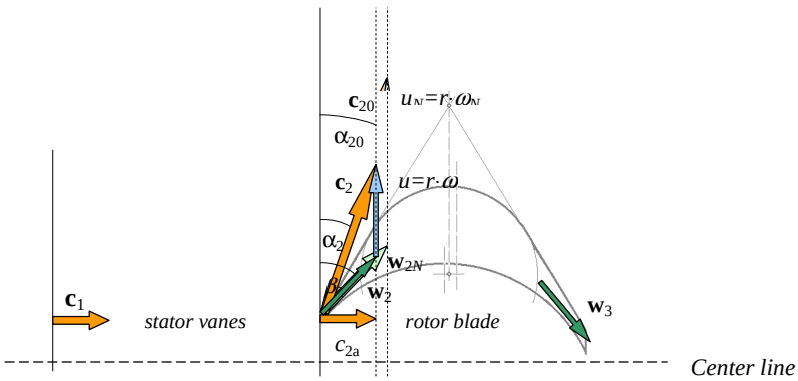

Figure 8. Modified rotor speed distribution at non-nominal flows.

This means that the re-compression at the governor exit does not involve shocks, or that they may be ignored. The losses should be considered through an experimental coefficient of efficiency. Then the local conditions are indicated by the set of equations

$$A_1\rho_1 c_1 = A_2\rho_2 c_2\,, \qquad (\textit{mass conservation}) \tag{9}$$

$$\frac{c_1^2}{\sin^2\alpha_2}\left(\frac{\rho_1}{\rho_2}\right)^2 + L^2\left(\frac{\rho_2}{\rho_1}\right)^{\kappa-1} = c_1^2 + L^2\,, \qquad (\textit{Bernoulli}) \tag{10}$$

where L denotes the maximal (limiting) speed of the air through the isentropic expansion,

$$L^2 \equiv \frac{2\kappa}{\kappa-1} R_1 T_1\,.$$

It manifests as if the speed at stator exit were lower than the one in steady expansion, up to the value c_2, limited by the circular frequency ω and blades' direction β through the triangle relation (7). Note: the unsteady value for the velocity inclination α_2 is greater than the nominal value α_{2N} and should result from the set of four equations (7)-(10). They are complete for determining the four unknowns of the macro-problem. As a direct check, for a virtual case with no deviation of the velocity within the governor ($\alpha_2=\pi/2$), $\sin\alpha_2=1$ and the Bernoulli equation (10) shows that no expansion takes place into the stator ($\rho_1/\rho_2=1$), consequently no energy release into the rotor could occur.

For convenience, in the computational scheme the circular frequency ω is replaced by the local speed c_2. The time dependent values of the parameters stand for the conditions at tower entrance (x=0) in the numerical scheme described in (Cirligeanu et al., 2010).

THE GEOTHERMAL GRAVITY DRAUGHT EFFICIENCY FOR LAFDED

Grounded on the above mentioned computational scheme the geothermal power plant has an optimal efficiency when the heating of the draught air comes to around 200^{0}C (Figure 9), which means a complete fit with the geothermal condition around Lac Assal, Djibouti. To derive the efficiency the basic equation of motion of the air within the tower becomes (Rugescu, 2005)

$$\frac{\Delta p(\ell)}{g\rho_0\ell} \equiv \frac{1+r-k}{1-r}\cdot\frac{\dot{m}^2}{2g\ell\rho_0{}^2A^2} + \frac{\Delta p_f(\ell)}{g\rho_0\ell} - r = 0\,. \tag{11}$$

For small values of the friction loss the equilibrium mass flow rate becomes

$$\frac{\dot{m}^2}{2g\ell\rho_0{}^2A^2} = \frac{r(1-r)}{1+r-k}, \tag{12}$$

or slightly greater only than the value in the previous limit model (Unger, 1988).

When the friction losses are considered, the accurate value for the quadratic mass flow rate results from the second degree equation (11),

$$a\left(\frac{\dot{m}}{\dot{m}_\ell}\right)^2 + b\,\frac{\dot{m}}{\dot{m}_\ell} - r = 0, \tag{13}$$

where at the nominator a reference free-fall mass flow rate appears,

$$\dot{m}_\ell = w_\ell\,\rho_0 A,$$

based on the Torricelli free-fall velocity $w_\ell{}^2 = 2g\,\ell$ and the constants are

$$a = \frac{r/R}{w_\ell{}^2\rho_0{}^2A^2}, \qquad b = \frac{32\,\nu_0}{AD^2\,g\rho_0}\left(\frac{T_w}{T_c}\right)^{1.7}. \tag{14}$$

or a slim, tall stack of $\ell/D = 70/2$ the contribution of friction is very small,

$$b/a = 2\%,$$

surely indicating that the actual difference between the non-friction flow and the real flow is smaller than ~0.05%. Consequently the non-friction result in (12) should be considered accurate enough. Its quadratic form shows the known fact that the heating of the inner air presents an optimal value and there exist an upper limit of the heating where the flow stack ceases. From the formula (12) it results that the non-dimensional quadratic mass flow rate R^2 is in fact the squared ratio of the exhibited stack entrance speed w_1 over the free-fall speed w_ℓ, due to constant cross-section area of the stack,

$$R^2(r) \equiv \left(\frac{w_1}{w_\ell}\right)^2 = \frac{r(1-r)}{1+r-k}, \qquad R^2(r) \equiv \frac{\dot{m}^2}{w_\ell{}^2\rho_0{}^2A^2} = \frac{r(1-r)}{1+r-k}. \tag{15}$$

The entrance speed exhibits a maximum at the theoretically optimal heating r_{opt},

$$\mathrm{d}R^2/\mathrm{d}r = 0, \qquad r_{opt}{}^2 + 2(1-k)\,r_{opt} - (1-k) = 0, \tag{16}$$

$$r_{opt} = -(1-k) + \sqrt{(1-k)(2-k)}.$$

The optimal heating for the standard air appears at a relative density reduction

$$r_{opt} \equiv (\rho_0 - \rho)/\rho_0 = 0.392033,$$

meaning an equal increase of the absolute temperature of (1+r) times, when the normal air temperature should be raised with around 200ºC above 27ºC to achieve a maximal discharge, independent of the stack geometry. These values are an optimal response to the craft balance between the drag of the inflated hot air and its buoyant force, due to Archimedes' effect (Unger, 1988).

The behavior of the chimney flow for various heating intensities of the airflow, in the limit case of equal far stagnation pressures (FSP), is reproduced in Figure 9. The denoted curve is the other limiting case of equal static pressures (ESP) at the chimney's exit rim.

The free mass flow rate in formula (12) presents two roots where the flow ceases, at its origin $r = 0$ and at a maximal limit $r = 1$. These can not and do not hang on the exit assumptions, while the optimum heating point

does. Stack permeability is slightly higher for FSP. The above integral theory, thus, also allows for assessing the velocity increase at the tube entrance w_1.

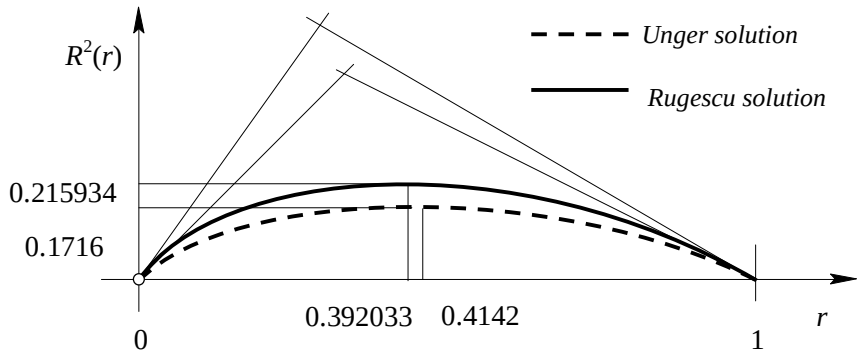

Figure 9. Stack discharge R^2 versus air heating intensity r.

The maximal value of the speed in the zone 1 from above is

$$w_{1\max} = R_{\max} \cdot w_{\ell}\,, \tag{17}$$

depending on the tower's height through the Torricelli speed w_{ℓ}. For the same example of a 70*m* tall tower the maximal constant area velocity of the entering air is roughly

$$w_{1\max}\sqrt{2g\ell \cdot R_{\max}^2} = \sqrt{1372.931 \cdot 0.2159} = 17.2 \ \ m/s.$$

After the heating the velocity should increase $(1+r)$ times, to the otherwise moderate value of $w_2 = 20.9$ *m/s*., denoting very low air turbulence, if any at all.

The accelerating potential in a largely contracted nozzle goes in this case to more than 20 times the w_1 value, namely to the considerable boost of 340 *m/s*. Taller towers may contribute to further improvement of this potential. The rarefaction of the airflow in the nozzle, combined with its limited diameter, shows that such an aerodynamic rig is turned to small values of the Reynolds number rather, but this is the very realm where the aero-acoustics of noise generation is significant. We have no desire whatsoever to create a noise pollution macro-problem in the small ecosystem-state of Djibouti!

Both numerical simulations of ducted airflow and experimental measurements on a scale model were called in support of the above estimations.

CONCLUSION

The efficiency of the Lac Assal Freshwater Distillatory and Energy District's proposed gravity draught power-plant is quite obvious, and when coupled with existing supplies of naturally-heated saline hot water from local underground geothermal resources, it represents a very powerful means of providing electricity in remote regions like, typically, the Republic of Djibouti's Lac Assal region. The capacity of the power-plant is great enough to

simultaneously secure seawater desalination and, subsequently, a reliable civilian freshwater supply over a large section of the ecosystem-nation. Our estimates show that an urban habitat of ~10,000 people may be served by a medium-size, draught power-plant, like the one considered in detail above. The application of that macro-project solution to the Lac Assal region, in the form of our proposed LAFDED seems especially useful.

REFERENCES

***, The Djibouti Geothermal Project, 2008.

Backer, H., Clin, M and Lange, K (1973) Tectonics in the Gulf of Tadjura. Marine Geology 15: 309-327.

Bolonkin, AA and Cathcart, RB (2007) Inflatable 'Evergreen' dome settlements for Earth's Polar Regions. Clean Technologies and Environmental Policy 9: 125-132.

Brisou, J, Courtois, D. and Denis, F (1974) Microbiological Study of a Hypersaline Lake in French Somaliland. Applied Microbiology 27: 819-822.

Cathcart, R.B. and Badescu, V. (2004) Architectural Ecology: A Tentative Sahara Restoration. Int. J. of Environmental Studies 61: 145-161.

Cathcart, R.B. (2008) Kra Canal (Thailand) excavation by nuclear-powered dredges. International Journal of Global Environmental Issues 8: 248-255.

Chideh, A.F., Pilot Project for Energy and Mining Economic Beneficiation from Assal (Djibouti) Geothermal and Mineral Resources, Geothermal Resources Council GRC-2006 Annual Meeting, Tuesday, September 12.

Cirligeanu, R., Rugescu, R. D., Bogoi, A. (2010), TRANSIT code for turbine flows in solar-gravity draught power plants, Paper GT2010-22518, *Proceedings of the ASME International Conference on Gas Turbines*, June 14-18, 2010, Glasgow, Skotland, UK.

Gandillon, P (1931) Amenagement et mise en valuer de la cote Francaise des Somalie. Memoires de la Societe des Ingenieurs Civils de France 84: 967-977.

Gasse, F. and Fontes, J-C. (1989) Palaeoenvironments and Palaeohydrology of a Tropical Closed Lake (Lake Asal, Djibouti) Since 10,000 yr B.P. Palaeogeography, Palaeoclimatology, Palaeoecology 69: 67-102.

Günter, H., In hundert Jahren – Die künftige Energieversorgung der Welt, *Kosmos, Gesellschaft der Naturfreunde, Franckh'sche Verlagshandlung*, Stuttgart, 1931.

Hassan, ESM (1961) Power from the Sea. Proc. Amer. Soc. Civil Engineers 87: 21-27.

Le Grain, L (1955) Remarques au sujet de la centrale hydro-solaire de lac Assal: Autres possibilities d'utilisation de ce lac. La Houille Blanche 10: 207-210.

Mugnier, C.J. (2008) Grids and Datums: Republic of Djibouti. Photogrammetric Engineering & Remote Sensing 74: 1183-1185.

Poole, L., Jun 22, 2010, Geothermal Companies Vie for African Development Contracts, renewableenergyworld.com.

Rowland, J.V., Baker, E., Ebinger, C.J., Keir, D., Kidane, T., Briggs, J., Hayward, N. and Wright, T.J. (2007) Fault growth at a nascent slow-spreading ridge: 2005 Dabbahu rifting episode, Afar. Geophys. J. Int. 171: 1226-1246.

Rugescu R. D., *Thermische Turbomaschinen*, ISBN 973-30-1846-5, Ed. D. P. Bucharest, Ch.7, 2005.

Rugescu, R. D., Demos T. Tsahalis, "Improved unsteady approach to gravity draught power plants", *Proceedings of the International Workshop on Acoustics and Vibration-IWAVE2007*, Cairo, Egypt, September 8-9, 2007

Rugescu, R. D., Chatcat, R., Rugescu, D. R., Electricity and Freshwater Macro-project in the Arid African Landscape of Lac Assal, Eighth International Conference on Structural Dynamics, EURODYN-2011, Leuven, Belgium, 4-6 July 2011.

Schuiling, R.D., Badescu, V, Cathcart, R.B., Soud, J. and Hanekamp, J.C. (2007) Power from closing the Red Sea: economic and ecological costs and benefits following the isolation of the Red Sea. Int. J. Global Environmental Issues 7: 341-361.

Strahan, D. (2009) Green Grid. New Scientist 201: 42-45.

Unger, J., *Konvektionsströmungen*, B. G. Teubner, ISBN 3-519-03033-0, Stuttgart, 1988.

Vigny, C., de Chabalier, J-B, ruegg, J-C, Huchon, P., Feigle, K.L., Cattin, R., Asfaw, L. and Kanbari, K. (2007) Twenty-five years of geodetic measurements along the Tadjoura-Asal rift system, Djibouti, East Africa. Journal of Geophysical Research 112: B06410.

Whetstone, GA (1954) La Houille d'Or. Water Power 6: 272-274.

INFRASTRUCTURE DEVELOPMENT IN GEOTHERMAL FIELDS: A CASE STUDY FOR MENENGAI GEOTHERMAL PROSPECT, KENYA

Wilson Rutinu
Geothermal Development Company, P.O Box 100746-00101 - Nairobi, Kenya
rougo@gdc.co.ke, wrutinu@gdc.co.ke

ABSTRACT

The world over is gearing towards exploring and harnessing of renewable energy. This is because green energy development is the theme towards reduction of green house gases and hence reduce global warming. Geothermal energy is one of the green energy and Kenya in particular has a potential over 7,000 MWe along in the Kenya Rift. Kenya is therefore exploring and harnessing this renewable and promising geothermal energy. To develop this immense potential, a lot of infrastructure development is required. Geothermal fields are naturally located in very steep and rugged terrains with no meaningful, or none at all and therefore logistical arrangements are required in the development of infrastructure in a geothermal field. Normally accessibility of geothermal potential areas is difficult until these fields are opened up to ease mobility into and within the prospects. There are various infrastructural development that are required in a geothermal field before actual drilling can be undertaken. These include; Access roads network, water supply connections, well pads and circulation ponds construction, electricity connections and provision of lay down areas. This paper therefore discusses these critical infrastructural development and an approximate cost of each task. It also describes the challenges encountered from access road provision until the drilling phases of geothermal wells.

INTRODUCTION

Geothermal resource development comprise the following principal activities

Stage 1: Geothermal Resources Assessment

Stage 2: Resource Development

Stage 3: Electric Power Generation

Figure 1 shows the stages of geothermal development in details. After the surface exploration is completed and the exploration wells are sited, a lot of infrastructure work is normally carried out for drilling of the first well to be realised. In Kenya like elsewhere in the world, geothermal prospects are located on remote areas and therefore the whole work is done form scratch. The chapters that follow expound on the infrastructural work that is carried out in a geothermal prospect, taking into consideration Menengai geothermal prospect as a practical case.

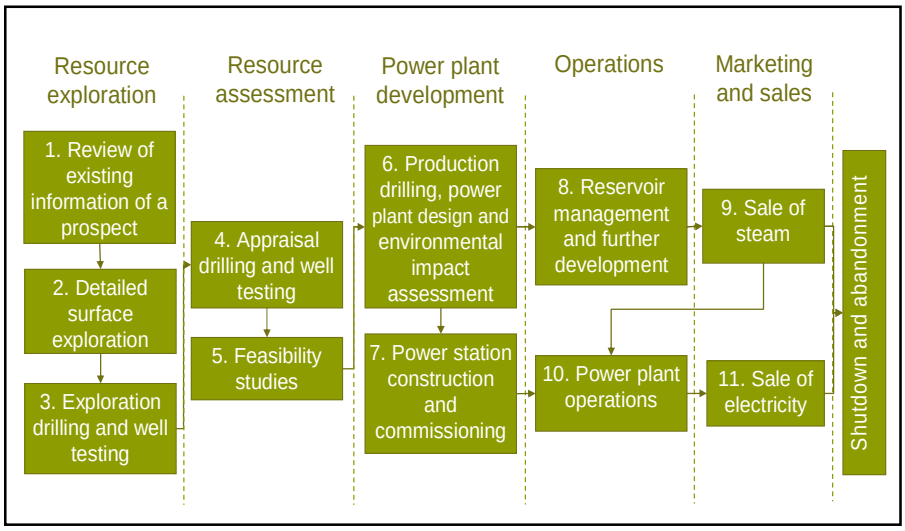

INFRASTRUCTURE WORK

Access roads network.

In order to ease mobility within a geothermal field, access roads network is vital. Due to the lugged nature of these geothermal fields, cutting of these access roads take quite a lot of time, money and machine power. Strong earth moving equipment are required to cut and flatten these roads. Bulldozers are the initial earthmoving equipment that require to be engaged to clear the bushes and remove surface rocks and soil. After the bulldozer has finished that, graders are used to grade the roads to final finish, cut mitre drains and give the roads required slope. Tipper trucks are then used to dump murram along the roads while a grader follows to spread it uniformly along the entire road. Vibratory roller compactor then follows to compact the spread murram while water bowsers move along to water the murram for better bonding. These roads sometime may pass very steep gullies and culverts are therefore constructed at the bottom of the gully to allow storm water pass without washouts.

As the access road enters Menengai caldera, a hard base rock was encountered which could not be cut using a bulldozer. This made us to engage a licensed qualified company to do blasting of this section of the road. After blasting, bulldozers were engaged to remove the rocks fragments and hence the steep gradient was drastically reduced.

Water supply connection

Drilling of geothermal steam cannot be achieved if water is not available in plenty. One drilling Rig consumes as much as 2000 litres per minute of water. Menengai geothermal prospect, which GDC is geared to developing from initial stages possess a lot of challenges as far as water is concerned. Unlike areas like Olkaria and Eburru, whose proximity to lake Naivasha give the two fields a very big advantage as far as geothermal development is concerned, Menengai geothermal field is very different. In this field, there are no streams neither is there fresh water lake.

GDC had to look for other ways of getting water in Menengai. One option was to drill water boreholes in order to get adequate water for drilling needs. Seven boreholes were drilled and commissioned and very impressing results indicated that water yield is in the range of 12-60 m^3 per hr in these boreholes. When the six (6) boreholes will be connected, we expect a total output of 264 m^3 per hr. This translates to 4400 litres per minute. Table 1 below shows the details of the six boreholes.

Table 1: Parameter of the 6 boreholes drilled in Menengai caldera

	Borehole 1	Borehole 2	Borehole 3	Borehole 4	Borehole 5	Borehole 6
Drilled Depth- Mtrs	200	105	135	50	50	55
Cased Depth- Mtrs	155	105	130	48	48	52
Water Rest Level- Mtrs	22.6	56.2	43.7	18.2	19.7	18.1
Proposed Pump setting level- Mtrs	100	86	115	40	38	40
Flow rate- m^3/hr	60	12	12	60	60	60
Pump size	6"	4"	4"	6"	6"	6"

GDC approached Nakuru Water and Sanitation Services Company (NAWASSCO) and was allowed to connect into their main using 4 inch GI pipes. From this connection NAWASSCO committed to supply a minimum of between 80-100 m^3 per hr. This again translate to 1500 litres per minute.

With these two sources of water on our reach, were are assured of about 5900 litres of water per minute and therefore we are confident that with the two Rigs drilling in Menengai, the GDC can confidently proceeds with the projects of putting up storage reservoirs tanks, water pump stations and electric sub-station as we anticipate power line connection into the caldera by Kenya Power & Lighting Company (KPLC)

A contract to supply, construct and commission five reservoir tanks each of capacity 4 million litres is underway. This will give us a total installed capacity of 20 million litres. To illustrate what this mean to two anticipated rigs; Two Rigs consume 4000 litres per minute, it will therefore take 5000 minutes to drain all the tanks assuming no

inflow. This will translate to 83.3 hrs or 3.5 days. That is how big the tanks capacity we boast of! Atypical tank is shown in figure 2.

Figure 2: A typical steel panels bolted tank

Use of brine water from discharging wells is our future option when excavating of cooling ponds/pans is complete. Due to the porous nature of Menengai field, lining of these ponds is very critical on the inner part to stop water percolation. Plans are underway to procure pond liners. A contract for water pump station is also underway whereby a pump house will be build, three massive booster pumps will be supplied, one running, one on standby and one spare. Five submersible pumps will also be installed. Each booster pump will have a capacity to pump 270 m^3 per hr (4500 litres per minute) of water. That means we require 14.8 hrs to fill one reservoir tank. It also implies that one booster pump can feed the two rigs with water requirement even when there is total loss in circulation.

Well pads and circulation ponds.

A wellpad is a well prepared flat area where a drilling rig and accessories are placed during drilling process. There are different sizes of wellpads depending on the number of cellars that needs to be constructed onto it and the size of a rig. Generally, common standard size rig requires a pad measuring 110 m long by 70 m wide for one cellar. For any additional cellar, 35meters are added to the pad length. Therefore a pad of three cellars require 180m length, i.e 80 m by 180 m. This is just a general guideline and it's not cast on stone. It should be noted that rigs are of different sizes meaning that pads may vary from rig to rig. Cellars are constructed concrete pit where drilling mad is retained during spud-in process. In normal drilling process, drilling fluid from the well return back to the cellar and is drained through the cellar drain into the circulation pond.

Table 2: Typical cost estimate and infrastructural requirements for a 140 MW power plnt

MAIN ACTIVITIES	OPTIONS	REQUIREMENTS	QTY	UNIT	HRS/FUEL REQUIRED	UNIT COST (KShs)	TOTAL COST (KShs)	RECURRENT COSTS (KShs)
WATER SUPPLY	OPTION 1A (Usage of brine)	Excavation of 12,000 M^3 holding ponds	2	pc	600 Hrs	12,000	7,200,000	
		EPDM material & Accessories and installation	12	pc		1,805,137	21,661,644	
		Hardcore to cover EPDM	1,200	ton		1,500	1,800,000	
		Victaulic water pipes	450	pc		21,060	9,477,000	9,477,000
		Victaulic couplings	450	set		3,198	1,439,100	1,439,100
		Sub-mersible pumps	2	pc		250,000	500,000	
		Booster pumps	2	pc		1,000,000	2,000,000	
		Diesel Generators	2	pc		2,000,000	4,000,000	
		Diesel consumption	10	lts	1440 litres	75	1,080,000	1,080,000
		Transport cost for 30 days	9000	km		30	270,000	270,000
		Supervisors allowances	2	each	30 days	3,000	180,000	180,000
		Engineer's allowances	1	each	30 days	4,000	120,000	120,000
		Hire of Casuals	20	each	240 Hrs	135	648,000	648,000
	Sub-Total						**50,375,744**	**13,214,100**
	Option 2A (Metered)	Victaulic water pipes	450			21,060	9,477,000	9,477,000
		Victaulic couplings	450			3,198	1,439,100	1,439,100
		Metered cost of water(lts)	4,000		1440 litrs	0.0750	432,000	432,000
		Transport cost for 30 days	9000	km		30	270,000	270,000
		Supervisors allowances	2	each	30 days	3,000	180,000	180,000
		Engineer's allowances	1	each	30 days	4,000	120,000	120,000

		Hire of Casuals	10		240 Hrs	135	324,000	324,000
	Sub-Total						**12,242,100**	**12,242,100**
	Option 3A (Drill boreholes)	Purchase of 5 acres land	5			1,500,000	7,500,000	
		Drill boreholes	5			2,500,000	12,500,000	
		Victaulic water pipes & fittings	50	Km		4,360,966	21,804,829	21,804,829
		Pump Station	1			57,000,000	57,000,000	
		Reservoir tanks	5			35,000,000	175,000,000	
		Electricity connection (33kv)	1			24,000,000	24,000,000	
		Sub-Station	1			26,000,000	26,000,000	
		Control & switching room	1			1,200,000	1,200,000	
		Transport cost for 30 days	9000	km		30	270,000	270,000
		Supervisors allowances	2	each	30 days	3,000	180,000	180,000
		Engineer's allowances	1	each	30days	4,000	120,000	120,000
		Hire of Casuals	10		240 Hrs	135	324,000	324,000
							522,142,287	**894,000**
CONSTRUCTION OF ACCES	Option 1B (Using own equipment)	D8 Bull Dozer	1		500 litres	75	37,500	37,500
		Motor Grader	1		200litres	75	15,000	15,000
		Vibratory Roller	1		100 litres	75	7,500	7,500
		Water Bowser	1		140 litres	75	10,500	10,500
		Tipper Trucks	2		140 litres	75	10,500	10,500
		Wheel loader	1		70 litres	75	5,250	5,250
		Hire of Casuals	3		120 litres	135	48,600	48,600
	Sub-Total						**134,850**	**134,850**
	Option 2B (Using hired equipment)	D8 Bull Dozer	1		40 Hrs	12,000	480,000	480,000
		Motor Grader	1		40 Hrs	7,500	300,000	300,000
		Vibratory Roller	1		40 Hrs	6,000	240,000	240,000
		Water Bowser	1		40 Hrs	1,289	51,560	51,560
		Tipper Trucks	2		40 Hrs	1,678	67,120	67,120

		Wheel loader	1		40 Hrs	10,500	420,000	420,000
		Hire of Casuals	3		120 Hrs	135	48,600	48,600
Sub-Total							**1,607,280**	**1,607,280**
CONSTRUCTION OF DRILL SITES AND CIRCULATIONS PONDS	Option 1C (Own equipment)	Back Hoe Excavator	1		50 litres	75	3,750	3,750
		D8 Bull Dozer	1		500 litres	75	37,500	37,500
		Motor Grader	1		200 litres	75	15,000	15,000
		Vibratory Roller	1		100 litres	75	7,500	7,500
		Water Bowser	1		140 litres	75	10,500	10,500
		Tipper Trucks	2		140 litres	75	10,500	10,500
		Wheel loader	1		70 litres	75	5,250	5,250
		Fencing of well pad & pond and landscaping	1	each			100,000	100,000
		Hire of Casuals	10		120 hrs	135	162,000	162,000
	Sub-Total						**352,000**	**352,000**
	Option 2C (Hired equipment)	Back Hoe Excavator	1		20 Hrs	7,000	140,000	140,000
		D8 Bull Dozer	1		160 Hrs	12,000	1,920,000	1,920,000
		Motor Grader	1		120 Hrs	7,500	300,000	300,000
		Vibratory Roller	1		120 Hrs	6,000	240,000	240,000
		Water Bowser	1		120 Hrs	1,289	51,560	51,560
		Tipper Trucks	2		120 Hrs	1,678	67,120	67,120
		Wheel loader	1		120 Hrs	10,500	420,000	420,000
		Fencing of well pad & pond and landscaping	1	each			100,000	100,000
		Hire of Casuals	10		120 Hrs	135	162,000	162,000
Sub-Total							**3,260,680**	**3,400,680**
GRAND TOTAL FOR MOST VIABLE OPTIONS FOR INITIAL ONE SITE(3A+2B+2C)							**330,906,789 (US$4,136,335)**	
GRAND TOTAL FOR MOST VIABLE OPTIONS FOR EACH ADDITIONAL SITE (1A+2B+2C)								**18,222,060 (US$227,776)**
COST ESTIMATE FOR INFRASTRUCTURE DEVELOPMENT FOR 30 WELLS							877,568,589 **(US$10,969,608)**	**877,568,589**

(ENOUGH FOR 140MW PLANT)	

Electricity connections

With the anticipated contracts for putting up of water pumps station and supply of booster pumps and sub-mersible pumps, electricity connection is vital because these pumps require power to run them. Two contracts has already been given for electricity connection. One of them is to connect a high voltage (HT) line of 33 KV into the caldera. This was given to the only power company authorized to distribute power, the Kenya Power & Lighting Company. This company will establish wayleaves thereafter connect the HT line. The second contract involves construction of a transformation and switching power sub-station. This sub-station will transform the voltage from 33 KV to 3.3 KV and to 415 V. This is because booster pumps motors are rated at 3.3 KV while sub-mersible pumps are rated at 415 V. Power is also required for lighting and workshop jobs (Figure 4). GDC will however construct metering and switching control room for KPLC and also GDC use. GDC will carry out all civil works required in the sub-station and also do fencing of the entire sub-station, which is a requirement by KPLC.

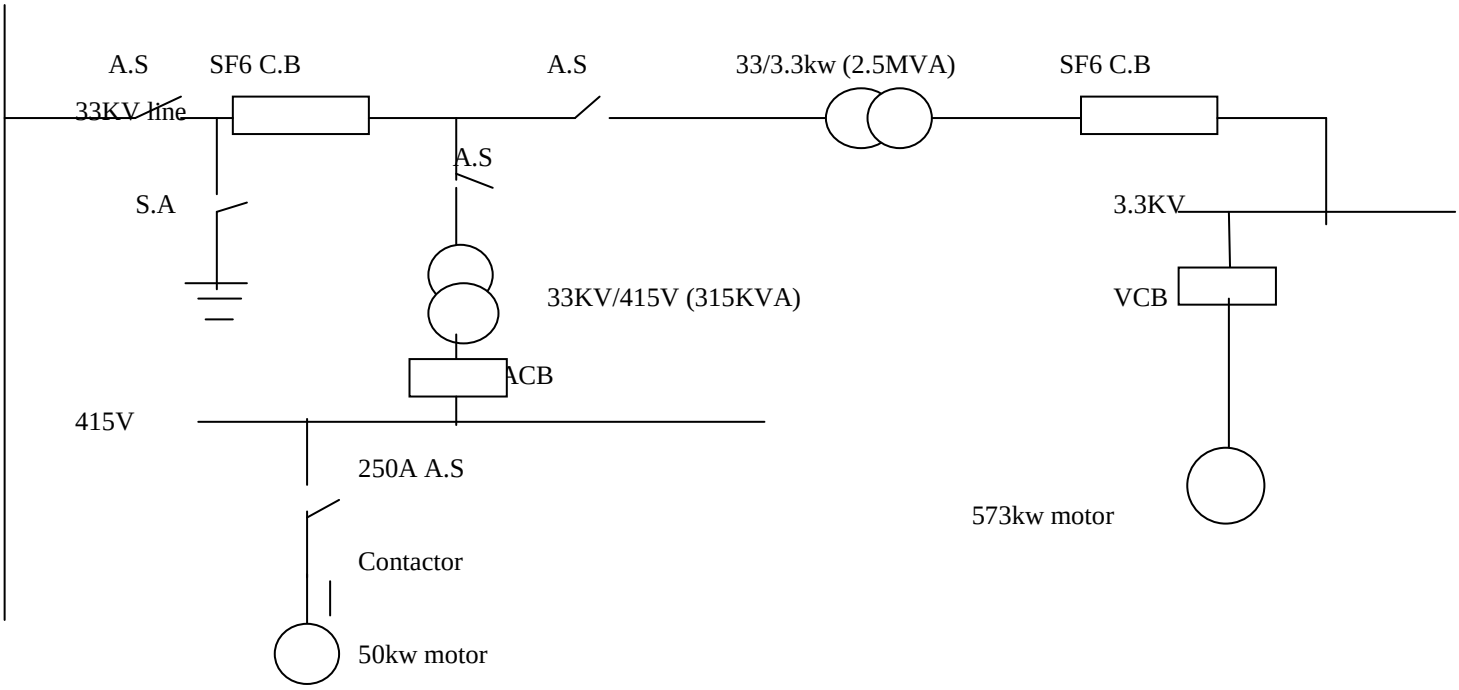

Key:

A.S – Air break switch, S.A – Surge arrestor, VCB - Vacuum Circuit Breaker, ACB – Air Circuit breaker. C.B – Circuit Breaker

Figure 4: Line Diagram for the Substation

Provision of laydown areas

There are so many materials and equipment in a geothermal field that require to be secured in a save area. Laydown areas or storage yards are made for storage of these materials and equipment. These areas are leveled and murram is applied then compacted so that heavy equipment and trucks can be able to deliver materials inside the yard. Perimeter chain link fencing is thereafter constructed around these areas, to secure the materials and equipment. The cost of construction of laydown areas is above the cost indicated in the table above. After all these are said and down is when you may expect to see something like a land rig below;

Figure 5: A land Rig in operation on a well pad.

THEME VII

TRAINING AND CAPACITY BUILDING

UNU-GTP AND GEOTHERMAL TRAINING FOR AFRICA

Lúdvík S. Georgsson
United Nations University Geothermal Training Programme
Orkustofnun, Grensásvegi 9, Reykjavík, Iceland
lsg@os.is

ABSTRACT

The United Nations University Geothermal Training Programme (UNU-GTP) has operated in Iceland since 1979 offering six month annual courses for professionals from developing countries. The aim is to assist developing countries with geothermal potential in capacity building in order to make the countries self sufficient in expertise for geothermal development. The training is tailor-made to suit the needs of the home country. Since 2000, the possibility has also opened for some UNU Fellows to extend their studies to MSc level with the six months training adopted as an integral part (30 out of 120 ECTS). In 2008, the possibilities were expanded further to include PhD studies.

As a contribution to the UN Millennium Development Goals, the UNU-GTP has expanded its activities with "annual" workshops/short courses in Africa (started in Kenya in 2005), Central America (started in El Salvador in 2006), and Asia. The events have been organized in cooperation with local energy agencies responsible for geothermal development. The aim is not only to increase capacity building, but also to further geothermal cooperation and to reach out to countries with interest in geothermal development which have not yet received quality training. Discussions are now underway with interested financial partners, looking at the feasibility of this developing into regional geothermal centres, under the UNU-GTP umbrella. An off-spring has also been the decision of UNU-GTP in offering short courses that can be tailor-made to the needs of a client from a developing country with local or external sponsors, with the first such events taking place in 2010.

Africa is a major cooperating partner of the UNU-GTP and a priority area within the UN system. Amongst the 452 UNU-GTP graduates (1979-2010), 129 or 29% have come from twelve African countries. Moreover, 12 of 25 UNU MSc-graduates are from 5 countries of Africa. The first two UNU PhD-Fellows are also Kenyans. Kenya is the leading country in geothermal development in East Africa, and many of their specialists have been trained in Iceland. The close cooperation between UNU-GTP, on one hand, and KenGen and more recently also GDC, on the other, has been the key to the successful annual Short courses given in Kenya from 2005, from which all countries in the region with geothermal potential have benefitted. The UNU-GTP expects to see other African countries succeed in geothermal development and is determined to continue to provide the training opportunities that the region needs.

Keywords: Geothermal Training, Short Courses, Africa

INTRODUCTION

The United Nations University (UNU) was founded in 1975 with an aim to build a global university, with special focus on assisting developing countries. Its headquarters are in Tokyo, but teaching is conducted in various centres around the world. The Geothermal Training Programme is operated within Orkustofnun - the National Energy Authority of Iceland. Orkustofnun became an Associated Institution of the UNU in 1978 and the UNU Geothermal Training Programme (UNU-GTP) has been in operation since 1979.

The aim of the UNU-GTP is to assist developing countries with significant geothermal potential to establish groups of specialists in geothermal exploration and development. This has been done by offering 6 months intensive training in the various fields that are needed in the exploration and development of geothermal resources. An MSc programme was initialized in 2000 in cooperation with the University of Iceland, and a PhD programme was opened in 2008, also in cooperation with the University of Iceland, providing more advanced academic opportunities in geothermal sciences or engineering. From 2005, core funding has also been secured for additional training efforts, taking the training to the developing countries, through regular workshops/short courses hosted in cooperative countries on different continents, as a part of efforts related to the UN Millennium Development goals. Finally, this has also opened up possibilities on offering short courses fulfilling special needs of a paying customer, with the first such courses held in 2010.

The paper describes the operations of the UNU-GTP with special reference to the activities and needs in Africa.

GEOTHERMAL TRAINING IN ICELAND

Since 1979, the UNU-GTP has held annual six month courses for professionals from developing countries. Nine specialized lines of training are offered: Geological Exploration, Borehole Geology, Geophysical Exploration,

Borehole Geophysics, Reservoir Engineering, Chemistry of Thermal Fluids, Environmental Studies, Geothermal Utilization and Drilling Technology (*www.unugtp.is*). Each trainee attends only one specialized line of study. The trademark of the training is to give university graduates engaged in geothermal work intensive on-the-job training in their chosen fields of specialization. The trainees work side by side with geothermal professionals in Iceland. The training is tailor-made for the individual and the needs of his institution/country. Table 1 shows the time schedule for the training.

A significant part of the practical training is conducted in connection with individual research projects. In most cases the participants bring with them data from geothermal projects in their home countries, but sometimes the research projects are integrated with geothermal exploration or utilization projects that are in progress in Iceland at the time of training. The project topic is always selected with respect to the status in the home country of the participant. All project reports have been published by the UNU-GTP, and since 1994, reports have been collected in the annually published book "Geothermal Training in Iceland", with the international publishing code (ISBN 978- 9979-68 / ISSN 1670-7400). Copies of the book can be obtained upon request. The reports are mailed regularly to former UNU Fellows and many of the leading geothermal institutions in developing countries. The complete reports can also be accessed from the home page (*www.unugtp.is*) in a pdf version.

Table 1: Time schedule for the six month specialized courses at UNU-GTP

Week	Geological Exploration	Borehole Geology	Geophysical Exploration	Borehole Geophysics	Reservoir Engineering	Environmental Studies	Chemistry of Thermal Fluids	Geothermal Utilization	Drilling Technology
1 2 3 4 5	Lecture course on all main aspects of geothermal energy exploration and utilization, practicals and short field excursions								
6 7 8 9 10	Field geology Maps and photos Structure analysis Hydrogeology	Drilling Petrological logging Alteration Mineralogy	Resistivity methods Thermal methods Magnetics Gravity	Course on well logging and reservoir engineering including: Logging and well testing practises Reservoir physics Reservoir simulation Tracer tests Computer programs		EIA Project planning Chemistry Physics Biology Monitoring Revegetation Health and safety	Sampling of fluids and gas Scaling and corrosion Analytical methods Thermodynamics Geothermometers	Heat transfer and fluid flow Control systems	Drilling equipment Drilling procedures Well design Safety Management Rig operations
11 12			Excursion to the main geothermal fields of Iceland						
13 14	Field work in deeply eroded strata	Aquifers Modelling	Data processing techniques	Logging methods Data evaluation	Responses to exploitation	Gas dispersion and abatement	Water rock interaction	Design of plants and systems	Cementing Completion
15 16 17 18 19 20 21 22 23 24 25 26	Project and report	Project and report	Project and report	Project and report	Project and report	Project and report	Project and report	Project and report	Project and report

Participants for the 6 months training are selected by private interviews during a site visit to the country in question, where a UNU-GTP representative assesses geothermal fields, research institutions and energy utilities. Candidates must have a university degree in science or engineering, a minimum of one year practical experience in geothermal work, speak English fluently, have a permanent position at a public energy company, utility, research institution or university, and be under 40 years of age. Participants from developing countries have received Fellowships financed by the Government of Iceland and the UNU that cover international travel, tuition fees, and per diem in Iceland. Other international agencies, such as The UNDP, the International Atomic Energy Agency (IAEA) and more recently a few other institutions have also financed fellowships for a few trainees through the years.

Since the foundation of the UNU-GTP in 1979, 452 scientists and engineers from 47 countries have completed the annual six month specialized courses offered (Figure 1). Of these, 42% have come from countries in Asia, 29% from Africa, 15% from Latin America, and 14% from Central and Eastern Europe. The largest groups have come from China (75), Kenya (53), Philippines (31), El Salvador (30), Ethiopia and Indonesia (27). In many countries, UNU-GTP graduates are among the leading specialists in geothermal research and development.

For the past few years, the regular funding of the UNU-GTP has allowed financing of six months training of about 18-20 UNU Fellows per year, with additional 1-3 UNU Fellows per year being financed through other sources, at least partially. However, our current set-up in Iceland, makes it possible to accept a few additional fellows if financed through external sources. This is reflected in the largest group to date in 2010, with 28 UNU Fellows, 8 of whom (6 Kenyans and 2 Nicaraguans) are mainly financed through other agencies. Figure 2 shows the UNU Fellows of 2010, 13 of whom come from Africa. The statistics show that the participation of African fellows has gradually grown and has reached 33% for the past 10 years (2001-2010), and half of those participating in the last 2 years have come from Africa (see Figure 1). This reflects the high current priority of Africa at UNU-GTP, as in the UN system in general.

The aim of establishing an MSc programme in cooperation with the University of Iceland (UI) was to go a step further in assisting selected countries in building up their specialist groups and to increase their geothermal research capacity. Since 2001, 25 former UNU Fellows (China 1, Djibouti 1, El Salvador 2, Eritrea 1, Ethiopia 2, Indonesia 3, Iran 3, Jordan

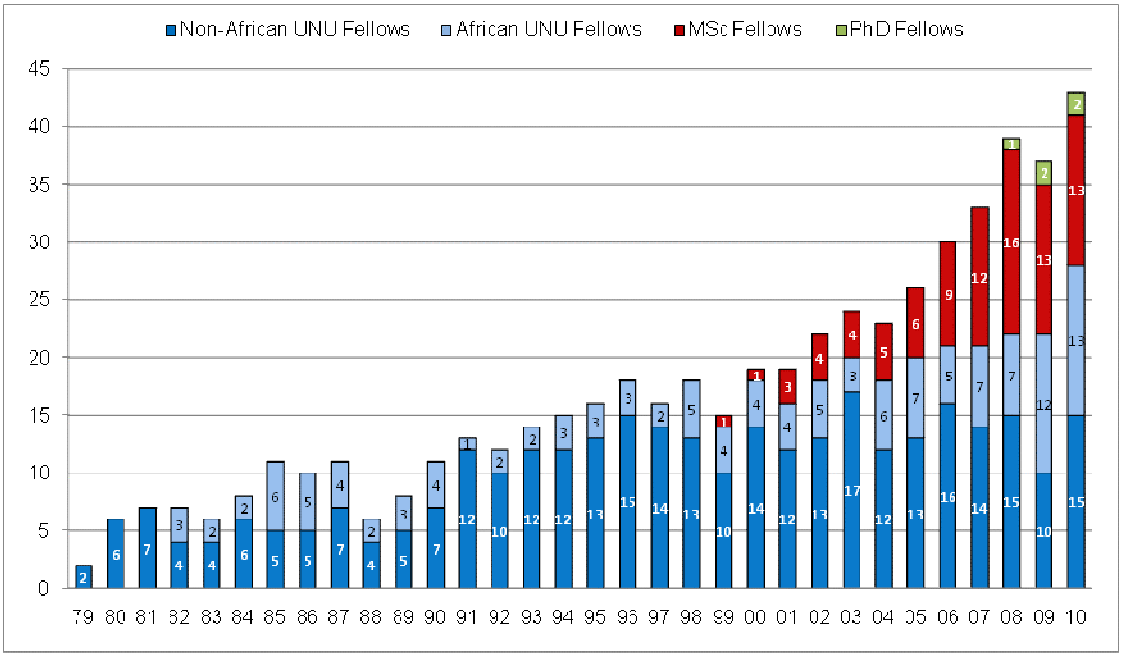

Figure 1: Number of UNU Fellows being trained and doing studies in Iceland 1979-2010 – the share of Africa for each year of the 6 months training is emphasized

1, Kenya 7, Mongolia 1, Philippines 2, and Uganda 1) have completed an MSc degree in geothermal science and engineering through the UNU-GTP MSc programme with 12 or 48% coming from Africa. In addition, eight are doing their MSc studies in Iceland in the autumn of 2010, 3 of whom come from Africa. The six months training at the UNU-GTP fulfils 25% of the MSc programme credit requirements (30 of 120 ECTS). The MSc theses have been published in the UNU-GTP publication series, and can also be obtained from the UNU-GTP webpage (*www.unugtp.is*). All of the MSc Fellows have been on UNU Fellowships funded by the Government of Iceland.

Figure 2: UNU Fellows in Iceland for 6 months training in 2010

Four former UNU Fellows, all of whom come from Africa, have now been admitted to PhD studies at the University of Iceland, with the first two admitted in the academic year 2008-2009. The two first ones are on UNU Fellowships (both from Kenya) while the other two (from Djibouti and Eritrea) are funded through other sources in Iceland.

For a more detailed description of the general operations of the UNU-GTP see Fridleifsson (2010) or the UNU-GTP webpage (*www.unugtp.is*).

SHORT COURSES IN AFRICA

Introduction

At the UN Summit Meeting on Sustainable Development in Johannesburg in 2002, the Icelandic Government announced that its contribution to the goals of the conference would be to finance increased operations of the UNU-GTP to enhance the use of geothermal resources for power production, thus, allowing the UNU-GTP to expand its capacity building activities, through workshops and short courses in geothermal exploration and development in selected developing countries. At the International Conference for Renewable Energies in Bonn in 2004, this contribution to the UN Millennium Development Goals was outlined further, and targeted to comprise annual workshops / short courses in East Africa to start in 2005, in Central America to start in 2006, and in Asia to start later (Fridleifsson, 2004). From the year 2005, the Government of Iceland has secured the necessary core funding for the UNU-GTP to carry out these plans.

The courses/workshops are set up in a selected country in the target region through cooperation with local energy agencies / utilities and/or earth science institutions, responsible for exploration, development and operation of geothermal facilities in the respective countries. In implementation, the first phase has been a week long workshop during which decision makers in energy and environmental matters in the target region have met with the leading local geothermal experts and specially invited international experts. The status of geothermal exploration and development has been introduced and the possible role of geothermal energy in the future energy mix of the region discussed. The purpose has, on one hand, been to educate key decision makers in the energy market of the respective region about the possibilities of geothermal energy and increase their awareness of the necessity for more effort in the education of geothermal scientists in the region, and, on the other hand, to further the cooperation between specialists and decision makers in the different countries. The workshop is followed by “annual” specialized short courses for earth scientists and engineers in surface exploration, deep exploration, production exploration, environmental studies and production monitoring etc., in line with the type of geothermal activity found in the respective region, and the needs of the region.

Presently, Workshops for Decision Makers have been held for East Africa (in Kenya 2005), for Central America (in El Salvador 2006) and for Asia (in China in 2008). Specialized Short Courses have since been held annually in Africa (Table 2) and almost annually in Central America, with the next courses scheduled to be held in Africa and Central America in late 2009 / early 2010. Material presented and written for these events has been published on CDs and is also available on the website of the UNU-GTP (*www.unugtp.is*). These series of Short Courses are expected to develop into sustainable regional geothermal training centres.

The African series of Short Courses

During the planning of the first Workshop, the priority region was East Africa with its huge and to a large extent unused potential for geothermal power development, and urgent need for development. Cooperation was sought with the Kenya Electricity Generating Company – KenGen. Kenya has been the leading African country in geothermal development, with 167 MWe on-line in 2009, expected to go beyond 200 MWe in 2010 (Simiyu, 2010), and KenGen has been the main authority in charge of that development. UNU-GTP had also had a long and fruitful cooperation with KenGen through its training activities. Hence, it was clear that KenGen had the knowledge and capability to act as a strong and active partner in this project. A cooperation contract was signed in early 2005. The Lake Naivasha area in the southern part of the Kenyan rift was chosen as the main site for the Short Courses, due to the vicinity of the active Olkaria high-temperature geothermal system and its geothermal power plants. In 2009, the newly formed Geothermal Development Company – GDC in Kenya, which has taken over many of the responsibilities of KenGen as well as staff members, came in as an additional cooperation partner. The cooperation has generally meant that the costs of all invited foreign participants (travels and accommodation) and non-local lecturers (salaries, travels and accommodation) are covered by the UNU-GTP and the Icelandic Government, while the costs of the local Kenyan participation and some of the local arrangements are born by KenGen, and from 2009 also GDC. KenGen and GDC have proven to be first-class hosts and have made excellent arrangements for the Workshop and Short Courses.

The first course in Africa ("*Workshop for Decision Makers on Geothermal Projects and their Management*") was held in Kenya in November 2005 in cooperation not only with KenGen, but also ICEIDA (Icelandic International Development Agency) and UNEP (United Nations Environment Programme). The 5 day Workshop was held after six nations in East Africa with good geothermal potential had decided to join forces and increase their cooperation in geothermal research and development within the so-called African Rift Geothermal Facility (ARGeo). Here the UNU-GTP had accepted to play a leading role in guiding and implementing the capacity building component of ARGeo, and the Workshop was intended to be the first step in that process.

The aim of the Workshop was, as outlined above, to get together high-level decision makers from the energy companies / institutions in the region, to make them better informed about the main phases of geothermal development and what kind of manpower, equipment, and financing is needed for each phase, and analyse what was available in the region. Participation was by invitation only, as has been for all other events. High-level decision makers from five of the six ARGeo countries (Eritrea, Ethiopia, Kenya, Tanzania, and Uganda, but missing Djibouti) attended the Workshop, plus lecturers from Ethiopia, Iceland, Kenya and The Philippines. As listed in Table 2, 30 participants attended including the local lecturers that were active in all phases of the Workshop. In addition, 4 Icelandic lecturers attended the event and 1 from the Philippines (Table 3). Figure 3 shows the participants and lecturers.

From the good attention of the participants and their active participation in the discussion, it was clear that the Workshop achieved its aim, and that there was indeed need for increased capacity building in the region. Sixteen papers were written, presented and distributed as conference proceedings and on a CD-ROM (Fridleifsson et al., 2005).

Table 2: Participants in the Workshop and Short Courses in East Africa 2005-2009

Country	Kenya 2005*	Kenya 2006	Kenya 2007	Kenya 2008	Uganda 2008	Kenya 2009	Total
Algeria			1				**1**
Burundi				2	1	2	**5**
Congo				1	1		**2**
Djibouti		2	1	2	3	2	**10**
Egypt			1				**1**
Eritrea	2	3	2	2	1	2	**12**
Ethiopia	5+2	3	1	2	3	3	**19**
Kenya	6+9	10	13	18		21	**77**
Rwanda			2	2	1	3	**8**
Tanzania	2	2	2	2	4	3	**15**
The Comoros			2			2	**4**
Uganda	4	3	3	2	5	3	**20**
Zambia				2	2	2	**6**
Yemen			2	2	1	2	**7**
Others					2		**2**
Total	**30**	**23**	**30**	**37**	**24**	**45**	**189**

* The second number shows African lecturers, most of whom also

participated fully in other parts of the Workshop

One of the results of the Workshop was that the Short Courses in East Africa should focus on surface exploration which was the field acutely needed for most countries in the region. These Short Courses have been an annual event since 2006. Table 4 gives an overview of the events, while Table 2 shows the participation from various countries and Table 3 lists the lecturers. The first Short Course was the 10 day "*Short Course on Surface Exploration for Geothermal Resources*" held in November, 2006. The purpose was to give "a state of the art" overview of the methods used in surface geothermal exploration, and discuss the status and possibilities of geothermal development in East Africa. This was achieved through a first half with scientific lectures covering the three important fields of surface exploration of geothermal resources, i.e. geology, geophysics and chemistry of thermal fluids, including many case examples, while the second half included presentations and discussions on the status of the

Figure 3: Participants in the Workshop for Decision Makers on Geothermal Projects and their Management held at Naivasha, Kenya, November 14-18, 2005

Table 3: Lecturers in the UNU-GTP Workshops and Short Courses in East Africa 2005-2009

Short course / Workshop	Total	Home country	Neighbour. countries	Internat.	Iceland	UNU-Fellows
Kenya 2005	16	9	2	1	4	8
Kenya 2006	20	11	5	0	4	15
Kenya 2007	25	16	4	0	5	18
Kenya 2008	28	19	5	0	4	23
Uganda 2008	15	1	7	2	5	8
Kenya 2009	35	27	4	0	4	26

exploration in the different countries and practical training including field demonstrations and use of computer programs. The Short Course was very well received and from the results of an assessment meeting of all participants and lecturers during the last day, it was clear that the Short Course had been a success. The basic model was one that should be repeated but suggestions were made of improvements and additions.

Table 4: UNU-GTP Workshops and Short Courses held in East Africa 2005-2010 as a part of the UNU Millennium Development goals

Event	Main site	Dates	Duration (days)
Workshop for Decision Makers on Geoth. Projects & their Man.	Naivasha	Nov. 14-18, 2005	5
Short Course on Surface Exploration for Geothermal Resources	Naivasha	Nov. 13-22, 2006	10
Short Course II on Surface Exploration for Geothermal Resourc.	Naivasha	Nov. 2-17, 2007	16
Short Course III on Exploration for Geothermal Resources	Naivasha	Oct. 24 - Nov. 17, 2008	25
Short Course on Geothermal. Project Management & Developm.	Entebbe	Nov. 20-22, 2008	3
Short Course IV on Exploration for Geothermal Resources	Naivasha	Nov. 1-22, 2009	22
Short Course V on Exploration for Geothermal Resources	Naivasha	Oct. 29 - Nov. 19, 2010	22

During the last 5 years, the annual Short Course at Naivasha has gradually developed into a more general course on geothermal exploration. In 2007, a few days of field work and demonstrations were added at the start of the course. This part has been held at Lake Bogoria in the Central Kenyan rift and has been entirely handled by the KenGen/GDC staff. And in 2008, 4 days of project work were added at the end of the course, which at that time had become 3½ week long. This model was followed in 2009. The topic of the Short Courses has also gradually broadened by adding varying types of lectures to its content, including environmental science, resource assessment, project planning, drilling technology, well logging, well siting and an introduction to geothermal power plants. As an example, Table 5 shows the set up of the *"Short Course IV on Exploration for Geothermal Resources"* held in November 2009. Figure 4 shows the participants in the 2009 Short Course. The 2010 Short Course is planned to be in a similar mould.

Presentations and papers specially written for the Short Courses have been published on CDs and distributed to participants, lecturers and others interested (Georgsson and Simiyu, 2006; Georgsson et al., 2007; Georgsson et al., 2008a; Georgsson et al., 2009).

Table 5: The structure of "Short Course IV on Exploration for Geothermal Resources "held at Lake Bogoria and Naivasha, Kenya, November 2009

Dates	Programme	No. lectures	Prac-ticals	Lecturer/Supervisor		
				Local	Neighb.	Iceland
1. Nov.	Arrival at Lake Bogoria					
2. Nov.	Introductory lectures	8		8		
3.-6. Nov.	Site visits to geothermal areas and geothermal field work		X	8		
7. Nov.	Site visit and drive to Lake Naivasha		X			
8. Nov.	Geothermal energy, power plants, drilling, etc.- Lectures	5		4		2
9. Nov.	Geothermal activity and geology – Lectures & mapping	6	X	3		1
10.-11.No.	Geophysics – Lectures & interpret.	14	X	3		2
12. Nov.	Chemistry of thermal fluids – Lectures and interpretation	8	X	2		1
13. Nov.	Practical sessions in geophysics and chemistry		X	4		2
13. Nov.	Hydrology, resource assessment,	4		4		

	logging and well siting					
14. Nov.	Excursion – Olkaria geothermal field, power plant and drilling rigs			2		4
15. Nov.	Environmental science – lectures and measurements	5	x	6		1
16.-17. No.	Status of geothermal in E-Africa – Planning projects	15	x	3	5 (+ 5)*	
18. Nov.	Case examples	5	x	1		3
19.-21. No.	Project work in groups		x	7		3
22. Nov.	Project presentations, course review, closing ceremony	(8)	x	1		1
23. Nov.	Departure participants – Instructors assessm. meeting					

* Trainees from countries outside ARGeo gave lectures on geothermal in their countries, shown in parentheses

Figure 4: Participants in the 2009 Short Course with the Olkaria II power plant in the background

A special addition in November 2008 was the "*Short Course on Geothermal Project Management and Development*". This three day event, given in Entebbe, Uganda, was co-organized by the UNU-GTP, KenGen and the Ministry of Energy and Mineral Development (DGSM) in Uganda. The timing and location of the Short Course was scheduled prior to the ARGeo C-2 conference to strengthen this event. ARGeo may not have developed into the forum it was scheduled to become but its biannual conferences have become very important venues for cooperation and exchange of ideas and information for the geothermal community in East Africa, and are worthy of good support. The Short Course was mainly aimed at high level managers/employees in ministries / energy companies / research institutions in East Africa. The participants came from 10 countries in East Africa and Yemen (Table 2). Teaching and organization was partially in the hands of experts from Kenya, Ethiopia and Uganda, all former UNU Fellows, and partially in the hands of five Icelandic and two international experts in geothermal utilization and development from El Salvador and the Philippines (Table 3). The lectures

(Georgsson et al., 2008b) and project work covered the status of geothermal energy in the world, with emphasis on East Africa, phases of geothermal development, resource assessment and geothermal project planning and management. The intention was to promote and improve focus in planning of geothermal projects in the region to move the development of geothermal resources into the production stage. The course was well received and seemed to add an important piece to the capacity building in the region.

Participation in the Short Courses in Kenya has increased with every year, not least due to the big pressure on capacity building in Kenya itself, needed for its intended fast-tracking of geothermal development in the next few years. New countries have also been added to those invited most years, and in some cases, like for D.R. Congo, Rwanda, The Comoros, Yemen and Zambia, they were participating for the first time in UNU-GTP events. Yemen has been included despite being on the other side of the Red Sea and thus in Asia, as it has common geological features with East Africa. The highest number of participants in a single event is 45 for the 2009 Short Course, and the total number of participants is now reaching close to 200 persons (Table 2). Similarly, the number of lecturers has increased with the length of the Short Courses as can be seen from Table 3, which also shows that most of the African lecturers/supervisors are former UNU Fellows trained in Iceland.

Results of the Short Courses

The Short Courses in East Africa have certainly proven to be a valuable addition to the capacity building activities of the UNU-GTP in Africa. They are now established as a good first training opportunity for young African scientists and engineers engaged in geothermal work. They have been given an introduction to state-of-the-art exploration techniques for geothermal resources and the possible development of this valuable renewable energy source. In total, 157 Africans (including Yemen) participated in the Short Courses during 2006-2009 compared to a total of 34 UNU Fellows from Africa (including Yemen) being trained for 6 months in Iceland during the same period. Furthermore, the Short Courses have become a new channel to the more advanced training in Iceland with the strongest participants showing their ability and strength, and thus opening the possibility to be selected to go for training in Iceland. There are now many examples of good participants in the Short Courses being selected for the 6 months training in Iceland. And in four cases it has even led to MSc studies in Iceland (Georgsson et al., 2008c; Fridleifsson and Georgsson, 2009), first of whom completed his MSc in April 2010.

The Short Courses have also been an important element towards increased cooperation between the countries in East Africa. Here, Kenyans have mainly been in the role of the donor, while countries like Rwanda, The Comoros and Zambia, have utilized their knowledge and contracted them for local exploration projects. Similarly, geothermal exploration projects financed by ICEIDA, e.g. in Djibouti and Eritrea, have been carried out partly with the assistance of a multinational group including their neighbouring countries.

The UNU-GTP foresees a further development of the Short Courses in Africa, and hopes that in the near future they may develop into a permanent school for geothermal training. Additional countries may also get entrance to the courses though most countries in East Africa blessed with considerable geothermal potential have now already sent some participants to the Short Courses.

For a further description of the Workshops / Short Courses of the UNU-GTP see Georgsson (2010) or the UNU-GTP webpage (*www.unugtp.is*).

Customer-designed short courses

The latest capacity building service of the UNU-GTP has been to offer customer-designed short courses in developing countries, done for the first time in 2010. This new service of the UNU-GTP has been triggered by an urgent need for training in countries planning fast-tracking of geothermal development, while it has also been an offspring of the regular training and Short Courses and the material prepared there. This has proven a good opportunity for some countries/institutions in need of a rapid capacity building process, beyond what UNU-GTP can service under its conventional operations, and which have themselves the strength or the support of external mechanisms to finance such events. The paying customer defines the outline of the Short Course, while UNU-GTP is a guarantee of the quality of the content. The first such courses have been held in 2010 for four different customers in 3 countries. The contents have varied from general geoscientific courses to geothermal drilling, or scaling and corrosion in geothermal installation.

RESULTS OF THE UNU-GTP TRAINING FOR AFRICA AND FUTURE PLANS

UNU-GTP has, through its training programme in Iceland, given 129 Africans the opportunity of intensive 6 months training in geothermal sciences or engineering, since its start in 1979. In recent years, with larger groups and higher priority to Africa, its share has risen to about 29%, of the total. If we, however, look at it in a shorter

term, during the last 10 years, the African participation has been 33%, while during the last 2 years, half of the UNU Fellows have come from Africa, or 25 out of 50, some though financed through external sources. The large majority of the UNU Fellows from Africa is still active in geothermal exploration and development.

High priority has also been given to Africa in selection of candidates for MSc and PhD studies in Iceland on a UNU-GTP Fellowship. To date 25 MSc Fellows have completed their studies at the University of Iceland, of which 12 (48%) are Africans. The first 2 PhD Fellows are both Kenyans, and two additional former UNU Fellows have now also started their PhD studies at the University of Iceland (from Djibouti and Eritrea), both funded through Icelandic sources.

With the Millennium Workshops and Short Courses, the UNU-GTP has reached a much wider audience than before. Almost 200 African scientists and engineers (including Yemen) have participated in these Series during 2005-2009 (Table 2), and about 40 additional individuals from the region have lectured in the events. This can be compared with the 38 UNU Fellows from Africa and 3 from Yemen that received 6 months training in Iceland during the same period.

The Short Courses have also opened up new connections. In East Africa, key geothermal scientists in the region are lecturing and supervising the young and promising scientists, with the knowledge thus being transferred from one generation to the next. They have also created bonds and friendship between individuals with different background and across boundaries, which can only help the development of geothermal in the region.

An important part in the development of these Series is also how they have come to act as a channel to the more advanced training in Iceland for some of the best participants. Many of the East Africans participating in the Short Courses have now come for 6 months training in Iceland and a few have already continued for MSc studies.

Most important is though that these Series are expected to develop into a sustainable regional geothermal centre under the umbrella of the UNU-GTP. The idea is now under discussion and external financing partners have shown interest in participating and turning this into reality. The idea has also been presented and accepted at the headquarters of the United Nations University in Tokyo. Here the financial crisis may have delayed action but hopefully this can be seen turning into reality during the next two year.

In 2010, the UNU-GTP has also opened a new service in offering customer-designed short courses. This has been a good opportunity for some countries in a fast-tracking developing mode of geothermal, which have had themselves the strength or had the support of external mechanisms to finance it. The first such courses have been held in 2010 for four different customers in 3 countries. The UNU-GTP foresees that service of this type may become an important part of its operations in the near future.

The financial crisis in the world has hit Iceland badly. In recent years, the operations of the UNU-GTP have almost solely been financed by the Government of Iceland (>90%). Even though the Government has emphasized that development aid through UNU-GTP has a high priority, some cut-downs are foreseen, which may affect the operations of the UNU-GTP to some extent in the near future, after a long period of continuous expansion. The 6 months training in Iceland is the cornerstone of the UNU-GTP operations and will continue to be so along with the more advanced studies for an MSc or a PhD degree. The UNU-GTP Millennium Series of Short Courses will though certainly get its fair share, and will be continued as possible with East Africa having a priority here. Expansion is unfortunately hardly in the framework until the financial climate in Iceland has improved, except based on external financing, which though seems to be a realistic possibility despite the difficult international economic climate.

REFERENCES

Fridleifsson I.B. 2004: Geothermal energy training in Iceland of professionals from developing countries. *Presented at the International Conference for Renewable Energies, plenary session "Best-Practice Examples and Success Stories", Bonn, Germany,* 4 pp.

Fridleifsson, I.B., 2010: Thirty one years of geothermal training in Iceland. *Proceedings of the Word Geothermal Congress 2010, Bali, Indonesia,* CD, 10 pp.

Fridleifsson, I.B., and Georgsson, L.S., 2009: Geothermal short courses, Iceland's contribution to the UN millennium goals. *Paper presented at the Annual Meeting of Orkustofnun (in Icelandic),* Orkustofnun, report, 31-43.

Fridleifsson, I.B., Georgsson, L.S., and Mwangi, M.M., (eds.), 2005: Papers presented at *„Workshop for Decision Makers on Geothermal Projects and their Management"*. UNU-GTP and KenGen, Naivasha, Kenya, November 14-18, 2005. UNU-GTP, CD SC-01.

Georgsson, L.S., 2010: UNU Geothermal Training Programme - Taking the training to the developing countries. *Proceedings of the Word Geothermal Congress 2010, Bali, Indonesia,* CD, 9 pp.

Georgsson, L.S., Holm, D.H., and Fridleifsson, I.B., 2008c: UNU-GTP and geothermal capacity building in Africa. *Proceedings of the ARGeo C-2 Conference, Entebbe, Uganda,* 12 pp.

Georgsson, L.S., Holm, D.H., Simiyu, S.M. and Bahati. G. (eds.), 2008b: *Papers and presentations at „Short course on Geothermal Project Management and Development"*. UNU-GTP, KenGen and MEMD-DGSM, Entebbe, Uganda, November 20-22, 2008. UNU-GTP, CD SC-08.

Georgsson, L.S., Holm, D.H., Simiyu, S.M. and Mariita, N. (eds.), 2008a: *Papers and presentations at „Short Course III on Exploration for Geothermal Resources"*. UNU-GTP and KenGen, Naivasha, Kenya, October 24 –November 17, 2008. UNU-GTP, CD SC-07.

Georgsson, L.S., Holm, D.H., Simiyu, S.M. and Ofwona, C., (eds.), 2007: *Papers and presentations at „Short Course II on Surface Exploration for Geothermal Resources"*. UNU-GTP and KenGen, Naivasha, Kenya, November 2-17, 2007. UNU-GTP, CD SC-05.

Georgsson, L.S., Mariita, N., and Simiyu, S.M., (eds.), 2009: *Papers and presentations at „Short Course IV on Exploration for Geothermal Resources"*. UNU-GTP and KenGen, Naivasha, Kenya, November 1-22, 2009. UNU-GTP, CD SC-10.

Georgsson, L.S. and Simiyu, S.M., (eds.), 2006: *Presentations at „Short Course I on Surface Exploration for Geothermal Resources"*. UNU-GTP and KenGen, Naivasha, Kenya, 12-22 November 2006. UNU-GTP, CD SC-02.

Simiyu, S.M., 2010: Status of geothermal exploration in Kenya and future plans for its development. *Proceedings of the Word Geothermal Congress 2010, Bali, Indonesia,* CD, 11 pp.

DEVELOPING CRITICAL HUMAN COMPETENCIES IN GEOTHERMAL ENERGY TECHNOLOGY

Peter Omenda and Silas Simiyu
Geothermal Development Company Ltd
P. O. Box 100746 -00101, Nairobi
Corresponding author: pomenda@gdc.co.ke

ABSTRACT

Geothermal energy is anticipated to play an important role in meeting the global energy demand in the coming century. Geothermal in Africa is expected to compete with other renewable energy sources, in particular solar. However, the rate of geothermal development in Africa has been slow partly due to lack of trained human resources in geothermal technology and risk funds. This paper looks at the need to develop critical human competencies in Eastern Africa required for accelerated geothermal development in the region. Among the areas with inadequacies within the East African Rift Countries include geology, geochemistry, geophysics, reservoir engineering, drilling, steam-field engineering, power plant operation and maintenance and environmental management. The paper recommends that an aggressive training programme needs to be put in place to address the identified training needs. The recommended training should include overseas training for degree and diploma certificates; short courses of one to four months duration, and local and foreign internships The Geothermal Development Company and KenGen are proposed as local organizations that can support training via internships.

INTRODUCTION

Training in geothermal technology that started in 1970 at the International School at Pisa (Italy) and at Kyushu University (Japan) were non-degree overview type courses. These lasted between 9 and 2 months in Pisa and 4 months in Kyushu. This decade saw a rapid expansion of geothermal projects in developing countries sponsored by international and bilateral aid. Overview teaching, however, could not cope with demand for specialized and academic type training. At the request of the UN Development Programme (UNDP) and with the support of the NZ Ministry of Foreign Affairs (MFA), the Geothermal Institute (GI) was established in 1978 at the University of Auckland (UA). Its purpose was to offer a post-graduate, 10 months academic Diploma course for earth scientists and engineers (Hochstein, 2005). However, UA course was suspended between 2003 and 2006 but resumed in 2007 with post graduate certificate course in geothermal technology (Newson et al., 2010). The Pisa school has not held its annual course since 1993 due to drastic cuts in government financing, but has occasionally held short courses (1-3 weeks) in developing countries while the International Group Training Course at Kyushu University was closed in 2001.

After the University of Auckland training programme, a 6-months training course in geothermal technology was initiated at Reykjavik (Iceland) in 1979 as part of a United Nations University training programme (Friðleifsson, 2010). The United Nations University-Geothermal Training Program (UNU-GTP) currently trains masters and PhD students in collaboration with the University of Iceland. Despite the availability of these courses, trained manpower in Africa over the year's number only about 329 out of which some have retired while others work in foreign countries. This, therefore, calls for a new approach to fast track training of additional 460 technical staff to provide the needed human capital to drive the Eastern Africa's agenda of generating additional 4,000MW from geothermal sources by 2020.

WORLD GEOTHERMAL RESOURCE USE

On a global scale geothermal resources constitute a small, yet rapidly growing, energy resource. It is a very important renewable energy source for many countries. In the year 2010 geothermal energy constituted about 0.75% of the annual worldwide energy consumption (IEA, 2009). Geothermal resource has been identified in more than 80 countries and utilization of the resource had been recorded in 76 countries in the world. Geothermal energy, as natural steam and hot water, has been used for decades to generate electricity, in space heating and industrial processes. In 2010 a total of 25 countries were generating electric power from geothermal resources (Bertani, 2010) and 78 countries were using geothermal energy directly (Lund et al., 2010). The world installed electrical capacity from geothermal resources is 10,715 MWe (year 2010). Installed capacity of electricity from geothermal sources is expected to reach over 18,500 MWe by 2015 (Bertani, 2010). The global thermal capacity of non-electrical uses (greenhouses, aquaculture, and district heating and industrial processes) is 121,696GWh/yr (Lund et al., 2010).

GEOTHERMAL USE IN AFRICA

Among African countries only Kenya and Ethiopia have been generating electricity from geothermal sources. Kenya commissioned its first plant (45MW) between 1981 and 1985 while Ethiopia commissioned an 8.5MW plant in 1998. Kenya has since installed further 160MW at Olkaria giving her a total installed capacity of 205MW. Additional 4MW off grid plants have been installed to directly supply agricultural industry. Ethiopia commissioned its first 8.5 MWe geothermal plant in 1998 at Aluto in the Lakes District (Teklemariam et al., 2000). Exploration for geothermal resources has been conducted to varying extent in Cape Verde, Djibouti, Eritrea, Tanzania, Uganda, Zambia, Malawi, Rwanda, Egypt, Comoros, Tunisia, Algeria, DRC and Burundi.

Many African countries have made some direct uses of their geothermal resources. These countries are Algeria, Egypt, Ethiopia, Kenya, Tunisia, and Zambia. Tunisia, which is one of the world leaders in the use of geothermal energy for greenhouse heating and irrigation, is currently leading in Africa with about 110 hectares of greenhouses (Mohamed, 2003). In Kenya, Oserian Development Company, a flower-growing firm utilizes geothermal energy to heat 50 hectares of greenhouses. Other African countries are keen to exploring their geothermal resources both for direct applications and electricity generation. Kenya plans to add 3,000 MW of geothermal power by 2020 while the other eastern African countries plan to install 1,000 MW.

GEOTHERMAL TRAINING IN AFRICA

The UNU-GTP is at present the only international graduate school offering specialized training to diploma and degree levels in all the main fields of geothermal science and engineering (Friðleifsson, 2010). University of Auckland offers post graduate certificates and also intends to offer degrees in geothermal technology in the near future (Newson et al., 2010). From the geothermal development plans of eastern African countries, more than 460 personnel need to be trained in all aspects of geothermal development including exploration, drilling, reservoir management, environmental management and power plant operations and maintenance. To this end, UNU-GTP commenced post graduate certificate short course in Kenya on geothermal exploration.

The first course was held in Kenya in 2005 in collaboration with Kenya Electricity Generating Company (KenGen) and the UNEP/GEF African Rift Geothermal project (ARGEO) with participants from Kenya and neighbouring countries with geothermal resources. The teaching was a blend of Icelandic experts and former UNU Fellows in eastern Africa. The current version of the course lasts three weeks and is co-sponsored by the Government of Iceland, KenGen and Geothermal Development Company Limited (GDC).

As part of its aggressive plan to develop steam equivalent to 5,000 MWe by year 2030, GDC plans to set up a training facility for its staff. The training facility will handle short courses that include exploration techniques (geology, geochemistry, and geophysics), drilling technology, reservoir studies, environmental management and safety, utilization and power plant operation and management. These courses will typically last three weeks to three months. Detailed plan about the centre is covered in another manuscript in this conference's proceedings.

TRAINING PROGRAMS FOR THE FUTURE

To meet the required trained human capacity to develop geothermal resources in eastern Africa, both traditional training programs and other capacity building programs need to be utilized at the same time. It is hoped that UNU-GTP program and the scholarship thereof will continue to be offered to deserving African countries. Recent survey by Teklemariam (2010) indicated that the region would need four hundred and sixty (460) trained experts to post graduate diploma and another fifty (50) to M.Sc. and PhD degrees by year 2013. The UNU-GTP and higher degree graduates would form the core of trained experts in various countries and who can be relied upon to further train other graduates in their countries (Friðleifsson, 2010). African trained personnel have successfully been used for the short courses held in Kenya since 2005. They Africans comprise the bulk of the trainers.

To further fast track capacity building, GDC recently hired consultants from UNU-GTP to undertake local training of their graduates and technicians on exploration methods. The courses covered include geology, geophysics, and geochemistry. Theory and practical aspects were covered over a period of 30 days and included actual field work. Forty graduates and technicians underwent through the course. The course had a great impact on the trainees as they are now able to deploy field equipment and undertake basic interpretations. Additionally, it was cost effective to bring in three consultants than take fort trainees to Iceland for similar training. GDC plans to continue with that approach to develop critical mass of trained personnel in exploration, drilling, reservoir and modeling.

GDC is also working on plans to train some staff through local or foreign internship with renowned laboratories and/or projects. It is anticipated that the attachment to the experts would provide international exposure and

work ethics required for rapid geothermal development. GDC is seeking internships in Iceland, New Zealand and USA for its staff. Conversely, GDC and KenGen having well developed capacity in exploration, drilling and geothermal power plant operation and maintenance should offer internship to graduates and technicians from eastern African countries to learn from their experiences.

ArGeo stakeholders meeting held in Nairobi in March 2010 resolved that the African rift countries should strive to incorporate teaching of geothermal technology in the local universities (Teklemariam, 2010). The syllabus would follow similar curriculum for MSc degree in geothermal technology programs to those of the Institut Teknologi Bandung, Indonesia (Saptadji, 2010). The curriculum would include courses in exploration (geology, geochemistry, geophysics), drilling technology, management and economics of geothermal, geothermal energy utilization, geothermal production engineering, geothermal reservoir studies (modeling and simulation), environmental management, direct utilization and power plant operation and management.

REFERENCES

Bertani, R. (2010). Geothermal Power Generation in the World 2005 – 2010 update report. *Proceedings, World Geothermal Congress 2010, Bali, Indonesia.*

Fridleifsson, I.B. (2010). Thirty one years of Geothermal Training in Iceland. *Proceedings of World Geothermal Congress 2010. Bali, Indonesia*.

Hochstein, M.P (2005). 25-year Geothermal Institute (University of Auckland, 1979-2003), *Proceedings, World Geothermal Congress 2005 Antalya, Turkey*.

IEA (2009). Key World Energy Statistics 2009. International Energy Agency, Paris, France.

Lund, J. W., Freeston, D. H., Boyd, T. L. (2010). Direct Utilization of Geothermal Energy 2010 Worldwide Review. *Proceedings of World Geothermal Congress 2010. Bali, Indonesia*

Mohamed, M.B. (2003). Multiple integrated use of geothermal resources in Kebili region, southern Tunisia. *Proceedings, International Geothermal Conference, Reykjavik, Iceland*

Newson, J. A., O'Sullivan M.J. and Zarrouk, S.J. (2010). Postgraduate Geothermal Training in New Zealand. *Proceedings of World Geothermal Congress 2010. Bali, Indonesia*

Saptadji, N. M. (2010). Geothermal Education for supporting geothermal development in Indonesia. World Geothermal Congress 2010, Bali, Indonesia.

Teklemariam, M. (2010). Training needs assessment for Eastern African countries. *Report prepared for AU, Addis Ababa, Ethiopia*

Teklemariam, M., Beyene, K., Amdeberhan, Y., and Gebregziabher, Z. (2000). Geothermal development in Ethiopia. *Proceedings, World Geothermal Congress 2000,* Japan.

CHALLENGES OF HUMAN CAPACITY BUILDING: GDC'S EXPERIENCE

IRENE N. ONYAMBU (MRS.)
GEOTHERMAL DEVELOPMENT COMPANY LTD
P. O. BOX 100746 – 00101, NAIROBI, KENYA
ionyambu@gdc.co.ke

ABSTRACT

The East African Rift System, which is estimated at having over 15000MWe of clean geothermal energy, covers eleven countries among them being the Republic of Kenya. The development of this high and largely untapped resource has been very slow in Kenya. The country's first 15 MWe unit of the 45 MWe electric power generating plant was commissioned in 1981. It has been operating since then and has proven reliable and economical, running at 98% availability (Ng'ang'a, 1998). The total installed geothermal capacity in the country currently stands at 128 MWe.

Demand for electricity has been on the rise and future growth projection in Kenya requires that urgent initiatives are undertaken to ensure electric energy capacity addition is adequate to cover this demand. One key initiative undertaken by the Government of Kenya is the establishment of Geothermal Development Company Ltd (GDC) as a special purpose vehicle to accelerate the development of geothermal energy resources in the country.

GDC, incorporated on the 2nd of December 2008, robustly began operations in Mid 2009 with the appointment of key members of the top management. With the entrance of GDC into the Kenyan energy sector, there is need, more than ever, to *build capacity* in order to adequately and effectively harness this environmentally friendly resource – the geothermal resource.

INTRODUCTION

Kenya, having been among the first in Africa to tap geothermal energy for the purpose of electric power generation, has made strides, albeit small, in the development of human capacity in the field of geothermal development. Skilled personnel in the areas of resource assessment, exploration, drilling and reservoir engineering, for example, are lacking in Kenya and in Africa as a whole, hence the need for the implementation of comprehensive and systematic human capacity building programmes and initiatives so as to effectively harness this clean natural resource.

What then is the meaning of Capacity Building

Interviews and conversations with a few employees of GDC confirm that the term Capacity Building is at best, loosely defined. Some respondents referred to it as 'staff development', others said it was 'anything that strengthens organizations while others called it,'developing networks with NGOs for financial aid.

Capacity Building encompasses all the above descriptions and more. The definition that will be adopted in this paper is as follows:

> **"Capacity Building refers to activities that are designed to improve the performance of an organization by strengthening its employees, leadership, management and overall administration"**

To clarify this definition further, Capacity Building includes:

a) ***Institutional and Legal Framework Development;*** making legal and regulatory changes to enable organizations and institutions to enhance their capacities.
b) ***Organizational Development;*** the elaboration and management of relationships between and within the different organizations and sectors.
c) ***Human Resource Development;*** the process of equipping individuals with the understanding, skills and access to information, knowledge and training that enables effective performance

CAPACITY BUILDING: THE CASE OF GDC.

Legal and Regulatory Framework Development – The Birth of GDC

The government of Kenya in its endeavor to respond to the anticipated growth of electricity demand from the current 1,080 MWe to 10,000 MWe by 2030, saw the need for rapid geothermal development through the creation of GDC. GDC is a 100% government owned State Corporation under the Ministry of Energy mandated to add 4,000MWe of geothermal power in the next 20 years. As a result of these legal and regulatory changes within the energy sector in Kenya, to say that GDC hit the road running is an understatement. GDC is airborne

at crusing speed and altitude so as to accelerate the delivery of not just 4,000MWe but 5,000 MWe by the year 2030. Capacity building therefore, in terms of the legal and regulatory framework in Kenya saw ***the birth of GDC*** for geothermal resource development and utilization.

Organizational Development – Managing Stakeholder Relations

For GDC, capacity building is a long-term continuous process in which all stakeholders participate in order to improve governance, leadership, mission & strategy, administration (i.e HR, Financial Management and Legal matters) project management, fundraising and income generation, partnerships and collaborations, evaluation, marketing and positioning. As an organization, the ***managment of stakeholdder relations*** is key for the realization of high level organizational development.

The institutional arrangement in the electricity sub-sector in Kenya comprises several companies whose overall activties generally fall under Resource Development, Electricity Generation, Electricity Transmission and Electricity Distribution. The Electricity Regulatory Commission under the Ministry of Energy manages and coordinates activities of these organizations.

There are also other stakeholders whose relations GDC must embrace and conciously develop and maintain: the communities around our operational sites. There are 15 high potential sites that have been identified. These are:- Suswa, Longonot, Olkaria, Eburru, Menengai, Arus-Bogoria, Korosi, Paka, Lake Magadi, Badlands, Silali, Emuruangongolak, Namarunu and Barrier. A number of these sites are located in remote parts of the country with high poverty levels and whose way of life is nomadic in nature due unfavourable and unpredictable weather conditions. Ethnic tension is rife in some of the communities where these high potential sites are located.

The diagram below shows the high potenstial sites to be explored by GDC vis a vis climatic conditions.

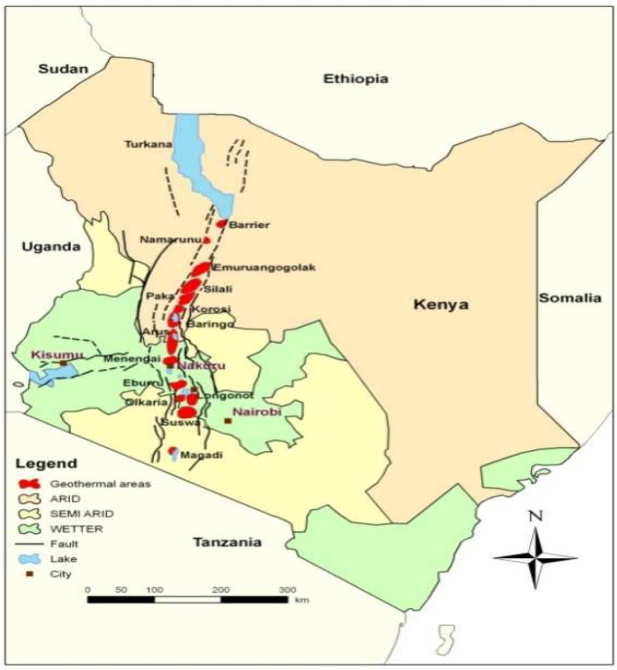

Diagram 1

GDC's approach in ***managing stakeholder relations*** has been through their engagement so as to understand their expectations on the issues most important to them and map them against our business priorities. GDCs priority focus areas include support for education, income generating activities/job-creation projects, environmental management initiatives, provision of clean water & sanitation and preservation of art, culture and sports.

Human Resource Development - Through Training

In Kenya, adequate numbers of trained and skilled personnel in the geothermal industry are lacking. GDC has a strong technical workforce of about 420 staff. The following initiatives are being used to develop staff capacity at GDC.

Human Capacity Building Plans & Initiatives at GDC - *Mitigation Measures*

In order to brigde the skills gap indicated in ***Table 3*** above, it is envisaged that GDC's staff capacity building will be achieved through various means as indicated below.

Collaboration with Overseas Institutions

Collaboration with various institutions such as BRGM (France), UNU-GTP (Iceland), University of Auckland (New Zealand), University of Kyushu (Japan), BGR (Germany), IRIS (USA), ICS-UNIDO (Trieste & Pisa, Italy), University of Manila (Philipines), University of Aberdeen (Scotland) and University of Potsdam (Germany) will enhance lead to the transfer of knowledge from experts in the geothermal industry to employees on GDC. This shall include both formal training and on-the-job training.

Participation at Major Geothermal Related Workshops & Conferences

Participation in various geothermal forums both locally and internationally has gone a long way in improving our employees' understanding of various concepts in the geothermal field in addition to keeping them abreast with the latest developments in this area. Furthermore, employees at GDC are encouraged to submit papers and make presentations at regional and global conferences and summits hence further clarifying their understanding of the subject matter during research and paper preparation and eventual presentation.

Coaching & Mentoring

Coaching and Mentoring are ways of building human capacity within an organization. At GDC, the prinicipals of ***Coaching*** (transfering of knowledge through instruction and training) and ***Mentoring*** (one-on-one wholistic staff development) are of paramount importance in order to build human competencies within the workforce. Line managers and supervisors are encouraged and will continually be required to identify talents amongst their new engagements with a view to building and developing them to achieve higher levels of performance. This in turn will lead to skills and competency improvement.

Instutionalizing of Performance Culture

Human Capacity Building programmes go hand in hand with employee performance. GDC has embraced a culture of performance right at the on-set with the use of the Balanced Score Card approach whereby key deliverables in a given year are directly linked to the overall score card of the organization. This way each employee knows what is expected on him and strives to meet each of their targets by the end of the agreed period. It is during performance assessment interviews that skills gaps are identified and corrective measures taken to improve performance.

Provision of Attractive Performance Rewards & Incentives

As part of GDC's performance culture, an attractive performance incentives scheme has been developed to reward exceptional performance. We believe that exceptional performance must result in exceptional rewards. Hence, as employees seek to achieve and even surpass performance targets, their skills consequently get sharpened and enhanced. This in turn translates to improved human capacity within the organization.

Employee Self Development

An environment in which employees are encouraged to actively develop themselves provided it does not interfere with their duties, must exist if Human Capacity Development is to thrive. At GDC, several employees who received scholarship in technical studies have been given time off (unpaid leave) by the company to pursue further training overseas so as to build capacity within GDC.

Talent Management Initiatives

It is said that talent is sometimes like a parachute. If it is not there, you may not need it again! In order to retain talent once identified and developed, one has to manage it, so as to help reduce the risk of mass exodus of skilled technical personnel to competitor companies whether locally or overseas. At GDC, cost effective short-term incentives such as provision of paid day offs, commendation letters, dinner with the management team and employee of the year awards shall be employed to management her desired talent. Long-term and more costly incentives include use of flexi-time for high performers, annual overseas holidays with spouse & children and repayment of staff outstanding loans just to mention a few.

Establishment of a Regional Geothermal Training Institute

Establish a state-of-the-art Geothermal Training Institute that will make the access of specialized training locally available. This institute will also facilitate the transfer of knowledge especially in technical and other specialized areas.

Challenges

In any human capacity building programme, there will always be challenges and GDC is not an exception.

Legal/Regulatory Framework

Challenges in Legal/Regulatory Framework Development have been in the

i. Acquisition of land at potential sites
ii. Acquisition of property eg office blocks, rigs etc, critical for operations

Organizational Development

Challenges in Organizational Development:

i. Effective management of stakeholder relations
ii. Effective management of Donor/investor relations

Human Resource Development

Challenges here include:

i. Development of Systems & Structures from scratch
ii. Managing Diversity
iii. Creating the desired culture

CONCLUSION

In conclusion, capacity building encompasses a country's human, scientific, technological, organizational, institutional and resource capabilities. It is the creation of an enabling environment with appropriate policy and legal frameworks, intitutional development and human resource development and the strengthening of managerial systems.

Capacity building initiatives are not done over night neither are the results realised at once. It is a long-term, continuing process, in which all stakeholders participate for the good of all.

The journey to build capacity in the geothermal industry has just began GDC. It is a journey that will see us through challenges that we shall bravely overcome and learn from, in order to deliver cheap electric energy to Kenyan citizens and beyond.

ACKNOWLEDGEMENT

Acknowledgement goes to the CEO & MD of Geothermal Develpment Company, for his support and provision of information and data used to complete this paper. I also acknowledge Dr. Peter Omenda and the Corporate Planning team for providing relevant literature & material used in this paper.

REFERENCES

Dr. Silas M. Simiyu & Martin N. Mwangi, Geothermal Education in Africa – Past Experience and Future Prospects

Dr. Silas M. Simiyu, Development of a Geothermal Training Centre in Kenya. Workshop for Decision Makers on Geothermal Projects and Management organized by UNU-GTP and KenGen, Naivasha, Kenya, November, 2005.

Dr Peter Omenda, 2010: Training Schedule & Estimated Budget. Department of Infrastructure and Energy, African Union Commission, April 2010.

Pacifica F. A. Ogola, UNU-GTP Fellow (2009-2012). Paper presented at the World Geothermal Congress, 2010.

Geothermal Development Company: Capacity Building Plan (2009 – 2011)

Geothermal Development Company: Corporate Social Responsibility Policy & Guidelines, 2010.

CAPACITY BUILDING, THE GDC EXPERIENCE

Rose Ougo Tindi
Geothermal Development Company,
P.O Box 100746-00101. Nairobi, Kenya
rougo@gdc.co.ke

ABSTRACT

Realisation of organisation growth and attainment of competitive advantage is only through filling the skill gaps that exist in an organisation. Capacity Building is much more than training and includes; Human Resource Development, Organizational Development and Institutional and legal framework development. The challenge for a new organisation like the Geothermal Development Company (GDC) is to attain a leverage in the Energy sector by having a skilful and competent workforce who have the requisite skills to help the organisation attain competitive advantage. From inception it is therefore critical to define a skill inventory by carrying out a detailed assessment of the skills that exist and projecting the required skills in five years so as to have a basis for capacity building indigenous qualified and technically competent employees with a bias in geothermal generation and reservoir engineering is a scarce resource in Kenya. Growing staff shortage in core corporate areas necessitates that we develop a comprehensive training program geared towards attaining the key competences, more so getting institutions that offer the kind of training required for the geothermists are rare. This therefore necessitates sourcing from outside Kenya institutions that offer the unique skill and competence in geothermal technology in resource exploration and drilling. GDC has been able through the Company's Training Committee to structure training after extensive research by and by visiting institutions that offer the requisite skill. This paper therefore will primarily focus on capacity building, the modalities to groom employees to bring their best and to share our GDC experience of an effective and appropriate capacity building. A fundamental goal of capacity building is to enhance the ability to evaluate and address the crucial questions related to policy choices and modes of implementation among development options, based on an understanding of environment potentials and limits and of needs perceived by the company.

INTRODUCTION

Because of the dynamic nature of management, the skills associated with it often become outdated with the passage of time. Because most aspects of management can only be learned through practical exposure rather than academic discourse, it is necessary for organizations to have in place systems that continually updates managers at all levels on the emerging and developing management trends.

Capacity building is a response to this need for a continuous professional development within an organization's management. It essentially involves systematic development of management competencies and devising best methods for the development of skills at all managerial levels to meet the organization's requirements and future needs. This, of course, takes place after a careful analysis of present and future management requirements and an assessment of existing and potential management skills within the organization.

For capacity building to be effective, it should be designed and mainstreamed to meet the overall corporate goals. To achieve this, capacity building programmes should derive their specific and measurable objectives from the broad corporate goals. This is done by breaking down these broad goals into unit or departmental objectives and then further into individual objectives.

RATIONALE FOR CAPACITY BUILDING

It is the human resources of an organization that manages all the other resources – time, material, financial and so on - towards achieving corporate objectives. This reason alone, if not any other, makes it have the biggest impact on the success of any organization. It is therefore imperative that high quality management development is vital for the success of an organization.

Ideally, appropriate management development strategies provide a vehicle for imparting new values attitudes, skills and knowledge. This is key to the successful management of all of a company's resources towards achieving its short and long term objectives. Capacity building that changes peoples' thinking and understanding should precede, or be part of, training programmes. If managerial training is limited to specific tasks, procedures and current assignments, it does no qualify to be called management development as it does not meet long term needs for career development, succession planning and organizational survival, growth and profitability.

The pressure of increasing liberalization and globalization of most economies, coupled with rapid changes in technology, necessitate a well structured management development policy.

BACKGROUND TO GDC

Geothermal Development Company is a limited liability company whose mandate is to develop Geothermal Resources with core functions that include exploration, drilling, assessing and developing geothermal resources for power generation and other direct uses. Prior to October 2009, the only power generating companies in Kenya were KenGen (a State Parastatal) and independent power producers. In line with the challenges of a new company and in anticipation of further liberalization, the company defined its vision as "To be the world leader in the development of Geothermal Resources" and its mission as "To develop 3000 MW from Geothermal Resources by 2020".

As a result, the management of GDC embarked on a programme of building a new, vibrant image of an efficient and highly responsive organization. This is based on the premise that the success and public image of the company will depend largely on the quality of service delivered to both internal and external customers. One of the primary mechanisms identified as key to the branding process was capacity building of employees both of the managerial and non-managerial cadres.

CAPACITY BUILDING AT GDC

As mentioned earlier, GDC's mission is "To develop 3000 MW from Geothermal Resources by 2020". A capacity development policy has been developed and documented based on the philosophy that people are the most valuable asset and the attainment of corporate objectives depends on how efficiently and effectively the staff carry out their responsibilities (GDC Training Policy April, 2010).

The policy document states that the success of the Company essentially depends on the quality of its people. GDC shall develop the skills of all its employees to create high level of motivation and performance, to allow them to reach their full potential. This policy aims at having a well trained, highly skilled, knowledgeable and competent staff.

It is the policy of the company to promote the development of skills, knowledge and attitudes of its human resources in the most equitable and efficient manner by:

1. efficiently allocating the necessary human, material and financial resources;
2. systematically planning its training based on short and long term needs of the; company for the improvement of its services to customers and the fulfillment of its skill requirements;
3. evaluating programmes regularly to determine the extent to which training and development activities are contributing to the achievement of company objectives;
4. making training an integral part of the human resource management process

The policy document further states that GDC's training mission is "to enable the company achieve its objectives through staff capacity development by enhancing requisite knowledge, skills and attitudes''. Its specific objectives are to:

- develop staff capacity for efficient and effective performance of their jobs;
- prepare staff for career development and succession;
- inculcate the desired corporate work culture;
- induct all new staff to company operations;
- help staff adapt to change

CHALLENGES FACED IN THE DRIVE FOR CAPACITY ENRICHMENT

The challenge for a new organization like, Geothermal Development Company, is to attain a leverage in the Energy sector by having a skilful and competent workforce who have the requisite skills to help the organization attain competitive advantage.

It has therefore been critical, right from inception, for GDC to define a skill inventory by carrying out a detailed assessment of the skills that exist and projecting the required skills in five years so as to have a basis for capacity building. Indigenous qualified and technically competent employees, with a bias in geothermal generation and reservoir engineering, are a scarce resource in Kenya.

Growing staff shortage in core corporate areas has necessitated that we develop a comprehensive training program geared towards attaining the key competences, more so when we take into account the fact that local or regional institutions that offer the kind of training required for the engineering cadre is rare. This therefore

necessitates sourcing from institutions outside Kenya that offer the unique skill and competence in geothermal generation and drilling.

With the assistance of the Chief Executive Officer we have been able, through the Training Committee, to structure our training programmes after researching extensively by visiting institutions that offer the requisite skills.

Benefits of systematic management development include the provision of the skilled managerial manpower for the organization's long term needs, improved skills, knowledge and attitudes, improved individual, unit and corporate performance and greater commitment of staff as a result of improved motivation and better employee relations.

Measuring behaviour change is a challenge. The New Zealand Association of Training and Development (NZATD, 1998) has identified six steps that must be in place to ensure behavioural change. These are:

1. recognition by participants of the need to change behaviour;
2. understanding by participants what exactly is the required behaviour;
3. self assessment of the participant's skill level – compared to that of a high achiever;
4. practice the skill and gain feedback;
5. job application and goal setting to transfer the skill back to the job;
6. follow up and support to monitor the learning

According to Kinlaw (1950), capacity building helps employee's to fulfill their roles and perform their functions in ways that are consistent with the company's goals and is crucial for organizational success. He further argues that training and development is linked to empowering people with the following key competencies to help them meet those organizational goals.

1. Business competencies such as skills for:-
    - thinking, planning and acting strategically;
    - understanding economics of the company, that is profit, debt, share value and others;
    - managing financial resources;
    - developing business skills;
    - changing environments and markets
2. Performance improvement competencies such as skills for:
    - technical mastery of job tasks;
    - designing improvement projects;
    - tracking and measuring personal performance;
    - tracking and measuring supplier performance;
    - tracking and measuring customer satisfaction
3. Personal Competencies such as skills for:
    - thinking analytically and using a variety of rational problem solving methods;
    - facilitating the empowerment of self and others;
    - managing continuous learning for self;
    - being a superior team leader;
    - being a superior team player and member;
    - managing interpersonal conversations and interactions for positive results;
    - coaching others;
    - influencing others

LINKING CAPACITY BUILDING TO ORGANIZATIONAL VISIONS, MISSIONS AND OBJECTIVES

According to Burners (1996), capacity building as a mechanism for change is unlikely to succeed on its own. This is because it concentrates on the individual and does not go up to the organizational level. Burke (1980) complements this by arguing that, although capacity building may lead to individual changes, there is scant evidence that attempting to change the individual will in turn change the organization. For capacity building to be effective it must, therefore, be linked to the corporate vision and mission.

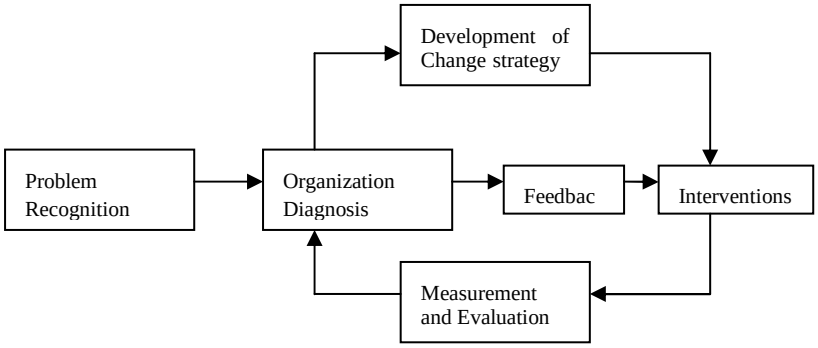

Figure 1*: Organizational Diagnosis*

CAPACITY DEVELOPMENT: A CASE FOR GDC

GDC has redefined its needs in terms of the skills required, skills that need to be developed and those that need to be nurtured in order to achieve our corporate mandate. Redefining organization structure so as to have lean and effective optimal staff establishment that can function effectively and position GDC as a global leader in capacity enrichment is the highlight of our training policy.

DEVELOPMENT OF A REGIONAL GEOTHERMAL TRAINING INSTITUTE IN KENYA

James Wambugu
Geothermal Development Company, P.O Box 100746 -00101, NAIROBI, KENYA
jwambugu@gdc.co.ke

ABSTRACT

Kenya and the East African region countries are endowed with vast, non-polluting geothermal energy resource occurring along the East African Rift System. In Kenya, the potential is estimated at over 7,000-10,000MWe. The development of this enormous resource has, however, been slow mainly due to lack of expertise in geothermal resource development, lack of proper equipment and lack of adequate funding. Taking into consideration the present and especially the future demand of developing this green indigenous source of energy, specialists in the fields of exploration, exploitation and utilization of geothermal energy will be required. The Geothermal Development Company Ltd (GDC) has taken a bold step in establishing of a Geothermal Training Institute (GTI) to offer courses in geothermal technology in Kenya in order to address this problem. GDC has few well trained professionals in all fields that will be used as resource persons. In addition, GDC will have fields, laboratories, workshops and equipments including drilling rigs to handle the training effectively. GDC in collaboration with United Nations University-Geothermal Training Program (UNU/GTP) and Kenya Electricity Generating Company Limited (KenGen) have successfully held short courses on Geothermal exploration in Kenya before and therefore it has the necessary experience. The courses that will be offered at the Geothermal Training Institute will include, short courses of 2-3 months mainly for practicing professionals leading to certificates, medium term courses of 3-6 months for advanced training leading to awards of diploma certificates and long term courses of 6 months to 2 years specifically tailored for research students pursuing geothermal related disciplines in Sciences and Engineering. GDC is already developing the curriculum in collaboration with UNU/GTP.

INTRODUCTION

The East African countries of Burundi, Comoros, Djibouti, Ethiopia, Eritrea, Kenya, Malawi, Rwanda, Tanzania, Uganda and Zambia all lie in the highly volcanic East African Rift. The East African Rift is a zone where the earth's interior heat escapes to the surface as manifested by volcanic eruptions and geothermal manifestations (hot springs, fumaroles, geysers). This indicates the presence of a remarkable geothermal potential in the region and therefore presents an opportunity for major geothermal power developments in these countries. A brief update of geothermal development in the countries within the region is outlined below.

Kenya

Kenya was the first country in Africa to tap geothermal energy for electric power generation.

Exploration for geothermal energy started in the early fifties when two wells were drilled at Olkaria. In 1970, the UNDP and the Kenya Power and Lighting Company (KPLC) carried out an extensive exploration program in the Kenya Rift. This survey identified Olkaria as the best candidate for exploratory drilling. Kenya's first 15 MWe unit of the 45 MWe electric power generating plant was commissioned in 1981. It has been operating since then and has proven reliable and economic, running at 98% availability (Ng'ang'a, 1998). The total installed geothermal capacity in the country currently stands at 209 MWe. High potential fields run along the Kenyan rift from North–South with an estimated potential of 7,000-10,000 MWe. The potential fields are shown in figure 1. A brief update of geothermal development in Kenya is outlined below.

Of the 16 potential prospects, only Olkaria field has been partially developed currently generating about 209 MWe. The main reasons for this is mainly due to; lack of adequate and well trained personnel (expertise) to carry out geothermal resource exploration and development, lack of equipment required for carrying out the work and also inadequate financial resources to carry out the work.

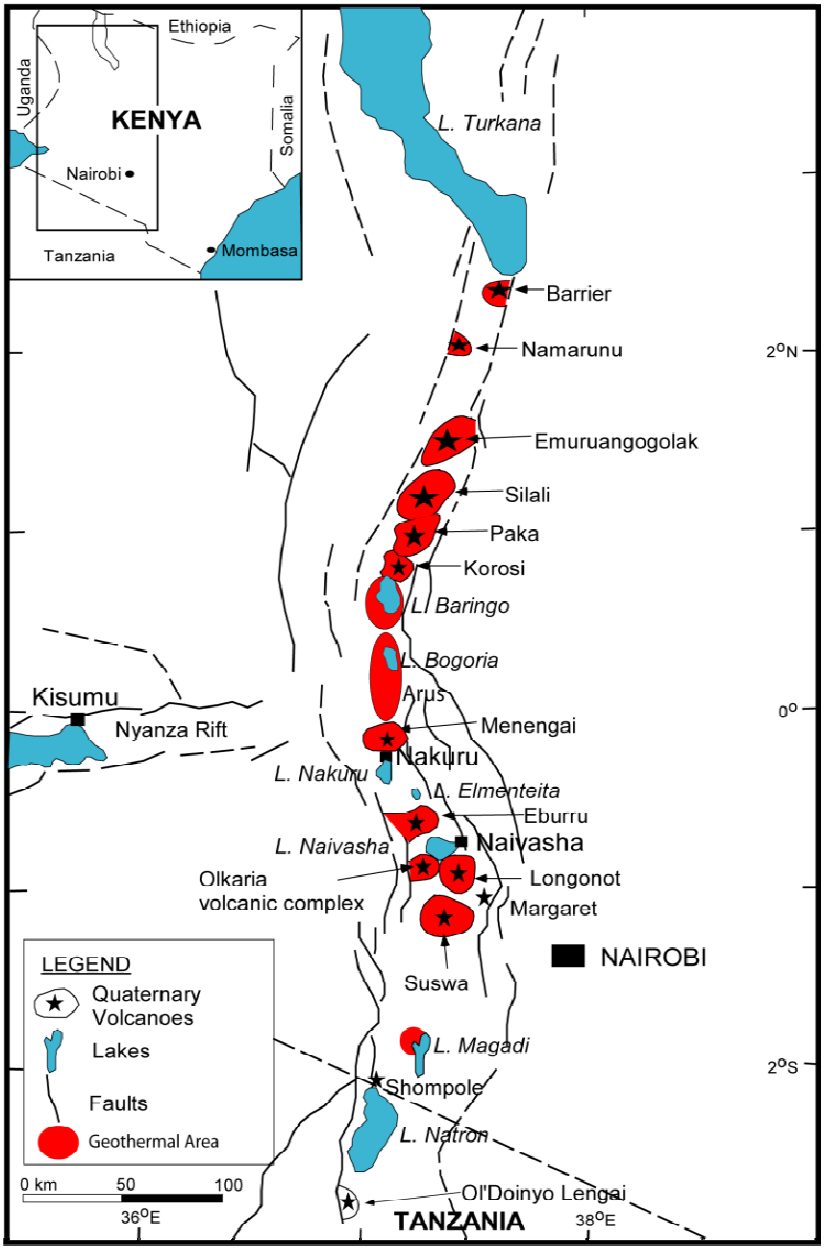

Figure 1: Geothermal prospects along the Kenyan rift**.**

Ethiopia

Ethiopia started a long-term geothermal exploration undertaking in 1969 and over the years a good inventory of the possible resource areas within the Ethiopian Rift has been built. Exploration work peaked during the early to mid-eighties when exploration drilling was carried out at Langano (Lakes District). A 7.2 MWe net capacity pilot plant was installed in the area in 1999 (Teklemariam, 2003). It operated for a short while before encountering operational difficulties that are essentially due to lack of appropriate field and plant management skills.

Zambia

In Zambia, reconnaissance survey has been carried out on geothermal areas since 1950's. A mini geothermal pilot power plant of 200 KW capacity was installed on the basis of limited exploration work. The plant, however, never became operational due to lack of trained manpower. Plans are in place to restore the plant and make it operational.

Djibouti

In Djibouti, much effort has been expended since the seventies, in view of developing the country's indigenous energy resource. About six exploratory wells have been drilled in the Assal geothermal field and intercepted a very high temperature system. However, due to the high salinity of the encountered fluids, the resource development has been delayed. The high salinity could be due to the close proximity of the Assal field to the Gulf of Aden.

Uganda

A reconnaissance survey has been carried out on geothermal areas of Uganda, starting in 1935 when the first documentation of hot springs was made. Recent geoscientific studies have focused on three geothermal systems, Buranga, Katwe and Kibiro, all located in the active volcanic belt in the western rift. No drilling has been done in Uganda.

Eritrea

The Eastern lowlands of Eritrea are of potential geothermal interest, and first priority was given to the Alid Volcanic center for exploration as it has numerous manifestations in the form of hot springs and fumaroles. Detailed geoscientific investigations are underway in this prospect area indicating geothermometry reservoir temperature of about 250ºC.

The rest of the countries have not made much progress in the exploration and development of this enormous, untapped resource estimated at over 7,000-10,000 MWe in the East African Rift. Currently more than 220 MWe has been installed in the region and out of these, the only operational power plants are in Kenya representing about 209 MWe (99%).

NEED FOR ESTABLISHMENT OF A GEOTHERMAL TRAINING INSTITUTE (GTI) IN THE EAST AFRICA REGION

The key issues for the exploration and development of this enormous green energy in the East African countries are financing and technological transfer. There are opportunities for utilizing this largely untapped source of energy in East Africa and therefore specialists in the fields of exploration, exploitation, and utilization will be required.

Currently there are less opportunities for geothermal training than there were in the 1980's and 1990's. The UNU-GTP is at present the only international graduate school offering specialized training in all the main fields of geothermal science and engineering. Two international schools were established in 1970 in Italy and in Japan and in 1978, two more were established in Iceland and in New Zealand. Unfortunately the Pisa school in Italy has not held its course since 1993 due to drastic cuts in government funding however, it has occasionally held short courses (1-3 weeks) in developing countries. The International Group Training Course at Kyushu, Japan was discontinued in 2001 while the Diploma course at the University of Auckland in New Zealand was also discontinued in 2003 due to withdrawal of government financing. Current geothermal professionals in Kenya and the region have been trained in these graduate schools. Nevertheless, still there are few trained professionals in geothermal related areas because such kind of training is only available abroad. This is expensive for these countries and it is difficult to train many people, hence the need to have local training.

Geothermal Development Company Limited (GDC) of Kenya is mandated to carry out exploration and development of geothermal resources and also to built capacity for geothermal development in terms of human resources and equipment on behalf of the Government of Kenya. GDC intends to widen its scope and mandate to the larger East African Region and African Continent as a whole. This can only be achieved through training of regional personnel and by equipping and operating laboratories and engineering workshops. To achieve this, GDC intends to establish a Geothermal Training Institute (GTI)

The creation of a GTI in Kenya will therefore be an important contribution to address the technical capacity and confidence barriers through shared experience and technical assistance in geothermal exploration, exploitation and utilization in the region. The 12-week course will give valuable orientation and practical hands on training in field operations and how to carry out specific tasks in laboratories. The African Rift Geothermal Facility (ARGeo) under establishment by UNEP has strongly recommended the creation of such an institution and has offered its support (Malin, 2001).

MISSION AND OBJECTIVES

The Mission of the Geothermal Training Institute will therefore be to pursue the establishment of an organized skill training and skill-improvement system for the specialists in the field, within the context of the growth of use of geothermal energy development in the African Region.

The main objective of the Geothermal Training Institute is capacity building in promoting geothermal energy resource development and utilization in the region. The primary aim is to assist African countries with significant geothermal potential to build up groups of specialists that cover most aspects of geothermal exploration and development.

SCOPE AND MANDATE OF THE TRAINING INSTITUTE

The scope and mandate for the proposed Geothermal Training Institute will be;

- To train all cadres of staff in all disciplines related to geothermal exploration, development and utilisation (Capacity building)
- To offer relevant courses (for staff involved in geothermal development)
- The Institute will be affiliated to the United Nations university
- The Institute will Initiate institutional collaborations with other re-known geothermal schools for exchange of programs and students.
- To establish and Manage a geothermal information system.
- To establish and manage a technical advisory Assistance program

LOCATION OF THE INSTITUTE

It is proposed that the Geothermal Training Centre be established in Nakuru, Rift Valley Province, Kenya because of the following factors:

- Close to known and well-studied geothermal systems, which will provide hands on training in all phases of geothermal development from geothermal exploration to operation of power plants.
- Easy availability of trained staff in most aspects of geothermal exploration and development to offer practical examples.
- Easy travel access by road and air for staff from all areas of the region both as trainees and trainers and for conferences
- Existence of infrastructure e.g. laboratories and equipment and experienced operators. This will assist the proposed center to take-off faster
- Due to the central locality in the Kenyan Rift Zone, easy accessibility to new geothermal prospects and to the already developed geothermal fields at Olkaria, opportunities are available for geothermal professionals in the region to work with experienced consultants on attachments. Consultancy work in areas of reservoir management, optimization studies and drilling operations will greatly assist in technology transfer

ADMNISTRATIVE SETUP OF THE TRAINING INSTITUTE

The administration set-up can be in a combination framework similar to the UNU-GTP in Iceland and the former Geothermal Training Institute in New Zealand, but adapted to local conditions. The following management structure is recommended for the GTI:

- The GTI: The Institute should be autonomous in its operations. However, it should work in close collaboration with organizations in the host country that are involved with geothermal development and the UNU-GTP.
- The Director: The director will be in charge of the day-to-day operations of the facility. It is recommended that the director (who will work with a designate director) be seconded from the UNU-GTP to set up the operations of the Institute. He/She is expected to hand over to the designate director with time.
- The Study Board: The director will be answerable to a study board that shall include representatives from stakeholders and member countries. The board will decide the timetable of operations for the Institute and program development to suit their individual country needs. On the board there will also be representatives from UNU-GTP and other universities at advisory level.
- Resource Personnel: These should not be permanent employees of the Institute and when required should be hired from member countries depending on their expertise and other geothermal experts from around the world.
- Maintenance and Operation personnel: A small maintenance and operation personnel should be hired by the board or seconded by stakeholders to the center.

The training complex will have the following facilities:

- Administrative block which will host GDC offices.
- A demonstration centre where uses of geothermal energy will be demonstrated with an aim of sensitizing people (potential users) on the benefits of using geothermal energy.
- Scientific Laboratories and engineering workshops where all the fabrications and analysis of samples will be done. The laboratories will be well equipped to cater for the needs and requirements for geothermal users. When fully operational the laboratories will be a part of income generating unit for GDC by serving customers from other institutions.
- Lecture rooms for training students and staff.
- Accommodation hostels for hosting students and staff during training.
- GDC staff canteen.

TRAINING AND CURRICULUM TO BE OFFERED

It is proposed that the Centre be set up to offer training in all basic aspects of most geothermal technology disciplines. The Centre will provide the required training needs for each member country and will have limited introductory theory and practical classes to those who do not have previous training in geothermal technology. This can be undertaken to certificate or diploma levels with time and in such a case, the Centre would need to be affiliated to a recognized educational institution of higher learning. Practical hands on training on various aspects of geothermal technology will be provided for staff already involved in geothermal work in their home countries but lacking equipment.

Course at the Geothermal Training Institute will be offered as follows;

- Short courses (2 weeks – 3 months)- mainly for practicing professionals leading to certificates
- Medium term (3-6 months) – advanced training leading to awards of diploma certificates
- Long term (6 months – 2 years) – tailored for research students and strictly on geothermal science and engineering
- Sponsorships – from development partners (AFD, JICA, USTDA, BGR, UNU/GTP etc)

SELECTION OF CANDIDATES

A consultancy firm will be engaged to assess the requirements of each ARGeo member country. In consultation with the ARGeo team members, the firm will make use of the results of the sub-regional assessments, available Country Strategy Papers (CSP's) of the countries in the region to identify training and capacity building needs.

However, the GTI students shall mainly come from African countries that have developed projects for the utilization of geothermal resources but are facing a shortage of trained manpower. The number of students who will register for the program will depend on the number of places designated by the Study Board. Candidates must have at least a diploma or its equivalent in science or engineering, one-year geothermal experience, working knowledge in English, and be permanently employed by a specific institution. The candidates will be interviewed with a view of selecting students with interest, knowledge, and development potential in the field.

Admission of students will come from the region with a larger proportion from Kenya. Students from outside the region may be considered on merit and the Category of students to be divided into two:

- ✓ Graduate professionals (with degree certificates)
- ✓ Technician professionals (with diploma certificates)

Both fresh and experienced graduates and students attached from local universities will be also admitted.

FUNDING

The initial estimated cost of financing of the Training Institute is U$ 5,000,000 and this will be raised from:

Fund raising from stake holders:

- ✓ GoK (providing/buying land)
- ✓ GDC funds (internally generated when fully operational)
- ✓ Donors (Development partners: AFD, JICA, UNU/GTP, BGR),
- ✓ Collaboration with other international geothermal organizations:
- ✓ International Geothermal Association (IGA)
- ✓ GDC is already the patron of the Geothermal Association, Kenya and can easily request assistance from IGA
- ✓ From UNU-GTP (mainly to run the programs)

Taking into consideration the economic resources of the countries in the region, the candidates who qualify to secure a place for admission will receive a fellowship. The fellowship will cover the tuition, living and travel expenses in Kenya and a return ticket to their respective countries. This will be co-financed by GDC, UNU-GTP, AFD, BGR, JICA and other multilateral donors, and bilateral agencies.

PLANS FOR ESTABLISHING THE TRAINING COMPLEX

GDC is in the process of securing land and other infrastructural facilities to put up the institute and once this is done, the procurement of required equipment will follow shortly.

The Curriculum for the institute is being developed by the United Nations University in collaboration with GDC and financial pledges have been given by development partners (AFD, JICA, USTDA, UNU) totaling to U$ 9,500,000

TIMELINES FOR PLANNED ACTIVITES

Activity	Start date	End date	Remarks
Procure land	May 2010	June 2010	On-going
Proposal	June 2010	June 2010	Presented
Procure Design Consultants	July 2010	Sept. 2010	Open tendering
Design (Architectural) and approval	October 2010	Dec. 2010	Open tendering
Construction including tendering	January 2011	June 2011	Open tendering
Equipping	June 2010	May 2011	Sourcing of equipment on-going
Commissioning	August 2011	August 2011	-

The proposed development will take place in phases.

REFERENCES

Fridleifsson I. B., 2005: Capacity building in geothermal energy technology for professionals in ARGeo countries. *ARGeo SC meeting Addis 2005.*

Malin P. E., 2001: Establishment of a Geothermal Resources Center to accelerate development in the East African region. *GEF/UN Draft Proposal.*

Ng'ang'a J. N., 1998: Status of geothermal development in Kenya. *United Nations University 20th Anniversary Workshop 1998.* 29-38

Teklemariam, M., 2003: *Overview of Geothermal Utilization and Potential in East Africa, East African Rift System.*

APPENDIX

TABLE 1: Curriculum and approximate time schedule of courses to be offered at the Geothermal Training Centre

Week No.	Geological Exploration and Borehole Geology	Geophysical Exploration	Borehole Geophysics and Reservoir Engineering	Environmental studies and Chemistry of Thermal fluids
1	Introductory lectures on all main aspects of geothermal energy exploration, exploitation and utilization including practicals and short field excursions			
2	Introduction to geological field mapping methods and borehole geology. Alteration mineralogy, XRD and Fluid Inclusions	Introduction to geophysical methods (Gravity, Resistivity, Magnetics and Seismics)	Introduction to Logging and Well Testing Practices. Reservoir Physics, Simulation Studies, Tracer Tests and Computer Programs	Introduction to EIA, Monitoring, Afforestation, Brine Disposal Geochemical Sampling & Analytical Methods, Geothermometers
3				
4				
5	Excursion to major geothermal fields in Kenya. Visits to direct (greenhouses, spas and plant drying facilities) and electric generation plants			
6	Data processing and project report writing.			
7				

THEME VIII

ECONOMICS FINANCING, PRIVATE SECTORS

NOTE ON THE PROGRAMME FOR INFRASTRUCTURE DEVELOPMENT IN AFRICA (PIDA)

Mr. Bernard BARANDEREKA,
Consultant- Energy Expert, AU CommissionEmail :
baranderekab@africa-union.org; berbarandereka@yahoo.fr

ABSTRACT

PIDA is an initiative of the African Union Commission, the African Development Bank and the New Partnership for Africa's Development (NEPAD) Planning and Coordinating Agency. It covers the 4 sectors, Energy, Transport, Information & Communication Technology and Water (Trans-boundary). PIDA will be implemented in two major steps: (i) study step and (ii) implementing steps of the results of the study.

The main objective of PIDA is to maximize efforts and use of resources and to enable African stakeholders to speak with one voice on the basis of a common agenda and common vision for infrastructure development.

The specific objectives of the PIDA study are to enable African decision-makers to:

- Establish a strategic framework for the development of regional and continental infrastructure based on a development vision, strategic objectives and sector policies;
- Establish an infrastructure development programme articulated around priorities and phases; and
- Prepare an implementation strategy and process including, in particular, a priority action plan.

Thus, a number of studies will be conducted with the aim of providing African decision-makers with analytical and decision-making tools for the formulation of policies, priority infrastructure development programmes and related implementation strategies and processes.

The outcomes of the PIDA study phase are:

- Continental Sector Policies;
- Regional and Continental Infrastructure Programs and Projects;
- Priority action plans;
- Funding measures and monitoring and evaluation processes.

The duration of the PIDA study is eighteen (18) months. The PIDA sector studies practically began on 20 May 2010 following the selection and signature of contract with a Consortium of Consulting Firms led by SOFRECO and mobilization of resource. The total budget of the PIDA Study is estimated at 7.781 million Euros.

The timeframe for implementation of PIDA under consideration is up to 2030, and is phased as follows: 2010-2015 for the short-term and priority action plan, 2016-2020 for the medium-term, and 2021-2030 for the long-term.

PIDA was launched officially on 24 July 2010 in Kampala, during a side event of the fifteenth (15th) Ordinary Session of the Assembly of the African Union.

The previous African Union Summits, particularly those of January 2009 on the development of Transport and Energy and January 2010 on the development of Information and Communication Technologies, supported the strengthening of infrastructure in Africa and notably endorsed PIDA as a program for integrating all regional and continental initiatives.

Referring to the presentation made by the PIDA Sponsors during the ceremony, African leaders reiterated their support to the initiative and called PIDA stakeholders including Regional Economic Communities, Member States, Specialized Institutions and Africa's Development Partners to support PIDA and participate in its implementation.

Energy sector

Although Africa is well endowed with hydropower and other energy resources, only a small fraction of its potential has been developed.

PIDA will deliver an energy strategy that will emphasise energy security through development of energy mix, cooperation and integration and joint use of trans-boundary water resources. Priority Action Plan will be based on regional approach that explores opportunities for regional integration through integrated regional power infrastructure network development.

The future of power trade depends on the health of the power sector in key exporting countries, endowed with exceptionally large and low-cost energy resources, such as hydropower and geothermal resources.

The technological mix and volume of investment required, policy and regulatory environment to be put in place, market liberalization and inter regional trade policies to achieve the vision will be outcome of PIDA. The rolling Priority Action Plan will be holistic with linkages to the other subsectors to lead to transformation of African Economies.

OVERVIEW OF STATUS, STRATEGY AND GAPS IN THE COUNTRIES OF THE EAST AFRICAN RIFT SYSTEM (EARS) FOR DEVELOPMENT OF THEIR GEOTHERMAL ENERGY RESOURCE

Meseret Teklemariam (Ph.D)

ABSTRACT

The **EARS** is an important zone of the world where the heat energy of the interior of the earth escapes to the surface in the form of volcanic eruptions, earthquakes and the upward transport of heat by hot springs and natural vapor emanations (fumaroles). Consequently, EARS possesses a remarkable geothermal energy potential. Using today's technologies, EARS has the potential to generate more than 15,000 MW of power from geothermal energy.

The main **challenges** for the development of this huge indigenous geothermal resources in the EARS are: (i) lack of appropriate policy and regulatory framework to attract private developers in the region; (ii) Lack of adequate skilled manpower and equipment for geothermal exploration and development; (iii) large upfront cost of geothermal resource exploration and development; (iv) Risks associated with Resource exploration and power development; and (vi) Risks associated with investment in power development projects.

At present, the EARS countries are individually at different stages of exploration and development. For example: (i) Burundi, Comoros, DRC and Zambia are at reconnaissance stage of exploration; (ii) Rwanda, Tanzania, Uganda and Eritrea are from semi detailed to detailed stages of exploration; (iii) Djibouti is at detailed investigation; (iv) Ethiopia is from detailed to Power development stage (Pilot Plant); and (v) Kenya is at most advanced stages of power development.

Consequently, the strategic objective of each country for the next 5 years varies according to its status of development. A brief over-view indicates that in the next 5 years, the EARS countries have the following groups of strategic targets: (i) Burundi, Comoros, DRC and Zambia to identify geothermal prospect areas; (ii) Tanzania to perform detail investigations; (iii) Rwanda, Uganda and Eritrea to perform detailed investigation and pilot power plant construction and development; (iii) Djibouti to develop about 50 MWe; (iv) Ethiopia to develop about 125 MWe and (v) Kenya to develop about 880 MWe.

Feedback and information collected from countries of the EARS revealed specific gaps (Except Kenya) to meet their strategic objectives. These include: (i) Inadequate skilled manpower; (ii) Inadequate field and laboratory equipment for carrying out geothermal exploration, development and Utilization of the resource; (iii) Inadequate technical and financial assistance as well as private sector participation to explore and develop about 1000 MWe power from geothermal energy resource in the region in the coming 5 years.

THE BUSINESS VALUE OF SERVER VIRTUALIZATION: THE GDC CASE

Charles Sitonik
Geothermal Development Company, P.O Box 100746 -00101, NAIROBI, KENYA
csitonik@gdc.co.ke

ABSTRACT

In today's competitive global economy, organizations need to be poised to respond faster to market changes, customer demands, and growth opportunities. In today's enterprise data centers, for example, it is not uncommon to find servers with utilization rates as low as 5 to 15 percent and storage with utilization rates of less than 50 percent. On the other hand, energy expenditures are going up due to high-density servers, storage power and cooling costs. While data center costs are increasing, the utilization of information technology (IT) assets, including servers and storage devices is very low. Today's x86 computer hardware was designed to run a single operating system and a single application, leaving most machines vastly underutilized. Since the advent of client-server technology, x86 server configuration has been the standard architecture and norm in most organizations. This technology meant that IT administrators spend so much time managing servers rather than innovating. Further, about 70% of a typical IT budget goes towards just maintaining the existing infrastructure, with little left for innovation and provision of quality services. The nature of GDC's business is complex - in terms of operations, locations and logistics. This scenario calls for robust solutions be put in place in order to meet user and business expectations. To do this, the need for an agile IT infrastructure cannot be over emphasized, one that is built to deliver better business outcomes. This paper, therefore, will discuss how GDC intends to overcome these challenges while improving the efficiency and availability of IT resources and applications. It will discuss how GDC will get more value and a higher return on investment by moving away from the old "one server, one application" model and embracing the modern solutions based on blade architectures. The paper will also discuss how, combined with the quickly maturing x86 hypervisor technologies, the synergy of blade architectures and virtualization offers the ability to dramatically increase utilization of server investments, boost uptime, provide a more resilient and available infrastructure, and roll out new infrastructure and services more quickly.

INTRODUCTION

In today's competitive global economy, organizations need to be poised to respond faster to market changes, customer demands, and growth opportunities. In today's enterprise data centers, for example, it is not uncommon to find servers with utilization rates as low as 5 to 15 percent and storage with utilization rates of less than 50 percent. On the other hand, energy expenditures are going up due to high-density servers, storage power and cooling costs. While data center costs are increasing, the utilization of information technology (IT) assets, including servers and storage devices is very low.

Today's x86 computer hardware was designed to run a single operating system and a single application, leaving most machines vastly underutilized. Since the advent of client-server technology, x86 server configuration has been the standard architecture and norm in most organizations. This technology meant that IT administrators spend so much time managing servers rather than innovating. Further, about 70% of a typical IT budget goes towards just maintaining the existing infrastructure, with little left for innovation and provision of quality services.

The nature of GDC's business is complex - in terms of operations, locations and logistics. This scenario calls for robust solutions be put in place in order to meet user and business expectations. To do this, the need for an agile IT infrastructure cannot be over emphasized, one that is built to deliver better business outcomes.This paper,therefore, will discuss how GDC intends to overcome these challenges while improve the efficiency and availability of IT resources and applications. It will discuss how GDC will get more value and a higher return on investmentbymoving away from theold "one server, one application" model and embracing the modern solutions based on blade architectures. The paper will also discuss how, combined with the quickly maturing x86 hypervisor technologies, the synergy of blade architectures and virtualization offers the ability to dramatically increase utilization of serverinvestments, boost uptime, provide a more resilient and available infrastructure, androll out new infrastructure and services more quickly.

The latest IT and e-Business trends have brought in essential changes that allow businessesoperate in real-time information environment. It is no surprise that information relevancy, timelessand accuracy are specific issues which need specific emphases in order to understand andhaving proper insights in any business dynamics, in decision support, problem solving, reducinguncertainties and taking risks.

In his white paper entitled ***"Understanding the Business Value of x86 Virtualization and the Benefits of Virtualization - Optimized Hardware"***, Gary, Chen et al argues that Virtualization delivers compelling business

value today, increasing by a factor of threethe number of users supported per server, improving availability of servers, enablingapplication scalability, and reducing costs across the board.

CURRENT SCENARIO

In the one year that GDC been in operations, a lot of investment has gone into developing a robust ICT infrastructure. The QA & ICT Department has developed policies and a roadmap in an effort to drive all processes and provide quality services which are aligned to the overall corporate strategy.

Five servers are currently in operation within the organization as described in the table below. All servers are of varying capabilities and features. Two Linux-based servers are running specialized Geochemical and Geophysical systems respectively.

Table 1

Server Make	**Location**	**Role**
Dell PowerEdge	Nakuru Office	GIS
Dell PowerEdge	Taj Towers	MS Exchange
HP Workstation	Nakuru Office	Geochemistry data processing and interpretation
HP Workstation	Nakuru Office	Geophysics data processing and interpretation
HP Pro	Riverside	MS TMG (Firewall, content management)
HP Pro	Taj Towers	MS TMG(Firewall, content management)
Hp Pro	Taj Towers	Phone Call Billing
HP Pro	Taj Towers	Domain Controller

In addition, six IBM BladeCenterservers are currently being assembled, installed and configured for the ERP System implementation. SAP business applications paired with BladeCenter servers allow businesses of all sizes to benefit from relevant, timely information with simple management, excellent performance and rock-solid reliability. With SAP Business Suite and SAP Business All-in-One on IBM BladeCenter servers, GDC will have the scalability to meet the dynamic needs of your business while reducing carbon footprint - without sacrificing application performance.

Four of these servers will be located at the primary site at GDC Riverside office while two will be at the Nakuru secondary site.

THE NETWORK

The current GDC topology is as shown in the figure below. Due to the rapid expansion and new systems being introduced, plans are currently in place to replace the link with high performing fibre connection at Riverside, Taj and Nakuru offices. This is especially to cater for the real time replication between the ERP servers at Riverside and Nakuru.

Understanding Virtualization:

Virtualization is a technique for hiding the physical characteristics of computing resources to simplify the way in which other systems, applications, or end users interact with those resources. Virtualization lets a single physical resource (such as a server, an operating system, an application, or storage device) appear as multiple logical resources; or making multiple physical resources (such as storage devices or servers) appear as a single logical resource. An application such as VMWare or Microsoft Virtual PC can let Windows run Linux or other applications and vice versa on a virtual PC.

Figure 1: Network Topology

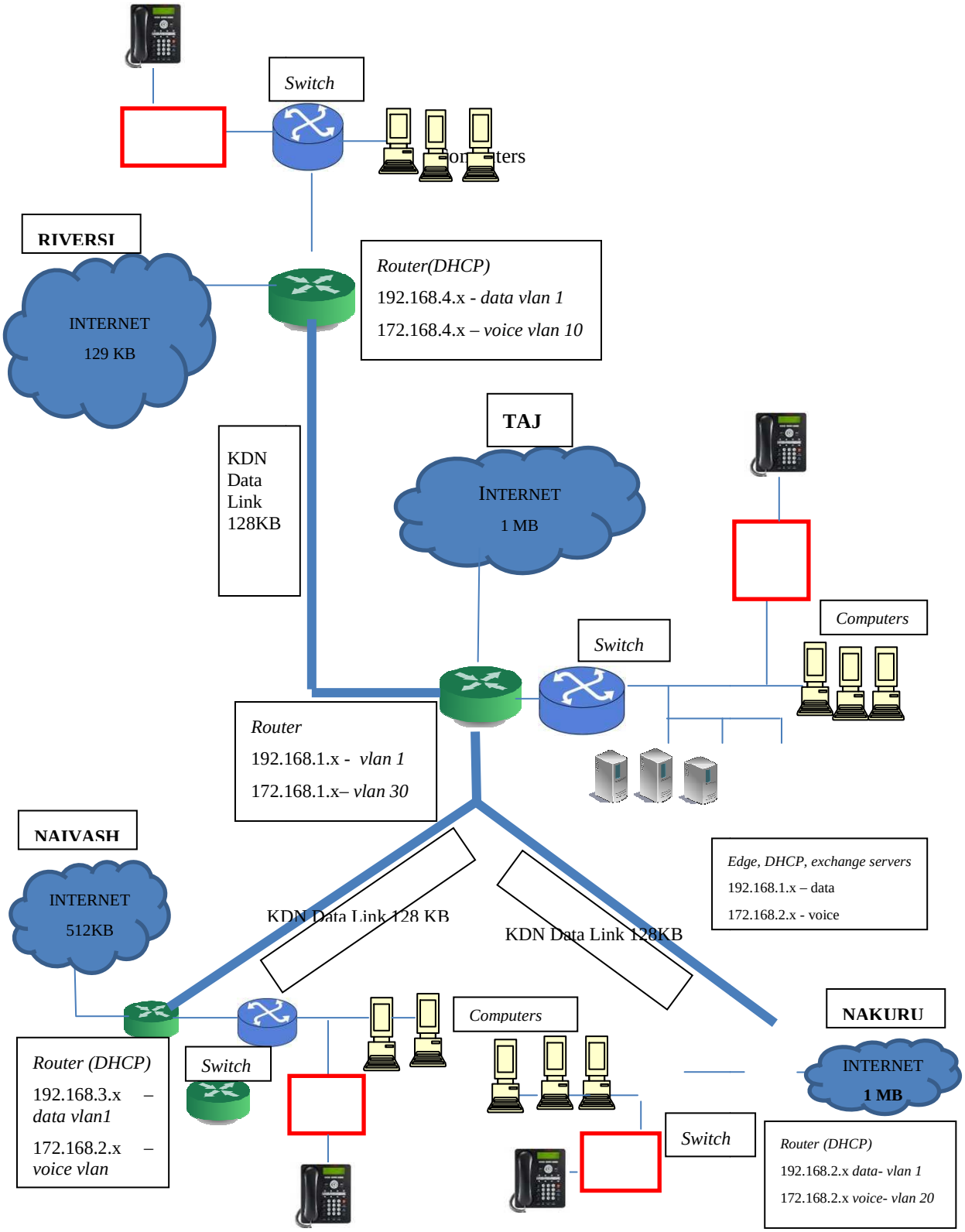

Server virtualization, the most common, is the masking of server resources, including the number and identity of individual physical servers, processors, and operating systems, from server users. The server administrator uses a software application to divide one physical server into multiple isolated virtual environments. The virtual environments are sometimes called virtual private servers, but they are also known as guests, instances, containers or emulations.

Virtual machines are based on the host/guest paradigm. Each guest runs on a virtual imitation of the hardware layer. This approach allows the guest operating system to run without modifications. It also allows the administrator to create guests that use different operating systems. The guest has no knowledge of the host's operating system because it is not aware that it's not running on real hardware. It does, however, require real computing resources from the host - so it uses a hypervisor to coordinate instructions to the CPU. The hypervisor is called a virtual machine monitor (VMM). It validates all the guest-issued CPU instructions and manages any executed code that requires addition privileges. VMware and Microsoft Virtual Server both use the virtual machine model.

The paravirtual machine (PVM) model is also based on the host/guest paradigm -- and it uses a virtual machine monitor too. In the paravirtual machine model, however, the VMM actually modifies the guest operating system's code. This modification is called porting. Porting supports the VMM so it can utilize privileged systems calls sparingly. Like virtual machines, paravirtual machines are capable of running multiple operating systems. Xen and UML both use the paravirtual machine model.

Virtualization at the OS level works a little differently. It isn't based on the host/guest paradigm. In the OS level model, the host runs a single OS kernel as its core and exports operating system functionality to each of the guests. Guests must use the same operating system as the host, although different distributions of the same system are allowed. This distributed architecture eliminates system calls between layers, which reduces CPU usage overhead. It also requires that each partition remain strictly isolated from its neighbors so that a failure or security breach in one partition isn't able to affect any of the other partitions. In this model, common binaries and libraries on the same physical machine can be shared, allowing an OS level virtual server to host thousands of guests at the same time. Virtuozzo and Solaris Zones both use OS-level virtualization.

Server virtualization can be viewed as part of an overall virtualization trend in enterprise IT that includes storage virtualization, network virtualization, and workload management. This trend is one component in the development of autonomic computing, in which the server environment will be able to manage itself based on perceived activity. Server virtualization can be used to eliminate server sprawl, to make more efficient use of server resources, to improve server availability, to assist in disasterrecovery, testing and development, and to centralize server administration.

The potential for virtual server consolidation is extremely attractive to companies that specialize in providing and managing their client's network resources.

Any organization might face the challenges brought on by dozens - or even hundreds - of servers, but these companies can easily fill a data center with systems dedicated to their various clients.

THE BUSINESS VALUE OF VIRTUALIZATION

This paper presents a detailed analysis of the value proposition associated with moving from an unvirtualized environment to a basic virtualization scenario or an advanced virtualization deployment.The figures used in this analysis were the results of a study done by an American research firm, International Data Corporation (IDC) and published in a white paper Gary, Chen et al ***"Understanding the Business Value of x86 Virtualization and the Benefits of Virtualization - Optimized Hardware"***. The discussion demonstrates the benefits GDC will earn by implementing virtualization.

Users per Server, ICT Manager

Figure 1 shows the direct impact of increasing the number of workloads on servers that are using virtualization software. Merely moving from an unvirtualized infrastructure to a basic virtualization infrastructure boosts the number of users per server from 140 to 882. Likewise, because of the reduced hardware management requirements, the number of users per ICT infrastructure manager increases from approximately 2,300 to over 3,500.

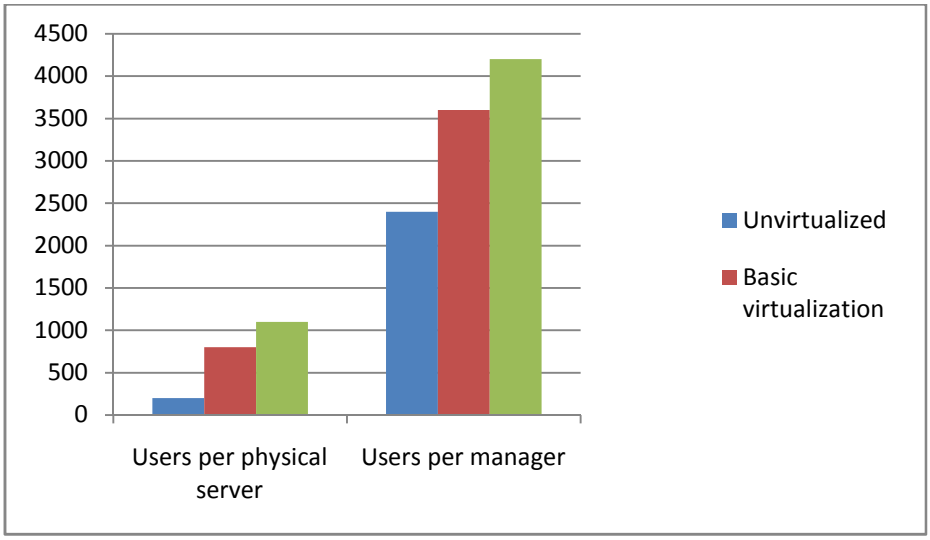

FIGURE 1

* The IT infrastructure manager is responsible for regression test, configuration and releasemanagement, incident/problem resolution, security, storage, capacity, and availabilitymanagement.

Source: IDC's Business Value of Virtualization Research, 2009

Servers per Manager, Downtime, Time to Launch, Time to Upgrade/Migrate

Figure 2 below provides several additional metrics that illustrate the impact of moving to avirtualized infrastructure. The number of physical servers per manager increases from17 in an unmanaged, unvirtualized environment to over 25 in a basic virtualizationenvironment and almost 30 in an advanced virtualization infrastructure.

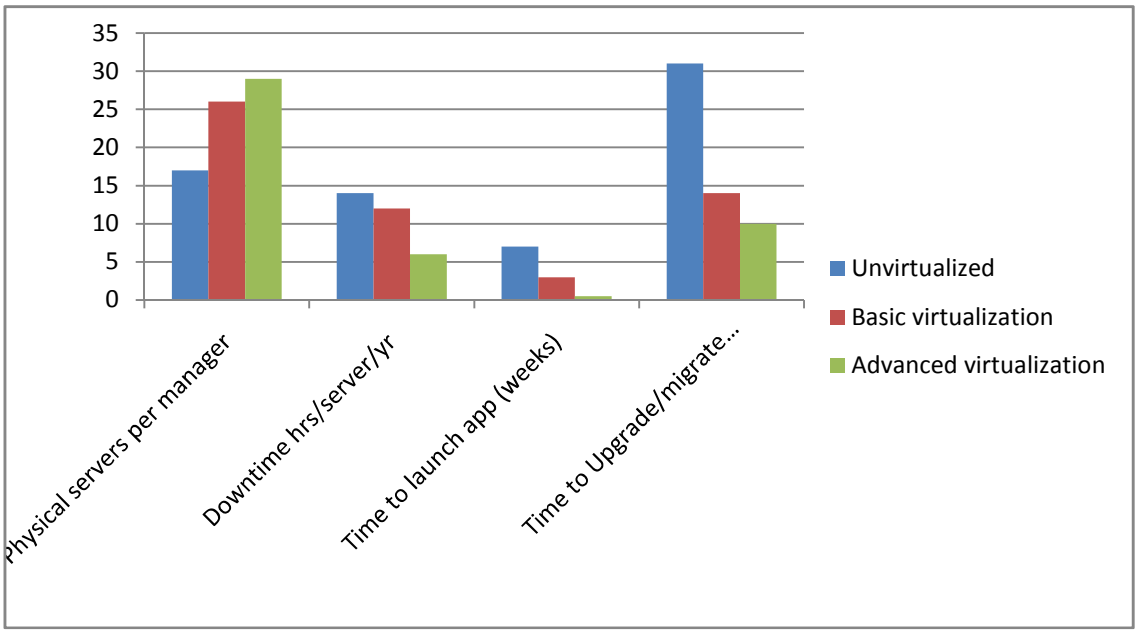

FIGURE 2

* The IT infrastructure manager is responsible for regression test, configuration and release management, incident/problem resolution, security, storage, capacity, and availability management.

Source: IDC's Business Value of Virtualization Research, 2009

Figure 2 includes the first business value elements that go beyond hard TCO data - the reduction of downtime hours on an annual basis and the significant reduction in time to launch applications. While there are multiple contributors to this downward shift, a few items stand out:

- More standardized configurations of servers. Because a virtualized environment requires a level of standardization of the underlying operating system, it becomes easier to drive uptime through consistent configuration and patching of server operating system. No longer does each operating system require one or more unique drivers that are specific to a particular hardware configuration; instead, all operating systems map to the same portfolio of drivers provided by the virtualization software. This also helps ease the deployment of new applications because the underlying operating system is far more likely to be in a known and well-understood configuration. In addition, the ability to clone and replicate VMs from approved templates ensures exact configurations.
- Ability to migrate workloads easily. In the case of downtime reduction, operating systems can be moved from one server to another to facilitate repairs or maintenance, avoiding the lengthy downtime normally associated with that service. In the past, operating systems were tightly married to the underlying hardware, making it impossible to move the workload to an alternate server on a short-term basis. Even without live migration, it is possible to suspend an operating system and its workload, relocate it to another physical server, and bring it back up in only minutes. With live migration and advanced software, migrations can be made with no user-perceptible downtime.
- Ability to snapshot and replicate operating systems for test and configuration purposes. When IT deploys new applications, it now becomes possible, with little more than some mouse clicks, to replicate environments that can be used for testing and experimentation. "Trialing" a new application in a server operating system becomes easy and virtually risk free. This improves the speed and quality of software testing, allowing production deployments to launch faster.

Annual Costs per User

Except for software licensing schemas that enable unlimited instances per processor - for example, Windows Server 2008 Data Center allows unlimited OS instances perprocessor in a server - software costs generally remain consistent, or are evenslightly higher, after the move to a fully managed infrastructure. Hardware and staffing costs falldramatically in a move to a basic virtualizationscenario, and even further in advanced virtualization. In parallel, lost user productivity, the cost of downtime, drops mostsignificantly during a move from basic virtualization to advanced virtualization deployment.

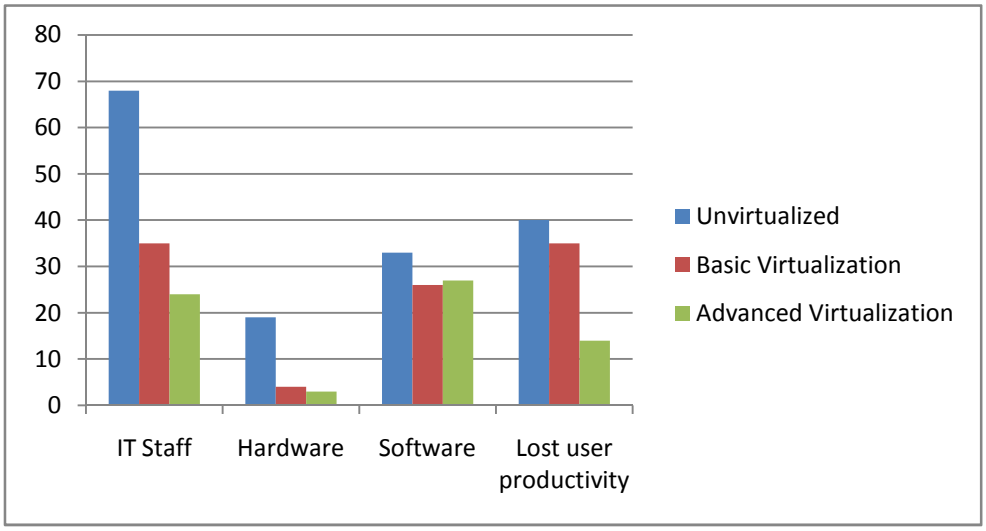

FIGURE 3

* IT staff costs include full life-cycle support and deployment for hardware, storage, operating system, and applications.

Source: IDC's Business Value of Virtualization Research, 2009

This indicate that the use of increasingly standardized operating systemimages deployed on hypervisors (with increasingly common sets of drivers anddevices) leads to more stable environments, a key contributor to the reduction incosts associated with supporting servers and the basic operating systemconfigurations run on those servers.

Cost Reduction

ICT labour cost savings can exceed 50% merely by a move to basic virtualization and over 70% in an advanced scenario.While hardware cost reductions are roughly equal across different levels ofvirtualization. An advanced virtualization scenario delivers reductions incosts due to downtime that are over 30 percentage points greater than those of abasic virtualization deployment. This cost savings alone, along with the less tangiblebusiness value that comes from greater systems availability, would likely justify muchof the investment costs associated with deploying an advanced virtualization environment.

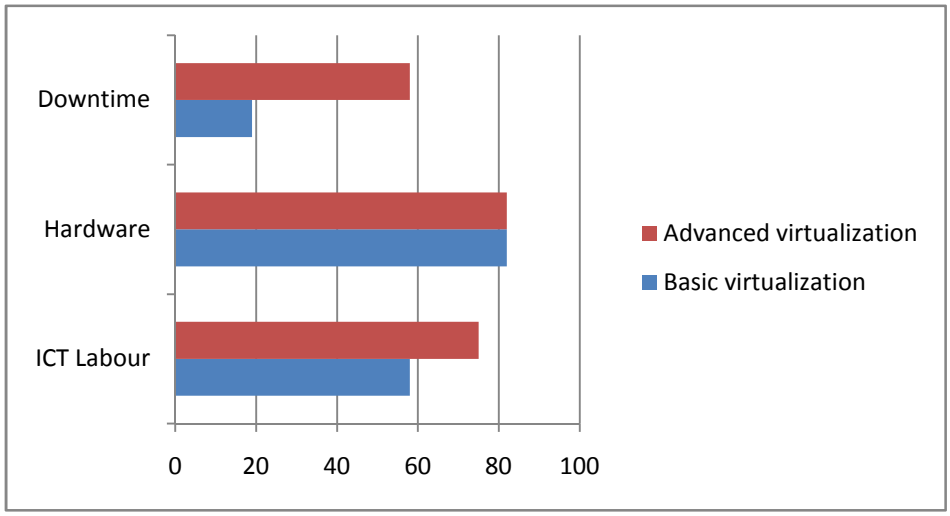

FIGURE 4

Source: IDC's Business Value of Virtualization Research, 2009

Agility Enhancement

There arebusiness benefits that come from using a management solution inan advanced virtualization environment. While initial deployment and/or redeploymentcosts are marginally reduced for an advanced virtualization deployment, it is possibleto achieve 36 points of incremental benefit from using management tools in anadvanced virtualization deployment, when used for the deployment of new software.Of course, even for a basic virtualization deployment, the cost savings versus thoseof an unvirtualized environment are dramatic.

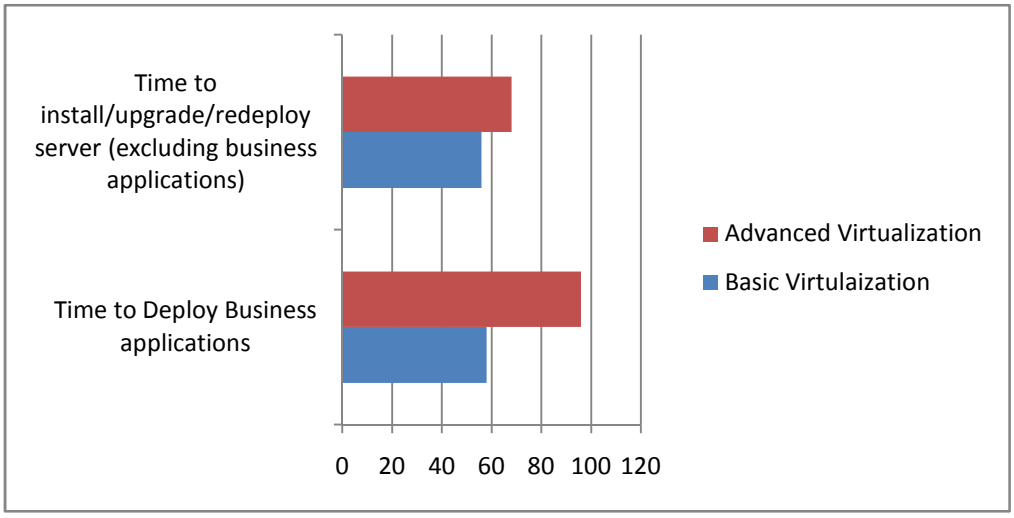

FIGURE 5

Source: IDC's Business Value of Virtualization Research, 2009

Annual TCO

Figure 6 presents an overall view of the annual TCO, comparing the three deployments. Customers moving from an unvirtualized environment to a basic virtualizationenvironment can lower their total annual costs by 39% per user per year. Organizations that move to advanced virtualization will realizea 59% cost savings per year per user compared with an unvirtualized environment.

These cost savings are dramatic and illustrate the reason why virtualization adoptionis pervasively sweeping the industry.

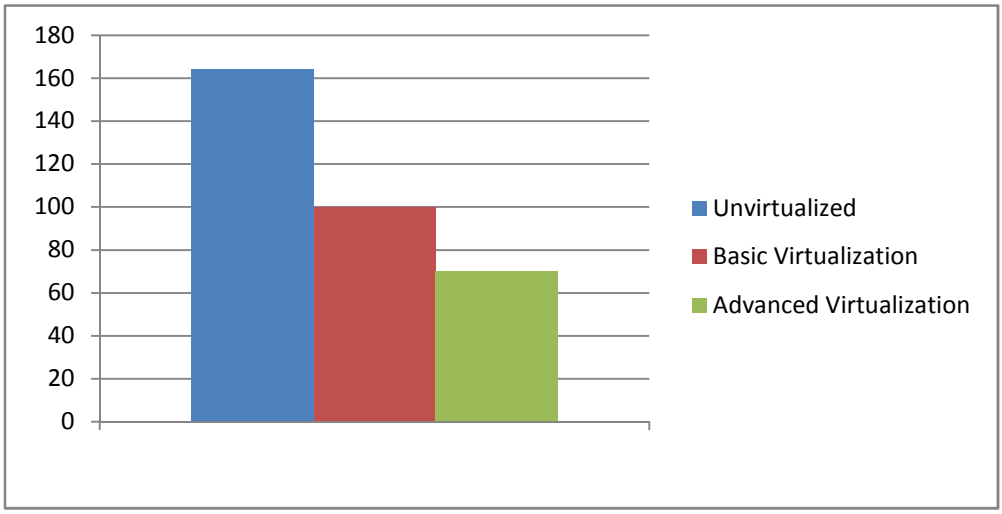

FIGURE 6

Source: IDC's Business Value of Virtualization Research, 2009

Return on Investment Calculations

By deploying basic virtualization GDC will realize costs savings of $163per user over three years with a total investment of $28 per user. An average company deploying basicvirtualization could see an ROI of 486% and payback in less than half a year - threeto four months - including deployment time. This is a very significant ROI for arelatively low-cost, low-risk initiative.

In the advanced virtualization scenario, average benefits increase by over 25%(primarily through enhanced ICT operations and user productivity cost reductions),while costs per user decline due to lower hardware costs.

CHALLENGES/OPPORTUNITIES

Any new technology faces challenges, and these challenges are usuallycounterbalanced against interesting new opportunities that the new technology canaddress. Virtualization software and the associated systems management tools thatenable an advanced virtualization deployment certainly face these factors.

Challenges

Moving from distributed to consolidated infrastructure - The data presentedin this paper clearly illustrates the business justification for moving toa virtualized infrastructure. With any new technology, the return always comesafter the investment. Therefore, an investment and executive backing are neededto spend money to save more money later.

Aligning and/or minimizing management tools in use - Most organizationshave multiple management tools in their infrastructure, along with proponents ordepartments that will resist consolidation aboard a smaller number of tools.

Consolidating version inconsistencies - Moving to an advanced virtualizationinfrastructure mandates having relatively high degrees of consistency in thevirtual servers that run on the infrastructure. This goal, as attractive as it sounds,is inconsistent with the deployments at a typical company. Therefore, thephysical-to-virtual migration/consolidation activities are not as simple,straightforward, and easily accomplished as the advertisements often suggest.

Up-front investment avoidance- While consolidating ona virtualized platform will certainly provide a positive ROI over time, many ICTdepartments may have difficulty securing the capital required to invest in the newsystems. Some ICT managers may find it easier to simply purchase a few moreservers to support what applications they need to in order to get them throughthe economic downturn rather than purchase, potentially expensive, systemsonto which to consolidate their infrastructure. Hardware costs alone can beenough to deter investment. However, additional software licensing costs for theleading virtualization applications can add up-front expense. Larger environmentswill also often incur additional up-front cost for more sophisticated managementtools to manage both physical and virtual environments.

Reeducating ICT on best practices - As with any new technology, there is arequired learning curve to understand best practices. For example, customersthat were once used to operating a diverse infrastructure with many different OSimages will need to adapt to working with a small number of standard images.Many of the previous issues found by having these diverse deployments, such asBIOS or DLL issues will no longer be as apparent. Instead, ICT will need todevelop skills around configuration of virtual machines and management of avirtual environment. Challenges lie in learning new license/usage compliancerules as well as transitioning skill sets from OS management to systems,configuration, and virtualization management.

I/O latency and throughput - One of the biggest limitations for virtualizing certain workloads such as databases was I/O performance, a traditionally weak area of hypervisor performance. Software hypervisor optimizations have been made over several versions but now increasingly are accelerated by hardware. System chipsets, NICs, and HBAs are being designed with new I/O features that work well with VMs, relieving resource contention, providing QoS, reducing latency, and increasing overall throughput to allow even I/O-intensive applications to be virtualized.

More fault tolerant systems - Consolidating servers has the effect of making each server more mission critical than if it hosted only one OS and application. A server failure now means that multiple systems are affected.

Opportunities

User density increases dramatically - The average user density grows by a factor of six on a per-server basis, while the number of users per server manager almost doubles.

Availability increases (Disaster Recovery) - A side effect of virtualization is that system availability goes up even for the most basic configurations of a virtualized infrastructure. The real benefit comes from an advanced virtualization scenario in which downtime drops by 50%.

Service-level noncompliance decreases - Once virtualized, an application that needs more scalability can be moved to a server that can fulfill that requirement with little more than a few clicks of the mouse.

Cost decreases - Cost reductions occur across the board and especially in hardware (80%), but with future deployments, customers can move to server operating systems that offer unlimited virtualization rights, extending their savings dramatically in many cases.

Focus on reducing hypervisor overhead - Advances in CPU and their corresponding chipsets now accelerate and offload many hypervisor functions, reducing overhead significantly. Over time, the overhead for virtualization is expected to drop to near zero.

Increased robustness - New CPU architectures are packing more cores per socket and allow for very large system memory capacities, the two main factors that determine how many VMs a given server can host.

Agility benefits - While agility benefits come first and foremost from having asolid management system in place, layering that solid management tool set ontop of a virtual infrastructure multiplies those benefits.

Green IT benefits - Moving to a virtualized infrastructure that reduces the numberof physical servers has a direct impact on power and cooling requirements andassociated carbon emissions. Even better, moving to a virtualized x86infrastructure may delay or eliminate the need for datacenter expansion. Forsome organizations, it may actually lead to datacenter consolidation.

Future-proofing (cloud computing readiness) - Virtual machines allow ITadministrators to get used to maintaining a logical environment as opposed toindividual 1:1 configurations. This will help to ease their transition to a cloudcomputing model that is based heavily in virtual assets, a trend that IDC expectsto greatly proliferate in the near future. In addition, virtualization of theinfrastructure is a key step to evolving to an internal cloud architecture, which will drive higher efficiency with the datacenter and enable interfacing with externalclouds.

IT consolidation - With virtualization, many physical servers and storage units can be consolidated into one virtual server or storage pool. This can result in a 10:1 or greater ratio of virtual servers on a single physical server. This helps stop physical server and storage sprawl and solve the problem of devices that are under-utilized, consume too much space, and cost too much to power, cool, and maintain.

Development and testing - Virtualization can also improve the efficiency of test and development environment. With virtualization, multiple operating systems and versions can be run on fewer servers and workstations. This helps support complex development and testing environments with limited resources.

CONCLUSION

Virtualization delivers compelling business value today, increasing by a factor of fivethe number of users supported per server, improving availability of servers, enablingapplication scalability, and reducing costs across the board.

The business case is clear and the options abound. In particular, the introduction ofmodern virtualization solutions based on advanced system architectures - which canoffer both intelligent configuration and management and the ability to sense, predict,and enable the replacement of failing hardware components before they causesystem shutdown - can help promote uptime and efficient resource usage,particularly when used in direct combination with the high-quality hypervisorsavailable on the market today.

These same technologies can lower costs directly through an immediate reduction ofpower and cooling costs and subsequently deliver a long-term benefit through lowerICT administrative costs that continue to benefit GDC year after year. These benefits accrue for integratedvirtual and physical management solutions available in the newly acquired IBM'sSystem BladeCenter virtualization portfolio.

GDC will gain better utilization of serverresources and reductions in acquisition, deployment, and power and cooling costs.Further, the long-term benefits of reducing staff costs and increasing business agilityleads to other long-term benefits that will continue for years to deliver returns on the investment required to put this solution in place.

THEME IX

ENVIRONNEMENT, SOCIAL, LEGAL AND ECONOMICAL ASPECTS

THERMAL INFLUENCE OF SURFACE DISPOSAL OF HOT GEOTHERMAL WASTEWATER ON AQUATIC ECOSYSTEMS: WITH EXAMPLES FROM ICELAND

Gabriel N. Wetang'ula[1, 2, 3] and Sigurdur S. Snorrason[1]
[1]*Faculty of Life and Environmental Science, University of Iceland*
[2]*United Nations University-Geothermal Training Programme*
[3]*Geothermal Development Company, P. O Box 17700, Nakuru, Kenya*
Emails: gwetangula@gdc.co.ke, ganw@unugtp.is,

ABSTRACT

Disposal of hot wastewater from a standard steam cycle power plant directly into an existing natural waterway inevitably leads to an increase in temperature. This changes various physical–chemical properties of water, such as density, viscosity, surface tension and solubility of gases. The influence of heating on aquatic ecosystems is ambiguous, and at different levels of heating it may be both positive and negative. The most important ecological factor is then to limit excessive heat dumping which will exceed the buffer capacity of the aquatic ecosystem. Of the many environmental factors influencing an ecosystem probably none exerts a more profound influence than temperature. Nesjavellir geothermal co-generation power plant in SW-Iceland utilizes high temperature geothermal fluid for production of electricity and hot water for district heating. The plant wastewater is either pumped into shallow drill holes or disposed off in a stream, which finds its way into a freshwater Lake. Result of water temperature measurements done to determine the extent of thermal influence show that large volume of geothermal effluent (40.9°C - 84.0°C) disposed of has caused a rise in both summer and winter temperature at lake shoreline outflow sites. Summer temperature was in the range of 11.7°C - 27.3°C with definite outflow sites temperature being in the range 23.4-27.3°C. During winter temperature at Varmagja varied from 0.6°C on the ice edge to 26°C at the mouth. To minimize local effects deep reinjection of geothermal wastewater and further cooling of the condensed steam was recommended.

INTRODUCTION

Aquatic ecosystems are composed of the biological community (producers, consumers and decomposers), the physical and chemical (abiotic) components and their interactions. Within aquatic ecosystems, a complex interaction of physical and biochemical cycles exist, and changes do not occur in isolation. Aquatic ecosystems thus undergo constant change. However ecosystems have developed over a long period of time and organisms become adapted to their environment. In addition, ecosystems have an inherent capacity to

withstand and assimilate stress based on their unique physical, chemical, and biological properties. Nonetheless, systems may become unbalanced by natural factors, which include drastic changes in climatic variations or by factors due to human activities. Any changes especially rapid ones, could have detrimental effects (CCME, 2001).

Adverse effects due to human activities, such as release of toxic chemicals in industrial effluents, may affect many components of aquatic ecosystem, the magnitude of which will depend on both biotic and abiotic site-specific characteristics. In evaluation aquatic ecosystems are always viewed as whole units, not in terms of isolated organisms affected by one or few pollutants (CCME, 2001). As effluents are released into the environment through natural processes or human activities, they may enter aquatic ecosystems and partition into particulate phase. These particles may remain in the water.

Heated wastewater discharge effects on aquatic communities

Thermal pollution has been directly associated with the development of the heat and nuclear power engineering, whose operating objects discharge large volumes of warmed water into water reservoir (Beznosov and Suzdaleva, 2001).

If hot wastewater from a standard steam cycle power plant is released directly into an existing natural waterway it inevitably leads to an increase in temperature. This changes various physical–chemical properties of water, such as density, viscosity, surface tension and solubility of gases. The influence of heating on aquatic ecosystems is ambiguous, and at different levels of heating it may be both positive and negative. The most important ecological factor is then to limit excessive heat dumping which will exceed the buffer capacity of the aquatic ecosystem. Of the many environmental factors influencing an ecosystem probably none exerts a more profound influence than temperature.

Due to its pivotal role in biological activity (development, growth and reproduction) temperature has long been recognized as an important environmental factor in both terrestrial and aquatic ecosystems. Seasonal temperature differences, characteristic of higher latitudes, strongly influence the biological activity of aquatic

organisms and establish cyclical patterns that often mediate the scope of each activity. Over the long-term, changes to the thermal regime of the surrounding environment can effect the evolutionary, physiological and behavioural responses of individual organisms (Begon et al., 1990).

Temperature directly influences the metabolic rates, physiology, and life-history traits of aquatic species and helps to determine the rates of important community processes such as nutrient recycling and productivity (Allen, 1995). Thermal loads can cause negative processes in local areas of aquatic environment, such as over growth of blue-green algae deteriorating the water quality, change in the composition of plankton and dynamics of its numbers, disruption of fish and other aquatic communities. Fluctuation in water temperature induces behavioural and physiological responses in aquatic organisms. Permanent shifts in temperature regimes can render formerly suitable habitat unusable by native species.

Because of ecological importance of lake temperature, preventing or mitigating anthropogenic thermal degradation is a common concern for resource managers (Poole and Berman, 2001). In serious cases a permanent increase in water temperature levels can result in a complete change of the community whereby high temperature tolerant species take over. In milder cases water temperatures variations among sites may create differences in the physiological and behavioural advantages among aquatic organisms hence influencing their competitive ability and distribution as indicated by the study of Taniguchi et al. (1998) showing that changes in competitive ability (measured as food consumption and aggression) could be temperature mediated.

Many studies have shown the effects of thermal discharges on aquatic communities. Squires et al. (1979) study of water temperature increases caused by thermal discharges in the Provo River in Utah, USA found a unique algal community which was attributed to this thermal discharge. Flora displayed an overall similarity in specific composition but with zonation related to local environmental conditions.

Esterly (1975) study of thermal effluent effects on the benthos of Thomas Hill Reservoir, Missouri, USA found maximum surface water temperature was 37 ºC while bottom muds varied between 8-29 ºC. Numerical abundance and biomass of benthos were greater in the control Arm than in the hot water Arm but heated water had no apparent deleterious effects on the benthos.

Hickman and Klarer (1975) showed that thermal discharges caused an increase in the standing crop size of the epiphyton associated with sedges, *Scripus validus* and the mean primary productivity also increased. Thermal discharges were also found to cause changes in species composition and dominance in algal communities.

Klarer and Hickman (1975) monitored water temperature, dissolved oxygen and water chemistry in a lake receiving heated water and found no large variations in these parameters except for water temperature and dissolved oxygen levels among the stations.

Phytoplankton species have also an optimum temperature where growth rate is maximal. The growth rate of phytoplankton generally increases with temperature only within a certain temperature range, and the temperature dependency of the growth rate differs among species. Species found growing at a higher temperature usually have a higher optimum temperature (Suzuki and Takahashi, 1995).

A study at Madras Atomic Power Station, India showed that thermal discharge affects benthic communities in three ways; reduction in composition of the assemblages; increased abundance of the so-called opportunistic or ephemeral species and alteration of population dynamics of the most abundant species. Death of almost all the macrofauna and flora species was observed during the hot season in an area impacted by the heated effluents. Much of the area that showed consistent thermal effects on benthic community structures (Suresh et al., 1993).

The response of freshwater algae to temperature change have also been summarized by DeNicola (1996) and include a variety of effects that have been studied at the cellular, population and community level. Individual responses are highly dependent upon the variability in the physicochemical environment and spatio-temporal pattern in species distribution. Physiological responses to temperature include changes in concentrations of photosynthetic and respiratory enzymes, changes in cell quota and nutrient uptake, as well as alterations in fatty acids and proteins. Individual populations have been shown to exhibit minimum, maximum and optimal temperatures for growth that contribute to species composition and diversity and eventually lead to seasonal succession.

Temperature changes beyond threshold levels can also have variable effects on aquatic insect communities diapause induction as a function of endocrine processes; hatching success which decreases at low or high extremes; larval growth, adult size and fecundity for which temperature has influence on the rate of feeding, assimilation and respiration, food conversion efficiencies and enzymatic kinetics; voltinism[3] ; and timing of

[3] Number of generations per year based on larval growth rate.

adult emergence which may be premature or delayed depending on temperature increase or decrease (Sweeney and Vannote 1981).

High but sub-lethal temperature can affect fish in a number of ways. The effects may reflect metabolic inefficiencies, susceptibility to disease and toxic effects of pollutants, changes in behavioural patterns, intra- and inter-specific competition, predator-prey relationships, community composition and parasite-host relationships (Dickerson and Vinyard 1999).

A study of ecological effects of hot water discharge of a steam electric generating plant in Crystal River, Florida on fishes found that species abundance was higher at non-affected sites than affected station (Grimes and Mountain, 1971).

Carr and Giesel (1975) found that both the numbers and biomass of juvenile fish in the thermally affected creeks were 3-10 fold smaller than those obtained from the creek at ambient temperature.

A study of the thermal effluent effects on the community structure and nursery function of fish in an estuary showed decreasing numbers of species with decreasing distance from the thermal outfall (Jones et al., 1996). The thermal effluent only affected the species compositions in the inner estuary, and estuary-opportunistic species. During winter/spring months, thermal effluent attracted some fish species to the warmer waters of the inner estuary. The extended growth season for such species and significantly higher growth rates promoted premature movement out of the inner estuary. The latter effects were postulated to lead to alteration of the population structures of the species by increasing their vulnerability to heavy localized fishing intensity, aggregation of natural predators and point-source pollution.

In a study Mosquitofish from thermally affected stations (28 to 40ºC) and unaffected sites (12 to 29ºC) for reproductive activity, sex ratios, size at sexual maturity, percentage of fat, and size structure. Bennett and Goodyear (1978) showed that mean brood size of populations from thermally affected areas generally varied inversely with water temperature.

Stauffer et al. (1974) studied the distribution of fish in two rivers in relation to thermal discharges from a fossil fuel power plant. They noted a slight decrease in diversity indices for stations located in the thermal discharge. The results showed that while a number of species were not affected; others avoided high temperatures but others were attracted to high temperatures.

Exposure to thermal effluents can possibly compromise gametogenesis in fish (Luksiene et al., 2000). High temperature in Swedish and Lithuanian thermal effluent areas influenced gametogenesis of female perch *Perca fluviatilis*, roach *Rutilus rutilus* and pike *Esox lucius* negatively, indicating reduced reproductive capacity.

In the mitigation of effects arising from heated water discharge on aquatic communities, the most important ecological factor will then be to limit excessive heat dumping that might exceed the buffer capacity of the aquatic ecosystem as a way of eliminating the profound influence of temperature on such communities.

1.2 Nesjavellir co-generation power plant and Lake Thingvallavatn

Nesjavellir co-generation power plant is located in the Nesjavellir geothermal field, a high enthalpy geothermal system within the Hengill Central Volcano in south-western Iceland, on the south of Lake Thingvallavatn (Fig. 1). Thingvallavatn is a rift lake of high conservational value (Jónasson, 1992), fed 90% by underground springs with main springs entering in the north at a temperature of 2.8-3.5°C. Warmer groundwater enters the lake in the southwest from the Hengill geothermal area (Ólafsson, 1992). Geothermal investigations at Nesjavellir commenced in 1946, however, it was not until 1986 that a decision was made to harness the geothermal heat for district heating in Reykjavík (Gunnarsson *et al*. 1992). By 1990, 14 production boreholes had been drilled, and all except one were successful. That year the Nesjavellir power plant was commissioned, generating about 100 MW_t, by producing about 560 l/s of 82°C hot water for district heating. In 1995 the capacity was expanded to 150 MW_t and in 1998 to 200 MW_t and the production of 60 MW_e of electricity commenced (co-generation plant).

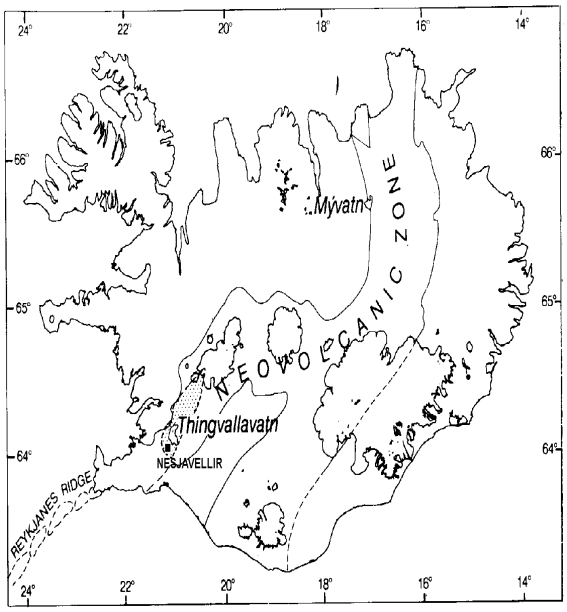

Figure 1. Location of Nesjavellir geothermal co-generation plant and Lake Thingvallavatn

The co-generation power plant has two functions. The first is to produce electricity with the geothermal steam. The second is to heat cold groundwater for district heating. Figure 2 shows the general design of the plant. The electricity production phase is a steam cycle design currently generated by three steam turbines, each 30 MW. The steam is condensed in a tubular condenser and cooled to approximately 55°C with cold groundwater. The condensate is disposed of in shallow boreholes in the nearby lava field. The cooling water is pumped from a shallow fresh-water aquifer (Gramelur) in the lava field 6 km away from the power plant. The temperature of the cooling water is 5-7°C. The cooling water is heated to about 55°C in the condensers, and then piped through heat exchangers, for final heating to 87°C, using the 192°C hot geothermal water from the separators. In the heat exchangers the geothermal water is cooled to 55°C (Gislason, 2000). Used and unused brine at flow rate of 115-143 kg/s at 46 - 100°C are discharged in the nearby Nesjavellir stream that disappears into Nesjahraun lava at Lækjarhvarf. About 126-140 kg/s of condensate at 48-68°C and 343-1776 l/s of cooling water at 49-69°C is also discharged into shallow drillholes that connects to surface groundwater (Wetang'ula and Snorrason, 2003). This mixes with groundwater, which flows some 3.8 km to the lake Thingvallavatn. Present installed capacity is 90 MW_e and 200 MW_t. The project aim was to evaluate the thermal effects of geothermal wastewater disposal on Lake Thingvallavatn water temperature at the out flow points.

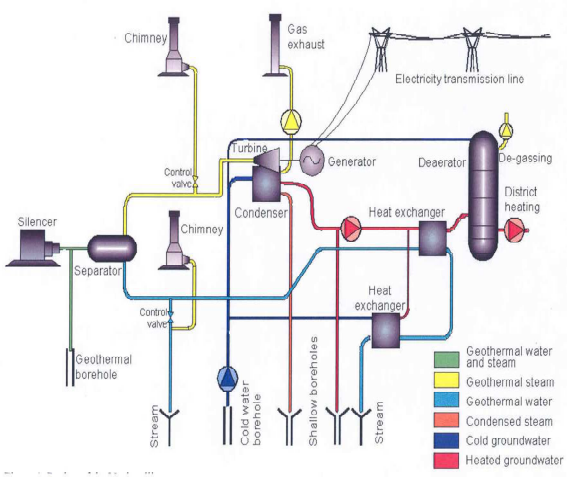

Figure 2. Nesjavellir geothermal co-generation power plant flow diagram.

METHODOLOGY

Beginning in June 2003 water sampling was initiated to describe spatial variability in the water quality at various study sites along the shore of Lake Thingvallavatn, Iceland influenced by geothermal outflow. Temperature mapping was carried out on the southern shoreline of the lake (Fig. 3) to determine geothermal water outflow sites by use of digital thermometer (Cole Palmer).

Approximately ten sites were verified as definite outflow points of warm wastewater into Lake Thingvallavatn. The sites represented a gradient of the influence of geothermal wastewater on Lake Thingvallavatn water quality.

Temperature and conductivity transect measurements

During transect mapping, a YSI 650 Multiparameter Display System logger (YSI Environmental) was used to measure temperature (accuracy ±0.15, resolution 0.01°C), specific conductivity (accuracy ±0.5% of reading +0.001 mS/cm, resolution 0.001 or 0,1 mS/cm), dissolved oxygen – mg/L (accuracy 0 to 20 mg/L: ±2% of reading or 0.2 mg/L, whichever is greater, 20 to 50 mg/L: ±6% of reading, resolution 0.01 mg/L), pH (accuracy ±0.2 unit, resolution 0.01 unit) and depth (accuracy ±0.02 m). The parameters were logged along three sections of three different transects at both Varmagja and Eldvik starting from the mouth.

RESULTS

Water temperature and conductivity

The results for summer 2003 water temperature measurements at definite outflow sites along the shoreline of Lake Thingvallavatn from Markagjà to Gràmelur are as shown in figure 3. The lowest and highest outflow sites water temperature was 16.8 and 27.2 ºC at sites 1 and 2 respectively. Water temperature at other outflow sites sampled was within a temperature range of 23.4-25 ºC.

Conductivity of water at the outflow sites was lowest at site 1 (210µs) and highest at site 8 (322 µs) with a spatial increase in conductivity from site 1 through site 10 (Table 1). Conductivity at sites 7-10 was much higher compared to sites 1-6 (Fig. 4).

Variation in conductivity and water temperature with depth at two sites; Varmagja and Eldvik based on summer 2003 transect measurements show a general trend of conductivity and water temperature decrease with increasing depth. Temperature profiles taken at 10 m, 25 m, 50 m and 75m mark along three different transect (Va T1, Va T2 and Va T3) from the mouth of Varmagja (Transect Va T2, Fig. 5) show a decrease in water temperature as one moves further away from the mouth. At 10 m from the mouth, there is no pattern in water temperature with depth with the water temperature being in the range 14-25 ºC (Fig. 5a).

Water temperature decreases with increasing depth and distance from mouth of Varmagja at the profile points for transects. This was also true with the temperature profile of other Varmagja transects Va T3 and Va T1.

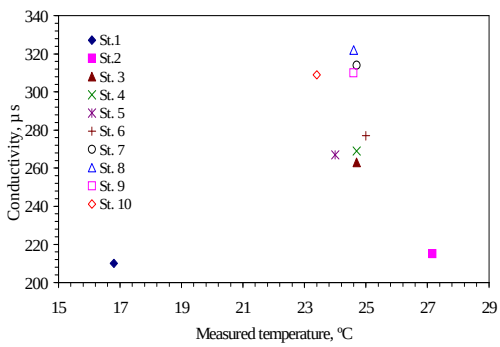

Figure 4: Relationship between conductivity and water temperature at major outflow sites

Table 1: Conductivity and water temperature at various major geothermal water outflow sites (July 2003)

Point	Conductivity (µs)	Temperature (°C)
Site 1	210	16.8
Site 2	215	27.2
Site 3	263	24.7
Site 4	269	24.7
Site 5	267	24
Site 6	277	25
Site 7	314	24.7
Site 8	322	24.6
Site 9	310	24.6
Site 10	309	23.4

The winter temperature profiles at Varmagja also decrease with increasing depth and distance from the mouth. For example point V2 which is just close to the mouth had a surface (30 m depth) temperature in the range of 5-26ºC. At profile points V4, V5 and V6 a layer of warm water is floating on cold water as indicated by drop in temperature with increasing depth. Points V3 and V7 which were closer to the ice edge had lower temperature of < 1ºC at a depth of 2 m which however increased to 3.5-4.0 ºC at 3-3.5 m depth (Fig. 7). Winter surface water temperature around Varmagja were high at the mouth but decreased with decreasing distance to the ice sheet (see Fig. 6**)**. The temperature range at Varmagja was 0.6 ºC near the ice edge to 26 ºC at the mouth. Water temperature at Varmagja outflow site was 27.92 ºC. All points previously measured in the summer were ice free despite most part of the lake having frozen.

DISCUSSION

Variation in water temperature and conductivity at outflow sites

From the temperature measurements at the various sites along southern shoreline of Lake Thingvallavatn, it is evident that the inflow of warm water has elevated the springs temperature in relation to the overall lake temperature which is usually varies between 6-11 °C in summer and 0°C in winter reading. At most outflow sites, the water temperature have increased more than two folds the average lake temperature. Results from the temperature profile transects taken at both Varmagja and Eldvik show a similar trend in water temperature increase. A few meters from outflow sites into the lake, there is a drop in water temperature from top to bottom showing that the warm geothermal wastewater is floating atop the cold lake water. The volume increase in warm wastewater disposal from the power plant is seen in elevated water temperatures at the thermally affected springs from Varmagjá towards Eldvík. This was emphasizes by the fact that during winter when most parts of the lake had frozen forming a thick ice sheet, most section around Varmagja and Eldvik were ice free. There surface water temperature decreased with decreasing distance for the mouth of the outflow sites to the ice edge. Judging by elevated temperatures in drill holes (Hafstað, 2001) at the edges of the warm water tounge, the elevated summer and winter water temperatures at outflow sites further to the south of Eldvík is not a surprise.

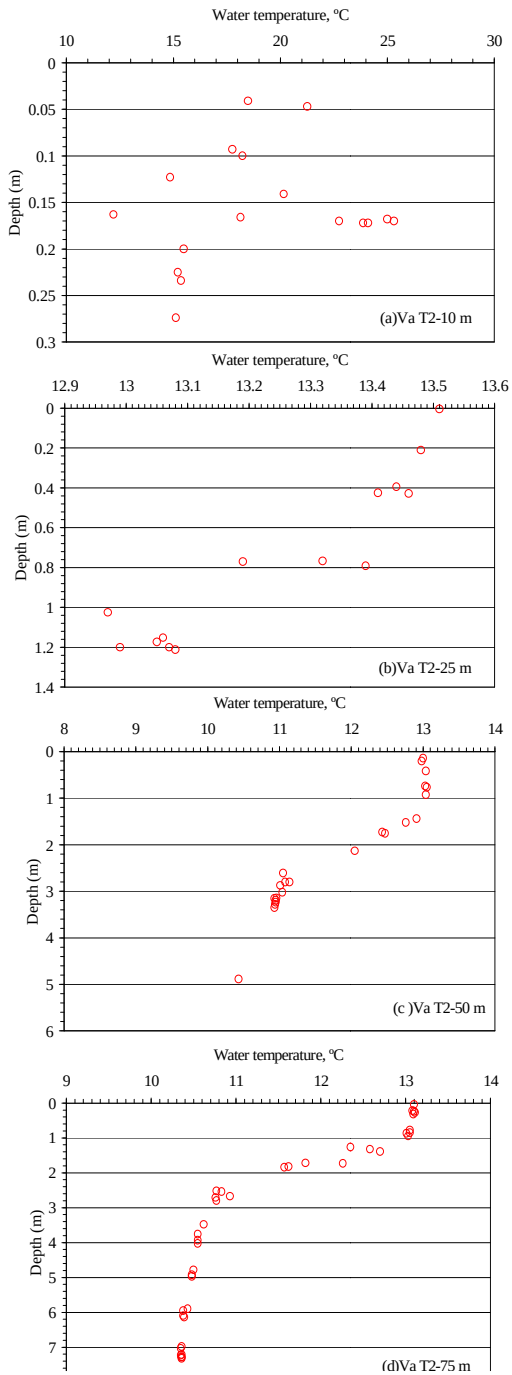

Figure 5. Summer (2003) temperature profiles on transect 2 at Varmagjá. Profiles were situated at 10, 25, 50 and 75 m distance from the outflow sites.

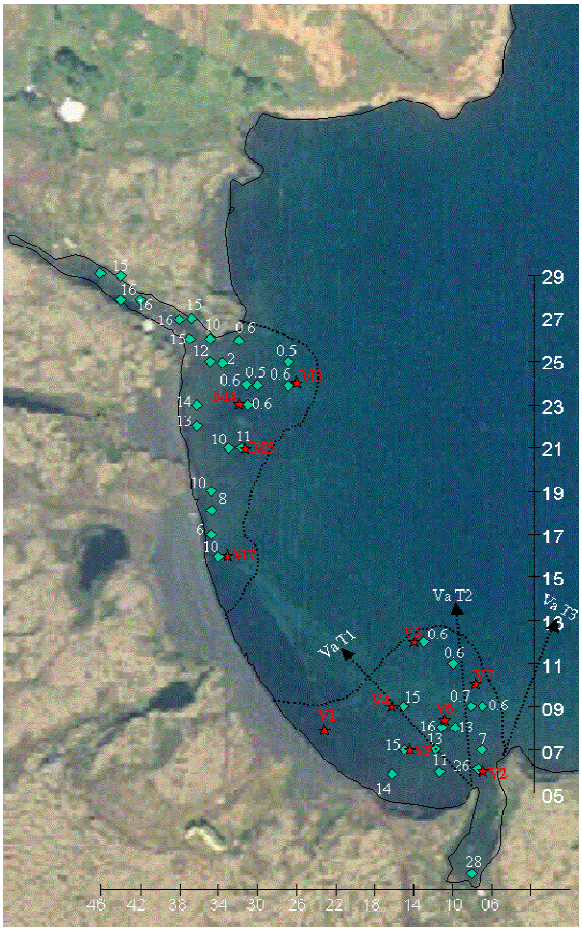

Figure 6. Water temperature measurements at Varmagja and Markagjà. Diamonds = surface temperature in winter 2004, stars = winter 2004 temperature profile points, Va T1 = temperature profile measurements along a transect in summer 2003.

The effects of elevated outflow sites temperatures on Thingvallavatn will only be on a local scale (see Fig. 5). In calm weather tongues of warm water floating on the surface may form temporarily. Such layering is likely to break down quickly due to wave action when the wind picks up. Any large scale effects of elevated spring temperature on the Thingvallavatn ecosystem are not expected. Efficient water mixing (Snorrason, 1982) causes temperature drop to the normal lake temperature a few meters away from sites of outflow. Hence, the normal cold water adapted benthic algal communities will not be affected (Jónsson, 1992). However, changes can be expected to the benthic communities of plants and animals in the nearest neighbourhood of the outflow sites, particularly in Varmagjá, which, due to it's isolation from the lake, is somewhat sheltered from wave action.

Water conductivity of at both Varmagja and Eldvik also decreases with an increase in depth. Electrical conductivity of water being a measure of total dissolved solids (TDS) in water implies that the higher conductivity of the upper water layer is indicative of its TDS content. This high TDS content could be attributed to the geothermal outflow input which also concurs with the earlier supposition that the geothermal wastewater is floating on the cold lake water. There is also a general increase in water conductivity with an increase in water temperature. Apart from wastewater being a major source of ions that have increased the water conductivity of the lake, rock composition (geology) will also determine the chemistry of the watershed soil and ultimately the lake.

Atmospheric input of ions in this case will be relatively minor except if the lake was near a coastal zone where ocean water may increase the salt load of dry aerosol and wet deposition.

CONCLUSION AND RECOMMENDATIONS

After the start of electricity generation at the Nesjavellir Power Plant increased discharge of hot water has lead to a marked temperature rise, - from 11.7 – 27.3°C, of geothermally affected lakeside springs.

Efficient, wind driven mixing of spring water with lake water (Snorrason, 1982) precludes any large-scale effects of elevated temperature and chemical concentrations in affected springs. Hence, any biological effects are expected to be strictly localized. Despite of this, the high conservational value of Thingvallavatn and its surroundings calls for stringent wastewater management. The amount, temperature and chemical composition of wastewater and potentially affected lakeside springs should be closely monitored. The local biota at spring sites should be assessed for effects of increased temperature and chemical effects. To minimize local effects deep reinjection of geothermal wastewater and further cooling of the condensed steam was recommended.

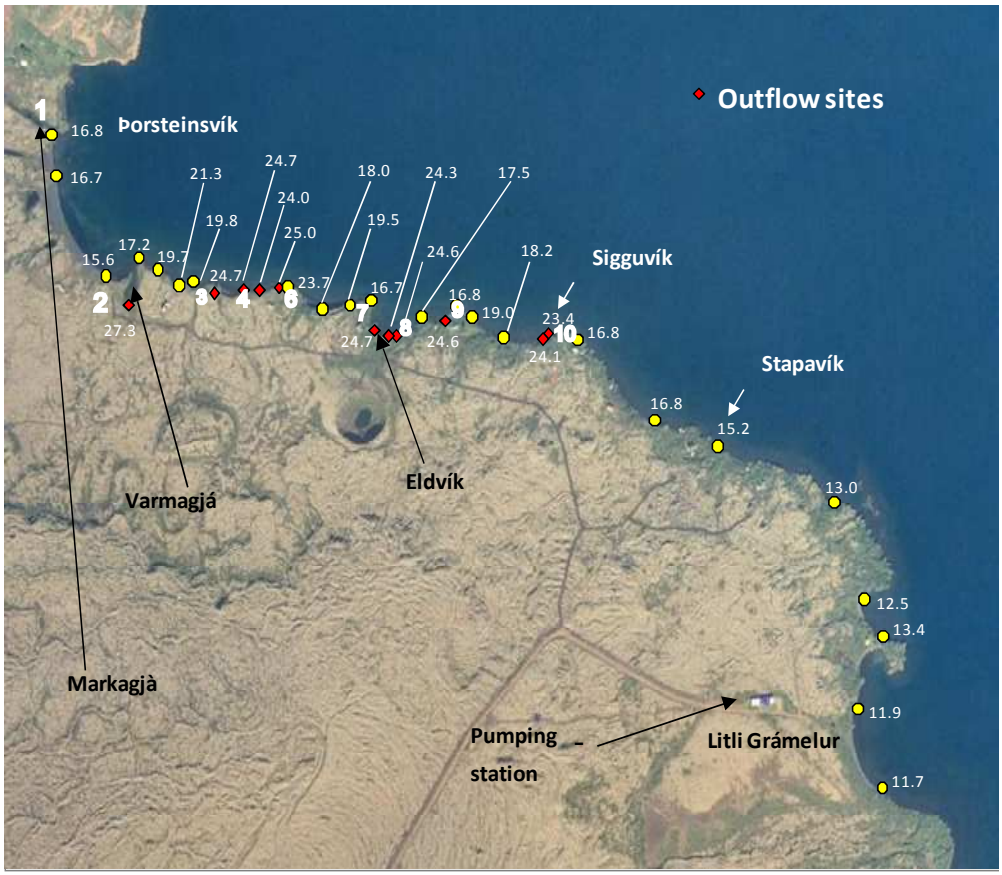

Figure 3. Spatial variations in water temperature along the southern shoreline of Lake Thingvallavatn. Red diamonds = Visible geothermal outflow sites, Yellow dots = Points with no visible outflow flows

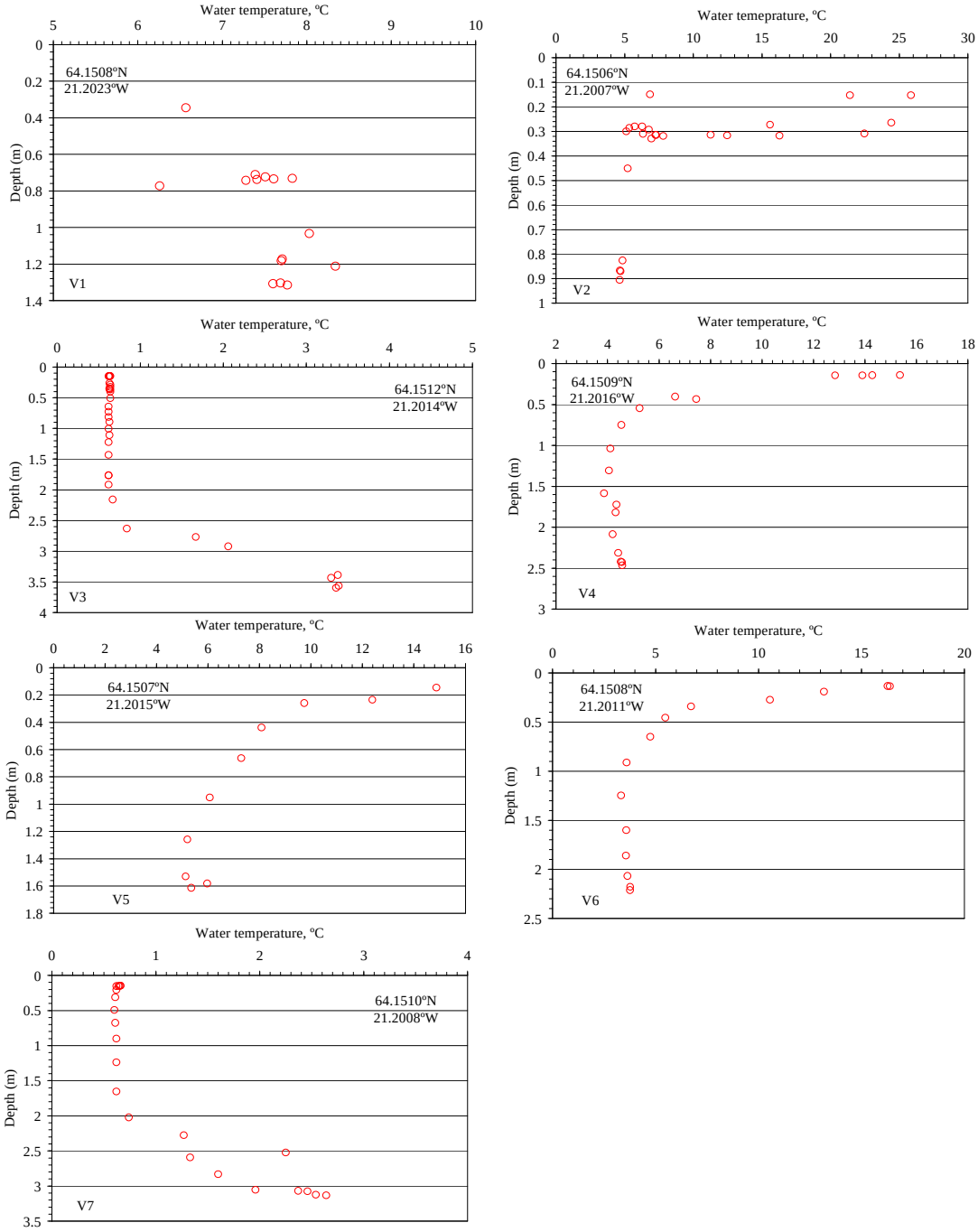

Figure 7. Winter (2004) temperature profiles at Varmagjá. Refer to Figure 6 for the locations.

REFERENCE

Allen, J.D. (1995). Stream ecology: structure and function of running water. Chapman & Hall, New York, 388pp.

Begon, M., J. L. Harper and C. R. Townsend. (1990). Ecology: individuals, populations and communities. Blackwell Scientific Publications, Cambridge, MA. 945 p.

Bennett, D.H, Goodyear, C.P (1978). Response of Mosquitofish to Thermal Effluent Energy and Environmental Stress in Aquatic Systems, Selected Papers from a Symposium, held at Augusta, Georgia November 2-4, 1977. CONF-771114. p 498-510, DOE EY-76C-09-0819.

Beznosov, V. N. and A. L. Suzdaleva (2001) Temperature Decrease in the Surface Water Layer of a Reservoir as an Example of Environmental Thermal Pollution. Water Resources 28(4),396-398.

Carr, W.E.S and Giesel, J. T (1975). Impact of thermal effluents from steam electric station on a marshland nursery area during the hot season. *Fishery Bulletin* Vol. 73, No. 1, 67-80.

CCME (Canadian Council of Ministers of the Environment). (1999). Canadian environmental quality guidelines, Winnipeg. Updated 2002.

DeNicola, D. M. (1996). Periphyton responses to temperature at different ecological levels. Pages 150-183 *in* R. J. Stevenson, M. L. Bothwell and R. L. Lowe (eds.) Algal ecology. Academic Press, New York.

Dickerson, B. R. and G. L. Vinyard. (1999). Effects of high chronic temperatures and diel temperature cycles on the survival and growth of Lahontan cutthroat trout. *Trans. Am. Fish. Soc*.128, 516-521.

Esterly, C.W (1975). The Effect of a Thermal Effluent on the Benthos of Thomas Hill Reservoir, Missouri. National Technical Information Service, Springfield VA 22161 as PB-264 835,ofiche. M.S. Thesis, 63 p,. OWRT B-039-MO(5), 14-31-0001-3296.

Gislason, G., (2000). Nesjavellir co-generation plant, Iceland. Flow of geothermal steam and non-condensable gases. *Proceedings of World Geothermal Congress 2000, Kyushu-Tohoku, Japan, 585-590.*

Gunnarsson, A. Steingrimsson, B.S., Gunnlaugsson, E., Magnusson, J. and Maack, R., (1992). Nesjavellir Geothermal Co-Generation Power Plant. *Geothermics*,21 (4), 559-583.

Hafstad, H. T. (2001). Nesjavellir: Temperature measurement in wastewater run-off area. Orkustofnun, report ÞHH-2001-13 (in Icelandic) 18pp.

Hickman, M and Klarer, D. M. (1975) The Effect of the Discharge of Thermal Effluent from a Power Station on the Primary Productivity of an Epiphytic Algal Community. *Br. phycol. J*. 10, 81-91.

Jónasson, P.M., ed. (1992). Ecolology of oligotrphic, subarctic Thingvallavatn, Iceland. *Oikos*.

Jones, G.K., Baker, J.L., Edyvane, K., Wright, G.J (1996). Nearshore fish community of the Port River-Barker Inlet Estuary, South Australia. 1. Effect of thermal effluent on the fish community structure, and distribution and growth of economically important fish species. *Marine & Freshwater Research* , vol. 47, no. 6, pp. 785-799.

Jónsson, G.S (1992). Photosynthesis and production of epilithic algal communities in Thingvallavatn. *Oikos, 64*, 222-240.

Klarer, D. M., Hickman, M. (1975) The effect of the thermal effluent upon the standing crop of an epiphytic algal community. *Hydrobiol*. Vol. 60, no. 1, pp. 17-62.

Luksiene, D., Sandstrom, O., Lounasheimo, L., and Andersson, J. (2000). The effects of thermal effluent exposure on the gametogenesis of female fish. *Journal of Fish Biology* 56, 37-50.

Ólafsson, J. (1992). Chemical characteristics and trace elements of Thingvallavatn. *Oikos, 64*, 151-161.

Poole, G. C. and Berman, C.H. (2001). An ecological perspective on in-stream temperature:Natural heat dynamics and mechanisms of human-caused thermal degradation. *Environmental Management* 27 (6), 787-802.

Snorrasson, S. (1982). *The littoral ecosystem and the ecology of* Lymnaea peregra *in lake Thingvallavatn, Iceland*..University of Liverpool, Ph.D thesis, Liverpool, 429pp.

Squires, L.E; Rushforth, S.R; Brotherson, J.D (1979). Algal Response to a Thermal Effluent: Study of a Power Station on the Provo River, Utah, USA. *Hydrobiologia* 63, (1), 17-32.

Stauffer, J.R., Dickson, K.L., Cairns, J (1974). A field evaluation of the effects of heated discharges on fish distribution. Water Resources Bulletin, Vol. 10, No. 5, 860-876.

Suresh, K., Ahamed, M. S., Durairaj, G. and Nair, K. V. K. (1993) Impact of power plant heated effluent on the abundance of sedentary organism, of Kalpakkam, east coast of India. *Hydrobiologia* 268, 109-114.

Suzuki, Y. and Takahashi, M. (1995). Growth responses of various diatoms isolated from various environments to temperature. *J.Phycol*. 31, 880-888.

Sweeney, B. W. and R. L. Vannote. (1981). *Ephemerella* mayflies of White Clay Creek: bioenergetic and ecological relationships among six coexisting species. *Ecology* 62, 1353-1369.

Taniguchi, Y., Rahel, F.J., Novinger, D.C. and Gerow, K.G., (1998). Temperature mediation of competitive interactions among three fish species that replace each other along longitudinal stream gradients. *Canadian Journal of Fisheries and Aquatic Sciences, 55*, 1894-1901.

Wetang'ula, G.M.N and Snorrason, S.S (2003). Ecological risk assessment of Nesjavellir co-generation plant wastewater disposal on Lake Thingvallavant, SW-Iceland. *Proceedings of International Geothermal Conference 14th – 17th September 2003, Reykjavik, Iceland.*

CHALLENGES IN PROVISION OF ADMINISTRATIVE SERVICES IN AN ACCELERATED GEOTHERMAL DEVELOPMENT PROCESS

Purity Gituma
Geothermal Development Company Ltd,
P.O. Box 100746 – 00101, Nairobi.
pgituma@gdc.co.ke

ABSTRACT

Geothermal Development Company (GDC) is a state owned corporation in the Ministry of Energy and was incorporated in the year 2008 with a mandate to fast track geothermal resource development in the country. The estimated potential in the Kenya rift is over 7,000-10,000 MWe and the Company is expected to realize development of up to 5,000 MWe in the next 20 years. The Company has been in operation since September 2009 and currently has a staff of 403 and the capacity is set to increase as operations increase. GDC has four operational offices in Nakuru, Naivasha and two in Nairobi. The Company is currently involved in drilling at Olkaria Domes, infrastructure development in Menengai and surface exploration work in Silali, Korosi, Paka and Homa Hills have been completed. The rapid employee expansion and increased geothermal development activities means increased responsibilities which the Administration Department is charged with. Administration has faced challenges like lack of adequate facilities, lack of sufficient vehicles for transport and parking spaces, lengthy procurement process, limited funds, poor supervision and coordination of staff, lack of communication, diversity of staff and overlapping of duties. Administration department has taken a remedial step to ensure that the functions run smoothly through established of administration management systems. Administration department has come up with rules to guide her operation. This paper therefore discusses the challenges faced by administration in providing the required services to facilitate efficiency and effectiveness in geothermal development operations and capacity expansion within the Company in order to realize its goal of 5,000 MWe geothermal by 2030.

Keywords: Administration, function, Service

INTRODUCTION

Administration

Organizations are increasingly seeking proper administration to effectively and efficiently manage performance in the operations. GDC, in her efforts to fulfill its mandate of delivering 5000 MWe to Kenyans in the next 20 years and play vigorous role of realization of the vision 2030, has engaged effective administrative machinery in its operations (Steam publication January-March 2010 pg.3).

The Administration Department is concerned with providing support services in organizations. It is regarded as a top level function of policy making, but this is too narrow a definition for administrative management that includes the office side of business. Therefore administration is the act of management in companies that undertakes responsibilities for office work on a day to day basis. Bovee, C.L., Business Communication Today, 7thed. (2003).

The Role of Administration

There are a number of descriptions of the administrative function but quite often it is the oil that keeps a business rolling efficiently. Without a workable administrative system organization's operations can come to halt *(http://EzineArticles.com)*.

In GDC administration is mandated to undertake the following functions:-

i) Ensuring conducive and secure working environment
ii) Facilitating effective communication both internally and externally
iii) Ensuring effective and efficient transportation services for its employees
iv) Maintenance of office furniture, equipment and fittings
v) Provision of hospitality service to staff
vi) Utility management for the Company

CHALLENGES FACING ADMINISTRATION

Provision of adequate facilities and appropriate physical condition

An organization strives to ensure smooth running of all its functions to achieve its goals and objectives. Administration department provide adequate facilities and appropriate physical conditions for productivity. In GDC, administration department ensures a conducive working environment through identification and acquisition of relevant office services, office furniture, equipment and fittings, office settings, decoration, heating, ventilation, lighting, noise control and provision of safety measures. Bovee, C.L.: Business Communication Today, 7thed. (2003).

An organization strives to ensure smooth running of all its functions to achieve its goals and objectives. According to Saun David in the article:

> *"Office furniture is one of the most important Business Decision" When a company begins working on a plan, one of the furthest things from their mind is what kind of office furniture the company needs. They are focusing on business plans, strategies, and ways to market to their potential customers. By ignoring their office furniture, many companies are losing out on much more productive work that could be earned by their employees.*
>
> *Employees will sit in chairs and at desks for 8 hours a day. Imagine sitting on an uncomfortable chair for 40 hours out of your week? Employees already would rather be somewhere else instead of being productive for the employer. Many people develop serious conditions relating to their back and spine because of un-proper sitting techniques and chairs that just aren't good enough (http://Ezine-articles.com)*

GDC has mandated administration to ensure employee's needs on office furniture, equipment and fittings and general office environment are taken care of. Administration liaise with its customers/or other departments and compiles needs base requests and prioritizes them. Administration also identifies appropriate furniture based on need analysis for the entire company. This forms the basis of raising a Purchase requisition to supply chain department.

Administration department is faced with a challenge on provision of adequate facilities through slow procurement process that recommends purchase from the lowest bidder who does not necessarily provide the best quality products.

Rapid Growth in staff and Company Operations

The operations of GDC have expanded very fast and spread rapidly. This has put pressure on the department in provision of office space, furniture, hospitality service, transport and communication, security and clean environment. So far some areas have no established offices for the administration to effectively discharge duties and provide fully for all staff needs. There is an increase on demands on property management due to increase in number of acquired facilities.

Inadequate Transport and Parking Space

Transport is an essential requirement in any organization *(http://Ezine-articles.com)*. Administration manages the company vehicles including allocation, scheduling, fuelling, and maintenance and taking care of drivers' welfare. It coordinates all transport logistics within the company and its areas of operation especially the drilling sites at Olkaria and Menengai. Vehicles are used to ferry employees to different field activities and sites for research and exploration, meeting stakeholders and projects monitoring. All these require proper planning to ensure that operations are carried out as per demand by various users making it possible to realize the company's mandate.

Administration faced the challenge of provision of sufficient transport service for staff as the company could not purchase sufficient vehicles at inception. The company also faced challenge of lack of sufficient parking space since acquisition of office space was done hurriedly and lacked future considerations.

Securing for Hospitality Services

Hospitality services are managed by Admin *(http://Ezine-articles.com)*. These include: - clean drinking water, tea, and meals. Water is a basic necessity for human kind. Administration ensures unlimited supply of clean drinking water for all staff. GDC's Headquarter office is located far off the central business area making it necessary to engage services of hotelier to cater for day meal for its staff. To reduce on time wastage looking for hotelier services this is a relief to the company to capitalize on the manpower fully without time wastages hence a step towards the 5000 MWe by 2030.

However it is faced with the challenge of procuring for these services through competitive bidding as is the requirement. Since some of the services were acquired through mutual agreement it becomes a challenge for finance to make payment and as a result delayed payments occurred.

Maintenance of equipment, furniture and fittings

It is the responsibility of Administration department to manage buildings and maintenance of equipment, furniture and fittings. It also ensures that buildings meet government regulations on health and safety standards. It therefore maintains GDC asset inventory and keeps a record on when the company's equipment are due for servicing. It ensures servicing is done without delay to avoid breakdown of essential services that could lead to delay or failure in operations. In discharging the above duties it faces challenges while identifying the service providers. It is a requirement to use pre-qualified suppliers for the service while most never qualified or apply for qualification process for their firms.

Management of Utilities

Administration also monitors the utilities to avoid misuse and ensures payment in time to avoid unwarranted disconnections. It manages the proper usage and payment of electricity, telephone, water, sewerage, sanitation, rents and rates. This ensures smooth flow of work without disruptions due to discontinuation of supplies e.g. power, water and electricity. Administration personnel initiate the payment of their settlement through finance department. The process of payment may sometime time rendering administration to seek for ways of explaining the delay to suppliers hence a challenge.

POOR SUPERVISION & COORDINATION OF STAFF

Due to vast distances involved between field offices and the headquarters it is difficult to coordinate provision of services and monitor staff output on a daily basis as well as oversee productivity of staff under their supervision. Appleby, R.C.: Modern Business Administration, 6th edition (1994).

HIGH DEMAND FOR STAFF TRAINING

Induction and On-job training are quite necessary especially for first time employees for this equips them with commensurate skills to ensure effective and efficient execution of assignments.. However, during training the department is denied of the adequate human resource thus slowing down the implementation of plans including service delivery to other departments.

COMMUNICATION

Communication is conveying of information and/or data from one person (sender) to another (receiver). Communication is an essential tool in organizations in that it facilitates flow of information as work necessitates for effective and efficient performance (*John Harrison (1999) 4th Edition office procedures pg.129).*

GDC being an expanding company with regional offices in various parts of the country requires proper choice of channels for communication, equipment and coordination to effectively communicate to its customers.

Communication equipment like telephone took time before installation at the initial stages of operation rendering administration department with a challenge of communication.

SLOW PROCUREMENT PROCESS

It is a government requirement that any purchase goes through a procurement process. The regulation requires that quotations are sought for certain threshold and others are advertised for open tendering. These processes are time consuming and limiting. It takes a lot of time for procurement of any sizeable service is completed thus hampering timely provision of services and especially during emergencies. This is a great a challenge to the administration department which wishes to provide goods or services immediately they are requested for.

DIVERSITY OF STAFF

The department has also faced a challenge in that most of the management staff was former employees of Private and government Parastatal. They have diverse office culture backgrounds, and their orientations are quite different. In administering to their needs, administration department is faced with challenges to satisfy their demands.

OVERLAPPING OF DUTIES

Owing to lack of defined policy and having staff from diverse work backgrounds, there tends to be overlap in duties with some departments assuming the duties of others e.g.ICT & QA taking up duties of Administration after installation of telephone system they assumed the role of administering in allocation of entitlement and budget which is an Administration function.

CONCLUSION

GDC being a state corporation all its operations are governed by government rules, regulations and procedures. An example is the adherence to the PPOA in acquisition of all the needs ranging from property, equipment and services. The procedure involved is too slow bearing in mind that the company is new and procurement of equipment need to be quick to fast-track the mandate of 5000 MWe by 2030. However, we have slowly but timely managed to overcome the challenges through projection of our future needs based on the strategic plan and capitalizing on shared ideas, views and opinions (open door policy) to come up with uniform policies, processes and needs. The challenges facing administration of services in an accelerated geothermal development process are unique and uncommon to new organizations. Our company is faced with the following challenges due to the ever changing need to continually review on policies, procedures and processes:-

1. Lack of proper operating systems, rules, procedures and practices.
2. Provision of essential services to fast growing staff and company operations.
3. Lack of proper supervision and coordination of staff
4. High rate of staff training needs
5. Slow procurement process
6. Overlapping duties

Diversity of staff in an organization call for timely & effective support in the direction of operating for their business to function efficiently. It's therefore prudent to embrace a high level of policy formulation to accommodate administrative support project like outsourcing of some administrative activities which as a result has led to cost-effective without compromising on a quality. Formulation of a middle ground for all is essential to the benefit of the company.

ACKNOWLEDGEMENT

The author would like to thank the organizers of the conference for providing/giving a platform/forum to exchange knowledge on the challenges facing administration in an accelerated Geothermal Development Process and chart the way forward. The author would also wish to thank Geothermal Development Company for giving an opportunity to participate in the conference. I would also wish to thank my colleagues who encouraged me to write on the topic and others who took time to read the paper and provide some corrective criticisms. Thank you all.

REFERENCES

Bovee, C.L.: Business Communication Today, 7thed. (2003).

Appleby, R.C.: Modern Business Administration,

John Harrison 6thed. (1999) and 4th Edition office procedures pg.129)

Steam publications Issue 1 January-March 2010

Geonews in-house bulletin Aug 1-15, 2010

Oxford Advanced Learner's Dictionary of current English 7th Edition

Business Communication Today By Bovee Thill Schatzaman

Modern Business Administration sixth Edition by Robert Apple by Office Procedures 4th Edition by John Harrison

Internet - http://Ezine-articles.com

EMPOWERING COMMUNITIES LIVING WITHIN GEOTHERMAL AREAS IN THE KENYAN RIFT

Pascal Manan
Geothermal Development Company Ltd, P. O. Box 17700 Nakuru 20100
pmanan@gdc.co.ke

Empowering of local communities now has to be detached from the dependency syndrome in order to ensure sustainability and self reliance for the development of the communities. This paper describes how GDC is working towards empowerment of the communities living along the Kenyan geothermal prospects areas. The processes is geared towards ensuring sustainability, equitability, profitability, acceptability and durability. This all round empowerment can only be achieved through community involvement on one hands, use of the government departments/administration and local community leaders on the other hand. This model of community empowerment is based on knowledge and community education to ensure that the community members know their resources well and their weakness in terms of productivity and to ensure that they are fully involved before company financing to make sure that they are attached to the projects that are undertaken in order to guarantee their sustainability. Empowering the local communities requires specialized staff in order to ensure that the geothermal representative built close tie with the local community members to ensure that during empowerment and resource distribution there are laid out structures for conflict resolution to reduce cases of conflict arising from scarcity of Community participation in community development is the starting point in order to achieve tangible community empowerment, it is also crucial for companies harnessing for geo thermal resources to have a method of performance monitoring and evaluation in order to gauge how effective the company efforts are to the communities and to assess the impacts of the use of resources through developing performance indicators and use of local leaders to ensure that the empowerment program has achieved its optimum desired effect at the end of the day .

CORPORATE SOCIAL RESPONSIBILITY (CSR) IN GEOTHERMAL DEVELOPMENT: THE CASE OF THE GEOTHERMAL DEVELOPMENT COMPANY (GDC), KENYA

Ruth Musembi
Geothermal Development Company Ltd -P. O. Box 100746 -00101, Nairobi
rmusembi@gdc.co.ke

ABSTRACT

The World Business Council for Sustainable Development defines corporate social responsibility as the continuing commitment by business to behave ethically and contribute to economic development while improving the quality of life of the workforce, their families, the host community and the society at large. Having been in operation for over a year now, GDC has developed a CSR policy and strategy that focuses on five areas: education; economic empowerment, environmental management; health and sanitation; and arts, culture & sports.

Our community investment programme aims at creating a symbiotic relationship between GDC and host communities geared towards improving their quality of life. The GDC CSR model entails empowering communities to utilize local resources for improved livelihoods. communities will benefit from GDC's presence as well as from the direct utilization of geothermal resources where applicable. In order to ensure that we continuously maintain GDC's brand visibility, GDC sponsors worthy causes in the society, not necessarily within our areas of operations. Such include support to deserving educational cases, promotion of professional advancement or co-sponsoring strategic initiatives. In all cases sponsored projects fall within GDC's CSR focus areas. GDC recognizes the need to deliver services in an environmentally sustainable manner. The company has developed a strategy to safeguard the environment. In most of the geothermal areas in Kenya, the environment has been degraded and trees have been cut, leaving the soil bare and open to erosion. GDC is engaging in rehabilitation of forest cover in water catchment areas and in and around geothermal sites. Overall, GDC is committed to undertaking its operations in a sustainable manner. With regard to workplace practices, GDC recognizes employees as the Company's most important asset and promotes equal employment practices, gender equity, and health and safety, and offers a competitive pay and benefits package.

INTRODUCTION

I recently bumped into this quote, "Geothermal fuel - like the sun and the wind - is always found where the power plant is. Therefore, economic benefits remain in the region…" At the Geothermal Development Company (GDC) in Kenya, we intend to share the benefits of geothermal development with our host communities by creating a symbiotic relationship between GDC and host communities. CSR is an important activity to any businesses nationally and internationally. The term is often used interchangeably with other terms such as Corporate Citizenship and Corporate Social Investment (CSI). It is also linked to the concept of Triple Bottom Line Reporting (TBL), used as a framework for measuring a company's performance against economic (profits), social (people) and environmental (planet) parameters. The World Business Council for Sustainable Development defines CSR as the continuing commitment by business to behave ethically and contribute to economic development while improving the quality of life of the workforce, their families, the local community and the society at large. The key elements of corporate social responsibility include:

i. **Responsibility for good corporate governance and ethical business practices** –compliance with national and international laws, regulations and standards; efforts to prevent bribery and corruption; and the establishment of a code of conduct that ensures that the company goes beyond legal compliance.
ii. **Responsibility for people** – This includes product and employee safety programmes to ensure that consumers and people involved in the sourcing, production and distribution of products are not placed at risk; safeguarding human and labour rights which may include equal opportunities, non-discrimination, prevention of child labour, freedom of association and fair wages within the workforce and fairness along supply chains.
iii. **Responsibility for environmental impacts** –maintaining environmental quality, adopting clean and eco-efficient business processes, sharing environmental technologies and engaging in addressing environmental challenges such as climate change and biodiversity protection.
iv. **Responsibility for communities** – efforts to contribute to broader social and economic benefits in host communities, for example: building local business linkages; increasing access to essential products and services for poorer communities, such as credit, farming technology, water, energy, medicines,

education, information technology; and so on. These contributions to development should be part of a company's core business operations.

THE BUSINESS CASE FOR CSR

In today's tough business environment no company can afford to undertake CSR without consideration of its value in meeting corporate objectives. Critics of CSR wonder why a company should spend its resources to fund CSR activities. Others argue that profitability and good corporate citizenship are mutually exclusive. To the contrary, there is growing evidence that by doing business in a socially responsible manner, companies can greatly enhance stakeholder relationships thereby obtaining a "license to operate" and support for the company's business goals, leading to profitability. In the long run the company earns great monetary and non- monetary benefits. A company can incur huge losses by "getting it wrong" in terms of economic, social and environmental performance yet there exist business and societal benefits of "getting it right."

Well designed CSR programmes can reap immense mutual benefits by:

i. improving relationships and goodwill with the community
ii. enhancing business performance and the company's long-term survival
iii. enhancing corporate brand visibility and a caring image of the company
iv. contributing to government's poverty eradication programmes
v. providing opportunities to build relationships with partners

THE GDC CSR POLICY STATEMENT

At GDC we have adopted the World Business Council for Sustainable Development definition of CSR as the continuing commitment by business to behave ethically and contribute to economic development while improving the quality of life of the workforce, their families, the local community and the society at large. The key elements of corporate social responsibility include:

Our CSR programmes go beyond philanthropy and entail taking responsibility for four key elements of CSR: responsibility for good corporate governance and ethical business practices; responsibility for people; responsibility for environmental impacts; and responsibility for communities. The GDC CSR policy is guided by the following principles:

i. **Corporate Alignment** – All our CSR activities are aligned with business plan which is be aligned with national priorities as outlined in Vision 2030.
ii. **Management Commitment-** At GDC considers CSR is core business. The CSR committee is chaired by the Chief Executive Officer with a budget allocated annually.
iii. **Good corporate governance and ethical business practices** – Our operations comply with national and international laws, regulations and standards; we have established a code of conduct that ensures that GDC goes beyond legal compliance
iv. **Sustainability** - We focus on initiatives that contribute to capacity building and improved quality of life. CSR projects are implemented in such a manner as to ensure that the beneficiaries are able to sustain the ongoing viability of the project;
v. **Community Involvement & Partnerships** – We build relationships with host communities and ensure that communities and beneficiaries of CSR projects are actively consulted in the process of project selection, implementation and evaluation. In the planning and execution of CSR projects, GDC may partner with reputable organizations capable of generating mutually beneficial brand visibility and capacity building outcomes;
vi. **Environmental responsibility** - GDC undertakes its operations in a manner that safeguards the environment;
vii. **Responsibility for people/employees -** GDC ensures employee safety at work; fair wages/benefits; safeguards human & labour rights and ensures fairness along supply chains
viii. **Quick-Win Sponsorship** - In order continuously maintain GDC's brand visibility, we sponsor worthy causes in the society; not necessarily within our areas of operations. Such include supporting deserving educational cases, promotion of professional advancement or co-sponsoring strategic initiatives. However, the proposed projects must fall within GDC's CSR focus areas;
ix. **Professional approach to CSR** – Officers with CSR responsibilities are trained and exposed to exchange programmes, conferences and workshops in order to enhance their capacity.
x. **Continuous improvement** – GDC monitors CSR performance against set targets for improvement.

GDC'S CSR APPROACH

In line with this CSR policy, the corporate planning and budgeting process makes provision for resources required for the implementation CSR activities. In the current budget, a substantial sum has been set aside for implementing initial projects. Lessons learned from this year's experience will form the basis for an enhanced budget next year. We have engaged stakeholders to understand their expectations on the issues most important to them, and we have mapped these against our business priorities. We are in the process of selecting appropriate CSR programmes for the first year.

At the corporate level, the PR and Communication department has the ultimate responsibility for coordinating, and providing advice and guidance on CSR matters. The Manager, PR and Communication develops an annual work plan that is presented to the CSR Committee for approval.

Area managers champion CSR projects in their areas. In conjunction with the Environment, Safety and Community Liaison department, they propose suitable projects, develop a budget and present it to the Manager, PR and Communication for compilation. All proposed projects are guided by the approved corporate CSR policy and guidelines.

Project proposals are appraised on a monthly basis by a CSR sub-committee comprised of the PR and Communication (PRC), Environment, Safety and Community Liaison (ESCL) departments and a representative of the Area where the project will be implemented. The appraisal report is then tabled with recommendations to the CSR committee for approval.

Area Managers, in collaboration with Community Liaison Officers, supervise the implementation of the approved CSR projects to ensure successful implementation. They submit regular reports for inclusion in the CSR annual report.

This policy is communicated to staff and will reviewed every two years. The PR and Communication department will annually document progress towards CSR targets and objectives, and include it in the corporate annual report which will be published and made widely available to staff and stakeholders.

The Manager, Internal Audit is responsible for monitoring the compliance and effectiveness of CSR measures, as part of ongoing internal audit programme.

GDC'S CSR FOCUS AREAS

Education

GDC supports education for children in the areas where we operate. Our support may include infrastructure development such as the establishment of model schools through the rehabilitation of existing educational institutions or establishing new ones as the case may be; provision of school equipment and supplies; or support for school feeding programmes for children in hunger spots using locally produced foods. We also educate parents on the benefits of education particularly among nomadic communities. We believe that these efforts will contribute towards the Millennium Development Goal two (2) of achieving universal access to primary education by 2015.

Economic empowerment

We focus on income generation and job-creation projects, with the primary focus on youth and women. Some initiatives may include improving food productivity through technology transfer such as the replenishment of soil nutrients for smallholder farmers on lands with nutrient deficient soils, through distribution of fertilizers and seeds.

We also encourage communities to form cooperatives through which they may supply products to our rig camps and offices. Through our feeder roads we are improving food transport to local markets thus ensuring trade links to urban markets. We will assist communities establish drying and storage systems to ensure food produce do not go to waste.

We will diversify economic activity in rural areas by encouraging fish farming and eco-tourism through the establishment of community-managed heated spas, hotels, golf course, and touristic sites all utilizing geothermal resources.

Our choice of this focus area is in line with the Millennium Development Goal one (1) on the eradication of extreme poverty and hunger by 2015 that creates the imperative for all sectors - corporate, civil society and government - to collaborate in income generation, food security, job creation and poverty alleviation initiatives.

Environmental Management

Reducing our impact on the environment is a priority. We recognise the need to deliver services in an environmentally sustainable manner (MDG 7) and to include concern for the environment in all our activities. By reducing waste in our business processes, we will as well reduce operational costs and increase profits.

GDC therefore:

- **Promote office energy efficiency** through initiatives such as fitting timer switches to ensure lights are not left on overnight, adding movement and daylight sensors to ensure lights are only on when needed, installing energy-efficient bulbs, fitting flow restrictors to water taps, and maximising natural light in our buildings,
- **Practise sustainable IT**- Personal and network IT equipment account for a large proportion of our energy use. GDC will cut the energy used by ensuring that power management features are enabled on all IT equipment,
- **Manage print waste** by combining copiers, printers and scanners in one device; removing printers from desks to a central location and minimising the number of printers in use; implementing default settings to save energy, ink, toner and paper (e.g. double-sided printing and black and white settings); reduce waste in procurement of ink, toner and paper, and where possible negotiate recycling arrangements with manufacturers of ink and toner cartridges,
- **Increase forest cover** by establishing tree nurseries, re-planting degraded areas and water catchments as well as supplying tree seedlings to communities.
- **Undertake environmental awareness projects** (e.g. clean-ups, awareness campaigns etc)
- **Get involved in disaster relief programs** (e.g. community assistance during floods, drought relief etc)

Water and Sanitation

Clean water not only sustains life but prevents water-borne diseases. GDC supports the rehabilitation of water pans or sinking of boreholes to ensure supply of clean water for the communities. GDC will also support projects aimed at rain water harvesting in schools and health centers.

With regard to health, GDC will facilitate local communities' access to affordable health care. This will include free distribution of bed nets and anti-malaria medicine for all children in areas with malaria as well as access to the GDC clinics within our rig camps. We will also promote the "ABCs" of HIV/AIDS management.

Preservation of Art, Culture and Sports

GDC works with communities to enhance sports, arts and culture. Such initiatives may be used to foster peace between communities and competitiveness among schools. GDC may sponsor sporting events for the aim of enhancing our brand visibility and for fundraising in support of CSR projects, sports, arts and culture in our areas of operation.

MONITOR AND EVALUATION OF PROJECTS

Annual audit of projects will be conducted to assess project implementation and determine adherence to stated objectives. Deliverables and conditions of significant funding will be agreed with the beneficiaries. Direct periodic contacts will be maintained with the project beneficiaries to assess their development impact.

CORPORATE SOCIAL RESPONSIBILITY (CSR) COMMITTEE

The CSR Committee is established to administer the CSR policy. It approves the annual CSR work plan and receives quarterly reports on progress made. However, quick-win sponsorships are approved administratively by the Managing Director/CEO. The CSR committee is made up of all heads of departments and is chaired by the Managing Director/CEO.

Annexes

FUNDING GUIDELINES

GDC funds projects that are to be implemented in Kenya by legally constituted and registered community based organizations (CBO) or non-governmental organizations working within our areas of operation. Funded

CBOs/NGOs must have strategic partnerships with community leaders and administration in order to ensure community buy-in.

GDC defines a project as a set of activities organized in response to an identified need that aims to achieve specific objectives within a specific time frame and budget which leads to sustainability.

Eligible organizations will submit proposals in the prescribed format to the GDC headquarters or Area offices by post or via email. Applications forms are available in GDC offices or they may be downloaded from the GDC website www.gdc.co.ke. Applications for funding will follow the prescribed format. Received applications will be acknowledged within 10 working days of receipt and a decision taken within three (3) months of acknowledgement. The proposals will be structured as follows:

PROJECT PROPOSAL FORMAT

- **Project name**
  A statement of the name of the project, the organization implementing the project, contact person and contact information: physical address, postal address, phone number and email address.
- **Project background and executive summary**
  This is a brief overview and summary of the project. It should provide a credible statement that describes your organization and establish the significance of the project.
- **Problem statement**
  A statement of the need/challenges identified the rationale for addressing these challenges and the conditions to be changed by the project.
- **Project objectives**
  A description of the intended outcome of the project stated in a SMART manner (Simple, Measurable, Accurate, Realistic and Time Bound). The proposal must also indicate what difference the project will make.
- **Strategic fit into GDC's CSR key focus areas**
  A statement of how the project fits into one or more of the GDC's five CSR focus areas.
- **Project implementation plan**
  A description of the project implementation activities, stakeholders' participation, and partners involved in the implementation, if any.
- **Beneficiaries**
  A statement of the direct beneficiaries of the project and a description of what difference is envisaged in their lives.
- **Timeframe**
  An indication of how long the project is going to last from inception to successful completion.
- **Detailed costing**
  An indication of the total cost of the project and a detailed budget.
- **Sustainability**
  An indication of how the project will sustain itself beyond GDC's intervention after the funding period.
- **Impact of GDC's intervention**
  A description of the multiplier effects through jobs to be created, skills to be developed, increased utilization of and market for local resources etc.
- **Evaluation**
  A statement of how the project implementers will determine if the objectives of the project have been met and a statement of the people to be involved in the project evaluation.

CRITERIA FOR APPRAISAL OF PROPOSALS

Project proposals are appraised on a monthly basis by CSR sub-committee comprised of the PR and Communication (PRC), Environment, Safety and Community Liaison (ESCL) departments and a representative of the Area where the project will be implemented. The appraisal report is then tabled with recommendations to the CSR committee for approval. The funded projects must meet the following criteria:

- GDC funds projects in any of our five (5) focus areas: Education; Improved Livelihoods, Environmental Management; Health and Sanitation; and Arts, Culture & Sports.

- Projects funded must have a developmental approach that is intended to build capacity in communities and should eradicate dependency;
- Projects should take an affirmative approach bias with women, and the youth getting priority;
- Individuals may not be funded. Funding must benefit a wider community or groups with common objectives and purpose;
- Partnerships with other businesses, government and communities are encouraged, while promoting GDC's identity for its interventions;
- Funding agreements must outline expectations and deliverables on both sides (GDC will enter into a formal agreement – standard forms to be developed) and
- The process of allocating funds and grants must be open and transparent (grant application forms to be made available to all applicants).

REFERENCES

World Economic Forum and the Prince of Wales International Business Leaders Forum, 2002 online at http://www.weforum.org/pdf/GCCI/GCC_CEOstatement.pdf

"The Business Case for Corporate Citizenship" online at www.weforum.org/corporatecitizenship or at www.environment-risk.com

"The Power to Change: Mobilising board leadership to deliver sustainable value to markets and society", The Prince of Wales International Business Leaders Forum & SustainAbility, 2001.

Corporate Social Responsibility: ASOCIO (Asian- Oceanian Computing Organization) Policy Paper June 2004 online at http://www.weforum.org/pdf/GCCI/GCC_CEOstatement.pdf

United Nations Conference on Trade and Development. Disclosure of the Impact of Corporations on Society: Current Trends and Issues. New York: United Nations, 2004. online at www.unctad.org/en/docs/iteteb20037_en.pdf

The PR and Communication department and the Community Liaison team at GDC.

BIODIVERSITY CONSERVATION AND GEOTHERMAL DEVELOPMENT

Thecla M. Mutia
Geothermal Development Company Ltd, P. O Box 17700-20100, Nakuru, Kenya
tmutia@gdc.co.ke

ABSTRACT

Major geothermal prospects occur in fragile ecosystems constituting a rich tapestry of all forms of life and the ecosystems that they are part. Ensuring intra and intergenerational equity in geothermal development is critical for conservation of biological diversity. Relative to the variety of habitats, biotic communities and ecological processes in the biosphere, biodiversity is an important pre-requisite for all forms of life to exist as it provides valuable ecosystem services. Nevertheless, there exist several threats to biodiversity and biodiversity conservation including loss of habitat, overexploitation, pollution, and climate change. To mitigate this, several environmental concerns including binding, non binding and local agreements involved in achieving biodiversity conservation are reviewed in this paper with case examples from the Olkaria geothermal power project, situated within the Hells Gate National Park in Kenya.

Keywords: Biological diversity, biodiversity conservation, sustainable development

INTRODUCTION

One of the key components crucial in economic and social development is energy. The current energy exploration and use has resulted in environmental changes with significant local and regional effects, a concern that caught the attention of many countries in the Earth Summit. Today, more than 1.6 billion people worldwide have no access to electricity and approximately three billion people depend on traditional biomasses as their energy supply for cooking and heating (Advisory Group on Energy and Climate Change Report, 2010), hence a challenge. Biodiversity loss and global warming threats continue to place an increasing demand for environmental compliance hence the need for environmentally sound energy systems to attain global prosperity. Presently, the shift is toward clean renewable energy sources among which geothermal power is the most attractive because of its relatively benign nature (De Jesus, 1997). Enhancing the sustainability of geothermal development will therefore ensure viable energy for the future whilst maintaining the integrity of the natural environment.

The Kenyan rift, forming part of the eastern arm of the African rift, harbors the great wealth of geothermal resources in fragile and critical habitats. A unique success is the continued existence of the Olkaria geothermal power project amidst a complex self sustaining biophysical functional unit; the Hells Gate National Park in Naivasha. The challenge facing the Kenyan government is to continue developing the geothermal resource for power generation whilst maintaining and sustaining the delicate biodiversity, however several environmental management measures have been implemented with continuous follow-up to enhance conservation

Biodiversity Conservation: benefits and losses

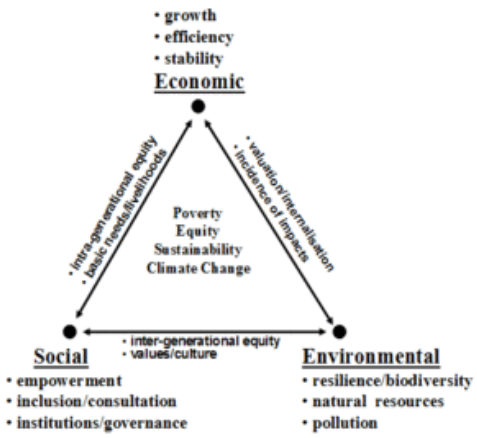

Figure 1: Sustainable development triangle (Modified from Munasinghe 1994a)

The manifestation of biodiversity is the biological resources (genes, species, organisms, ecosystems) and ecological processes of which they are part. Biological diversity is therefore essential in supporting human life, and is central to the relationship between man and nature. A number of ecological goods and services are directly and indirectly derived from biodiversity including air quality balance, determination and regulation of climate and biogeochemical cycles, environmental change indicators, environmental purification and protective services. Other biodiversity values include utilitarian for example, industrial raw materials and aesthetics.

In parallel with human development and economic expansion has come a greater reliance on products and resources originating from the world's biodiversity. However, this increase in the extent and range of use of biodiversity has generally not taken into account natural regeneration rates of biodiversity, and thus over-use has resulted in the

degradation of natural systems and loss of components of biodiversity. The major cause has been human mismanagement of biological resources often stimulated by mis-guided policies and faulty institutions resulting in habitat destruction, overexploitation, invasive species, pollution, climate change, human over population, and overharvesting.

Optimal utilisation and development of natural resources ensures both intra and inter-generational equity hence environmental sustainability (figure 1) and biodiversity conservation. The Brundtland Commission, 1987 defines sustainable development as development that ´meets the needs of the present generation without compromising the ability of the future generations to meet their needs´ (UNCED, 1992a). Sustainable development therefore is living within the Earth´s capacity at a given time and has been observed that economic policies that do not consider environmental concerns lead to deteriorated environments. On the other hand, environmental policies that ignore economic realities limit opportunities to raise resources for environmental rehabilitation and enhancement (International Chamber of Commerce, 1992).

In this light, sustainable development is not a moral call. It is a necessity for human and natural survival. A safe, environmentally sound, and economically viable energy pathway that will sustain human progress into the distant future is clearly imperative. It will require new dimensions of political will and institutional cooperation to achieve it.

BINDING AND NON BINDING AGREEMENTS

Binding, non-binding international and local significant guiding principles need to be integrated in any kind of development to foster sustainability. It is critical to understand and observe strict adherence to vital environmental legislation in the course of geothermal development in relation to exploration, drilling, power plant construction, operations and decommissioning. These legislations often specify standards with which the project must comply and sometimes may delay implementation due to lengthy licensing processes or public consultation requirements. Implementing agencies should guard against any environmental liabilities as they may have adverse financial implication on the total project cost. In this context, key regulations that need to be understood and observed include:

- **Environmental Impact Assessment regulations** (National legislation and guidelines, WB Operational policy **(OP) 4.01**, **OP/BP/GP 4.02**, Environmental Action Plan; **OP 4.07).**
- **National and donor emission standards for air, noise and water quality requirements** (WB guidelines on air and Noise emissions, WHO water quality requirement, National and local bylaws requirement, Water Resources Management; OP 4.09, Conventions on climate change)
- **Local and international legislation in relation to biodiversity conservation** incase the project is located in the critical habitats**. (WB OP/BP/GP 4.04,** Natural Habitats, Convention on Biological Diversity).
- **National and international policy on resettlement/relocation and compensation** of people if necessary. (**WB OP/BP 4.12,** Involuntary Resettlement, National Resettlement Policy).
- **Identification of key stakeholders and public consultation and disclosure** methods within the national environmental legal framework (**OD 4.20,** Indigenous Peoples**; and OPN 11.03,** Cultural Property, National disclosure methods**)**.
- **Occupational health and safety rules related to geothermal development.**
- **Local council bylaws.**

In Kenya, the Olkaria I (45Mwe) and II (70Mwe) geothermal power projects' development took place before the enactment of the Environmental Management and Coordination Act (EMCA), 1999. They were however implemented and have been operating in line with the legal requirements of the World Bank, World Health Organization (WHO), EMCA, 1999 and other existing legislations. Full EIA's were undertaken and appropriate environmental management plans put in place. The first experience in application of the national law on geothermal projects in Kenya was the Olkaria III Project and Olkaria II Unit 3 (35Mwe) (Ogola, 2005).

Convention on Biological Diversity, 1992

The Convention on Biological Diversity is a binding agreement that was inspired by the world community's growing commitment to sustainable development. Signed by 150 government leaders at the 1992 Rio Earth Summit, the Convention on Biological Diversity (CBD) is dedicated to promoting sustainable development (Article 1). It provides a comprehensive document underlining the principles (Article 2) of biodiversity conservation and sustainable use at the global scale with the objective to ensure sustainable use and conservation of biological resources, as well as fair distribution of benefits related to biodiversity and genetic resources (**www.cbd.int/convention**, 2010). The Convention also highlights the relationships between conservation, sustainable use of natural resources and sustainable human development. In ratifying the CBD, the

Parties to the Convention undertake a commitment to implement the Convention at a national level in contribution to achievement of its goals and objectives at a global level. Kenya ratified the Convention in the year 2000 (**http://www.cbd.int/information/parties.shtml**, 2010).

CBD and renewable energy

CBD has put a major emphasis on the need to factor sustainability into development choices to mitigate climate change, a significant threat to biodiversity conservation. According to the Inter-governmental Panel on Climate Change (IPCC), an average temperature rise of more than 1.5 to 2.5°C would put 20% to 30% species at risk of extinction. Renewable energy development is therefore encouraged due to its minimal effects on climate change, however CBD stipulates continuous mitigation and monitoring to minimise any likely effects on biodiversity (Secretariat for CBD, 2009).

Aim for conservation and no net loss of biodiversity

The biodiversity-related Conventions are based on the premise that further loss of biodiversity is unacceptable. Biodiversity must be conserved to ensure it survives, continuing to provide services, values and benefits for current and future generations. The International Association for Impact Assessment (IAIA), 2005 recommends the following approach to help achieve *no net loss* of biodiversity:

- Avoid irreversible losses of biodiversity.
- Seek alternative solutions that minimize biodiversity losses.
- Use mitigation to restore biodiversity resources.
- Compensate for unavoidable loss by providing substitutes of at least similar biodiversity value.
- Seek opportunities for enhancement.

BIODIVERSITY CONSERVATION IN GEOTHERMAL DEVELOPMENT

The current environmental measures for geothermal projects minimize habitat destruction and therefore, the loss of biological diversity. The measures include: i) an environmental impact assessment prior to project implementation that already integrates biodiversity considerations; ii) avoidance of rare, endangered or threatened species in earthworks; iii) minimization of openings; iv) directional drilling that allows compact work areas which are standard practices in geothermal development and minimize impacts on habitats (De Jesus, 2007). The recent procedure of redirecting emissions during well testing to avoid brine spray and defoliation proved helpful for projects in forest locations and is highly recommended (Tuyor, et al., 2005).

Chapter 9 of the Rio Declaration of 1992 declared that geothermal is an environmentally advantageous energy option basically due to its benign emissions. It is against this background that geothermal can be considered a green energy resource as it addresses the following key environmental concerns

Climate change

Losses in biodiversity are highly attributed to climate change, a global catastrophe resulting from global warming due to green house gas emissions. Today, climate change is a universal concern closely linked to energy utilization and sustainable development. The goal of the UN Framework on Climate Change Convention (UNFCC) of 1992 is the "stabilization of Greenhouse Gas (GHG) concentrations in the atmosphere at a level that would prevent dangerous anthropogenic interference with the climate system… within a time frame sufficient to allow ecosystems to adapt naturally..." (UN, 1992). Carbon dioxide (CO_2) emissions represent the main GHG known to cause global warming. In 2005, according to the G8 Conference (2005) about 200 scientists from thirty (30) countries discussed the latest research on climate change. They confirmed the link between the concentration of GHGs in the atmosphere and the increase in global temperature levels. A change of 2°C (3.6°F) was defined as the threshold to avoid the serious effects of global warming. This translates to a ceiling of 550 parts per million CO_2 equivalent by volume in the atmosphere (De Jesus, 2007). Among the known geothermal emissions, only carbon dioxide and methane are known to be GHGs. Their levels are however much lower from geothermal production compared to those of fossil fuels.

Kyoto Protocol, 1997 and Clean Development Mechanism (CDM)

The increase in deployment of geothermal energy will have a large net positive effect on the environment in comparison with the development of fossil fuels. This is in harmony with the Kyoto resolutions on global climate change. The convention requires developed countries and those in transition economies to reduce their GHG emissions by 5% of their 1990 level (UN, 1997). The agreement allows the joint cooperation of developed countries to abate GHGs and for industries to trade their emissions based on their permit ceiling. During

production, geothermal power plants emit insignificant amounts of CO_2, SO_2 and absolutely no nitrogen oxides in comparison to thermal plants. These small quantities from geothermal plants are not emitted during power production as a result of combustion but are natural constituents of a geothermal reservoir. The gases eventually vent into the atmosphere under natural conditions although at much lower rates (Goff, 2000). The nature of the geothermal reservoir and technology employed determine the amount of Non Condensable Gases that may be released into the atmosphere. For instance, binary plants emit virtually no gases because it is a closed loop system using heat exchange method. Dry steam and flashed steam plants emit water vapor containing these gases. However, the process of re-injecting the geothermal fluids back into the reservoir diminishes the possible release of gases into the atmosphere. In low temperature utilization, CO_2 found in geothermal fluids could prove beneficial in direct use greenhouse applications as a growth stimulant. Studies indicate that increased CO_2 concentration from the normal level of 300ppm to approximately 1000ppm can raise crop yields by up to 15% (Dunstall and Graeber, 2004). The Oserian Flower Farm in Kenya operating a geothermal plant with an installed capacity of 4Mwe and 16 Mwt successfully injects CO_2 in the greenhouses to increase the rate of photosynthesis and production.

CDM, a concept that allows developed countries to offset their GHG emissions by investing in emission reduction projects in developing countries enables emission reduction targets to be achieved cost effectively while developing countries receive sustainable development and technology transfer benefits. The Olkaria III Phase II 36MWe (Orpower 4) geothermal project in Kenya is a recipient of a *CDM* facility for the period 2009-2015 with an average emission reduction of 171,265 tonnes of CO_2. With the expected capacity expansion plan for geothermal energy in Kenya, most of the earmarked geothermal projects are expected to be *CDM* or comply with the requirements of the next protocol (Ogola, 2010).

Critical Habitats

Most geothermal resources in the world are located in remote scenic, wild and protected areas hence a challenge to developers. Current international opinion however indicates that authorities now recognize that development may be considered in protected areas. The International Union for the Conservation of Nature (IUCN) prescribes the exclusion or the declaration of special zones for areas that are needed to maintain services to human settlements (IUCN, 1986).

Geothermal development and wildlife conservation

Kenya's geothermal resource is located within the Rift Valley. Some of the fields with geothermal prospects are in densely populated areas, while others are within national parks. The Olkaria power plants (area 80km^2) located in Hells gate National Park (68km^2) are a typical example of power development and wildlife conservation compatibility. This area was gazetted as a park in 1984 after construction of Olkaria I power plant. This has been perceived as the best decision made by the conservationist at that time in view of the fact that the area was going to be opened up following the construction of a power plant. The land is characteristic of rugged terrain, volcanic hills, valleys, gorges, boulders and highly altered weathered rocks. Vegetation is mainly shrubs and short trees dominated by several species of *Acacia* and *Euphorbia*. There are also a wide variety of succulents in the area and some unique plants capable of withstanding high temperatures. Some of the seen animals include Maasai giraffe *(Giraffa reticulata)*, warthogs (*Phacochoerus aethiopicus*), zebras (*Equus burchellis)*, Coke's hartebeest *(Alcephalus buselaphus)*, thompson's (*Gazelle thomsonii*) and grants gazelles (*Gazelle grantii)* and buffaloes (*Syncerus cafer)*. Others include water buck, baboons, monkeys, African jackal; hippopotamuses, and leopards with about 103 bird species including vultures, tawny eagles, verreaux's eagles, augur buzzards, secretary birds and swifts. The land is mainly used for geothermal activities, wildlife conservation and ranches. Lake Naivasha, a freshwater lake that gained international Ramsar recognition in 1989, and Mt. Longonot are major scenic sites within close proximity attracting both local and international tourism, education and research.

As part of the Environmental Impact Assessment recommendations, Kenya Wildlife Service (KWS) and KenGen have since then developed a Memorandum of Understanding (MoU) to govern geothermal power operations within the park. Orpower 4 (Independent Power Producer) also has a MoU with KWS. The Geothermal Development Company (GDC) Limited of Kenya which kicked off its geothermal development activities late 2009 is also seeking to establish a MoU with KWS and KenGen to facilitate conservation efforts against development in bid to develop the underway 140Mwe geothermal power plant at the Olkaria IV field. KWS and other conservationists major concerns due to geothermal development in the park include; effluent disposal, emissions, animal accidents (traffic), habitat loss, blockage of seasonal animal migration corridors, noise and odour. To minimize such impacts, several studies which included establishment of animal migratory routes, breeding grounds, tourist circuits, protected plants and wildlife species were carried out and implemented. Operations have maintained conservation of the unique scenic features and wildlife species within the park. Steam pipelines on major animal routes are looped to provide easy movements for the wildlife such as

giraffes within the park. High voltage lines and silencers are a potential danger to birds and as such they were constructed to avoid right angle crossing of known bird flying routes. To avoid animal accidents in the park, a speed limit of 40km/h is observed while game proof fencing is done to keep the animal away from brine pools.

In managing the park KWS personnel monitor the patterns of animal movement and carry out quarterly animal census in addition to their regular research. Environmental Audits are also conducted by KWS within the park and follow-up reports with mitigation measures to be implemented are sent to the KenGen environment offices for action. The geothermal power plants have therefore not altered significantly the ecology of the surrounding National Park.

Figure 2: Olkaria II 105 MWe Plant, Naivasha Kenya

Generally, an average geothermal power plant is estimated to use between one to eight (1-8) acres of land per megawatt, compared to 5-10, and 19 acres per megawatt for nuclear and coal power plants respectively. On the other hand, large hydropower requires over 275 acres of land per megawatt for an adequate size reservoir (De Jesus, 2007). However, the effect of geothermal resource development on land depends on a number of interacting factors, namely characteristics of reservoir, type of extracted fluid, type of application, size of the plant and terrain. In addition, ancillary supportive infrastructure for geothermal resource exploitation such as access roads and power transmission lines imposes additional impact on the terrestrial environment.

The declaration of geothermal projects as ecotourism sites in Bacon-Manito, Albay-Sorsogon in the Philippines because of its heart of the geothermal field (De Jesus, 2007) is proof that the utilization of geothermal energy does not contribute to the earth's deterioration. Other sites include the Hoshino, a resort in Japan using geothermal heating, the Great Geysir, the Surtshellir lava cave, the Deildartunguhver hot spring of Iceland and Rotorua of New Zealand, to name a few.

Toxic Wastes

The concern for toxic wastes and transboundary movements led to the signing of the Basel Convention (1989). Under this treaty everyone is encouraged to manage the wastes as close as possible to the source of its generation. Geothermal operation can be compliant with this international prescription as geothermal effluents in liquid dominated fields may be reinjected back into its reservoir, ensuring in situ waste management. Reinjection has been adopted for brine disposal in more than 44 fields (Stefansson, 1997). It is a standard practice that Kenya has started adopting to prevent contamination of the environment. The mineral extraction of silica, zinc, lithium, manganese, caesium, rubidium and rare metals has been studied in Salton Sea and Mammoth Springs in California, U.S.A. with some results (Bloomquist, 2006). Sorption membranes using resins to remove boron have been reported (Yilmaz et al., 2005). Hypersaline brines and supersaturated steam may contain high levels of chemicals that can generate solid wastes. These wastes may be reduced to soluble forms for reinjection. Thiobacilli is used as a bioremediation method to dissolve, separate or immobilize hazardous geothermal sludge (De Jesus, 2007). Countries utilizing geothermal energy also adopt best practices in the management of its solid wastes and no utilizing country has been reported to export wastes to other countries.

Displacement of people

Infrastructure projects have yielded global concern about dislocation of people and the related social costs. To address the socio-economic and physical dislocation in cases when these are inevitable, appropriate involuntary resettlement packages must be negotiated with the affected households, to include replacement of structures, amenities and livelihoods. De Jesus, 2007 avers that the objectives of resettlement are to: i) relocate houses to areas where residents are not exposed to physical, health, and security hazards; ii) ensure that affected households are fully and justly compensated for any crop and property damages; and iii) help the relocated households regain and improve their standard of living on the settlement sites. In negotiating with the affected population, the community is assisted in gathering facts and perceptions, understanding their situation, developing common solutions and agreeing on a mode of collaboration with the geothermal developer.

Geothermal Projects in Kenya, have adopted the same practice with the involvement of government surveyors to assist in giving a baseline resource value upon which negotiations are open and conducted with the displaced persons.

Indigenous People (IP)

The people´s way of life and origin is vital in defining their identity and thus needs special attention based on international consensus. The UN Declaration on the Rights of Indigenous Peoples (IPs) affirms that IPs are equal to all other people and that the UN is convinced that the IPs have suffered historic injustices through dispossession of their lands (UN, 2007). Thus, the UN recognizes the urgent need to respect and promote the inherent rights of the IPs to their lands, territories and resources and their need to have control over the developments affecting them. Issues such as encroachment of geothermal projects into the ancestral lands of indigenous communities, desecration of their sacred sites and the destruction of IP traditional ways of life are due to the growing awareness of the IPs as distinct peoples who have the right to self-determination. The current practices in geothermal development and utilization are compliant with these prescriptions of the UN declaration. In Kenya, social benefits have been derived from geothermal development along with cultural conservation. The Olkaria geothermal project lies within the vicinity of the Maasai community who form the indigenous community of the area living at the periphery of the project on private land. Their cultural aspects have to a lesser extent been affected by geothermal operations due to their minimal interactions with the proponents. However, through corporate social responsibility implemented by the geothermal developers several benefits are accrued to the locals including piped water services, employment, education, transport, social afforestation and health facilities. The geothermal proponents foster a bottom – top approach where they engage the communities' voice in any kind of planning to ensure social acceptability of their projects, consequently encouraging participatory rural appraisal and cultural acknowledgement and respect.

CONCLUSION

Geothermal energy is an environmentally advantageous energy option basically due to its minimal environmental impacts. Understanding the nexus between biodiversity conservation and geothermal development presents a unique case of compatibility thereby promoting environmental sustainability. This is viable with appropriate integrated environmental advocacy including monitoring, mitigation measures and legislation with local and international support. With the global call for protection and conservation of the environment, investments in geothermal projects must be given support as they are the next best alternative to green the economy thus fostering biodiversity conservation.

ACKNOWLEDGEMENTS

The author would like to thank colleagues at GDC, KenGen, KWS and UNU-GTP Iceland for their fruitful information, discussions and papers referred to herein.

REFERENCES

Basel Convention on the Control of Transboundary Movements of Hazardous Wastes and Their Disposal, March 22, 1989.

Bloomquist, R.G; 2006, Economic benefits of mineral extraction from geothermal brines. Washington State University Extension Program, 1-6.

Brundtland Commission; 1987, *Our Common Future*, Oxford: Oxford University Press. ISBN 0-19-282080-X 383pp

Convention on Biological Diversity, 1992, Convention on Biological Diversity http://www.cbd.int/convention/, Updated on 2010-08-04

Convention on Biological Diversity; 1992, List of Parties, http://www.cbd.int/information/parties.shtml, Updated on 2010-08-04

De Jesus C. A; 1997, *Environmental Sustainability of Geothermal Development*. Energy Sources, 19: 35 – 47

De Jesus, C. A; 2007, *Environmental aspects of geothermal utilisation: a global perspective*, Short Course on Geothermal Development in Central America – Resource Assessment and Environmental Management, UNU-GTP and LaGeo, San Salvador, El Salvador, 25 November – 1 December, 2007. 1-10

Dunstall, M and Graeber, G. 2004. *Geothermal carbon dioxide for use in greenhouses*. Geo-heat bulleting Vol.18, p 1-14.

Government of Kenya; 1999, Environmental Management and Co-ordination Act of Kenya, government printers, Nairobi, Kenya

Goff, S. 2000: *The effective use of environmental impact assessments (EIAs) for geothermal development projects.* Proceedings of World Geothermal Congress 2000 Kyushu - Tohoku, Japan, May 28 - June 10, 2000.

International Association for Impact Assessment; 2005, *Biodiversity in Impact Assessment*, IAIA Special Publication series No. 3, pp 65

International Chamber of Commerce; 1992, *Policy paper No. 4: Energy and the protection of the atmosphere*. Report presented to UNCED, Brazil, 4 pp

International Union on Conservation of Nature (IUCN); 1986, *Management of protected areas in tropics.*

Munasinghe, M; 1994a. '*Sustainomics: a transdisciplinary framework for sustainable development'*, Keynote Paper, Proc. 50th Anniversary Sessions of the Sri Lanka Assoc. for the Adv. of Science (SLAAS), Colombo, Sri Lanka. *Policy*, p13-28

Ogola, P. F. A; 2005, *Environmental and social considerations in geothermal development*, Workshop for Decision Makers on Geothermal Projects and Management, UNU-GTP and KenGen Kenya, 14th -18th November, 2005,1-12

Ogola, P. F. A; 2010, *Geothermal energy, climate change and gender in Kenya***,** Proceedings World Geothermal Congress 2010 Bali, Indonesia, 25-29 April 2010

Secretariat of the Convention on Biological Diversity (2009). *Biodiversity, Development and Poverty Alleviation: Recognizing the Role of Biodiversity for Human Well-being.* Montreal, pp 52. http://www.cbd.int/doc/bioday/2010/idb-2010-booklet-en.pdf

Stefansson, V; 1997, *Geothermal re-injection experience*. Geothermics, 26, 99-139.

Tuyor, J.B. et al., 2004: *Impacts of geothermal well testing on exposed vegetation in the Northern Negros Geothermal Project*, Philippines. Geothermics, 34, 252-265.

United Nations Conference on Environment and Development; 1992a, *The Global Partnership for Environment and Development*. UN Press,Geneva

United Nations Secretariat–Generals; 2010, Advisory Group on Energy and Climate Change Report: Energy for a Sustainable Future, summary report and recommendations, Newyork7 - 9

United Nations; 1992 a. UN Framework on Climate Change.

United Nations; 1992 b. UN Conference on Environment and Development.

United Nations; 1997. Kyoto Protocol on UN Framework on Climate Change.

United Nations; 2007. UN Declaration of the Rights of Indigenous Peoples.

Yilmaz, I., Kabay, N., Brjyak, M., Yüksel, M., Wolska, J., Koltuniewicz, A; 2005, A submerged membrane-ion exchange hybrid process for boron removal. 2nd Membrane Science and technology Conference of Visegrad Countries, Poland, Sept 18-22, 2005.

THE NEED FOR ENHANCED ENVIRONMENTAL AUDITING OF GEOTHERMAL PROJECTS. A CASE STUDY OF KENYA ELECTRICITY GENERATING COMPANY LTD (KENGEN).

Ms. Pacifica F Achieng Ogola,
Environment Officer, Kenya Electricity Generating Company Ltd, P. O. Box 47936 00100, Nairobi, Kenya.

ABSTRACT

Increasing legislative, financial and community awareness of environmental issues have led to the rethinking of the role and responsibilities of government and private sector in environmental management in Kenya. Consequently, both private and public organizations are forced to be accountable for their actions. In order to guard against environmental litigation and liabilities, organizations are not only adopting voluntary environmental management systems like ISO 14001:2004 but doing regular environmental audits. The implementation of voluntary standards like ISO is also included in the government performance contracts of all government agencies. Financiers/lending institutions are also insisting on environmental audits to avoid the risk of investing in projects with potential environmental liabilities and public rejection.

In order to increase capacity in power generation, KenGen has opted for geothermal capacity expansion. These geothermal projects will be implemented in a setting of heightened environmental awareness and legislation. Moreover, environmental issues of geothermal development are not obvious to the environmental regulators and elites outside geothermal field.

The paper discusses the need for enhanced environmental responsibility and audits in the implementation of KenGen geothermal projects. The paper also highlights the company experience in auditing and its role in supporting/influencing the regulatory environment in which the planned geothermal projects will be implemented.

Key words: Environmental Auditing, Geothermal Projects, KenGen

INTRODUCTION

Over the years, considerable efforts have been made in development, generation and utilization of hydropower, thermal, wind and other forms of renewable energy in Africa. However, little effort has been made in development of geothermal energy and hence information on geothermal energy is not easily known to most elites and regulators outside the geothermal field. In contrast, basic environmental and technological information about other forms of renewable and thermal energy are often well known and understood.

To enhance capacity expansion in Kenya, KenGen in its new strategic vision has made deliberate effort to focus on geothermal capacity expansion. The government of Kenya also allocated Kshs 54 billion (USD) in the current budget (2008/2009) for geothermal development to support the strategy. The strategic direction for the company and the country as a whole in energy development is clearly geothermal. The geothermal strategy will be implemented in an environment of heightened environmental awareness in Kenya. The increased knowledge and awareness of environmental issues have led to a rethinking of the role and responsibilities of both government (and their associated agencies) and the private sector.

To demonstrate environmental responsibility, the Kenyan government enacted a National Environment Management and Coordination Act (EMCA 1999) and associated regulations. The new legislation created the National Environment Management Authority (NEMA). Among the new regulations created was the Environmental Impact Assessment (EIA) and Environmental Audit (EA) regulations 2003. Whereas EIA is meant to identify significant impacts at the planning stage, the audit regulation was drawn with the aim of ensuring that projects comply with the recommendations of the EIA and good environmental management practice and that projects implemented after the formulation of EIA regulation put in place measures to comply with environmental requirement.

In the wake of the new regulations and heightened environmental awareness in the country, both private and public sectors are introducing environmental management systems to ensure that they are systematically setting policies for continual improvement in environmental performance and are achieving the policy objectives. Furthermore, voluntary accreditation schemes like ISO 14001:2004 have been introduced in the government performance contracts to enable organizations obtain external confirmation of the adequacy of their environmental management systems and recognition that they are operating such systems. Consequently, the resources spent by both sectors on environmental management and Corporate Social Responsibility (CSR) has

increased, and both businesses and government bodies are forced to look for more cost-effective ways of dealing with compliance issues through environmental auditing.

Environmental awareness among financial institutions both nationally and internationally has also increased and more stringent. The pressure and scrutiny by these institutions has given the government and businesses the impetus to give environmental issues closer consideration. The World Bank has also developed guidelines for environmental audits in industrial projects, which is documented in the pollution prevention and abatement handbook 1998. The guidelines can be used in auditing geothermal project expansion activities.

According to United Nations Environment Program (UNEP) report on environmental due diligence of renewable energy (including geothermal), procedures for environmental due diligence of Renewable Energy Technologies (RETs) are poorly defined and financiers must often adopt *ad hoc* procedures for environmental review. Although most renewable energy technologies are environmentally sound in theory, all of them can have negative impacts on the environment if poorly planned hence the need for auditing and mitigation. The UNEP report has well define criteria for environmental due diligence for geothermal power projects.

Consequently, environmental audit though still at infancy stage, is becoming the next important environmental management tool after EIA in Kenya and the world at large.

DEFINING "ENVIRONMENTAL AUDITS''

There are several definitions of environmental audits one of them is as described by the International Chamber of Commerce (ICC)**:**

The systematic examination of the interactions between any business operation and its surroundings. This includes all emissions to air, land, and water; legal constraints; the effects on the neighboring community, landscape and ecology; and the public's perception of the operating company in the local area. Environmental audit does not stop at compliance with legislation. Nor is it a 'green-washing' public relations exercise. Rather it is a total strategic approach to the organization's activities.[4]

In a nutshell, the short term objectives of the audits are to determine compliance with environmental laws and regulations, to determine conformance with internal environmental policy, to assess strengths and weaknesses of a facilities environmental management systems, and to assess level of environmental awareness and communication while the long term objectives are to improve environmental compliance and management, and to build supporting financial programs and budgets appropriate for environmental compliance requirements.

Types of environmental audits vary in scope and objective. Types of environmental audits as used in the context of this report include the following:

- Environmental due diligence or liability audits
- Environment Management Systems (EMS) Audits (ISO 14001:2004)
- Regulatory compliance audits
- Environmental Management Plan Audit (as recommended in the EIA)
- Financial audits of environmental performance

The above audits can be combined. Environmental audits are undertaken by independent environmental or specialist consultants or suitably trained internal company staff, depending on the purpose of the audit.

The nature and scope of details can be defined in various ways; different kind of individuals skills are involved; terms of reference for examination may differ; approaches and techniques are still continuing to emerge; and there are different ways of reporting the results and suggest ways for improvement.

ENVIRONMENTAL AUDITS EXPERIENCE IN KENGEN

Despite the fact that EIAs were done prior to implementation of power projects in KenGen, environmental audits were not done until the year 2003 after the establishment of the environmental audit and compliance enforcement section. Just like other departments in the company, the environmental audit section must understand its new role in achieving geothermal growth within the environmental legal framework and ensuring that the projects are regularly audited to enforce compliance and avert liability.

The company has therefore undergone regulatory compliance audits since 2003, thus complies with environmental audit regulatory requirement of self-audits. The reports are submitted to NEMA for scrutiny on an annual basis. It is worth noting that the initial regulatory audits were done under some legislation gaps which were bridged after 2006 i.e. Water Quality Regulation 2006, Waste Management Regulation 2006 (both came

4 www.iccwbo.org/policy/environment/

into force in April 2007) and more recently Air Emission Regulation in 2008. Copies of the audit reports are also submitted to the Energy Regulatory Commission (ERC) whose mandate includes ensuring environmental health and safety compliance in the electric power industry. The Energy Regulatory Commission despite developing audit protocols for geothermal projects are yet come up with specific environmental standards for geothermal projects and the sector as a whole as these were omitted in the above regulations. The role of environmental audit section under the regulatory management division is to influence formulation and publishing of these standards.

Most recently, the company underwent an EMS ISO 14001:2004 certification audits. The audits which were conducted by Kenya Bureau of Standards are expected to continue biannually while internal audits are expected on a quarterly basis. The implementation of ISO 14001:2004 began in 2007 and is in its final stages. Under ISO 14001:2004 management systems requirements, all divisions identified and documented their significant aspects, objectives and targets, developed environmental management programs with timelines and documented operational procedures for controlling the significant aspects. Duties are responsibilities of environmental management within each division/section have been allocated. The ISO 14001 approached has improved not only documentation of environmental processes and procedures but heightened the need for compliance.

External environmental audits on the company in the recent past include; Energy Regulatory Commission (ERC) audits for regulatory compliance, Kenya Bureau of Standards (KEBs) audits for EMS ISO 14001:2004, one environment and risk assessment audit in 2007 (for insurance), at least two environmental due diligence (for the Initial Public Offer (IPO) and the shelved Secondary Public Offer (SPO) done in 2006 and 2007 respectively. This was in bid to offload Government shares in KenGen to the public through the Nairobi Stock Exchange (NSE) (30% in the IPO and 19% in the SPO). In the due diligence process, environmental audit reports formed the main reference documents besides the EIAs. The company has also continued submitting annual environmental audit reports to the World Bank Clean Development Mechanism (CDM) group for the Olkaria II unit III Geothermal project. The World Bank also subjected the same project to an environmental audit in 2004 as pre-funding condition since it is an extension of an existing project (Olkaria II). Lending institutions will often require an environmental audit in order to avert the risk of environmental liabilities and to assess appropriate cost of mitigation on unavoidable impacts. In the past two-years external financial auditors of KenGen have also captured environmental performance review and compliance audits as part of their audit program.

KenGen is currently sourcing for funds through a financial arranger to finance the upcoming projects including geothermal. Part of the financial arrangement process includes environmental due diligence on past and future projects. Since the new corporate strategy is dominated by geothermal expansion, the financiers are keen on environmental performance of geothermal projects. To objectively assess this, all environmental audit reports and EIAs are currently being reviewed by the assessor for financial arranger.

In this environment of intensified environmental audits and a corporate strategy which focuses on geothermal expansion, KenGen needs to take a proactive role in ensuring enhanced environmental compliance of its geothermal projects through regular monitoring and audits. The need for this compliance as based on the company's experience is further discussed below.

THE NEED FOR ENHANCED AUDITING OF GEOTHERMAL PROJECTS IN KENGEN

Locations of geothermal plants

Most geothermal manifestations occur within protected areas and Kenya is not an exception. Just like the Olkaria Geothermal Plants which are located in Hellsgate National Park, the new geothermal potential areas are also located in wildlife and/or forest protected areas e.g. Eburru, Menengai, Longonot, Suswa among others. Opening up of new areas for geothermal expansion within protected areas will require enhance auditing to ensure that all the geothermal activities are controlled and monitored as required. Since most of these spots act as retreat areas and scenic tourist sites, the environmentalists and the financiers alike will be interested in the environmental management plan set-up throughout the project life. The environmental impact assessment and environmental audit recommendations will be expected to create harmony with the wildlife conservation, forest management, tourism and geothermal exploitation. To ensure compliance, both internal and external environmental auditing must be conducted and most significant aspects unique to each area identified and controlled throughout the project cycle.

Need for holistic environmental management through audits

There is a tendency for the EIA to focus on scientific, ecological and social impacts of geothermal projects. While these are important, audit results have shown that other significant environmental aspects are usually

overshadowed. Thus environmental management as stipulated in the EMPs is not holistic. For instance, most common omissions in the EIAs captured as significant aspects during audits, include energy consumption (office and power station), paper consumption, domestic water and waste management, sewage water management, ergonomics, house-keeping, water conservation, emergency preparedness procedures during operation, motor vehicle fuel use and consumption and consumption of other materials etc. Since geothermal energy is considered green, its total impact on environment beyond the EIA must be understood and mitigated. Regular environmental audits must therefore be conducted to ensure that the operators are collecting the relevant environmental data as prescribed, and that the data is properly documented and available and total impact on environment accounted for.

Bridging of weaknesses and gaps in environmental legislation and policy

The Kenyan regulation is relatively new and so is the National Environmental Management Authority (NEMA) that was established in 2003. Though NEMA plays a critical role in approval of projects and in this regard geothermal projects, a lot is still not known about geothermal by the regulators. The NEMA officers who are charged with the issuance of licenses and review of environmental audit reports are usually bogged down with documentation of several other permits without necessarily looking into the details of the EIA or audit reports. The new regulatory management section of KenGen strives to ensure EIA and Environmental Audit reports are not just submitted and shelved but helps the permit writer to understand the operations of geothermal energy in totality before any approval is given. KenGen therefore have opened channels of communication with the regulator and makes effort to present projects to the regulator during or before submission. Some geothermal terminologies which are not understood by the regulators are also explained.

Some of the national regulations as discussed above have not captured applicable requirements for geothermal projects and power sector in general. The task of creating power industry specific environmental regulation therefore lies with the Energy Regulatory Commission (ERC). These gaps should be bridged to ensure value adding auditing. The results of the past audits and monitoring records can be used to create suitable standards based for Kenyan geothermal fields and acceptable international best practice.

The regulator cannot develop these standards without a clear understanding of geothermal operations. The regulatory management division in KenGen and environmental audit section in particular now intends to see the audit results being used in identification of gaps and weaknesses in the implementation of the environmental laws in as far as power projects and especially geothermal projects are concerned in order to provide in-put or further clarifications in future reviews.

Establishment of strategic partnerships with key institutions and groups

The road to achieving the corporate strategy will not be smooth without strategic partners. Present geothermal audits and impact assessment studies must also identify complexities of, and cooperation required in, environmental governance of geothermal projects. This shall include identification of environmental issues which cover more than one institution, and the need to harmonize issues among these institutions, increase coordination and cooperation among them, and to ensure adequate communication and legal enforcement in as far as geothermal projects are concerned. Previously, under the Olkaria Geothermal project, KenGen mainly dealt with the Kenya Wildlife Service (KWS), however, with the expansion of geothermal projects outside Olkaria, new government institutions like Kenya Forest Service (KFS) are now playing a major role in access to geothermal sites as in the case of Menengai and Eburru geothermal project among others. As a result, KenGen has to develop a new Memorandums of Understanding (MoU) and license arrangements with stringent environmental management conditions. The consequences of going against the conditions stipulated in the license include withdrawal of the license. Though geothermal operations might not be evicted from the forest or wildlife conservation area, prudent environmental management as part of good governance will be required on the part of KenGen.

Currently, the audits also include checking compliance with conditions stipulated in the MoU between KenGen and Kenya Wildlife Service (KWS), community complaints records etc. similar audits will be done under the new MoU and license agreements with the KFS.

Overspecialization of environmental experts

In most instances, environmental professionals are always blinded by their expertise and often pay less attention to other fields. The environmental audits create opportunity for different experts coming together on a regular basis to inspect diverse environmental aspects of the project thus giving a broader knowledge of information. Environmental audit teams in KenGen are selected from different professional background, which include various environmental disciplines, engineers, human recourse officers, finance officers among others. The

multidisciplinary approach that has now been adopted through the EMS ISO 14001:2004 system is expected to give a holistic approach to environmental management in the company. The role of each division in environmental management has been identified, documented and tasks assigned to all persons whose activities impact on environment. Environmental audits can thus be used as a means to enhance capacity development in environmental management throughout the company.

Impact of environmental management on KenGen share price in the Nairobi Stock Exchange (NSE)

Since the turn of the new millennium, several companies in Kenya started trading freely in the Nairobi Stock Exchange. The highest entry into the Nairobi Stock Exchange was witnessed after the successful KenGen IPO (Initial Public Officer), which was concluded in May 2006. Companies that followed the KenGen IPO include Safaricom Ltd, Scan Group, Stanbic Uganda, Access Kenya, Kenya-Re, and Eveready among others. KenGen's entry into the stock market mandates it to publish and circulate annual reports to shareholders with a disclosure on environmental management. As part of preparations for the IPO and SPO, two environmental due diligence were conducted to assess the company's credibility in environmental management. During data collection for environmental due diligence, it was easy for the lawyers to identify risks associated with hydro and thermal power plants than with the geothermal plants. Previous environmental audit reports played a key role in highlighting some of the environmental concerns associated with geothermal plants.

Potential environmental catastrophes can have a direct impact not only on the company image but on the share price, hence the emphasis on environmental risk assessment and emergency preparedness in the due diligence process. The some of the key areas assessed during the due diligence include type community complaints, environmental litigation in court, notices from the environment regulators, previous emergency situations, possibilities of material liabilities, contractual liabilities, correspondences with regulatory authorities, health and safety, insurance and general expenditure on environmental safety, risk management among others.

Geothermal Clean Development Mechanism (CDM) projects

A meeting of the framework convention on climate change in 1997 established the Kyoto protocol, which sets firm targets for green house gases emissions for developed countries. Also agreed at Kyoto is clean development mechanism (CDM) which allows developed countries to meet targets for reducing emissions by gaining certified credits from projects undertaken in developed countries. The twin objectives of CDM are emission reductions in developed countries and accelerated sustainable development in developing countries.

Geothermal projects are classified as potential CDM projects. Clean development mechanism is thus an impetus to adoption of geothermal energy in Kenya. However, to meet the CDM criteria, a project has to satisfy a number of requirements; such as environmental, technological among others. A successful project is one which links energy and socioeconomic aspects, meets needs, uses appropriate technology, is reliable, sustainable and economically viable. Olkaria II unit III is a classic Kenyan example of such. Currently, Olkaria II has an installed capacity of 70MW consisting of two units of 35MW each. The project has potential of an additional third unit of 35MW which will use the excess steam. The Unit III component of the project is expected to generate 125,000 tCO2-equivalent annually up to 2014and is expected to start generating CERs by October 2010.

Since the acceptance of the project by World Bank and UNFCCC as a potential CDM project in 2006, KenGen has been submitting environmental audit reports to the bank on an annual basis and has continued working on the social component of the project. Currently, an independent validator has been appointed to certify the emission reductions that will be generated from the project. Once again, all environmental audit reports of geothermal operations were collected for scrutiny. In order to submit sound CDM projects that can pass validation and verification processes, the evidence of continual improvement in the current project must be provided. Environmental auditing is expected to bring about continual improvement and KenGen hopes that the systematic improvement of environmental management of KenGen geothermal projects will be seen in the audit reports. Continual improvement can only be achieved through regular auditing and implementation of the mitigation.

Lessons learnt from the current geothermal CDM project must be incorporated in the project idea note (PIN) or project design document (PDD) of the future geothermal CDM projects. Lessons from environmental audits will also act as valuable source of information to guard against penalties of non-compliance with the monitoring and project performance requirements.

If a company has no robust environmental auditing systems of CDM projects in place, it will not meet the CDM requirements. Currently there is a need for capacity building in KenGen for monitoring and auditing CDM projects as the company plans to generate CERs from the proposed geothermal projects

Public accountability & enhance stakeholder relationship

The new geothermal expansion strategy will mean opening up of new areas with different environmental set-up from the Olkaria Geothermal project. The Company is more likely to meet more organized communities with different cultures and demands from the Maasais of Olkaria. The expansion of geothermal projects will increase interaction with these communities and the the public at large. Thus the enhanced environmental audits should start as soon as drilling works starts. The audits of the new projects should be flexible and dynamic and try as much as possible to collect new information, which is unique to the area other than assuming that the outcome will simply be the same as Olkaria geothermal project. If properly controlled, accountability will be enhanced and conflict with the local community reduced.

Review of the actual operating environmental performance of the plant in relation to its original design parameters.

As the geothermal power plant ages, the performance decreases and the environmental parameters as designed change. The environmental audits should assess the plants performance in the relation to the age and identify deviations from the original design parameters. Some of the environmental audit considerations at this stage should include inspection of the emergency management equipment, waste water facilities, plant efficiency and its ability to cope with the risks, environmental concerns arising from operation and maintenance of the plant, occupational health & safety of workers among others. The environmental audit should recommend energy efficiency, technology review and optimization of resources where necessary.

CONCLUSION

KenGen capacity expansion strategy will require proactive regulatory management of all aspects of geothermal development and especially environmental management. With the new regulatory management division and a well defined environmental section in place, the company will be able to provide leadership to the regulators and the relevant ministries. The company has already made a stride in improving its environmental management system by adopting the ISO 14001:2004 standards. As part of continual improvement process, all divisions will be expected to identity two best practices in environmental management to improve their procedures in bid to control significant aspects. An annual budget is provided for implementation and maintenance of the system.

Despite the fact that annual environmental audits is a mandatory legal requirement for companies, the pressure to do so is very low because the NEMA does not have manpower and capital to enforce the regulation. KenGen has taken a proactive role in engaging NEMA and other stakeholders in its environmental undertakings. This engagement has opened up channels of communication which will be important in implementation of future projects and developments of new environmental standards. KenGen also implements relevant environmental regulations as good environmental management practice.

Environmental audit is at a crucial stage of development as a disciple in Kenya and its future will be shaped by standards that environmental professionals will evolves. There is still need for capacity building for auditing geothermal projects especially where the audits are external (done by a third party who may not understand all the intricacies of geothermal operations). KenGen is expected to play a major role in opening up geothermal as a known and leading alternative source of energy.

STATUS AND STRATEGIC FRAMEWORK IN GEOTHERMAL DEVELOPMENT IN ETHIOPIA

Solomon Kebede
Geological Survey of Ethiopia
Geothermal Exploration and Assessment Core Process
P.O.Box 40069, Addis Ababa, Ethiopia, e-mail solo450354@yahoo.com

ABSTRACT

The significance of Geothermal Power within Ethiopia has long been recognized. Under a programme that began in 1969, geo-scientific studies have been conducted in a number of Ethiopian fields and over sixteen areas have been identified in the Ethiopian Rift Valley to have Geothermal Resources suitable for electricity generation. From these areas it is recognized that a total of about 5000 MWe geothermal energy could be developed. So far deep drilling has been undertaken in Aluto Langano (1982 to 1985) and Tendaho (1993 to 1998) and detailed surface exploration has been nearly completed in four other areas. A 7 .3 MWe net capacity pilot plant has been installed at Aluto, currently generating about 5MWe. Feasibility study for the expansion of the Aluto Langano Geothermal power has been recently completed with the Japanese Overseas Development Assisstance. The study indicated expansion of the Aluto Geothermal power to additional 35MWe is feasible.

Accordingly, as an initial step to develop the 35MWe, it is planned to drill four deep appraisal wells in 2011 with the Japanese technical assistance and the World Bank loan. The government encourages private sector investment in Geothermal exploration and development. Attractive feed in tariffs and incentive packages are in the process of being implemented.

Within the Ethiopia's long range power plan, geothermal is now recognized as offering an important (potential) input to the Ethiopian grid as it is base-load and climate independent. Irrespective of future hydro developments, geothermal's contribution to energy security at times of drought is considered critical. The generation development plan consists mainly of hydro projects. However generation from Wind and Geothermal power plants are foreseen to compliment the hydro. By 2015 it is planned to generate 75 MWe geothermal power from Aluto Langano and by 2018 it is anticipated to generate a total of 450 MWe from five other geothermal areas in the Rift. The order of priority for geothermal development in these areas is: Aluto Langano, Tendaho, Corbetti, Abaya, Dofan-Fantale and Tulu Moye

INTRODUCTION

Ethiopia started long-term geothermal exploration in 1969. Over the years, an inventory of the possible resource areas within the Ethiopian sector of the East African Rift system, as reflected in surface hydrothermal manifestations has been built up. The inventory work in the highland regions of the country is not complete but the rift system has been well covered. Of the about 120 localities within the rift system that are believed to have independent heating and circulation systems, about two dozen are judged to have potential for high enthalpy resource development, including for electricity generation. A much larger number are capable of being developed for non-electricity generation applications such as in horticulture, animal breeding, aquaculture, agro-industry, health and recreation, mineral water bottling, mineral extraction, space cooling and heating, etc. (UNDP, 1973).

Since the late 1970's, geo scientific surveys mostly comprising geology, geochemistry, and geophysics, were carried out at, from south to north, the Abaya, Corbetti, Aluto-Langano, Tulu Moye and Tendaho prospects (Teklemariam and Beyene, 2005). In addition, a reconnaissance survey of ten sites in the Central and southern Afar has been carried out, some of these being followed up by more detailed surface investigation. The prospects and fields discussed here are shown in Figure 1.

Due to various factors that determined where the first geothermal power plant would best be located, detailed exploration work was decided to commence in the Lakes area of the rift system during the 1970's. The ICS was already being extended into this region of load growth. The best prospect areas from the technical point of view were located in the Afar which had then been poorly endowed with essential infrastructure and local load demand to support power development. The present circumstances however favor resource development also in the Afar region.

Exploration work peaked during the early to mid 1980's when exploration drilling was carried out at Alutu. Eight exploratory wells were drilled with five of these proving productive. During 1993-98, exploration drilling was also carried out at Tendaho. Three deep and three shallow wells were drilled and geothermal fluids were encountered in the 200-600m-depth range.

Resource utilization was delayed until 1999. The 7.3 MWe net capacity pilot plant installed at Aluto has faced operational difficulties that are essentially due to the lack of the appropriate field and plant management and operation skills. The plant was then put back in to operation after problem identification and rehabilitation of the plant was carried out at the Aluto-Langano geothermal field.

Figure 1 Location of Geothermal Prospects in Ethiopia

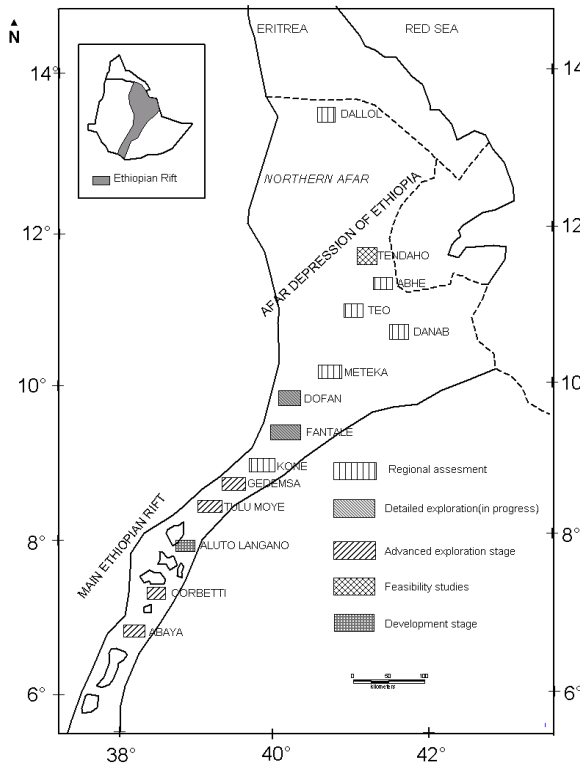

During the three decades that geothermal resource exploration work was carried out in Ethiopia, a good information base and a good degree of exploration capacity, in human, institutional and infrastructure terms, has accumulated, ensuring that selected prospects can be advanced to the resource development phase much more rapidly than before.

The exploration work to date has been carried out by the Geological Survey of Ethiopia (GSE) but has benefited from a number of technical cooperation programs. The most consistent over the long term had been support by UNDP, which also helped in creating other technical capacities of the GSE. The European Development Fund financed the overseas cost of the exploration-drilling project that resulted in the discovery of the Alutu resource. The development cooperation program of the Italian Ministry of Foreign Affairs provided the funding for the offshore costs of the surface and drilling exploration of the Tendaho prospect. The reconnaissance survey of the Afar was sponsored by the Petroleum Exploration Promotion project financed by IDA during the 1980's. The IAEA is assisting the GSE in the isotope geochemical study of hydrothermal fluids and in the process is providing training and experience in the application of the technique in geothermal investigations. IAEA also provided technical advice and equipment. The German Geological Survey (BGR) assisted in Geophysical investigations (MT) of the Tendaho deep geothermal Reservoir during 2006-07. The specialized geothermal science and technology training programs in Japan, Italy, New Zealand, Iceland and Kenya (in cooperation with United Nations University- Geothermal Training Programm of Iceland and Kenyan Generating Power Company) contributed in human resource training and development.

WORK DONE IN GEOTHERMAL EXPLORATION AND DEVELOPMENT

The explored prosects are at various stages of exploration and include: (i) More advanced prospects where exploration drilling has been conducted (Aluto Langano and Tendaho), (ii) Prospects where surface exploration is relatively at higher level (Corbetti, Abaya, Dofan, Fantale and Tulumoye), and (iii) Prosects where surface exploration is at lower level and warrant further exploration in the future (Kone, Meteka, Teo, Danab and L. Abe).

The More Advanced Prospects

Only two prospect areas have been subjected to exploration drilling to date.

The Aluto-Langano Geothermal Field

Detailed geological, geochemical and geophysical surveys were carried out in the Langano area during the late 1970's and early 1980's. Results showed the existence of an underground fluid at high temperature with evidence of long time residence in zones occupied by high temperature rocks (ELC, 1986). The objective then was to locate an economically exploitable geothermal reservoir.

Two wells (LA3 and LA6) drilled on the Aluto volcano produced 36 and 45 T.P.H. geothermal fluid at greater than 300°C along a fault zone oriented in the NNE-SSW direction. Two wells drilled as offsets to the west (LA4) and east (LA8) of this zone respectively produced 100 and 50 T.P.H. fluid with a lower temperature. LA5, drilled in the far SE of the earlier two wells was abandoned at 1,867m depth due to a fishing problem but however later showed a rise in temperature over an extended period of time. LA7 was drilled in the SW but could discharge only under stimulation, being subject to cold-water inflow at shallow depth. The earliest wells drilled in the prospect were drilled outside the present limits of the reservoir area, to the south (LA1) and west (LA2) of the area drilled later.

A 7.3 MWe pilot geothermal plant was installed in 1999 utilizing the production from the above exploration wells. The plant has not been fully operational due to reasons that have to do with the lack of operational experience. But now the plant is partially rehabilitated and put back into an operation of about 5 MWe.

The Tendaho Geothermal Field

Geothermal exploration was carried out in the Tendaho area with economic and technical support from Italy between 1979 and 1980. Between 1993 and 1998, three deep (about 2,100m) and three shallow exploratory wells (about 500m) were drilled and yielded a temperature of over 250ºC. The Italian and Ethiopian governments jointly financed the drilling operation in the geothermal field. A preliminary production test and techno-economic study indicated that the shallow productive wells could supply enough steam to operate a pilot power plant of about 5 MWe, and the potential of the deep reservoir is estimated about 20 MWe.

Based on this and further studies, the Ministry of Mines and Energy is currently working on Tendaho for progressing it towards development. The recent upgrade of a trunk highway through the Tendaho area will help facilitate such exploration and development. In addition, the Ethiopian government plans to extend the country's main 230KV transmission line to Semera, which is within ten km of the drilled wells at Dubti.

Prospects where Surface Exploration is Relatively at Higher Level

Over the years, a number of prospects have been subjected to surface investigation: geology, geochemistry and geophysics and the shallow subsurface has been investigated by drilling at a few of the prospects. They are mostly located in the MER, especially in its most recent zones of tectonic and magmatic activity, the different sectors of the discontinuous WFB. The more important areas are Abaya, Corbetti, Tulu Moye, Dofan and Fantale.

The Abaya Geothermal Prospect Area

Abaya is located on the northwest shore of Lake Abaya, about 400 km south by road from Addis Ababa. The Abaya prospect exhibits a widespread thermal activity mainly characterized by hot springs, fumaroles and altered ground. Spring temperatures are as high as 96 °C with a high flow rate. Integrated geo scientific studies (geology, geochemistry, and geophysics) have identified the existence of a potential geothermal reservoir with temperature in excess of 260°C (Ayele et al., 2002). Further geophysical studies including drilling of shallow temperature gradient wells are recommended here.

The 132 KV transmission line to Arba Minch to the south starts at the Wolayta Soddo substation located about 40 km distance to the NNW of the prospect. This raises the prospect for development of the resource once it is adequately explored, including by drilling.

The Corbetti Geothermal Prospect Area

The Corbetti geothermal prospect area (Figure 1) is located about 250 km south of Addis Ababa. Corbetti is a silicic volcano system within a 12 km wide caldera that contains widespread thermal activity such as fumaroles and steam vents. Detailed geological, geochemical and geophysical investigations conducted in the Corbetti area indicate the presence of potential geothermal reservoirs with temperatures exceeding 250°C. Six temperature gradient wells have been drilled to depths ranging from 93-178m (Kebede, 1986). A maximum temperature of 94°C was recorded. Detailed shallow temperature distribution surveys and geochemical surveys have conducted in 2009-2010. The data so far collected shows the probable existence of a deep reservoir with temperatures exceeding 250 °C.

A 132 KV power transmission line passes within 15 kms of the prospect and is the main trunk line to Southern Ethiopia, to towns along the two branches of the highway to Kenya.

The Tulu Moye Geothermal Prospect Area

The area is characterized by volcanism dating from Recent (0.8 –0.08 Ma) to historical times. Volcanism involved the extrusion of per alkaline felsic lava associated with young tensional and transverse tectonic features dating from (0.1 –1.2 Ma) with abundant silicic per alkaline volcanic products (Di Paola, 1976) in the Tulu Moye-Gedemsa prospect area. This suggests the existence of a deep seated magma chamber with a long residence time. The area is highly affected by hydrothermal activity with the main hydrothermal manifestation being weak fumaroles, active steaming (60-80°C) and altered ground. The drawback of the hydrothermal manifestations is related to the relatively high altitude of the prospect area and the considerable depth to the ground water table. During 1998-2000, integrated geological, geochemical and geophysical studies including shallow temperature gradient surveys (150-200m) , confirmed the existence of potential geothermal reservoirs with a temperature of about 200°C (Ayele et al., 2002) and delineated target areas for further deep exploration wells.

This prospect area is located close to the koka and Awash II and III hydro-electric power stations, the associated 230 and 132 KV substations and transmission lines.

The Dofan Geothermal Prospect Area

Geological, geochemical, and geophysical investigations in the Dofan geothermal prospect (Figure 1) show that the area is characterized by a complex volcanic edifice that erupted a considerable volume of pantelleritic lava from numerous eruptive centers between 0.5-0.2 Ma (Cherinet and Gebreegziabhier, 1983). The presence of several hydrothermal manifestations (fumaroles and hot springs) within the graben, together with an impervious cap, needs to be regarded with high priority for further detail exploration and development (Teclu, A, 2002/2003).

The area is located about 40 km from the high voltage substation at the Awash town.

The Fantale Geothermal Prospect Area

The Fantale geothermal prospect is characterized by a recent summit caldera collapse, felsic lava extrusions in the caldera floor and widespread fumarolic activity, suggesting thereby the existence of a shallow magma chamber. Active tensional tectonics form fissures up to 2m wide near the volcanic complex. Ground water discharge to the system is assured by the proximity of the area to the western escarpment. The results of an integrated interpretation of previous data suggest that the area is potentially prospective for future detailed geothermal resource investigations. Therefore, due to the presence of an impervious cap rock, the western part of the prospect particularly deserves to be investigated during a more detailed geothermal exploration program. In this view, the Geological Survey of Ethiopia has carried out detailed geological, geochemical and geophysical investigations in order to delineate and select target areas for deep exploration wells.

Prospects where Surface Exploration is at Lower Level

The strategic exploration and development plan deals with a total of six geothermal project areas which had been selected on the basis of proximity to areas of economic activity and the national power grid. However, past work has shown that there are several other attractive prospects that are suited for pursuing in the long run.

During the 1980's, reconnaissance geological, geochemical and geophysical investigations have been conducted at Kone, Meteka, Teo, Danab and L. Abe areas that are found in a zone extending between the southern and northern Afar geological provinces (Elc, 1986). Meteka and Teo hold promise for the discovery of economically exploitable geothermal resources at high temperature and warrant detailed surface investigation, followed by exploration drilling. The Lake Abe area warrants further investigation in a wider exploration context that encompasses areas in the eastern part of Tendaho graben and the Lake Abe prospect in Djibouti. These resource areas were not investigated in detail so far, as their large distances from electricity load centers and the national grid accord them lower priority. With advancing economic activity in southern and central Afar as well as in the eastern part of the country, these prospect areas should prove useful for power supply both within the region and to the national grid in the longer-term.

The prospects that have been dealt with under reconnaissance stage are located to the north of 12°N latitude and comprise terrain that is at the most advanced stage of rift evolution in the eastern Africa region and holds a much greater potential for geothermal resources than any other region of equivalent size. This region should be considered as a prime target area for future exploration and development. With the improving availability of the economic development infrastructure in the region, the power-supply system in the load growth areas of northern Ethiopia would benefit from geothermal power generating facilities located in this part of the country.

From these long-term points of view, reconnaissance and preliminary surface evaluation works should commence in the not too distant future in the regions of southern and central Afar, north of 12°N latitude, in order to raise the available level of knowledge regarding the resource areas and to provide the necessary information that is required for long-term planning.

CURRENT GEOTHERMAL ACTIVITIES AND FUTURE STRATEGIES

Current Activities

Currently the following geothermal activities are being conducted in Ethiopia:

- A three year project entitled Strategic Geothermal Resource Assessment in the Ethiopian Rift Valley has started in 2009. The target areas of assessment are Tendaho, Aluto Langano, Corbetti and Abaya. Geo scientific studies including: (i) geological, (ii) geochemical, (iii) geophysical (MT, TEM, Gravity and Magnetics) and (iv) Reservoir Engineering studies are being conducted in these areas. The objectives of the project are to locate and identify areas (sites) for deep drilling by acquiring data that can supplement the already available ones, and upgrade and synthesize all existing information in order to establish a geothermal exploration conceptual model for future feasibility studies. The surface geo scientific studies at Tendaho are being assisted by the German Geological Survey.
- In order to expand the Aluto Geothermal Resource to its full potential, a study on the power development at the Aluto Langano geothermal field in Ethiopia (Phase I) has been conducted by GSE and Japanese consultants as part of "FY2009 Studies for Economic Partnership Projects in Developing Countries " promoted by the "Ministry of Economy, Trade and Industry of Japan (METI)" and that was entrusted to West Japan Engineering Consultants Inc. (West JEC) through Ernst & Young Shin Nihon LLC and the Japan External Trade Organization (JETRO) (Ernst & Young LLC et.al, 2010). The objective of the study was to assess the capacity of the geothermal resource to generate electricity and to determine the technical and eco-financial feasibility of the project. This was done by integration all the existing information and of the execution of MT geophysical survey. The study outlined subsequent two phases for the Expansion and power development. In Phase II the drilling and testing of appraisal

wells will be conducted and preparation to conduct this phase are on going and in the third phase drilling of additional wells and construction of a 35 MW plant is planned.

Future Strategies

Rationale for Strategy

During the past several decades, Ethiopia faced repeated cases of impending or actual power shortages. Reliance on hydro-power has exposed the Ethiopian power sector to the vagaries of periodic drought as it limited the power that could be generated. Consequently, it is planned to diversify the power generation mix. Specifically, this will be done through utilizing indigenous energy resources that are economically competitive, reliable and have a low environmental impact. According to worldwide experience, geothermal resources meet these criteria. Indeed, geothermal is known to be a cheaper energy source. Besides, in Ethiopia it is more intensively studied compared to other renewable resources.

Currently, the desire to increase geothermal development and utilisation in Ethiopia is on account of the:

- Critical role of energy in socio-economic development of the country
- Energy demand growth
- Rural Electrification focus
- Increasing world oil price
- Vulnerability to drought of the hydro power (currently, the main energy supply)
- Availability of a Clean Development Mechanism (CDM)
- Readily available local qualified geoscientists and engineers and equipment (Deep drilling Rigs etc..), for geothermal exploration and development and
- Existence of identified potential geothermal prospect areas

Strategic Plan for Geothermal Development

Six areas which are at advanced stage of exploration are selected as a prime target of near future Geothermal Development of the country. From these areas it is recognized that a total of about 450 MW geothermal energy could be developed in the next 8 years. It is known that the development of geothermal resources is generally more expensive than for a similar capacity hydro electric scheme on a $/kW installed basis. Within Ethiopia however, the level of exploration drilling that has been completed at Aluto and Tendaho, and the potential availability of existing drilling equipment should assist in reducing the cost of the next phases of development

The main criteria for prioritization of various prospect areas for undertaking further exploration and development are: (i) State of advancement of exploration level (Technical); (ii) The relative strategic location (proximity to the existing National grid as an economical factor), and; (iii) Population density of the areas (GSE and EEPCO, July 2008).

Based on these main criteria, the following geothermal prospect areas have been selected (in order of priority) for further exploration and development: (i) Aluto-Langano, (ii) Tendaho (iii) Corbetti, (iv) Abaya, (V) Dofan and Fantale and (vi) Tulumoye

The strategies in each geothermal prospect area are developed in terms of:

- Additional work required to fill knowledge gaps;
- Estimated time to complete the work;
- Estimated potential (MWe) of the field; and
- Required input to implement the project (Human resource, Finance, equipment).

The projected electrical potential of these areas is tabulated in Table 1.

Table 1: Projected output of six selected geothermal prospects in Ethiopia

No.	Prospect Area	Estimated out put (MWe)	Estimated time to develop (Years)
1.	Aluto-Langano Geothermal Field	≈ 75-100	3-5
2.	Tendaho Geothemal field	≈ 100	4-5
3.	Corbetti Geothermal Prospect area	≈ 75-100	5-6
4.	Abaya Geothermal Prospect Area	≈ 100	5-6
5.	Dofan and Fentale Geothermal Prospect area	≈ 60	5-6
6.	Tulu Moye Geothermal Prosepect Area	≈ 40	5-6
	Total	450	

REFERENCES

Ernst & Young ShinNihon LLC, Japan External Trade Organization (JETRO) and West Japan Engineering Consultants, Inc., 2010: STUDY ON GEOTHERMAL POWER DEVELOPMENT PROJECT IN THE ALUTO LANGANO FIELD, ETHIOPIA Prepared for the Ministry of Economy, Trade and Industry, Japan,

GSE and EEPCO, July 2008: Project Pipeline Proposal on Ethiopian Geothermal Resources Exploration and Development in Ethiopia.

Teklemariam, M. and Beyene, K., 2005: Geothermal Exploration and Development in Ethiopia, Proceedings of the World Geothermal Congress, WGC 2005, Antalya, Turkey.

Teclu, A., 2002/2003: Geochemical studies of the Dofan Fantale Geothermal Prospect Areas, South Afar, Internal Report, GSE.

Ayele.A,, Teklemariam, M., and Kebede, S., (2002): Geothermal Resources Exploration in the Abaya and Tulu Moye- Gedemsa Geothermal Prospects, Main Ethiopian rift, Compiled Report.

Electroconsult (ELC), 1986: Geothermal Exploration Project- Ethiopian Lakes District, Exploitation of Langano-Aluto Geothermal Resources, feasibility report, ELC, Milano, Italy.

Kebede, S., 1986: Results of temperature gradient survey and geophysical review of Corbetti geothermal prospect, EIGS.

Cherinet, T. and Gebreegziabhier, Z., 1983: Geothermal geology of the Dofan and Fantale area, (Northern Ethiopian rift), Geothermal Exploration Project, EIGS.

United Nations Development Programme (UNDP), 1973: Investigation of geothermal resources of Power development Geology, Geochemistry and Hydrogeology of hot springs of the east African Rift System within Ethiopia, DP/SF/UN 116-technical report, United Nations, New York, 275 PP.

THEME X

GEOTHERMAL COST - SIDE EVENT

POLICY IMPLEMENTATION TO ENABLE ACCELARATED GEOTHERMAL DEVELOPMENT

R. Gordon Bloomquist, Ph.D.
Nevada Geothermal Power, Inc.

ABSTRACT

Policy implementation can be a very strong tool when it comes to encouraging the development and financing of geothermal energy projects. Developers and especially financiers are unwilling to invest large amounts of money in projects that carry undo legal, institutional, regulatory and environmental risks. In order to facilitate and accelerate geothermal development countries should look carefully at policies related to the granting of and terms of concessions or leases, market policies including such things as long term power purchase agreements and feed in tariffs, incentive programs and last but not least policies relative to foreign investment. Creating a very positive climate that encourages development is essential if geothermal development is to realize its potential.

Key Words: geothermal, investing, policy development, power purchase agreements

INTRODUCTION

The worldwide potential for geothermal development is tremendous, innovative design has solved most of the issues surrounding the development of hydrothermal resources and yet the geothermal industry continues to grow at a relatively slow pace. If the geothermal resource potential is as significant as most experts estimate and if we truly have solved most of the technological problems, why is it that we do not see a tremendous accelerated growth of the industry? In much of the developing world and if we take Africa as an example we find that the estimated potential in East Africa could exceed 20,000 MWe, the need for power is increasing exponentially and yet geothermal development outside of Kenya is more or less nonexistent. There has to be other factors that deter development and discourage investment. The most likely deterrent is an almost total lack of an institutional, legal and regulatory environment that provides the needed safeguards, incentives and framework that is required by international developers and investors. It is thus of paramount importance that each and every country access their policies, regulatory and institutional framework, incentive programs and climate for foreign investment in order to accelerate geothermal development, achieve energy goals and ultimately move the country into a much more economically progressive and sustainable position. The facilitation of private investment in geothermal energy requires that governments create a legal, institutional and regulatory environment that is truly conducive to large-scale investment by the private sector. Through the establishment and implementation of such reforms, countries take a proactive role in creating an environment that is conducive to foreign investment and ultimately to ensuring that development of the nations geothermal resources will take place.

ACCESS

Although government estimates of geothermal resource potential are often extremely encouraging, the private sector needs to be able to obtain a lease or concession that provides not only the initial access to the resource area required to undertake detailed reconnaissance, exploration and reservoir confirmation activities; the lease or concession must also provide for long term development and operation rights should a developable resource be discovered.

Providing access requires the development of comprehensive geothermal statutes, which address all aspects of leasing and exploration as well as the provisions of project development rights.

The first task is to define “Geothermal” and place it into the context of existing water, mineral and land rights.

Is it water, mineral or Sui Generis (unique unto itself)?

The second is to determine who owns that resource. Is it the holder of the:

- Water rights?
- Mineral estate?
- Surface estate?

Access can be provided through:

- Exploration permits
  - Exclusive or non-exclusive
  - Convertible or non-convertible to a lease/concession
- Non-competitive leases/concession
- Competitive leases/concession
  - Cash bonus bids
  - Royalty bids

Leasing terms must also be well defined in statute.

- The duration of primary exploration permit or lease/concession and whether or not it is extendable and with what terms
- Fees: Rentals and royalties
- Work requirements
- Environmental compliance

ACCESS TO A ROBUST AND FAIR MARKET REQUIRES:

Although we often focus our attention on ensuring that the private sector has access to the resource area and long term development and operational rights, it is really access to market that allows developers to raise the significant risk capital that is required to carry out exploration, reservoir confirmation drilling, production drilling and ultimately power conversion facility construction and operation. In order to ensure access to market governments need to provide for the following:

- Empowerment of private partners to engage in the generation of electricity or supply of thermal energy.
- Authority for public entities to enter into legally-binding relationships designed to provide a firm, reliable stream of payments to support private project financing.
- Authority for the private party to have a legal entitlement to payments made by the ultimate consumer of the goods/services provided.
- A level playing field relative to the provision of power by private vs. public suppliers.
- A transparent regulatory framework with regulatory agency independence from influence by government, electricity suppliers, or customers.
- Market power abuse prevention.
- Clear contract dispute resolution procedures.
- Government mandated renewable portfolio standards.

The Power Purchase Agreement (PPA) must obligate the energy purchaser to purchase enough power or thermal energy from the project to support project debt.

The agreement must provide a firm commitment at a specified revenue level or levels not subject to material charges or offsets.

Key provisions include:

- A fair price which may include a capacity component to cover fixed costs and an energy component to cover variable costs.
- A term that fits with the projected construction and operation schedule and at a minimum equal to the term of financing.
- Significant flexibility in terms of the on-line date.
- Significant flexibility relative to the ability to nominate output under the contract (up or down).
- Details of interconnection requirements and charges, design and construction requirements, equipment and monitoring, and continuation of services if an outage occurs.
- Protection against changes in project economics due to changes in environmental laws.
- Assurance that the PPA will not be subject to continuing government revisions.
- An obligation to continue capacity payments (at a level sufficient to cover debt service) during force majeure periods.

GOVERNMENTAL INCENTIVE PROGRAMS

If developers have both resource access as well as market access it is still extremely difficult to secure required equity financing and nearly impossible to obtain any form of conventional financing for upfront exploration and

reservoir confirmation drilling. If countries are truly interested in and committed to the development of indigenous geothermal resource development to help meet further demand for electricity and/or thermal energy it is imperative that incentive programs be initiated that either provide a mechanism for risk sharing between the government and the private investor or provide some form of risk mitigation instrument such as risk mitigation insurance against failure of exploration or reservoir confirmation drilling. Once an economically viable resource has been discovered, governments can continue to play a strong supportive role through the tax policy and in some cases guaranteed loans.

Government policies that can encourage and accelerate geothermal development and aid in the securing of financing include:

- Availability of government grants for exploration and/or development.
- Government cost sharing of exploration costs.
- Risk mitigation insurance for exploration and/or development drilling.
- Government backed guaranteed loans for project development.
- Provision of investment and/or production tax credits.

THE INVESTMENT CLIMATE

Developing and enacting comprehensive geothermal statutes and establishing sound energy related policy, although critical, is usually insufficient to attract private sector investment and project development. Developers and more importantly investors are extremely reluctant to commit to project development and financing in countries where there is no substantial history and experience of private sector energy project development and operation. To overcome this, governments can proactively focus on the enactment of statutes that provide the private sector with safeguards that improve the investment climate. Of critical importance are the following:

- Removal of foreign ownership prohibitions or limits.
- Providing authority to do business, including confirmation of legality of ownership vehicles, and removal of restrictions, if any, on changes of ownership control.
- Codification of all required government approvals, permits, licenses, etc., and mandated government support of the expedited processing of all required approvals, permits, and licenses.
- Establishment of an agency or office with the mandate to serve as a “one stop” shopping center for all required approvals, permits and licenses.
- Providing protection against uninsurable force majeure events such as war, insurrection, terrorism, general strikes, etc.
- Clear delineation of tax and customs statutes.
- Establishment of protections governing availability of foreign exchange, currency convertibility and exchange rate coverage.
- Provisions against expropriation.
- Provisions for import and export tariff relief.
- Expedited clearance of all goods.
- Clarification of employment laws, including use of expatriates.
- Intellectual property protection:
  - Registration of rights
  - Enforcement of rights
- Clearing defined dispute resolution, including:
  - Governing law
  - Location of proceedings
  - Arbitration or courts
  - Sovereign immunity
  - Enforcement of judgments

CONCLUSION

Geothermal development is per say a very high-risk venture with no assurance that significant expenditures in exploration and reservoir confirmation drilling will result in the discovery of a resource that can be economically developed. Because of this both developers and investors must have assurances that once a developable resource has been discovered that this investment can result in the generation of significant revenue to cover debt service as well as an acceptable rate of return on investment. Governments can play a very significant role in providing developers and investors with required access to resource areas, access to markets

and an attractive investment climate. It is clear that developers and investors are as concerned about the business climate in any given country as they are about the resource potential. Investments flow to those countries that have seriously considered the needs of private sector investment, instituted necessary reforms, enacted comprehensive geothermal statutes and have a policy that encourages private sector energy development, renewable energy development and most importantly geothermal energy development.

SELECTED REFERENCES

R. Gordon Bloomquist, 2010, *Facilitating Geothermal Development Through Policy Implementation*. Proceedings – Open Seminar on Low-Carbon Energy Supply Policies for APEC. Tokyo, Japan.

Bloomquist, R. Gordon, Susan Petty and Roger Wagner, 2007, *Geothermal Risk Mitigation Instrument and Incentive Program.* The World Bank, Washington, D.C.

Bloomquist, R. Gordon, Matthew H. Brown and Jennifer A. DeCesaro, 2005, *State Policy Options-Geothermal Leasing*. National Conference of State Legislatures, Denver, Colorado.

Bloomquist, R. Gordon, Matthew H. Brown and Jennifer A. DeCesaro, 2005, *State Policy Options-Geothermal Policy*. National Conference of State Legislatures, Denver, Colorado.

Bloomquist, R. Gordon, Matthew H. Brown and Jennifer A. DeCesaro, *2005 State Policy Options-Defining and Characterizing Geothermal Energy.* National Conference of State Legislatures, Denver, Colorado.

Bloomquist, R. Gordon, 2005, *The Evolution of U. S. Policy Designed to Encourage Geothermal Development.* World Geothermal Congress 2005 Proceedings, Antalya, Turkey.

Knapp, George M. 2005, *Financing Geothermal Projects: Short Course number 4*, World Geothermal Congress Proceedings, 2005, Anatalya, Turkey.

Bloomquist, R. Gordon, 2003, *United States Geothermal Policy-Provision of Access and Encouraging Project Development.* International Course on the Sustainable Use and Operating Policy of Geothermal Resources, International Geothermal Conference, Reykjavik, Iceland.

Bloomquist, R. Gordon and George Knapp, 2002, *Economics and Financing in Geothermal Energy*, UNESCO Chapter 9, Editors M.H. Dickson and M. Fanelli.

Bloomquist, R. Gordon, 1995, *National Geothermal Policy and Regulation in the United States.* Proceeding, World Geothermal Congress 1995, Florence, Italy.

Bloomquist, R. Gordon, 1995, *Understanding the Lenders' Criteria for Funding.* Pre-Congress Short Course Proceedings, World Geothermal Congress 1995, Pisa, Italy.

Bloomquist, R. Gordon, 1992, *Financing Geothermal Projects-Small Geothermal Resources-A Guide to Development and Utilization*. UNITAR/UNDP Centre on Small Energy Resources, United Nations.

Bloomquist, R. Gordon, 1986, *A Review and Analysis of the Adequacy of the U.S. Legal, Institutional and Financial Framework for Geothermal Development*. Pergaman Press.

GEOTHERMAL ENERGY DEVELOPMENT OF L. ABBE AND CDM FOR DJIBOUTI

D Chandrasekharam[1,2] and Varun Chandrasekhar[2]
[1.] *Department of Earth Sciences, Indian Institute of Technology Bombay, India*
[2.] *GeoSyndicate Power Pvt. Ltd., Mumbai*

ABSTRACT

Lake Abbe geothermal province is located within the Afar depression and is one of the active geothermal provinces in Djibouti. The lithological and tectonic configuration of Lake Abbe geothermal systems appears to bear strong similarity to Tendaho geothermal systems located in the Ethiopian Rift, towards NE of Lake Abbe. Lake Abbe is part of ther Awash river basin and the entire surface run off of Awash discharges in to this lake. The geochemical signature of the Lake Abbe geothermal waters is similar to the surface thermal springs and bottom hole thermal waters of Tendaho geothermal province. A conservative estimate of 15 to 20 MWe for the thermal province reported. By using tapping all the geothermal provinces, Djibouti can become energy independent and improve the socio-economic condition of the rural as well as urban population and earn about 9 million euros under certified emision rate through clean development mechanism

INTRODUCTION

The Republic of Djibouti occupying an area of 23180 sq.km is located above the 'Horn of Africa" adjacent to the Red Sea (Fig 1a) It is occupies a strategic position in the East African Continent due to the presence of natural harbour. The essential commodities to all the East African countries land in Djibouti port and transported over land. The population density of the country is about 14 persons/km^2, most of them concentrated in Djibouti town. The country is bordered by Ethiopia and Somalia in the SE. Although the coastal plain is ~ 25 km wide, Ghoubet Kharab bay at Gulf of Tadjoura separates the sea from SE-NW depression land. This part of the land is 155 m below the sea level. The western part of the country is dominated by several SE-NW trending ridges formed due to linear faults that rsulted due to the tectonic configuration of the AFAR triangle and are dominated by basaltic flows. The only river basin in Djibouti is the L Abbe, located toward the south western part of the country that receives drainage from Awash river (Fig 1b).

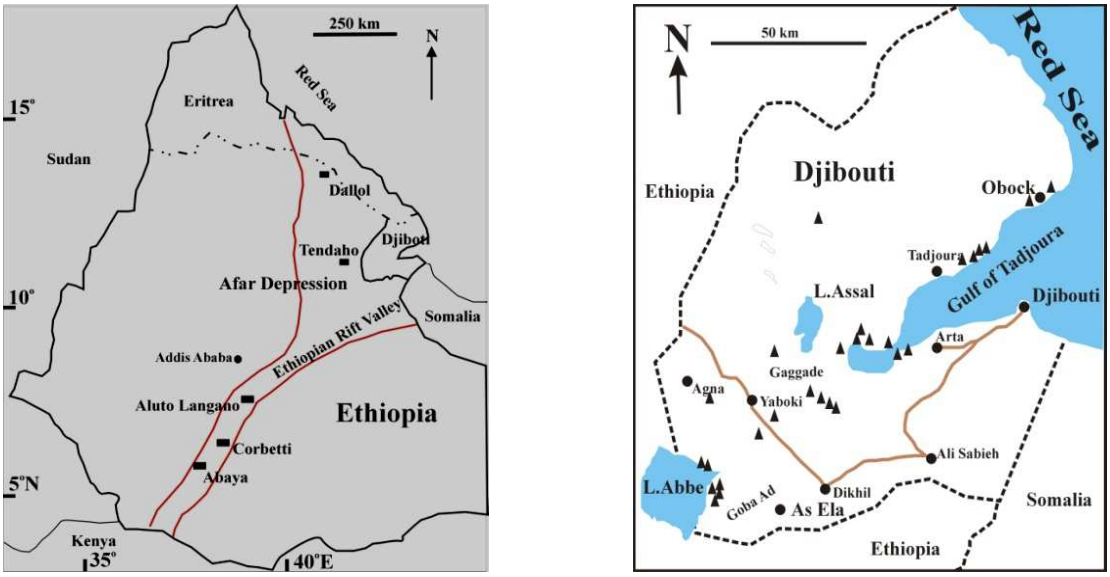

Figure 1: **a).** Map showing the major geothermal fields in the East African Rift valley and **b)** geothermal springs in Djibouti.

The main source of electric power in Djibouti is diesel, imported from the developing countries. The unit cost of electric power is about US 20 cents. Djibouti, being located within the East African Rift system, is endowed with excellent high enthalpy geothermal energy resources. The country can be energy independent if the geothermal resources are utilized both for power production and space heating and cooling. The socio-economic status of the rural communities in the country can be uplifted through this energy source.

TECTONIC SETTING OF THE GEOTHERMAL SYSTEM AROUND L. ABBE

The Afar Depression is loci of active volcanism and tectonism and extends SW in to Ethiopia as the East African Rift. Afar and the EAR host a large number of thermal springs that resulted due to active magmatic activity. This region is one of active spreading ridge since 30 Ma represented by a series of volcanic flows of age ranging from Recent to > 4 Ma (Barberi and Varet, 1977, Varet and Gasse,1978) has given a detailed account on the geological information on the Afar (including EAR and Djibouti). A geological cross section of the lithological Formations across the EAR extending from West of Tendaho to the western banks of Lake Abbe is shown in figure 2.

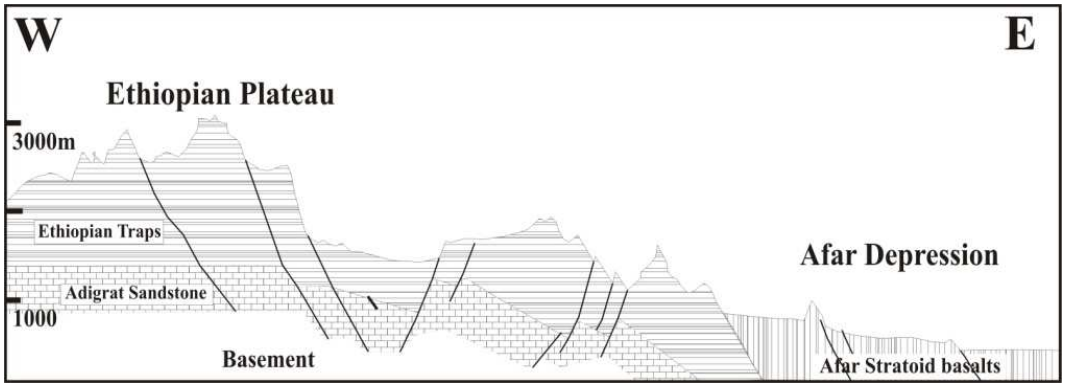

Figure 2: Lithological section across the Ethiopian plateau (Western flank of the rift valley) and Afar depression (up to western bank of Lake Abbe). Modified from (Barberi and Varet, 1977, Varet and Gasse, 1978).

Although Djibouti and Ethiopia are divided politically, the geologically the stratigraphic sequence found on either side of L. Abbe is same and a part of this sequence is shown in figure 2. The Ethiopian Plateau basalts on the western side of L. Abbe continue towards East of the lake and form the oldest basalt sequence in Ali Sabieh horst in Djibouti. Pre-Tertiary sandstone (Adigrat Formation) and limestone Formations underlying below the Ethiopian Plateau basalts continue towards East and lie below the Afar Stratoid basalts extensively outcropping around L. Abbe. All the basalts are dissected by series of parallel NW-SE trending faults. Being within the zone of a spreading zone, the entire L. Abbe zone experiences very high heat flow represented by a large number of boiling thermal springs and fumaroles. Considering the location of the Tendaho geothermal field and the stratigraphic configuration of litho units and drainage systems, the L. Abbe geothermal field is no way different from that of the Tendaho system located a few kilometres away from the L Abbe geothermal field. In fact, as seen from figure 3, the L. Abbe geothermal systems appears to be a part of the Tendaho geothermal system, considering the surface and subsurface geology, tectonic setting and surface manifestations.

GEOCHEMICAL SIGNATURE OF L. ABBE GEOTHERMAL PROVINCE

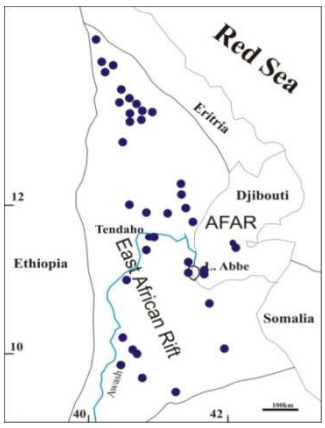

The L. Abbe geothermal province hosts more than 20 thermal springs with issuing temperature varying from 70 to 98 °C with a flow rate varying from 40 to 45 L/s. Majority of the springs are characterised by tall travertine mounds, aligned parallel to the regional structural trend (figure 3). The fumarolic activity is seen at the top of several travertine mounds (Figure 4) deposited over boiling springs.

The geochemical signature of the L Abbe area is very similar to the thermal springs around Tendaho as shown in figure 5a. On the Giggenbach's Na-K-Mg diagram (Figure 5b) the L. Abbe thermal springs fall near the Tendaho Thermal springs area within the partial equilibrium field.

Figure 3: East African Rift and Afar showing the location of thermal springs and the Awash River (modified after Ali, 2001).

Figure 4. Travertine mounds around Lake Abbe and fumarolic activity over the Travertine mound.

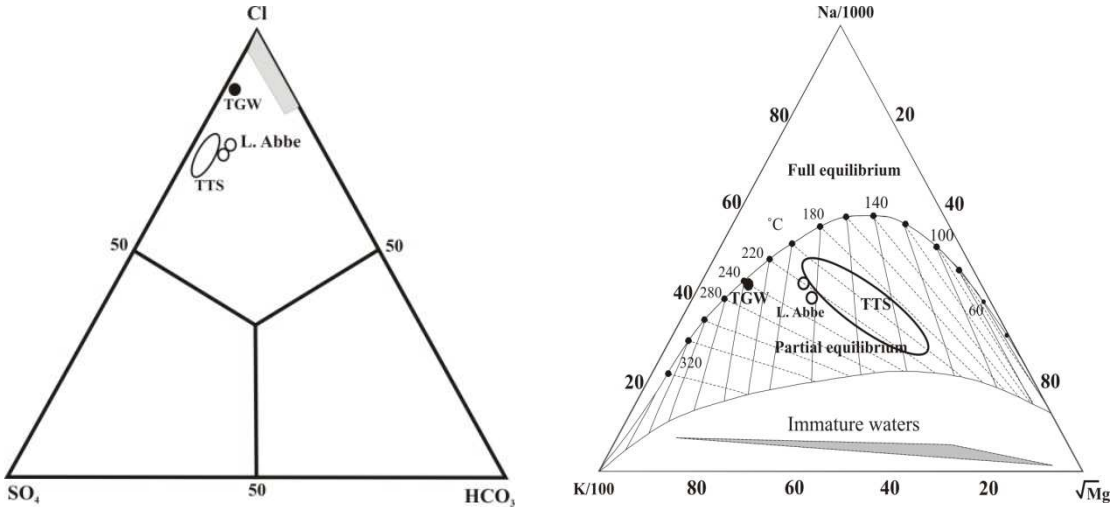

Figure 5 a) Position of Lake Abbe thermal waters with respect to Tendaho thermal springs and Tendaho geothermal well and **b)** position of Lake Abbe geothermal waters on the Giggenbach's (Giggenbach, 1988) Na-K and Mg diagram indicating the reservoir temperatures. TGW: Tendaho geothermal well; TTS: Tendaho thermal springs

DISCUSSION

The Afar Triangle, that hosts Lake Abbe geothermal field, is a part of the active East African Rift system, extending from the Gulf of Tadjoura to Lake Victoria, curing the entire Ethiopian country. The Assal rift extending from the Red sea through the Gulf of Tadjoura, is spreading at the rate of 30 mm/year and is propagating westwards (Courtillot et al., 1980,1984.). The Afar Triangle encloses several active tectonic elements such as normal faults open fissures associated with basaltic volcanism extending age from 1 to 4 Ma (Corti, 2009, Wolfendenm et al., 2004). The NW trending Tendaho rift is a part of the Erta Ale Manda active rift system that extend to the Lake Abbbe geothermal province. Lake Abbe, falling within this rift is filled with lacustrine and alluvial sediments followed by the Afar Stratoid basalts. The Awash River, originating from the elevated SW region (~ 1700 m above mean sea level) of the Ethiopian rift floor, flows towards lower regions in the NE discharging in to Lake Abbe.

As evident from figure 5, the Lake Abbe geothermal waters are very similar to Tendaho geothermal field. The position of the lake Abbe thermal waters close to the Tendaho geothermal field in figure 6 indicates mixing of waters from both basalt as well as sandstone aquifers, like what has been documented for Tendaho region. Reservoir temperatures, as indicated by Na-K-Mg geothermometers (Figure 5b) around 200 °C. Considering the flow rate and estimated reservoir temperature for Lake Abbe, and the transmissivity of the sedimentary (10

m^2/h to 163 m^2/h) and Stratoid basalt aquifers (20 m^2/h to 800 m^2/h; Jalludin, and Razack, 2004) and assuming conditions similar to modelled Tendaho geothermal field (Battistelli et al., 2002) the Lake Abbe geothermal province should be able to generate minimum (conservative) of 15 to 20 MWe (~ 120 x 10^6 kWhr) per a group of 3 to 4 wells tapping both basalt and sedimentary geothermal aquifers. Although both sandstone and limestone aquifers lying below the Stratoid basalts are grouped as sedimentary aquifers, as evident from the volume of travertine mounds found around Lake Abbe, contribution of CO_2 by the limestone aquifer to the geothermal system appears to be greater relative to the sandstone and basalt aquifers.

Djibouti is currently generating about 260 million kWhr (50 MWe) of electricity through diesel thus emitting 1.76 million metric tons of carbon dioxide. For a small country like Djibouti this amount is quite large. The country's per day consumption of diesel is about 13 thousand barrels (http://www.estandardsforum.org). In addition to the existing diesel power generators, the country is planning to augment it electricity supply by installing four 5 MWe diesel generators shortly. The future demand may exceed 120 MWe

According to the preliminary estimates discussed above, development of Lake Abbe geothermal field alone can save about 120 x 10^6 kg of CO_2 there by earning over one million euros under CER (Certified Emission Rate; about 10 euros /tCO_2). Thus the country can geopower its rural regions and become power independent. Both socio-economic status of the rural Djibouti and economic status of the urban Djibouti can be augmented if all the geothermal resources are put to use. If the geothermal potential of Assal is also considered, which is estimated to be of the order of 100 to 150 MWe (Reykjavík Energy report-unpublished, 2008) then the country can generate both from Lake Abbe and Lake Assal geothermal fields ~900 x 10^6 kWhr thus earning about 9 million euros under CER. The country can also earn revenue by supplying electric power to neighboring countries like Somalia and Eritrea.

REFERENCES

Ali, S. 2001. Geochemistry of the Tendaho geothermal field, Ethiopia**.** Stanford Geothermal workshop

Barberi, F. and Varet, J., 1977. Volcanism of Afar: small-scale plate tectonics implications. Geol. Sot. Am. Bull., 88:1251-1266.

Battistelli,A., Yiheyis, A., Calore,C.,Ferragina,C. and Abatneh, W. 2002. Reservoir engineering assessment of Dubti geothermal field, Northern Tendaho Rift, Ethiopia. Geothermics 31, 381–406.

Corti, G. 2009. Continental rift evolution: From rift initiation to incipient break-up in the Main Ethiopian Rift, East Africa. Earth Sci. Rev., Earth-Science Reviews 96 (2009) 1–53

Courtillot, V., Galdenao, A. and Le Mouel, J.L. 1980. Propogation of an accreting plate boundary: a discussion of new aeromgnetic data in the gulf of Tanjurah and south Afar. Earth. Planet. Sci. Lett., 47, 144-160.

Courtillot, V., Acache, J., Landre, F., Bonhommet, N., Montigny, R. and Feraud, G. 1984. Episodic spreading and rift propogation: new paleomgnetic and geochronologic data from the Afar nascent passive margin. J. Geophy. Res, 89, 3315-3333.

Gigenbach, W. F. 1988. Geothermal solute equilibrium. Derivationof Na-K-Mg-Ca geoindicators. Geochim. Cosmochim. Acta, 52, 2749 - 765.

Jalludin, M. and Razack, M. 2004. Assessment of hydraulic properties of sedimentary and volcanic aquifer systems under arid conditions in the Republic of Djibouti (Horn of Africa). Hydrology Jour., 12, 159-170.

Salahadin Ali, 2001. Geochemistry of the Tendaho geothermal field, Ethiopia**.** Stanford Geothermal workshop

Wolfenden, E, Ebinger, C., Yirgu, G., Deino, A. and Ayalew, D. 2004. Evolution of the northern Main Ethiopian rift: birth of a triple junction. Earth Planet Sci. Lett., 224, 213– 228.

http://www.estandardsforum.org/system/briefs/250/original/brief-jibouti.pdf?1277490973

Geothermal energy in the least cost electricity sector planning in Djibouti

Idriss Ahmed Hared
Renewable Energy Lab, Djibouti Centre for Studies and Research

The Republic of Djibouti imports oil to meet its energy demand in the electricity sector. Heavy fuel fired Diesel power plants are run for the baseload and peak demand of electricity. The production cost of the kWh is high (because of oil) and the retail price can reach such level of 32 cents US $ per kWh for some kind of consumers. The government of Djibouti has a strong commitment to develop indigenous energy resource of the country.

The Republic of Djibouti is well endowed with geothermal energy and the development of this resource is a key target for Djibouti.

In this paper we propose a least-cost planning model of the electricity sector in Djibouti in the period 2010-2030. An energy demand and power demand forecasting for the analysed period are first derived based on the historical trend and taking into account future loads that will be added (cement plant load, seawater desalination plant load).

We analyse several electricity generation options which are geothermal option, Diesel option, interconnection with Ethiopia option, CSP option and wind option. All costs are integrated in the model (capital cost, fuel cost and O&M cost). Because of no fuel, geothermal energy is part of the optimal solution.

Keywords : geothermal, least-cost planning, demand forecasting

DRILLING CHALLENGES TOWARDS COST EFFECTIVE DRILLING IN KENYA

Stephen Kangogo
Drilling Engineer
Geothermal Development Company Ltd, P.O. Box 100746- 00101 Nairobi Kenya

ABSTRACT

The objective of drilling is to reach the target depth at the lowest cost, highest degree of safety and minimum damage to the formation. There are several factors which hinder the achievement of this goal; financial support, lack of drilling technical capabilities, lack of experienced crew, few drilling training schools in the world to offer specialized course in drilling, poor research in the drilling industry, no locally available drilling materials. Other challenges include lack of locally available drilling contractors or drilling service providers hence high cost of mobilising fee from overseas. Drilling cost contributes a large portion of total investment in geothermal development; in Kenya. It is estimated that drilling contributes in excess of 65% of the total cost of steam field development for power generation. This paper therefore discusses and challenges encountered while carrying out drilling in Kenya.

KENYA'S OPPORTUNITIES IN CARBON TRADING: A FOCUS ON THE ENERGY SECTOR

Benjamin Kubo, Tecla Mutia, Kennedy Moss and Patrick Oyugi
Geothermal Development Company Ltd, P. O. Box 1770 Nakuru, 20100
E-mail: bkub@gdc.co.ke

ABSTRACT

The idea of carbon trading exists as a product of increasing awareness of the need for controlling emissions attached with the understanding that in order to progress, a monetary value needs to be positioned along with the environmental importance. The Kenyan administration attaches high priority to Carbon Development Mechanism (CDM), which is seen as an instrument for mobilizing investments in the country and advancing the development of new industrial projects. National CDM guidelines had already been developed shortly after the turn of the millennium. Practical project implementation has, however, made slow progress so far, as it is still hampered by a number of factors. Above all, these include lack of information about the scope of CDM on the part of prospective project developers and insufficient technical and institutional capacity. Although Kenya already has quite a substantial number of projects in the pipeline, including some that have already been approved by the competent national authority (NEMA), as at October 2007, only one has been registered with the CDM Executive Board (EB), the UN body responsible for the international approval of CDM projects. The current CDM projects stem largely from the energy sector with a major potential in the geothermal sector. Only three were in the process of validation in October 2007. Regarding international registration by the EB, the 35-MW power station project of the leading sugar producer Mumias Sugar Company Limited for electricity generation from sugarcane bagasse is rated as the most advanced. This paper illustrates key opportunities presently available in Kenya's energy sector for carbon trading and some challenges that the sector is facing. It draws attention to viable market opportunities in the energy sector that potentially could engender lofty investment income.

Keywords: CDM, Carbon trade, Greenhouse gases, Geothermal Energy.

INTRODUCTION

Energy and the Environment

It is now accepted worldwide that the globe is warming to such an extent that the livelihoods of large swathes of the world's population are under serious threat. Violent and frequent storms wreck people's habitats; unpredictable weather drastically changes conditions for agriculture; new health threats emerge. As a result, awareness of global warming is increasingly influencing views all over the world. The main cause of global warming is rapidly increasing carbon dioxide emissions; primarily the result of burning fossil fuels despite international agreements to reduce such emissions.

To manage these risks responsibly, the stock of greenhouse gases in the atmosphere should be held below some target level and brought down from there. Linking energy development to climatic degradation has affected this sector calling for appropriate mitigation measures and now international communities have opted for environmentally friendly sources of energy. It is said that one thing that we have really broadly started to appreciate more is that climate is not an environmental issue. Climate change is a systematic and fundamental issue about the way our economics work and the way we get our energy.

Energy development: Dynamics of Energy Demand

World usage of energy of all types has been increasing at an average annual rate of 2.6 percent per year since the 1960s (Spiegel & McArthur, 2009). The price may as well rise and fall from time to time, particularly as the financial meltdown of 2008 played itself out and the global downturn disclosed. But no matter how prices vary in the short term, the adamant growth in energy use will continue over the long term. Slower growth in the developed world will be offset by faster growth in developing nations.

Kenya, like most sub-Saharan African countries face a major challenge in trying to attain their development and social obligations because of inadequate modern energy services. Low levels of electricity access in sub-Saharan Africa demonstrate this deficiency as an estimated 17% of the region's population, and less than 5% of rural areas are electrified (Davidson & Sokona, 2002). This situation needs to change if sub-Saharan Africa is to be economically competitive with other developing regions of the world and realize its sustainable development goals.

Energy for the future

Demand for renewable energy sources is also going to increase, but for the foreseeable future it will be limited, by the industry's ability to provide it at competitive costs (Spiegel & McArthur, 2009). Key factors that has led to the substantial growth in the renewable energy industry includes; the high fossil-based energy costs related to increased demand and uncertainties in supply; economies of scale and falling capital equipment costs for alternative technologies, improving both yield and efficiency, and thereby improving, competitiveness; legislative action by governments worldwide; greater public awareness of environmental concerns, particularly regarding greenhouse gas (GHG) emissions associated with fossil fuels; the Kyoto Protocol, through which certain countries have committed to reduce GHG emissions, and which in turn motivates those governments to implement policies that decrease the use of fossil-sourced energy and increase the use of alternative technologies.

Increase in nuclear-generating capacity in most nations alongside their long-term outlook is still unclear. Renewables, given the current trend lines, seem unlikely to play a large role in the energy transformations between now and meeting 2030. What would be needed for either of these carbon-free alternative energy sources to grow rapidly enough to make noteworthy inroads into fossil fuels' share of electricity generation is a big, unrelenting push from governments.

Carbon trade

Carbon finance should be a "win-win" opportunity for Africa and in particular, Kenya, and its investors: a way to promote new development initiatives, such as renewable energy projects, while reaping financial benefits and effectively responding to climate change. Kenya possesses abundant natural resources in the energy sector suitable for sustainable energy production. The lack of existing energy infrastructure, particularly in Sub-Saharan Africa, makes it possible to leapfrog the emission-intensive stage of economic development to clean technologies. While the continent is well endowed with renewable energy prospects (solar, wind, geothermal, biomass, hydro), only a very small proportion of the sources is currently exploited. For example, as Figure 1 shows, only 7% of hydroelectricity and less than 1% of geothermal potential is exploited.

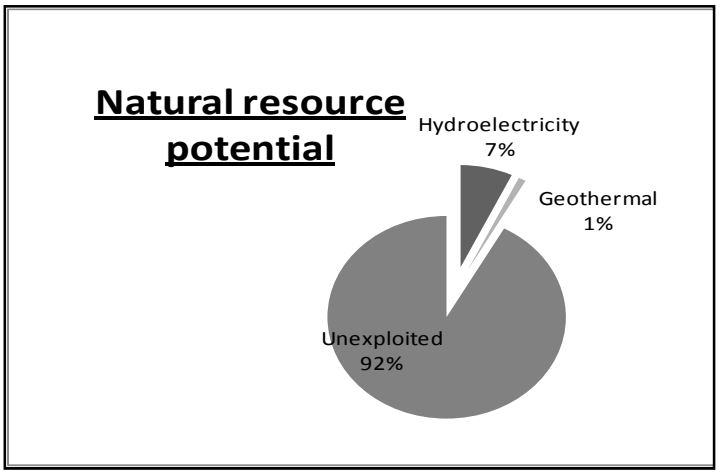

Figure 1: Natural resource potential in Kenya (IEA, 2007)

Analysis of the International Energy Agency's (IEA) most recent (2007) statistics shows that although renewable energy makes up 16 percent of all Africa's energy sources used for power generation, the vast majority comes from combustible renewables and waste. In addition, less than one percent of the total figure is made up of hydro electricity. Other forms of renewable energy in the continent (geothermal, solar, tide and wind) are negligible (International Energy Agency- World Energy Balances, 2009).

POLICY INTERVENTION

Kyoto Protocol

The Kyoto Protocol ratified in 2005, commits many developed countries, defined as Annex I countries, to reduce their greenhouse gas emissions to specific targets. The Protocol defined the Clean Development Mechanism as a mechanism to help these industrialized countries to reduce the costs of meeting their targets by buying certified emission reductions (CERs) generated from projects implemented in developing countries. The

quantification of the CERs, generated by different projects, is made using a methodology that provides all the steps to determine the emissions reductions in an accurate and conservative way.

Kenya National Guidelines on CDM

The National Environment Management Authority (NEMA) in collaboration with the Ministry of Environment is the National Designated Authority (NDA) which handles all CDM activities in Kenya. In 2001, NEMA formulated Kenya National Guidelines on CDM to ensure that CDM projects are environmentally effective and sustainable. This required CDM projects to be based on principles of equitable allocations with focus on non-greenhouse gas emitting technologies especially non-carbon renewable energy technologies (GoK, 2001).

Environmental Management and Coordination Act (EMCA) 1999

The Kenyan Government enacted EMCA to consolidate environmental statutes within a single framework law to enhance environmental management in the country. The law provides for environmental impact assessment and environmental audits for all projects likely to have adverse negative impacts on the environment. NEMA has further developed Environmental Impact Assessment and Environmental Audit regulations, 2003 to further guide the implementation of EIA/A. The process ensures sustainable development while maintaining environmental integrity which directly addresses climate change challenges.

Kenya's Vision 2030

In preparation to curb climate change, the government came up with the Carbon offset scheme to exploit opportunities within the Kyoto Protocol on the establishment of voluntary carbon markets to promote conservation and compensation for environmental services. To integrate planning approaches and improve overall governance of the environment by 2012, at least five CDM projects per year in the next five years should be attracted (GoK, 2007).

KENYA'S OPPORTUNITIES IN CARBON TRADING: ENERGY SECTOR

The current interest to reduce emissions of CO_2 worldwide gives a new boost for renewable energy development in Kenya, hence an additional source of revenue. (Muusya & Ojoo-Massawa, NEMA). The Ministry of Energy, Kenya is therefore taking a deliberate strategy to pursue renewable sources of power from the indigenous geothermal, wind and hydro sources.Kenyan companies are losing out on the global carbon emissions trade, where industrialized nations invest in clean energy projects in poorer nations and in return get offset credits which can be used towards emissions goals or sold for profit. In the energy sector, several projects qualify as CDM projects. This include gas-fired power generation, hydro-electricity to replace coal fired power stations, co-generation (biomass or fossil fuel based), other renewable types of energy (geothermal, wind, photovoltaic, biomass, biogas), and use of forest and agricultural wastes to generate electricity and heat.

KenGen, Green Belt Movement, Mumias Sugar Company, East Africa Portland Cement are some of the Kenyans companies engaged in carbon market projects. KenGen's strategy for green energy is focused on the geothermal sector with planned projects in its portfolio estimated to generate 5 million tonnes of CERs/yr in 2019, which are to be developed through carbon financing. (Simon N., 2009).

Geothermal Energy

Study results reveal that geothermal power production has a significant environmental advantage over burning fossil fuels for electrical power production. Electrical production from geothermal fluids results in an order of magnitude less CO_2 per kilowatt-hour of electricity produced compared to burning fossil fuels. Thus, the data clearly demonstrate that increased geothermal utilization can help Kenya reduce greenhouse gas emissions, assisting National Climate Change Technology Initiative goals while helping to meet increasing power demands. Kenya is in a position to take advantage of carbon finance mechanisms to expand investment in (and access to) energy. The potential of geothermal energy sources is great, with an estimated potential of 4,000MW by 2030 (Geothermal Development Company Ltd (GDC), Kenya). With the empowerment of scientists and engineers in the geothermal field in Kenya and the vast geothermal resource in the Kenyan Rift, the opportunities in carbon trading in the energy sector are quite enormous.

Development of geothermal projects in Kenya faces a number of barriers and these can be partly offset by CDM revenues. While various opportunities continue to arise for Kenya to increase its clean energy projects after ratification of the Kyoto Protocol, KenGen's/GDC, Olkaria Geothermal Project is pursuing its capacity expansion programs with a focus on projects that generate less greenhouse gas emissions.

This expansion can help Kenya to meet the growing power demands as well as securing energy independence. However, some projects face barriers that prevent them from being carried out if they are not registered as CDM activities. Being a registered CDM project activity, and negotiating a CER purchase agreement, has both financial and institutional benefits that enhance the viability of the project. In particular, the Olkaria II expansion project faced four main barriers i.e. investment, tariff, financing and transaction/financing cost barriers (Kollikho, 2007). The third extension phase of the Olkaria II geothermal power station financed by the World Bank has also progressed quite far. Capacity is being increased from 70 MW to 105 MW. For this project, KenGen has already signed an emission reduction purchase agreement (ERPA) with the World Bank's Community Development Carbon Fund for 900,000 tons of CO_2 equivalent. Among others, the Kreditanstalt für Wiederaufbau (KfW) has expressed interest in financing the future fourth extension phase, a project amounting to US$ 150 million.

The country's will in establishing the Geothermal Development Company GDC, to pave way for development of all the geothermal prospects in the Kenyan Rift and realizing the 4000MW by the year 2030, is a move towards the attainability of the carbon reduction and carbon finance.

The Eburru geothermal power station is another CDM project in preparation (expected annual electricity generation of 21 GWh; with an anticipated carbon dioxide equivalent savings according to KenGen of 13,400 tons a year). Ormat (Africa's first privately funded geothermal plant), the US geothermal developer, currently producing 48MW (Olkaria III) is also expected to qualify from the CDM. Olkaria IV, a 140MW plant funded by the Kenyan Government and KfW, is in the planning stage (Hackenbroch *et al.*, 2007).

Geothermal investments promise to enhance energy unit sales

Based on the KenGen report 'Geothermal Development in Kenya, 2006' geothermal power occupies about 11% of the electricity sub-sector and has huge potential for growth (estimated at 4,000MW in Kenya). Kenya has emerged as one of the leaders in Africa in exploiting this form of renewable energy and the Geothermal Development Company was created in 2009 to explore, appraise and undertake steam production. This form of generation is crucial to the generation mix because of its high (94%) load factor (the ability to generate a consistent energy supply from installed capacity). The expected new tariffs on new geothermal projects are also considerably higher than hydro and ranging between KShs 7.00 to KShs 8.20 per kWh. However, despite the massive potential to impact KenGen's top-line growth the ability to fund these projects (high upfront costs) as well as the complexity of the development process represents the biggest headaches. The management estimates that they could earn up to US$1.29 million (Kshs100 million) in CDM revenue from the new projects (Olkaria II 3rd unit and Eburu) through the emerging carbon credits market (Faida Investment Bank, 2009).

Table 1: Installed Geothermal Capacity in Kenya (GDC, 2010)

Project	Capacity Installed (MW)	Year Commissioned	Additional (MWe)	Year Expected
Olkaria I	45	1981 -1985	140	2012
Olkaria II	70	2003	35	May 2010
Olkaria III	48	2000, 2009	50	2013
Olkaria IV	-	-	140	2012
Oserian	4	2004, 2006	-	-
Eburru	-	-	2.5	2010
TOTAL	**167**		**367.5**	

Hydropower

Hydropower is Kenya's main energy source. In the years immediately following World War II (1939-45), Kenya met the increased demand for electricity mainly through the use of fuel oil to provide thermal power. Since 1950, hydroelectric capacity has been dramatically increased, and new hydroelectric schemes have been developed. Kenya has an installed capacity of 737 MW, which is 73.4% of the KenGen's installed capacity. The bulk of this electricity is tapped from five generating plants along the River Tana. Projects in validation as CDM projects include; Sondu Miriu hydropower station for the annual generation of 330 GWh of electricity, Sang'oro hydropower station Lake Victoria (21.4 MW; planned CO_2 equivalent reduction of 57,400 t. Other CDM projects include the Redevelopment of Tana Power Station Project of 130.3 GWh; 83,200 tons CO_2 equivalent a year and the optimization of the Kiambere power station of 60 GWh; 38,300 tons CO_2 equivalent

annually. Research findings indicate that the 2009-13 expansion of hydro capacity will result in only half the potential to raise unit sales as compared to the geothermal projects due to the existing tariffs. KenGen estimates that they could earn up to US$1 million (KShs 80 million) in CDM revenue from the new hydro projects (through the emission reductions purchase agreement signed with the World Bank) (Faida Investment Bank, 2009).

There are also significant endowment sites for small hydros (mini or micro hydros) which are suitable to rural energy demand patterns. The current known potential for mini and micro hydro is estimated to be 300 MW. A number of pilot projects in the area of mini and micro hydro have been implemented to assess the viability of such systems and create the impetus for accelerated exploitation of the mini/micro hydro resource (Hackenbroch *et al.*, 2007).

This CDM project has improved livelihoods by creating employment and business opportunities for the Kenyan people. But recent droughts have slashed capacity at Kenya's main dams, forcing shutdowns and leading to reliance on costly diesel-powered generators, which in turn have pushed up energy bills.

Wind Energy

Wind has been identified as a clean, inexpensive source of energy. Inventions have been made that can harness the energy of the wind and put it to practical use. Wind generated electricity ought to be installed on the grounds that it is already profitable at the present energy prices. Wind energy has been used in Kenya primarily for water lifting since the beginning of the 19th century but its use declined with the advent of oil fired internal combustion engines, which are flexible and more convenient to use. However, with the rising cost of oil, the exploitation of wind energy is becoming increasingly more attractive particularly in areas remote from the grid and oil supply outlets.

To promote investment in wind energy generation, the Ministry of Energy recently completed preparation of a broad National Wind Atlas (www.energy.go.ke/renewable energy). In addition, the Government is promoting the development of wind-diesel hybrid systems for electricity generation under rural electrification programme in areas remote from the national grid. In the meantime, a total of 550 Kilowatts are installed in Ngong and Marsabit, generating about 0.4 gigawatt-hours (GWh) of electrical power, which has been approved by the Kenya Designated National Authority; NEMA as CDM Projects (Hackenbroch *et al.*, 2007).

Co-generation using bagasse and other opportunities

Co-generation using bagasse as a primary fuel is common practice in the domestic sugar industry in Kenya. The industry comprising seven sugar companies produces an average of 1.8 million tonnes of bagasse with fibre contents of about 18% by weight annually. Out of this quantity, about 56% is used in co-generation using an installed capacity of 25 MW and the balance disposed at cost. Mumias, the only registered CDM project in Kenya, is the only sugar company among the seven factories that is self-sufficient in electricity production and has the capacity to export about 2 MW of surplus power to the national grid). A bagasse-based electricity generation project in a joint venture with the Chemilil Sugar Company Ltd. (25 MW; 67,400 tons CO_2 equivalent a year) is in the offing as an additional CDM Project (Hackenbroch *et al.*, 2007).

Other projects have already been approved by the Kenyan Designated National Authority as CDM projects include; the Kipevu (Thermal) Combined Cycle Project (223 GWh an annual 142,500 ton CO_2 equivalent and several industrial projects in the area of fuel switch (the largest being at the Michimukuru/Kiegoy Tea.

CDM Project Portfolio, Kenya

Table 2: CDM (Energy Sector) Project Portfolio in Kenya, January, 2010

	PROJECT	STATUS
1.	35 MW Bagasse Based Cogeneration Project" by Mumias Sugar Company Limited (MSCL) Ref 1404	Registered
2.	Sondu Miriu Hydro Power Project	Validation -re issued
3	Olkaria II Geothermal Expansion Project	Validation on
4	Redevelopment of Tana Hydro Power Station Project	Requested Validation
5	Optimisation of Kiambere Hydro Power Project	Requested Validation

6	6 MW Bagasse Based Cogeneration Project by Muhoroni Sugar	Requested Validation
7	Olkaria III Phase 2 Geothermal Expansion Project in Kenya	Requesting Registration

(DNA – CDM Kenya, 2009)

BARRIERS/RECOMMENDATIONS TO CDM ENERGY PROJECTS IN KENYA

Whilst the opportunities have been stressed, there are however significant challenges. One of the most significant is population growth and rapid urbanization, which will put additional pressure on planning (including spatial planning) for a lower carbon future. These drivers will increase demand on energy, food and water, leading to increases in emissions. This means that opportunities for implementing lower carbon alternatives needs to be an integral element of the planning and policy making system. Grantham Research Institute (2009) summarizes other barriers that need to be overcome to increase uptake of low carbon technologies to include:

- Economic / market barriers (e.g. no finance, poor commercial case). This includes relatively high cost of equipment and services (Phillipines vs. Kenya in Geothermal development) and limited ability to access internationally available "sustainable energy financing", from the Global Environment Facility (GEF) and various other financing schemes. Price distortions and high initial capital costs is also a disadvantage
- Low levels of information (statistics and data), awareness including baseline and methodological constraints for renewable energy and programmatic CDM. This is due to limited availability of comprehensive and well-documented data sets on the dissemination of energy efficient systems in the region and their potential benefits in the economic development of the region,
- Political instability, inadequate policies (regulatory framework), plans and weak dissemination strategies for renewable energy
- Technical problems of use in-country due to renewable energy and energy efficiency industry infancy. Technical knowledge is needed to build a critical mass of policy analysts, economic managers and engineers who will be able to manage all aspects of efficient systems development.
- Inadequate skills, knowhow and research developments
- Limited institutional capacity and infrastructure
- Limited local private sector participation

To overcome the barriers the following recommendations (Karekezi and Kithyoma, 2005) need to be implemented:

- Build local capacity in developing CDM project activities and adoption of appropriate technologies.
- Clear and well defined policies, plans and good governance
- Support to CDM project financing and replication
- Improve information sharing /technology transfer and training.

CONCLUSION

Kenya has contributed very little to global warming itself, but is heavily affected by possible climate changes. The current interest to reduce emissions of CO_2 worldwide gives a new boost for geothermal development in Kenya. Geothermal energy is a clean, renewable and environmentally friendly energy source having greater resource and economic potential. However there is quite some scope for more CDM projects in the energy sector and a variety of measures in the pipeline. Implementation has thus been hampered by a number of factors including; absence of framework legislation, inadequate institutional, financial, technical and personnel capacity on the opportunities afforded by CDM.

REFERENCES

Davidson O. and Sokona Y., 2002: A new sustainable energy path for African development: Think bigger act faster, EDRC, Cape Town and ENDA, Dakar.

Grantham Research Institute, 2009: Possibilities for Africa in global action on climate change, Grantham Research Institute on Climate Change and the Environment.

Hackenbroch. I, Wiekert.M, Cosack. C, (2007) CDM Market Brief, German Office for Foreign Trade

International Energy Agency, 2006: IEA Key World Energy Statistics. Extracted from; www.iea.org/Textbase/nppdf/free/2006/Key2006.pdf.

International Energy Agency, 2009: Key world energy statistics.

Jane H., and Michael H., 2008: Green - Your place in the new energy revolution. Palgrave Macmillan Publishers.

José A.R., and José L.H., 2007: Economics and financing for geothermal projects in Central America. Lectures on geothermal in Central America.

Karekezi, S. and Kithyoma, W., 2005: Sustainable Energy in Africa: Cogeneration and Geothermal in East and Horn of Africa—Status and Prospects, Nairobi, AFREPREN/FWD and Heinrich Boll Foundation Regional Office for East and Horn of Africa (HBF).

Kollikho P. 2007: CDM potential from a geothermal perspective - A case study of Olkaria II 3rd unit, Kenya. Short Course II on Surface Exploration for Geothermal Resources, organized by UNU-GTP and KenGen, at Lake Naivasha, Kenya, 2-17 November, 2007.

Kyoto Protocol to the United Nations Framework Convention on Climate Change < http://unfccc.int/resource/docs/convkp/kpeng.pdf >

Muiruri. A, (2009) Equity Market Research: Kenyan: Energy Sector – Electricity Generation (KenGen), Faida Investment Bank, Nairobi

Muusya A. M., and Ojoo-Massawa E. : Clean development mechanism project development in Kenya, NEMA.

National Petroleum Council, July 18, 2007: Draft Report, "Facing the Hard Truths about Energy: A comprehensive view to 2030 of global oil and natural gas."

NEPAD-OECD Africa Investment Initiative, (2009): Boosting Africa's energy sector through carbon finance. Ministerial meeting and expert roundtable.

Olle N., Niclas H., Robert Ö., 2006: Carbon Trading: A critical conversation on climate change, privatisation and power. Development dialogue no. 48. September 2006

Republic of Kenya (2000) Environmental Management and Co-ordination Act (EMCA), 1999, Government Printers, Nairobi

Republic of Kenya (2001) Kenya National Guidelines on the Clean Development Mechanism. Nairobi

Republic of Kenya (2007) Kenya's Vision 2030. Nairobi

Rohan B., Chris G., Alice H., Michael L., Virginia S.O., Alice T., and Eric U., 2008: Global trends in sustainable energy investment 2008. Analysis of trends and issues in the financing of renewable energy and energy efficiency. United Nations Environment Programme and New Energy Finance Ltd.

Simon N., 2009: Mentoring to empower African CDM project developers – an electric utility's experience. Experience and current approach of the CBNet Team.

Spiegel E., and Mcarthur, N., 2009: Energy Shift; Game-Changing Options for Fueling the Future. McGraw-Hill Publishers.

UNEP (2008), 12th Session of the African Ministerial Conference on the Environment: Financing Climate Change Mitigation – With Special Focus on Africa, Johannesburg, South Africa

Willy A. S., 2008: Clean development mechanism, carbon finance and geothermal applications. Workshop for Decision Makers on Direct Heating Use of Geothermal Resources in Asia, organized by UNU-GTP, TBLRREM and TBGMED, in Tianjin, China, 11-18 May, 2008.

www.ecoseed.org

www.point carbon.com

REGULATORY FRAMEWORKS AND THEIR IMPLICATIONS IN GEOTHERMAL DEVELOPMENT PROJECTS - THE CASE OF KENYA.

Cornelius Ndetei
Kenya Electricity Generating Company, P.O. Box 785-20117 Naivasha, Kenya
cndetei@gmail.com; cndetei@kengen.co.ke

ABSTRACT

In Kenya, several Acts of Parliament regulate and guide use of geothermal and other natural resources in a sustainable way. The laws that deal specifically with geothermal development are Environmental Management and Co-ordination Act of 1999 (EMCA 1999) and the Geothermal Resource Act of 1982 and its supplementary legislation of 1990. Other regulations do not refer specifically to geothermal development but, due to their implications, affect geothermal development at various stages in various ways. These include Energy Act of 2006, Wildlife Conservation and Management Act, Kenya Forest Act of 2005, Occupational Health and Safety Act of 2007, Public Health Act, Local Government Act, Water Act of 2002 and Physical Planning Act of 1999. Geothermal development is also guided by World Bank environmental and social safeguard policies such as the Operation Procedures on environmental assessment, natural habitats, indigenous people and involuntary resettlement. In addition, Kenya is a signatory to various international treaties and protocols which dictate environmental management approaches. Some of these treaties/conventions include the Ramsar Convention, 1994 Convention on biological diversity, Kyoto protocol to the United Nations Framework Convention on Climate Change and Vienna Convention on the protection of ozone layer among others. Presented in this paper are the significant pieces of environmental legislation necessary to fast-track geothermal development in Kenya.

Key words: Environmental legislations, safeguard policies, conventions.

INTRODUCTION

Geothermal energy is considered as a clean, safe, renewable, sustainable and environmentally friendly benign source with opportunities for carbon trading. Further to being indigenous source of energy, it generates continuous and reliable baseload power and offers modular incremental development to remote sites. Though the initial capital needed for development of a geothermal power plant is high, the operation and maintenance costs are low compared to other energy sources.

In Kenya, power demand exceeds the supply, and the current demand growth is 8%. The Kenyan rift is endowed with vast resource of geothermal exceeding 7,000 MWe (Simiyu, 2010), and capable of meeting the electricity demand in Kenya for the next 20 years. Currently, only 202 MWe has been harnessed at Olkaria field with Kenya Electricity Generating Company generating 150 MWe, Orpower 48 MWe and Oserian 4 MWe. The Least Cost Power Development Plan (2008-2028) prepared by the Government of Kenya indicates that geothermal plants have the lowest unit cost and therefore suitable for base load and thus, recommended for additional expansion. In view of meeting 2030 vision, the Kenyan government has recognized the importance and reliability of geothermal energy, and plans to increase the power to 1500 MWe by 2020 and to 4000 MWe by 2030 (Simiyu, 2010).

There are about 14 geothermal fields/prospects located in the Kenyan rift (Mwangi, 2006). The prospects from south to north are Lake Magadi, Suswa, Longonot, Olkaria, Eburru, Badlands, Menengai, Arus Bogoria, Lake Baringo, Korosi, Paka, Silali, Emuruangogolak, Namarunu and Barrier (Simiyu, 2010) as indicated in figure 1. Out of these fields, it's only Olkaria that has been developed. The other fields are at various exploration stages ranging from reconnaissance studies to advanced surface exploration and Eburru field has had exploration wells drilled

Majority of these geothermal fields are located in remote scenic, wild and protected areas such as in national parks, game sanctuary, forest reserves and ramsar sites. Part of the greater Olkaria geothermal field is located inside Hell's Gate National Park. The park was gazetted in 1984, after development of the 45 MWe Olkaria I power station in 1981. Olkaria field has been developed by the Kenya Electricity Generating Company (having developed Olkaria I, II and now in the progress of

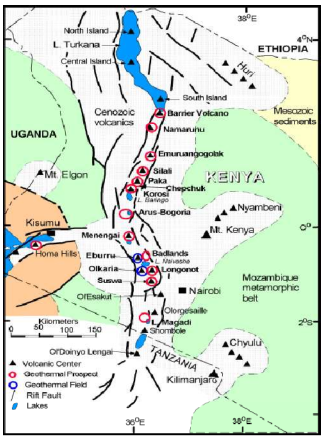

Figure 1: Geothermal fields in Kenya

developing Olkaria IV) and Orpower (developed Olkaria III). Apart from Olkaria IV which is located in a private land, Olkaria I, II and III sub-fields are all located within a national park. The field is also situated near

Lake Naivasha which is a ramsar site and near flower farms. Hence there is need for sound legal and regulatory framework.

It is imperative to comply with environmental legislations at the various phases of geothermal development including exploration, drilling, power plant construction, operations and decommissioning. Failure to adhere to these legislations at any stage of development may lead to delays in the project implementation, adverse financial implications or even abandonment of the project. Hence it is of essence to understand the necessary environmental legislations in relation to geothermal development particularly in Kenya.

LEGISLATIVE FRAMEWORK FOR GEOTHERMAL DEVELOPMENT

There are more than 77 statutes in Kenya which relate to environment. The paper summarizes key environmental legislative requirements for a geothermal project in the country. For ease of discussion, these legislative requirements have been divided into three major parts namely Kenya environmental legislation, World Bank safeguard policies and relevant international conventions and treaties.

KENYA ENVIRONMENTAL LEGISLATION

In Kenya, several Acts of Parliament regulate and guide use of geothermal and other natural resources in a sustainable manner. The laws that deal specifically with geothermal development are Environmental Management and Co-ordination Act of 1999 (EMCA 1999) and the Geothermal Resource Act of 1982 and its supplementary legislation of 1990. Other regulations do not refer specifically to geothermal development but, due to their implications, affect geothermal development at various stages in various ways.

Environmental Management and Co-ordination Act of 1999 (EMCA 1999)

With the enactment of the environmental management and Co-ordination Bill in December 1999, the institutional framework for environmental management was strengthened. The Environmental Management and Co-ordination Act (EMCA) of 1999 provided for the establishment of an environment agency known as National Environment and Management Authority (NEMA) which has been operational since 2002. The authority has been mandated to supervise and coordinate all environmental activities within the country and is the principal instrument of the government in implementation of all policies relating to the environment.

EMCA 1999 supersedes all other environmental legislations and provides "for the establishment of an appropriate legal and institutional framework for the management of the environment". The Act governs Environmental Impact Assessment (EIA) studies and the second schedule of the Act lists project that require EIA studies. More information concerning NEMA environmental regulations are contained in publications by republic of Kenya (1999 and 2003).

The Environmental (Impact Assessment and Audit) Regulations 2003: The environmental Impact Assessment (EIA) is a critical examination of the effects of a project on the environment. The goal of an EIA is to ensure that decisions on proposed projects and activities are environmentally sustainable. Environmental Audit (EA) is the systematic documentation, periodic and objective evaluation of activities and processes of an ongoing project. The goal of EA is to establish if proponents are complying with environmental requirements and enforcing legislation. The purpose of EA is to determine the extent to which the activities and programs conform to the approved environmental management plan. An initial environmental audit and a control audit are conducted by a qualified and authorized environmental auditor or environmental inspector who is an expert or a firm of experts registered by the Authority.

Environmental Management and Co-ordination (Waste Management) Regulations 2006: These regulations outline requirements for handling, storing, transporting and treatment/disposal of all waste categories including industrial waste, hazardous and toxic waste, pesticides and toxic substances, biomedical wastes and radioactive substances.

Environmental Management and Co-ordination (Water Quality) Regulations 2006: The regulations provide for the protection of lakes, rivers, streams, springs, wells and other water sources. The objective of the regulations is to protect human health and the environment. The regulations also provide guidelines and standards for discharge of poisons, toxins, noxious, radioactive waste or other pollutants into the aquatic environment.

Environmental Management and Co-ordination (Controlled Substances) Regulations 2007 (Legal Notice No. 73 of 2007): The Controlled Substances Regulations defines controlled substances and provides guidance on how to handle them. These regulations make it mandatory for industries and other stakeholders in ozone depleting substances trade to obtain a licence to import these substances. Under these regulations, NEMA will be publishing a list of controlled substances and the quantities of all controlled substances imported or exported

within a particular. The list will also indicate all persons holding licenses to import or export controlled substances, with their annual permitted allocations.

Environmental Management and Co-ordination, Conservation of Biological Diversity (BD) Regulations 2006: These regulations apply to conservation of biodiversity which includes conservation of threatened species, inventory and monitoring of BD and protection of environmentally significant areas, access to genetic resources, benefit sharing and offences and penalties.

Kenya has a large diversity of ecological zones and habitats including lowland and mountain forests, wooded and open grasslands, semi-arid scrubland, dry woodlands, inland aquatic, and coastal and marine ecosystems. In addition, a total of 467 lake and wetland habitats are estimated to cover 2.5% of the territory (KPLC, 2010). In order to preserve the country's wildlife, about 8% of Kenya's land area is currently under protection.

Environmental Management and Co-ordination (Noise and Excessive Vibration Pollution Control) Regulations 2009: This law has given general prohibitions on excessive vibrations, and permissible noise levels. It gives provision related to noise from certain sources such as from motor vehicle, construction at night and noise, excessive vibrations from construction, demolition, mining or quarrying sites.

Environmental Management and Co-ordination (Wetlands, Rivers Banks, Lake Shores and Sea Shore Management) Regulations 2009: These regulations include management of wetlands, wetland resources, river banks, lake shores and sea shores.

Environmental Management and Co-ordination (Fossil Fuel Emission Control) Regulations 2006: Apply to all internal combustion engine emission standards, emission inspections, the power of emission inspectors, fuel catalysts, licensing to treat fuel, cost of clearing pollution and partnership to control fossil fuel emissions used by the proponent.

Geothermal Resources Act of 1982 and its supplementary Legislation of 1990

The Act focuses on the drilling and licensing of geothermal wells while taking into consideration the need to dispose the waste products from the geothermal processes appropriately. The regulations stipulate the procedures to be followed by those who wish to explore, drill, extract and utilize geothermal resources.

The Act has provisions on authority for geothermal resources and states that all ownership of all geothermal resources under any land is vested with the Government. The minister for energy is responsible for declaring any area a geothermal resources area and grants the authority or licence to search for geothermal resources or to drill and extract geothermal resources and to do all that is necessary for the conduct of those operations.

Energy Act No. 12 of 2006

The Act establishes an energy regulatory commission, which is the main policy maker and enforcer in the energy sector. This commission among other things shall be responsible for issuing all the different licenses in the energy sector, prescribing the licensing processes, setting and enforcing energy policies, collecting and disseminating energy data and public education and enforcing energy conservation. With this act, all the different aspects of energy e.g. electricity, petroleum and renewable energy are brought under one ambit.

The Act prescribes the manner in which licences shall be obtained for generating, transmitting and distributing electricity. The licence is required if generation is more than 1MWe or the power requires a transmission system from the generation site to the consumption site or the power will be distributed to the public.

The Act in Section 67 establishes a rural electrification authority which is mandated to facilitate access to electricity in rural areas, promote development of renewable energy and levy a fee on all electricity sold for the rural electrification fund.

The Wildlife Conservation and Management Act, Cap 376

This Act consolidates and amends laws relating to the protection, conservation and management of wildlife in Kenya. The main objective is to ensure that wildlife are managed and conserved in a manner that yields optimum returns in terms of scientific, cultural, aesthetic and economic gains, while at the same time taking into account the varied forms of land use and the inter-relationship between wildlife and other land uses. The Act establishes the Kenya Wildlife Service (KWS) as the implementing agency. Under this Act, KWS and KenGen has a Memorandum of Understanding concerning use, management and conservation of Hell's Gate National Park.

The Kenya Forest Act 2005

The Kenya Forests Act, 2005, allows for the sustainable development of a forest in collaboration with institution. Part II (Administration) of the Act, Sec. 4(f) states that; 'The Kenya Forest Service shall collaborate with individuals and private and public research institutions in identifying research needs and applying research findings.'

The Occupational Safety and Health Act No. 15 of 2007

This Act applies to all workplaces where any person is at work, whether temporarily or permanently. The purpose of this Act is to secure the safety, health and welfare of persons at work, and protect persons other than persons at work against risks to safety and health out of, or in connection with, the activities of persons at work. The Act also provides for the establishment of the National Council for Occupational Safety and Health. Some of the areas addressed by the Act include machinery safety, chemical safety, health, safety and welfare special provision.

Public Health Act 1986 Cap 242

The Act regulates activities that may be detrimental to human health. Part IX section 115 of the Act states that no person/institution shall cause nuisance or condition liable to be injurious or dangerous to human health. Section 116 requires Local Authorities to take all lawful, necessary and reasonably practicable measures to maintain their jurisdiction clean and sanitary to prevent occurrence of nuisance or condition liable for injurious or dangerous to human health. Part XII, section 136, states that all collections of water, sewage, rubbish, refuse and other fluids which permit or facilitates the breeding or multiplication of pests shall be deemed nuisances and are liable to be dealt with in the matter provided by the Act.

3.8 Local Government Act (cap 265)

Section 163 (e) allows the County Council to prohibit all businesses, which may be or become a source of danger, discomfort, or annoyance due to their noxious nature through smoke, fumes, dust, noise, or vibrations. Section 165 allows the local authority to refuse to grant or renew any license which is empowered in this act or any other written law on the grounds that the activity does not conform to the requirements of any bylaws in force in the area of such local authority or the granting of the license would be contrary to the public interest.

3.9 The Water Act 2002

The Water Act 2002 provides the legal framework for the management, conservation, use and control of water resources and for the acquisition and regulation of right to use water in Kenya. It also provides for the regulation and management of water supply and sewerage services. In general, the Act gives provisions regarding ownership of water, institutional framework, national water resources, management strategy, requirement for permits, state schemes and community projects. Part IV of the Act addresses the issues of water supply and sewerage.

Part II section 18 of the Act provides for national monitoring and information systems on water resources. Sub-section 3 allows the Water Resources Management Authority to demand from any person or institution, specified information, documents, samples or materials on water resources. Under these rules, specific records may need to be kept by a factory operator and the information thereof furnished to the authority.

Section 73 of the Act allows a person with license (licensee) to supply water to make regulations for purposes of protecting against degradation of water sources. Section 75 and sub-section 1 allows the licensee to construct and maintain drains, sewers and other works for intercepting, treating or disposing of any foul water arising or flowing upon land for preventing pollution of water sources within his/her jurisdiction.

Physical Planning Act, 1999

This is the main Act that governs land planning and all proposed developments must be approved by the respective Local Authority and certificates of compliance issued accordingly. The Local Authorities are empowered under Section 29 of the Act to reserve and maintain all land planned for open spaces, parks, urban forests and green belts. The same section allows for the prohibition or control of the use and development of land and buildings in the interest of proper and orderly development of an area. Section 30 states that any person who carries out development without development permission will be required to restore the land to its original condition. The section also states that no other licensing authority shall grant license for commercial or

industrial use or occupation of any building without a development permission granted by the respective local authority.

WORLD BANK SAFEGUARD POLICIES

Besides the national legislations, there are guidelines that govern the development of geothermal resources and particularly those tied to conditions on funding geothermal projects. The World Bank has developed guidelines for pollution prevention and abatement measures as well as emission measures that are acceptable to the bank (World Bank Group, 1998)

Environmental Assessment (Operational Policy, OP 4.01)

The objective of this policy is to ensure that Bank-financed projects are environmentally sound and sustainable, and that decision-making is improved through appropriate analysis of actions and of their likely environmental impacts (World Bank, 1989). This policy is triggered if a project is likely to have potential (adverse) environmental risks and impacts on its area of influence. OP 4.01 covers impacts on the natural environment (air, water and land); human health and safety; physical cultural resources; and trans-boundary and global environment concerns.

Natural Habitats (Operational Policy, OP 4.04)

This policy recognizes that the conservation of natural habitats is essential to safeguard their unique biodiversity and to maintain environmental services and products for human society and for long-term sustainable development. The Bank therefore supports the protection, management, and restoration of natural habitats in its project financing, as well as policy dialogue and economic and sector work (World Bank, 1989). The Bank supports, and expects borrowers to apply, a precautionary approach to natural resource management to ensure opportunities for environmentally sustainable development.

This policy is triggered by any project (including any subproject under a sector investment or financial intermediary) with the potential to cause significant conversion (loss) or degradation of natural habitats, whether directly (through construction) or indirectly (through human activities induced by the project).

4.3 Indigenous Peoples (Operational Policy 4.10)

The objective of this policy is to ensure that the development process fosters full respect for the dignity, human rights, and cultural uniqueness of indigenous peoples. The policy ensures that adverse effects during the development process are avoided, or if not feasible, ensure that these are minimized, mitigated or compensated. The policy also ensures that indigenous peoples receive culturally appropriate and gender and inter-generationally inclusive social and economic benefits.

4.4 Involuntary Resettlement (Operational Policy 4.12)

The objective of this policy is to avoid or minimize involuntary resettlement where feasible, exploring all viable alternative project designs. The policy is applied to assist displaced persons in improving their former living standards, income earning capacity, and production levels, or at least in restoring them and encourage community participation in planning and implementing resettlement. The policy also provides assistance to affected people regardless of the legality of land tenure (World Bank, 1990). The policy covers not only physical relocation, but any loss of land or other assets resulting in relocation or loss of shelter, loss of assets or access to assets, loss of income sources or means of livelihood, whether or not the affected people must move to another location. It also applies to the involuntary restriction of access to legally designated parks and protected areas resulting in adverse impacts on the livelihoods of the displaced persons.

RELEVANT INTERNATIONAL CONVENTIONS AND TREATIES

Kenya is a signatory to several international treaties and conventions that would need to be adhered to in implementing any geothermal project and are geared towards environmental protection and conservation. The most important treaties and conventions are hereby discussed.

The Ramsar Convention

The Ramsar Convention on Wetlands is primarily concerned with the conservation and Management of Wetlands and Kenya ratified the convention in June 1990. Wetlands are defined by the convention on Wetlands or the Ramsar Convention (1971) as: “Areas of marsh, fen, peat land or water, whether natural or artificial,

permanent or temporary with water that is static or flowing, fresh, brackish or salty, including areas of marine water the depth of which at low tide does not exceed six meters". Parties to the convention are also required to promote wise use of wetlands in their territories and to take measures for the conservation by establishing nature reserves in wetlands, whether they are included in the Ramsar list or not.

The 1994 Convention for Biological Diversity

The convention aims the conservation of biological diversity, the sustainable use of its components and fair and equitable sharing of the benefits arising out of the utilization of genetic resources. Following on from this Convention, and in accordance with the precautionary approach contained in Principle 15 of the Rio Declaration on Environment and Development, the *Biodiversity Protocol* contributes to ensuring an adequate level of protection in the field of the safe transfer, handling and use of living modified organisms resulting from modern biotechnology that may have adverse effect on the conservation and sustainable use of biological diversity, taking also into account risks to human health, and specifically focusing on transboundary movements.

The 1992 United Nations Framewok Convention on Climate Change (UNFCCC)

The UNFCCC has established an ultimate objective of stabilizing green house gases emissions at a level that would prevent anthropogenic interference with global climate. In order to achieve the convention's objectives, the *Kyoto Protocol* was drawn in 1997, where the developed nations agreed to limit their green house gases emissions to levels to 5% below 1990 levels by year 2012.

Vienna Convention for the Protection of the Ozone Layer.

Intergovernmental negotiations for an international agreement to phase out ozone depleting substances concluded in March 1985 with the adoption of the *Vienna Convention for the Protection of the Ozone Layer.* This Convention encourages intergovernmental cooperation on research, systematic observation of the ozone layer, monitoring of ChloroFluoroCarbons (CFC) production, and the exchange of information. The *Montreal Protocol on Substances that Deplete the Ozone Layer* was adopted in September 1987, and was intended to allow the revision of phase out schedules on the basis of periodic scientific and technological assessments. The Protocol was adjusted to accelerate the phase out schedules. It has since been amended to introduce other kinds of control measures and to add new controlled substances to the list.

Convention on the Conservation of Migratory Species of Wildlife Animals

Also known as *Bonn Convention* and is intended to ensure that migratory species of wild animals spelt out on appendix I and II to that convention are protected from extinction. The convention requires intergovernmental cooperation to ensure that the species are allowed to migrate as their nature and their habitat is preserved. The convention was adopted on 23rd June 1979 and came to force on 1st November 1983.

Convention on International Trade in Endangered Species

Came in force on 1st July 1975 after being adopted on3rd March1973.The Convention regulates international trade in wild plants and animals that are at risk of extinction as a result of trade. The convention seeks to control trade not only in live species but also in dead specimen and their derivatives.

United Nations Convention to Combat Desertification (UNCCD)

Kenya ratified the convention on 24th June 1997. The purpose of the convention is to address problem of land degradation by desertification and the impact of drought particularly in arid and dry semi-humid areas.

CONCLUSION

Kenya has not met its' energy requirements despite the vast geothermal resources in the country. Geothermal energy has numerous benefits as compared to other sources of energy and the Kenyan Government has considered geothermal power as the least-cost. As has been experienced, geothermal resource can coexist with other land uses and a clear illustration is Olkaria power station which has been operational since 1981 and is located within Hell's Gate National Park.

Most of the geothermal resources in Kenya are located in protected and sensitive areas. The country is rich in biodiversity and it's imperative to preserve and conserve the environment for sustainable development. Environmental legislations play a very important role in ensuring that geothermal resources are exploited in a sustainable manner, taking into consideration the environment and the future generations.

REFERENCES

KPLC, 2010: ESIA report. environmental and social impact assessment for the proposed Olkaria-Narok-Bomet-Sotik and Kisii-Sondu 132kv Transmission Lines. 168 pp

Mwangi M.N., 2006: Environmental and socio-economic issues of geothermal development in Kenya. A paper presented in the Workshop for Decision Makers on Geothermal Projects in Central America, organized by UNU-GTP and LaGeo in San Salvador, El Salvador, 26 November to 2 December 2006. 12pp

Republic of Kenya, 1999: The environmental management and co-ordination Act, No. 8 of 1999. Government printer, Nairobi. 117pp

Republic of Kenya, 2003: Legislative supplement no. 31, legal notice no. 101: The Environmental (Impact Assessment and Audit) Regulations, 2003. Government printer, Nairobi. 35pp

Simiyu S.M., 2010: Status of geothermal exploration in Kenya and future plans for its' development. Proceedings world geothermal congress 2010 Bali, Indonesia, 25-29 April 2010, 11 pp

World Bank, 1989: Operational directives for environmental impact assessment. World Bank

webpage www.worldbank.org

World Bank, 1990: World Bank operational manual OD 4.30 June 1990 9pp Webpage www.ifc.org/ifcext/.../OD430_InvoluntaryResettlement.pdf

World Bank Group, 1998: Pollution prevention and abatement handbook. Toward cleaner production. World Bank, Environment Department, Washington, DC, 471 pp. Webpage www.worldbank.org

COSTING OF GEOTHERMAL WELLS

Reuben Ngosi
Geothermal Development Company Ltd, P.O BOX 100746 – 00101, NAIROBI
rngosi@gdc.co.ke

ABSTRACT

Well cost forms a major cost component of the total cost of developing any geothermal development project. Due to this fact, it becomes a key consideration in the determination of the economic viability of a geothermal field. Well costs are generally categorized into two components; Tangible and intangible drilling costs. Tangible drilling costs are mainly cost of equipment that become a permanent part of the well and include Well Casings, Wellhead Equipment and Casing Setting Equipment, while intangible costs refer to money spent primarily for services. In addition, one formula of cost monitoring, during drilling, has been suggested. This formula can be a useful tool in ensuring that acceptable variation in the actual drilling costs and planned drilling costs. It can be deduced that well costing is of vital importance since it can help quantify the substantial cost associated with development of any geothermal project thus enabling adequate budgeting/financing. It can also help investigate the costs of drilling and completion of wells and relate those costs to the economic viability of the geothermal project. In addition, since well costs usually contribute a big percentage of the total project cost, determination of the selling price of energy produced will be easy if the well cost is accurate. From well costing records, it is possible to carry out analysis using drilling-costs-with-depth for various regions and couple them with energy-recovery-with-depth as they relate to various regions. Obviously, areas with relatively low drilling costs will have greater return on investment.

INTRODUCTION

Costing of geothermal wells help quantify the substantial cost associated with development of any geothermal project. It will also help to investigate the costs of drilling and completing of wells and relate those costs to the economic viability of the geothermal project. In addition, well costs contribute a big percentage in determination of the selling price of energy produced. From well costing records, it is possible to carry out analysis using drilling-costs-with-depth for various regions and couple them with energy-recovery-with-depth as they relate to various regions. Obviously, areas with relatively low drilling costs will have greater return on investment.

The objective of drilling is to reach the target depth or pay zone at the lowest cost, highest degree of safety, and minimal degree of damage to formation. To achieve this, two requirements must be satisfied. The first is proper design of the well program, which includes evaluating the formation, coring and testing. The second is proper choice of a drilling rig, which includes the ability to reach the target depth rapidly and economically with the highest degree of safety. The well program is 40 percent of the well costs. The remainder of the cost is proportional to the time for drilling, which includes rig day rate, rental tools, etc.

Proper well planning is key to optimizing operations and minimizing expenditures. To minimize the cost of drilling, it is imperative to gather sufficient information of the area to be drilled, such as:

- Cost of surrounding wells
- Geology to be encountered to reach target depth
- Casing requirements – Surface casing depth, Production casing
- Objective of the well – Hole Size
- Other well activities such as well logging, Cores and well testing.

Some information sources like bit records and rig inventory can be very useful in determining cost-effective procedures in drilling a well.

GENERAL OVERVIEW OF GEOTHERMAL WELL DRILLING IN KENYA

Geothermal wells in Kenya are drilledto a depth of about 3000m, vertical and directional (depending on a geothermal prospect) and temperatures of over 300^0C are encountered. High capacity drilling rigs (2000HP) are used in order to reach the target depth.

The planned drilling duration is approximated at 60 days to complete a well and the average cost of drilling is about 6.5 MUSD (using a drilling contractor), however, if own rigs are used, the drilling cost can be much less.

With directional drilling technology many wells (3-5) can be drilled on one platform (same pad). In addition, directional drilling intercepts as many structures as possible thus enhancing permeability. The kick off point

(KOP), where deviation starts, is normally 400m. The maximum deviation angle is 20 degrees built at a rate of 3 degrees per 30m.Deviationsurvey is done at KOP and after every single drilled during angle build up.

Coring is done only where the stratigraphy of the area is not known, but for well-known areas, it is done only if need arises or at the request of the Rig Geologist.

Cuttings samples are collected at 2 m interval, half a liter sample of both inflowing and out flowing drilling fluids are collected after every 50 m interval. Geo-sweeps are carried out with the request of the Rig Geologist if mixing of the cuttings is suspected.

Anticipated drilling problems at various hole sections are usually tackled using advanced drilling techniques and adopting practices from past experiences. Problems like cave in(s), lost circulation, Washouts, are normally comprehensively addressed in the drilling program and possible solutions techniques recommended.

TYPICAL GEOTHERMAL WELL DESIGNS

Directional well design

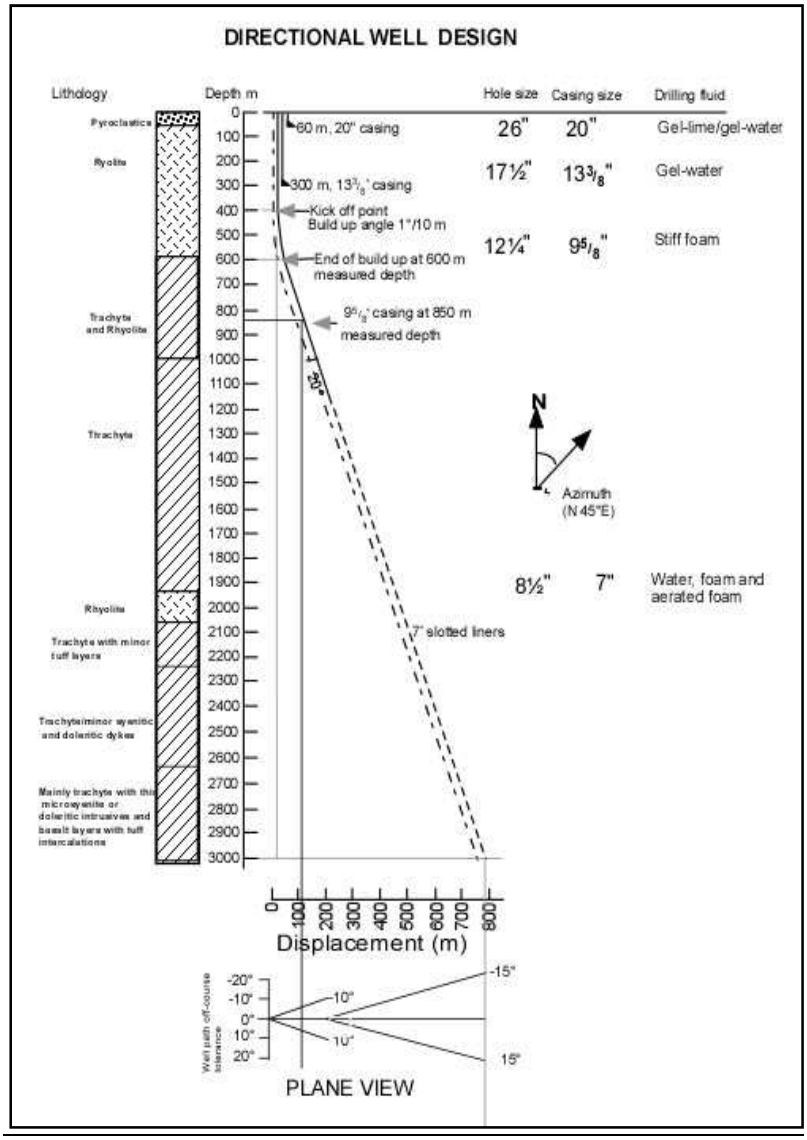

Vertical well design

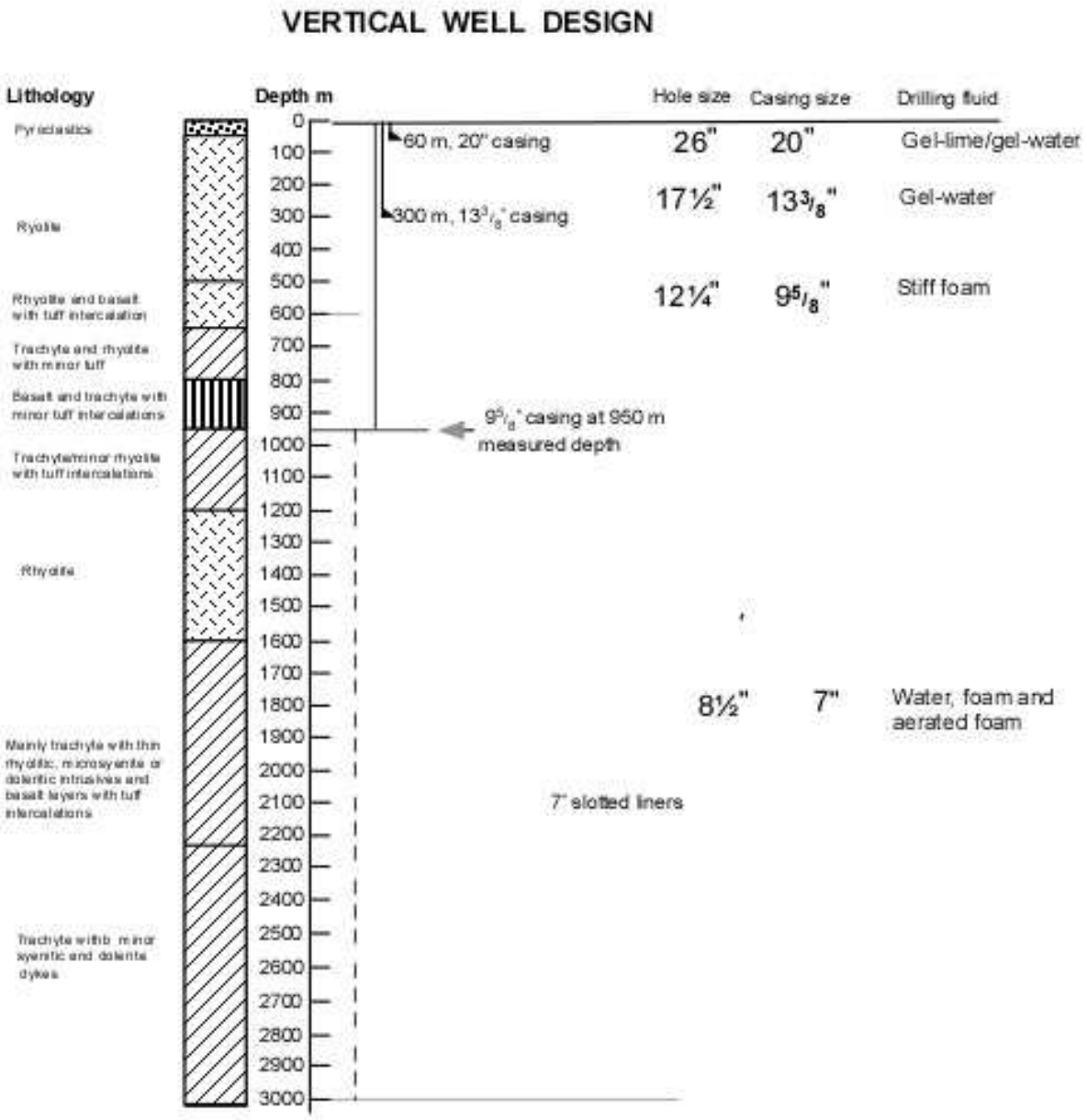

Planned Drilled Depth Vs Drilling Days

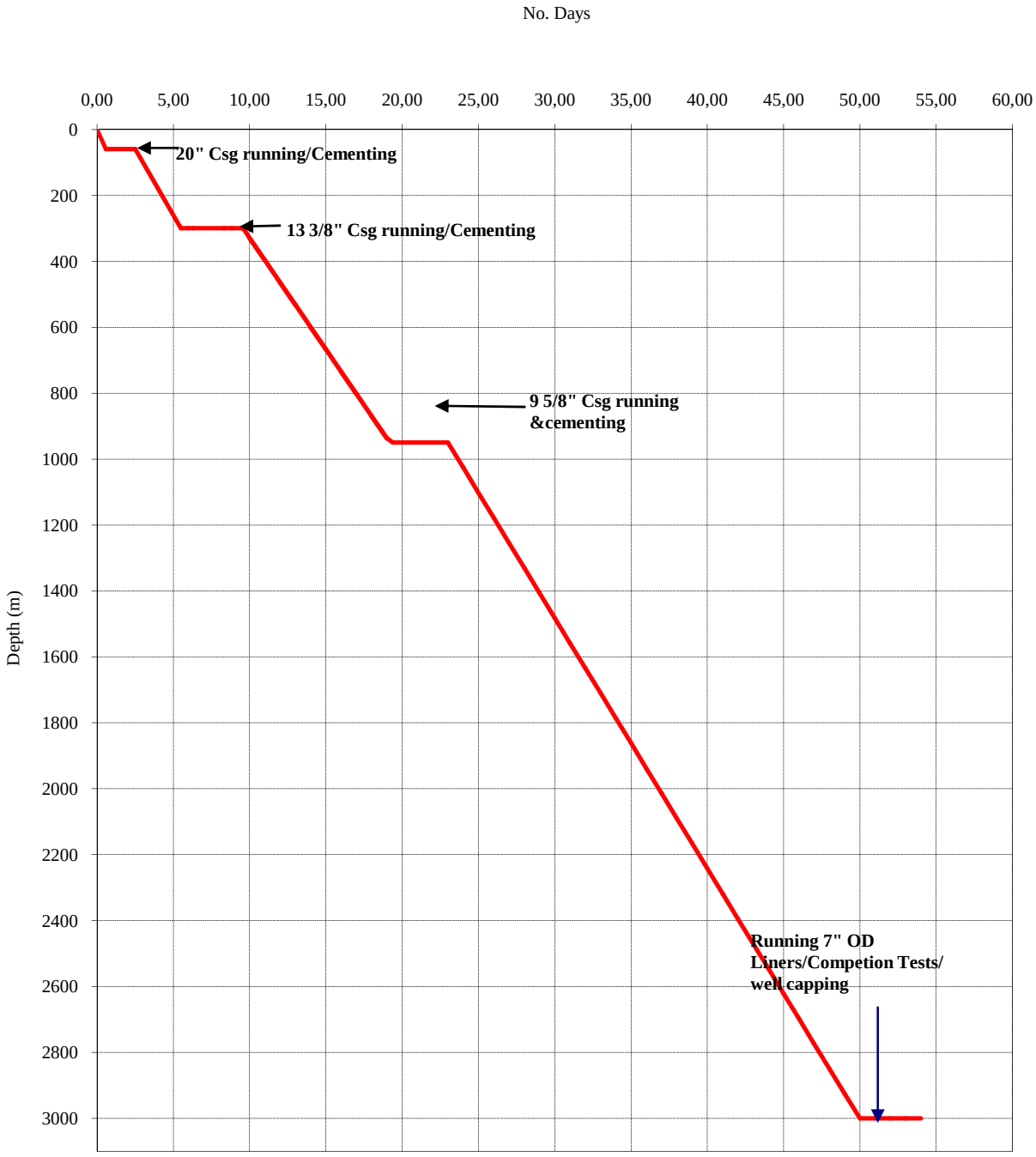

GEOTHERMAL WELL COSTING

Well costs are generally categorized into two components; Tangible and intangible drilling costs. Tangible drilling costs are mainly cost of equipment that become a permanent part of the well while intangible costs refer to money spent primarily for services.

Tangible Drilling Costs (TDC)

These are expenditures for property that has salvage value and generally is equipment or capital costs.

Examples of such expenditures include:

- Well Casings;Surface Casing, Anchor Casing, Production Casing & Slotted Liners
- Wellhead Equipment; Casing Head Flange (CHF), Master Valve, Side Valves
- Casing Setting Equipment; Guide shoe, Casing Hangers, Centralizers, Stop collars.

Intangible Drilling Costs (IDC)

These are expenditures for items that are not tangible. By far the most significant factor in estimating intangibles is drilling time. Interpretation of offset well data yields a depth –versus - days drilling time curve. In addition to day-work charges, some of the most prominent intangible costs are wages, mud, bits, cement, fuel, repairs, hauling and supplies necessary for the drilling and recompletion of the well and the preparation of such well for production.

Other Examples of such costs include:

- ground clearing, drainage construction, location work, road making, temporary roads and ponds, surveying and geological works;
- drilling, completion, logging, cementing of wells;
- hauling mud and water, perforating and supervision overhead;
- Legal cost, damages, insurance;
- Directional drilling services,Plugging
- Environmental costs;
- Logging, coring and wireline services;
- Rig Mobilization and de-mobilization, Transport;
- Contract Labour & Services
- Tools services

Authorisation For Expenditure (AFE)

The authorization for expenditure (AFE) is an estimate of the total cost of drilling a well. It is normally the first steps in drilling a well so that the approximate cost of drilling the well can be known even before the drilling of the well begins. It is however paramount to note that there is no guarantee that the cost of well the drilled will be close to the estimated cost in the AFE. Nevertheless, drilling companies or operators are obligated to provide themselves, investors and all potential stakeholders with a reasonable estimate of the well cost, hence the need for the AFE. If, for some reason, during the drilling of a specific well the operator knows that the total cost of a well is going to exceed the estimated cost in the AFE, it is considered good practice to issue a supplementary AFE, for approval from investors or stakeholders. On some wells there may be several supplementary AFEs.

.

WELL COSTING

WELL NO: ……..
INTERNAL ORDER:…….
FIELD NAME: ……..
COST CENTRE:……
AREA: .....

WELL LOCATION: ……
DATE SPUD: .....
ELAVATION:…….*masl*
DATE COMPLETE: ……
TARGET:
DRILLING DAYS: …….
DEPTH: ……..*m*
CONTRACTOR: ……
RIG: …….
PROJECT:……

TANGIBLE WELL COSTS

	ITEM DESCRIPTION		QTY	UNIT	UNIT COST (USD)	TOTAL (USD)
1	20 " CASING	20" Casing	54.00	m	452.00	24,408.00
		Casing Shoe	1.00	pc	687.00	687.00
2	13⅜ "CASING	13⅜ " 68 lb/ft Casing	22.04	M	227.00	5,003.08
		13⅜ " 54.5 lb/ft Casing	286.38	M	195.00	55,844.10
		Casing Shoe	1.00	Pc	287.00	287.00
		Float collar	1.00	Pc	642.30	642.30
		Top plug	1.00	Pc	385.00	385.00
		Centralizer	8.00	Pc	101.00	808.00
		Stop collar	8.00	Pc	25.25	202.00
3	9⅝ " CASING	9⅝ " 47 lb/ft Casing	1,192.99	M	156.00	186,106.44
		Casing Shoe	1.00	Pc	227.30	227.30
		Float collar	1.00	Pc	502.40	502.40
		Top plug	1.00	Pc	198.00	198.00
		Centralizer	27.00	Pc	90.30	2,438.10
		Stop collar	27.00	Pc	22.58	609.53

	ITEM DESCRIPTION		QTY	UNIT	UNIT COST (USD)	TOTAL (USD)
4	7"Liners	7" 26 lb/ft Casing-Plain		M		
		7" 26 lb/ft Casing-Slotted		M		
5	Wellhead Equipment	Casing Head Flange, 13 3/8"	1.00	Pc	7,988.00	7,988.00
		10" Class 600 Master Valve	1.00	Pc	28,583.00	28,583.00
		10" Class 900 Master Valve		Pc	-	-
		Adaptor Flange, API 6A	1.00	Pc	3,820.00	3,820.00
		2 1/16" Side Valve, 5000 psi	2.00	Pc	7,640.00	7,640.00
		R-57 Ring Gasket C600	1.00	Pc	120.00	120.00
		R-53 Ring Gasket C600	1.00	Pc	120.00	120.00
		R-24 Ring Gasket	2.00	Pc	70.00	70.00
TOTAL TANGIBLE COSTS						

This is a case study where all tangible costs of a well are recorded in a simple spreadsheet.

INTANGIBLE WELL COSTS

	ITEM DESCRIPTION		QTY	UNIT	UNIT COST (USD/KSHS)	TOTAL (USD/KSH)
1	MUD & MUD	Drilling Bentonite	32.50	Ton	653.00	21,222.50
		Lime: Ca(OH)2	-	Ton	1,200.00	-
		Starch	1.50	Ton	1,834.20	

	ITEM DESCRIPTION		QTY	UNIT	UNIT COST (USD)	TOTAL (USD)
	MATERIALS					2,751.30
		Caustic Soda	3.50	Ton	1,341.00	4,693.50
		Calcium Chloride	-	Ton	540.00	-
		Sodium Chloride	-	Ton		-
		CMC		Ton	3,067.00	-
2	LCM MATERIALS	Walnut Shells		Ton	757.40	
		Mica-Flakes		Ton	1,088.50	
		Total Cement for 20" Csg	18.00	Ton	13,189.20	237,405.60
		Blended Cement	18.0	Ton		
		Neat Cement	-	Ton		
		Wyoming (2% BWOC)	0.4	Ton	1,088.50	391.86
		Mica Flakes (3% BWOC)	0.5	Ton	1,088.50	587.79
		Total Cement for 13-3/8" Csg	38.16	Ton	13,189.20	503,299.87
		Blended Cement	21.40	Ton		
		Neat Cement	16.76	Ton		
		Wyoming (2% BWOC)	0.43	Ton	1,088.50	465.88

	ITEM DESCRIPTION		QTY	UNIT	UNIT COST (USD)	TOTAL (USD)
3	CEMENT & CMT ADDITIVES	Mica Flakes (3% BWOC)	0.64	Ton	1,088.50	698.82
		ITEM DESCRIPTION	**QTY**	**UNIT**	**UNIT COST (USD/KSHS)**	**TOTAL (USD/KSH)**
		Fluid Loss (0.65% BWOC)	0.14	Ton	11,515.50	1,601.81
		Friction Reducer (0.3% BWOC)	0.06	Ton	4,941.50	317.24
		Retarder (0.1% BWOC)	0.02	Ton	7,857.40	168.15
		Total Cement for 9-5/8" Csg	80.56	Ton	13,189.20	1,062,521.95
		Blended Cement	46.40	Ton		
		Neat Cement	34.16	Ton		
		Wyoming (2% BWOC)	0.93	Ton	1,088.50	1,010.13
		Mica Flakes (2% BWOC)	1.39	Ton	1,088.50	1,515.19
		Fluid Loss (0.65% BWOC)	0.30	Ton	11,515.50	3,473.07
		Friction Reducer (0.3% BWOC)	0.14	Ton	4,941.50	687.86
		Retarder (0.1% BWOC)	0.05	Ton	7,857.40	364.58
4	ROCK BITS	26" Bit	0.25	Pc	12,285.00	3,071.25
		17-1/2" Bit	0.00	Pc	16,330.00	-
		12-1/4"Bit	3.00	Pc	9,145.00	27,435.00
		8-1/2" Bit	10.00	Pc	5,700.00	57,000.00
5	DIESEL	DIESEL	468,000	Lts	83.56	39,106,080.00
6	OTHERS	Corrosion Inhibitor	drums	drums	710.90	
		Pipelax	drums	drums	700.00	

	ITEM DESCRIPTION		QTY	UNIT	UNIT COST (USD)	TOTAL (USD)
		Casing Dope13⅜ "Casing	1.00	Tin	120.75	120.75
		Baker Lock13⅜ "Casing	1.00	Tin	73.63	73.63
		Casing Dope9⁵ ⁄₈ " Casing	1.00	Tin	120.75	120.75
		Baker Lock9⁵ ⁄₈ " Casing	1.00	Tin	73.63	73.63
		Casing Dope 7" Liner		Tin		
		Rig mobilization and De-mobilisation				
		Survey and Permits				
		Well Services				
		Legal matters				
		Water Supply				
		Transport				
		Drilling operations (daily rates,)				
		Cementing Service				
		directional drilling Services				
		Insurance				
		Tools and Equipment Rent				
		Drilling Supervision				
		Contract Labour and Services				
TOTAL INTANGIBLE COSTS						

DISCUSSION

There is no guarantee that the estimated cost in the AFE will be anywhere close tothe actual cost of the drilled well. This is because during drilling, hole problems are encountered resulting to extend drilling times and thus increased drilling cost.

Daily drilling costs can be monitored so as to maintain the actual cost as close to the estimated cost as much as possible.Estimates of total drilling expenditures for each day can be recorded so that any abnormal variation in the daily estimates can be picked and investigated. The sum of the daily estimates of drilling expenditures over the drilling period should give the approximate cost of drilling the well.

The following equation can be used to determine estimates of drilling costs for any period considered appropriate, either hourly, daily or per bit basis.

$$C_t = \frac{B + C_r (t + T_r)}{F}$$

Where:

C_t = Total drilling cost, $/ft.

B = Bit Cost, $.

C_r = Rig cost, $/hr.

t = Total on-bottom time, hr.

T_r = Round trip time, hr.

F = total ft. /bit

Bit cost B, is easy to estimate. The total on-bottom time, t, is the total time on-bottom with the bit, and includes string connection time. Round trip time, T_r, is the total time necessary to pull and rerun a bit.The total footage per bit, F, is easy to determine. The hourly rig operating costs, C_r, may be difficult to determine but can be estimated from:

- Daily maintenance expenditures
- Drilling practices i.e. Pump pressures, RPM, WOB etc.such practices will impact on rig operating costs (fuel, repairs etc.)
- Rig rental rate.

An accurate record of drilling expenditures of the tangible and intangible drilling costs will give the total well cost. Monitoring the daily drilling expenditures will ensure that the actual drilling costs compare favorably with the AFE costs.

SUMMARY AND CONCLUSION

Costing of geothermal wells can be a fairly simple task if one has a clear understanding of all activities and operations involved from well planning up to when it is completed. If that is the case, it will be possible to factor all costs associated with the drilling of a geothermal well to obtain an accurate figure of the well cost.

It is also imperative to note that proper and reliable record keeping is vital when doing well costing. Therefore this calls for systematized controls of all documents related to costs of items spent on the well so that determination of the well cost can be as accurate as possible.

The level of supervision by engineers, geologists, and operating personnel is also an important contributing factor to accurate well costing. This is because these personnel play a major role in data and record management processes.

Accurate well costing help quantify the substantial costs associated with development of geothermal projects. It will also help to investigate the costs of drilling and completing of wells and relate those costs to the economic viability of the geothermal project. In addition, well costs contribute a big percentage in determination of the selling price of energy produced. From well costing records, it is possible to carry out analysis using drilling-costs-with-depth for various regions and couple them with energy-recovery-with-depth as they relate to various regions.

REFERENCES

Moore L.Preston, (1986)Drilling Practices Manual, 2nd Ed, Pennwell Publishing Company.

2003 Joint Association Survey on Drilling Costs, 2005, American Petroleum Institute.

Chilingarian G., and R. Vorabutr 1983, Drilling and Drilling Fluids, Appendix G, New York, Amsterdam: Elsevier,

A NEW KFW FUNDING AND RISK MITIGATION SCHEME FOR GEOTHERMAL PROJECTS IN THE EAST AFRICAN RIFT VALLEY - STRATEGY AND STRUCTURE"

Katrin Kessels (KfW)
Horst Kreuter (GeoT, GeoThermal Engineering GmbH)
James Muir (SKM, Sinclair Knight Merz)
Marietta Sander (BGR, Bundesanstalt für Geowissenschaften und Rohstoffe, Hannover)

ABSTRACT

Eastern Africa has an estimated geothermal resource potential of over 7,000 MWe. Development of these resources presents the opportunity to address issues like the reliability of power supply, low cost power production and low carbon emissions in the electricity sector and support economic development. Many international and regional organisations recognise this opportunity, yet progress remains slow. The high upfront costs and risks associated with exploration drilling remain the greatest obstacles. In addition, investment in the geothermal sector is still hindered by unsupportive regulatory, institutional and financial conditions in some countries.

KfW Entwicklungsbank (KfW) -supported by BGR- appointed Sinclair Knight Merz (SKM) and GeoT to design a feasible risk mitigation facility ('the Facility') that assists public and / or private investment in early-stage geothermal drilling in Ethiopia, Kenya, Rwanda, Tanzania and Uganda. The Facility will reduce geothermal exploration drilling risk by supporting two key activities:

- Surface studies to determine the optimal location of exploration wells at the most promising geothermal prospects
- Drilling of exploration wells at the most promising geothermal prospects to assist developers secure finance for subsequent exploration or appraisal wells.

A limited stakeholder consultation process was undertaken seeking comments on the Facility Concept. Views were received from a range of public and private organisations across the region. These were broadly supportive of the principles of the Facility and also highlighted how the Concept could be improved. Subsequent to this, the Concept was further refined over the course of meetings between AUC, KfW and SKM in Addis Ababa, 9th – 13th August 2010.

Establishment of the Facility is supported by two main documents: Operational Guidelines which provide guidance for the AUC on establishing and operating the Facility; and the Developer Manual which provides guidance to those applying to the Facility.

An indication of the total funds required has been determined through the development of different scenarios. Under the Base Case, support is provided to eight surface studies and five exploration drilling programmes. Of the drilling programmes, two secure finance for subsequent exploration or appraisal wells.

Présidence de la République
République de Djibouti

Centre d'Etudes et de Recherches de Djibouti
B.P. : 486 – DJIBOUTI – République de Djibouti
Tél : (253) 35 27 95 / Fax : (253) 35 48 12
Email : cerd@intnet.dj ; argeo-c3-djibouti@intnet.dj – Site web : www.cerd.dj